NATIONAL AERONAUTICS AND SPACE ADMINISTRATION

Technical Report 32-1460

Volume I

Mariner Mars 1969 Final Project Report

Development, Design, and Test



FACILITY FORM 602
N71-15484 (ACCESSION NUMBER)
(PAGES)
CR-115875 (NASA CR OR TMX OR AD NUMBER)
(THRU)
63
(CODE)
31
(CATEGORY)

JET PROPULSION LABORATORY
CALIFORNIA INSTITUTE OF TECHNOLOGY
PASADENA, CALIFORNIA

November 1, 1970

NATIONAL AERONAUTICS AND SPACE ADMINISTRATION

Technical Report 32-1460

Volume I

Mariner Mars 1969 Final Project Report

Development, Design, and Test

JET PROPULSION LABORATORY
CALIFORNIA INSTITUTE OF TECHNOLOGY
PASADENA, CALIFORNIA

November 1, 1970

Preface

The work described in this report was performed by the technical divisions of the Jet Propulsion Laboratory, under the cognizance of the *Mariner* Mars 1969 project.

This is Volume I of the three volumes that constitute the final report of the *Mariner* Mars 1969 project. The three volumes correspond, in chronological order, to the three principal activities of the project:

(1) The preparation and preflight phase for the dual spacecraft mission, *Mariner VI* and *Mariner VII*, from December 1965 through March 1969 is described in Volume I. The project management, planning, and mission analysis are presented in Part 1; the development, design, and testing of spacecraft system and subsystems are detailed in Part 2; and the launch and earth-based systems are covered in Part 3.

(2) The conduct of the flight phase of the mission from February–March 1969 to October 1969 is presented in Volume II. A summary of the events of the entire flight phase and the flight path report are given in Part 1; the launch phase is discussed in Part 2; and Part 3 covers the space flight phase, including details of spacecraft system and subsystem performance.

(3) Postflight scientific analysis of the mission scientific data is given in Volume III. The project scientist's report is provided in Part 1 and some experimenters' interpretations are included in Part 2.

A comprehensive report of the tracking and data system support to the mission will be provided in a separate report.

Acknowledgment

This volume was compiled from administrative, engineering, and scientific, data contributed by many people. Acknowledgment is given to the following JPL personnel for their direct contributions:

W. C. Apel
C. M. Ashley
D. L. Brunn
W. H. Chitty
M. C. Clary
R. L. Crabtree
J. E. Earnest
D. D. Gordon
D. E. Griffith
N. H. Herman
L. M. Hershey
R. J. Holman
J. R. Hyde
J. B. Ingles
R. H. Josephs
C. E. Kohlhase
C. C. La Baw
W. J. Lane
E. A. Lawmann
D. W. Lewis
K. W. Linnes
J. L. Mc Gillicuddy
E. S. Mc Millan
D. Montgomery
G. E. Nichols
J. F. Park
L. G. Parker
J. A. Plamondon
D. C. Preska
N. A. Renzetti
E. L. Royal
W. J. Schatz
D. M. Schofield
R. F. Stott
D. W. Swenson
H. J. Wilkeyson
J. H. Wilson
A. Wiltsey
J. L. Wolfe

This volume was compiled by J. H. Wilson under the direction of G. P. Kautz and J. R. Casani.

Contents

Part 1. Project and Mission

Introduction 3

Project Background and History 6

Management 14

Mission Design, Analysis, and Engineering 31

Part 2. Spacecraft System

Spacecraft System Design 69

Engineering Mechanics 107

Science Subsystems 157

Telecommunications System and Subsystems 237

Guidance and Control 325

Propulsion and Pyrotechnic Subsystems 396

Environmental Test Program 421

System Test and Prelaunch Operations 445

Test Support Equipment 462

Reliability and Quality Assurance 505

Part 3. Launch and Earth-Based Systems

Launch Vehicle System 531

Mission Operations System 542

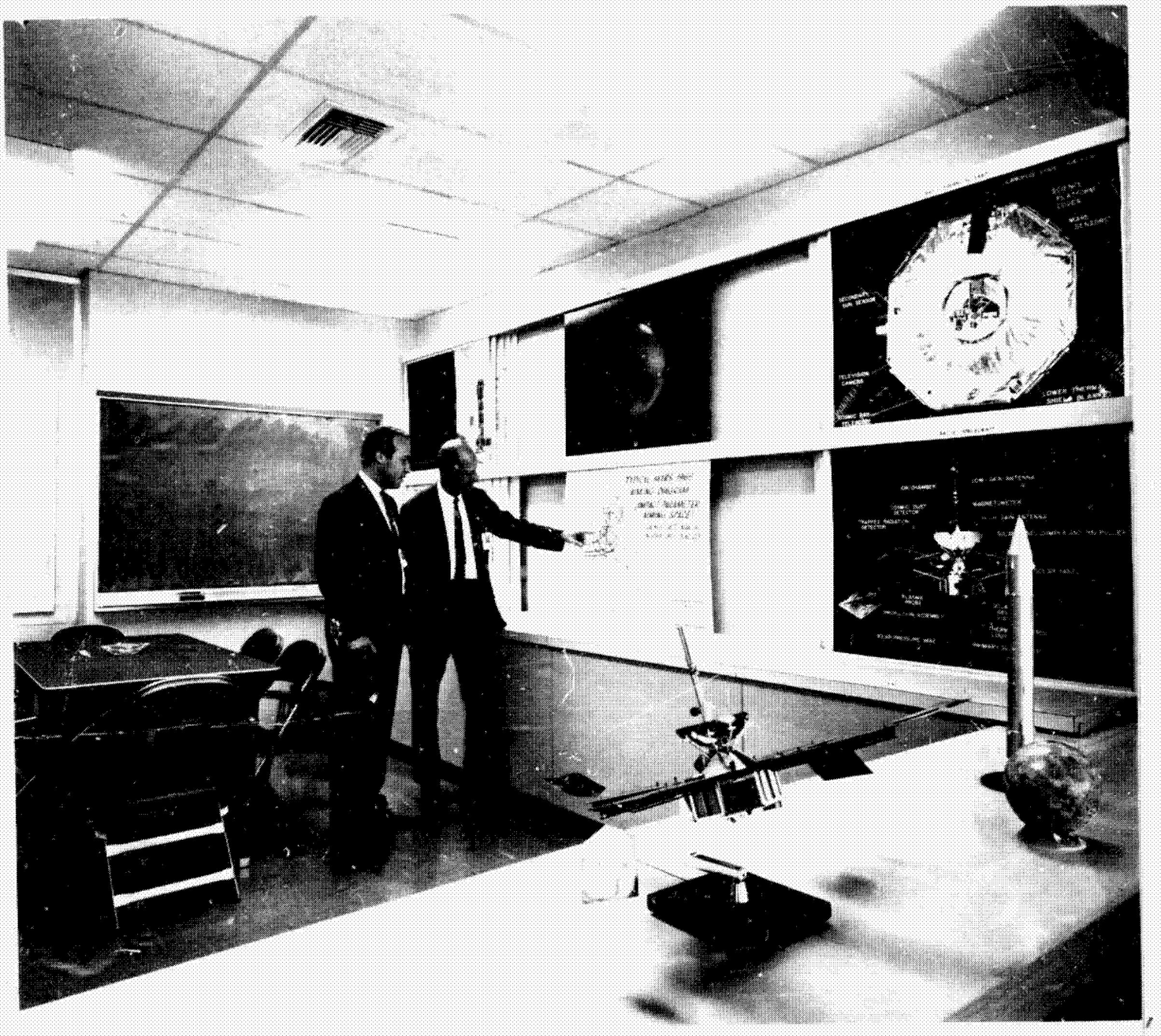
Tracking and Data System 584

Glossary 603

Abstract

This is the first of three volumes of the *Mariner* Mars 1969 Final Project Report. This volume describes the pre-operational activities including planning, development, design, manufacture, and testing. Volume II describes the performance of the mission by flight and Earth-based elements during the launch and space-flight phases. Volume III deals with the scientific program, including experiment results.

The *Mariner* Mars 1969 project was organized around four functional systems: (1) the *Mariner* spacecraft, based on *Mariner C* design, (2) the *Atlas/Centaur* launch vehicle, (3) the Tracking and Data Acquisition System, and (4) the Mission Operations System. Four spacecraft were prepared: one proof test model, two flight spacecraft, and a spare. The spacecraft were divided into nineteen functional subsystems which were subcontracted by JPL and the launch vehicles were adapted and built by a contractor under the cognizance of the NASA Lewis Research Center.



Part 1. Project and Mission

PRECEDING PAGE BLANK NOT FILMED

Introduction

When the *Mariner* Mars 1969 project was established at the end of 1965 and during early 1966, it was assigned to the Jet Propulsion Laboratory (JPL) under contract to the National Aeronautics and Space Administration (NASA). In addition to project management, JPL was given the responsibility for the spacecraft system, mission operations, and tracking and data acquisition (TDA). The Lewis Research Center (LeRC) of NASA was made responsible for the *Atlas/Centaur* launch vehicle system.

I. Objectives

Objectives of the *Mariner* Mars 1969 project were:

(1) To conduct flyby missions in order to make exploratory investigations of Mars which will set the basis for future experiments, particularly those relevant to the search for extraterrestrial life.

(2) To develop technology needed for the succeeding Mars missions.

A tentative objective concerned with inflight solar-system investigations was removed from consideration by NASA early in science planning and experiment selection, when it was decided to concentrate the scientific mission on the planet Mars.

II. Technical Approach

The technical approach chosen for the project was to rely heavily on existing technology, in particular elements of the *Mariner* Mars 1964 efforts and *Atlas/Centaur* as used in support of *Surveyor*, with modifications and novel features as necessitated by mission characteristics and objectives. Some of the governing factors and constraints which helped define approach and design were:

(1) The 1969 launch opportunity, with the various features and differences from 1964, and similar absolute time limitations.

(2) The funding and manpower limitations.

(3) The demonstrated *Mariner C* spacecraft design, which had carried out the *Mariner IV* mission in 1964 and 1965.

(4) The existing *Atlas/Centaur* launch vehicle system, then beginning to support *Surveyor* missions.

(5) The scientific data from the limited scope of the *Mariner IV* mission.

(6) The future-mission-oriented objectives.

The determination of the scientific experiments, made by NASA with the advice of the project and the recommendation of the Space Science Board, was very influential in mission, spacecraft, and operations design. The experiment teams included representatives of university, industrial, and government laboratories. The experiments selected ranged from extensions of existing study programs to bold new investigations, and called for the return of some thirty times more information then previously collected from any other planet.

Two spacecraft* were to be launched from Cape Kennedy between mid-February and early April 1969, on type I trajectories giving a transfer time of four to six months. The same scientific experiments were to fly on each spacecraft. The dual launch was for the two purposes: (1) reliability, to increase the probability that scientific data would be returned from Mars, and (2) scientific, to improve the scientific return by purposefully coordinating the two planetary passes. The prospect of studying seasonal variation by observing the same region at two widely separated times was considered and abandoned in favor of observing a larger area, with considerable overlap under different lighting conditions, from the equator of Mars to the south pole in two passes five days apart. Observation of the planet at longer range during the approach to the close pass was suggested early in the planning, as well as scan control to provide multiple-swath coverage instead of the single swath obtained by *Mariner IV*. Both of these features were realized in the design, through the adoption and thorough application of design features and operational techniques, notably in communications and programmed control and sequencing, which were essentially novel in this project.

III. Management Approach

The *Mariner* Mars 1969 project was organized around four functional systems:

(1) The *Mariner* spacecraft, based on the *Mariner C* design but with many modifications undertaken to meet the 1969 mission objectives and to accommodate the change of launch vehicle, as well as to enhance reliability, and to reduce cost.

(2) The *Atlas/Centaur* launch vehicle, whose increased injection energy permitted both a large increase in spacecraft weight (over *Mariner C*) and a large increase in launch opportunity (over 1964), and whose improved injection accuracy was expected to simplify some aspects of mission design.

(3) Tracking and data acquisition, which included some elements of the Air Force Eastern Test Range (AFETR) and Manned Space Flight Network (MSFN) during the launch phase, but was based on committed elements of the Deep Space Network (DSN) in California, Australia, South Africa, and Spain for the remainder of the mission.

(4) Mission operations, a complex of mission-independent and mission-dependent hardware and software, and operational personnel to conduct the mission.

Each of these systems was responsible to design (or adapt), develop and construct (or commit), test, and operate its portion of the project or mission. Each is discussed (from design through final testing) in a separate portion of this volume.

Other project elements, active as appropriate at the system level but represented on the project staff, were mission design, analysis, and engineering, reliability and quality assurance, science, and management control and administration. With the exception of science, which is covered in Volume III, each of these curricula is discussed in a separate section of this report.

The *Mariner* spacecraft is further divided functionally into nineteen subsystems (see Table 1), of which four are scientific instruments supporting four of the experiments (two experiments required no peculiar flight equipment).

Each subsystem, or in some cases major portions of the subsystem, were developed and manufactured by subcontractors, under the cognizance of the appropriate technical divisions of JPL. The spacecraft, in turn, were assembled and tested under the cognizance of the project engineering division of JPL.

Four spacecraft were prepared: a proof test model (PTM) spacecraft, two flight spacecraft, and a spare spacecraft. The spare spacecraft, although fully tested as a flight item served the purpose of providing spare subsystems which were fully qualified in the flight environment.

*After the successful launches, described in Volume II, the flights and spacecraft were formally designated *Mariner VI* and *Mariner VII* (in the order in which they were launched). Before launch, the flight sequences were referred to as *Mariner F* and *Mariner G* respectively; the actual flight hardware spacecraft being prepared for launch were designated M69-3 and M69-2 respectively.

Table 1. *Mariner* Mars 1969 subsystems

Subsystem	Subcontractor
Radio frequency	Philco-Ford Corp., Space & Reentry Systems Division
Flight command	Motorola Government Electronics Division
Telemetry	Texas Instruments Inc.
Data storage	Texas Instruments Inc.
Power	Electro-Optical Systems
Central computer and sequencer	Motorola Government Electronics Division
Attitude control	Honeywell, Inc.
Scan control	Honeywell, Inc.
Structure	Northrop Space Laboratories, Northrop Corp.
Cabling	—
Mechanical devices	—
Temperature control	TRW, Inc.
Propulsion	TRW, Inc.
Pyrotechnics	Electro-Optical Systems
Data automation	Litton Systems, Inc.
Television	Electro-Optical Systems
Ultraviolet spectometer	University of Colorado. Laboratory for Astroscience & Space Physics
Infrared spectrometer	University of California Space Science Laboratory, Berkeley
Infrared radiometer	Santa Barbara Research Center

The launch vehicles were adapted and built by contractor under LeRC cognizance, and were tested and accepted before delivery to the launch site. There, after further testing, they and the spacecraft were tested jointly, and in due course were counted down for launch.

Committed elements of the tracking and data system (TDS) were negotiated, prepared (and mission-peculiar equipment was integrated), trained, and tested at various levels, under the cognizance of the TDS manager. Elements of AFETR and MSFN supported launch-phase flight operations. The Deep Space Instrumentation Facility (DSIF) stations tracked the spacecraft in the deep space phase. Other DSN elements, which were committed to and prepared for *Mariner* Mars 1969, included portions of the Space Flight Operations Facility (SFOF) and communications links, such as NASCOM.

The Mission Operations System (MOS) was designed and constructed in a more disciplined manner than previously, resembling spacecraft design. It reached a greater level of complexity, owing to the nature of the mission and the flexibility inherent in the spacecraft system. Many new computer programs were written, tested, and certified, and a considerable variety of equipment was accommodated. Operations could not be conducted on a 24-hour basis because of manpower limitations. There had to be considerable interaction between mission design and MOS design before compatibility and feasibility could be established.

Once the flight mission was underway, and the early phase of each flight gave way to the interplanetary cruise, it was time for the final refinement of the encounter stage of mission design and the reflection of this in updated programming of the spacecraft central computer and sequencer by command, and training and testing of the MOS/TDS team. This extension of preflight preparation into the flight phase (in time) is the only postlaunch activity which falls within the scope of Volume I.

Project Background and History

Mariner Mars 1969 was developed and operated in a continuum of predecessor *Mariner* missions, related lunar missions, concurrent *Pioneer* and manned lunar missions, and plans and requirements for subsequent Mars projects. From the predecessor efforts, both *Mariner* and *Surveyor*, the project extracted spacecraft, launch-vehicle, test, and operational technology data. With the concurrent missions, it shared tracking and some of the operational facilities. Various types of information were required from time to time for the support of future missions, and the *Mariner* Mars 1969 objectives were designed for this function. Thus, the context and background against which the project existed had a strong influence upon it.

Novel characteristics of the project were not limited to mission and spacecraft design. The concentration of scientific objectives on the dual Mars encounter brought forth operational design, coordination, planning, and testing efforts of greater complexity and depth than required in the previous planetary efforts. The scope and depth of design control and reliability and quality-assurance efforts were increased for this project.

Although the requirements and plans for *Mariner* Mars 1969 evolved a great deal over the three years of the preflight phase, the direction of the trend did not change. From the beginning, the evolution was in the direction of the future-mission-oriented project objectives, and of increasing the data return from Mars. In spite of (or perhaps partly because of) the relatively long preflight period, as the launching period approached, some compromises had to be made in hardware delivery schedules. These compromises caused compressing of the system test schedule and even though there were difficulties encountered in the latter phase, the launch readiness dates were met. *Mariner VI* was launched on the first day of its launch period, and *Mariner VII* lifted off within three days of the opening of its launch period. Although both encounter sequences (with options) were programmed at launch, the final design of the dual encounter was completed and programmed by earth command during the flight phase, subject to last-minute modification based on near-Mars data inputs.

I. Summary of the *Mariner* Series

The *Mariner* Mars 1969 project was assigned to carry out the sixth and seventh launches in the *Mariner* series; it was the fourth project of this kind. However, two prior *Mariner* projects which had begun study, design, and development efforts did not culminate in launch or flight.

In early 1959, JPL was assigned a technical role in the *Vega* project. This role included development of an upper stage of the launch vehicle and a planetary-mission spacecraft (with the goal of attempting a Mars mission in 1960 and a Venus mission in 1961) which could be adaptable for lunar missions. At this time the early *Pioneer* missions, utilizing small spin-stabilized spacecraft barely capable of lunar flyby or solar orbit, represented the outer reach of the operational mission capability.

The demonstrated performance of the *Atlas/Agena* vehicle, and the potential of *Atlas/Agena B* (a restartable version), led to the cancellation of the *Vega* space-vehicle project. The *Ranger* spacecraft and mission, embodying a number of *Vega* characteristics, were joined to the new vehicle for lunar missions scheduled for 1962, with two engineering test launches in 1961. Though for a variety of reasons the early *Ranger* missions failed to achieve their objectives, they provided a pioneering demonstration of fundamental mission and system features which were soon to characterize the *Mariner* series as well as the following and more successful lunar missions.

The most important of these was three-axis attitude stabilization, using gyros and celestial sensors, switching amplifiers, and cold-gas jets. This permitted orienting solar panels for electrical power and thermal shields for temperature control, relative to the Sun; high-gain communications antennas toward the Earth; and selected scientific instruments to their targets of interest. It also permitted spacecraft turns and accurately vectored thrust maneuvers. Other characteristics of this spacecraft generation were an extensive ground command capability and a large number of engineering as well as scientific telemetry measurements. Except where the circumstances could not be predicted, as in the trajectory-correcting thrust maneuver, the ground commands served principally as back-up to the outputs of a central sequencer; a computer, part of the same subsystem, governed the maneuver in response to ground commands.

During the same period, the *Mariner A* and *Mariner B* projects were begun in turn, designing larger-scale and far more elaborate spacecraft intended to be launched by the *Atlas/Centaur* vehicle during the 1962 Venus and 1964 Mars opportunities respectively. In some respects the *Mariner* Mars 1969 project represents a matured realization of *Mariner B*.

Launch vehicle schedule difficulties precluded both *Mariner A* and *Mariner B*, in turn; *Atlas/Agena*-scale spacecraft were quickly developed for each opportunity. *Mariner R*, initiated in mid-1961 and representing a fusion of *Ranger* and *Mariner A* technology, resulted in the successful *Mariner II* Venus flyby at a 21,000-mile closest approach on December 4, 1962. This first interplanetary mission conducted both in-flight cruise science and planet-scanning experiments, and lasted about three months before contact was lost with the spacecraft.

The *Mariner C* effort, which became the *Mariner* Mars 1964 project, drew upon *Mariner R* and *Mariner B* spacecraft art, and an improved *Atlas/Agena* vehicle, to meet the greatest challenge yet posed to an unmanned space mission: an eight-month flight to within about 6,000 miles of Mars. The highly successful *Mariner IV* mission conducted eight scientific experiments, obtaining data on the interplanetary medium and near the planet, including the first close-up television pictures of the surface. The spacecraft survived and operated long past the Mars encounter, finally loosing power three years after launch. In contrast to *Mariner R*, which could be described as an interplanetary *Ranger* configuration, *Mariner IV* exhibited the general design pattern which was to characterize *Mariner* spacecraft for many years to come, particularly *Mariner* Mars 1969.

The central body was octagonal, with electronic assemblies and the onboard propulsion system occupying the eight bays. Four hinged solar panels radiated from the octagon; on the anti-solar face a scan platform for the TV camera was mounted, and on the opposite side the omnidirectional antenna and fixed high-gain reflector antenna were attached. The spacecraft was capable of maintaining continuous two-way radio contact with the Earth, for turnaround ranging and doppler tracking and for the return of scientific and engineering telemetry. The large mass of data obtained by the TV camera was stored by an onboard tape recorder for reduced-rate playback to Earth. The flight path was designed to permit Mars to occult the spacecraft from Earth, so that scientific data concerning the atmosphere could be derived from study of the extinction and emergence of the radio signal.

Concurrent with the evolution of spacecraft and mission design in the *Vega/Ranger/Mariner* sequence came the growth and development of ground tracking and operational systems. It had early been recognized that for deep-space missions, highly sensitive steerable antennas (essentially radio telescopes) were required, and that for continuous long-range coverage a network of

three such stations, appropriately spaced in longitude, was normally sufficient. By the time of the early *Ranger* lunar flights, such a network (with stations at Goldstone, California, Johannesburg, South Africa, and Woomera, Australia) was operating at frequencies in the L-band, and was controlled from a space flight operations complex at JPL. *Mariner II* also operated in this regime, with command messages sent from the JPL complex through the appropriate station to the spacecraft, and telemetry traveling the return path.

By the time of *Mariner IV*, the existing Deep Space Instrumentation Facility (DSIF) stations had evolved in design, new antennas had been added, and a new Space Flight Operations Facility (SFOF) housed network control and communications, tracking and telemetry processing equipment, and the mission control team. The standard operating frequency was in the S-band at this time. By the end of *Mariner IV* operations, a single 210-foot-diameter advanced antenna system station had joined the network of 85-foot antennas. These antenna stations, which were then sited in Spain, Africa, Australia (two sites), and Southern California (four stations), were routinely supporting lunar, planetary, and interplanetary missions; assigning tracking time to as many as four spacecraft on a shared-pass basis. In addition, these stations were conducting various radar-astronomy and technology efforts.

A second generation of *Pioneer* missions, managed by the Ames Research Center of NASA, which operated spin-stabilized spacecraft in solar orbits from 0.8 to 1.1 astronomical units, was beginning, its experiments studying fields and particles in the interplanetary medium. A next-generation planetary program called *Voyager* had been conceived some time before, with the goal of orbiting and possibly landing on Mars and Venus. A *Voyager* project was established in 1965, to orbit and land on Mars. Fiscal considerations led to postponement of the first mission to 1973 and, eventually, to cancellation of the project. Consideration of the eight-year interval from *Mariner IV* to *Voyager*, and of the need for more Mars data than provided by *Mariner IV* to support *Voyager* planning, led in turn to the study of a Mars mission at the *Mariner* scale in 1969. At the same time a plan was initiated to adopt residual hardware, including the spare spacecraft from *Mariner* Mars 1964, for a Venus mission in 1967. This low-cost mission was to advance the study of Venus and of planetary missions and spacecraft technology; the successful *Mariner V* effort thus became an additional demonstration precursor, with *Mariner IV*, for the 1969 Mars project.

The fast turnaround required of the first three *Mariner* projects is worthy of note. Each was authorized, on the basis of pre-project studies and some existing technology, after one planetary launch opportunity, and scheduled for launch at the very next opportunity. The two Venus missions had about a year to prepare for launch; the Mars effort had less than two years. *Mariner* Mars 1969 was the first planetary project to develop over a longer interval, more than three years from initial authorization to actual launch.

II. Origin and Early History of *Mariner* Mars 1969

The Project was formally authorized December 22, 1965, by TWX from the NASA Associate Administrator, Office of Space Science and Applications (OSSA), to the Deputy Director of JPL; this was followed by a contractual Task Order, No. RD-59 to Contract No. NAS 7-100, with the same effective date, issued February 1, 1966. During this interval the project office was established and planning began on the basis of the following tentative technical assumptions and ideas:

(1) Dual launch, using *Atlas/Centaur* with minimum change from *Surveyor* configuration, and Mars flyby encounter.

(2) *Mariner* Mars 1964 spacecraft type, with changes allowed for the purposes of reducing cost (some design features of the 1964 mission achieved very low weight at high cost), improving reliability, and meeting mission objectives.

(3) Direct use of ground equipment from *Mariner* Mars 1964, as used and modified by the 1967 mission.

(4) Shorter flight time than during the 1964 mission, and shorter communication distance at encounter.

(5) Greater electrical power demand at encounter than in 1964, and encounter closer to the Sun than in 1964.

(6) Planning-purposes scientific payload features:

  (a) Improved TV resolution and coverage (probably two cameras).

  (b) Increased data storage requirement.

  (c) Improved occultation experiment.

  (d) Ultraviolet and/or infrared spectrometer.

(e) Similar but improved fields and particles instruments.

(7) Technology experiments related to *Voyager*.

The mission objectives were fourfold at this stage. The primary and secondary objectives were essentially the same as those to which the mission was ultimately designed, with the addition of Mars-related observations unrelated to the search for life, and the acquisition of information on the interplanetary medium.

The project approval document deleted the third objective, which was essentially covered by the primary objective of "exploratory investigations," but retained interest in the interplanetary environment. It indicated that the spacecraft was to be in the 800-lb class, and specified JPL as project management agency and system manager for all systems except launch vehicle, which was assigned to Lewis Research Center. The procurement of two flight spacecraft and one proof test model, with other test models and critical assemblies, and of two *Atlas/Centaur* launch vehicles, was also specified.

During the first few months spacecraft subsystem procurement planning was a major activity, concurrent with system and mission design. The development of spacecraft functional requirements, selection of the scientific payload, and a number of general project requirements for subcontractors began at this time. Table 1 contains a chronological listing of the *Mariner* Mars 1969 preflight events. Experiment proposals were solicited and received by the Space Science Board, operating as an advisor to OSSA. An atmospheric entry probe was proposed, and rejected; since this could have a significant effect on project planning and spacecraft design, the project was advised of the rejection in February. Another early payload decision, to reject interplanetary fields-and-particles experiments and concentrate on Mars, was communicated for the same reasons in April. The payload selection was formally concluded and announced on May 26, 1966.

Thus by mid-1966, the initial inputs necessary to the design of the mission and project systems had been assembled. The mission profile and system functions and configurations defined at this early point are clearly recognizable in the eventually realized *Mariner* Mars 1969 project and mission.

Fiscal constraints imposed successively on the project each fiscal year caused the deferral of certain completion and delivery milestones from one year to the next, requiring the revision of integration and testing schedules. The deletion of many spacecraft test and spare articles and the redirection of MOS design were caused by the fiscal constraints.

As the program evolved the scientific possibilities of the mission (once the payload and certain potential spacecraft capabilities were known) led to many reconsiderations and expansions of the science mission and requirements. The design of the encounter phase of flight, the introduction of high-rate telemetry on an experimental basis, and an increased utilization of the scan control subsystem (for the instrument platform) and the programmable computer of the CC&S subsystem (both new designs for 1969), together with advances in DSN utilization and MOS design, were strongly influenced by this scientific growth.

The impact of the science payload on the spacecraft configuration was first generally realized at the second project quarterly review in September 1966, when a mockup of the scan platform was unveiled. At this time the moving mass on the scan platform was expected to total 130 lb, compared to less than 20 lb for *Mariner IV;* this part of the spacecraft design could no longer be considered a minimum-change repetition of *Mariner* Mars 1964.

The direct-ascent launch mode was formally selected in October 1966. The use of a powered-phase yaw maneuver (called a "dog-leg" ascent trajectory) was found to permit a 56-day launch period.

The project development plan was in preparation through much of 1966. A draft went out for comments in midyear, and the final draft was circulated for signature in late September. The experimenters' agreements were signed during the same period, and were appended to the project development plan when it was released in November. All areas of management were covered by the various general agreements and plans contained in and appended to the project development plan; the operations plan was necessarily unspecific, and as expected was superseded by a later revision in late 1968.

Table 1. Preflight chronology

Month/year	Day	Event
December 1965	22	Project authorized by TWX from NASA, OSSA.
February 1966	1	NASA Task Order RD-59 to contract NAS7-100, effective December 22, 1965, issued by NASA Resident Office to JPL. *Mariner* Mars 1969 authorized and funds allocated.
	11	Spacecraft system design team first meeting.
	28	NASA project approval document, Code 84-840-816, subject *Mariner* Mars 1969 project, submitted by OSSA associate administrator, approved by NASA deputy administrator.
April 1966	7	Experiment candidates restricted to Mars-oriented investigation, NASA TWX.
	8	Procurement approach approved by NASA.
	12	First project quarterly review.
	18	Type I trajectory, February–April 1969 launch period selected.
May 1966	2	Procurement instructions document and spacecraft system change control plan released.
	4	Spacecraft system design control document preparation requirements released.
	5	Spacecraft system engineering drawing requirements released.
	10	Release of Phase I procurement RFPs began (continued through November 1966)
	18	Project action item list started.
	26	Scientific Experiment complement selected by NASA.
June 1966	8	Project development plan first draft completed.
	16	Use of two launch pads (complex 36A and 36B).
	29	Selection of first spacecraft subsystem contractor.
	30	Mission plan first discussed with principal investigators.
July 1966	1	Revision of spacecraft system change control plan.
	18	Spacecraft system functional design review.
	20	Spacecraft/launch vehicle hardware-integrate panel, first meeting.
	31	Mission requirements first draft completed.
August 1966	17	Performance, trajectories, and guidance panel first meeting.
	25	Initial memorandum of agreement on spacecraft/TDS/MOS interface at DSIF stations.
	31	Quality assurance program plan released.
September 1966	1	Project development plan (PDP) final draft completed.
	15	Second project quarterly review.
	22	Environmental test program requirements released.
	23	PDP final signoff started.
October 1966	12–20	Direct ascent launch period of February 16, 1969 to April 4, 1969 defined.
November 1966	2	First spacecraft subsystem task order issued for structural forgings.
	8	Planetary quarantine study completed and presented to NASA.
	15	Full-scale spacecraft configuration mockup completed.
	18	Project policy and requirements released.
	21	Spacecraft functional requirements completed (first issue). Mission plan document first draft completed. MOS/TDS schedule (first issue) released.
	29 (to 12/1)	Mission and spacecraft system design review: Higher telemetry rates proposed and discussed, culminating in high-rate telemetry study.
December 1966	5	Planetary quarantine criteria established by NASA/OSSA.
	13	Third project quarterly review: design delay from experiment requirements noted.
	15	Procurement instructions revised.
	28	Distribution of PDP.
January 1967	10	Mission operations design team first meeting.
	12	Mars arrival dates of August 1, 1969 and August 10, 1969 assigned for planning purposes.
	27	Subsystem preliminary design reviews begin (continue to March 21, 1967).
February 1967	28	High-rate telemetry (block-coding, 16.2 k bits/s rate) adopted as "experimental" encounter and playback data-return mode.
March 1967	1	Phase I contracting completed.
	2	MOS software design team first meeting.
	9	Project/mission briefing for launch vehicle contractor.
	21	Spacecraft subsystem preliminary design reviews completed (supplemental and OSE reviews continue to May 16, 1967).
	28–29	Fourth project quarterly review and experimenters' meeting.

Table 1 (contd)

Month/year	Day	Event
April 1967	5	Second iteration of spacecraft functional requirements completed (TV last).
	12	Temperature control flux monitor deleted from spacecraft design for lack of funds (returned May 10, 1967).
May 1967	10	*Mariner* Venus 67 temperature control model received for rework to *Mariner* Mars 1969 design.
	16	High-rate telemetry functional design review (last late preliminary review).
	31	Environmental estimates.
June 1967	15	Phase I spacecraft subsystem contracts all definitized.
	27–28	Fifth project quarterly review and experimenters' meeting.
July 1967	1	Support instrumentation requirements document Rev. 1 (signed off by NASA). *Atlas*/*Centaur* mission-peculiar engineering studies completed, flight article design and fabrication start.
	7	MOS/TDS functional design review.
	13	Spacecraft subsystem detail design reviews start (continue through November 1967).
	15	Project redirection to meet FY68 fiscal constraints: deletion of type-approval-test units, revision of proof test model and flight-hardware delivery schedules, reduction of OSE, test models, documentation, etc. Spacecraft/MOS interface control document released.
	31	Preliminary trajectory characteristics released.
August 1967	1	Quality assurance working organization established.
	4	NASA support plan released.
	24	Quality assurance program plan released.
September 1967	1	Spacecraft/DSIF telecommunications interface control document.
	10	Approach guidance subsystem deleted for fiscal reasons.
	15	Spacecraft detail design reviews completed.
	20	Spacecraft test and operations plan initial release (additional release and revision continued through operations.
October 1967	1	Space flight operations plan. (Revised February 12, 1968 and September 2, 1968.)
	3	Project/mission briefings to subsystem contractors begin (continue for a few months).
	10–11	Sixth project quarterly review and experimenters' meeting.
	24	Flight plan approval request transmitted to AFETR.
November 1967	—	AC-19 *Centaur* engines delivered.
	2–22	MOS comprehensive modifications proposed and studied.
	28	Launch vehicle system design review.
December 1967	1	Change control applied to all design and design control documentation.
	6	Flight plan approval (conditional).
	8	First spacecraft octagon structure delivered.
	13	Project problem list established.
January 1968	—	MOS/TDS redirection and reprogramming in response to fiscal constraints.
	15	First OSE delivered to SAF.
	15	Spacecraft detail drawings and specifications completed.
	17	PTM octagon delivered to SAF for assembly.
	22	Completion of spacecraft preliminary design phase (end of regular meetings, spacecraft design team).
February 1968	13–14	Seventh project quarterly review.
	15	Temperature control model tests in space simulator completed.
March 1968	—	AC-20 *Centaur* engines delivered.
	13	Spacecraft/launch vehicle match/mate tests.
	22	DSN *Mariner*/*Pioneer*/*Apollo* tracking-schedule coordination meeting.
	22–28	First spacecraft system test (PTM).
April 1968	12	Spacecraft/Launch Vehicle pyrotechnic design verification.
	15	Final spacecraft PTM hardware delivery.
	10–18	Second spacecraft system test (PTM).
	25	AC-19 *Centaur* final assembly.
	26	Start of space simulation (PTM).

Table 1 (contd)

Month/year	Day	Event
May 1968	7	Preferred Mars arrival date selection by principal investigators (July 31, 1969 and August 5, 1969).
	20	Planetary quarantine plan. Completion of PTM space simulation.
	21–22	Eighth project quarterly review.
	22	Release of Mission Plan. Delivery of first flight spacecraft structure (M69-2) to SAF.
	28	AC-19 *Atlas* buyoff.
June 1968	3–7	PTM vibration testing.
	5	AC-19 *Centaur* checkout and acceptance.
	15	AC-20 *Centaur* final assembly.
	18	Delivery of second flight spacecraft structure (M69-3) to SAF.
July 1968	12	AC-20 *Centaur* checkout and acceptance.
	20	AC-19 mission peculiars installed.
	23	First flight spacecraft (M69-2) started *system tes* .
	29	AC-20 *Atlas* acceptance.
August 1968	15	Space flight operations test plan released.
	20	AC-20 mission peculiars installed.
	23	M69-2 space simulation began, continues to September 17, 1968.
	26	SFOP revision 2 released.
	28	AC-19 composite test and data review completed.
	29	FPAC software acceptance began (completed November 15, 1968).
September 1968	1	Spacecraft separation testing and AC-19/adapter test.
	3	SPAC software acceptance began (continued to November 9, 1968).
	13	First encounter sequence design review.
	15	Space (M69-4) flight hardware delivered to SAF.
	17	AC-19 *Atlas* arrives at Cape Kennedy.
	17–18	Ninth project quarterly review.
	19	MOS test readiness review.
	23	M69-3 space simulation began, continued to October 18, 1968.
	26	Project science review.
	29	AC-19 *Centaur* arrives at Cape Kennedy.
October 1968	3–4	AC-19 *Atlas* and *Centaur* erected on Pad 36A.
	11	AC-20 composite test and data review completed.
	15	Planetary quarantine plan approved by NASA Headquarters. Launch period utilization and constraints document.
	20	NASA support plan (Revision 2) released.
	28	Deep Space Stations 12, 41, ground communications facility operational for *Mariner* Mars 1969.
	30	DSN real-time data processing and simulated data conversion center operational.
	31	M69-4 space simulation began (continued to November 22, 1968).
November 1968	1	SFOF operational for *Mariner* Mars 1969.
	12	Second encounter sequence design review.
	12	AC-20 *Atlas* arrived at Cape Kennedy.
	14	Spacecraft/MOS compatibility test, real-time encounter sequence, M69-4 in simulator, CTA-21 in service.
December 1968	6	AC-20 *Centaur* arrived at Cape Kennedy.
	10–11	Spacecraft preshipment acceptance review.
	11–13	AC-20 *Atlas* and *Centaur* erected on Pad 36B.
	12	Tenth project quarterly review.
	15	Deep Space Station 62 operational for *Mariner* Mars 1969.
	16	MOS/TDS data system operational (except DSS 14 portions).
	17–20	M69-2 and M69-4 shipped to Cape Kennedy.
	31	*Atlas/Centaur* final guidance equations.
January 1969	2–6	M69-3 shipped to Cape Kennedy.
	5	MSFN facilities and AFETR tracking facility operational for *Mariner* Mars 1969.
	17	M69-2 final system test at Cape.
	18	AC-19 and AC-20 checkouts on pad complete.
	20	MOS software acceptance.
	21	M69-4/AC-19 joint flight acceptance composite test.
	23	M69-3 final system test at Cape.
	24	M69-4/AC-20 joint flight acceptance composite test.

Table 1 (contd)

Month/year	Day	Event
February 1969	3–4	Launch readiness review, Cape Kennedy, systems at Cape.
	6	Launch readiness review, NASA Headquarters, general.
	14	Launch readiness review, JPL, deep-space MOS/TDS functions.
	—	Accidental depressurization of Atlas 5402 during AC-19/M69-3 test; reassignment of AC-20 to *Mariner F* launch.
	17	AC-20 composite readiness test.
	18	M69-3 mated to AC-20.
	19	Deep Space Stations 51, 71 operational for *Mariner* Mars 1969
February 1969 (contd)	19–20	*Mariner F* launch-phase operational readiness test.
	20	New *Atlas* for AC-19 arrives at Cape Kennedy.
	22	*Mariner F* launch readiness verification.
	25	*Mariner VI* launch.
	25–26	AC-19 re-erected on Pad 36A.
March 1969	19–20	*Mariner G* launch-phase operational readiness test.
	20	*Mariner G* launch readiness verification.
	27	*Mariner VII* launch.

Management

The *Mariner* Mars 1969 project was managed in accordance with the management plan set forth in the project development plan (PDP). The PDP was prepared under guidelines provided in NASA Management Instruction 4-1-1 and other NASA policies. Subsidiary management planning was accomplished through the use of planning documents which were issued by JPL and encompassed, among other things, MOS/TDS, quality assurance, reliability, and system level operations.

I. Organization

The organizational structure and management responsibilities for *Mariner* Mars 1969 were explicitly defined by the PDP. Project management responsibility was assigned to JPL and organized around four functional systems described in the Introduction: spacecraft, mission operations, tracking and data acquisition, and launch vehicle. Two of the systems were relatively project-independent; launch vehicle tracking and data acquisition, which were parts or applications of ongoing NASA mission-support programs, and were technically adapted to *Mariner* Mars 1969 by a process of selection and/or modification. Their system management was provided similarly, drawing upon the respective existing organizations. The other two systems, like the *Mariner* Mars 1969 mission itself, required a process of design, development, and manufacture. The management of these two systems, therefore, took a somewhat different form, oriented toward this start-to-finish progressive sequence.

The *Mariner* Mars 1969 project office was established at JPL, reporting administratively to the lunar and planetary projects (later flight projects) office, and technically both to it and to a counterpart *Mariner* Mars 1969 program office within the NASA Office of Space Science and Applications (OSSA). Staff management within the project assumed four functional areas of responsibility:

(1) Mission analysis and engineering.

(2) Science.

(3) Project control (and administration).

(4) Reliability (assumed by representative of reliability and quality assurance office).

In addition, the spacecraft system and Mission Operations System managers were members of the project

office, administratively and technically responsible to the project manager. The other two system managers had dual responsibility, to this project and to other programs. Figure 1 sketches the general organizational relationships which governed the management of the project.

The basic principle defining the organization of JPL is technical or professional discipline; the majority of personnel and groups supporting *Mariner* Mars 1969 efforts within JPL were members of various technical divisions. Each of these divisions assigned a full-time division representative to the project to assume responsibility for the efforts of the division for the Project. The organization of JPL (as of March 1968) is given in Fig. 2.

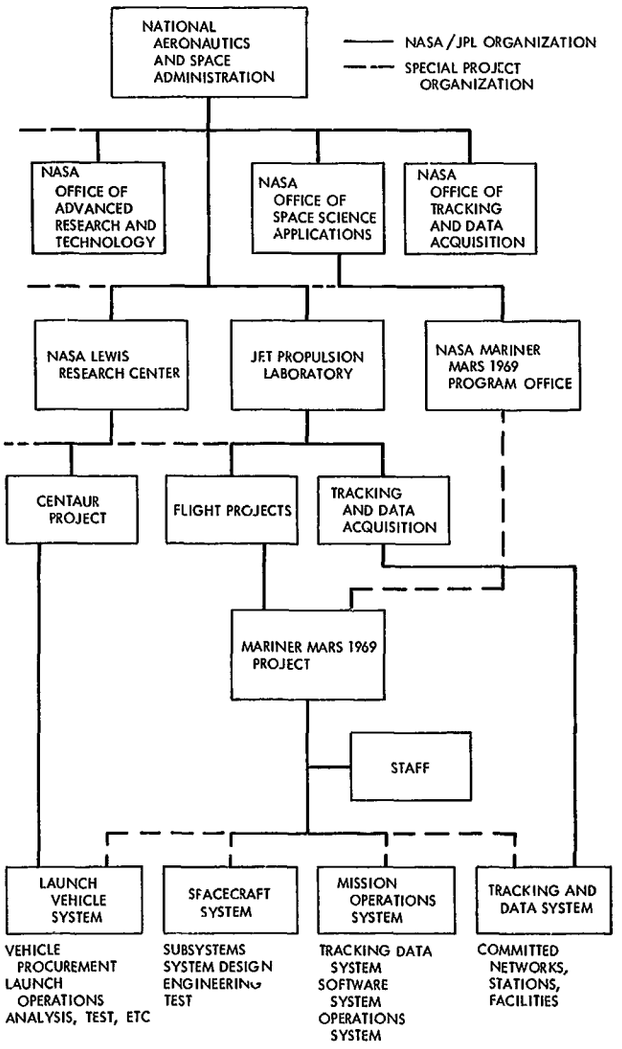


Fig. 1. General organizational relationships

Virtually all divisions, including service and support elements, participated to some degree in the activities of the project.

Thus, the Project organization *in toto* contained largely JPL elements, with NASA Headquarters elements at the program level, and NASA LeRC elements in the launch vehicle system. Industrial contractors were broadly involved, not only in launch vehicle manufacture and preparation and spacecraft subsystems development and manufacture, but, in launch operations at Cape Kennedy and network operations in the Deep Space Instrumentation Facility (DSIF) and Space Flight Operations Facility (SFOF). Also, university, government, and industrial laboratories were involved in the experiment efforts.

The project organization, including the project office and assigned JPL technical and support division elements, grew to a peak population of about 600 people in March 1968. A chart of this organization at that time is given in Fig. 3. The organizations of the NASA OSSA and LeRC (as of late 1969) are given in Figs. 4 and 5.

Principal contractor to LeRC for *Atlas/Centaur* launch vehicle manufacture and preparation was General Dynamics/Convair, San Diego, California. For the spacecraft, each subsystem was manufactured under contract to JPL by an industrial contractor as listed in Table 1 of the Introduction to this volume. The project organization (Fig. 3) shows the assignment of JPL technical managers, cognizant engineers, and cognizant contract negotiators from the appropriate divisions for the various subsystems. After subsystem acceptance and delivery to JPL (together with appropriate operational support equipment) the spacecraft were assembled and tested at system level under cognizance of the operations managers and test teams.

The scientific experiments of the mission were proposed and conducted by principal investigators and their co-investigator teams (Table 1), under contract to JPL. The project scientist and a number of cognizant scientists (also known as experiment representatives) served to coordinate the interests and efforts of the experimenters and the project. The scientific instruments carried on the spacecraft were designed, developed, and manufactured using a management technical approach similar to that used for engineering subsystems of the spacecraft.

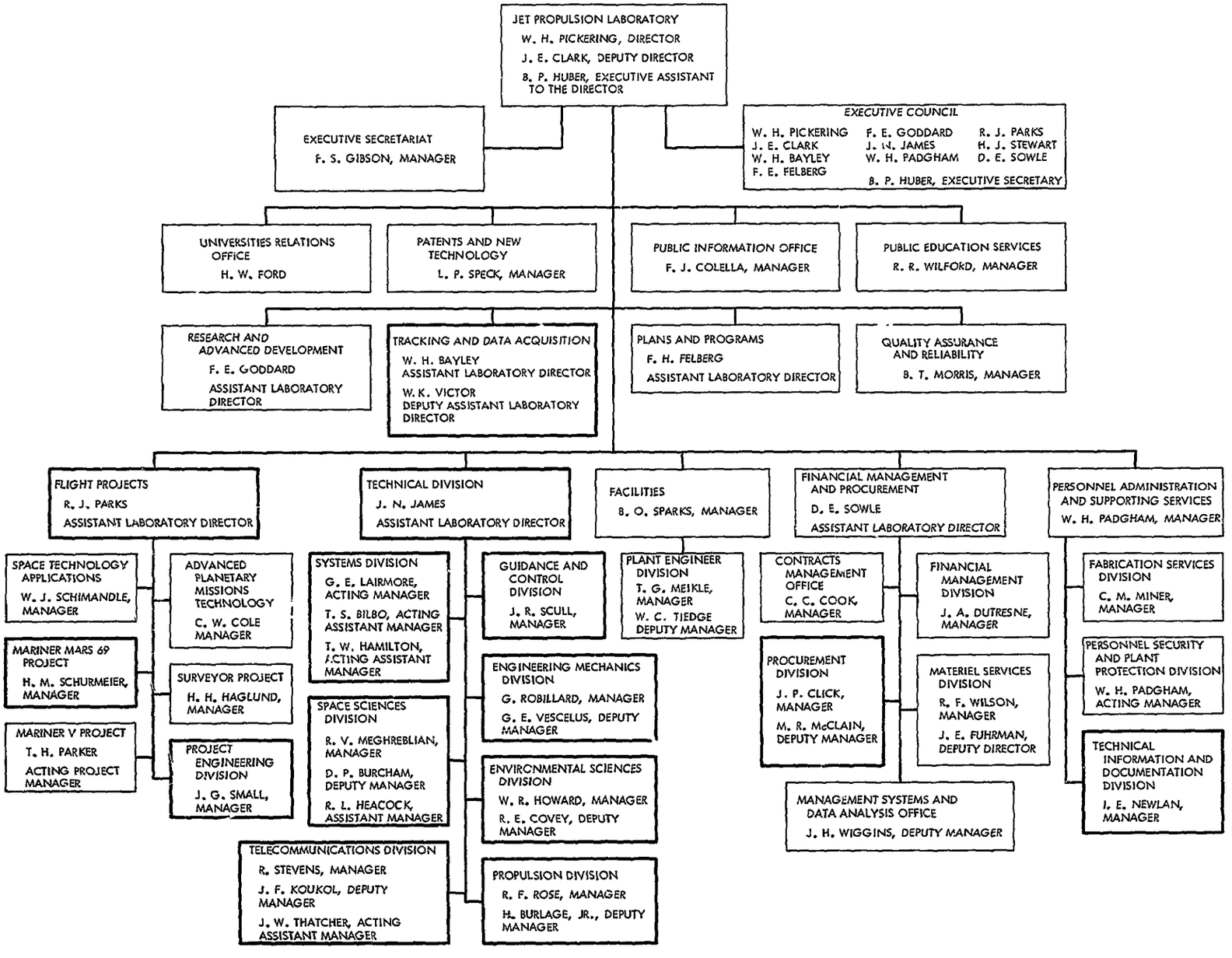


Fig. 2. Jet Propulsion Laboratory organization

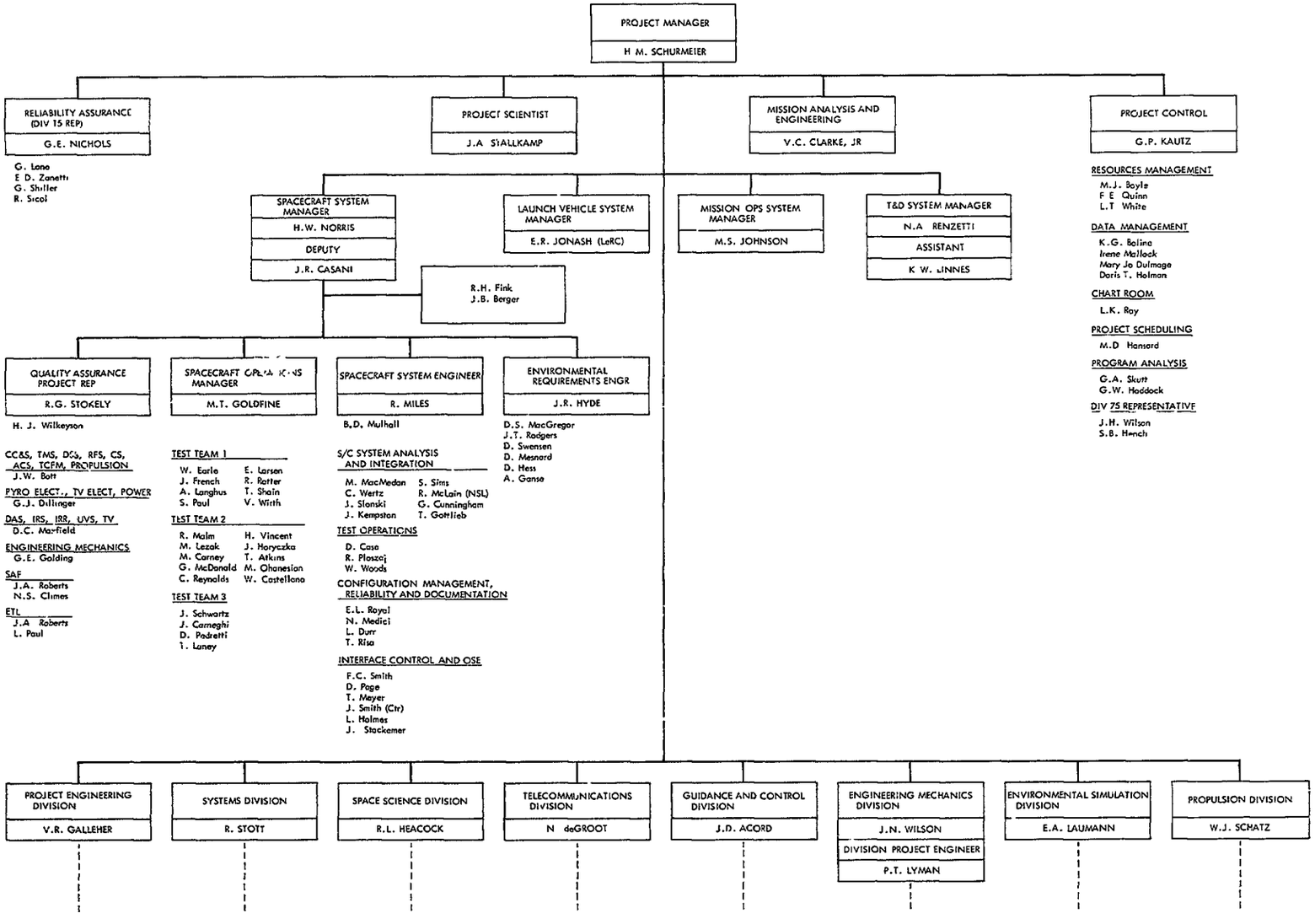


Fig. 3. *Mariner* Mars 1969 project organization and JPL support

LAUNCH VEHICLE PERFORMANCE AND INTEGRATION
L. T. Shaw
S R. Schofield
H Schneider
W. Lane
A N. Williams

MISSION ENGINEERING AND SCIENCE INTEGRATION
T. Migliori
G Cunningham
B. Sorensen
T. Gottlieb

FLIGHT OPERATIONS
B. Dysart
J. Slonski
B.D. Mulhall

ENVIRONMENTAL REQUIREMENTS SUPPORT
D. Wiksten

NATURAL SPACE ENVIRONMENT
A Beck

ELECTROMAGNETIC INTERFERENCE
D. Frankos

STCDS
C. Cleven
D. Lame (Ctr)

DOCUMENTATION
J. Ingles
R. Enfeld
E. Nave
H. Reisenger

TEST ANALYSIS AND PLANNING SUPPORT
J. Beckert
R. Collins

MISSION DESIGN AND ANALYSIS
J.S. Reuyl
+C.E. Kohlhase
C.Z. Schissell
A. Hirshberg

FLIGHT PATH PROGRAM DEVELOPMENT
J.K. Campbell
R.T. Mitchell
T.H. Thornton
H. Macomber
F. Sturms
J.E. Freeman (Ctr)

FAPC DESIGN AND SUPPORT
H.J Gordon
J.E. Ball
J A Borras
S. Reinbold
S. Wong

COMPUTER DATA SYSTEMS
+W. Wolin
R. Ollivier
H M. Doupe
R. Polczynski
M. Barr ick

DATA SYSTEMS PROGRAMMING
E. Holloway
D.J. Adams
P.K. Rubin
A.D. Schoepke
J. Schoeni

DAS CHECKOUT DATA SYSTEM
R. Rice

SFOF OPERATIONS PROGRAMMING
+E. Pyle
F.W. Miller
J.H. White
W. Levine
G. Blake
D.E. Casperson
E.V. Schultz
J. Womast
J.H. Donhauser
P. Pace
J.H. Weidner
G. Wanczuk
E. Sundquist
L. Meredith
M. Schneider

SFOF OPERATIONS ENGINEERING
+R. Crabtree
R.B. Rung
G. Textor
N. Ausman
H.E. Hielscher
F.J. Walker
W.N. Jensen
C. Rodriguez
M. Goble
C. Morgan

CELESTIAL MECHANICS
J. Anderson

EXPERIMENT INTEGRATION AND SUPPORT
A.G. Herriman

INSTRUMENT INTEGRATION AND SUPPORT
+L.G. Parker — R. Ebbett
H. Canvel — J. VanZomeren
R. Gasteiger — E. Seeger
W.L. Momsen — D. Kiefer
C.W. Odd — W. Hodges
V. O'Brien

DATA AUTOMATION
*H. Friedman — A. Calabrese
+J. Wolfe — J. Shephard
++J. Boyd — J. Patterson
M. Dudley — E. Kirchhoff
J. Wooddell — C. Kopper
J. Collier — J. DeJong
T. Shain — D. Johnson
F. Baron — J. Kent
J. Brown — J. Padilla
D. Bailey

TELEVISION
*+D. Montgomery — W. Sl ..h
+R. Blackwell — R. Sloan
++J. Heie — P. Squires
+L. Adams 168/227 (Optics Eng.) — W. Stratton
L. Snyder — J. Cutts
C.C. LaBaw — G. Danielson
R. Hastings — H. Rosenberg
D. Sm ith — J. Mahoney
R. ' ng — P. Salomon
J. Dufresne — J. Fenske

INFRARED SPECTROMETER
*+L.W. Carls
+++D. Bethel
F. Kuperstein
T Foster (Berkeley)
B Jones
R. Holman

UV SPECTROMETER
*+E. McMillan
++O. Raper
+++D. Bethel
T. Perkins
R. Newell
J. Farrar

INFRARED RADIOMETER
*+D.K. Schofield
++E. Miner
+++D. Bethel
D. Griffith
M. McMillan

SCIENCE DATA HANDLING
G.M. Smith — D. Gordon
+E. Buckley — R. Borrell
W. Spuck — E. Goldyn
H. Eyerly — G. Holmlund
L. Fairchild

VIDEO DATA PROCESSING
*G. Tatsuka — G. Peterson
K. Taylor — V. Tuck
J. Fulton — J. Morecraft
F. Billingsley — R. Brundt
S. Silver — H. Frieden
J. Lindsley

OPERATIONS SUPPORT EQUIPMENT
G.M. Smith — C. Bode
+R. DelNegro — M. Clary
F. Charles — J. Schantzen
J. Barney — W. Wade
F.A. Tomey — J. Lucks
J. Beard — W. Wilson
D. Bell — K. McGraw

MARINER TELECOMMUNICATIONS SECTION
R.B. Harker
T.C. Sorensen

SYSTEMS
*+A.J. Spear — J. Hong
R. Edelson — B. Larman
G. Garrison — F. Stuhr
W. Gillmore — W. Allen
C. Hamilton — V. Ruzicka
C. Harris — W. Tisdale

TRANSPONDER AND POWER AMPLIFIER
*D.L. Dakan
+++D. Chase
S Burks
E Culp

Transponder
+N. Evans — N. Lambert
R. DeSantis — G. Wood
P. Batelaan — S. Zingales

ANTENNA AND MICROWAVE COMPONENTS
L.M. Hershey

Antenna Assembly
+A. Brejcha — C. Smith
D. Lewis — P. Watters
H. Martin — C. Wong
W. Kessler

SAF OPERATIONS
G. Barbani
D. Hughes
C. Paul

COMMAND
*W. Leflang — W. Chitty
+R. Rakunas — F. Stolarik
+++W. Shaffner — H. Good
E. Hilbert — J. Park
G Mays — L. Koga
N. Yamell

TELEMETRY
*W.E. Arens — C McCreigh
+++P. Ryken — G. Crawford
J. Birch — R. Springer
M. Crawford
R. Manaker

DATA STORAGE
*W.C. Apel — J. Neilsen
+R. Harrington — W. VanKeuren
+++E. Reiz — H. Stovall
L. Berg — V. Tyree
G. Bullock — R. Zenone
R. Grumm — M. Deese

STAFF
R. Boon's
J. Brimhall
J. Daniels
E. Fujimoto
L. Myers
O. Irvin
J Jones
D. Mix
C. Squire

ANALYTICAL DESIGN
R.V. Morris
+J. Miller
J. Rhoads
E. Suggs
J Fehsenfeld
P. Lecoq
G. Pace

OSE AND SUPPORT ENGINEERING
J L. Savino
D L. Ross
+E. Lindeman
Equivalent persons

CC&S OSE
+M. Ebersole
R. Otamura
C. Moore
A. Shain

POWER OSE
+R. Anker
K Musson
K. Toomath
D. Pasbrey

ATTITUDE CONTROL AND SCAN CONTROL OSE
+D. McFarlane
(2)W. Moore
J. Billitti

CENTRAL COMPUTER & SEQUENCER
*W. Scott — W. Brocksieper
+N.H. Herman — S. Deese
++O. Figueroa — D. Lord
E. Greenberg — W. Cook
R. Robinson — M. Hoppe
R. Carder — S. Lingon
A. Miyoshi

POWER
P. Goldsmith — A. Schulze
*H.L. Johnson — A. Uchiyama
+R. Josephs — P. Brisendine
++C. Sears — S. Krouse
T.J. Williams — J. Person
R. Rowe — W Long
E. Sequeira — A. Schloss
K. Dawson — J. Goldsmith
L. Whitcomack — A. Phillips
D. Bowen

ATTITUDE CONTROL/ SCAN CONTROL
G. Sweetnam — L. Schmidt
*K. Russ — J. McGillicuddy
+D.P. Meyer — R. Shrake
+++D. Weckerle — L. Sidwell
R. Rathcke — R. Uematsu
T. Almaguer — W. Packard
W. Goss — L. Keen
T. Verner — W. Salmi
R.H. Summers — O. Duffy (Ctr)
L. Bouvier — G. Courvitte
R. Crawford — D. Boyd
G. Perkins — J. McLauchlan
D. Carpenter — E. Koch
W. Charlan

MECHANICAL SYSTEMS
J Q. Spaulding
R J. Spehalski
A. Delgadillo
D.E. Hayes
L. Arthur

STRUCTURE
+R.J. Spehalski
+E.J. Dieckman
E. Floyd
F. Locatell
R. Norman
W. Layman

FLIGHT CABLING
+S. Dennis
D. Moore
A. Prisk

OSE/STC CABLING
+P. Sottosanti
Equivalent persons

OSE/LC CABLING
+W. Pierce
R. Sipos

ULCER
+B. Wagoner
W. Cook (Ctr.)

TEMPERATURE CONTROL
+D.W. Lewis
H. vonDelden
R. Becker

MECHANICAL DEVICES
+F. Goodwin
T. Thostesen
R.W. Kocsis
G. Coyle
D C. Miller

L/V MECHANICAL INTERFACE
F. Goodwin

MATERIALS SUPPORT ENGINEERING
C. Savage
V. Lardenoit

ELECTRONIC PARTS ENGINEERING SUPPORT
R. Scott
S. Sollock

APPLIED MECHANICS SUPPORT
H. Holbeck — J. Chen
R. Freeland — J. Chisholm
C. Larson

MECHANICAL TECHNICIAN SUPPORT
T. Bickler

DESIGN AND SPECIFICATION SUPPORT
R.W. Fuller
S. Kennedy

ELECTRONIC PACKAGING ENGINEERING SUPPORT
E.J. Dieckman — R. Dawe
R.C. Mayne — F. Lane
J. Caster — A. Franzon
J. Cox (Ctr) — A. Lawson
G. Hayashida

LIAISON SUPPORT
D. Scherff
R. Howell
W. Lewis

INSTRUMENTATION
+J. Wise — J. Hawkes
G. Wiker — J. Roelvink
T. Fisher — J Pozego
J. Nielson — V. Doty
R. Taylor — C. Burgessor.
R. Hansen — D. Loguirato
D.E. Lewis — R. Purves
K. Sutherland — A. Torres
J. Kendall — C. Hankenzee
W. Mushigan — K MacDavid
C. Dunlap — J. Watstein
A. Engel — F. Hiraoka
A. Gigger — J. Rogers
S. Rumsey — R. Whiteman
C. Sydnor — K. Wilbert
D. Griffin — W Brown
R. Harrison — L. Tewes
E. Adams — R. King

ENVIRONMENTAL TEST LABORATORY
+E. Gregory — J. Martinez
F. vanBiene — W. Matney
H. Dundas — P. Miller
C Nelson — H. Roe
D. Morrison — D. Ross
R. Daniel — J. Stoker
D. Waggle — A. DeMarchi
R. Woodbury — W. Reynaud (ETS)
J Cooper — G. Berry
C. Fee — R. Cadwallader
J. Andrews — M Johnson
W. Andrews — C. Klose
R. Blaydes — N. Webster-Zieher
A. Carnevale — D. Rupnik
P. Chapman — E. Adams
C. Hayes — C. Nussey
F. Johnson — A. Beers
B. Walker

SPACE SIMULATORS
+L. Dyckman

PYROTECHNICS
+J.E. Earnest

Electroexplosive Devices
A.J. Murphy
*S.N. Prescott

Pyro Electronics
*I.D. Quinn
Z.T. Wujcicki

Pyro OSE
W.G. Collins
R.J. Graham

Analysis
W.S. Wuest

PROPULSION
*+W.H. Tyler
L.B Mattson
T.R. Metz
P.I. Willson

Combustion Devices
D.D. Evans

Feed System
L. Toth

Analysis and SPAC
R.W. Rawley

IR SPECTROMETER SUPPORT

Valves and Dump System
R.S. Weiner
E. Ramvary

ATTITUDE CONTROL OSE

OSE Support
D.L. Boyer

* TECHNICAL MANAGER
\+ COGNIZANT ENGINEER
++ EXPERIMENT REPRESENTATIVE
+++ COGNIZANT NEGOTIATOR

Fig. 3 (contd)

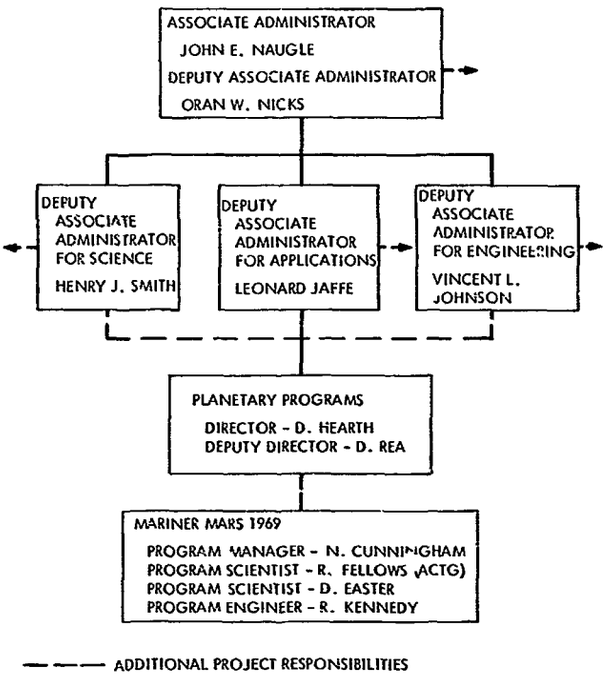


Fig. 4. NASA Office of Space Science and Applications management directly concerned with *Mariner* Mars 1969

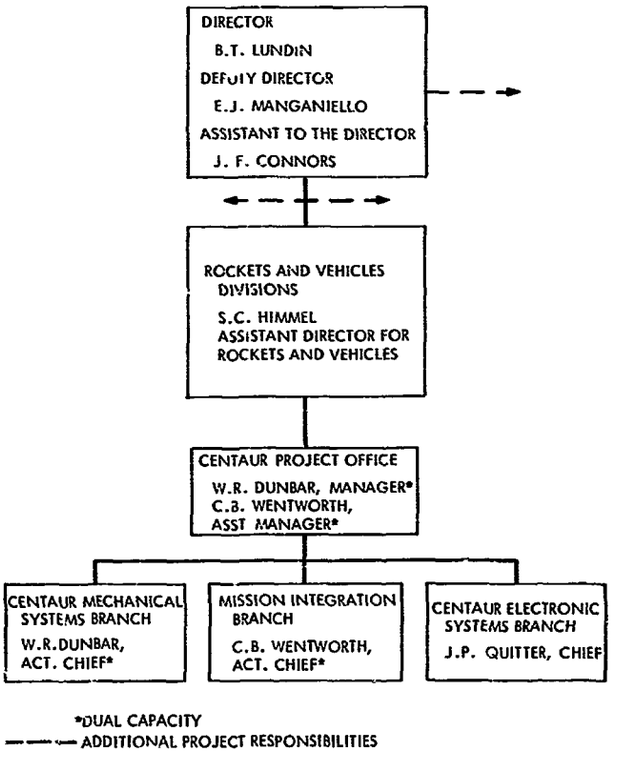


Fig. 5. *Mariner* Mars 1969 Launch Vehicle System management responsibilities at NASA Lewis Research Center

Table 1. Experimenter teams

Investigator	Affiliation
Television experiment	
R. B. Leighton[a]	California Institute of Technology
B. C. Murray	California Institute of Technology
R. P. Sharp	California Institute of Technology
N. H. Horowitz	CIT/Jet Propulsion Laboratory
A. G. Herriman	Jet Propulsion Laboratory
R. K. Sloan	Jet Propulsion Laboratory
A. Young	Jet Propulsion Laboratory
M. E. Davies	Rand Corporation
C. Leovy	University of Washington
B. A. Smith	New Mexico State University
Infrared spectrometer experiment	
G. C. Pimentel[a]	University of California (Berkeley)
K. C. Herr	University of California (Berkeley)
Ultraviolet spectrometer experiment	
C. A. Barth[a]	University of Colorado
F. C. Wilshusen	↓
K. Gause	
C. B. Hord	
K. K. Kelley	
R. Ruehle	
J. B. Pearce	University of Colorado
E. F. Mackey	Packard-Bell Electronics Corporation
W. G. Fastie	Johns Hopkins University
Infrared radiometer experiment	
G. Neugebauer[a]	California Institute of Technology
G. Munch	California Institute of Technology
S. C. Chase	Santa Barbara Research Center
S-band occultation experiment	
A. J. Kliore[a]	Jet Propulsion Laboratory
G. Fjeldbo	Stanford University/JPL
S. I. Rasool	NASA Goddard Institute of Space Studies
Celestial mechanics experiment	
J. D. Anderson[a]	Jet Propulsion Laboratory
W. L. Martin	Jet Propulsion Laboratory
[a]Principal investigator	

Three interface panels operated in support of *Mariner* Mars 1969. One, the Tracking, Telemetry, and Communications Panel, was an inter-project effort, serving *Surveyor, Lunar Orbiter, Pioneer, Voyager,* and two *Mariner* Projects; the other two were chartered for *Mariner* Mars 1969. They both covered the launch vehicle interface, one concerned with performance, trajectories, and guidance, and the other with the hardware interface.

II. Management Responsibilities

The chain of responsibilities in connection with *Mariner* Mars 1969 was given in Fig. 1. Ultimate responsibility for the project rested, of course, with NASA. The Associate Administrator, OSSA, is responsible to NASA general management for the planning and direction of a related group of research and development activities, including a number of flight projects, of which *Mariner* Mars 1969 was one. The Director of lunar and planetary programs and the Assistant Director, planetary flight programs, are successively delegated responsibilities which included the project; the *Mariner* Mars 1969 Program Manager was directly responsible within OSSA for management of the effort.

Management responsibility for the project was formally assigned to JPL in a document attached to the PDP. The broad responsibilities assigned were as follows:

(1) Integrating the several systems of the project, assuring that such overall systems engineering activities as may be necessary are carried out.

(2) Ensuring that oversights and omissions in any aspect of the project are detected and corrected in time to minimize cost overruns, schedule delays, and technical failures.

(3) Identifying project requirements which have not been anticipated in the PDP and actively taking steps as may be necessary to obtain solutions to these needs.

(4) Recognizing the responsibility and authority of the Director of LeRC, for the procurement, modification, and integration of the launch vehicle, for the launch of the *Atlas/Centaur* vehicle, and for the launch-to-injection tracking and instrumentation in support of the launch vehicle.

Corresponding assignments for system management responsibility were formalized in the same way. A memorandum of agreement with each principal investigator, signed by the project and program managers and the investigator, and the charters of the interface panels and working groups were similarly documented as attachments to the PDP.

Specific management responsibilities for the four system managers, as prescribed in the PDP, are listed in Table 2. Project staff management responsibilities are listed in Table 3.

Table 2. System management responsibilities summary

Spacecraft System	Launch Vehicle System	Mission Operations System	Tracking and Data Acquisition System
Spacecraft and operational support equipment (OSE) development and procurement, including upper adapter and separation system	Launch vehicle and aerospace ground equipment modification and procurement	Mission Operations System and mission-dependent equipment organization, development, and procurement	Providing tracking, telemetry, and data acquisition support as required by project through SIRD, and establishing and defining appropriate DSN configuration
Spacecraft change control	LVS change control	MOS change control	Ensuring adequacy of DSN change control
Spacecraft and OSE documentation	LVS documentation	MOS documentation	TDS documentation
Spacecraft scheduling	LVS scheduling	MOS scheduling	TDS scheduling
Spacecraft system reliability and quality assurance programs	LVS reliability and quality assurance programs	MOS reliability and quality assurance programs	Ensuring adequacy of DSN reliability and quality assurance programs
Spacecraft prelaunch testing and operations including test and operations plan	LVS prelaunch testing including test planning	MOS prelaunch testing and training including space flight operations plans	TDS prelaunch testing and training including test planning
Commitment of spacecraft launch readiness	Commitment of LVS launch readiness	Commitment of MOS launch readiness	Commitment of TDS launch readiness
Staffing and assuring technical proficiency of SPAC team for mission operations	Plan and direct launch operations	Plan and direct mission operations	Operational support of MOS
Support postflight analysis and evaluation of spacecraft performance	Postflight analysis and evaluation of LVS performance	Postflight analysis and evaluation	Support postflight analysis and evaluation
Reporting (technical and management)	Reporting (technical and management)	Reporting (technical and management)	Reporting (technical and management)
Launch Vehicle System (LVS)/ spacecraft interface prime responsibility	LVS/spacecraft interface support and participation	SIRD prime responsibility and MOS inputs to PRD	SIRD and PRD review and assistance; SIRD response
MOS/spacecraft interface participation	Inputs to project requirements document (PRD), support instrumentation requirements document (SIRD), and other project/AFETR interface activity	MOS/spacecraft interface prime responsibility	DSIF/spacecraft interface participation
DSIF/spacecraft interface prime responsibility	LVS/AFETR interface	LVS/MOS interface prime responsibility	Monitoring requirements on tracking and data-acquisition facilities for consistency
	LVS/MOS interface participation		
	LVS performance and trajectory analysis		

Table 3. Project staff management responsibilities summary

Mission analysis and engineering manager	Reliability assurance staff engineer	Project scientist	Project control manager
Project and mission requirements (mission plan and requirements document, program requirements document, etc.)	Assessing adequacy of system and subsystem reliability and quality	Assistance in defining scientific objectives, evaluating experiments, and recommending experiments for payload	Development and maintenance of project master plan and detailed project schedules for all systems, hardware, and software
Project/mission documentation planning	Independent mission and spacecraft system reliability and failure analysis studies	Developing appropriate science schedule	Establishing and ensuring the existence of detailed plans throughout project structure
Monitoring and assessment of system interfaces	Recommending measures to improve probability of mission success	Communicating with principal investigators and establishing contractual relationships between them and project	Establishment and maintenance of detailed records of current status and schedules
Launch vehicle liaison and planning	Monitoring system and subsystem tests	Approval of instrument functional requirements, ensuring accurate reflection of requirements of approved experiments	Central control of project programming actions
Launch vehicle guidance and trajectory interface	Correlation of system and subsystem reliability activity	Actual source of scientific information affecting spacecraft and ground-data-handling equipment design	Maintenance of project chart room and conference center
AFETR trajectory and inflight range safety interface	Design review board participation	Preparation of final mission scientific-results report	Project configuration-management support
Trajectory design, orbit determination, and maneuver analysis	Preparation and implementation of reliability-assurance program (in consonance with NPC-250-1)	Staffing and assuring technical proficiency of mission operations space science analysis and command team	Project data management
Staffing and assuring technical proficiency of mission operations, flight-path analysis, and command team	Auditing and evaluation of all portions of system reliability plans and activities	Assessing, maintaining, and ensuring scientific adequacy of project elements	Assurance of expeditious communication of project policy and activity within the project and with JPL management, NASA headquarters, government agencies, and industries
Project functional design tradeoff studies	Participation in acceptance and certification of flight hardware, flight spacecraft, and support equipment		Provision of project resource status and analysis data
Launch constraints	Monitor all subcontractors' inspection, parts selection and application, and packaging procedures		Preparation of program obligation plan and project management record
Mission success probability assessment	Develop, audit, and approve system and subsystem reliability-assurance program plans and appropriate documentation		Contractual-management guidance of subsystem contracts
Representing project on Centaur performance and trajectory panel; tracking, telemetry, and communication panel, and spacecraft/launch vehicle interface panel	Implement program for failure reporting, analysis, corrective action, and correction verification		Overall contractual surveillance of subcontractor performance
Planetary quarantine analysis and certification			Assistance in formulating new procurement efforts and plans
			Advising and participating with NASA to establish secondary responsibilities with government procurement, inspection, material, or audit agencies assigned to major subcontractors
			Participation in planning, preparation, and presentation of project documentation and reports inside and outside JPL and NASA
			Project audit and analysis

Division representatives were assigned to the project from the project engineering division and each technical division, and, in addition, from procurement, quality assurance and reliability, and technical information and documentation. Each representative was responsible to the project manager (procurement and technical information division representatives to the project control manager) for project activities within his division. He was responsible for applying division resources, within the funds and manpower available, for project work and for meeting project commitments in accordance with approved operating plans. Specific responsibilities of the division representatives at that time included:

(1) Reviewing project guidelines and requirements and clarifying tasks and areas of effort to permit preparation of divisional staffing and operating plans as required to support the project.

(2) Planning and coordinating the implementation of those portions of the project requirements assigned to his division.

(3) Compiling information from appropriate section managers and project office personnel, and preparing an overall division plan for support of the project in terms of staffing requirements and job numbers.

(4) Informing all line management personnel in his division about all aspects of the project that will aid in carrying out line responsibilities.

(5) Acting to ensure that his division technical and scheduling interfaces are being resolved.

(6) Management of all project activities within his division, including budgetary and technical; overseeing preparation and maintenance of flow plans, schedules and budgets, and work authorization releases; and reporting status of these functions to concerned division and project management.

(7) Coordinating the review and modification of the project plan within the framework of the division line organization.

(8) Handling all day-to-day project affairs within the scope of the established plans.

(9) Continuously monitoring all division work in support of the project, keeping the concerned project and division management elements informed about approved changes to plans, the status of activities as compared to plans, and promptly reporting to the division manager any problems (existing or potential) within the division that could affect the meeting of project commitments.

(10) Taking the initiative to bring together the appropriate project and division management elements in all instances where it is evident a situation may exist that could adversely affect the attainment of project objectives, or where a significant redirection of division efforts in support of the project is required.

(11) Taking the initiative to ensure that the division implements approved project staffing plans.

Areas of responsibility associated with specific JPL divisions were defined essentially by technical discipline as follows:

(1) The project engineering division was responsible for spacecraft system design, environmental requirements, system assembly and test, and spacecraft/launch vehicle interface and integration.

(2) The systems division was responsible for mission analysis (later a function of the data systems division, when it was formed) and software and other operational-support functions.

(3) The space science division was responsible for experiment and project science support and for the data automation subsystem and the four scientific instrument subsystems.

(4) The telecommunications division was responsible for telecommunications-link systems analysis and integration as well as the radio frequency, command, telemetry, and data storage subsystems.

(5) The guidance and control division was responsible for the power, attitude control, central computer and sequencer, and scan control subsystems.

(6) The engineering mechanics division was responsible for mechanical design and engineering support, the structure, mechanical devices, cabling, and temperature control subsystems.

(7) The environmental simulation division was responsible for environmental test operations.

(8) The propulsion division was responsible for the propulsion and pyrotechnic subsystems.

III. Operations

Management and coordination of project activities were carried out using a variety of tools, the principal elements of which were documentation and meetings.

A. Management Documentation

The basic management documents used in *Mariner* Mars 1969 were the following:

(1) *Project development plan.* As described previously, the PDP was the fundamental plan and agreement defining all areas of the project. Published in late 1966, and signed off by JPL, LeRC, and OSSA Management, as well as the project and system managers, the PDP governed the project management planning through the Mars mission without revision, except that a supplement containing an expanded and updated coordinated operations plan was issued in late 1968.

(2) *Project policy and requirements.* The project policy and requirements document detailed JPL-internal interpretations and expansion of the PDP, dealing with all JPL pre-mission activities, approved by concerned JPL management and signed by the project manager. Released in early 1967 after many iterations, negotiations, and reviews, this document was never revised.

(3) *Work breakdown structure, master schedule, and organization chart.* Published and revised periodically as required (the schedule and organization chart were reissued monthly), these working documents helped to frame and define the activities of the project. The work breakdown structure served as the basis for the *Mariner* Mars 1969 chart of accounts and for the subject-indexed data management master file. The organization chart served also as the project directory and the basis of manpower planning and monitoring.

(4) *Monthly project management reports.* These reports contained status-vs-plan analysis of schedules (project and system), financial and manpower plans, and other matters of management. The master project schedule cumulated from these documents is given in Fig. 6.

(5) *Spacecraft system plans and requirements.* These documents included the quality assurance plan, document preparation requirements, engineering drawing requirements, the change control plan, environmental test program requirements, the design review program, the test and operations plan, and a number of more technical requirements that dealt with specific tasks and aspects of system management as indicated by the titles.

(6) *MOS/TDS management plan.* This was a general, integrated two-system plan, revised once, providing for the development and testing of hardware, software, and operational elements (some mission-peculiar and some committed by the TDS), supported by a number of development, test, and operations plans, including a multi-volume DSN operations plan.

(7) *Interface control documents.* These documents included a spacecraft/DSIF telecommunications document, a spacecraft/MOS document, spacecraft/*Centaur* launch vehicle hardware requirements, and spacecraft/*Centaur* interface schedules in the area of performance, trajectories and guidance, and a hardware document. These frequently revised documents, aided interface management and coordination and defined technical integration arrangements.

A number of other specialized management documents, including the data management plan, and many subsystem-level requirements and plans, supported the management of various specific activities.

B. Meetings

The meetings which served as management media for *Mariner* Mars 1969 are considered in two categories: working meetings, conducted regularly, and reviews, conducted occasionally. The project quarterly reviews combined aspects of both types.

The quarterly reviews were conducted about every three months beginning in April 1966, which was close to the inception of the project, until October 1969, which was after completion of the Mars mission. These meetings served as a status review for JPL and project management and the NASA OSSA Program Office and simultaneously as a working meeting characterized by the exchange of information, requirements, and action items. The reviews were normally held in a facility large enough to accommodate all interested personnel, taking one or two days to cover all aspects of the project. The twelve quarterly reviews were documented.

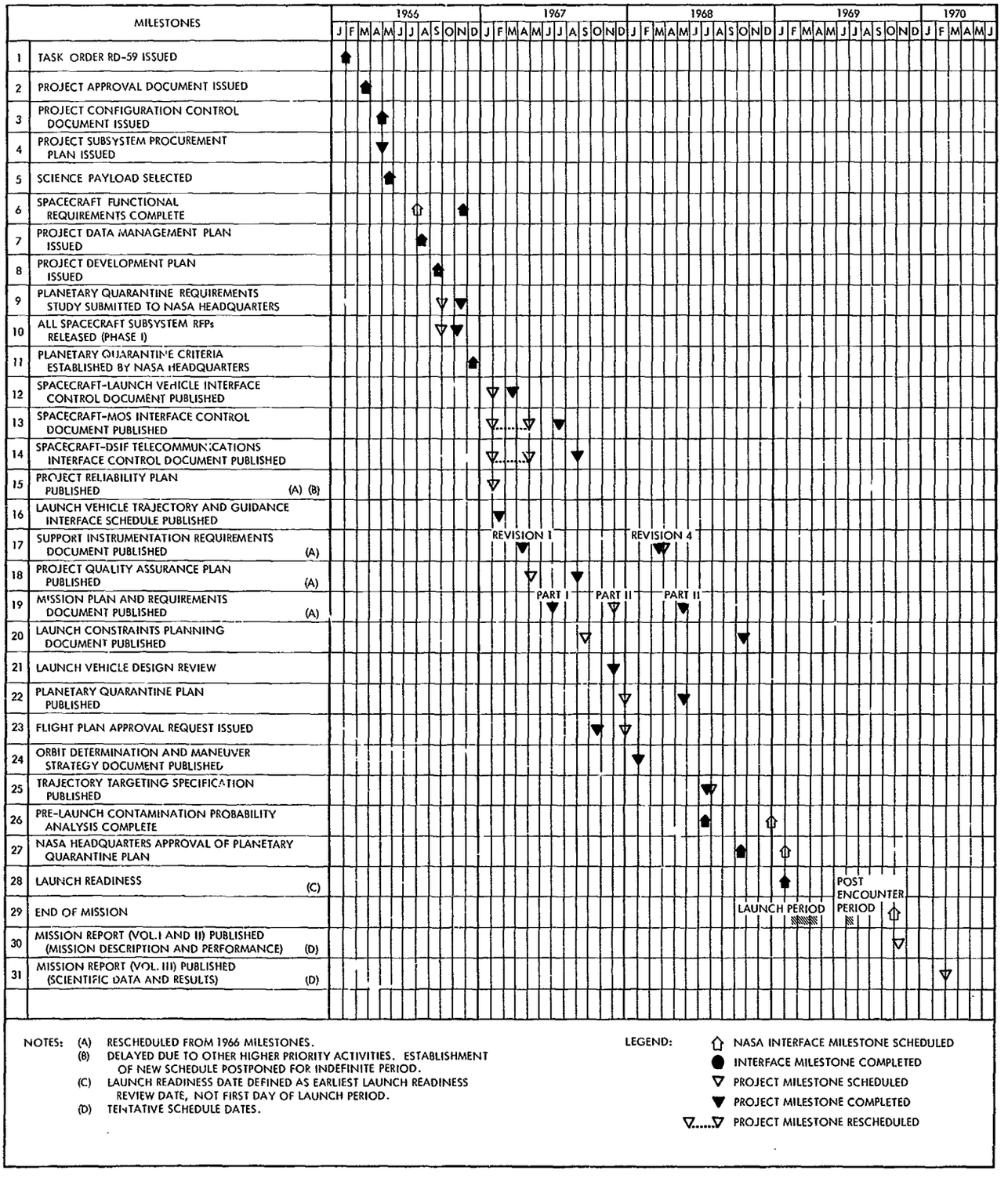


Fig. 6. Master project schedule

Regular project meetings were conducted weekly from the beginning through mission conclusion. Participants included the project management and staff, the division representatives, and interested or concerned managers and personnel. The agenda varied with the phase of project activity, from concentration on design documentation through contractor development and manufacture status to delivery, assembly, and test of flight hardware and MOS software, and, finally, to flight operations progress. Because of the nature of the project and its systems, mission design and spacecraft development and test tended to dominate the discussions and negotiations of the project meetings. The meetings were documented in widely-circulated minutes, to which were attached such useful records as a running list of open action items, a schedule of other meetings such as design reviews, and the "problem list." The problem list, a powerful management tool, was initiated on December 13, 1967 as a record of problems which could place the mission in jeopardy, in the judgment of the project manager. A total of 24 problems were identified during the life of the project; they were referred to division managers and others of similar level for high-priority solution. The problem list is shown in Table 4.

Weekly project staff meetings, attended by the JPL system managers and the staff managers, were conducted by the project manager. These meetings were not documented regularly, but the major agreements and positions reached within them were individually published as appropriate.

Various design teams (spacecraft, MOS, software, encounter sequence, etc.) met regularly during their appropriate tenures to manage specific design efforts. The minutes of these meetings were regularly taken, as a rule. In the pre-operational and operational phases, various series of operations-oriented meetings were conducted. For the most part, these were not recorded directly.

Preliminary, design, and hardware or acceptance reviews were conducted at system and subsystem levels. These reviews consisted of presentations to a board, usually supported by much backup documentation, followed by recommendations forwarded by the board to the project or concerned system manager. Their purpose in general was threefold: first, to bring independent and senior judgment, in the form of the review board, to bear on all aspects of the system or subsystem; second, to assure consideration of the internal and interface characteristics by the appropriate management and engineers

Table 4. Project problem list

No.	Problem	Date recognized
P-1	Radio PTM schedule	1/68
P-2	IRS PTM schedule	1/68
P-3	TV PTM schedule	1/68
P-4	UVS PTM schedule	1/68
P-5	CC&S, FCS integrated circuit failures	3/68
P-6	A/C relay failure	3/68
P-7	Tape belt failures	4/68
P-8	Radio flight unit schedule	4/68
P-9	IRS flight unit schedule	4/68
P-10	TV flight unit schedule	4/68
P-11	TV integrated circuit failures	4/68
P-12	Radio capacitors	4/68
P-13	IRS gas tanks	5/68
P-14	Tape deck vibration	6/68
P-15	TV shutter	6/68
P-16	STCDS	6/68
P-17	TCP computer	7/68
P-18	TV test schedule	8/68
P-19	IRS film drive	10/68
P-20	Radio quality	11/68
P-21	IRS cryostat	11/68
P-22	Tape Degradation	11/68
P-23	Radio Flight anomalies	4/69
P-24	TV AAC Inversion	7/69

(the presentors); third, to uncover and deal with residual or new problems.

The spacecraft system design review program established the plan for the subsystem and system reviews within its scope, including purposes, framework of agenda, responsibilities of participants, and disposition of the review results. Stated specific objectives of this program included:

(1) Improvement of the product.

(2) Assurance of consideration of interfaces with other elements of the project and that compatibility did in fact exist.

(3) Assurance of complete compatibility of the item under review with system (or mission) requirements.

(4) Evaluation of the design to determine that the best design had been achieved within the program constraints.

(5) Periodic re-evaluation of the design against current information and requirements.

(6) Exposure of design concepts to technically competent personnel as early as possible to assure a workable and reliable product and to eliminate incorrect assumptions or inefficient design concepts.

A composite schedule of the formal reviews conducted during the performance of the program is given in Fig. 7.

C. Resources

Funding and manpower considerations were influential in the development of the *Mariner* Mars 1969 project. Some design changes from *Mariner IV* to the baseline 1969 configuration were undertaken to reduce cost, and some design options were not chosen for the same reason. Careful value/cost tradeoffs were a part of each stage of the design and development process.

Resources for the launch vehicle system and TDS were allocated and applied outside the *Mariner* Mars 1969 organization. Launch vehicle developments and the *Centaur* project in particular were the responsibility of the NASA Office of Advanced Research and Technology. The Deep Space Network and other TDS elements were the responsibility of the NASA Office of Tracking and Data Acquisition, and resource management for these elements were conducted through the respective line-organization channels.

Funding and manpower allocations for project management and the spacecraft and MOS elements came through the Office of Space Science and Applications to the JPL project management center and were dispensed there in accordance with approved plans. Each budget and plan was developed in a division/project negotiation, with extensive review preceding approval by JPL management. Costs and manpower within these limitations are summarized for the active life of the project in Table 5. The trend in the estimated cost-to-completion, with changes annotated, is given in Fig. 8. It may be

Table 5. Funding and manpower allocations

Fiscal year	Dollars allocated, thousands				Manpower allocation, JPL
	Project management	Spacecraft	MOS	Total	
1966	328	3,558	4	3,950	36
1967	1,113	28,623	394	30,130	257
1968	1,871	59,468	1,251	62,590	532
1969	1,289	20,930	3,081	25,300	445
1970	576	2,285	1,641	4,502	79
Total	5,237	114,864	6,371	126,472	1,349

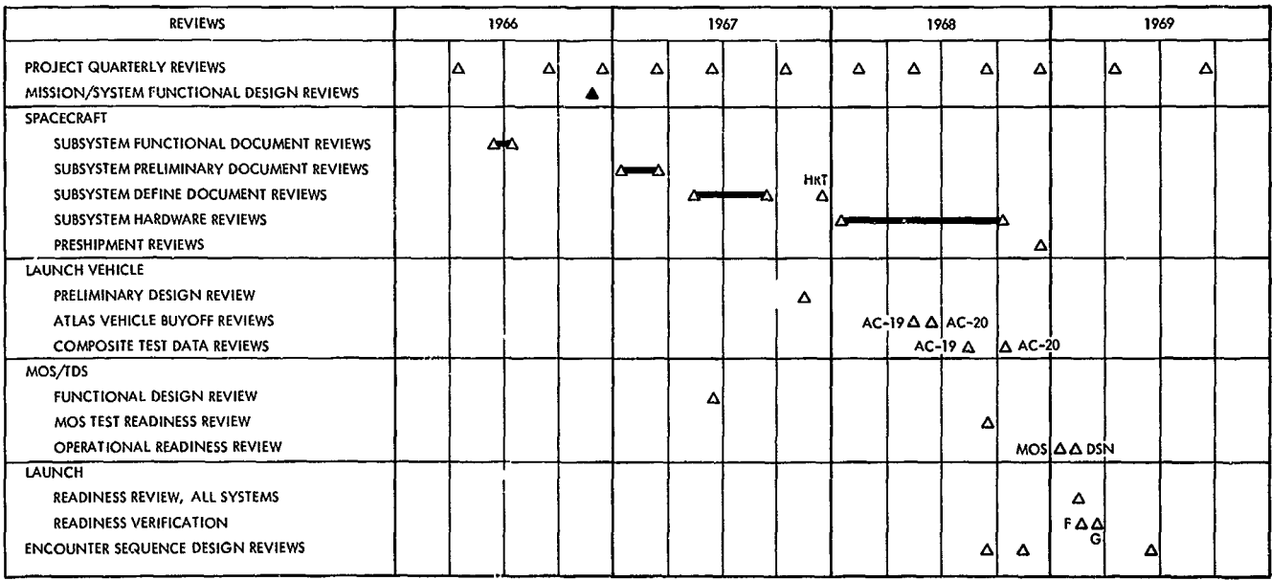
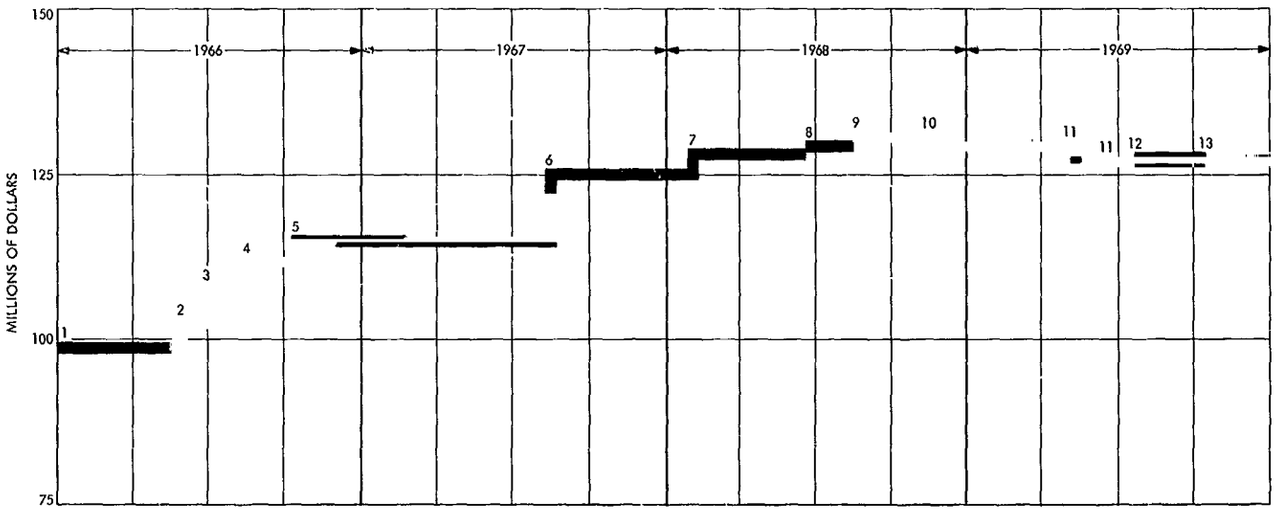


Fig. 7. Schedule of formal reviews



REASON FOR PLANNED COST CHANGE

1. PRELIMINARY ESTIMATE BASED ON MISSION SIMILAR TO MARINER MARS 1964.
2. HEADQUARTERS INCREASE TO ACCOMMODATE SELECTED SCIENCE PAYLOAD.
3. JPL ESTIMATES UPDATED TO INCLUDE SELECTED SCIENCE PAYLOAD AND INCREASED SPACECRAFT ESTIMATES.
4. TO COVER INCREASES IN SUBSYSTEM COSTS AS INDICATED BY CONTRACT NEGOTIATIONS AND PROPOSALS.
5. DUE TO SURVEYOR H-J CANCELLATION. MARINER MARS 1969 TO ASSUME SPACE SIMULATOR CHARGES.
6. INCREASE TO COVER UNDERESTIMATION OF CONTRACT COSTS, PIECE PARTS PROBLEMS, DOD COMPETITION, AND EXPERIMENT-RELATED ITEMS, AS WELL AS JPL IN-HOUSE COSTS.
7. INCREASE DUE TO CONTRACTOR UNDERESTIMATION OF PHASE II HARDWARE COSTS, LATE DELIVERIES, AND SOME CONTRACTOR SALARY RATE AND OVERHEAD INCREASES.
8. INCREASE IN ESTIMATE TO COMPLETE.
9. INCREASE PER PROGRAM OBLIGATION PLAN GUIDELINES.
10. DECREASE IN PROGRAM OBLIGATION PLAN GUIDELINES BASED UPON CONTINUING INCREASE OF SUBCONTRACT COSTS FOR FIRST HALF OF FY69. THESE EXPECTED INCREASES DID NOT MATERIALIZE.
11. DECREASE IN ESTIMATE TO COMPLETE.
12. INCREASE IN JPL APPLIED COSTS PLUS SOME FY70 PROJECT COST INCREASES.
13. DECREASE IN PROJECT GUIDELINE AMOUNT TO ACCOMMODATE INCREASE IN MARINER MARS 1969 SHARE OF HQ IMPOSED TAX.

Fig. 8. Cost trend analysis

observed that early increases were associated with the selection of the scientific payload and the determination (by NASA) to go ahead with it, and that later increases were associated with the progressive realization of subsystem contractor and spacecraft change costs.

D. Spacecraft procurement

The *Mariner* Mars 1969 project approval document had provided that "the capabilities of industry . . . be utilized . . . to the maximum extent possible by contracting for subsystems or elements of the spacecraft and supporting equipment." This approach was executed by subsystem contracts technically managed by the technical divisions responsible for the various subsystems, and negotiated and administered by the procurement division.

Requirements and instructions for the initiation of these procurements were provided in the *Mariner* Mars 1969 subsystem procurement instructions. Proposals were requested and submitted, and source evaluation and selection were undertaken according to accepted criteria. Different types of contracts were offered, and different phasing schemes were established, according to the scope and content of the contracted efforts. The resulting contracts are listed in Table 6. The subsystem procurement operations are shown in Fig. 9.

Table 6. Major subsystem contracts

Subsystem	Phase	Contractor	Contract number	Contract type	Period of performance	Technical manager	Cognizant JPL division
Engineering mechanics	I	Northrop Corp, Nortronics	951690	CPAF[a]	8/3/66 – 12/31/69	J. N. Wilson	Engineering mechanics
Engineering mechanics	II	Northrop Corp, Nortronics	951691	FFP/TO[b]	9/1/66 – 3/1/69	J. N. Wilson	Engineering mechanics
Computer and sequencer	I A and B	Motorola	951711	CPFF[c] > Purchase Complete	9/12/66 – 4/15/67	W. F. Scott	Guidance and control
Computer and sequencer	II A and B and III	Motorola	951816	CPFF	12/6/66 – 12/1/69	W. F. Scott	Guidance and control
Telemetry	I	Texas Instruments	951697	CPFF/AF[d]	9/23/66 – 12/31/69	B. Kim	Telecommunications
Telemetry	II	Texas Instruments	952026	CPFF	8/1/67 – 9/15/68	B. Kim	
Data storage	I	Texas Instruments	951735	CPFF/AF	9/23/66 – 2/1/68	R. Harrington	
Data storage	II	Texas Instruments	952079	CPFF	8/1/67 – 7/30/68	R. Harrington	
Radio	I	Philco Corp.	951729	CPFF/AF	8/22/66 – 11/1/69	D. Dakan	
Radio	II	Philco Corp.	951888	CPFF/AF	7/28/67 – 7/25/68	D. Dakan	
Command	I	Motorola	951700	CPFF/AF	9/8/66 – 7/1/69	R. Rakunes	
Command	II	Motorola	952042	FFP	8/1/67 – 7/20/68	R. Rakunes	Telecommunications
A/C and scan	I	Honeywell, Inc.	951701	CPFF/AF	9/9/67 – 9/30/69	K. Russ	Guidance and control
A/C and scan	II	Honeywell, Inc.	951701	CPFF/AF	7/28/67 – 4/30/69	K. Russ	Guidance and control
Data automation	I	Litton Systems, Inc.	951797	CPFF	12/6/66 – 9/15/67	H. Friedman	Space science
Data automation	II	Litton Systems, Inc.	951797	CPFF	9/22/67 – 5/6/68	H. Friedman	Space science
Pyro electronics	I	Electro-Optical Systems, Inc.	951866	CPFF/AF	1/16/67 – 6/1/69	J. Quinn	Propulsion
Pyro electronics	II	Electro-Optical Systems, Inc.	951866	CPFF/AF	12/4/67 – 6/30/68	J. Quinn	Propulsion
Power	I	Electro-Optical Systems, Inc.	951881	CPFF/AF	1/25/67 – 11/30/69	H. Johnson	Guidance and control
Power	II	Electro-Optical Systems, Inc.	951881	CPFF/AF		H. Johnson	Guidance and control
Propulsion	I	TRW Systems, Inc.	951806	CPFF	2/22/67 – 8/30/67	W. Tyler	Propulsion
Propulsion	II	TRW Systems, Inc.	951806	CPFF	8/28/67 – 8/30/68	W. Tyler	Propulsion

[a]CPAF: Cost plus award fee

[b]FFP/TO: Firm fixed price/task order

[c]CPFF: Cost plus fixed fee

[d]CPFF/AF: Cost plus fixed fee plus award fee

Table 6 (contd)

Subsystem	Phase	Contractor	Contract number	Contract type	Period of performance	Technical manager	Cognizant JPL division
IR spectrometer	I	University of California, Berkeley	951722	Cost reimbursement	8/31/66 – 5/1/70	W. Carls	Space science
IR spectrometer	II	University of California, Berkeley	951722	Cost reimbursement	9/15/67 – 8/1/68	W. Carls	
TV electronics and integration	I	Electro-Optical Systems, Inc.	951788	CPFF	12/16/66 – 6/30/68	D. Montgomery	
TV electronics and integration	II	Electro-Optical Systems, Inc.	951788	CPFF/AF	4/1/67 – 10/1/68	D. Montgomery	
IR radiometer	I	Santa Barbara Research	951789	CPFF	11/11/67 – 7/21/68	D. Schofield	
IR radiometer	II	Santa Barbara Research	951789	CPFF	8/31/67 – 7/21/68	D. Schofield	
UV spectrometer	I	University of Colorado	951790	Cost reimbursement	11/28/66 – 10/13/67	E. McMillan	
UV spectrometer	II	University of Colorado	951790	Cost reimbursement	8/4/67 – 8/1/68	E. McMillan	Space science

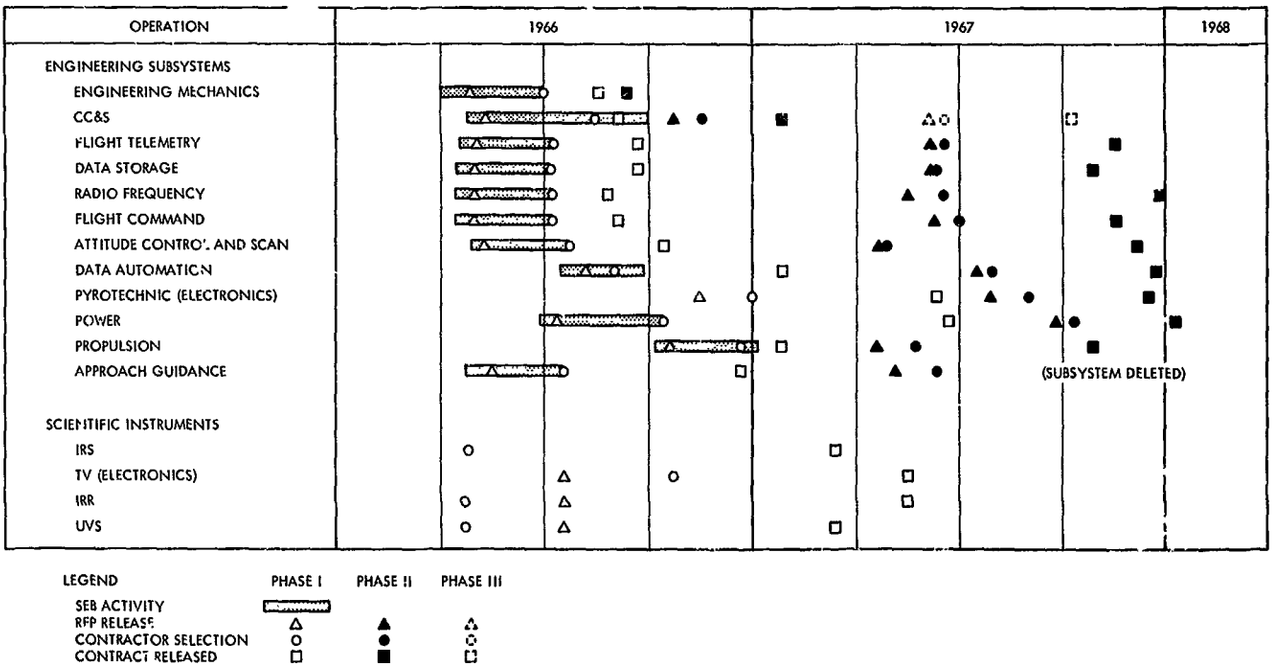


Fig. 9. Subsystem procurement operations

Mission Design, Analysis, and Engineering

I. Mission Planning

The Mariner Mars 1969 mission design was the result of a number of broad inputs coming mainly from the project approval document and the scientific objectives and experiment complement. The project approval document prescribed mission objectives and outlined the technical approach. It also specified the launch of two 850-lb-class spacecraft by *Atlas/Centaur* launch vehicles, from AFETR, during the 1969 Mars opportunity, toward flyby encounters with the planet. The science payload selected was planet-oriented; there was no "cruise science." Requirements of the other two project systems, mission operations and tracking and data acquisition, and the NASA planetary quarantine policy, were additional inputs, as were the appropriate physical conditions.

Mission requirements arose from characteristics of the four systems, as affected by the project guidelines and the appropriate policies, and by the scientific program. The principal guideline was to use existing systems so far as possible, changed only to achieve the mission, improve reliability, and minimize cost. The main thrust of the scientific program was to maximize the return and quality of the Mars data. In a number of cases, especially in spacecraft and Mission Operations System (MOS) design, mission requirements reflected back into system design, bringing about significant increases in capability.

A number of scientific questions about Mars were generated by the *Mariner IV* mission and by scientific gatherings in the 1965–67 period, sponsored in part by NASA. With regard to the surface, for example, it was asked whether the present surface is the result of a long steady-state process or an episodic history which might once have included a denser atmosphere and the presence of liquid water. In addition the seasonal changes of albedo and color in some light and dark areas were pondered.

The *Atlas/Centaur* launch vehicle system, used for the first time in a planetary mission in 1969, presented a number of new features to the *Mariner* program. Its payload capability and injection accuracy represented a significant advance over prior vehicles. It had single-burn and double-burn capability, and was able to perform a yaw maneuver during the ascent. Use of the *Centaur/Surveyor* nose fairing provided adequate space for the *Mariner* spacecraft.

Characteristics of the *Mariner* spacecraft, based principally on 1964–65 flight experience, included relatively long operating life, three-axis attitude stabilization through celestial and inertial references and cold-gas thrustors, inflight course corrections through a small onboard rocket engine, solar electrical power, two-way communications through fixed spacecraft antennas, onboard fixed and programmable computing and sequencing, scientific instrument pointing control (relative to spacecraft attitude), and onboard science data storage. The programmable spacecraft computer was a new feature; in addition, a multichannel telemetry system with engineering data rates of 8⅓ and 33⅓ bits/s, science rates of 66⅔ and 270, and an experimental high-rate channel with 16.2 kbits/s was introduced.

Mission operations and tracking and data acquisition characteristics (the two systems were fused in operation and, to a lesser extent, in design) included the capability of the world-wide Deep Space Network, which had tracked *Mariner IV* to a distance of 192 million miles on the 85-ft antenna network, with the 210-ft-diameter antenna at the Goldstone site, which formed an essential part of the experimental high-rate telemetry link. A much greater capability for real-time telemetry and operational response was available to the 1969 mission; in conjunction with the programmable spacecraft computer, a much greater flexibility in operational sequence design was possible. This was particularly evident in the design of the Mars encounter.

The characteristics in detail of the project systems are described in succeeding sections of this report.

Two launches, two flights, and two Mars encounters were planned for *Mariner* Mars 1969. The hardware elements were to be identical for the two, but the conditions were to be different. The launches would be scheduled relatively far apart during the launch opportunity; and the encounter conditions were to be established, according to the desires of the experimenters, to maximize the return from either one or two successful flyby passes.

Scientific experiment requirements would affect the timing and placement of the flyby, the velocity relative to the planet, and the altitude. The desire to conduct the flyby over Goldstone defined a time of day for encounter. The presence of the S-band occultation experiment prescribed a flight path in which the desired occultation occurred.

Thus, there were to be multifaceted interactions between the principal investigators, the spacecraft design team, the launch vehicle system, MOS, TDS, and mission design, in the course of the parallel design and definition processes.

II. Trajectory Design

A. Hyperbolic Departure

Consider the simple two-body situation depicted in Fig. 1. It is well known that, in the presence of only gravitational forces, the projectile will travel along a trajectory which describes one of the conic sections. If the projectile is launched horizontally, but with a low velocity, its path will describe an ellipse whose apoapsis is at the location of the cannon. By increasing the launching velocity until it is equal to

$$\frac{\sqrt{\mu}}{R}$$

the projectile can be placed in a circular orbit about the attracting body. Further increases in the launch velocity will cause the projectile to travel in an ellipse whose periapsis is at the cannon. When the launch velocity is increased to

$$\frac{\sqrt{2\mu}}{R}$$

the "escape velocity," the projectile will travel along a parabola and will only be slowed to zero velocity by

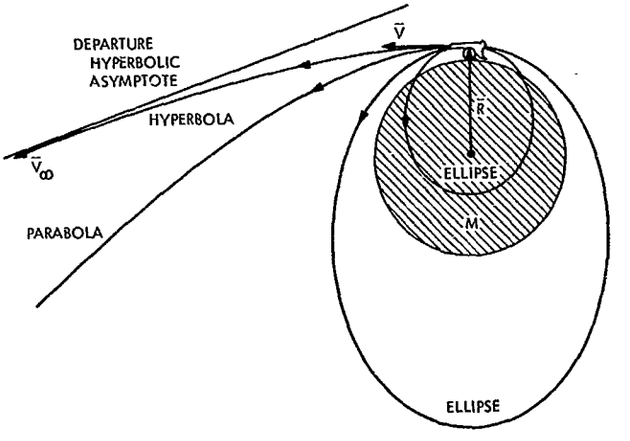


Fig. 1. Two-body conic sections

the time it has reached an "infinite" distance from the attracting body. If the launch velocity is increased beyond the escape velocity, the projectile will travel along a hyperbola and will still possess a residual velocity $\mathbf{V}_\infty$, known as the hyperbolic excess velocity, after reaching an infinite distance.

One of the most common parameters (Refs. 1 and 2) used by the trajectory designer is C_3, sometimes referred to as the vis-viva energy, which is equal to twice the total energy per unit mass. The equation for C_3 is shown in Fig. 1. When $C_3 < 0$, the launched object will remain in a capture orbit about the attracting body. When $C_3 = 0$, the object will just barely escape along a parabola and, when $R = \infty$, $\mathbf{V}_\infty = 0$. When $C_3 > 0$, the launched object will reach an infinite distance and will still possess a residual velocity whose magnitude is $\mathbf{V}_\infty = \sqrt{C_3}$. In order to launch a spacecraft to Mars, it is necessary to vectorially add $\mathbf{V}_\infty$ to the Earth's heliocentric velocity vector in order to achieve the required heliocentric transfer ellipse to Mars.

B. Type I vs Type II Transfers

Figure 2 illustrates the basic trajectory design chart for the 1969 Mars opportunity. This chart indicates the C_3 requirements over a broad span of launch and arrival dates, for both type I and type II transfer trajectories. Type I trajectories have total heliocentric central transfer angles (from Earth at launch to Mars at encounter) of less than 180 deg, whereas type II transfers have transfer angles around the Sun of more than 180 deg but less than 360 deg. Also shown in Fig. 2 are dashed time-of-flight contours and, along the right-hand ordinate, earth-to-Mars communication distances at encounter as a function of arrival date.

For a separated spacecraft weight of about 850 lb, the *Atlas/Centaur* launch vehicle can inject the spacecraft at a C_3 as high as about 27 km^2/s^2. Referring to Fig. 2, it can be seen that an extremely large span of launch and arrival date possibilities are available for this energy capability. This situation is quite different from the previous *Mariner* missions which, because of the reduced payload capability of the *Atlas/Agena* launch vehicle, had to be launched during the period around minimum C_3. Thus, for the *Mariner* Mars 1969 mission, the trajectory designer had a wide range of possible transfer and encounter geometries to investigate and understand. This section discusses the narrowing process that was carried out to determine the preferred trajectory selection region.

During the first quarter of 1966, the question arose regarding whether to launch both spacecraft on type II transfers, both on type I, or perhaps a mixture. An examination of the type II trajectory region revealed that, for arrivals after early September 1969, and for launches after late December 1968, the encounter geometry with Mars was not compatible with the requirements of the TV and S-band occultation experiments. In order to fly by the illuminated face of Mars for the TV pictures, an aiming point on the direct side of Mars had to be chosen, but this would not have permitted passage of the spacecraft through the earth occultation zone which required an aiming point on the retrograde side of Mars. Also, optimum lighting angles generally did not occur near closest approach. Finally, the later arrival dates exhibited larger trajectory error sensitivities, longer flight times, and greater communication distances at encounter.

But the question remained regarding the high-energy type II transfers with arrival dates earlier than September 1969, and launch dates earlier than late December 1968. These type II transfers did have acceptable (but by no means optimum) encounter geometries at Mars. However, there were four undesirable properties of these trajectories. First, it was felt there would not be adequate time after the FY 1967 funds became available to reliably develop, fabricate, and test the spacecraft to meet a launch as early as November or December of 1968. Second, as the trajectories would have required high C_3 values in the range of about 20 to 27 km^2/s^2, the mission would have been more sensitive to variations in launch vehicle performance and spacecraft weight. Third, the type II trajectories could only have been achieved by using the two-burn (parking orbit) powered ascent mode which was considered slightly less reliable than the direct ascent mode which was available for the type I transfer trajectories. Fourth, as these type II trajectories initially departed inside the orbit of the Earth, a third antenna would have to have been added to the spacecraft to provide the required coverage.

When considering a mixed mission (one type II launch followed about three months later by a type I launch), it was further realized that either (1) the two spacecraft would have required different designs to accommodate the different transfer and encounter geometries or (2) a more complex single design would have been necessary to afford compatibility with both transfer types.

In summary, primarily as a result of schedule concerns, it was decided to eliminate the type II transfer trajectories from further consideration. This decision was made

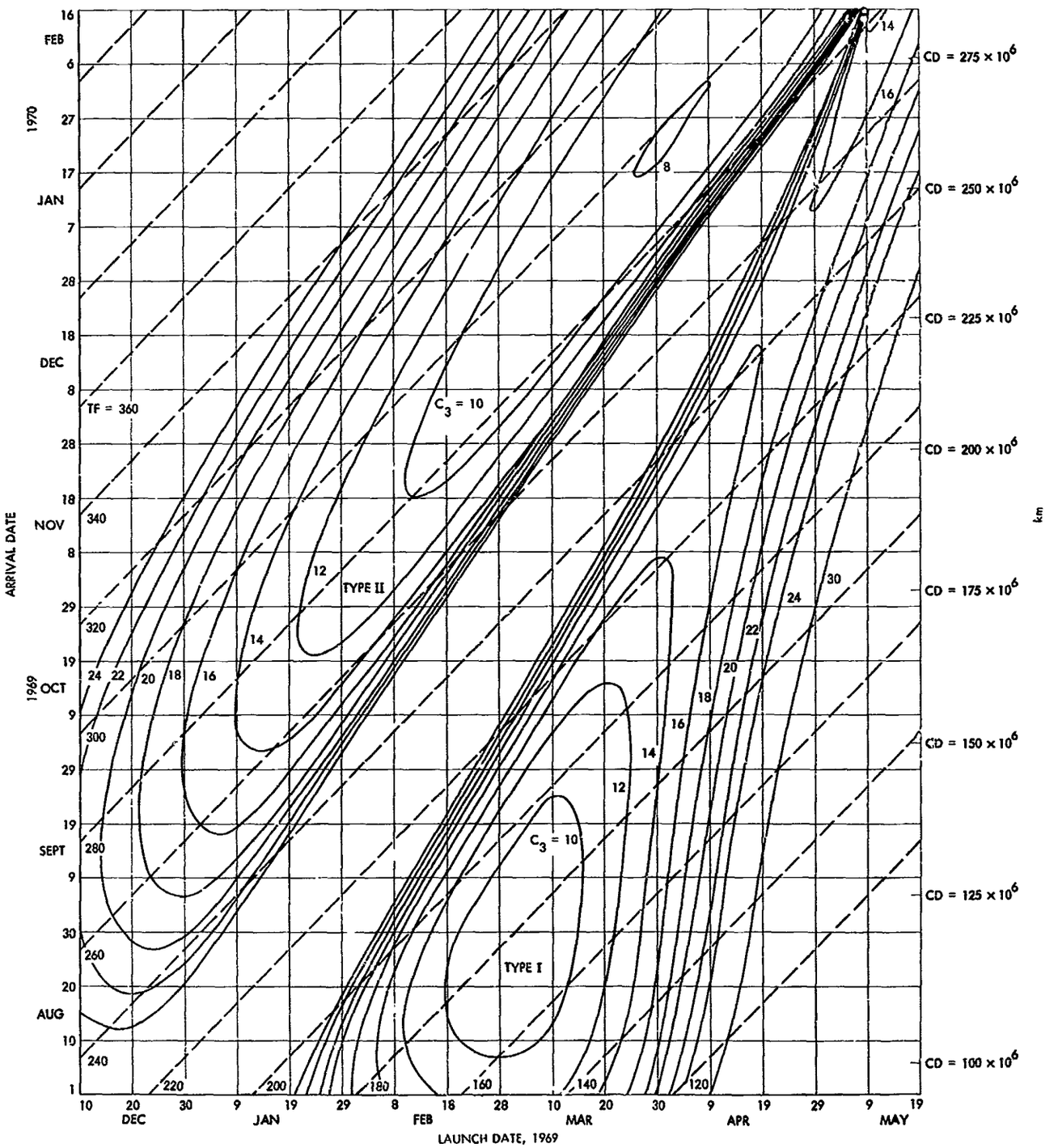


Fig. 2. *Mariner* Mars 1969 basic trajectory design chart

in April 1966. It was also known at that time that the type I transfer trajectories exhibited more favorable transfer properties and encounter geometries with Mars.

C. Trajectory Selection Criteria and Process

Referring to Fig. 2, it can be seen that a very large span of launch and arrival date possibilities still existed for type I transfer trajectories with C_3 values as large as 27 km^2/s^2. There was still the question of how the mission designer selects a preferred region interior to this large possibility space. This selection process was carried out in the following three phases:

(1) Establish gross trajectory selection boundaries.

(2) Determine preferred Martian longitudes for science viewing.

(3) Refine selection by applying other mission considerations.

1. Selection analysis. The gross boundaries for the trajectory selection space are shown in Fig. 3 and will now be discussed. The right-hand, or closing-launch-date, boundary is established by the maximum value of C_3 which the *Atlas/Centaur* launch vehicle can achieve for an 850-lb separated spacecraft weight. The left-hand, or opening-launch-date, boundary is established by two considerations, both of which are related to obtaining acceptable communications between the Earth and the spacecraft. The more important of these two considerations is related to the geometrical fact that, when DLA (the declination of the departure geocentric hyperbolic asymptote, Φ_s; see Fig. 4) is more negative than about −43 deg, the spacecraft will pass, during the first several days after injection, too near or below the ground masks of the northern hemisphere deep space tracking stations at Goldstone, California, and Madrid, Spain.

The other, but lesser, communications consideration is associated with the location of antennas on the spacecraft. The spacecraft has two fixed (not movable) antennas. The low-gain antenna provides only slightly more than a hemispherical coverage pattern on the solar-cell side of the spacecraft, and is used to communicate with the Earth during the early and middle portions of the flight to Mars. The high-gain antenna, which has a much narrower beam width, is used to communicate with the Earth during the approximate period from one month prior to encounter with Mars until two months after encounter. The science data is played back to the Earth

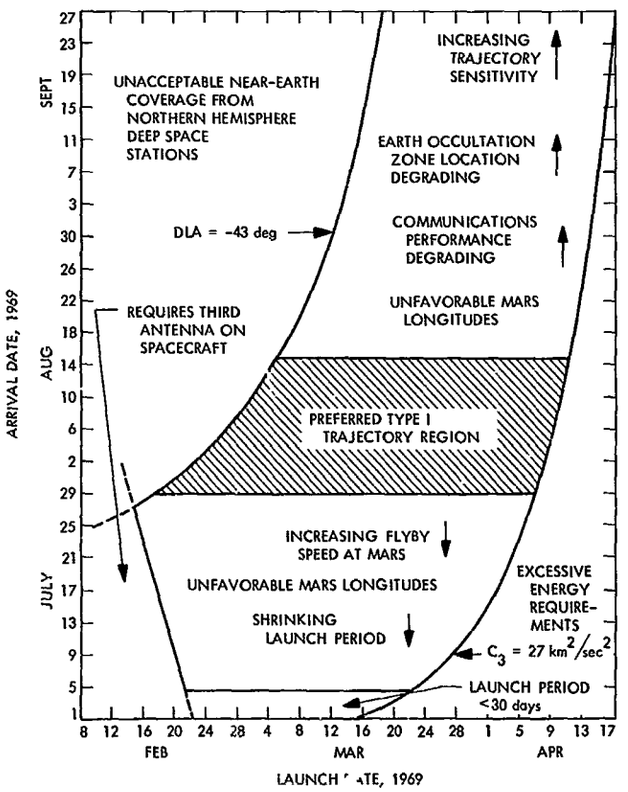


Fig. 3. Type I trajectory selection space

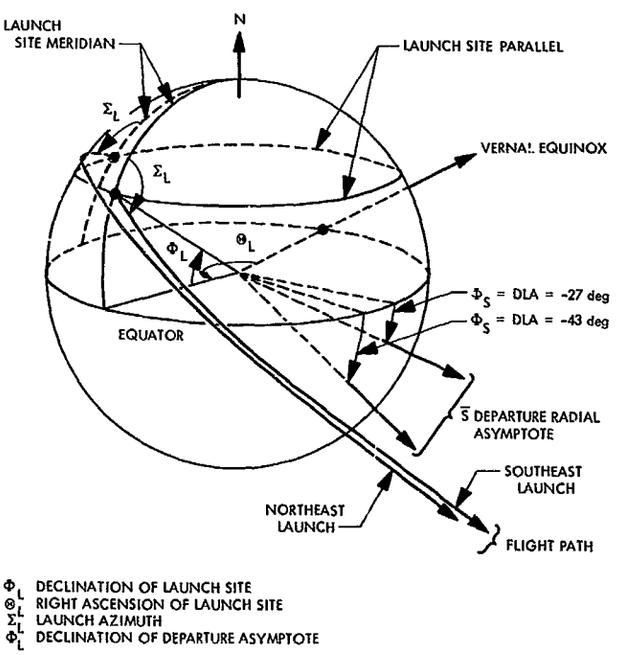


Fig. 4. Departure launch geometry

over the high-gain antenna. The ability to use a fixed high-gain antenna results from the fact that the direction to the Earth, in a spacecraft-fixed coordinate system, changes by only 5 to 10 deg over a period of a few weeks near encounter.

Returning now to Fig. 3, the words "requires third antenna on spacecraft" appear to the left of one of the boundary contours. In this region of the trajectory space, the trajectory initially departs inside of the orbit of the Earth around the Sun. This causes the Earth to lie on the dark side of the spacecraft and at extremely weak signal points within the low-gain antenna pattern. Thus, for trajectories in this region, it would be necessary to add a third antenna to the spacecraft to provide coverage when the Earth is not within the beam widths of the low-gain and high-gain antennas.

The earliest arrival date boundary of about July 4, 1969, was established by the requirement for at least a 30-day duration launch period. No firmly established latest arrival date boundary was shown in Fig. 3; however, it was estimated to occur (for reasons which will be covered later) in the last half of September 1969.

2. Mars longitude, arrival date, and science viewing. Having established the gross trajectory selection region boundaries by the above considerations, it was appropriate to determine what scientific preferences existed for selecting arrival dates within the broad span from early July to mid-September 1969. When questioned on this matter, the scientific investigators expressed a preference to view that face of Mars containing those longitudes within about ± 90 deg from the Mars prime meridian (which passes through Meridiani Sinus). However, this desire, by itself, did not constrain the selection of arrival date until it was combined with the desire to arrive at a specific time during an Earth day. This latter condition was imposed by the following three considerations:

(1) The strong desire to use the 210-ft antenna (DSS 14) at Goldstone, California, to enhance the mission return.

(2) The desire to have an adequate amount of time before encounter to take corrective action, if necessary, using the 100-kW transmitter at Goldstone.

(3) The desire to perform the S-band occultation experiment over the Deep Space Stations at both Goldstone and Woomera, Australia.

An analysis of the above three criteria resulted in a preferred arrival time (closest approach) of approximately 2 h after Mars crossed the zenith meridian at the Goldstone station. Some variation was allowed in this time and will be discussed later.

Next, preferred arrival date regions were established based upon the criteria that the spacecraft would cross the Mars prime meridian at a time when the subspacecraft point would be 30 deg (favorable scene illumination) from the terminator, and the assumption that the areocentric closest approach would be at 2 h past Goldstone zenith. The resulting arrival date periods were in the vicinities of June 27, August 1, and September 5. As a result of the slightly different rotational rates of Earth and Mars, the sub-spacecraft traces would move 9.2 deg to Mars' east (in this discussion Mars longitude is measured positive to Mars' east, which is in the direction of Mars' rotation about its spin axis) for each day of delay in the arrival date. Thus, in order to obtain a favorable view of any longitude within the ± 90-deg band, it may be necessary to adjust the arrival date by up to ± 10 days about each of the three reference dates noted above. An additional adjustment of 1 to 5 days may also be necessary to accommodate differences in the near-Mars aiming point and in the instrument pointing directions.

The late-June arrival period was eliminated from further consideration as a result of the limited launch period duration and the extremely high flyby velocities at Mars. However, the alternatives remained regarding the two preferred arrival periods of early August and early September: (1) send both spacecraft to the early-August arrival period, (2) send both spacecraft to the early-September arrival period, or (3) send one spacecraft to each arrival period. The last of these alternatives was considered for reasons of attempting to observe seasonal changes on Mars by having the two spacecraft arrivals separated by 35 days. However, this alternative was eventually dropped for the following reasons:

(1) Studies indicated that it would be difficult to reproduce a sufficiently identical viewing geometry for the two arrivals to ensure the observation of a seasonal change in the surface feature characteristics.

(2) There was a strong desire to view both the region near the edge of the southern polar cap and the region near the equator containing the greater number of dark and light surface feature variations.

(3) Additional complexity would have been incurred in trying to achieve identical spacecraft designs which would still accommodate the larger geometry variations associated with widely separated arrival dates.

It was thus decided to send both spacecraft to either the early-August arrival period or the early-September arrival period and, also, to select different aiming points at Mars for the two flyby passes. The early-August arrival period was selected for reasons summarized in the next phase of the trajectory selection process.

3. ***Refining the selection.*** Referring to Fig. 3 it can be seen that several trajectory properties would begin to degrade for arrival dates after late August of 1969. The Earth-Mars communication distance would be increasing at a rate of about 900,000 km per day of delay in arrival date. For September and later arrivals, the location of the Earth occultation aiming zone would move into a region that would be less compatible with the range of flyby geometries desired by the TV, infrared spectrometer, and infrared radiometer experiments. Finally, for September and later arrivals, trajectory sensitivities would begin to increase appreciably as a result of the increasing flight times to Mars. Thus, the decision was made to send both spacecraft to the early-August arrival period, at which time it would be spring in the southern hemisphere of Mars. As a result of a preference to view those longitudes near and to the east of the prime meridian (these longitudes included such surface features of interest as Meridiani Sinus, Hellas, Hellespontus, and Syrtis Major), an arrival period of August 1 through August 10 was initially selected. The spacecraft design was then tailored to this period. However, several months subsequent to this selection, the scientific experimenters expressed a desire for a somewhat greater flexibility in the choice of arrival dates. A study was then conducted to determine how much of an expansion in the arrival date period could be accommodated by the existing spacecraft design. As a result of this study, the arrival date period was expanded to cover the interval from July 29 through August 15, 1969. This is the preferred arrival date period that has been identified in Fig. 3. Within this period, two different arrival dates were chosen for the two spacecraft. One arrival date was selected for a near-equatorial flyby trajectory, while the other arrival date was selected for a more southerly flyby trajectory which views the regions in the vicinity of the southern polar cap edge. In order to avoid excessive loading of the mission operations activities during the critical flyby phases of the two spacecraft, a constraint was established that the two chosen arrival dates must be separated by at least 5 days.

In May 1968, the scientific experimenters expressed a preference for an arrival date of July 31 for the near-equatorial pass and August 5 for the southerly pass arrival date. It was decided to target (have *Centaur* guidance tapes prepared for) 13 launch days for each of these two preferred arrival dates. In addition, 50 other launch date/arrival date combinations were targeted over the preferred trajectory region shown in Fig. 3. Thus, should any new data indicate, at some future date, a sound reason to change the above arrival date preference, a certain amount of flexibility would exist to accommodate such a change.

4. ***Launch geometry constraints.*** The launch geometry was strongly dependent upon the launch site latitude (Φ_L) and departure asymptote declination (Φ_s). In 1969, the preferred type I trajectories exhibited highly negative values of Φ_s, ranging from -43 deg early in the launch period to -27 deg near the end of the launch period. Referring to Fig. 5, this occurs primarily as a result of:

(1) Launch occurring in the spring when the Earth's equatorial plane is about 23.5 deg above the heliocentric velocity vector of the Earth.

(2) Mars being nearly at its maximum departure south of the ecliptic plane for the desired arrival dates.

(3) The fact that, in order to rotate the resultant heliocentric velocity vector of the spacecraft through, say, 2 deg, the hyperbolic excess velocity vector leaving the Earth must be inclined some 20 deg to the ecliptic plane.

Whenever $|\Phi_s| > |\Phi_L|$, utilization of a band of launch azimuths symmetric about 90 deg east of north would not allow the trajectory plane to contain the departure asymptote, unless a plane-change maneuver would be used to increase the inclination of the trajectory plane. The amount of this geometrical restriction on launch azimuth for planar trajectories is shown in Fig. 6. For Φ_s as negative as -43 deg, planar trajectory launch azimuths between 54 and 126 deg could not be used. For launch azimuths north of 54 deg, parking-orbit (two-burn) ascent trajectories would have to be used to satisfy the larger travel angles between the launch site and the departure asymptote. Whereas for launch azimuths south of 126 deg, the direct-ascent (one-burn) mode can be utilized because of the smaller angles between the launch site and departure asymptote (see Fig. 4).

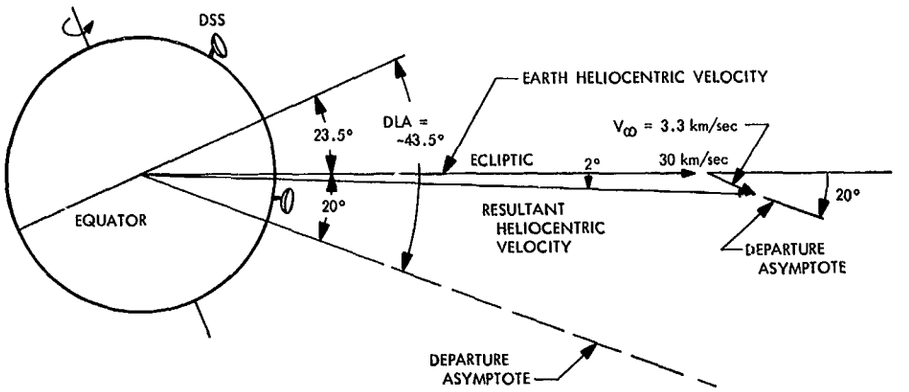


Fig. 5. Large negative departure asymptote declination

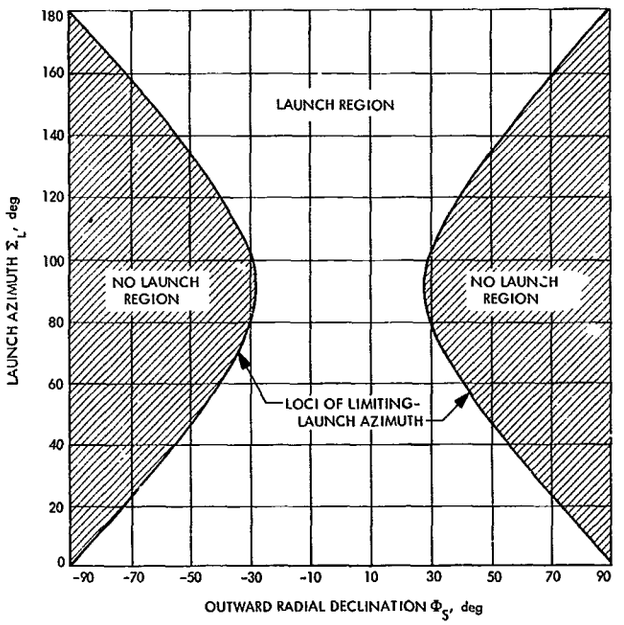


Fig. 6. Launch azimuth restrictions vs departure asymptote declination for planar launch trajectories

In order to launch the spacecraft from Cape Kennedy, either (1) a launch azimuth had to be used that would allow the spacecraft to travel in a plane containing both the launch site (at launch) and the departure asymptote, or (2) a dog-leg plane-change maneuver would have to be utilized. Since the asymptote was approximately fixed in inertial space and the launch site was rotating, it was necessary for either the launch azimuth or the dog-leg maneuver size to be varied continuously through the launch window (Ref. 3). Also, as the Earth rotated during the launch window, the angle between the launch site and the departure asymptote would vary. This would have to be compensated for by either varying the parking-orbit length, in the case of a two-burn launch, or by varying the pitch profile, for a one-burn launch. In the latter case, as the total burn arc was nearly constant (about 30 deg central angle), the spacecraft would be injected at different true anomalies (i.e., at different radial angles from perigee) along the departure hyperbola. Maximum performance capability for a direct-ascent launch would be realized when injection occurred at a positive true anomaly of about 5 deg. The launch window length available for a direct-ascent launch was usually limited by performance reductions associated with injecting too far from the optimum true anomaly or, in some cases, by launch azimuth restrictions.

In October 1966, it was decided to choose the southeast direct-ascent launch mode over the northeast two-burn launch mode. The reasons for this decision were primarily the increased launch vehicle reliability and the improved near-Earth tracking coverage. Also, ample launch window durations were available as a result of the excess launch vehicle performance associated with launching a relatively light spacecraft. Although, as a result of AFETR range safety restrictions on launch azimuth, permission was not granted to use the large southeast planar trajectory launch azimuths. In fact, Range Safety requested that the *Mariner* Mars 1969 project not use launch azimuths south of 108 deg east of north, even though prior missions had obtained waivers to go to 115 deg, if required. The key word here is "required," and, inasmuch as adequate launch period and launch window durations were still available, the *Mariner* Mars 1969 project accepted the 108-deg launch azimuth restriction. By not launching south of 108 deg, the Bahama Island range safety destruct line would not be threatened.

As a result of the above launch azimuth restriction, dog-leg (plane change) ascent trajectories utilizing yaw-right maneuvers had to be flown during much of the launch period in order to achieve the large inclinations of the final geocentric trajectory plane. Use of a dog-leg maneuver to increase flight plane inclination is shown in Fig. 7. In designing the powered-flight trajectories, the launch vehicle system contractor planed to utilize the following three categories of powered ascent:

(1) Category I trajectories are planar profiles used when launch azimuths of 108 deg or less are required.

(2) When the planar azimuth heading necessary to reach a particular inclination is greater than 108 deg and less than or equal to 115 deg, a category II trajectory is utilized. This type of trajectory initiates flight with a 108-deg launch azimuth and yaws shortly after booster engine cutoff (BECO + 8 s) to the desired azimuth heading.

(3) If the desired inclination requires a planar azimuth heading in excess of 115 deg, a category III trajectory is used. Category III trajectories begin with 108-deg launch azimuth, an intermediate yaw is made to a 115-deg parallel azimuth heading initiated at BECO + 8 s, and then a final yaw maneuver starting shortly after *Centaur* main engine start (MES + 4 s) aligns the vehicle with the desired final heading.

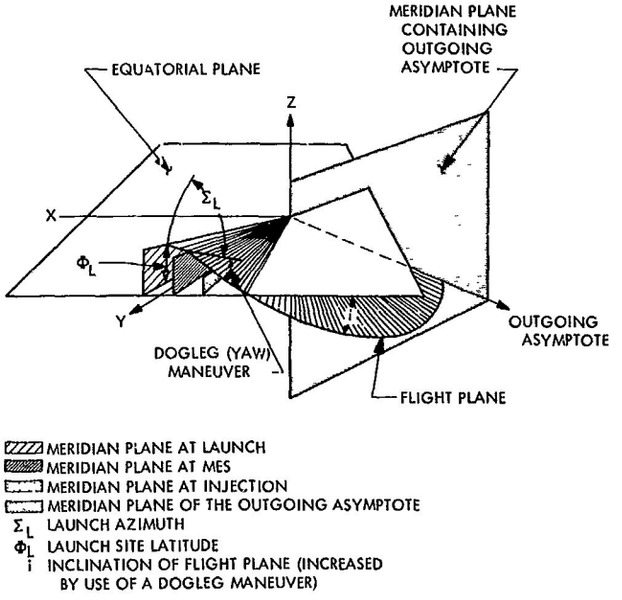


Fig. 7. Dog-leg maneuver to increase inclination

Use of the category III trajectories does not threaten the Leeward Island destruct line. The amount of vehicle yaw for the category II and III trajectories is referred to as yaw index, which is related to the inclination of the geocentric hyperbola as shown in Fig. 8. Yaw index equals the yaw rates multiplied by the yaw times, and is thus approximately equal to the total yaw angles turned during the powered flight. Category II trajectories have yaw indices ranging from zero to 9.25, where a yaw index of 9.25 corresponds to an equivalent parallel azimuth heading of 115 deg. Category III trajectories execute an intermediate yaw (index of 9.25) at BECO +8 s, and perform the remaining yaw maneuver at MES +4 s. In order to provide ample clearance of the Leeward Island destruct line, a maximum category III yaw index of 25 was established for the *Mariner* Mars 1969 launches.

Figure 9 illustrates the ground tracks associated with the three powered-flight categories. As progress is made through both the launch period and the daily launch windows (a decision had been made to limit the daily launch windows to a maximum of one hour), different regions as depicted in Fig. 9 are utilized. For a late-February launch, a yaw index of about 22 would typically

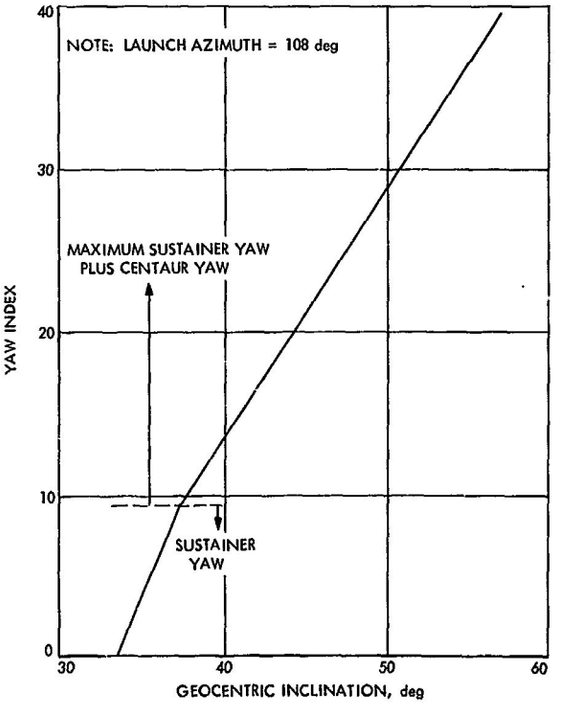


Fig. 8. Yaw index defined

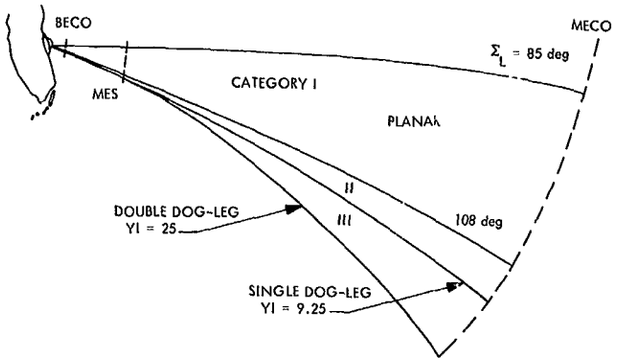


Fig. 9. Powered trajectory categories

be flown at window open, and yaw index would slowly diminish as time advanced through the window such that, by window close, the yaw index would be about 16. For a late-March launch, window open would typically exhibit a planar launch azimuth of about 103 deg, increasing slowly to 104 deg by window close.

Figure 10 depicts the altitude-vs-ground range behavior for different values of injection flight path angle.

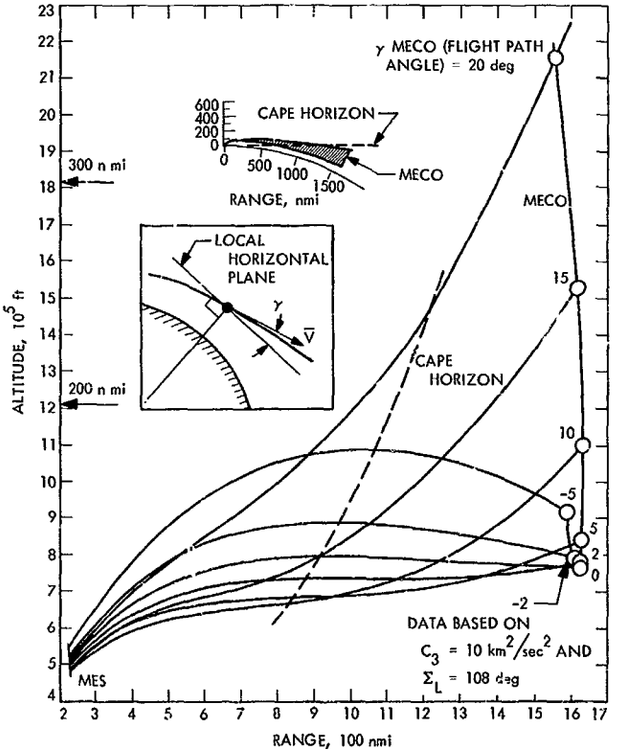
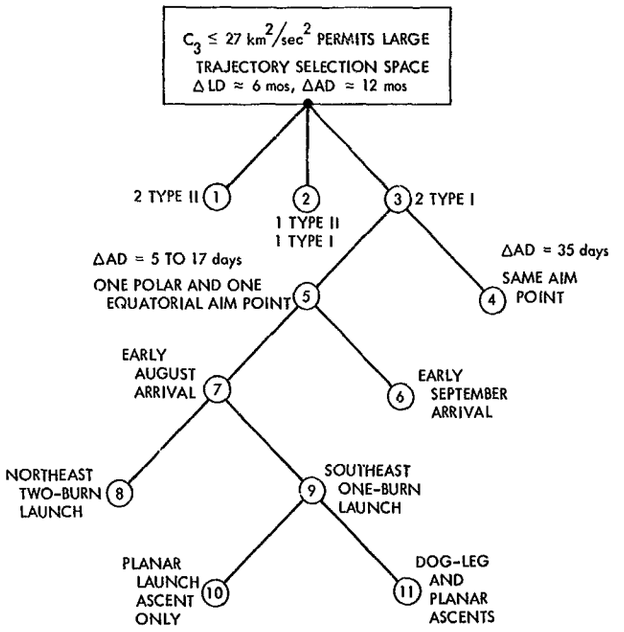


Fig. 10. Powered ascent altitude profiles

Typical values of injection flight path angle lie between 10 and 16 deg for the early-launched, yawed trajectories. For the late-launched, planar trajectories, this range is shifted towards slightly smaller values of path angle. The high *Mariner* Mars 1969 injection altitudes not only satisfied spacecraft aerodynamic heating limitations, but also improved the tracking and telemetry coverage from the ground stations. More detailed information on the design of the *Mariner* Mars 1969 powered-flight trajectories may be found in Ref. 4.

5. Trajectory selection summary. A wide variety of mission and trajectory design tradeoffs have been discussed above. The associated decision-making process is summarized in Fig. 11.



(1) SCHEDULE TIGHT (LESS FAVORABLE GEOMETRY)

(2) SCHEDULE TIGHT (MORE COMPLEX SPACECRAFT DESIGN)

(3) FAVORABLE SCHEDULE AND GEOMETRY

(4) LOW CHANCE OF OBSERVING SEASONAL CHANGES (ADDED COMPLEXITY IN SPACECRAFT DESIGN)

(5) OBSERVE EACH OF THE DIFFERENT SURFACE FEATURE TYPES (SIMPLER SPACECRAFT)

(6) GEOMETRY AND COMMUNICATIONS PERFORMANCE DEGRADING

(7) MAXIMUM LAUNCH PERIOD. BEST BALANCE BETWEEN MANY TRADEOFFS

(8) SLIGHT DEGRADATION IN NEAR-EARTH TRACKING COVERAGE AND ASCENT RELIABILITY

(9) IMPROVEMENT IN ITEM (8) AND AMPLE LAUNCH PERIOD

(10) VIOLATES AFETR RANGE SAFETY FOR EARLY LAUNCH DATES

(11) SATISFIES RANGE SAFETY AND LAUNCH PERIOD DURATION STILL ACCEPTABLE

Fig. 11. Trajectory selection decision process

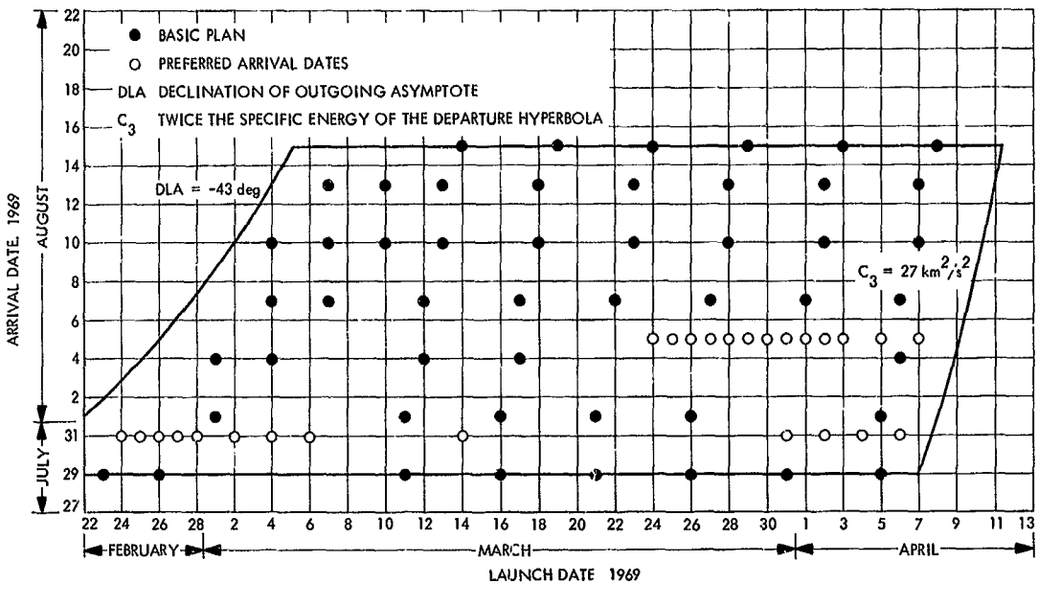


Fig. 12. Launch/arrival targeting plan

6. Launch date/arrival date plan. In order to give the principal investigators adequate flexibility to make use of new information gained from Earth-based observations of Mars, several launch date/arrival date combinations were targeted (i.e., launch guidance tapes were prepared) over the preferred Type-I trajectory space. These points are shown in Fig. 12. Preferred arrival dates of July 31 and August 5 were selected for the equatorial and southerly aiming points, respectively. It was planned that the first launch occur as early as possible, between about February 24 and March 6, and go for the earlier arrival date; whereas, the second launch should occur as late as reasonable, between about March 24 and April 7, and should go for the later arrival date. Other desired conditions were that the second launch not occur earlier than 10 days after the first maneuver of *Mariner VI*, that the second maneuver (if required) for *Mariner VI* not occur earlier than 10 days after the first maneuver for *Mariner VII*, that closest approach of each spacecraft occur at 1 hour 55 minutes (±40 minutes) after zenith at DSS 14, and that key spacecraft activities be separated in time to minimize excessive loading of the MOS facilities.

III. Aiming Point Selection

A. Aiming Plane Defined

The near-Mars aiming point is specified by either (B, θ) or by ($\mathbf{B}\cdot\mathbf{R}$, $\mathbf{B}\cdot\mathbf{T}$) shown in Fig. 13. The aiming vector **B**, customarily referred to as the impact parameter* vector, lies in the areocentric trajectory plane and goes from the center of the target to the approach asymptote. The magnitude of **B** is a measure of how much the spacecraft would miss the center of a massless planet. The approach asymptote direction, indicated by the unit vector **S**, is in the same direction as the vector difference between the spacecraft heliocentric velocity and the target (Mars) heliocentric velocity, at the time when the spacecraft is entering the gravitational sphere of influence of the target planet. The unit vector **T** is normal to **S** and parallel to the ecliptic plane. The unit vector **R** lies in the southern celestial hemisphere and completes the right-handed coordinate system. As may be seen in Fig. 13, it is possible to map various flyby conditions into contours in the aiming (**R**, **T**) plane. For example, all aiming points selected within the Earth occultation zone will have the property that the spacecraft will fly through the Earth occultation cone, which is the region within which the Earth will not be in view of the spacecraft.

Finally, the ($\mathbf{B}\cdot\mathbf{R}$, $\mathbf{B}\cdot\mathbf{T}$) aiming coordinates also facilitate guidance studies and calculations, as these particular coordinates vary in a more nearly linear manner in the presence of prior orbit perturbations than do such aiming coordinates as, for example, periapsis distance and orbital inclination.

*Originally used in Rutherford scattering experiments in physics.

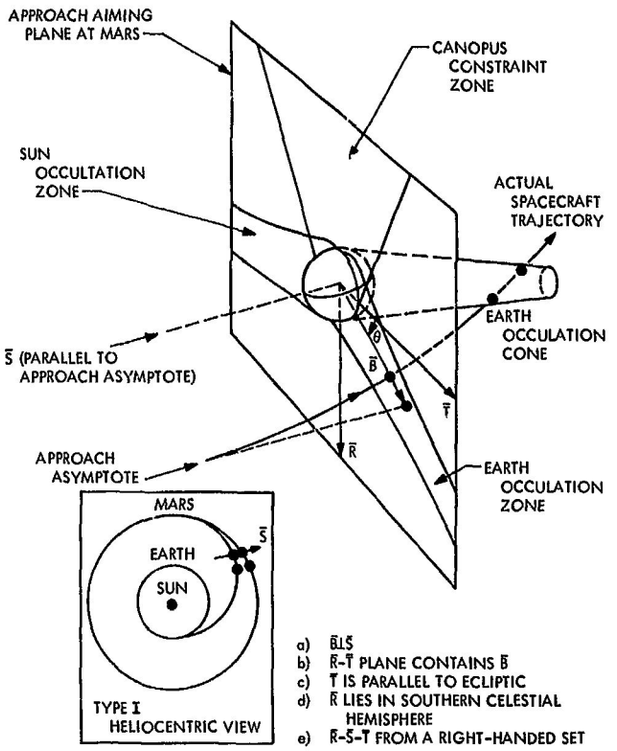


Fig. 13. Definition of aiming plane

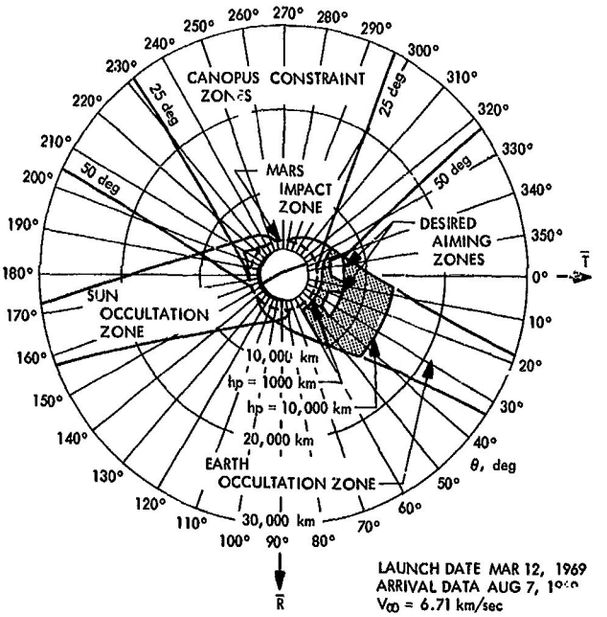


Fig. 14. *Mariner* aiming zones

Gross aiming point boundaries for the *Mariner* Mars 1969 mission were established as follows:

(1) The flyby periapsis altitude shall not be closer than 1000 km nor further than 10,000 km from the Mars surface.

(2) The aiming point shall be in the Earth occultation aiming zone in order to permit conduct of the S-band occultation experiment.

(3) The Canopus stray-light constraint shall not be violated (in order to prevent possible loss of Canopus lock when passing over or near the bright side of Mars).

(4) In order to prevent excessive dispersal over the southern polar cap, $\theta \leq 60$ deg.

The shaded region shown in Fig. 14 is contained within the aiming point boundaries, defined above. Within the shaded region, two clear aiming zones are shown. These smaller aiming zones represent the preferred aiming regions for the polar-cap and near-equatorial flyby trajectories. Each of these preferred aiming zones was initially centered at a periapsis altitude of approximately 3000 km (*Mariner* IV flew by at 9850 km from the surface). Subsequent to this early aiming point selection, the nominal *Mariner* VI periapsis altitude was raised to 3200 km, and the *Mariner* VII altitude raised to 3100 km.

B. Rationale for Selection of Different Aiming Points

It was rationalized that by the use of different aiming points for the two spacecraft, it would be possible to obtain scientific data from each of the different characteristic surface feature types. These different types would include the light and dark surface features (located mainly in the central latitudes), the southern polar cap, the thaw regions near the cap edge, and features that may be affected by the "wave of darkening." Selection of a southerly aiming point ($20° < \theta < 35°$) would permit coverage of the last three of the above feature types, while selection of a more equatorial aiming point ($-10° < \theta < 0°$) would permit good coverage of the many light and dark surface feature variations near the equator.

In addition to viewing the cap edge and thaw regions, the southerly aiming point would also permit viewing of Hellespontus and Hellas. Hellespontus is potentially interesting as it has historically darkened just after the polar cap has begun to recede. Hellas was also of interest as it seems to possess certain similarities to the polar cap. The scientific experiments were

designed and coordinated to yield maximum value return for the two preferred aiming zones shown in Fig. 14.

C. Flight Path Control

As the launch vehicle guidance was not of sufficient accuracy to ensure that the spacecraft would pass through the desired aiming region shown in Fig. 14, the spacecraft was designed with the capability of performing a maximum of two inflight trajectory correction maneuvers, if necessary, to pass through the desired region. Through the use of precision Earth-based radio tracking data, the orbit of the spacecraft was estimated. If a sufficient departure from the desired flight path was determined to exist, commands were to be calculated and transmitted to the spacecraft to execute a corrective maneuver. The spacecraft was to accomplish this correction by first making gyro-controlled precision turns from its Sun-Canopus reference cruise attitude, followed by the hot firing of its 50-lb thrust, liquid monopropellant (anhydrous hydrazine), rocket motor to provide the necessary velocity increment.

This corrective maneuver capability was required in order to ensure an acceptable pre-launch probability of achieving a satisfactory encounter. The likelihood of achieving such an encounter at injection is essentially zero for two reasons. First, because of normally occurring in-tolerance injection errors, the resulting dispersions at encounter are much larger than the acceptable encounter region. Second, in order to satisfy the planetary quarantine constraint, it was necessary to target the spacecraft approximately 20,000 km from the nominal desired final aiming point at injection. Similarly, although it was not anticipated that the first maneuver aiming point would have to be biased to satisfy the planetary quarantine constraint, in-tolerance execution errors associated with this maneuver were sufficiently large to lead to a reasonable probability of requiring a second maneuver. Although the *Atlas-Centaur* is the most accurate launch vehicle used to date, and could have satisfied the requirements of some previous interplanetary missions with no maneuvers, the stringent accuracy requirements placed on the *Mariner* Mars 1969 mission required the capability of executing two maneuvers for each spacecraft.

A considerable amount of effort went into pre-mission maneuver strategy studies in order to maximize the probability of executing successful maneuvers, and to prepare operations personnel for various contingency plans. An important part of maneuver strategy is the injection targeting procedure. The process of injection targeting includes selecting the spacecraft separation direction, the *Centaur* deflection direction, and aiming points for pre- and post-separation and post-deflection. Some of the considerations that go into selecting these values are as follows:

(1) Spacecraft separation direction.

- (a) Send the spacecraft toward the planet and the launch vehicle away from the planet.
- (b) Point the low-gain antenna toward the lower hemisphere (containing the Earth) for rapid acquisition of signal.
- (c) Orient to acquire the Sun before entering the shadow of the Earth.
- (d) Avoid pointing sensitive instruments toward the Sun.

(2) Launch vehicle deflection direction.

- (a) Minimize probability of the launch vehicle impacting the planet.
- (b) Insure that the launch vehicle is deflected in a manner so that it will not collide with the separated spacecraft.
- (c) Insure that deflection exhaust gases do not impinge on the spacecraft.
- (d) Insure that the launch vehicle does not come within the field-of-view of the spacecraft Canopus sensor.

(3) Aiming point selection (at injection).

- (a) Minimize the velocity increment required to remove injection bias.
- (b) Bias arrival time to be consistent with (a) above.
- (c) Insure that a nominal maneuver violates no constraints on the maneuver sequence.
- (d) Attempt to aim so that the midcourse maneuver will be in a direction which will cause maximum maneuver execution errors to map parallel to the limb of the planet.

During operations, the final midcourse aiming points were selected by the principal investigators as a function of orbit determination and expected maneuver execution errors so as to maximize the value of the

scientific experiments and minimize the likelihood of needing a second maneuver.

A number of constraints exist which must be taken into consideration when calculating midcourse maneuvers. These constraints appear as limitations on the turns that can be made, the time the maneuver is to be performed, and the possible aiming points that can be selected.

A list of the major considerations affecting the design of the *Mariner VI* and *Mariner VII* maneuvers follows:

(1) Due to the CC&S design, turns had to be equal to or greater than 0.18 deg, and not larger than approximately 360 deg, and the minimum motor burn time had to be 0.05 s with the maximum burn time no greater than 102.35 s.

(2) The maneuver had to be performed so the Earth range and cone angle would allow telecommunications throughout the maneuver. (This constraint was a very important consideration for these missions, and was a factor in deciding to perform the first midcourse maneuver on *Mariner VI* quite soon after launch.)

(3) A firm constraint in designing any maneuver is that enough tracking data have been obtained and processed to give an orbit estimate that will not improve appreciably by taking more data.

(4) The star acquired by the Canopus tracker had to be known prior to the maneuver computations.

(5) The total velocity correction capability for either spacecraft was about 56 m/s.

(6) In order to avoid damage to the ultraviolet spectrometer, the infrared spectrometer and the TV-B camera, it was necessary that the pitch turn lie within the range of −79.5 deg to +180 deg. (The 180-deg constraint was necessary to prevent damage to the instruments during reacquisition.)

(7) It was a desirable constraint for reliability reasons that the Sun not pass through the Canopus sensor field-of-view, which would activate the Canopus sensor sun shutter.

(8) It was desirable, if convenient, to limit the pitch turn to lie in the range ±67 deg. (This was to prevent the power system from using the battery during the maneuver.)

(9) Due to the geometrical configuration of the spacecraft, an inaccessible cone exists about the plus and minus pitch axes within which the thrust axis cannot be pointed. (The half angle of this cone was 1.085 deg for *Mariner VI* and 1.2625 deg for *Mariner VII*.)

Studies at JPL, by R. T. Mitchell and S. K. Wong, have indicated that, with a single midcourse correction, the *a priori* probability of passing through the small interior wedge-shaped region shown in Fig. 14 is 75% or better. If a second corrective maneuver is performed, the *a priori* probability is increased to 99% or better.

Figure 15 illustrates the relative sizes of various aiming zones which have been selected for prior flyby missions to Mars and Venus. As the orbit determination and midcourse guidance technologies developed, it became feasible to accept tighter aiming regions at the planets to enhance the value of the planetary science data returned.

To ensure an acceptably high probability of being able to deliver the spacecraft to the small aiming zone windows shown in Fig. 14, requirements had to be placed on the orbit determination estimation errors and spacecraft maneuver execution errors. The orbit determination accuracy requirements (and design goals) are

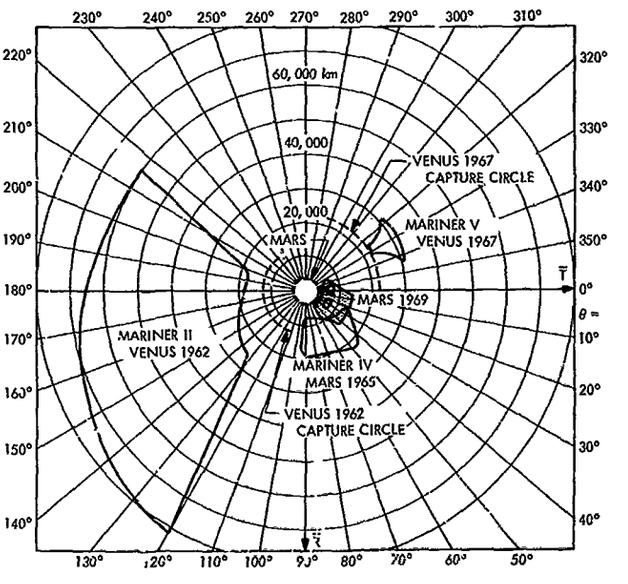


Fig. 15. Relative sizes of different mission aiming zones

Table 1. Three-sigma orbit determination requirements for *Mariner* Mars 1969

Time at which orbit estimate is calculated	Magnitude and time of prior orbit corruptions	Uncertainty[a] in magnitude of B, km	Uncertainty[a] normal to B and in R, T, plane, km	Uncertainty[a] in time of encounter min
Injection + 5 days	Spacecraft injection by *Centaur*	±1300[b] (800)[c]	±1500 (600)	±9 (4)
Injection + 30 days	Midcourse execution error of $\sigma_X^* = \sigma_Y^* = \sigma_Z^* = 0.1$ m/s at injection + 5 days	1100 (600)	1300 (600)	6 (3)
Encounter − 30 days	Midcourse execution error of $\sigma_X^* = \sigma_Y^* = \sigma_Z^* = 0.1$ m/s at injection + 5 days	800 (500)	800 (250)	6 (2)
Encounter − 6 h	Midcourse execution error of $\sigma_X^* = \sigma_Y^* = \sigma_Z^* = 0.01$ m/s at encounter − 30 days	500 (150)	390 (100)	2.0 (0.3)
Encounter + 15 days	Midcourse execution error of $\sigma_X^* = \sigma_Y^* = \sigma_Z^* = 0.01$ m/s at encounter − 30 days (IRS pressure vessel blow-down uncertain)	30 (1)	30 (1)	0.07 (0.002)

[a]Assume nominal $\mathbf{B} = 7200$ km, and $-20° \leq \theta \leq 40°$.

[b]Maximum allowable error.

[c]Numbers in parentheses are design goals.

summarized in Table 1. The requirements shown at encounter minus 6h and encounter plus 15 days are derived from science platform pointing requirements as opposed to spacecraft delivery accuracy requirements. In regard to spacecraft maneuver execution errors, the maximum allowed three-sigma error in controlling the magnitude of the maneuver velocity increment was to not exceed the larger of 0.036 m/s or 4.0% of the velocity increment magnitude. The maximum allowed three-sigma velocity error along each of two orthogonal axes normal to the velocity increment was to not exceed the larger of 0.036 m/s or 3.0% of the velocity increment magnitude. Design goal accuracies were also specified and were quite a bit smaller than these basic requirements.

Figures 16 and 17 illustrate what was believed (before launch) to be the three-sigma *a priori* dispersion ellipsis at Mars associated with one and two trajectory correction maneuvers. Figure 18 shows a more conventional representation of the equatorial flyby given in Fig. 16, as set up on a trajectory modelling device designed by C. E. Kohlhase and D. A. Tito.

IV. Planetary Quarantine

It has been agreed that the study of extraterrestrial life is a dominant scientific objective of the exploration of space. In fact, a great many individuals and scientific groups regard the search for extraterrestrial life as the primary objective of space exploration. The detection of life forms or elements of life forms on other planets would undoubtedly be considered one of the greatest discoveries of all times, since it could be a great step toward answering the many questions concerning the origin of life.

As a result of both their own concern and the recommendations of the international Committee on Space Research (COSPAR), NASA has made the following policy statement:

> Outbound automated spacecraft and planetary exploration programs shall not, within probabilities established by issuances implementing this policy, transport terrestrial life to the planets until it is determined that life does or does not exist on the planet and the character of existing life is explored, including potential hazards to earth of future returning missions.

Articles often appear in the news media concerning the question of life on Mars. In a late 1967 news article, Dr. M. K. Nadel, a biologist from Space-General Corporation, forthrightly predicted that life would be found on Mars. On the other hand, Horowitz et al. (Ref. 5) point out that the Martian environment is a very hostile one by terrestrial standards. This hostility arises from the dryness, lack of oxygen, low temperatures, and high ultraviolet

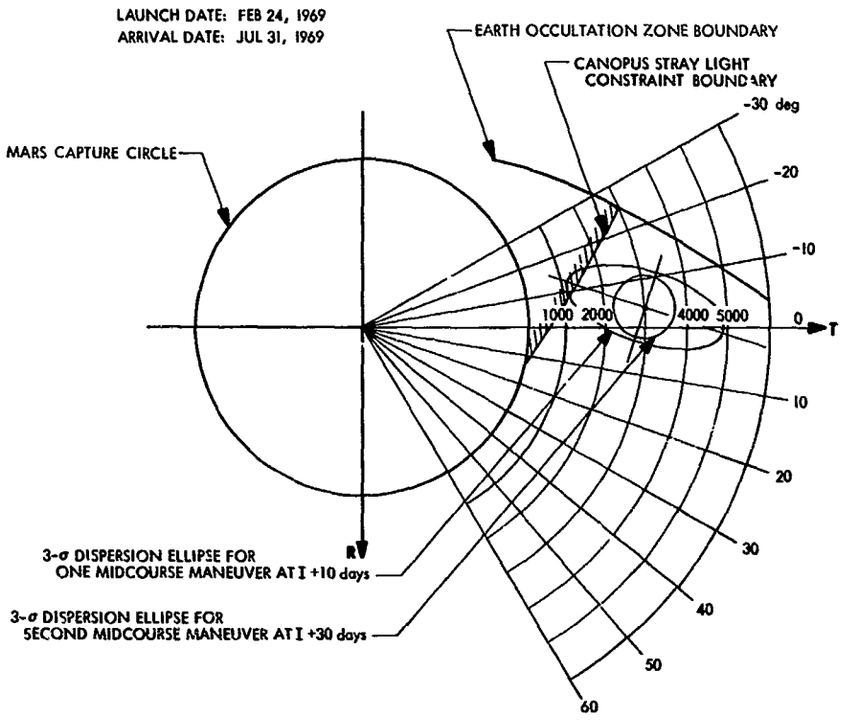


Fig. 16. Pre-launch *Mariner VI* aiming point and *a priori* maneuver dispersion ellipses

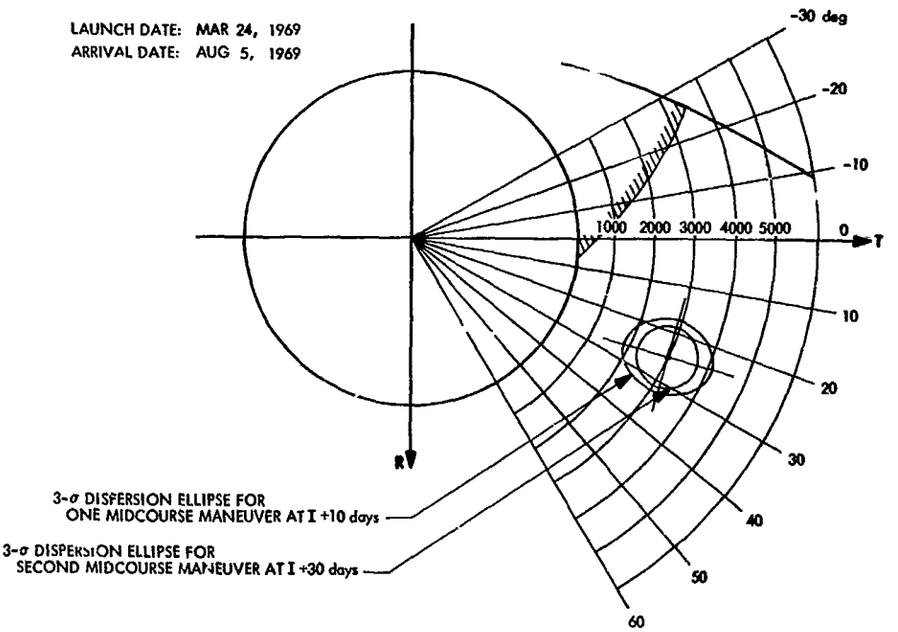


Fig. 17. Pre-launch *Mariner VII* aiming point and *a priori* maneuver dispersion ellipses

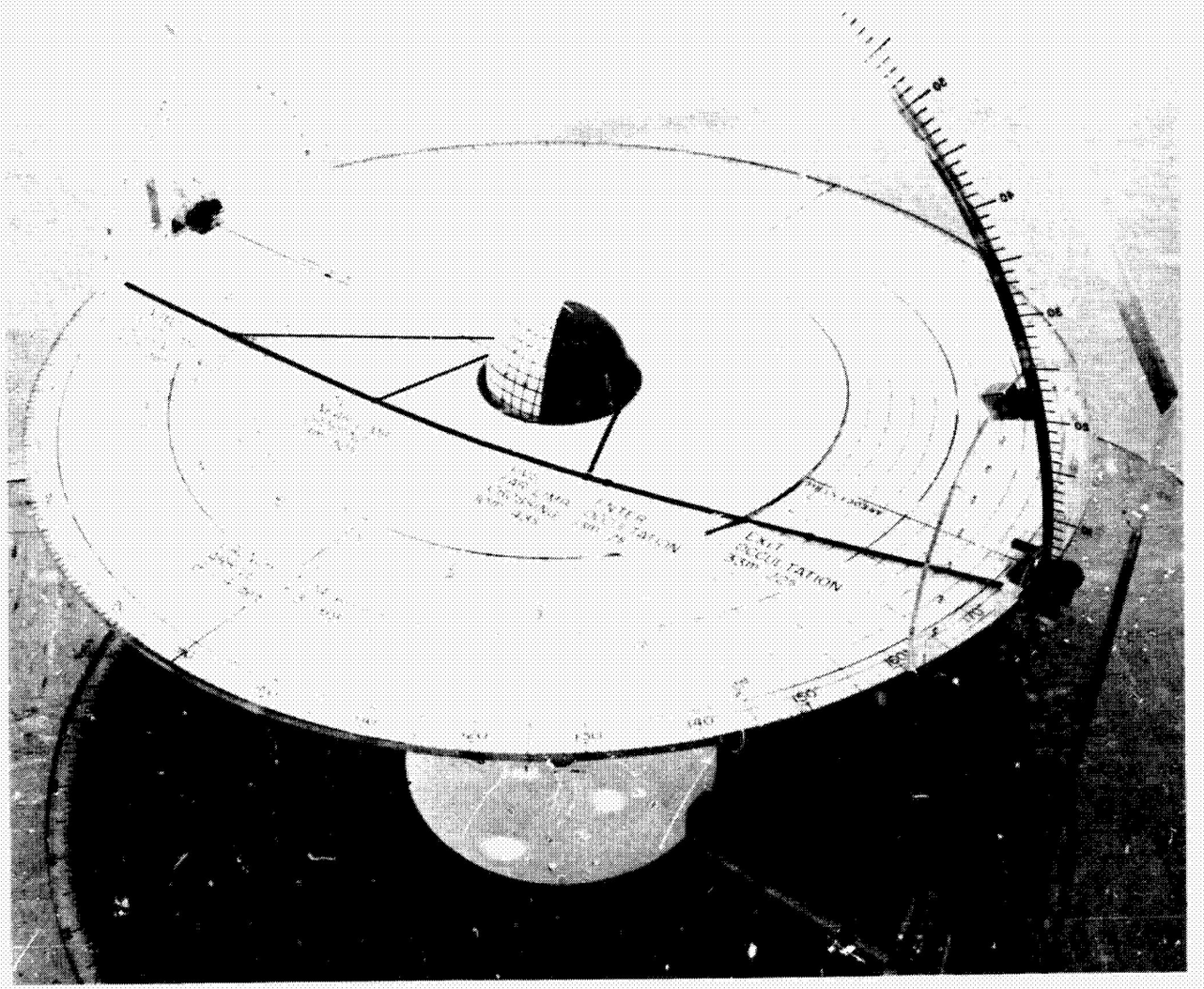


Fig. 18. Typical near-equatorial flyby trajectory

flux at the surface. This does not preclude, of course, the existence of life forms that have evolved on Mars, but it does imply that contamination of Mars from Earth-based organisms should be difficult.

It is impossible to conduct a program of interplanetary exploration without incurring some risk of biological contamination. The mere fact that an object is launched from the Earth into space implies a small chance of contamination. The magnitude of this risk is most conveniently expressed using the concepts of probability theory. Based upon a maximum acceptable probability (Ref. 6) of 10^{-3} that Mars will be contaminated prior to the successful completion of an adequate spectrum of biological experiments, the probability of Mars contamination by any single mission must be held to a very small number. For the *Mariner* Mars 1969 mission, NASA has stated that the probability that Mars will be contaminated shall not exceed 6×10^{-5}. This is simply twice the 3×10^{-5} number which NASA originally allocated for each of the two *Mariner* Mars 1969 launches. The restatement of 6×10^{-5} for the mission was made to permit the option of allocating unequal portions of the 6×10^{-5} to each launch should this be advantageous from a mission standpoint. The basis for the original 3×10^{-5} number is COSPAR resolution number 26, which was passed at the May 1964 COSPAR meeting in Florence, Italy.

It is important to define what is meant by the term "contamination." Contamination can be defined as the release and subsequent growth of one or more viable terrestrial microorganisms on the planetary surface, within the planetary subsurface, or in the planetary atmosphere. It is possible to impact Mars with either large populations of organisms (unsterilized *Centaur* stage or *Mariner* spacecraft) or very small populations (various effluxes such as attitude control gas, spalling, outgassing, propulsion system exhaust, and micrometeroid ejecta). The total allowed probability of Mars contamination by the 1969 mission is allocated between the two launches and, for each launch, among the launch vehicle, the spacecraft, and the efflux sources.

Since the launch vehicle and the *Mariner* spacecraft would not be guided perfectly, dispersions from the nominal aiming point would occur. If these dispersions were of sufficient size to cause a larger-than-acceptable probability of impact, then the nominal aiming point would have been biased further from Mars. For the *Mariner* Mars 1969 mission, it was necessary to bias the launch vehicle injection aiming point away from the desired flyby point. However, it was not necessary to bias the subsequent spacecraft maneuver aiming points. Additional information related to contamination control may be found in Ref. 7.

For each launch, the probability of contaminating Mars may be expressed in the simple equation form:

$$P_c = P_c(LV) + P_c(SC) + \sum_i P_c(SP_i) \qquad (1)$$

where $P_c(SP_i)$ is the probability that Mars is contaminated by one or more organisms from the ith small population source (or category).

In regard to possible contamination from impact of the launch vehicle or spacecraft, Fig. 19 illustrates the possible impact modes. The symbol ① stands for the first midcourse (MC) maneuver, ② for the second maneuver, and Ⓐ for an attitude control valve which might stick open and give the spacecraft an unwanted trajectory change. It can be shown that only five (encircled in Fig. 19) of the eighteen branches are non-negligible and, of these, P_{L2} and P_{S10} are probably the dominant contributors. Injection biasing and midcourse maneuver strategies were chosen to optimally satisfy the planetary quarantine constraints for the large population sources.

Referring to the right-hand side of Eq. (1), the expression for the probability of contaminating Mars with organisms ejected from a small population source is:

$$P_c(SP_i) = 1 - [1 - P_c(SP_i, j)]^{n(i)} \qquad (2)$$

where

$P_c(SP_i, j)$ is the probability of contaminating Mars with the jth organism ejected from the ith source, and $n(i)$ is the number of organisms contained in or on the ith source.

$$P_c(SP_i, j) = \sum_k P_c(SP_i, j, k) \qquad (3)$$

where

$P_c(SP_i, j, k)$ is the probability that the jth organism will be expelled from the ith source on the kth day and that it will subsequently contaminate Mars.

$$P_c(SP_i, j, k) = P_{E_i} P_{SE_i} P_{T_{i,k}} P_{SS} P_{SA} P_R P_{SD} P_{BC} P_G \qquad (4)$$

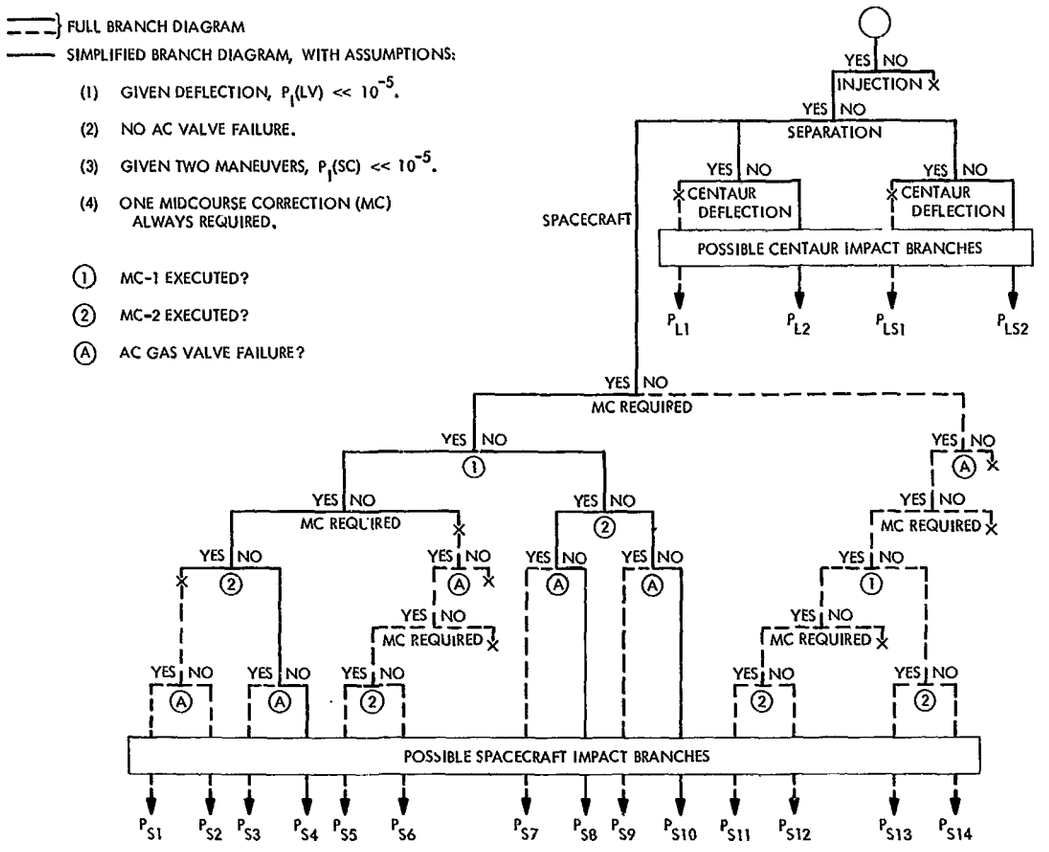


Fig. 19. Full branch diagram of probability of *Centaur* and/or spacecraft impact

where

P_{E_i} is the probability that the jth organism is ejected from the ith source on the kth day.

P_{sE_i} is the probability that the organism survives the ejection process.

$P_{T_{i,k}}$ is the probability that the organism is ejected on a trajectory that results in subsequent impact with Mars.

P_{SS} is the probability that the organism survives in the space environment until it reaches Mars.

$P_{S,1}$ is the probability that the organism survives the atmospheric entry heating.

P_R is the probability that it is released into the atmosphere or onto the surface of Mars.

P_{SD} is the probability that the organism survives dispersal on the planet.

P_{BC} is the probability that it is released in a region that provides a favorable biological climate.

P_G is the probability that it grows and replicates in the Martian environment.

Launch vehicle and spacecraft ejecta are classified as "small population" sources. They are placed in this category because of the relatively small number of organisms that are expelled at any time. The small population sources that have been identified are:

(1) *Centaur* attitude control engine exhaust products.

(2) *Centaur* vernier engine exhaust products.

(3) *Centaur* main engine blowdown products.

(4) Material outgassed from the *Centaur*.

(5) *Centaur* surface material; e.g., material dislodged directly or spalled as a result of micrometeoroid impacts.

(6) Material outgassed from the spacecraft.

(7) Spacecraft midcourse motor exhaust products.

(8) Spacecraft surface material.

(9) Spacecraft attitude control gas.

(10) Infrared spectrometer coolant gases.

Using the most conservative (pessimistic) assumptions, only sources (5), (8), and (9) proved non-negligible. Their worst-case *a priori* probabilities of contamination were estimated at approximately 5×10^{-8}, 2×10^{-6}, and 1×10^{-6}, respectively. It was through these calculations and certain other considerations that the following P_c allocation between the large and small population sources was selected. On a per launch basis, 2.4×10^{-5} was allocated to the large population sources, and 0.6×10^{-5} was allocated to the small population sources.

V. Mission Requirements and Desires

For a mission consisting of several scientific experiments, each experiment may be considered to have a set of basic requirements and also a set of desires. The set of basic requirements defines those items that must be satisfied for an experiment to be performed and the resulting data be interpretable. Such items as power levels, optical alignment accuracies, thermal control requirements, data rates, etc., fall into this category of requirements. The second category consists of those items that determine and affect such things as the scope of the experiment, the attainment of specific primary and secondary objectives, and the applicability and generalization of the results obtained to other situations. Certain requirements of this class are mandatory for the accomplishment of specific objectives; others may be expressed as being desirable in various degrees. Thus, the following sets of scientific requirements and engineering constraints (Table 2) may be thought of as competing characteristics, from which the tradeoffs

Table 2. Scientific requirements and engineering constraints

Experiment	Experiment requirements	Engineering constraints
Visual imaging	(1) Location of the centers of several pictures must be below the edge of the polar cap for the polar scan trace. (2) Scan trace should cross a maximum number of light and dark surface features. (3) Flexible pointing capability of scan platform until just before encounter is required. (4) Aim point altitude should allow sufficient overlap (at least 10%) for the low resolution pictures (camera TV-A) so that there will be areas covered by both a red and green filter picture from camera TV-A; a high resolution picture from camera TV-B then falls in the overlap. (5) At least 24 pictures shall be taken on the lighted side of Mars for each spacecraft. (6) Wide angle camera coverage should be selected to include a maximum of the known types of Martian surface features. (7) Overlapping wide-angle pictures of the limb from each spacecraft are desired. (More precisely, the lower atmosphere above the limb is of interest, since the actual limb line is not the same for two subsequent photographs.) (8) Some stereo coverage, obtained by covering the same area with two different platform cone angles, is desirable. However, a large amount of such stereo coverage is not desired as this would diminish the total area covered at km resolution. (9) Except for the limb photographs, pictures taken at highly oblique view angles should be avoided since the ground resolution of such pictures is degraded.	(1) Since the TV cameras are shuttered alternately every 42.24 s by mechanical shutters, the cameras should be subjected to no more than about 72 h cumulative running time during the mission. (2) In the event a failure-mode operation must be adopted during encounter, thermal imbalance between the camera TV-B (narrow-angle) optics and the camera TV-B head should be avoided, since out-of-focus pictures may result. (3) Science power turn-on should be so timed as to insure, within the limits of the encounter uncertainties, that a blue filter will be in place on the camera TV-A (wide-angle) during the shuttering of the first near encounter picture.

Table 2 (contd)

Experiment	Experiment requirements	Engineering constraints
Infrared radiometry	(1) The scan must not cross terminator while on the polar cap. (2) Measurements on dark side of planet are required and are of utmost importance. At least 6 min of dark-side data is desired. (3) Scan trace should be nearly perpendicular to the terminator at terminator crossing. (4) The IRR shall be boresighted with the camera TV-B to within ± 0.3 degree of the optical axis. (5) The IRR track across the terminator should be continuous for at least 10 deg and preferably 15 deg on both sides of the terminator.	The IRR places no engineering constraints on the design of the encounter sequence.
Infrared spectroscopy	(1) Equatorial scan trace is preferred to the polar scan trace, since the long-wave-length channel depends upon thermal radiation from the planet. (2) Trace should cross several light and dark surface features. (3) Slant range should be as small as feasible. (4) IRS swaths should not overlap after platform slews, as IRS "stereo" is undesirable. (5) Data recording is to begin at a minimum altitude of 400 km above surface. (6) Significant amount of dark side viewing at not too oblique angles is required. (7) Data recording until 60 s past dark limb crossing is necessary. (8) Scan traces should follow closely the narrow angle TV and IRR scan traces to allow possible correlation of results. (9) The terminator crossing should be as close to equator as feasible.	(1) The two detectors in the instrument shall be cooled to $\leq 40°K$ (22°K desired) for the Channel 1 detector, and $\leq 175°K$ (155°K desired) for the Channel 2 detector during the near encounter data gathering period. In order to ensure this, the instrument radiation plate should not be exposed to any heating transient after encounter E−12 h. Also, Channel 1 cooling must begin 18–24 min before scanning the upper atmosphere. (2) Because excessive risk is involved in operating the IRS scan motor for extended periods, the IRS motor start command has been divorced from the science power turn-on and coupled with the blowdown command for the IRS cooldown. (3) Because of the general cooling requirements of the IRS, the cruise heater should be turned off and the electronics on no later than encounter −48 h. (The electronics provide a lesser heat load than the cruise heater in this instrument.)
Ultraviolet spectroscopy	(1) Range must be as small as possible at limb crossing, particularly at the lighted limb, so experiment may be carried to lowest possible altitude before instrument gain is reduced. (2) Slit is to be aligned to within 3 deg of local horizontal plane at 100 km altitude with a confidence level of 90%. (3) Data recording is to start at a minimum of 1000 km above bright near limb. (4) Scan trace should be as near to the subsolar point at near limb crossing as feasible but, in no case, further than 30 deg away. (5) Scan traces should fall as close as possible to traces of the other instruments. (6) One-third of the experiment value should be allotted to detecting N_2 above bright limb. (7) Recording of data until 2 min after dark limb crossing is desirable in order to look for night airglow. (8) For each spacecraft, obtain two bright limb crossings, if feasible. Whenever the UVS is slewed off the planet for a second trace through the atmosphere, the swing-back altitude shall be at least 600 km.	(1) If the near encounter strategy involves collecting the upper atmospheric data by the UVS after the cone angle change back to 90 deg has been made, at least 30 s must be allowed for the N tube in channel 2 to recover from the excessive dark current induced by viewing the bright planet. In terms of altitude, this means the view axis of the UVS must be brought back to not less than 600 km above the limb. (2) A critical constraint imposed on the spacecraft design is to preclude the possibility of having any N_2 ejected into the UVS field-of-view.

Table 2 (contd)

Experiment	Experiment requirements	Engineering constraints
S-band occultation	(1) Radio beam tangent points at entrance and exit of occultation should be widely separated in absolute value of latitude: maximize $\|\|\Phi_{en}\| - \|\Phi_{ex}\|\|$ (2) Absolute value of difference between solar zenith angle at tangency points at entrance and exit should be as large as possible. (3) Average of distances from tangent points at times of occultation is desired to be less than 20,000 km. (4) Deep Space Station (DSS) elevation angles should be at least 15 deg and as high as possible. (5) Obtain views from both DSS 41 and DSS 14 during occultation.	For purposes of this experiment, the spacecraft radio is considered to be a science instrument. It is important that no major power changes, such as turning on gyros or switching the traveling wave tube (TWT) from low to high-power, be made after approximately encounter −10 h. Even minor power changes should be avoided where possible after the start of near encounter. The resultant change in temperature of the auxiliary oscillator crystal, if not stabilized by the time of occultation exit, will jeopardize the reacquisition of the radio signal and hence the S-band occultation results.
Celestial mechanics	(1) Periapsis of spacecraft trajectory should be as close to Mars as feasible. (2) Lower approach speeds (V_∞) are desirable. (3) Short time of occultation is preferred. (4) Tracking line-of-sight (Earth-to-spacecraft) to lie within areocentric trajectory plane of motion is desired.	(1) Minimizing length of IRS gas blowdown and associated orbit perturbation uncertainties is desired. (2) A specified amount of control over tracking data quantity and quality should be achieved.

necessary to assemble an optimal scientific mission have been made.

VI. Encounter Sequence Planning and Design

It was realized, as the mission planning progressed, that the encounter sequence as originally conceived was quite conservative and a very substantial increase in science data return could be realized. A re-evaluation of the encounter sequence was begun with emphasis on using the spacecraft and ground systems to maximum utility. Three new generations of encounter sequence design, culminating in design reviews, were conducted: two prior to launch and one during the flight phase. The initial mission design effort had been reviewed in late 1966. The new encounter sequence effort, embodying the essential elements of the sequence flown, was reviewed in September 1968. A thorough rework of this effort produced the sequence described in this section and programmed into the spacecraft prior to launch. The review and revision effort continued in the flight phase, and a final review was conducted. This effort resulted in the development of mission encounter sequences which would enhance the mission return if the condition of the spacecraft would permit it, yet retain the conservative aspects of the original sequence to guarantee science data return in the event of unforeseen problems. The new sequences were to rely heavily on the experimental high-rate telemetry system. Further, ingenious programming of the CC&S within available core space afforded reliable execution of a much more complex sequence.

A. Standard and Conservative Sequences

It was decided that the general encounter mission plan should consider two major types of missions, the standard mission and the conservative mission. The phrase "standard mission" is defined to mean that mission which is planned to be executed if supported by certain controlling factors. The key controlling factors are:

(1) Science return and value.

(2) Condition of flight spacecraft.

(3) Results of supporting ground testing of the spacecraft and various subsystems.

(4) In-flight determination of communications, power, and temperature control performance margins.

(5) Availability and performance of the DSN facilities.

(6) Operational complexity required to execute and the capability of handling non-standard events.

There was to be one standard mission applied in almost the same way to each spacecraft. For convenience of operational planning, the standard mission was divided into a number of phases of activity, each considering and covering both spacecraft. With the exception of operational deviations necessitated by nonstandard events, the launch, midcourse, and cruise phases had the same profiles for *Mariner F* and *Mariner G*.

In the standard mission (see Fig. 20) the far-encounter period lasts about two to three days, during which time series of full-disk pictures of Mars are recorded and then played back at daily intervals over the high-rate telemetry system to the DSN 210-ft antenna at Goldstone California. Near-encounter operations begin about 35 min before encounter (closest approach) with the initiation of active cryogenic cooling of the detector of the infrared spectrometer. About 20 min later, two TV cameras, a radiometer, and two spectrometers begin taking planetary data. These data are variously transmitted directly to Earth, recorded in digital format, and recorded in analog form, according to their nature. The instrument scan platform is pointed at Mars and slewed in accordance with a sequence programmed in the spacecraft.

When the TV swath has crossed the day/night terminator, picture recording ceases, but the other instruments continue taking and recording dark-side data out to and slightly beyond the dark limb, about 10 min after closest approach. Occultation of the spacecraft by Mars begins near this time and lasts about 25 min. Occultation data are obtained on the tracking stations at entry and emergence. Tracking data obtained throughout encounter, as well as during the rest of the flight, contribute to a celestial-mechanics experiment. Following occultation, near-encounter scientific data recorded on two tape recorders are played back, and the spacecraft is then returned to the cruise mode.

Suppose, however, that it became necessary to execute an encounter and playback sequence which would be operationally simpler than the same phase of the standard mission, but which would still be capable of meeting the primary mission objective. From this consideration, as a backup to the standard mission, in the event of degraded capability or anomalies early in the encounter phase, a conservative mission was designed and programmed into each spacecraft, to operate on an automatic basis or by selection. It consisted of fewer far-encounter TV pictures, a normal near-encounter, and a normal-rate playback. Neither high-rate telemetry nor ground-command capability was required to complete the conservative mission. The conservative mission sequence was to be the same for each spacecraft.

The standard mission sequences were designed with built-in decision points. Before passing these points, the past performance of the spacecraft could be surveyed and its ability to successfully perform the next sequence of events determined. If it was decided that the spacecraft or the ground system could not support the continuance of the standard sequence, the decision point allowed a shift to the built-in conservative sequence.

Each of the mission sequences were further divided into three periods. The far-encounter period began with science-instrument turn-on and extended to about 1 h before closest approach. The near-encounter period began at this time and continued until occultation, and the playback period began when the CC&S issued the begin-playback command during occultation. Playback then continued until all data had been recovered from the data storage subsystem.

In line with the *Mariner* philosophy, the encounter was to be as automatic as possible, consistent with the intent to include decision points as discussed above. Ground commands were to be used where necessary but with the following restrictions. The receipt of any ground command must not make the spacecraft dependent upon another ground command in order to successfully complete the mission. If ground command capability were lost, the spacecraft would revert to the most conservative sequence. Ground commands would be separated as much as possible for ease of MOS operation and the verification of spacecraft state changes prior to the transmission of additional ground commands. Ground commands would be used to back up time-critical onboard functions. There would be reduced dependence on the time criticality of ground commands.

As many commands as possible were to be automatically initiated by the CC&S. In fact, the entire near-encounter sequence was to be under the complete control of the CC&S with no ground commands required. It was desired that the CC&S programs for each spacecraft be as identical in structure as possible, and have their memories loaded at launch. The dependence between the near-encounter and far-encounter portions of the programs was to be minimized. The MOS was to continually update the variable parameters with the best available trajectory information and science strategy.

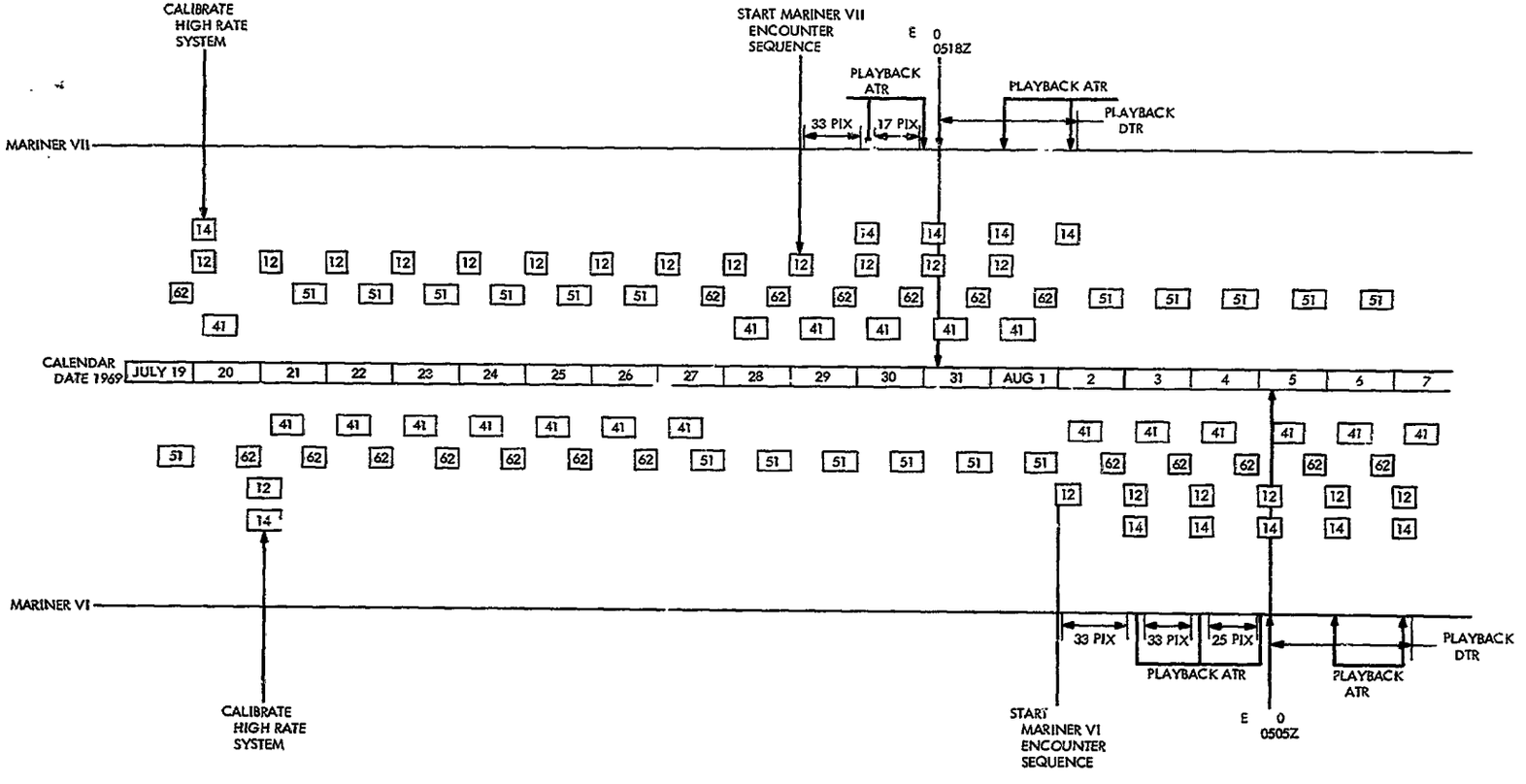


Fig. 20. Standard mission encounter profiles

The most important aspect of the encounter sequences was to be the failsafe backup events included in the sequences. These would be automatic events issued by the CC&S which would cause the spacecraft to enter a safe mode for continuing operations if a failure to transmit or receive a ground command occurred. These events include erasing the analog tape recorder (ATR), slewing the scan platform to the near-encounter position, and stopping ATR playback. In addition, contingency plans were developed in parallel with the standard sequences for what were considered to be the most likely failure areas: loss of ground command capability, an inoperative scan platform, and a negative high-rate-telemetry margin.

Finally, Table 3 summarizes some of the specific features of the conservative and standard mission plans. It can be seen that the standard far-encounter sequence for *Mariner G* is more ambitious than that planned for the first-arriving *Mariner F*. Additional details of the far and near-encounter sequences are contained in the next two subsections.

Table 3. Summary of the differences between mission plans

Mariner Mars 1969 plans	Description	Utilization
Conservative plan	8 far-encounter TV pictures from encounter — 22 h to encounter — 12 h with no playback until after encounter.	Stored in CC&S at launch. Automatically executed if ground command not available.
Standard plan for *Mariner F*	33 far-encounter pictures from encounter — 48 h to encounter — 28 h with ATR playback using high rate mode. 17 far-encounter pictures from encounter — 22 h to encounter — 7 h with ATR playback using high rate mode.	To be stored in the CC&S of both spacecraft at launch. Planned to be used on *Mariner F* but requiring ground command and minimum CC&S reprogramming after launch.
Standard plan for *Mariner G*	33 far-encounter pictures from encounter — 72 h to encounter — 52 h. 33 far-encounter pictures from encounter — 47 h to encounter — 27 h. Both ATR playbacks via high rate mode. 25 far-encounter pictures from encounter — 21 h to encounter — 4 h with playback via high rate mode before encounter.	Requires partial reprogramming of CC&S after launch.

B. Far-Encounter Mission Design

During the time period from about 72 h to 4 h before encounter, it was planned to take several narrow-angle TV pictures of Mars. The TV principal investigator expressed the desire (see Table 2) that the actual pictures obtained meet, as a minimum, certain coverage requirements. These requirements are listed from the most to the least important requirement as follows:

(1) Full-planet coverage (all longitudes).

(2) Coverage of those areas which will be subsequently covered at higher resolution during the near-encounter scan phase.

(3) Coverage of Syrtis Major, Elysium, and Trivium Charontis.

(4) Coverage of the *Mariner IV* area.

(5) Coverage of Mars' moons, Phobos and Deimos.

Regarding the surface feature areas, it was necessary to decide under what geometrical conditions the best pictures could be expected. As picture resolution was to be relatively coarse for the far-encounter pictures, it was felt that the best pictures would result when the feature would be photographed within about 30 deg of the subspacecraft point. Figure 21 illustrates the best times for photographing the areas of interest, for the preferred July 31 and August 5 arrival dates. Closest approach to Mars is assumed at 1 h 55 min past Goldstone zenith. It can be seen that the conservative eight-picture sequence fails to meet the two highest priorities, whereas the standard *Mariner F* and *Mariner G* far-encounter picture sequences more than satisfy the first four priorities.

In the case of the two moons of Mars, refer to Fig. 22 for an explanation of the times shown in Fig. 21. A higher value was assigned for taking a picture when the

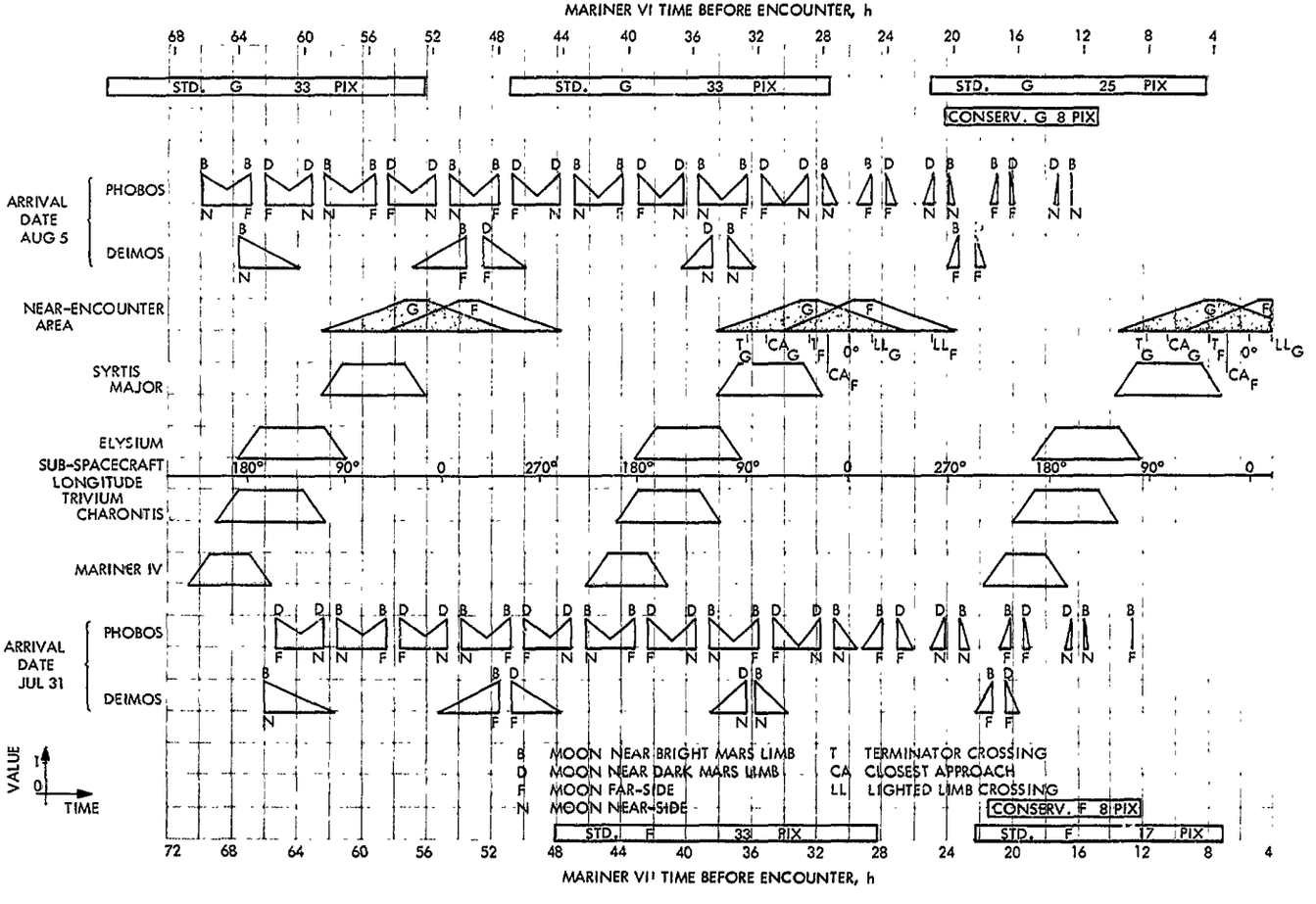


Fig. 21. Favorable times for obtaining various types of far-encounter TV picture coverage

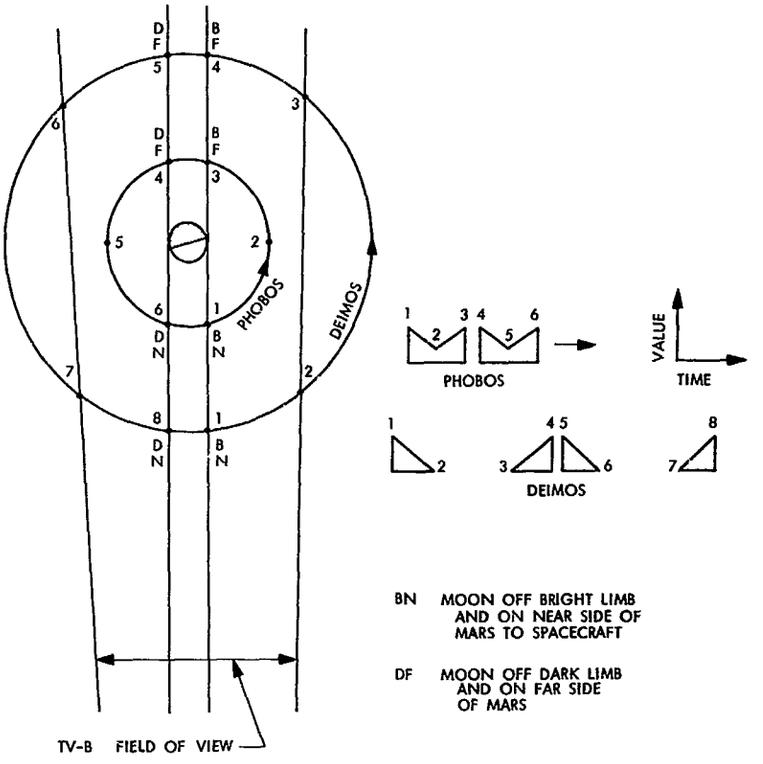


Fig. 22. Method of value assignment for location of Mars' moons

moon would be near one of the planet limbs than when it would be near the edge of the narrow-angle camera (TV-B) field-of-view. This was done because of the greater possibility of missing the moon, as a result of pointing errors in the FEPS/TV-B system, when the moon would be near the edge of the TV-B field-of-view.

The standard far-encounter sequences for both spacecraft consisted of recording narrow-angle TV pictures of the planet as the spacecraft approaches. The FEPS is designed to point the TV-B camera at the planet, and the CC&S is to command the analog recording of one TV frame approximately every 37 min until all four tracks of the ATR are filled. The pictures are played back over the high-rate telemetry system to DSS 14. *Mariner VI* was to nominally record one full tape load of 33 far-encounter pictures and one half tape load of 17 pictures before the near-encounter period. *Mariner VII* was to nominally record two full ATR tape loads plus an additional 25 pictures before near-encounter.

The sequences were designed so that each spacecraft would be conditioned for TV picture recording over DSS 14. The automatic sequence would then be performed over the Australian and Spanish stations, and the spacecraft readied for playback during the next pass at DSS 14. Following the high rate playback, the ATR would be erased and the scan platform returned to the far-encounter position for further picture recording, or left in the near-encounter position for the initiation of the near-encounter sequence. The data storage subsytsem is empty at the beginning of near-encounter.

Major features of the far-encounter sequences included digital TV data returned at high rate while the spacecraft would be over DSS 14 and still recording analog pictures. Far-encounter analog recording would always be stopped at AEOT=4 (the fourth end of track) so that one fail-safe analog erase command would completely erase the tape. The scan platform would be turned on to first slew to the near-encounter position so that, if a failure occurred, it would be in the optimum position for the most valuable mission data. In selecting 17 as the number of pictures in the last far-encounter group from *Mariner VI*, and 25 for *Mariner VII*, a trade-off was made between the number of pictures that could be played back and the amount of time required to condition the spacecraft for near-encounter.

Finally, Figs. 23 and 24 illustrate the appearance of Mars in selected far-encounter pictures for the standard *Mariner F* and *Mariner G* picture sequences. Far-encounter coverage of the gross near-encounter picture swath regions is also apparent in several of the pictures. It is useful to correlate Figs. 23 and 24 with Fig. 21.

Late in the mission planning, a small adjustment was made to the last 17 *Mariner F* picture times in order to try to catch both Phobos and its shadow on the planet surface. This objective was planned for far-encounter pictures 40 and 41. Figure 25 is a computer-drawn plot which shows the expected appearance of picture 40.

C. Near-Encounter Mission Design

The far-encounter TV picture sequences have been previously discussed and constitute significant scientific value. However, the majority of the scientific and mission value return was anticipated during the near-encounter phase, when all instruments were to perform higher-resolution measurements of the Martian environment. The following is an over-simplified description of the key near-encounter events. At about 35 to 40 min before encounter (closest approach), cryogenic cooldown of the IRS is initiated either by ground command or by NAMG-1 (narrow angle Mars gate number 1). Approximately 20 min later, the analog tape recorder and the

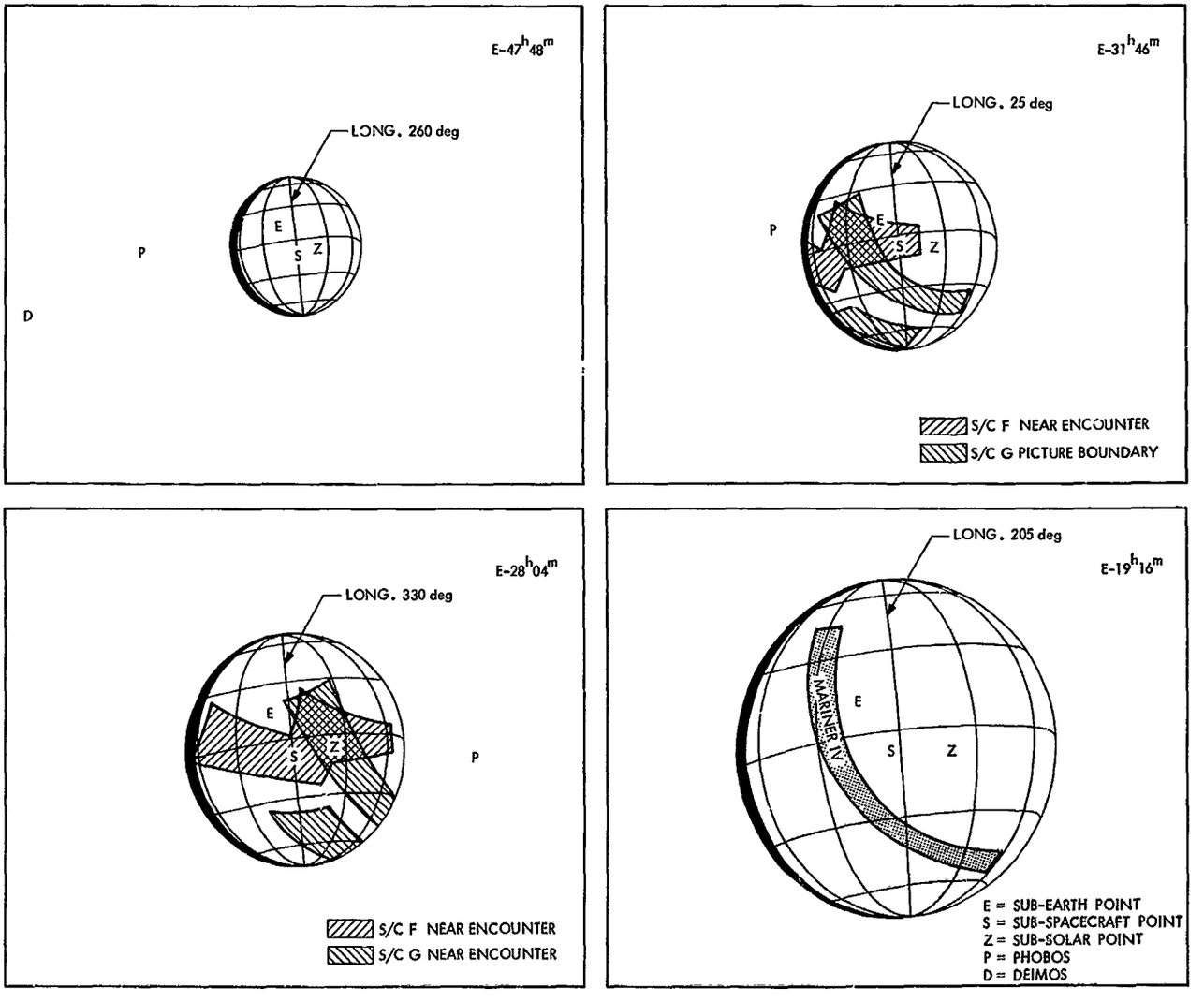


Fig. 23. Selected far-encounter pictures from the standard *Mariner VI* sequence

digital tape recorder (DTR) are started by the appropriate signal from the logic network. The relative timing of N6DAS, DC-16, and NAMG-2 has been chosen to ensure that the appropriate wide angle TV picture will be counted as near-encounter picture 1 (subsequent platform slews follow frame readout starts of specified picture numbers). In addition, the occurrence of NAA is so timed as to assist such other goals as recording high-altitude UVS and IRS measurements, obtaining (in association with DC-25, science power turn on) the desired color filter for picture 1, recording a total 25 to 33 TV pictures on the lighted side of Mars, and obtaining other timing goals which may be desirable.

Alternate wide and narrow angle TV pictures are recorded at 42.24 s intervals. The CC&S counts TV frame starts and, at prescribed times, causes the scan platform to be slewed to a new pointing position. The recorders stop automatically at their fourth end-of-track signal and are then ready for playback. DSS 14 is the prime station for encounter, and all encounter science data are nominally returned in real time via the high-rate telemetry link. The non-TV instruments continue taking data out to and slightly beyond the dark limb, about 10 min after closest approach. Occultation of the spacecraft by Mars occurs within a few minutes after dark limb crossing and lasts for about 25 min.

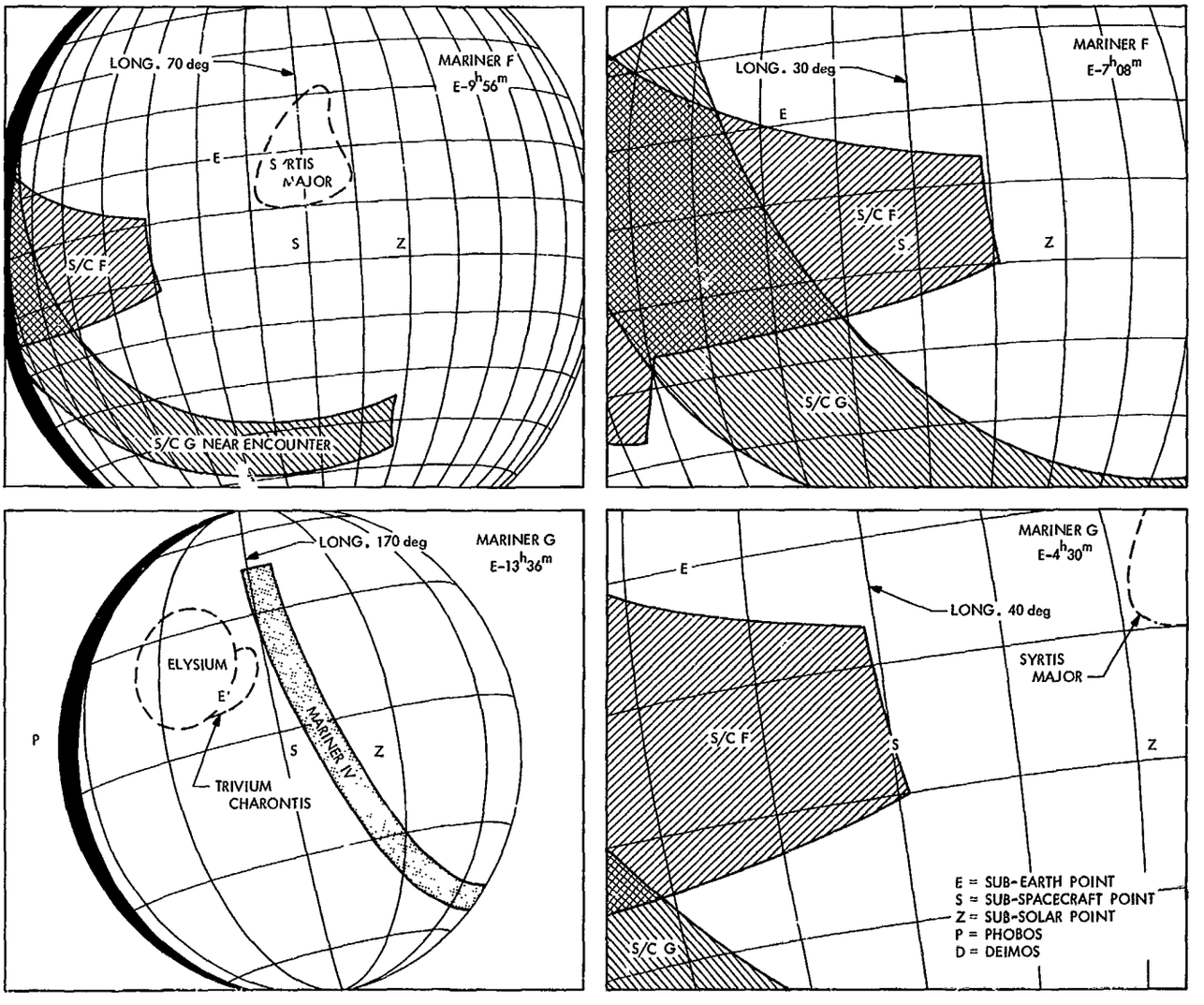


Fig. 24. Selected far-encounter pictures from the standard *Mariner VI* and *Mariner VII* sequences

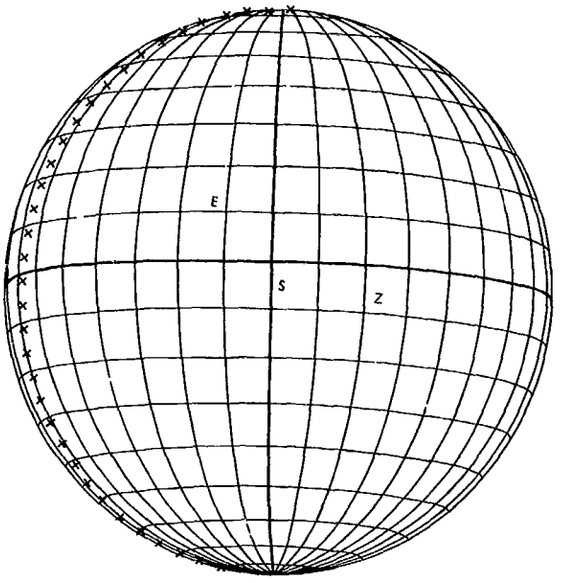


Fig. 25. Computer-drawn plot of the expected appearance of picture 40

During the occultation period, the CC&S issues a start playback command, and the DTR begins to playback. A slight amount of data are lost during the occultation, but these data are played back twice more. DTR playback is interrupted during the next two DSS 14 passes, in order to playback the ATR at high rate. After the DTR has played back all tracks twice, it begins transferring the analog data from the ATR to the DTR and playing back each DTR tape load until commanded to stop from the Earth.

VII. Platform Pointing

A. Instrument Offsets on Scan Platform

The relative pointing directions of the instruments were chosen to best carry out the objectives of all experiments. The two TV cameras are boresighted to place the high resolution coverage in the overlap areas formed by the wide-angle camera coverage. This works as required since the narrow-angle (TV-B) and wide-angle

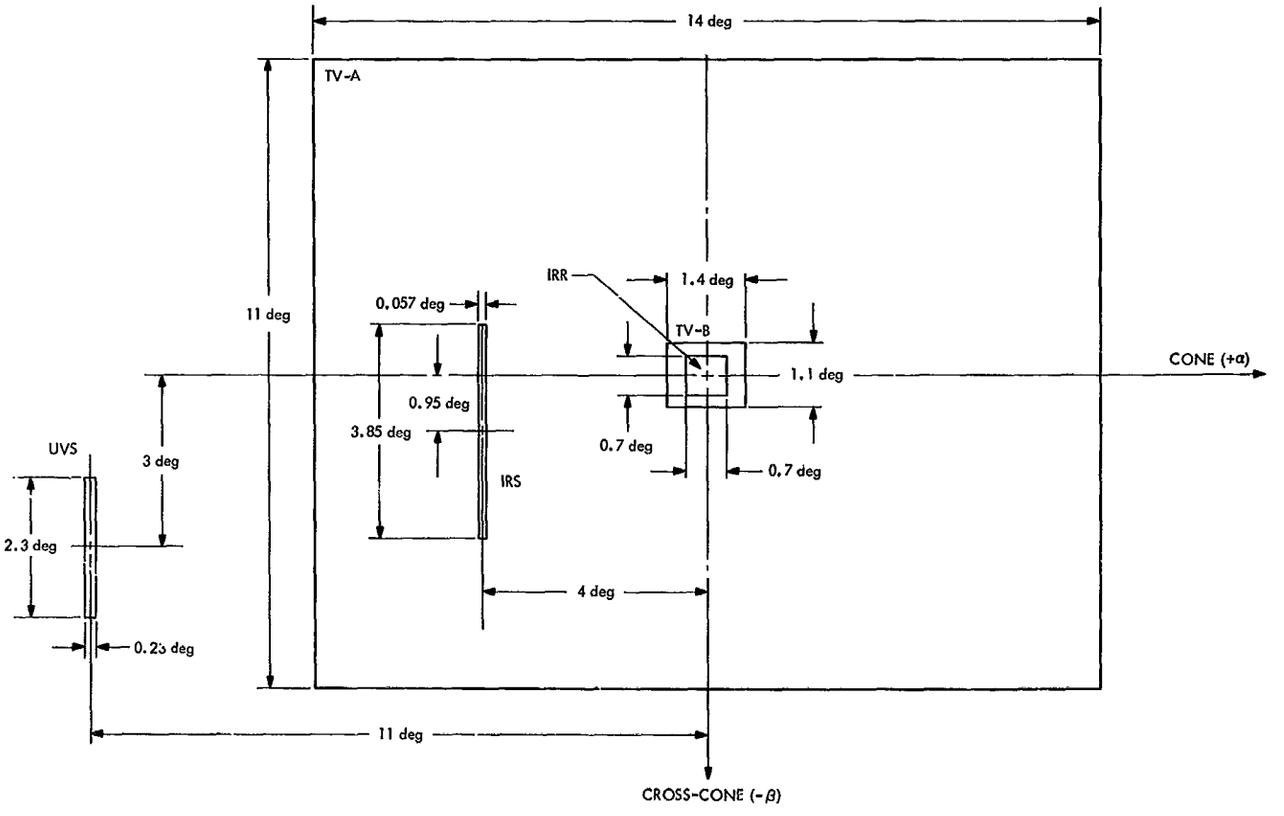


Fig. 26. Relative fields-of-view and instrument pointing directions

(TV-A) camera exposures alternate. The IRR is boresighted with the TV cameras so that IRR coverage within the high resolution TV coverage is assured.

The IRS pointing direction is offset −4 deg in cone angle so that, when the TV crosses the limb and data recording begins, the IRS is looking at a region at least 400 km above the limb. To assure IRS coverage of the areas on the planet covered by the high resolution TV and the IRR, the IRS pointing direction is offset +0.95 deg in cross cone.

The UVS pointing direction is offset −11 deg in cone so that, when data recording begins, the UVS will be looking at an altitude of at least 1000 km. To obtain the best possible overlap with the coverage of the other instruments on the surface, the UVS is offset +3.0 deg in cross cone. The relative pointing directions of the instruments are shown in Figs. 26 and 27.

B. Platform Viewing Directions

Finally, it is important to discuss the selection of the platform viewing directions during each near-encounter pass that are expected to best satisfy those scientific desires previously specified. The scan platform can be slewed in 1-deg steps over a fairly broad range of cone angle and clock angle. The manner in which these angles

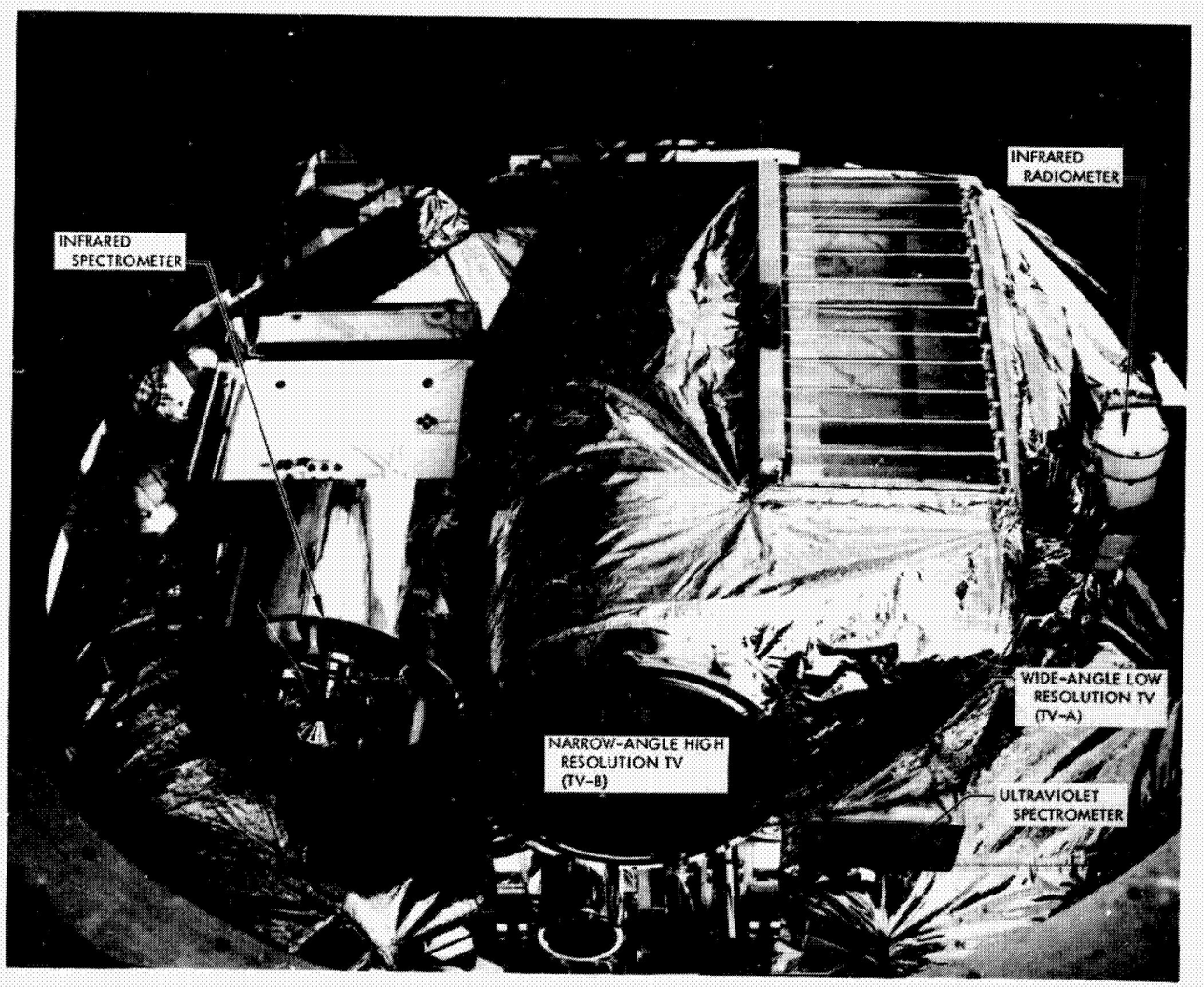


Fig. 27. Scan platform

are measured is defined in Fig. 28. Platform slews are initiated by the CC&S shortly following frame readout starts of selected picture numbers. The picture numbers, the number of one-degree cone-angle steps, and the number of one-degree clock-angle steps are stored in the CC&S memory and can be updated from the ground during the flight.

Up until a few weeks before encounter, the planned instrument swaths across Mars were those shown in Fig. 29. Note how the different swaths overlap to permit cross-correlation of results. A few days before the *Mariner VI* encounter, the *Mariner VI* slewing strategy was altered slightly, and the final strategy will now be explained in some detail. It was planned that *Mariner VI* take 25 pictures of the lighted side of Mars during the near-encounter pass. The odd-numbered frames are wide-angle (TV-A) pictures, and the even-numbered frames are narrow-angle (TV-B) pictures. Picture 1 was to be shuttered approximately 13 min and 59 s before encounter (closest approach), and picture 25 was to be shuttered approximately 2 min and 55 s after encounter. The pictures would be spaced at 42.24 s intervals. Four different platform-viewing orientations would be utilized during the TV portion of the flyby pass. The factors which dictated each of these platform positions will now be summarized briefly.

The initial platform cone angle was selected such that (at the initial clock angle used) the digital tape recorder (DTR) would start at the appropriate time and, also, the first picture would be a suitable wide-angle picture of the limb. By the word "appropriate" it is meant that the DTR would still be running some 30 s to 60 s after the IRS viewing axis had crossed the dark limb (at the final platform-cone and clock-angle position). This was done to ensure recovery of the dark-side data on the DTR in the event that the real-time high-rate (16,200 bit/s) channel did not function properly. The initial platform clock angle for the first swath was selected so that (for the initial cone angle used) the UVS viewing slit would be aligned with the local horizontal at an altitude of 100 km above the bright limb. A sufficient number of pictures would be taken along this first swath to ensure that the trailing UVS field-of-view had scanned the lower atmosphere, had crossed the limb, and had even passed a small distance across the planet surface.

Approximately 8 s after the shuttering of frame 8, the CC&S would instruct the platform to slew to its second position. A negative slew in clock angle was chosen to carry the instrument viewing axes to the north in order to view such interesting surface features as Margaritifer Sinus, Oxia Palus, Meridiani Sinus, and a small part of the western side of Sabaeus Sinus. The amount of clock-angle slew was limited so that some overlap would be maintained with the last picture swath across the lighted side. The platform had to be slewed after picture 13 in order to carry the UVS back off the limb to a sufficient altitude where it could make a second scan of the atmosphere.

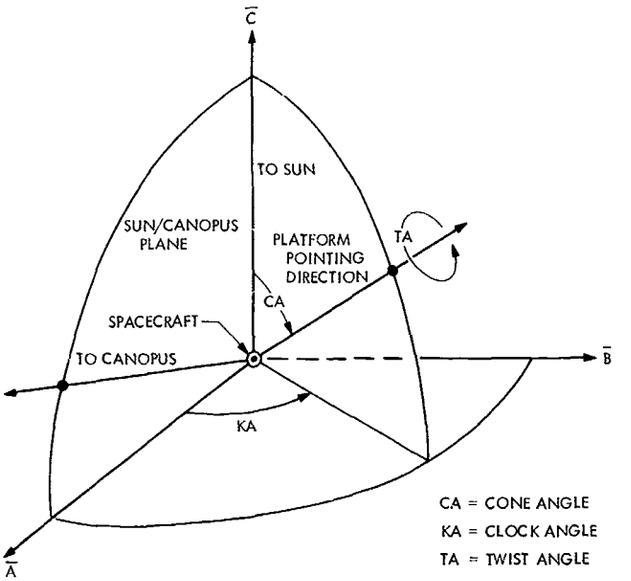


Fig. 28. Cone angle, clock angle, and twist angle defined

The third platform orientation was therefore determined by slewing to the final cone angle position (≈100 deg) and that clock angle position which would again align the UVS slit with the tangent plane at 100-km altitude above the bright limb. This slew-back also provided the UVS with its shortest slant-range view of the atmosphere above the limb. In order to again give the UVS ample time to scan the atmosphere, cross the limb, and pass onto the planet surface, the next platform slew would not be made until 8 s after picture 17 had been shuttered.

After picture 17 had been shuttered, the platform clock angle was to be diminished by 2 deg, thus, moving the instrument traces slightly to the north on Mars. This fourth platform position was chosen to accomplish three objectives: (1) maintain some overlap with frames 11 and 13, (2) view the southern boundary and most of Sabaeus Sinus, and (3) obtain a good pass completely

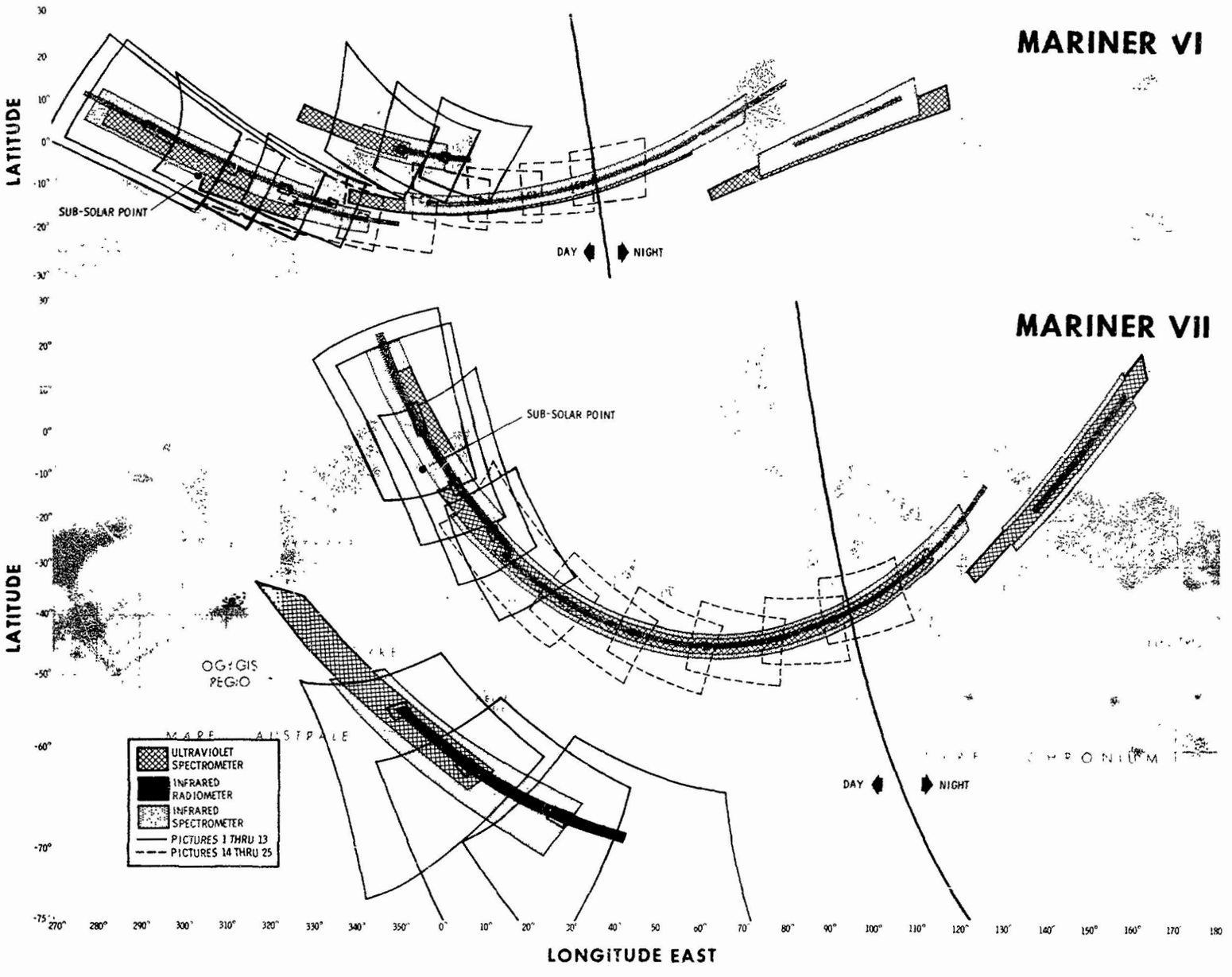


Fig. 29. *Mariner* Mars 1969 scientific planetary scans

across Syrtis Major on the dark side with the IRR and IRS. A final platform slew would be performed on the dark side (after frame 32) in order to view Libya and extend dark-side viewing time for the non-TV instruments.

Since the high-rate channel subsequently worked successfully for *Mariner VI* far-encounter and near-encounter (and for *Mariner VII* far-encounter), and because the actual far-encounter pictures further increased the interest in the southern polar cap, it was decided to take more near-encounter pictures for *Mariner VII* with as many of these as reasonable on the southern polar cap. The initial platform cone angle was therefore increased to about 135 deg in order to start the sequence properly and fill the analog tape recorder with 33 pictures of the lighted side of Mars. Picture 1 was to be shuttered approximately 20 min and 26 s before closest approach, and picture 33 was to be shuttered approximately 2 min and 6 s after closest approach. The pictures again would be spaced at 42.24 s intervals. Four different platform viewing orientations were used during the TV portion of the flyby pass. The factors which dictated each of these platform positions will now be summarized briefly.

The initial cone-angle value was based upon knowledge of the time the TV would cross the terminator (with the platform slewed back to cone angle $\approx$ 100 deg, clock angle $\approx$ 234 deg), and assuming that initial value of platform clock angle which would properly align the UVS slit projection at 100-km altitude above the bright limb. The initial platform position also resulted in obtaining very desirable coverage of Meridiani Sinus under different viewing conditions than had been present during the second *Mariner VI* near-encounter platform position. A sufficient number of pictures would be taken along this first swath to ensure that the trailing UVS FOV had scanned the atmosphere, had crossed the limb, and had passed a short distance across the planet surface.

Approximately 8 s after picture 9 had been shuttered, the CC&S would instruct the scan platform to slew to its second position in order to view the southern polar cap. This required a very large positive clock slew of 33 deg, as well as a positive cone slew of 9 deg. The chosen cone and clock angles (cone angle $\approx$ 144 deg, clock angle $\approx$ 250 deg) would give all instruments the opportunity to view the regions north of the cap boundary, to make the transition across the thaw region and cap boundary with continuity, to progress well onto the cap, and, finally, to obtain wide-angle pictures (frames 17 and 19) of the terminator while on the polar cap. The platform had to be slewed after picture 20 in order to carry the UVS back off the limb to a sufficient altitude where it could begin a second scan through the atmosphere.

The third platform position was therefore determined by slewing to the final cone angle position ($\approx$100 deg) and that clock angle value ($\approx$234 deg) which would again align the UVS slit with the tangent plane at 100-km altitude above the bright limb. This slew back also provided the UVS with its shortest slant-range view of the atmosphere above the limb. Motion along this third swath would continue for a sufficient time to permit the UVS to complete its scan of the atmosphere and, in addition, to permit the TV and IRR to cross the western boundary of Hellas, and for the trailing IRS to cross most of Hellespontus. At this point, the IRS experimenter requested a 5 deg clock slew to the north in order to cross Hellas at slightly warmer latitudes. Pictures 21 through 27 were taken along the third platform swath.

Approximately 8 s after picture 27 had been shuttered, the CC&S would instruct the platform to slew north to its fourth position. In this position, the remaining TV pictures, 28 through 33, would be taken with much of picture 33 covering the dark side across the terminator. Motion along this swath would continue until 8 s after picture 37 had been shuttered, at which time the CC&S would issue instructions for a final clock angle slew of the platform of +21 deg. Performance of this final clock slew would delay the occurrence of excessively oblique viewing angles and extend dark-side coverage for the non-TV instruments.

References

1. Clarke, V. C., Jr., *Design of Lunar and Interplanetary Ascent Trajectories,* Technical Report 32-30. Jet Propulsion Laboratory, Pasadena, California, March 15, 1962.

2. Bollman, W. E., "The Engineering Design of Interplanetary Ballistic Trajectories," *AIAA* Paper No. 63-414, presented at Yale University, August 1963.

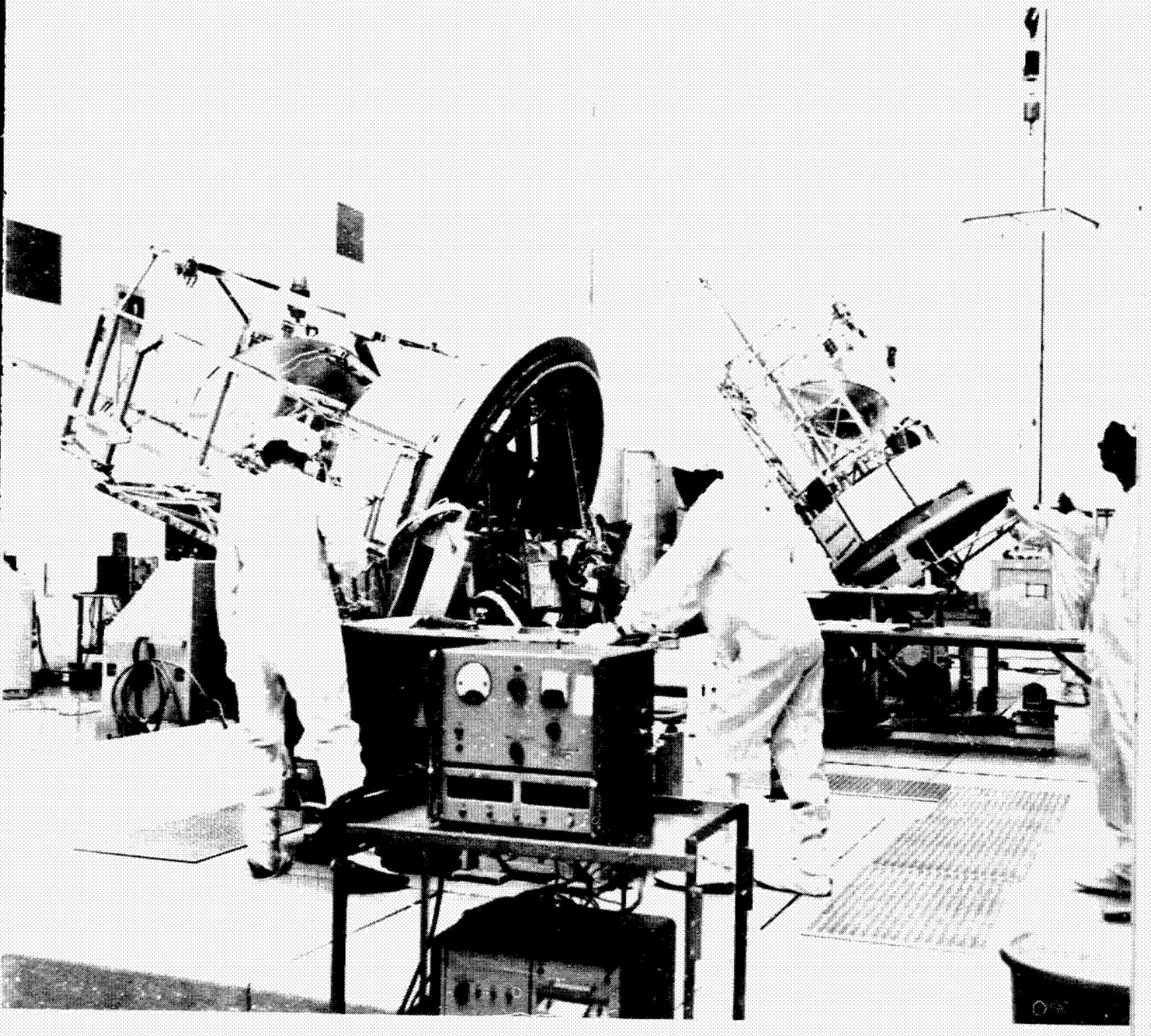
3. Kohlhase, C. E., "Launch-on-Time Analysis for Space Missions," *ARS Progress in Astronautics and Rocketry: Guidance and Control, Vol. 8,* pp. 3–20. Edited by R. E. Roberson and J. S. Farrior, Academic Press, New York, 1962.

4. Kohlhase, C. E., "Mariner Mars 1969 Flight Path Design and Mission Analysis," *AIAA* Paper No. 68-134, presented at Jackson, Wyoming, September 1968.

5. Horowitz, N. H., et al., "Planetary Contamination I: The Problem and the Agreements," *Science, Vol. 155,* March 24, 1967.

6. Light, J. O., et al., "A Discussion of the Planetary Quarantine Constraints," Paper Presented at *COSPAR Symposium on Space Science,* Vienna, 1966.

7. Craven, C. W., and Wolfson, R. P., *Planetary Quarantine,* Technical Report 32-1216. Jet Propulsion Laboratory, Pasadena, California, December 15, 1967.



Part 2. Spacecraft System

PRECEDING PAGE BLANK NOT FILMED

PRECEDING PAGE BLANK NOT FILMED

Spacecraft System Design

I. Introduction

The *Mariner* Mars 1964 spacecraft design was used as a basis or baseline for the development of the *Mariner* Mars 1969 configuration. Even in their final configurations, there are many similarities.

In early 1966 the design philosophy adopted for the baseline *Mariner* Mars 1969 was based upon minimum modifications to the *Mariner* Mars 1964 design. Changes were to be made only to:

(1) Improve reliability.

(2) Reduce costs.

(3) Meet mission objectives.

Nevertheless the design underwent an extensive evolution, resulting in a spacecraft which has many design features and capabilities markedly different from *Mariner* Mars 1964.

Principal differences in this design from *Mariner C*, the *Mariner* Mars 1964 spacecraft design, were a modified structure, a large science payload, a greater scan capability, a more complex encounter sequence, an increased data-storage capacity, increased electrical-power handling, a programmable CC&S, an approach guidance subsystem, and no cruise-phase science. The design was changed with respect to scientific equipment by deleting all *Mariner* C science, by adding the new TV, ultraviolet spectrometer, infrared spectrometer and radiometer, and by replacing the data automation subsystem with a wholly new design.

The science payload was to contain no instruments which operated during the cruise phase of the mission, that is, no interplanetary experiments. Thus, the data mode for the launch and cruise phases was to consist solely of engineering data called the cruise data mode. Since neither a magnetometer nor a particle detector was to be included, there would not be a rigid project requirement for magnetic cleanliness and absence of radioactive materials.

In the *Mariner* Mars 1969 design, as on all *Rangers* and *Mariners*, the sequencing through the mission phases was to be primarily controlled by onboard logic. The design selected was a programmable sequencer, with a 128-word core memory. This programmable sequencer, with a memory which could be updated or modified by ground command, allowed a versatility in mission operations heretofore unobtainable in *Ranger* and *Mariner* missions.

The spacecraft was designed to be automatic; that is, to be capable of operating from launch to the end-of-mission without the use of ground commands, with the exception of the trajectory correction maneuver. Critical functions which were to be automatically initiated on board the spacecraft in a nominal mission were also backed up by ground command capability.

II. Design Management

A. System Design Team

A team made up of senior-level design people was formed by selecting at least one such person from each subsystem represented on the spacecraft and making it function as a spacecraft design team. The major purpose of this design team was to establish a system design and to ferret out major problems inherent in the original mission studies.

On the *Mariner* Mars 1969 spacecraft, system level support was provided on a continuing basis during both test and operations. Surveillance was made of all major milestone activities at: (1) SAF, (2) environmental test sites, (3) hardware reviews, (4) calibration checkouts, and (5) AFETR for all prelaunch activities. This support meant that system engineers were always present and thereby were able to more effectively provide the type of support required. Specific functions performed in many of these support roles included verification of complex spacecraft system states, resolution of subsystem interface problems, and analysis of raw and computer generated test data.

B. System Design Control Documentation

1. Spacecraft and operational support equipment design books

The spacecraft design book and its companion operational support equipment design book served as the documented control mechanisms for systems level design control:

Level 1–Introduction and general information

Level 2–System characteristics and restraints (project level)

Level 3–System level functional requirements

Level 4–Subsystem level functional requirements (one per subsystem)

Requirement documents were made via formal drawing change procedures. Either the new revision issue or a copy of the Engineering Change Instruction (ECI), depending on whether or not the change was incorporated immediately was released to design book users.

2. Interface drawings. Interfacing end circuits between subsystems were required to be described on common circuit data sheet (CDS) drawings. CDSs necessarily are released early in the life of a project, and, if not released early, are useless.

There were additional interface control drawings that were the mechanical design equivalent of the circuit data sheet interface control drawing. This mechanism gave the spacecraft system engineer a way of retaining visibility of the packaging design of the spacecraft.

3. Engineering change control. After the design was frozen, engineering change control was put into effect; this meant that there was a review and approval of all changes requested against released system level documentation, including waivers and ECIs. Also, there was a system and responsibility to follow up on the incorporation of approved hardware changes. The purpose of this was to control the design and ensure that hardware and documentation agree.

4. Telemetry channel assignment. The task of spacecraft telemetry channel assignments was a system optimization problem of maximizing the value of telemetry data received through the proper assignment within the commutation scheme. Before the requirement for this was placed in a level 3 functional requirement document it was handled as a spacecraft system design team task assignment because of its importance. Many changes were made in the commutation scheme since the design was iterated several times.

5. Spacecraft functional block diagrams. The spacecraft functional block diagram was really three documented listings which together contained all subsystem interfaces controlled by the spacecraft system design group.

The three lists were as follows: (1) spacecraft interfaces, (2) OSE interfaces, and (3) spacecraft-OSE interfaces. The day-to-day control mechanism involved updating a computer program with card decks. The program was run on the 1620 computer and the output was a printout formatted for direct IBM reproduction into the functional requirement.

6. Power profiles. A key mechanism in controlling the design was to have a power profile which showed power requirements for all spacecraft system states and modes. By updating a card deck, the spacecraft systems design group could produce a computer printout which reflected a detailed power demand breakdown for each mission phase on all possible spacecraft status. The results of this were placed in a level 3 functional requirement for formal documentation control.

A greater amount of scrutiny was required during SAF testing when actuals observed did not always agree with the allocations. However, with slight program update changes, a new run could be made to provide several different types of power profile data of varying detail and uses. Although this program was somewhat more sophisticated than the block diagram program explained above, it too was basically simple. This program was converted to FORTRAN V for UNIVAC 1108 computer use on remote batch terminals that operate in a time sharing mode.

7. Mass properties. The *Mariner* Mars 1969 spacecraft system design area retained control of mass properties and analytically determined weight and center-of-gravity values for *each* 1969 spacecraft that was assembled. The calculations were for several spacecraft configurations and were generated from raw weight data found in quality assurance SAF logs on parts weighed as they entered SAF.

The calculated weights were obtained by a computer program which performed summation of all component parts and/or black box weights.

Although the final spacecraft weighing was done at AFETR the line item weights were actually measured in SAF at JPL Pasadena. The many measurements required were made, out of necessity, on different days, by different people and on different measuring equipment. In addition, some line item weights were estimated.

Therefore, considering the error sources involved, it was significant that the calculated spacecraft mass properties closely correlated with the measured spacecraft values made at SAF.

In addition, the program would also calculate and print moments and products of inertia values (in slug-feet squared). By reliance solely on actual measured mass properties at the spacecraft systems level the constraint is that it was not practical to physically measure more than about two different spacecraft configurations.

The development of a spacecraft weight control matrix proved to be a very useful tool on *Mariner* Mars 1969. This was a two-dimensional matrix of spacecraft subsystem equipment weights versus physical location on the spacecraft. This matrix had information on spacecraft mass properties and was handy as an aid to control weights per allocations to each subsystem.

The weight summary was also a one page report which summarized weight in subtotals such as science, scan platform rotated weight, science support subsystems, engineering subsystems, etc.

8. Launch and hold criteria document. Inputs to the launch and hold criteria document had to be made by spacecraft system personnel and these inputs had to be coordinated by the spacecraft test director and the spacecraft system engineer. Similar inputs to the preparation of that document had to be provided by both the launch vehicle and Mission Operations System personnel. The spacecraft launch and hold criteria classified each telemetry measurement and unbilical function into two categories for making decisions. The two categories are (1) mandatory, or (2) primary. Both the cognizant subsystem engineer and the spacecraft system engineer must sign approval to each measurement criteria.

C. Configuration Control

When the project documents and plans were prepared for configuration control of the 1969 project, only modifications resulting from the minimum changes and the new payload were expected from the *Mariner* Mars 1964 design. However, the lack of availability in 1966 for parts used several years earlier in the 1964 design was one major factor in the decision to make major iterations to the old design. The consequence was that the spacecraft design was not as mature at the start of the phase II activity as originally expected. The result was that a number of minor corrections had to be incorporated in the design drawings and specifications.

First, the design documentation was classified into design control and design documents (see Table 1). Changes to design control documents required engineering change requests (ECRs) following their initial release.

Table 1. Classification of design/control documents

Documents	
Design control	**Design**
Functional requirements	Assembly drawings
Design requirements	Detail drawings
Interface control drawings	Detail specifications
Circuit data sheets	Manufacturing process specifications
Thermal data sheets	Parts lists supporting the drawings
Project parts control lists	Parts specifications (including requirements, procurement and screening specifications)
Electronic packaging specifications	Acceptance test procedures
Type approval and flight acceptance test specifications	

Flight hardware was manufactured only to formally released design documents and ECIs were required to track changes to the design documents. On December 1, 1967, ECRs were required on changes to all design and design control documentation. At that time most of the errors and minor corrections had been made and a reasonably accurate set of documents were available when the PTM subsystems started delivery into SAF on January 2, 1968.

D. Control of System Interfaces

The interfaces between the spacecraft system and the other major systems in the project were defined and controlled through use of three interface control documents:

(1) Spacecraft-DSN communications interface document

(2) Spacecraft-MOS interface document

(3) Spacecraft-launch vehicle interface document

In general, each interface control document was accompanied by a compatibility test plan which defined a series of tests designed to demonstrate the degree to which the interface requirements defined in the interface control document had to be reflected in the hardware.

The telecommunication interface between the spacecraft system and the DSIF was defined to consist of the following:

(1) The spectrum characteristics of the uplink transmission from the DSIF stations to the spacecraft including the carrier and the ranging and command modulation.

(2) The spectrum characteristics of the downlink transmission from the spacecraft to the DSIF stations including the carrier and the ranging and telemetry modulation.

(3) The spectrum and hardline characteristics of the modulation signal from the spacecraft to the DSIF transmitters.

(4) The combined effects of the characteristics parameters of the spacecraft and the DSIF necessary to guarantee performance.

The spacecraft/MOS interface was defined in the command link and in the telemetry link between the SFOF and the spacecraft.

The command link interface includes: (1) the processing and punching of a paper tape containing coded commands (CC) or quantitative commands (QC) by the telemetry and command processor (TCP) and (2) the loading and verification of prepunched paper tapes containing direct commands or TCP punched tapes containing CC or QC into the read, write, verify (RWV). Descriptions of the commands and the punched paper tape formats control these two points of the interface.

The interface in the telemetry link exists in the TCP, where the spacecraft telemetry data is received for processing. Data rates, data modes, and data formats control this point of the interface.

The spacecraft-launch vehicle interface was defined to include certain physical and functional aspects of the spacecraft and launch vehicle equipments.

The normal in-house ECR procedure applied only to the spacecraft design book and subordinate documentation. Special revision and change control procedures were developed for the interface control documents.

The following procedure was employed to effect changes to the text of the interface control documents:

(1) The system desiring a change had to request approval of the change by the other system and will provide available information supporting the need for a change.

(2) When satisfactory agreement was reached, the change had to be approved by the two system managers.

(3) The *Mariner* Mars 1969 spacecraft system manager was responsible for publication of amendments to the document.

(4) Revisions to the document could include only mutually agreed-upon amendments. Each document revision was to be numbered sequentially.

E. Control of CC&S and Spacecraft Mission Interfaces

The many CC&S interfaces with the rest of the spacecraft and the role the CC&S plays in flight operations were such that a complex system integration activity was required to verify the design. Also, later but prior to each launch, there were several system level functions required in the process of establishing launch readiness. These functions were to:

(1) Provide initial known event times and system level flight program constraints for generating CC&S programs.

(2) Assist in the generation and checkout of launch tapes. (These tapes contain data generated by the COMGEN computer program used to update the onboard CC&S prior to launch.)

(3) Assist in making the CC&S load and verify checks of computer memory.

(4) Provide system level inputs to establish CC&S constraints in the overall launch and hold criteria requirements.

III. Initial (Baseline) System Design

The task of the system design team was to establish what the minimum changes entailed. Certain changes were recognized and were planned for, while others were put under consideration.

A. Configuration Selection

The spacecraft system design activity resulted in two configuration layouts. The first contained a fixed high-gain antenna, a scan platform, and data storage capacity consistent with an assumed science payload. The second configuration had a two-position, moveable high-gain antenna, a scan platform, and data storage subsystem consistent with the requirements for another assumed science payload.

The fixed high-gain antenna configuration, selected later, was initially thought to involve a period of communication blackout on the order of about a week plus a gray-out period of a month or more occurring during the latter part of the cruise phase. A two-position moveable high-gain antenna, although it was never used, was a configuration that eliminated this undesirable characteristic.

The spacecraft system was initially committed to a design goal weight of approximately 835 lb with a 10% contingency, which included everything forward of the *Centaur* field joint. The final total weight of 908.03 lb was a marked increase over the *Mariner* Mars 1964 weight of 575.6 lb.

The science payload selection and a decision on whether or not to use type II trajectories constituted two key problems affecting the spacecraft system. The design of practically every subsystem was affected by the selection of the science payload. The selection of the science payload had to be accomplished by the target date of May 16, 1966, to avoid serious problems in the areas of both spacecraft design and procurement.

The use of type II trajectories impacted the spacecraft system both in the design of the spacecraft and the spacecraft planning schedule. The type II trajectory launch period opened about 3½ mo before the type I. The time allotted in the spacecraft schedule, from the start of fabrication to delivery to AFETR, could not be shortened, therefore the initiation of fabrication for a type II trajectory spacecraft would have to start 3 to 4 mo ahead of initial scheduling.

The use of type II trajectories was thought to require a third antenna to be incorporated in the configuration, in addition to the low- and high-gain antennas. This third antenna would have had to be moveable, with at least two positions.

Operating under the minimum-change guidelines and design philosophy, a baseline spacecraft design was conceived, together with a baseline flight profile. The spacecraft subsystems are shown in Fig. 1. with the detail conceptual-design changes listed in Table 2.

B. Baseline Flight Profile

The initial flight profile represented an advance from the *Mariner* Mars 1964 profile even though this spacecraft design was also for a flyby mission. Like the spacecraft design, the flight profile continued to change from 1966

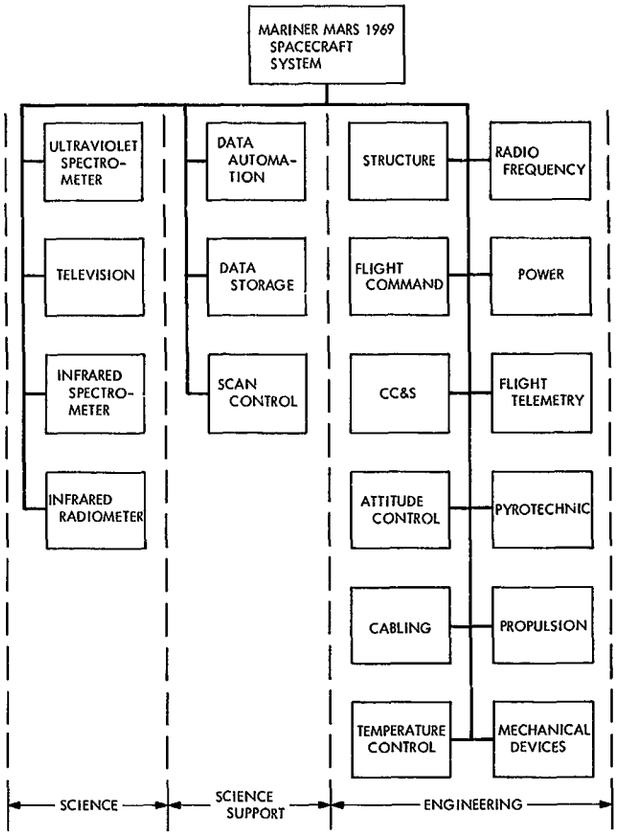


Fig. 1. *Mariner* Mars 1969 spacecraft subsystems

to 1969. The initial (baseline) flight profiile was outlined as follows.

1. Launch phase. In the launch phase, each of the two *Mariner* Mars 1969 spacecraft was to be boosted into the interplanetary transfer trajectory toward a Mars encounter by the *Atlas-Centaur* launch vehicle. The substitution of the *Centaur* stage for the *Agena* stage imposed new requirements on the spacecraft design, and during launch subjected the spacecraft to a new acoustical and vibrational environment. The launch profile could be either parking orbit or direct ascent. The shroud was the *Surveyor* design and RF transparent. As two travelling wave tube (TWT) power amplifiers were to have been incorporated in the radio subsystem for which there was to be one power mode, the flight profile at that time assumed that TWT power would be on, and radiating 10 W of RF from liftoff.

At the termination of the launch phase, the spacecraft was to be separated f ⁻ the *Centaur* launch vehicle, on

Table 2. Initial *Mariner* Mars 1969 design changes from *Mariner* Mars 1964 design

Subsystem	Design change[a]
Structure	Modify structure to accommodate changes to other subsystems Relocate umbilical connector Redesign packaging for bays 3 and 7 Move propulsion equipment outboard Interface with *Centaur* launch vehicle
Radio frequency	Two TWT power amplifiers TWT power-up at launch Move receiver equipment from bay 5 to bay 6 Receive on low-gain antenna only
Telemetry	Change telemetry channel assignments Incorporate new data modes Three bit rates: 66⅔, 33⅓, 8⅓ Process digital data from approach guidance and CC&S
Flight command	Reassign isolated switch outputs to direct commands
CC&S	New memory-oriented programmable sequencer Redundant capability for maneuver sequencing
Attitude control	Canopus sensor modifications Add stray light sensor; delete Earth detector Repackage attitude control electronics
Power	Redesign boost-regulators Redesign inverters Incorporate timing reference Redesign battery charger Redesign power distribution logic Incorporate four secondary Sun sensors N-on-P solar cells
Mechanical devices	Redesign scan platform for two-degrees-of-freedom Redesign scan platform for increased science weight
Temperature control	Temperature control power to scan platform Add temperature control flux monitor; delete absorptivity standard Modify temperature control surfaces as required

[a]No changes were anticipated for the propulsion subsystem, a new subsystem was planned for the approach guidance, and a new design for the science subsystem.

Table 2 (contd)

Subsystem	Design change[a]
Cabling	Redesign cabling to *Mariner* Mars 1969 requirements
Data storage	Delete *Mariner* C video storage subsystem Incorporate *Mariner* Mars 1969 data storage subsystem Digital recorder Analog recorder Record and playback electronics Analog-to-digital converter for data transfer
Scan control	Control for two-degrees of-freedom platform Closed loop servo for far encounter Open loop control for near encounter Open loop control for UVS
Pyrotechnic	Delete current to scan cover solenoid Add UVS cover squib Add IRS gas bottle squibs

command from the *Centaur*. The use of the *Centaur* required a new mechanical and electrical interface. The adapter was to use the *Mariner C* design at the separation plane, and the *Surveyor* design at the field joint, with JPL maintaining design responsibility down to the field joint. The use of the *Surveyor* shroud required that the spacecraft umbilical lines be routed down through the adapter and out the *Centaur* umbilical island.

2. Acquisition phase. Following separation from the launch vehicle, the spacecraft was to acquire the Sun, and immediately commence Canopus acquisition. No magnetometer roll calibration as performed on *Mariner C* would be required, for no magnetometer was included in the *Mariner* 1969 science payload. The Canopus tracker was to incorporate an adaptive gate for star brightness which could be successively lowered by cyclic command from the CC&S until a celestial object, hopefully Canopus, was acquired. Then the spacecraft would center into the cruise phase of the mission.

3. First cruise phase. The spacecraft was to start the cruise phase transmitting engineering data at 33⅓ bits/s over the low-gain antenna. During the flight, the cone angle of the Canopus tracker was updated by programmed command by the central computer and sequencer (CC&S). When the communications performance dropped to the sum of the negative tolerances, the CC&S would command the telemetry subsystem to lower the bit rate to 8⅓ bits/s. When the communications performance dropped again into greyout, this time at 8⅓ bits/s, and after several days in greyout, the CC&S would command the radio subsystem to switch the power amplifier to the fixed high-gain antenna. The communications performance would rise rapidly at 8⅓ bits/s on the high-gain antenna, and after a suitable performance margin had been obtained, the telemetry bit rate would be switched to 66⅔ bits/s, the bit rate which at that time was planned for the encounter mode, and the first part of the playback mode.

4. Maneuver phase. The cruise phase was to be interrupted early in the flight in order to perform the first of two possible trajectory correction maneuvers. As on *Mariner C*, the capability for a second maneuver was to be provided for in the design. On *Mariner* Mars 1969, redundancy in the maneuver logic was to be present, in that the CC&S would have a separate fixed sequencer for the maneuver functions.

In the tandem maneuver mode, the CC&S would compare the output of the programmable sequencer against the output from the fixed sequencer. In the event of a discrepancy, the maneuver would be automatically aborted. The capability would exist, by ground command, to select the correctly functioning part of the CC&S and to repeat the maneuver sequence.

5. Second cruise phase (and approach guidance). Ten days prior to arrival at the planet, an approach guidance subsystem was to have been turned on, this being the last event of the cruise phase of the mission.

An approach guidance subsystem was to have been assigned so as to optically track the center of the planet Mars during the time from 10 days until 12 h before encounter. The cone and clock pointing angles to the center of Mars were to have been measured in the spacecraft reference system. Those angles, in conjunction with the Sun and Canopus sensor error signals would be telemetered to the ground where they were to have been processed and used in an orbit determination program to compute the near planet trajectory of the spacecraft.

6. Far-encounter phase. Both the near-encounter and the far-encounter was to be conducted in the encounter date mode at 66⅔ bits/s. The encounter data mode of *Mariner* Mars 1969 was to be analogous to the cruise data mode of *Mariner C* in that 140 bits of engineering data would be followed by 280 bits of science data.

There would be no data mode equivalent to the all-science data mode 3 of *Mariner C*.

At the start of the far-encounter sequence, the scan control, the television, the infrared radiometer, and the data automation subsystems would be energized. The scan platform would have 2 degrees-of-freedom, one in cone and one in clock, and would provide support to the two-camera television subsystem, the infrared spectrometer, and the infrared radiometer. After the science instruments warmed up, and sufficient time has passed for the mission operations system to evaluate the performance of the spacecraft in the far-encounter mode, the scan platform would be commanded from the erected near-encounter position with cone angle equal to approximately 120 deg, to the far-encounter position. Once the planet brightness was above threshold for the far-encounter planet sensor, the scan control subsystem would switch from open-loop pointing to a closed-loop mode and servo on the planet. A series of far-encounter TV pictures would be taken by the narrow-angle television camera starting at the time of closest approach minus 48 h and continuing to the time of closest approach minus 12 h. The picture data would be stored on a *Mariner C*-type tape recorder using an analog recording scheme. At the conclusion of the far-encounter sequence, the scan platform would then be commanded back to the near-encounter position.

7. ***Near-encounter phase.*** The near-encounter sequence was to commence several hours prior to closest approach. At that time all the science instruments would be energized. The scan platform was fixed at a cone angle of 120 deg, a position identical on both spacecraft and fixed at one of a number of selectable clock positions. The clock position could be stepped by ground command through a number of discrete positions in 3-deg increments. Thus no servo sensor or closed-loop planet tracking was presently envisioned for the near-encounter sequence.

About 20 min prior to the start of near-encounter data taking, cooling of the infrared spectrometer detectors would be initiated by CC&S command. When the planet came within the view of the narrow-angle television camera, near-encounter data taking would commence.

Because of the large increase in the required amount of data storage, due not only to the increased number of TV pictures, but also to the increased number of lines and elements per picture, a new mechanization was proposed for the data storage subsystem. The new mechanization made a 30-fold increase in data storage, from 5.2×10^6 bits on *Mariner C* to 1.8×10^8 bits for *Mariner* Mars 1969. The mechanization consisted of two *Mariner-C* type endless loop tape recorders. One recorder stored 2.3×10^7 bits in digital form; the other recorder stored 1.6×10^8 equivalent bits in an analog manner.

During the near-encounter data taking sequence, the scan platform would be slewed from a cone angle of 120 deg to a cone angle of approximately 90 deg, in order to extend the duration of the sequence. The data taking was to continue until both the analog recorder and the digital recorder were full.

8. ***Occultation.*** About 1 min after the data-taking stopped, the spacecraft was to enter occultation, and be occulted from Earth for approximately ½ h. After exit from occultation, several hours of engineering data would be required for engineering analysis of the spacecraft by the mission operations system, prior to the start of the playback phase of the mission.

9. ***Playback phase.*** The original conceptual design of the *Mariner* Mars 1969 playback phase was considered more complicated than *Mariner C* in that periodically, roughly every 3 days when transmitting at 66⅔ bits/s, data would be transferred from the analog tape recorder, through an analog-to-digital converter, and re-recorded on the digital machine.

The playback phase was to begin at a bit rate of 66⅔ bits/s, until the communication performance starts to degrade, and then the bit rate would be commanded to 33⅓ bits/s for the rest of the mission.

The initial mission plan called for playback of the recorded data once, which at 66⅔ bits/s would require 35 days, assuming 2 h of engineering telemetry per day.

IV. Design Evolution

A. Spacecraft Design Changes During Development Cycle

The period of time between the documentation of the initial *Mariner* Mars 1969 spacecraft system design and launch was nearly 3 yr. That period was used to develop, test and verify the adequacy of the design to successfully accomplish the mission. As a result there were many design changes, both the detail and functional type. The changes discussed in this section were system level in that they affected subsystem interfaces, system logic or operational practices. A system level change may also be

a change that is totally within the confines of one subsystem if the change affects one or more of the following system design areas:

(1) Spacecraft power allocations or profile.

(2) Spacecraft weight or CG location.

(3) Telemetry channel assignment.

(4) Mission capability.

(5) Mission Operations System (MOS) or Deep Space Network (DSN) interfaces.

The major system level changes that were incorporated during the development cycle prior to shipment to Cape Kennedy are listed in sequence of occurrence by affected subsystems, but not chronologically from subsystem to subsystem.

1. Structure subsystem. The high-gain antenna was modified to a circular aperture type. When higher bit rates were selected to minimize data retrieval time, it followed that the performance could be increased for the shorter playback period by changing the antenna pattern.

The 6-mil solar panel cover glass was replaced with 20-mil cover glass. The purpose of this substitution was to provide more protection against solar panel solar flare damage. This incorporation adds approximately 25 W to the capability of the solar panels in the case of maximum solar flare damage.

2. Radio frequency subsystem. The difficulty in procuring a 10-W TWT amplifier (TWTA) tube similar to the tube used for *Mariner C* led to the selection of an available TWT with output power levels of 20 and 10 W, respectively. This change increased the feasibility of higher playback rates and also block coding.

The overcurrent circuit was changed to prevent possible on-line hang-up of an overcurrent TWTA. Fuses were added, and the overcurrent detection and correction circuit was modified to prevent the catastrophic loss of the spacecraft in the event the RFS would switch over to a shorted TWT.

An RFS false-lock problem was recognized but the risk was minimized since it was decided that it could be handled through operational procedures on the ground.

3. Flight command subsystem. The 1.5 dB improvement in subsystem performance, 0.99 probability-of-lock on the first correlation (vs 0.3 for *Mariner C*), and a maximum acquisition time of 9.5 min (vs 30 min for *Mariner C*) were the reasons for incorporating the automatic acquisition detector in the 1969 FCS.

For purposes of redundancy, additional interface circuitry was added between the FCS and the CC&S to provide two separate paths for coded commands to reach the CC&S. One path led to the fixed sequencer and the other led to the computer.

4. Central computer and sequencer subsystem. The CC&S controlled the scan platform slew operation through the DAS. A change was made to obtain direct CC&S control of scan pointing. This allowed greater flexibility in timing the slew operations, and permitted a functionally redundant means for backup of the slew commands (ground command), as well as simplifying the DAS.

An *internal-abort* signal transferred the CC&S computer out of the maneuver routine and back into the cruise routine. Ground command maneuver abort signal DC-13 now performs the same function.

Spare relays were utilized to add the following onboard CC&S command capability: N10—platform cone slew positive; N11—platform cone slew negative; F3—analog erase; P2—playback mode. Command N5 (near-encounter terminate) was modified so it no longer changes FTS data mode.

Single word readout of the CC&S was made an open action item since this capability was needed if CC&S were inhibited for some reason. Later it was incorporated in the software.

5. Power subsystem. Before the addition of the redundant 2.4-kHz inverter, a number of single failures in the main inverter could result in the catastrophic loss of the spacecraft. Other changes were as follows:

(1) Battery test load (DC-50) was added.

(2) Power distribution module was reconfigured to accommodate temperature control changes.

Boost enable/inhibit indication was implemented on channel 224 ($-Y$ solar panel current), so when the boost circuit in power was inhibited (DC-37) channel 224 reads high data number (DN) or noise. It was still possible to determine the $-Y$ solar panel current from other measurements, but with slightly degraded accuracy.

Signal DC-3 was made to no longer turn science power off when starting playback. Potential power subsystem problems resulted from encounter turn-on causing a transient share mode but no major change was incorporated.

A fuse box was added to the power subsystem to house the fuses for the spacecraft temperature control heaters. Location of the fuses at the power source provides the maximum fusing protection by protecting against shorts in the cabling as well as in the heaters. It also provided a single access for heater fuse inspection and replacement during system test and launch operations.

A new command titled *heater power switch* was incorporated. This new command toggled the dc thermostatic heaters which were under the science platform thermal blanket between the dc buss and the battery. It provided the capability to improve the solar panel power margin during encounter, if circumstances dictate. It also provided a means for inflight checks on the condition of the battery.

The voltage fail-sense circuitry in the power subsystem was moved from the output of the 2400-Hz inverter to the output of the booster regulator. This change improved the capability of the fail-sense circuitry to sense out-of-tolerance voltage conditions.

6. Pyrotechnic subsystem. A current-limiting resistor was added to reduce turn-on transient at separation because pyro turn-on transients at spacecraft/launch-vehicle separation exceeded specification. A fix was made to limit the turn-on transient.

7. Propulsion subsystem. The use of a spontaneous catalyst, instead of the bipropellant start technique used on *Mariner C*, greatly simplified the operation of the propulsion subsystem, thereby increasing system reliability.

A new mounting of the propulsion unit offset the decrease in weight caused by the change to spontaneous catalyst, resulting in a net gain in weight.

8. Attitude control subsystem. Gyro turn-off DC-40 was incorporated to disable a malfunctioning gyro without having to disable the Canopus brightness gate.

Jet vanes and ring assembly were redesigned to improve accuracy of maneuver.

Turn-on of the Canopus tracker was delayed from spacecraft/launch-vehicle separation (PAS event) to a later time to ensure complete outgassing of the tracker prior to application of high voltage.

The attitude control pitch and yaw deadbands were reduced in half without any increased gas consumption, thus providing better antenna alignments and improved instrument pointing accuracies.

The gyros-on event to flight telemetry subsystem (FTS) was eliminated.

9. Flight telemetry subsystem. New FTS changes to design were:

(1) The elimination of the PN sync channel from the composite telemetry signal.

(2) Only DAS data was allowed on data channel A during the encounter mode.

(3) Engineering data was restricted to data channel B at 8⅓ or 33⅓ bits/s.

a. FTS synchronization. The removal of the PN sync channel greatly simplified the FTS by removing all sync interfaces between the FTS, the data storage subsystem, and DAS. The power which was allocated for the sync channel now used for data channels, thereby further increasing performance.

b. High rate channel. A block coder with a capability of 16.2 k bits/s was added to provide a high rate channel. The use of more than one data channel permits continuous monitoring of spacecraft performance in the playback data mode, eliminates the complex switching previously required to interrupt playback to monitor spacecraft performance, and increases the quantity of real time science that can be transmitted in the encounter mode.

c. Subframe sync. The replacement of the 7-bit sync word by a 15-bit PN sequence for subframe synchronization was necessary since, with the elimination of the sync channel, there was a high probability of false synchronization on seven consecutive ones which might appear anywhere in a subframe.

d. Engineering rates. Deletion of the 66⅔ bits/s engineering rate simplified the FTS design without compromising any measurement sampling requirements.

e. Subcommutation identification. A high-rate word was made to identify the medium and low-deck positions of the commutator. This permitted the replacement of the low-deck sync words with data measurements and enabled the ground decommutator to obtain total frame sync during one subframe time.

f. Timing reference. The 480-kHz crystal oscillator was included in the FTS because: (1) the 2400-Hz signal could not be conveniently used to generate the higher frequency for the sub-carriers, and (2) the 307.2-kHz signal available within the power subsystem was also not a frequency which could be conveniently counted down to the required sub-carrier frequencies.

g. Elimination of the ground telemetry subsystem. Bit synchronization and decommutation was performed by the telemetry and command processor (TCP). The use of bit synchronization in the TCP resulted in a performance increase of 0.9 dB in the engineering channel.

h. Mixer-amplifier redesigned to improve signal-to-noise ratio. Faster rise and fall times improved signal-to-noise ratio for high-data-rate link.

i. Isolation amplifier for PAS added in event counter 3. PTM tests showed that the PAS/FTS interface shorted out event counter 3, and blocked all future counts to that channel.

j. Circuit changed to inhibit all alert pulses after the first issued to CC&S upon receipt of DC-2 (CC&S readout). Formerly, when FTS was in the CC&S computer readout mode, it sent alert pulses every 4.2 s to CC&S. The FTS logic was modified to only issue one alert pulse. This simplifies the computer readout program.

10. Data storage subsystem. New changes to design were:

(1) Direct digital playback of the data stored on the analog tape recorder at a rate of 16.2 kbits/s using block coding.

(2) Real-time transmission of the data stored on the digital tape recorder at a rate of 16.2 kbits/s using block coding.

(3) Elimination of the slow record speed (8.1 kbits/s) of the digital tape recorder.

(4) Only one digital recorder playback speed.

a. Playback rate. The 270 bits/s playback rate was selected for better compatibility with the overall telecommunication design. This rate shortened the playback period for all data from one spacecraft to 8 days. The elimination of the second rate simplifies the overall design.

b. Digital record rate. Deletion of the slow record mode on the digital recorder simplified the data storage subsystem motor design and the DAS timing and control logic.

c. Digital recorder playback. To increase the reliability of obtaining all the UVS, IRS, TV, and IRR data recorded on the digital tape recorder during encounter, the first playback of this recorder will be repeated. This data gets erased during transfer of data from the analog recorder.

d. Analog data playback. The block coder permits the direct digital playback of the analog recorder data through an analog-to-digital converter. This provided an alternate path for data retrieval thus increasing mission reliability.

e. Data storage subsystem input power. The deletion of the 400-Hz power to the data storage subsystem was possible because the subsystem internally generates the frequency required to drive the two-phase motors.

f. Power switching. The redesigned spacecraft logic made it possible to turn off data storage subsystem power during the cruise phase.

g. Dual co-belt replaced with single pressure belt. A single pressure belt improved the fidelity of the data storage subsystem.

h. Data storage. A data phase-lock loop was added to replace the zero-crossing detector.

11. Data automation subsystem and science data

a. DAS encounter timer. The encounter timer was deleted primarily because of the inflexibility of a hardwired timer.

b. Encounter science data return capability added. Block coding permitted the transmission in real time of the 16.2 kbits/s data which was being recorded on the digital tape recorder. This provided an alternate path for retrieving the data and thus increased mission reliability.

Circuitry was added to turn on the data storage subsystem power upon receipt of CC&S command P1. This incorporation formed a part of the means used to remedy a spurious command problem which existed between the DAS and the data storage subsystem.

12. Scan control subsystem and scan platform

a. Near-encounter clock references. By eliminating one of the two near-encounter clock position reference potentiometers, the scan control subsystem was simplified, and two QCs as well as two umbilical functions were eliminated.

b. Scan cone step under CC&S control capabilities added. The CC&S can now incrementally slew the platform in cone, as well as clock.

A structural interference between the scan platform and the buss which restricted the motion of the scan platform in certain cone-clock angles was eliminated, thereby permitting the elimination of the slew sequencing logic in the scan control subsystem.

In order to reduce the forces imparted to the scan platform when being unlatched, a pneumatic system was designed to latch it in four places at the same time. Release of the platform is effected when either CC&S command C5 or ground command No. 45 causes one valve-squib to fire, releasing compressed gas.

13. Temperature control. In the temperature control area, white paint was used on the back of the solar panels rather than black paint in order to maintain the solar panel temperatures during ascent heating within acceptable limits. A heat pipe was proposed to be added to the face of the radio bay to reduce the thermal gradients across the face of the bay which will reduce the temperature on the traveling wave tube.

The heat pipe medium was changed from H_2O to NH_3 and louvers on bay III were replaced with a thermal shield. Later the heat pipes were eliminated due to the TWTA temperature being lower than originally expected and the heat pipe being less effective than estimated.

Louvers were added for platform temperature control, ac and dc heaters were reconfigured, a DC-34 backup heater was added, as was a plastic insert in the scan clock tube, and the thermal design of the scan platform was optimized as follows:

(1) Heaters were changed in the TV circuit.

(2) Heaters were added to the platform structure.

(3) The use of the DC-34 was redefined from IRS to platform backup.

14. Science subsystems

a. TV covers. TV optical covers were included to protect against lens degradation due to contamination or particle impingement. Later the TV-B cover on the narrow-angle TV optics was deleted.

b. Infrared spectrometer. The material of the H_2 tank was changed from inconel to aluminum.

c. UVS cross-cone pointing angle changed from −4.8 to −3.0 deg. Analysis of planet scan traces by use of the planetary encounter geometry and science instrument scans (PEGASIS) program revealed that a −3.0 deg offset in cross-cone produced a more favorable planet scan for the UVS.

d. Promethium 147. Promethium 147 was eliminated from the spacecraft design as a source of heat because of its incompatibility with the ultraviolet spectrometer and electrical heaters were used to replace it.

e. UVS dc heater removed. Changes to the temperature control design of the platform, including the addition of louvers on the UVS, deleted the requirement for a heater in the UVS.

f. IRS strain gages and wires added to monitor H_2 pressure on pad. It is possible, by means of the launch complex Equipment, to monitor the pressure of the H_2 and N_2 high pressure bottles of the IRS.

g. IRS gas-cooling vent nozzle relocated. The IRS gas-cooling vent nozzles were relocated from the sides of the octagon to the ends of the bridge tube on the scan platform. This was necessary in order to meet the requirements on the uncertainty in the magnitude of the thrust produced by the exhaust gas.

h. Cover-removal function deleted. As a followup to the deletion of the ultraviolet spectrometer covers, the pyrotechnic cover-removal function that was to be used was deleted also.

i. New motor-start signal. Due to a cold-welding problem in the infrared spectrometer motor gear train, the motor could not be operated for 48 h in a vacuum

environment. This posed a problem since all the science instruments were turned on at 48 h before encounter. To solve this problem, the signal from narrow-angle Mars gate No. 1, scheduled occurs at approximately 35 min prior to encounter, was thereby used to start the motor while at the same time initiating the cooldown. Ground command No. 49 backs up the narrow-angle Mars gate signal.

B. Encounter Sequence Design Changes During Development Cycle

1. Far-encounter functional design

a. The old far-encounter sequence (prior to August 1968). The old far-encounter sequences were:

(1) A nominal sequence of eight pictures was recorded on 4-h centers between $E - 40$ and $E - 12$ h.

(2) Optional sequences of three sets of 32 pictures were recorded on 39-min intervals between $E - 72$ and $E - 4$ h (all far-encounter pictures were played back prior to near encounter) and two sets of 32 pictures were recorded on 39-min intervals between $E - 72$ and $E - 28$ h. All 64 pictures were played back prior to $E - 24$ h and eight pictures were recorded on 103-min intervals between $E - 24$ and $E - 12$ h.

b. Disadvantages of old sequences. The disadvantages were:

(1) Nominal sequence pictures on equal intervals do not allow picture-area selection.

(2) Optional sequence for 96 pictures was not completed until $E - 54$ min.

(3) They required extensive in-flight CC&S reprogramming in order to execute either optional sequence.

(4) Loss of ground command during either optional sequence would cause loss of near as well as far-encounter data and pictures.

c. The new far-encounter sequence. The new far-encounter sequence was:

(1) A nominal sequence of eight pictures was recorded on arbitrary intervals between $E - 23$ h and anytime prior to $E - 7$ h.

(2) An optional sequence of 17 pictures was recorded on periodic intervals between $E - 23$ h and anytime prior to $E - 7$ h.

(3) Extra sequences of two sets of 33 pictures were recorded on 37-min intervals between $E - 72$ and $E - 28$ h. All 66 pictures were played back prior to $E - 24$ h. At $E - 24$ h either the nominal sequence or the optional sequence could be implemented.

d. Merits of the new sequence. The new sequence permits the following:

(1) Basic sequences are programmed into CC&S prior to launch. The optional or extra sequences can be initiated in-flight by only sending one or two DCs.

(2) Science power is not cycled on/off. Power always remains on.

(3) The sequences always protect the near encounter sequence in case ground command is lost.

(4) More time is given to MOS operations in preparation for the near encounter sequence.

(5) It allows for selecting the picture area for each of the eight nominal pictures by allowing the recording of the eight nominal pictures to be at arbitrary times.

(6) There is integrated use of CC&S commands with ground commands to reduce the number of DCs required.

2. CC&S program for encounter operations

a. Nominal sequence. An eight-picture nominal sequence results if there are no ground commands.

b. Optional sequence. An optional sequence replaces the nominal sequence if DC-32 is received anytime prior to $E - 24$ h. This results in:

(1) Seventeen pictures taken on 59-min centers.

(2) Automatic erasure inserted just prior to near-encounter for protection.

c. Extra sequences. An extra sequence is enabled and selected by a CC-pair and DC-13. This results in:

(1) Thirty-three pictures taken on 37-min centers.

(2) Automatic erasure inserted just prior to nominal/optional sequence for protection.

(3) Extra sequence decision independent from optional sequence decision.

(4) Extra sequence is repeatable.

3. Development for nominal/optional extra capability.

The development resulted in:

(1) An approach evolved toward integrated sequencing routines.

(2) A cycle generator evolved which was used for extra sequence, optional sequence, and near-encounter slewing.

(3) The computer-only maneuver capability was deemphasized.

V. Spacecraft System Description

A. Spacecraft Design

The spacecraft system proved to be capable of achieving 10^{21} different logic states. A breakdown of subsystem states is given in Table 3, and state diagrams are presented in the various functional discussions in succeeding paragraphs.

The most prominent cause of the majority of the changes was the new science payload and the new scan platform for pointing the planetary science experiments. (See Fig. 2.)

Mariner Mars 1964 had had a small, single-degree-of-freedom science platform. *Mariner* Mars 1969 had a larger platform with 2 degrees-of-freedom. Actually, the scan platform was almost a separate spacecraft but required the use of the octagon as a source of support for power, communications, and logic as well as shade from the Sun. The platform was supported rigidly to the octagon during the launch period, but in flight it was released so that its only structural tie was through the support bearings.

The mission required the platform be pointable anywhere within the range of an 101- to 165-deg cone angle, where 0 deg is the spacecraft Sun vector, and a 90- to 305-deg clock angle, where 0 deg is the center of bay 8.

The elements of the scan subsystem mounted on the scan platform were: the clock and cone scan drive actuators; the far-encounter planet sensor (FEPS); and two narrow-angle Mars gates (NAMG). The science instruments mounted on the platform were: the ultraviolet spectrometer (UVS); the wide-angle television camera (TV-A); the narrow-angle television camera (TV-B); the infrared spectrometer (IRS), which includes the

Table 3. *Mariner* Mars 1969 spacecraft logic states by subsystem

Subsystem name	States	
	Units	Subsystem
Structures subsystem		1
Major logic state	1	
Radio frequency subsystem		64
10/20 W	2	
Exciter 1/2	2	
TWTA 1/2	2	
Low/high antenna	2	
One/two way track	2	
Ranging on/off	2	
	$2^6 =$ 64	
Flight command subsystem		7
Major logic states	7	
Power subsystem		288
Power chain main/standby	2	
Battery test load on/off	2	
Platform heater 2 on/off	2	
Charger on/off	2	
Booster off/enable/boost	3	
Power source battery/share/panel	3	
Science on/off	2	
	$2^5 \times 3^2 =$ 288	
CC&S		7,680
Processor major states	6	
Maneuver modes	5	
Flag flip-flops (8 of 9)	256	
	$6 \times 5 \times 256 =$ 7,680	
Flight telemetry subsystem		40
Redundant processor	2	
Engineering data/CC&S readout	2	
Engineering data rate	2	
Data modes	5	
	$2^3 \times 5 =$ 40	

Table 3 (contd)

Subsystem name	States	
	Units	Subsystem
Attitude control subsystem		768
Major logic states	16	
Cone angle states (5 + 3)	8	
Tracker low gate	3	
CC&S Y-2 input flip-flop	2	
	$16 \times 8 \times 3 \times 2 =$ 768	
Pyro subsystem		8
Midcourse position 1/2	2	
Midcourse enable/ inhibit	2	
NAMG enable/ inhibit	2	
	$2^3 =$ 8	
Cabling subsystem		2
Separation connector in/out	2	
Propulsion subsystem		2
Burn/no burn	2	
Temperature control subsystem		1
Major logic state	1	
Mechanical devices subsystem		6
Pyro arming switch	2	
Separation initiated timer	3	
	$2 \times 3 =$ 6	

Subsystem name	States	
	Units	Subsystem
Data storage subsystem		14
Major logic states	14	
Data automation subsystem		4
Major logic states	4	
Scan subsystem		8
Major logic states	8	
Ultra-violet spectrometer subsystem		1
Major logic states	1	
TV subsystem		16
Read camera A/B	2	
Shuttering enable/ inhibit	2	
Shutter positions open/closed	2	
Camera A cover on/off	2	
	$2^4 =$ 16	
Infra-red spectrometer subsystem		4
Cooldown/cruise mode	2	
Disk position	2	
	$2^2 =$ 4	
Infra-red radiometer subsystem		6
Major logic states	6	
Total number of system logic states (Obtained by multiplying together the number of states of each subsystem)		1.0×10^{21}

monochromator-telescope, the gas bottles, and the IRS gas disposal system (IRS vent); and the infrared radiometer (IRR). The weight of all sensors, the cone actuator, and the science instruments which move with the platform was roughly 122 lb. Some of the sensors and instruments required thermal and/or electrical isolation from the platform.

The octagon structure is the central body of the spacecraft, providing a cavity into which the electronics are mounted and acting as a rigid frame to which the scan platform, solar panels, antennas, and miscellaneous equipment are mounted, Fig. 3. The *Mariner* Mars 1969 octagon structure was derived from the *Mariner* Mars 1964 structure, the only major difference being the heavier

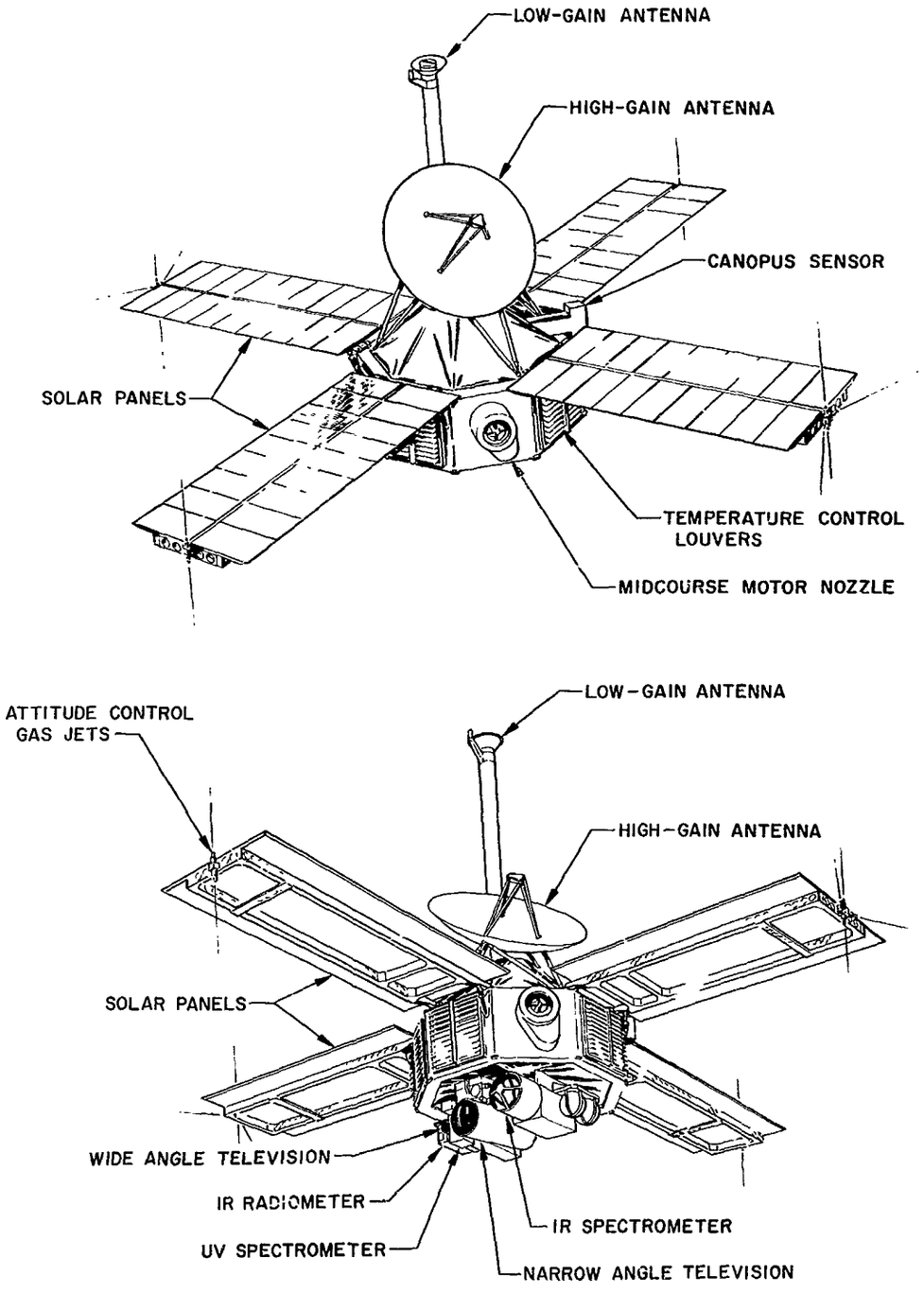


Fig. 2. *Mariner* Mars 1969 spacecraft

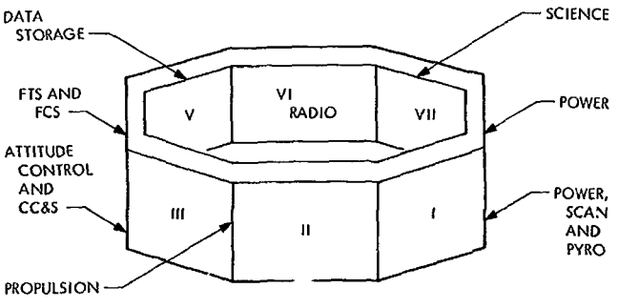


Fig. 3. *Mariner* Mars 1969 octagon structure

scan platform attachment and a new adjustable midcourse motor mounting scheme.

An adapter structure raised the spacecraft high enough to locate the platform between the octagon and the launch vehicle. The extent that the spacecraft could be raised was limited by the nose fairing dynamic envelope and the size of the solar panels.

The solar panels were similar to the *Mariner* Mars 1964 design in construction. The area was increased and the spars were spaced further apart to attach to the outboard corners of the octagon. They were tip-latched and damped similarly to the *Mariner* Venus 67 design. The latches were released by pyrotechnically actuated pin-pullers after which the panels were driven to the cruise position by clock springs and latched to the cruise dampers which were mounted on the octagon structure.

The high-gain antenna was located 24 in. above the octagon. The appropriate pointing direction was determined from the trajectory studies, and a single fixed position proved adequate. The antenna was supported with an aluminum truss structure to clear the solar panels (in their folded position) and the equipment mounted on top of the octagon.

The mechanical configuration is shown in Fig. 4. The spacecraft weight breakdown by location and subsystem, is given in Table 4.

The superstructure and the entire top (sunlit) surface were blanketed with multilayered insulation. This insulation, which also covered the bottom of the spacecraft and most of the instruments on the platform, was part of the temperature control design. The octagon thermal design was similar to that of 1964 except that some of the equipment in the bays was relocated to achieve a better distribution of power. The platform thermal design was different from that used in the 1964 design. The 1969 platform was treated as an independent temperature control problem. It was thermally isolated from the octagon and its temperature was independently controlled using thermal shields, louvers, and electrical heaters.

Two engineering experiments initially entered into the configuration of the spacecraft: the temperature control flux monitor (TCFM) and the planetary approach guidance. The flux monitor was a cone radiometer located at the end of the low-gain antenna so that it had a clear view of the Sun with no view of the spacecraft.

The approach guidance experiment was to view both the Sun and the planet during the period just prior to encounter. This instrument was later dropped from the design before its integration into the design was complete. A functional block diagram of the spacecraft is given in Fig. 5.

B. Spacecraft Power

Spacecraft electrical power is obtained from two sources. The first source consists of four solar panels using N-on-P silicon solar cells with a total active area of 83 ft^2 which can provide at least 449 W of power at encounter. The second source is a 1200 Wh sealed 18-cell rechargeable, silver-zinc battery which furnishes power for limited time periods when the solar panels cannot view the Sun, as during launch and maneuvers.

The main regulated power for the spacecraft is obtained in the following manner: raw dc power from either source is boosted up to 56 V and regulated by the booster regulator. The main 2.4-kHz inverter takes this regulated dc and changes it into a square wave of 50 rms. This power is then switched to various subsystems in response to commands either from the CC&S or the flight command subsystem (FCS).

The battery was to be kept charged by the battery charger, which could be commanded on or off from the ground. A separate boost circuit was also provided which continually monitored the raw dc supply voltage, and if a share mode condition was detected in which the battery was unnecessarily supplying part of the total power, then the boost mode circuitry would return the entire load to the solar panels. The logic state diagram for the power subsystem is shown in Fig. 6.

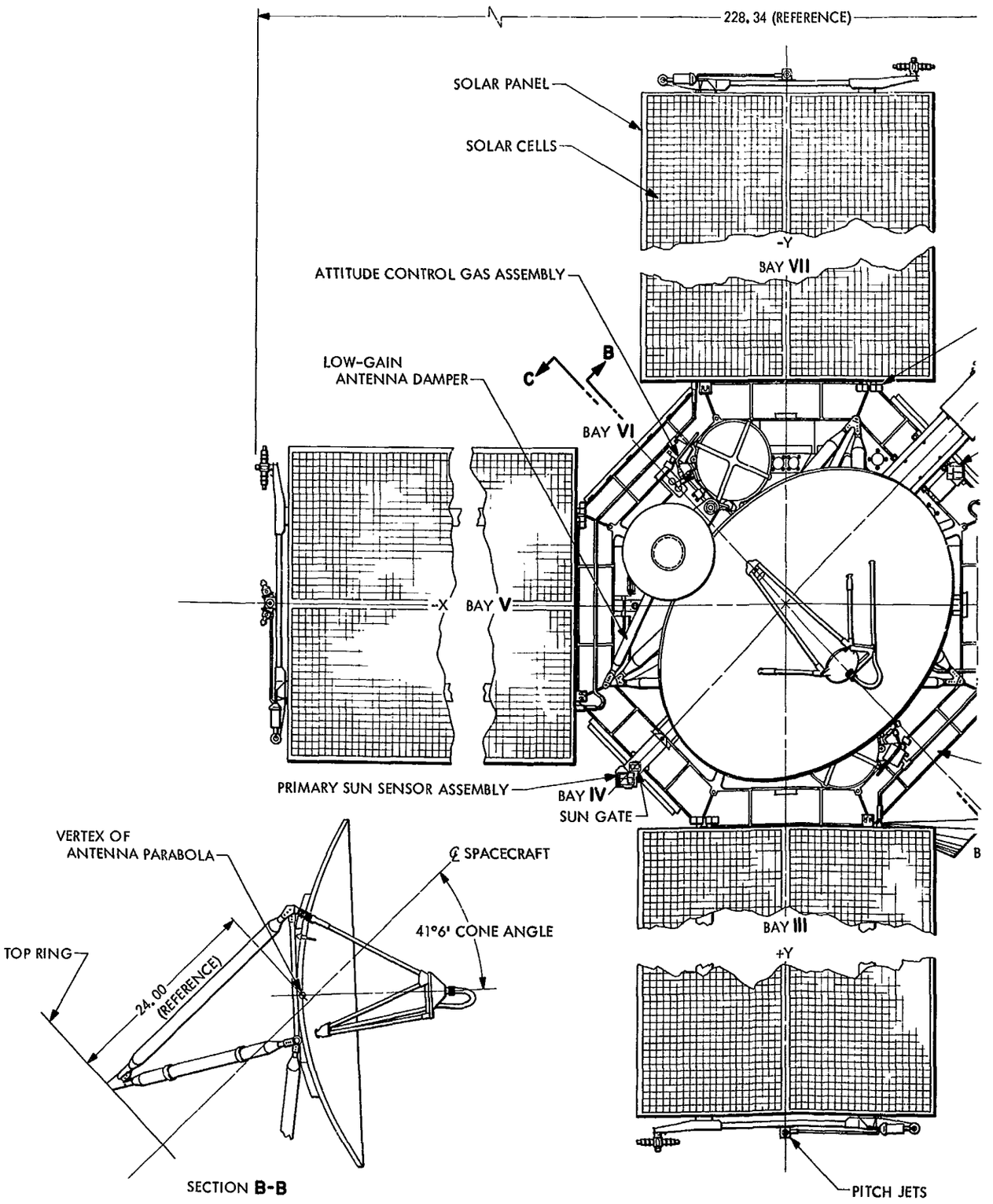
Table 4. *Mariner* Mars 1969 spacecraft[a] weight summary: subsystem vs assembly

Subsystem		Assembly group weight, lb																				Totals, lb		
		Structure	Spacecraft adapter	Scan platform	Miscellaneous assemblies	Electronic assembly I	Bay II	Electronic assembly III	Electronic assembly IV	Electronic assembly V	Electronic assembly VI	Electronic assembly VII	Electronic assembly VIII	Battery assembly	Solar panels	Attitude control gas assemblies	Attitude control sensors	Antenna assemblies	Thermal control assemblies	Pyro devices	Cable assemblies	M69-1 subsystem weight	Contingency	Allocated weight
Structure	01	50.10	55.50	.08	.08	5.00		6.91	4.59	4.80	6.80	6.71	5.06	4.88	57.20		.82	9.00			2.22	219.75		
RFS	02										52.08							.54			1.27	53.89		
FCS	03								8.78													8.78		
Power	04					12.36							24.22	29.38	50.40							116.36		
CC&S	05							19.88														19.88		
FTS	06								20.85													20.85		
Attitude control	07						3.95	18.82								28.30	10.03				2.20	63.30		
Pyro	08		.88	.15		7.95	.60													84		10.42		
Cabling	09		5.85	6.98	1.21	5.47	1.67	5.25	7.37	3.99	2.92	5.24	1.75							2.28	15.34	65.32		
Propulsion	10						42.78															42.78		
Temperature control	11			3.54	.25	5.07	2.60	1.35	1.35	1.35	.80	1.30	1.35						7.26			26.22		
Devices	12		8.19	46.59	3.72										1.36			1.39				61.25		
Data storage subsystem	16									36.44												36.44		
DAS	20											13.56										13.56		
Scan	31			10.57		8.75																19.32		
UVS	34			34.28																		34.28		
TV	36		.12	35.54								14.02										49.68		
IRS	37			38.39																		38.39		
IRR	38			7.56																		7.56		
Totals		50.10	70.54	183.68	5.26	44.60	51.60	52.21	42.94	46.58	62.60	40.83	32.38	34.26	108.96	28.30	10.85	10.93	7.26	3.12	21.03	908.03	29.13	937.16

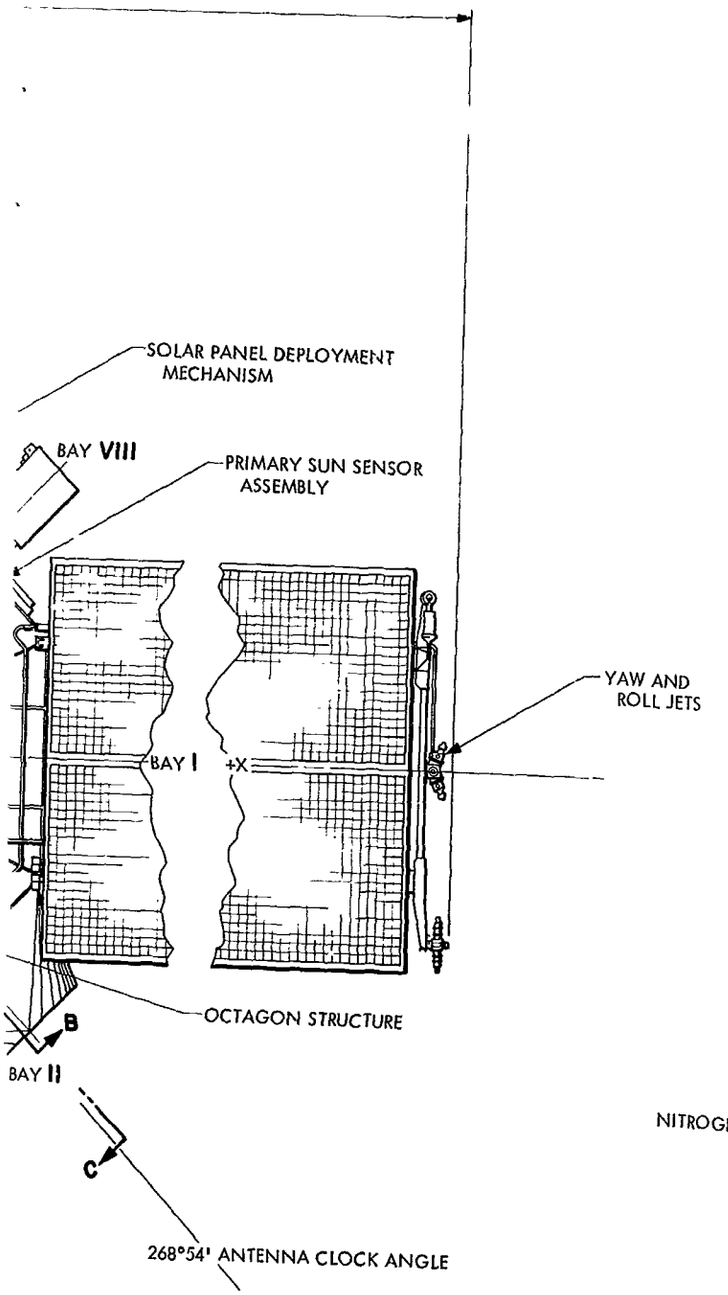
[a]Proof-test-model spacecraft

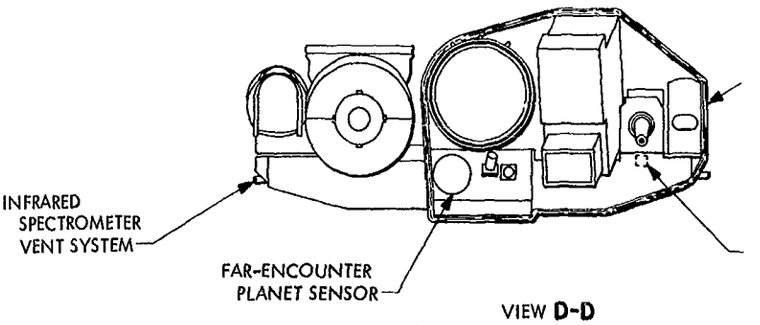
Recap:

Separated spacecraft	837.49
Spacecraft adapter	70.54
Total spacecraft	908.03

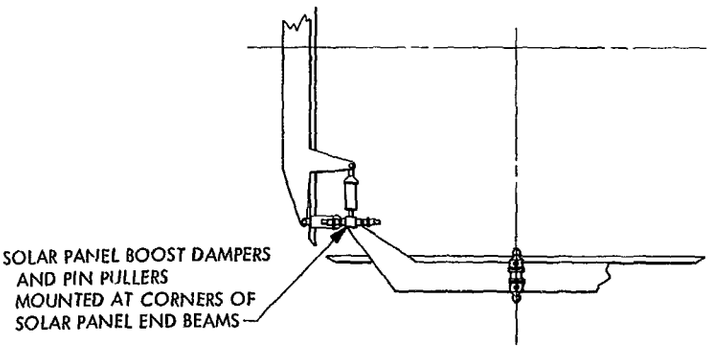


FOLDOUT FRAME 1

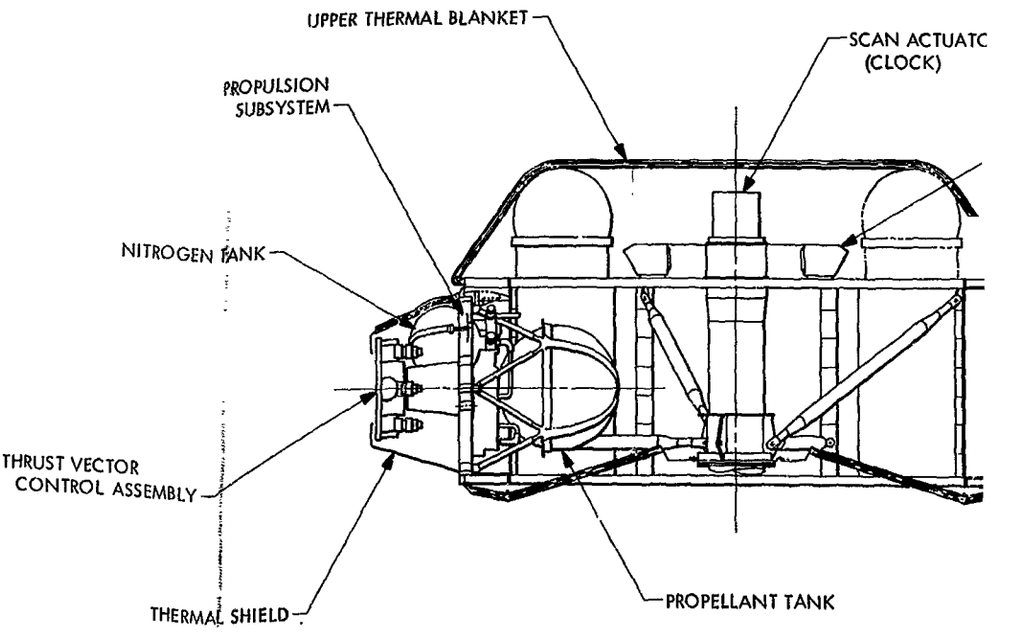




VIEW **D-D**
(ROTATED 84° COUNTERCLOCKWISE)
(LOUVER OMITTED FOR CLARITY)

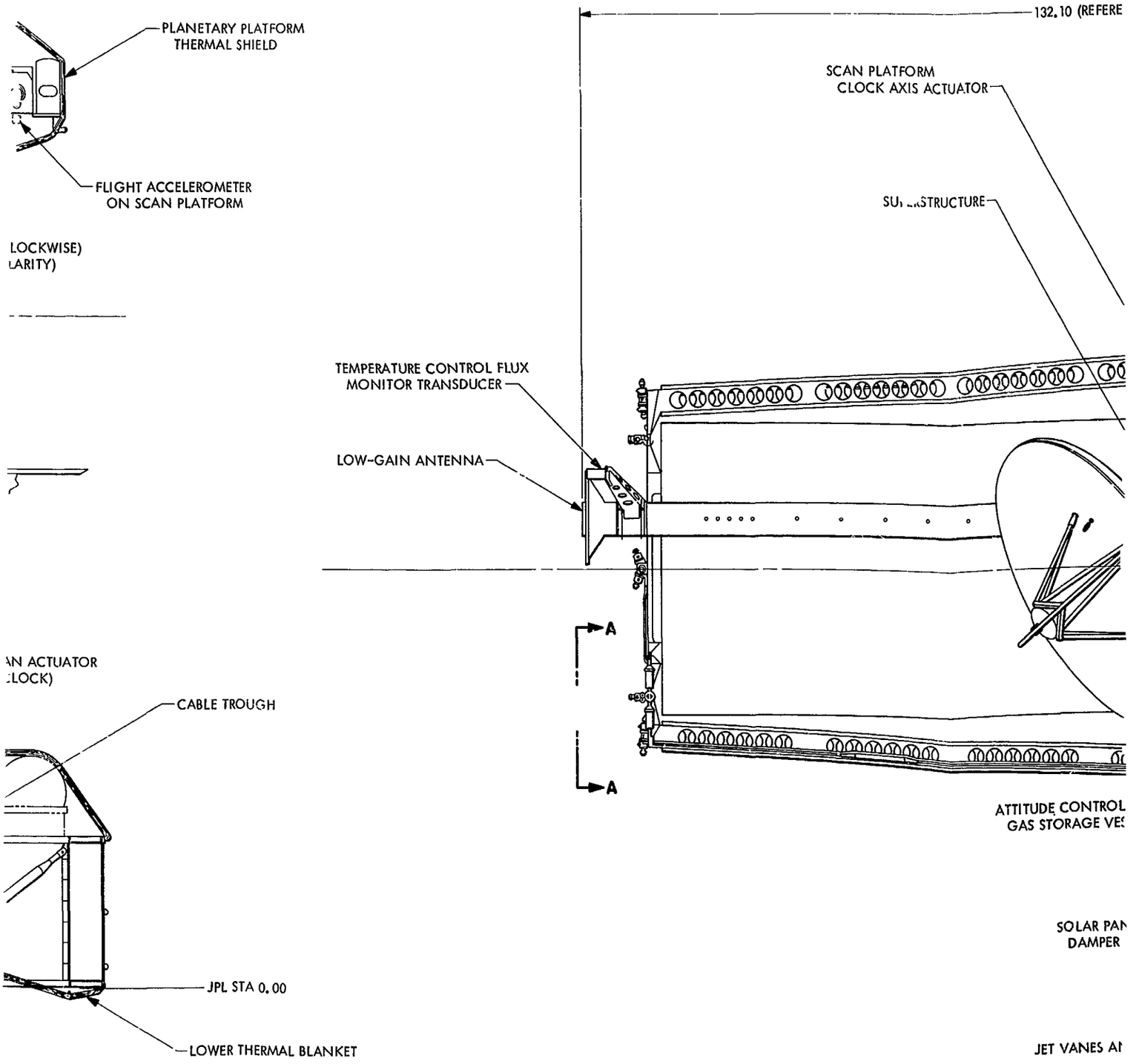


VIEW **A-A**



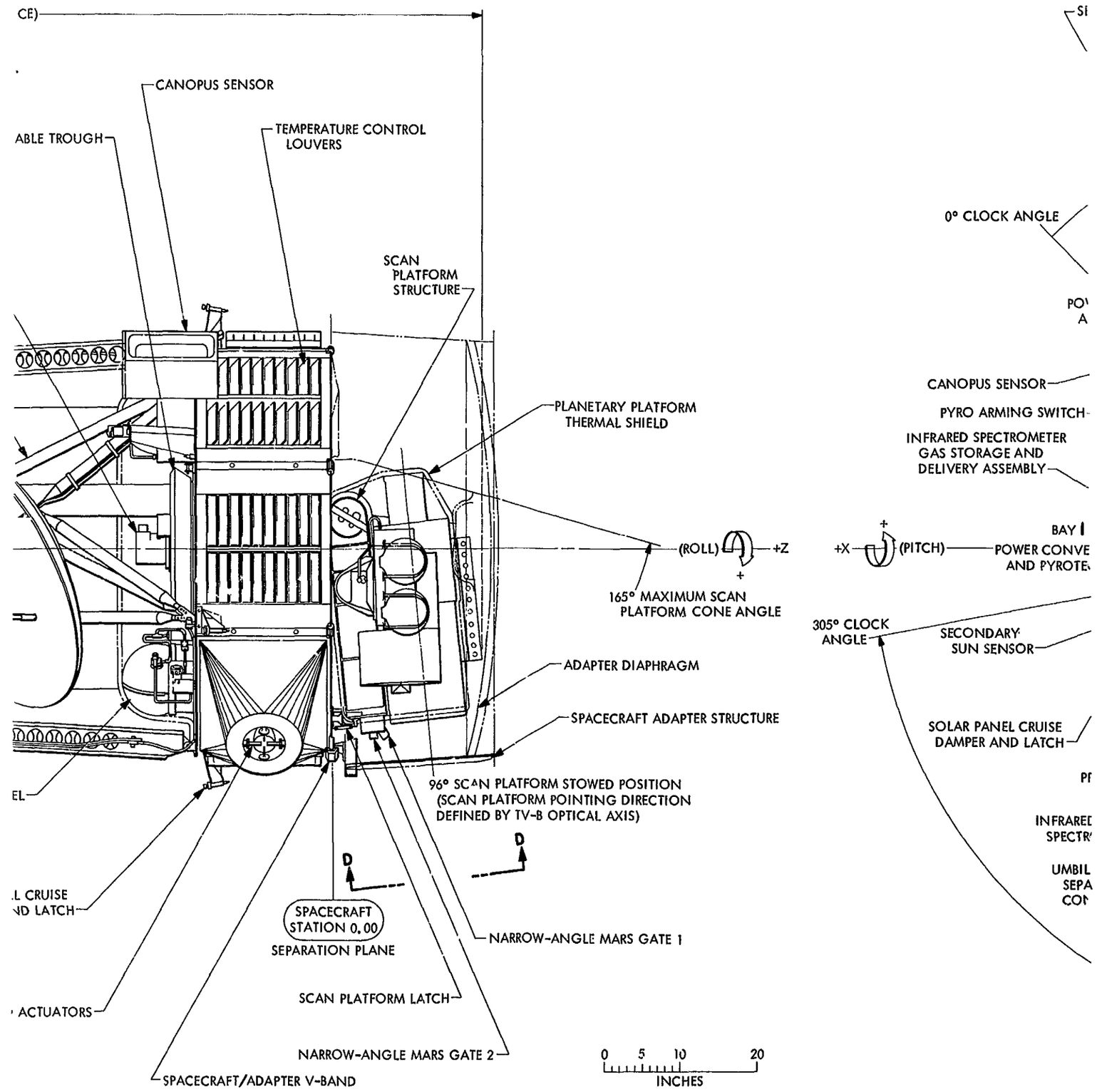
SECTION **C-C**
(ROTATED 135° CLOCKWISE)

FOLDOUT FRAME
2



FOLDOUT FRAME

3



FULLOUT FRAME 4

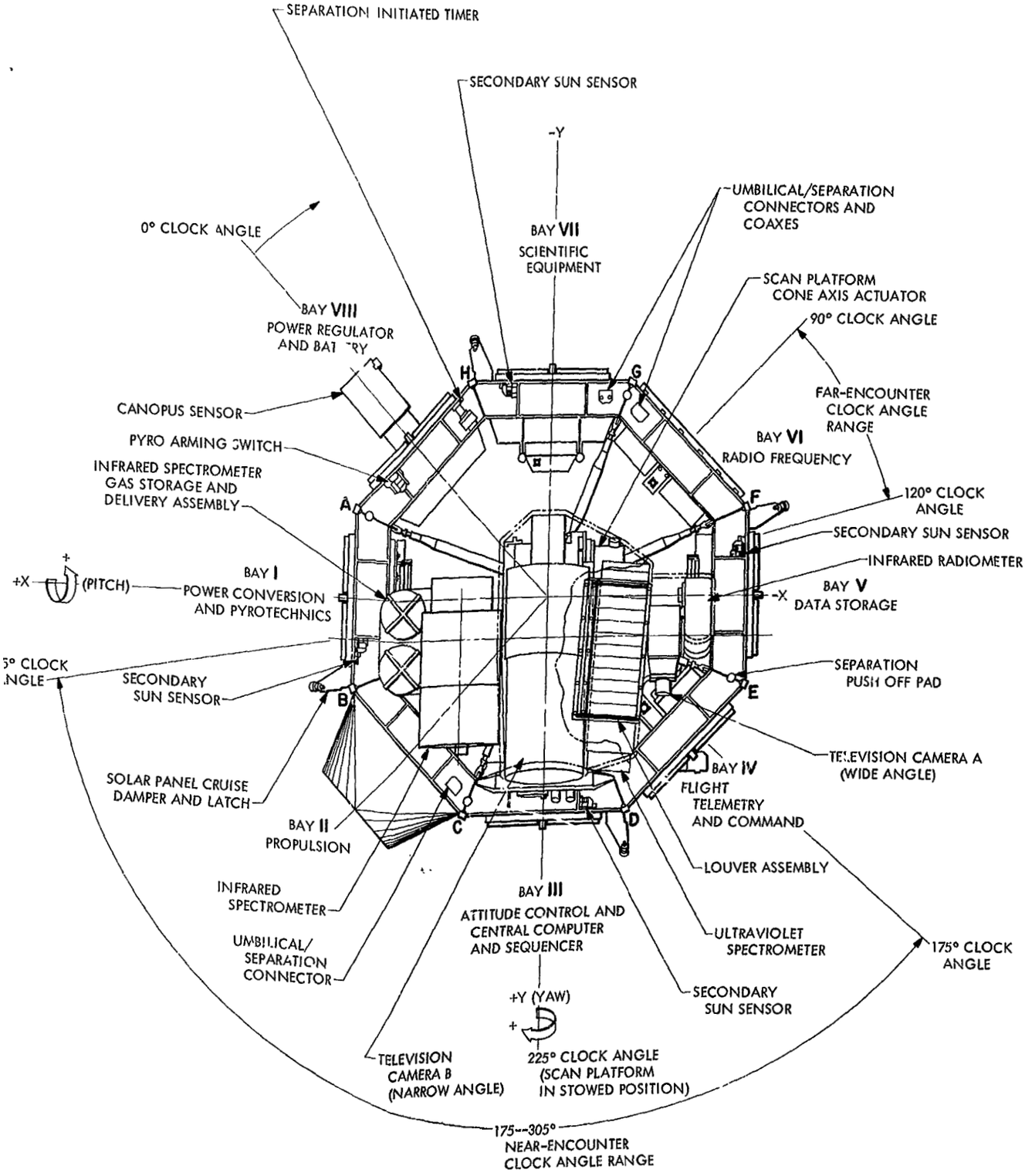


Fig. 4. *Mariner* Mars 1969 mechanical configuration

FOLDOUT FRAME 5

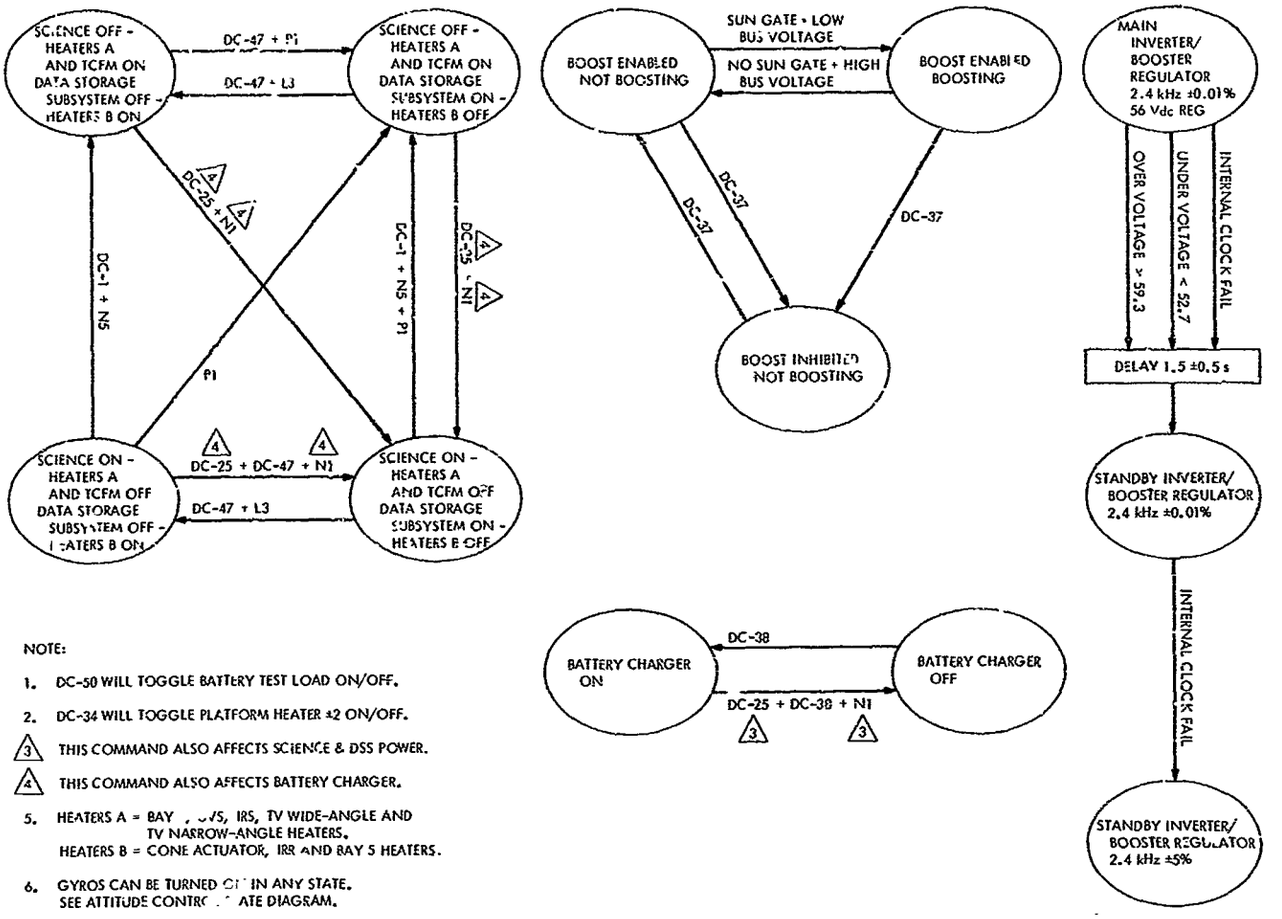


Fig. 6. Power subsystem state diagram

C. Thermal Design

The thermal design of the spacecraft was based on achieving a complex energy balance between the energy received from the Sun and that thermally radiated to the space environment. To achieve this balance, the design included isolation from solar heating, minimum resistance to heat transferred within the octagon enclosure and thermally regulated heat emission both from the octagon and from the science platform.

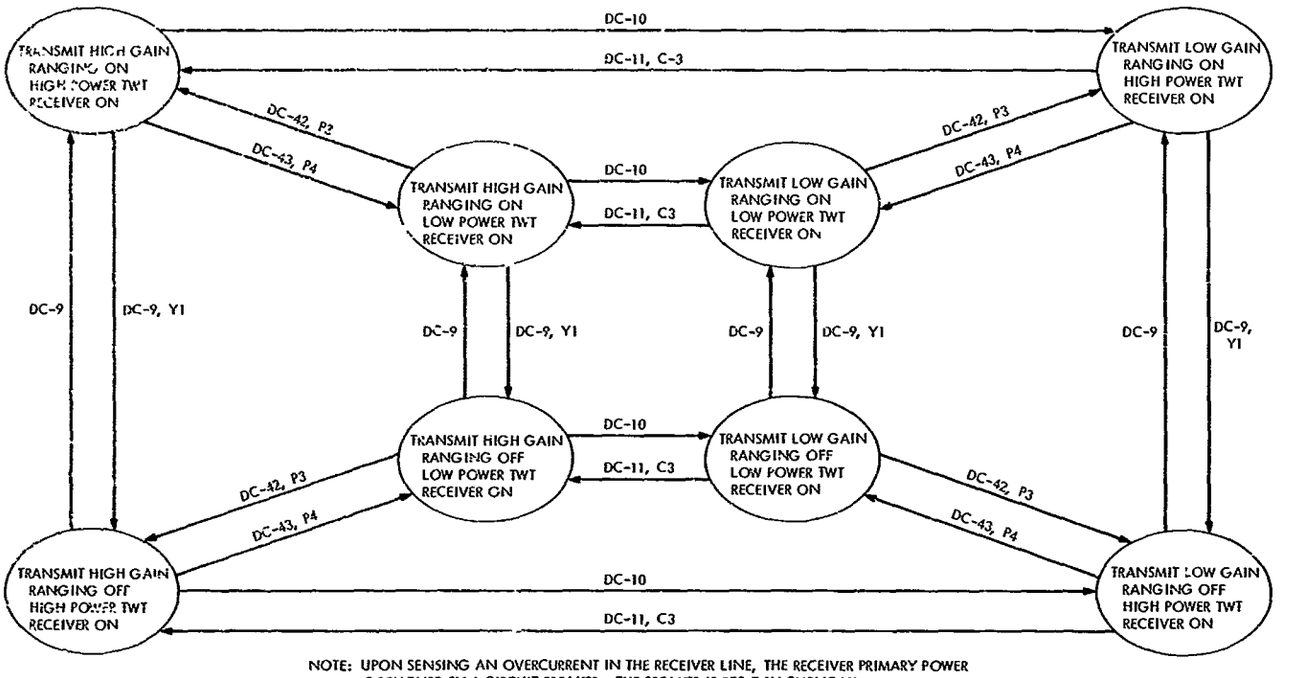
The isolation from solar heating and the reduction in heat losses to the space environment were accomplished through multilayered aluminized teflon thermal blankets, polished metal thermal shields, surface finishes, and paint patterns. Excessive heat generated by equipment was radiated to the space environment through thermally-actuated, variable-emittance louvers located on the bays and the science platform. Electrical heaters located in two of the bays and in the science platform were to provide the necessary additional heat during certain portions of the mission. Direct command capability exists to turn on and off some of this heat in the science platform.

One new item of temperature control hardware was flown for the first time on a spacecraft: a temperature control flux monitor. The temperature control flux monitor is a thermal flux radiometer which gives an accurate inflight measurement of the incident solar flux. This data was to provide a standard for future simulator testing and spacecraft design.

D. Command and Control

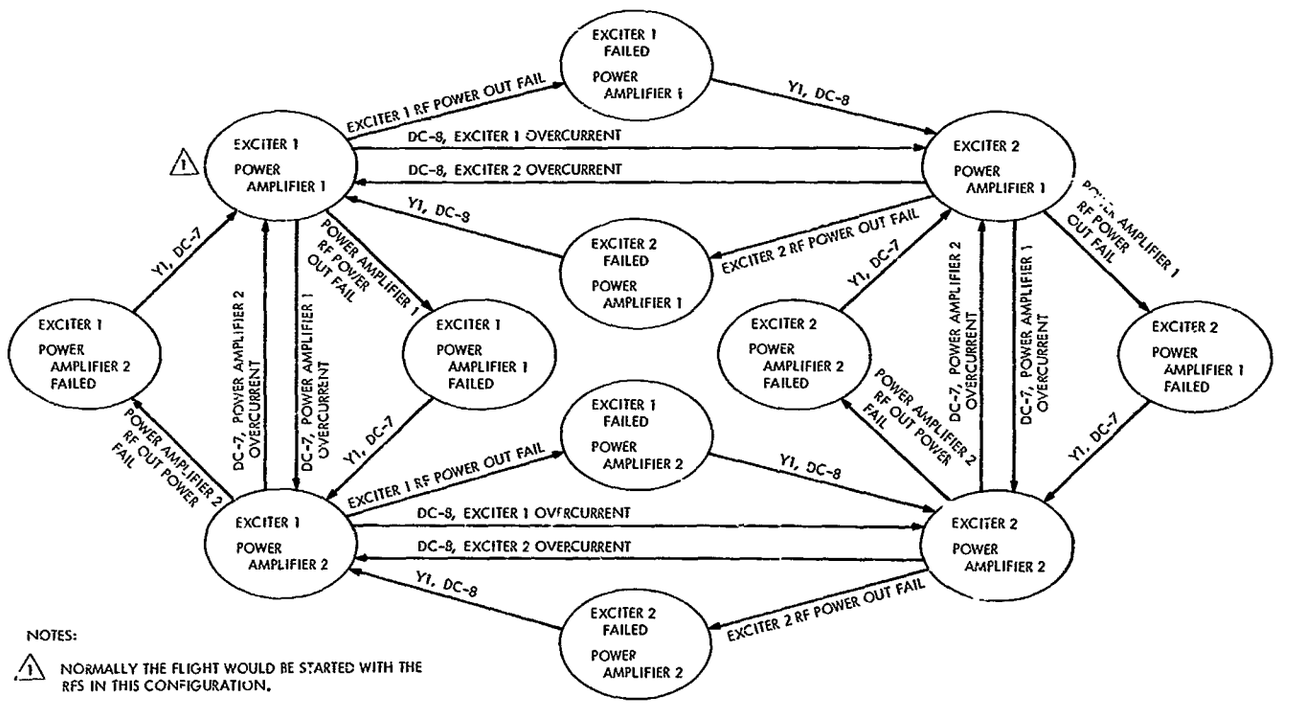
The two engineering subsystems which are principally responsible for commanding spacecraft events are the FCS and the CC&S. The FCS provides the spacecraft with the means to accept ground-initiated commands.

PRECEDING PAGE BLANK NOT FILMED



NOTE: UPON SENSING AN OVERCURRENT IN THE RECEIVER LINE, THE RECEIVER PRIMARY POWER IS REMOVED BY A CIRCUIT BREAKER. THE BREAKER IS RESET BY CYCLIC Y1.

a. RFS STATES



NOTES:

1. NORMALLY THE FLIGHT WOULD BE STARTED WITH THE RFS IN THIS CONFIGURATION.
2. Y1 ALSO HAS EFFECT OF TURNING OFF RANGING IF ON, DESCRIBED MORE FULLY ON SHEET 1.

b. FAILURE MODE SWITCHING

Fig. 7. *Mariner* Mars 1969 RFS state diagram

The FCS accepts command subcarrier information from the spacecraft receiver and demodulates and decodes these signals into commands which are provided as isolated switch closures to the recipient spacecraft subsystem.

The radio frequency subsystem (RFS) receives an S-band signal containing command and ranging information from the DSIF and transmit back to the DSIF at a different frequency an S-band signal modulated with telemetry and ranging information. The receiver is a narrow-band, double-superheterodyne, automatic-phase-control receiver which operates continuously and is always connected to the low-gain antenna. It detects the ranging signal and the composition command signal, and when it is receiving a signal the voltage controlled oscillator synthesizes the frequency of the transmitted signal. The RFS logic state diagram is shown in Fig. 7.

Three types of commands are processed by the FCS: direct commands called DCs, coded commands called CCs, and quantitative commands called QCs. Direct commands are used to back up critical spacecraft functions which are automatic, to select alternate modes of operation, to choose redundant elements, to initiate the midcourse maneuver, and to perform a variety of other functions. The spacecraft used 50 out of a possible 53 direct commands. Coded commands, of which there are five varieties, are used to interface with the CC&S. Quantitative commands are used to step the scan reference angles in the scan control subsystem a variable number of fixed increments. There are four of these, each with 18 possible magnitudes. Brief description of each command by command type are given in Tables 5, 6, and 7.

The command bits and reference frequency are transmitted to the spacecraft along with a bit synchronization in the form of a pseudonoise (PN) code. The command detector first locks onto the reference frequency in a phase-lock loop. The incoming PN code is then compared to an identical PN code which is generated in the command detector. This code is frequency coherent with respect to the incoming PN code because it is driven by the reference frequency, but it normally will not be phase coincident. If the codes are not coincident in phase, the spacecraft-generated PN code is incremented by one phase bit each second until they reach coincidence, resulting in command detector lockup. An inhibit signal is then removed from the command decoder and the detected command bits are decoded and commands issued.

Table 5. Direct ground commands

Symbol	Name	Destination	Comment
DC-1	Cruise mode	Power	DAS, science, and scan encounter power off. Heater power on.
		Data storage subsystem	During record mode: turns off power to the record motor and places data storage subsystem in ready mode.
			During playback: stops playback in data storage subsystem.
		Pyrotechnic	Disables IRS cooldown.
		FTS	Selects cruise data mode.
DC-2	CC&S readout select	FTS	With successive transmissions, initiates CC&S memory readout, or selects engineering telemetry on the engineering channel.
DC-3	Playback mode	Data storage subsystem	Initiates playback of data off digital recorder (Playback 1 mode).
			Stops analog-to-digital transfer.
		FTS	Places the FTS in the playback 1 mode.
DC-4	Analog-to-digital data transfer	Data storage subsystem	Initiates transfer of data from analog recorder to digital recorder. Effective only if data storage subsystem is in the playback 1 mode.
DC-5	Data rate switch	FTS	In any data mode, toggles the engineering channel data rate between 8⅓ and 33⅓ bits/s.
DC-6	FTS redundant elements switch	FTS	Selects alternate redundant elements in the FTS.
DC-7	Power amplifier switch	RFS	Selects alternate TWT.
DC-8	Exciter switch	RFS	Selects alternate exciter.

Table 5 (contd)

Symbol	Name	Destination	Comment
DC-9	Ranging on-off	RFS	Turns on ranging if off, and vice versa.
DC-10	Transmit low	RFS	Selects low-gain antenna for transmission.
DC-11	Transmit high	RFS	Selects high-gain antenna for transmission.
DC-12	Adaptive gate step	Attitude control	Successively steps lower Canopus brightness gate to lower values. When minimum setting is reached, next command resets lower gate to its maximum setting.
DC-13	Maneuver inhibit	Attitude control	Inhibits CC&S output commands to attitude control, and initiates sun and Canopus reacquisition.
			Turns on attitude control subsystem if CC&S L2 and PAS fail to do so.
		Pyrotechnic	Inhibits CC&S propulsion start and propulsion shutoff commands to pyro.
		CC&S	Resets fixed sequencer.
			Places maneuver logic in non-tandem mode. Sets flag flip-flop No. 6.
DC-14	Maneuver enable	Attitude control	Enables CC&S output commands to attitude control.
			Turns off attitude control subsystem if DC-13 was used to turn it on.
		Pyrotechnic	Enables CC&S propulsion start and propulsion shutoff commands to pyro.
DC-15	Canopus gate override	Attitude control	Removes Canopus brightness gate thresholds.
			Turns off gyros, if gyros were on only because of absence of Canopus acquisition signal.
DC-16	Planet acquisition	DAS	Initiates near-encounter sequence.
		Data storage subsystem	Starts recording on analog and digital recorders.
DC-17	Canopus cone angle step	Attitude control	Advances cone angle to next position.
DC-18	Inertial roll control/ step	Attitude control	Gyros on. Places roll axis under inertial control. Positive roll increment on subsequent transmission.
DC-19	Canopus roll control	Attitude control	Resets DC-15, DC-18, DC-20, and DC-40. Initiates Canopus acquisition if roll axis not under sensor control.
DC-20	Roll control inhibit	Attitude control	Inhibits roll axis control.
			Turns off gyros, if gyros were on only because of absence of Canopus acquisition signal.
DC-21	Roll search/step	Attitude control	Turns on gyros. Forces sensor off light source, and begins Canopus search.
			Subsequent to DC-18, produces a negative roll increment.
DC-22	Digital tape track switch	Data storage subsystem	Steps digital tape machine to next track and steps digital end-of-tape counter.
DC-23	Analog tape track switch	Data storage subsystem	Steps analog tape machine to next track and steps analog end-of-tape counter.
DC-24	(Spare)		
DC-25	Encounter phase	Power	DAS, data storage subsystem, science, and scan encounter power on. Heater power off.
			Turns off battery charger.
		FTS	Selects encounter 1 data mode.
		Scan	Selects initial near-encounter references.
			Disables far encounter planet sensor.
		Data storage subsystem	Places data storage subsystem in ready mode.
DC-26	Near-encounter sequence enable	DAS	Enables TV-PIV and NAMG-2; places DAS in near encounter mode.
		—	Spare actuator.
		Pyrotechnic	Enables IRS cooldown.

Table 5 (contd)

Symbol	Name	Destination	Comment
DC-27	First maneuver start	CC&S	Initiates tandem or fixed sequencer maneuver routine, depending on the state of CC&S maneuver logic.
		Pyrotechnic	Selects first maneuver devices.
DC-28	Far-encounter position	Scan	Selects far encounter references. Enables far encounter planet sensor.
		Data storage subsystem	Enables far encounter logic; effective only if data storage subsystem is in the ready mode.
DC-29	Second maneuver start	CC&S	Initiates tandem or fixed sequencer maneuver routine, depending on the state of CC&S maneuver logic.
		Pyrotechnic	Selects second maneuver devices.
DC-30	Computer inhibit	CC&S	Inhibits computer output actuators. Halts computer operation. Resets all flags. Places power monitor relay in the SET (nominal) condition.
DC-31	Computer enable	CC&S	Enables computer output actuators. Starts computer operation after a DC-30. Resets all flags.
DC-32	Computer maneuver initiate	CC&S	Initiates a computer-only maneuver routine if the CC&S logic is in the non-tandem standby mode. Sets the flag flip-flop No. 5.
DC-33	Tandem maneuver	CC&S	Places CC&S logic in the tandem standby mode. Enables the tolerance detector.
DC-34	Platform heater No. 2	Power	Toggles scan platform back-up heater off/on. Nominally off.
DC-35	Far encounter planet sensor control	Scan	Switches platform control into far encounter planet sensor loop.
DC-36	Far TV picture	DAS	Records a TV picture on analog tape machine.
*DC-37	Boost mode enable/ inhibit	Power	Enable function is subject to sun gate signal.
DC-38	Battery charging on-off	Power	
DC-39	Analog erase	Data storage subsystem	Effective only when data storage subsystem is in the ready mode.
DC-40	Gyros off	Attitude control	Forces gyros to turn off in spite of any inputs to the gyro control OR gate. Reset by DC-19.
DC-41	Platform cone slew	Scan	Slews scan platform to final cone angle position.
DC-42	TWT high power	RFS	Switches TWT to its high power output mode.
DC-43	TWT low power	RFS	Switches TWT to its low power output mode.
DC-44	Block coding on-off	FTS	Effective only if FTS in an encounter or a playback data mode.
		Data storage subsystem	Effective only if the data storage subsystem is in a playback data mode.
DC-45	Platform unlatch	Pyrotechnic	Permanently releases latch on scan platform.
DC-46	TV covers deploy	TV	
DC-47	Data storage subsystem power on-off	Power	
DC-48	Science off precondition		
		IRR	Preconditions TV, and IRR for power turn-off.
DC-49	IRS cooldown	Pyrotechnic	Starts gas-cooling of IRS, and start IRS motor.
DC-50	Battery test load	Power	Assesses battery by toggling battery test load off/on.

Table 6. Quantitative ground commands

Symbol	Name	Destination	Comment
QC-1	Cone angle positive step	Scan	Positively steps cone angle reference value 1-18 increments.
QC-2	Cone angle negative step	Scan	Negatively steps cone angle reference value 1-18 increments.
QC-3	Clock angle positive step	Scan	Positively steps clock angle reference value 1-18 increments.
QC-4	Clock angle negative step	Scan	Negatively steps clock angle reference value 1-18 increments.

Table 7. Coded ground commands

Symbol	Name	Destination	Comment
CC-1	Computer load	CC&S	Used to program computer. First of a pair if CCs required for programming the computer.
CC-2	Computer load	CC&S	Used to program computer. Second of a pair of CCs required for programming the computer.
CC-3	Word interrogate	CC&S	Effects single-word memory readout in the CC&S.
CC-4	Sequencer load	CC&S	Used by fixed sequencer to enter maneuver parameters.
CC-5	Tolerance detector disable	CC&S	Used to disable the tolerance detector, which inhibits the CC&S when the input power drops out of tolerance.

The logic state diagram for the command detector and code commands is shown in Fig. 8.

The other subsystem capable of commanding spacecraft events is the CC&S. Figure 9 shows the CC&S with its functional interfaces. Basically, the CC&S is a special purpose computer which has extreme flexibility and can be reprogrammed in flight. Its primary purpose is to provide event actuation at certain times which are specified prior to launch. In addition, while in flight, there is the capability of adjusting event times, making major sequency changes, and issuing real-time commands. Real-time CC&S commands (Table 8) are accomplished by modifying the CC&S program in flight to immediately issue a desired event. There were many non-standard events that could not be commanded by the FCS but could be commanded by the CC&S, so the real-time command capability added additional flexibility to the spacecraft design. The logic state diagram for the CC&S processor is shown in Fig. 10.

The CC&S design included a fixed sequencer which was similar to the *Mariner* Mars 1964 maneuver sequencer. It could be used to provide redundancy during the trajectory correction maneuver. In the nominal

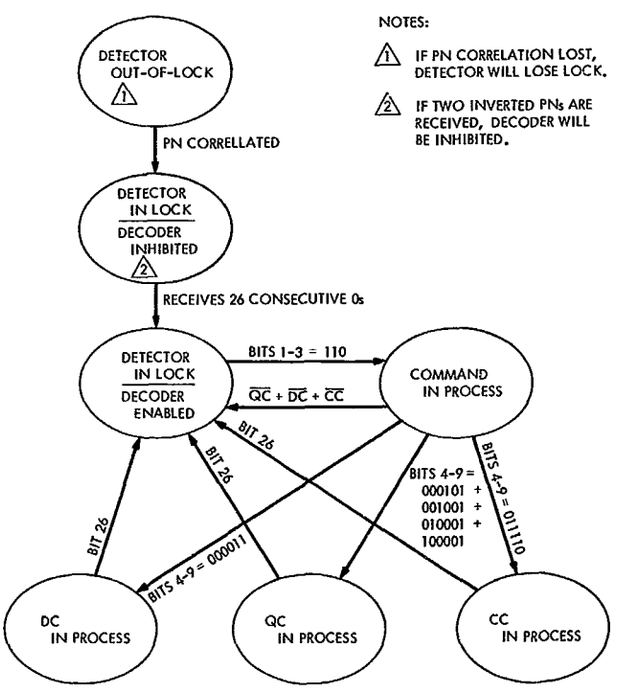


Fig. 8. Command detector and coded command logic state diagram

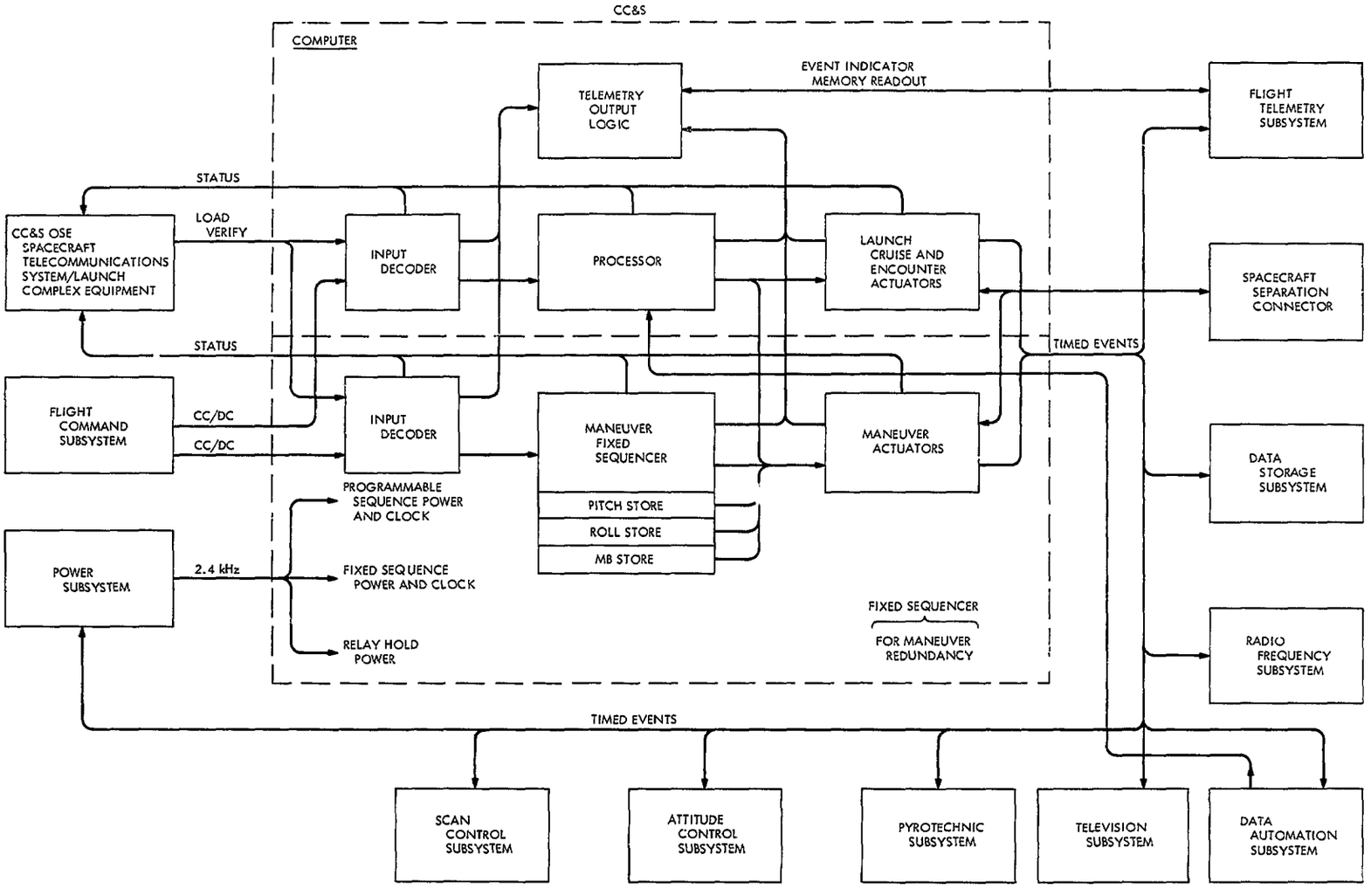


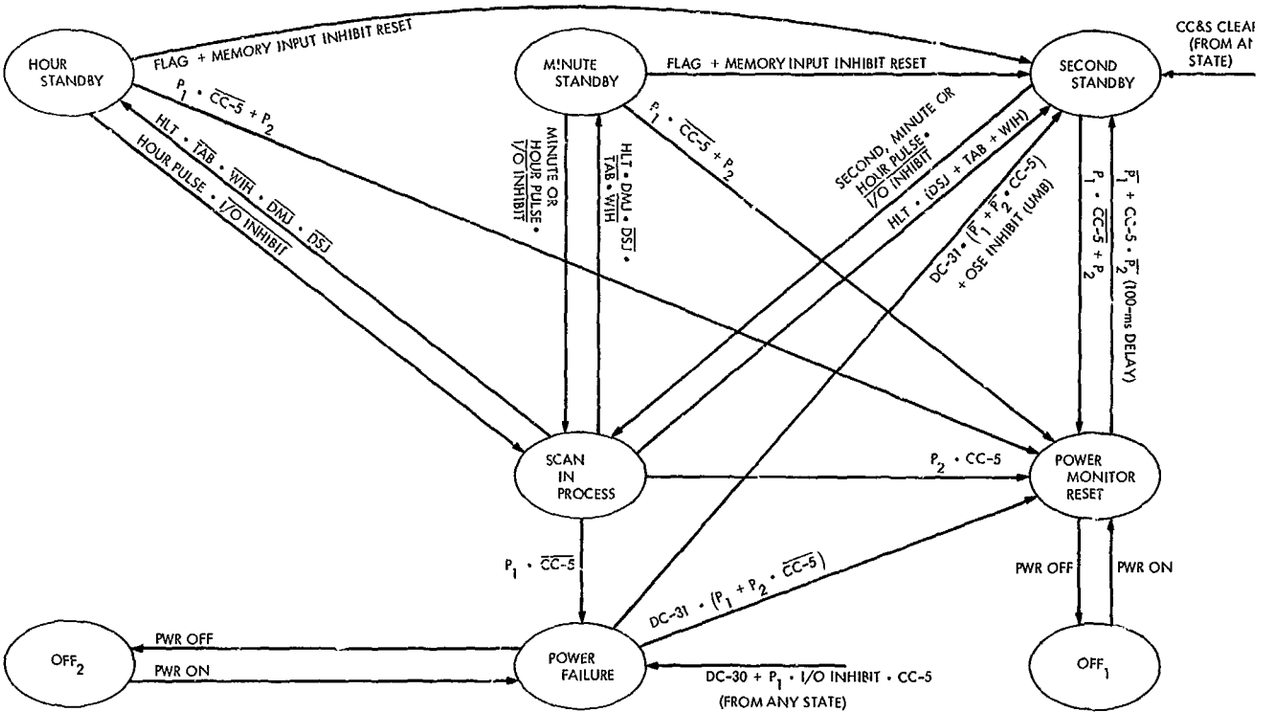
Fig. 9. CC&S functional interfaces

Table 8. CC&S commands

Symbol	Name	Destination	Comment
Launch			
L1	Solar panel deploy	Pyrotechnic	Unlatches solar panels for deployment.
L2	Canopus sensor on	Attitude control	Allows Canopus sensor 2.4-kHz power to come on. Turn on sun acquisition circuits if they are off.
L3	DSS power off	Power	
L4	Attitude control on	Attitude control	Turns on attitude control except for the Canopus sensor.
Maneuver			
M1	Gyros on	Attitude control	Turns gyros on for warm-up.
M2	All axes inertial	Attitude control	Places all axes under inertial control.
M3	Turn polarity set	Attitude control	Sets polarity of roll or pitch turn.
M4	Pitch turn	Attitude control	Executes pitch turn.
M5	Roll turn	Attitude control	Executes roll turn.
M6	Propulsion start	Pyrotechnic	Fires propulsion-start squibs.
M7	Propulsion shutoff	Pyrotechnic	Fires propulsion-stop squibs.
Cruise			
C1	Canopus cone angle step	Attitude control	
C2	8⅓ bits/s data rate	FTS	Switches the engineering channel data rate to 8⅓ bits/s.
C3	Transmit high	RFS	Switches transmitter to high gain antenna.
C4	(Unassigned)		
C5	Platform unlatch	Pyrotechnic	Permanently releases latch on scan platform.
C6	33⅓ bits/s data rate	FTS	Switches the engineering channel data rate to 33⅓ bits/s.
C7	Engineering telemetry select	FTS	During CC&S memory readout, selects engineering telemetry on the engineering channel and does not affect data mode. When CC&S memory readout is not in effect, this command selects the cruise data mode.
Encounter			
Far-encounter phase			
F1	Far-encounter position	Scan	Erects platform to far-encounter position. Enables far-encounter planet sensor.
		Data storage subsystem	Enables far-encounter logic. Effective only if data storage subsystem is in the ready mode.
F1	Far TV picture	DAS	Records a TV picture on analog tape recorder.
F2	Analog erase	Data storage subsystem	Same as DC-39.

Table 8 (contd)

Symbol	Name	Destination	Comment
Near-encounter phase			
N1	Encounter phase	Power	Science instruments, DAS, data storage subsystem, and scan encounter power on. Heater power off. Battery charger off.
		Data storage subsystem	Places data storage subsystem in ready mode.
		FTS	Selects Encounter 1 data mode.
		Scan	Erects platform to initial near-encounter position.
			Disables far-encounter planet sensor.
N2	(Unassigned)		
N3	Platform clock slew	Scan	Slews scan platform by sending a variable length pulse train.
N4	Final platform cone position	Scan	Slews scan platform to final cone-angle position.
N5	Near-encounter terminate	Power	Science, DAS, and scan encounter power off. Heater power on.
N6	Near-encounter	DAS	Enables TV-PIV and NAMG-2; places DAS in near encounter mode.
		Pyrotechnic	Enables IRS cooldown.
N7	TV cover deploy	TV	
N8	Analog recorder stop	Data storage subsystem	
N9	Digital recorder stop	Data storage subsystem	
N10	Platform cone slew positive	Scan	Slews scan platform positively by sending a variable length pulse train.
N11	Platform cone slew negative	Scan	Slews scan platform negatively by sending a variable length pulse train.
Playback			
P1	Playback 1 and science off	Data storage subsystem	Initiates playback of data off digital recorder.
		Power	DAS, science and scan encounter power off. T/C power on. Data storage subsystem power on.
P2	Playback 1 mode	Data storage subsystem	Initiates playback of data off digital recorder.
P3	TWT high power	RFS	
P4	TWT low power	RFS	
Cyclic			
Y1	Test radio	RFS	Switches exciters or power amplifiers in the event of a failure. Turns off ranging.
Y2	Adaptive gate pulse	Attitude control	Decreases level of lower Canopus brightness gate.



NOTES:

1. $P_1 \Leftarrow$ POWER 20% LOW.
   $P_2 \Leftarrow$ POWER X% LOW;
   X IS UNSPECIFIED CONSTANT > 20.
2. OSE INHIBIT SIGNAL ALSO STOPS COMPUTER CLOCK.
3. DSJ, DMJ, TAB, WIH, WOH AND HLT ARE PROGRAM INSTRUCTIONS THAT MAY BE ENCOUNTERED DURING SCAN.
4. DC-30, DC-31 AND CC-5 ARE GROUND COMMANDS.
5. STATES OFF_1 AND OFF_2 DIFFER ONLY IN CONDITION OF POWER FAILURE RELAY. $OFF_1 \Rightarrow$ RELAY RESET, $OFF_2 \Rightarrow$ RELAY SET
6. IF AN EVENT STROBE OCCURS THAT IS NOT DUE TO A DSJ OR WOH INSTRUCTION, COMPUTER CLOCK PULSES WILL BE INTERRUPTED TO THE PROCESSOR UNTIL CORRESPONDING DELAYED EVENT STROBE OCCURS.

Fig. 10. CC&S processor state diagram

maneuver sequence, the computer and the fixed sequencer was designed to operate in tandem. However, if there were a disagreement on any maneuver event, except burn stop, an internal abort would be issued and the spacecraft would reacquire the Sun and Canopus. In case there were a failure in either the computer or the fixed sequencer, a maneuver could still be performed using either one alone.

The computer memory consists of 128 22-bit words. While memory loading could be accomplished in less than a minute using the operational support equipment (OSE), inflight loading requires a minimum of two min/word, excluding transmission time. The 22 bits of memory data for each word were contained in the variable field portion of two coded commands.

E. Scientific Instrument Sequencing and Data Automation

The four scientific instruments and the recording functions of the data storage subsystem are controlled and sequenced, and the science data are processed for direct or delayed transmission to Earth, by the data automation subsystem (DAS), as shown in Fig. 11. The DAS is on when science power is turned on (DC-25 command or CC&S N1). The instruments and experiments are discussed in Part 1, Mission Design, Analysis, and Engineering, in Table 2.

The data automation function involves responding to ground-command, CC&S, and sensor outputs by actuating and changing various instrument and tape-recorder functions accordingly. In turn the DAS receives, codes, formats, buffers, and releases the science data stream to flight telemetry or data storage.

The low-rate 280-bit format, identified by a PN sequence, includes radiometer science data intermixed with selected data on all instruments and spacecraft status, to be transmitted at 66⅔ bits/s in real time. The combined 972-bit format adds all spectral data and every seventh TV picture element to the low-rate format, and is routed via high-rate telemetry (16.2 kbits/s) to Earth in real time and/or to the digital tape recorder for later playback. The TV science format of 6804 bits/frame contains all picture elements and is routed to the analog tape recorder for later playback. Frame counts are maintained.

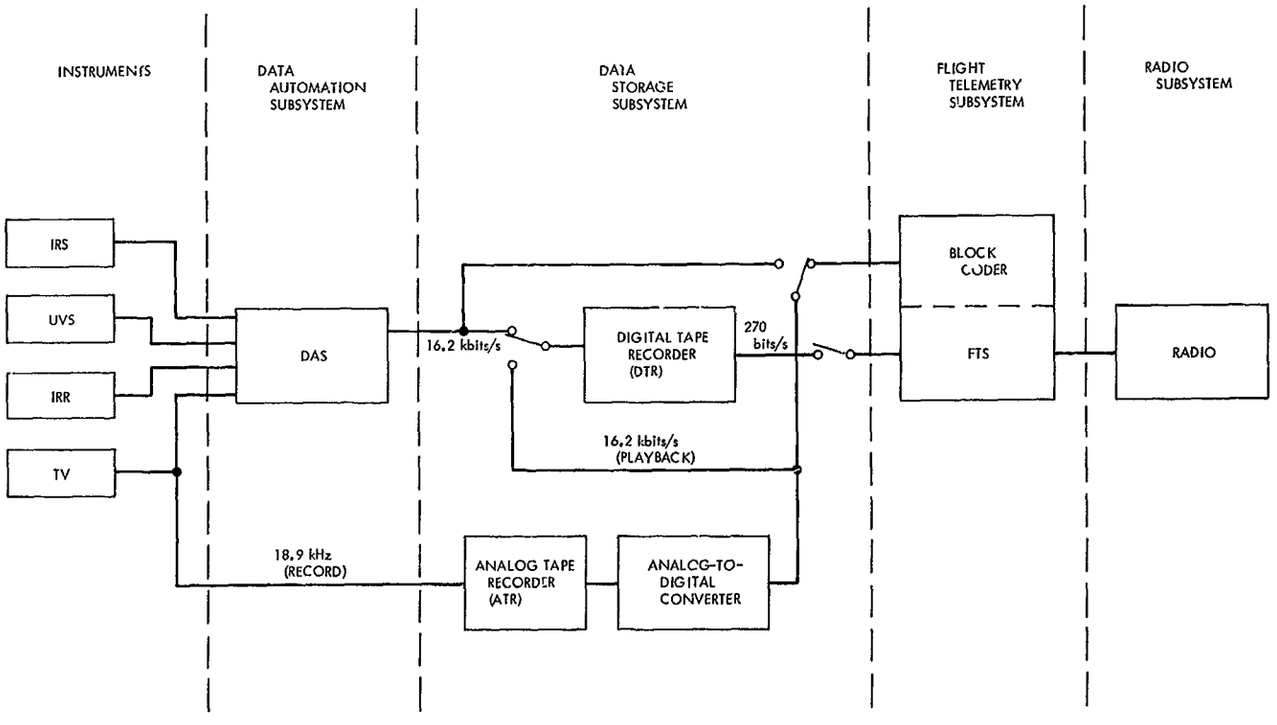


Fig. 11. Scientific instrument sequencing and data transmission

Various clock and sync functions for the TV cameras, in addition to switching and other command functions, are also provided.

F. Spacecraft Data Sources and Modes

The three data channels are:

(1) The engineering channel.

(2) The science channel.

(3) The high-rate channel.

The engineering channel is always on, regardless of what the FTS data mode is. The plan was to use the science channel during the nominal encounter and playback phases of the mission. The high-rate channel, which employs special block coding technique to provide a data rate of 16.2 kilobits/s, was designed to be used during the optional encounter and optional playback phases. Neither the science channel nor the high-rate channel was used during the launch, maneuver, and cruise portions of the mission. There was no sync channel, since the bit synchronization function was to be performed by the telemetry and command processor at the DSN stations.

The 1969 data system capability included five different data rates. Data carried on the engineering channel was to be transmitted at 8⅓ bits/s or 33⅓ bits/s at any time. Encounter data and playback data carried on the science channel are transmitted at 66⅔ and 270 bits/s, respectively. The block-coded data carried on the high-rate channel in the standard encounter or playback phases is transmitted with a symbol rate of 86.4 k symbols/s, the information rate being 16.2 kbits/s.

The data sources for the FTS on the spacecraft are the CC&S for memory readout, the spacecraft subsystems for engineering telemetry, the DAS for real-time TV and science, and the data storage subsystem for recorded TV and science. It should be noted that there were several partially or fully redundant data paths in the system.

TV data could be transferred in analog form from TV to the analog tape recorder, while at the same time every seventh analog sample was to be digitized and sent to the DAS, where it was multiplexed with science data from the ultraviolet spectrometer, the infrared radiometer, and the infrared spectrometer and sent to the digital tape recorder at 16.2 kbits/s.

The same 16.2-kbits/s data being recorded on the digital tape recorder could be transmitted simultaneously over the high-rate channel in the standard encounter. In the conservative encounter, some of the 16.2-kbits/s science data is transmitted in real-time at 66⅔ bits/s.

In the playback phase, the recorded analog TV data could be recovered either via the digital tape recorder or, as an option, directly from the analog to digital converter.

The conservative encounter mode was called the encounter 1 data mode. In this mode, the spacecraft telemetry is carried on the engineering channel at 33⅓ bits/s (8⅓ bits/s is possible if necessary to improve the engineering channel reception). Science data was to be sent down on the science channel at 66⅔ bits/s. This data consists of all the infrared radiometer data plus selected samples of the ultraviolet spectrometer and infrared spectrometer data. In the meantime analog TV data is recorded on the analog tape recorder at a rate of 18.9 kHz. Every seventh analog sample is digitized and sent to the DAS at 16.2 kbits/s. The DAS time-multiplexes this digital TV data with all the science instrument data and sends this composite format to the digital tape recorder.

The standard encounter mode was called the encounter 2 data mode. This data mode is very similar to the encounter 1 data mode except that the 66⅔ bits/s science data is deleted in favor of the 16.2 kbits/s composite science format. That is, the science plus TV data being recorded on the digital tape recorder is also block coded and transmitted on the high-rate channel.

The conservative playback mode was called the playback 1 data mode. The engineering channel carrier is at 8⅓ bits/s, while the science channel carries data from the digital tape recorder at 270 bits/s. After double playback of the data that was originally recorded on the digital tape recorder, the data that was on the analog tape recorder is analog-to-digital converted and recorded on the digital tape recorder. Seven analog to digital transfers are required in order to digitize the analog data in its entirety. In this mode it takes approximately 8 days to return all the analog data.

The playback 2 data mode, which was the standard method returning the analog recorder data, is designed so that the output of the analog-to-digital-converter is fed directly into the FTS, where it is block coded and

transmitted over the high-rate channel. In this mode, all the analog data can be returned in less than 3 h. Again, in this mode, as in all the other data modes, spacecraft telemetry or CC&S memory data is being transmitted on the engineering channel.

The FTS was designed to perform the general functions of formatting the engineering and science data according to defined modes of operating and of generating a multiple-data-channel composite telemetry signal which modulates the RF carrier. It provides three data channels and makes provisions for data rate, data mode, and modulation index switching. The FTS has a redundant chain which contains a second sync generator, analog to digital converter, and data processor which can be switched in by ground command if the primary chain fails.

The engineering-telemetry commutated-channel functions are described in Table 9.

Table 9. Telemetry channels real-time engineering telemetry assignments

Channel	Measurement	Subsystem
High deck		
100, 101, 102	PN sequence (15 bits) and subcommutation index (6 bits)	Flight telemetry
103	20X deck (subcommutated channel)	—
104	21X deck (subcommutated channel)	—
105	Pitch gyro rate/pitch fine sun sensor	Attitude control
106	Yaw gyro rate/yaw fine sun sensor	Attitude control
107	Roll gyro rate	Attitude control
108	Canopus intensity	Attitude control
109	Command detector monitor	Flight command
110	22X deck (subcommutated channel)	—
111	Receiver static phase error (SPE)	Radio frequency
112	Pitch position	Attitude control
113	Yaw position	Attitude control
114	Roll position/roll search rate	Attitude control
115	Receiver AGC, coarse	Radio frequency
116	PS&L output voltage	Power
117	Thrust chamber pressure	Propulsion
118	Event counters No. 1 and No. 2	Flight telemetry
119	Event counters No. 3 & No. 4	Flight telemetry
Medium deck		
200	Scan clock position, coarse	Scan control
201	Scan cone position, coarse	Scan control
202	30Y deck (sub subcommutated channel)	—
203	Main/standby inverter output voltage	Power
204	Main/standby inverter output current	Power
205	400-Hz inverters input current	Power
206	Battery voltage	Power
207	Scan cone reference angle/cone position, fine	Scan control
208	FEPS cross-cone error signal	Scan control
209	FEPS cone error signal	Scan control
210	Exciter output drive	Radio frequency
211	40Z, 41Z decks (sub subcommutated channel)	—
212	42Z, 43Z decks (sub subcommutated channel)	—
213	High-gain antenna drive	Radio frequency
214	Low-gain antenna drive	Radio frequency
215	Main 2.4-kHz inverter input current	Power
216	Battery charger output current	Power
217	Receiver AGC, fine	Radio frequency
218	Data storage subsystem status channel 2	Data storage
219	Data storage subsystem status channel 2	Data storage
220	CC&S timing of events	CC&S
221	+X panel current	Power
222	−X panel current	Power
223	+Y panel current	Power
224	−Y panel current	Power
225	Battery output current	Power
226	Main/standby booster/regulator input current	Power
227	Scan clock reference angle/clock position, fine	Scan control
228	Data storage subsystem status channel 2	Data storage
229	Data storage subsystem status channel 2	Data storage
Low deck		
300	Power switching and logic (PS&L) current to radio frequency subsystem and heaters	Power
301	Status monitor	Flight telemetry
302	TWT anode II voltage and TWT indicator	Radio frequency
303	Temperature-control flux monitor (TCFM) measurement No. 1	Temperature control
304	TCFM measurement No. 2	Temperature control
305	TCFM measurement No. 3 (Guard temperature)	Temperature control
306	Exciter supply voltage and exciter indicator	Radio frequency
307	Adaptive gate setting	Attitude control
308	TWT helix current	Radio frequency
309	Canopus cone angle	Attitude control

Table 9. (contd)

Channel	Measurement	Subsystem
Low-low deck		
400	Frame number	Flight telemetry
401	Temperature reference	Flight telemetry
402	Data storage status channel No. 1	Data storage
403	Spare (digital)	
404	VCO temperature	Radio frequency
405	Battery temperature	Power
406	Sun sensor temperature	Attitude control
407	Canopus sensor temperature	Attitude control
408	Propellant tank temperature	Propulsion
409	Platform yoke temperature	Devices
410	Infrared radiometer engineering temperature	Infrared radiometer
411	Bay 1 temperature	Structure
412	Bay 3 temperature	Structure
413	Bay 5 temperature	Structure
414	Bay 7 temperature	Structure
415	TV-A vidicon temperature	Television
416	Ultraviolet spectrometer detector temperature	Ultraviolet spectrometer
417	Infrared spectrometer electronics temperature	Infrared spectrometer
418	TWT No. 1 base temperature	Radio frequency
419	+Y inboard panel temperature	Power
420	CC&S status monitor	CC&S
421	Scan latch gas pressure	Devices
422	Local oscillator drive	Radio frequency
423	Standard cell voltage	Power
424	Standard cell current	Power
425	Radiation resistant cell current	Power
426	+X/+Y N_2 pressure	Attitude control
427	−X/−Y N_2 pressure	Attitude control
428	Propellant tank pressure	Propulsion
429	Propulsion N_2 tank pressure	Propulsion
430	Auxiliary oscillator temperature	Radio frequency
431	Propulsion N_2 tank temperature	Propulsion
432	Bay 4 temperature	Structure
433	TWT No. 2 base temperature	Radio frequency
434	Bay 8 temperature	Structure
435	TV-B vidicon temperature	Television
436	TV-B optic[illegible]ture	Television
437	Infrared spectrometer radiator temperature	Infrared spectrometer
438	−X/−Y N_2 temperature	Attitude control
439	+Y outboard panel temperature	Power

The data storage subsystem is composed of two tape recorders (one digital and one analog) which store on magnetic tape data channeled from either the TV subsystem or the DAS. In the playback mode, the digital recorder reproduces data previously recorded on it (either directly or via an analog to digital converter) for transmission to Earth via the FTS system and the RFS in a form (analog or digital) and at rates which are consistent with the telemetry constraints. The logic state diagram for the data storage subsystem is shown in Fig. 12.

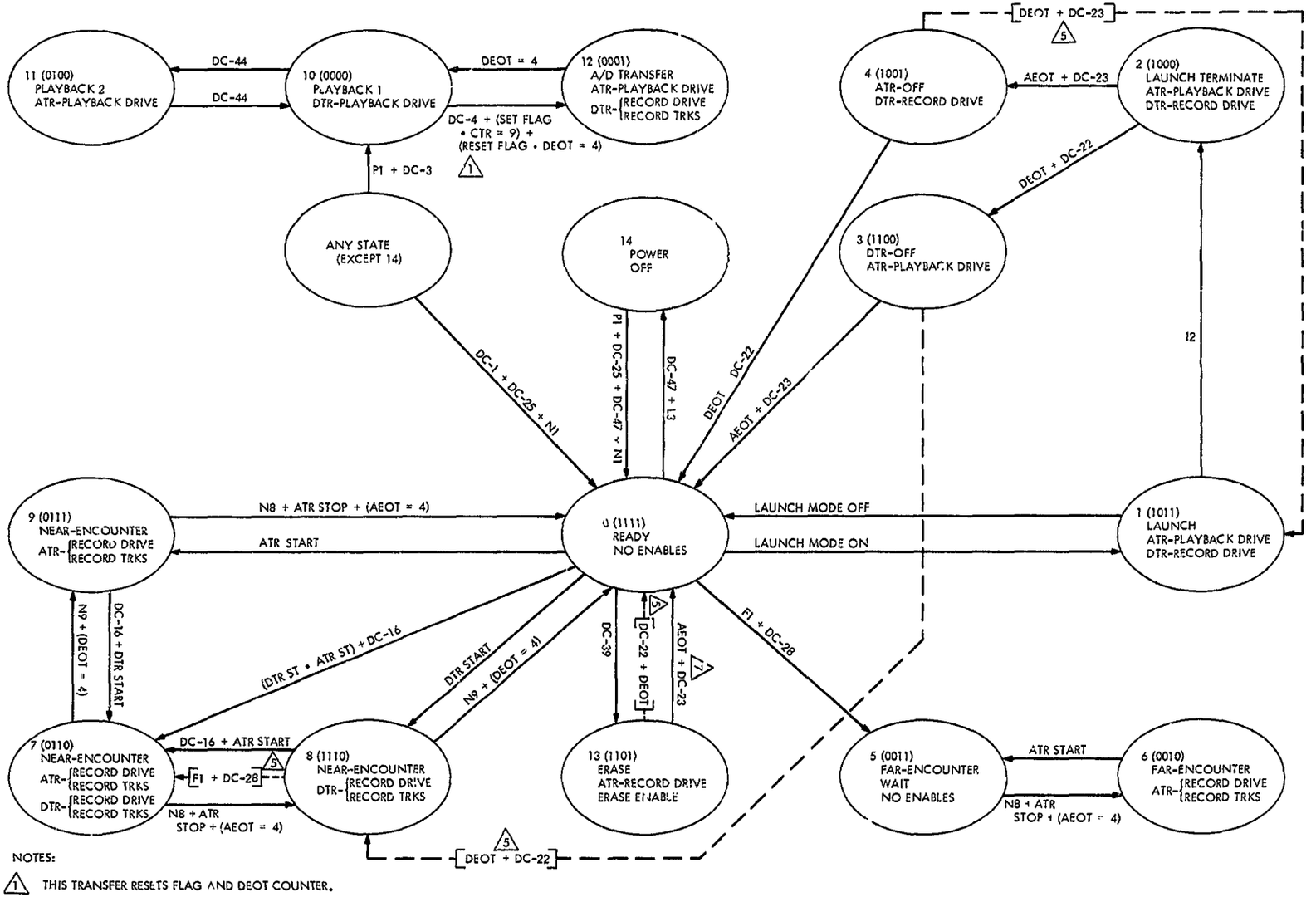
G. Spacecraft Attitude and Scan Platform Control

The spacecraft attitude-control subsystem is very similar to the old *Mariner* Mars 1964 design. It provides the spacecraft with three-axis stabilization and control. Three single-degree-of-freedom gyros are included to provide inertial sensing during initial stabilization and commanded maneuvers. Sun sensors were strategically placed to provide position information relative to the pitch and yaw axes, and a similar type Canopus sensor was provided to give position information relative to the roll axis. The attitude control subsystem logic state diagram is shown in Fig. 13.

Control torques about the three control axes were generated by the expulsion of cold nitrogen gas except during engine firing, when the control torques are generated by jet vanes located in the motor exhaust. Switching amplifiers control the expulsion of the nitrogen gas because they have a built-in deadband causing the spacecraft to maintain a position limit cycle. During the cruise limit-cycle operation the gyros were to be turned off and simulated rate signals derived from passive networks.

The scan control subsystem was a two-degrees-of-freedom, electromechanical, feedback control system which was designed to point the scientific instruments at specific areas on the planet during the encounter phase of the mission.

The general features of the scan control subsystem included: (1) two identical actuator units which consist of a servo motor, a slip clutch, and a gear train to drive the 180-lb platform 215 deg in clock and 64 deg in cone; (2) four electromechanical reference units used to store predetermined and (in two cases), updateable platform pointing angles; (3) servo electronics to drive the actuators, (4) a far-encounter planet sensor, which is an electro-optical device used to track the planet; and (5) two narrow-angle Mars gates, used in succession to initiate near-encounter events.



NOTES:

1. THIS TRANSFER RESETS FLAG AND DEOT COUNTER.
2. POWER ON RESETS EOT COUNTERS AND SETS TO READY STATE.
3. DC-22 AND DC-23 ALWAYS STEP THEIR RESPECTIVE EOT COUNTERS.
4. ENTERING STATES 7, 8 OR 9, SET FLAG AND RESET AUXILIARY COUNTER (NINE COUNT). AUXILIARY COUNTER BEGINS TO COUNT DEOTs IN STATE 10.

Fig. 12. Data storage subsystem state diagram

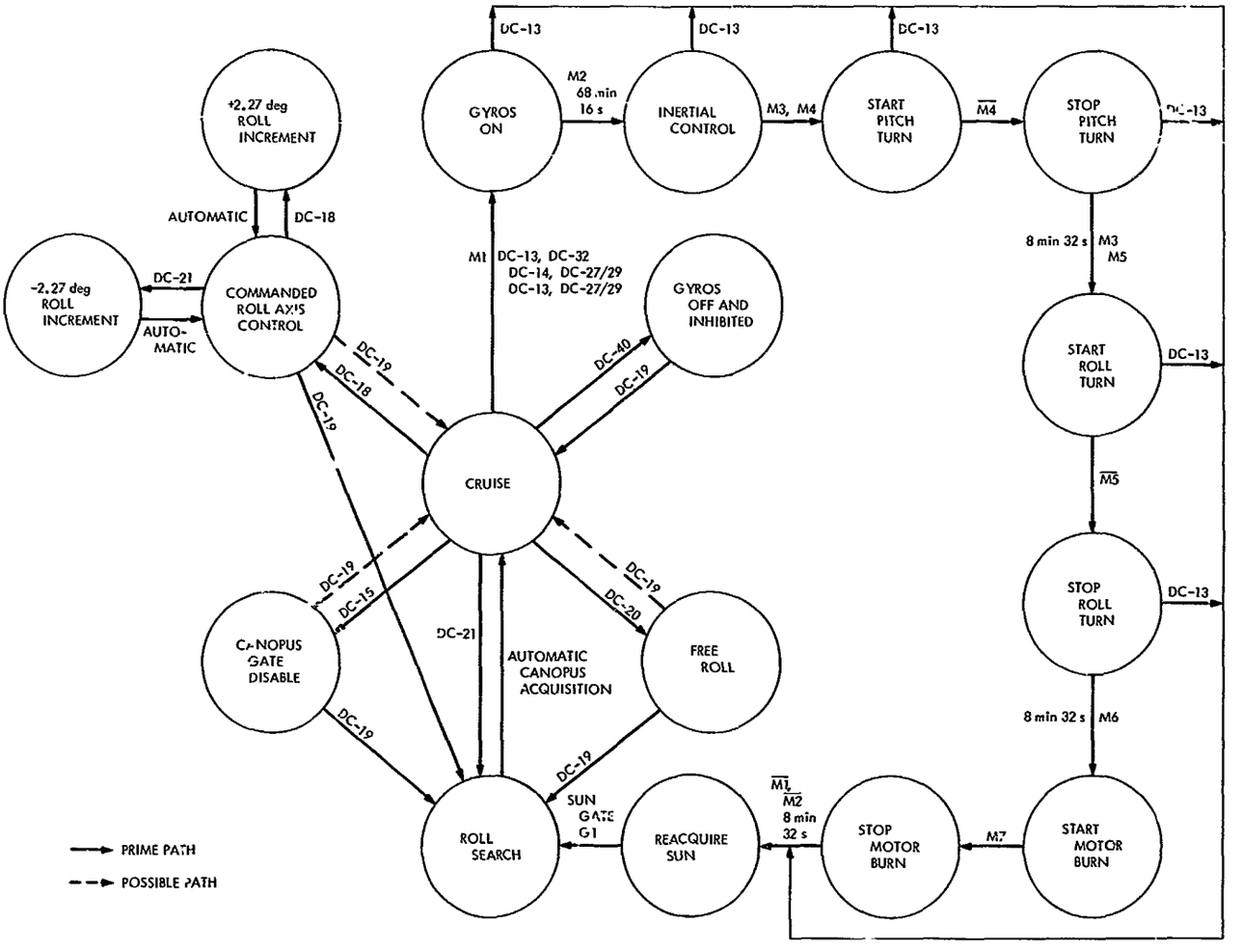


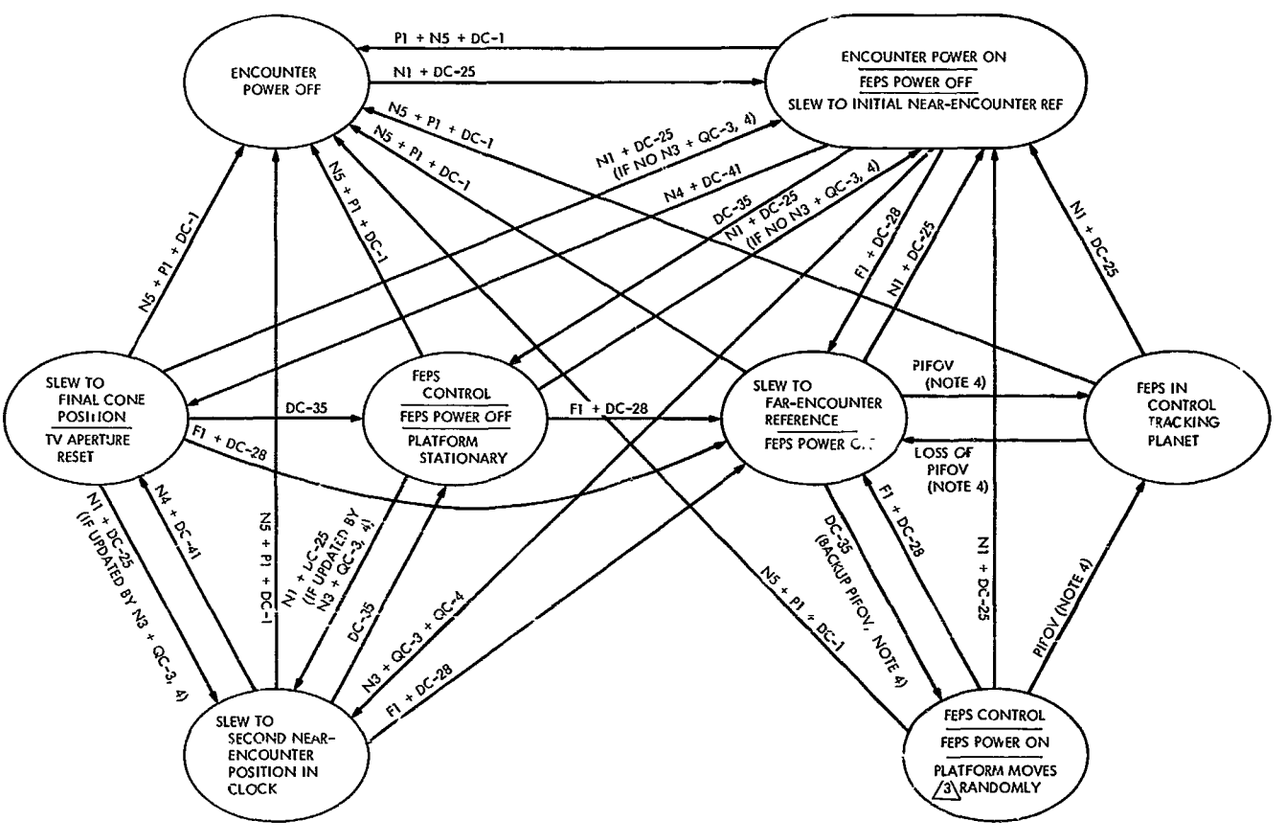
Fig. 13. Attitude control subsystem state diagram

There were two modes of operation of the scan control subsystem. First, in the far encounter mode, from $E - 48$ to $E - 12$ h, the FEPS tracks the center of brightness of the planet by providing two error signals to the scan electronics. Then next, after the time of $E - 12$ h, the scan control subsystem was designed to operate in the near encounter mode in which the platform pointing angles are derived from the near encounter reference units. These units (pots) stored angles that could be updated either by ground command or CC&S command. The logic state diagram for the scan control subsystem is shown in Fig. 14.

H. Pyrotechnics and On-Board Propulsion

The pyrotechnic subsystem provides the energy storage and switching required to activate the pyrotechnic-operated devices. Capacitor banks were utilized for energy storage and semiconductors used to switch the energy from the capacitors to the devices to be fired. The pyro initiated events included the deployment of the solar panels, starting the IRS cooldown and the start of both trajectory maneuvers. The pyrotechnic subsystem was completely redundant in every operation.

The propulsion subsystem was very similar to the *Mariner* Mars 1964 design. It was located in bay 2, and was a constant thrust rocket utilizing a liquid monopropellant, anhydrous hydrazine. It provided the thrust capability for trajectory correction maneuvers. Two maneuver capability was realized by the inclusion of ganged explosive valves, with two parallel branches of normally closed and normally open valve groups in the high pressure gas and fuel lines.



NOTES:

1. THIS DIAGRAM DOES NOT INCLUDE ANY NAMG STATES.
2. QC-1, 2 OR N10, 11 CAN BE USED TO UPDATE CONE REFERENCE ANGLES AND QC-3, 4 OR N3 CAN BE USED TO UPDATE CLOCK REFERENCE ANGLES, AT ANY TIME DURING MISSION.
3. WITH NO LIGHT SOURCE, i.e., FEPS NOT VIEWING PLANET, FEPS OUTPUT IS ±1.0 V. PLATFORM WILL MOVE WHEN REFERENCE UNIT (POTS OR FEPS) PROVIDES OUTPUT OF 0.1 V OR GREATER. THEREFORE, PLATFORM WILL MOVE RANDOMLY IN THIS STATE.
4. PLANET IN FIELD-OF-VIEW.

Fig. 14. Scan control subsystem state diagram

I. Spacecraft Redundancy

This subsection lists the spacecraft redundancy that is designed into various subsystems of the 1969 spacecraft system design.

Block redundancy is the identical duplication of equipment, whereas functional redundant elements provide alternate methods of achieving the same result.

1. Functional redundancy. Functional redundancy on the spacecraft was largely incorporated into control functions and data paths.

2. Block redundancy. The following items were redundant:

(1) RFS exciters, exciter power supplies, and isolators.

(2) RFS TWT amplifiers, dc/dc converters, and output RF filters.

(3) Coded command input lines from FCS to CC&S.

(4) Power booster-regulator/2.4-kHz inverter strings, which include crystal oscillator frequency sources.

(5) FTS analog-to-digital converters, synchronizers, and data processors.

The synchronizer in (5) consists of:

(a) 480-kHz oscillator

(b) Count-down chain

(c) Sync generator

The data processor in (5) consists of:

(a) Science data selector

(b) Engineering multiplexer

(c) Channels A, B, and C modulators

(d) Subcarrier mixer

(e) Output amplifier

(6) Attitude control cold gas tanks, plumbing, and jets

(7) All pyro squibs are either dual bridge wire (squib actuated values) or redundant single bridge wire squibs (pin-pullers). The functions initiated by redundant actuation are:

(a) Release V-band

(b) Deploy solar panels

(c) Start propulsion burn (two sets of values)

(d) Stop propulsion burn (two sets of values)

(e) Unlatch scan platform

(f) Release IRS cooling gas

(8) Pyro control units.

(9) Separation connector functions:

(a) CC&S output enable

(b) DSS launch mode terminate

(c) RFS TWT power on

Disconnecting either separation connector will actuate these functions.

(10) Solar panel deployment springs.

(11) Scan control reference potentiometers: the near-encounter and far-encounter reference potentiometers cover the same range and are identical in design. They are redundant to a certain extent since the near-encounter potentiometers can be commanded to position the platform in the far-encounter position. The converse is not true since far-encounter potentiometers can be commanded in flight.

(12) DAS crystal oscillators.

Engineering Mechanics

I. Introduction

The engineering mechanics subsystems included the spacecraft structure, the cabling, and the temperature control and mechanical devices. In addition, the engineering mechanics discipline was responsible for the mechanical and thermal design and testing of the system and for studies and testing in related fields.

II. Structure Subsystem

The structure subsystem comprised two areas of hardware for the *Mariner* Mars 1969 program. Elements of the structure subsystem such as the basic octagon, the solar panel structures, and the science platform structure were considered primary structures. The remaining hardware consisted of the electronic assembly structures (chassis), which were installed within the octagonal bus structure, and the associated assembly handling and shipping equipment hardware.

A. Spacecraft Adapter

The spacecraft adapter attached the spacecraft to the forward structure (*Centaur* adapter) of the *Atlas/Centaur* boost vehicle and positioned the spacecraft base above the *Centaur* adapter forward flange. The spacecraft adapter was a cylinder 52 in. in diameter by 21 in. high, composed of the following main elements:

(1) The lower flange, made of a rolled aluminum angle section, carried the bolt pattern that allowed attachment of the spacecraft adapter to the *Centaur* adapter.

(2) The skin, made of 0.025-in. aluminum sheet, stabilized by vertical hat sections, formed the cylinder that provided the shear and torsional stiffness required of the adapter.

(3) The eight vertical longerons, machined from aluminum bar, provided rigid points for attachment of the eight spacecraft feet to the adapter and smoothly delivered the concentrated spacecraft attach loads into the shell structure of the adapter.

(4) The top ring, a rolled aluminum channel section, stabilized the top of the cylindrical skin and longerons and provided a convenient mounting surface for miscellaneous bracketry.

(5) The thermal diaphragm, consisting of a fiberglass skin coated with a 1-in.-thick layer of urethane foam, formed a thermal barrier between the *Centaur* tanks. (The cryogenic temperatures of the tanks would be detrimental to the spacecraft science instruments.)

No significant problems were encountered during the adapter fabrication, and testing was completed with no failures.

B. Octagon Structure

The octagon structure was the central body of the spacecraft, providing a cavity into which the electronics were mounted and acting as a rigid frame to which the scan platform, solar panels, antennas, and miscellaneous equipment were mounted. The *Mariner* Mars 1969 octagon structure was derived from the *Mariner* Mars 1964 structure, the only major difference being the heavier scan platform attachment and a new adjustable midcourse motor mounting scheme.

The scan platform support structure, a structurally redundant truss of 1-in.-diam swaged aluminum tubing, provided mounting points and roll axis bearings for the 130-lb scan platform, carrier of all the planet-oriented instruments for the *Mariner* Mars 1969 mission.

All of the magnesium structure elements were treated with the Dow 17 anodic coating process, which proved to be more durable than the Dow 7 used in previous programs. The Dow 17 coating gives the magnesium a pale green color and is electrically insulating.

A good deal of difficulty was experienced in the early adjustable motor mount fabrications because of the curved serrated adjustment pads. A technique similar to that used to cut gears was finally adopted, and the parts were successfully fabricated. Installation of the motor mounts into the octagon structure presented some difficulty because of the alignment tooling design.

There were no failures in the octagon structure during the *Mariner* 1969 test program.

C. Scan Platform

1. Description. The planet-oriented instruments flown on the *Mariner* Mars 1969 mission imposed the requirement for a two-degree-of-freedom gimballed platform to which the science instruments and planet sensors were mounted (Fig. 1).

The mission required that the platform be pointable anywhere within a cone angle of 101 to 165 deg, where 0 deg is the spacecraft sun vector, and a clock angle of 90 to 305 deg, where 0 deg is the center of bay VIII.

The elements of the scan subsystem that were mounted on the scan platform were: the clock and cone scan drive actuators, the far encounter planet sensor (FEPS), and two narrow-angle Mars gates (NAMG). The science instruments mounted on the platform were the ultraviolet spectrometer (UVS), the wide-angle television camera (TV-A), the narrow-angle television camera (TV-B), the infrared radiometer (IRR), and the infrared spectrometer (IRS). The IRS included the monochromator-telescope, the gas bottles, and the IRS gas disposal system. Some of the sensors and instruments required thermal and/or electrical isolation from the platform.

In addition to the sensors and instruments listed above, two heaters, an accelerometer, and an alignment mirror were mounted on the platform. A cable harness for power, pyrotechnic, accelerometer, and science signals had to be routed from the bus cable trough through the two axes of articulation to the items mounted on the platform. The torques experienced by the scan subsystem during spaceflight had to be less than 40 in.-lb to give acceptable scan subsystem pointing direction offsets.

The spacecraft configuration dictated the platform location underneath the bus. In the launch configuration, the platform extended down into the spacecraft adapter. The platform was required to have adequate clearance to exit from the adapter upon spacecraft separation.

To transfer the launch loads directly to the bus, the platform was locked to the bus during the launch phases. Upon platform latch release, the restraint was slowly removed and the entire platform translated 0.060 in. along the clock axis in the +Z direction. Once released, the platform was attached to the bus through the gimbal only.

The platform can be divided into three basic areas: the platform instrument frame, the gimbal, and the latch. The gimbal contained both degrees of freedom, clock and cone. The platform clock axis coincided with the spacecraft Z axis. The gimbal was made of three primary pieces: the clock tube, isolation sleeve, and clock cone adapter (gooseneck). The clock tube passed through two sleeve bearings in a tube in the bus and was restrained by a thrust bearing acting on a flange on the clock tube. The upper half of the thrust bearing was spring-loaded to permit the 0.060-in. axial movement when the platform was

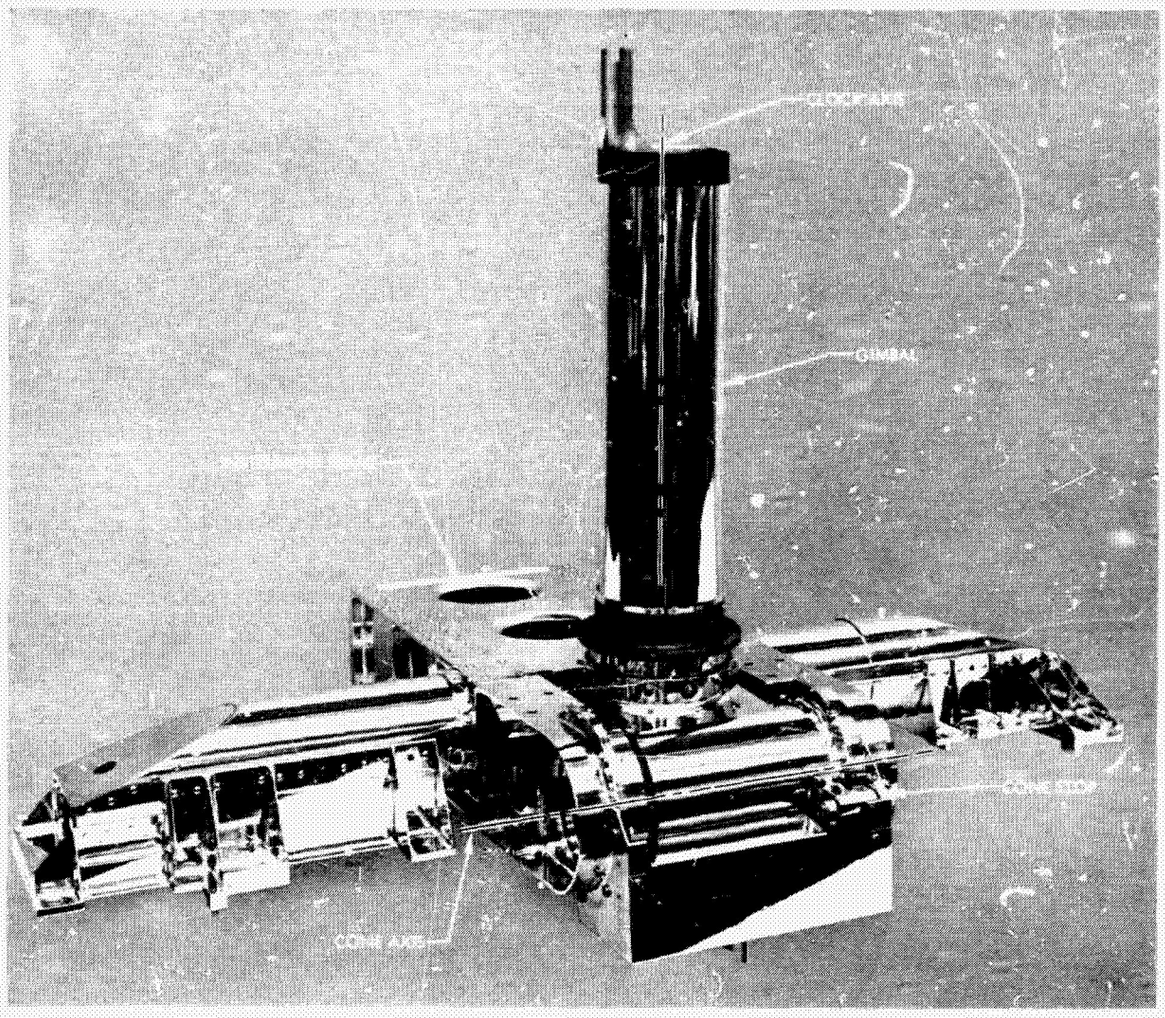


Fig. 1. Scan platform structure

latched. The clock actuator was mounted on an adapter on the octagon upper ring and drove the clock tube by an arm that rode in a slot in a tongue in the tube.

The scan platform gimbal is shown in Fig. 2. The clock tube fitted into the fiber glass isolation sleeve, which fitted into the gooseneck. A combination radial and thrust bearing was pressed into one end of the gooseneck and the outside diameter of the gooseneck at the opposite side served as the shaft of the other cone radial sleeve bearing. This latter bearing was fastened to the instrument frame, as was the cone axis bearing adapter which fitted into the combination radial and thrust bearing. The cone actuator was mounted on the instrument frame and drove the platform through a drive arm which fitted into a slot in a bracket riveted into the gooseneck.

The bearings are a nominal 0.014-in. layer of a Teflon-filled asbestos matrix bonded on aluminum. The bearing material was chosen for low friction, stability in space environment, and reliability. The bearings ran on hard-anodized aluminum surfaces.

The instrument frame (Fig. 3) was a box section with a tube passing transversely through the center. This configuration was chosen to permit rapid recovery from any design changes in instrument or sensor look directions. The primary instrument, TV-B, to which all other instrument and sensor look directions were referenced, was located on the box section. The other instruments were mounted on brackets fastened to the tube. The box section was composed of two side beams and an outboard beam, all of which were machined, two sheet metal surface skins,

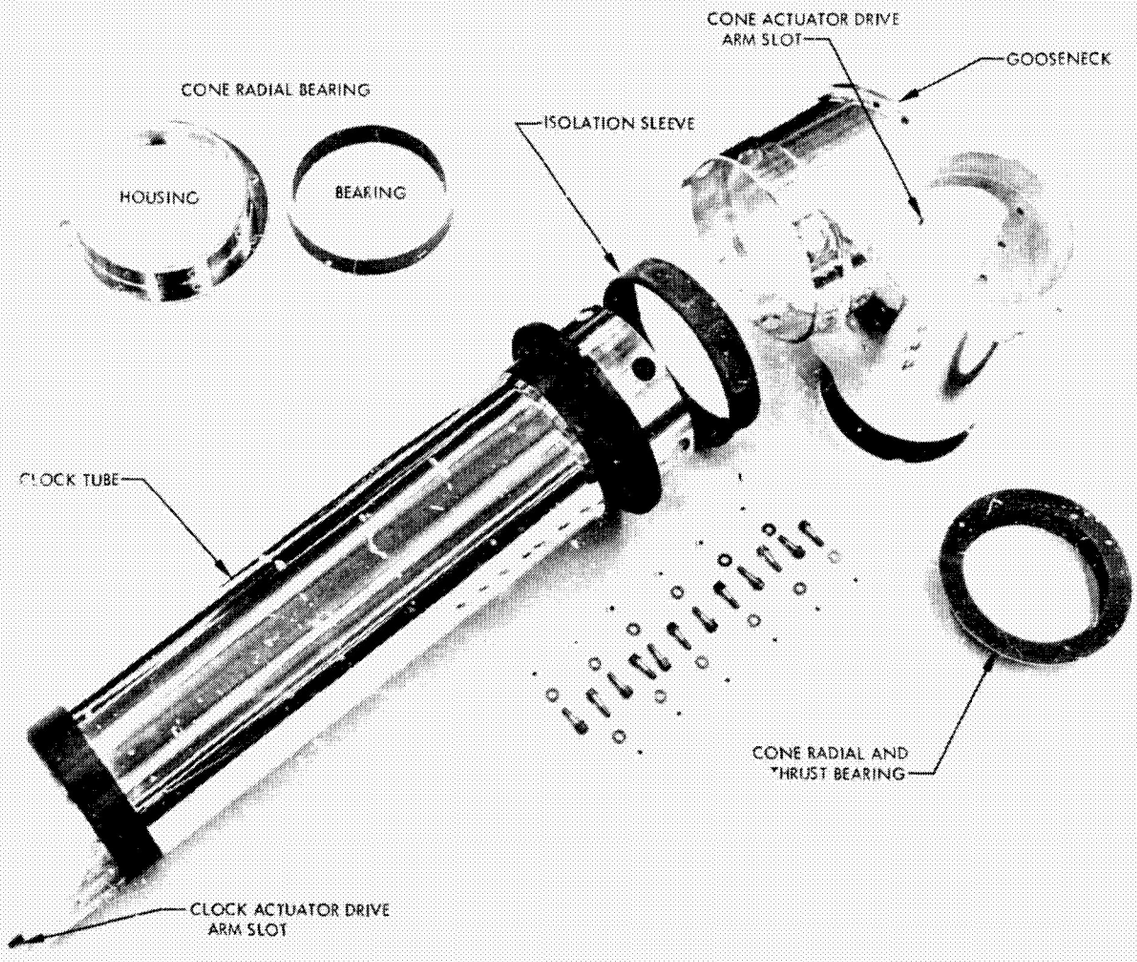


Fig. 2. Scan platform gimbal

and two sheet metal transverse webs. The instrument tube was 4 in. in diameter with $\frac{1}{8}$-in. walls in the center third and $\frac{1}{16}$-in. walls at the outboard ends. The brackets mounted on the tube were designed to be stiff within themselves and to rely only minimally upon the instrument tube for strength. The result was a stronger assembly, with the brackets and tube reinforcing each other.

The top side of the ends of the instrument tube were relieved, or beveled, at 18 deg to provide clearance to the lower thermal shield. To maintain the tube's rigidity at the ends, these large cutouts were bridged by end closures.

The instrument mounting and alignment surfaces are shown in Fig. 4. As has been mentioned, the TV-B was mounted on the bottom of the instrument frame box section. The instrument was electrically isolated from the platform by 4 hard-anodized aluminum washers, with the bolts isolated by fiberglass shoulder bushings. The TV-B was aligned on the platform by pushing fiberglass pads on the rear of the instrument against two dowel pins. (In the inspection of the instrument and sensor mounting planes and angles, all measurements were referenced back to the plane established by three of the TV-B isolation washers and to a line tangent to the two dowel pins.)

The IRS was located on a bracket on the instrument tube, with the monochromator-telescope adjacent to the TV-B and the gas bottles on the outboard end. The monochromator-telescope was electrically and thermally

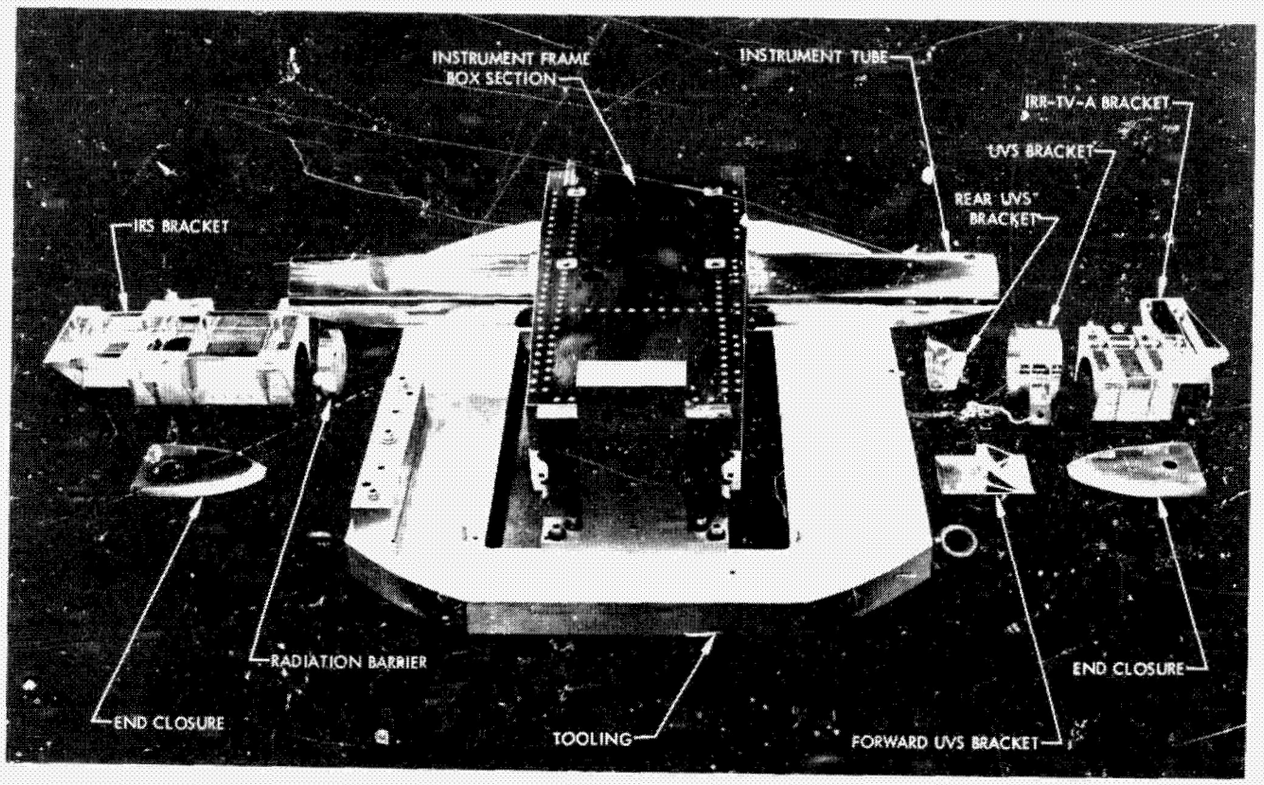


Fig. 3. Instrument frame box section with instrument tube and brackets

isolated from the platform by hardware provided by the experimenter. Because the IRS must run at a much lower temperature than the other instruments, great effort was made to reduce heat flow to the instrument. The instrument was positioned on the platform by setting the distance from the side of the instrument to two platform dowel pins. This 0.100-in. [illegible]ng prevented heat flow into the instrument. The IRS [illegible]ostat protruded from the instrument beyond the mounting plane, requiring a 2.00 × 2.81-in. hole through the IRS bracket and into the instrument tube. To prevent the cryostat from "seeing" the warm end of the instrument tube, a radiation barrier was installed inside the tube approximately where the tube entered the box section. The gas bottle assembly was bolted directly to the platform with the position set only by the four mounting bolts.

The IRS vent is a [illegible]-in.-diam tube inside the instrument tube, parallel to the cone axis. The vent tube is rigidly mounted at two central points and restrained at the ends at the free state position. This vent configuration was chosen to permit a completely aligned and pretested unit to be installed, rather than having two nozzles and plumbing bolted on, with consequent concern about thrust axis alignment and balanced thrusts.

The UVS was mounted next to the TV-B opposite the IRS. The forward and aft feet rested on brackets bolted to the left beam of the box section and were pushed against two dowel pins for alignment. The third UVS foot rested on a bracket on the instrument tube. Since no electrical or thermal isolation was required, the UVS was bolted directly to the platform.

Outboard of the UVS was the bracket upon which the TV-A and IRR were mounted. The IRR was set back from the TV-A to provide clearance to an umbilical island in the adapter. Both instruments were aligned by pushing each against two shoulders on the bracket. Both the IRR and the TV-A were electrically isolated from the platform. The TV-A had fiber glass pads against the alignment shoulders, rested on a fiber glass washer, and had the bolts isolated by fiber glass shoulder bushings. The isolation of the IRR was specified after initial platform design. The mounting isolation was similar to that of the TV-A except that the

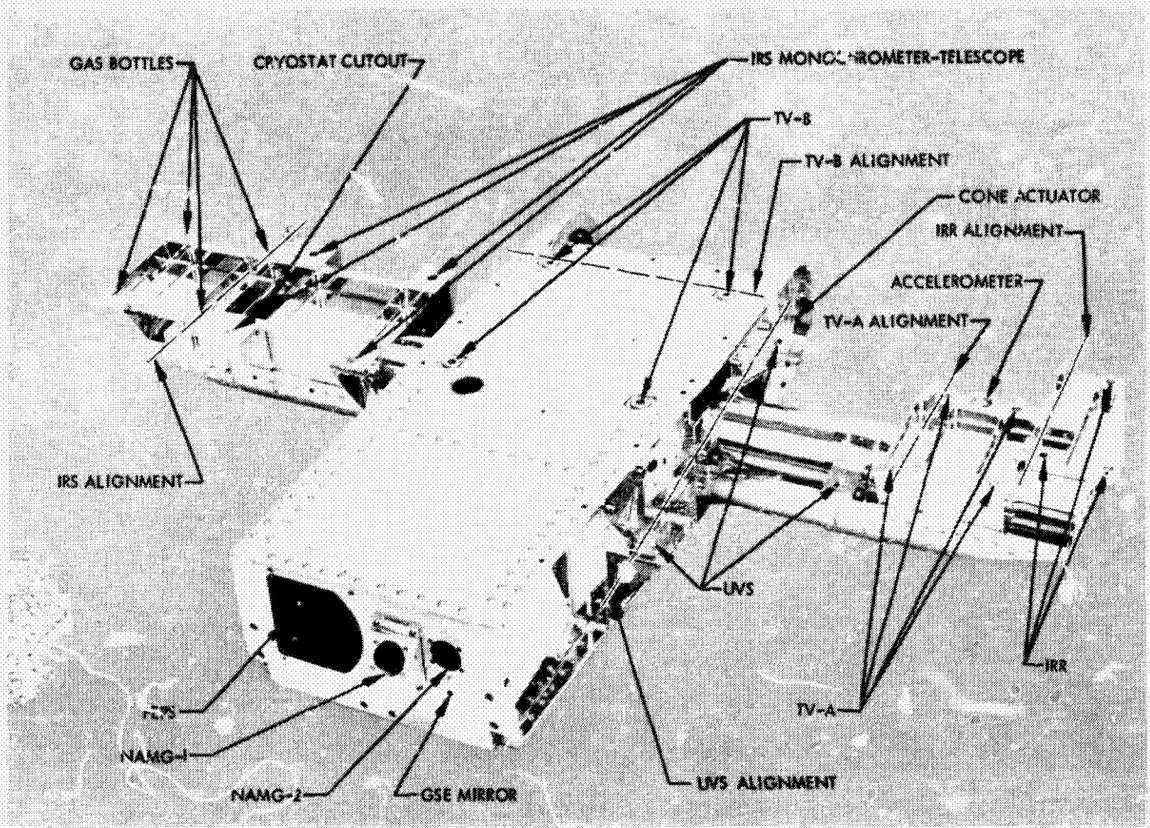


Fig. 4. Instrument and sensor mounting points

fiber glass at the alignment interface was on the platform shoulders.

The FEPS was mounted inside the box section, looking out forward through the outboard beam. Alignment was given by two shoulders. The NAMGs were mounted on the front of the outboard beam, aligned only by the bolt pattern. The NAMG-1, which started IRS cool-down, was mounted on a wedged block which, in turn, was bolted to the outboard beam. The NAMG-2, which started the near-encounter sequence, was bolted directly to the outboard beam. A mirror, which was used during alignment measurements, was bolted to the outboard beam and was rotationally constrained by a dowel pin. The mirror was used as a reference line during instrument checks and was removed for flight.

The platform flight accelerometer was mounted on the IRR–TV-A bracket by the rear of the TV-A. Two thermal control heaters were mounted on the left beam, and a temperature transducer was located in the gimbal gooseneck.

The two scan actuators fitted into shallow, close-tolerance bores and were located at a specified angle by dowel pins.

The routing and support of cabling from the bus to the platform was a problem. The original intent was to separate power, pyrotechnic, signal, and scan wires into four bundles to reduce cross talk and noise in the signal lines. For simplicity and to reduce torque required to turn the cable bundle, the harness through the gimbal was a loose single bundle that flared between the mounting points to prevent cross talk. The cable harness was gathered from various points on the bus at the port in the clock actuator adapter. The harness then made a 90-deg bend to align with the clock tube and passed through the interior of the tube down to the gooseneck. In the gooseneck, the bundle made two 90-deg turns to the cone axis and exited at the rear of the IRS. From this point, the harness spread outward to the instruments, sensors, heaters, accelerometer, and cone actuator. The movements of the gimbal axes were accommodated in the harness by

torsion rather than by bending. The harness was tied to the bus at the top of the clock tube and to the gooseneck at the bottom of the clock tube, with a combination bumper-guide in the center. The harness was fixed with respect to the cone axis in the gooseneck. Attach points and supports were placed at intervals along the platform to restrain the cabling.

Thermal control considerations resulted in the provision of (1) polished external surfaces to reduce heat losses, (2) black paint on the interior of the box section to increase internal heat transfer, (3) the radiation barrier inside the instrument tube, (4) the isolation sleeve in the gimbal to reduce heat flow between the bus and platform, and (5) nylon hook and pile fasteners bonded on exterior surfaces for attaching thermal shields.

As described before, the platform instrument frame was tied to the spacecraft bus during launch. After the first midcourse maneuver, the platform restraint was removed by a pneumatic latch mechanism. As the platform was released, it moved away from the bus along the clock axis for 0.060 in. The spring-loaded thrust washer followed this movement until the outer edge of the thrust washer rested against the clock axis split cap bearing. The platform movement remaining after the thrust bearing was seated provided the thrust axial clearance necessary for smooth operation. The rotational movement of the platform was constrained to the specified operational envelope by mechanical stops. The location of the two clock stops was fairly critical because the actuator position potentiometers became unstable about 1 deg beyond the stops. The cone axis stop had a dual range. The platform was stowed at a cone angle of 96 deg. The stop was set slightly below this angle to prevent the platform from coming up into the bus. The platform was able to slew the entire clock range at a cone angle of 96 deg without striking the bus. However, the platform operational cone envelope was 101 to 165 deg. Therefore, when the platform cone angle passed 101 deg, the cone stop pin dropped off a shelf into a slot with cone limits of 101 to 165 deg. The platform was prevented from returning to the stowed position until the pin was retracted manually.

2. Testing. The platform structure was tested in the bus after installation for smooth, low-torque operation, using a mockup actuator and a dial torque wrench. During systems tests of the scan subsystem, the platform was driven by the actuators and the operation was noted. Each flight unit was operated, although through small movements, in the space simulator. The thermal qualification of the platform was done during the thermal control model tests, both in separate platform thermal studies and on the spacecraft bus in the 10-ft simulator. The platform was subjected to proof loads during the development test model vibration testing without damage. It was found that the accelerations were one-half of the predicted levels. The platform was type-approval qualified on the proof test model (PTM) during the PTM vibration and thermal testing. Similarly, flight approval qualification of the flight units was on the flight spacecraft during vibration and space simulator testing.

3. Problems. It was found that the PTM platform had tilted with respect to the bus after extensive testings—systems, vibration, and space simulation. Examination showed that the box section was undamaged; therefore all distortion was in the gimbal. Upon examination, the bolts joining the clock tube and thermal isolator were found to have enlarged their holes (they no longer had a press fit), but this did not account for the tilt. It was found that the gimbal is relatively weak when an access cover is removed and it is surmised that the damage occurred during a period of systems testing when the cover was not installed. As a result of the discovery that the cover is structural and not just a dust cover, the thickness was increased from 0.020 to 0.063 in. and it was specified that the cover must be installed during testing. The elongation of the bolt holes in the fiber glass isolation sleeve was traced to testing in the Spacecraft Assembly Facility; M69-3 was undamaged both prior to and after vibration, and the development test model had much less damage than the PTM although the former experienced much higher vibration levels. It was found that the platform can impose 2100 in.-lb torque across the isolator joint in one system test configuration. The solution was to install bushings to increase the area in bearing and to warn the Spacecraft Assembly Facility about the possibility of damage during extreme testing.

The running torque of the PTM platform in clock motion was found to be excessive during testing. The problem was traced to the thrust bearing, which was distorting and dragging on the clock tube flange. The solution was to increase the shim thickness to give adequate thrust bearing clearances.

The platform cone angle range capabilities in the loaded configuration in a 1-g field were lower than expected. It was found that the actuator slip torque, combined with the frictional load due to gravity and actuator arm thrusts, gave very limited ground test capability in cone angle, on the order of 10 deg from gravity dead center.

D. Superstructure

The antenna support structure for the *Mariner* Mars 1969 mission was less complicated than the *Mariner* Venus 67 structure, since the antenna did not require articulation. The *Mariner* Mars 1969 superstructure did not vary greatly from the *Mariner* Venus 67 structure, in that it consisted of swaged and polished aluminum tubing riveted to machined aluminum end-fittings.

Assembly of the superstructure was accomplished by supporting the machined end fittings in their relative positions by accurate machine tooling and by riveting the tubes to their fittings. The only problem encountered during fabrication was a rivet that could not be drawn because of inadequate gun clearance. This rivet was replaced with a chemically expanded type.

The superstructures were completed ahead of schedule and were tested with no failures.

E. Cable Trough Assembly

The *Mariner* Mars 1969 cable trough was an eight-sided polygon constructed from aluminum sheet metal formed into a channel.

The structure housed the spacecraft upper cable ring and was mounted on the top of the octagon. The sheet metal segments were spot-welded together and were secured to the octagon structure by machined aluminum clips riveted to the trough.

No particular difficulty was encountered in fabricating the cable trough; however, a late change caused a connector location to be shifted. This made it necessary to patch the existing hole and relocate the mounting. No structural degradation was associated with these modifications, and the cable trough passed its structural test requirements

F. High-Gain Antenna Structure

The high-gain antenna structure is composed of the parabolic reflector and the feed support truss.

In previous spacecraft programs, which used essentially the same parabolic reflector design, the certification of bond quality on honeycomb core-to-face skin bond lines was based largely on sample coupon testing and visual verification of bonding preparation. To assure the discovery of any low-strength bonding and of any voids in the bond line, a method of pressurizing the *Mariner* Mars 1969 high-gain antenna honeycomb structure was developed that proof-loads the core–face–skin bond line, thereby certifying it to be structurally sound.

When this inspection method is applied to heavy honeycomb structures with thick face skins (0.016 in. or greater), it will detect only very large voids in the bond line. Its primary usefulness in this case is that of general proof-loading of the bonded joints. By contrast, when the pressure inspection method is applied to thin-face-skinned honeycomb (0.005 in. or less, as in the high-gain antenna), it can detect voids as small as 0.10 in. in diameter, thus providing significant new information about the bond line in addition to the simple *go, no-go* results of the proof pressure loading.

The pressure testing of the high-gain antenna honeycomb structure was achieved by (1) simultaneously sealing the edge of the honeycomb sandwich with a core fill material and potting copper-tube pressure taps into the edge seal and then (2) injecting air into the sandwich through the pressure taps. A few seconds were required for the pressure in the sandwich to equalize through the perforated core; then the face skins were inspected for bulges, which indicated bond-line voids. The entire process required approximately 1 day and replaced a less informative ultrasonic inspection method requiring approximately the same length of time.

Following fabrication, the high-gain antennas were tested for qualification. No difficulties were encountered in qualifying the high-gain antennas.

G. Low-Gain Antenna Structure

The low-gain antenna is mounted on the top of the octagon structure similar to the *Mariner* Mars 1964 and *Mariner* Venus 67 designs. In the *Mariner* Mars 1969 design the antenna was 95.25 in. long and extended above the solar panels when the spacecraft was in the boost configuration. The structure consisted of a 25-mil-wall, 4-in.-diam aluminum tube supported parallel to the spacecraft roll axis by two spring dash pots struts and pin-jointed at the base. The 4-in. tube was the wave-guide, which radiated directly through a cruciform-shaped aperture at the tip.

Because the technique for fabricating the tubular low-gain antenna was developed on earlier programs, no difficulty was experienced with the *Mariner* Mars 1969 units. Fabricated antennas were qualified without difficulty.

H. Solar Panels

The construction and attachment of the *Mariner* Mars 1969 solar panels were similar to those of the previous *Mariner* solar panels.

During production of the solar panel structures, a very serious problem was discovered by routine quality assurance testing of adhesive peel strength. Production peel-test sample results and an extensive laboratory-controlled peel-test program supported the conclusion that a structurally unacceptable bond joint (bonding failure) can result even though procedures reflecting current industry standards are followed for cleaning and bonding aluminum. The acid etch solution, when mixed exactly to specification in clean glass containers, has randomly produced weak bond joints (less than 10% of normal joint peel strength). These low-peel-strength bond joints exhibit a dangerous lack of resistance to bond-line fracture propagation. Unfortunately, sufficient data to specify an etch solution that will consistently produce high-peel-strength bond joints in aluminum structures are not available at present.

The random nature of the bonding failure made it possible that a weak structural bond could have occurred in any of the bonded structures, even though the associated process control bonding samples were of good quality. Since no immediate solution to the bonding problem existed, the *Mariner* Mars 1969 solar panels were fabricated using the existing cleaning and bonding procedures and then proof-loaded in such a manner that the critical bond joints were certified to be structurally sound.

No problems were experienced during qualification testing of the solar panels.

III. Electronic Packaging Structure

A. Introduction

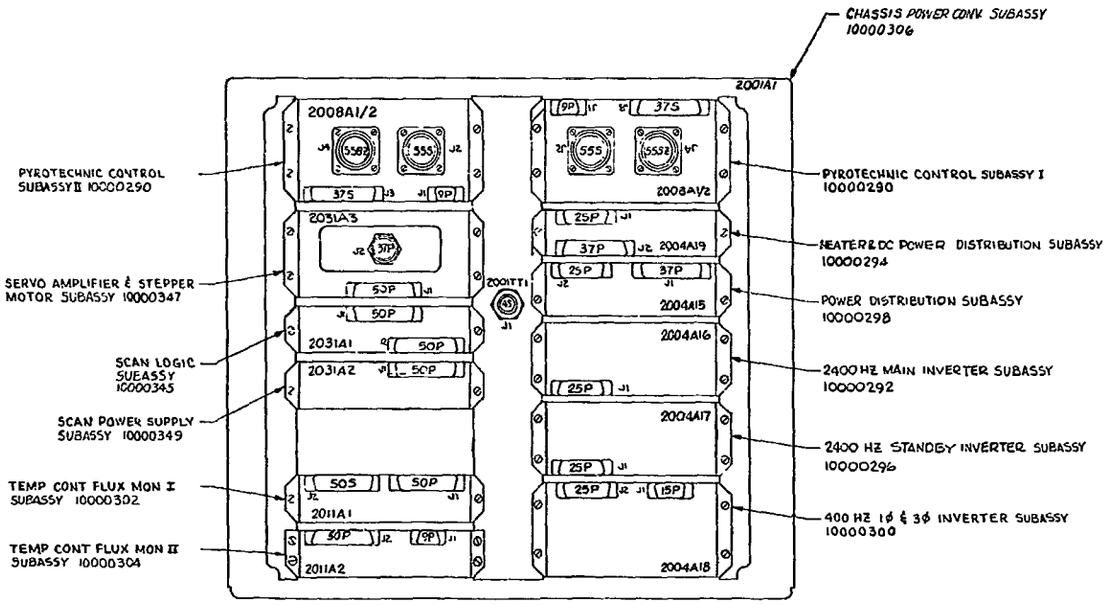
Each major electronic assembly mounted within the octagonal bus was made from at least three types of hardware: chassis assembly structure, cable harness assembly, and electronic subassemblies. Frequently, the electronic subassemblies from more than one subsystem required placement within a single electronic assembly; for example, electronic assembly (EA) I contained electronic subassemblies from four subsystems for *Mariner* Mars 1969: power, scan control, pyrotechnic, and temperature control flux monitor (TCFM). Accordingly, all electronic assemblies installed within the spacecraft octagon were given a structure subsystem reference designation (for example, EA I). Figure 5 shows the reference designations and the layout of the electronic assemblies within the *Mariner* Mars 1969 octagonal structure.

Three different configurations were used for the octagon electronic assemblies: EA I, IV, V, and VI used a modified *Mariner* Mars 1964 integrated shear plate design, while EA VIII (power regulator) was a completely new modular design for *Mariner* Mars 1969. A new plug-in equipment electronic assembly was developed for use in EA III (attitude control/central computer and sequencer) and EA VII (scientific equipment). (Because bay II housed the spacecraft propulsion subsystem, there was no EA II.) The design and development of the new plug-in equipment EAs were undertaken primarily to develop more volume (20%) for use by the electronic subsystems in EA III and VII.

B. Integrated Shear Plate Electronic Assemblies

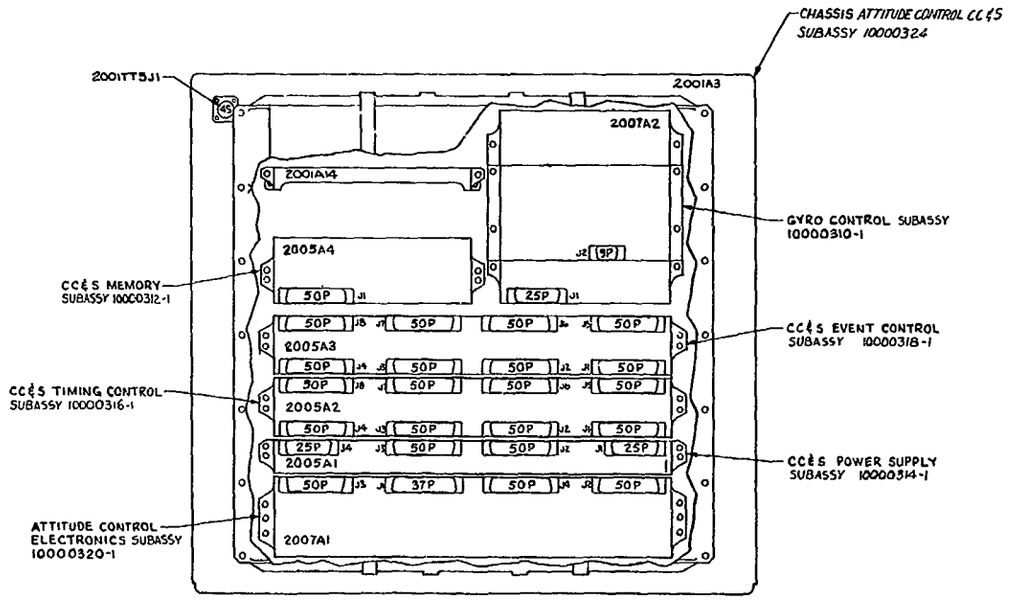
The integrated shear plate electronic assembly concept was first developed by JPL for the *Mariner* Mars 1964 program as a lightweight, structurally efficient EA design. The integral shear plate of the EA chassis is utilized as a load-bearing primary structural member by the spacecraft octagonal bus; the integrated shear plate EA chassis is also used for temperature control by conducting heat within the overall electronic assembly and by radiating heat into space.

Major changes were made in the mechanical design of the integrated shear plate EA for *Mariner* Mars 1969. The shear pin fasteners were deleted at each of the four corners of the chassis at the interfaces with the spacecraft octagon inboard longeron flanges and the corner shear pins were replaced with screws in order to withstand additional tension forces. There were two reasons for making this change: (1) the new *Mariner* Mars 1969 EA configuration in bays III and IV required threaded fasteners in the four corners of the inboard longeron flanges and it was desirable to have identical interfaces between all the EAs and the octagon, and (2) adding the screws at the inboard corners of the chassis improved the mechanical integration between the integrated shear plate EA and the spacecraft octagon structure, thus improving the overall dynamic performance of the *Mariner* Mars 1969 integrated shear plate EA in comparison with the *Mariner* Mars 1964 design. The EA cable harness support assembly, which carries the EA cables, was redesigned to decrease fabrication costs, increase physical reliability, and increase operational flexibility.



POWER CONVERSION/PYRO CONTROL
ELECTRONICS ASSEMBLY I
10000140 2001EA1

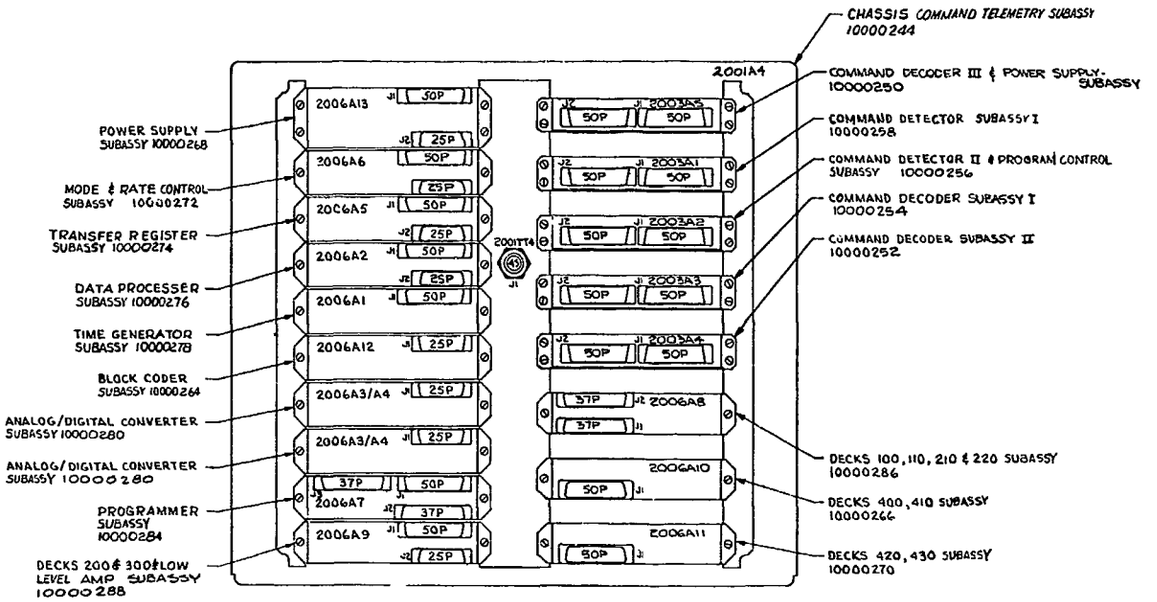
(WIRING HARNESS, POWER CONVERSION SUBASSY
10000307 REMOVED FOR CLARITY)



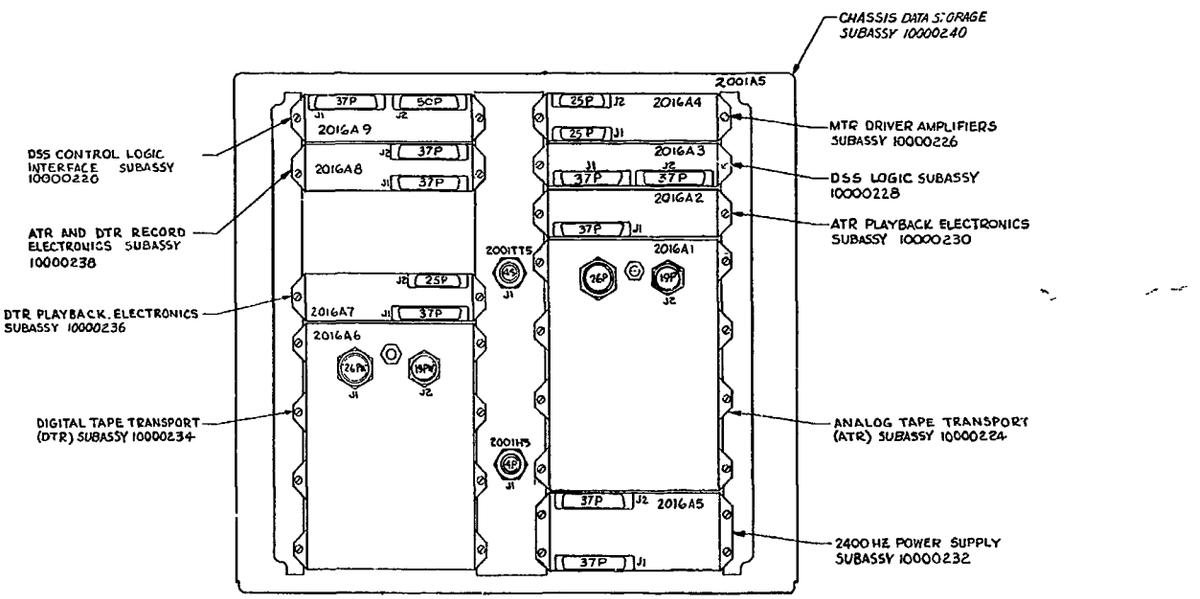
ATTITUDE CONTROL/CC&S
ELECTRONIC ASSEMBLY III
10000150 2001EA3

(INSIDE WEB OF CHASSIS AND WIRING HARNESS
ATTITUDE CONTROL CC&S SUBASSY
10000326 REMOVED FOR CLARITY)

Fig. 5. Electronic packaging layout

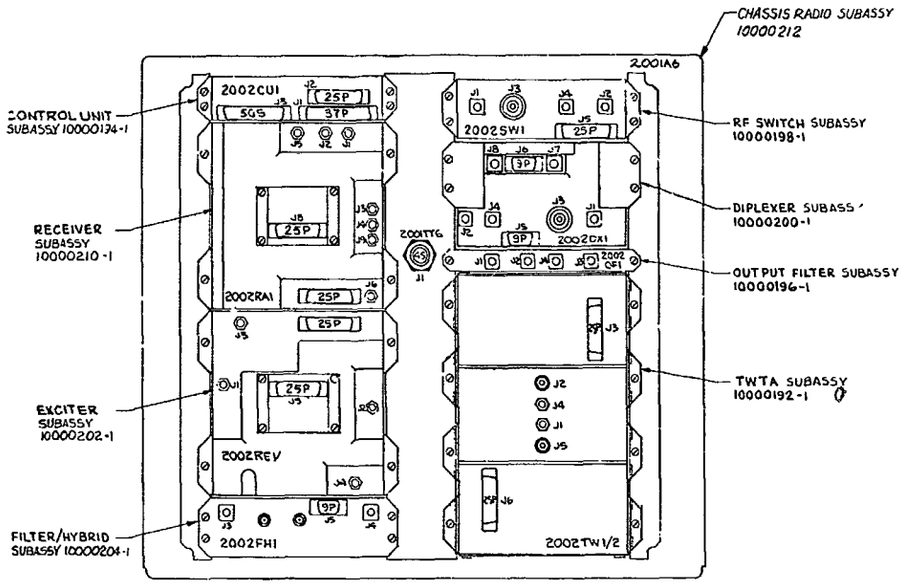


COMMAND/TELEMETRY
ELECTRONIC ASSEMBLY IV
10000144-1 2001EA4
(WIRING HARNESS, CMD/TELEMETRY SUBASSY REMOVED FOR CLARITY) (10000245)



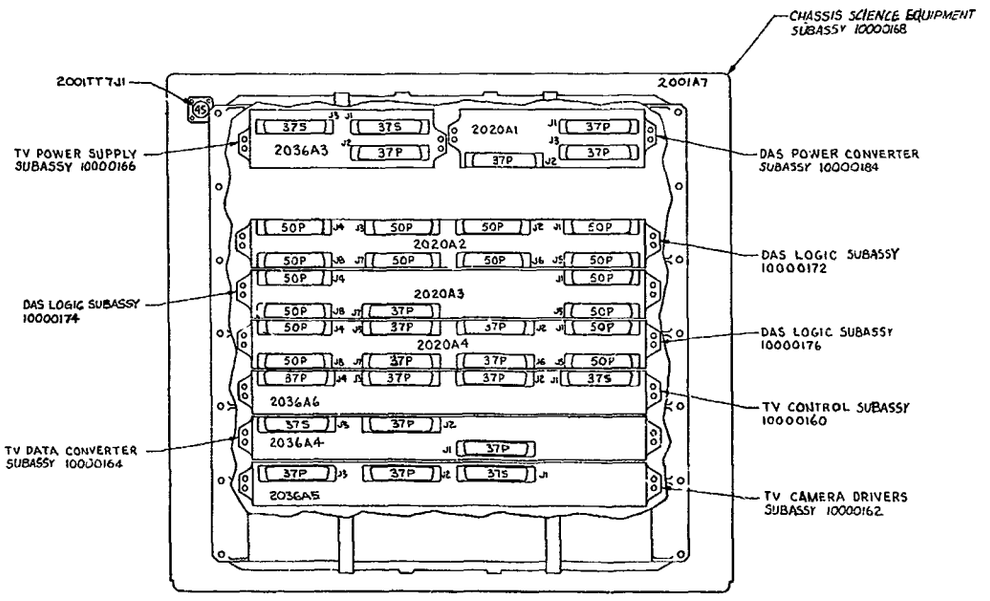
DATA STORAGE
ELECTRONIC ASSEMBLY V
10000146 2001EA5
(WIRING HARNESS, DATA STORAGE SUBASSY 10000241, REMOVED FOR CLARITY)

Fig. 5. (contd)



RADIO ASSEMBLY VI
10000148 2001EA6

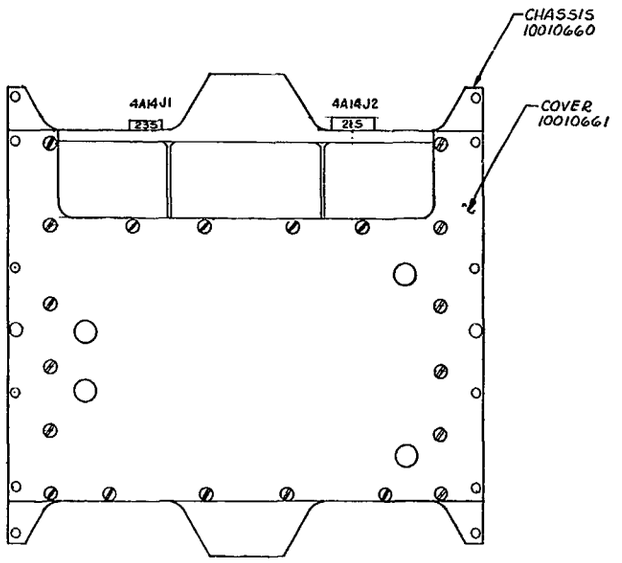
(WIRING HARNESS, RADIO SUBASSY
10000217 REMOVED FOR CLARITY)



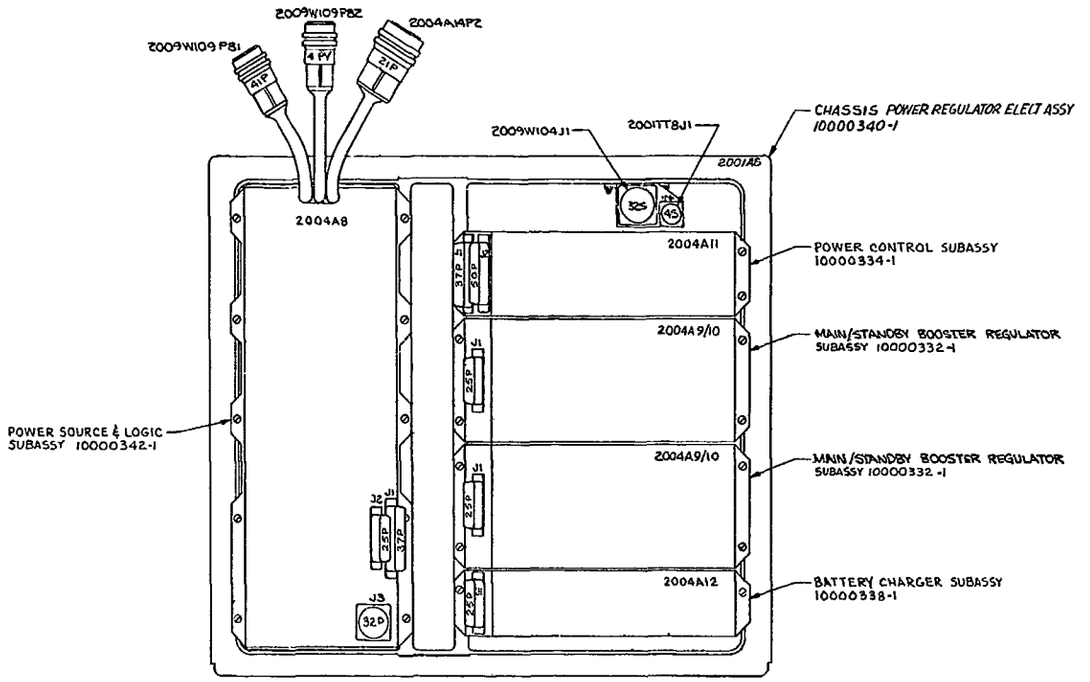
SCIENTIFIC EQUIPMENT
ELECTRONIC ASSEMBLY VII
10000142 2001EA7

(INSIDE WEB OF CHASSIS AND WIRING HARNESS SCIENCE
EQUIPMENT REMOVED FOR CLARITY) (10000168)

Fig. 5. (contd)



BATTERY ASSEMBLY
(LOOKING INBOARD)
10000154 2004A14



POWER REGULATOR
ELECTRONIC ASSEMBLY VIII
10000152 2001EA8
(WIRING HARNESS, POWER REGULATOR SUBASSY
10000341 REMOVED FOR CLARITY)

Fig. 5. (contd)

C. Plug-In Equipment Electronic Assemblies

It became apparent early that the *Mariner* Mars 1969 spacecraft configuration (based on the *Mariner* Mars 1964) would not adequately house the required electronic equipment, and that new packaging configurations would be required. The volume requirements became critical for the attitude control/central computer and sequencer and science equipment (data storage and data automation/television) electronic assemblies (EA III and EA VII respectively).

The following description briefly summarizes the design of the new plug-in electronic assemblies.[1]

The new *Mariner* Mars 1969 plug-in equipment electronic assembly was designed for a high degree of mechanical integration within the octagonal spacecraft structure. This integrated design concept was also a feature of the *Mariner* Mars 1964 electronic assembly, which utilized the chassis structure as an integrated shear plate for the octagonal structure.

Figure 6 shows the plug-in electronic assembly installed in a typical bay within the spacecraft octagonal structure. The separate outer shear plate fastens to the outboard flanges of the longerons and the outboard flanges of the upper and lower ring structures; the chassis fastens to the inboard longeron flanges. The mechanical integration of electronic subassemblies within the chassis and shear plate structures is more effective than that of previous JPL spacecraft designs.

[1]A more complete description is given in *Flight Projects*, Space Programs Summary 37-53, Vol. I, pp. 21–29. Jet Propulsion Laboratory, Pasadena, Calif., Sept. 30, 1968.

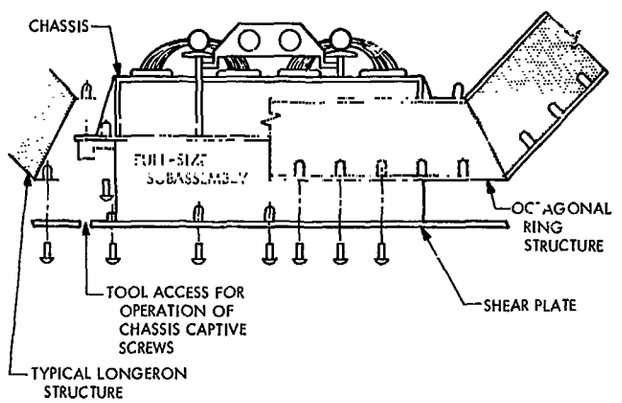


Fig. 6. Installation of plug-in electronic assembly into octagonal structure bay

D. Discussion of Individual Assemblies

1. Power conversion pyrotechnic control, electronic assembly I. Electronic assembly I contained electronic subassemblies from the power, scan control, temperature control flux monitor, and pyrotechnic subsystems; Fig. 5 identifies the various subassemblies.

Severe problems occurred with this EA during vibration testing. Apparently, there was coupling of resonances between the test fixture and the EA, and one chassis was actually cracked during type approval level testing. A new vibration fixture is being developed for future programs, and it is felt that use of the new (and stiffer) fixture will eliminate problems that have occurred in the past.

2. Command/telemetry, electronic assembly IV. Electronic assembly IV contained the subassemblies comprised in the flight telemetry subsystem and flight command subsystem.

One major problem occurred during the initial vibration testing of this EA; a large space was left initially on one side of the EA between subassemblies of the flight command subsystem and flight telemetry subsystem. This space was left to allow for possible growth of either electronic subsystem. The dynamic characteristics of the initial EA configuration were unacceptable, and the electronic subassemblies were repositioned for more equal spacing. Subsequent vibration testing showed a marked improvement in the dynamic performance, and the final EA configuration is shown in Fig. 5.

3. Data storage, electronic assembly V. The data storage subsystem is contained completely within EA V. Figure 5 shows the overall EA configuration. The integrated shear plate EA design relies inherently on the electronic subassemblies for stiffening since they are used as load-bearing members.

A unique problem occurred in the design of EA V because of the mechanical design of the two hermetically sealed tape transport subassemblies. Normally, the outboard surfaces of the electronic subassemblies are tied to the integrated EA thermal/shear plate with screws, but the tape transport units were spaced away from the thermal/shear plate and supported only by their "ear" flanges; this design feature was carried over from the tape transport design for *Mariner* Mars 1964, and use of the 1964 design was a constraint for the *Mariner* Mars 1969 tape transport envelope. Initially, both tape transports were positioned at the lower end of EA V, but when it was

discovered that the transport subchassis could not be tied into the chassis shear plate, the analog tape transport was moved up far enough to install a more conventional subassembly below it (see Fig. 5). Vibration testing qualified the resultant design with no outstanding problems.

4. Radio, electronic assembly VI. The radio electronic assembly was somewhat unusual for *Mariner* Mars 1969 because of the relatively high power dissipation of the power amplifier and because of the high packaging density (compared with the *Mariner* Mars 1964 radio). The thermal design approach that was taken for the *Mariner* Mars 1969 radio EA was to attempt to design the chassis for low temperature gradients. A heat pipe was developed as a backup effort for use, if required, to further reduce thermal gradients in the EA chassis. Final temperature measurements indicated that the design of the chassis was satisfactory thermally and that the heat pipes were deleted from the design of the radio EA. The radio EA was the heaviest of the *Mariner* Mars 1969 electronic assemblies and there was some concern about the mechanical integrity of the chassis under type approval vibration conditions. An EA I chassis had previously failed under type-approval-level vibration because of a coupling of resonances between the EA and the vibration test fixture. Fortunately, the resonant frequencies of the radio EA were enough lower than those of EA I to adequately decouple from the test fixture resonances; the *Mariner* Mars 1969 EA VI (radio) dynamic characteristics were excellent during vibration testing. The radio subsystem could not be contained within a single electronic assembly for *Mariner* Mars 1964 and approximately one-half of an adjacent EA was used to contain the receivers and associated power supply. For *Mariner* Mars 1969, the requirement was to package the entire radio subsystem within one EA because the adjacent data storage subsystem required an entire EA due to the addition of the second tape transport. The entire radio subsystem was repackaged because of functional changes, to incorporate two new TWT power amplifiers and to contain the entire radio subsystem within a single EA. The packaging efficiency was improved for the entire subsystem, and density improvements were highest for the receivers, the exciter, and the associated power supplies.

5. Power regulator, electronic assembly VIII. The power regulator assembly was packaged as a unique variation of the integrated shear plate EA design concept for both the *Mariner* Mars 1964 and *Mariner* Mars 1969 programs. Because EA VIII and the battery had to share a single bay, the height of EA VIII was severely limited in comparison with that of other EAs.

For the *Mariner* Mars 1964 spacecraft, the power regulator was packaged within a single chassis and no modular subassemblies were used. The difficulty of this concept occurred during fabrication and checkout; the unit required excessive time periods for these activities. It was decided to package the power regulator in a modular form factor for *Mariner* Mars 1969 in order to gain the attendant advantages—easier fabrication, quicker checkout, and improved operational considerations. Because of the previously mentioned height constraint for EA VIII, the new subassemblies were limited to approximately 3.2 in. in height, and a completely new electronic subassembly design configuration had to be developed.

The thermal characteristics of the new EA VIII chassis were excellent and no modifications were required during initial development testing. Some minor improvements were made to improve the dynamic characteristics after the initial developmental vibration testing. The top plate of the chassis center box beam was initially attached only by screws. The resonant frequency of the EA at the center of the box beam was only 240 Hz when the assembly was vibrated in the Y axis (perpendicular to the plane of the shear plate). The mechanical integration of the box beam was improved by adhesive bonding the box beam top plate to the chassis: the resonant frequency increased to 260 Hz. This 20-Hz increase in resonant frequency was significant because the vibration input levels dropped to 4.5 *g* rms from 7.5 *g* at 250 Hz. The overall dynamic performance of EA VIII was excellent in all three axes, partly because of the new vibration fixture that was designed for this unit. The fixture was very rigid, and there was no apparent coupling of resonances between the fixture and electronic assembly.

E. Electronic Assembly Handling and Shipping Equipment

The shipping equipment required for electronic assemblies was of the same design that was used for *Mariner* Venus 67 (see Fig. 7). The electronic assembly is fastened within a rigid handling fixture, and the fixture is in turn supported within a hermetically sealed and close-fitting inner container. The inner container is then fitted within an outer container for environmental protection during shipment; the outer container has a very thick resilient foam inner liner (Fig. 7) for isolation of the electronic equipment from a shock or vibration environment.

The electronic assembly handling fixture is shown in Fig. 8. This unit is a modification of the *Mariner* Mars 1964 design; two rectangular bars (with lightening holes) were

added to stiffen the assembly and to more precisely support and align the EA chassis during installation of subassemblies. Two round rods were installed between the end plates of the fixture, and connector dust caps were attached to the rods by clamps. The pigtailed cables of the EA cable harness assemblies were thereby supported by engaging each circular connector to the corresponding hard-mounded dust cap.

Satisfactory handling and shipping equipment for electronic subassemblies had not been designed and developed by JPL for previous programs and it was decided to develop this hardware for the *Mariner* Mars 1969 Program. A design concept utilized for previously designed

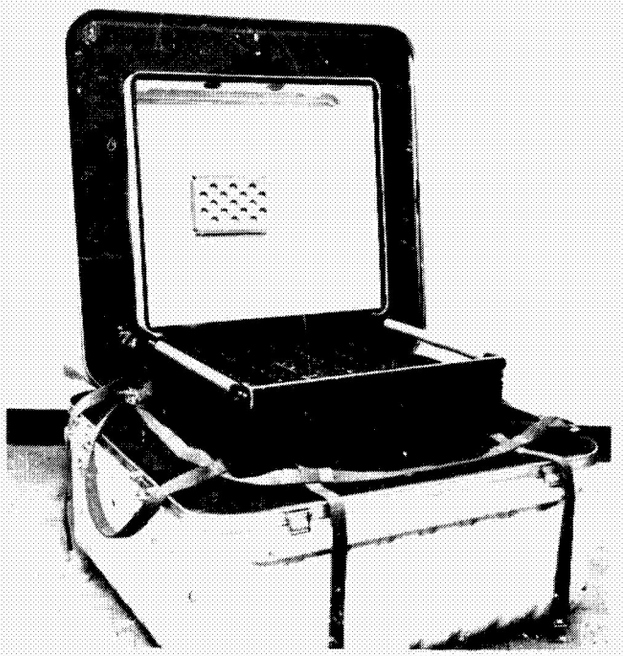


Fig. 7. Electronic assembly shipping equipment

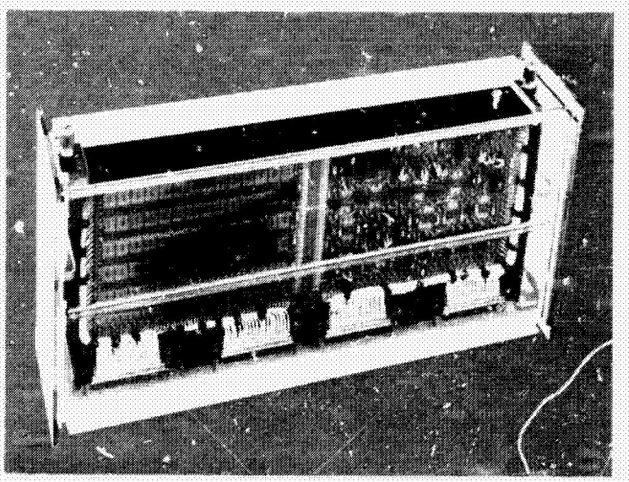


Fig. 9. Full-size subchassis handling frame

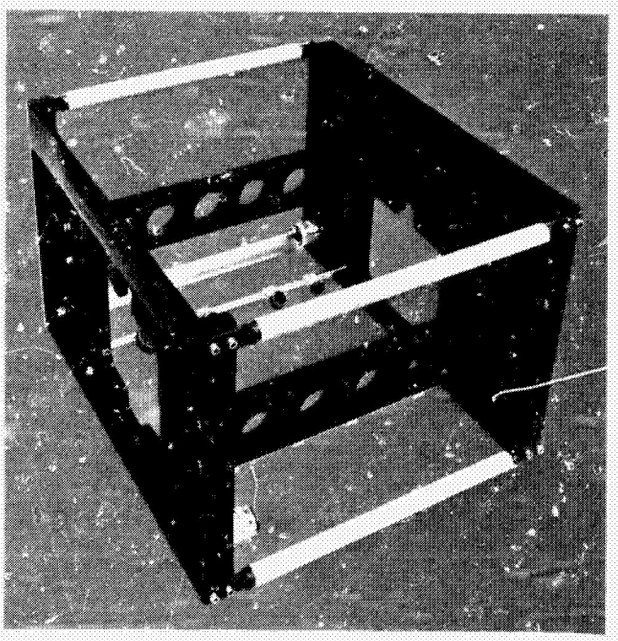


Fig. 8. Electronic assembly handling frame



Fig. 10. Electronic subassembly transportation system

JPL handling (not shipping) equipment was followed. Plastic side frames were designed which could be attached to either the new *Mariner* Mars 1969 type of subassembly (14 or 6.5 in. wide) or to the *Mariner* Mars 1964 type. The capability to install clear plastic protective covers within grooves in the side frames was a new feature of the design. Figure 9 shows the new handling frames and covers installed on a full (14-in.-wide) subassembly. The handling frames fit closely within matching grooves in the associated inner containers (Fig. 10). The inner container may be used during in-plant fabrication and checkout for protection from handling and contamination. The inner container in turn fits within the resilient foam liner of the outer container, which is used for environmental protection during transportation, etc. The outer container is large enough to accept two half-sized subassemblies.

IV. Cabling Subsystem

A. Introduction

The *Mariner* Mars 1969 spacecraft cabling is similar to designs on earlier *Mariner* vehicles. It consists of upper and lower ring harnesses, electronic assembly harnesses, platform and adapter harnesses, and miscellaneous peripheral harnesses.

Standard spacecraft cabling design approaches were taken. Consideration was given to the requirements for mechanical strength, environmental protection, electrical function, and accessibility during construction, rework, and test. In addition, various unique design innovations were incorporated in several of the harness assemblies to accommodate physical and electrical characteristics peculiar to the *Mariner* Mars 1969 spacecraft.

B. Description

The upper and lower ring harnesses interconnect the eight electronic assembly bays and provide interface for the umbilical functions, the solar panel power, some science platform functions, the sun sensing functions, and other peripheral cabling.

The science scan platform harness services all the instruments mounted on the platform and makes the necessary connection between the science instruments and associated electronics located in the electronic assembly bays.

The *Centaur* adapter harness carries the umbilical functions from the lower ring harness to the adapter island. It also accomplishes required circuit interruption for initiation of several system functions at spacecraft/adapter separation. Other system signal and power control functions use the several peripheral harnesses which are integrated with the spacecraft.

The upper ring harness (Fig. 11) is divided into three separate cables for carrying noisy signal, quiet signal, and power distribution functions. The cables are individually mounted within a single support tray, providing both physical separation for ease of fabrication and installation and electrical separation for control of electromagnetic interference. Other design features, such as selected lay length in twisted wire configurations and 90 deg crossovers in the mounting methods, further enhanced isolation within the ring assembly.

Forty hard-mounted and seven pigtailed connectors are used in the harness assembly, requiring 1290 separate contacts. Because of the relocation of the attitude control gas bottles to the top surface of the bus for attachment, it was necessary to design a new ring tray. During this design, the structure of the ring and its attachments to the bus were greatly improved.

The primary use for the lower ring harness is to carry the umbilical functions between the electronic assemblies and the inflight separation connectors on the spacecraft.

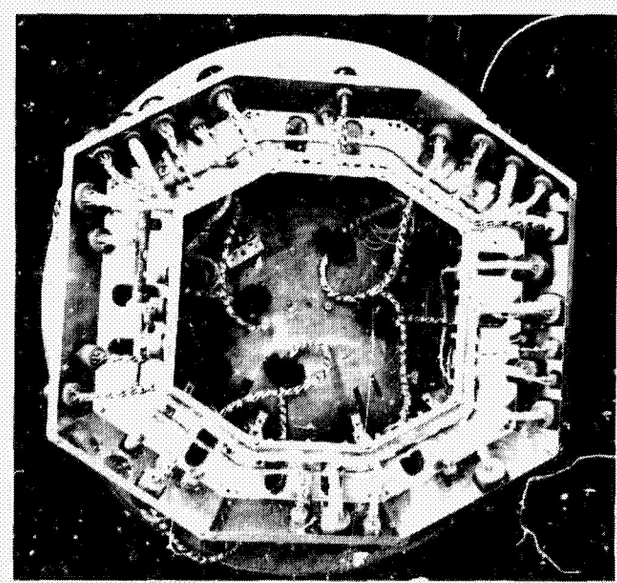


Fig. 11. Upper ring cabling harness

It also interconnects the lower connectors of the electronic assembly harnesses, the secondary Sun sensors, separation-initiated timer, and pyrotechnic arming switch. The in-flight connectors carry all the umbilical functions plus selected systems functions that are actuated upon separation of the spacecraft from the *Centaur*. Two connectors of 63 pins each and a separate connector for the two coaxial cables were used. This configuration reduced the weight by about 40% and the cost by more than 80% when compared with connectors used in earlier *Mariner*-type spacecraft.

Because of the excursions of the science platform, the lower ring harness had to be made smaller and relocated. The harness itself was modified to resemble a nearly closed C, permitting it to be installed and removed with the platform in place. The new harness was attached to the inner periphery of the lower octagonal structures by means of Ty-raps through nylon pillow blocks on the structure. This eliminated the use of cable clamps, washers, and screws and allowed the harness to lie closer to the structure.

The electronic assembly harnesses were of three different types. Type A (Fig. 12) was similar to the *Mariner* Mars 1964 design except that the cable support bracket was redesigned to allow separation of the bracket tubes from the center post. This design change permitted the removal of individual harnesses when the electronic assembly was shared by several subsystems.

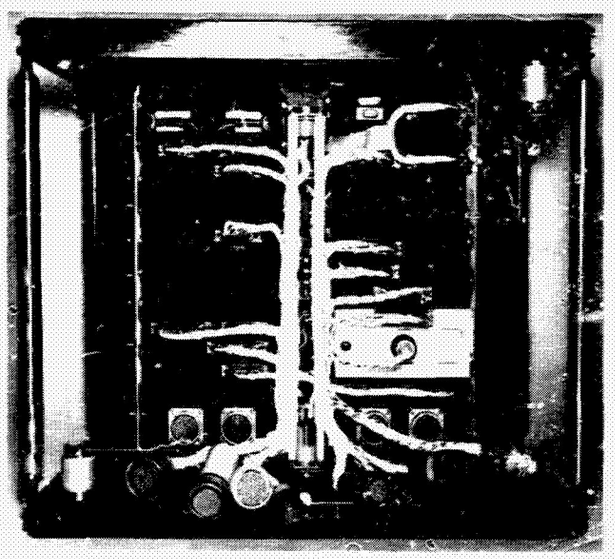


Fig. 12. Type A electronic assembly cable harness

Type B (Fig. 13) is a rack-and-panel type of design with the harness connectors (Hi-Rel rectangular D type) float-mounted on the inboard surface of a bathtub-type chassis. The subchassis are then "plugged" into the main chassis from outboard and covered with a shear plate for support and protection. The inboard surface of the main chassis is supported by two rails machined as a part of the chassis. The cables are supported on these rails by Ty-raps attached through rectangular holes in the base leg of the rails. At each end of the chassis a keystone-shaped plate is bolted to the ends of the rails to provide a surface on the upper end for the operational support equipment connectors and on the lower end for the lower ring interface connectors.

Type C (Fig. 14) is used in bay VIII only.

The science platform cabling harness is composed of four cables: (1) the science harness connecting the platform science instruments to the science electronics in bay VII; (2) the power harness, which supplies instrument power through the upper ring; (3) the scan control harness interconnecting the two scan actuator motors, the clock motor on top of the platform support tube, and the cone motor on the platform perch tube, with its associated

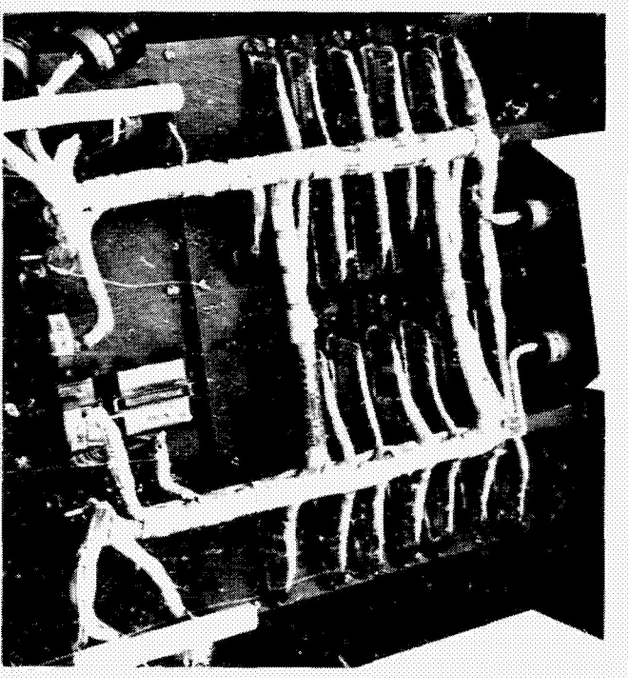


Fig. 13. Type B (rack-and-panel) electronic assembly cable harness

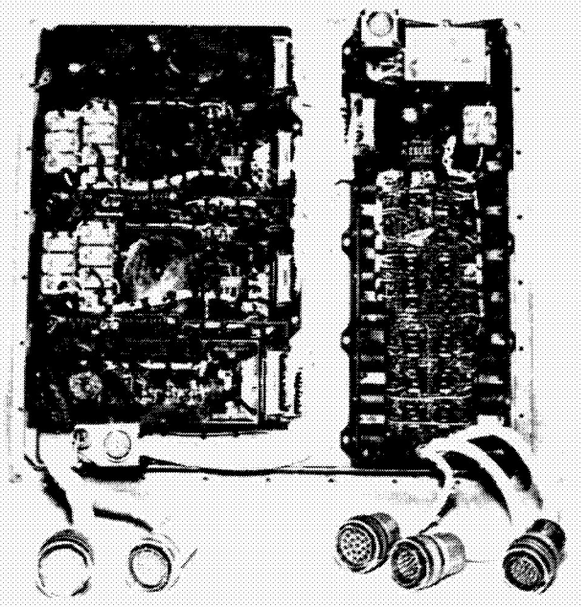


Fig. 14. Type C electronic assembly cable harness

electronics in bay I; and (4) a pyrotechnic cable connecting the IRS cooling gas valves to the pyrotechnic firing unit in bay I.

The size and complexity of the science platform and the attendant large excursions of the science instruments caused interferences with the lower end plates of the electronic assembly harnesses, requiring them to be relocated. The solution to this problem was to move the direct-access connectors to the upper bracket in all the bays. In turn, this required relocation of the connectors, already mounted in the upper bracket plates, to new supports on the spokes of the bus and on the upper ring tray.

A study of the science platform cabling installation was made using a mockup constructed of transparent plastic. All mechanical articulating members were simulated, and tests were made to determine the torque required to position the scan platform against the resistance of cable twist. Optimum cable mounting and support methods were also determined.

C. Documentation

Drawings and indentured parts lists were created for all individual harnesses and cables, and assembly drawings were created for those groups of harnesses which were joined together to form an assembly. The harnesses discussed above are shown in the spacecraft cabling master block diagram (Fig. 15) and the spacecraft adapter cabling block diagram (Fig. 16).

Several tests and studies were made during the *Mariner* Mars 1969 cabling design. A study to evaluate the incorporation of a low-cost noise monitor in the spacecraft cabling was carried out by Northrop Space Laboratories. The report concluded that the cost of suitable recording devices and their maintenance would be excessive in relation to the usefulness of the data obtained. A study of isolation and interference problems created by the cable twist and by grounding and shielding techniques was performed during the early stage of the cabling design. Other EMI tests associated with the scan platform cabling were made, and a scan platform cable articulation torque requirements study was also performed.

D. Fabrication

All harnesses were fabricated on three-dimensional fixtures and verified on a full-sized spacecraft mockup. Flight-approved cable supports were used whenever possible to reduce excessive handling of the cables. The fixtures were arranged so that the flight connectors on the harnesses were mated only once with the fixture connectors during fabrication and inspection, and all probing and/or testing was done through a connector and jumper assembly.

Peripheral cables were fabricated on the mockup spacecraft bus, while fabrication and routing of the cabling on the science platform and spacecraft adapter were done on special fixtures supplied for that purpose. Thus, the routing and fabrication were accomplished and proved simultaneously.

The upper ring harness was fabricated within a flight cable support tray mounted on a special handling fixture. The testing of the harness was done while the harness was still in the handling fixture.

The lower ring harness was fabricated in a manner similar to that used for the upper ring harness.

A summary of cabling subsystem engineering is given below:

Number of cables per spacecraft	33
Total cable weight, lb, for spacecraft	62.29
Adapter cable weight, lb	5.5
Electrical connectors in cables	392
Problem failure reports	27

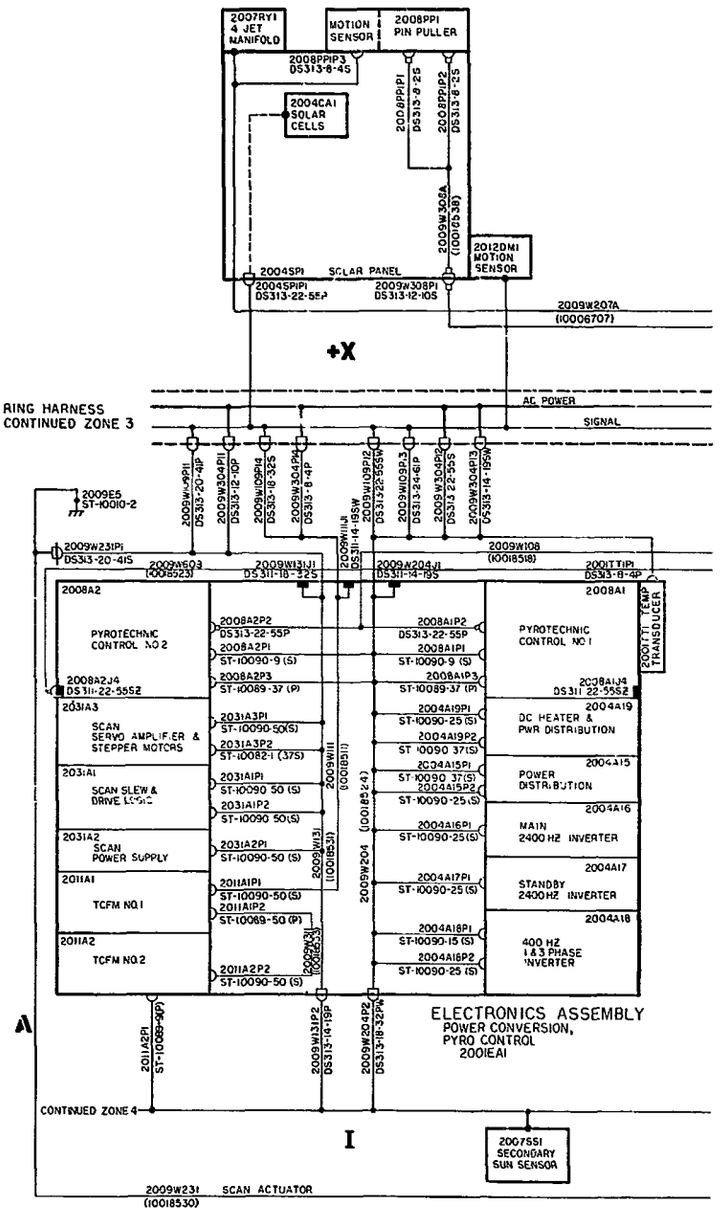


Fig. 15. Spacecraft cabling master block diagram

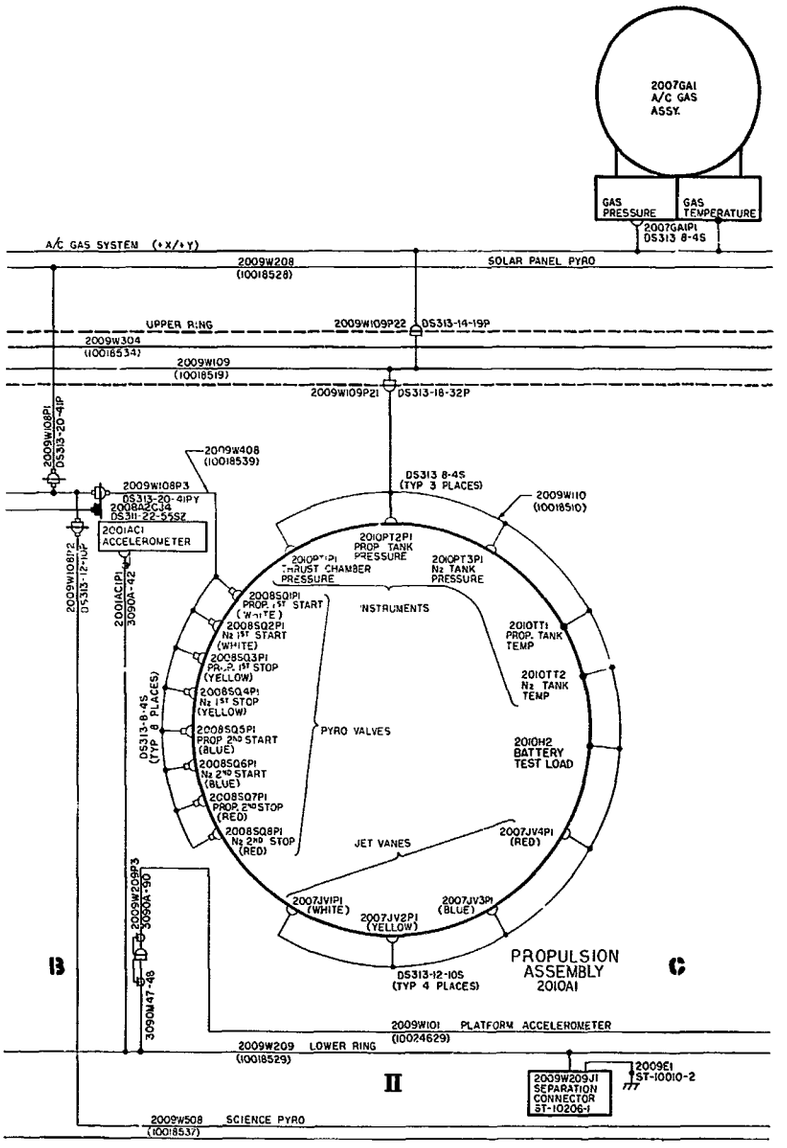

2007GAI
A/C GAS
ASSY.
GAS
PRESSURE
GAS
TEMPERATURE
2007GAIP1
DS313 8-4S
A/C GAS SYSTEM (+X/+Y)
2009W208
(10018528)
SOLAR PANEL PYRO
UPPER RING
2009W109P22
DS313-14-19P
2009W304
(10018534)
2009W109
(10018519)
2009W109P21
DS313-18-32P
2009W108P1
DS313-20-41P
2009W408
(10018539)
2009W108P3
DS313-20-41PY
2008A2C-34
DS311-22-55SZ
2001AC1
ACCELEROMETER
2009W108P2
DS313-12-10P
2001AC1P1
3090A-42
DS313 8-4S
(TYP 3 PLACES)
2009W110
(10018510)
2010PT2P1
PROP TANK
PRESSURE
2010PT1P1
THRUST CHAMBER
PRESSURE
2010PT3P1
N2 TANK
PRESSURE
INSTRUMENTS
2008SQ1P1
PROP 1ST START
(WHITE)
2008SQ2P1
N2 1ST START
(WHITE)
2008SQ3P1
PROP 1ST STOP
(YELLOW)
2008SQ4P1
N2 1ST STOP
(YELLOW)
2010TT1
PROP. TANK
TEMP
2010TT2
N2 TANK
TEMP
DS313 8-4S
(TYP 8 PLACES)
2008SQ5P1
PROP 2ND START
(BLUE)
2008SQ6P1
N2 2ND START
(BLUE)
2008SQ7P1
PROP 2ND STOP
(RED)
2008SQ8P1
N2 2ND STOP
(RED)
PYRO VALVES
2010H2
BATTERY
TEST LOAD
JET VANES
2007JV4P1
(RED)
2007JV1P1
(WHITE)
2007JV2P1
(YELLOW)
2007JV3P1
(BLUE)
DS313-12-10S
(TYP 4 PLACES)
PROPULSION
ASSEMBLY
2010A1
B
C
II
2009W209P3
3090A-90
3090W47-48
2009W101 PLATFORM ACCELEROMETER
(10024629)
2009W209 LOWER RING
(10018529)
2009W209J1
SEPARATION
CONNECTOR
ST-10206-1
2009E1
ST-10010-2
2009W508 SCIENCE PYRO
(10018537)

Fig. 15. (contd)

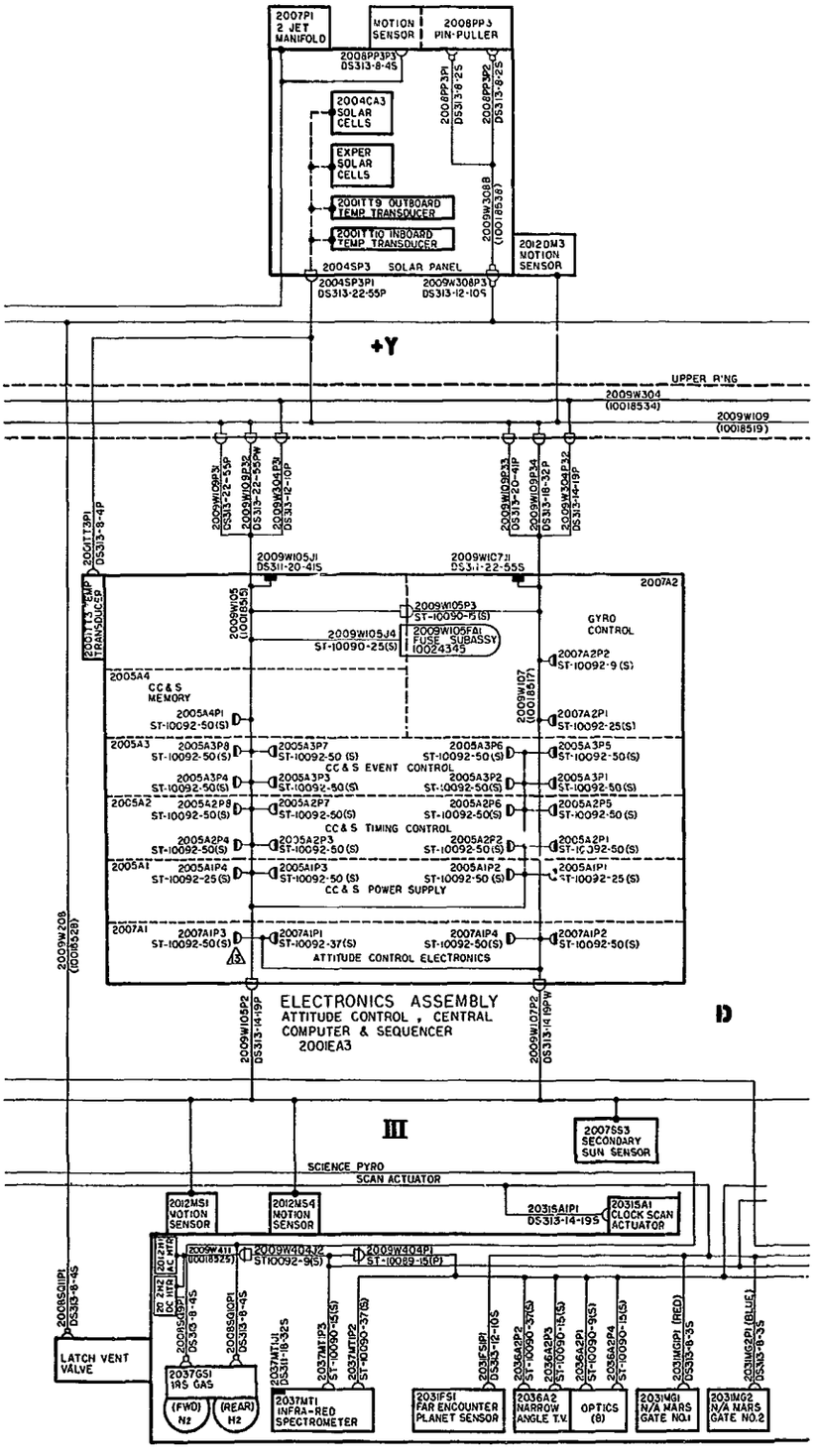

2007P1
2 JET MANIFOLD
MOTION SENSOR
2008PP3
PIN-PULLER
2004CA3
SOLAR CELLS
EXPER SOLAR CELLS
2001TT9 OUTBOARD TEMP TRANSDUCER
2001TT10 INBOARD TEMP TRANSDUCER
2004SP3 SOLAR PANEL
2012DM3
MOTION SENSOR
+Y
UPPER RING
2009W304
2009W109
2007A2
GYRO CONTROL
2005A4
CC&S MEMORY
CC&S EVENT CONTROL
CC&S TIMING CONTROL
CC&S POWER SUPPLY
2007A1
ATTITUDE CONTROL ELECTRONICS
ELECTRONICS ASSEMBLY
ATTITUDE CONTROL, CENTRAL COMPUTER & SEQUENCER
2001EA3
III
2007SS3
SECONDARY SUN SENSOR
SCIENCE PYRO
SCAN ACTUATOR
2012MS1
MOTION SENSOR
2012MS4
MOTION SENSOR
2031SA1
CLOCK SCAN ACTUATOR
LATCH VENT VALVE
2037GS1
IRS GAS
(FWD) N2
(REAR) H2
2037MT1
INFRA-RED SPECTROMETER
2031FS1
FAR ENCOUNTER PLANET SENSOR
2036A2
NARROW ANGLE T.V.
OPTICS (8)
2031MG1
N/A MARS GATE NO.1
2031MG2
N/A MARS GATE NO.2

Fig. 15. (contd)

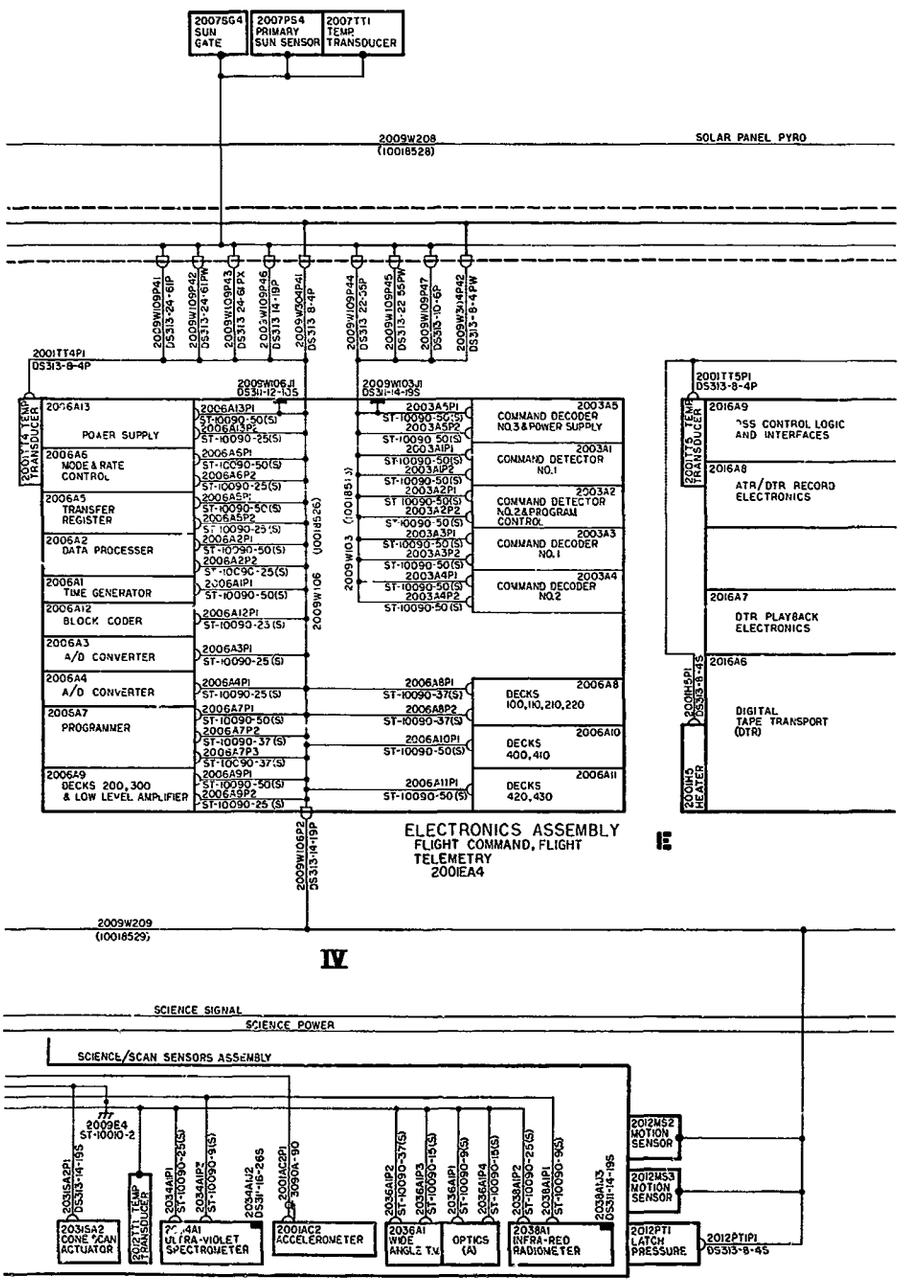

2007SG4 SUN GATE
2007PS4 PRIMARY SUN SENSOR
2007TT1 TEMP TRANSDUCER
2009W208 (10018528)
SOLAR PANEL PYRO
2001TT4P1 DS313-8-4P
2009W106J1 DS311-12-135
2009W103J1 DS311-14-195
2006A13 POWER SUPPLY
2006A6 MODE & RATE CONTROL
2006A5 TRANSFER REGISTER
2006A2 DATA PROCESSER
2006A1 TIME GENERATOR
2006A12 BLOCK CODER
2006A3 A/D CONVERTER
2006A4 A/D CONVERTER
2006A7 PROGRAMMER
2006A9 DECKS 200, 300 & LOW LEVEL AMPLIFIER
2003A5 COMMAND DECODER NO.3 & POWER SUPPLY
2003A1 COMMAND DETECTOR NO.1
2003A2 COMMAND DETECTOR NO.2 & PROGRAM CONTROL
2003A3 COMMAND DECODER NO.1
2003A4 COMMAND DECODER NO.2
2006A8 DECKS 100, 110, 210, 220
2006A10 DECKS 400, 410
2006A11 DECKS 420, 430
2001TT5P1 DS313-8-4P
2016A9 SSS CONTROL LOGIC AND INTERFACES
2016A8 ATR/DTR RECORD ELECTRONICS
2016A7 DTR PLAYBACK ELECTRONICS
2016A6 DIGITAL TAPE TRANSPORT (DTR)
ELECTRONICS ASSEMBLY FLIGHT COMMAND, FLIGHT TELEMETRY 2001EA4
2009W209 (10018529)
IV
SCIENCE SIGNAL
SCIENCE POWER
SCIENCE/SCAN SENSORS ASSEMBLY
2009E4 ST-10010-2
2035SA2 CONE SCAN ACTUATOR
2034AI ULTRA-VIOLET SPECTROMETER
2001AC2 ACCELEROMETER
2036AI WIDE ANGLE T.V.
OPTICS (A)
2038AI INFRA-RED RADIOMETER
2012MS2 MOTION SENSOR
2012MS3 MOTION SENSOR
2012PTI LATCH PRESSURE
2012PTIP1 DS313-8-4S

Fig. 15. (contd)

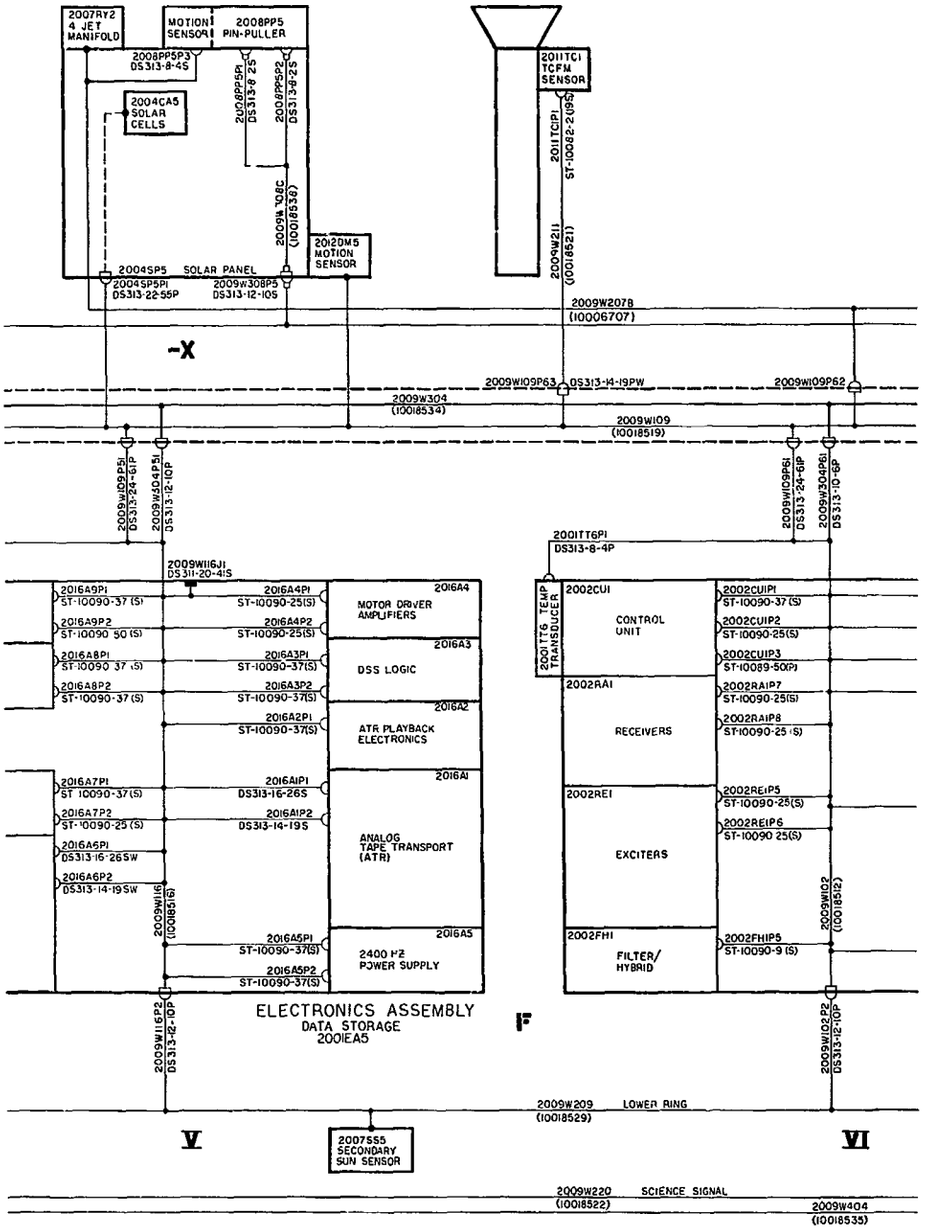

2007RY2
4 JET
MANIFOLD
MOTION
SENSOR
2008PP5
PIN-PULLER
2008PP5P3
DS313-8-4S
2004CA5
SOLAR
CELLS
2008PP5P1
DS313-8-2S
2008PP5P2
DS313-8-2S
2009W108C
(10018538)
2012DM5
MOTION
SENSOR
2004SP5 SOLAR PANEL
2004SP5P1
DS313-22-55P
2009W308P5
DS313-12-10S
2011TC1
TCFM
SENSOR
2011TC1P1
ST-10082-2(9S)
2009W211
(10018521)
2009W207B
(10006707)
-X
2009W109P63
DS313-14-19PW
2009W109P62
2009W304
(10018534)
2009W109
(10018519)
2009W109P5
DS313-24-61P
2009W304P5
DS313-12-10P
2009W109P6
DS313-24-61P
2009W304P6
DS313-10-6P
2001TT6P1
DS313-8-4P
2009W116J1
DS311-20-41S
2001TT6 TEMP
TRANSDUCER
2016A9P1
ST-10090-37 (S)
2016A9P2
ST-10090 50 (S)
2016A8P1
ST-10090 37 (S)
2016A8P2
ST-10090-37 (S)
2016A4P1
ST-10090-25(S)
2016A4P2
ST-10090-25(S)
2016A4
MOTOR DRIVER
AMPLIFIERS
2016A3P1
ST-10090-37(S)
2016A3P2
ST-10090-37(S)
2016A3
DSS LOGIC
2016A2P1
ST-10090-37(S)
2016A2
ATR PLAYBACK
ELECTRONICS
2016A7P1
ST 10090-37 (S)
2016A7P2
ST-10090-25 (S)
2016A6P1
DS313-16-26SW
2016A6P2
DS313-14-19SW
2016A1P1
DS313-16-26S
2016A1P2
DS313-14-19S
2016A1
ANALOG
TAPE TRANSPORT
(ATR)
2009W116
(10018516)
2016A5P1
ST-10090-37(S)
2016A5P2
ST-10090-37(S)
2016A5
2400 HZ
POWER SUPPLY
2009W116P2
DS313-12-10P
2002CU1
CONTROL
UNIT
2002CU1P1
ST-10090-37 (S)
2002CU1P2
ST-10090-25(S)
2002CU1P3
ST-10089-50(P)
2002RA1
RECEIVERS
2002RA1P7
ST-10090-25(S)
2002RA1P8
ST-10090-25 (S)
2002RE1
EXCITERS
2002RE1P5
ST-10090-25(S)
2002RE1P6
ST-10090 25(S)
2002FH1
FILTER/
HYBRID
2002FH1P5
ST-10090-9 (S)
2009W102
(10018512)
2009W102P2
DS313-12-10P
ELECTRONICS ASSEMBLY
DATA STORAGE
2001EA5
F
2009W209 LOWER RING
(10018529)
V
2007S55
SECONDARY
SUN SENSOR
VI
2009W220 SCIENCE SIGNAL
(10018522)
2009W404
(10018535)

Fig. 15. (contd)

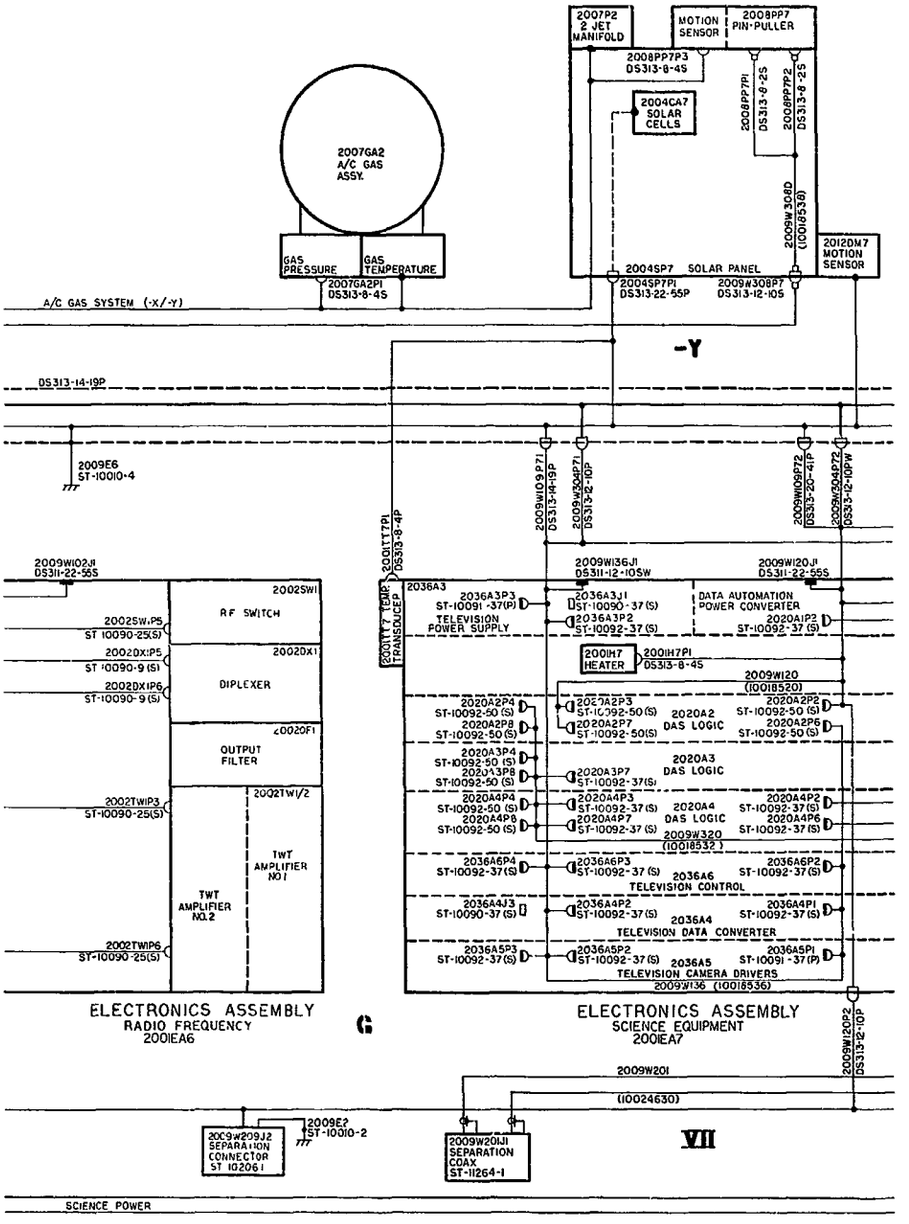

2007P2
2 JET
MANIFOLD
MOTION
SENSOR
2008PP7
PIN-PULLER
2008PP7P3
DS313-8-4S
2004CA7
SOLAR
CELLS
2008PP7P1
DS313-8-2S
2008PP7P2
DS313-8-2S
2007GA2
A/C GAS
ASSY.
GAS
PRESSURE
GAS
TEMPERATURE
2007GA2P1
DS313-8-4S
2004SP7 SOLAR PANEL
2004SP7P1
DS313-22-55P
2009W308P7
DS313-12-10S
2009W308D
(10018538)
2012DM7
MOTION
SENSOR
A/C GAS SYSTEM (-X/-Y)
-Y
DS313-14-19P
2009E6
ST-10010-4
2009W109P71
DS313-14-19P
2009W304P71
DS313-12-10P
2009W109P72
DS313-20-41P
2009W304P72
DS313-12-10PW
2009W102J1
DS311-22-55S
2001IT7P1
DS313-8-4P
2001IT7 TEMP.
TRANSDUCER
2036A3
2009W136J1
DS311-12-10SW
2009W120J1
DS311-22-55S
2036A3P3
ST-10091-37(P)
2036A3J1
ST-10090-37(S)
DATA AUTOMATION
POWER CONVERTER
TELEVISION
POWER SUPPLY
2036A3P2
ST-10092-37(S)
2020AIP2
ST-10092-37(S)
2001H7
HEATER
2001H7P1
DS313-8-4S
2009W120
(10018520)
2002SW1
RF SWITCH
2002SW1P5
ST-10090-25(S)
2002DX1
2002DX1P5
ST-10090-9(S)
DIPLEXER
2002DX1P6
ST-10090-9(S)
2020F1
OUTPUT
FILTER
2020A2P4
ST-10092-50(S)
2020A2P8
ST-10092-50(S)
2020A2P3
ST-10092-50(S)
2020A2P7
ST-10092-50(S)
2020A2
DAS LOGIC
2020A2P2
ST-10092-50(S)
2020A2P6
ST-10092-50(S)
2020A3P4
ST-10092-50(S)
2020A3P8
ST-10092-50(S)
2020A3P7
ST-10092-37(S)
2020A3
DAS LOGIC
2002TWIP3
ST-10090-25(S)
2002TWI/2
TWT
AMPLIFIER
NO.1
TWT
AMPLIFIER
NO.2
2020A4P4
ST-10092-50(S)
2020A4P8
ST-10092-50(S)
2020A4P3
ST-10092-37(S)
2020A4P7
ST-10092-37(S)
2020A4
DAS LOGIC
2020A4P2
ST-10092-37(S)
2020A4P6
ST-10092-37(S)
2009W320
(10018532)
2002TWIP6
ST-10090-25(S)
2036A6P4
ST-10092-37(S)
2036A6P3
ST-10092-37(S)
2036A6
TELEVISION CONTROL
2036A6P2
ST-10092-37(S)
2036A4J3
ST-10090-37(S)
2036A4P2
ST-10092-37(S)
2036A4
TELEVISION DATA CONVERTER
2036A4P1
ST-10092-37(S)
2036A5P3
ST-10092-37(S)
2036A5P2
ST-10092-37(S)
2036A5
TELEVISION CAMERA DRIVERS
2036A5P1
ST-10091-37(P)
2009W136 (10018536)
ELECTRONICS ASSEMBLY
RADIO FREQUENCY
2001EA6
G
ELECTRONICS ASSEMBLY
SCIENCE EQUIPMENT
2001EA7
2009W120P2
DS313-12-10P
2009W201
(10024630)
2009E2
ST-10010-2
2009W209J2
SEPARATION
CONNECTOR
ST 10206-1
2009W201J1
SEPARATION
COAX
ST-11264-1
VII
SCIENCE POWER

Fig. 15. (contd)

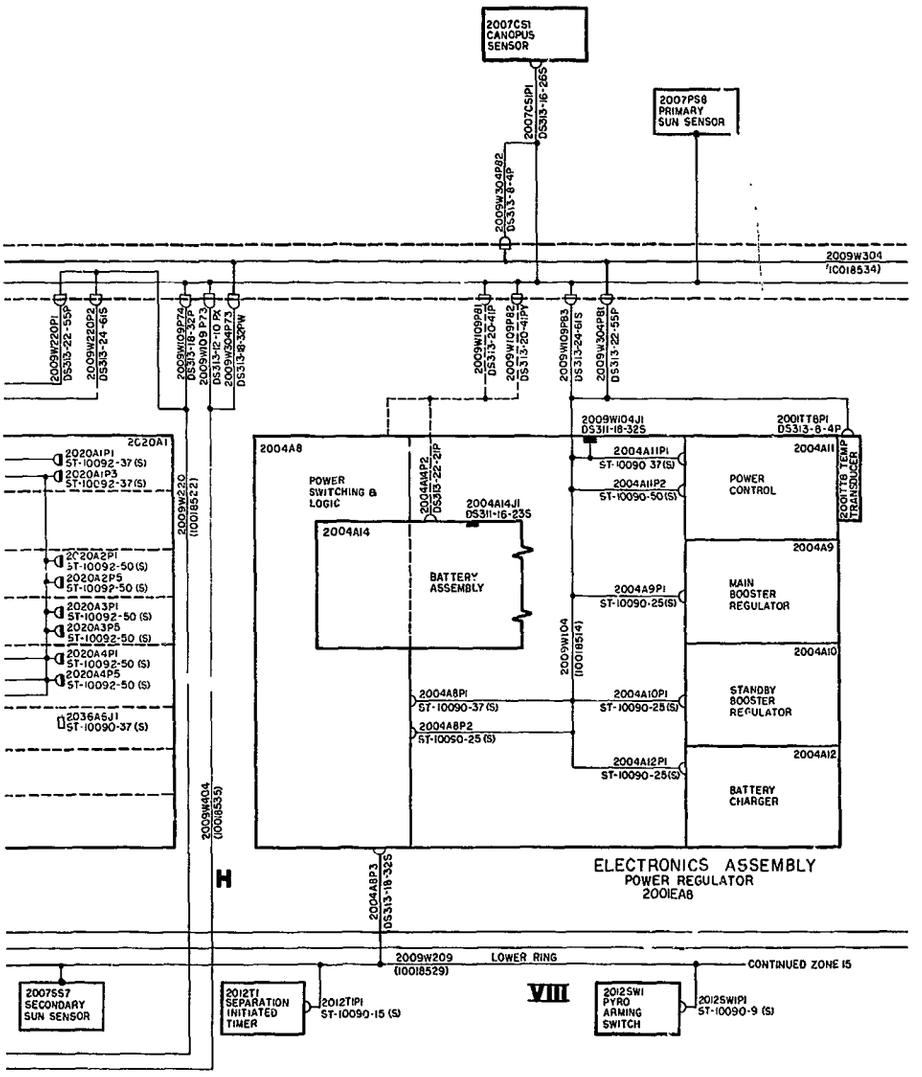

2007CS1
CANOPUS
SENSOR
2007CS1P1
DS313-16-26S
2007PS8
PRIMARY
SUN SENSOR
2009W304P82
DS313-8-4P
2009W304
(10018534)
2009W220P1
DS313-22-55P
2009W220P2
DS313-24-61S
2009W109P24
DS313-18-32P
2009W109 P23
DS313-12-10 PX
2009W304P73
DS313-8-32PW
2009W109P81
DS313-20-41P
2009W109P82
DS313-20-41PY
2009W109P83
DS313-24-61S
2009W304P81
DS313-22-55P
2009W104J1
DS311-16-32S
2001IT6P1
DS313-8-4P
2004A11P1
ST-10090 37(S)
2004A11P2
ST-10090-50(S)
2001IT6 TEMP
1124139062R
2004A11
POWER
CONTROL
2004A9
MAIN
BOOSTER
REGULATOR
2004A9P1
ST-10090-25(S)
2004A10
STANDBY
BOOSTER
REGULATOR
2004A10P1
ST-10090-25(S)
2004A12
BATTERY
CHARGER
2004A12P1
ST-10090-25(S)
2004A8
POWER
SWITCHING &
LOGIC
2004A14P2
DS313-22-21P
2004A14J1
DS311-16-23S
2004A14
BATTERY
ASSEMBLY
2004A8P1
ST-10090-37(S)
2004A8P2
ST-10090-25(S)
2009W104
(10018514)
2020A1
2020A1P1
ST-10092-37(S)
2020A1P3
ST-10092-37(S)
2020A2P1
ST-10092-50(S)
2020A2P5
ST-10092-50(S)
2020A3P1
ST-10092-50(S)
2020A3P5
ST-10092-50(S)
2020A4P1
ST-10092-50(S)
2020A4P5
ST-10092-50(S)
2036A6J1
ST-10090-37(S)
2009W220
(10018521)
2009W404
(10018535)
H
2004A8P3
DS313-18-32S
ELECTRONICS ASSEMBLY
POWER REGULATOR
2001EA8
2009W209
(10018529)
LOWER RING
CONTINUED ZONE 15
VIII
2007SS7
SECONDARY
SUN SENSOR
2012T1
SEPARATION
INITIATED
TIMER
2012T1P1
ST-10090-15 (S)
2012SW1
PYRO
ARMING
SWITCH
2012SW1P1
ST-10090-9 (S)

Fig. 15. (contd)

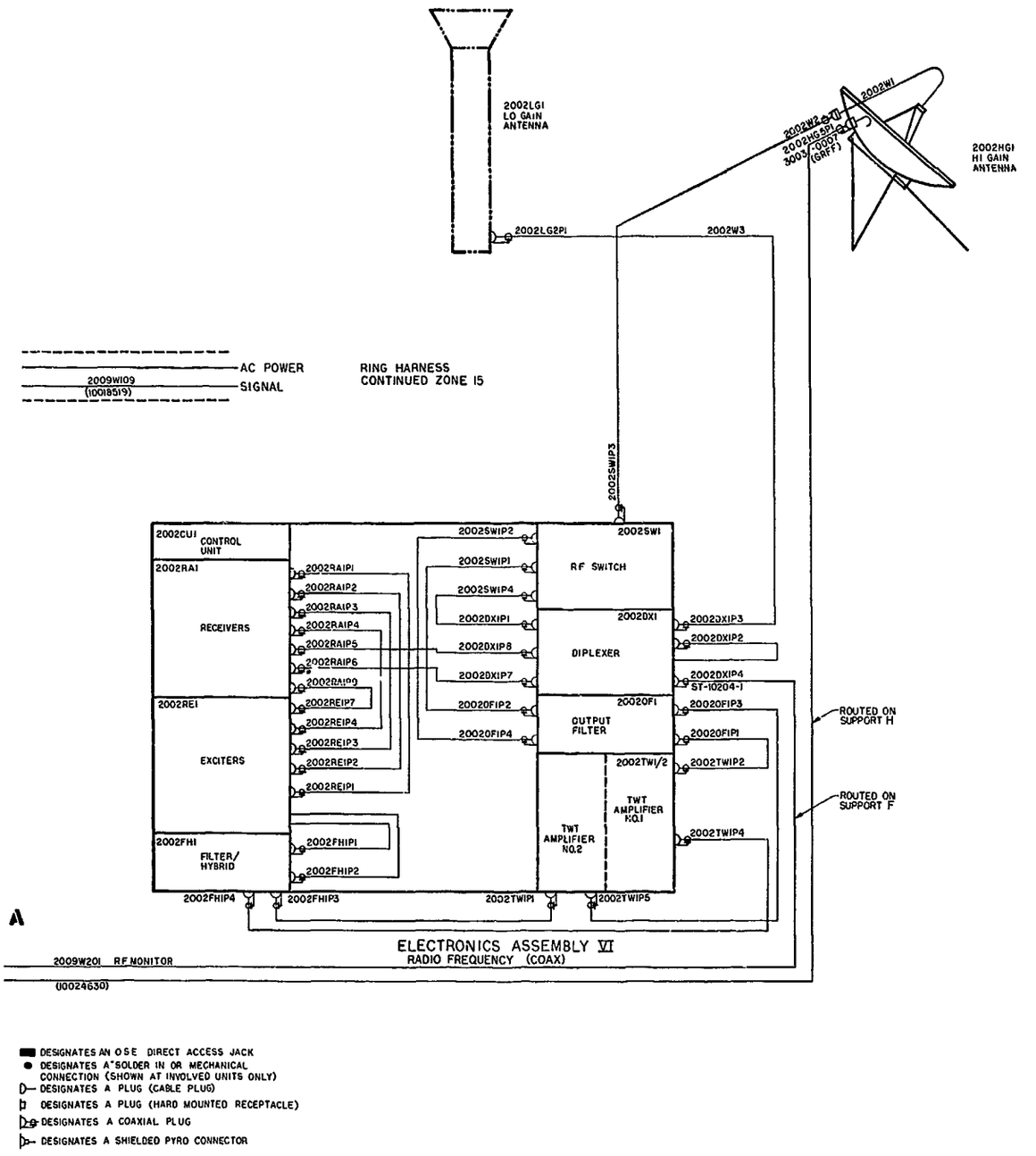

2002LG1
LO GAIN
ANTENNA
2002W1
2002HG1
HI GAIN
ANTENNA
2002LG2P1
2002W3
AC POWER
SIGNAL
2009W109
(10018519)
RING HARNESS
CONTINUED ZONE 15
2002SWIP3
2002CU1
CONTROL
UNIT
2002RA1
RECEIVERS
2002RE1
EXCITERS
2002FH1
FILTER/
HYBRID
2002SWIP2
2002SWIP1
2002SWIP4
2002DXIP1
2002DXIP8
2002DXIP7
20020FIP2
20020FIP4
2002SW1
RF SWITCH
2002DX1
DIPLEXER
20020F1
OUTPUT
FILTER
2002TW1/2
TWT
AMPLIFIER
NO.1
TWT
AMPLIFIER
NO.2
2002DXIP3
2002DXIP2
2002DXIP4
ST-10204-1
20020FIP3
20020FIP1
2002TWIP2
2002TWIP4
ROUTED ON
SUPPORT H
ROUTED ON
SUPPORT F
2002RAIP1
2002RAIP2
2002RAIP3
2002RAIP4
2002RAIP5
2002RAIP6
2002RAIP9
2002REIP7
2002REIP4
2002REIP3
2002REIP2
2002REIP1
2002FHIP1
2002FHIP2
2002FHIP4
2002FHIP3
2002TWIP1
2002TWIP5
A
ELECTRONICS ASSEMBLY VI
RADIO FREQUENCY (COAX)
2009W201 RF MONITOR
(10024630)
DESIGNATES AN OSE DIRECT ACCESS JACK
DESIGNATES A SOLDER IN OR MECHANICAL CONNECTION (SHOWN AT INVOLVED UNITS ONLY)
DESIGNATES A PLUG (CABLE PLUG)
DESIGNATES A PLUG (HARD MOUNTED RECEPTACLE)
DESIGNATES A COAXIAL PLUG
DESIGNATES A SHIELDED PYRO CONNECTOR

Fig. 15. (contd)

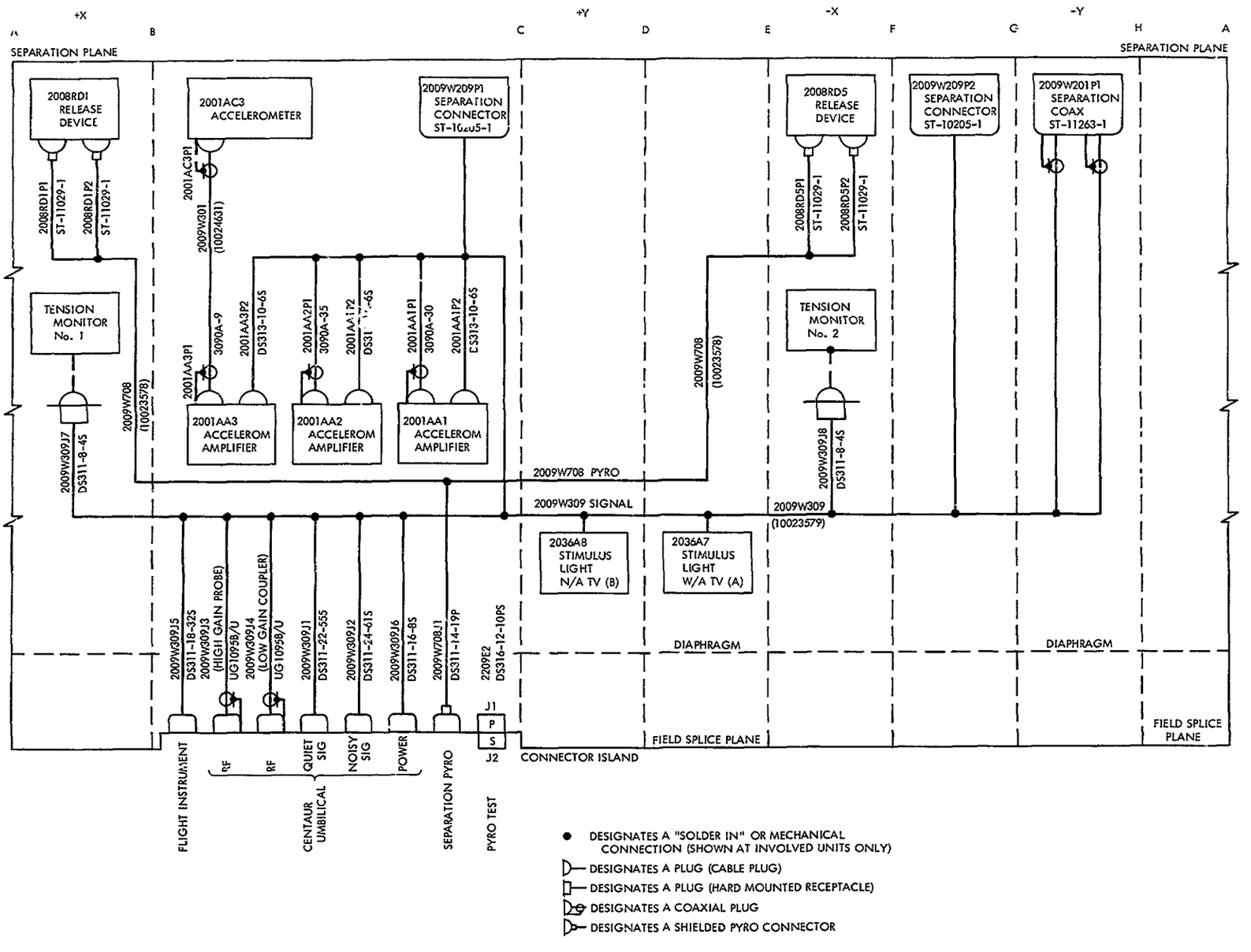


Fig. 16. Spacecraft adapter cabling block diagram

The problem area most frequently encountered was in handling of the harnesses. Prior to the time when the connectors are mated, the mating surfaces must be closely inspected for any interference such as bent pins or foreign materials. Several matings were made to connectors with bent pins, causing punctures in the inserts of the mating part. In some cases replacement of the connectors was required.

A breakdown of the total cable weight is given in Table 1.

Table 1. Cable weight breakdown

Bay	Type	Weight, lb
I	Scan	1.86
	TCFM electronics	0.49
	TCFM interconnect	0.195
	Power conversion/pyrotechnic control	2.70
II	Propulsion pyrotechnics	0.915
	Thrust vector control assy. and propulsion sensors	0.77
III	Central computer and sequencer	3.53
	Attitude control	1.65
IV	Flight command subsystem	2.34
	Flight telemetry subsystem	4.48
V	Data storage	3.5
VI	Radio frequency subsystem	2.55
VII	Data automation	1.3
	Data interconnect	2.05
	Television electronics	1.83
VIII	Power regulator	1.95
	Upper ring power (not potted) Upper ring signal (not potted)	13.5
	Lower ring (not potted)	3.1
	RF monitor lower ring	
	Pyrotechnics distribution	1.90
	Solar panel pyrotechnics	1.12
	Solar panel squib	1.32
	Pyrotechnic direct access	0.94
	Platform accelerometer Scan platform pyrotechnics Scan platform power Scan platform signal Scan platform actuator	7.09
	Adapter signal Adapter pyrotechnics Adapter accelerometer	5.5
	TCFM sensor	1.21
	Total weight	67.79

V. Temperature Control Hardware

A. Introduction

Temperature control of the *Mariner* Mars 1969 spacecraft was accomplished by utilizing both active and passive methods. The active category included the louver assemblies, and ac and dc heaters; the passive category included superinsulation blankets, polished aluminum shields, and surface finishes. This article discusses the removable external hardware that was not delivered to the Spacecraft Assembly Facility as part of another subsystem.

The temperature-control subsystem for the *Mariner* Mars 1969 spacecraft was composed of 3,791 parts, divided into 81 separate assemblies, and weighed 20.5 lb. Of this weight, approximately 15 lb were louvers, polished aluminum shields, and support hardware. The remaining 5.5 lb were superinsulation thermal blankets.

Thermal blankets, shields, and louvers covered approximately 95% of the 48-ft^2 surface of the spacecraft bus. All but one instrument on the science scan platform were enclosed by a superinsulation blanket with an approximate 18-ft^2 surface area. Items outside the shielding, e.g., solar panels, antennas, and attitude-control gas jets, were passively controlled by surface finishes (Fig. 17).

A description of the thermal design of the spacecraft, temperature distribution, and power profiles is given in Ref. 1.

B. Thermal Shields

The term "thermal shields" is used to describe the insulating materials protecting the perimeter of the spacecraft. Low-emittance (approximately 0.05) thermal shields (0.016-in.-thick 6061-T6 aluminum) covered the high-emittance PV-100 paint where required to reduce radiation from the spacecraft bus. Five basic configurations were used to cover areas not occupied by louvers (Fig. 17). The interchangeability of these bolt-on shields provided an emittance-adjustment capability that could be used to adjust temperatures as a result of simulator testing. Except for minor configuration changes, the shields were of the same type used on the *Mariner* Mars 1964 and *Mariner* Venus 67 spacecraft.

C. Thermal Blankets

The superinsulation thermal blankets were made of alternating layers of aluminized mylar and nylon net; Teflon was used for the outer layers. There were 17 such

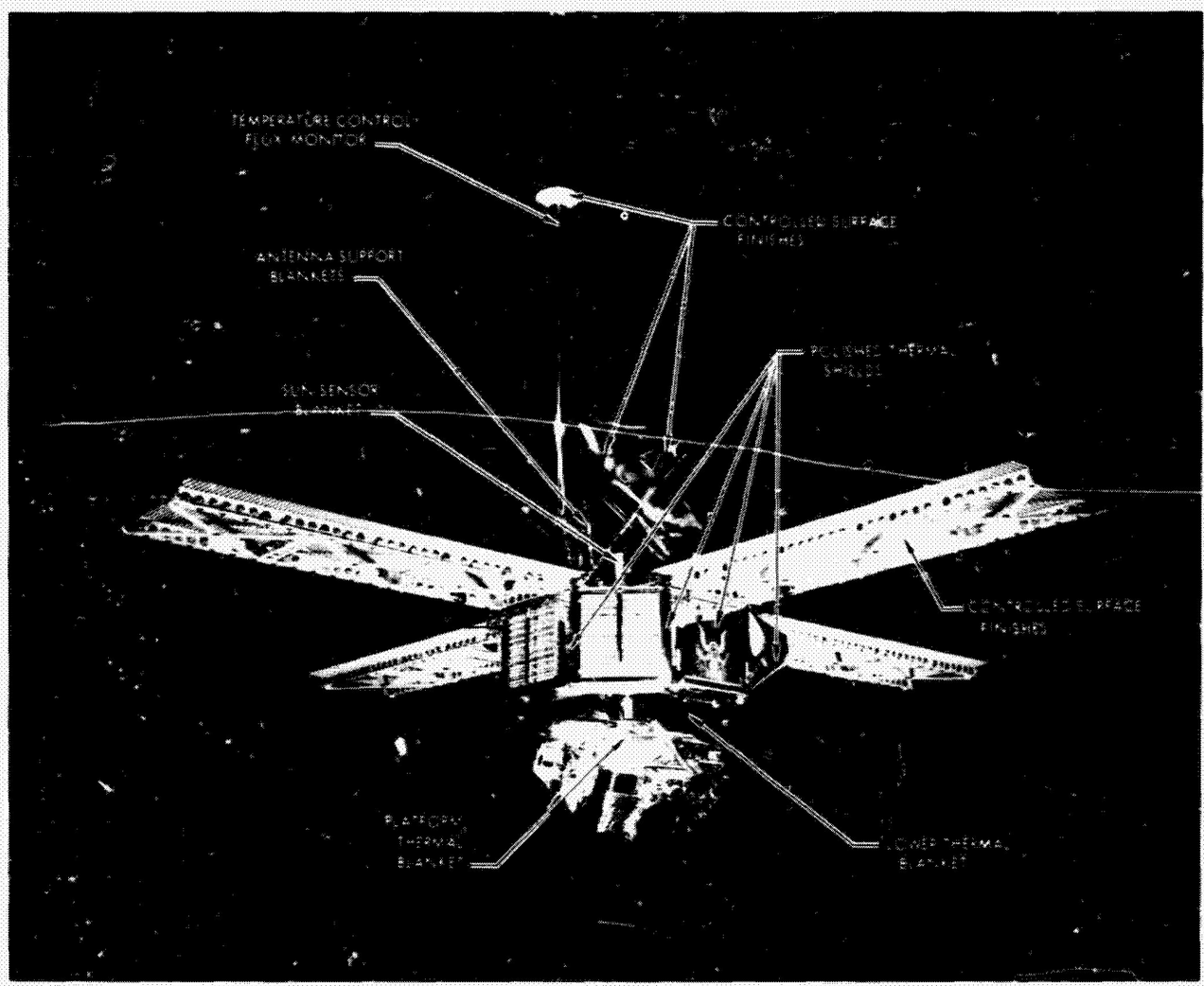


Fig. 17. Flight spacecraft thermal shield configuration

assemblies on the *Mariner* Mars 1969 spacecraft, the three major assemblies being the upper, lower, and scan-platform blankets. The upper thermal blanket was the largest (approximately 19 ft²) and the heaviest (2.1 lb). The smallest was approximately 3 in.² and weighed about 0.03 lb. The upper blanket was on the normally sunlit side of the spacecraft while the lower and scan-platform blankets were on the dark side. All blankets were designed to provide a light-weight adiabatic boundary; however, the primary function of the upper shield was to prevent the spacecraft from absorbing solar energy.

The scan platform and science instruments were not thermally slaved to the bus. Therefore, it was necessary for the blanket to conserve the internally-dissipated power to maintain temperatures at acceptable levels. The usual goal of super insulation is to achieve the lowest possible effective emittance. The scan-platform blanket design, however, deviated somewhat from this concept. Since the internally-dissipated power was fixed, as were the desired instrument operating temperatures to satisfy requirements including power-failure modes, the effective emittance of the blanket was designed to be within the range of 0.03 to 0.05, although 0.001 may have been possible.

Separate scan-platform thermal tests were conducted prior to the completion of the temperature control model. These tests determined the thermal characteristics of various blanket designs that differed in construction details.

1. Design criteria. The blanket configurations for the *Mariner* Mars 1969 spacecraft were geometrically complex and thermally compromised to fit the well-balanced spacecraft design required to meet the mission requirements. The compromises consisted primarily of protrusions through the blankets by structures, instruments, mechanical devices, and cabling. The cutouts required in the blanket lower its performance and divorce it from theoretical analysis or correlation with laboratory sample data. For these and other reasons, the temperature control subsystem was designed and developed with the aid of full-scale thermal mockup testing.

The first consideration in design of the superinsulation shielding was maintenance of proper temperature levels within the spacecraft during its voyage to Mars. Since shielding performance was verified on each flight spacecraft during approximately 500 h of simulator testing, performance in space was dependent upon repeating the thermal characteristics of the earth-bound testing. The thermal blankets were subjected to many environments, including installation and removal cycles in the time between simulator testing and space operation. The insulation system selected was the least sensitive to repeated handling and installation differences.

2. Materials. All the superinsulation blankets were constructed of the same basic materials. The Mylar was coated on both sides with vacuum-deposited aluminum having a resistivity measurement of 1–3 Ω/in.^{2} Both ¼- and ½-mil thicknesses of Mylar were used.

The nylon net separator was Sears Roebuck & Co. type 36H-1008H. This all-nylon net was constructed of multistrands of approximately 0.001-in.-diam monofilament. The hexagonal holes had an approximate 0.060-in. diameter; the net was 0.005–0.007 in. thick. The net's relatively tight weave assured both a uniform separator performance and the capability of conforming physically to the configurations and enduring handling. Although the net weighed about 16 g/yd^2, twice that of some other candidate materials, the blanket effective conductivity was not appreciably increased.

The outside layers of the blankets were 1-mil, aluminized FEP Teflon type A. One side only was coated and had a resistivity of 1.0 ±0.25 Ω/in.^{2} When used with the Teflon side out, the absorptance-emittance ratio of 0.24 lowered the sunlit-surface temperatures to within material limits, which in turn reduced the temperature difference through the blanket.

Other construction materials used were commercially-available Dacron thread, Kapton tape, Velcro closure strips, and aluminized glass tape. The tape adhesive was a pressure-sensitive silicone type with low out-gassing characteristics.

3. Fabrication. Because the outer 1-mil Teflon layer of the upper blanket was expected to approach 430°F during ascent heating, the first four layers of Mylar under the Teflon were ½-mil thick to increase the heat capacitance; the remaining seven layers were ¼-mil thick. Twelve layers of nylon net were used to separate the Mylar sheets. Each layer of the blanket was fabricated from two pieces of material, which overlapped approximately 12 in. in the center corresponding to the area of the blanket covering the attitude-control gas bottles. In that area, the unit loading on the blanket was highest and the double thickness lowered the conductivity through the blanket. A 1-mil aluminized Teflon sheet on each side with the Teflon side out finished the blanket lay-up.

The configuration of the upper blanket (Fig. 18) was such that flat-pattern construction was possible. Full-size paper patterns developed on the spacecraft were used as a cutting guide. In addition to the flat-pattern configuration, several closures flaps and an insert for the Canopus sensor were required. All the edges were bound with aluminized glass tape and a Velcro closure strip was sewn to the perimeter.

The lower blanket was also fabricated from a flat pattern in the same manner as the upper shield (Fig. 19).

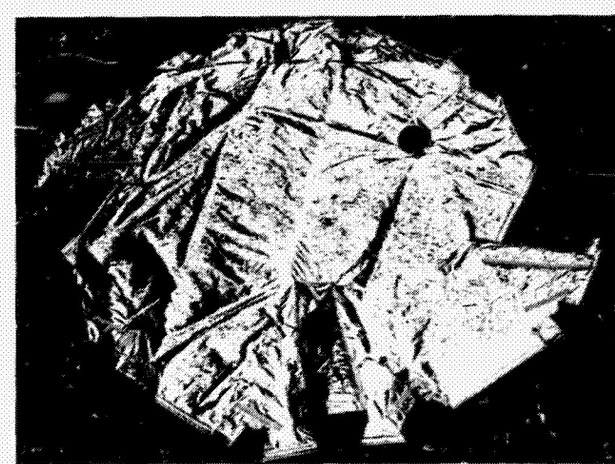


Fig. 18. Upper blanket configuration

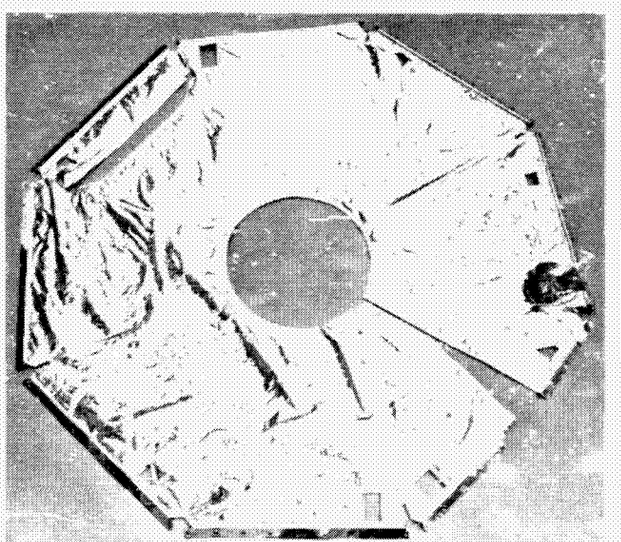


Fig. 19. Lower blanket configuration

Seven layers of ½-mil Mylar were alternated with eight layers of net, which, along with the two outside Teflon layers, completed the lay-up. This blanket was attached to the perimeter of the spacecraft by metal strips hand-sewn to the blanket. The radial opening in bay VII performed three major functions: it was necessary for installation, allowed the blanket to conform to a conical shape, and provided access to the scan latch mechanism. The circular center portion was retained by a groove in the mating polished aluminum shield attached to the scan-platform support structure. The blanket opening was tied together with Dacron cord and adjusted to a diameter that would be retained in the groove. This type of installation also provided a blanket-tightness adjustment to compensate for fabrication tolerances.

The scan-platform blanket configuration (Fig. 17) departed from the conventional flat pattern construction. The complex contours resulted in an excessive number of seams when trying to form the blanket from a flat-pattern development. In this instance, the seams caused excessive thermal shorts and unacceptable blanket performance. The method developed for fabricating the scan-platform blanket avoided through seams. This method required a model of the configuration envelope that was to be covered by the blanket. The temperature-control model (TCM) scan-platform mockup was used to develop the blanket construction model.

The platform volume to be covered was wrapped with tape (Fig. 20). The wrap directions could change the scan

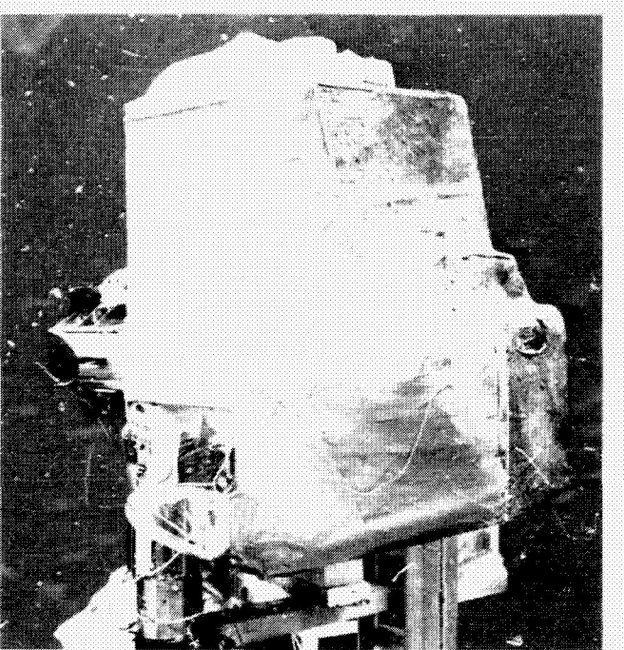


Fig. 20. Tape-wrapped TCM scan platform

platform contours at intersecting planes; consequently, many wrappings and unwrappings were necessary to achieve an acceptable configuration. The taped surface was then coated with papier-maché to form a mold, which was later removed in two parts and finished by filling it with a polyurethane foam and smoothing the outside with a plaster compound.

The construction of the blanket then proceeded one layer at a time, starting with the inside 1-mil Teflon layer and alternating seven ½-mil aluminized Mylar layers with eight nylon net separators. Each layer was fabricated with a random number of pieces and the joints were overlapped and taped together on approximately 4-in. centers. The joints of each successive layer were staggered so that no two layers were alike. The seams on the outside layer of Teflon were sewn together and reinforced with aluminized glass tape. The blanket was then removed from the mold for edge finishing and the addition of Velcro closure strips.

A number of small blankets are also used for insulating or shading specific areas of the spacecraft. These include the antenna-support blankets, the Canopus-sensor blankets, and the solar-panel hinge shades.

The high-gain antenna support structure on the sunlit side of the spacecraft was a potential source of solar

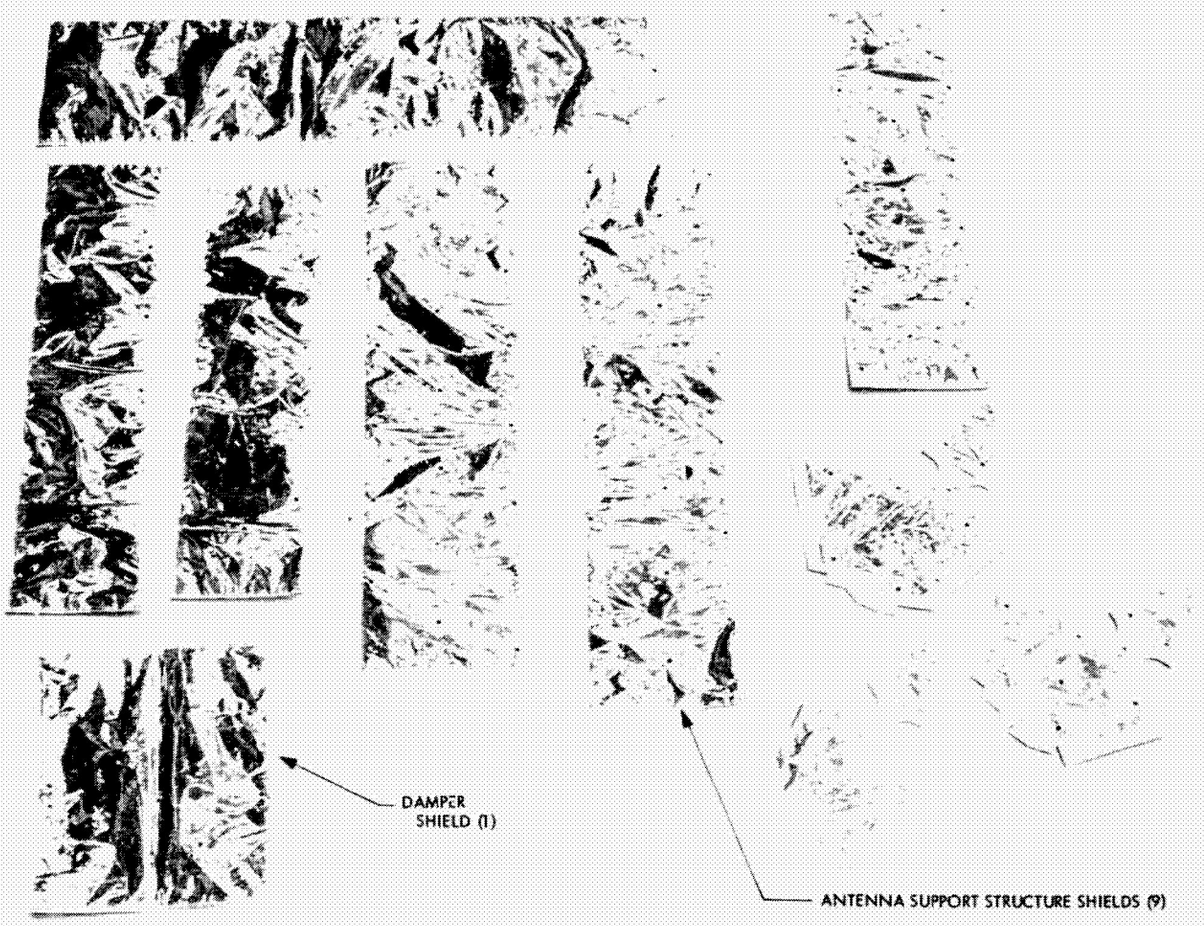


Fig. 21. High-gain antenna support structure thermal blankets

energy input to the bus. To reduce this input, nine blankets were used to cover the structure tubes and attach fittings (Fig. 21). These blankets were constructed of seven ½-mil layers of aluminized Mylar, eight nylon net separators, and two 1-mil Teflon sheets on the outside. The blankets were wrapped around the tubes approximately 1-½ times and then tied on with Dacron tie cord. The blankets used to cover the base fittings (Fig. 21, lower right) were installed in a "boot-type" configuration and secured by a Velcro closure strip.

The Canopus-sensor housing was bolted to the upper ring of the bus and enclosed by the upper blanket. However, the baffle box on the sensor extended beyond the bus perimeter and two separate blankets were required on that section. Because of its location, the top of the baffle box was exposed to solar radiation and the bottom to space, causing a 145°F temperature gradient from top to bottom. With that large a gradient, there was a possibility of warping the thin aluminum structure. To reduce the gradient, a multi-layer shield, approximately 6 × 8 in., was located on the sunlit side. It was constructed of nine layers of ½-mil aluminized Mylar, 10 layers of nylon net and two outside sheets of aluminized 5-mil Teflon, used to stiffen the blanket, with the Teflon side out. The 5-mil Teflon stiffening was necessary because of a potential stray-light problem that involved one of the primary sun sensors. The close proximity of the sun sensor to the baffle box (Fig. 22) subjected it to solar illumination reflected from the top surface of the Canopus baffle shield. Therefore, it was necessary to keep the reflecting surface

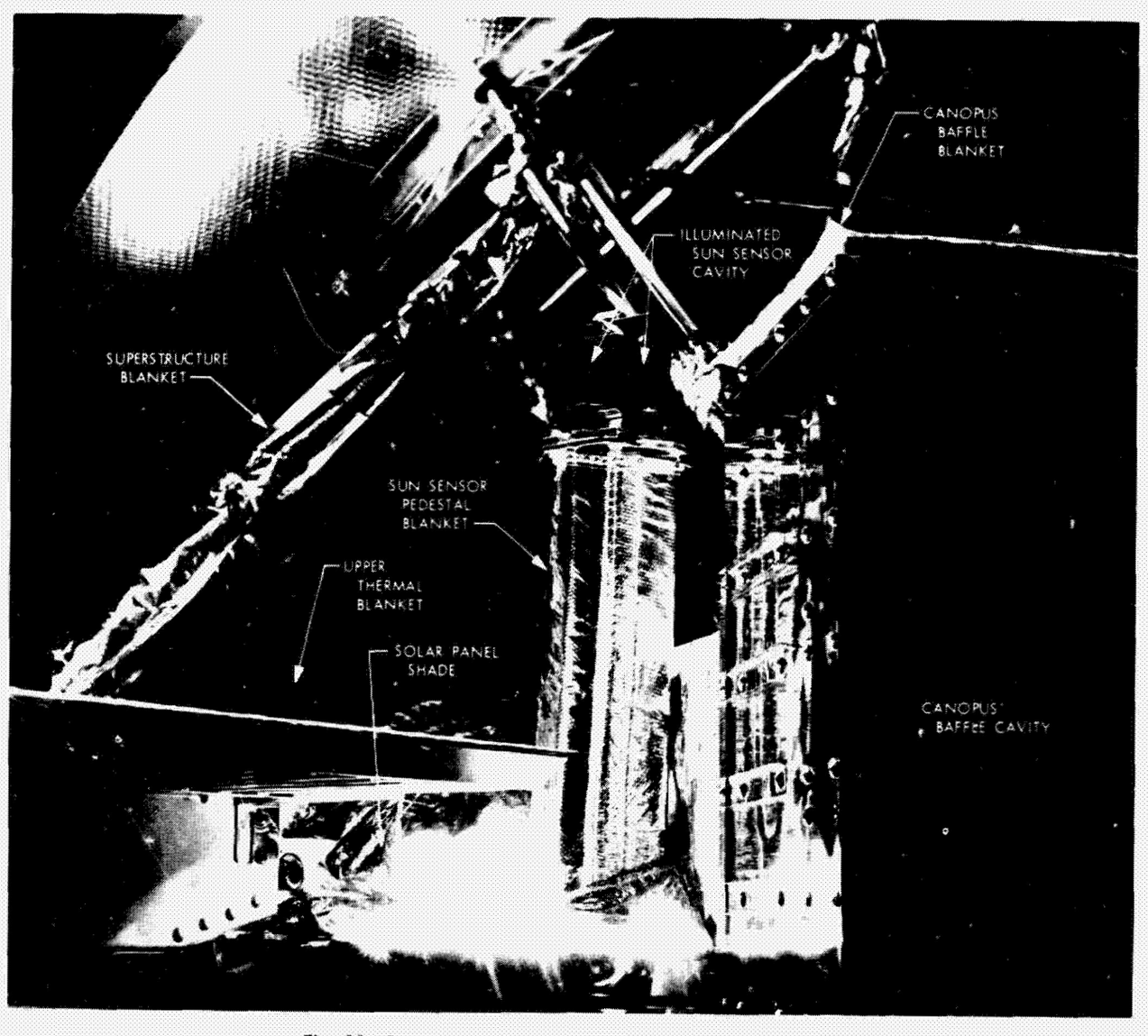


Fig. 22. Sun sensor/Canopus baffle box shield interface

flat and in a plane such that it would not reflect sunlight into the sensor. An "X" was sewn in the middle of the shield (Fig. 23, left) to prevent the outer layer from assuming a convex shape, which was a possibility during the launch phase when multi-layer blankets typically balloon. The shield was attached to the baffle by five 0.63 × 1-in. Velcro closure strips that also perform as thermal isolators.

The other blanket (Fig. 23, just above the Canopus baffle shield) required for the Canopus sensor baffle assembly was on the sun detector. This unit had no internal dissipated power and was subject to large temperature excursions when the spacecraft went off the sun line. A surface coating, in this instance, was impractical so a multi-layer blanket was used. Because of the size (approximately 3 $in.^2$) and intricate nature of the detector, it was not practical to use nylon net for this blanket; 10 layers of hand-crinkled ¼-mil aluminized Mylar with 1-mil Teflon outer layers were used instead. The blanket was installed on the detector using Dacron-thread drawstrings secured in the edges of the blanket.

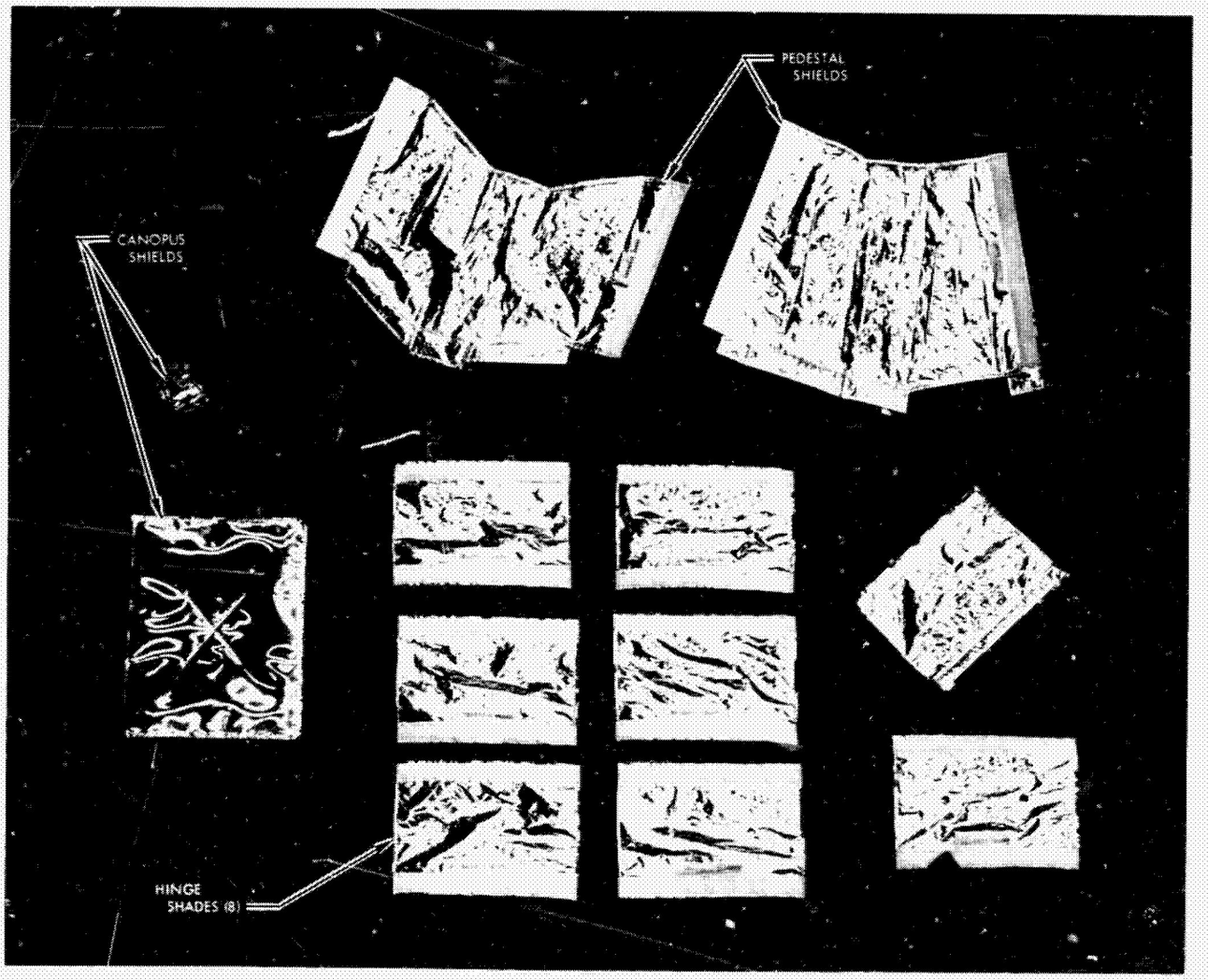


Fig. 23. Spacecraft shields

There were eight solar-panel hinges located on the sunlit side of the spacecraft bus, each of which protruded above the plane of the upper blanket and exposed a considerable area to the sun. At one hinge point on each panel, there was a flex joint for the attitude-control gas system, and, at the other, there was a microswitch assembly to indicate the deployment of each solar panel. Because of the difficult interface presented, the upper blanket could not effectively insulate these areas (Fig. 22). The next-best approach was to shade the area and eliminate the direct solar input. Although this was done, some solar energy was still conducted and radiated to the bus by the solar-panel structure.

The shades were constructed of two layers of 1-mil aluminized Teflon and two layers of nylon net. They were 4.50-in. wide, 6.00-in. long, and weigh 5 g each (Fig. 23). A Velcro closure strip was used to attach one edge to the solar panel and the opposite edge to the upper blanket. Prior to solar-panel deployment, the shade was stowed in a folded configuration against the upper blanket. The motion of the solar panel during deployment pulled the shade into position over the hinge assembly.

4. Handling and packaging. All handling of the multilayer blankets, including spacecraft installation and removal, inspection, and packaging for shipment, was accomplished by temperature-control cognizant personnel. The spacecraft-installation sequence required experience in blanket handling and final adjustment of closures to satisfy configuration and thermal performance. The flexible and fragile construction of the blankets rendered them easily damaged by mishandling. Incorrect installation procedures subjected other subsystems to damage as well. One such occurrence was a wire broken due to repeated bending during the upper blanket installations. Therefore, an awareness of handling limitations for all subsystem interfaces was developed by the temperature-control personnel.

The temperature-control hardware was packed for shipment in the same containers used for the *Mariner* Venus 67 Project. The method of packaging, also the same, consisted of placing the blankets in linen-lined canvas protectors (Fig. 24) prior to sandwiching them between layers of foam rubber in the aluminum containers. A method for folding the larger blankets was developed to avoid creasing the blankets in critical areas.

The canvas protectors were also used as work surfaces to inspect and prepare the blankets for spacecraft installations. The linen cloth provided a clean, low-static electrical charge surface that the blankets would not adhere to.

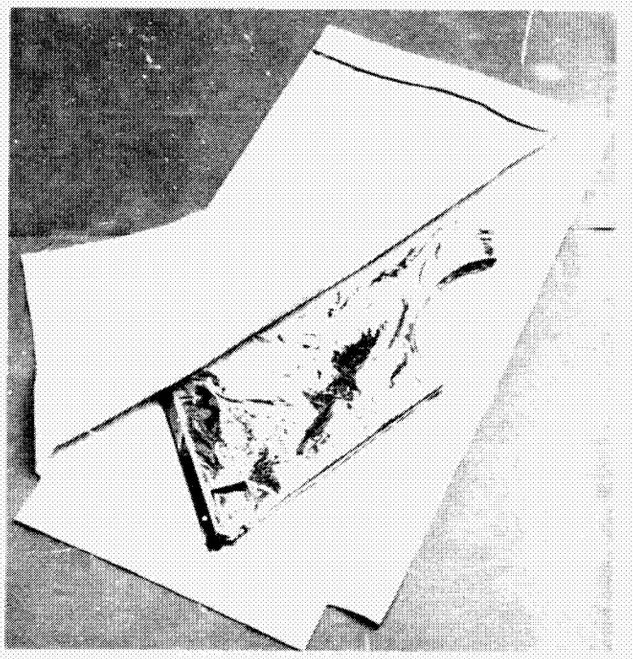


Fig. 24. Canvas-protected lower thermal shield

5. Blanket and shield testing. In constructing the thermal blankets, 0.25-in.-diam vent holes were punched on 6-in.-minimum centers in all blanket layers except the outer Teflon surface. The venting is necessary to allow the air trapped within the blanket to escape during the launch phase. A series of balloon tests were conducted to verify the venting capability of the blankets. In the worst case, inadequate venting could result in popping the blankets like toy balloons. A more realistic result would be distortion and the exposure of portions of the spacecraft.

For this series of tests, a prototype upper and lower blanket were installed on the TCM bus without solar panels, antennas, louvers, scan platform, cabling, and other equipment that would not affect the results. Voids caused by missing hardware, such as the propulsion unit, were completely sealed to assure a conservative test. The upper blanket was of more concern than the lower because of the greater configuration changes from the previous *Mariners*. For this reason, the bus was placed in the JPL 7 × 14-ft vacuum chamber so that pictures of the upper blanket could be taken through the available viewing ports. The lower blanket was observed through an obstructed port in the opposite end.

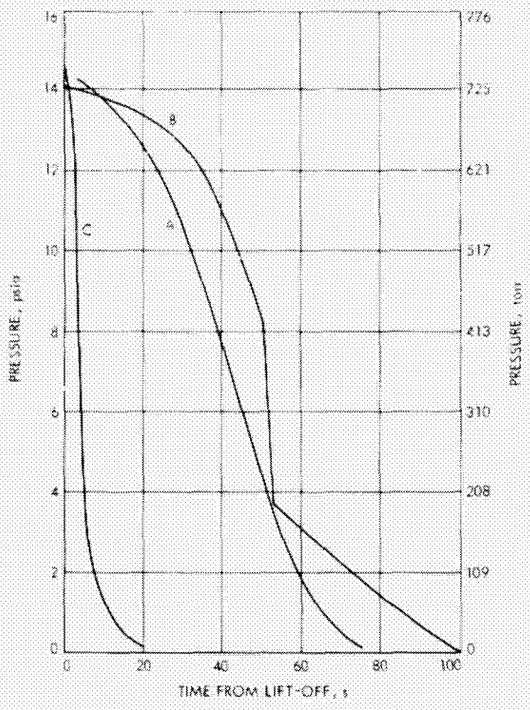


Fig. 25. Thermal blanket ballooning test pressure profiles

The three pressure profiles used are shown in Fig. 25. The first run (curve A) was the curve indicated by the *Mariner* Venus 67 type approval (TA) test. The second run (curve B) was the simulated *Atlas Centaur* profile and the last (curve C) was the maximum rate profile. The blankets survived all of the tests and the results indicated that other subsystems would not be affected by the ballooning. The maximum ballooning (Fig. 26) occurred at approximately 70 torr in all three profiles. The maximum rate occurred between 400 and 600 torr and was approximately 150 torr/s.

The scan-platform blanket was similarly tested during the later platform temperature tests in the 7×14-ft vacuum chamber. At that time, the pumpdown at the beginning of one test was run at the maximum rate. The thermal performance before and after a ballooning test appeared to be unchanged.

Later in the program, a problem arose when it was discovered that the upper blanket came in contact with the solar panels in bays III and VII. At that time, it was decided to investigate the effect of blanket ballooning on the problem. It would have been very difficult to evaluate the problem by looking through the ports of a chamber since such information as area in contact, location, unit loading, and effect of relative motion between the contacting surfaces was required to fully evaluate the situation. Therefore, a balloon test of a different nature utilizing the DTM spacecraft with two solar panels installed was conducted to obtain the required data. The DTM upper blanket was pressurized with dry nitrogen with the vent holes taped closed to simulate the ballooned configuration it would assume during launch (Fig. 27). Indications were that this type of test was highly successful and conservative for the purpose. The test indicated that the blanket would contact the solar panel, but with no detrimental effects to either subsystem.

A two-part test was conducted to investigate possible stray light interference with celestial sensors and science instruments. The completed TCM spacecraft was used for these tests conducted in the JPL Celestarium.

The first part of the test was to determine the existence of problems in both the Canopus sensor and the primary sun sensors. This involved directing the available 30-in.-diam sunlight bundle onto different portions of the spacecraft to find the worst-case conditions. Figure 22 illustrates one of the potential problem areas. The location was the top of the bus at bay VIII where the Canopus baffle box and one of the primary sun sensors was located. Here, reflection from the baffle box partially illuminated two cavities of the sun sensor. As shown in the photograph, the Canopus baffle cavity is completely black. Other items of interest in this figure are the illuminated edges of the Canopus baffle shield, the solar-panel hinge shade, and the antenna support-structure blankets. The second part of the test involved measurements of light reflected off the scan-platform blanket onto adjacent science instruments. A collimated light source was used with intensities at the blanket ranging from 214 to 2415 cd/ft^2. The light source was directed at the blanket from both the instrument line-of-sight and increments to 67 deg off the line-of-sight. At the conclusion of the two-part test, the result indicated no serious problems with any of the subsystems.

The temperature-control shields and blankets were TA and flight-acceptance (FA) tested on each spacecraft. The TA tests were performed on the proof test model (PTM). During the PTM test cycle the shields and blankets were subjected to space, vibration, acoustic, and handling environments. Prior developmental tests qualified the shield system for ballooning, sun-shade deployment, stray light, and materials. Another informal part of the qualification, realized from the PTM test cycle, involved the blanket



Fig. 26. Thermal blanket ballooning at 70 torr



Fig. 27. Area of solar panel and thermal blanket contact during simulated ballooning

installation and assembly compatibility with the spacecraft preparation sequence. Several assembly sequence revisions were necessary and resulted in minor changes to the blankets. At the conclusion of the PTM type approval test cycle, the superinsulation blanket design was released for flight fabrication.

The FA testing of the shields and blankets was performed on the flight spacecraft. Approximately 250 h of temperature data, including five different mission modes, were recorded from simulator testing. Each flight spacecraft was tested with its assigned shield system. This method was used to correlate more accurately flight and test data by eliminating shield performance differences.

D. Louver Assemblies

1. Spacecraft bus louvers. With the exception of minor changes to simplify fabrication and installation, the five sets of louvers on the bus were identical to those used on the *Mariner* Mars 1964 and *Mariner* Venus 67 Projects. Fourteen sets of louvers built in 1963 were rebuilt for use on the *Mariner* Mars 1969 TCM and DTM spacecraft; an additional 22 sets were fabricated for flight spacecraft use. The major modification was the revision of the hole pattern for the mounting screws. This revision eliminated the need to remove the 22-blade assemblies to install or remove the unit from the spacecraft. Therefore, the louver assembly remained intact from testing to flight. The elimination of the partial disassembly improved the reliability and decreased the probability of damage to the unit. The operating temperature range of all the bus louver assemblies was 55–85°F.

2. Testing of the bus louvers. Many tests, such as package drop, humidity, thermal shock, vacuum/temperature, and life tests, were omitted on the new *Mariner* Mars 1969 louvers because of their likeness to previously qualified units.

Tests were performed to verify the integrity of each unit rather than qualify the design. The FA vibration tests were performed on each louver assembly prior to final temperature performance testing. The FA vibration levels were slightly higher than previous *Mariner* requirements, but within *Mariner* Mars 1964 and *Mariner* Venus 67 TA levels. The increased vibration levels were a result of using the *Centaur* upper stage instead of the *Agena*. The final test was performance on the flight spacecraft during the space-simulator testing.

3. Scan platform louvers. The louver assembly used on the scan platform (Fig. 28) was half of a standard set used on the bus, except the operating temperature range was 0–30°F. The shift in temperature range was accomplished by preloading the spiral-wound bimetal actuators. The general qualification criteria were the same as for the bus louvers, except that the vibration levels at the platform location were higher.

The half-set of louvers was fabricated from standard bus louver parts, except for the omission of the 11-blade assemblies and one support assembly.

4. Modification problems. The first problem encountered in modifying the bus louver design for the scan platform was blade preloading against the full-open stop above 30°F. Initial vibration tests were conducted on the unit at approximately 70°F, which was consistent with the launch environment. The preload forced the blades past the stops because of deflections that occurred during the peak input of 20 *g* rms. This problem did not exist on the bus louvers because the blades were at an intermediate position at 70°F. The deflections were decreased to an acceptable level by using a stiffer mounting bracket (Fig. 28).

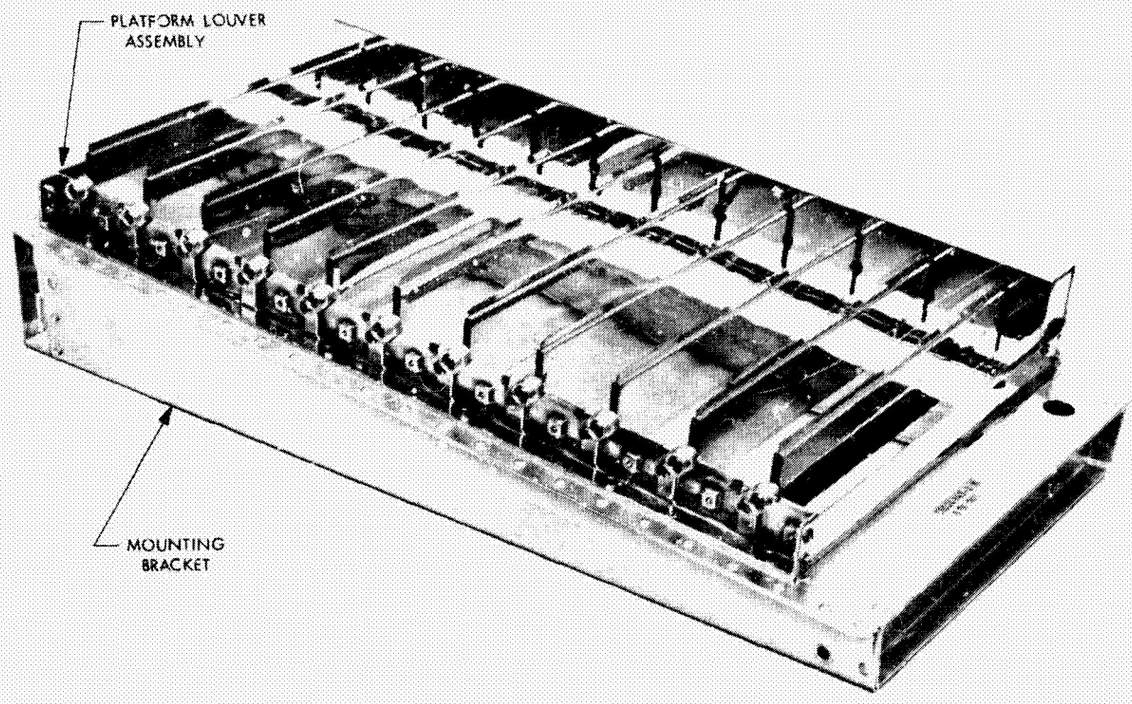


Fig. 28. Scan-platform louver assembly and mounting bracket

The second problem was associated with stress-relieving of the bimetallic actuator when subjected to vibration. Under this stressed condition, the temperature versus angle characteristics of the actuator changed. In subsequent testing the change was repeatable and constant at 2°F or 7 deg of blade rotation. To compensate for this shift in temperature versus angle, the initial louver calibrations were biased for proper operation after the vibration testing.

A third problem was associated with the inspection for excessive hysteresis in the blade bearings. During final assembly, the blade position at temperatures above 30°F precluded hand-operation of the blades for visual bearing inspection. For this reason, the half-set louver assembly was first assembled and tested for operation at 55–85°F, after which the 11 blades were removed and replaced subsequent to rotating the actuator 180 deg CCW.

5. Testing of the scan-platform louvers. The component-level FA testing consisted of two temperature-performance tests and vibration tests in the three spacecraft axes. In all qualification testing, the platform louver assembly and mounting bracket were tested as one unit.

A temperature-performance test was conducted prior to vibration testing to confirm the calibration and operation of the assembly. The FA vibration test maximum level was 13.3 *g* rms between 40 and 1000 Hz for the platform louvers, as opposed to 9.0 *g* rms between 600 and 2000 Hz for the bus louvers. The higher levels at the lower frequencies were of most concern because the louver design had not been previously qualified at these levels.

A final temperature test was conducted after FA vibration testing. The louver assembly was cycled from 70 to 0 to 70°F in a dry nitrogen atmosphere. Visual surveillance confirmed the louver opening-and-closing operation between 0 and 30°F.

The flight spacecraft space-simulator testing provided the final verification of louver operation. The spacecraft orientation in the chamber also provided an opportunity to observe the scan platform louvers in operation. This

was the last time the louvers were subjected to temperatures within their operating range prior to flight.

VI. Temperature-Control Flux Monitor

A. Introduction

This article presents a brief description of the flight adaptation of a JPL-developed absolute cavity radiometer for the *Mariner* Mars 1969 spacecraft. The flight adaptation of this instrument, called the temperature-control flux monitor (TCFM), was designed and fabricated by TRW Systems for JPL.

The TCFM was flown as part of the *Mariner* Mars 1969 temperature control subsystem. Its flight objectives were: (1) to compare spacecraft ground-test thermal performance with flight performance referenced to solar flux, (2) to establish a reliable radiometric standard for future spacecraft solar-simulator testing, (3) to obtain a more accurate measurement of integrated solar flux, and (4) to support the *Mariner* Mars 1969 temperature-control subsystem.

The TCFM transducer was at the tip of the omnidirectional antenna, provided an unobstructed view of the sun (Fig. 17); the electronics were located in bay I. The TCFM utilized 7 W of power, weighed 4.5 lb, and occupied a volume of 108 in.^{3}

B. Description

Basically, the TCFM consisted of a transducer, an electronic controller for the transducer, spacecraft interface electronics, and ground-test operational support equipment.

Figure 29 shows a cross-section of the transducer. Incident integrated radiation was received and measured within the conical cavity. The cavity was surrounded by a thermal guard that provided a reference for the conical receptor and restricted all heat interchange to the aperture. Platinum thermometers, reference resistors, and electrical heaters were located on the cone's internal surface and in the structure of the guard. The thermometers and reference resistors form several sets of Wheatstone bridges and were used to sense and control, through the heaters, the cone and guard temperatures.

The operation of the transducer is as follows. Through the use of the controller, a bridge, and a heater, the guard is maintained at a preselected temperature. Using a second bridge wherein one leg is located on the cone and

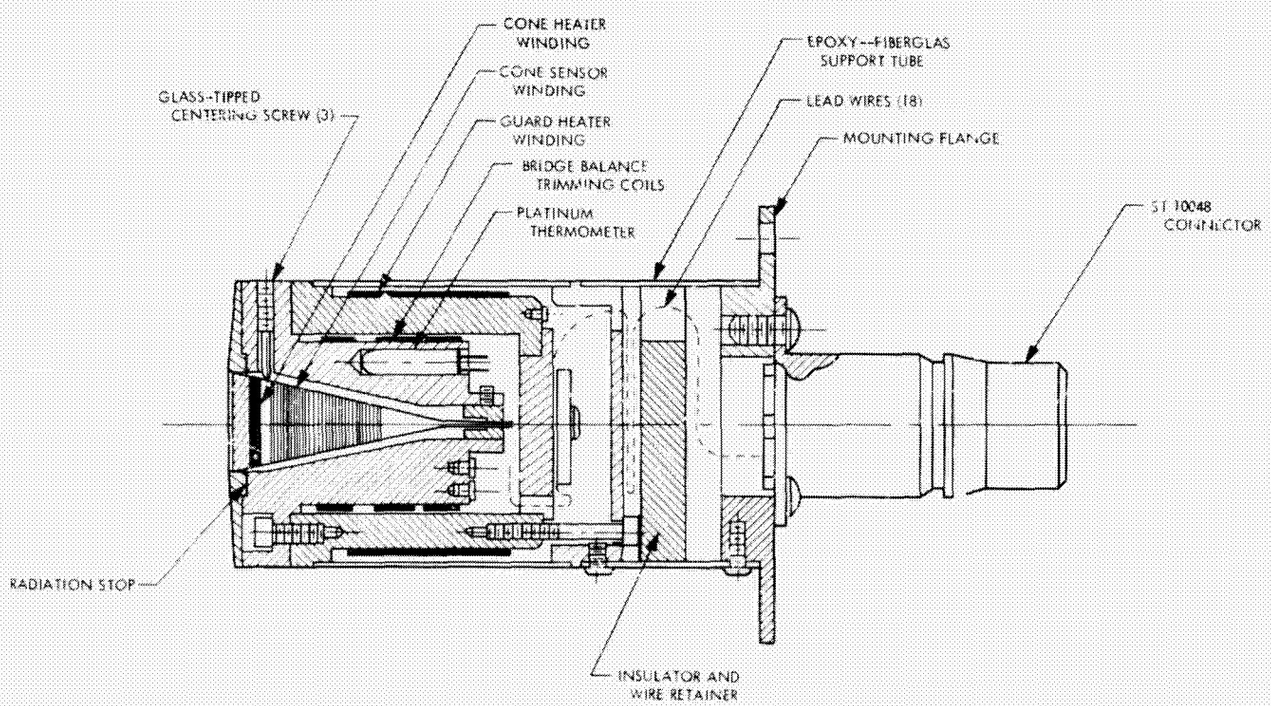


Fig. 29. The TCFM transducer

the other in the guard, power to the cone heater is controlled slaving the cone temperature to the preselected guard temperature. The power required to slave to cone temperature is measured, and the unknown radiation entering the cone is determined from

$$I_{unk} = \frac{\epsilon}{\alpha_s} \sigma T^4 - \frac{P}{\alpha_s A}$$

where I_{unk} is the unknown radiation, σ is the Stefan–Boltzmann constant, T is the preselected guard temperature, P is the electrical power to the cone, A is the cone aperture area, and ϵ and α_s are the effective radiation properties of the cone.

C. Flight Design

Only minor modification of the laboratory transducer design was necessary for flight adaptation of the TCFM. As a result of the telemetry interface, in conjunction with the desired goals of the TCFM, a significant area of design centered around the control electronics. Specifically, the accuracy placed upon the TCFM was set so that the measurement error was less than ±1.5%. Considering all sources of error, the maximum error in measured cone power had to be less than ±0.5% to maintain a total error of less than ±1.5%. Now, consider that the word size of a *Mariner* Mars 1969 telemetry channel is 7 bits, which alone would produce a minimum uncertainty of ±1%. In addition, if the data is input to telemetry as analog data, the analog-to-digital conversion produces another ±1% uncertainty. Thus, it becomes evident that the data must be input in digital form and that a larger than 7-bit word is needed. Therefore, a 10-bit word that spreads 5 bits each into two 7-bit channels was selected. The remaining 4 bits of the available 14 bits were used to telemeter the magnitude and direction of the cone bridge error signal, thus providing a data validity indication. Additionally, since the guard temperature would oscillate within the deadband of the guard bridge error detector, a third 7-bit analog input channel was used to independently measure these oscillations.

Since digital formatting to telemetry was required, it became apparent that digitizing the whole of the controller would result in the least complications. Referring to Fig. 30, the operation of the controller was as follows: An error signal from either the cone or guard bridge, resulting from a lack in null of either, was amplified. This amplified analog signal was digitized in a four-stage log amplitude-to-digital converter. The output of the converter caused a 10-bit register to count in the most significant bit in relationship to the triggered stage of the converter. The direction of the count depended upon the phase of the bridge error signal (all bridges were ac excited). The binary number in the 10-bit register, via control logic and gates, dictated the length of a power pulse supplied to a nulling heater for the bridge. A power pulse was generated once each frame, or every 0.213 s. Once bridge null was achieved, the binary number in the register did not change and both proportional and integral control were achieved. The voltage of the power pulse was held by regulation to 0.01%. Consequently, since the heater was of constant resistance, the length of the power pulse was exactly equivalent to the power. This length, the number in the 10-bit cone register, was thus telemetered. Each time the 10-bit register was updated, the 10-bit binary word was parallel shifted into two 7-bit registers with each 7-bit register receiving 5 of the 10 bits. Additionally, the digital error output of the log converter was shifted into the two remaining bits of each shift register to form a 4-bit error word consisting of 1 bit for the error direction and 3 bits for the error magnitude.

The shift registers were used to prevent clearing of the 10-bit register at telemetry read-out. Logic element timing was achieved by using the rise of the 2400-Hz square-wave spacecraft power supply as a clock. Much of the circuitry was common to both the cone and guard and the common elements were time shared. To measure set-point temperature oscillations in the deadband between the first-stage error triggering of the converter, an independent temperature deviation measurement was provided and telemetered. This circuit was analog with digital conversion taking place in the telemetry subsystem.

D. Testing

In addition to the standard series of type-approval and flight-acceptance testing typical of all *Mariner* Mars 1969 electronic equipment, laboratory tests were conducted to verify the accuracy of the instrument. Over 1000 h of operating time on each assembly established confidence that the operational characteristics of each instrument were understood and that the bridge thermometers were not subject to drifting. A perfect preflight simulation was not possible in at least two areas: (1) the spectral response of the black cone, and (2) the effect, if any, of the degradation effects of the space environment. Based on the material tests that could be conducted, appropriate values were included in the error analysis. As a further protection against changes due to the space–solar environment, the data were considered to be most accurate about 2 days after launch. By this time, it was expected that the launch

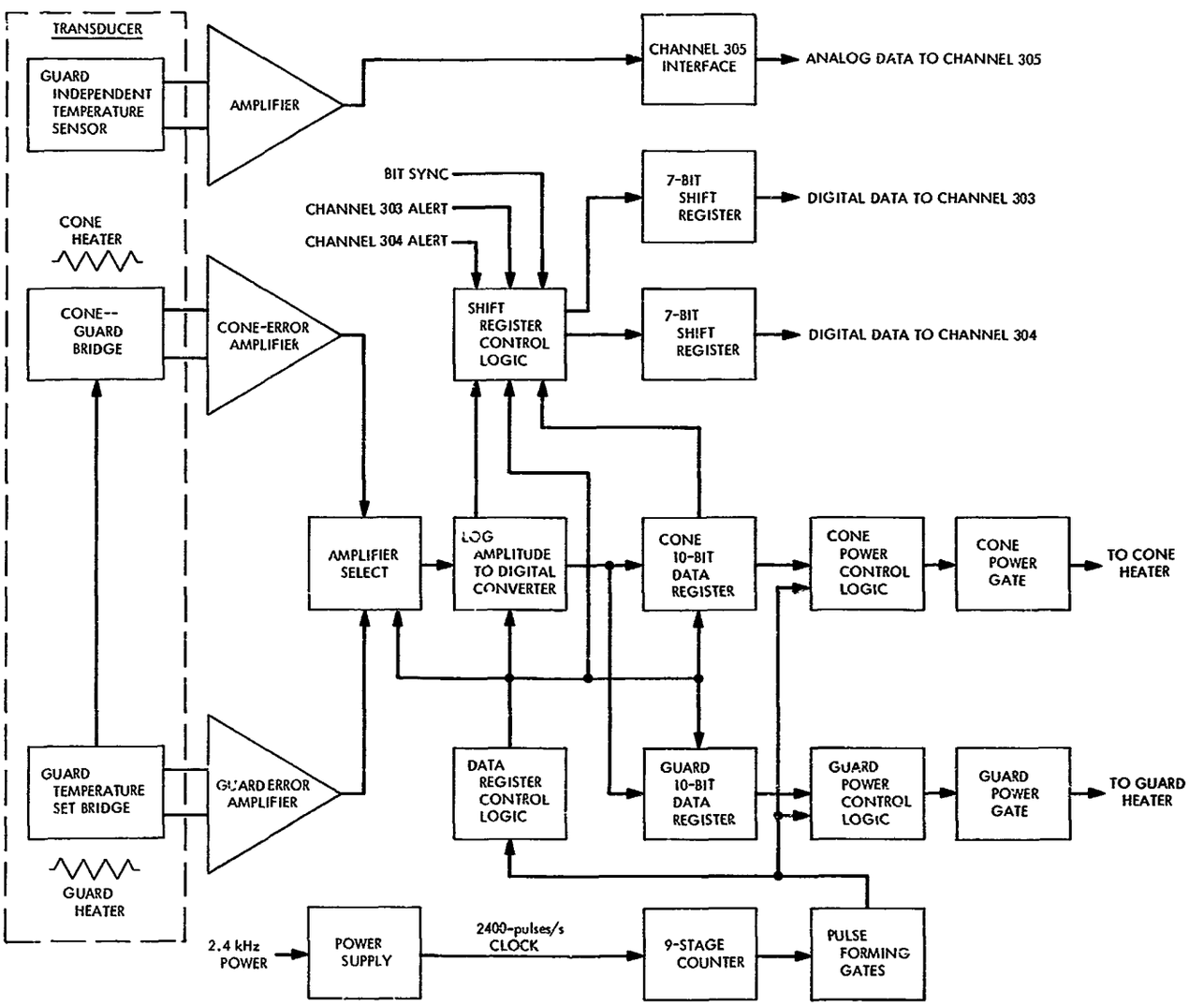


Fig. 30. The TCFM time-shared dual digital controller

transients and the effect of earth's radiation would have become negligible.

VII. Mechanical Devices Subsystem

The mechanical devices subsystem consisted of eight types of mechanical, electro-mechanical, or pneumatic devices. These had the general characteristic that they were not part of a closed-loop control system which operated on an error signal feedback. These systems contained mechanical devices such as motors, relays, sensors, etc., but were considered parts of other subsystems. For example, the cone and clock drive motors were part of the scan control subsystem.

A. Scan Platform Latch Assembly

1. Design philosophy. The scan platform was latched to the main equipment compartment during the launch and first maneuver periods to minimize the design loads for the structure members and drive mechanisms, and to assure a minimum of dynamic interaction between platform structure and the autopilot during the trajectory correction maneuver. To minimize the effect of the residual strain energy, two general criteria were set forth. First, the platform would be attached as directly to the main structure as possible, paralleling, if possible, any secondary structure, bearings, or actuators. Second, the release of the platform would be such that any unavoidable strain energy would be released slowly.

2. Design. The aforementioned criteria resulted in a design which held the scan platform in its stowed or launch position by means of four pneumatic latch mechanisms manifolded together to obtain parallel release. The location of the latch points were roughly the four corners of the basic box structure of the platform, thus forming a broad base for load transfer to the bus structure. Latch preload was applied by pressurizing the manifold to engage "T" bar latches at a serrated interface as illustrated in Fig. 31. Piston areas were chosen to give preloads of approximately 5700 lb force at each inboard location and 1600 lb force at the outboard latches when pressurized to 1500 lb in.^{2} This preload, in conjunction with the serrations, guaranteed no joint separation or slippage within the design loads expected at the platform.

Platform latch release was initiated by firing a normally closed pyrotechnic valve which allowed manifold venting to space. To minimize the resultant torque reaction on the spacecraft, venting was accomplished through a sintered plug restrictor to limit flow rate and was discharged overboard through a balanced T-fitting. The 4-in.^{3} manifold was vented from 1500 lb/in.^{2} to the nominal unlatching pressure of 100 lb/in.^{2} in approximately 30 to 60 s. Piston return springs were sized to allow the outboard latches to disengage slightly before the inboard latches. This was done to ensure that the 0.060-in. Z axis translation of the platform to clear the serrations during release would not cause undesirable torques on the cone axis actuator.

Latch pressure was monitored through spacecraft telemetry as an engineering measurement. This status measurement was chosen instead of an event indication to allow system test and on-pad monitoring of possible leaks which could cause a launch hold. In addition to pressure, microswitches at each latch were wired in series to give an event indication when all latches have released.

3. Latch testing. Due to the small 4-in.^{3} volume of the latch manifold, considerable attention was given the design and verification of a leak-tight assembly. The requirement to maintain the fill pressure of 1500 lb/in.^{2} through an estimated 4 wk of encapsulation and launch environment in addition to maintaining an inflight pressure of no less than 1200 lb/in.^{2} for the 6-mo cruise phase was a concern early in the design.

To verify the approach, many early tests were performed to select the proper seals, geometry, cleanliness, and required surface finish for the eight dynamic seals and three static seals utilized in the design. These tests were completed successfully with the decision being to use standard Viton O-rings in conjunction with Parker Parbak backup rings for the dynamic seals and standard flare tube connections with copper gaskets for the static seals. Utilizing the inspection and assembly procedures developed, no detectable leakage has occurred in any test or flight assembly over the duration of the *Mariner* Mars 1969 Program.

As mentioned, welding procedures were also established to guarantee leak-tight weldments at the 12 joints in the assembly. Numerous weld samples were prepared to verify an acceptable joint design with radiographic and cutaway sections being inspected for proper penetration and homogeneity of the weld. As was true in the seal design effort, the joint configuration and welding procedures employed resulted in a test history of no leakage.

Tests on the latch assembly installed on the DTM and flight spacecrafts include vibration and thermal-vacuum qualification at the system level as well as live pyrotechnic valve release tests on each assembly. The only problems

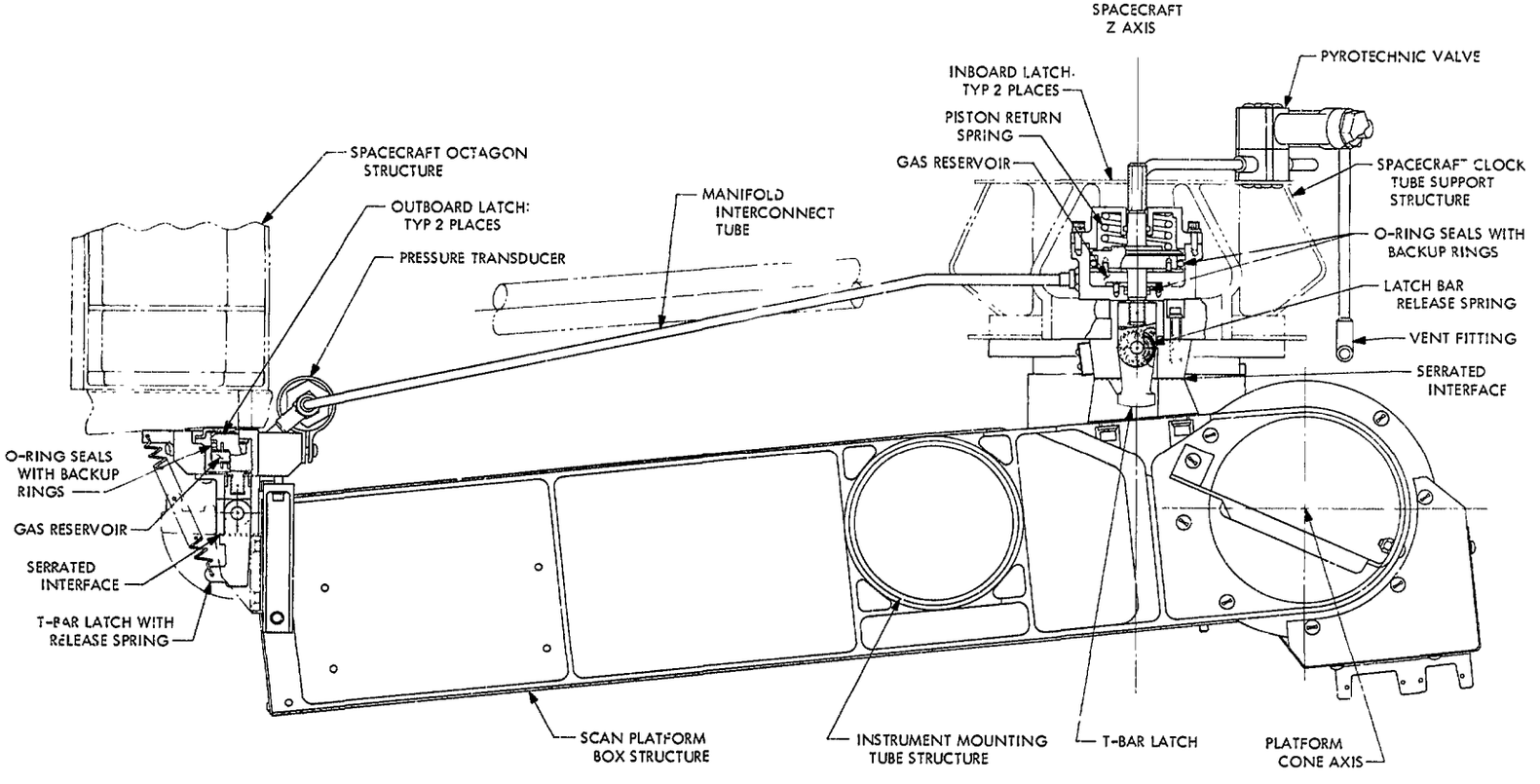


Fig. 31. *Mariner* Mars 1969 scan platform latch installation

noted were the post-fire integrity of the pyrotechnic valve which exhibited tendencies to leak following actuation and to discharge squib debris into the manifold due to blow-by. The former problems were remedied by the addition of electron beam case welding and by replacing the metal crush gasket with a seal using a Viton washer with a stainless-steel center hub. The latter blow-by, although not eliminated by valve redesign, was minimized to an acceptable level by incorporating prefilters in the manifold vent restrictor. Test results on the modified valve with filters indicated that the effect on manifold venting time was less than a 10-% increase due to debris. No debris were detected downstream of the restrictor filter.

B. Separation Initiated Timer

The primary function of the separation initiated timer (SIT) was to provide a time delay between arming and firing the pyrotechnics subsystem. This allowed the capacitors to acquire the required charge. The SIT consisted of a spring-loaded hydraulic timer and a set of electrical switches. The switch end of the timer shaft protruded from the timer and held the switches in the energized position (Fig. 32). The other end rested against the adapter. When separation occurred, the shaft moved slowly under the influence of the timer spring and hydraulic damping. The switches moved to the de-energized position (Fig. 32) sequentially as the switch end of the shaft withdrew into the timer body.

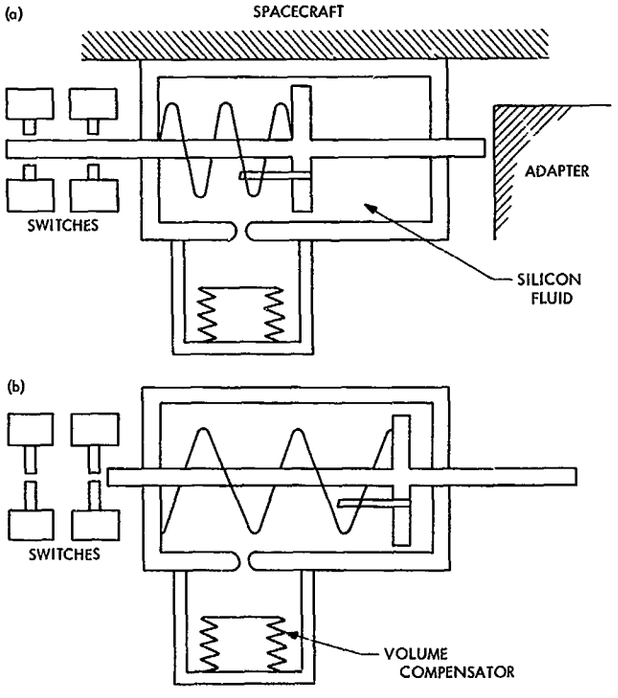


Fig. 32. Separation-initiated timer

The *Mariner* Mars 1969 SIT is only slightly different from the *Mariner* Mars 1964 SIT. Two modifications were made to the latter design: (1) a bellows-type volume compensator was added, and (2) a simple circuit was removed. Tests on the *Mariner* Mars 1964 SIT showed that high temperatures produced high pressures in the hydraulic fluid. No leakage occurred, but the volume compensator was added to the *Mariner* Mars 1969 design to increase the allowable temperature range and assure adequate sealing.

The *Mariner* Mars 1964 SIT contained a resistive-capacitive circuit to prevent a blocking of the event registers by the closed switch contacts. This was removed from the *Mariner* Mars 1969 SIT design and combined with the rest of the pyrotechnic circuitry; it was packaged in a more standard manner and the mechanical and thermal environments were better controlled.

The SITs left over from previous programs were modified for use on mock-up spacecraft, but all flight units were new. Assembly and testing of the new hardware revealed several problems. Most of these were extremely minor and were corrected by part modifications or assembly procedure changes. An erratic closed-circuit resistance problem, however, recurred throughout the qualification program, and is described below.

The specifications required that the closed-circuit resistance be no more than 100 mΩ. For a normal switch, the resistance was found to be about 20 mΩ including the contact resistance of the SIT connector, the mating connector, and the wiring in the SIT. It was found that the resistance of such a switch would vary from actuation to actuation over the range of 20 to 300 mΩ. The switches had all passed the screening specification (75 mΩ max) and were all 7 mΩ.

The bridges used to measure closed-circuit resistance in the SIT applied a maximum of 6 and 11 V, to an open circuit, and supplied 175 and 215 mA through the closed contacts. A two-wire system was used. Investigation showed that if the resistance was measured as described the switch resistances were erratic and varied up to nearly 300 mΩ; however, the resistance did not get higher as the switches were repeatedly actuated. In addition, if the resistance was measured at 1 A, the value would be the "normal" 7 mΩ.

Since all the SIT circuits operate properly with 10 Ω in place of the closed-circuit switches, the "high-resistance" SITs were accepted for spacecraft use.

Only one SIT problem was reported during all system testing. During a space simulator test, the SIT failed to furnish the last two switching events. Investigation showed that the remote SIT actuator was improperly installed and prevented the SIT shaft from extending fully.

C. Pyrotechnic Arming Switch

The pyrotechnic arming switch (PAS) had two primary functions: (1) arming the pyrotechnic subsystem (turning it on), and (2) initiating the sun acquisition sequence. The PAS consisted of four microswitches and two leaf springs mounted in a housing. When the spacecraft was mated to the adapter, the switches were held in the energized position (Fig. 33). Upon separation, the springs and microswitches were released and the PAS moved to the deployed configuration.

The only significant difference between the *Mariner* Mars 1964 and *Mariner* Mars 1969 PAS designs was the addition of the inner spring (Fig. 33). Switch chatter was a problem in the *Mariner* Venus 1967 Project which used an unmodified *Mariner* Mars 1964 design. The outer spring, the only spring in the *Mariner* Mars 1964 design, had two broad leaves, each of which actuated two microswitches. The inner spring had four narrower leaves so that each switch was individually actuated. There was no switch chatter problem on *Mariner* Mars 1969.

The only problem of significance revealed by qualification testing was the erratic resistance problem previously described for the SIT. One instance of handling damage occurred during system testing. This was a consequence of the lightweight construction of the PAS, and no changes were made.

D. V-Band Assembly

1. Introduction. The spacecraft was attached to the launch-vehicle/spacecraft adapter at eight points by V-blocks held in position by a circumferential stainless-steel band. The entire assembly is called the V-band assembly. A single attach point is shown in Fig. 34. A tension of 2500 lb was applied to the circumferential band by two turnbuckles. At the attach points, this tension becomes a radial force; through the wedging action of the V-blocks, it becomes an axial force, clamping the spacecraft and the adapter together. Separation was accomplished by pyrotechnically releasing the circumferential band at two points, thus allowing the blocks to retract simultaneously.

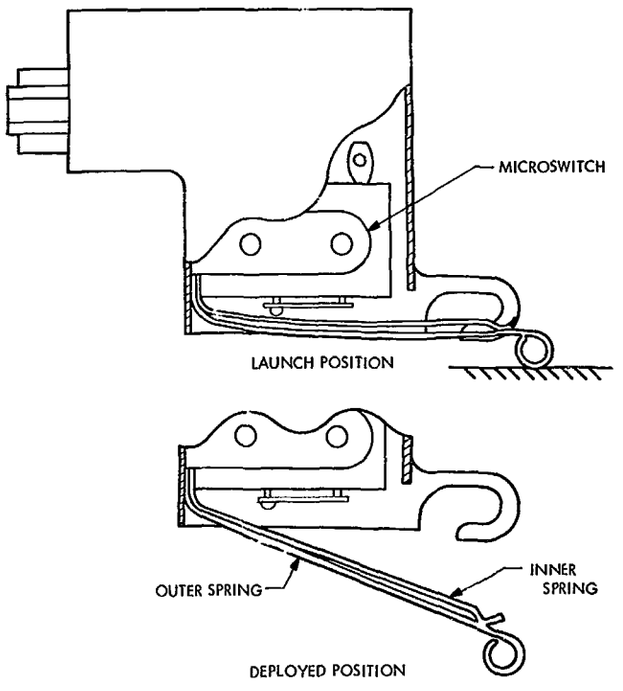


Fig. 33. Pyrotechnic arming switch

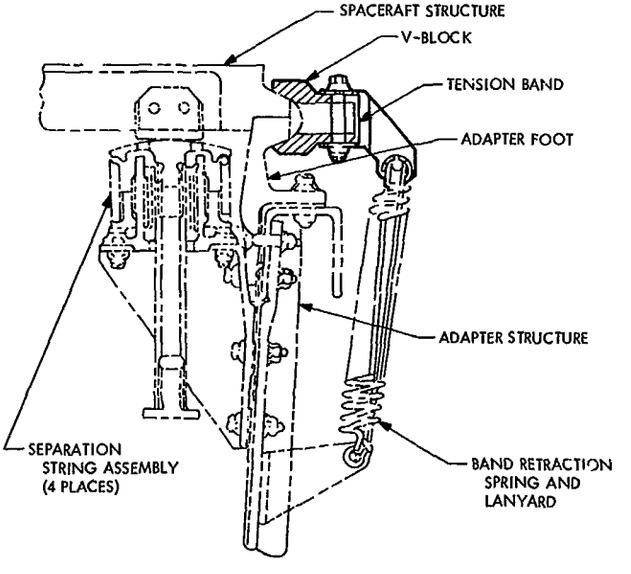


Fig. 34. Spacecraft separation joint

2. Design modifications. The V-band release method was first used on the *Mariner IV* and was again flown, unmodified, on *Mariner V*. The design of this system was, at that time, under the control of Lockheed Missiles and Space Company with the delivery and installation of this hardware being under their cognizance. Although JPL assumed direct responsibility of this area for *Mariner* Mars 1969, the basic design was kept intact with only minor modifications.

The change from an *Agena* final stage on the *Mariner* Mars 1964 and *Mariner* Venus 67 to the *Centaur* for the *Mariner* Mars 1969 made it necessary to revise the adapter interface. The *Mariner* Mars 1969 adapter design combines many of the spacecraft-interface features of the previous *Mariners* and most of the launch-vehicle-interface features of the *Surveyors*.

The most noteworthy design change resulted from a new, but subsequently relaxed, requirement that the V-band be tensioned to 3000 lb instead of the previously established 2500 lb; this requirement resulted primarily from a consideration of a heavier *Mariner* Mars 1969 spacecraft. The band material was changed from 7075-T6 aluminum alloy to A286 high-strength steel, and the turnbuckle size was increased from ¼ to 5/16 in. diam. The pyrotechnic release devices, although considered marginal at this tension, were retained to minimize development effort and take advantage of previous test and flight data. However, as a result of subsequent testing, which indicated some degree of tension relaxation in the device, the design requirements were reappraised and modified to the original 2500-lb tension specified on previous *Mariner* programs.

3. Qualification testing. The V-band assemblies completed a series of developmental type-approval, and flight-acceptance tests. All bands were statically proof-loaded to 3450 lb a minimum of six times. Type-approval vibration testing of a complete development test model and proof test model spacecraft mounted on flight adapters with both 2500- and 3000-lb tensions was successfully completed with only the previously mentioned load relaxation being noted.

Static and dynamic separation tests were performed with a fully configured spacecraft using the flight-type V-band. Approximately 21 pyrotechnic releases were logged with accelerometer, rate gyro, and fastax movies being used to record data. In all cases, including tests using only one pyrotechnic release device and one squib, the V-band properly released, allowing the spacecraft to separate.

E. Solar Panel Boost Dampers

The solar panel boost dampers for *Mariner* Mars 1969 remained essentially unchanged in concept from the *Mariner* Venus 67 design. Past experience with this particular damping concept on *Mariner* Mars 1964 and *Mariner* Venus 67, and results of later investigations helped to obviate some inherent problems peculiar to this design.

The dampers are designed to provide the following functions: (1) tip-to-tip latching of the solar panels in the stowed position, (2) damping of the natural vibration modes of the solar panels, and (3) support of the static loads associated with the solar panels. The larger and somewhat heavier solar panels of *Mariner* Mars 1969 necessitated increases in the static spring rate of 40 lb/in. (vs 20 lb/in. for *Mariner* Venus 67) and in the maximum allowable stroke to ±0.6 in. (vs ±0.3 for *Mariner* Venus 67). The damper consisted of two concentric tubes and a coaxial extension-compression spring with a viscous damping fluid contained in the annulus by seals seated in the piston body. The damper configuration is shown in Fig. 35. The damping force was provided by the shear stress generated in the annulus as the damping fluid flowed relative to the cylinder.

Experience has shown that the cross-sectional squeeze on the seals is a critical parameter. Too little squeeze results in seal damage. Excellent results with minimum seal deformation were obtained with seals having a modified cruciform cross section and under a cross-sectional squeeze of approximately 20%. During the course of testing forty-eight units, there were no cases of fluid leakage or excessive seal wear. Damping characteristics remained

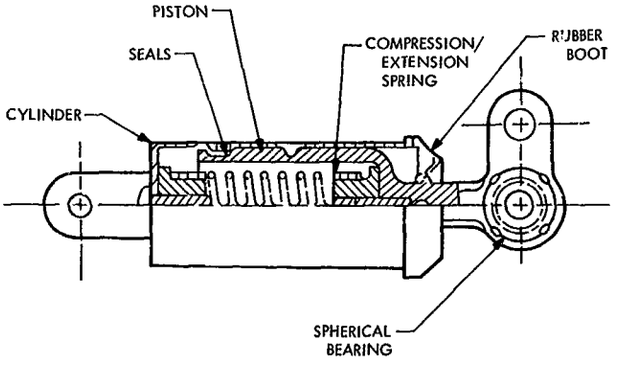


Fig. 35. Damper configuration

essentially unchanged after six months of storage and testing.

The only problem was that several units exceeded the specified force levels during testing; this was traceable to tolerance buildup in the seal glands. Remedial action consisted of modifying specification requirements and replacing parts where necessary.

F. Low-Gain Antenna Dampers

The low-gain antenna dampers positioned the low-gain antenna and damped its dynamic response. These devices were large scale reproductions of the solar-panel boost dampers and behaved in exactly the same manner. The upper damper, extending from a point on the superstructure, had a spring constant of 200 lb/in.; the lower damper from the bay IV–bay V corner of the octagon, had a spring constant of 800 lb/in. and made an angle of approximately 30 deg with the antenna axis. The axis of the dampers intersected each other on the axis of the antenna so that no torques were imparted to the antenna. The dampers were sealed with O-rings. There were no problems or failures associated with the low-gain antenna dampers during the course of the program.

G. Solar Panel Cruise Dampers and Latches

The solar panel cruise dampers for *Mariner* Mars 1969 were the same as those employed on *Mariner* Venus 67 and *Mariner* Mars 1964. The bracket configuration was modified to accommodate repositioning of the solar panels. The cruise dampers were designed to provide the following functions:

(1) Absorb the kinetic energy of a deployed solar panel.

(2) Position the deployed solar panel.

(3) Damp solar panel oscillations during the midcourse motor firing.

The cruise dampers consisted of two springs and a dash-pot in parallel. The damping force is generated by displacing a piston through a viscous, incompressible fluid. The effective spring constant and damping coefficient of each unit had to be determined to ensure adequate energy absorption capability and proper vibration control of a deployed panel. The spring constant of 530 lb/in. (±10%) was determined by force measurements at fixed displacements and zero velocity. Since the expected damped first-mode frequency of a deployed solar panel is 1.5 Hz, the units were actuated at fixed amplitude and at three measured frequencies between 1 and 3 Hz; i.e., at three distinct velocities. With the spring force and imposed velocity known, the peak force on each force-versus-time recording enabled calculation of an effective damping coefficient. The nominal measured damping coefficient was in the range of 65 lb/in. This method bypassed the problems of performing phase angle measurements at low frequencies or of evaluating less than ideal decay curves. Damper characteristics can be determined accurately with a minimum of operation time. Figure 36 shows a sample of the test data.

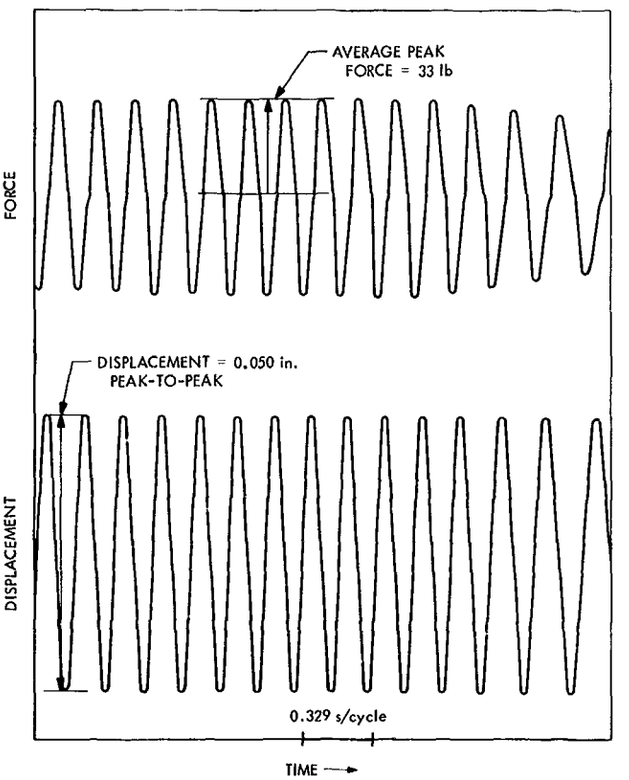


Fig. 36. Solar panel cruise damper test results

In all cases where fluid leakage was observed, the problem was directly traceable to seals and glands damaged during seal installation. Surface refinishing and seal replacement constituted the corrective actions required.

VIII. Engineering Support

Engineering mechanics tasks supporting *Mariner* Project activities included the mechanical and thermal design of the spacecraft, design documentation, materials, packaging, and parts engineering, and mechanical testing at system and lower-tier levels. These tasks and sustaining activities are described in Refs. 2–10.

Electronic packaging engineering support included design methods and processes, material and hardware selection for electronic equipment, electromechanical engineering, manufacturing processes, connector and wire selection, and high-voltage design support. Two work areas of special interest concerned the use of the JPL stick module for packaging integrated circuits and the mechanical design of the TV camera head.

Materials engineering support included a number of specific tasks and studies. Some of these studies included evaluations of conversion coatings for magnesium alloys.

References

1. *Flight Projects*, Space Programs Summary 37-55, Vol. I, pp. 5–18. Jet Propulsion Laboratory, Pasadena, Calif., Jan. 31, 1969.
2. *Flight Projects*, Space Programs Summary 37-52, Vol. I. Jet Propulsion Laboratory, Pasadena, Calif., Jul. 31, 1968.
3. *Flight Projects*, Space Programs Summary 37-53, Vol. I. Jet Propulsion Laboratory, Pasadena, Calif., Sep. 30, 1968.
4. *Flight Projects*, Space Programs Summary 37-54, Vol. I. Jet Propulsion Laboratory, Pasadena, Calif., Nov. 30, 1968.
5. *Flight Projects*, Space Programs Summary 37-55, Vol. I. Jet Propulsion Laboratory, Pasadena, Calif., Jan. 31, 1969.
6. *Flight Projects*, Space Programs Summary 37-56, Vol. I. Jet Propulsion Laboratory, Pasadena, Calif., Mar. 31, 1969.
7. *Flight Projects*, Space Programs Summary 37-57, Vol. I. Jet Propulsion Laboratory, Pasadena, Calif., May 31, 1969.
8. *Flight Projects*, Space Programs Summary 37-58, Vol. I. Jet Propulsion Laboratory, Pasadena, Calif., Jul. 31, 1969.
9. *Flight Projects*, Space Programs Summary 37-59, Vol. I. Jet Propulsion Laboratory, Pasadena, Calif., Nov. 31, 1969.
10. *Flight Projects*, Space Programs Summary 37-60, Vol. I. Jet Propulsion Laboratory, Pasadena, Calif., Jan. 31, 1970.

Science Subsystems

I. Introduction

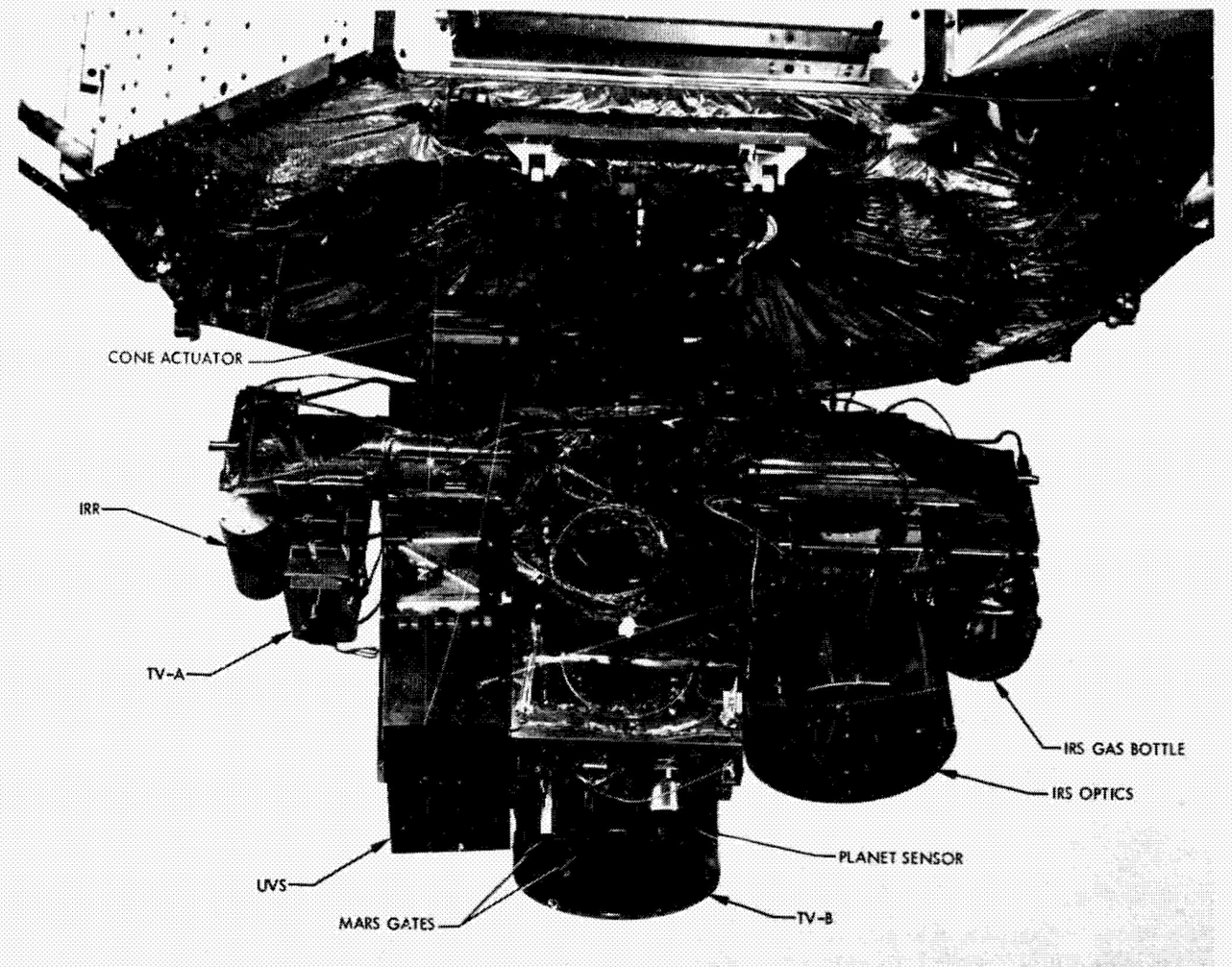
The *Mariner* Mars 1969 science payload consisted of four scientific instruments and the data automation subsystem. They are listed in Table 1. The experiments are Mars-oriented in that their design emphasizes planetary data rather than interplanetary data. Figure 1a shows equipment location and orientation; Fig. 1b is a simplified block diagram of the science subsystems.

A. Science Payload Incorporation

Incorporation of the science payload into the *Mariner* Mars 1969 spacecraft actually began before the payload was selected. On the basis of selected "typical" payloads, estimates of required resources were made. By the time the actual payload was chosen, the scope of the eventual effort was established. The spacecraft designs which evolved from these early efforts were

Table 1. *Mariner* Mars 1969 science instrument characteristics

Instrument	Physical characteristics			Data characteristics			
	Weight, kg	Power, W	Operating temperature range, °C	No. of sensors	Sample rate	Sample size, bits	Data accumulation rate, bits/s
IRS	17.5	8	−50 to +30	2	Each sensor every 15 ms	10	1.33×10^3
IRR	3.5	3	−20 to +30	2	Each sensor every 2.1 s	10	9.5
TV	20.5	32	−25 to +40	2	1) Every 65 μs	8	123×10^3
					2) Every 370 μs	6	16.2×10^3
UVS	16	15	−20 to +20	2	Each sensor every 5 ms	8	3.2×10^3
DAS	6.5	18	0 to +55	—	Accept above data and output two simultaneous streams		



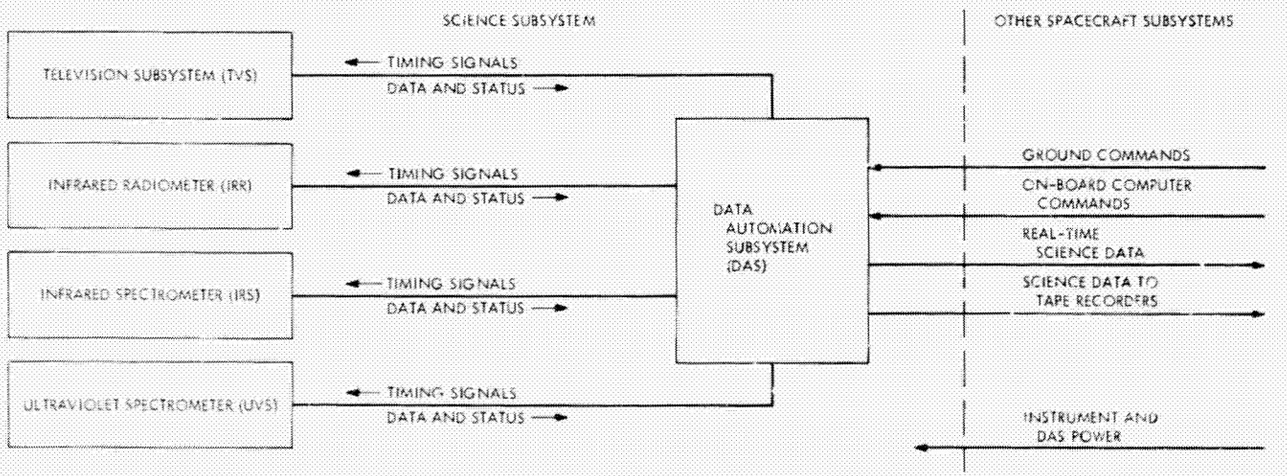


Fig. 1. Science subsystems: (a) equipment location and orientation, (b) simplified block diagram

directly influenced by the scientific instruments. The combination of an assumed payload and the spacecraft to support that payload constituted a discrete spacecraft design. Eight or nine such designs were pursued to varying degrees before the final payload, and therefore the design, was selected. Subsequent to that time, some refinements and changes were made, but the payload itself remained constant.

The basic planetary-oriented mission guidelines bound the selection of the payload and formed the fundamental constraints upon the payload. But within this broad definition the spacecraft for many reasons constrained the range of choice for payload design.

1. Spacecraft constraints. Because the *Mariner* Mars 1969 spacecraft was to draw heavily upon experience gained in the *Mariner C* program, many of the initial constraints were a direct result of the earlier *Mariner* legacy. Since the basic spacecraft configuration was to be the same as *Mariner C*, the packaging and available volume for equipment mounted in the bays was also expected to be the same. The volume limitations for several subsystems, such as data storage, presented serious problems. Despite the *Mariner C* starting point, the potential of the selected payload began to exert pressure for changes which led to the most advanced planetary vehicle yet attempted. In the development of the final mission design, the payload constrained the spacecraft to a greater extent than it was itself constrained.

Other initial constraints of note were the spacecraft telemetry rate (8⅓ and 33⅓ bits/s) and the data storage capacity (2×10^7 bits). The telemetry format specified required that science and engineering data share the single transmitted data stream. The incorporation of gaseous cooling of the infrared spectrometer (IRS) detector and the attendant necessity for dumping the released gas generated a new set of constraints. Any gas venting imbalance must not induce torques on the spacecraft above an acceptable minimum, and the vented gas must not interfere with the measurements of any other instrument.

2. Instrument-generated constraints. The science instrument payload placed a set of requirements for support from the spacecraft. The usual requirements were present with the *Mariner* Mars 1969 payload that accompany any payload: appropriate power, sufficient packaging volume, proper temperature environment, structural soundness, unobstructed view in desired directions. The *Mariner* Mars 1969 payload, however, introduced new unique requirements. The television subsystem, with its expanded picture format, placed greater emphasis on data storage capabilities. The need for cryogenic cooling of one IRS detector required the incorporation and handling of high-pressure gases. The radiative cooling of the other IRS detector created surface cleanliness problems new to this mission. The extraordinary capability of the high-resolution TV subsystem permitted pictures of Mars to be taken starting many hours before encounter which, in turn, necessitated special instrument pointing.

Through an iterative process these and other items caused the spacecraft design to evolve beyond *Mariner C*. A two-degree-of-freedom articulating mount for the instruments was one result. An extra tape recorder for data storage was added, and the density and recording technique were changed to increase capability. The packaging design for bay-mounted science equipment was changed to accommodate the required volume.

In addition, the solar panels were enlarged to provide the increased power demands of the new spacecraft design, and the command subsystem was expanded to include more command[illegible] a more complex mission. Additional effects were felt in the flight telemetry subsystem, which was almost completely redesigned, two extra data streams and increased telemetry rates being added to keep pace with the data that could be accumulated by the science subsystem.

B. Resource Allocation and Maintenance

This section and those to follow will treat the various topics from the point of view of the Science Project Engineer.

1. Data. Mariner C had one data stream shared by engineering and science. On *Mariner* Mars 1969 it soon became apparent that such a system would not suffice. Accordingly, the science and engineering data streams were separated and an additional science data stream was added. The system was configured in such a way that the engineering data could not be interrupted and either of the science streams could be selected. This meant science data no longer had to be synced to the engineering telemetry, but could adopt any reasonable rate. It was decided not to change the science data frame size, but to increase the rate by sampling more often. In addition, the second channel capability for science data meant the high-rate digital science data could also be transmitted concurrent with engineering data. Table 1 contains some characteristics of the science data.

There are three science data formats: (1) real-time, (2) high-rate digital, and (3) composite analog video. Each format evolved from an attempt to satisfy the individual experimenter's data requirements. Response time, desired resolution (data and spectral), field of view, relative spacecraft/Mars velocity (smear), and instrument cycle time were typical of the considerations involved in deciding when and where a given instrument would be sampled. To be sure, the end result often represented a compromise, but it was one which all parties could accept. It was also necessary to insure that an acceptable amount of engineering data on instrument performance be included in the telemetered format to permit evaluation of the accompanying science data.

2. Physical characteristics. Table 1 lists pertinent physical characteristics of the science subsystems. Both power and weight were limited early in the project. Largely because the scientific instruments were unable to meet the limited power allocations, the power system on the spacecraft was modified to increase its capacity. Other important characteristics as well as power were specified as early as possible and then were monitored on a continuous basis for conformity. Several necessary changes were made after all the ramifications were understood.

3. Schedule. As an aid for those responsible for instrument development and to meet project requirements, important schedule milestones were identified and progress toward meeting these milestones was reported. During the period of highest activity, progress was reported weekly. Management review meetings were held with several of the subsystem groups in order to achieve adequate visibility of project and science subsystem problems.

4. Fiscal considerations. Several means of effecting economies were used for items in common use. A centralized source or integration of activities was utilized by a single agency where such action could be taken. Several of these are discussed later. Two examples are the flight electrical connectors, which were dispensed by a central source, and electronic components, which were procured and screened by JPL, thus relieving the instrument supplier of such activities.

C. Design Definition

With the payload selection, the required spacecraft support for that payload could be established and the necessary resources allocated. Then the task of forming an integrated set of sub-systems began.

1. Integration. Selection of the science subsystems was founded on previous experience. All but the infrared spectrometer (IRS) had earlier flight experience on other spacecraft upon which to base the instrument design. The IRS was JPL-developed to a sufficient degree that incorporation on the spacecraft was not expected to be difficult. In spite of these backgrounds, all the *Mariner* Mars 1969 instruments experienced significant design development and integration problems. Several integration problem areas are discussed below.

The standard JPL technique for referencing electrical signals is to collect the signal current-carrying returns within a subsystem into a single isolated ground line and carry it to a central point on the spacecraft where it is connected to the chassis grounding system. All subsystem chassis must, therefore, be kept insulated from the circuitry they contain and are grounded to the spacecraft at their mounting points. However, from past experience and contemporary investigation it has been found that better noise rejection and signal-to-noise characteristics can often be obtained by electrically tying the signal returns to the chassis and isolating the chassis from the spacecraft except through the single point grounding system. The subchassis then acts as a reference potential shield for noise-sensitive circuits.

Again drawing upon experience from previous projects, an all-digital interface criterion was established. This approach has been superior to systems which transmit voltage levels (analog signals) from one subsystem to another. Low-level noise susceptibility is eliminated, and the problems involving the uncertainty during the design phase of the eventual signal path length and cabling interactions are minimized. Instead, through the use of an analog-to-pulse-width converter (A/PW), any voltage can be converted to a pair of pulses whose separation interval is directly proportional to the voltage input. The transmission of these fast pulses, coupled through noise rejection circuits at the receiving end, has proven to be a reliable data interfacing technique. The particular converter in use was developed by the data automation subsystem engineers and has been improved several times. It can be used in either a unipolar or bipolar mode and can resolve input voltages into 1024 parts. Each of the science instrument interfaces carrying science data and most of the instrument engineering data were handled with A/PW converters.

In addition to cable drawings prepared for science use and project-prepared circuit data sheets, a new means of identifying and controlling interfaces between elements of the science subsystems was introduced.

These were functional interface definitions which provided information found nowhere else to describe the function and routing of each signal passing between two subsystems and, where appropriate, to specify the relationship between signals. These definitions were particularly helpful during the earlier stages of the system design and prevented many troublesome problems which had plagued earlier projects.

The problem of protecting the spacecraft power subsystem also received considerable attention. Ultimately, the UVS, TVS, and IRS used active current-limiting, the IRR used fuses, and the DAS was direct-wired without protective devices. As a series element in terms of science data return, the DAS was judged to be a critical element to the mission.

2. ***Liaison.*** Instead of having each cognizant engineer separately negotiate his cabling interface with the cable shop, the collection of science subsystems was treated as a system in achieving the preliminary cable design. This is a reasonable approach, since the majority of connections to the science subsystems are with other science subsystems. Some economy in cabling was realized by this approach, particularly with the cables between the instruments and the DAS.

The combination of the DAS hardware and that part of the TVS which was located in the spacecraft bus outgrew the volume available utilizing the *Mariner C* standard packaging design. Therefore, it was decided to adopt a new packaging design which had been developed by the engineering mechanics division. This necessitated some redesign of the DAS, with an impact upon the interconnection scheme being utilized. It was fortunate, however, that sufficient flexibility existed in cabling layouts to accommodate the new approach.

The new bus electronics bay design was itself the source of some concern. In the previous design, the modules could be installed and removed without special tools; the new design required specially designed fixtures and tools for inserting and removing modules. However, once the users gained proficiency in the use of these fixtures, the advantages of the new design were obvious. Perhaps the most useful was the ability to remove and replace modules without disturbing the cable harness.

As in the case of the platform-mounted hardware, packaging experts were consulted concerning the platform-mounted instruments. Since these instruments were all attached to the same structure and were subjected to the same environmental input, this work was coordinated as much as was practical.

Within practical limits an attempt was made to provide uniform reliability and quality assurance (QA) support to the cognizant engineers. The actual support which each of the instruments received depended upon the apparent need at the time. It is certain that budget and manpower constraints were factors in limiting such support.

3. ***Documentation.*** To help formalize the design of the science subsystems, several intermediate documents suitable for data transfer to project-level documents were utilized. Two notable examples were science system drawings, which provided information for spacecraft cabling drawings, and science interface sheets, which were the basis for the project circuit data sheets. Both of these documents were prepared earlier than their project-level counterparts. Another such science document was the functional interface definition discussed earlier. In this case, however, there was no comparable project document.

In addition, special assistance and direction were given to the instrument cognizant engineers for the generation and maintenance of the functional and design requirements and the environmental test specifications. Engineering change requirements (ECRs) and problem/failure reports (PFRs) were reviewed, as were circuit data sheets, thermal data sheets and interface control drawings. This important activity helped to emphasize the importance of all levels of documentation while lessening the load on the subsystem cognizant engineer wherever possible.

D. Qualification Support

Full qualification of the spacecraft hardware at all levels from piece parts to the assembled spacecraft is a recognized JPL goal. Payload integration support was given to this effort whenever common elements by all or several of the science instruments were involved.

1. ***Piece parts and components.*** Two items already mentioned are examples of piece parts and components used by all subsystems and which were centrally distributed. These were the electrical connectors and the A/PW converters. These were received from the supplier after qualification to rigid performance and workmanship specifications, and were, in turn, distributed to

the instrument suppliers. Engineering temperature transducers were handled in the same way, and since these items were accompanied by appropriate identification data, a complete history file was maintained for later configuration checks.

2. *Subsystems.* The value of actually performing interface testing with an early model DAS and each of the science instruments has been demonstrated many times in the past. This activity was again undertaken on the *Mariner* Mars 1969 project, and the results were satisfying. The breadboard DAS was interfaced with the prototype models of the instruments. Several problems were identified and corrected while such work was comparatively easy to accomplish. This setup was also used to verify the flight subsystems/operational support equipment (OSE) interfaces.

As support to the cognizant engineers, all special cables needed for environmental or special testing at the subsystem level were provided by the payload integration personnel. This insured that special requirements imposed by these uses would be fulfilled without unduly burdening the cognizant engineer. Assistance was also provided in the design and procurement of special jigs and fixtures used in subsystem environmental testing.

3. *Spacecraft.* On-pad operation to verify the launch integrity of the science subsystems were performed. To obtain meaningful results, it was found necessary to provide remote input stimuli for the TVS. The most convenient location for the stimuli was the spacecraft adapter. The necessary equipment was designed, built, and subjected to flight qualification tests by payload integration personnel and is representative of the support supplied by the science project engineering staff when responsibility cannot conveniently be assigned to any one subsystem.

System-level support was provided several other exercises involving test spacecraft such as the thermal control model (TCM) and structural test model (STM). A particularly significant series of tests to study the effects of stray light on the platform-mounted instruments was performed using the TCM spacecraft and science instruments. Another very important series of tests included measurements of the relative lines of sight of the science instruments and planet sensors for each flight-configured spacecraft. This latter effort is discussed separately in the following section.

E. Sensor Instrument Alignment Verification

As *Mariner* Mars 1969 passed Mars, the instruments on the scan platform were positioned to view the proper target areas on the surface of the planet. This required that they be positioned on the pla form with the proper angular alignment relative to each other and to the scan platform. Because of the importance of this alignment, verification measurements were made just prior to flight with the instruments mounted on the scan platform in their final configuration. The measurements were made by determining a line of sight (LOS) for each instrument and by measuring its vertical and horizontal offsets relative to that of the narrow-angle television subsystem (TV-B)—the reference pointing direction of the scan platform. Mission constraints required that the angular offsets of the instruments be within ± 0.3 deg of their specified value and that they be known to ± 0.1 deg.

1. *Method of measurement.* In the case of the nonimaging instruments, the LOS of an instrument is defined as the center of its field of view (FOV) and can be computed from the angular limits of the FOV. These limits are readily found by means of a collimator mounted in a transit base. The collimator simulates a distant source and can be effectively translated across the FOV by turning angularly. Since the position of the source in the FOV can be determined by watching the electrical output of the instrument as a function of the angular position of the collimator in the transit base, the limits are those positions at which the output diminishes to zero as the source leaves the FOV. In the case of the imaging instruments (TV-B and TV-A), the LOS is defined as the direction of those parallel rays brought to focus at the center fiducial mark on the face of the vidicon tube. It is found directly by stimulating the camera with a crossline reticle, adjusting the collimator angularly to bring the cross line into coincidence with the center fiducial mark.

Once the LOS of an instrument and that of TV-B is found and measured in the coordinates of the transit, the angular offset between them can be measured by referring them to a common reference plane and normalizing their angular readings. Using a mirror as the reference plane, this can be done very accurately by positioning the collimator in front of the instrument, aligning it to the instrument, and then referring to the mirror by autocollimation. To make the mirror easily accessible to the collimator during the alignment of each of the instruments, it is positioned to the side of the platform approximately vertical and perpendicular

to the LOS of TV-B. To minimize the size and cost of the mirror, the transit is constrained to move vertically and horizontally in a plane directly in front of the platform and roughly normal to the LOS of TV-B by mounting it on a movable carriage supported by a vertically adjustable rail. Maintaining the horizontal plane of the transit level during all measurements permits the measurements to be referred to TV-B in a common coordinate system.

The relationship between the LOS of TV-B and the normal to the reference mirror need be measured only once to permit the offsets of all the instruments relative to TV-B to be determined, provided the angle mirror and the scan platform do not move with respect to each other. This is an advantage, since finding the LOS of TV-B is an exacting and time-consuming process. Sometimes, however, the platform is moved relative to the reference mirror during tests and data is lost. To prevent this, a small reference mirror called the planetary platform mirror is rigidly attached to the front of the platform and its normal is also referred to the LOS of TV-B by autocollimation. This provides a fixed directional reference, independent of motion between the platform and the angle mirror, to which the LOS of each of the instruments can be quickly referred, greatly reducing the measuring time required when an instrument is changed from one spacecraft to another and its offset remeasured.

2. ***Discussion of method.*** The method described has the advantage of being independent of mechanical tolerances except for the surfaces of the reference mirrors. For example, it is not necessary to translate the transit of an optically level guide rail or optical bench or to align the rail precisely to either the scan platform or the angle mirror. Its dependence, instead, on autocollimation to a common, optically flat reference plane makes it flexible and more accurate and the instrumentation less expensive. Its main limitation is that it is tedious and time-consuming to define the FOV of many of the instruments because of the low sampling rates in their electrical outputs.

3. ***Description of hardware.*** The collimator used for the measurements was specially designed and custom-mounted in a standard transit base. It has reflecting off-axis optics to enable it to operate over a wide IR to UV spectral range and to avoid a central obscuration, a focal length of 18 in., a 3-in. aperture, and is fitted with a microscope and a removable beamsplitter for autocollimation. The stimulus is provided by three separate sources: a mercury lamp for the UV range, a soldering iron filament for the IR range, and a variable-intensity quartz-iodide lamp for the intermediate range. The size of the source presented to the instruments is adjustable over a wide range by interchanging reticle disks containing holes of different size.

The collimator was supported in a standard transit base to permit accurate angular measurements at low cost. The transit base was selected to accommodate the largest collimator diameter practical and was equipped with a bearing-mounted spindle to guard against overloading. Precision vertical and horizontal circles and 30-second leveling vials permit accurate angular readout and leveling. In operation, it rides on an aluminum tooling bar supported on an adjustable stand.

A 3×8-in. angle mirror, with the front surface flat to ¼ wavelength of light, was chosen to provide the reference plane. It was made oversize and mounted independently on a separate instrument stand to accommodate all the instruments without being moved.

4. ***Measurement accuracy.*** The measuring accuracy of this system is about ± 2 min of arc: roughly equal to the resolution of the instruments, i.e., their ability to register small changes in the position of the collimator source or target. This resolution is the main limiting factor in these measurements; although smaller errors due to inaccuracies in the graduations of the angle rings on the transit and imperfect resolution during autocollimation to the reference mirrors are also present. The accuracy of the rings is ± 20 sec of arc; autocollimation can be repeated to about ± 10 sec of arc.

5. ***Measurements made.*** Measurements were taken both at the SAF and AFETR. Those at SAF were taken on all the spacecraft (M69-1, -2, -3, -4) prior to vibration-testing in the environmental test laboratory; in addition, postvibration measurements were made only on M69-2 and M69-3. However, swapping of instruments from one spacecraft to another after the initial verification required additional measurements for each configuration. In most cases, each measurement was repeated and the average of two readings recorded to avoid possible measuring errors.

6. ***Results.*** Many improvements in measurement technique were made and the accuracy of the measurements at AFETR increased as a result of the experience with measurements made at SAF. The measurements indicate

good repeatability where instruments were merely removed from the platform and replaced. Mechanical alignment errors proved to be less than the measuring error, and no appreciable error was noted even after vibration-testing, which indicates good stability of the optical axis. Offset changes were noted, however, as a result of switching instruments from one scan platform to another and from realignments of the optical axis of the IRR and IRS prior to the AFETR measurements. Changes due to switching instruments were of the order of a few minutes at most; but when combined with changes in the optical alignment of the IRR and IRS they exceeded the required tolerances. It might also be noted that alignment discrepancies arose in the case of the IRS because of inadequate definition of the LOS of the instrument. This occurred because the instrument had two channels with overlapping fields of view, one of which was inoperative at systems test temperatures, resulting in an ambiguous definition of its LOS.

7. Recommendations. If similar measurements are made of future spacecraft instruments, more accurate determination of the FOV of each instrument and its measuring resolution and detector characteristics prior to SAF tests should be made and recorded to speed SAF and AFETR alignment testing. In addition, the optical alignment of an instrument should be accurately measured to permit the effect of alignment caused by changing an instrument from one spacecraft to another to be predicted.

Because of the time required for alignment measurements, it may be decided to minimize them on future programs. If this is done, care should be taken to guard against undetected optical alignment changes. Final alignment accuracy is dependent upon the mechanical tolerances of the completed spacecraft scan platform and the optical alignment of the instruments. While experience shows that the mechanical alignment can be repeatable, the optical alignment did change on those instruments which underwent an additional optical alignment calibration between the SAF and AFETR tests. To insure against such errors, a detailed inspection and verification of the vendor's alignment should be checked at JPL before the instrument is mounted on the spacecraft scan platform.

II. Data Automation Subsystem

The data automation subsystem (DAS) serves as the data handling system for the science payload. It controls and sequences the science instruments, converts the resulting science data into digital form, provides temporary (buffer) storage, codes and formats the data into 28-word (10 bits per word) frames, and routes the data to both the flight telemetry subsystem (FTS) and data storage subsystem for direct or delayed transmission to earth. The DAS exchanges commands with other subsystems aboard the spacecraft which pertain to the operation of the science payload.

The *Mariner* Mars 1969 DAS (Fig. 2) consists of a power converter subassembly, an interface circuit subassembly (discrete components), and two integrated circuit logic subassemblies. Six analog-to-pulse-width converter (A/PW) modules located in the scientific instruments are remotely controlled by the DAS and are considered part of the DAS. Each subsystem employs 488 discrete components (17 in the power converter) and 653 integrated circuits installed on 12 laminated multilayer (PC) boards. The 12 multilayer boards are placed in three 6×14-in. subassemblies and the power converter components in one 2×6-in. subassembly using a total volume of 541 in.^{3} The subsystem weighs 13.65 lb and requires approximately 18 W of 2.4-kHz ac power. The DAS internal harness (interconnection) contains 284 wires, the external harness (input/output) 149 wires; combined they weigh 3.38 lb.

A diagram of the DAS and its interfaces with the various subsystems on-board the spacecraft is shown in Fig. 3. The major inputs to the DAS are data from the four scientific instruments shown on the left side of Fig. 3. The major output from the DAS consists of data which have been accumulated from the various instruments and properly formatted. The three destinations for the data from the DAS are the flight telemetry subsystem, the data storage subsystem, and the television subsystem.

A. Data Streams

The DAS produces three data streams throughout the far-encounter and near-encounter phases of the mission. There is no cruise science included. The three data streams are 66⅔ bits/s real-time data to FTS, 16.2 kbits/s digital data to the data storage subsystem, and 18.9 kbits/s with analog coding to the television subsystem. The formats of these data streams remain the same throughout both encounter portions of the mission. The major difference between the DAS far-encounter and near-encounter operation is the cycling of the data storage subsystem recorders.

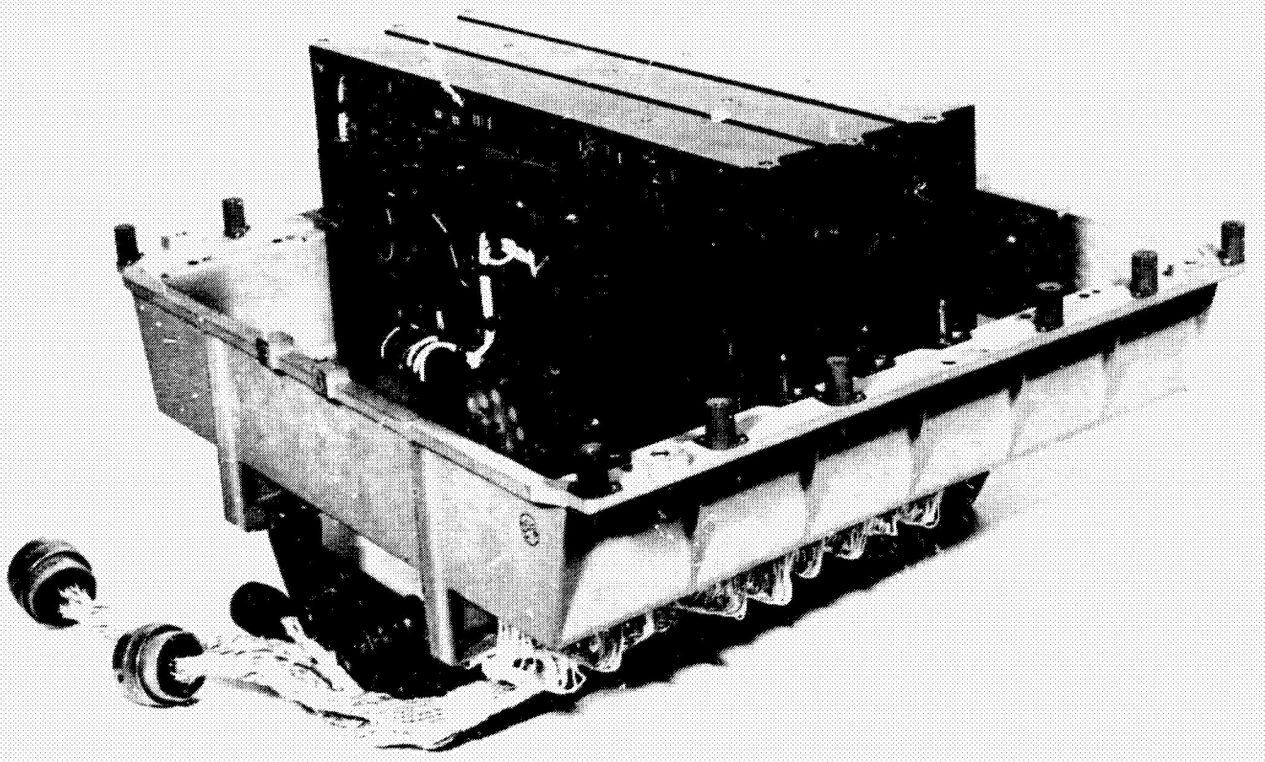


Fig. 2. Data automation subsystem

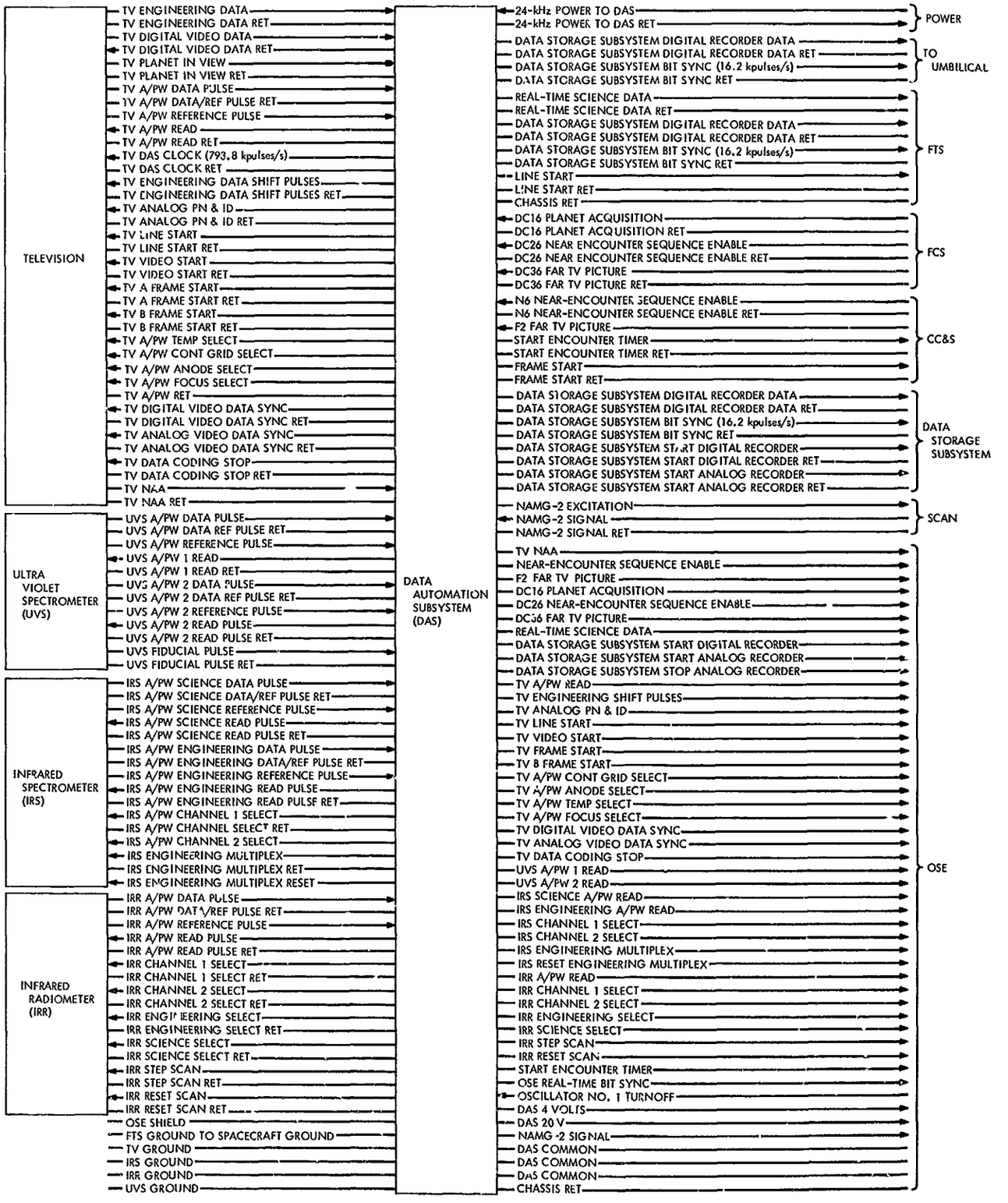
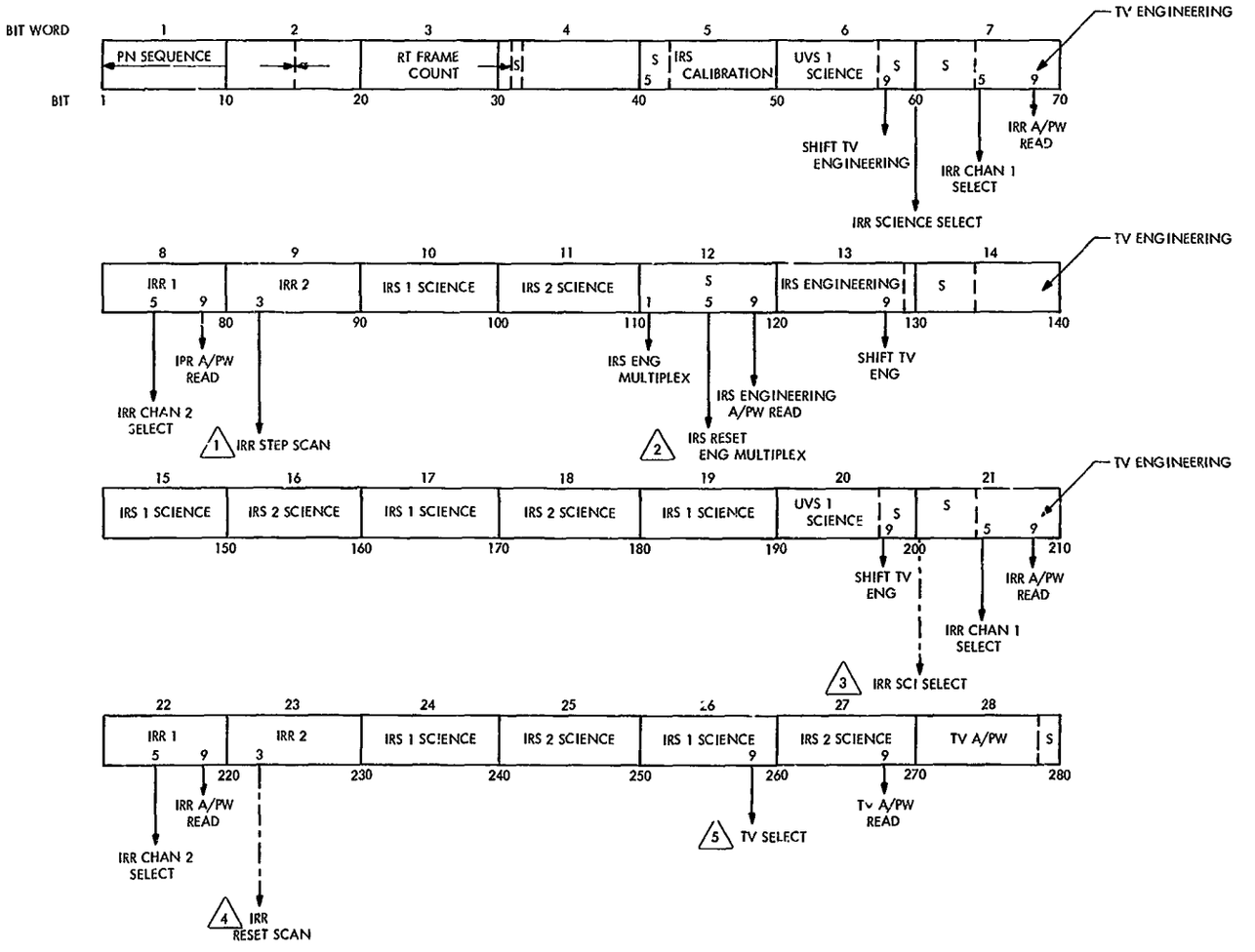


Fig. 3. Data automation subsystem interfaces

1. Real-time data format. The DAS real-time (RT) data format is shown in Fig. 4. A description of the RT words is given in Table 2. The science data words are from 1 to 16 bits in length. However, the DAS word length is 10 bits. There are 28 DAS words per RT frame.

Status bits are included in the RT frame format to indicate the time of receipt or transmission of certain functions and to permit evaluation of the DAS performance throughout the mission. The status bit locations in the RT frame are shown by an S in Fig. 4 and a description of each bit is given in Table 3.

2. 16.2-kbits/s digital data format. The digital recorder data format is composed of A/PW samples, digital TV coding, and digital TV video data. The TV video data is received as return-to-zero pulses (16.2 kpulses/s) and "ORed" directly with the digital data generated by the DAS. The digital recorder format indicating the data stream structuring is shown in Fig. 5.



NOTES:

ALL COMMANDS SHOWN OCCUR EVERY FRAME UNLESS STATED OTHERWISE

S = STATUS BITS

1. OCCURS DURING FRAMES 2, 9 AND 10. REPEATED EVERY 15 FRAMES (63 s)
2. OCCURS ONCE EVERY 10 FRAMES (42 s)
3. ONCE EVERY 15 FRAMES; NINTH FRAME REPLACED BY IRR ENG SELECT
4. OCCURS ONCE, FRAME 1, EVERY 15 FRAMES (63 s)
5. SEPARATE SELECT LINES FOR TV TEMP., TV CONTROL GRID, TV ANODE, AND TV FOCUS. ONE LINE SELECTED EVERY FRAME. CYCLE REPEATED EVERY 25.2 s

Fig. 4. Real-time data format

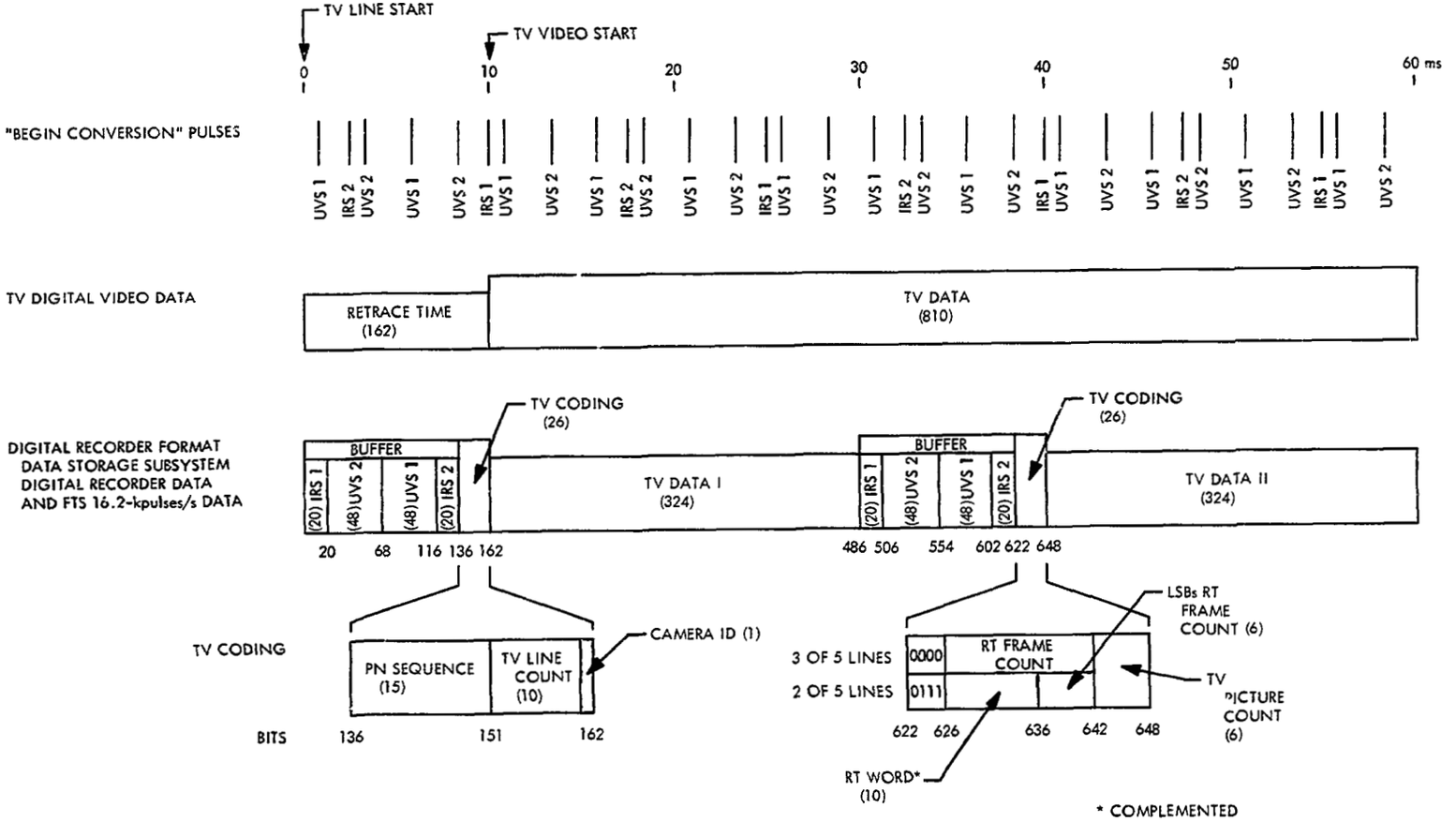


Fig. 5. Generation of the digital recorder format

Table 2. Data automation subsystem real-time word description

Abbreviations	Data format word	Description
PN Seq	1, 2	The 15-bit pseudonoise sequence used to identify the beginning of each RT data frame. The sequence is 000011101100101
RT Frame Count	2, 3	The count of the number of RT frames (4.2-s periods) from power on reset
A/PW Calib	4	The monitor of the DAS master oscillator frequency. The 793.8 KHz is counted between two adjacent trailing edges of the 2.4-KHz power
IRS Calib	5	The 8-bit indication of where in the IR spectrum the IRS science words of this RT frame occurs
UVS1-Sci	6, 20	The 8 most significant bits of an integration of the 20 consecutive UVS1 science samples occurring 0.905 s after the UV fiducial pulse
TV Eng	7, 14, 21	The 6 bits of the TV subsystem status
IRR1	8, 22	The 10-bit A/PW bipolar data with 1-bit sign for IRR channel 1
IRR2	9, 23	The 10-bit A/PW bipolar data with 1-bit sign for IRR channel 2
IRS1 Sci.	10, 15, 17, 19, 24, 26	The 10-bit A/PW bipolar data with 1-bit sign for IRS channel 1
IRS2 Sci.	11, 16, 18, 25, 27	The 10-bit A/PW bipolar data with 1-bit sign for IRS channel 2
IRS Eng.	13	The 9-bit A/PW unipolar measurement which is multiplexed (in IRS subsystem) between 10 IRS internal voltages
TV A/PW	28	The 9-bit unipolar measurement which is multiplexed (in TV subsystem) between 4 TVS internal voltage

The digital data inserted into each TV line consists of four science measurements, TV coding, and real-time data words. Each line is 60 ms long and contains 972 bits. The real-time data was previously described. The data samples inserted into each TV line are identical except where the RT frame count and RT word is inserted. The timing relationship between each TV line and the real-time word intervals is such that 2 out of 5 TV lines contain one RT 10-bit word and 3 out of 5 lines contain the 16 bits of RT frame count. During the RT word lines, the 6 least significant bits of the RT frame count are inserted. Both the RT frame count and RT words are preceded by a 4-bit code used to identify the two groups of data. Since the sampling rates of the science data are slower than the output rate and the RT format data is asynchronous with the TV line, this data must be buffered prior to recording.

3. 18.9-kbits/s analog coding format. The analog coding format is transmitted as an 18.9-kpps burst of 64 bits to the TV, where it modulates the TV carrier and is sent to the analog recorder. This 64-bit burst occurs every 60 ms at the start of a TV line. The total TV line as presented to the data storage subsystem contains 1134 bits. Figure 6 shows the analog coding format.

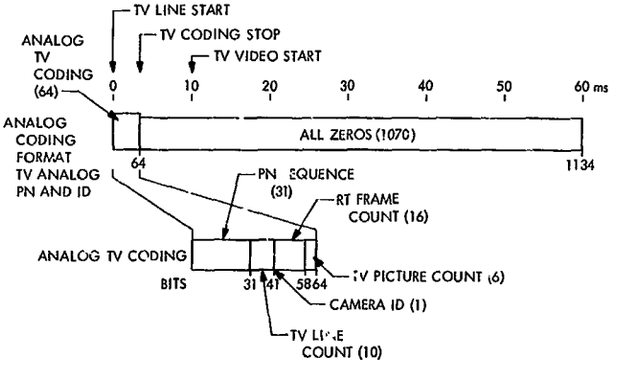


Fig. 6. Analog coding format

B. Internal system operation

A functional block diagram of the overall DAS is presented in Fig. 7. The science data and instrument engineering data enter into four A/PW counter/control blocks. The control and sequencing signals to the instruments exit from basically the same control logic blocks. The 2.4-kHz power signal is converted to dc power and as a clock signal for the real-time logic. The commands received from the CCAS and FCS are used to control the encounter operation of the DAS.

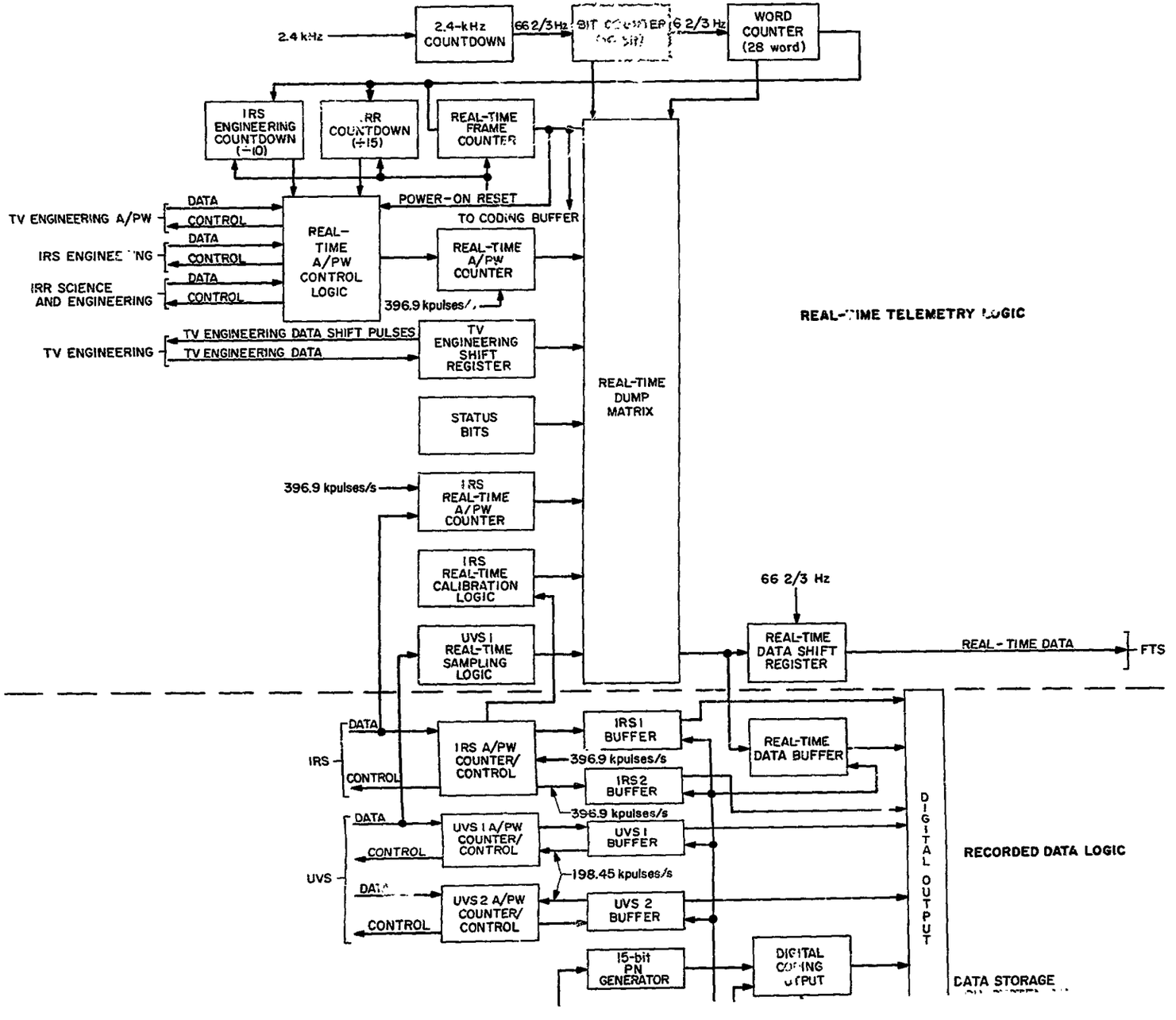
Most of the data inputs are received at the DAS in the form of a time period between two pulses on separate lines. These pulses are generated by A/PWs located in the instruments. The time period is converted to a binary equivalent in the A/PW counters. This converted data is immediately inserted into the RT format and/or buffered for later recording by the data storage subsystem. The

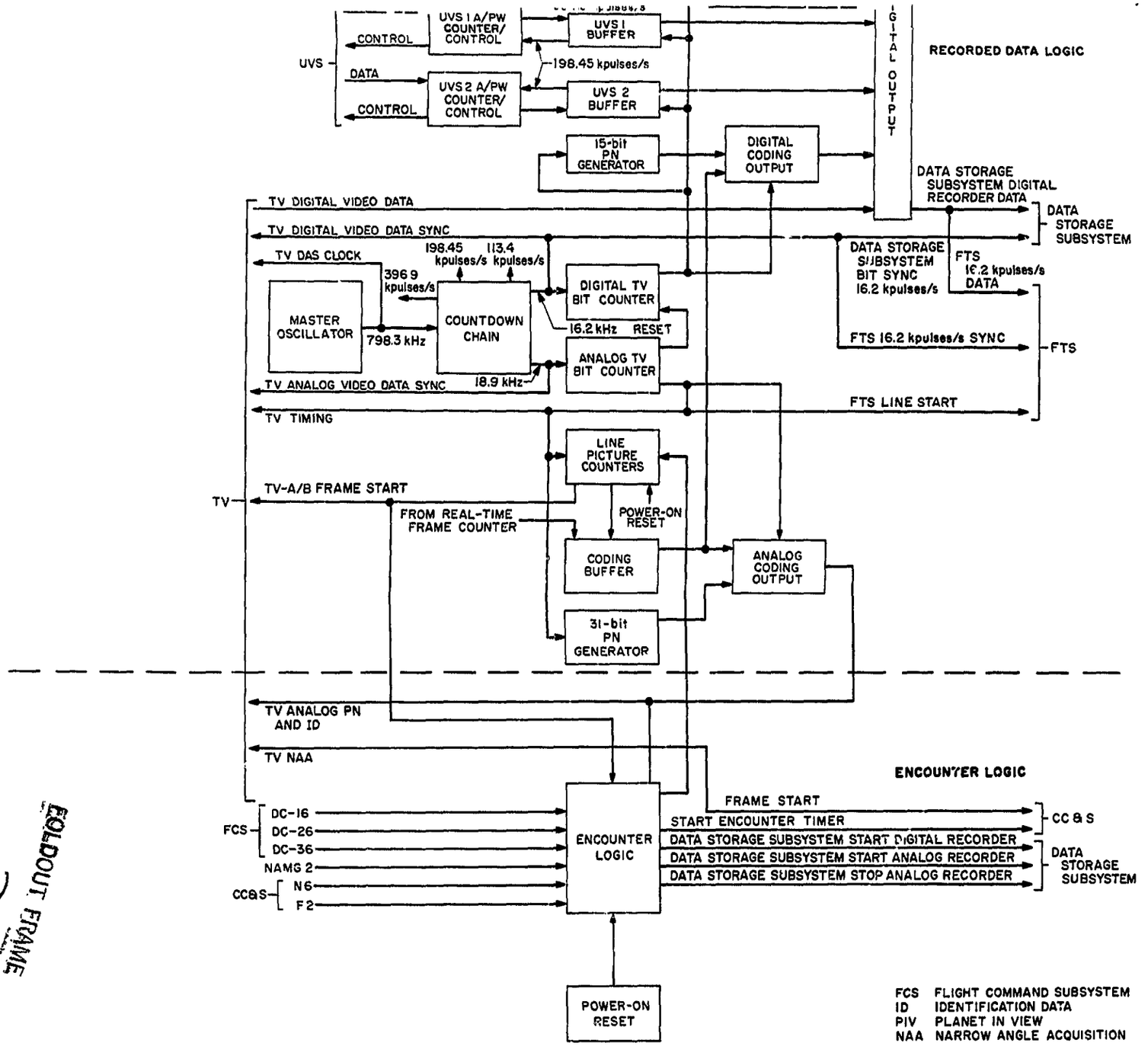
Table 3. Data automation subsystem real-time status bits

Word	Bit	Function	Notes
4	2[a]	N6 received	"1" indicates receipt of N6; enables the near-encounter sequence
5	1	F2 received	Bit toggles with receipt of each F2; command to take far TV picture
5	2[a]	DC-16 received	"1" indicates receipt of DC-16 —ground command to back up N6 and DC-26; enables the near-encounter sequence
6	9	TV-PIV received	Function deleted; bit will be a "0"
6	10	DC-36 received	Bit toggles with receipt of each DC-36—ground command to back up F2; command to take far TV picture
7	1	Spare	Bit will be a "1"
7	2[a]	DC-26 received	"1" indicates receipt of DC-26 —ground command to back up N6; enables the near-encounter sequence
7	3	Spare	Bit will be a "1"
7	4	Camera ID	A direct monitor of TV camera ID bit will be a "1" for camera B vidicon and a "0" for camera A vidicon
12	1	NES enabled	"1" indicates the DAS encounter mode has been enabled (by N6, DC-26, or DC-16)
12	2	NAMG-2 received	"1" indicates NAMG-2 level is present at DAS
12	3, 4	Digital video monitor	Monitor of bits 485 and 486 of a TV line occurring in RT word 11; indicates output of video data from TV
12	5, 6	CC&S start encounter sent	2-bit count, counting once for each time DAS sends signal to CC&S
12	7	Oscillator status	"1" if prime oscillator is being used, "0" if secondary oscillator is being used
12	8, 9, 10	DAS serial No.	Hardwired to identify each individual DAS Data SN Spacecraft 001 SN-1 M69-3 010 SN-2 M69-2 011 SN-3 M69-4 100 SN-4 PTM 101 SN-5 Prototype
13	10	Stop analog recorder sent	Bit toggles each time stop analog tape recorder signal is sent
14	1, 2, 3, 4	Start analog recorder sent	4-bit count, counting once for each time DAS sends start analog tape recorder signal
20	9, 10	Power monitor	2 bits indicating gross range of DAS power supply voltage: 10 indicates $V_{cc} > 4.28$ V 00 indicates 3.17 V $< V_{cc} < 4.86$ V 01 indicates $V_{cc} < 3.59$ V
21	1, 2	Start digital recorder sent	2-bit count, counting once for each time start digital recorder/TV NAA is sent
21	3	IRS engineering reset	Bit is "1" once every 10 RT frame (normally "0") indicating reset signal sent
21	4	Spare	Bit will be a "1"
28	10	IRR scan motor reset	Bit is "1" once every 15 RT frames (normally "0") indicating reset signal sent

[a]Bit is power-on-reset to zero. Signal normally received by the DAS once. However, the status bit is implemented to toggle each time the signal is received.

FOLDOUT FRAME





FOLDOUT FRAME 2

Fig. 7. Data automation subsystem, functional block diagram

PRECEDING PAGE BLANK NOT FILME

TV digital video data is received by the DAS in order to insert the science data in the proper sequence for recording on the digital tape recorder. This is shown in Fig. 5.

The DAS functional operation can be separated into three logic groups: real-time telemetry logic, recorder data logic, and encounter logic. The real-time logic contains counters for timing (generated from the 2.4-kHz clock), data formatting and instrument control, data dump matrix, and real-time output shift register. The 66⅔ bits/s data stream from the shift register is sent to the FTS.

The recorder data logic contains a 793.8-kHz oscillator, countdown chain for timing and control, data buffers, and digital output circuitry for the 16.2 kbit data and sync sent to both the data storage subsystem and FTS.

The encounter portion is made up of control logic that accepts automatic or ground commands from which a series of special commands and controlling functions is generated from the start of far encounter to the end of the encounter phase (Fig. 8). These special signals are for control of the analog and digital recorders and the CC&S encounter timer.

C. Logic Type

The integrated circuits (IC) logic family used in the *Mariner* Mars 1969 DAS was made up of the Signetics Corporation 100 and 400 series devices. These include both diode transistor logic (DTL) and transistor transistor logic (TTL). The Signetics Corporation integrated circuits were initially used and proven to be flight worthy devices on the *Mariner* Venus 67 mission. Integrated circuits are considered to be inherently more reliable than the sum of the parts and interconnects they replace. Using an average of 35 components per IC (the number is based on 7 device types used in the DAS), the number of components contained in the DAS becomes 653 ICs × 35 + 488 discrete components = 23,343 components.

Two nand gates, two nand/nor gates, one flip-flop, one gate expander, and one line driver make up the seven

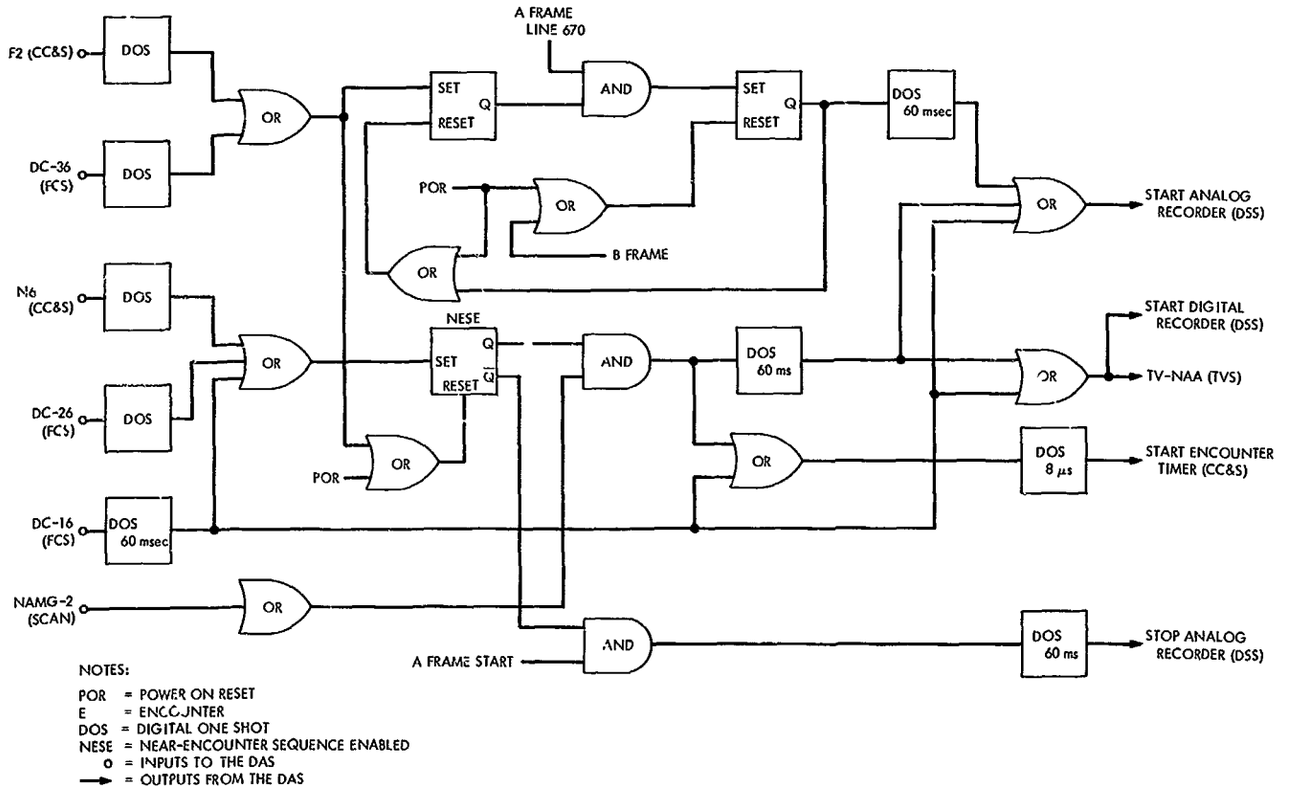


Fig. 8. Data automation subsystem, functional encounter logic

device types used. The prime difference between the two nand gates and the two nand/nor gates is the number of inputs and the output drive capability.

The procurement philosophy used for the *Mariner* Mars 1969 DAS integrated circuits was the same as that employed for the *Mariner* Venus 67 ICs. However, the IC specifications were upgraded, certain inspection and test criteria were added, and the vendor management section was expanded for the *Mariner* Mars 1969 effort. The basic philosophy was to use very detailed specifications for both visual inspection and electrical requirements, resident inspectors at the IC vendor under JPL direction to monitor vendor inspection points, a full-time program manager at the vendor, and strict and comprehensive liaison between JPL engineering and the program manager.

D. Multilayer Printed Circuit Boards

A packaging scheme for an integrated-circuit DAS requires an approach tailored to accept close lead spacing and device form factor as well as a means for interconnecting discrete component interface circuits and to satisfy weight, volume, and maintenance requirements. Multilayer laminated printed circuit boards satisfy these requirements with good flexibility and reliability.

The requirements and processes were developed and put into practice during the *Mariner* Venus 67 program and were upgraded and refined during the *Mariner* Mars 1969 program. An increase of approximately 30% in packing density of ICs was realized by the 1969 over the 1967 design. Mechanical design constraints were documented and enforced which "designed in" the capability of changing interconnections after assembly by making all internal functions accessible. Etch-cut and magnet wire rework processes were used to incorporate changes. Studies performed following the 1969 effort show that IC density can be increased further by approximately 80%.

The use of photomicrograph acceptance of plated-through holes was employed to identify and control process variables. Holes were sectioned around the periphery of each board, and two photomicrographs of the worst-case holes were submitted for acceptance. Photomicrographs were demonstrated to be a powerful tool in the control of multilayer board reliability. There were no multilayer board problems at the subassembly level on the 1969 DAS program.

E. Subsystem Testing

System acceptance tests were conducted at -10 and $+65°C$ with $\pm 10\%$ voltage margin. These tests were performed at the contractor's facility prior to delivery as part of the contract requirement. After component delivery, verification of acceptance was performed with bench checkout equipment (BCE). Complete temperature/voltage margin tests were conducted with the PDP-7 computer prior to and following all TA and FA environmental tests and again prior to delivery to Cape Kennedy. The PDP-7 provides a more comprehensive and timely test of the DAS by comparing actual events and measurements with their expected time of occurrence and values. The results of the PDP-7 tests revealed that the subsystem margins had changed by less than the resolution of the test equipment used. No DAS failures were encountered during the TA or FA environmental tests or life tests performed on the flight units.

F. Systems Testing

Science instrument integration and compatibility tests were performed with the breadboard DAS. Similar tests were performed with all spacecraft subsystems except two prior to any DAS hardware delivery to the Spacecraft Assembly Facility (SAF). System integration tests on a science subsystem level were conducted by the JPL Science Division prior to hardware delivery. Both the breadboard and the prototype units supported this effort. The prototype DAS was used to support calibration of the UVS flight instruments at Goddard Space Flight Center.

All flight configuration hardware was tested on the spacecraft. The prototype served as a substitute for the PTM until PTM delivery. Spacecraft testing revealed one interface problem that resulted in a DAS logic change. This problem occurred between the DAS and the TV subsystem and was found to be a logic timing problem.

The *Mariner* Mars 1969 DAS was found to be much less sensitive to external noise during both the subsystem and system testing than previous designs flown. This sensitivity characteristic was the result of much stricter logic design rules, larger functional blocks of logic contained in each subassembly, and fewer interconnections between logic subassemblies. Only minor anomalies were encountered during systems testing and no failures occurred.

III. Ultraviolet Spectrometer Subsystem

The ultraviolet spectrometer subsystem (UVS) measures the density and scale height of atoms, ions, and molecules in the upper atmosphere of Mars (60- to 600-mi range), the Rayleigh scattering in the lower atmosphere, and the ultraviolet reflectivity of the planet surface.

The instrument was designed, developed, and built by the University of Colorado Laboratory for Atmospheric and Space Physics under the direction of the experiment team in collaboration with the JPL Space Sciences Division. The UVS consists of an occulting slit telescope having a focal length of 25 cm and a scanning monochromator to provide wavelength resolution to two photomultiplier tube (PMT) sensors. The UVS scans the ultraviolet spectrum from 1050 to 1900 Å in the second order and from 1750 to 4350 Å in the first order. Each of the two PMT sensor output signals is separately amplified and conditioned for compatibility to the spacecraft data automation subsystem (DAS). During the spacecraft far-encounter mode, only the Lyman-alpha hydrogen data (1216 Å) is selected for radio transmission in real-time by the DAS. Logic circuits are used within the DAS and the UVS to synchronize the DAS to the appropriate position of the UVS scan grating for wavelength selection of the Lyman-Alpha data.

A phototransistor is employed behind and at each end of the preslit of the telescope in the UVS to separately detect the sunlit limb of Mars. These limb detectors are used to expand the dynamic range of the UVS data system and to assist in defining the scale height of the Martian atmospheric data as sampled by the UVS.

A. Spacecraft Interface

1. Data. Two analog channels are used in the UVS. Channel 1 covers the UV spectral range between 1050 and 1900 Å; Channel 2 covers the range between 1600 and 4350 Å. Each analog channel output is separately connected to an analog-to-pulse-width converter (A/PW) housed in the UVS. The UVS data interface with the DAS is at the output of the A/PW. The full-scale analog input voltage to each A/PW is + 6 V. For protection, diodes are used at each analog output to limit the A/PW input voltages at approximately + 6.8 and − 0.6 V. The A/PW data interrogations from the DAS are alternated between each channel every 2.5 ms, each channel being read out once every 5 ms. Each analog output sample is converted to an 8-bit binary word, a decimal number of 255 being representative of an analog output of 6 V.

The equally spaced DAS real-time data frame word numbers 6 and 20 have been assigned for the Lyman-alpha data. The DAS real-time data frame length is 4.20 s, and the total UVS scan cycle is 3.00 s (synchronized with the spacecraft 2400-Hz power); therefore, about two-thirds of the real-time UVS data received is redundant. The UVS transmits a fiducial pulse to the DAS that initiates a 0.905 s delay prior to enabling an 11-bit counter in the DAS (only the 8 most significant bits are used). The counter accumulates UVS data for a period of 100 ms (mechanized by counting 20 of the A/PW interrogation pulses which occur each 5 ms). The Lyman-alpha resonance line (appearing on the analog output in triangular form about 50 ms wide at the base) is approximately centered within the time period of the DAS counter. Since there is no other significant data appearing within the UVS during the DAS 100-ms counting period, the peak height of the Lyman-alpha data is interpreted as being:

$$\frac{8 \times DNa - 20 \times DNb}{5}$$

where

- *DNa* is the decimal number accumulated in the DAS counter
- *DNb* is the background decimal number determined from acquired spectrum high-speed data
- 8 represents the number of used bits in the DAS counter
- 20 samples are accumulated in the DAS counter for each word
- 5 samples are half the samples taken at the base of the Lyman-alpha data triangle

The DAS counter is mechanized to indicate an output decimal number of 255 if the counter is in the accumulation process when the data frame readout occurs. The timing relationship between the UVS, the DAS counter, and the counter readout is dependent on logic states at the time of science power turn-on. If the related times are such that a decimal number of 255 does occur, it will appear regularly once every fifth data frame. The real-time UVS data is displayed in SFOF on a 100-word/min teletype receiver using format number 455. Only

UV data words number 6 and 20 are available from the spacecraft at the real-time data rate of 66⅔ bits/s.

At the high-speed data rate (16.2 kbits/s) all UVS data is transmitted, including UVS engineering measurements. Of the 3.00 second UVS scan cycle 180 ms is used to return the scan grating back to the scan-start position. In turn, 140 ms of the grating flyback time is used to mix UVS engineering measurements with the analog outputs. The engineering measurements made during each grating flyback are shown in Table 4.

Table 4. Grating flyback engineering measurements

Measurement	Analog output		Per scan	
	DN	Voltage	Duration, ms	Number of A/PW readouts
Channel 1				
Zero data level	6	0.141	40	8
Gain calibrate	190	4.471	40	8
Optical temperature 1	189	4.447	20	4
Optical temperature 2	189	4.447	20	4
PMT high voltage	194	4.565	20	4
Channel 2				
Zero data level	5	0.118	40	8
Gain calibrate	182	4.282	40	8
N-PMT temperature	190	4.471	20	4
Regulated +15-V supply	202	4.753	20	4
PMT high-voltage (normal)	145	3.412	20	4
PMT high-voltage when viewing lighted surface of Mars	50	1.177		

The above measurements are from the UVS model on board the M69-2 spacecraft stabilized at an operating temperature of +70°F. Little or no UV data is expected on channel 1 at the time that the UVS limb detectors are excited; therefore, the limb data is transmitted on this data channel. When the lighted limb of Mars is first viewed by limb detector 2, a 50-ms pulse is transmitted on channel 1 (10 data readouts); a 90-ms pulse is transmitted when the lighted limb is first viewed by limb detector number 1 (18 data readouts). The amplitude of either pulse at the channel 1 A/PW input is 2.5 V (a decimal number of 107). The time difference between the two pulses is translated into the orientation of the UVS field of view relative to the Martian limb. The logic in the UVS is such that all other channel 1 data and measurements are automatically muted during the transmissions of limb data pulses. All the while that either or both of the limb detectors view the lighted portion of the Martian disc, the high voltage across the 541N photomultiplier sensor (channel 2) will be held at about 1100-V (tube current gain of about 10^3). The N-tube high voltage otherwise will be held to about 1800 V, having a current gain of 10^6. All high-rate, quick-look spectrum plots are available from recorded data tapes. Recorded magnetic tapes of the high-rate data will be used for data reduction and processing.

The flight telemetry subsystem (FTS) channel 416 engineering temperature transducer is mounted on the UVS cable trough bulkhead, approximately in the middle of the X and Y axes, just beneath the platform thermal-control louver panel. This measurement is transmitted directly by the FTS during cruise and encounter modes. The predicted temperature at encounter is about +30°F.

2. *Physical.* The UVS maximum power consumption from the spacecraft 2400-Hz supply is 15.0 W. The power factor is 0.96. The used power in the UVS is distributed as follows: sensor electronics (including high-voltage power supplies), 7.0 W; logic electronics, 3.7 W; grating drive motor, 4.1 W; motor drive electronics, 0.2 W. The UVS is not fused; however, an instantaneous current limiter is employed between the spacecraft supply and the UVS power transformer. A 5-μF Mylar capacitor is connected in series with one side of the 2400-Hz power line as a precaution to prevent passage of a dc component in the event of a piece-part failure on either side of the capacitor. The current limiter prevents an excess of 150% current increase for any condition within its response time of 1 ms. The UVS power turn-on current transient is from 120 to 200% above the static current level for a period of about 10 μs.

During the cruise mode, science (including the UVS) power is not applied. In order to keep the shrouded science instruments warm enough for power turn-on, cruise mode electrical heaters are used in these instruments. The UVS electrical heater consists of three parallel-connected resistors, located appropriately in the UVS for proper heat distribution, that consume 12.0 W of power from the spacecraft 2400-Hz supply.

The total instrument weight of each UVS model delivered varied between 34 lb 2 oz and 35.0 lb, the

difference being in component parts and potting materials. For example, the packaged weight difference between phototube sensors alone may vary as much as 100 g. An active thermal-control louver panel is attached to the UVS surface as shown in Fig. 9. The science platform aluminum-mylar thermal blanket is solidly attached to the perimeter of the louver panel.

B. Design

1. Electrical. Refer to the block diagram shown in Fig. 10. Two PMTs are used to view the monochromator output. Each PMT has a similar high-voltage power supply, integrator amplifier, and analog-to-pulse width converter (A/PW). One PMT is an EMR type 541G, having a lithium fluoride window and a cesium iodide photocathode capable of viewing the spectrum from 1750 to 1900 Å in the first order and from 1050 to 1900 Å in the second order. The other PMT is an EMR type 541N, having a sapphire window and a bialkali photocathode capable of viewing the spectrum from 1900 to 4350 Å. Each PMT is packaged with its dynode resistors in a stainless steel can, vacuum-filled and vacuum-cured with Stylgard 183. Concentration of dielectric fields about the PMT within the packaging container is minimized.

The output of each PMT is fed to an integrating polystyrene capacitor of about 10^{-9} F, having a useful signal voltage storage range of approximately 200 μV to 50 mV. The capacitor is reset by a field-effect transistor (FET) switch initiated by the DAS A/PW read command once every 5 ms, appropriately delayed by the UVS logic. The integrating capacitor output voltage is buffered from the following sample and hold circuits by a high input impedance FET source follower operating at about unity gain and having a low output impedance.

Since unknown dc offsets may occur to disturb the true data level, the output of the FET source follower is capable of being switched with FETs to two separate data hold circuits. With appropriate FET switching signals from the UVS logic, one hold circuit captures the minimum integrator voltage charge (data zero level) for a given data point; the other hold circuit captures the

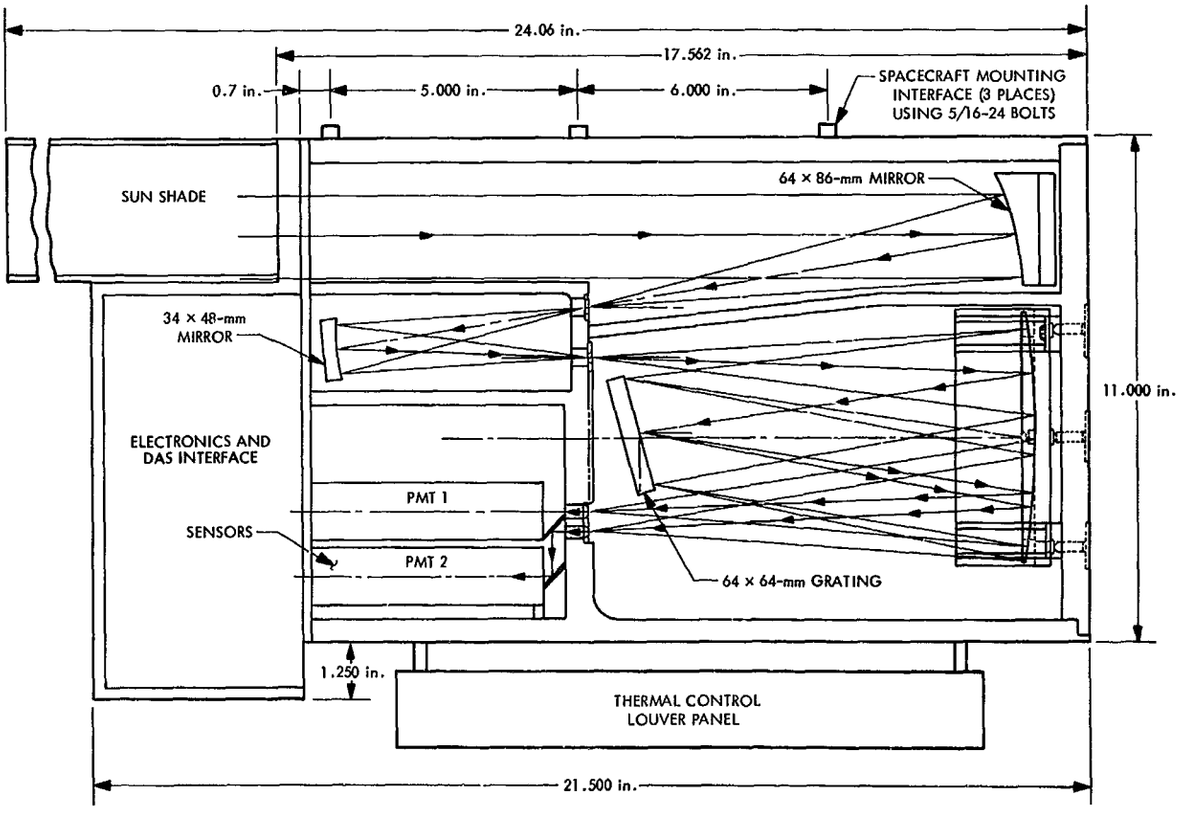


Fig. 9. Ultraviolet spectrometer, physical configuration

maximum integrator voltage charge for the same given data point. The output of each hold capacitor is fed to separate operational amplifiers, the difference in output voltage being the true data amplitude referenced to circuitry common returns. Then the true data amplitude is switched with an FET by UVS logic command to store and hold this data level until sampled by the DAS. An additional operational amplifier is used to isolate and buffer the DAS A/PW from the last data storage capacitor.

Each PMT has a separate identical high-voltage power supply. Since PMT current gains are not necessarily identical, the high-voltage converters are driven by a high-voltage control amplifier to preset the high voltage to the required level of ultraviolet sensitivity. The control amplifier for the 541N PMT supply requires an additional input from either planet limb sensor to increase the dynamic range of that data channel. When the limb sensor detects the abrupt increase in light level, as the bright limb of Mars comes into the UVS view, a logical voltage is applied to the control amplifier driving and holding the N-PMT potential to about 1100 V and reducing the PMT gain. The 541N high voltage returns to about 1800 V when both limb sensors view the dark side of Mars.

Circuit logic is used in the UVS to gate the analog data FET switches with the appropriate timing using the DAS A/PW read commands as the reference. In addition, the grating fiducial initiates UVS logic to insert three UVS temperature transducer outputs (scale-down high-voltage readings, analog electronic calibrations, and amplifier drift status) into the two analog data channels during the flyback time (180 ms) of the scan grating. The fiducial logic also provides the DAS with a transformer isolated 10-μs signal to synchronize the DAS for the selection of the Lyman-alpha resonance line at 1216 Å for real-time transmission. The planet limb sensors alignment data is inserted into the analog-G data channel at the time the UVS views the Martian limb. The low-voltage power supply provides low bus voltage to electronic circuits; the ±15-V supply for the A/PWs is regulated to a minimum of ±10%. The supply also provides synchronizing signals for the grating drive motor. The power supply operates from the spacecraft power of 100-V, peak-to-peak 2.4-KHz square wave over the parameter variation requirements specified.

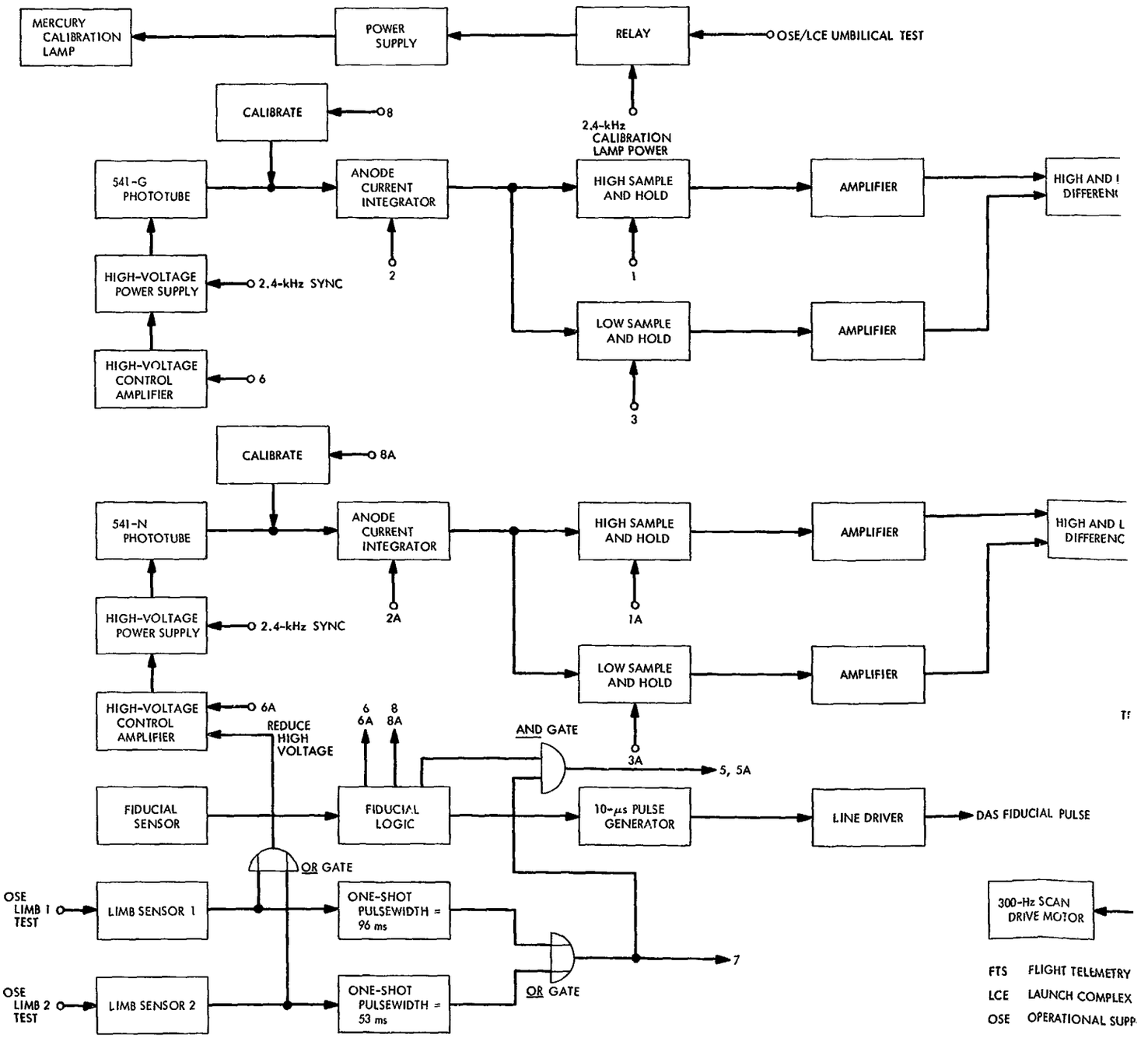
2. Mechanical. The mechanical portion of the UVS instrument consists of a chassis, optical mirrors, optical scan grating, scan drive motor, scan drive mechanisms, light baffling, planet limb detectors, and temperature sensors. The chassis is machined from a block of aluminum and contains the remaining mechanical portions of the UVS. Figure 9 shows the physical configuration of the instrument.

The optical axis of the ultraviolet spectrometer is offset from the TV line-of-sight at an angle of 3.0 ±0.3 deg in cross cone and −11 ±0.3 deg in cone. These angles are known to ±0.1 deg. This offset is designed to provide the maximum overlap between the TV-A and the UVS, and to satisfy the requirement that the UVS viewing axis be greater than 1000 km above the Martian limb when the near-encounter data recording is initiated.

The instrument has an unobstructed view of the planet and will image a portion of the planetary limb that is 0.04 by 0.004 rad of arc onto the entrance slit of the spectrometer. The image of the slit in space 100 km above the planet surface should be parallel (within ±3 deg) along its length to the tangent-to-the-planet surface at the subimage point.

In order to minimize stray light, a sunshade and baffle assembly, which restricts the field-of-view at the primary mirror to approximately 1 deg, is included as part of the instrument. The wavelength scan grating is ruled with 2160 lines/mm. The grating is rotated by a spring-loaded cam follower and a motor-driven cam. The cam is contoured so that one nearly linear wavelength scan will be 2.82 s in duration with approximately 0.18 s to return the grating to the begin-scan position. The grating wavelength position is identified and mechanically indexed with a fiducial wheel.

The grating cam is driven by a 300-cycle, 2-phase synchronous motor with a 300-cycle, 34 V, peak-to-peak square wave derived from the 2.4-kHz UVS power supply via a divide-by-eight counter. The motor speed is 9000 rev/min and drives a 18:1 planetary gear reduction assembly to provide a rotational speed of 500 rev/min. The motor and gear assembly is enclosed in one sealed housing, employing a sealed bearing at the output of the speed reducer. The output of the motor speed reducer is connected to a planocentric drive assembly having a 25:1 speed reduction and providing a rotational speed of one revolution per 3 s to the grating cam. A bellows is employed between the planetary gear assembly and the planocentric drive to contain bearing lubrication. A ball check valve, a filter, and a vent line are attached



FOLDOUT FRAME

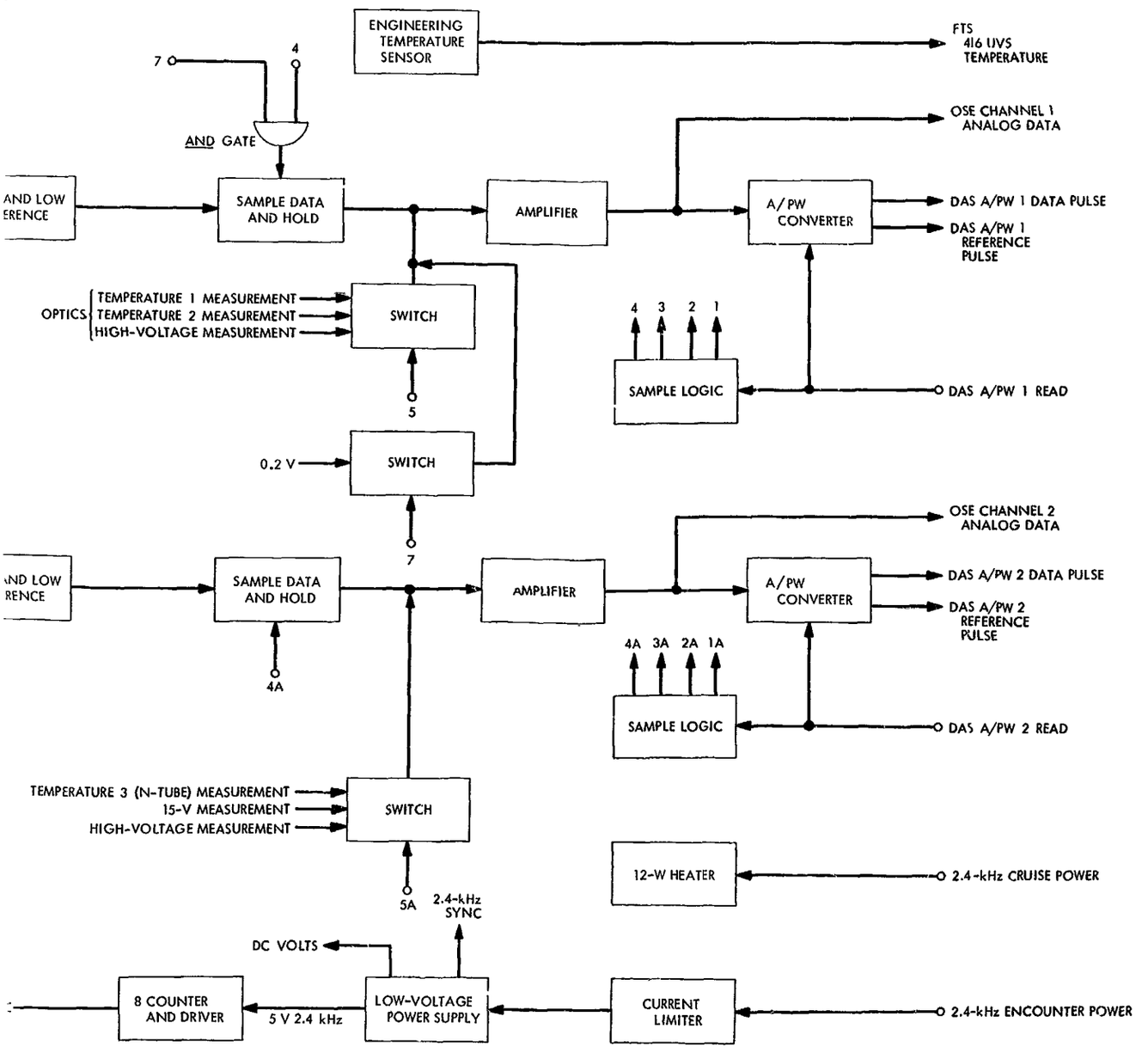


Fig. 10. Ultraviolet spectrometer, functional block diagram

FOLDOUT FRAME 2

to the motor case to relieve pressure differential strain on the bellows. The ball check valve is designed to close at 1.0 psia. As a precaution to the venting of contaminants, a porous bronze filter is used in the vent line to prevent the escape of any lubricating oil. The scan drive assembly has successfully completed operating 2500 h (75 million bellows revolutions) in a vacuum environment.

C. Design Development

1. Electrical. The original design required the use of an ultraviolet stimulus mounted inside of the UVS near the aperture. The stimulus was a low-pressure mercury argon penray lamp. The lamp was to have been operated remotely from the launch complex equipment via the launch pad umbilical cable. It was found that the lamp ignition time was lengthy, taking as long as 20 min. Because the lamp had been in darkness for a long time, the lamp gas took a long time to ionize. Later, it was proven that the stray light, due to the physical presence of the lamp, caused the field of view to be excessively large. As a result, the stimulus lamp was removed from the UVS. The TV stimulus, attached to the shroud, easily excites the UVS 541N sensor. This, along with UVS engineering measurements present in the normal high-rate data, permitted adequate on-pad tests.

Initially, the scan motor drive voltage was ± 12.5 V. This voltage was originally set low to keep the UVS power consumption low. However, the operating torque was too close to design margin. To overcome this difficulty, the operating voltage was increased to ± 17.0 V, increasing the overall UVS power consumption from 13 to 15 W. The motors were subsequently screened at ± 24 V (operating temperature at ± 24 V is 0.9°F higher than that measured at ± 12 V). All other affected components were designed to operate well above this new voltage and current levels.

When the flight units were fabricated, it was found that because of excessive inductive ringing of the fiducial signal, multiple fiducial markers appeared. This anomaly created multiple UVS engineering measurements per scan cycle and caused the DAS Lyman-alpha data counter to reset to zero during the accumulation process. It was found that the magnetic field of the fiducial magnets in the flight units was about 5 times greater than the earlier proof test and prototype UVS models. To correct the problem, a 9-Ω swamping resistor was connected in shunt with the magnetic pickup inductor, reducing the undesirable ringing amplitude below the fiducial logic threshold.

2. Optical. The preslit was changed from 3×10 mm to 3×12 mm to decrease the sensitivity to mechanical disturbance. Lengthening the slit did not degrade spectral resolution. The monochromator exit slits were changed in length only. Both slit lengths were originally 0.394 in. One was changed to 0.315 in. and the other to 0.472 in. This was done to allow the ultraviolet light to cover nearly the maximum diameter of the phototube photocathodes. The fields of view of the original limb detectors were found to be too broad. A two-element lens system ahead of each phototransistor detector replaced the one-element system. The measured results proved satisfactory.

3. Mechanical. The original phototube anode lead (single-conductor coaxial cable) broke loose within the phototube package during environmental vibration tests. Changing the design of lead attachment solved the problem.

The light baffle assembly was acoustically too noisy during environmental vibration tests, causing the shake table limiters to abort the tests. Changing the light baffle assembly snubber attachment design reduced baffle noise to an acceptable level.

The scan drive unit required some redesign. The original bellows material was too brittle and would rupture during environment vibration tests. The material was changed to pure nickel. This solved the vibration problem; however, in a vacuum environment, the bellows would overexpand owing to the pressure differential. This latter problem was solved by employing a pressure relief valve for the bellows. The valve was set to close at 1 psia and to outgas rapidly above 1 psia. The 1-psia bellows pressure is maintained to contain internal lubrication (vapor pressure of the lubricant is well below 1 psia).

The original harmonic drive (scan drive output speed reducer) was unsuccessful because of mechanical binding. The required minimum tolerances could not be maintained during manufacture. The harmonic drive assembly was replaced with a planocentric gear assembly. Later, the planocentric needle bearings became cocked relative to the shaft. Cocking increased with wear and eventually bound the shaft. The needle bearing assembly was replaced with one utilizing ball bearings. The new ball bearing assembly required 2½ times less torque (18 oz-in.) than the previous needle bearing. After this modification, there were no further scan drive problems.

PRECEDING PAGE BLANK NOT FILMED

Table 5. Proof test model TA tests

Completion date, 1968	Test	Remarks
3/5	Vibration	Fractured scan drive bellows
3/9	Vibration	Fractured bellows. Phototube anode leads broke at tube termination
3/22	Vibration	This test conducted with flight-type thermal louvers attached. Only anomaly was fractured bellows
4/26	Vibration	DTM tested new bellows design—bellows passed test
8/28	Vibration	Last TA test. Lost one UVS mounting insert. Shaker system could not duplicate expected flight dynamic characteristics
3/23	Pyrotechnic shock	Tested with fractured bellows
4/29	Pyrotechnic shock	DTM tested bellows. Test passed
8/13	Pyrotechnic shock	PTM passed
4/12	Explosive atmosphere	Passed using prototype UVS
3/25	Thermal/vacuum	Channel 2 electrical failure at −40°C
4/7	Thermal/vacuum	For FA duration
9/30	Thermal/vacuum	For TA duration. Passed
8/9	Static acceleration	Passed
8/23	Acoustic	Passed
11/15	Humidity	Passed

Table 6. Flight acceptance tests, flight units

Completion date, 1968	Test	Remarks
	UVS SN 001	
5/14	Vibration	Passed
5/19	Thermal/vacuum	Passed
7/12	Vibration	New planocentric ball bearings used. Motor connector demated during test
7/17	Vibration	Passed
	UVS SN 002	
6/28	Vibration	Cover plate screw came out. UVS mounting bolt loosened during test
6/28	Vibration	Passed
7/2	Thermal/vacuum	Passed
11/22	Vibration	Passed. Retested due to discovery of fractured solder joints. Test included new planocentric bearings
	UVS SN 003	
6/14	Thermal/vacuum	Passed
6/19	Vibration	Capacitor C_1 came loose from circuit board
7/10	Vibration	Passed
11/18	Vibration	Passed. This test used new planocentric bearings.

D. Qualification

1. Subsystem environmental tests. A dynamic test model (DTM) was fabricated using spare parts and simulated masses to be mechanically and physically similar to the PTM and flight units. The DTM was designed for special vibration and shock tests and for qualification of the tests and test equipment prior to exposure of the PTM to that environment. The PTM was subjected to type approval (TA) tests as shown in Table 5. The flight units were subjected to Flight Acceptance (FA) environmental tests shown in Table 6.

2. Subsystem life tests. Two separate tests were performed, one with the UVS PTM and one with the scan drive assembly. The PTM, after completing the TA thermal/vacuum tests, remained in the vacuum chamber for two additional weeks at +70°F. The unit was operated for 5 h per day (70 total operating hours during the 2-week test). The scan drive assembly was vibrated to TA levels in the DTM and then operated continuously for 800 h at ambient temperature and pressure. Afterwards, the scan drive unit successfully operated for 2500 h in a vacuum environment from 10^{-7} to 10^{-9} torr. The cam and cam follower wear were measured to be less than 0.001 in.

3. Systems test anomalies. Testing anomalies were as shown in Table 7.

IV. Television Subsystem

A. Design Philosophy

The television experiment parameters were chosen to best accomplish the scientific objectives within the constraints imposed by the mission profile and the limitations of a practicable subsystem configuration.

These scientific objectives, as set forth in the experiment proposal prepared in 1966, were derived, in part, from two new sources. First, the National Academy of

Table 7. Test anomalies

UVS SN	Date	Spacecraft	Anomaly
Prototype	2/4/68	M69-1	UVS stopped operating for a few min. Cause unknown
Prototype	2/23/68	M69-1	UVS engineering measurement out of spec. UVS temperature too high; dc heater that was to have been disconnected was still connected
UVS stimulus	4/30/68	M69-1	Inverter transistors shorted in stimulus. Improved operating margins
PTM	5/18/68	M69-1	Planocentric bearing frozen. Changed from needle to ball bearings
001	6/20/68	M69-2	Internal stimulus took 12 min to ignite. The stimulus was eventually removed from the UVS
003	7/12/68	M69-2	Double fiducial markers. Fiducial magnet mounted in reverse direction
PTM	3/24/68	M69-2	Gassy N-phototube
003	10/30/68	M69-2	High voltage unstable. Cracked solder joints found
PTM	10/23/68	M69-1	Noisy high voltage. Poor solder joint
001	7/25/68	M69-3	Double fiducial marker due to foreign magnetic material on fiducial magnet
003	1/15/69	M69-4	Analog operational amplifier offset drifted out of tolerance Amplifier board replaced with PTM amplifier. SN 003 amplifiers replaced with nonflight-acceptable amplifiers and placed in PTM UVS. M69-4 is the spare; was not flown.

Sciences Summer Study of 1965 included a section on Mars entitled "Recommended Priorities in the Early Stages of Investigation." Secondly, the *Mariner IV* television experiment produced new scientific information about the planet which led to a concentration of scientific objectives for future planetary photographic explorations.

The NAS study cites a "photographic three-color reconnaissance of surface and clouds" as of being high priority. In addition, it cites as a specific objective "the identification and classification of major physiographic and surficial features of the planet, including a distinction between permanent and variable surface features over a significant fraction of the planetary surface. Particular attention should be paid to determining differences in environmental conditions from place to place." Photographic exploration of the planet, particularly combined with boresighted, high-sensitivity infrared radiometry to determine surface temperature, is the most promising way to accomplish the identification and classification of the major surficial features of the planet and also to help determine the differences in environmental conditions from place to place.

The *Mariner IV* TV experiment indicated that Mars has a more lunar-like surface than many people had thought was the case before the experiment. However, it left open two very important questions which are directly pertinent to the future biological explorations of the planet. First, is the present surface the result of a more or less steady-state condition that has prevailed for a very long period of time? Or is it the most recent in an episodic history which may have included at one time a much denser atmosphere, perhaps including liquid water on the planet itself? Secondly, what is the difference between the light and dark areas of Mars which undergo seasonal transitions in albedo and, possibly, also color?

These aims and questions combined with the general objective of overall scientific exploration with special emphasis on biological exploration led to the establishment of the scientific objectives for the 1969 Mars flyby. These objectives were: (1) to determine the general physiography over much of the planet at a resolution significantly better than that obtainable from the ground and to topographically categorize the basic light and dark areas and perhaps learn more about why they undergo seasonal variations, (2) to further explore, both geographically and in resolution, this unknown planetary surface for additional clues as to its origin, and, (3) to obtain sufficient coverage at a suitable resolution to distinguish, on the basis of crater morphology and other criteria, between and episodic and a continuous history.

In addition to establishing the scientific objectives for the experiment, the experiment proposal further defined an instrument configuration. Very simply, the configuration proposed, and that which ultimately was developed, consisted of a wide-angle, medium-resolution camera, a companion narrow-angle, high-resolution camera, and a common set of supporting electronics exclusive

of a data storage system. In order to effect a set of specific hardware performance requirements, the scientific objectives were translated into engineering rationale.

Translated into specific terms which were applicable to the functional design of the television instrument, the scientific objectives, as stated above, implied the following requirements:

(1) The best possible resolution should be obtained with the high-resolution camera.

(2) The signal-to-noise ratio attained in the high-resolution camera should be as high as that in the *Mariner IV* pictures, under similar Mars brightness conditions, but not significantly higher at the expense of geometric resolution.

(3) Consecutive wide-angle pictures must overlap sufficiently to include the narrow-angle pictures within the overlap region to permit correlation of high- and medium-resolution data obtained during encounter. For the same reason, the difference in ground resolution between the wide- and narrow-angle cameras should be a minimum while still permitting the wide-angle camera overlap and the highest possible resolution with the narrow-angle camera.

(4) The total coverage with the wide-angle camera during encounter should be a maximum consistent with the requirement to minimize the resolution difference between cameras.

As a result of tradeoff studies involving mission, spacecraft, and resource constraints, a set of operational and performance requirements was established. These requirements, as implemented in the flight instruments, are set forth in Table 8.

The *Mariner* Mars 1969 imaging instrument was developed under several constraints which had a major impact in terms of influencing the design configuration that ultimately evolved.

The data received from *Mariner IV*, which photographed Mars on July 14, 1965, had significant impact relative to the handling of the video information within the instrument. In particular, the *Mariner IV* data indicated that the Martian surface was of low contrast on the order of 2:1 within each picture that was obtained. To observe more clearly the surface feature detail, the instrument was designed to enhance the scene contrast by increasing the percent modulation of the video signal by a factor of 3. The slow variation in the contrast of Mars further allowed a degree of data compression which was accomplished by transmitting the two most significant bits (MSB) of the digital video data over a time-sampled telemetry channel. Their periodic return to earth resulted in only a small compromise in data accuracy during the image reconstruction process.

Table 8. *Mariner* Mars 1969 TV experiment requirements

Parameter	Wide-angle camera	Narrow-angle camera
Closest approach altitude, km	*Mariner VI*, 3500 *Mariner VII*, 3200	*Mariner VI*, 3500 *Mariner VII*, 3200
Closest approach velocity, km/s	7.5	7.5
Optics aperture, mm	9.55	216
TV line density, TV lines/mm	73.3	73.3
Smear (min), m	675 m	45
Effective focal length, mm	52.5	508
Best ground resolution, m/TV line (0.7 Kell factor)	1110	115
Focal ratio	5.5	2.34
Optics transmission number	6.36	3.85
Exposure time, ms	90 and 180	6 and 12
Number of lines/frame	704	704
Number of active elements/line	945	945
Image size, mm	9.6 × 12.5	9.6 × 12.5
Coverage at closest approach (nom), km	*Mariner VI*, 840 × 975 *Mariner VII*, 760 × 890	*Mariner VI*, 84 × 95 *Mariner VII*, 76 × 85
Overlap at closest approach, %	*Mariner VI*, 13 *Mariner VII*, 12	None
Field of view, deg	18 diagonal	1.8 diagonal

At the outset of the imaging instrument development, the tape recorder technology precluded consideration of space-qualified digital recorders with storage capacity in excess of approximately 2.3×10^7 bits. The need to store data in excess of these limits resulted in the use of both an analog tape recorder to achieve a high-storage capability and a digital tape recorder to store precision digital video data. This compromise configuration represented the optimum storage capacity with the constraints dictated by the technology available at the time.

The instrument data handling philosophy was heavily influenced by the computer-oriented image-processing capability of the Image Processing Laboratory (IPL). As a result of the capability, greater liberties were taken in terms of simplifying the instrument video processing requirements, thereby placing the demands on the ground processing facilities to achieve the sophistication in image reconstruction.

The process of implementing the functional description by translating the functional design into actual hardware commenced in December 1966. At this time, a contractor was engaged to assist JPL in the detail design of the electronics aspects of the instrument. JPL retained the total responsibility for, and cognizance of, the optics and shutter designs as well as the selection, procurement, and test of the vidicon image sensors.

The hardware requirements called for the development of a breadboard model, a prototype model, a type approval model, a proof test model (PTM), and three flight models. Resource limitations midway in the program resulted in the elimination of the type approval model, with the PTM then being required to serve this function in addition to its original role.

In addition, two developmental models of the television instrument were fabricated to aid in certain investigative efforts related to the spacecraft performance. In conjunction with the JPL Engineering Mechanics Division, a structural test model (STM) was fabricated to serve in assessing the structural integrity of the spacecraft. A thermal control model (TCM) also was developed in conjunction with the Engineering Mechanics Division, which provided a unit which was thermally equivalent to the flight models. Tests conducted with the TCM spacecraft allowed a determination of temperature conditions throughout the spacecraft and the television instrument as a function of the mission profile.

The development schedule governing the design, test and fabrication efforts is shown in Table 9.

As a result of a delayed commitment to a detail design, which in turn created parts procurement delays, coupled with management and manufacturing difficulties, the delivery of hardware including the flight units was late.

It is significant to note that the prototype experienced a 5-mo delay in delivery. As a result, the prototype evaluation effort was insufficient in terms of time, thus precluding a thorough determination of design deficiencies.

Table 9. Television unit development schedule

Unit	Completion	
	Required	Actual
Prototype	3/8/67	8/25/67
Proof test model (PTM)	12/15/67	2/28/68
Thermal control model (TCM)	8/30/67	11/15/67
Flight unit 1	3/1/68	5/17/68
Flight unit 2	3/15/68	5/24/68
Flight unit 3	4/1/68	6/21/68

The consequence was that design deficiencies were not determined until much later in the program, when the time required to institute corrective measures critically impacted both the spacecraft schedule and the instrument subsystem tests and calibrations.

Concurrent with the contractor-assisted electronics design and breadboard fabrication, an optical design study, as well as a vidicon selection activity, was pursued by JPL. The optical design study concluded that, for the narrow-angle camera, a refractive system would exceed the weight allocation whereas several reflective designs appeared possible. Two optical designs were pursued through the engineering model stage. An equal-radii Schmidt–Cassegrain system was developed by JPL, with a contractor undertaking a catadioptric design utilizing Ross correctors. While both units met the optical requirements, the contractor-developed unit exceeded the weight limitations and the cost constraints for the flight units. The JPL design was used in the final instrument configuration.

The sensor selection effort involved the test and evaluation of several GEC-type slow-scan vidicons, with photoconductors similar to that used on *Mariner IV* but utilizing an all-magnetic electron gun. Based on the evaluation of these vidicons employing variations in photoconductor compositions, a GEC type 1342-010 was selected for the final instrument configuration.

The contractor concluded the phase I portion of the subsystem contract with the successful completion and delivery of the prototype model television instrument and three units of bench checkout equipment (BCE). The contractor expended approximately 48,000 engineering man-hours developing the prototype design, including all designs and drafting related to packaging the bus electronics. All electronic components for the prototype

were supplied by the contractor. JPL supplied certain major components of the BCEs since such components were available from the *Mariner IV* television development effort. All remaining BCE components were supplied by the contractor.

Phase II of the subsystem contract provided the PTM and three flight models. The contractor had the total manufacturing responsibility for the bus electronics, whereas JPL built and tested all optical systems including shutters. These optical systems were installed on the instrument after the instrument was delivered by the contractor. JPL supplied all screened components to the contractor for the manufacturing process and provided resident engineering personnel to support the manufacturing effort.

The flight vidicon procurement responsibility was retained at JPL, the sensor being installed in each instrument following its delivery to JPL. Test activities at the contractor's facility were thorough but necessarily limited, inasmuch as the vidicon and optics were installed at JPL. The contractor conducted tests which completely characterized the bus electronics and certain elements of each camera head as a function of temperature.

The subsequent test and calibration activities included all environmental tests related to both flight acceptance and type approval test activities as well as all tests conducted with the instrument on the spacecraft. Additional information pertaining to the test activities as well as the calibration efforts are discussed in subsequent subsections.

B. Major Development Problems

The *Mariner* Mars 1969 television instrument experienced some rather significant problems during the course of the development and test activities. While not the direct cause of these problems, the fact that the instrument design effort was initiated at such a late date relative to the hardware delivery requirements created a condition wherein the effect of the development problems was compounded in light of the short time available for investigation and corrective action. The impact of those problems is exemplified by the fact that a special engineering group was formed in July 1968 for the express purpose of investigating and correcting the major design deficiencies existing in the instrument at that time.

Development and development-related problems which can be termed significant in the evaluation of the instrument and are worthy of note and comment in this report were experienced in the following areas:

(1) Circuit design review.

(2) Integrated circuits.

(3) Contractor manufacturing capability.

(4) 2N4044 transistors.

(5) Wide-angle shutter.

(6) Light source RFI damage.

A detail design review was conducted in January 1967 to assess the adequacy of the instrument design prior to proceeding with the prototype and PTM fabrication. A number of specific recommendations resulted from the review, including a recommendation for a thorough circuit review. While certain specific circuits were critically analyzed subsequent to the review, the development schedule, coupled with the existing manpower, precluded the required comprehensive circuit analysis. Those design deficiencies which subsequently developed and which could have been corrected had a comprehensive review been conducted are as follows:

(1) Camera gain sensitivity to potentiometer value changes.

(2) Phase shift of 18.9-kHz carrier at high luminance levels.

(3) Dark current clamp inadequacies.

(4) Requirement for μA709 input limiting.

(5) Susceptibility of planet-in-view (PIV) circuitry to switching transients.

(6) 2N2920 overstress in dc restorer application.

(7) Improper AGC gain setting resulting in inadequate AGC control range and improper operation by the cuber.

(8) "Latch-up" susceptibility of μA709 operational amplifiers.

(9) Excessive turn-on power dissipation in power supply 2N3251 transistors.

The deficiencies noted above, along with others of a lesser nature, were identified as a result of the instrument testing program and ultimately rectified. However, the overall impact on schedule and flight hardware rework required to accomplish these corrections introduced

undue risk to the spacecraft test program and diminished the hardware reliability to some undetermined degree.

Each television instrument incorporated a total of 384 Fairchild integrated circuits (ICs) distributed by part type as follows:

IC type	Quantity
6040	276
6041	91
6042	17

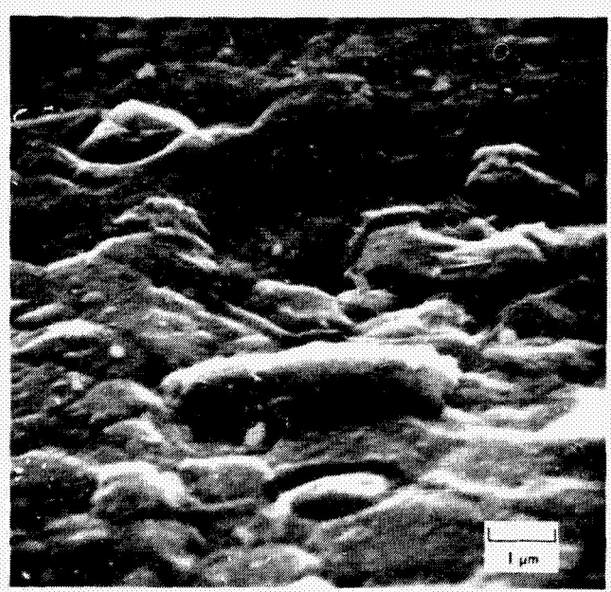
In September 1967 a total of 2244 units (1599 6040s, 536 6041s, and 109 6042s) were procured by JPL for use in the TV control and data converter subassemblies. These devices were screen-tested by Fairchild in accordance with the JPL specification.

As a result of multiple integrated circuit failures occurring during the fabrication of the PTM, a major investigation was undertaken. This investigation revealed that the largest percentage of failed devices experienced failure as a result of an electrical open circuit caused by an open metalization at various IC contact windows. A typical example of an open window failure is evident in the photomicrograph shown in Fig. 11. The open window problem was felt to result from improper material gradation at the window step or transition coupled with an improper heating schedule to accomplish the metalization.

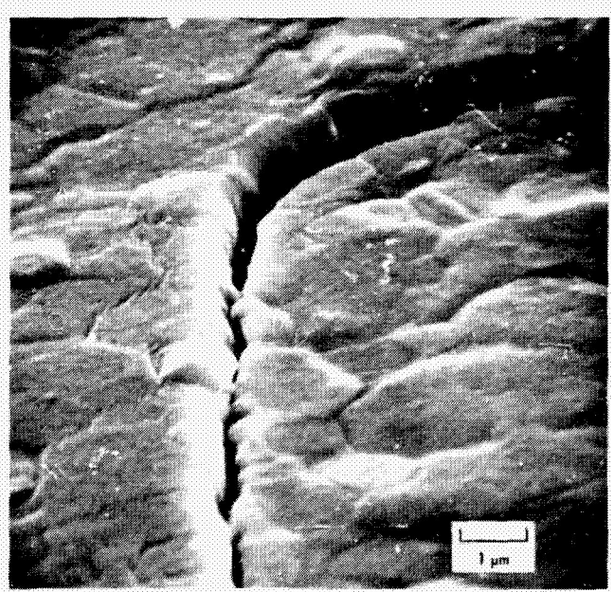
Inasmuch as the integrated circuit failures continued to occur during the flight article fabrication process (failure rate was on the order of 1%) a second set of ICs was procured. All units of this second procurement were subjected to an intensive 100% screening process at Continental Testing Laboratory in addition to the screening at Fairchild. This additional screening involved multiple thermal cycles and extensive parametric measurements. These new integrated circuits were to be retrofitted into the flight units had the failure rate of the devices in the flight units continued beyond the fabrication and initial test activities. Additionally, spare ICs were fabricated into sticks and subjected to a 1000-h life test under thermal cycling conditions.

The integrated circuits in the flight units were not replaced by the devices from the second procurement for the following reasons:

(1) Only one failure of a questionable nature occurred after the initial tests of the integrated circuits.



FAIRCHILD INTEGRATED CIRCUIT PROPER WINDOW METALIZATION (9350×)



FAIRCHILD INTEGRATED CIRCUIT IMPROPER WINDOW METALIZATION (9350×)

Fig. 11. Example of open window failure

(2) The second procurement ICs were termed equal in terms of window metalization to the ICs in the initial procurement. (Time had not permitted the manufacturer to correct the metalization process.)

However, the devices were fabricated into sticks and subjected to all acceptance testing and put on life test at room temperature. No failures occurred during the life test process.

The overall IC investigation yielded the following conclusions:

(1) The greatest failures, all types, occur during thermal cycling (typically −65 to +125°C). Steady-state temperatures do not induce failures.

(2) "Open window" types of failures represented the greatest majority of failures.

(3) Intensive screening was not 100% effective in reducing the "open window" failures in flight devices.

(4) The greatest number of failures following screening, all types, occurred at the first application of power following the stick build process.

(5) There is no evidence to indicate that "open window" failures have a time relationship beyond the stick fabrication and acceptance test phase.

Item 4 implied that some mechanism involved in the stick build process induced some number of "open window" failures. Studies and surveys conducted by two independent groups failed to identify any technique or manufacturing practice that would cause or initiate the "open window" failures.

Future use of integrated circuits will involve 100% screening, including thermal cycling, extensive examination of windows with the scanning electron microscope, and a thorough investigation of all processes involved in the assembly of the devices into sticks or onto printed or multilayer boards.

The manufacturing problems experienced during the early stages of the fabrication phase, particularly with the PTM, indicated a lack of depth in terms of manufacturing processes and techniques on the part of the subsystem contractor. This factor resulted in a several-month delay in hardware delivery, which contributed to the late test and evaluation activities. Considerable effort was spent training the manufacturing personnel on such items as soldering, proper component board cleaning, wire dressing and connector assembly, to mention but a few. Resident JPL engineering personnel were required to maintain the necessary fabrication quality of the hardware.

During the manufacturing of the PTM and the flight units and continuing into the testing phases of these units a large number of 2N4044 transistor failures were experienced. An investigation was undertaken to determine the nature of the failures and to institute corrective action. While the exact failure mechanism was not unquestionably defined, the following factors caused all 2N4044s to be replaced with 2N2920 devices in the flight units on a retrofit basis following the fabrication of the flight units:

(1) Sensitivity of the 2N4044 to damage (a 3:1 degradation of h_{FE} and an increase of base leakage of up to 10,000 to 1) by electrostatic discharge from personnel during handling.

(2) Sensitivity of the 2N4044 to circuit transients due to the limited reverse base current rating and a 10-mA collector current rating.

The replacement with the 2N2920 devices was based on the following factors:

(1) Relative immunity of the 2N2920 to any possible circuit transients due to a 30-mA collector current rating and the absence of a reverse base current rating.

(2) Immunity of the 2N2920 to damage by electrostatic discharge from personnel during handling.

(3) Relative tolerance of the 2N2920 to ball bond deficiencies present in all gold-ball-bonded devices.

Following the replacement process, no failures of the 2N2920s were experienced during any phase of testing including TA level thermal/vacuum qualification tests.

Tests conducted on the television instrument on the PTM spacecraft within the solar simulator revealed a design deficiency in the wide-angle shutter mechanism. This design deficiency was manifested by intermittent shutter operation at elevated temperatures, generally after a substantial number of cycles (20,000 or more) had been accumulated on the shutter.

Subsequent investigations carried out on spare units revealed excessive friction, particularly with regard to the filter wheel bearings and the pawl/latch interface.

After extensive evaluation of potential changes, including mole-sink tests for 100,000 shutter cycles on spare shutters under thermal variations, a series of design changes was incorporated. All flight shutters were retrofitted with the following changes:

(1) The material of the pawl which engages the cog on the filter wheel was changed from anodized aluminum to Delrin AF.

(2) All bearing material in the mechanism was changed from Teflon to Delrin AF.

(3) The latch devices which engaged the cog to prevent over-travel following the shutter actuation were changed from a cylindrical configuration to a T-bar form, which decreased the mass and reduced latch bounce.

(4) The actuating solenoid design was changed to incorporate a core material and case construction which minimized the residual magnetism and allowed a faster plunger release time.

In addition to the above changes, all flight shutters, as part of their calibration and acceptance tests, were subjected to mol-sink tests for a duration of 10,000 shutter cycles. Following the adoption of these changes and test methods no further failures were experienced.

During the course of FA thermal/vacuum testing of the SN 002 flight unit, several malfunctions or anomalies in performance were observed almost simultaneously. Following a thorough investigation it was determined that several small-geometry solid-state devices, including a Fairchild integrated circuit had failed. These devices failed in circuits related to the A/PW commutator, the wide-angle shutter, and the reset function.

It was hypothesized that a voltage transient had induced the failures. Circuit design modifications were incorporated in the affected circuits in order to afford transient immunity. However, subsequent thermal/vacuum tests on the SN 003 instrument resulted in similar failures.

Following another investigation it was determined that the ignitors, used in the xenon light sources which provided the illumination for the optical stimulus, when ignited in the existing ground circuit configuration, introduced large voltage transients on the television ground network.

A program was initiated to filter the igniter circuits for all the light sources and associated power supplies as well as to reconfigure the ground arrangement such that adequate isolation existed between the television ground, the light source igniter ground, and the thermal/vacuum chamber ground. In addition, all turn-on procedures were modified to incorporate precautionary measures to preclude the introduction of ground loops.

Following the incorporation of these changes, no further transient induced failures were experienced.

C. Instrument Description

In support of the visual imaging experiment, JPL developed a television instrument. This instrument design drew heavily on the technology and experience generated during the development of the camera system for the *Mariner IV* mission to Mars as well as those cameras developed for the *Ranger* and *Surveyor* spacecraft.

As an extension of these previously developed technologies for planetary photography, the television instrument for *Mariners VI* and *VII* incorporated both digital as well as analog video data processing to achieve photometric precision and high spatial resolution within the constraints of the storage capacity of the spacecraft tape recorder. This dual-data format, in conjunction with rudimentary data compression methods, combined to form an instrument whose output data format depended totally on a computer-oriented image reconstruction process to achieve the scientific objectives.

This instrument (Fig. 12) consists basically of two separate camera heads each containing a vidicon image sensor, its attendant electronics, and independent optical systems with companion shutter mechanisms. Further, the instrument contains a common set of electronic circuit assemblies which perform the various amplification, conversion, timing, and scanning functions necessary to derive image data in a form suitable for storage and transmission to earth. Companion subsystems to the television instrument are the data automation subsystem (DAS), which provides basic timing, data processing, and general housekeeping functions for all the scientific instruments, and the data storage subsystem. The data storage subsystem consists of an analog tape recorder

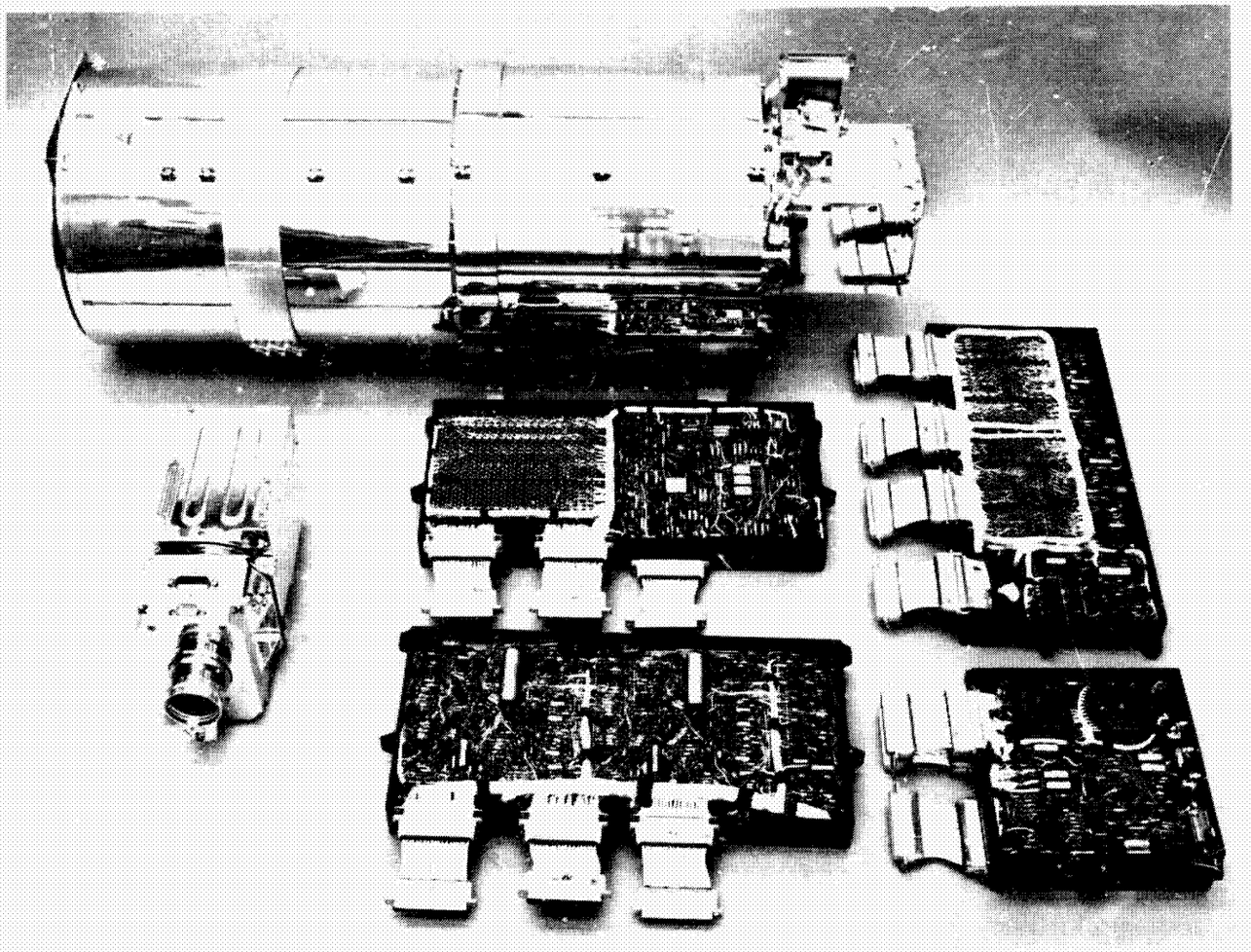
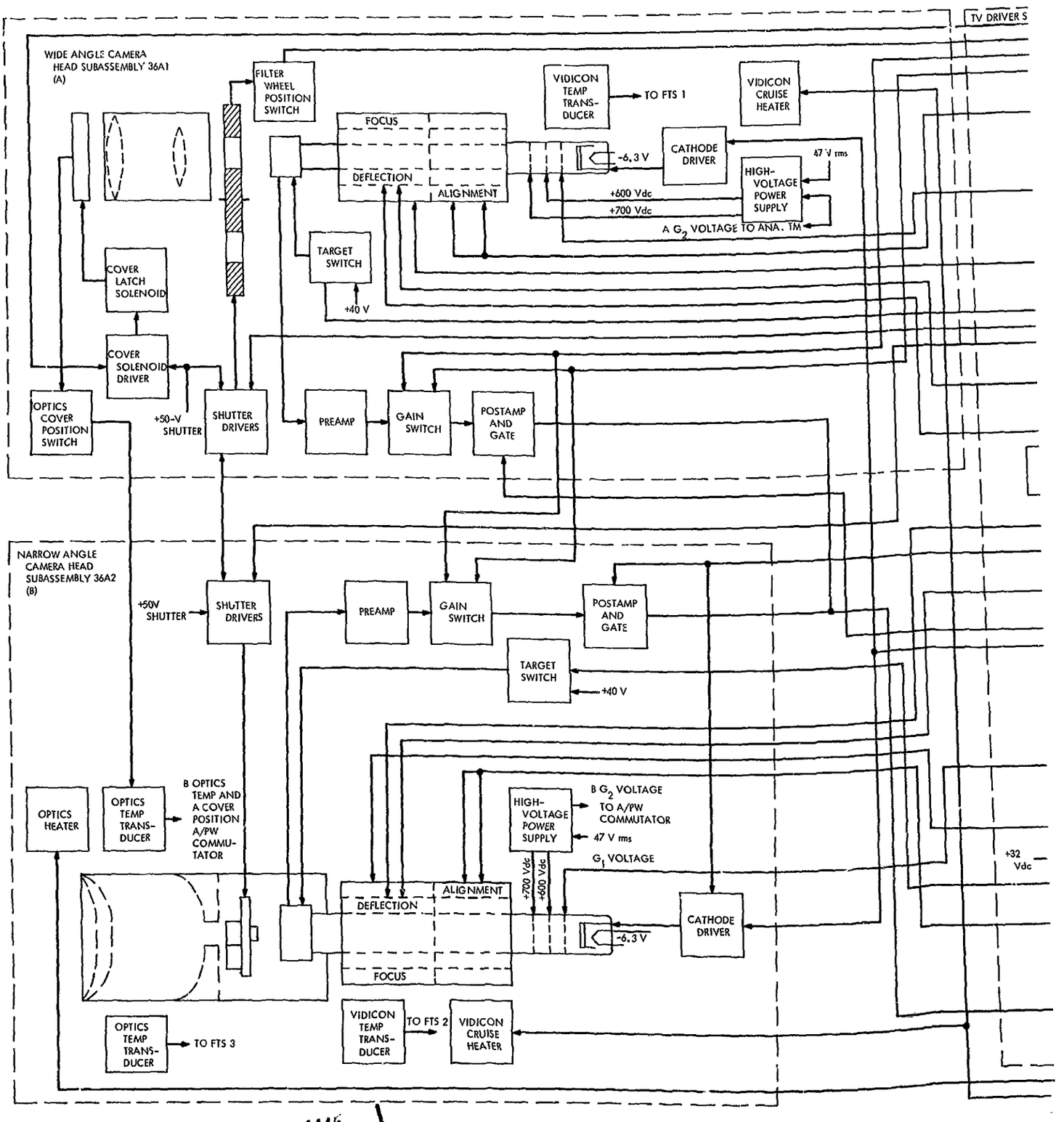


Fig. 12. Television instrument

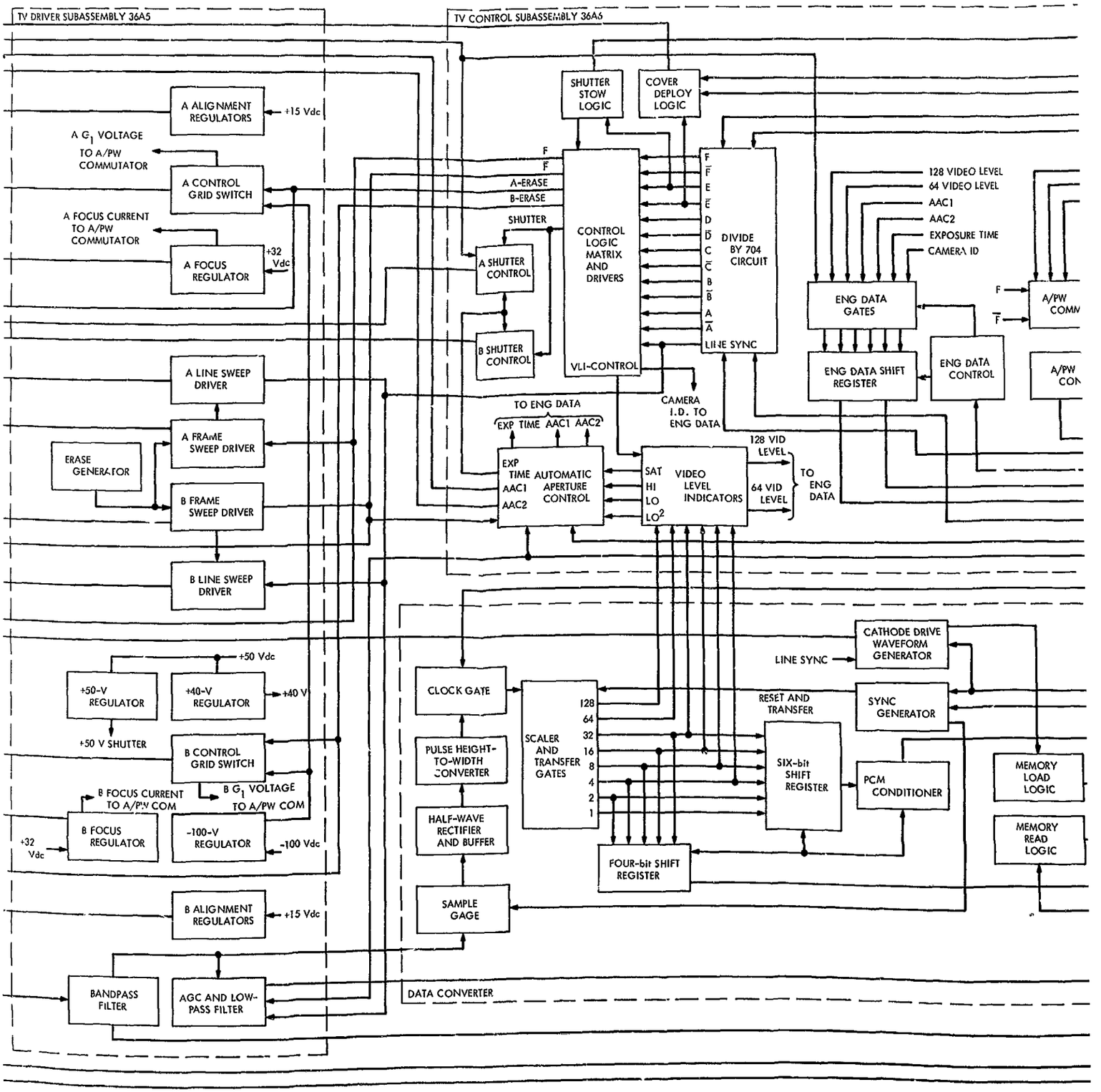
and a digital tape recorder, both of which function to store video data prior to transmission to earth.

1. Functional electronics description. The functional description of the electronics is keyed to the overall system block diagram, which indicates location of function, signal flow, and the various support functions required for systems operation (Fig. 13). For purposes of description, it is convenient to separate the electronics into six major sections: "signal chain," system timing, vidicon control functions, engineering data, power supply, and miscellaneous functions.

a. Signal chain. The function of the components comprising the "signal chain" is to take the image information from the vidicon, process the video signal, and format this signal for recording on a digital recorder (through the DAS) and on an analog recorder, both in the data storage subsystem. The digital data channel samples and records every seventh picture element in each line. It is dc-coupled and preserves photometric information. The format of the digital video picture raster and the format of each digital TV line are shown in Fig. 14. In contrast, the analog channel processes the entire picture for recording on the analog tape recorder. Low-frequency information is suppressed in the analog channel to allow pre-emphasis of high-frequency data. As shown in Fig. 15, one line of recorded data on the analog channel contains analog video information, a pseudonoise and identification code (PN and ID), and a digital memory dump of the preceding line. The digital memory serves to provide a coarse redundancy to every seventh element digital video in the event this



FOLDOUT FRAME



FOLDOUT FRAME 2

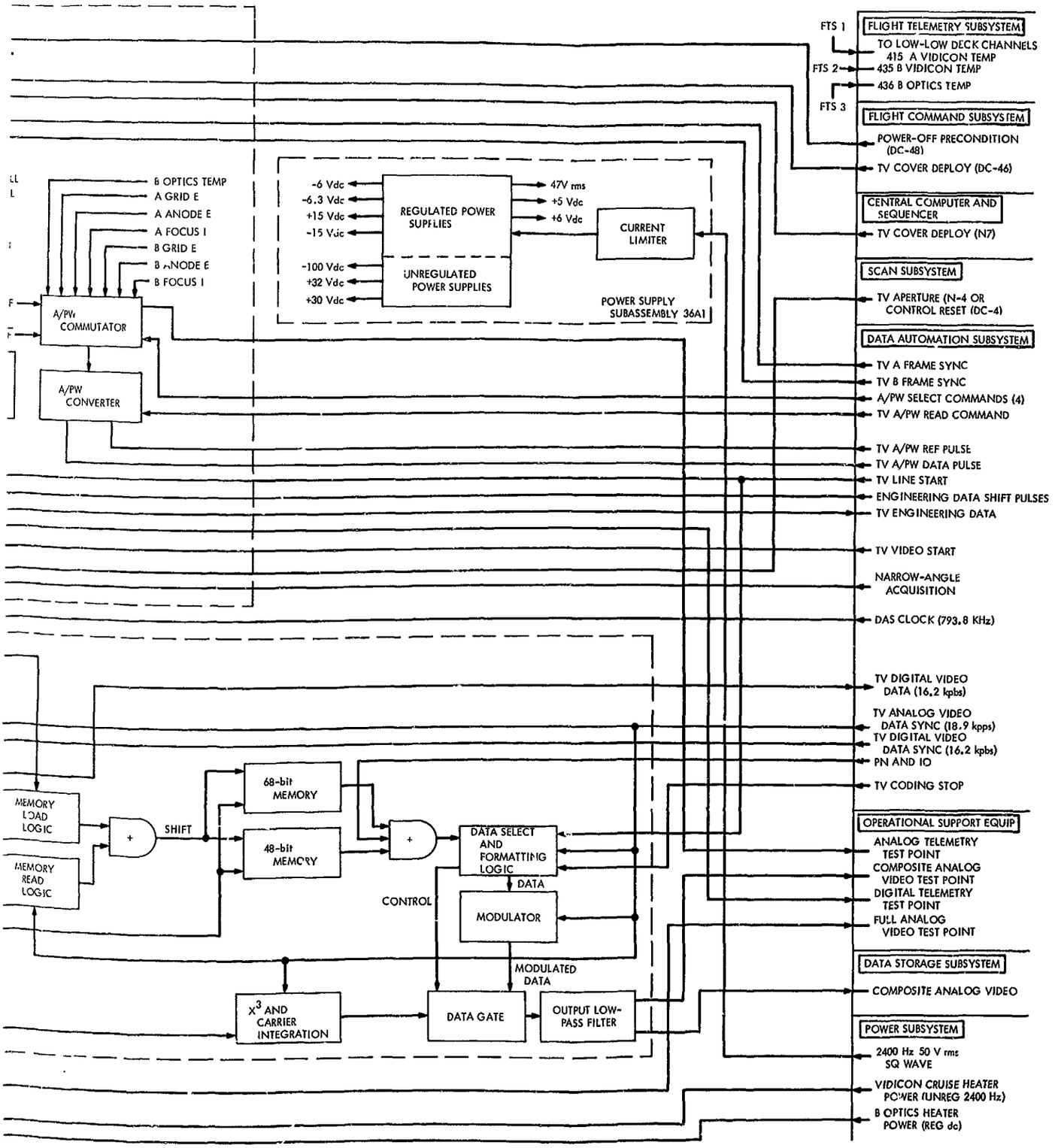


Fig. 13. Television subsystem, block diagram

FOLDOUT FRAME 3

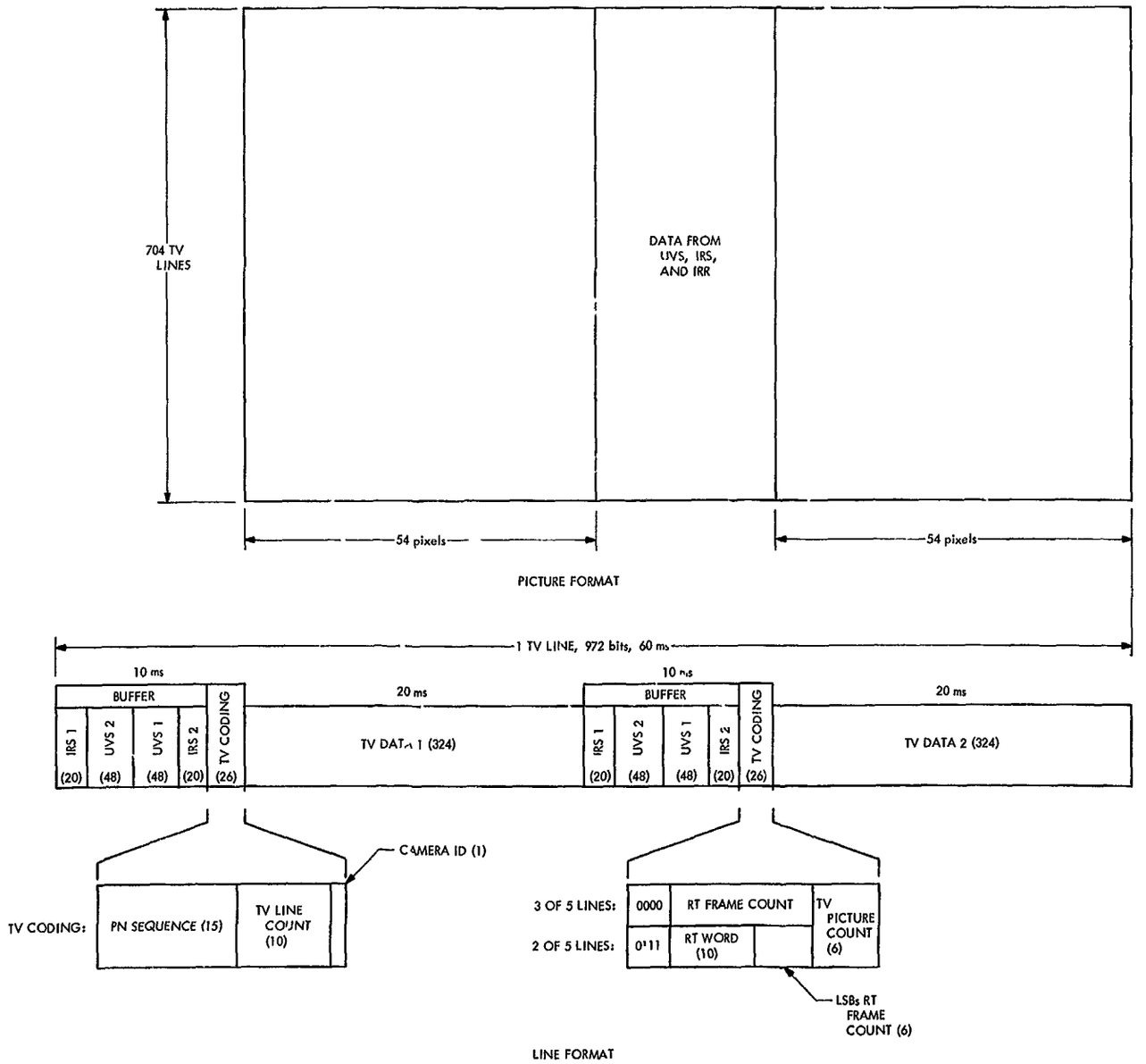


Fig. 14. Digital video line and picture format

PRECEDING PAGE BLANK NOT FILMED

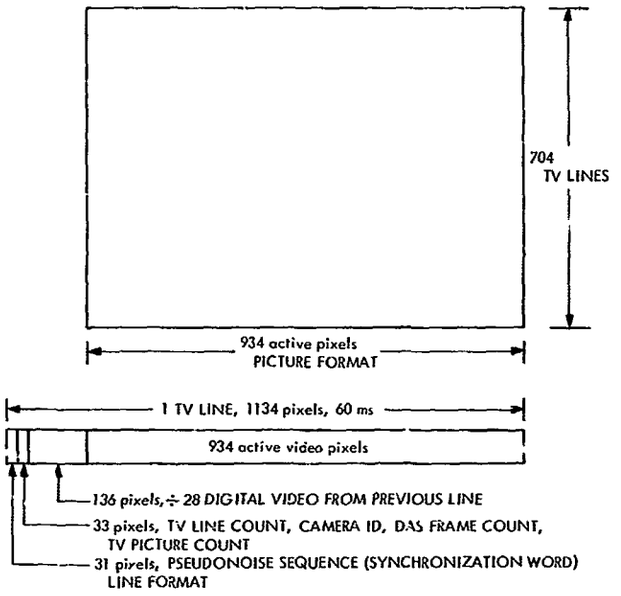


Fig. 15. Composite analog video line and picture format

data is lost on the digital recorder in the data storage subsystem. It further provides data during the middle 20% of each digital TV picture when other science data is being inserted for recording purposes. The digital memory stores a 4-bit representation of every twenty-eighth picture element in each television line. On this basis, each line is represented in the memory by 34 4-bit samples for a total memory load of 136 bits per line.

The automatic aperture control (AAC) circuitry in the near-encounter mode automatically adjusts the signal chain gain by setting the exposure time (shutter speed) and the variable attenuator gain. These adjustments are based on previous picture information. The AAC is considered part of the signal chain since it is effectively a sampled data feedback loop operating within the signal chain.

The "signal chain" is separated into five segments to facilitate its functional description: the camera head signal chain, the signal chain common path, the digital signal chain, the analog signal chain, and the AAC operation.

b. Signal chain, camera head. The camera head signal chain (Fig. 16) takes the vidicon output and amplifies it to a level suitable for transmission to the bus electronics. The signal at the vidicon output is a pulse-amplitude-modulated current signal with a pulse rate of 18.9 kpulses/s. Each output current pulse represents the magnitude of 1 pixel (picture element) and typically has an amplitude of 2×10^{-9} A, full scale. The output pulse rate of the vidicon is controlled by the cathode chopping signal, which is present during the active line read time. The preamplifier presents a virtual ground current summing mode for the vidicon output. It has a 3-dB bandwidth from approximately 1 to 45 kHz and treats the vidicon output like an AM-modulated signal with a center frequency of 18.9 kHz.

The gain switch which follows the preamplifier is controlled on a picture-by-picture basis by the automatic aperture control circuitry. It has four gain states, $A_{00}=0.208$, $A_{01}=0.352$, $A_{10}=0.595$, and $A_{11}=1.00$. Following the gain switch is a third-order low-pass filter which has a 3-dB cutoff frequency of 37.5 kHz. Its primary function is to attenuate harmonics of the 2400-Hz power supply noise, which are higher in frequency than the upper sideband of signal information. Attenuation of this noise is required to minimize cross modulation of signal and noise in the postamplifier.

The postamplifier provides the final signal amplification in the camera head, generating a 4-V, peak-to-peak, full-scale output. Feedback limiting is used around the postamplifier to limit the output amplitude swing. This protection insures that the remaining signal chain electronics operates in a linear mode over the range of input signal conditions.

Following the postamplifier is a unity gain video switch which is switched at the frame rate. Thus, the A camera video switch is on during the A frame and off during the B frame, while the converse is true for the B camera video switch. The video signals from the two camera heads become common on the scan platform and are routed to the common signal chain.

c. Signal chain, common path. The common path signal chain components (Fig. 17) form the inputs to both the analog and the digital signal chains and are located in the TV driver. To improve the signal-to-noise ratio of the modulated signal, the input bandpass filter is incorporated to attenuate signal and noise outside of the desired passband. Only the fundamental carrier with its information-carrying sidebands is unattenuated. The third- and higher-order harmonics of the square wave carrier, together with their respective sidebands which are located outside of the passband of the filter, are therefore highly attenuated.

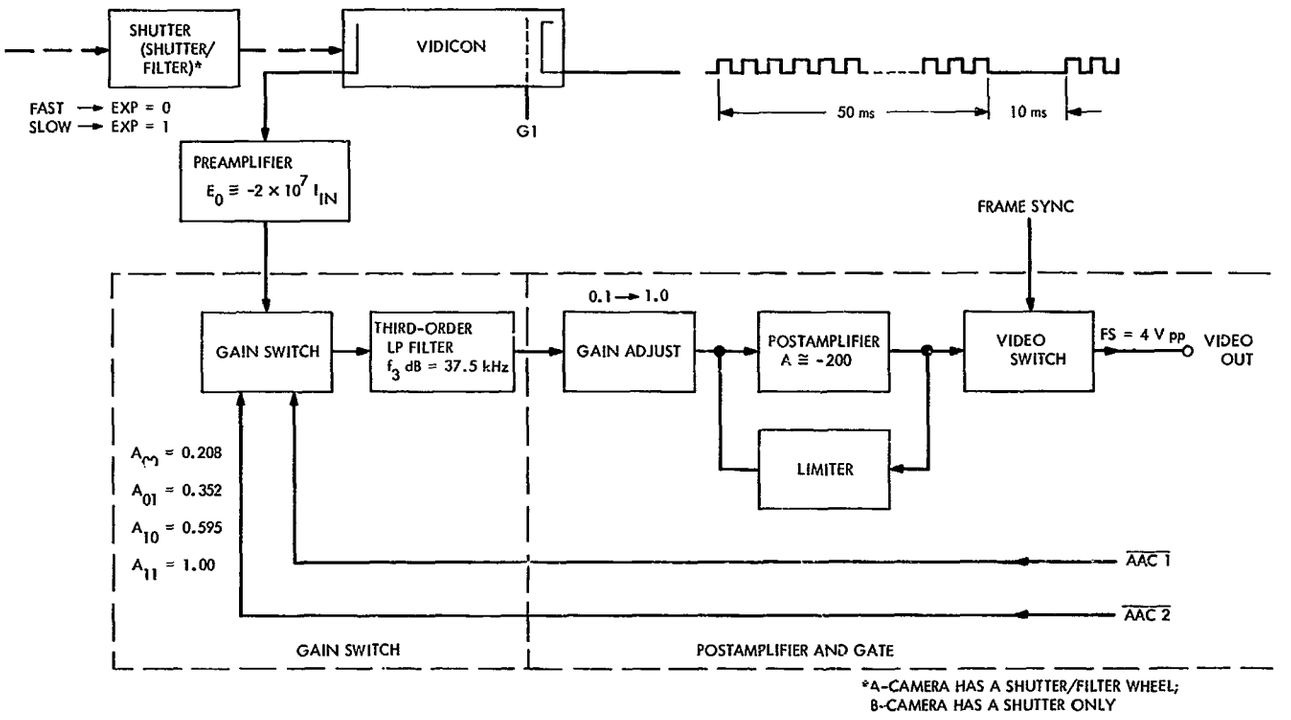


Fig. 16. Signal chain, camera head

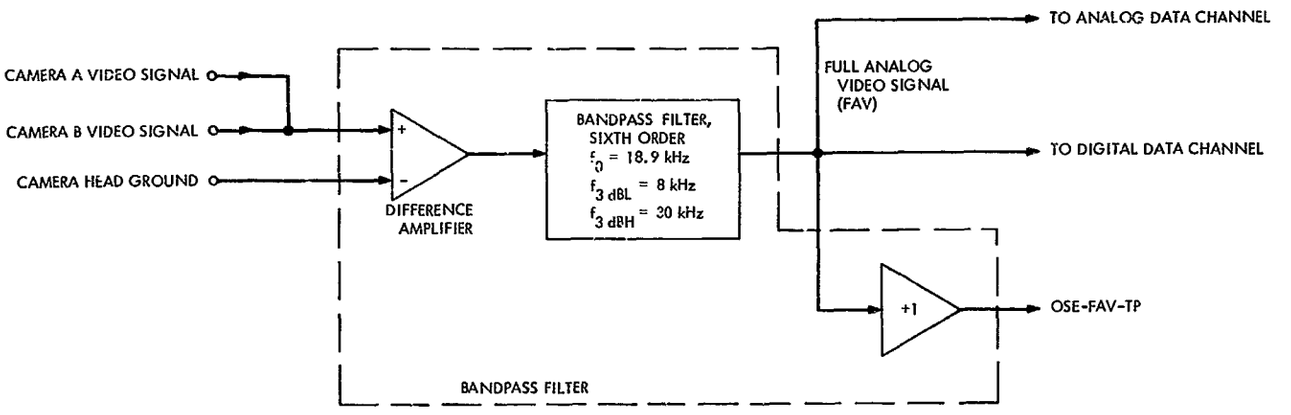


Fig. 17. Signal chain, common path

The output of the bandpass filter is routed to the analog and digital signal chains as well as to an output buffer which drives an OSE test point. This signal is referred to as a full analog video (FAV) signal and is an important reference point in TVS calibration.

d. Digital signal chain. Figure 18 shows that every seventh pixel is sampled by the 2.7-kHz sample rate frequency. Phasing of the cathode chopping signal on the vidicon is adjusted such that a single cycle of 18.9-kHz carrier is selected by the sample gate. This single cycle is then half-wave-rectified with the positive half of the cycle going into a pulse-height-to width converter.

The pulse-height-to-width converter is the input stage of an 8-bit A/D converter. Remaining positions of the converter are the 3-input and gate, the 8-stage scalar, and the overflow inhibit circuitry. The output of the A/D converter is sampled every seventh pixel, transferring the least-significant 6 bits into a 6-stage shift register which is being shifted at a 16.2-kbits/s rate. The serial output of the 6-bit register forms the TV digital video data.

The digital video data, therefore, is comprised of the 6 least significant bits (LSBs) of the 8-bit representation of every seventh picture element along each horizontal line of the raster. The 2 most significant bits (MSBs) representing levels 128 and 64 are provided on a sampled basis (every 17.5 TV lines) to the DAS, which in turn inserts the status of these bits in a real-time DAS word located in the digital video stream.

The suppression of the 2 MSBs creates a unique transfer function condition for the digital video data stream. With reference to Fig 19 it is seen that a continuous linear transfer curve constituting the relationship between digital level and input light level is transformed into four equal sawtooth segments each of which has a maximum amplitude one-fourth the maximum level achieved in the 8-bit analog-to-digital conversion. An

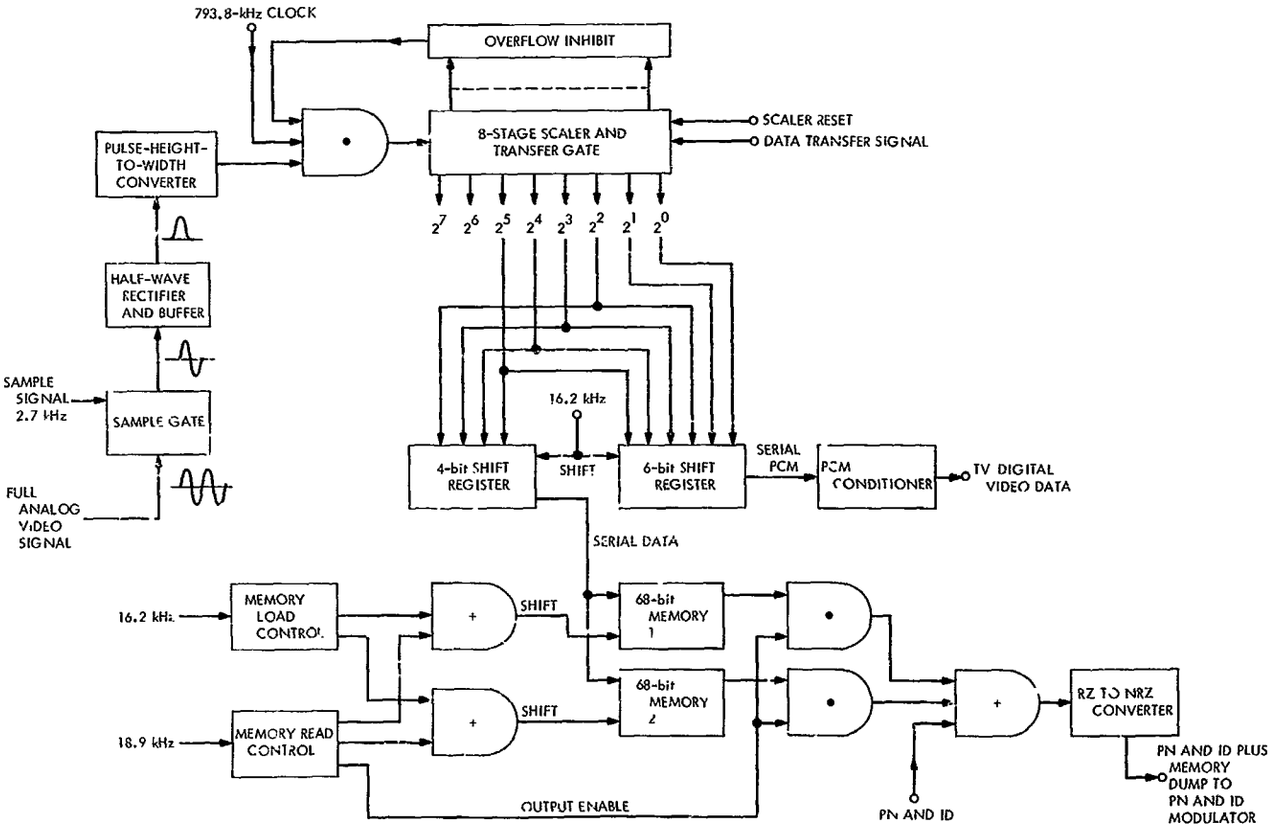


Fig. 18. Digital signal chain

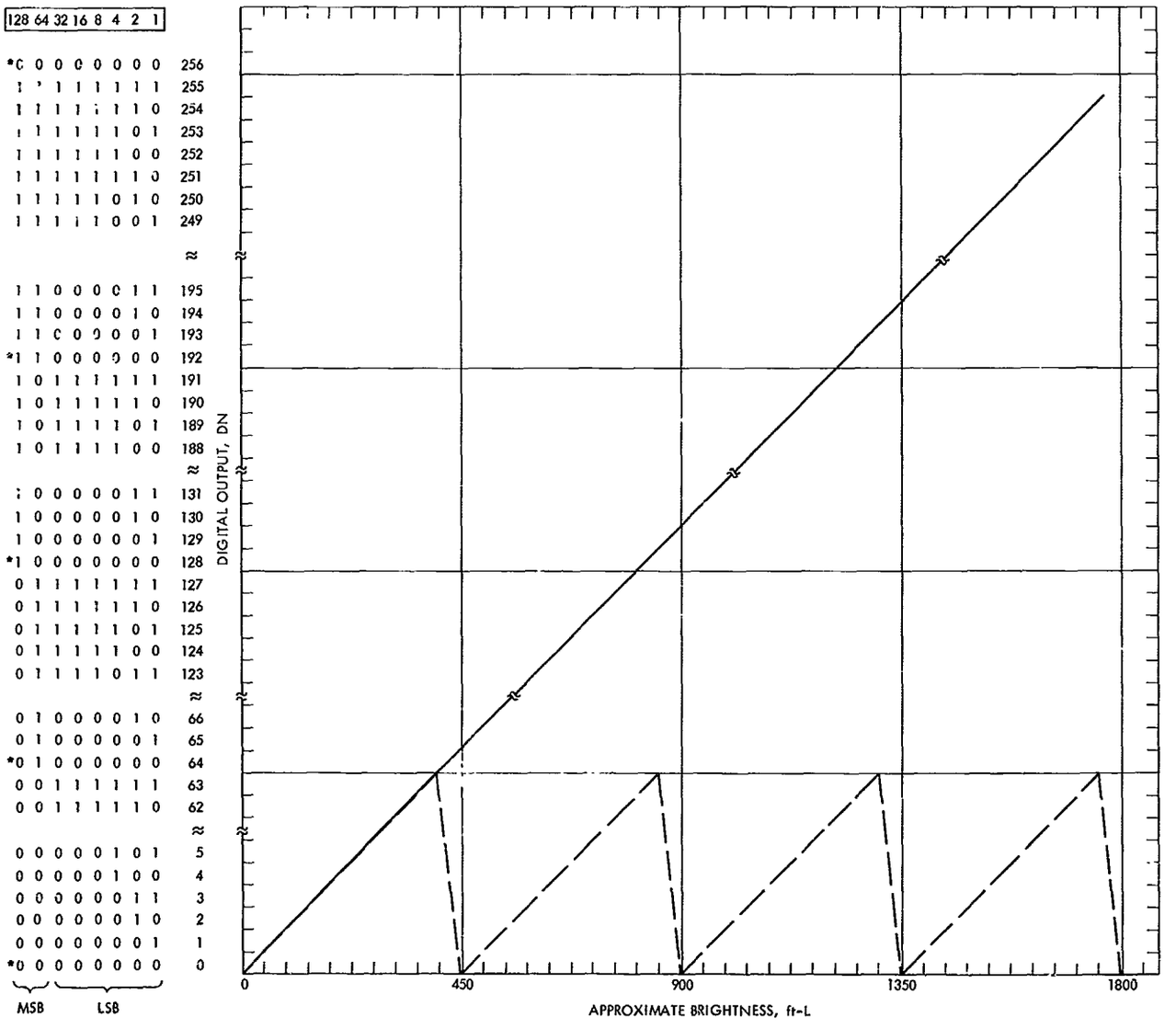


Fig. 19. Digital video data transfer function

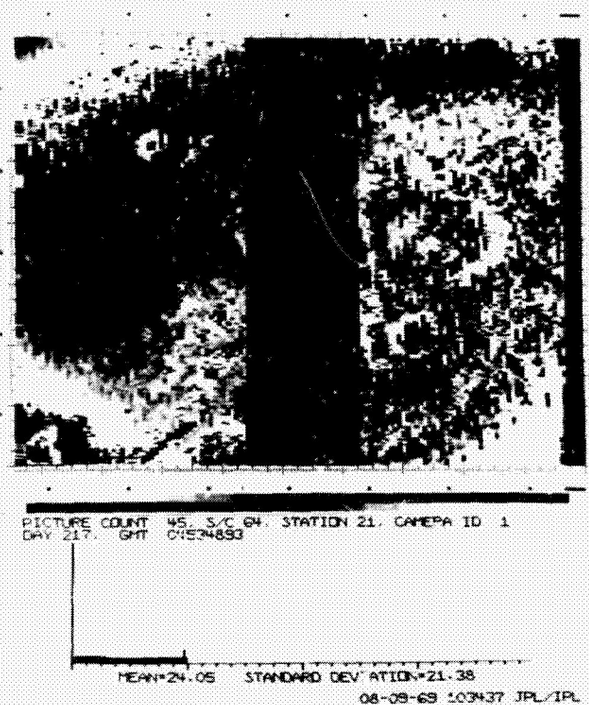


Fig. 20. Digital video data

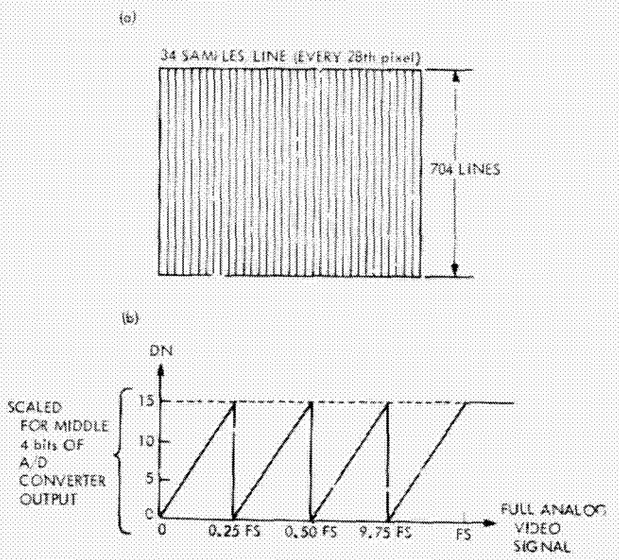


Fig. 21. Memory data: (a) picture format, (b) transfer function

examination of the 6 LSBs in the table associated with Fig. 19 shows them to be identical and equal to zero at the levels 0, 64, 128, 192 and 256. This fact creates the segmented nature of the transfer function. A representative picture depicting the character of digital video data is shown in Fig. 20. Restoration of the most significant bits during the ground image reconstruction process is required to place the picture elements into the correct quadrant and hence give them the proper brightness value.

Simultaneous with the transfer of data into the 6-stage register, the 4 middle bits of the word are transferred into the 4-bit shift register, which forms the data input stage to the two 68-bit memory units. Data flow into the 68-bit memories is controlled by the memory load control logic, which generates shift signals allowing every twenty-eighth 4-bit word to be stored in the memory.

The 136-bit memory (2×68) is loaded with 34 4-bit words per line. The memory is then dumped at an 18.9-kHz bit rate at the beginning of the next line into the analog data stream. During this time, the PN and ID code from the DAS is also inserted into the analog data stream. The memory data picture format and transfer function are shown in Fig. 21.

e. Analog signal chain. The analog signal chain (Fig. 22) optimizes the full analog video (FAV) data for recording on an analog tape recorder in the data storage subsystem. To achieve adequate fidelity on the analog tape recorder and to achieve a contrast enhancement of the viewed scene, the video signal modulation index must be increased prior to recording. This is accomplished by first passing the FAV signal through an AGC network, creating a relatively constant carrier amplitude. The AGC acts somewhat like a variable-gain notch filter centered at 18.9 kHz which attenuates dc and low-frequency video components and passes high-frequency video components, amplified by whatever factor is required to raise the carrier level to its nominal output value. The AGC action generates some distortion which is effectively removed by a fifth-order low-pass filter following the AGC amplifier. The AGC action described above holds for the near-encounter mode only. In the far-encounter mode, the AGC cannot be used because of the change in contrast between the planetary disk and space. Since the expected light levels (and therefore video signal levels) were somewhat defined, the AGC amplifier is locked into a fixed gain mode, which gives the required output carrier level to the cuber circuitry.

For modulation indices of less than 10% (which is the range expected), the cuber effectively increases the percent modulation of the AM video signal by a factor of 3. The output of the cuber is summed with an 18.9-kHz carrier signal to insure that a carrier signal will always

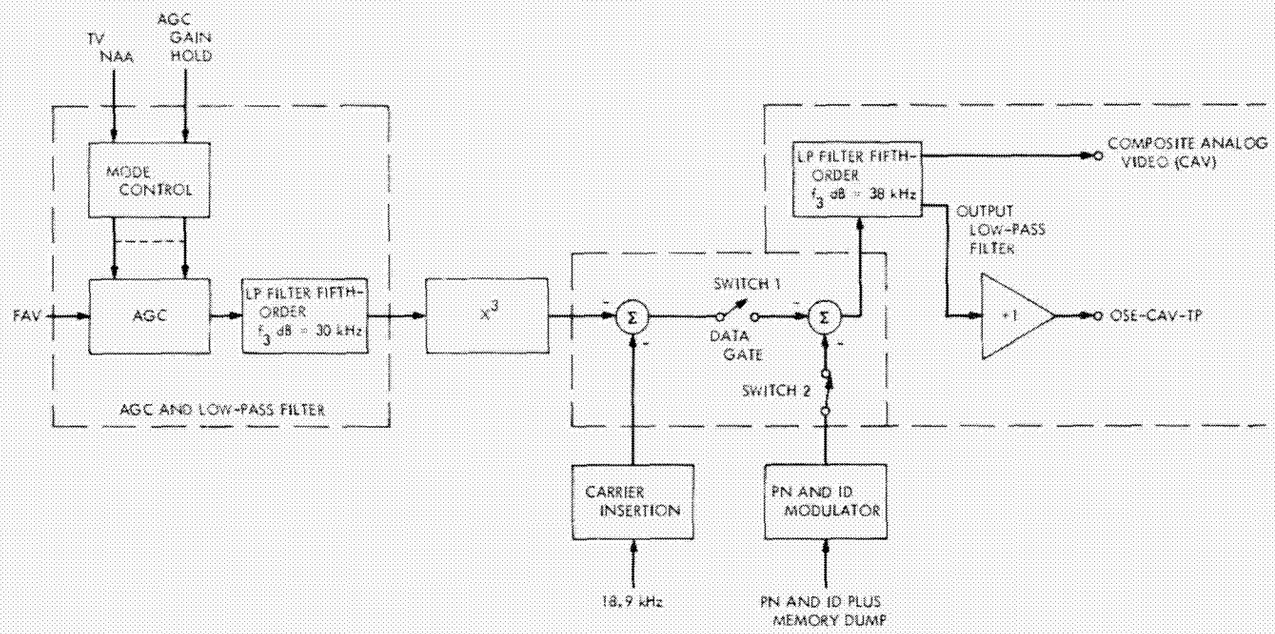


Fig. 22. Analog signal chain

be present at the recorder input for synchronizing purposes when the video signal amplitude goes to zero.

The data gate sequentially switches between the video plus camera signal and the PN, ID, and memory dump data. These switched signals generate the composite analog video (CAV) signal, which contains synchronization, line coding, and memory dump data as well as analog video. A picture representative of the CAV format is shown in Fig. 23. Prior to entering the output low-pass filter, the composite signal contains a multitude of odd harmonics resulting from the cubing action on the video. The filter attenuates all undesired components, leaving an AM modulated sine wave as the composite analog video (CAV) output.

f. Automatic aperture control. In the far-encounter mode, the automatic aperture control (AAC) circuit (Fig. 24) is locked into minimum-gain configuration in which the gain switch in the camera head is set to a gain of 0.208 and the shutter is set to "fast" shutter. The AAC is not used in far-encounter. In near-encounter the video level indicator (VLI) for AAC operation samples the digital video A frame picture as shown in Fig. 25. Based on this sample, the AAC gain and exposure time are set for the next B and A frames. The gain and exposure setting updatings are based on the AAC gain switching algorithm shown below (DN = digital number):

DN	
$X < 32$	$\overline{\text{low}^2}$
$32\,X < 128$	$\overline{\text{low}^2}$
$128\,X < 192$	low
$192\,X < 251$	high
$X \geq 251$	saturation

If a DC-41 or N-4 command is sent, the AAC gain is reset to the minimum state, 5, at which time it will commence adjusting according to the algorithm.

During the AAC period, the VLI for AAC operation is enabled. This period is 88 lines in duration. The VLI integrates on a line-by-line basis on one of five bins. In particular, the VLI receives 54 every seventh samples per line and determines the signal average based on a minimum of 41 or 75% of the samples.

Only the highest recorded value is used to set the AAC. Therefore, at the end of the VLI sample period the highest average value of the video signal, on a line basis, is recognized to be in one of the five bins listed

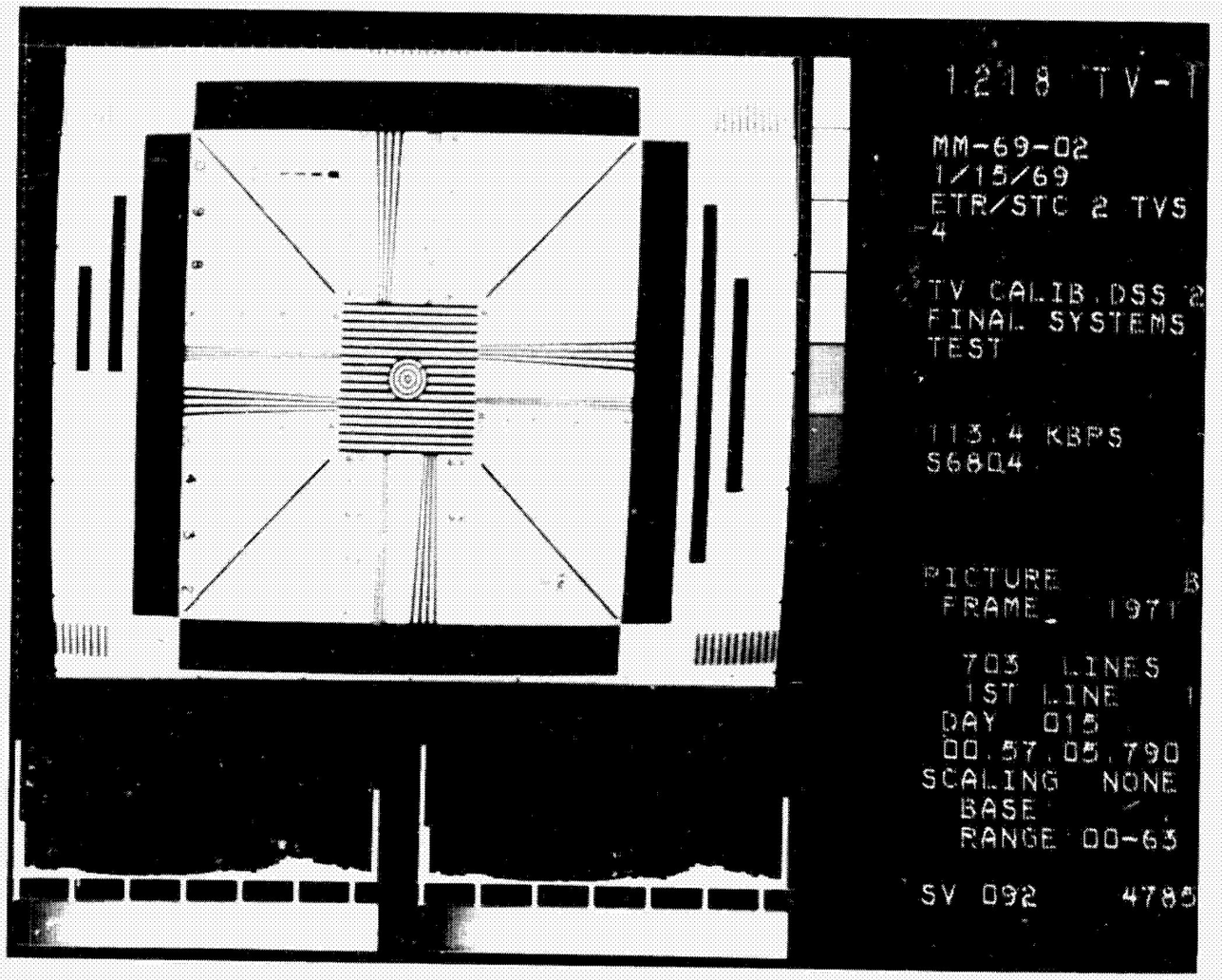


Fig. 23. Composite analog video picture format

above. The resultant signal is manipulated by the AAC control logic to set the storage registers A and B exp, B-AAC-1, B-AAC-2, and A-AAC-1 and A-AAC-2. The storage registers are set to the states indicated by the algorithm.

g. System timing. All primary synchronous TVS timing functions are provided by the DAS. These functions, other than TVS engineering data timing, are:

(1) DAS clock (793.8 kHz).

(2) TV analog video data sync (18.9 kpulses/s).

(3) TV digital video data sync (16.2 kpulses/s).

(4) TV coding stop.

(5) A-frame Start.

(6) B-frame Start.

(7) Line start.

(8) Video start.

The first four timing functions in the list are used exclusively in the signal chain; the remainder are used to generate TV control timing. The majority of the TV control timing is derived from a 704-line counter which counts from line rate down to frame rate. A-frame start and B-frame start are used to synchronize the frame logic and to generate a *frame start* signal which comes at the beginning of each frame.

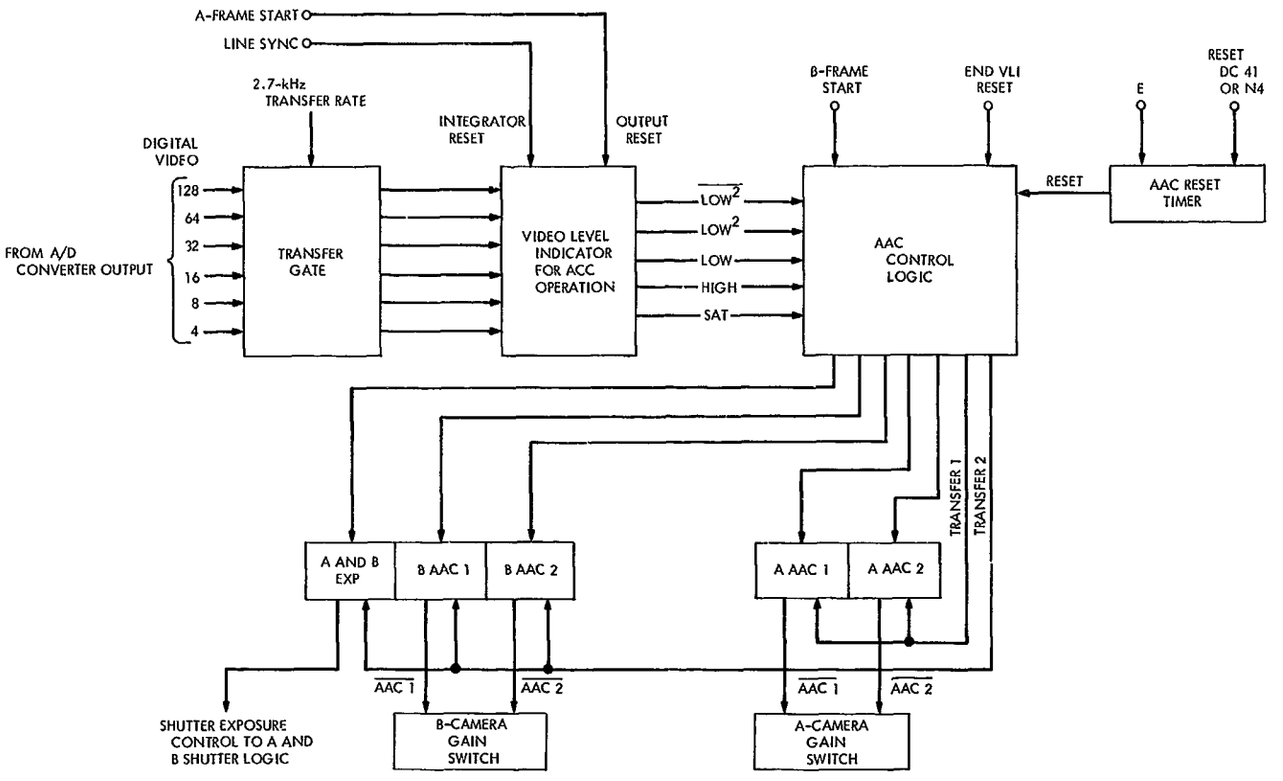


Fig. 24. Automatic aperture control operation

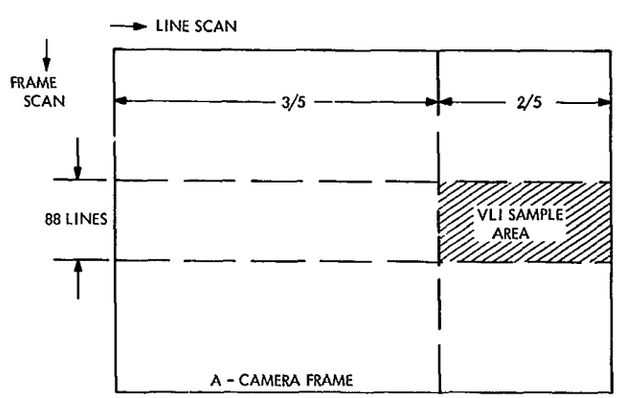


Fig. 25. Digital video sample

System startup is controlled by the power-on reset generator and startup generator. Approximately 300 ms after power is turned on, a system reset pulse is generated which places all critical logic in a known initial condition. The startup generator forces both A and B cameras into an erase mode for the first 7 frames after startup. The A and B camera shutter circuitry is controlled by the AAC exposure control, shutter logic, and $\overline{F}$ or F logic, respectively. Shutter speed is a function of the AAC exposure control state. The shutter speeds (in ms) are:

TV-A Camera	TV-B Camera
Fast: 90	Fast: 6
Slow: 180	Slow: 12

The power-off command timer inhibits the shutters at the end of a frame following the asynchronous receipt of a DC-48 power-off conditioning command. Receipt of this command insures that the shutters will not be falsely activated (and possibly left open) when the TVS power is removed.

Cover deploy commands are routed through a timer to insure that the cover deploy command arrives at a time when the cover can be safely actuated. Safe actuation is dependent on the energy storage of the shutter drive capacitors, which function as energy sources for the cover deploy solenoid.

h. Vidicon control function. The vidicon control function supplies all the peripheral signals and functions required for operation of the vidicon. These may be separated into two broad categories: static vidicon support signals, and dynamic control signals. Static vidicon support signals include inputs from the alignment current regulators, focus current regulator, and high-voltage power supply. Dynamic elements of the vidicon control are the remainder of the functions in the vidicon control function block diagram (Fig. 26).

The vidicon, as described in other sections, employs magnetic deflection and focus. All coil supplies are controlled current devices located in the TV driver subassembly. The focus current regulator supplies a constant current of approximately 75 mA to focus the electron beam on the vidicon target surface. Two alignment current regulators supply alignment current to two coils which are in quadrature with each other. Proper adjustment of alignment current in the two coils minimizes vidicon shading.

The frame and line sweep circuits deflect the vidicon electron beam to produce a raster scan of 704 lines per 42.24-s frame. Both the frame and line sweep drivers operate in a triggered mode. The frame sweeps alternate between read and erase, with complementary timing for the A and B cameras. When the A frame sweep starts a read cycle causing the beam to scan from top to bottom of the vidicon targets in the 42.24-s A frame, the B camera frame sweep is erasing from bottom to top of the vidicon in approximately 28 s. During erase, a 30-kHz dither signal is applied to the frame sweep current, causing it to fluctuate back and forth approximately one line width as the beam is horizontally scanned across the vidicon. Also, during erase the sweep deflection amplitude is increased approximately 20% over that used in the read mode. This insures that the preceding picture is erased as completely as possible.

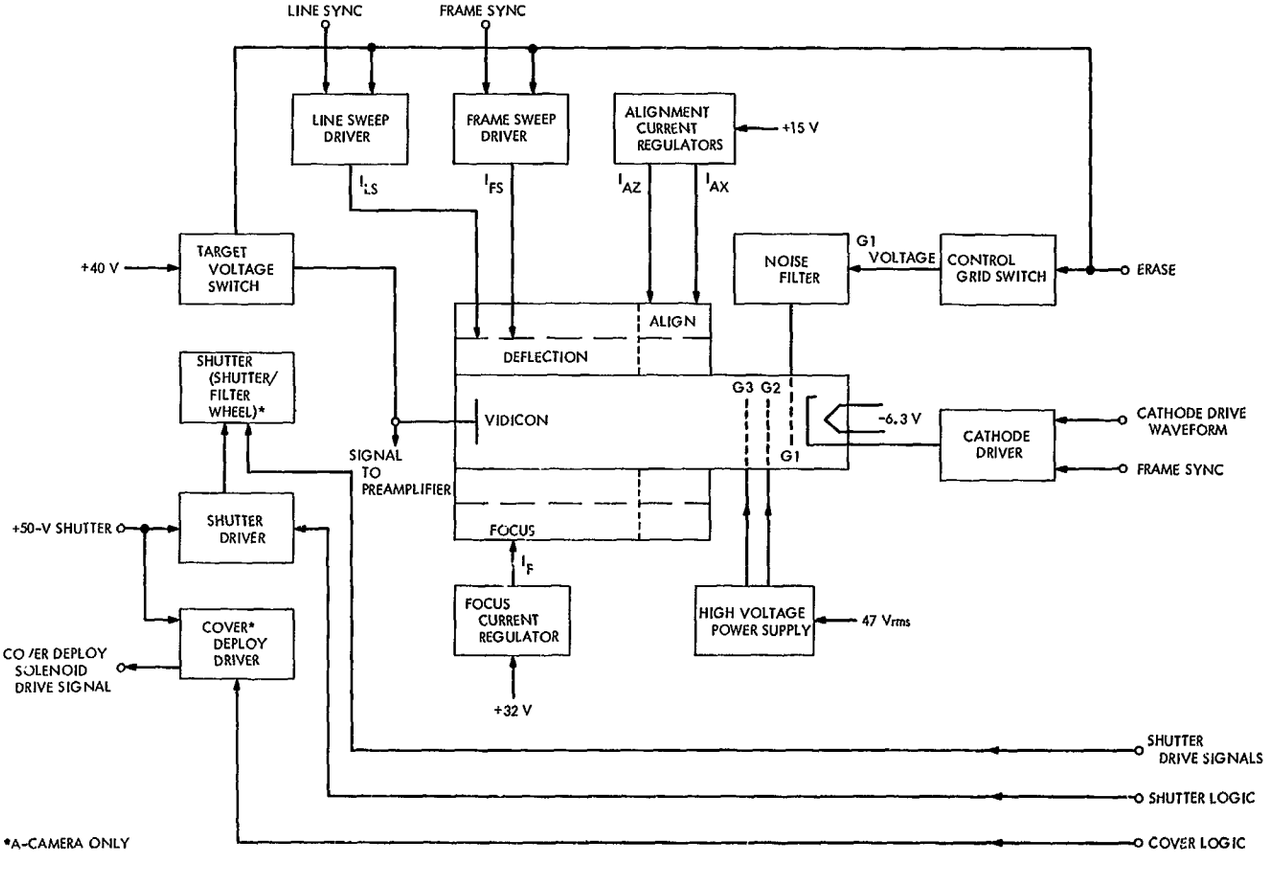


Fig. 26. Vidicon control functions

The line sweep driver generates the current waveform on a line-by-line basis. During erase, the sweep magnitude is increased, as in the frame sweep, causing a 20% overscan in the horizontal direction.

The high-voltage power supply module converts a regulated 47-V rms square wave into voltages for grids G2 and G3 on the vidicon. A majority of the electron beam generated by the vidicon cathode is collected by the accelerating grid G2. The portion of the beam which passes through G2 is collected either by G3 or the vidicon target. Therefore, G2 can draw microamperes of current while G3 only nanoamperes. The G2 and G3 voltages are a function of the vidicon read and erase modes. In the read mode, when the beam current is chopped and relatively low, the voltage at G2 is approximately 600 V and the voltage at G3 is approximately 710 V. During erase, the beam is turned on continuously at a higher beam current. This causes the G2 and G3 voltages to drop to 570 and 708 V, respectively, causing some defocusing of the vidicon.

The cathode driver generates a 0 to 6-V square wave cathode chopping signal at an 18.9-kHz rate. During line retrace time, the cathode chopping signal is positive, turning off the beam, while during erase the chopping signal is also inhibited to provide a constant beam current.

The control grid switch and noise filter provide the vidicon with a control grid voltage (G1 voltage), which is switched for the A and B cameras. Both read and erase voltages (V_{RA}, V_{FB}, V_{EA}, and V_{EB}) are optimized for each vidicon. The noise filter is a low-pass filter which bypasses any noise picked up on the G1 voltage line to camera head ground.

The target voltage switch changes the dc potential on the vidicon target from approximately 12.5 V during a read cycle to 13 V during an erase cycle. The voltage difference between the target read and target erase voltage controls the vidicon gain.

The shutter on camera head B and the shutter/filter wheel on camera head A provide the vidicon exposure time on a picture-by-picture basis via the AAC exposure control. Operation of the B camera shutter is described as follows. The shutter driver drives the two bidirectional shutter solenoids. One exposure is developed per camera read frame. The shutter is so constructed that the dual blade shutter reverses direction each frame. The first pulse to shutter coil 1 opens the aperture. A second pulse to shutter coil 2 closes the aperture. The difference in time between the two pulses determines the exposure period. At the next frame, the coil sequence and current are reversed, thereby causing another exposure and returning the shutter blades to their first position. The shutter solenoid drive voltage is 50 V. A capacitor network acting as an energy storage device is used to eliminate the requirement for high peak current drain from the power supply.

The A camera shutter/filter wheel combination not only provides exposure time, but changes the filter in front of the A camera at the same time. The filter sequence is as follows: red, green, blue, and green.

The shutter driver circuit develops two shutter solenoid drive pulses per camera read frame. The time difference between initiation of these two pulses determines the shutter exposure time. The shutter drive logic from the TV control subsystem initiates the shutter open and close pulses. Logic is also included to sense the position of the shutter and produce only one shutter drive pulse in the event the shutter malfunctions and remains in the open state.

The cover deploy driver is actuated only once during the mission. Once the cover is deployed there is no mechanism for resetting it other than manual repositioning.

i. Engineering data. Engineering data in the TVS is monitored by two separate data channels. An analog engineering data monitoring function is employed to measure primarily analog data points. The analog output is converted to pulse width information before being transmitted to the DAS. A digital data channel is used to monitor digital data points in the TVS. A description of each of these data channels follows.

As shown in Fig. 27, seven analog points are routed to a commutator which selects a given input sequentially on an A/PW select signal command from the DAS. The commutator is advanced through the sequence; B optics temperature, G1 voltage (A or B), anode voltage (A or B), and focus current (A or B). The A or B following the sampled parameter indicates that during an A frame the A camera data point is read out while during the B frame the B camera data point is read out.

The digital engineering data channel monitors 6 bits of TV engineering data, as shown in Fig. 27. Data is sampled by the transfer function which enters the data bits into a 6-bit shift register. The transfer and readout

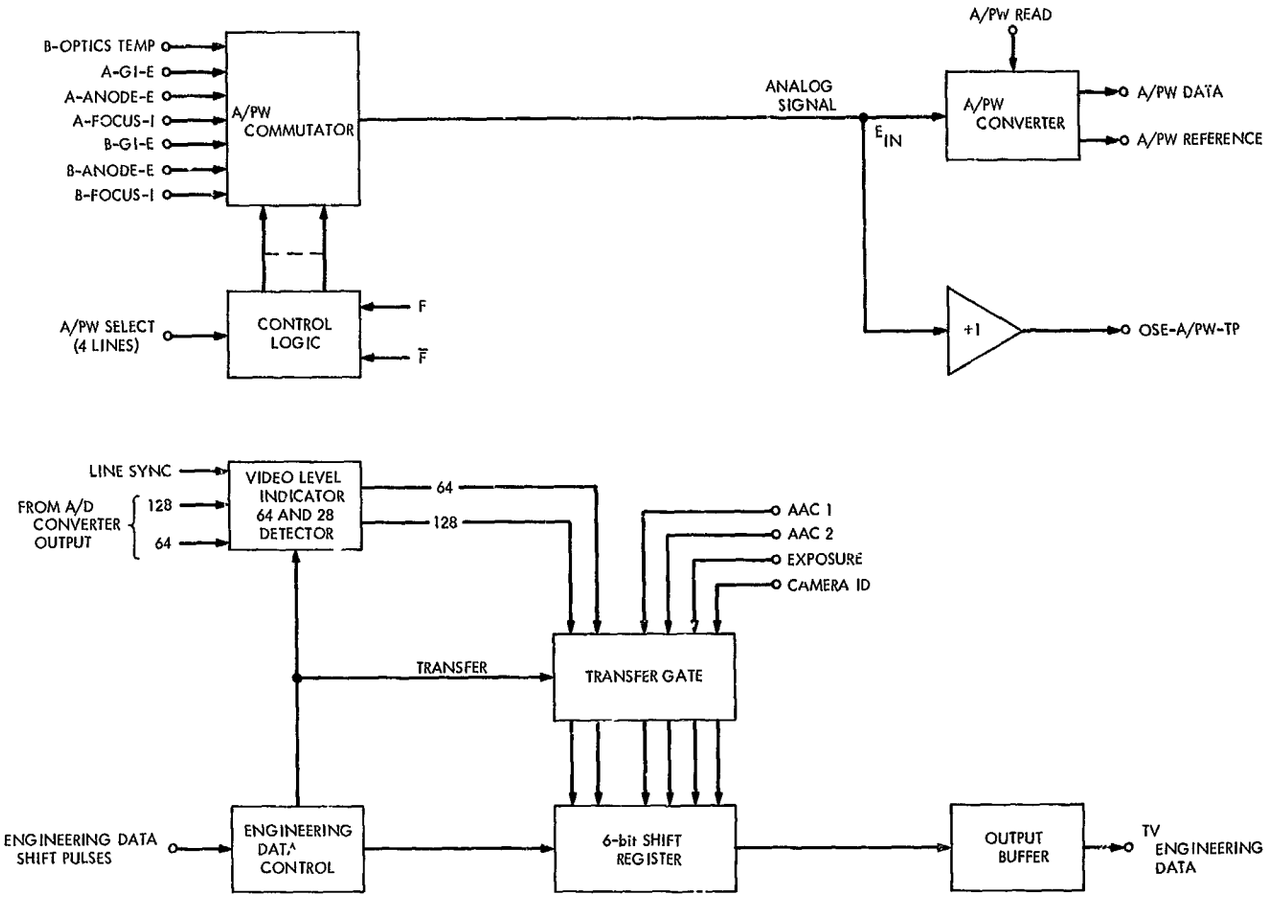


Fig. 27. Engineering data

of data to the DAS is effected by a burst of 7 pulses at a 2.4-kHz rate. These pulses are known as the engineering data shift pulses. The first pulse transfers the data into the shift register, while the 6 remaining pulses dump the digital data in serial format into the DAS. Four of the inputs to the shift register are directly sampled data points; the remaining 2, 128 and 64 video are derived from the digital video picture. Between engineering data samples, each line of video is sampled to see if more than 5% of the line has a video level which falls in the range:

$$64 \text{ video level bit} \qquad 64 \geq X < 128, X > 192$$

$$128 \text{ video level bit} \qquad X \geq 128$$

If this condition is met by any line in the sample, the 64 bit and/or the 128 bit is set to the one state, which it holds until readout.

j. Power supply. The power supply provides +5, +6, −6, −6.3, −15, +15, +32, +40, +50, −100, and 47 V rms ac for TVS operation. The selection of these voltages was based on circuit and vidicon voltage requirements as well as on overall power supply efficiency considerations. Input current limiting is used to protect the spacecraft against failures in the TV subsystem (other than in the current limiter). This limiter limits input current at 150% of the maximum normal input. Regulation is required for all voltages, with the exception of the +32 V used in the focus current regulators and the +50 V used to charge the solenoid energy storage capacitors All output voltage regulators use the series configuration for the pass transistor.

k. Miscellaneous functions. The miscellaneous items not covered in the previous system descriptions are the cruise and optics heaters and the vidicon temperature transducers. Each vidicon has an ac 2400-Hz cruise

heater associated with it. During the spacecraft cruise mode, power is supplied to these heaters to maintain the desired vidicon temperatures. During encounter, when the vidicons are on, the cruise heaters are turned off. The power dissipated by this heater is 8 W and is equal to that power consumed by the camera head when the subsystem is on. Power control is external to the TVS.

The TV-B optics has a dc strip heater which is used to minimize the thermal gradient along the barrel of the telescope. Power is applied continuously to this heater directly from the power subsystem.

Each camera head has a vidicon temperature transducer mounted near the vidicon target. These transducers are read out directly by the flight telemetry subsystem (FTS).

2. *Vidicon.* The vidicon used in the *Mariner* Mars 1969 television is a type 1342-010 manufactured by General Electrodynamics Corporation and is shown in Fig. 28. It is used to convert the optical image input into an electronic signal output. The vidicon can be divided into two basic blocks: the electron optics and the target.

The electron optics generates, initially shapes, and controls the current in the scanning electron beam. The electron optics consists of five elements: filament, cathode, control grid, accelerator, and mesh. The low-power filament heats the cathode, whose emitted electrons are attracted by the positive accelerator. The electron flow to the accelerator, however, is limited by the negative control grid, which is between the cathode and the accelerator. Of the electrons which do reach the accelerator, which is at a 600-V potential, a low percentage pass through a small pin hole in the accelerator called the limiting aperture and are accelerated down the length of accelerator tube toward the target. At the end of the accelerator is another electrode, called the mesh, which is held at a 700-V potential. It is a fine screen which also aids in accelerating the electrons toward the target. After the electrons pass through the mesh they begin decelerating from the 700-V potential on the mesh to the 10-V potential on the target.

The target operation is best described by considering the target as a plane containing an infinite number of capacitors each in parallel with a light-dependent resistor. One side of all the capacitor–resistor networks is connected together and is brought outside the tube as the target lead. This lead is connected through a 20-MΩ load resistor to a 10- to 15-V potential (optimum potential varies for each tube). The other sides of all the networks are isolated from each other and exposed to the electron beam. As the electron beam is swept across the target, it charges the beam side of each network to the potential of the cathode, zero V. The target lead side of each network is at the potential of the target supply.

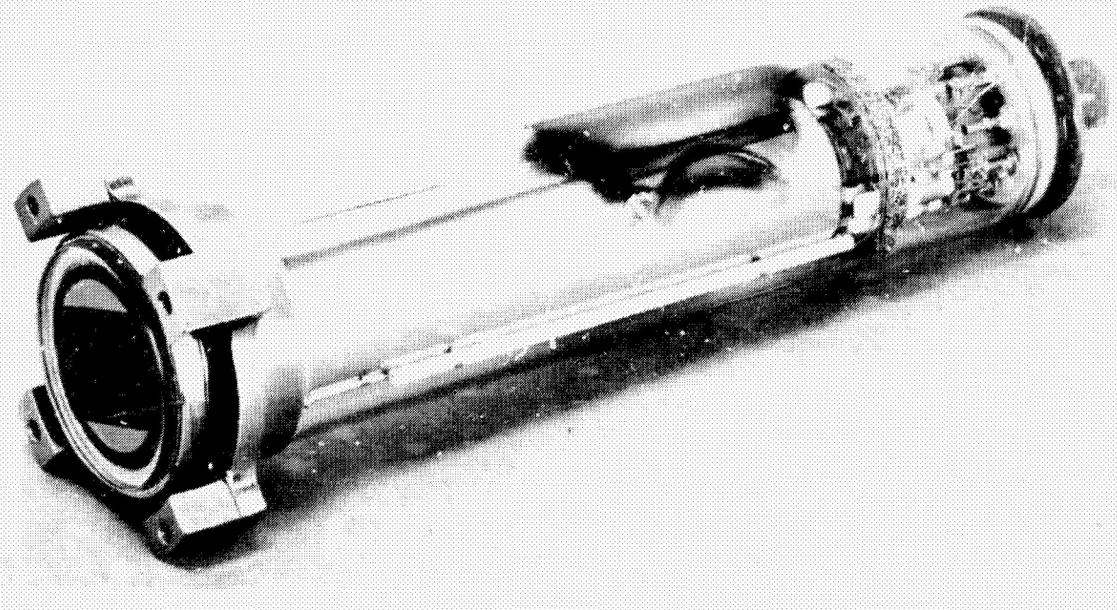


Fig. 28. Vidicon

The capacitor in each network, therefore, is charged to a potential between 10 and 15 V. When light is exposed to the target, the light-dependent resistor in each network discharges a portion of the charge on the capacitor in proportion to the intensity of the light illuminating the resistor. As the electron beam is again swept across the target it charges each network back to its original potential. To do this, however, requires current to flow from the beam into each network. The amount of current flow is also proportional to the light which illuminated the target and is sensed in the network's return leg by the target load resistor. There it is converted into an analog voltage (which is proportional to the light striking the vidicon) for amplification and further signal processing. A typical light transfer characteristic curve showing the relationship between light input and current output is shown in Fig. 29.

The photoconductor is a type of doped selenium, and its response varies as a function of the spectral content of illuminating light source. The response to specific wavelengths of light is shown in Fig. 30.

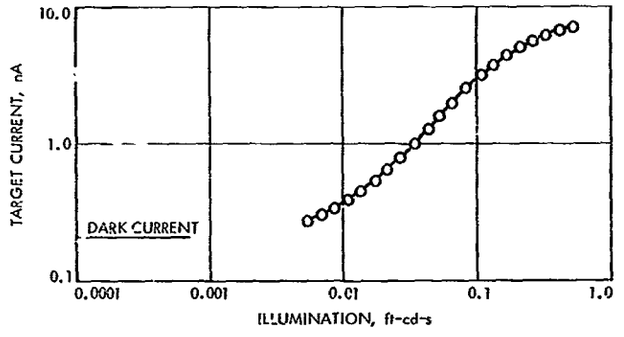


Fig. 29. Typical light transfer characteristics

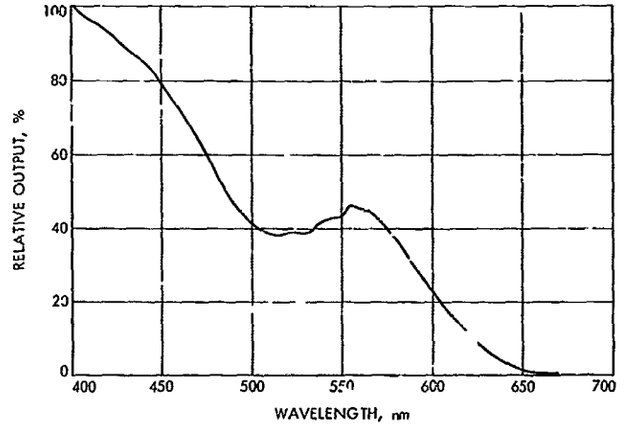


Fig. 30. Typical spectral sensitivity characteristics

On the faceplate of the vidicon, a thin layer of nichrome is deposited before the photoconductor is deposited. The nichrome acts as an optical barrier (it has an optical transmission of less than 0.1%) and prevents certain areas of the photoconductor from being illuminated. The nichrome configuration provides a black reference mask on both edges of the raster format and a reseau containing 49 square reticle marks. The black mask serves to provide a reference for optical black as a means of determining the dark current level of each image. The reseau provides a reference matrix used in the process of correcting the received images for electronic distortions. The mask shape and reseau configuration are shown in Fig. 31.

3. Wide-angle optics. The optical system for the wide-angle camera is a commercial camera objective, remounted into a lens barrel specifically designed to survive the spacecraft environment. The lens consists of six refracting lens elements, two of which comprise a cemented doublet. In the commercial mount the lens has a maximum relative aperture of *f*/2.0; however, in the *Mariner* Mars 1969 flight configuration the lens is stopped down to *f*/5.5. Figure 32 gives the lens schematic, which shows the lens elements, their positions, and the position of the focal plane.

The optical characteristics of the lens are listed as follows:

(1) Focal length: 2.07 in.

(2) Geometrical *f*/No.: 5.50.

(3) *T*-number (effective *f*/No.): 6.36.

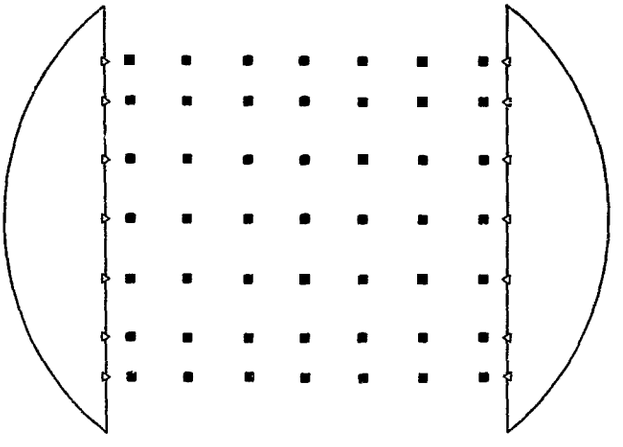


Fig. 31. Vidicon mask shape and reseau placement

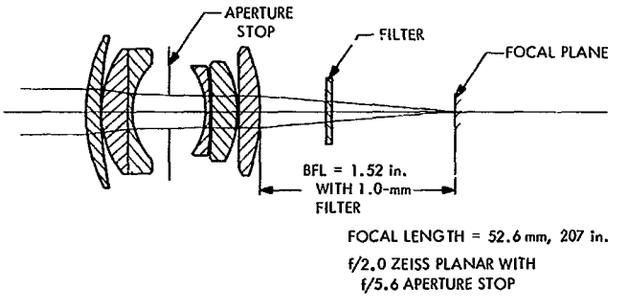


Fig. 32. Optical diagram, wide-angle camera

(4) Field size: 0.378 × 0.494 in.

(5) Maximum angular field: 9.0 deg off axis.

(6) Minimum low contrast resolution over the full field: 160 plus line pairs/mm.

(7) MTF: the sine wave response of the lens at 40 cycles/m is 57% on axis.

Physical characteristics of the lens are as follows:

(1) Size: 5.5 × 4.2 × 4.4 in. long.

(2) Thermal control surfaces: all of the exterior metallic surfaces are polished aluminum.

Mechanical characteristics of the lens are as follows:

(1) Lens barrel.

(2) Lens cover and latch assembly.

(3) Chassis.

(4) Thermal cover.

(5) Barrel holder.

The lens barrel houses the six lens elements and is made of 416 stainless steel to closely match the coefficient of thermal expansion of the glass lens elements. This is necessary because the lens is subjected to a wide temperature range. A fixed-diameter aperture stop is machined in the barrel obviating the use of a variable iris. The dimensions of the lens seats and spacings in the commercial mount are duplicated in the flight mount. Focusing threads are machined into the outer diameter of the barrel, and mating threads are machined in the barrel holder. The lens is focused by rotating the lens barrel in the barrel holder. Locking rings lock the barrel in position after the lens is focused.

A removable transparent lens cover is provided on the wide-angle camera to protect the lens from possible contamination from any outgassed products surrounding the spacecraft during flight. The cover consists of a quartz window, a frame which supports the window, and a solenoid latch mechanism. The window frame is spring-loaded about a shaft and locked in position in front of the lens by the latch mechanism. Upon command, a pulse is sent to the solenoid latch mechanism, which releases the frame. The spring-loaded frame then rotates, swinging the cover window from in front of the lens. A cam surface on the frame actuates a microswitch when the cover is fully deployed, producing a telemetry signal which indicates that the cover has deployed.

4. Narrow-angle optics. The optical system for the narrow-angle television camera is a Schmidt-Cassegrain telescope of 20-in. focal length. It consists of three optical elements: A Schmidt corrector plate, with the aspheric figure on the front surface, an oblate spheroid concave primary mirror, and a spherical convex secondary mirror. Figure 33 shows how the light passes through the corrector plate, reflects off the primary mirror, then off the secondary mirror, and passes through the central hole in the primary mirror, coming to a focus approximately 3 in. behind the vertex of the primary mirror. Nearly all of the image formation is accomplished by the two mirrors. However, a simple two-mirror system was inadequate to achieve the optical performance required. The low-power corrector lens was required to minimize the inherent optical aberrations of a two-mirror system in order to achieve the required optical performance.

The optical characteristics of the system are listed as follows:

(1) Effective focal length: 19.87 in.

(2) Clear aperture: 8.50 in.

(3) Geometrical *f*/No.: 2.34.

(4) *T*-number (effective *f*/No.): 3.85 (for "white" light).

(5) Field size: 0.378 × 0.494 in.

(6) Maximum angular field: 0.9 deg off axis.

(7) Minimum low contrast resolution over the full field: 130 line pairs/mm.

Physical characteristics of the system are as follows:

(1) Weight: 21 lb.

(2) Size: 10.75 in. in diameter by 24.90 in. long.

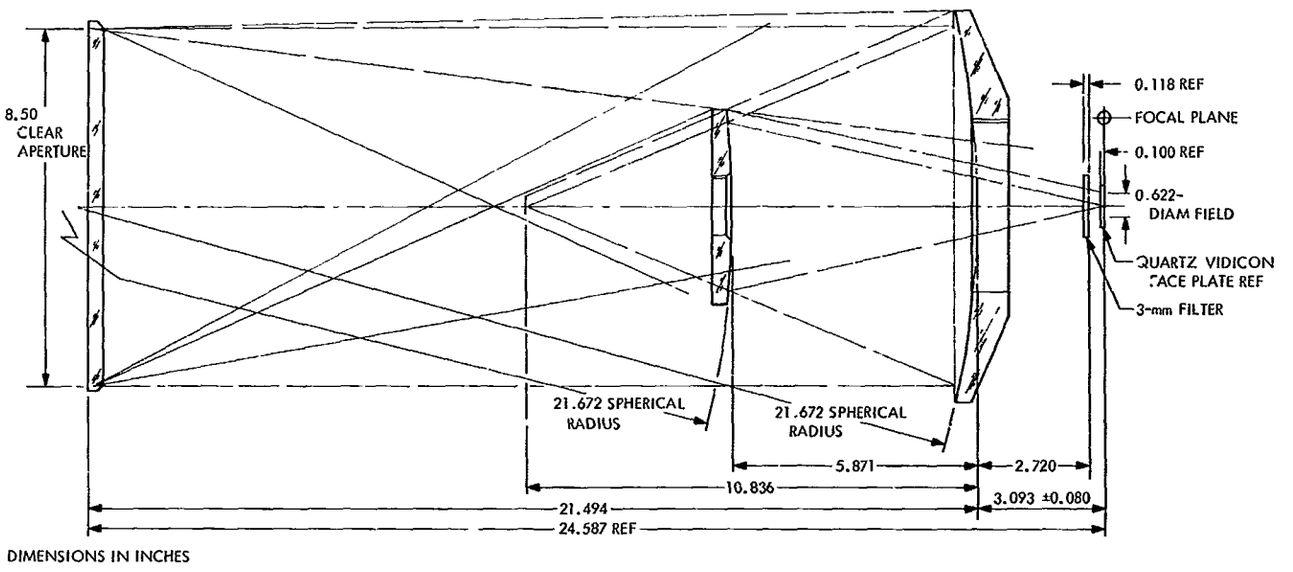


Fig. 33. Optical diagram, narrow-angle camera

(3) Thermal control surfaces: All of the exterior metallic surfaces are polished aluminum. The corrector plate is coated with an infrared reflecting (transparent in the visible spectrum) gold coating.

The mechanical structure of the optical system consists of eight major elements:

(1) The optical elements: corrector plate, primary mirror and secondary mirror.

(2) Optical element mounts.

(3) Spacer rods.

(4) Chassis structure.

(5) Front support structure.

(6) Base tube structure.

(7) Extender tube structure.

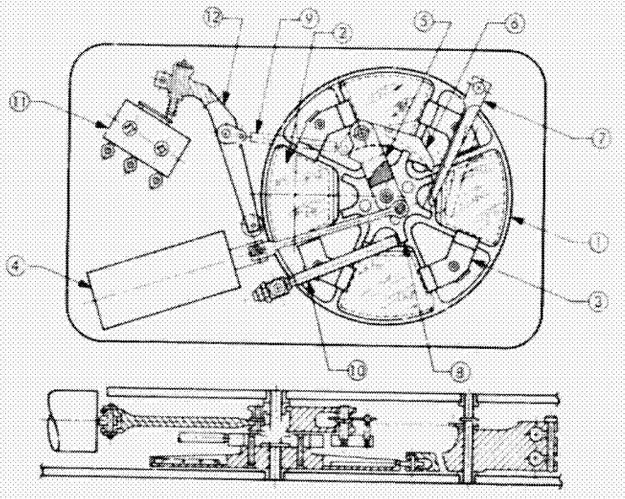
(8) Secondary spider.

The optical elements are fabricated from fused silica (fused quartz), the mirrors from a mirror-grade fused quartz and the corrector from a high-quality, optical-grade fused quartz. Both the primary and secondary mirror mounts and associated hardware are fabricated from Invar 36. The spacer rods, which separate the mirrors, are fabricated from super Invar. All of the rest of the major structural elements are fabricated from aluminum alloy.

5. Wide-angle shutter. The wide-angle (A) shutter is shown in Fig. 34. The filter wheel (1) has four openings with radial edges 45 deg apart, each of sufficient size to clear the light path from the lens to the vidicon. Each opening is covered by a glass filter (2) retained by spring clips (3). The filter wheel can be indexed by 45-deg increments. Each such indexing cycle is started by an electrical pulse from the A shutter drive circuitry.

Except during an exposure, the filter wheel is in the closed position, with the opaque web between filters obscuring the aperture. When the wheel is rotated 45 deg into the open position, light can pass through to the vidicon, but a further 45-deg rotation again obscures the aperture. The time during which the vidicon is exposed to light is controlled by the time between the two indexing cycles, which is in turn governed by the separation of the input drive pulses.

The pulse initiating an indexing cycle energizes the linear solenoid, thereby rotating the rocker arm (5) by means of the connector rod. The pawl (6), pivoted on the rocker arm is consequently driven to the position shown in phantom. In reaching this position, the pawl releases latch A (7) extends the drive spring (9), and then engages with the next cog. The shutter is now said to be "cocked." When the solenoid is de-energized, the linkage is returned to its original position by the drive spring, advancing the filter wheel 45 deg. During this



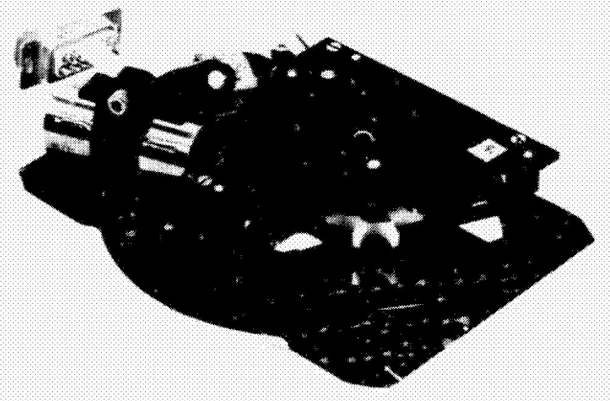


Fig. 34. Wide-angle shutter

travel, the latch follows the pawl inward and is in position to stop the filter wheel at the end of the stroke. The back latch B (10) ratchets over the cogs, preventing back motion of the wheel. Latch B can be adjusted to provide the optimum backlash for the mechanism.

Two microswitches (11) are provided as a sensing mechanism to determine improper shutter operation and initiate a corrective sequence. These switches are actuated by a spring-loaded follower arm which rides on the rim of the filter wheel. The rim is contoured to actuate the switches at points corresponding to the shutter open positions. The redundant switches are connected in parallel and provide an actuation signal to the shutter drive logic in the event the shutter half-cycles and comes to rest in the open position. The logic is such that the proper shutter sequence is again synchronous with the shutter drive pulses during the shutter actuation subsequent to the malfunction.

Shutter functional characteristics are as follows:

(1) Exposure time: the shutter operates in the camera with exposure times of 90 and 180 ms.

(2) Aperture: the clear aperture of the shutter is 0.50 × 0.60 in.

(3) Power: 50 V.

(4) Pulse width: 14 ms.

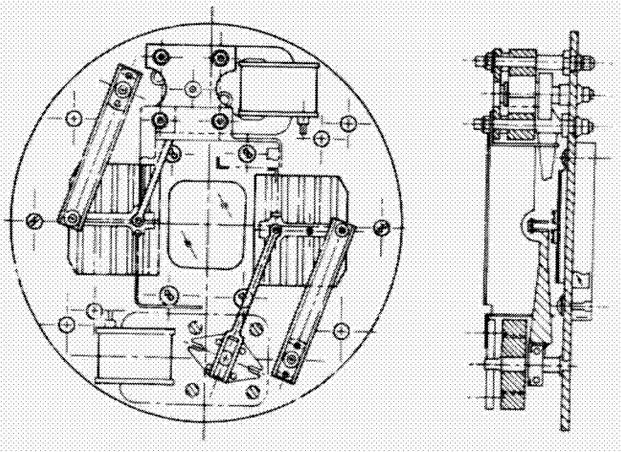
(5) Opening and closing time: 20 ms.

Shutter physical characteristics are as follows:

(1) Size: 5.0 × 4.05 × 1.30 in. thick.

(2) Weight: 264 g (0.70 lb).

6. Narrow-angle shutter. The narrow-angle (B) shutter (Fig. 35) is a two-blade focal plane shutter. Each blade



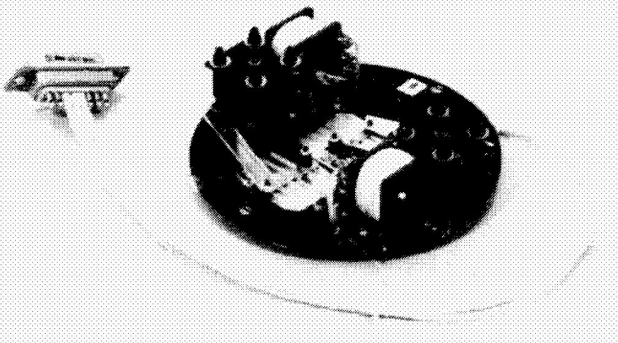


Fig. 35. Narrow-angle shutter

is powered by its own permanent magnet rotary solenoid. The solenoid coils have bifilar windings which enable the direction of the shutter blades to be reversed by switching the current from one half of the winding to the other half. The length of the exposure is controlled by the time interval between two pulses (an open pulse and a close pulse). The open pulse powers the "leading" blade and the close pulse powers the "trailing" blade.

Consecutive exposures are made with the blades moving in the reverse direction. The exposure sequence starts with the leading blade covering the aperture. The open pulse moves the leading blade, uncovering the aperture, and the close pulse moves the trailing blade, in the same direction, covering the aperture again. For the subsequent exposure, the direction and sequence of blade movement are reversed.

Shutter functional characteristics are as follows:

(1) Exposure time: the shutter operates in the camera with exposure times of 6 and 12 ms.

(2) Aperture: the clear aperture of the shutter is 0.790 × 0.670 in.

(3) Power: 50 V.

(4) Pulse width: 22 ms.

(5) Opening and closing time: 8 ms.

Shutter physical characteristics are as follows:

(1) Size: 3.5 in. diam × 1.10 in. height.

(2) Weight: 140 g (0.375 lb).

D. Calibration Objectives

The purpose of calibration is to determine as accurately as possible the relation between input stimuli and instrument output. Calibration serves the purpose of defining the functions which equate instrument output to input stimuli. Each individual instrument has its own calibration signature which must be accurately determined. It is necessary to know not only the instrument's response to input stimuli, but also its response to the environment in which it is expected to operate.

The calibration data is used to correct or compensate for irregularities of performance of components or circuits, to establish absolute photometric, radiometric, and geometric references, and to correct mission data to more accurately reflect the viewed scene. Mission data is convoluted with the known nonlinearities of the TV circuitry and the distortions and responsivities of the optics/vidicons to obtain pictures that are geometrically correct and photometrically accurate. Telemetry point calibration curves are used during mission operations as system performance monitors and aid real-time evaluation of nonstandard performance, if any.

The television instruments on the *Mariner* Mars 1969 spacecraft were each subjected to extensive calibrations. The requirements for these calibrations were established jointly with the experiment team and in consonance with the scientific objectives for the experiment. The calibration of the television instruments for the 1969 mission resulted in the recording of approximately 4137 pictures each in four different data types, yielding 16,548 calibration frames. Some 2000 magnetic tapes were required for storage of this data.

The procedures for the *Mariner* Mars 1969 calibration were based on past *Ranger*, *Mariner IV*, and *Surveyor* calibration experience. The calibrations were carried out, in each case, after all final engineering adjustments were made. The calibrations were divided into three major categories. The first category included component-level calibration. These calibrations included measurements to determine the spectral transmission of optical components, shutter exposures, optical focal lengths, sensitivity and relative spectral response curves of the vidicons, and measurements of the locations of vidicon fiducial marks. These component-level calibrations were essential to determine the unique properties of each component, and they served as an aid in the selection of the components which were able to meet the scientific objectives of the experiment. The chart in Fig. 36 illustrates the typical component-level calibrations, their predicted duration, and their dependence on proper vidicon selection prior to final assembly.

The second category of calibrations included those at the subsystem level and those in the thermal/vacuum environment. These calibrations were essential to determine the instrument properties in simulated space environment. There were six calibrations conducted at the subsystem level. These calibrations utilized the development support equipment (DSE) and were referred to as bench, baseline thermal/vacuum (T/V), Cold T/V, Encounter T/V, Hot T/V, and postbaseline T/V calibrations. These subsystem-level calibrations utilized test collimators, specially designed test targets, and extended source luminance stimuli. Information was obtained on

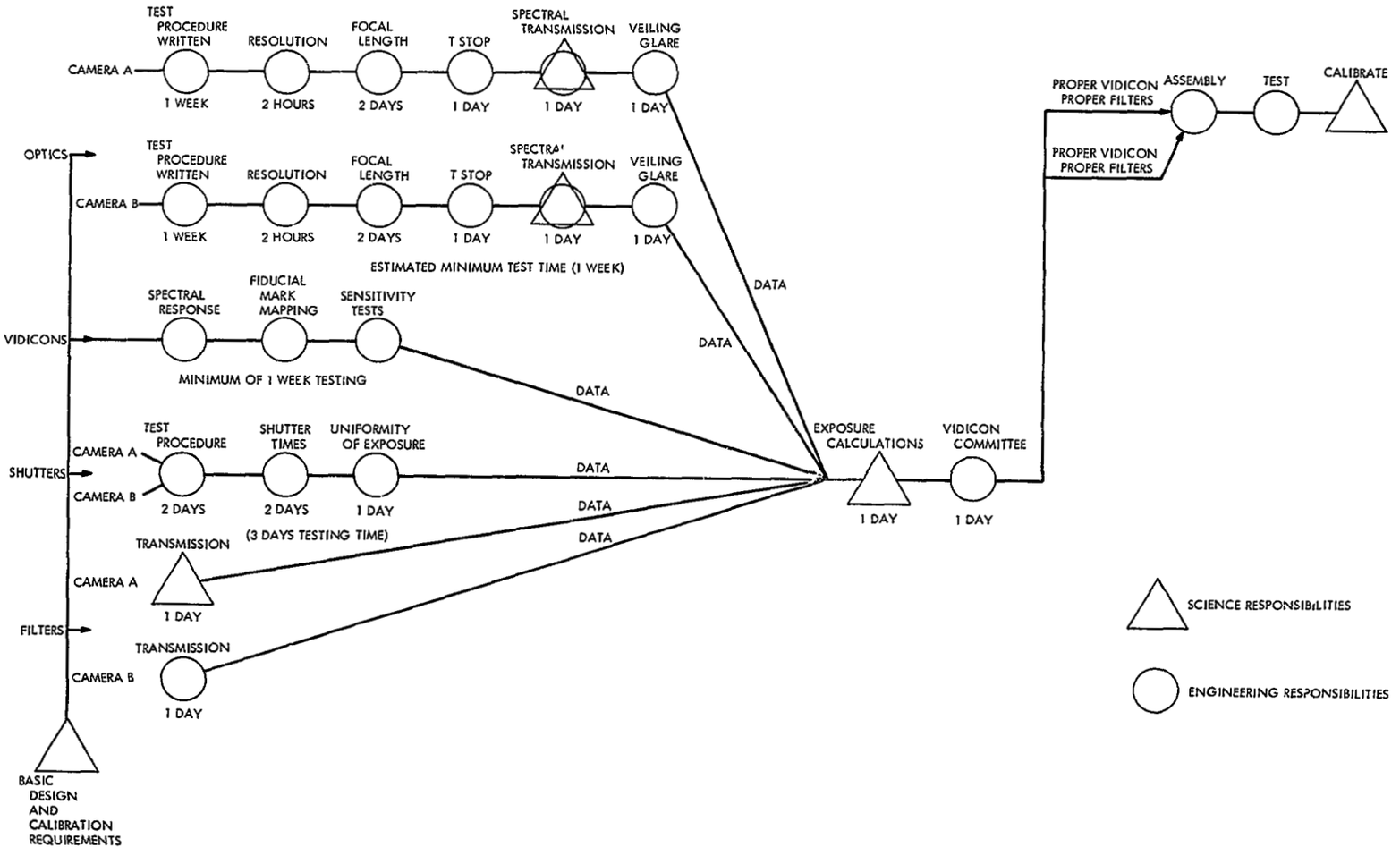


Fig. 36. Television subsystem component calibration and data flow requirements

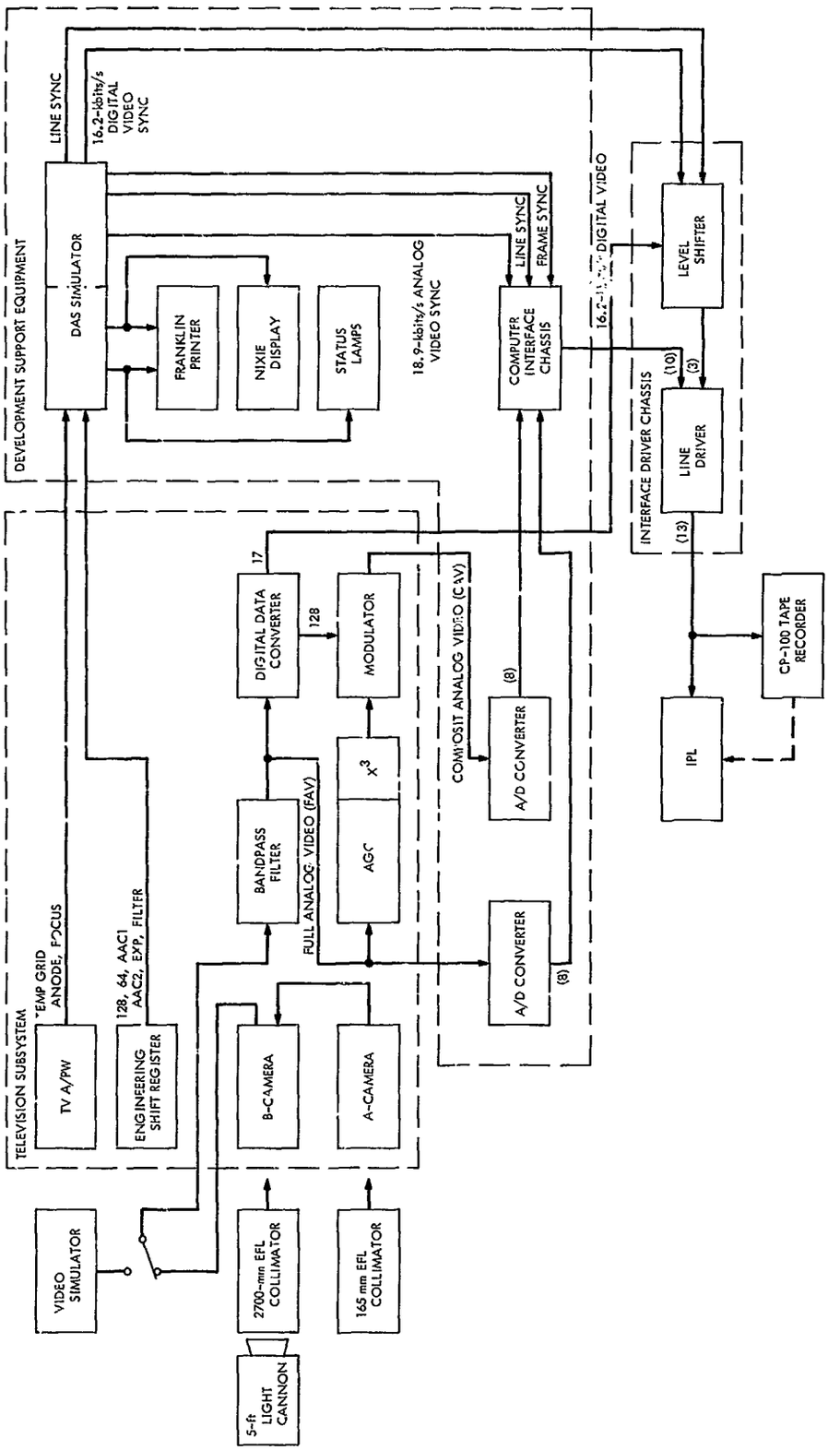


Fig. 37. Bench and thermal/vacuum calibration configuration

the sensitivity, erasure, resolution, temperature, and complete subsystem transfer characteristics. The bench and thermal/vacuum calibration test configuration is shown schematically in Fig. 37. In the DSE, analog video in "raw" or unprocessed form (FAV) and in AGCed and cubed form (CAV) is digitized and interlaced for transmission to the Image Processing Laboratory (IPL) via hardline or digital tape.

The third category of calibrations involved system-level calibrations which were performed on each instrument after integration on the spacecraft. These calibrations were designed to verify the previous calibrations and to characterize subsystem performance in the spacecraft environment. These calibrations were conducted at the Spacecraft Assembly Facility at JPL and again just prior to launch at AFETR. Since these tests are conducted by supplementing the system test setup, the data sources and processing equipment are described in the next section of this document.

E. Calibration Data

The material in this section was extracted from a voluminous collection of calibration test results that describe, in detail, the complete characterization of the TV cameras. This material was selected to provide a representative description of camera performance as experienced during the mission. The following data was obtained from each calibration:

(1) Environment profile and test log.

(2) Analog and digital telemetry printout.

(3) Magnetic tapes of FAV, CAV, and DV.

(4) Polaroid photos of A trace of center line of video frame.

(5) Polaroid photos of monitor display of selected frames.

To exercise all TVS functions and provide multipoint characterization the following image sources were utilized:

(1) Flat light field.

(2) Narrow-band interference filters.

(3) Complex sine-wave target.

(4) Leighton two-way grey scales.

(5) Vidicon sensitivity.

(6) Spectral response.

(7) Modulation transfer function.

(8) AGC and cuber response.

Additionally, various topographical scene targets were utilized to provide image reconstruction practice.

1. Spectral response. To obtain spectral response functions for the cameras, the measured relative response of each vidicon was multiplied by the measured transmittance of the filters with which it was used. The derived functions thus obtained were then compared with predicted scene spectra for various viewing phases of the mission. The spectra of both desert and polar-cap scenes viewed at close and distant ranges were normalized at 555 nm and compared at 5-nm intervals. Representative "near desert" curves are shown in Figs. 38 and 39. Subsequent to the convolution of the response and the scene, the filter factor, effective wavelength, and ratio of energy incident on the vidicon were calculated and tabulated with each curve.

2. Light transfer function. The light transfer curves (Figs. 40 and 41) depict typical data obtained during the calibration tests. In all cases, a uniformly illuminated diffuse stimulus was used to obtain the data. Since the filters did not have equal exposures, the wide-angle cameras actually have four unique light transfer characteristics. This spectral dependence is readily noted when the data is displayed as a function of subsystem operating temperature in the thermal/vacuum test results (typically shown in Fig. 42).

3. Modulation transfer function. The modulation transfer function (MTF) is defined as that function which will describe the system frequency and linear system modifications to an arbitrary input signal. That is, given a linear system such that the input excitation or signal is defined as $x(t)$ and the output as $y(t)$ we have

$$x(t) \text{ linear system } y(t)$$

Thus schematically one can depict this linear system in the frequency domain as

$$X(\omega) \quad \begin{matrix}\text{system transfer} \\ \text{in frequency domain}\end{matrix} \quad Y(\omega)$$

Now,

$$Y(\omega) = T(\omega)\, X(\omega)$$

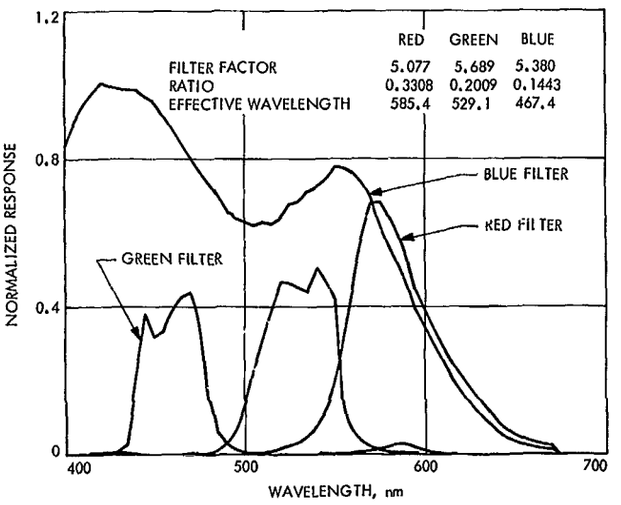


Fig. 38. Normalized response vs wavelength, *Mariner VII*

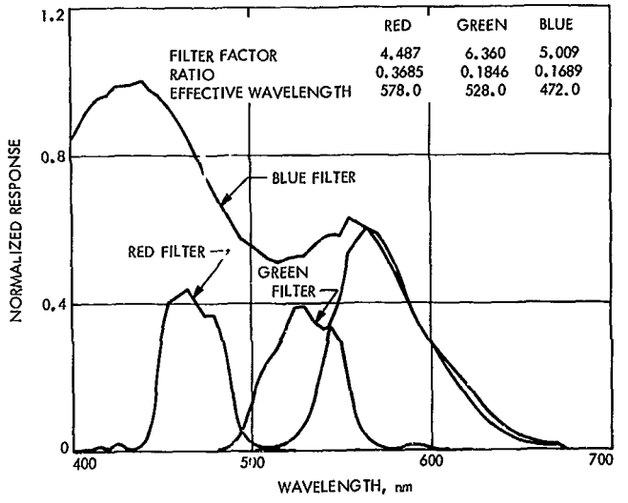


Fig. 39. Normalized response vs wavelength, *Mariner VI*

where $T(\omega)$ is defined as the modulation transfer function. This $T(\omega)$ is helpful in complicated systems in getting at certain quantities of interest. In optics, the MTF is directly related to the highest resolution one can obtain from an optical system.

The MTF can be characterized by putting in known signals of specific frequencies and measuring the output function $Y(\omega)$. This was accomplished in the *Mariner* Mars 1969 television system by producing test targets with low-contrast sine waves of various frequencies.

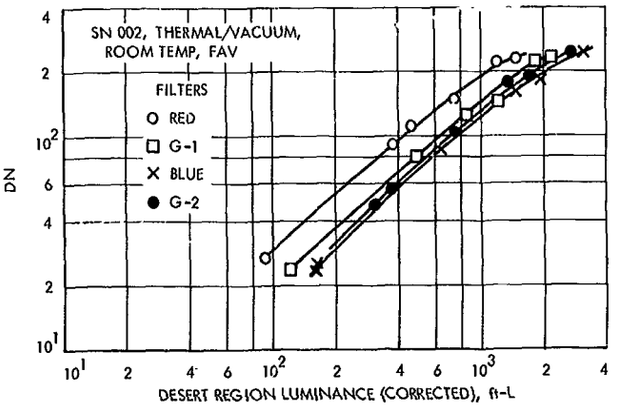


Fig. 40. *Mariner VII* light transfer characteristic, wide-angle camera

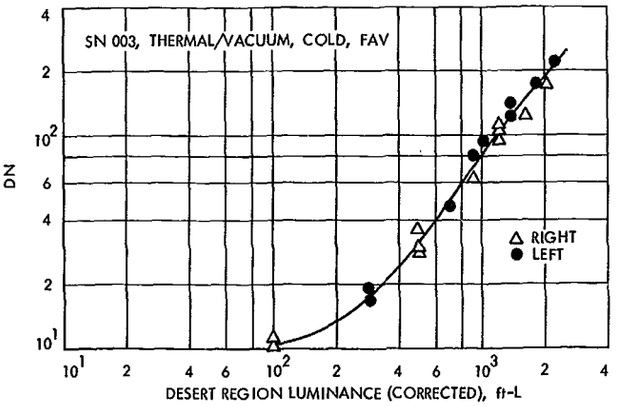


Fig. 41. *Mariner VII* light transfer characteristic, narrow-angle camera

These sine wave bursts were formatted in a complex sine array. The sine waves were located in the center and all four corners of the sensor format. The data depicted in this section (Fig. 43) was obtained from the central burst of sine waves only. The sine waves were produced on the test targets such that the maximum transmission was 60% and the minimum transmission was 40% with the nodes centered at 50%, which gives 20% modulation. This modulation was enhanced by the cuber circuit. Since high-contrast signals would tend to saturate when enhanced by the cuber circuit, the low-contrast sine waves were needed to characterize the MTF of the TV subsystem accurately.

The actual MTF of the system is dependent on the optics, the vidicon, and the electronics. The following data was reduced from various calibrations tests and has not been analyzed completely at this time. The

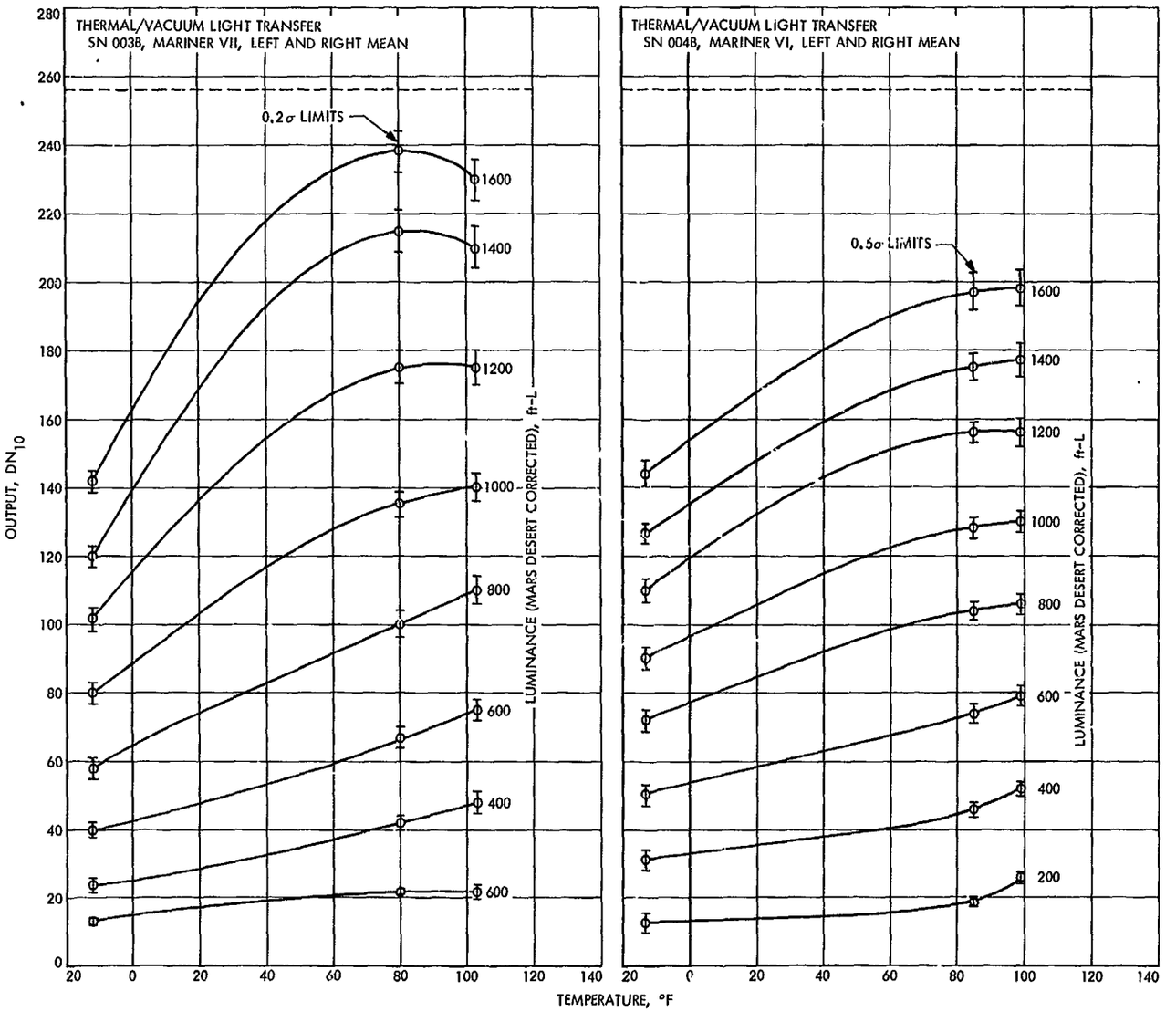


Fig. 42. Spectral dependence as a function of subsystem operating temperature

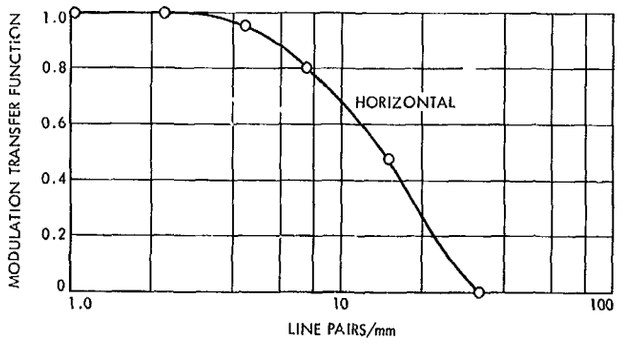


Fig. 43. Nominal horizontal modulation transfer function, *Mariner VI*, camera B, bench calibration

vertical and the horizontal response data were obtained by rotating the test target 90 deg.

4. CAV-DV transfer function. To characterize the cuber circuit response in terms of the system digitized video output, the composite analog video was compared with the digital video with an electrical ramp voltage inserted in place of the camera video. The transfer function between these two signals had to be known since the FAV would not be available during the mission and the DV would be required to provide information to restore the dc level to the analog-video. This data also provides a check on the cuber response.

F. Flight Acceptance Testing

To insure that each flight TVS would be able to withstand the launch and flight environments, each system was subjected to vibration and thermal/vacuum environments. The severity of the environment was intended to be realistic from a mission standpoint and was less severe than the type approval test levels (see previous section of this document).

The subassemblies were vibrated at predicted launch levels, both randomly and sinusoidally, in three axes. Performance was verified after each axis of vibration. The hardware was not operating during vibration tests.

The thermal/vacuum environment acceptance tests were combined with the thermal calibrations as an expedient. The TVS was placed inside a thermal/vacuum chamber which was provided with an optically flat window. This window allowed stimulation of the cameras with the calibration image sources. The TVS was operated at pressure 1×10^{-5} torr and at temperatures reflecting the predicted extremes of the actual mission.

G. System Testing

System testing had the following objectives:

(1) To verify TVS functional performance with respect to design specifications.

(2) To verify TVS performance stability with respect to previous subsystem and spacecraft system-level testing.

(3) To monitor the functional performance of the several series spacecraft subsystems through which the TVS must be commanded and through which the TVS data must be processed during mission operations. The spacecraft subsystems which are directly related to TVS command, data acquisition, and data recovery are power, radio, command, telemetry, data automation, data storage, central computer and sequencer, scan control, and temperature control.

Spacecraft system testing of the TVS flight hardware included:

(1) Initial system test at Spacecraft Assembly Facility (SAF).

(2) Post space simulation system test at SAF.

(3) Preshipment system test at SAF.

(4) Final system test at AFETR building AO.

A simplified TVS system test configuration is presented in Fig. 44.

The TVS system test procedure/playback sequence was designed to exercise the TVS through all of its far- and near-encounter functional modes and to generate adequate data for statistical analysis of the functional performance of the several series of spacecraft TVS data processing subsystems. As nearly as possible, this procedure remained unchanged during the several system tests. This provided a consistent set of data from which TVS performance stability was verified. The data processing facilities and hardware was used in support of TVS system test data generation/reduction are listed in Table 10.

During each system test a TVS representative was in attendance at the system test complex. As nearly as possible all real-time displayed TVS related data was analyzed in real time. Post-system test data analysis included a re-examination of the real-time displayed TVS hard copy, both line printer and photographic data,

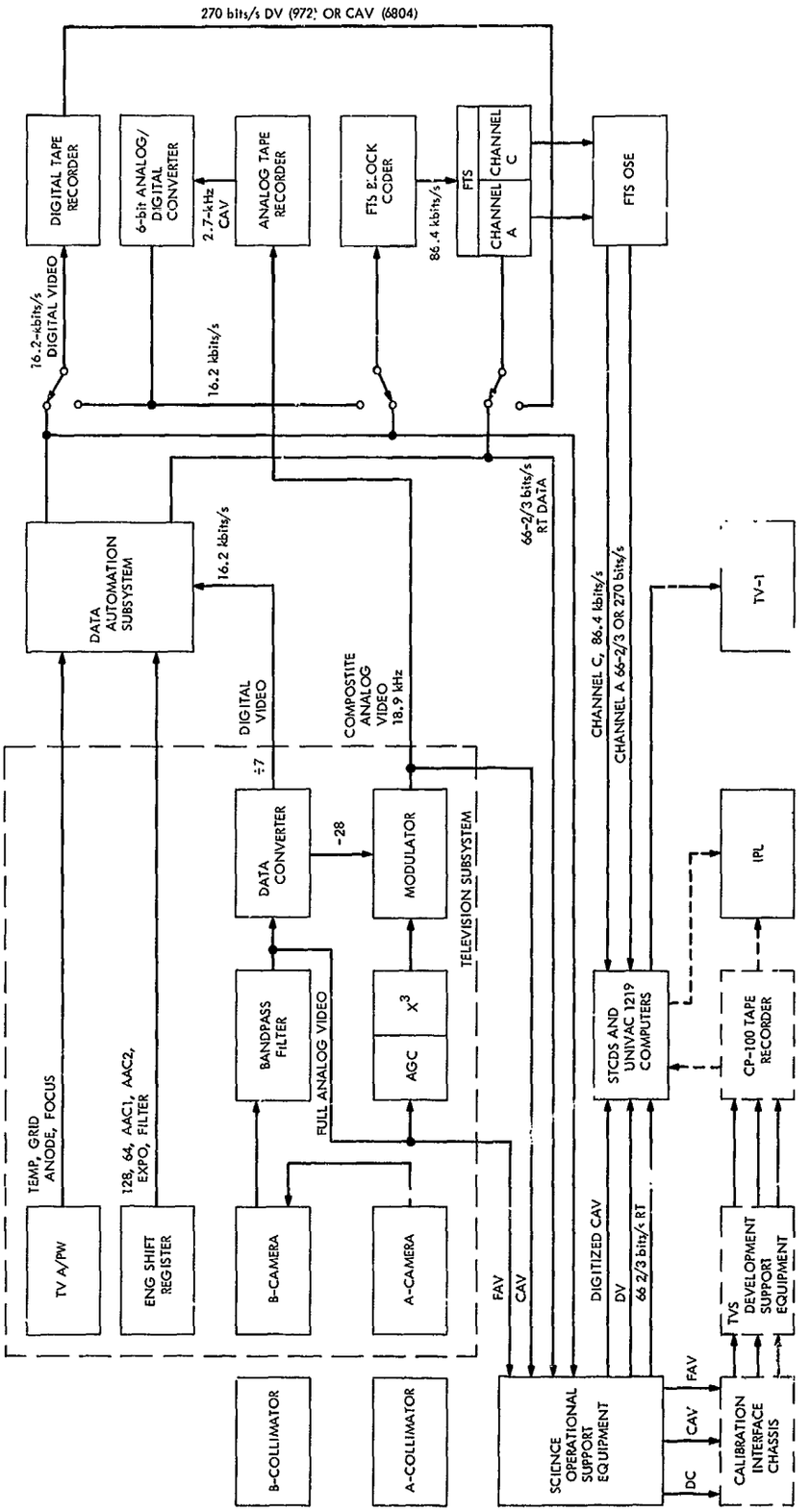


Fig. 44. Simplified TVS, system test and ca... ...ion configuration

Table 10. TVS system test data generation/reduction

Facility/hardware	Product
Science operational support equipment	Single line trace Polaroid photos
	Conrac monitor Polaroid photos
	Conrac monitor 35 mm negatives
System test complex data systems	Real-time line printer data
	Commands, status, events, TV engineering
	TV A/PW, error messages, and ATR playback sync status
	Non-real-time line printer data
	Tab listings of TV A/PW values
	Digital video ÷ 7 vs ÷ 28 logical comparisons
	Hardline digital video vs DTR playback digital video logical comparisons
	Hardline CAV PN-only amplitude histograms including Os and Is, mean and standard deviation
	Data storage subsystem ATR playback PN-only amplitude histograms including Os and Is, mean and standard deviation
Univac 1219 computer	Two-source video comparison plots of hardline CAV vs data storage subsystem ATR playback CAV
	Two-source video comparison printouts of hardline CAV vs data storage subsystem ATR playback CAV
	Two-source comparisons listed the mean and standard deviation of each video intensity level
TV-1	70-mm strip contact photos
	8 × 10 photos
	All photos included video intensity frequency histograms and gray scales

Table 11. Data analyzed for parameter verification

Data	Parameters verified
Real-time line printer data TV A/PW Engineering telemetry Commands, status, and events	Proper response of TVS as a function of both far- and near-encounter modes and stimulus levels
TV engineering 128-level video 64-level video AAC-1 AAC-2 Exposure time Filter position	
TV A/PW Temperature Grid voltage Anode voltage Focus current	Stability of listed parameters and proper sequencing of readouts between cameras A and B
Engineering telemetry Bay VII temperature A vidicon temperature B vidicon temperature B optics temperature	TVS temperature is within limits during system testing and is related properly to certain temperature-dependent TVS parameters
Commands, status, and events Commands Error messages Mode status of the various subsystems interfacing with the TVS TV picture and line count Out-of-sync messages during data acquisition and playback	Proper sequencing and response of TVS during commanding and automatic operation; out-of-sync messages were used as a gross measure of combined TVS/DSS performance
System test photo analysis Dark current Digital video sampling rate Raster/fiducial mark relationship Line width Raster skew Focus Dynamic range Coherent noise Random noise Vertical deflection Horizontal deflection Image retention Vidicon blemishes	Stability of listed parameters after each system test

along with evaluation of the non-real-time TVS related data products. The data analyzed for verification of specific parameters is detailed in Table 11.

Non-real-time A/PW tab listings and frequency histograms were examined to evaluate the stability of the A/PW measured parameters. Non-real-time logical comparisons were examined to verify proper TVS processing of the digital data, which was inserted into the analog video during retrace time, and to verify the integrity of video coding after processing by the data storage subsystem and the FTS.

Non-real-time, two-source analog video comparison printouts and plots were examined to evaluate data

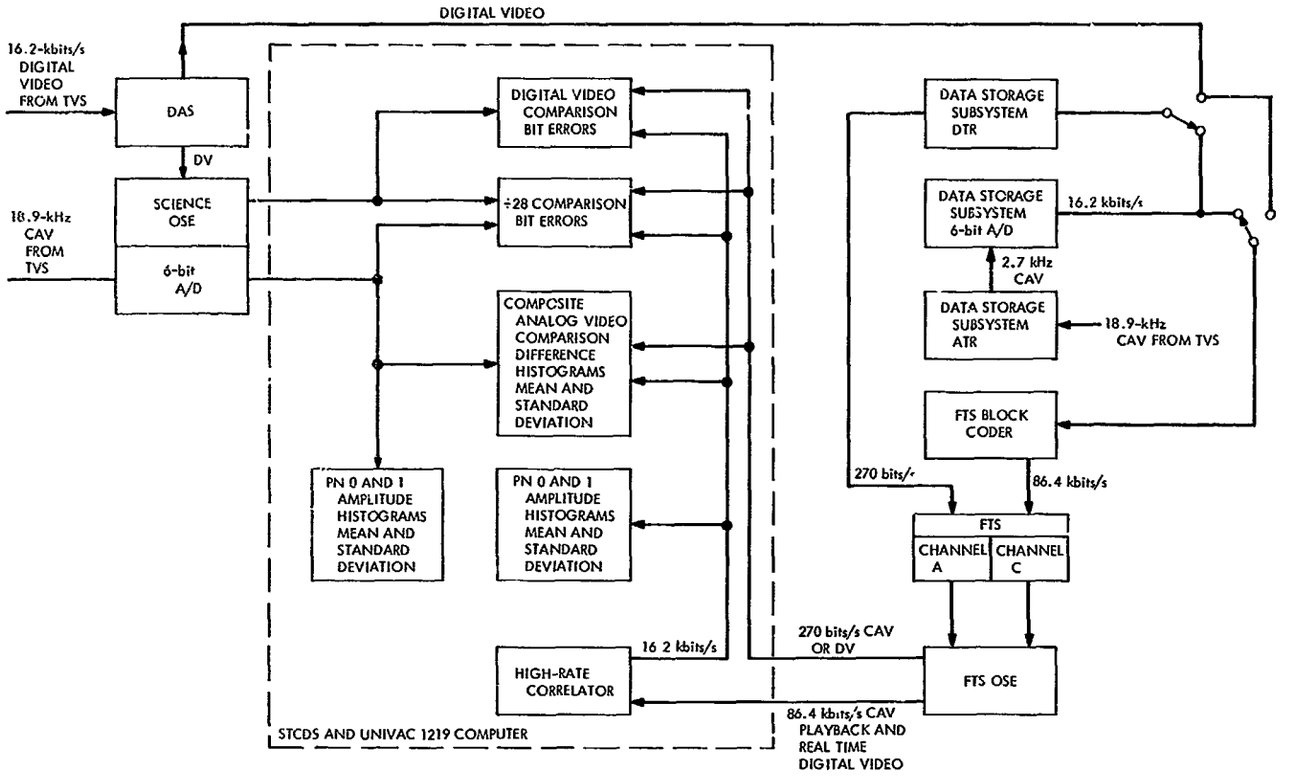


Fig. 45. System test video comparison

storage subsystem/FTS analog video processing. Also, PN-only histograms generated from TVS hardline CAV were compared with PN-only histograms of data storage subsystem/ATR playback as a gross measure of relative track to track ATR gain and gain linearity. A block diagram showing the various system test video comparisons is presented in Fig. 45.

V. Television Image Processing

The Image Processing Laboratory (IPL) provides support to the television experiment manager and, through him, to the project scientist and the television principal investigator for the quantitative digital processing of *Mariner* Mars 1969 television calibration data and flight imagery. Because of the nonlinear contrast emphasis electronics inherent in the television subsystem, digital processing is required to even approximately quantitative intensity measurements can be made on the television data. The full realization of the scientific objectives of the television experiment requires the additional careful correction for systematic noises, photometric nonuniformities and nonlinearities, geometric nonlinearities, and modulation transfer degradation of the television subsystem.

The Image Processing Laboratory of the Science Data Analysis Section is a facility consisting of a digital computer and special-purpose peripheral equipment, image scanning and display hardware, and the specialized software system designed for image manipulation and processing. The IPL is staffed with personnel specializing in image analysis, image processing technique development, hardware development, and operational support. A schematic diagram of the overall IPL configuration is shown in Fig. 46.

The major phases of the IPL support to the *Mariner* 1969 television experiment include preflight video subsystem calibration support, near-real-time flight image analysis support to the mission operations, and detailed postmission image analysis support to the television experiment team. Preflight calibration support includes participation in the design and preparation of special procedures and test targets, preliminary calibration data analysis for engineering evaluation, and the detailed

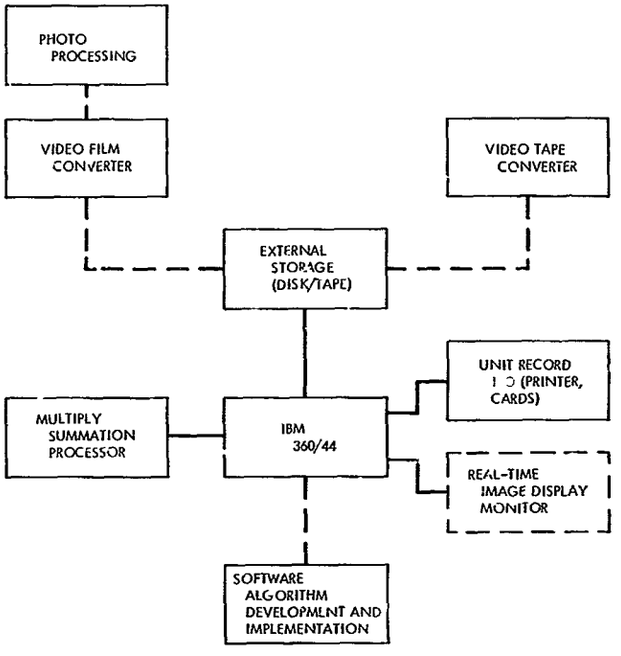


Fig. 46. Image Processing Laboratory configuration

reduction of calibration data for the quantitative restoration of flight imagery. Inherent in the preflight activities was the development of image processing techniques and software for the correction of *Mariner* 1969 unique video subsystem characteristics.

Near-real-time mission operations support includes the evaluation of pre-encounter video test data and the preliminary enhancement and restoration of selected flight imagery. This data was intended to provide information on the operation of the television subsystems relative to the photographic characteristics of Mars, with a possible impact on the encounter strategies of *Mariners VI* and *VII*.

The postmission image analysis phase includes the careful evaluation of preflight calibration data relative to *in situ* television subsystem operating characteristics and the detailed application of corrected calibration data to the restoration of quantitative aspects of the flight images. This work is in direct support of the television experiment team and the scientific evaluation of the *Mariner* 1969 photographs of Mars.

This report contains brief descriptions of the video subsystem data formats and characteristics as they relate to image processing, as well as a survey of the various aspects of *Mariner* Mars 1969 image processing and analysis. More detailed descriptions of the video characteristics and data formats can be found in the television subsystem and science ground data handling sections of this report.

A. Image Data Formats

Figure 47 is a simplified block diagram of the *Mariner* Mars 1969 video subsystem. Major subsystems are the TV subsystem (TVS), including the cameras, head electronics, video amplifiers, cuber, automatic aperture control (AAC), and the data storage subsystem, including the analog tape recorder (ATR), analog channel A/D converter, and digital tape recorder (DTR). Analog video is recorded in the analog mode on the ATR and digitized on playback, whereas digital video is digitized before recording on the DTR or transmission in real-time over the block coder.

1. Analog video, far-encounter mode. Composite analog video (CAV) first passes through an X^3 amplifier (cuber) for contrast enhancement, and is then recorded in the analog mode on the ATR. In the far-encounter mode, the automatic aperture control (AAC) is locked in its lowest gain state, and the automatic gain control (AGC) is inhibited. The CAV is digitized to 6 bits in the analog A/D converter; CAV frames contain every twenty-eighth digital video sample recorded on the ATR during camera retrace time.

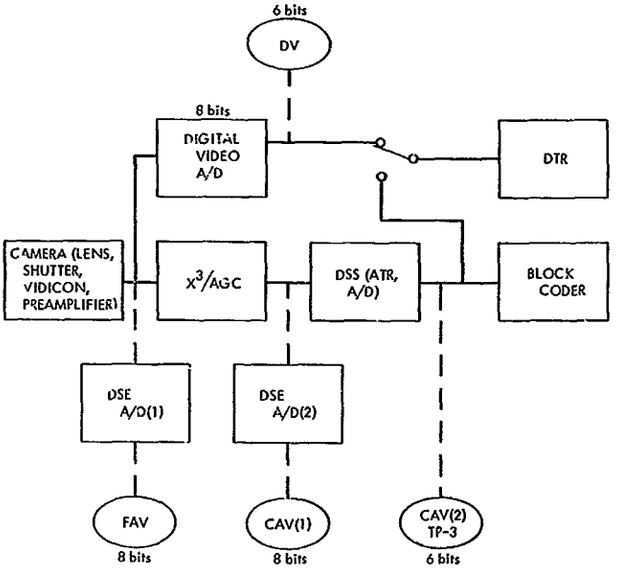


Fig. 47. Television image processing block diagram

2. Analog video, near-encounter mode. Near-encounter CAV, in addition to being acted upon by the cuber, is subject to two separate electronic gain adjustments. First, the AAC sets one of eight gain states, depending on the signal received from the AAC sense area in a previous A camera frame. Second, an AGC amplifier, acting in real-time, continuously adjusts gain to keep the CAV signal on the most sensitive portion of the cuber transfer curve. The AAC gain state information is transmitted in the science data stream, but no information is available on the state of the AGC; therefore, near-encounter CAV contains no photometric DC reference.

3. Digital video. Every seventh sample of the video data is digitized directly by a separate A/D converter in the television subsystem and encoded to 8 bits, of which the 6 least significant bits (LSB) are either recorded on the DTR and transmitted or transmitted directly over the block coder. In addition, every twenty-eighth sample is transmitted embedded in the CAV during the television retrace time. For each of these samples only the 4 central bits are transmitted; i.e., two LSBs and two MSBs are truncated. The digital video (DV) frames consisting of every seventh picture element also contain science telemetry introduced during the active line scan producing a "data bar" corresponding to the central 26 samples of each DV line. Therefore, of 134 possible DV samples per line, only 108 are transmitted. Near-encounter DV is, like the CAV, affected by the AAC gain state but is not affected by the AGC amplifier, thereby providing a reference for DC restoration.

4. Calibration data formats. Calibration data differs from flight data in three significant areas. First, all calibration data contains full analog video data (FAV), extracted upstream of the cuber and AGC and digitized externally in the developmental support calibration test equipment (DSE). Second, the calibration CAV is digitized in the DSE as opposed to the flight DSS. Third, the DV frames contain 134 samples per line (no data bar). These special formats were provided to allow adequate calibration of the camera systems and to isolate the transfer properties of the flight on-board processing electronics.

B. Calibration Data Processing and Analysis

Calibration data is necessary for the development and application of image processing techniques for the quantitative restoration of image intensity and geometry information. The general categories of system performance for which calibration data must be collected include noises and photometric, geometric, and modulation transfer function distortions. Each of the calibration tests described below was designed to provide information pertinent to a specific performance variable. A more complete discussion of calibration procedures and rationale can be found in the television subsystem calibration section of this report.

1. TVS calibrations. TVS calibration data was obtained on near- and far-encounter mode flat fields, geometric distortion and modulation transfer function targets, complex gray scale targets viewed in various orientations to provide residual image data, simulated lunar limb and low-contrast surface scenes, orbit determination test targets, narrow bandpass filter targets for spectral response characterization, and miscellaneous special tests designed to provide data on light leaks and out-of-field scattering. Nearly 6000 calibration frames were recorded; most of these were recorded on an analog tape recorder (Ampex CP-100) and converted to IPL formatted tapes by 1219/TV-1. Approximately 600 PTM frames were recorded directly by IPL, using a "hardline" data link to the thermal/vacuum test area. The SN 004 and SN 002 AFETR calibration CP-100 tapes were converted directly in IPL, approximately 400 frames in all.

2. Data storage subsystem calibrations. As shown in Fig. 47, the data storage subsystem includes the ATR and playback A/D converter. Since the ATR processes the analog video, the possibility of distortion exists, and calibration of ATR characteristics is necessary. The object of the data storage subsystem calibrations was to define noise characteristics, "flat field" transfer properties, and the modulation transfer function (MTF) for each of the four tracks of the ATR, outputs being measured in terms of DN produced by the playback A/D converter. Flat field transfer functions were obtained using an 18.9-kHz carrier at constant p-p voltage as the input. This data also served to statistically characterize the various noises. For MTF data, sine wave modulation up to 10-kHz was imposed on the carrier at various carrier voltages, and the output DN normalized to a response relative to that corresponding to the unmodulated carrier. Data storage subsystem coherent noise characteristics were measured by means of noise power spectra obtained using a fast Fourier transform algorithm; ATR dropouts were analyzed from a statistical point of view, using cross-correlation matrices. In addition to bench calibrations, flight and spare data storage subsystems were exercised in the systems tests as portions of the science payloads.

3. *System tests.* The SAF and AFETR calibrations, in addition to providing TVS calibration data in the formats discussed, produced flight-type data streams via the data storage subsystem, DTR, and spacecraft transmitters. These were played through a simulated station receiver using the CTA-21 system, thereby exercising the complete data recovery, logging, and reformatting loop which was employed in mission operations. The resulting Mission Operations System (MOS) IPL-formatted tapes, again produced by 1219/TV-1, were used by IPL to check out data acquisition software and exercise certain postencounter processing programs.

C. Flight Image Processing and Analysis

The processing of flight image data by IPL is summarized in Fig. 48. The various tasks indicated in the diagram can be assigned to one of four general categories, as listed in the following paragraphs. The first of these, reconstruction, receives the most attention in this discussion, since it involves the removal of the effects of *Mariner* Mars 1969 unique on-board processing, restoring the video data to the equivalent of the far-encounter mode (AAC clamped) FAV data obtained during calibration. Unlike reconstruction, the remaining three categories are not specific to *Mariner* Mars 1969, in that they are entirely analogous to similar corrections applied to previous flight data, including *Ranger, Surveyor,* and *Mariner IV.*

1. Reconstruction.

a. ATR and transmission defect removal. The ATR dropouts and transmission errors can cause portions of lines in the raw pictures to deviate significantly from adjacent lines producing short, vertically well-defined defects. These defects are, by the nature of the processes which produce them, always 1 pixel in vertical extent and a number of pixels in length. A program has been developed which recognizes and automatically repairs defects of this type. The repair consists of replacing the anomalous value by the average value of its neighbors in the preceding and following lines, respectively.

b. ATR transfer function decalibration. The ATR A/D converter produces some relative distortion of the CAV sample values from track-to-track. The transfer functions of the flight ATRs have been determined in data storage subsystem calibrations and these distortions can be removed from the flight data within the limits imposed by ATR stability.

c. MSB restoration. The effect of MSB truncation is indicated diagramatically in Fig. 49. It is obvious that MSB restoration can become quite difficult for active scenes. Restoration of MSBs to the DV using CAV data is possible in the far-encounter mode only since the AAC and AGC are then inoperative. Correlative CAV and DV will not, however, be received for most of the far-encounter sequence pictures; and so far-encounter MSB restoration will involve iterative procedures similar to those for near-encounter digital video.

Since the CAV contains no photometric reference in near-encounter mode, DV MSB restoration must be done independently, using CAV data as a subjective guide only. A program has been developed which makes a first pass at MSB restoration, based on internal data smoothness and consistency. The products of this processing are not perfect because of random ambiguities in applying the data smoothness criteria, and they must be iterated and adjusted by hand, using the correlative CAV pictures as a contextual guide. An interactive display console and its accompanying software system, developed to assist in this task, has been found to reduce the processing time required for MSB restoration by a significant factor. The difficulty of MSB restoration increases greatly with increasing scene contrast and activity. Once determined, the DV data numbers are used to provide an accurate photometric reference for the AGC reconstruction process.

d. Noise removal. Techniques have been developed for the removal of periodic noise from the video data. These techniques involve the generation of fast Fourier transform bandpass filters based upon the analysis of noise power spectra. Using two-dimensional filtering techniques, a noise pattern containing the periodic noise can be extracted from a picture. This pattern is then processed using a data-dependent modulation matrix obtained by least-square fitting of the noise to the video data. The product of this process, after suitable scaling, is subtracted from the raw picture to produce a coherent noise-free picture. The noise removal techniques are tedious, involving as they do a considerable amount of intermediate analyses to generate appropriate parameters for the various steps in the procedure. Furthermore, it was anticipated that the techniques would have to be applied on a per frame basis because of the variable character of coherent noise noted in the data.

e. Cuber effect removal. By means of a comparison of FAV and CAV calibration data, a cuber transfer function curve was generated for each of the camera systems.

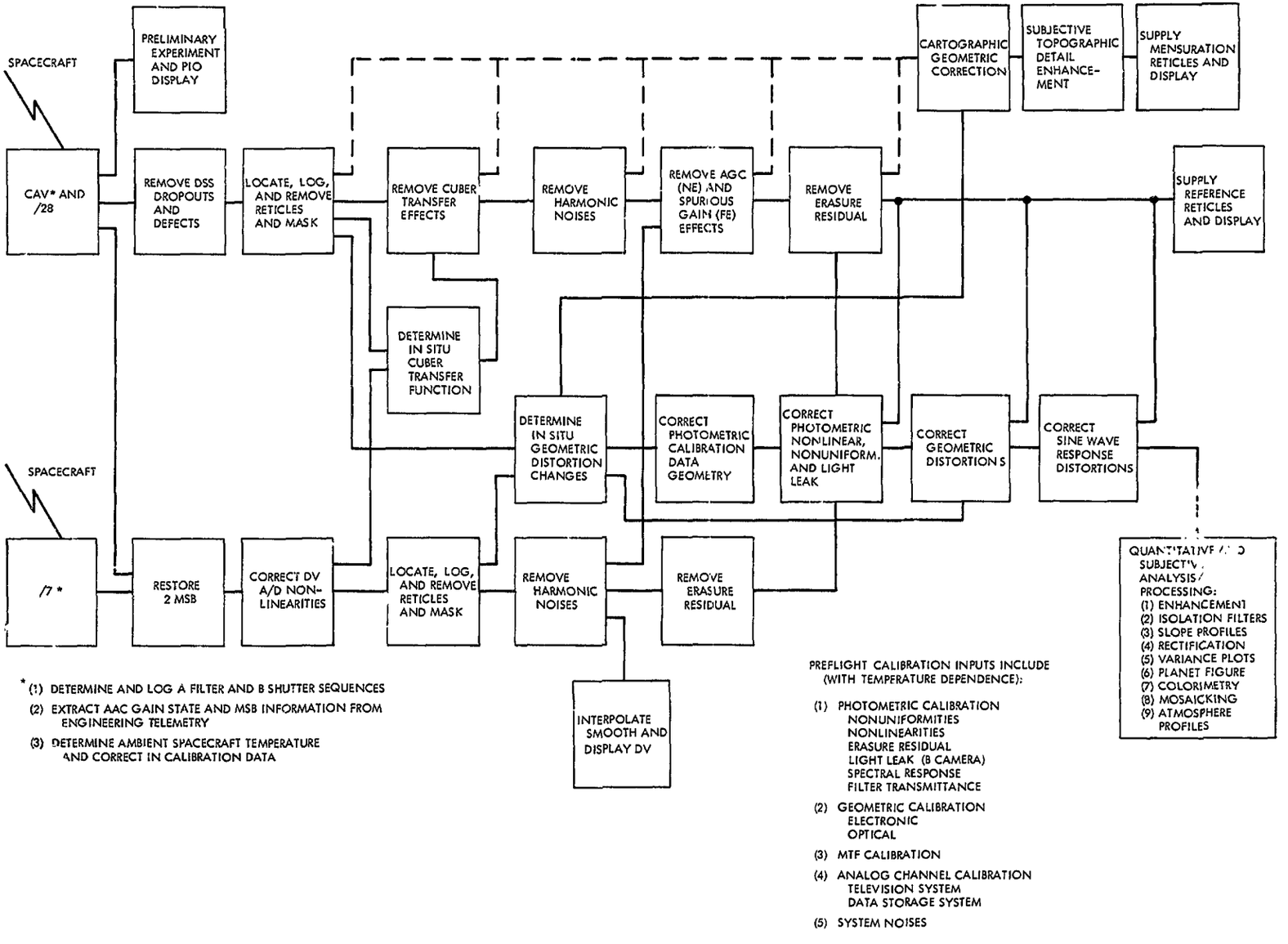


Fig. 48. Image Processing Laboratory encounter data flow

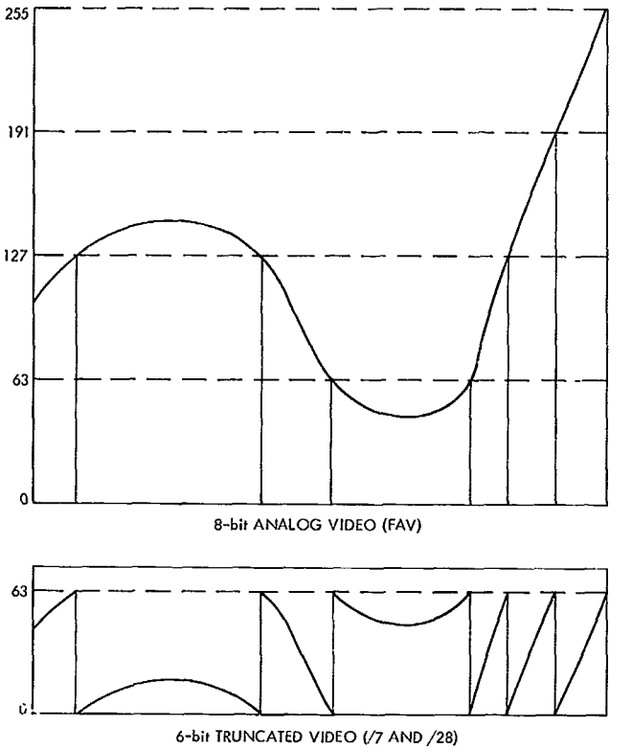


Fig. 49. Effect on MSB truncation

This curve was applicable to flight data for first-order cuber effect removal. It was considered possible to acquire *in situ* measurements during the far-encounter sequence to refine the cuber transfer curve for more accuracy in the cuber effect removal. This was to be accomplished by means of a comparison of CAV with corresponding DV after MSB restoration for those few pictures for which both CAV and DV are received. The success of these measurements was limted by the system noise levels in flight.

f. AAC gain effect removal. Near-encounter mode flat field tests were included in the calibrations in order to provide data on the relative magnitudes of the various AAC gain states. This data was obtained by means of adjusting input illumination levels in such a way as to cause the AAC to change gain states automatically. Comparison of the FAV output DNs with corresponding values obtained by interpolation to the same light values in the far-encounter mode FAV data provides a measure of the magnitude of the AAC gain state increments. After MSB restoration, DV data was corrected by the appropriate AAC gain state factor before being employed to restore a photometric reference to the CAV.

g. AGC effect removal. After restoration of MSBs and AAC gain state correction, DV is applied to CAV to remove AGC gain effects. This requires a knowledge of the DV-decubed CAV transfer function, obtained from calibration data and verified *in situ*. Since DV is every seventh relative to CAV, the granularity of the DV-generated gain field may in some instances be too coarse for accurate correction This effect is, of course, worse by a factor of 4 in the central region corresponding to the DV "data bar," where /28 samples must be used to generate the gain field. The development of techniques to accomplish the AGC correction therefore represented a significant portion of the IPL pre-encounter preparation.

h. Residual image removal. The final step in the reconstruction process is the removal of residual images resulting from incomplete erasure of the vidicon. FAV calibration data has been used to characterize the erasure residual properties of the several cameras. Residual image sensitivity maps have been generated for each of the flight vidicons, using data derived from crossed-complex gray bar targets and ascending-descending light-value flat fields. These maps have been found to be unique to the particular vidicon tested and unrelated to vidicon shading characteristics. Residual images typically do not exceed 10–15% of the previous exposure values, and can be corrected to within a few DN using the residual image sensitivity map as a modulation matrix to produce an effective residual picture which is then subtracted from the picture being corrected. Both the corrected and previous (residual-forming) pictures must first be restored to the equivalent FAV (i.e., reconstructed) before this technique can be applied.

2. ***Geometric distortion correction.*** Two categories of geometric distortion characterize a television camera system. First, there is the optical distortion which presents a distorted image to the vidicon. Second, an electronic scanning distortion is introduced in the vidicon itself. Calibration data is available by means of which these effects can be separated and measured and correction matrices generated. In the course of calibration data reduction preparatory to the generation of photometric correction techniques, a data-dependent raster shift was noted. This effect made electronic geometric distortion correction necessary before residual image removal techniques could be applied to the flight data. Therefore, the plan was to apply the electronic portion of the geometric distortion correction to the flight data immediately after AGC effect removal. To this end, a program which automatically logs reseau positions and generates electronic geometric distortion correction parameters was developed.

3. Modulation transfer function correction. In order to restore the definition of edge detail in the flight pictures, the high spatial frequency response of the television subsystem must be restored. Calibration data containing modulation transfer function (MTF) information was obtained on all flight vidicons, and used in the generation of appropriate sine-wave response correction filters. The test targets used to characterize MTF were produced by IPL, using computer-generated sinusoidal spatial frequency functions at a contrast range selected to avoid saturation effects.

4. Photometric decalibration. The recovery of photometric significance from DN values in all portions of the image format requires the analysis of flat-field calibration data on a pixel-by-pixel basis. The light transfer properties of the vidicon are characterized at each picture element for restoring accurate luminance values corresponding to DNs observed at each pixel. Programs for the determination and application of luminance corrections for each pixel were developed and applied to the far-encounter flat-field data. Temperature coefficients were determined from thermal/vacuum data, so that corrections to flight data could be adjusted to the vidicon temperature at which the data was collected.

D. Image Processing Laboratory Preliminary Products

Preliminary or "quick look" products anticipated for the period immediately following the *Mariner* encounter are described here. The products actually delivered in this period, which included approximate coherent noise removal, are described in Volume II of this report, as are all final processing steps and products.

VI. Infrared Spectrometer Subsystem

A. Introduction

The infrared spectrometer (IRS) was developed under a NASA study contract to Prof. George C. Pimentel of the University of California at Berkeley. These studies took place in 1965 and 1966, and in 1967 the contract for the *Mariner* Mars 1969 IRS instrument (Fig. 50) was executed.

B. Experimental Objectives

The IRS experimental objectives were as follows:

(1) Detect the presence and amount of all polyatomic atmospheric constituents, including those that suggest biochemical processes, affect the ambient surface temperature, and limit the ultraviolet light flux at the surface.

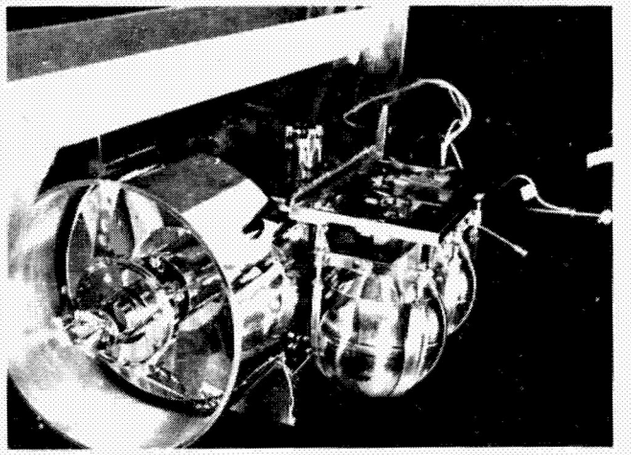


Fig. 50. Infrared spectrometer

(2) Determine the compositional variations of atmospheric constituents, particularly water vapor relative to geographic locale.

(3) Obtain data concerning surface composition, gas temperature, surface albedo, and surface temperature.

C. Constraints and Requirements

The following general requirements were requested to enhance the performance of the instrument:

(1) An equatorial scan trace was preferred to a polar scan trace.

(2) The trace should cross light and dark surface features.

(3) Instrument cooling must begin 18 to 24 min before upper atmosphere scanning.

(4) A significant amount of dark side viewing at not too oblique angles should be obtained.

(5) Scan traces should follow closely the narrow-angle TV scan trace to permit possible correlation of results.

(6) The terminator crossing should be as close to the equator as feasible.

1. Optical characteristics.

a. Optical pointing. The optical axis of the spectrometer was offset from the TV line of sight $+1 \pm 0.3$ deg in clock and -4 ± 0.3 deg in cone. This offset, designed to provide the maximum overlap between TV-B and the IRS, was consistent with the requirement that the

IRS viewing direction be greater than 300 km above the Martian limb when the TV axis crossed the limb.

b. Field of view. A circular aperture, 10 in. in diameter, had a 5-deg unobstructed view of the planet at encounter.

2. Thermal characteristics.

a. Monochromator and telescope. The telescope and monochromator were to be maintained at -38^{-10}_{+5} °C (235^{-10}_{+5} °K) during both cruise and encounter modes.

b. Pressure vessels. The pressure vessels required an unobstructed view of free space of sufficient solid angle to guarantee a temperature of -43 ± 15°C (230 ± 15°K) at encounter.

c. Radiation plate. The radiation plate required an unobstructed view of free space of sufficient solid angle to guarantee a temperature of -118 ± 5°C (155 ± 5°K) during encounter.

D. Description

The IRS instrument is composed of two major subassemblies: (1) Telescope–monochromator (including electronics) and (2) gas-delivery system. The monochromator-telescope is $11 \times 11 \times 20$ in. and weighs 25.3 lb. The gas-delivery system is $6 \times 7 \times 12$ in. and weighs 13 lb. Power required is:

(1) Cruise, 2400-Hz square wave: 4.5 W.

(2) Encounter, 2400-Hz square wave: 4.0 W.
400-Hz square wave: 3.8 W.

(3) Cruise and encounter, dc heater: 4.5 W.

The telescope assembly (Fig. 51) is an $f/2.3$ 10-in. Dall–Kirkham with a field of view of 5 deg. The mirrors are polished aluminum, Kanigen-coated, optically polished,

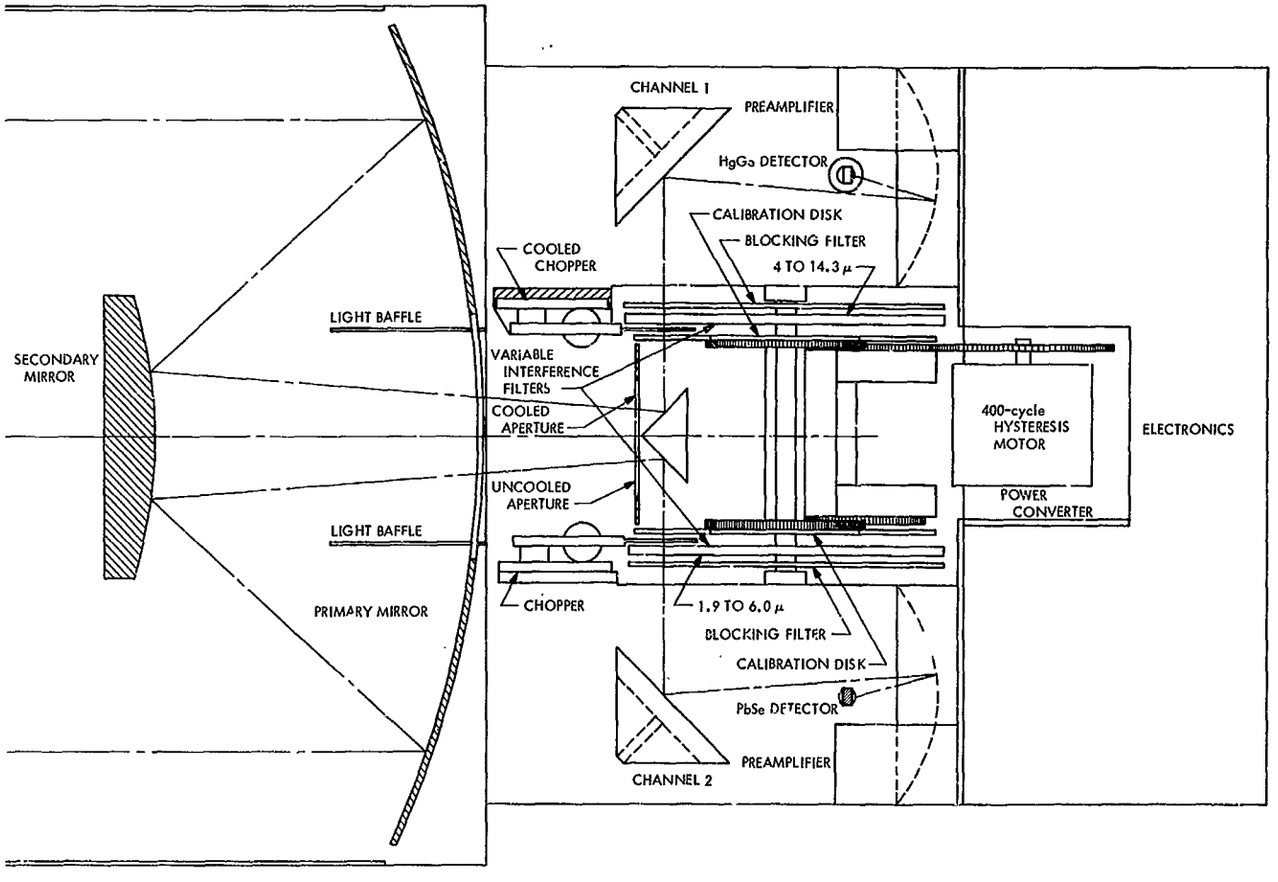


Fig. 51. Infrared spectrometer mechanical-optical layout

aluminized, and overcoated with a thin coating of SiO (silicon monoxide) ($\sim\lambda/10 = 500$Å). A 90-deg V-type beam-splitter divides the radiation into two channels. Channel 1 measures radiation from 4.0 to 14.3 μ, channel 2 measures from 1.9 to 6.0 μ. Radiation in each channel is passed through a filter disk and a calibration disk which are mounted on a common shaft continuously rotated by a drive motor. The rotation of the filter disks provides spectral scanning in each channel. After passing through the filters, the radiation reaches the two detectors. The channel 1 detector material is HgGe (mercury-doped germanium); channel 2 is PbSe (lead selenide).

1. Functional description. A separate blackened tuning fork modulates the radiation in each channel at frequencies of 500 and 550 Hz. The signal from each detector is fed to its associated preamplifier (Fig. 52), then to its synchronous filter and demodulator which integrates the signal and converts the ac voltage output of the preamplifier into a dc current to drive the log converter. The log converter and output amplifier linearly amplify the signal from the demodulator for all negative and small positive signals, and logarithmically compress it for the larger positive signals (approaching 6 V). The science multiplexer then selects either channel 1 or channel 2 data for presentation to the science A/PW converter, which changes the analog signal to a pulse-delay form for presentation to the DAS.

2. Calibration. Internal calibration is provided by the calibration disk, whose clear, opaque, polymer segments provide planet data, blackbody calibration, and wavelength calibration, respectively.

3. Cooling system.

a. Gas-delivery system. The channel 1 detector is cooled to 22°K by a two-stage nitrogen–hydrogen Joule–Thomson cryostat. The gases used in the cryostat are stored at 6000 psig in the nitrogen vessel and 5500 psig in the hydrogen vessel. The vessels are 85-in.^{3} titanium alloy 6Al-4V for nitrogen and 77-in.^{3} aluminum 2219 for hydrogen.

b. Radiation cooling plate. The channel 2 detector is cooled to 155°K by conduction to a radiation plate of 76-in.^{2} area.

4. Design evolution. During 1965, a laboratory bench model of the spectrometer was built and tested. Based upon this experience, a semiprototype, one-channel instrument was built in 1966. From these models, the design of the flight model evolved and a prototype instrument was built. The *Mariner* Mars 1969 infrared spectrometers contracted for in 1967 included an engineering prototype, a proof test model (PTM), and three flight instruments. The PTM was used for type-approval environmental testing.

5. Electrical interfaces. The electrical interfaces are shown in Table 12.

Table 12. Electrical interfaces

Subsystem-subsystem	From	To	Circuit name
004-037	Power	IRS	Encounter power, 2.4 kHz
004-037	Power	IRS	Cruise thermal power, 2.4 kHz
004-037	Power	IRS	Encounter power, 400 Hz, 1 phase
004-037	Power	IRS	DC thermal power
006-037	IRS	FTS	417 IRS electronics temperature
006-037	IRS	FTS	437 IRS radiator temperature
008-037	Pyrotechnics	IRS	IRS scan motor start
020-037	IRS	DAS	IRS A/PW science data pulse
020-037	IRS	DAS	IRS A/PW science reference pulse
020-037	IRS	DAS	IRS A/PW engineering data pulse
020-037	IRS	DAS	IRS A/PW engineering reference pulse
020-037	DAS	IRS	IRS science A/PW read
020-037	DAS	IRS	IRS engineering A/PW
020-037	DAS	IRS	IRS channel 1 select
020-037	DAS	IRS	IRS engineering multiplex
020-037	DAS	IRS	IRS reset engineering multiplexer
020-037	DAS	IRS	IRS channel 2 select
037-109	IRS	J-box	IRS pressure

6. Data format and telemetry bit rate. Science data consisted of alternate channel 1 and channel 2 samples. One sample was taken every 7.5 ms. Real-time data consisted of all engineering measurements and random sampling of the spectral data. Five samples of channel 2 data, six samples of channel 1 data, and 1 engineering measurement were taken in a 4.2-s interval asynchronous with the 10-s scan time. Seven real-time bits of each DAS frame represented the interval between the start of the frame and the first calibrate pulse. The total data rate was 1.33 kbits/s.

7. Mounting. The monochromator–telescope and the gas-delivery system are mounted to the spacecraft on the scan platform through mechanical mounts that provide thermal and electrical isolation.

E. Procurement

1. Parts. Most of the electronic parts, such as transistors, capacitors, diodes, and resistors were purchased by JPL and thoroughly screened before delivery to UCB. Some of the special components were purchased by UCB directly from the vendors: quality was assured by inspections both at the vendors and at UCB upon delivery. Some important components and the vendors are listed below:

Component	Vendor
Telescope mirrors and monochromator optics	Tinsley Laboratories, Berkeley, Calif.
Circular variable interference filters	Optical Coating Laboratories, Inc., Santa Rosa, Calif.
Motor	Gaylord Rives, Pasadena, Calif.
Cryostat	Air Products and Chemicals, Allentown, Penn.
Platings and coatings (gold)	Sel Rex, Los Angeles, Calif.
Gas regulators	Whittaker Corp., Los Angeles, Calif.
Gas vessels: nitrogen	Pressure Systems, Inc., Los Angeles, Calif.
hydrogen	Boeing Co., Seattle, Wash.
Manifold-pyrovalve	JPL/Pyronetics, Los Angeles, Calif.
Welded electronic modules	Philco, Palo Alto, Calif.
Printed circuit boards	Philco, Palo Alto, Calif.
Machine work	Reliance Tool and Die, San Jose, Calif. Associated Machining, Santa Clara, Calif.
Tuning forks	American Time Products, New York, N.Y.
Detectors	Santa Barbara Research Center, Santa Barbara, Calif.

2. Quality assurance. A quality assurance and reliability program was installed at the UCB to insure flight quality of the IRS instruments. A full-time JPL quality assurance engineer also participated in the fabrication and testing of the IRS instruments at UCB. Traceability, through the use of travelers, was kept on each part during the manufacturing of the instruments. Test records were kept where appropriate on materials such as potting compounds. All the electronic assemblies were inspected under a microscope, and each was photographed for a permanent record. Assembly, potting, and instrument testing were done in clean rooms to assure the flight integrity of each instrument. Also, some parts, such as mirrors and detectors, were maintained in a controlled humidity as well as clean atmosphere. The shipping of the instruments was accomplished in sealed carrying cases that were purged with dry nitrogen. During the design of the instruments and their first construction phases, reviews were held at JPL to determine the best parts, components, and construction methods.

F. Test Experience

1. Type approval testing. The TA tests were conducted at levels beyond the environment that the flight instruments were expected to experience at launch or in flight. The vibration testing was done at JPL and the thermal/vacuum tests of the instruments were done at UCB. Instrument failures occurred during both vibration and environmental testing, but fortunately all problems were solved before flight time. Some of these TA problems are listed below:

a. Vibration problems.

(1) Tuning fork vanes broke loose from their mounts.

(2) Log stack mounting broke.

(3) Cone snapped off of its legs.

(4) Tuning fork bent.

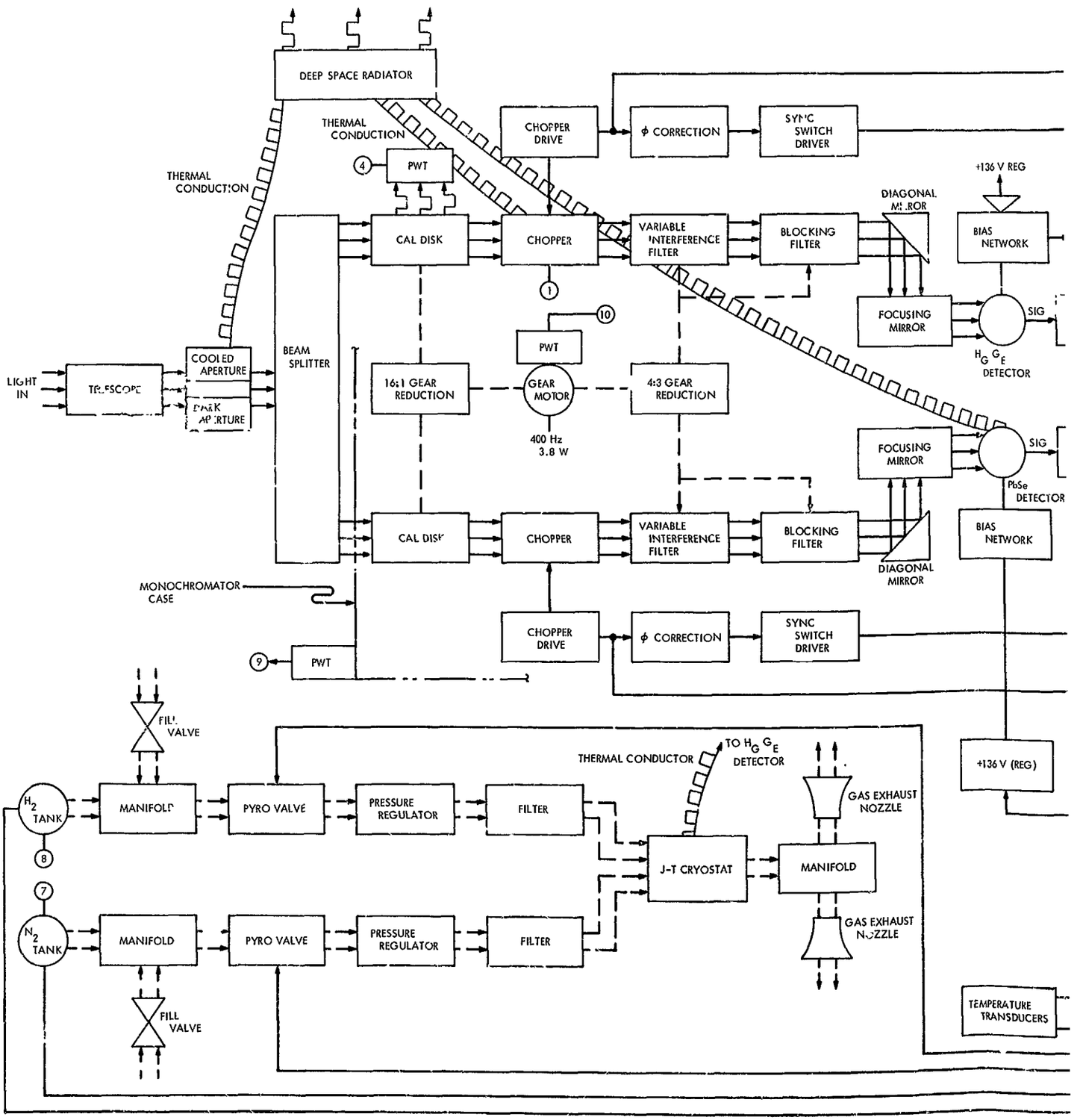
b. Other environmental problems.

(1) Particles in bearings caused gears to bind.

(2) Detector was noisy because of high temperature and humidity at SAF.

(3) Noise caused by dirt on slip ring.

(4) Mirror broke loose from its bonding.



FOLDOUT FRAME

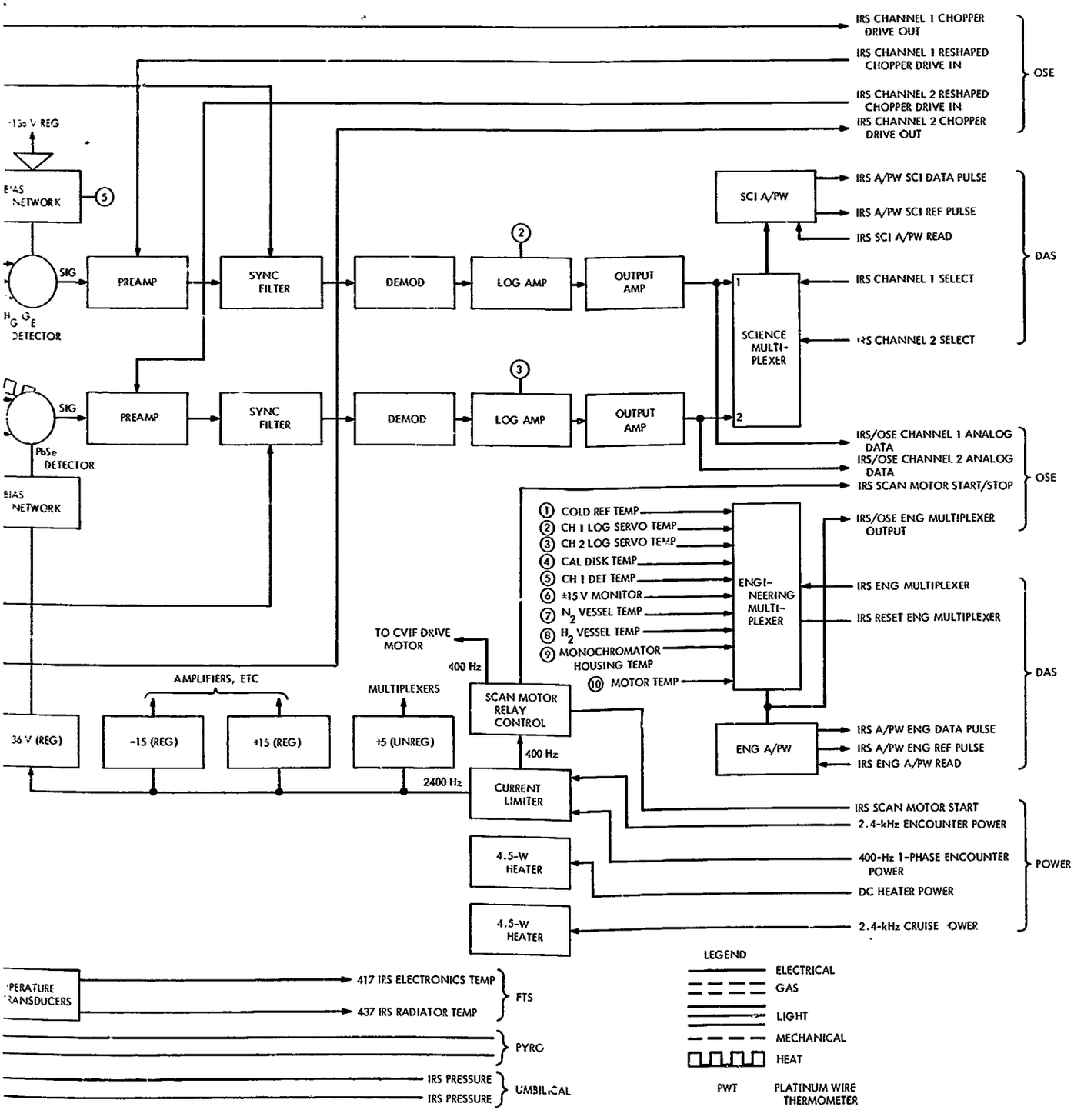


Fig. 52. Infrared spectrometer block diagram

FOLDOUT FRAME 2

PRECEDING PAGE BLANK NOT FILMED

2. *Flight acceptance testing.* The three flight units experienced only minor problems during the flight acceptance testing. However, during subsequent testing, several major problems did occur.

3. *System testing.* The system testing was conducted at four locations: (1) Spacecraft Assembly Facility (SAF), (2) JPL 10-ft space simulator, (3) JPL environmental laboratory, and (4) the JPL Facility at AFETR. Interfacing of the instrument with the spacecraft was effected at SAF, and system tests were performed to eliminate the problems of interreaction between the instrument and other elements of the spacecraft. Vibration of the spacecraft was done in the environmental laboratory. The 10-ft space simulator was used to create a vacuum and a cold environment for the spacecraft to simulate a mission to Mars. The vacuum and cold were also necessary conditions for test-firing the IRS cryostat. Several of the cryostat cooldowns were successful, but there were a number of failures caused by the cryostat plugging or the gear train locking up. At AFETR, final calibration of the instrument and system testing were accomplished.

4. *Problems.* Most problems were solved as the IRS instrument went through the preliminary stages of construction and testing. However, some were of major concern and would have affected the final data results. Some of these are listed below:

a. Cryostat. The proper cooling of the cryostat was probably the most significant of all the problems since it affected the channel I data and remained unsolved up to the final calibrations at AFETR. The cryostat plugged during tests in the space simulator at JPL and during the final instrument testing at UCB. The vendor was contacted and the cryostats were reworked, but during tests at AFETR the cryostats again plugged. Consultants from JPL were called in, and their review of the manufacturing process showed that the cryostat was being plugged by solder flux from the construction, followed by inadequate cleaning. Better manufacturing methods were introduced and although they were not completely satisfactory, it appeared that the probability of the cryostat working was greatly improved.

b. Gear train. The gear train, which turns the calibration disk, had undergone extensive test, but during space simulator tests it froze up because of improper materials and tolerances. Glass-filled Teflon bushings were substituted to correct the problem. Additional tests were conducted and no further problems were encountered.

c. Hydrogen gas bottle. Containment of the high-pressure hydrogen gas proved to be a serious problem. After the substitution of Inconel for titanium in the hydrogen vessel, it was reported that the Inconel 718 being used would be overly stressed by the high-pressure H_2 gas. Detailed testing by the Boeing Company revealed that a leak could develop in the Inconel 718 bottle for the particular high-pressure H_2 conditions. After appropriate testing it was decided to use aluminum 2219 alloy. Tests indicated that this alloy was not susceptible to the embrittlement problem.

VII. Infrared Radiometer Subsystem

A. Instrument Objectives

The objective of the infrared radiometer (Fig. 53) was to measure the equivalent blackbody temperature of selected areas on Mars. Measurements of the polar icecap may indicate whether it is composd of H_2O or CO_2 ice. Measurements across and beyond the terminator near the equator will provide a measure of the thermal inertia of the surface material and an indication of varying ground structure. The identification of cloud features of various kinds would also be facilitated by means of temperature discrimination.

B. Constraints

The basic instrument constraints were as follows:

(1) Weight: 7.5 lb max.

(2) Power: 3 W average from 2400-Hz source.

(3) Size: $3.2 \times 6.0 \times 9.0$ in.

(4) Operating temperature: from -30 to $+30$°C.

(5) Storage temperature: from -50 to $+55$°C.

Spacecraft constraints were as follows:

(1) Optical pointing: the instrument was to be boresighted with the TV to within $+0.3$-deg circle. Optical alignment between TV and IRR to be known within ± 0.1 deg.

(2) View of planet: a 20-cm² aperture was to have an unobstructed view of the planet subtending 0.7×0.7 deg.

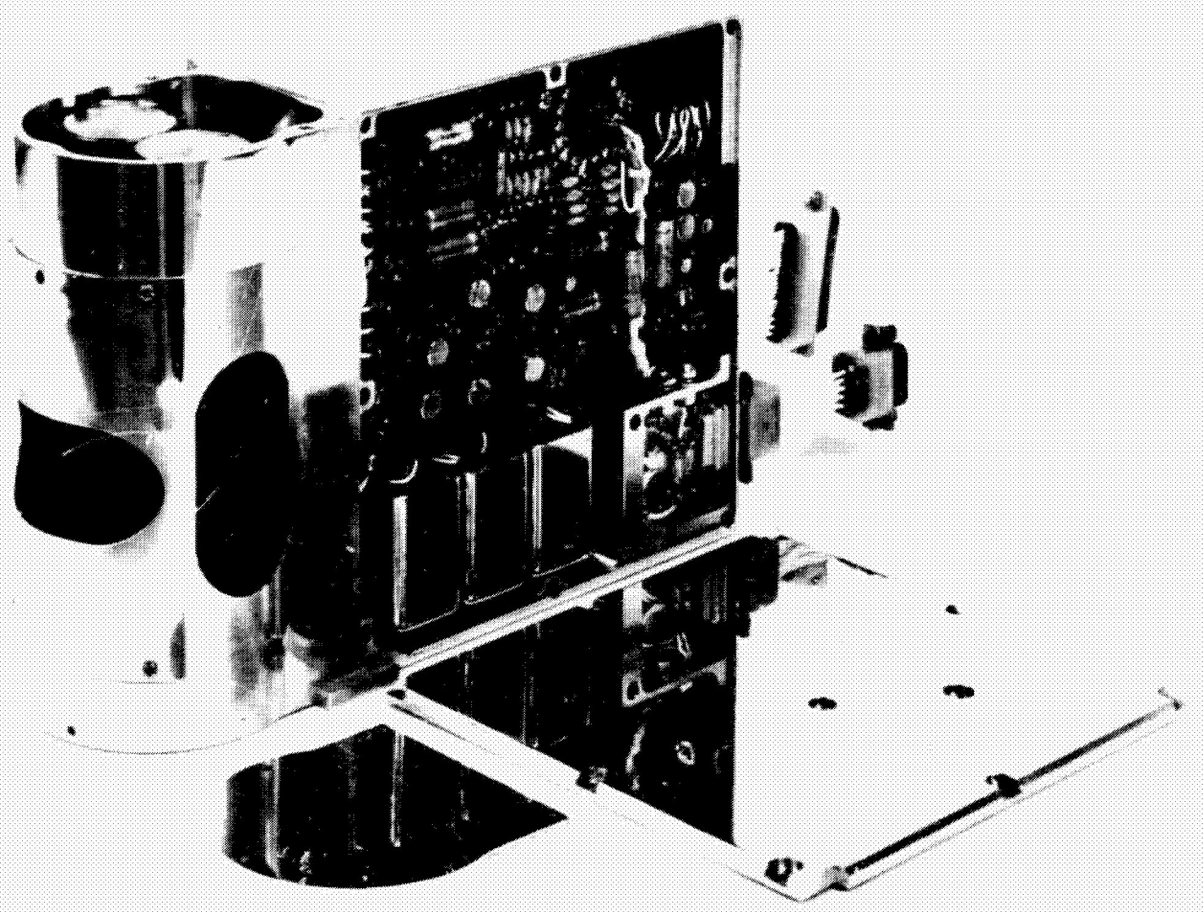


Fig. 53. Infrared radiometer

(3) View of empty space: a 20-cm² aperture was to have an unobstructed view of free space subtending 0.7 × 0.7 deg.

(4) Mirror positioning: the mirror was to be preset to the internal calibrate position prior to launch, so the optics and detectors could not be exposed directly to the sun during the mission. This preset operation could be initiated by FCS command DC-48.

(5) Instrument temperature at encounter: -10 ± 10°C.

(6) The instrument was to be mounted on the planetary scan platform through mechanical mounts that provided electrical isolation.

C. Instrument Description

The scan mirror (Fig. 54), driven by a bidirectional digital stepping motor, selects radiation to be measured from three sources:

(1) Space.

(2) Planet.

(3) Internal thermal reference.

Separate $f/0.85$, 1-in.-diameter aperture, refracting telescopes containing both detector and spectral filter provide two spectral channels, 8–12 μ and 18–25 μ, covering the temperature range 140–325°K. The radiation detectors are thin film thermopiles, each with five antimony–bismuth junctions. The photovoltaic output of each thermopile is electronically chopped by a voltage

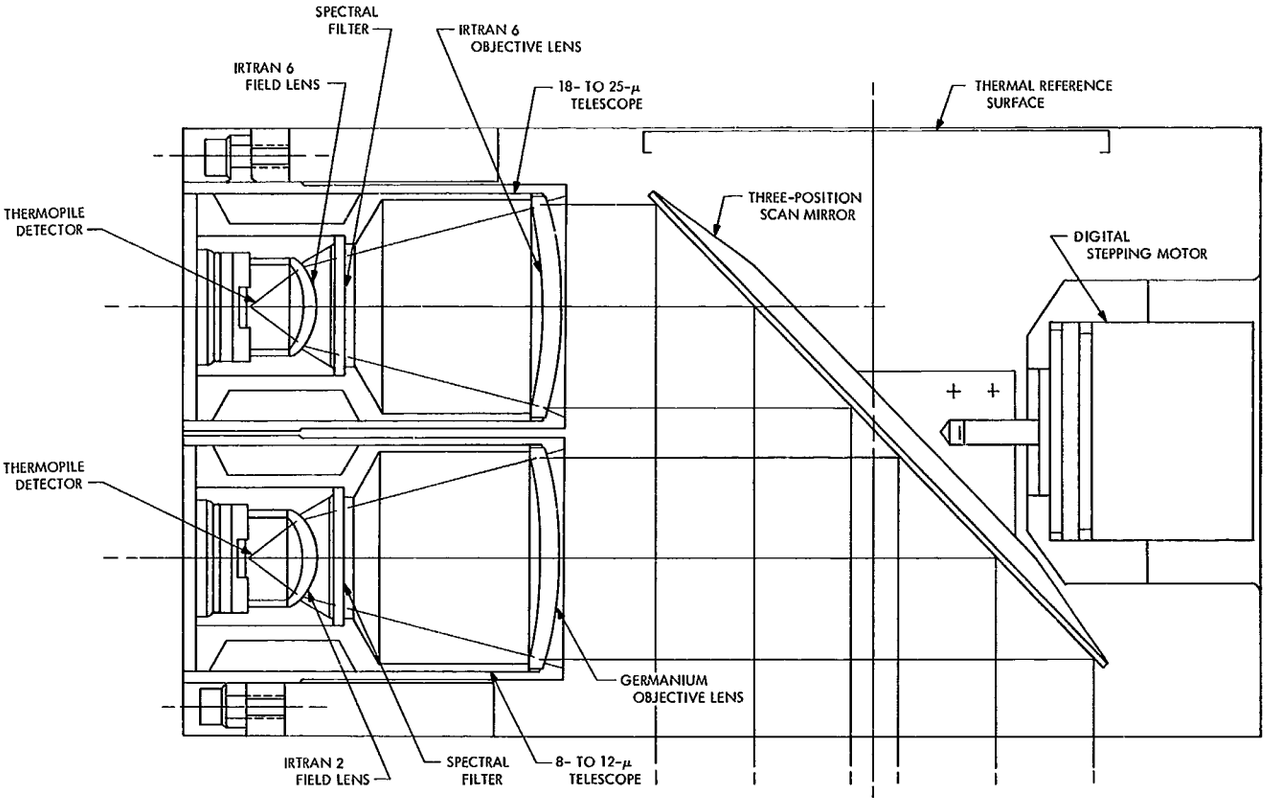


Fig. 54. Infrared radiometer, physical layout

doubling FET chopper, operating at 200 Hz. The resulting ac signal is then amplified and demodulated in a half-wave synchronous demodulator. Both chopper and demodulator are driven by a circuit which derives the 200-Hz drive signal by dividing down the 2.4-kHz power frequency.

A low-pass filter is used to determine the equivalent noise bandwidth of the system and filter out the 200-Hz ripple frequency. The filter bandwidth is 0.68 Hz and is sufficient to pass information for the frequencies of interest while restricting noise to an rms level of less than 0.1% of instrument dynamic range. The dc output of the low-pass filter goes to the memory-dc restore circuit, which causes the output of the system to be − 5 V when the scan mirror steps to the space position. This output corresponds to a zero input condition. During the 4.2-s interval that the scan mirror is in this position, the memory FET switch is closed, and the memory capacitor charges to a voltage level corresponding to the sum of the thermal and electrical offsets in the system at the time. At the end of the 4.2-s interval, the FET switch is opened and the mirror is stepped to the planet position. Because the memory capacitor is connected in the feedback loop of a high-gain operational amplifier, it has a time constant of many minutes. Therefore, as the planet is being viewed, the output of the system is the difference between the planet signal and the previously stored offset signal. Thus the output is proportional only to planet radiance; self-emission of the optics and electrical offset effects are removed.

The memory circuit is restored every 63 s, during which time the sag of the memory RC circuit is negligible. The temperature of the reference surface within the radiometer is seperately monitored by the thermister circuit. The outputs of the two data channels, reference surface temperature monitor and a power supply monitor, are combined in a single data output by the multiplexer circuit. The multiplexer and mirror step functions are controlled by the spacecraft DAS. The block diagram of the instrument is shown in Fig. 55.

1. Data flow. Each complete cycle is 63 s in length. It begins with a 4.2-s view of space, followed by a 27.3-s

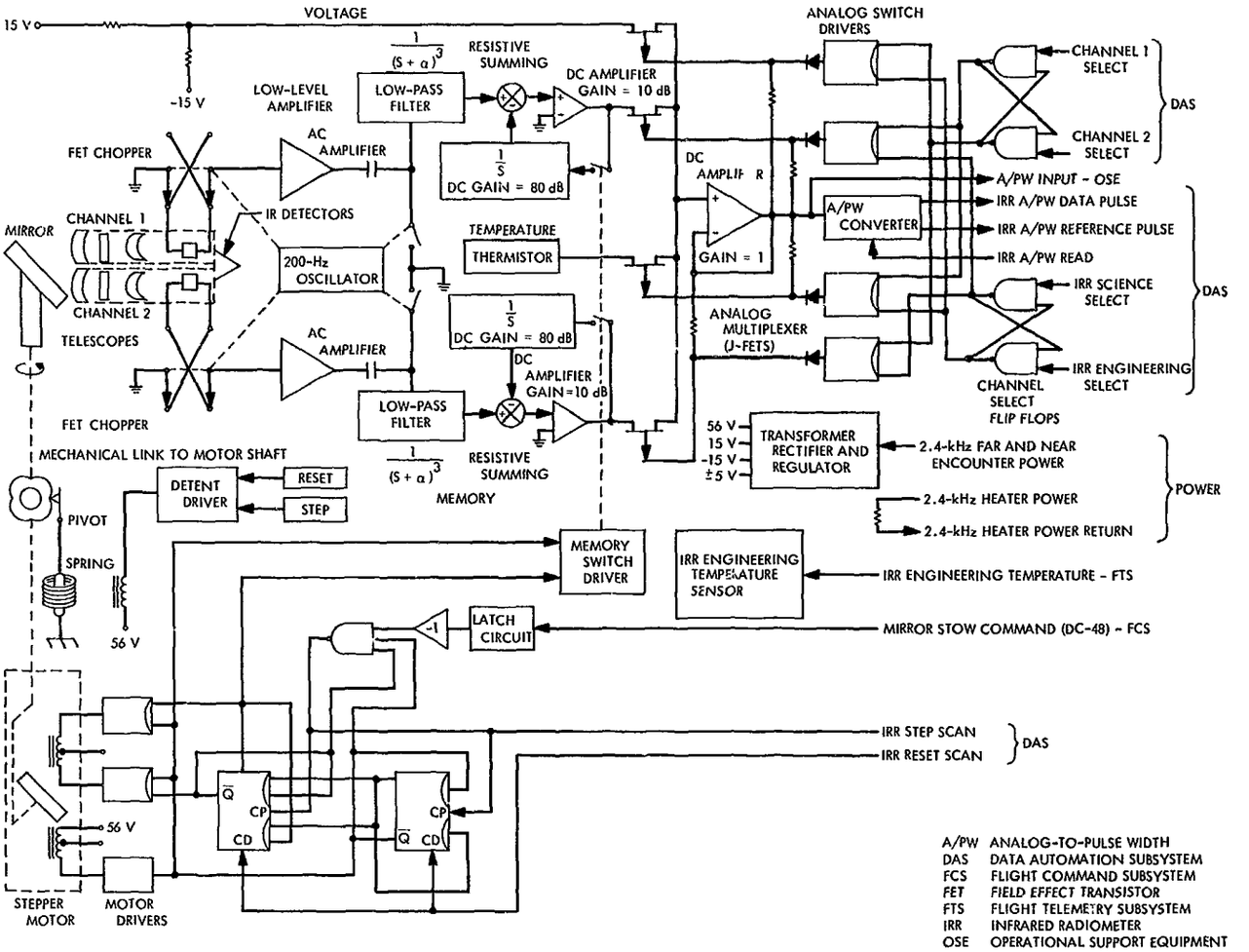


Fig. 55. Infrared radiometer, block diagram

view of the planet, followed by 2.1 s in the internal reference position, followed by 29.4 s of planet view.

Data samples are taken in pairs throughout the 63-s interval. Pairs occur 2.1 s apart; the interval between the samples in a pair is 150 ms. Each pair consists of a channel 1 sample and a channel 2 sample, except for the first two samples in the space interval which are temperature in channel 1 and power supply voltage in channel 2. Each sample is digitized to 10-bit accuracy. There are 600 bits each 63-s cycle, and the equivalent data rate is 9.5 bits/s. Data sampled during transmission of science data is transmitted in real-time. Data is seen as word 8, 9, 22, and 23 in the DAS real-time data format.

2. *Calibration.* Calibrations were performed in a vacuum chamber at 10^{-5} torr, with the instrument mounted in proper relationship to a radiometric calibrator. The calibrator consisted of two ribbed, extended source blackbodies. The one representing space was maintained continuously at LN_2 temperature (77°K) by a continuous flow of LN_2 through it. The one representing the planet was controlled by a blackbody. The heater acted in opposition to the LN_2-cooled coil attached to the blackbody through a thermal impedance, so that linear temperature control from 100 to 350°K was possible. The instrument was mounted on a temperature-controlled heat exchanger that controlled the instrument temperature at any point in the range −30 to +30°C.

Calibrations were made at 14 different planet blackbody temperatures between 107 and 327°K. At each of the 14 temperatures, 29 output readings were taken for each channel. The average of these readings was used to generate the transfer function of the system. Calibrations were performed with the instrument at −30, 0, and +30°C. In addition, cross-calibrations were made by holding the blackbody temperature constant and varying the instrument temperature between − 30 and + 30 in 10° steps. With this data, the transfer function of the instrument can be deduced for any instrument temperature in its range.

D. Design Development

The IRR design evolved from experience gained from the radiometer flown on *Mariner II* and concepts developed in the design of radiometers flown on *Nimbus* spacecraft. The instrument was developed and manufactured by the Santa Barbara Research Center.

The detector is a five-junction bismuth-antimony thermopile, evaporated onto a thin aluminum-oxide film supported by a annular sapphire disk 12.7 mm in diameter and 2.5 mm thick. The detector is suspended over a 1.8-mm hole in its center. The film is fabricated by anodizing aluminum foil and etching away the aluminum. The components of the detector are evaporated onto the film, giving a sensitive area 0.25 mm square. Masks are used for dimentional control.

Separate telescopes are used for each spectral channel. The 8- to 12-μ filter element produces a sharp spectral passband but also transmits at longer wavelengths. Therefore, Irtran 2, which is opaque to the longer wavelengths, was chosen for the objective lens. Germanium with an antireflection coating of zinc sulfide is used for the second lens. Uncoated Irtran 6 is used for both lenses in the 18- to 25-μ telescope. All of the optical elements are held in place by a semirigid epoxy adhesive.

The 6 × 8.5-cm scan mirror is machined of beryllium plated with electroless nickel, polished and aluminized. It is then coated with a protective layer of silicon monoxide. The mirror is mounted at a 45-deg angle, directly on the motor shaft of a size 11, 90-deg stepping motor. On the opposite end of the shaft is an electromagnetic detent mechanism which locks the mirror in each of the three allowed positions. The detent is 400-series stainless steel. The detent wheel material is DuPont Vespel SP-1 polymide resin, chosen for its low wear and self-lubricating properties in an space environment.

E. Procurement and Test History

1. Prototype. Type approval testing began November 14, 1967, and was completed on April 16, 1968, without significant problems. The prototype was installed on M69-4 from April 1969 to June 1969 for all system operations of the backup spacecraft.

2. PTM SN 001. Type approval and flight approval testing began March 1, 1968, and was completed August 14, 1968. Humidity, explosive atmosphere, and acoustic tests were waived. A total of 2664 h was completed in life test. Solar simulator vacuum testing, phases 1 and 2, was successfully completed on the PTM spacecraft. The unit completed all system tests while on the spacecraft.

3. SN 002 (flight unit). Flight approval testing began April 26, 1968, and was completed on May 7, 1968. On November 21, 1968, the unit successfully completed one axis (*X*) FA random to qualify rework. The unit completed all required system tests on M69-2.

The 002 unit was removed from the M69-2 as a result of a PFR. The unit was subjected to extensive EMI testing in the anechoic chamber at JPL. In addition, a 58-h thermal cycle test and a thermal gradient test were conducted.

4. SN 003 (flight unit). Flight approval testing began June 3, 1968, and was completed on June 11, 1968. On November 15, 1968, the unit successfully completed one axis (*X*) FA random vibration to qualify rework. Solar simulator vacuum testing, phases 1 and 2, was successfully completed on M69-3. The unit completed all required system tests on M69-3.

The SN 003 unit was aboard M69-2, which was launched March 27, 1969, from Cape Kennedy.

5. SN 004 (flight unit). Flight approval testing began July 8, 1968, and was completed July 12, 1968. On December 4, 1968, the unit successfully completed one axis (*X*) FA random vibration to qualify rework. Solar simulator vacuum testing, phases 1 and 2, was successfully completed on M69-4. The unit completed all required system tests on M69-4. This unit was aboard M69-3, which was launched February 24, 1969, from Cape Kennedy.

PRECEDING PAGE BLANK NOT FILMED

Telecommunications System and Subsystems

I. Introduction

This section describes the spacecraft telecommunications design, analysis, and test performed from mission conception to launch.

II. Major Spacecraft Telecommunications Design and Analysis Activities

A. Telemetry Design and Analysis

With the project decision to expand the TV picture-taking capability of *Mariner* Mars 1969, it became quickly apparent that the previous *Mariner* telemetry playback capability of 8⅓ bits/s must be increased in order to make possible reasonable data playback periods. At the same time, JPL Division 33 introduced the multi-mission telemetry concept: a hybrid software/hardware ground telemetry detection configuration with the flexibility to accommodate more than one mission design.

This telemetry configuration provided a more efficient detection of the telemetry data stream from the received noisy signal. It established data bit sync from the data signal itself and therefore required no transmission of a separate sync signal as was done in the past. It also allowed the simultaneous reception of two data signals, thus allowing the transmission of science data on one channel and continuous transmission of engineering on the other.

Analysis indicated that the playback data rate could be expanded to 270 bits/s, giving: (1) an increase in spacecraft power and antenna size; (2) the use of the multi-mission telemetry system; and (3) reduced communication range for the 1969 opportunity. This rate allowed a playback of the stored science data in approximately 10 days. In addition, an experimental coded high-rate channel was proposed at 16 kbits/s which made use of the increased sensitivity of the Goldstone 210-ft antenna. This would permit playback transmission time in less than 3 h, a substantial reduction in operation time. The high-rate channel also allowed direct playback out of the analog tape recorder through an A/D converter, bypassing the digital tape recorder. This reduced operational complexity, and was more reliable.

The project design incorporated both the multi-mission telemetry configuration and the high-rate channel. The resulting telemetry rates for each mission phase are listed in Table 1. In Table 2 a comparison of the channel parameters of the 270 bits/s and 16.2 kbits/s science channels with those of the *Mariner* IV 8⅓ bits/s science channels is given.

Table 1. Data rates for each mission phase

Data type	Mission phases		
	Cruise, bits/s	Encounter, bits/s	Playback, bits/s
Engineering data channel	8⅓ or 33⅓	8⅓ or 33⅓	8⅓ or 33⅓
Science data channel	—	66⅔ or 16,200	270 or 16,200

In developing the telemetry channel capabilities, a major attempt on *Mariner* Mars 1969 was made to pinpoint each channel parameter to its most exact value and to reduce the tolerances to a bare minimum. Out of this exercise new channel analysis and performance techniques evolved. Some of the most significant are described below.

In adjusting the telemetry modulation indices (allocating a certain percentage of the transmitted power to each of the carrier tracking, the engineering data and science data channels), a more quantitative and efficient approach was introduced. It took into account the interrelation of the carrier tracking loop with the telemetry detection process by explicitly identifying the degradation of the telemetry signal due to phase jitter in the carrier tracking loop. This technique permitted a better balance of the total power allocation and minimized the amount of received power necessary for adequate data detection, and at the same time guaranteed proper carrier tracking.

The station noise temperature and its tolerance, as used in channel design control tables in the past, were fixed and were based on worst case elevation angles. The *Mariner* Mars 1969 channel analysis updated the zenith noise temperature to take into account the actual noise temperature for the individual station elevation angles for each station-pass in the mission. This made the telemetry channel analysis station-oriented. The immediate results were a reduction in the sum of the negative tolerances and a differential in the nominal performance margin between southern and northern hemisphere stations because of the relatively larger antenna elevation angles for the southern stations.

A considerable amount of effort went into updating the initial telemetry predicts based on test results which included measurements made on each individual spacecraft during system and environmental testing. As well

Table 2. Comparison of parameters of *Mariner* 1969 and *Mariner* 1964 science channels

Parameter	1. *Mariner IV* 8⅓-bit/s channel		Δ	2. *Mariner* Mars 1969 270-bit/s channel		Δ	3. *Mariner* Mars 1969 16,200-bit/s channel	
P_T	8.9 W	+39.5 dBm	+3.10 dB	18.2 W	+42.60 dBm	—	18.2 W	+42.60 dBm
M		−5.3 dB	+3.50 dB		−1.80 dB	+0.46 dB		−1.34 dB
G_T		+20.1 dB	+0.11 dB		+20.21 dB	—		+20.21 dB
L_S	216×10^6 km	−266.2 dB	+6.84 dB	97×10^6 km	−259.36 dB	—	97×10^6 km	−259.36 dB
G_R	85 ft	+52.5 dB	—	85 ft	+52.5 dB	+8.50 dB	210 ft	+61.00 dB
L_R		−3.4 dB	+2.26 dB		−1.14 dB	+0.70 dB		−0.44 dB
S		−162.8 dBm	+15.81 dB		−146.99 dBm	−9.66 dB		−137.33 dBm
T_B	8⅓ bits/s	−9.2 dB/s	−15.11 dB	270 bits/s	−24.31 dB/s	−17.79 dB	16,000 bits/s	−42.10 dB/s
ST_B		−172.0 dBm/s	+0.70 dB		−171.30 dBm/s	−8.13 dB		−179.43 dBm/s
N_0	65°K	−180.5 dBm/Hz	—	65°K	−180.50 dBm/Hz	+4.10 dB	25°K	−184.60 dBm/Hz
ST_B/N_0		+8.5 dB	+0.70 dB		+9.20 dB	−4.03 dB		+5.17 dB
Required ST_B/N_0	5×10^{-6} BER	+5.2 dB	—	5×10^{-6} BER	+5.20 dB	+2.20 dB	1×10^{-2} WER	+3.00 dB
Margin		+3.3 dB	+0.70 dB		+4.00 dB	−1.83 dB		+2.17 dB

P_T = total transmitter power.
M = modulation loss.
G_T = antenna gain including circuit loss.
L_S = space loss.
G_R = receiver antenna gain.
L_R = receiver loss.
S = signal energy.
T_B = bit duration.
N_0 = noise spectral density.
BER = bit error rate.
WER = word error rate.

as being station oriented, the telemetry channel predicts now also became spacecraft oriented. The major impact of the predict update was that it made the nominal performance reflect the actual flight operational situation as closely as possible. This allowed accurate planning of key operational events such as switching transmitter power level, data rate, from low-gain to high-gain antenna, and the high-rate calibration periods. In a conflict with the *Apollo* program usage of the 210-ft Goldstone antenna, the high-rate calibration schedule was confidently moved back to an earlier date when it would be very close to threshold. This was possible because of accurate telemetry predicts which compared quite well with flight measurements throughout the cruise to Mars.

B. High-Gain Antenna Pointing

For the *Mariner VI* trajectories, the spacecraft cone and clock angle coordinates of the spacecraft-to-Earth vector changed slowly enough around encounter to allow reasonable high-gain antenna pointing to Earth with a fixed antenna position bolted to the spacecraft main frame.

The guidelines used in selecting the antenna boresite pointing position were:

(1) Maximize playback time after encounter.

(2) Provide at least 10 days of coverage on high gain before encounter in science encounter telemetry modes.

(3) Cover the arrival data window which extended from August 1 to August 10, 1969.

Figure 1 shows typical earth tracks across the antenna pattern for the antenna pointing position selected. A worst case pointing uncertainty of ±0.6 deg resulted because of attitude limit cycling and uncertainties in the sun sensor null location and the mechanical and electrical boresite positions.

C. Telecommunications Development Laboratory Implementation

When the *Mariner* Mars 1969 telecommunications system requirements were defined, it was apparent that a considerable amount of testing would be needed for design verification. In February 1967, work began on implementation of a system laboratory that would be capable of supporting both flight hardware and ground system equipment tests.

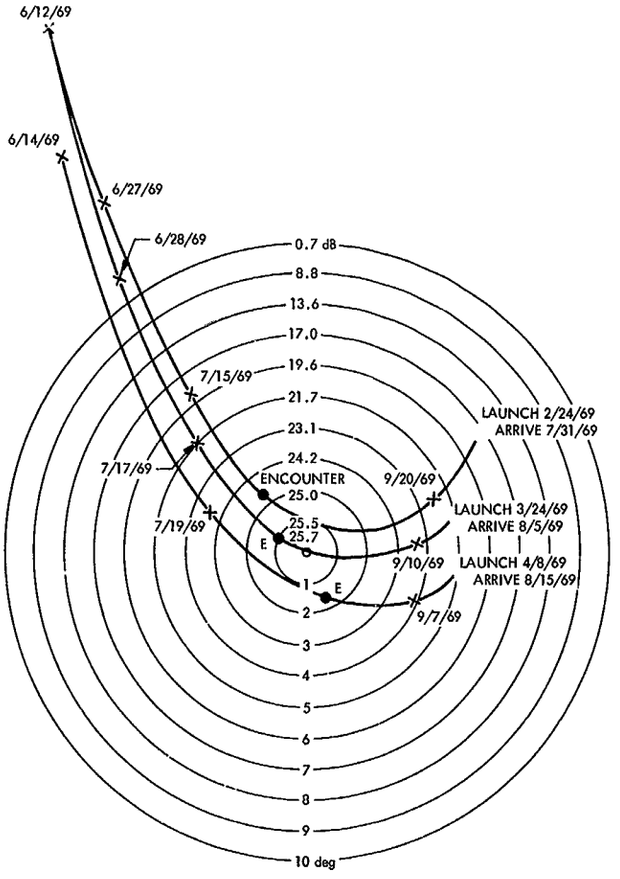


Fig. 1. Earth tracks across high-gain antenna pattern for typical trajectories

By September 1967 the first phase of the flight project telecommunications laboratory was completed and breadboard/prototype testing of flight hardware was in process. In parallel with this effort, a compatibility test area was being implemented to provide the ground station equipment necessary for complete testing of the overall telecommunications system. In January 1968, the flight project laboratory was integrated within this new facility to form the compatibility test area-21 (CTA-21). The facility provided all the necessary equipment for detailed compatibility tests in addition to allowing performance of separate ground/flight hardware tests.

Several special test devices were designed and built to permit measurement of critical parameters throughout the testing phase. Some of the devices developed were:

(1) A phase modulation index technique with an accuracy of ±0.5 deg.

(2) A demodulator which returned spacecraft data to baseband for real time bit error rate tests.

(3) A data source simulator for high-rate telemetry testing.

(4) An RF interface network for S-band transmissions between the spacecraft and CTA-21.

Commercial test equipment was utilized whenever possible to minimize costs and reduce time consuming development work.

III. Telecommunications Subsystem Tests

To facilitate early verification of the overall telecommunications system performance it was necessary to perform tests on the breadboard and prototype subsystems as individual units and in combination with mating units. The measurements performed on the individual subsystems were limited to obtaining those parameter values necessary for performance of the combined tests. In the case of the radio frequency subsystem more detailed breadboard and prototype tests were conducted to allow maximum utilization of the existing on-lab test facilities.

A. Breadboard Radio Tests

A breadboard version of the *Mariner* Mars 1969 transponder portion of the radio frequency subsystem was delivered to the systems test laboratory (STL) on October 5, 1967. Tests were performed during the period from October 5 through 21 at which time the unit was returned to the vendor. The following is a brief description of the tests performed and techniques used for obtaining the data.

1. Noise figure measurement. The combined preselector and S-band mixer noise figure was measured using a Hewlett-Packard (HP) 340B automatic noise figure meter and associated HP 349A noise source. The measured noise figure was 10.1 dB with an estimated accuracy of ± 0.5 dB. Design goal noise figure was $7.4^{+1.4}_{-1.1}$ dB. This goal was subsequently attained on the flight units.

2. Second IF predetection noise bandwidth. The receiver predetection bandwidth was measured and numerical integration of the normalized data yielded a noise bandwidth of 4,575 Hz with an estimated accuracy of $\pm 5\%$. This was within the design specification of 5.0 kHz $\pm 10\%$.

3. Strong signal open loop gain. Measurement of the phase lock receivers open loop gain was accomplished by use of a HP 8405A vector voltmeter (see Fig. 2). The RF input level was set to -80 dBm and the uplink frequency was adjusted to obtain zero volts static phase error at the loop filter output. The uplink frequency, voltage controlled oscillator (VCO) frequency and static phase error (SPE) voltage was recorded and the vector voltmeter phase angle set to zero. Next the uplink frequency was offset to obtain a 3.0 deg SPE as measured with the vector voltmeter and the resulting VCO frequency, SPE voltage and uplink frequency were recorded.

With the above data, several important receiver parameters were determined. The phase detector transfer function K_D is given by:

$$K_D \cong \frac{\Delta SPE}{\Delta \phi} \text{ V/deg}$$

$$K_D = \frac{0.90}{3.0} = 0.30 \text{ V/deg}$$

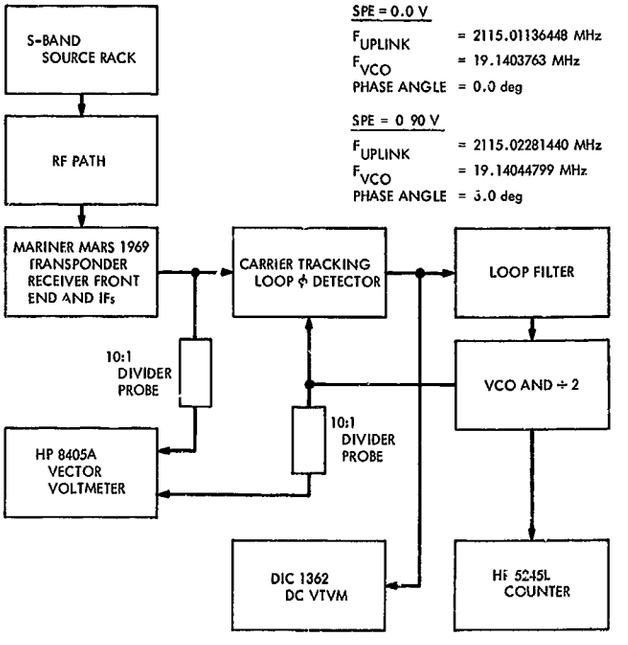


Fig. 2. Open loop gain measurement

The VCO transfer function K_V is given by:

$$K_V = \frac{\Delta VCO}{\Delta SPE} \text{ Hz/V}$$

$$= \frac{103.6}{0.90} = 115.1 \text{ Hz/V}$$

Strong signal open loop gain may be determined from the relationship:

$$G_o = (K_V)(K_D)(M)(\alpha)(360)$$

where

M = Receiver phase multiplication factor = 110.5

α = Limiter suppression factor = 1 for strong signal

Using the measured values of K_V and K_D, the open loop gain is:

$$G_o = (115.1)(0.30)(110.5)(1)(360)$$

$$G_o = 1{,}373.603$$

4. Strong signal loop phase modulation response and command output frequency response. The strong signal 1-H(S) response and command modulation output response was measured with satisfactory results.

5. Command output level vs RF input level. The command output level was measured with an uplink modulation frequency of 750 Hz (sine wave) at a modulation index of 1 radian peak over an RF input level ranging from −70 to −135 dBm. The results were satisfactory.

6. VCO frequency vs static phase error voltage. This measurement essentially determined the VCO linearity over the expected operating range. Results of this test were satisfactory.

7. AGC voltage vs signal level and threshold. The AGC voltage vs signal level characteristic measurement was satisfactory. Measured threshold was −151 dBm at the preselector input. Assuming a threshold loop noise bandwidth of 17 Hz, the calculated threshold as defined by zero dB SNR in the loop is

$$\text{Threshold} = (-174.0 + 10 \log 17) + \text{noise figure} + \text{limiter loss}$$

$$= -174.0 + 12.3 + 10.1 + 0.6$$

$$= -151 \text{ dBm}$$

The measured value was in agreement with the expected value.

8. Telemetry input modulation sensitivity and frequency response. Telemetry input modulation sensitivity and frequency response was measured with the transponder operating in auxiliary oscillator mode. The first carrier null (2.4 radians peak) was obtained at an input voltage level of 852 mVrms using a 24 kHz sine wave. Null depth was 41 dB. The modulator sensitivity was:

$$\text{Sensitivity} = \frac{2.4}{0.852 \times 1.414} = \frac{1.98 \text{ radians peak}}{\text{V peak}}$$

This value was approximately twice the specified value of 1.0 ±0.15 radians peak/V peak. This was subsequently corrected by the vendor. Modulator frequency response was satisfactory.

9. Ranging input modulation sensitivity and frequency response. Ranging input modulation sensitivity and frequency response was measured with the transponder operating in auxiliary oscillator mode (non-standard). The first carrier null was obtained at an input voltage level of 0.63 Vrms using a 500-kHz sine wave. Null depth was 42 dB. The modulator sensitivity is

$$\text{Sensitivity} = \frac{2.4}{0.63 \times 1.414} = \frac{2.69 \text{ radians peak}}{\text{V peak}}$$

Modulator frequency response was satisfactory.

10. Auxiliary oscillator phase deviation profile. Experimental tests were performed to determine if the auxiliary oscillator residual phase deviation was low enough to operate in conjunction with a ground receiver $2B_{LO}$ = 3 Hz. The test configuration is shown in Fig. 3. Baseline tests were first performed with the DSIF exciter/translater serving as the S-band signal source. The results of these tests are shown in Fig. 4. Next, the transponder breadboard operating in auxiliary oscillator mode was substituted and the results are shown in Fig. 4. During performance of these tests, it was noted that an excessive amount of 2.4-kHz modulation was present at the ground receiver dynamic phase error output. The problem was cured temporarily by physically separating the transponder power supply from the transponder. A permanent fix was devised by the vendor and was incorporated in the flight unit. These preliminary test results indicated the auxiliary would have difficulty operating with a 3-Hz tracking loop at low signal levels.

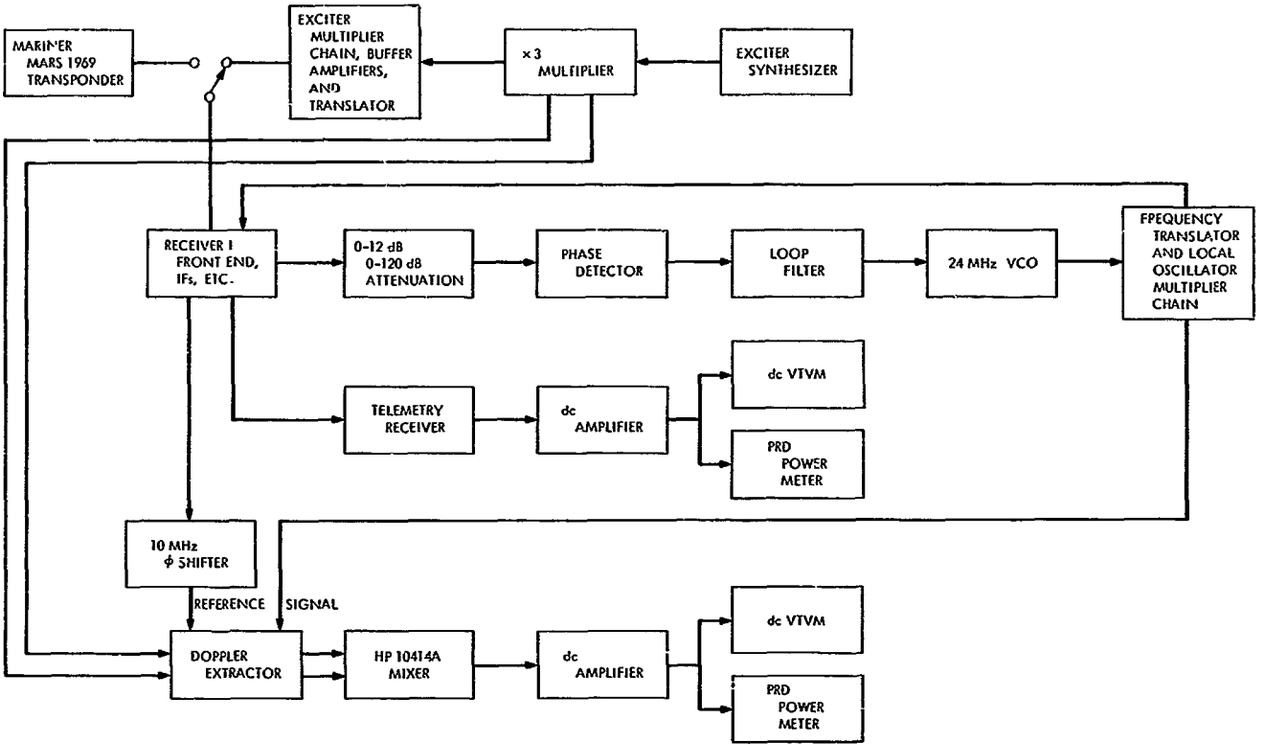


Fig. 3. Phase deviation profile measurement

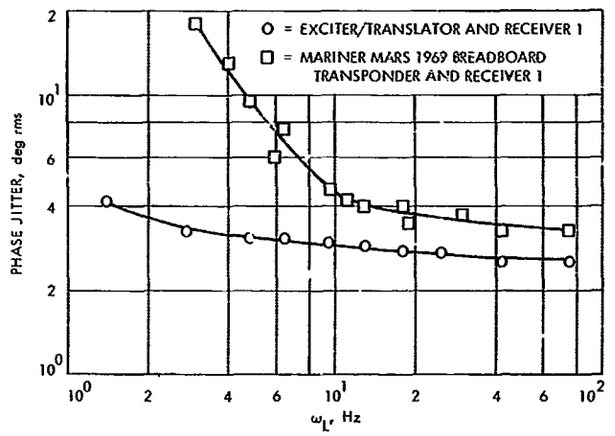


Fig. 4. Phase jitter vs loop bandwidth

B. Prototype RFS and FTS System Tests

The previously described transponder breadboard tests were of a very preliminary nature and did not yield information concerning the overall radio frequency subsystem (RFS) performance and its interaction with mating subsystems. This section gives a brief description of the tests performed on the RFS and flight telemetry subsystem (FTS) prototypes with the purpose of giving the reader an insight to the level and types of tests necessary to evaluating part of telecommunications link performance.

1. Scope. The tests were performed in the CTA-21 and the results reflect the RFS prototype compatibility between the FTS and DSIF interfaces. Limitations of tests are mentioned where the comments are applicable. Parameter discrepancies noted during the tests are listed and discussed in the conclusions.

2. Test data

a. RFS output power. Adequate tests could not be made in determining power outputs. First, traveling-wave tube amplifier 1 (TWTA 1) was not operative. Later the TWTA package was removed, repaired, and replaced. Attenuators were included into the hybrid filter/TWT lines which invalidated the readings shown herein. Further testing was desirable, but was incompatible with scheduling. Table 3 shows the power output data obtained before the TWTA package was removed and replaced and attenuators inserted.

b. Exciter output power. Power measurements were taken at the output of both exciter cables, as well as both

Table 3. Power output

TWTA measurements											
Mode		Antenna	Exciter	Power amplifier No. and power mode	Power output, dBm		Telemetry power monitor		Spectrum of carrier above noise level		
One way	Two way				One-way tracking	Two-way tracking	One-way tracking, mV	Two-way tracking, mV	Above two-way tracking, dB	Noise one-way tracking, dB	Remarks
1	4	Low	1	1-Low	TWTA 1 defective						
5	8	High	1	1-Low							
9	12	Low	2	1-Low							
13	16	High	2	1-Low							
17	20	Low	1	1-High							
21	24	High	1	1-High							
25	28	Low	2	1-High							
29	32	High	2	1-High							
33	36	Low	1	2-Low	38.88	38.91	693-696	696-699	45	45	Period ($T \approx 1$) s Spike in P_0 of $\approx$ 0.02 dB
37	40	High	1	2-Low	39.02	39.04	698-702	710-711	↓	↓	
41	44	Low	2	2-Low	38.90	38.93	692-695	702-704			
45	48	High	2	2-Low	39.02	39.04	700-702	715-716			
49	52	Low	1	2-High	41.33	41.33	739-742	740-742			Spike in P_0 not noticeable
53	56	High	1	2-High	41.82	41.82	777 —	777 —			↓
57	60	Low	2	2-High	41.73	41.73	757-758	757-758	↓	↓	
61	64	High	2	2-High	41.87	41.87	790 —	792 —	45	45	Spike in P_0 not noticeable

RFS measurements			
Exciter	Hybrid filter output (included cable to TWT), dBm		Exciter output to hybrid filter (cable included), dBm
	J3 ③[a]	J4 ④[a]	
1	19.45	19.45	23.89 ①[a]
2	19.75	19.45	23.40 ②[a]

[a]Numbers in circles represent measurement points shown in Fig. 5.

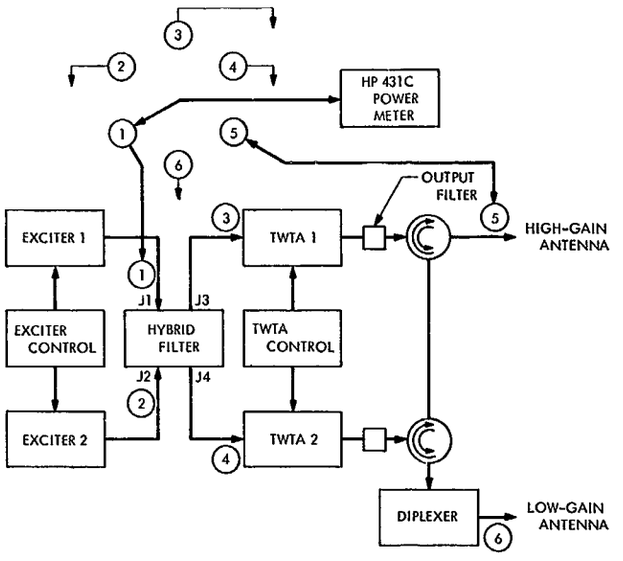


Fig. 5. RFS exciter power measurements

cables from the hybrid filter as shown in Fig. 5. Specifications require +24.5 dBm directly at the exciter output.

Exciter 1 was shown to be on the low side (+ 23.2 dBm). However, no loss measurements of exciter 1 output cable could be made to verify that exciter 1 was out of specification.

c. Modulation sensitivity. Modulation sensitivity was determined by measuring the sine wave rms value and obtaining a first null of the carrier. A modulation frequency was chosen to be in a flat response region around 260 kHz. Data recorded follows:

Exciter	Sinewave input to TLM, Vrms	Calculated modulation index, radians peak / V peak	Specified value, radians peak / V peak
1	1.69	1.01	1.00 ±0.015
2	1.43	1.19	1.00 ±0.015

Exciter 2 was out of the specified tolerance range. Exciter 1 and 2 subsystem test data from the vendor show 1.63 Vrms and 1.62 Vrms at 500 kHz to obtain a first null. This data would result in an out-of-tolerance condition of 1.04 and 1.05 radians peak/V peak sensitivity of exciters 1 and 2, respectively.

d. Modulation bandwidth and linearity. Telemetry bandwidth is defined by the highest frequency to maintain a 5% deviation from that of the 260-kHz value. Test data indicate a discrepancy from the specified 1.5-MHz minimum value. More details can be found in the conclusions at the end of this section.

A breadboard exciter (not RFS exciter 1 or 2 subsystem) was tested separately and was used to compare the modulation response of the RFS exciters. Assuming all exciter modulation responses to be similar, then the difference between the two results are due to the RFS harness and possibly the 50-ohm modulation source. A 1-ohm source should have been used.

The 3-dB modulation bandwidths were found graphically to be 5.1 MHz and 3.5 MHz for RFS exciters 1 and 2, respectively.

e. Spectrum analyzer and wave-analyzer data. The telemetry spectrums taken in the test configuration shown in Fig. 6 reveal the status of the following parameters:

(1) Amount of wanted energy into odd numbered sidebands (of high modulation index channels).

(2) Amount of unwanted energy into even numbered sidebands due to an asymmetric modulation waveform.

(3) Amount of wanted energy into the higher odd harmonics show the modulator frequency response to the highest frequency component of the telemetry input. This is a measure of modulation sensitivity at different modulation frequencies.

Comparisons were made of each distinguishable sideband with a theoretical maximum value. Predicted maximum values are calculated as follows:

Carrier suppression level:

$$\frac{P_C}{P_T} = 20 \log \cos \theta \cos \phi \qquad (1)$$

N^{th} sideband level:

$$\frac{P_{USB}BN}{P_T} = \frac{P_{LSB}BN}{P_T} = 20 \log_{10} \left[\frac{2}{n\pi} \sin \theta \cos \phi \right] \qquad (2)$$

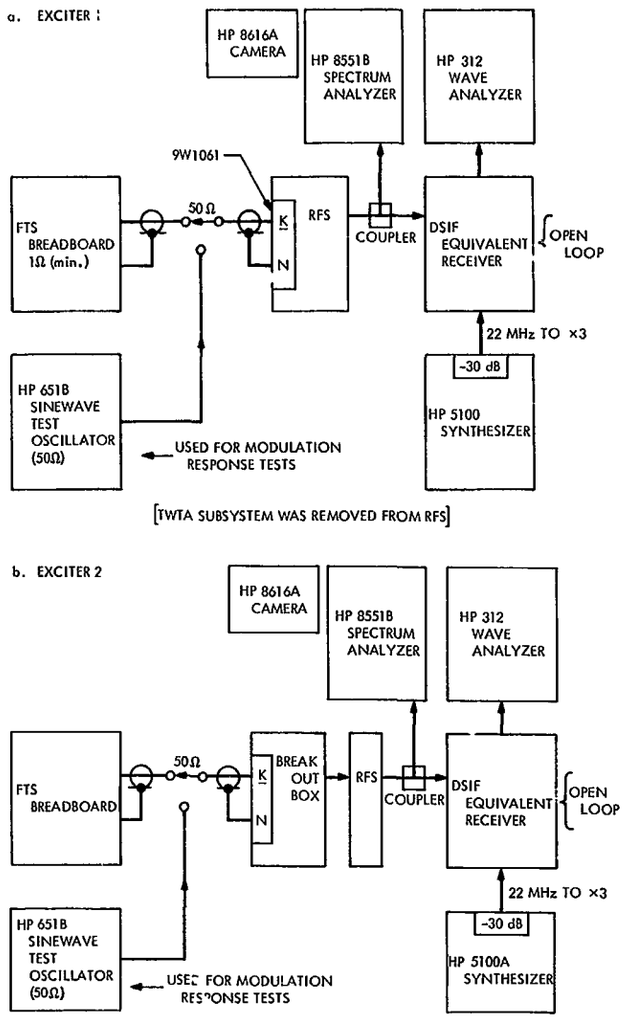


Fig. 6. RFS exciter telemetry test configuration

Where

θ = modulation index of the *wanted channel* N^{th} (upper or lower) sideband

ϕ = modulation index of the other channel ($\phi = 0$ if no other channel)

P_C = power at modulated carrier frequency

P_T = total power or power in unmodulated carrier frequency

$P_{USB}N$ = power in N^{th} upper sideband (N is odd)

$P_{LSB}N$ = power in N^{th} lower sideband (N is odd)

Equations (1) and (2) are used to compute the expected level of the carrier and sidebands below an unmodulated carrier reference.

For accuracy, the unmodulated carrier reference was recorded from wave analyzer data. The wave analyzer carrier suppression was then marked on each spectrum photograph.

Limitation as to both frequency and amplitude resolution prevented discerning channel B in the presence of channels C and A. These limitations are due to the following parameters:

(1) Higher modulation index on channels C and A than B.

(2) Much higher frequency on channel C.

(3) 3-kHz spectrum analyzer IF bandwidth.

(4) ± 2-dB amplitude accuracy of analyzer.

Analysis of spectrum photographs indicated satisfactory response characteristics.

f. Receiver auxiliary oscillator enable. This test assured that when the RFS receiver lost up-link lock on the carrier, the exciter internal auxiliary oscillator would be enabled. The receiver was first in-lock, then as threshold was exceeded, the exciter drive switched to auxiliary oscillator. When the auxiliary oscillator switched over a step change in output frequency was noted.

Exciter 1 and 2 auxiliary oscillator frequencies. Both RFS auxiliary oscillators were within specifications, Table 4.

Exciter 1 and 2 phase stability (with TWTA 2). Phase stability of the exciters as measured under strong signal conditions (−70 dBm) in one-way tracking mode into a test receiver ($2BL = 12$ Hz) produced approximately 3 deg peak error in each exciter. Specification of maximum phase stability was 10.8 deg. Both exciters were within specification.

Table 4. Oscillator frequency accuracy

Exciter	Actual frequency, MHz	Specification, MHz
1	2296.868770	2296.881711[a] to 2296.821993
2	2296.856059	

[a] 1.3 in 10^5 or ±29,859 kHz about 2296.851852 MHz.

3. *Receiver data*

a. Best lock frequency. By increasing and decreasing the carrier power near threshold, allowing the receiver to drop lock, then stabilize, then re-acquire the carrier, different thresholds were obtained around the best lock frequency. The data shown in Table 5 indicates best lock to be 2115.020,013,100 MHz ±3500 Hz. Specification require the best lock frequency to be between 2115.049,447,000 MHz and 2114.986,047,000 MHz. Specifications were met, but exact best lock frequency was somewhat ambiguous, viz. ±3500 Hz.

Table 5. Best lock data

Frequency, MHz	Threshold, dBm	Recapture, dBm
2115.030,016,600	−151.5	−147.5
18,000	−151.0	−147.0
14,400	−151.5	−148.0
13,100	−151.5	−148.5
10,900	−151.0	−148.0
12,200	−151.0	−148.0
2115.030,012,700	−151.5	−148.0

b. Static phase error calculations. The static phase error (SPE) experienced by the phase-lock-loop as the input frequency was varied to each side or the best-lock frequency is a measure of:

(1) VCO characteristics as linearity and gain.

(2) Phase detector symmetry.

(3) Phase detector bias.

Ideally, the VCO gain should be a straight line represented by the expression:

$$\pm V_{SPE} = \frac{\pm \Delta f}{K_{VCO} M} \tag{3}$$

Where

V_{SPE} = static phase error voltage (phase detector output)

$\pm \Delta f$ = change in frequency Hz about best-lock

K_{VCO} = VCO gain function Hz/V

M = loop multiplication constant

If the SPE deviates from Eq. (3) within a ±63 kHz range then poor VCO linearity can be expected. If non-symmetrical break-lock frequencies are shown, then an asymmetrical phase detector response can be expected, which includes phase detector bias. Generally, an asymmetrical break-lock condition exists, but as a percentage it is not as yet specified.

SPE data displayed good linearity over the frequency change region. In the negative frequency region, poor data was taken, but displayed a reasonable fit to Eq. (3). Break-lock asymmetry was calculated from the SPE data as follows:

$$\left| \frac{+\Delta f}{-\Delta f} \right| = \frac{110 \text{ kHz}}{130 \text{ kHz}} = \frac{1}{1.18} \text{ or about } 18\%$$

A graphical best fit of the SPE data to Eq. (3) shows: $K_V M$

$$K_V M = \frac{-\Delta f}{+\Delta V} = \frac{130 \text{ kHz}}{9.75 \text{ V}} = 13.44 \frac{\text{kHz}}{\text{V}}$$

Specification indicates $K_V M = (120 \pm 10)\ (110.5) =$ 13.26 kHz ±1.105 kHz to be needed. The gain was within specification.

c. Maximum break-lock frequencies. Specifications require ±63 kHz minimum break-lock frequency range at − 120 dBm. The RFS was tested at −70 dBm resulting in a loss of lock at −130 kHz and +110 kHz. A somewhat greater range was expected. The maximum change in frequency from best-lock is determined by the following relation:

$$\sin \phi = \frac{2\pi(\Delta f)}{G_{SS}} \tag{4}$$

Where

$G_{SS} = 1.67 \times 10^6 \frac{\text{deg}}{\text{deg/s}}$ strong signal loop gain

$\phi = 90$ deg maximum (or instability point)

Δf = frequency change from best-lock Hz

Then

$$\pm \Delta f = \frac{G_{SS}}{2\pi} = \frac{1.67 \times 10^6}{2\pi} = 268 \text{ kHz}$$

This value is not obtained in practice due to reference phase jitter, finite rate of change f as frequency is offset, and phase detector non-sinusoidal characteristics (which

includes dc offset and asymmetry). Though no specification is stated at −70 dBm, the +110 kHz and − 130 kHz break-lock frequency offset recorded are reasonable. However, the asymmetry could be objectionable due to lack of best-lock frequency definition.

d. AGC response test. The AGC test configuration is shown in Fig. 7. Due to the more logarithmic nature of the AGC amplifier, there is a deviation from a straight line response. As the signal level approaches threshold, a very rapid deviation from a straight line is experienced due to loss of phase reference which is established by the phase-lock loop and not due to the AGC loop. This is expected and should approach an asymptote of the threshold value shown here to be graphically −152 dBm.

e. Threshold. The RFS receiver threshold was calculated as follows:

$$\begin{aligned} \text{Reference temperature} &= 290^\circ\text{K} = t \\ -20\log_{10} Kt &= -173.0 \\ 20\log_{10} 2B_{LO} &= +13.0 \\ NF &= +7.6 \\ \text{Limiter loss} &= +0.7 \\ \text{Threshold} &= -151.7 \text{ dBm} \end{aligned}$$

Threshold was measured at the best lock frequency obtained (see Table 5) and found to be −151.5 dBm which corresponds favorably with the predicted threshold of −151.7 dBm.

f. Noise figure. The RFS noise figure measurement was 7.6 dB. A notable inaccuracy of ±0.5 dB is inherent with the test equipment used.

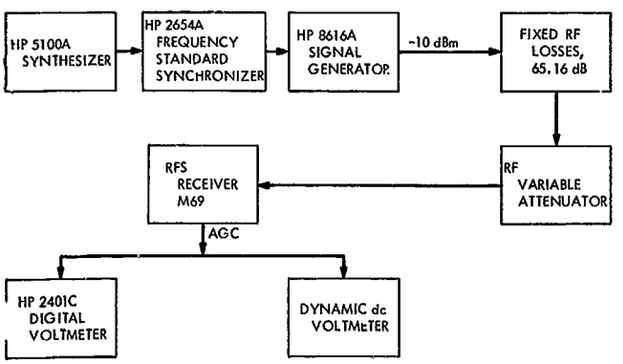


Fig. 7. AGC test configuration

g. Command output. For an up-link suppression of 2 dB when modulated with a 260-Hz sine wave, the receiver command output signal should be 630 mV nominal when measured into an 100 kΩ load at an input signal level of −70 dBm. The measured value was 470 mV.

Analysis indicates a 0.7 Vrms nominal with worst case conditions being 1 Vrms and 6.4 Vrms. This information shows the RFS prototype command output to be reasonable, but somewhat low.

4. Conclusions

The following discussion presents the parameter discrepancies that occurred during testing.

a. TWTA 1 failure. TWTA 1 measured no power output. The amplifier power output of TWTA 2 was measured, and then the TWTA package was removed, repaired, and replaced.

b. Modulation linearity. The exciter phase modulation sensitivity was specified to be within ±5% of the best straight line value from dc to 1.5 MHz. Test data showed both exciters to drop in sensitivity by 5% at 840 and 880 kHz for exciters 1 and 2, respectively. This was an out of tolerance condition.

A possible reason for the discrepancy, between the RFS prototype exciter test and the breadboard test, is the effects of the high capacitance in the RFS telemetry modulation leads. Three sets of twisted leads are used in the RFS harness for redundancy.

c. Modulation sensitivity. A modulation sensitivity of

$$\frac{1.01 \text{ rad (peak)}}{\text{V (peak)}} \text{ on exciter 1, and}$$

$$\frac{1.19 \text{ rad (peak)}}{\text{V (peak)}} \text{ on exciter 2, was measured.}$$

The specified value of

$$\frac{1.00 \text{ rad (peak)}}{\text{V (peak)}} \pm \frac{0.015 \text{ rad (peak)}}{\text{V (peak)}}$$

is needed at 260 kHz; exciter 2 was found to be too sensitive.

d. Receiver best-lock frequency ambiguity. Receiver best-lock frequency cannot be determined by the present methods within ± 3500 Hz. A possibility of a phase

detector unbalance exists, but was not verified. A unit level phase detector balance test was recommended.

C. Command Breadboard System Tests

The *Mariner* Mars 1969 FCS electro-mechanical breadboard was tested in the subsystem compatability test facility. The tests were intended to demonstrate compatability of the FCS and the remainder of the telecommunications system.

The tests consisted primarily of measurement of the bit error rates of the command data and sync channels, using extreme value theory techniques, for various conditions in the signal path. The most important objective of the test was considered to be the establishment of compatibility between the flight command system and the spacecraft RFS.

The up-link signal was obtained from an HP frequency synthesizer, modified to permit phase modulation of the generated signal. The frequency synthesizer output was used to drive an HP S-band signal generator combined with an oscillator synchronizer.

The tests performed were as follows:

(1) Confidence checks to assure that the command system was operating properly, i.e., proper lockup, signals at proper outputs, etc.

(2) Baseband tests (without RF link) to provide a point of comparison for further tests, to assure that the command system agreed with prior test data, and to demonstrate the validity of the extreme value theory techniques used for data analysis.

(3) Tests through the RF link (transponder) with signal levels and modulation indices adjusted such that the carrier component of the RF signal is 20 dB above threshold, with the signal to the flight command system at nominal threshold level. Under these conditions, no degradation of command system performance was expected, as compared to the baseband tests.

(4) Tests through the RF link with modulation indices and RF signal levels such that the transponder and FCS are operating at their nominal threshold conditions. Under these conditions, a degradation of approximately 1.4 dB was expected as compared to baseband tests and strong carrier RF tests. This degradation is due to limiter effects in the transponder and phase jitter in the transponder carrier tracking loop.

(5) Tests through the transponder, with the RF level and modulation indices set such that the system was operating at nominal threshold conditions, but with frequency offsets to produce static phase errors in the transponder carrier tracking loop of 10 and 15 deg.

(6) Tests using the transponder, with the RF power level set to nominal threshold operating conditions, but with varying modulation index, to determine an optimum modulation index.

The threshold conditions for the transponder and the command system are such that the command system will have a signal to noise ratio of 16.5 dB in a 1-Hz noise bandwidth, with the carrier tracking loop in the transponder operating at 8.0 dB above threshold. A degradation of 0.75 dB is expected in the command signal due to transponder phase jitter. The modulation indices were set such that the threshold requirements for the carrier tracking loop and for the flight command system were approached simultaneously, as the total RF power is varied.

1. Test configuration. A block diagram of the test configuration used for the *Mariner* Mars 1969 FCS tests is shown in Fig. 8. The *Mariner* Venus 67 transponder and *Mariner* Mars 1969 breadboard FCS plus necessary support equipment were located in a screen room which provided a minimum of 120-dB plane wave attenuation in the 2–3 GHz frequency range. All screen room input/output signals were carried by RG-58 A/U coaxial cables through a bulkhead connector panel. Composite command signals were generated by the modulator and fed to the S-band source rack. This rack was composed of an S-band signal generator phase locked to a frequency synthesizer via a microwave syncronizer. The synthesizer was modified to allow phase modulation from 0-300 kHz. The resultant modulated S-band signal was routed through a variable level precision RF path allowing control of the input level at the transponder preselector over the range of −70 to −196 dBm. The demodulated composite signal plus noise from the receiver was applied to the FCS which acquires sync and demodulates the command data.

Performance evaluation of the FCS was accomplished by use of extreme value theory techniques which required sampling of the command and sync channel matched filter outputs just prior to dump time. This was

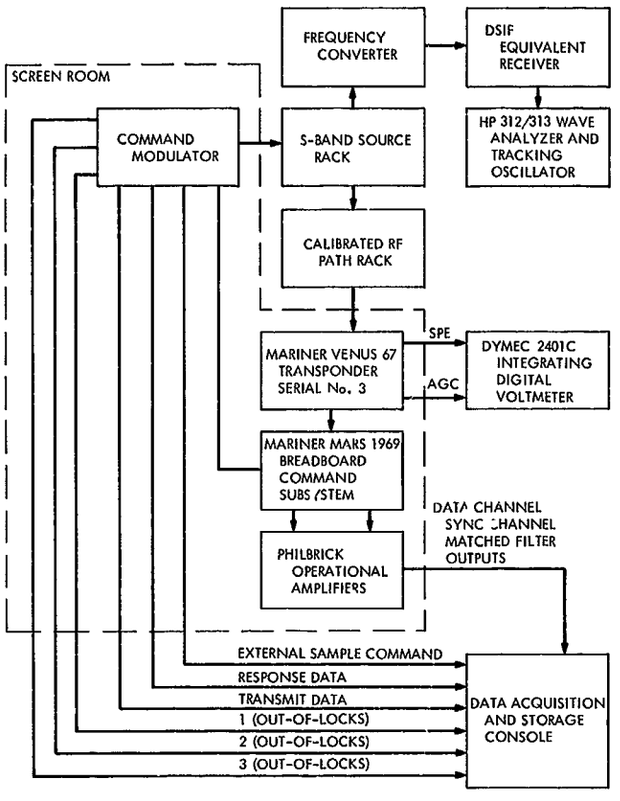


Fig. 8. Command breadboard test configuration block diagram

accomplished by use of the data acquisition and storage console (DASC) which was capable of sampling four analog channels and twenty four digital channels. The data are multiplexed, formated and recorded on magnetic tape in an IBM compatible format. The external sample command pulse for the DASC was derived from the command modulator and occurred approximately 250 μs prior to dump time. Thus for all practical purposes, the peak value of the matched filter outputs were recorded.

Functions recorded by the DASC were:

(1) Data channel matched filter output.

(2) Sync channel matched filter output.

(3) Transmit data.

(4) Response data.

(5) 1 O/L (out-of-lock).

(6) 2 O/L.

(7) 3 O/L.

(8) Bits in lock.

(9) Transponder AGC.

(10) Transponder phase detector output.

The matched filter outputs were isolated by operational amplifiers, which were specially modified to produce an input impedance in the order of 10^{13} ohms. The amplifiers assured that there would be negligible loading effects on the filter outputs. Certain FCS outputs were fed to gated flip-flops prior to application to the DASC. The flip-flops served as storage elements to permit recording of the data at sample time. To permit accurate modulation index settings and phase modulator calibrations, the S-band signal was up-converted and fed to the DSIF equivalent receiver. The 10-MHz 2nd IF linear output was monitored using a wave analyzer and associated tracking oscillator. This output level is directly proportional to carrier power when the receiver is operated in MGC mode, and therefore giving a measure of modulation index.

2. SNR measurement via DASC. Optimum techniques for measuring signal-to-noise ratios in the phase lock receiver were determined using a data acquisition system and computer for:

(1) The RF carrier-to-noise ratio at the IF output, by measurement of the characteristics of the "dynamic AGC" signal characteristics.

(2) The SNR of detected sinusoidal phase modulation.

The data acquisition and storage console (DASC) was the data acquisition system used in this determination, although results are applicable to similar systems.

The SNR measurements consisted essentially of sampling the receiver output signals at sample rates up to 10 kHz, performing analog-to-digital conversion of the samples, and recording the digitized samples on magnetic tape, all by means of the DASC. The tape was then read into a computer, and the data processed to obtain an estimate of the signal power and the noise power.

The test setup for measuring carrier-to-noise ratios is shown in Fig. 9.

Since we are generally more interested in the ratio of signal-to-noise spectral density, it is usually expedient to low-pass filter the coherent amplitude detector (CAD)

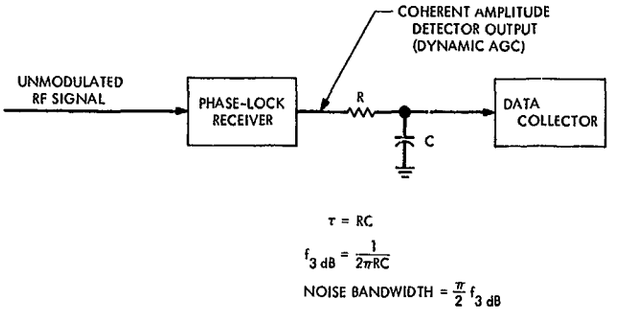


Fig. 9. Test setup for measurement of carrier-to-noise ratio

output before applying it to the DASC. This serves two useful purposes:

(1) It increases SNR, providing better accuracy.

(2) It provides a means of controlling the noise bandwidth of the noise spectrum, facilitating the determination of the ratio of signal-to-noise spectral density.

The ratio of signal power to noise spectral density is the same at the input and output of an ideal CAD.

The test setup for measuring the SNR of a detected sinusoidal phase-modulated subcarrier is shown in Fig. 10. In this instance, no filter is included, since the signal frequency must be applied to the DASC. The DASC sample rate in this case should be greater than twice the highest frequency at which there is significant power in the signal or noise spectrum. The output signal from the phase detector is assumed to be of the form:

3. Calibrations. A large portion of the available test time was spent in calibrating the various components of the test configurations shown in Fig. 8. The major areas of calibration were for S-band source rack modulator sensitivity, RF path, transponder, and command baseband.

4. Test results

a. Data analysis. The performance of the command system is normally evaluated in terms of the probability of executing a correct command, the probability of rejecting a correctly-received command, the probability of executing an incorrect command, and the probability of rejecting an incorrect command. These probabilities are in turn dependent upon the probability of a bit error in the command data channel, and the probabilities of sync channel in-lock, and out-of-lock indications, over the duration of a command word.

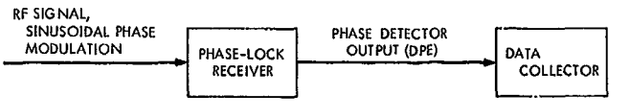


Fig. 10. Test setup for measurement of detected subcarrier-to-noise ratio

Normally, these various probabilities are determined by classical bit error tests, performed by counting bit errors under noisy operating conditions. In the command system, however, these classical bit error tests require excessive lengths of time, due to the low error rates encountered and the low data rate. To perform a classical bit error test on the command system under realistic threshold operating conditions requires approximately two weeks of operating time to find the bit error rate in the data channel, with reasonable confidence limits.

Due to the number of tests to be performed, and the relatively short time availability of the command system and associated hardware, other means were used to assess the performance of the command system. The use of extreme value theory techniques permits the estimation of bit error rates in both the data and sync channels, in test times of the order of one hour per test. Although these estimates are not sufficient to provide the complete evaluation of probabilities of executing correct commands, executing incorrect commands, etc., this data provides a convenient and useful means of evaluating the compatibility of the command system with the transponder, and of evaluating certain other effects, such as modulation index, and static phase error in the transponder carrier tracking loop.

An analysis of the techniques applied in this test program show that they are those which, with minor modifications in the computer programs, permit the use of tapes from the data acquisition system used in this program. Briefly, extreme value theory, as applied to the problem at hand makes use of voltages at the output of the matched filter of the command data and sync channels just prior to dump time. Under certain restrictions, the tail end of the probability distribution curve of these voltages is defined by a double exponential function of a linear expression of the voltage. The techniques of application, in this case, is to divide the test data into groups of 100 points, and choose the voltage nearest zero in each group of 100 points.

Approximately 32 groups of 100 points each were used in each test. This provided a set of data from which the parameters of the assumed probability distribution could be established. Once these parameters were determined, the bit error rate was estimated by extrapolating the distribution to the point of zero voltage, or the point at which the decision of the data state was reversed.

Test results by classical techniques were available from the Motorola test program of the command system breadboard. These results are shown on the accompanying curves (Figs. 11–13) to provide: (1) an evaluation of the extreme value techniques used; and (2) a reference in determining degradations resulting from the radio system and various other parameters of the test setup.

b. Direct tests. To provide an evaluation of the statistical techniques applied to the problem, and a point of reference for further tests, tests were first run on the FCS electro-mechanical breadboard without the radio link. The test setups and calibrations were explained previously.

Figure 11 shows the predicted probability of bit error in the data channel and the predicted probability of detecting a single out-of-lock condition, given that the loop is in-lock. The 90% confidence intervals for the various test points are also shown. (It should be noted that these confidence intervals are the intervals predicted by the statistics of the data only, and do not include the effects of errors in the equipment calibrations, inaccuracies in measurements, etc.) It is to be noted that the direct tests correspond very closely to those tests performed by classical techniques.

On Fig. 11, as well as the following figures, the results of bit error tests performed by the vendor on the FCS breadboard are shown for comparison. Test data (bit error rates) is shown for both the command data channel and the command sync channel, together with the

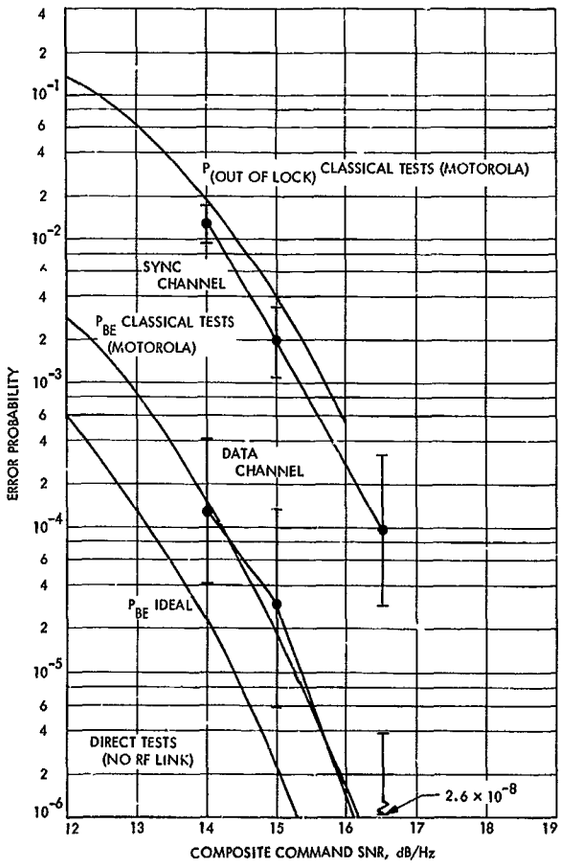


Fig. 11. Command system test curve, direct tests

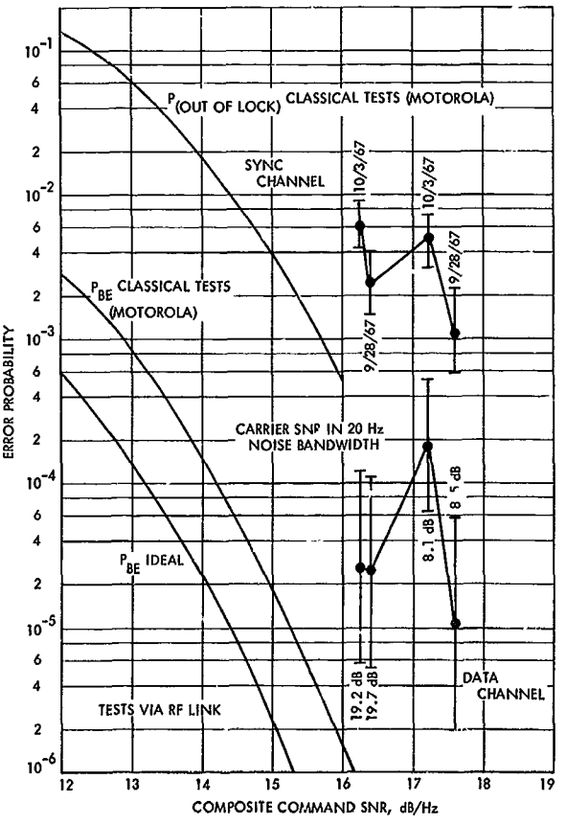


Fig. 12. Command system test curve, test via RF link

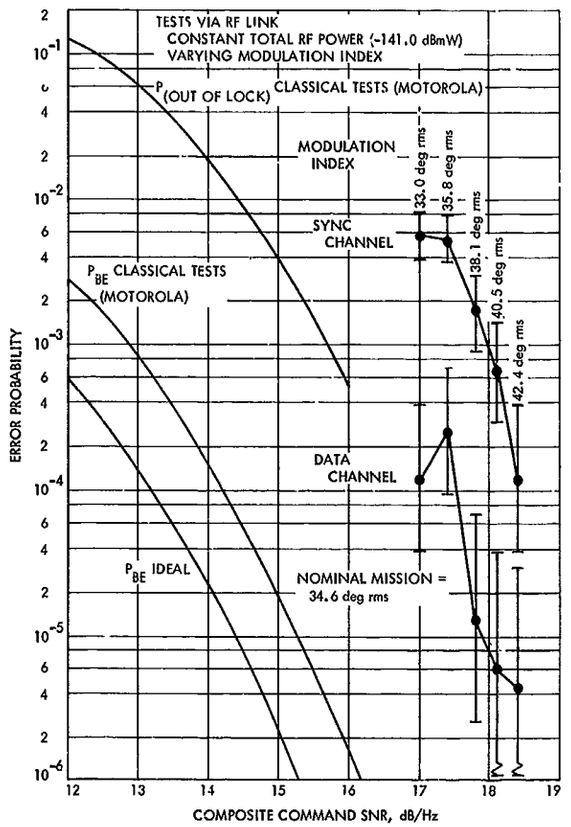


Fig. 13. Command system test curve, test via RF link, with varying modulation index

90% confidence interval as predicted by the extreme balue analysis. The predicted bit error is indicated by the small circles in the figures, while the 90% confidence intervals are indicated by the heavy vertical lines. The composite signal-to-noise ratio is the ratio of total useful command power to noise in a 1-Hz bandwidth, at the input to the transponder. Consequently the composite command signal to noise ratio on the figures does not account for degradation which may be produced by the transponder.

c. RF test, strong carrier. Tests were performed under conditions of a carrier level approximately 20 dB above transponder threshold, with the command signal to noise ratio at threshold conditions (16.5 dB in a 1-Hz bandwidth). The results of these tests were expected to be in agreement with those tests performed by direct baseband techniques, Fig. 11. The test results were not in agreement with the baseband tests (Fig. 11) but show an unexpected degradation of approximately 1.5 dB. This descrepancy is discussed in further detail in a later section of this report.

d. Threshold carrier. The remaining test data shown in Fig. 12 (the data labeled 8.1 dB and 8.5 dB carrier SNR in 20-Hz noise bandwidth) are the data resulting from tests with signal levels and modulation indices approximating conditions at nominal command threshold (16.5 dB composite command signal to noise ratio in a 1-Hz bandwidth, 8.0 dB carrier signal to noise ratio in the transponder tracking loop threshold noise bandwidth). It was expected that the data under these conditions would be degraded by 1.4 dB from similar data taken with strong signal conditions in the transponder tracking loop. Comparing the data (Fig. 12) for conditions of carrier level approximately 20 dB above threshold, and for carrier level approximately 8 dB above threshold, it is seen that a degradation of approximately 1.2 dB exists at the lower carrier levels, which is considered to be in excellent agreement with the predictions.

e. Static phase error in the transponder loop. Two tests were made to evaluate the effects of the static phase error in the transponder carrier tracking loop by offsetting the uplink frequency. The first test was made with a plus 9.0 kHz frequency offset, to produce a static phase error of approximately 15 deg, the second test was made with a frequency offset of −6.0 kHz to produce a static phase error of −10 deg. The tests were attempted at signal to noise ratios and modulation indices according to nominal command threshold condition, but difficulty was encountered in the first test in maintaining the transponder loop in lock for the duration of the test. Consequently, the total RF power was increased by 3 dB to maintain transponder lock. The test results are as follows:

Test	Frequency offset (S-band)	Carrier SNR in 20 Hz	Command SNR in 1 Hz	Data bit error rate	90% confidence interval		Sync bit error rate	90% confidence interval	
1	+9.020 kHz	11.04	20.04	7.5×10^{-3}	4.4×10^{-9}	1.3×10^{-6}	2.5×10^{-5}	5.4×10^{-6}	1.1×10^{-4}
2	−6.013 kHz	8.04	17.04	1.6×10^{-4}	6.0×10^{-5}	5.1×10^{-4}	3.9×10^{-3}	2.5×10^{-3}	6.0×10^{-3}

When the degradation of ST/N_0 from the ideal curve of the above data is compared with the data in Fig. 12, there appears to be no significant degradation in the command bit error rates due to transponder static phase error. Indeed, it appears that there is no significant command performance degradation from static phase error (at least due to frequency offset) as long as the carrier tracking loop remains in lock.

f. Variation of modulation index. The *Mariner* Mars 1969 modulation indices were determined by the assumption that the composite command signal to noise ratio in a 1-Hz noise bandwidth of 16.5 dB, and a carrier signal to noise ratio in a 20-Hz noise bandwidth of 8.0 dB, are required for command system operation. To evaluate the effects of lower carrier powers, tests were run with the total RF power level set to the nominal threshold conditions, while varying the modulation index. The results of these tests are shown in Fig. 13. As is seen from the figure, considerable improvement in command system performance is obtainable by increasing the modulation index, even though this results in carrier levels less than 8.0 dB from transponder threshold.

5. Conclusions. The test results show the command subsystem to operate as expected, when mated with the *Mariner* Venus 67 transponder, with two important exceptions: (1) there is an unexplained degradation of about 1.5 dB in all tests with the transponder, and (2) test results indicate that significant improvement in command threshold performance may be obtained by increasing the modulation index.

a. The unexplained 1.5 dB. Several tests were performed to determine the cause of the apparent 1.5-dB discrepancy with negative results. Time did not permit further investigation.

b. Effects of varying modulation index. The modulation index for the *Mariner* Mars 1969 command system was selected on the basis of (1) the composite command signal-to-noise ratio required at command threshold in a 1-Hz noise bandwidth is 16.5 dB, (2) a radio loss of 0.75 dB, due to transponder phase jitter is expected, (3) a loss of 0.65 dB is expected, due to limiter action, and (4) a carrier level of 8.0 dB above transponder threshold is required at command threshold. The modulation index was chosen, such that the command signal-to-noise ratio and the carrier level approached threshold requirements at the same RF power level.

To determine whether improved results could be obtained at different modulation indices, tests were run to determine the command bit error rates for a constant RF power level, but with varying modulation index. The results of these tests are shown in Fig. 13. It is seen from Fig. 13 that significant improvement in command performance, and presumably in command system threshold can be attained by increasing the modulation index above that which has been prescribed (34.6 deg rms). The use of modulation indices greater than the nominal mission indices (34.6 deg rms), however, results in carrier levels less than 8.0 dB above transponder threshold.

The test results here, however, indicate that such a situation does, nonetheless, increase overall command capability. As a consequence of these results and further analysis the command modulation index was increased.

D. FCS and RFS System Tests

This section describes the telecommunications system level testing done with the FCS detector breadboard unit in CTA-21 from April 16, 1968 to May 10, 1968. These tests were similar to the previous command breadboard system tests, and were designed to accomplish the following:

(1) Evaluate FCS performance when operating with the FCS operational support equipment (OSE), DSIF-equivalent transmitter, and spacecraft receiver resulting from variations in the following parameters:

  (a) RF power level

  (b) RF carrier SNR in $2B_{Lo}$

  (c) Command modulation indices

  (d) Spacecraft receiver SPE

(2) Verify FCS performance when operating with the read, write, verify (RWV), the DSIF transmitter, and the spacecraft receiver.

(3) Generate performance parameter values to be used in support of spacecraft assembly facility (SAF), environmental test laboratory (ETL), and AFETR spacecraft systems tests, as well as in SPAC for flight operations.

All of the above test objectives were met and satisfactory performance of the command link was demonstrated.

E. Telemetry Breadboard Tests

Telemetry tests at uncoded rates of 8⅓, 33⅓, 66⅔ and 270 bits/s were performed to confirm operational compatibility of the multi-mission telemetry (MMT) system with the *Mariner* Mars 1969 telemetry system. The complete operational loop, consisting of the *Mariner* Mars 1969 FTS breadboard, *Mariner* Mars 1969 RFS breadboard exciter, CTA-21 S-band receiver system, subcarrier demodulator assembly (SDA), telemetry and command processor (TCP) computer, and associated software were tested.

High-rate, block-coded telemetry tests at 16,200 bits/s were also performed using the same operational loop as used for the uncoded telemetry tests, with the addition of the high rate correlator and TCP software peculiar to the high rate system.

1. Test descriptions. The normal procedure used for measuring the performance of the telemetry subsystem was to set a series of ST/N_0 values and measure the overall system bit error rate (BER) performance using a classical (bit-by-bit comparison) technique.

The basic test configuration for measurement of the bit error rate is shown in Fig. 14. Although this figure illustrates the block diagram used for channel B tests, the channel A test block diagram is identical with the exception that for channel A data is not synchronous with the subcarrier; therefore, the bit sync source for the channel A tests was derived from an HP 5100A frequency synthesizer.

2. Preliminary tests. Preliminary telemetry bit error tests were conducted using software developed for checking bit sync algorithms. These tests were performed to confirm anticipated bit error performance, and also to compare the operational capability at three different bit sync bandwidths, 0.1%, 0.5%, and 1%. Table 6 gives a summary of the bit error tests indicating the observed performance at threshold as compared to the anticipated performance.

3. Operational BER tests. A second series of telemetry tests performed at CTA-21 were called the operational tests. These tests differed from the preliminary tests in that two production model SDAs had been installed at CTA-21, so that the CTA-21 was in a configuration similar to a normal DSIF station. The second difference was that the operational software was available and the tests were run using this software. Bit error rate tests were performed simultaneously on both SDAs in order to get an idea of how the two SDAs would compare.

Table 6. Summary of actual vs anticipated BER performance at threshold for preliminary tests

Bit rate, bits/s	Spacecraft mode	ST/N_0 for BER $= 5 \times 10^{-3}$		Performance degradation, dB	ST/N_0 setup tolerances, dB
		Anticipated dB	Actual dB		
8⅓	Cruise	+6.95	+7.65	0.7	±0.48
33⅓	Cruise	+6.05	+6.00	0.0	±0.48
66⅔	Encounter 1	+5.95	+6.40	0.45	±0.36
270	Playback 1	+5.50	+5.90	0.40	±0.36

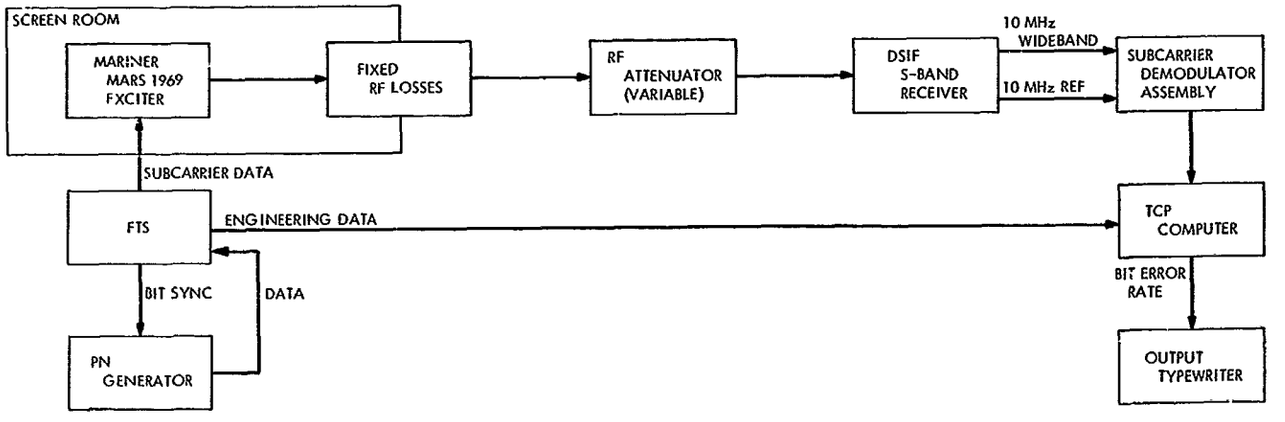


Fig. 14. Channel B bit error rate test block diagram

The test configuration used was identical to that described for the preliminary bit error tests in the previous section.

The measured bit error rate performance at 33⅓, 66⅔, and 270 bit/s was as anticipated.

IV. Telecommunications System Tests

A. Spacecraft Checkout Circle Testing

1. Monitoring and data collection. Performance monitoring was accomplished in the checkout circles at spacecraft assembly facility (SAF), building 248 (thermal/vacuum) and building 144 (vibration) with the subsystems installed on the spacecraft. In the SAF and during thermal/vacuum testing, quantitative data were obtained in addition to performance monitoring. Some of the parameter measurements of interest are as follows:

(1) RFS threshold

(2) AGC and SPE calibrations

(3) RF carrier suppression and sideband to carrier ratios (modulation indices checks)

(4) Receiver best lock frequency

(5) Auxiliary oscillator frequencies

(6) RF transmitted power levels

(7) Command VCO frequency

(8) Command lock statistics

(9) Command data channel bit error rates

Data from the above parameter measurements were necessary for assembling meaningful data record books. In addition, performance monitoring was instrumental in discovery and evaluating problems and failures. The problem of exciter sensitivity variation with temperature was discovered. Other major problems uncovered included an unexplained RF power output fluctuation and abnormal RFS local oscillator behavior with temperature. Review of the System Test Complex Data System (STCDS) computer print-outs along with recording of OSE readings provided the prime monitoring capabilities.

2. Special tests. Special tests were accomplished with the subsystems in the SAF, both on and off the spacecraft, ordinarily as required for trouble-shooting purposes. The most significant special tests performed were in connection with the adjustment of the RFS exciter modulation sensitivities. This was necessary after the telemetry modulation indices were found to be low for each spacecraft. This condition was the result of lower than required FTS modulation levels and RFS modulation sensitivities at delivery to SAF. In addition to special tests in SAF, the RFS units were tested individually at ETL to quantitatively determine the exciter sensitivity variation with temperature.

B. Spacecraft/CTA-21 Tests

1. Spacecraft assembly facility. Initial testing with CTA-21 while the spacecraft was in SAF provided general knowledge of the spacecraft/CTA-21 test set-up and experience on which to base later testing.

2. Environmental tests

a. General. Compatability test area-21 testing during spacecraft environmental tests consisted of measuring telemetry performance during thermal/vacuum testing in building 248 for each spacecraft. No CTA-21 testing was conducted during spacecraft vibration testing in building 144.

b. Test set-up. The test set-up is shown in Fig. 15.

c. Measurements. Telemetry parameters which were measured included:

(1) Subcarrier frequencies.

(2) Subcarrier acquisition times.

(3) Data bit rates.

(4) Bit error rates.

(5) Range delay calibrations.

The bit error rates testing was accomplished for all telemetry channels at the various data rates and under the following conditions:

(1) ST/N_0 variation.

(2) Combinations of primary and redundant spacecraft FTS data processors and RFS exciters.

(3) Combinations of one and two-way RF tracking and ranging on and off.

(4) Inclusion and deletion of a high pass filter in the CTA-21 subcarrier domodulator assembly (SDA).

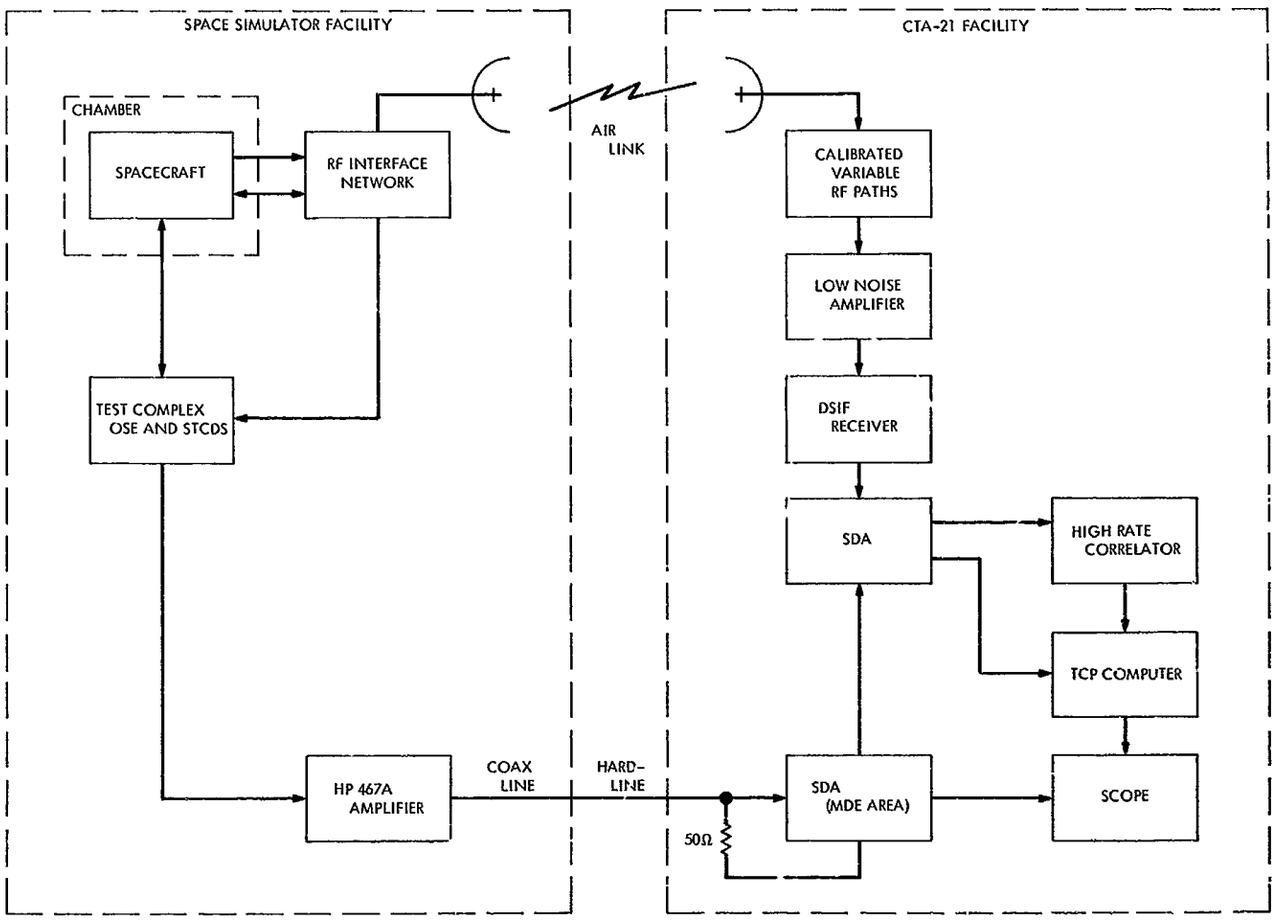


Fig. 15. Test setup in the 10-ft space simulator, with CTA-21 block diagram

Bit error rates were derived for the uncoded channels in real-time in the TCP computer by making a bit by bit comparison of RF and hardline transmitted data. Coded data via RF transmission was recorded at CTA-21 for nonreal-time processing with hardline data recorded at the building 248 System Test Complex (STC) to derive coded channel bit error rates.

d. Results. Measured subcarrier frequencies, subcarrier acquisition times and data bit rates were compared with the specified values and were found to be within the allocated tolerances. Measured bit error rates for the uncoded data channels with the SDA high pass filter removed (as for flight) were all within 1.5 dB (estimate of overall ST/N_0 accuracy) of the expected values. However, the 1.5-dB accuracy estimate does not includes variations in exciter sensitivities with temperature, which were known to occur but were not compensated for. Design control tables were tabulated for the RF links associated with each test mode in order to check the ST/N_0 values by comparing the calculated P_c and actual P_c (from measured AGC). Differences were less than 1 dB in most cases and did not exceed 2 dB in any case. It is noted that a definite degradation in performance occurred with the SDA high pass filter connected as a function of the data transition density and time. No BER results were obtained for the block coded data as the STC hardline data was not made available for comparison.

C. Compatibility Tests

Compatibility tests for *Mariner* Mars 1969 were extended from those conducted for previous missions. Actually, the breadboard telemetry tests, discussed previously, checked compatibility of the breadboard telemetry and radio subsystems with the DSIF multi-mission telemetry system.

Formal compatibility tests were conducted at JPL on the M69-1 proof test model (PTM) for 50 h, and M69-4 for 16 h. Compatibility verification tests at DSS 71 were conducted on M69-2,3, and 4 in an approximate 8-h test.

1. Proof test model compatibility tests. This test, officially titled the "*Mariner* Mars 1969 Spacecraft Deep Space Instrumentation Facility Interface Compatibility Test" was conducted from July 10 to 17, 1968.

A basic block diagram of the test setup is shown in Fig. 16. The PTM spacecraft (M69-1) was located at the spacecraft assembly facility. All telecommunications equipment was representative of the 1969 flight equipment, with the exception of the FTS output amplifier which was not the latest version. The affect of using this amplifier, which has rise and fall times of 0.5 μs, in comparison to flight unit rise and fall times of 0.1 μs, was to cause some modulation indices to fall outside specified values.

The test was performed via an RF air link to CTA-21. Telemetry subcarrier were brought by hardline from SAF to CTA-21. These subcarriers were demodulated to recover the telemetry bit stream, which was used as comparison data for bit error tests.

a. Radio subsystem tests

Best lock frequency. The best lock frequency was measured in two ways. First, the auxiliary oscillator inhibit function was used. In this mode the spacecraft transmits using the receiver VCO as a drive source. Thus the VCO rest frequency can be observed directly. A second technique was to locate the frequency at which uplink lock was achieved with minimum signal level.

The two techniques agreed to within 500 Hz at S-band. The best lock frequency was within specified tolerances.

Downlink threshold. The DSF receiver threshold was measured with the spacecraft in both one-way and two-way modes, in all telemetry modes, both radio exciters,

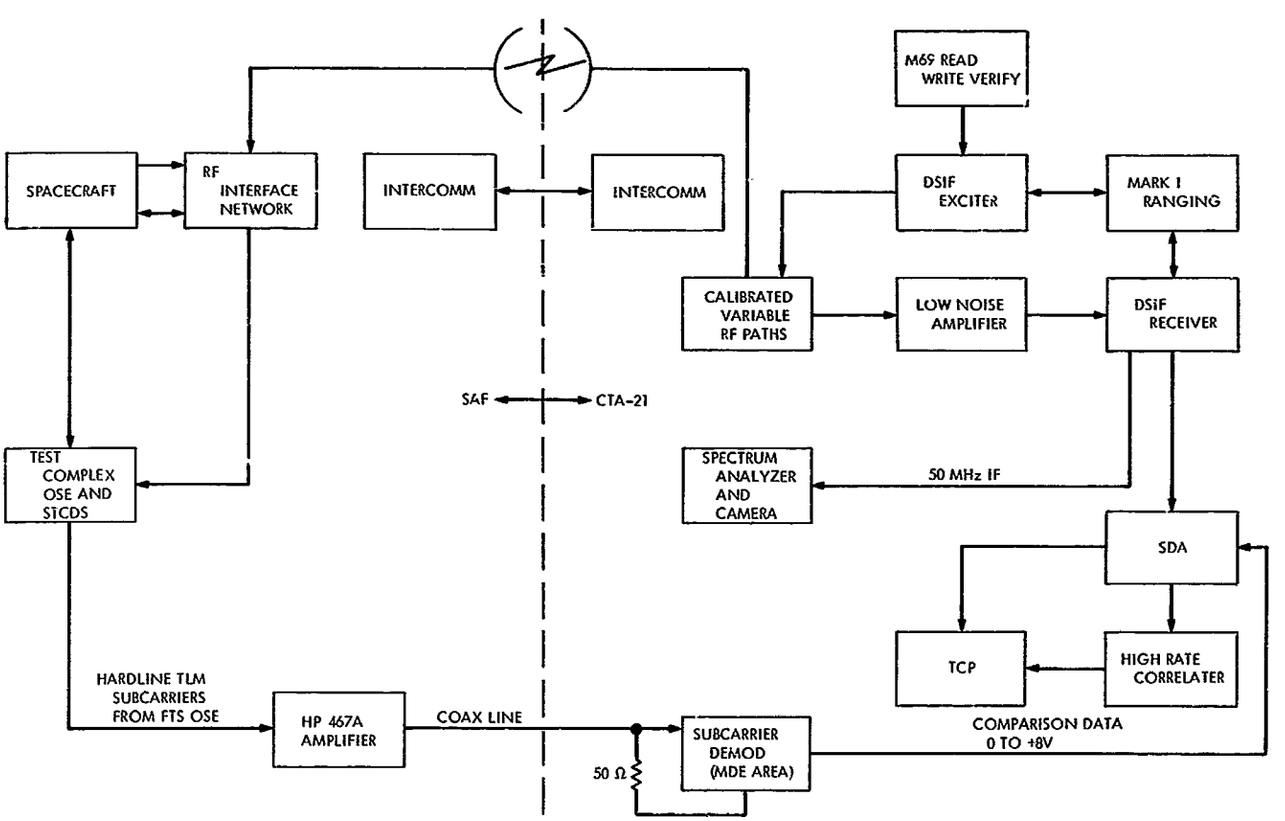


Fig. 16. Test configuration for PTM compatibility tests

and both telemetry output amplifiers. All measurements agreed within ±2 dB of anticipated threshold.

Uplink threshold. Uplink threshold was checked with the uplink unmodulated, with only command modulation, and with both command and ranging modulation. All measurements were within ±1.2 dB of anticipated threshold.

Downlink spectrum analysis. Downlink modulation indices were measured in all telemetry modes for both radio system exciters. With the exception of the channel C modulation indices, which were out of specification due to the non-flight FTS amplifier, all indices were in specification. No spurious signals were observed on the spectrum analyzer within 30 dB of the carrier.

Uplink spectrum analysis. The uplink spectrum was examined for spurious signals for three conditions: first with no modulation, second with only command modulation, and third with command and ranging modulation. No spurious signals were observed within 30 dB of the carrier.

Auxiliary oscillator frequency stability. Stability of auxiliary oscillator 1 was checked for a 30-min period after turn-on. During this time period the frequency change observed was 40 Hz, which was well within specifications.

b. Command tests

Polarity verification. The polarity of the transmitted command signal was verified by observing proper lock times with the correct polarity, while the command system was unable to acquire lock with the signal inverted at an uplink carrier power of 141 dBm, which is well above threshold.

Operational capability (strong signal). A series (ten total) of direct (DC), quantitative (QC) and coded (CC) commands were sent at strong signal best lock frequency, and at ± 25kHz, and ± 63 kHz from best lock. All commands were executed properly.

Operational capability (weak signal). A sequence (ten total) of DC, QC, and CC were transmitted at command threshold ($P_c = -146$ dBm) at best lock frequency, and at ± 8.6 kHz from best lock. All commands were properly processed.

Commanding with ranging. Ten commands were properly processed with ranging modulation and at command threshold.

Acquisition characteristics. Five lock acquisitions were observed, all at signal levels close to threshold. Three were at best lock frequency, and the other two were at ± 8.6 kHz from best lock. The average acquisition time was 5 min, 35 s. The longest acquisition was 8 min, 10 s. Maximum specified acquisition time was 12 min.

c. Telemetry tests

Bit error tests. Bit error tests for uncoded telemetry channels were performed using the classical technique of bit by bit comparison. The multi-mission telemetry system (MMT) output was compared with data run by hardline from SAF to CTA-21. Bit error rate tests were made at two ST/N_0 values in the test configurations shown in Table 7. Measured performance agreed with predicted to within estimated test tolerances of ± 1 dB except at 8⅓ bits/s, and one point in a one-way test. Time was not sufficient to locate the source of the problem. Later tests with flight spacecraft indicated proper performance.

Acquisition times. The time interval from receiver in-lock indication to SDA inlock indication was measured. For this test the SDA had previously been adjusted to the exact subcarrier frequency.

Bit sync loop lock time was measured from the start of the TCP bit sync program to the time that the computer derived bit timing pulse is within 1/10 of a bit time of the hardline data bit transitions. Abnormally long (compared to other data rates) acquisition times were observed at 8⅓ and 33⅓ bits/s.

Table 7 Bit error rate test configurations

RF mode	Telemetry mode	Bit rate, bits/s	Remarks
36	Cruise	33⅓	2 way RF, ranging off
36	Cruise	8⅓	
36	Encounter 1	33⅓	
36	Encounter 1	66⅔	
52	Playback 1	270	2 way RF, ranging off
37	Cruise	33⅓	1 way RF, ranging off
62	Cruise	8⅓	2 way RF, ranging on

Frame sync acquisition time is defined as the time from start of the TCP program to the printout by the computer of "frame-in-lock."

Data for the SDA, bit sync, and frame sync lock times are shown in Table 8. All tests were repeated five times at an ST/N_0 value of + 5 dB. No specifications are known, however, the times observed appeared not to be an operational problem.

Bit rates and subcarrier frequencies. All bit rates and subcarrier frequencies were measured and were within specifications

d. Ranging tests.

The polarity was confirmed as correct by evidencing valid range numbers.

e. Conclusions. The PTM compatibility test results indicate compatibility of the *Mariner* Mars 1969 spacecraft with the DSIF. The minor deficiencies noted in the tests were resolved in either additional CTA-21 tests or in later compatibility verification tests with flight spacecraft.

2. RF verification test of M69-4. The RF verification test of M69-4 (flight spare) was performed on Nov. 20, 1968. Located in the vacuum chamber, it was a 16-h test. The following individual tests were performed:

(1) Telemetry bit error tests (uncoded telemetry).

(2) Subcarrier and bit rate frequency measurements.

(3) Capability to process telemetry via the TCP in all modes (both uncoded and coded).

Table 8. SDA, bit sync, and frame sync lock times

Lock condition	Lock sync, s			
	8⅓ bits/s	33⅓ bits/s	66⅔ bits/s	270 bits/s
Average SDA lock time	28.2	6.7	24.4	14
Maximum SDA lock time	58	23	70	23
Minimum SDA lock time	9	1.6	5	7
Average bit sync lock	52.7	8.3	7.6	21
Maximum bit sync lock	62	9.5	12	44.5
Minimum bit sync lock	33	7.8	5.7	5.8
Average frame sync lock	19.75	6.2	4.2	
Maximum frame sync lock	42	8	5	
Minimum frame sync lock	5	5	2	

(4) Downlink spectrum analysis.

(5) Downlink threshold.

(6) Uplink threshold.

(7) Command operational verification at strong and weak signals, with and without offsets from best lock frequency.

(8) Tuning and acquisition at project specified rates.

(9) Auxiliary oscillator phase jitter, and frequency stability.

No incompatibility was observed except for an inability to tune the uplink at 10 Hz/s (S-band) with an uplink carrier power level of 144 dBm. The rate in the telemetry instruction manual was thus changed to 5 Hz/s. All measured parameter values were within test specifications.

3. RF verification tests of M69-2 and M69-3. These two RF verification tests were conducted with DSS 71 at the AFETR. The spacecraft were located in building AO. Tests performed were as follows:

(1) Telemetry performance tests (all modes).

(2) Subcarrier frequency and bit rate measurements.

(3) Telemetry processing capability (all modes).

(4) Downlink spectrum analysis.

(5) Downlink threshold.

(6) Uplink threshold.

(7) Ranging threshold.

(8) Tuning and acquisition at project specified rates.

No problems were encountered.

4. Special tests. During spacecraft testing, a basic incompatibility between one of the *Mariner* 1969 spacecraft telemetry modes and the operational configuration of the SDA was observed.

The spacecraft mode was the CC&S *single-word-read-out* mode in which single words are read from the CC&S memory upon receipt of ground commands at a minimum time interval of 1 min. Between each word the telemetry system transmits a continuous string of "zeros." Thus in this mode the telemetry data is very heavily biased with many more zeroes than ones.

The reaction of the SDA to this data sequence was as follows:

(1) Upon transfer to the CC&S mode, the SDA output moves to the infinite bit level of 1.5 to 2.0 V, since the SDA sees a series of zeroes for a minimum of one minute at the start of this mode.

(2) The SDA output is ac-coupled; therefore, as the output filter capacitor starts to charge toward the infinite bit value, the SDA output settles toward 0 V.

(3) The TCP computer will make normal data decisions at the infinite bit level but will start making additional decision errors as the SDA output settles toward 0 V. Upon reaching 0 V, the BER (with an input of all zeros) will be 0.5.

A series of tests were conducted to determine a fix for this problem. These tests also indicated that performance was degraded significantly if the telemetry data stream was biased even slightly from a 50% one-zero distribution. Figure 17 illustrates the results of a test comparing two SDAs, one ac-coupled and one dc-coupled. Commutated data from the FTS breadboard was used

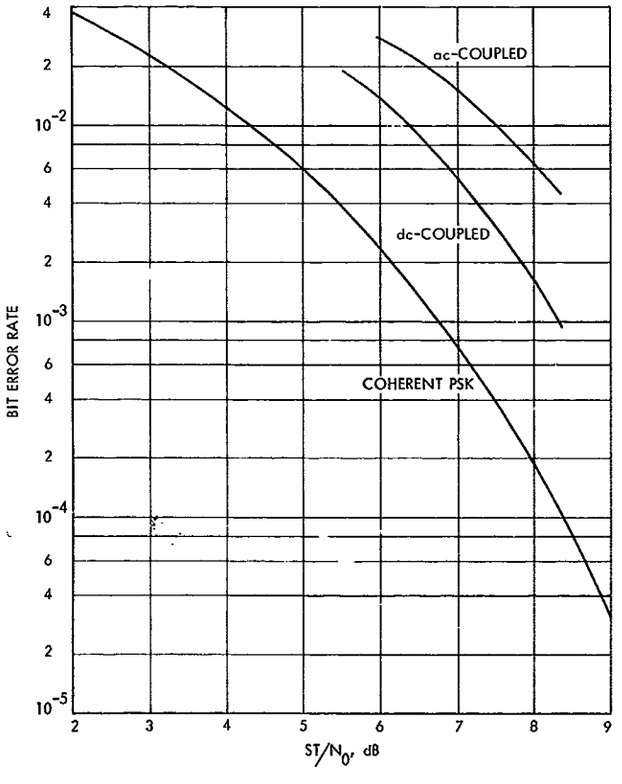


Fig. 17. Comparison of ac vs dc coupling for the SDA

with data words adjusted to provide approximately a 2–1 bias in favor of "one" bits over "zero" bits. This bias led to an approximate 1.2-dB degradation in performance for the ac-coupled SDA.

Another test, in which a data word of 1110101 was repetitively transmitted, indicated an approximate 2-dB degradation for an ac-coupled SDA, over the dc-coupled unit. As a calibration in this test a data stream of alternate ones and zeroes was used, giving identical performance for both SDAs.

These special tests also resolved a previously noted variation in bit error performance with the flight spacecraft with time, since it became obvious that the bit error rate, with the SDA ac-coupled, could be a function of the spacecraft configuration. In different configurations, the makeup of the data stream will be different.

Many additional tests were conducted with other data patterns, to confirm that the SDA could be operated dc-coupled without other problems being observed related to the dc coupling. Tests were also conducted to observe bit sync stability when no data transitions were observed over a long period of time.

The final decisions were:

(1) Change the SDA output from ac- to dc-coupling. This modification was incorporated in all SDAs by an engineering change requirement (ECR). Mission results were excellent.

(2) Limit the CC&S readout mode to 10 min since bit sync drift after this time will start to degrade the bit error rate.

5. *High-rate block-coded telemetry*

a. Test description. High-rate telemetry tests were initially conducted using the breadboard flight telemetry subsystem and the prototype high rate correlator. Later tests were performed using the field set correlators and confirmed the results presented here. The test block diagram is shown in Fig. 18. Two different test periods are discussed. The basic differences in test configuration for the two tests were:

Data format. During the first test period, tests were conducted with either the "all ones" or "all zeros" word transmitted continuously. This corresponds to subcarrier modulated with comma free vector or comma free vector bar.

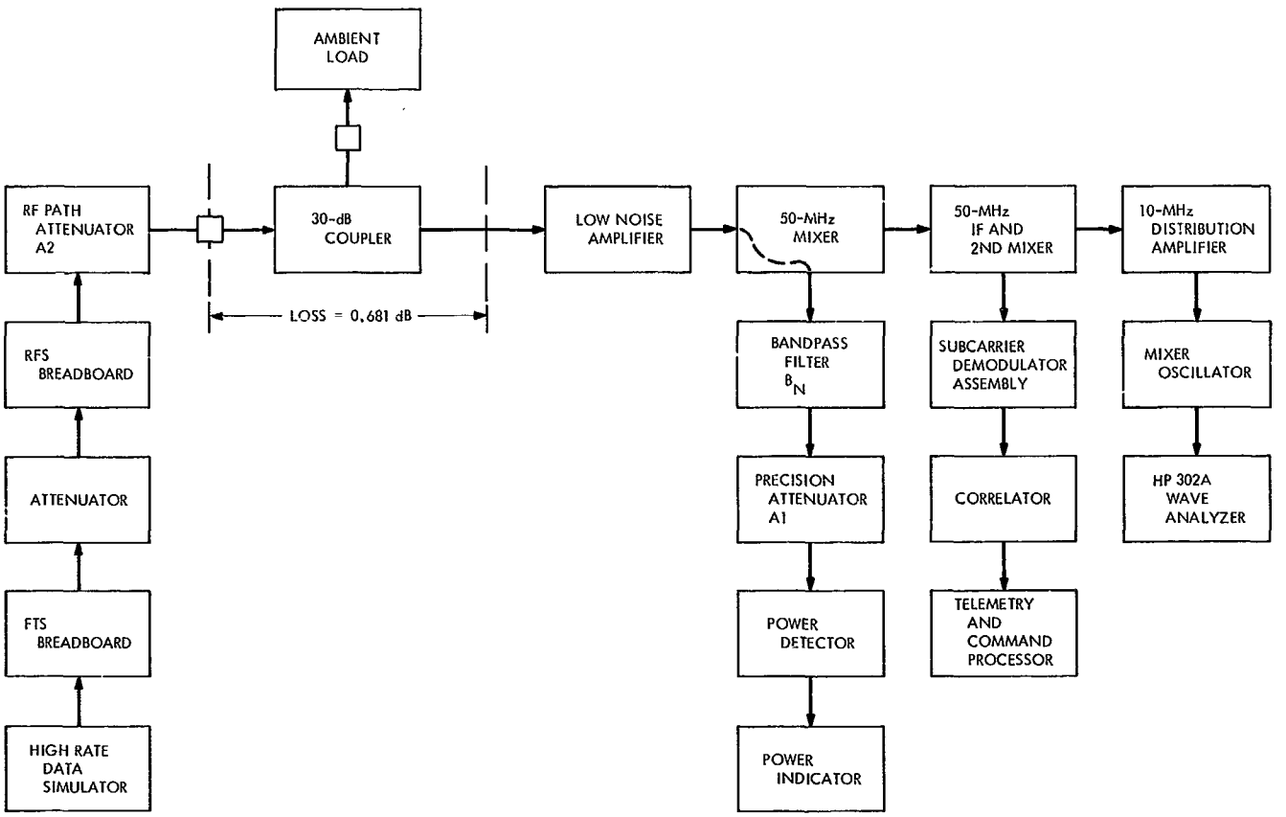


Fig. 18. High rate telemetry tests, block diagram

During the second test period, the FTS block coder was driven by a random sequence of words derived from a nine-stage PN generator. This word sequence was 512 data words long, with each word in the vocabulary repeated eight times during the sequence.

RF source. The *Mariner* Venus 67 exciter was used during the first test period and the 1969 exciter during the second. No noticeable difference in performance between the two sources was observed.

Signal-to-noise ratios were set up using the Y factor technique, which consists of measuring $S+N/N$ ratio in a precisely known bandwidth at 50 MHz. Description of this test technique was given previously.

b. Anticipated performance. For the high-rate demodulation system, including receiver, subcarrier demodulator, high-rate correlator, and associated software, a performance degradation of 0.4 dB was expected. Tests conducted by the DSIF as a buyoff of system performance indicated approximately 0.3 dB.

The major degradation caused by the breadboard FTS was due to subcarrier asymmetry. This asymmetry is 1.3% when in one data state and 3.9% in the other. This averages, assuming 50% probability of ones or zeros, to a 2.6% asymmetry. The loss in performance due to asymmetry is

$$\text{Loss in dB} = 10 \log \left(1 - 2\frac{\Delta T}{T}\right)$$

where T is the subcarrier period and ΔT is asymmetry For 2.6% asymmetry, the loss is

$$10 \log (1-0.052) = 0.23 \text{ dB}$$

It should be emphasized that the FTS performance specification on subcarrier asymmetry is 2%; thus, the FTS breadboard was outside system specifications.

Overall anticipated performance degradation from the theoretical perfect is then 0.4 = 0.23 or 0.63 dB total.

c. Test results. System performance is shown as plots of word error rate vs ST/N_0 in Tables 7 and 8. During the first tests shown in Fig. 18, system performance was checked only in the playback II mode, in which the channel C subcarrier at 259 kHz and the channel B subcarrier at 24 kHz are simultaneously modulating the RF carrier at modulation indices of 65 and 11.9 deg, respectively. Performance was within 0.1 dB of anticipated for all but one of the data points taken.

During the second series of tests, the overall performance was nominally 0.2 dB degraded from anticipated. Due to the possibility of degradation of the high rate demodulation system, it was requested that an internal loop test be made to confirm high rate performance. A performance degradation of 0.7 dB was noted, as compared to the previously observed 0.3 dB. It was thus concluded that the degradation due to operating with 1969 equipment was approximately the same as observed in test 1.

D. Operations at AFETR

A final series of telecommunications tests were performed at AFETR with the spacecraft in building AO (assembly facility), explosive safe facility (ESF), and on the pads. These tests are described in the following paragraphs.

1. Building AO. During system testing in building AO, monitoring of spacecraft performance was accomplished in the checkout circle and special measurements were made to obtain calibration data for launch predictions. Emphasis was placed on the following parameters:

(1) RF carrier suppression (modulation indices).

(2) AGC and SPE calibrations.

(3) RF power output levels.

(4) Receiver best lock and auxiliary oscillator frequencies as a function of telemetered temperature readings.

(5) Receiver threshold.

(6) FCS VCO frequency measurements.

(7) FCS and RFS threshold.

(8) FTS subcarrier frequencies and bit rates.

(9) Number of tape passes.

(10) ATR track gains and linearity characteristics.

2. Explosive safe facility. With the spacecraft in the explosive safe facility (ESF), a special trailer was instrumented adjacent to ESF to monitor hardline spacecraft functions such as RF power output. Also an RF link was established between ESF and building AO for transmission of telemetry data and commands. This permitted performance monitoring in the spacecraft checkout circle and at the instrumentation trailer.

3. On-pad

a. Transfer room. With each spacecraft on pad, a set of launch checkout equipment was located in the transfer room at the base of the tower. A calibrated RF hardline link connected the low-gain antenna probe at the umbilical connector to the launch checkout equipment. A transmitter in the transfer room was used to supply calibrated uplink levels to the spacecraft RFS for AGC checks. A power meter was used to monitor the RFS output power.

b. Blockhouse. A recorder was located in the blockhouse (some distance from the pad) for monitoring the spacecraft RF power output via the transfer room, after vacating the transfer room.

c. Checkout circle. RF links were established between building AO and the pads for precountdown and countdown operations. In addition, a hardline telemetry link was established from the spacecraft umbilical connector to the FTS OSEs in building AO. Parameters measured in the spacecraft checkout circle during precountdown included:

(1) Receiver SPE.

(2) RF carrier suppressions (modulation indices).

(3) Receiver best lock frequency.

(4) Auxiliary oscillator frequencies.

4. Spacecraft/DSS 71 tests. In addition to the spacecraft/DSS 71 compatibility tests with the spacecraft in building AO, DSS 71 participated in on-pad precountdown and countdown operations as well as miscellaneous testing with the spacecraft in building AO and at ESF.

a. Building AO. Monitoring of the spacecraft was performed at DSS 71 via an RF link during system testing primarily for collecting receiver and transmitted frequency data. In addition, spacecraft playback data was received and recorded for later processing.

b. On-pad. DSS 71 was utilized during precountdown and countdown operations as follows:

(1) Establish uplink with the spacecraft via an RF link (during precountdown) to verify command capability.

(2) Verify (during precountdown) receiver best lock frequency predictions generated from checkout circle calibrations.

(3) Verify (during precountdown and countdown) auxiliary oscillator frequency predictions generated from checkout circle calibrations.

(4) Receive spacecraft RF signal through lift-off for demodulation of telemetry and transmitted to the required users.

5. On-pad RF test links at AFETR. The RF air links between the spacecraft on pad 36A or 36B and each system test complex (STC) in building AO are shown in Fig. 19. In addition, the RF path between the spacecraft and the transfer room are shown. Direct radiation (uplink and downlink) occurs continuously through the RF transparent shroud in the case of the spacecraft low-gain antenna (LGA). The path to the umbilical tower antenna was primarily a back-up to the direct path when

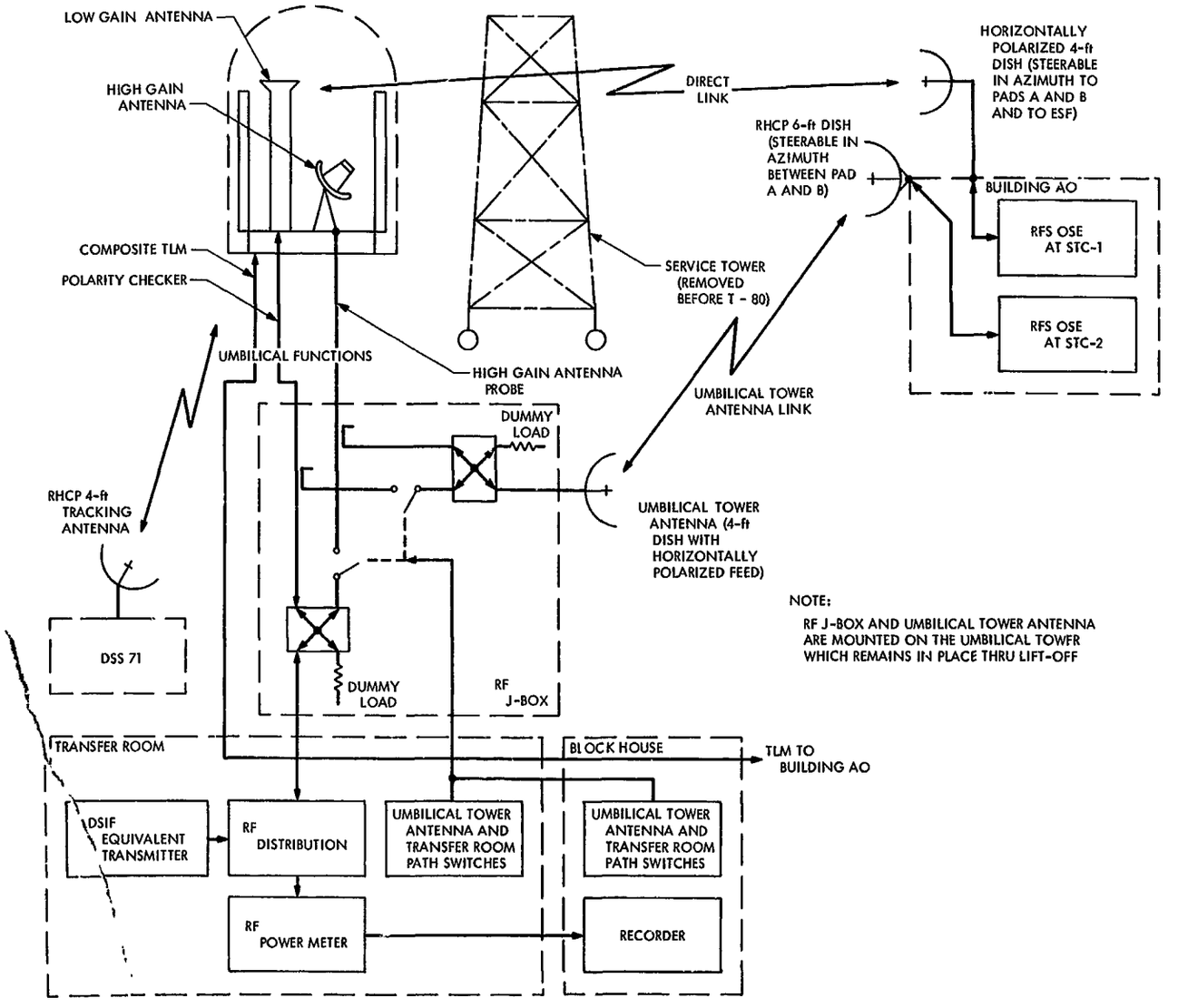


Fig. 19. RF link configuration for support of operations on pads 36A and 36B

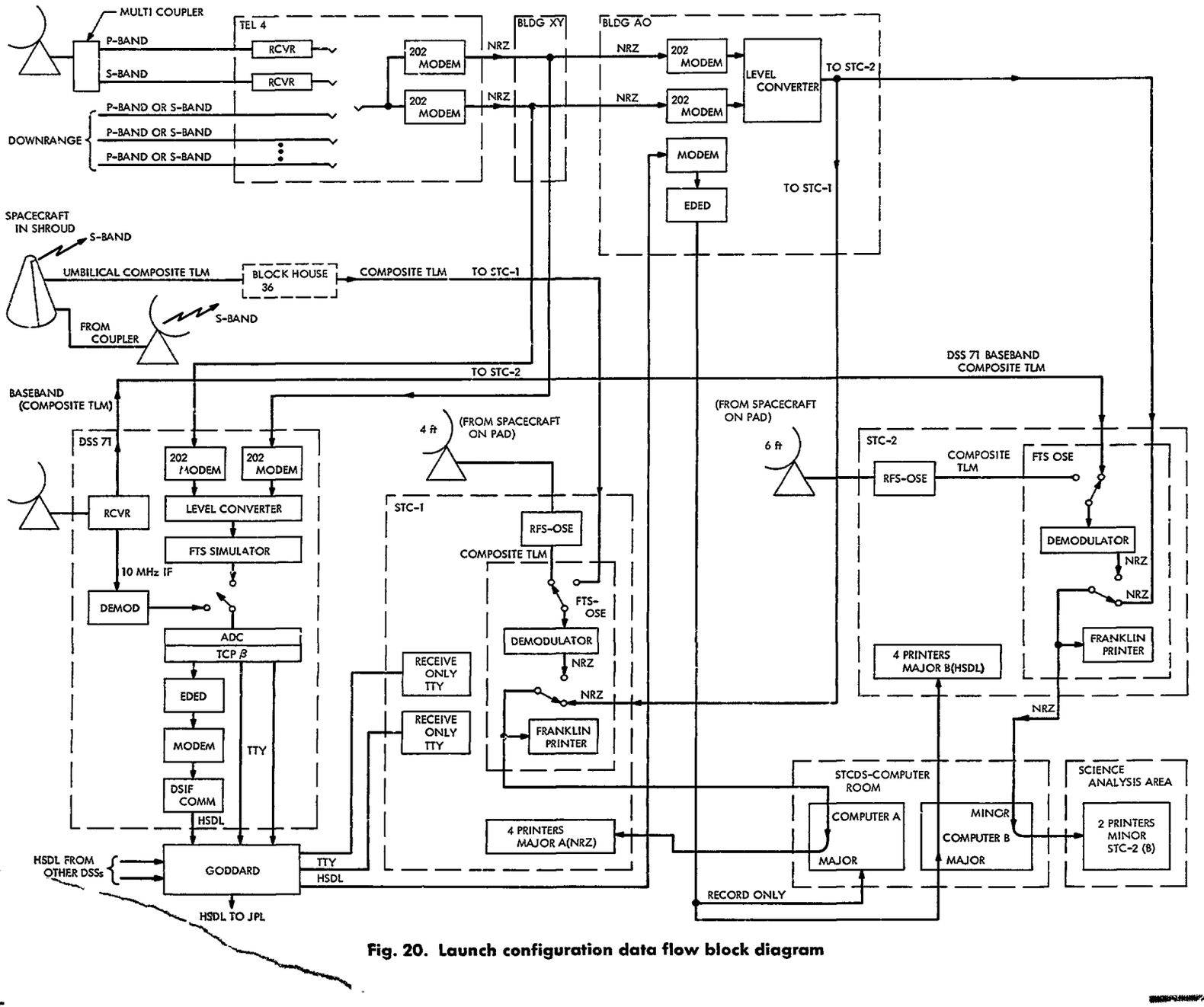


Fig. 20. Launch configuration data flow block diagram

the service tower was in place or at any time the direct path is subject to extreme variations. In the case of the spacecraft high-gain antenna (HGA), direct radiation was not possible due to the high directivity of the antenna and blockage by the solar panels in the stowed position. Hence, the path through the umbilical tower antenna was the only path for HGA downlink radiation (RFS does not receive via HGA). As shown in Fig. 19, STC-1 is connected to the 4-ft dish on the roof of building AO and STC-2 is connected to the 6-ft dish. Each antenna is repointed in azimuth for operation on pad 36A and pad 36B. The 4-ft dish also was repointed in azimuth for operation with ESF.

The RF air links between the spacecraft in ESF and STC-1 utilize a circularly polarized 6-ft dish at ESF and the horizontally polarized 4-ft dish at building AO. An RF downlink path from the spacecraft low-gain antenna polarity checker and high-gain antenna probe in ESF was also available to a power meter in the LCE trailer. No switching was required for any of the RF paths with the spacecraft in ESF.

6. Launch configuration data flow. The flow of telemetry data during countdown and following lift-off is shown in Fig. 20.

7. Countdown verification. Detailed procedures were followed during precountdown and countdown operations and called for immediate and positive responses relative to subsystem performance and readiness for launch. A special set of data sheets were generated to allow quick and formal documentation of measured data and rapid evaluation of its adequacy. The data sheets provided for pertinent information such as time, temperature, etc., as well as translation to desired units for quick comparison with pre-recorded expected values and limits of allowable variation. Launch operations were as expected for both spacecraft.

V. Radio Frequency Subsystem

The *Mariner* Mars 1969 RFS provides the communication link between the spacecraft and the ground-based DSIF. It consists of two major subassemblies; the antenna assembly with the high- and low-gain antennas and associated cables, and the radio assembly consisting primarily of a transmitter and receiver located in the electronics equipment bay VI in the spacecraft. The RFS provides the ability to:

(1) Receive the S-band radio frequency signal transmitted from DSIF.

(2) Demodulate from the RF signal the composite command signal and sends it to the command subsystem for direct commanding of the spacecraft.

(3) Demodulate the ranging signal transmitted from DSIF and condition it for retransmission.

(4) Transmit a modulated RF signal with a carrier which is phase coherent with either the received carrier or with an internally generated frequency source.

(5) Modulate the transmitted carrier with the composite telemetry signals from the flight telemetry subsystem.

(6) Modulate the transmitted carrier with the receiver detected ranging signal.

To accomplish these functions the RFS contains the subassemblies shown in the block diagram of Fig. 21. The nominal parameters of the RFS are given in Table 9.

Table 9. Nominal values of significant RFS parameters

Item	Parameter	Value
1	Receiver input frequency	2115 ± 5 MHz
2	Receiver tracking threshold	−153 dBm
3	Receiver tracking loop noise bandwidth at threshold	18 Hz[a]
4	Command channel noise bandwidth (single sided)	2.5 kHz
5	Ranging channel noise bandwidth (single sided)	1.5 MHz
6	Receiver noise figure	7.5 dB
7	Dynamic signal level range	−70 dBm to threshold
8	Transmit/receive frequency ratio	240/221
9	Transmitter output frequency	2295 ±5 MHz
10	Transmitter output power	
	(1) Low-power mode	8 W
	(2) High-power mode	16W
11	Telemetry and ranging channel modulation bandwidth	1.5 MHz
12	Power required	
	(1) 2.4 kHz 50 V	30 W
	(2) 25–50 Vdc TWT (high power/low power)	92/56 W
13	Weight of radio assembly	63 lb

[a]The actual value on *Mariner* Mars 1969 was approximately 13 Hz. The desired nominal value was not achieved.

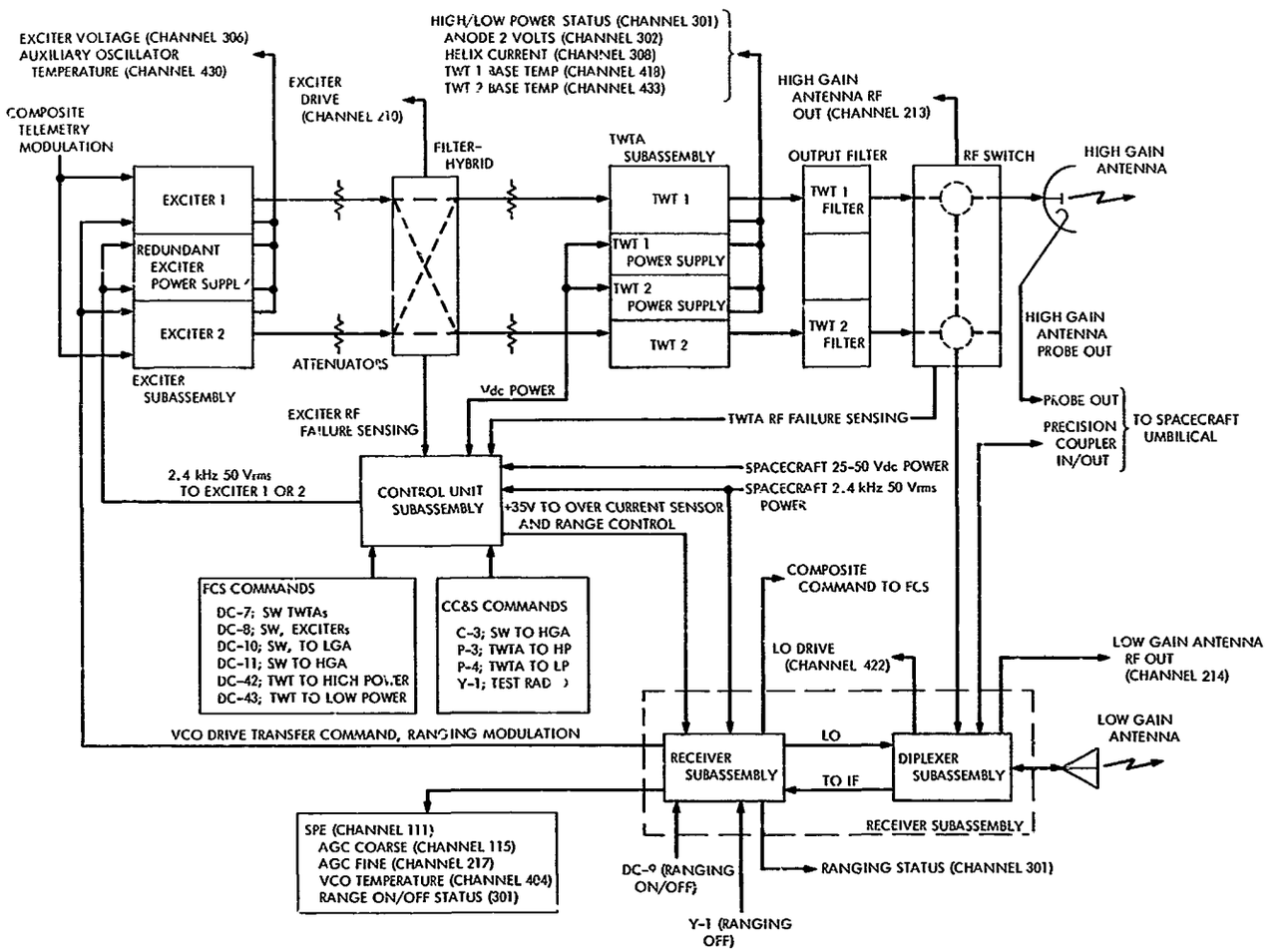


Fig. 21. Radio frequency subsystem block diagram

The *Mariner* Mars 1964 and *Mariner* Venus 67 RFS served as a design baseline for the *Mariner* Mars 1969 effort. The significant improvements made in the *Mariner* Mars 1969 RFS are:

(1) The receiver noise figure and threshold sensitivity were improved by 2–3 dB.

(2) Transmitter output power of over 16 W was achieved to support the high rate data at encounter.

(3) The receiver and exciter frequency stability was improved by a factor of about 2 to 1.

(4) The exciter modulation frequency response was improved by about 1.5 to one.

(5) To eliminate the interferometer effect of two receiving antennas. *Mariner* Mars 1969 receives only over the low-gain antenna.

(6) The RF filtering in the direct line from the transmitter was increased in order to protect the receiver against the possibility of the self-lock phenomena observed in *Mariner* Mars 1964.

(7) The RFS subassemblies were repackaged and required only one electronic equipment bay VI instead of one and one-half required on previous *Mariners.*

(8) The antenna radiation patterns were improved to enhance overall telecommunications performance.

The major design changes from *Mariner* Mars 1964/ *Mariner* Venus 67 were in the packaging, dual TWTA,

control unit, and power supplies for the receiver and exciter. Five receiver modules and all three exciter modules underwent major redesign, and the RF filtering and switching microwave components are new designs.

The procurement process for the RFS was substantially different from the previous *Mariners*. The *Mariner* Mars 1964 and *Mariner* Venus 67 RFSs were procured by separate subassemblies such as the antennas, receiver/exciter (transponder), microwave components, TWTA, cavity amplifier and control unit. The RFS was then assembled and flight tested as a subsystem at JPL. The radio subsystems, including the antennas, for *Mariner* Mars 1969 were procured from a single source. The vendor provided the flight acceptance testing of all units prior to delivery to JPL. The *Mariner* Mars 1969 contract was of the same cost-plus-fixed-fee type used on the previous programs, but had incentive fee awards for such performance items as RF output power, RF losses, delivery and mission performance.

A. Antenna Assembly

The *Mariner* Mars 1969 uses a low-gain antenna and a high-gain antenna with a parabolic reflector.

The low-gain antenna consists of a circular waveguide mode launcher, a circular wave polarizer and a radiating aperture. It produces a right-hand circularly polarized signal. A high temperature, semi-rigid coaxial cable assembly is provided for use between the antenna input connector and the diplexer on the RFS. Monitoring of low-gain antenna drive power is provided in the diplexer. Structural and electrical efficiency are achieved by using the low-loss waveguide as a support structure for the aperture.

The high-gain antenna, Fig. 22, consists of a 40-in. diam circular parabolic reflector, with a suitable left-hand circularly polarized feed and upper and lower cable assemblies between the feed and the RF switch in the RFS. A pickup probe is provided for power monitoring purposes.

A brief description of some significant characteristics of these antennas is given in Table 10.

A brief description of the design of the *Mariner* Mars 1969 antennas and a comparison with those on *Mariner* Mars 1964 follows.

1. Low-gain antenna. The original *Mariner* Mars 1969 low-gain antenna design philosophy was based upon the use of the 1964 design with no modifications. The latter was a simple design, but it had some fabrication problems; its conical feed and waveguide diameter had to be held to very tight tolerances or polarization losses would be high due to the use of a circularly polarized wave in the waveguide. Its return loss was high due to the manner in which the cruciform aperture was formed by crimping one end of the waveguide tube. An array of magnetic loops was required at the discontinuity in the aperture to suppress the resulting undesired mode.

The result was excessive man hours spent in fabricating the antennas. The 1964 antenna also had high back radiation due to currents on the outer surface of the circular waveguide.

Table 10. Antenna characteristics

Antenna	Size, in.	Weight, lb	Maximum gain, dB	Radiating pattern
Low-gain	95.25, long	4.7	8.0	Cardioid of revolution
High-gain	40, diam	5.2[a]	25.6	9.0 deg beam width at 3 dB

[a]Including feed assembly and cables.

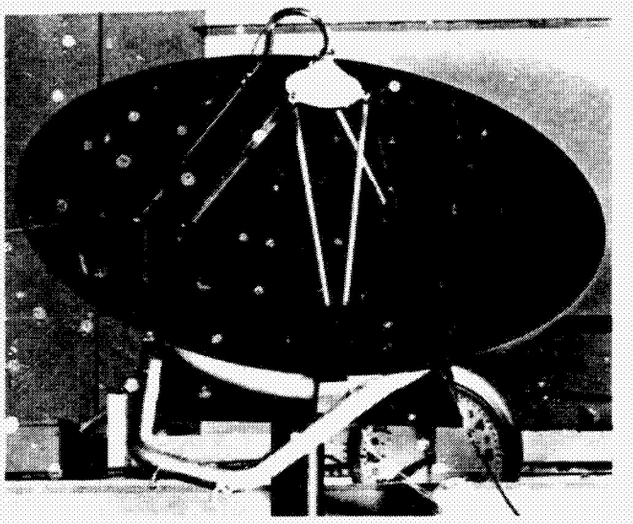


Fig. 22. High-gain antenna in test fixture

After analysis of the 1964 low-gain antenna performance and problems vs the 1969 requirements, the *Mariner* Mars 1969 design philosophy was decided upon as follows:

(1) Linear polarization was to be used from waveguide input to the aperture and converted to circular polarization at the aperture. This relieved tolerance requirements on the feed and waveguide since linear polarization is less susceptible to dimensional changes than circular polarization.

(2) The use of the low-gain antenna only to receive commands at encounter made it desirable to have as much gain as possible at the 40-deg cone angle then existent. The on-axis gain must exceed 5 dB and the 90-deg cone angle gain must exceed − 10 dB for midcourse maneuver.

(3) At least 5 dB gain through a 40 deg cone angle must be provided to support 8⅓ or 33⅓ bits/s engineering telemetry during launch and cruise. (The details of this requirement cannot be covered here; they are dependent upon the RFS and DSIF performance capabilities).

Four aperture designs were studied. The one selected yields the best overall performance at the receive frequency (2115 MHz). It has good on-axis gain and yielded the highest gain at 40-deg cone angle, while still above the minimum requirement at 90-deg cone angle. A thin metallic disk about the size of a quarter, inserted 1.1 in. into the aperture, reduced the VSWR to about 1.12 at 2115 MHz.

Figure 23 shows the *Mariner* Mars 1969 low-gain antenna. Figure 24 shows a comparison of the gain vs cone angle of the antenna designs, and Figs. 25 and 26 compare the ellipticity vs cone angle and VSWR vs frequency, respectively.

In summary, the *Mariner* Mars 1969 low-gain antenna provided adequate gain on-axis and at 40- and 90-deg cone angles and represented a distinct improvement

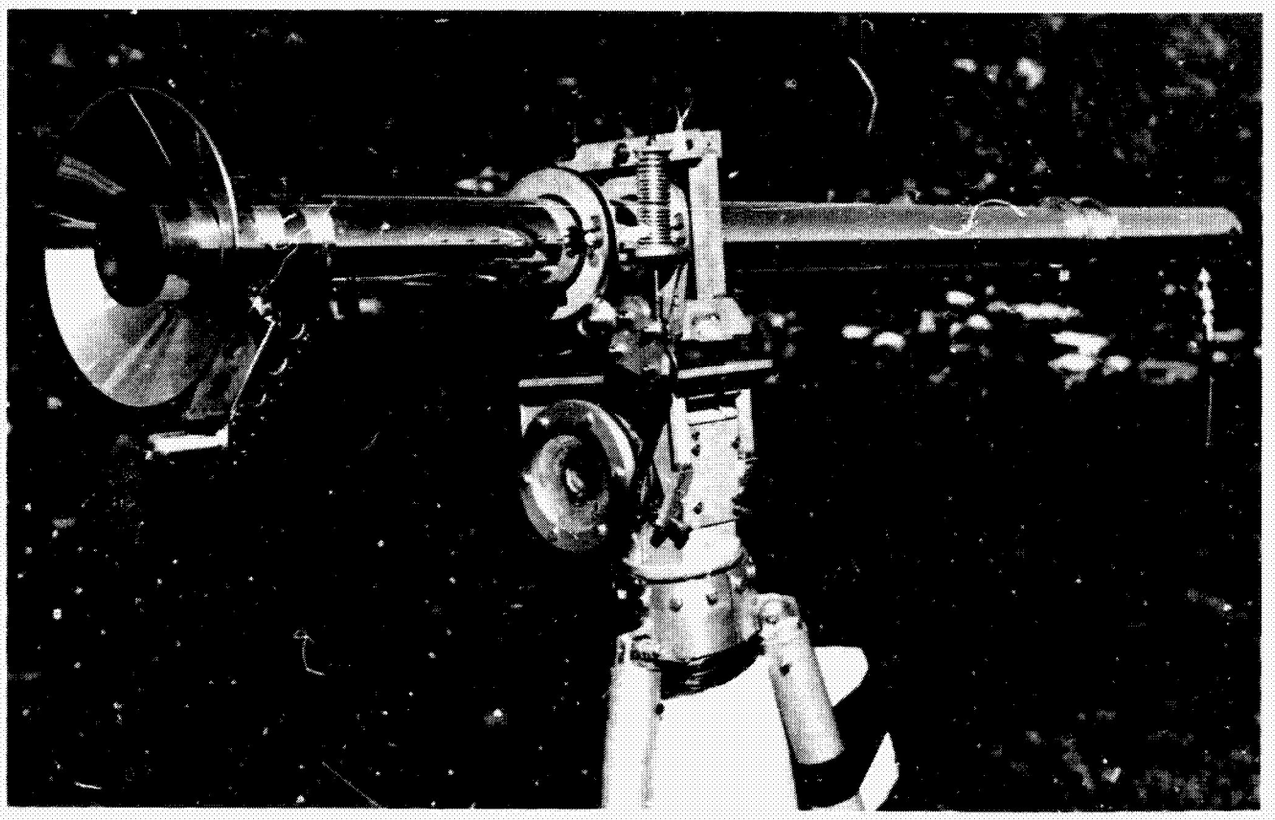


Fig. 23. Low-gain antenna in test fixture

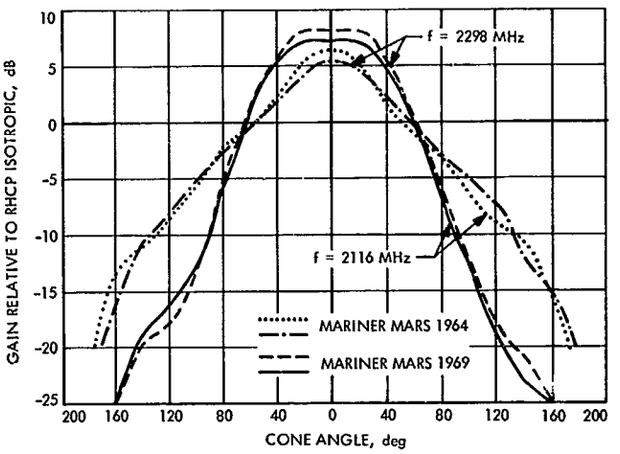


Fig. 24. Low-gain antenna gain vs antenna cone angle

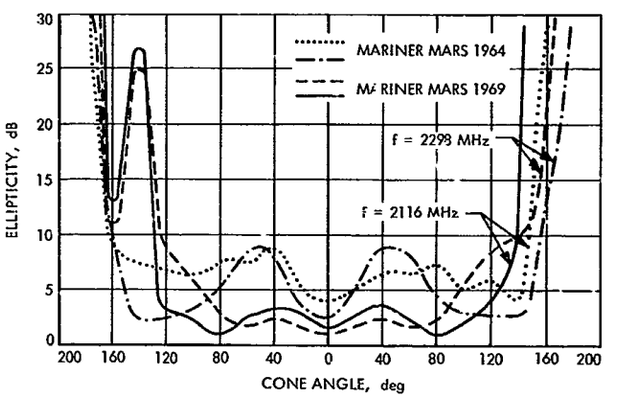


Fig. 25. Low-gain antenna ellipticity vs antenna cone angle

over the 1964 antenna in ellipticity vs cone angle and VSWR vs frequency. It was substantially easier and less costly to build to the required tolerances and provided more uniform gain from antenna to antenna. It operated well and reliably throughout the *Mariner* Mars 1969 program.

2. High-gain antenna. The 1969 high-gain antenna also used the 1964 design as a baseline. However, the *Mariner* Mars 1964 antenna gain was too low to support the higher data rate requirement and its gain contours did not fit the trajectory geometry. Consequently, fairly major design changes were required.

A study of the 1969 requirements led to design requirements as follows:

(1) The antenna should be fixed in position.

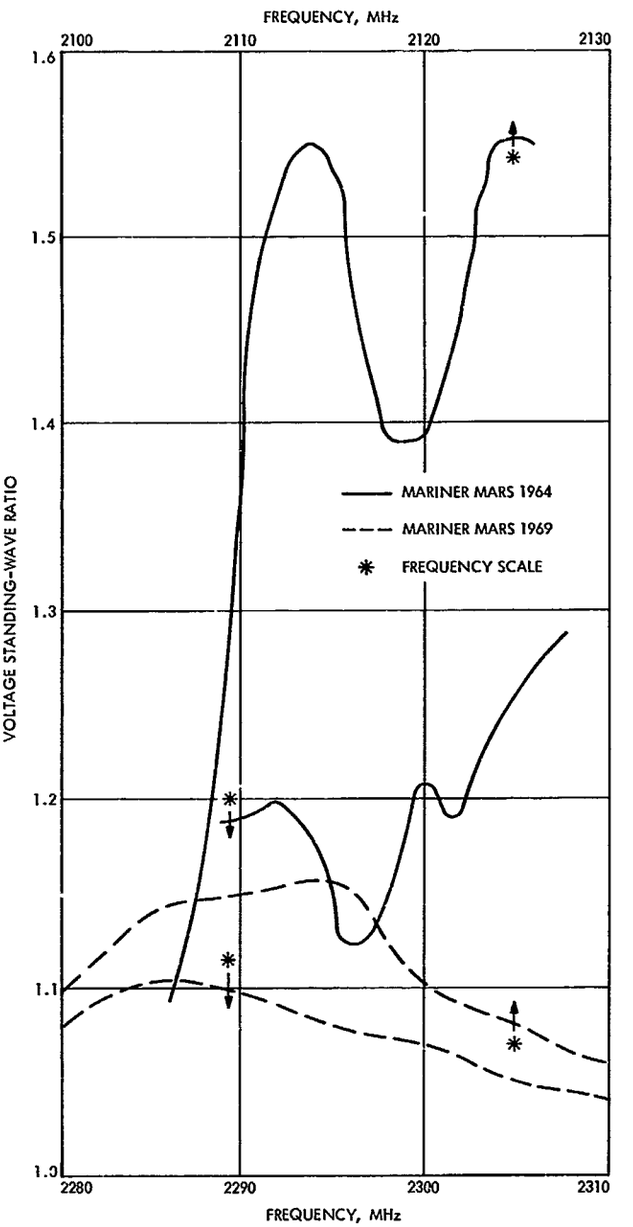


Fig. 26. Low-gain antenna VSWR vs frequency

(2) A circular reflector shape, 40 in. maximum diam was required.

(3) Antenna efficiency must be 59.7% minimum.

(4) Costs must be minimized; therefore, *Mariner* Mars 1964 tooling should be used where possible. This dictated that $f/D = 3.795$ in order to use the available reflector forming tool.

(5) To obtain the overall efficiency with the cost limitation, a fairly severe efficiency requirement was placed on the feed assembly.

Four turnstile feed configurations were studied to determine the effect of manufacturing variations and the best match to the fixed dish contour. The full-cone feed selected radiated approximately 93.7% of total power in the left-hand polarization component, of which 91.8% was intercepted by the dish. The 1969 antenna produced the uniform performance shown in Table 11. For comparison, the gain differences of the 1964 antennas was ±0.3 dB.

Table 11. High-gain antenna performance at 2298 MHz

Antenna	On-axis gain, dB	Efficiency, %	On-axis ellipticity, dB	VSWR
Proof test model	25.82	64.2	0.95	1.11
Mariner VI	25.92	65.7	0.85	1.02
Mariner VII	25.92	65.7	1.00	1.12
Spare	25.76	63.4	1.25	1.15

The feed position was made adjustable to compensate for expected dish contour variations. However, the dish tolerance was held to ± 0.010 in., so after fabrication of the first dish the feeds on the remaining antennas were preset to a position affording a compromise between peak gain, on-axis ellipticity and overall ellipticity vs cone angle.

The feed cable was carefully located for maximum efficiency. This entailed minimum cable length, minimum aperture blockage, and location in a single plane. Minimum impedance and cross-polarization affects were obtained by locating the cable 2.5 in. from the feed cone and in the plane of the longest turnstile elements.

The monitor probe loss was increased to 25 dB (from 20 dB) in order to reduce its effect on the cross-polarized component.

The *Mariner* Mars 1969 antenna provided the gain vs cone angle shown in Fig. 27. It represents a substantial improvement over the 1964 antenna. It fulfilled its function adequately and there were no problems encountered during fabrication, testing or flight.

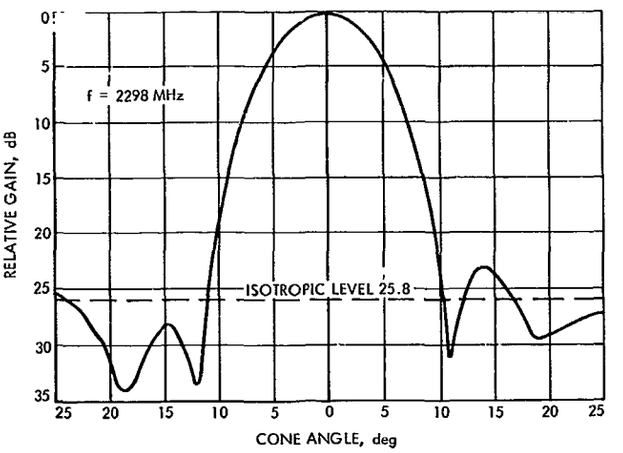


Fig. 27. *Mariner* Mars 1969 high-gain antenna gain vs cone angle

B. Radio Assembly

The radio assembly of the RFS occupies the entire electronics equipment bay VI on the spacecraft. The assembly and its components are shown in Fig. 28. The improvements in performance and the functions of the radio were discussed earlier.

For the program, five *Mariner* Mars 1969 radio assemblies were delivered. They are:

(1) The prototype—non-flight.

(2) The PTM (serial No. 1)—non-flight, type approval tested.

(3) The first flight (serial No. 002)—on *Mariner VII.*

(4) The second flight (004)—on *Mariner VI.*

(5) The flight spare (003)—on spare spacecraft.

The prototype radio was used to define the system design. Design documentation for the PTM and flight systems was based upon prototype performance. While the prototype performance was generally adequate, it was necessary to make design changes in some of the PTM modules. The design and test specifications were updated and revised after prototype tests were completed.

C. Telemetry Channels

A number of RFS parameters are telemetered during flight. These measurements provide engineering data for equipment performance evaluation and analysis. The indications of uplink signal strength, antenna RF drive

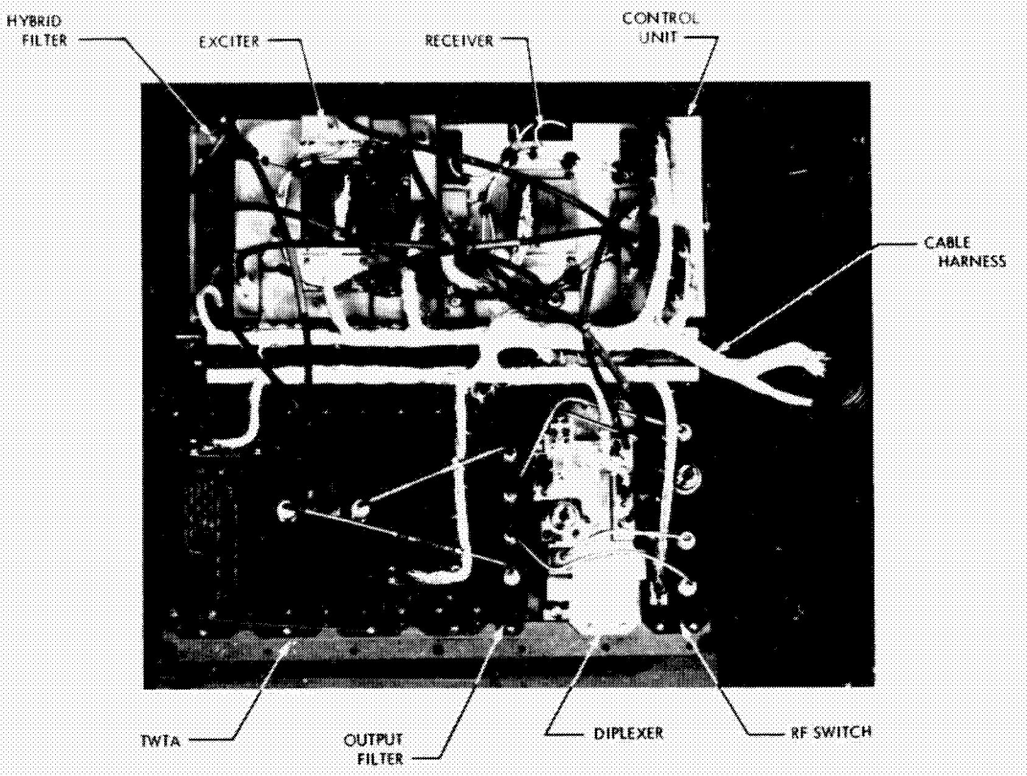


Fig. 28. *Mariner* Mars 1969 radio assembly and components

level and the temperature channels used to predict frequencies are operational functions in that they aid in tracking the spacecraft and provide information for telecommunications predictions. The channels are discussed below. While the telemetry channels as now mechanized are generally satisfactory, there are some minor changes (such as calibration) which could be made to considerably improve the accuracy and usefulness of some channels. Recommendations for these changes are made under the discussion of the affected channel.

1. Receiver static phase error, channel 111. This channel is a measure of the VCO control voltage and it indicates the receiver VCO operating frequency when the receiver is in lock. For the present RFS design, the channel is adequate, although it uses only 85% of the full range available. A design change to use the full channel capacity would increase its resolution.

2. Automatic gain control, channel 115. This channel indicates the spacecraft received signal level and that the receiver is in or out of lock. As now mechanized, this channel provides signal level data from −70 dBm to threshold (−153 dBm). Signal levels above −100 dBm are not experienced in flight and are considered less advantageous than the finer resolution which could be obtained if this range were reduced to −100 dBm to threshold. In addition, the 0- – 3-V channel is used over only a 2-V range as presently mechanized. By reducing the signal level range and utilizing the full channel capacity, a 2-to-1 improvement could be realized in resolution. Improvement of the calibration of this channel over the temperature range prevailing in flight would also permit more accurate signal level predictions.

3. Fine automatic gain control, channel 217. This channel indicates the receiver input signal level as does channel 115, but its range was supposed to be from −130 dBm to threshold. The minimum received carrier predicted through the mission (i.e., end of post encounter operations) is −135 dBm. Actual mechanization of the channel resulted in a range of −140 dBm to threshold. At these levels, the channel is noisy and hard to read as well as hard to calibrate accurately. For this range and for the mission signal

levels, this channel is useless, and could be more effectively used by another RFS or spacecraft function.

4. Exciter drive, channel 210. This channel measures the RF output power of the exciter and thus the drive to the TWTA. The typical maximum resolution of this channel per data number is 0.03 dB and the minimum is 0.06 dB. This is finer resolution than is required; something on the order of 0.1 to 0.3 dB would be adequate and would increase the range of the channel. The channel also drifts one data number for each 1 to 2°F of temperature change. This channel was calibrated only at room temperature and at FA temperature limits. Its usefulness under varying temperature conditions could be greatly improved if data were taken during the spacecraft space simulation tests. The temperature stability of the channel could be improved by redesign also.

5. RF drive monitor, HGA, channel 213. Channel 213 monitors the RF drive from the TWTA to the high-gain antenna. The approximate resolution of the channel is 0.1 to 0.3 dB per data number. The channel has the same temperature problem as channel 210.

6. RF drive monitor, LGA, channel 214. Channel 214 monitors the RF drive from the TWTA to the low-gain antenna. The resolution is about the same as channel 213 and has the same temperature stability problem as channels 210 and 213.

7. Status, channel 301. Channel 301 is a status channel and indicates the TWTA power mode (high/low power) and the ranging channel on/off status. The ranging on/off status is required; however, six other telemetry channels give indications of high or low power as well as the received signal strength at the ground station. This channel is not too important as a power indicator, but since it is an easily mechanized channel, it could be useful during a TWT failure.

8. TWTA second anode voltage, channel 302. Channel 302 indicates the second anode voltage of the TWTA. The voltage for each TWTA has a different center range so that the channel also indicates which TWT is on. The value of monitoring the second anode voltage is limited, but since it is an indirect measurement of the regulated + 20 Vdc of the TWTA, it is of some importance. The + 20 Vdc is used to generate more critical tube voltages such as the helix voltage of about 1400 Vdc. A more important use for this channel might be to monitor the TWTA cathode current or helix voltage.

9. Exciter −25 Vdc, channel 306. Channel 306 monitors the − 25 Vdc supply of the exciter and also indicates which exciter is on by using different voltage ranges for each exciter. The value of the channel is limited. The −25 Vdc is well regulated and the exciter will work properly at voltages well above or below this level. Typically, if the exciter voltage failed there would be no down-link signal to carry the telemetry information and a command to switch to the other exciter would be initiated immediately, either automatically or from the ground.

10. TWTA helix current, channel 308. Channel 308 monitors the TWTA helix current. This is an important parameter of the TWTA since almost any change from nominal operation of the TWTA will be reflected in the helix current (or more appropriately the beam interception current). However, the present resolution of the channel is about 0.15 mA per data number and this resolution is not required. Certain TWT phenomena can cause normal current changes of a few tenths of a milliampere. Also, the present range does not extend to a point where increased helix current would begin to indicate a potential TWTA failure.

11. Receiver VCO temperature, channel 404. Channel 404 monitors the receiver VCO temperature. This channel aids in the prediction of the receiver temperature variable best lock frequency. The channel's resolution could be increased from 1°F per data number to 0.2°F, to provide better measurement accuracy as well as better prediction of best lock frequency; this is discussed further elsewhere.

12. Auxiliary oscillator temperature, channel 430. This channel monitors the temperature and aids in the prediction of the one-way tracking temperature variable down-link frequency. Increased resolution of the channel would allow more accurate calibrations as well as better predictions of the one-way frequency. This is discussed in more detail elsewhere.

13. TWTA 1 and 2 base temperatures, channels 418 and 433. The temperatures are sensed at the output near the collector of the tube which is a critical temperature area.

14. Local oscillator drive, channel 422. Measurement is made of the level of the times-36 output to the first mixer in the receiver.

A telemetry relay module is common to both exciters. It provides the functions of conditioning the composite telemetry signal before reaching the phase modulator and of switching between two telemetry indications depending on which exciter is on. One of the switched signals is a monitor of the dc power supply voltage (channel 306). The temperature transducers located on each of the auxiliary oscillator modules are also switched (channel 430).

D. Receiver and Diplexer Subassemblies

The receiver and diplexer subassemblies form the narrow band, double conversion, automatic phase and frequency tracking spacecraft RFS receiver. When the receiver is phase locked to the transmitted uplink signal, it supplies an output frequency to the exciter which is phase and frequency coherent to the received signal. The exciter multiplies the frequency and phase by 120 for transmission at S-band. In this mode, the receiver and exciter form the transponder which coherently translates the frequency and phase of the received signal by a fixed ratio of 240 to 221. The transponder provides for coherent two-way doppler tracking of the spacecraft which permits an accurate method of determining the spacecraft trajectory. When the receiver is phase locked to a received signal which has been phase modulated with the composite command signal, the receiver demodulates the signal and sends it to the command subsystem for direct commanding of the spacecraft. The receiver also demodulates from the up-link signal the pseudo-random ranging code, amplifies and limits it and sends it to the exciter to be modulated on the downlink carrier. This permits precise measurement of the distance to the spacecraft.

The receiver performance characteristics are listed in Table 9 as the RFS receiving performance. Figure 29 is the receiver block diagram.

The receiver has a self-contained power supply which converts the spacecraft 2.4-kHz power to the dc voltages required by the receiver. The supply also provides a voltage to the first stages of the video amplifier module. This voltage turns the ranging channel on or off by a DC-9 signal or off by a CC&S cyclic Y-1. The turning off of the ranging channel by a Y-1 is a safeguard against the feedback observed on the *Mariner* Mars 1964 RFS which created self-lock. Self-lock can cause performance degradation or a complete loss of command and two-way tracking capabilities. A voltage is sent to an FTS status telemetry channel (301) indicating whether the ranging channel is on or off.

Five of the eleven receiver modules are completely redesigned from the 1964 to 1967 configuration. The video amplifier and the isolation amplifier modules of the ranging channel, the two IF modules, and the power supply have been completely redesigned. The diplexer RF filter replaces the 1964/1967 preselector bandpass type filter. All of the other modules also have some minor changes to improve reliability, increase RFI protection, improve performance stability in several areas, improve overall performance, eliminate spurious signals, and reduce the level of undesired harmonic signals.

E. Exciter Subassembly

The exciter subassembly consists of two identical and fully redundant S-band exciters. The output power of each exciter is divided in half by the hybrid filter and presented to the input of both of the redundant TWTAs. Thus, the exciters and TWTAs provide a fully redundant transmitter chain. The exciters are phase modulated by the composite telemetry signal for transmission of scientific and engineering information from the spacecraft. Figure 30 is a block diagram of one of the two exciters.

The RFS exciter represents a complete redesign when compared to the 1964/1967 design, although the functional operation is similar to the previous designs. The 1964/1967 design had two modules per exciter and multiplications of $\times 4$ and $\times 30$. The 1969 exciter has three modules per exciter and $\times 5$ and $\times 24$ multiplication. The redesign resulted in several improvements over the older system; the frequency variation of the auxiliary oscillator over the FA and TA temperature range was decreased; the auxiliary oscillator frequency change induced when transferring from VCO to auxiliary oscillator mode has been reduced by a factor of about 3, although no change at all was the design goal. An override of the transfer command circuitry was designed into the module [controllable from the system test complex equipment (STCE)] for the measurement of the rest (best lock) frequency of the VCO when the receiver is out of lock; variations in the S-band RF output level of the exciter have been reduced; spurious signals on the output are no longer present and the level of harmonically related components has been reduced; the phase modulation bandwidth has

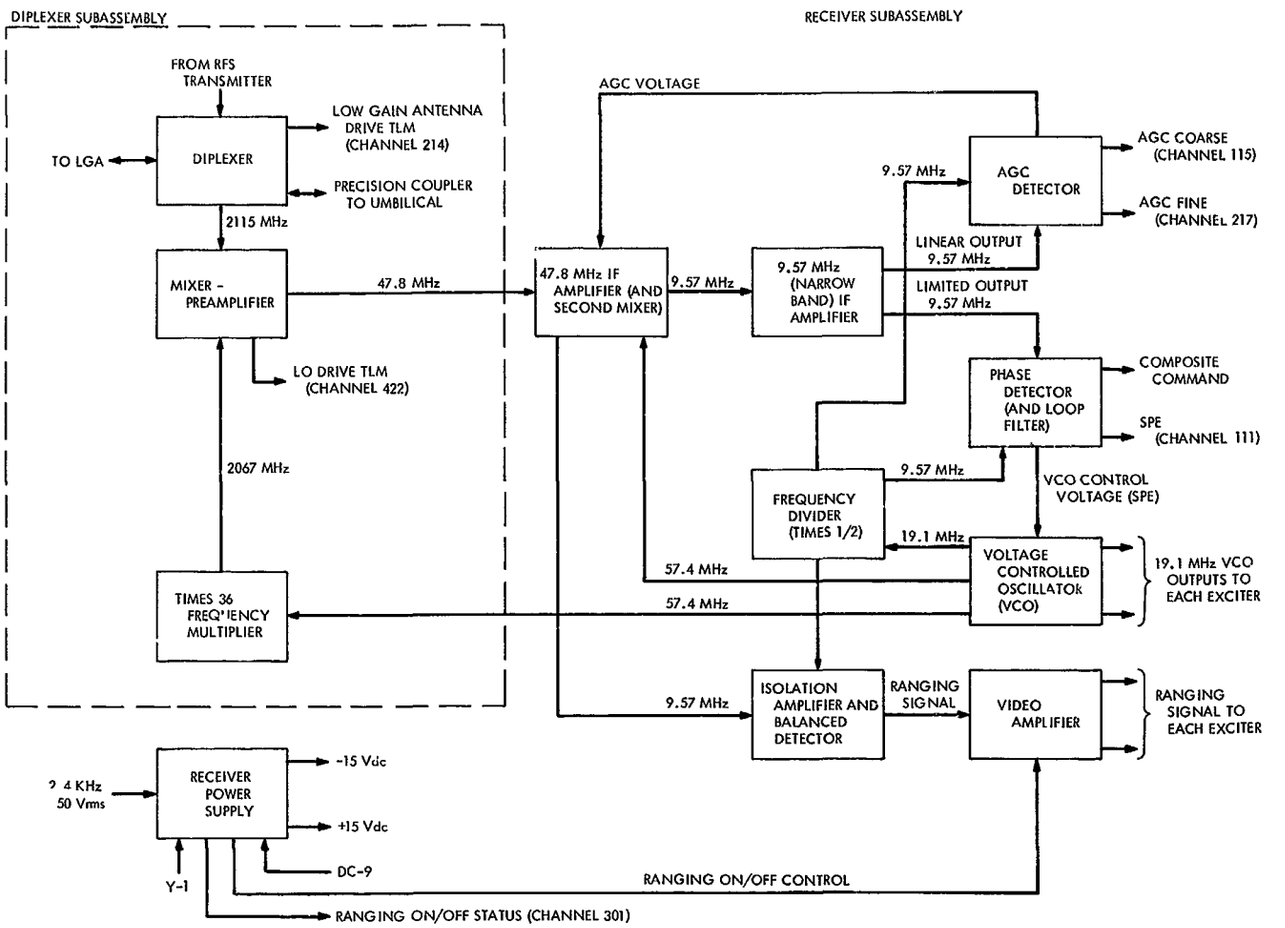


Fig. 29. Receiver block diagram

been increased and the overall modulation sensitivity characteristics improved; the power supply is also a complete redesign, has better regulation, and has lower ripple.

F. Control Unit

The control unit accepts direct commands from the FCS, the CC&S and the failure-sensing circuits in the RFS. It selects the appropriate RFS operating mode.

The functions of the control unit are:

(1) To switch the transmitter output to the high-gain or low-gain antenna upon receipt of a suitable command from the FCS or CC&S.

(2) To sense the TWTA and exciter power output level and if it is low, to switch to the redundant unit upon receipt of the CC&S Y-1 cyclic command.

(3) To sense overcurrent conditions in the TWTA and exciter power supplies and switch immediately to the redundant unit, and switch to either element upon receipt of a direct command from FCS.

(4) To select high or low-power output from the TWTA upon receipt of a command from the FCS or the CC&S.

The 1969 control unit design is based upon the 1964 unit, with added overcurrent, power mode switching and circulator switch bias current regulation. Many of the circuits were redesigned. The noise susceptibility of the exciter and TWTA control circuit was improved, and a dual redundant power supply was provided to improve reliability. Magnetic relays are used to provide

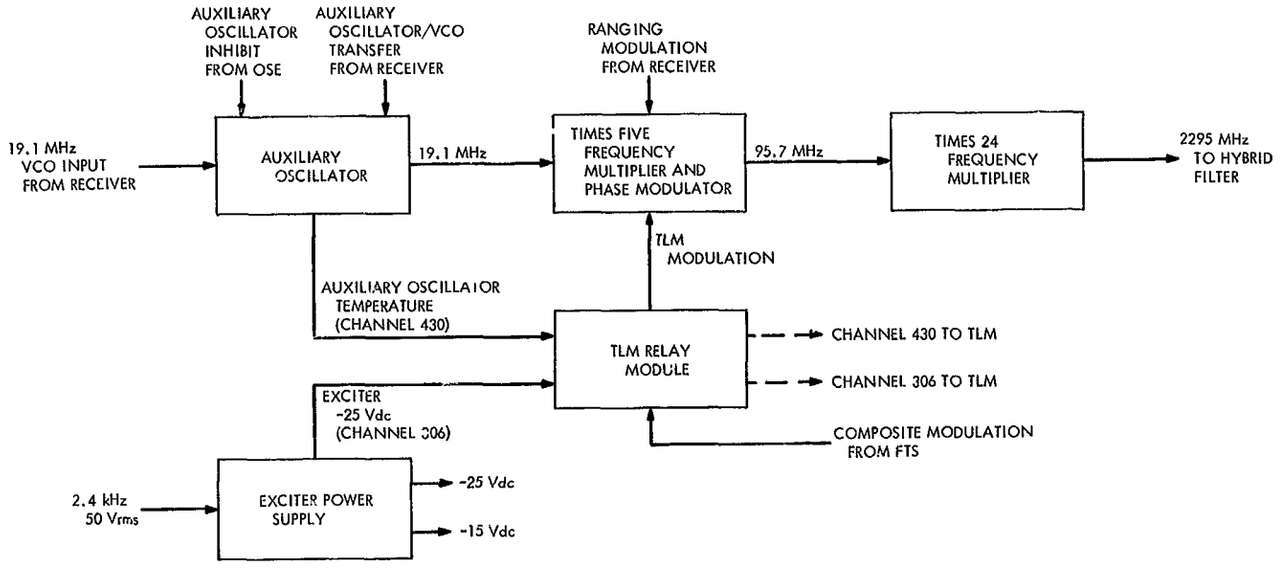


Fig. 30. Exciter block diagram

efficient switching and control, memory and isolation between functions. Figure 31 is a block diagram of the control unit.

Physically, the control unit consists of 16 welded, encapsulated cordwood modules and five relays mounted on a one-piece aluminum plate and frame. Originally, multiple layers of printed circuit boards were used to interconnect modules. Each module terminal pin projected through a tubelet mounted on the board nearest the modules. Connections were made between modules by welding a ribbon from each pin to its tubelet; a second ribbon connected the tubelet to the appropriate layer of the printed circuit board, a third connected the printed circuit to a tubelet which a fourth ribbon connected to the appropriate pin on the second module. Thus, four ribbons and eight welds were required to connect two terminals.

A broken ribbon during vibration testing of RFS serial-3 led to inspection of all control units. Large numbers of broken and fractured ribbons were found. As a result, all units were reworked using the soldered wire technique. All units were retested to flight acceptance limits. No further problems were experienced after rework of the control units.

The only recommendation for future programs is that the zener diode in the exciter level sensor power supply and the two zener diodes in the dual redundant power

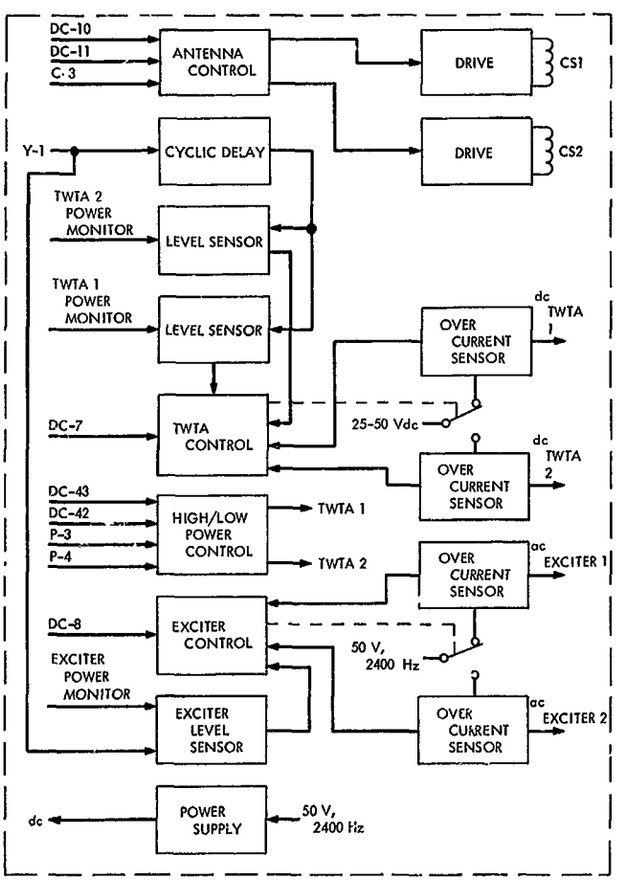


Fig. 31. Control unit block diagram

supply module should be made redundant so that an open circuit failure of any one diode will not affect the control unit performance.

G. Traveling Wave Tube Amplifiers

The TWTA consists of two TWTs, each with its encapsulated, modular, solid-state power supply; the block diagram for one TWTA is shown in Fig. 32.

The TWTA functions as a power amplifier of the phase modulated S-band signal from the exciter: it provides two output power levels, nominally 10 or 20 W by changing the voltages applied to the TWT helix, collector and first anode.

The 1964/1967 RFS had one TWT and one triode cavity amplifier, each with a separate power supply. Table 12 indicates the 1969 TWTA performance characteristics along with those of the 1964/1967 power amplifiers for comparison.

Mariners IV and *V* provided only TWT helix current or triode cathode current for telemetry. The 1969 TWTA has helix current (channel 308), second anode voltage (channel 302) and a power mode status indicator (channel 301). Like the prior design the TWTA output level is sampled by a diode detector which provides a voltage proportional to the RF level to the control unit. If the

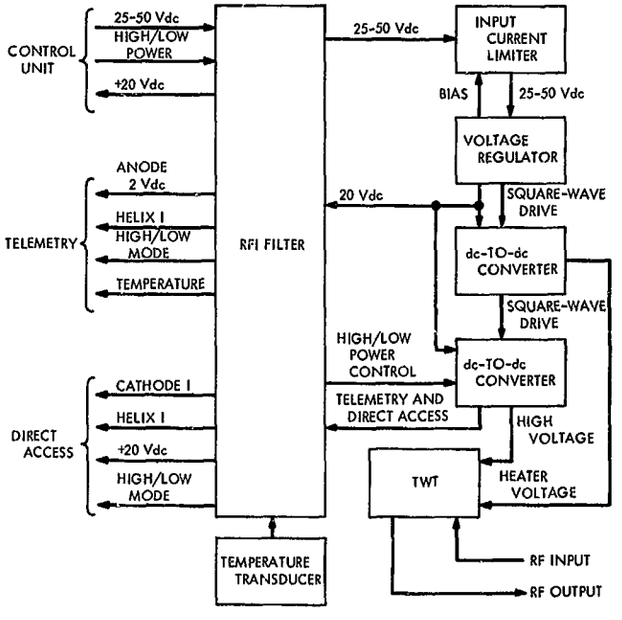


Fig. 32. TWTA block diagram

Table 12. TWTA major performance parameters

Data	*Mariner* Mars 1969	*Mariner* Mars 1964	
		TWTA	Triode
Size, in.	9.8 × 6.0 × 7.5	—	—
Weight, lb	19.2	4.8	4.0
Input RF drive, mW	50	30	500
Power output, W	20.5 (High power) 9.6 (Low power)	10	7.5
Overall efficiency, %	24	18	22
Power supply, Vdc	25 to 50	25 to 50	25 to 50

power drops below 2.5 W (nominal) a CC&S cyclic Y-1 will initiate a switch to the redundant TWTA. The 1969 incorporates a provision for failure switching in the event of an overcurrent as well as a backup set of fuses on the raw dc power line. If a TWTA draws current above a preset level, as sensed in the control unit, the overcurrent sensor automatically switches to the other TWTA. The 1964/1967 design only had fuses. The TWTs can also be switched by a direct command (DC-7).

Two of the TWTs developed air leaks due to cracks in their ceramic helix windows. In both cases, the cracks were believed to be due to thermal or mechanical shock.

Excessive noise and ripple voltage appeared on the dc primary power lines with some TWTAs at certain temperatures and line voltages. This voltage was generated in the voltage regulator module due to instabilities in the feedback loop regulating the output voltage. The effect was minimized by critically adjusting the 9 to 10 kHz switching frequency. Correction of this effect by improving the isolation in the regulator circuitry is recommended for future programs.

Helix current variations occurred in both high- and low-power modes. Generally, about a 10% change was observed. Four types of variations noted were:

(1) Step changes to above normal current lasting from a few seconds to many minutes.

(2) Upward jumps with immediate recovery recurring every few seconds.

(3) Occasionally, a burst of noise occurred on the helix current, lasting for a few seconds to a minute or more.

Some theories have been offered to explain the above phenomena, but it is thought that they are not well understood. Further investigation is indicated.

A fourth type of helix current variation occurs when the input signal is amplitude modulated. Such modulation was caused by the wide modulation spectrum with ranging on being distorted by the filter-hybrid which converted phase to amplitude modulation. Tests showed that helix current increased with the percentage modulation and frequency of the modulating signal. This can be avoided by adjusting the filter-hybrid so its passband is centered on the down-link carrier frequency.

Improvements in test methods should be considered as follows:

(1) Increased surveillance for the early detection of TWT malfunctions.

(2) Measurement of phase jitter before acceptance of the TWT for installation in the TWTA.

(3) Vibration testing with power applied to the TWT instead of with power off.

(4) Improved heater voltage setting and RF level measurement accuracy.

H. Microwave Components

The microwave components consist of the hybrid filter, output filter, RF switch and diplexer. The electrical characteristics of the microwave components are shown in Table 13. The hybrid filter, RF switch, and diplexer use stripline on polyphenelene oxide construction for the hybrid and all power monitors. Coaxial cavities are used in the other circuits.

The hybrid filter divides the power output from each exciter and furnishes drive power to both TWTs simultaneously through band-pass filters. It replaces the four-port dual circulator switch on *Mariner* Mars 1964 to which a low-pass, band-pass filter was added for *Mariner* Venus 67. Both used a separate attenuator to provide the proper power level into the TWTA and a single power monitor for telemetry and failure mode sensing. Attenuators are used in the hybrid filter input and output circuits to adjust the exciter drive to an optimum value for each TWTA, and to compensate for hybrid filter imbalance.

The output filter is used in the TWTA output circuit; it has minimum insertion loss at transmitter frequencies a band-reject filter at receiver frequencies, and a low-pass filter to attenuate transmitter output harmonics. The output filters on both 1964 power amplifiers provided only the band-rejection feature. On *Mariner* Venus 67 the filter was removed from the triode amplifiers output since it was not required to reduce the wideband noise to the receiver.

Table 13. Microwave component electrical characteristics

	Insertion losses, dB		
	Transmit[a]	Receive[b]	Rejection
Hybrid filter	4.5[c]	>100	>100 @ dc to 2117 MHz > 60 @ 2199.8 and 2391.8 MHz >100 @ 2477 to 4000 MHz > 70 @ 4000 to 10,000 MHz
Output filter	<0.3	>60	> 30 @ 2100 and 2125 MHz > 70 @ 4580 to 10,000 MHz
Diplexer			
LGA to receiver	> 100	< 1.2	>100 @ dc to 1988.4 MHz > 70 @ 1988.4 to 2048.4 MHz > 70 @ 4580 to 10,000 MHz
Transmitter to LGA	<0.3		
Transmitter to receiver		> 50	
			Reverse isolation
RF switch			Minimum / @ 25 ± 5°C
TWTA 1 to HGA	<0.35		>20 / >30
TWTA 2 to HGA	<0.7		>40 / >60
TWTA 1 to LGA	<0.7		>40 / >60
TWTA 2 to LGA	<0.35		>20 / >30

[a] 2290.2 to 2301.3 MHz.
[b] 2108.7 to 2119.2 MHz.
[c] Includes 3-dB power split.

The RF switch consists of two circulators making a four-port circulator switch. It provides a means of connecting either TWT to the high-gain or the low-gain antenna. A permanent magnet assures that TWTA 1 will be connected to the low-gain antenna with about 4.5 dB power loss in case the dc switch coil voltage supply fails. Failure sensing for the output of each TWT is accomplished at the input to each circulator, and the high-gain antenna telemetry power monitor is at the HGA output of the switch.

Mariner Mars 1964 was designed to receive on the high-gain antenna as well as on the low-gain antenna, so

a third RF switch section was required. Failure sensing was accomplished at the output of the first switch section, and RF power monitors were external to the output ports of the five-port switch.

The diplexer provides a band-reject filter at receiver frequencies between the transmitter output (RF switch) and the low-gain antenna, with a band pass filter at receiver frequency and a low-pass filter between the low-gain antenna and receiver (first mixer) input. The diplexer replaces the 1964/1967 bandpass (only) filter and separate coupler unit for telemetry and umbilical power sampling.

Two major problems were encountered. First, the diodes used in the level sensing and telemetry circuits were too low in voltage ratings. Many, but not all, had to be replaced prior to flight because they were burned out. Second, the boards were found to be cracked and crazed on the units remaining after flight. No failures were traced to this cause, but the condition is dangerous and the boards should be replaced.

I. RFS Performance and Test History

The purpose of the tests performed on the RFS by the vendor and JPL was to determine the flight readiness of the RFS as a part of the spacecraft system and its compatibility with other subsystems and the System Test Complex. In addition, operating procedures were verified and personnel trained.

In general, testing was performed at the module, subassembly and RFS level by the vendor. At JPL, the RFS was tested alone and in the spacecraft system; it was retested at module, subassembly and RFS level after rework. At the AFETR, it was tested alone and in the spacecraft.

1. Vendor tests. At the vendor's plant, the modules were aligned and bench tested, then conformally coated, readjusted and acceptance tested. Then subassembly (e.g., receiver and exciter) tests were run, followed by overall RFS assembly testing.

Test limits for flight acceptance (FA) were more severe than the anticipated environment in flight, and the type acceptance (TA) limits on the PTM were still more severe. Modules and major subassemblies were tested to FA (flight) or TA (PTM) temperatures at ambient air pressure and the complete RFS was tested in a vacuum. The temperature range was 0 to 60°C on *Mariner* Mars 1969 compared to 0 to 55°C on *Mariner* Mars 1964 for the FA limits. TA limits were −20 to +75°C for 1969 and −10 to +75°C for 1964. In flight the auxiliary oscillator temperature varied from about 19 to 30°C. Vibration test limits were also somewhat increased for 1969. FA and TA vibration tests were run on the overall RFS only.

The test specifications were improved versions of those used on *Mariner* Mars 1964 with more detail and more attention to systems problems and interactions, including RFI effects. The test procedures were similarly improved, but some tests were omitted in order to expedite deliveries.

2. JPL receiving tests. As each subsystem was received at JPL, it was subjected to bench checks to determine its power output and its cable and associated circuit losses from each TWTA to the antenna terminals on the RFS. The power output of all flight models exceeded the minimum (41.95 dBmW) required to earn maximum incentive award for the contractor. Cable losses also earned the contractor maximum award fees. This incentive was based upon a maximum loss of 0.95 dB from TWTA 1 and 1.40 dB from TWTA 2 to the high-gain antenna output terminal. After verification and calibration of STCE system performance, power output and cable losses, the OSE/RFS compatibility was verified and the initial checkout of the RFS was performed before mounting it on the spacecraft.

3. Spacecraft/RFS integration tests. The spacecraft/RFS integration tests achieved the following objectives:

(1) Verification of spacecraft/RFS/STCDS interfaces, and of interfaces with other subsystems.

(2) Measurement of the RFS power profile.

(3) Determination of the functional capability of the RFS as part of the spacecraft.

(4) Verification of RFS/DSIF compatibility.

(5) Determination of the operational readiness of the RFS OSE and its interfaces with the system test complex.

4. Subsystem tests. The objectives of the subsystem test were the evaluation of the performance of the RFS while operating with spacecraft power and in the systems environment, and to make a preliminary determination of any possible effects the RFS may have on the system environment.

The subsystem tests included all mission required modes and determined the ability of the RFS to perform according to its functional and design requirements. Variations of performance and interaction effects of the subsystem upon the spacecraft and vice versa were evaluated. Parameter variation tests were run to determine performance margins, and power profiles were measured.

5. Spacecraft/RFS mission compatibility tests. The spacecraft/RFS mission compatibility tests demonstrated that spacecraft and DSN telemetry and command data systems met mission requirements, that the ground system and personnel could operate the spacecraft satisfactorily, and that the flight telecommunications system and the DSIF were compatible.

After verification of all subsystems and interfaces, the mission tests were conducted. These tests included simulated launch, separation, acquisition, Earth and Mars cruise and playback, under hot and cold vacuum conditions. Engineering and command exercises were included, with attitude control, and midcourse maneuvers and science (at encounter) exercises.

6. Electromagnetic interference tests. Electromagnetic interference (EMI) tests were conducted on all flight models. The test consisted primarily of subjecting the spacecraft to an electromagnetic field simulating launch conditions.

7. DSIF compatibility tests. The objective of the DSIF compatibility tests with CTA-21 was to demonstrate functional and operational compatibility among all interfacing elements of the spacecraft and the DSIF. The tests were divided into two phases. For the phase I tests, a calibrated S-band link was provided between the spacecraft in SAF and the CTA-21 receiver exciter ranging (RER) subsystem, with additional hardlines to provide a source of data for bit error rate measurement. Calibrated attenuators in the simulated uplink and downlink signal paths provided known signal levels from threshold to −90 dBm at the receiver diplexer input and the DSIF receiver low-noise amplifier input.

After interface checkout and calibration of all elements of the system with the spacecraft in cruise mode, the RFS best-lock frequency was verified, the spacecraft receiver threshold was measured, and up-link lock reacquired with up-link signal offsets of ±1 and 2 kHz. The down-link threshold was also measured.

Then, with the spacecraft in encounter and playback mode the foregoing measurements were repeated. These measurements were made with the RFS in various modes to verify the performance of redundant elements and of the high and low-gain antennas. Ranging and command performance were also verified. Tracking and acquisition capabilities were determined, spectrum analyses were performed, and the down-link ranging and telemetry modulation indices and auxiliary oscillator frequencies and phase jitter were measured. The effects of SPE offsets and ranging modulation on the spacecraft command capability were also measured.

The phase II tests were conducted with the telecommunications subsystems located in the CTA-21 area. The objectives were the same as for phase I and the test setup similar except that a hardline was used instead of the S-band airlink. The tests performed were frequently a joint effort of the CTA-21 facilities and the telecommunications development laboratory at JPL.

Since the PTM was delivered at a later date than originally planned, it was necessary to use the prototype RFS for some of these tests. The test results indicated that the RFS was capable of meeting the mission requirements.

8. Miscellaneous tests. Vibration, weight and center of gravity, acoustic, simulated launch complex, electromagnetic interference and pyrotechnic shock tests were also performed on each spacecraft.

The PTM did not pass TA vibration tests at the vendor's plant due to trimmer capacitor failures described later. The PTM was reworked and reinspected at JPL. Modules and the overall RFS were retested on the bench and the RFS was retested at the TA vibration limits; the test results were satisfactory except for a drop in output power on TWT 1 of about 1.3 dB which occurred at 600 to 800 Hz while TA test limits were being exceeded. The cause and extent of the problem were not determined since the PTM was urgently needed to support system tests.

9. Proof test model life tests. It was planned that the PTM would be placed on life test as soon as PTM spacecraft tests were completed. However, the PTM was reworked and retested in vibration and thermal/vacuum (as described earlier), then substituted for flight models while they were undergoing rework. It was necessary to use the PTM at AFETR to check the set-up and for

interface tests in place of the spare RFS, since rework of the latter was not completed in time to make it available for this purpose. When the PTM finally became available, it was urgently needed by the *Mariner* Mars 1971 program and was transferred.

10. Recommendations for improvements in testing. Test teams for the 1969 program consisted generally of two men per subsystem. This does not provide adequate manpower for thermal/vacuum tests (which are run 24 h/day), occasional illness of a test team member or the proper recording and analysis of data.

It is recommended, first, that a third man be added to each RFS test group; this man should be capable of analyzing data, devising tests to resolve anomalous performance, and providing data necessary to close PFRs. Second, it is recommended that the data recording process be automated to a much greater extent than it has in the past. The RFS operational support equipment (OSE) should be made adaptable to drive a recorder with sufficient channels to analog record most direct access outputs and selected STCE functions on a suitable timing scale. Facilities exist and were used on *Mariner* Mars 1969 for the recording of telemetry data in the form of graphs. They should be revised somewhat to provide more readily usable data, and used during all tests.

In addition to planning which data shall be accumulated, and how it shall be done, the regular analysis of this data on an almost real time basis is important. Identification, storage, and retrieval of this data should also be carefully planned since many problems recur and require speedy review of old data.

One of the most important measurements made during the vibration tests was the amount of phase jitter introduced into the transponder by the shaker. This parameter is recorded (analog) from the down-link receiver's dynamic phase error (DPE) output. In order to make this measurement meaningful, no additional phase variations must be permitted in the measuring system; this includes the link between the transponder and its OSE. During the vibration tests of the 1969 PTM, an airlink configuration was used between buildings 144 and 248, resulting in an intermittent phase error of as much as 20 deg peak, even when the shaker was not in motion. Since the detectable threshold level is 6 deg peak, many of the measurements made during the test were clouded by this intermittent phase noise.

To avoid a repetition of this problem, it is recommended that all RF measurements between buildings 144 and 248 be made "hardline" using low-loss foam-filled cable similar to the type used with the roof-mounted antennas. At present a hardline power measurement is made between the low-gain antenna precision coupler output and the launch complex equipment (LCE) located near the shaker in ETL; the LCE provides an ideal point from which to couple the low-loss cable to the space chamber. Since the transponder's receiver operates from the low-gain antenna, a command capability from building 248 is assured. This low-loss cable should be installed in a permanent manner, suitable for use on the 1971 and other programs.

The spacecraft vacuum temperature test is perhaps the most valuable test performed on the RFS and allows very accurate prediction of in flight performance, if the test time is properly utilized. During the time spent in the chamber, several of the analog parameters can be measured accurately. Some of these include telemetry channel variations during the simulated launch, cruise and encounter. Best lock and down-link frequency predictions can be improved as well as predictions of the down-link short term frequency stability. These types of measurements performed under near flight conditions can greatly improve the predictions of RFS performance through all of the actual mission.

The flight radios on *Mariner* Mars 1964 were tested and calibrated at three temperatures. *Mariner* Venus 67 radio units were tested at 7 temperatures, with the result that in-flight data could be accurately predicted and compared to previous data. *Mariner* Mars 1969 was tested and calibrated at only three temperatures, similar to 1964. Accurate prediction of downlink frequencies is particularly desirable during a mission for rapid acquisition. Accurate knowledge of telemetry data is also valuable in the daily recognition and evaluation of any suspected performance anomalies in flight. Therefore, calibration of flight radios at several in-flight temperatures is recommended.

11. AFETR tests. Because of the inspection and rework of all three flight units just prior to delivery to AFETR, all three radios received some special testing at the Cape just prior to installation on the spacecraft. These tests were less comprehensive than those initially performed upon delivery of each RFS to JPL. One to two days were required to perform the required tests to verify that the RFS performance was acceptable.

The special tests were run to verify that the spacecraft was not damaged in transit from JPL. The test was divided into four parts: (1) a preliminary test that included special tests that could not be done during the normal testing sequence, (2) a detailed examination of the spacecraft during an accelerated mission sequence, (3) an encounter sequence at which time the radio was examined in detail, and (4) a playback sequence at which time the interface between date storage subsystem, FTS, radio FTS was verified.

The spacecraft was moved to the explosive safe facility after system test at building AO. A modified systems test was run with the RF link as the only command and data link. No direct access was provided. The spacecraft was encapsulated and precountdown tests were performed.

The spacecraft was moved from the ESF to pad 36 and mated with the vehicle. Compatibility precountdown tests were performed between the spacecraft, launch complex equipment (LCE), launch complex, launch vehicle, DSN, RF data link and building AC. A joint electromagnetic interference (EMI) and joint flight acceptance composite test (J-FACT) was performed with a precountdown test starting at $T - 230$ min with the spacecraft umbilical released at $T = 0$ and ending after verification of proper spacecraft operation. The precountdown test was conducted around a fixed sequence of events as opposed to a rigid time sequence. A composite readiness test (based on a time sequence) was conducted with all events occurring as they would at launch.

During testing at the AFETR there were indications of up-link signal acquisition with no transmitter on. There were also several minor anomalies including a recurrence of TWTA switching when spacecraft power was switched, described under problems and recommendations. Also, switching of antennas was falsely indicated when a TWT was switched from high- to low-power. A slow rise to full power was noted on one TWT, helix current variations were noted, low-gain antenna precision coupler output varied, and there were several anomalies caused by the launch complex equipment (LCE) and air links problems. These problems are described in more detail below.

There were four occurrences of receiver AGC indicating the presence of an up-link signal on RFS serial No. 4 when none was known to be present. While the resultant failure report was closed on a "cause unknown" basis, this condition could be related to a similar occurrence during vibration testing at JPL, and to the apparent self-lock and SPE offset of this radio in flight.

When the TWTA was switched from high to low power a transient of a few volts was produced on the + 20 V in the TWTA. (This 20-V supply is used to actuate the circulator switches, which switch antennas). The effect of this transient in the OSE sometimes caused momentary erroneous data to be printed by the STCDS, such as false indications that TWTA 1 was on instead of TWTA 2 or false antenna mode indications. Since this happened only a few times, and involved no risk (only inconvenience) it was not corrected.

TWT helix current variations on RFS serial No. 2 occurred during these tests. The variation was about 1 mA during high power operation of TWT 2, representing about a 15% increase above normal. This appeared to be the same effect, due to amplitude modulation of the TWT drive, observed earlier during JPL testing and later during the *Mariner VII* flight.

During the tests at AFETR, a slow rise (about 5 to 20 s after high voltage turn-on) to full power output was noted on TWT 2 of RFS serial No. 2. The cause could not be readily determined, so the TWTA assembly was removed for analysis and the TWTA assembly from RFS serial No. 3 (spare) RFS substituted. Tests of the TWT indicated it was performing exactly the same as during its acceptance test. A combination of very slightly reduced drive level, and TWT filament voltage very slightly low (but within specification limits) was determined to be the cause of the slow rise. Either the filament voltage was set slightly low initially and the slow rise overlooked on earlier tests, or the filament voltage had changed slightly. The TWTA power supply removed from serial No. 2 RFS was equipped with a new TWT and installed in serial No. 3 RFS, where it has been functioning normally.

The low-gain antenna drive monitor indicated a change in drive power when the antenna was connected in place of the dummy load, when the spacecraft was moved from place to place, or there was movement of people or equipment in the vicinity of the low-gain antenna. A definite pattern was established, with fairly uniform readings observed in any one location or with antenna off. Variations were over a range of slightly more than 1 db with lowest power indications occurring with solar panels on in the ESF and highest power indications occurring on the pad. These variations were

attributed to the change in VSWR occurring when the antenna was installed, and to the effect of objects near to the antenna, coupled with inadequate directivity of the directional coupler used to sense power. Temperature effects upon sensor circuit calibration tended to obscure these effects and had to be taken into account before the power output indication pattern could be established.

There was also an effect upon the output power recorded in the blockhouse caused by relative movement between the antennas on the spacecraft and the tower. This appeared at irregular intervals as a damped sinusoidal wave having a starting amplitude of up to about 0.5 dB, and died out after 6–10 Hz. The period of the sinusoid was about 1 Hz. The effect was observed on both high- and low-gain antennas, and was most pronounced when there was most activity on the tower. There appears to be no urgent reason to make design changes to reduce this effect as long as its cause and approximate magnitude are known.

The measurement of receiver threshold was difficult using the LCE with the spacecraft on the launch pad and people working in the vicinity. Threshold degradation of as much as 8 dB was observed. The cause of this condition was never determined. Possible causes are:

(1) Effects of proximity of people and equipment.

(2) Locally generated noise affecting the receiver.

(3) Excessive phase jitter in the LCE.

(4) Multipath transmission to the precision coupler via the hard-line cable and via the air path to the low-gain antenna, with reflections varying according to movement of people and equipment near the antenna.

12. Problems and recommendations. Many problems or design deficiencies were found in the radio during testing at the vendor plant and at JPL. For the most part, the problems were accepted as not being mission critical and no change was made, or "fixes" were made hurriedly in order to maintain schedules. The latter were usually not adequate redesigns. These problems resulted in 414 trouble failure reports (TFRs) at the vendor plant and 202 problem failure reports (PFRs) at JPL written against the RFS prior to countdown.

a. Problems during vendor testing. Test procedures were updated and much more detailed versions of the 1964 documents. The increased scope of the test procedures resulted in more and better data; however, further refinement is still recommended. Omission of RFI testing on the modules (included in the test specifications and procedures) in order to meet schedules resulted in failure to identify the false lock problem (described later) until too late to correct it.

The control unit test set had to be modified during the testing program.

A greater range of select at test (SAT) parts than planned was required. In the 16 T-frame modules comprising a transponder (with redundant exciters) there were 180 SAT parts. All of these modules required an excessive number of SAT parts and some component values required several changes before proper performance was achieved. The chance of damaging other components plus the amount of time required to make these changes could be reduced through better and more consistent design. Part of this design should include better accessibility of these parts. As an example, setting of the AGC coarse and fine telemetry channel voltages had to be done during the testing and alignment of the receiver. Since the resistors were buried under other components, they could not be changed without potentially damaging the module, and the change of values was extremely time consuming. As a result, the channels were never within the desired voltage ranges and in the case of the AGC coarse only 65% of the available channel range was useful.

Telemetry channel 210, monitoring the exciter drive level in the hybrid filter unit, is also adjustable to cover the range by means of an SAT resistor. It was improperly set on the flight models as well as on the PTM so that it read full scale (127 data numbers) at high temperatures on all units.

Module input impedances reacted on the previous module's output impedance; some had to be tuned in pairs to obtain enough driving power and stability. When interfaced, some modules exhibited bandwidth shifts, output power changes, and output instabilities. Usually these problems were resolved by a slight retuning, selecting another component, or just accepting minor deviations from desired receiver performance.

One example of the module interface problem is the times-36 ($\times 36$) multiplier. In alignment of this module, its S-band tuned cavity varactor multiplier output was tuned into a flat 50-ohm load. This output cavity is very susceptible to load changes. In one case, the

bandwidth was shifted over 2 MHz and caused changes in the × 36 output power. Serial No. 2 RFS (*Mariner VII*) × 36 multiplier was retuned into its mixer under normal operating conditions. This resulted in uniform drive performance over the FA temperature range and during flight. Other RFSs which were not retuned in this manner exhibited fairly large variations in drive level. The effect on threshold sensitivity of the largest variations in drive was too small to be measured accurately (about 0.3 dB) under flight conditions.

Modification of the test procedure to permit retuning the × 36 multiplier after mating with its mixer is recommended. In addition, the cause of the × 36 output variations (believed to be contact-finger variations on a tuning slug in its output × 3 multiplier circuit) should be investigated and corrected.

Interfacing problems also occurred in the exciter. One of the primary goals of the redesign of the exciter was to reduce the alignment time required to obtain the desired exciter performance. This goal was not achieved because of problems inherent in the design of the phase modulator and × 24. The design was adequate to obtain the improved performance required; however, several man-weeks were required to align the × 24. Sometimes a comparable amount of time was spent in almost completely realigning the exciter when the phase modulator and × 24 were mated. The × 24 always changed the phase modulation characteristics. In trying to retune the modulator and × 24, other exciter parameters were affected. The net result was that to obtain the desired exciter performance, several man weeks were spent in alignment and test of the exciter and because of delivery schedules, not enough time could be spent to optimize each exciter. As a result, the exciter was seldom within specification. The output power was typically 0.5-dB low and the output level stability was slightly out of specification at the temperature extremes. However, for the mission operating temperatures, the level stability was adequate, and with one exception, the exciter output was great enough to provide optimum drive for a TWTA; in that case, it was close enough to be acceptable.

Two major reliability problems were created by the excessive tuning required to align the exciters. Two transistor stages in the × 24 were frequently over-stressed or burned out due to excessive current drawn by these stages during the tuning process. Also, the excessive tuning of the small variable capacitors used extensively in the exciter (and receiver) caused short circuits in the capacitors due to metal particles scraped off of the tuning mechanism during tuning.

This problem was common to the receiver and exciter. It was a repeat of a serious component failure found in the 1964 RFS. Because of the large amount of tuning required on some modules, a small variable capacitor, used throughout the exciter and the receiver, received an excessive number of turns. The capacitor construction is such that the threads of the rotor and stator frequently galled and gold flakes and metal particles were dislodged. These metal particles caused shorts in the capacitor. The shorting of the capacitors was first observed during the vibration testing of the PTM RFS at the vendor plant. The capacitors were replaced by the same type of capacitor. The replacement capacitors received special screening and the threads were lubricated by a special grease. The number of turns on each capacitor was limited and the capacitor was replaced if this limit was exceeded.

As a result of the trimmer capacitor problem, the PTM did not pass acceptance vibration tests at the vendor plant. It was later reworked at JPL and retested to TA limits successfully.

b. Problems during JPL testing. Poor workmanship on the PTM and flight units resulted in twelve PFRs being written. The types of workmanship defects included transistor leads reversed, shielded wires pinched, ranging polarity reversed, cracked diodes, pinched wires with insulation damage, near shorts, failure to properly apply solithane, and various other examples.

Considerable doubt existed regarding the quality of the workmanship on the flight transponder modules as a result of these discrepancies found by JPL engineers and inspectors on the PTM and flight models, and of problems experienced during test. Consequently, it was decided to thoroughly inspect and rework the receiver and exciter power supplies, all exciter modules and the AGC, isolation amplifier, video amplifier and phase detector modules from the receiver in each flight unit.

Rework consisted of a thorough inspection and replacement of all defective or damaged parts, including resistors, diodes, capacitors, wiring, inserts, etc.; modules were interchanged between spare and flight units to put all doubtful units in the spare radio. Rework also included reprocessing of soldering, and adding solithane and stycast.

Many examples of poor workmanship were uncovered during the course of the inspection and rework of these modules, and those which could be were corrected or at least improved. There was, however, no fault found which could have caused a failure of the overall mission. Cracked diodes and unsoldered resistors were found in the ranging video amplifier which could have caused failure of the turnaround ranging system.

After rework, each flight radio module was retested at the module level, than assembled to the receiver and exciter subassembly level and tested, and finally assembled as an RFS and retested on the bench to FA limits. Following this test, each flight model was subjected to a thermal/vacuum test to FA limits, but for reduced time (36 h) and a random noise vibration test, also to FA limits but for only 21 s in one plane in order to verify the mechanical integrity of the RFS without undue stress on the flight radio.

During the test program a fundamental receiver design problem called "false-lock" was discovered. It is undesirable, but not mission-catastrophic. It only makes operations with the spacecraft slightly more difficult. Getting up-link receiver phase lock in the early phases of the mission would be made more difficult than it should be. The stations would be required to keep their transmitter power at a low level and might have to turn off their transmitter and try several acquisitions. These constraints were necessary only if the ranging channel was on.

The receiver has two servo-loops; one is the automatic phase control (APC) loop for coherent phase tracking, and an automatic gain control (AGC) loop for maintaining a constant carrier level in the receiver IF amplifiers. An undesired third loop in the receiver creates the false-lock phenomena. The modules which contribute the most to this problem are the ranging channel video amplifier, the receiver power supply, and the VCO. False-lock is defined as the receiver giving indications of phase lock acquisition to the uplink carrier when actually it is phase locked to a signal generated in the receiver by the externally generated carrier. The problem exhibits itself when an up-link carrier of a level of -110 dBm or above is received, but is not within the acquisition range of the phase lock loop. The input carrier frequency then mixes in the first and second mixers and results in the normal sinusoidal beat frequency in the IF amplifiers in the ranging channel. With the ranging channel off, there is little or no problem. However, if the ranging channel is on, this beat frequency enters the video amplifier and is amplified and limited. Inefficient filtering in this amplifier results in modulation of the beat frequency on the dc voltage which powers the video amplifier. The same dc voltage supplies the VCO. The modulation present on the dc power line in turn frequency modulates the VCO. Since the VCO is the primary frequency reference source for the receiver, the sidebands which result from the modulation are multiplied in amplitude relative to the carrier and mixed and finally become components in the receiver IF amplifiers.

One effect of these undesired sidebands is that for certain frequency and mixing conditions they exist at exactly the receiver acquisition frequency and the receiver acquires phase lock to them (false-lock). Also, if the undesirable sidebands are in a certain frequency range and of the correct amplitude, they cause the VCO frequency to change or be pushed away from its rest or zero control frequency (best lock). This pushing effect reduces the chances of obtaining phase lock of the receiver to the transmitted carrier. There are a few more effects caused by the false-lock problem but they are less troublesome than the VCO frequency pushing and the acquisition of lock to something other than the desired carrier.

The false-lock in the receiver is caused by three primary design factors. One is that the video amplifier output stages modulate the dc power line. A change in the output filtering to the power line and a redesign of the amplifier stages would reduce the modulation. The receiver power supply has a relatively high dynamic output impedance. Design changes exist which would reduce this impedance by a factor of 50 or more. This would reduce the modulation level on the power line. The VCO is susceptible to AC modulation on its input dc power line. A redesign including better low frequency filtering and a change in the internal regulator zener diode circuit for the VCO is required. Unfortunately, these relatively simple design changes could not be made for 1969 because of the late discovery of false-lock. Severe cost and scheduling impacts on the RFS would have been incurred if these changes had been made. False-lock fortunately can be tolerated since it only increases flight operational difficulties and does not affect mission performance.

The problem was avoided during operation by programming the ground transmitter power and carefully controlling the transmitter frequency during acquisition. The transmitter power level was chosen to keep the

spacecraft received signal level below − 100 dBm. The frequency was controlled within about one kHz of the best lock frequency.

During vibration testing of the spacecraft with serial No. 4 radio, an uplink signal was indicated by the spacecraft radio AGC when none could be accounted for. At that time, the spacecraft radio was connected by airlink to SAF and CTA-21 and it seemed probable that some extraneous signal could have been the cause. Therefore, the PFR was closed on a risk basis. It appears probable now that this might have been the first appearance of the anomaly which occurred again during testing at AFETR and during flight, when an uplink signal was indicated although none could be accounted for.

This apparent self-lock could have been due to an oscillation in one of the receiver modules; the most probable module is believed to be the mixer preamplifier. Such oscillations were observed during the design phase and a "quick fix" was applied. However, tests were less thorough than desired, and it seems possible an erratic oscillation could still be present.

If such an oscillation occurred near to ⅓ of the uplink frequency, it would be multiplied in the mixer and beat with the × 36 output to form a signal near to the IF. Such a signal could cause a self-lock to occur in a receiver having false lock capability.

In addition to the mixer-preamplifier, there are several modules which had stability problems in the past and still have not been properly redesigned. These are the × ½, the phase detector, the AGC detector, the × 36, the VCO modules and the × 24. One of the primary causes of instabilities resulting in spurious oscillation was the use of grounded-base transistor stages in several of the modules. This design was a carryover from the *Ranger* program and caused many problems. In several cases, these stages have oscillated and caused degraded receiver performance. The "fixes" utilized to eliminate the oscillations were not really redesigns, but minor circuit changes and were not always fully effective. One such oscillation in a grounded base amplifier stage in the phase detector of a flight receiver showed up during a special test on the RFS at JPL under cold temperature conditions. The PTM exhibited spurious oscillations in its VCO during thermal/vacuum testing. This was well after both units had undergone acceptance testing. With the present technology and design capabilities, there is no reason why this potentially dangerous design cannot be changed. Spurious oscillations also occurred in the receiver and exciter power supplies. A suitable correction was applied to all power supplies.

The modulation sensitivity was initially incorrectly set and it varied beyond specification limits with temperature variations. Two filter inductors of improper value caused the frequency response of the modulation input circuit to vary with frequency. The phase modulator circuit is unnecessarily complex. It is recommended that the phase modulator circuit be simplified, that temperature compensation be added, and that the input circuit frequency response be made more nearly flat, so that more accurate telemetry and ranging performance can be attained.

Switching problems sometimes occurred on the PTM and on the flight RFS when spacecraft power was switched from standby to main. The resulting power transient was sometimes sensed as an overcurrent failure to the TWTA and switching to the redundant TWT resulted. The addition of delay in the sensing circuits is recommended to prevent this from happening in future designs.

A new type of crystal was used for the VCO which resulted in reducing the maximum frequency change at temperature extremes. Unfortunately, it did not reduce the changes which occur over the limited RFS temperature ranges of the actual flight. For a limited temperature range, the previous VCOs drifted about 250 Hz/°F at S-band, and the new design is about the same. The relatively large shift in frequency with temperature makes it difficult to predict the best lock frequency of the receiver. This can and frequently does result in not acquiring two-way lock with the spacecraft in flight on the first try, especially at low receiver input levels.

The auxiliary oscillator frequency variations over the full temperature range have also been reduced. Unfortunately, over the range of temperatures of the RFS during the mission, the change of frequency is still about the same as previous *Mariner* RFSs (250 Hz/°F). This stability is acceptable for most of the mission, but during the exit from Mars occultation, the frequency should be known to a few Hz in order to reduce acquisition time. There are crystal and oscillator designs available which will reduce the change of frequency over the temperature range during the mission by several orders of magnitude. An easily implemented way of reducing

the frequency uncertainty, but not the best, is to increase the resolution of the telemetered temperature of the auxiliary oscillator. It is now 1°F per data number. By selecting a higher resolution temperature transducer calibrated over the RFS mission operating temperatures, the frequency uncertainty could be reduced from 250 to about 50 Hz.

An exciter failure occurred during environmental testing of serial No. 4 RFS. Without an apparent cause, the exciter output suddenly dropped on several occasions by 6 dB or more, slowly recovered partially, or recovered instantaneously when the exciter was switched off, then back on. Once a severe primary power line transient occurred during the exciter failure, and recovery was instantaneous.

This failure was similar to an effect which was observed during $\times 24$ module test when the $\times 24$ drive signal frequency was detuned, then brought back to normal frequency with the $\times 24$ circuits slightly detuned. The output carrier would drop in power by 6 dB or more and a spurious spectrum of signals spaced several hundred kHz apart would appear about the carrier. Turning off, then on again, the power to the $\times 24$ would cause instantaneous recovery. The downlink power increased slowly following the initial drop as the $\times 24$ temperature changed due to a change in power dissipated. This explanation of the probable cause of the anomaly must be considered speculative since no reason for the onset of the anomaly was found, and it could not be reproduced when the failed unit was subjected to varying temperature and voltage. The module was retuned, tested thoroughly and exchanged with an exciter from the spare (serial no. 3) RFS. There has been no recurrence of this anomaly.

A major problem during the spacecraft-RFS integration tests was the oscillation which occurred in the FTS due to an improper impedance match in the RFS telemetry input interface with FTS. This was corrected in the FTS. Corrections are recommended of the RFS/FTS interface in future programs.

During the EMI tests, interference was noted on telemetry channels monitoring TWTA drive, low-gain antenna drive, and high-gain antenna drive with the RFS in launch configuration. Some interference during actual launch conditions was anticipated, but did not occur. In addition to the EMI effects on the RFS in the spacecraft actually under test, on one occasion interference effects were observed on an RFS in a spacecraft in SAF which was adjacent to the one actually under test. It appears that the EMI test is considerably more severe than actual launch conditions, and reconsideration and revision of this test is recommended. In addition, the telemetry output circuits of the microwave components should be made less susceptible to interference.

Throughout the program, the ranging performance of the 1969 RFS was less than calculations indicated it should be at signal levels below about -95 dBmW. The discrepancy between measured and calculated performance increased with decreased uplink signal level, reaching about 5 dB at threshold. The cause of this degradation has been found to be asymmetrical clipping in the second amplifier stage of the video amplifier. Redesign of this module to correct this condition is recommended.

Two areas of marginal design still remain to be discussed in the RFS exciter. The telemetry relay module contains a relay which switches two telemetry channels. On several occasions, the flight spare RFS failed to switch the telemetry channels. The investigation of the problem revealed that the drive is too low to switch the relay reliably. Also, during testing of the RFS, the auxiliary-oscillator inhibit function was found to be faulty at low temperatures. A redesign of these two circuits is required.

VI. Flight Command Subsystem

A. Introduction

The *Mariner* Mars 1969 flight command subsystem (FCS) provides a remote control link with other spacecraft subsystems. Although in general, most commands that are decoded by the FCS are necessary to maintain planned operation and control of the spacecraft functions, some are provided for changing mission emphasis in case unusual or unexpected conditions occur. In extreme cases, the command link could even permit salvaging of the *Mariner* Mission if certain types of spacecraft failures were to occur.

All FCS commands fall into one of three categories: (1) the direct command (DC) for switching operations; (2) the quantitative command (QC), which provides a specified number of consecutive pulses to indicate magnitude; and (3) the coded command (CC), which gives detailed instructions to the CC&S.

The modulated command subcarrier information is furnished by the transponder receiver. This signal contains the command bits, a reference frequency, and a pseudo-noise (PN) bit synchronizing code.

Five complete 1969 FCS units were built by Motorola under contract to JPL. They include: a prototype, proof test model, spare and two flight models. All models have the same basic functional units as the FCS in *Mariner C* (*Mariner* Venus 67). These functions are: (1) command detector, (2) command decoder, (3) program control, and (4) power supply. While the *Mariner C* FCS had seven mechanically identical subassemblies, the 1969 FCS has only five (Fig. 33). Even though the size of the FCS had been reduced, the direct command capability was expanded to 53 DCs. This improvement in circuit density is mainly due to the conversion of many of the logic blocks to integrated circuits.

Another 1969 FCS innovation is the capability of automatic acquisition of the phase-locked loop (PLL) without adjustment of the ground reference frequency. The automatic acquisition detector simplifies acquisition and eliminates the possibility of false PN correlation points associated with PN synchronization.

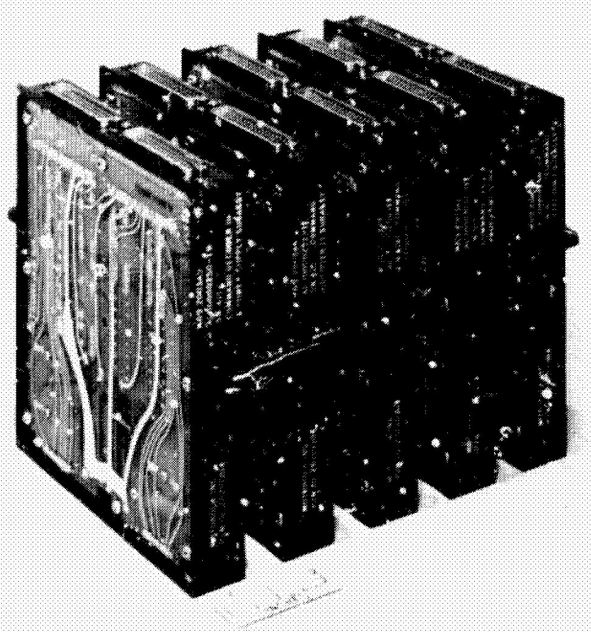


Fig. 33. Unmounted *Mariner* Mars 1969 flight command subsystem

B. Design as Flown

1. Command detector. The command detector provides three main functions: (1) establishes a phase coherent reference signal by locking a phase-locked loop (PLL) to the frequency-doubled transmitted-data subcarrier (PLL channel); (2) generates a detector *in-lock* signal, which indicates proper synchronization with the transmitter, and enables the decoder (lock channel); and (3) demodulates and detects, in the presence of noise, data bits that are transmitted from earth as a biphase-modulated sinusoidal subcarrier (command channel). The functional block diagram of the detector is given in Fig. 34.

The detector operates on a biphase-modulated data signal of $\pm\sin 2\pi f_s t$ added to a sync signal composed of a PN sequence, modulo-2 added to a square-wave signal at the clock frequency defined as $2f_s$. The composite signal may be expressed mathematically as $PN \oplus 2f_s \pm \sin 2\pi f_s t$. The subcarrier $\sin 2\pi f_s t$ is used instead of $\cos 2\pi f_s t$ to lessen the intermodulation problems between data and sync signals (Ref. 2). A summary of FCS detector operational data is listed in Table 14.

The phase modulation ambiguity is resolved by $\times 2$ multiplication in the PLL channel, and the loop is locked to the $\sin 2\pi f_s t + 90$ deg signal. The PLL signal is then used to provide a coherent reference for all phase detectors. Bit synchronization is obtained by correlating the transmitted $PN \oplus 2f_s$ with the FCS-generated $PN \oplus f_s$. Correlation is achieved by a discrete-step time search, in which the reference $PN \oplus f_s$ is compared against the received sync signal in the lock PN phase detector.

The search mode is initiated by the detector logic when three consecutive *out-of-lock* signals are received from the locked channel matched filter. The search logic

Table 14. FCS detector operational data

Parameter	Value
Modulation input	$PN \oplus 2f_s \pm \sin 2\pi f_s t$
Composite input signal, mV rms	$100 \pm 25\%$
Threshold signal-to-noise ratio, dB/Hz	16.5 ± 1
Input signal noise bandwidth, Hz	2350
Input impedance, kΩ	≥ 100
Probability of bit error at threshold	$\leq 10^{-5}$
Probability of in-lock indication at threshold	$2.25 \times 10^{-4} \pm 50\%$
Maximum detector lockup time, min	12.5

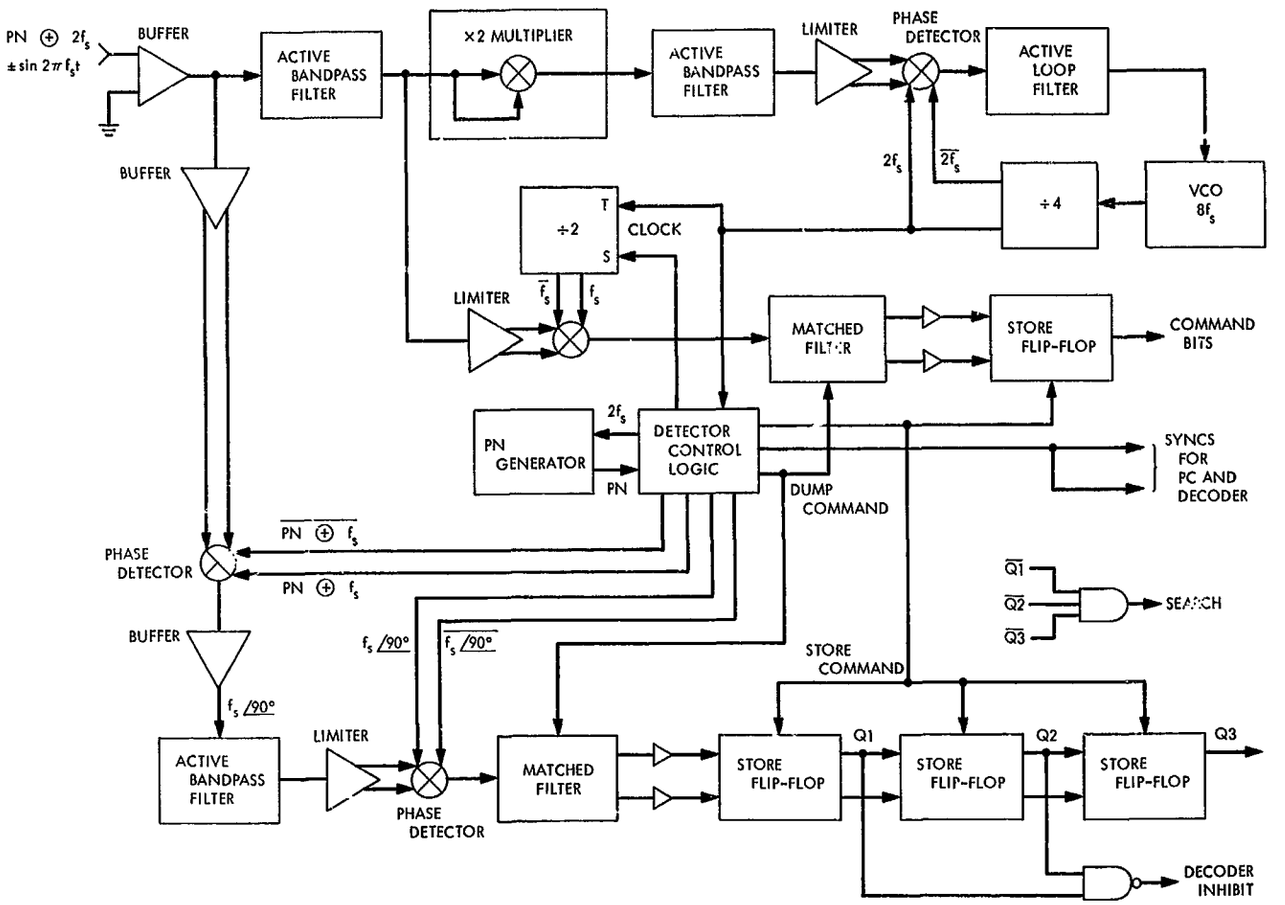


Fig. 34. Flight command subsystem detector functional block diagram

advances the code sequence one extra PN bit each cycle of the code, allowing the FCS code to overtake the ground code sequence. When the codes correlate, the PN phase detector produces an $f_s \angle 90°$ output, which is filtered in the f_s bandpass filter (BPF) to remove multiplication products. The $f_s \angle 90°$ signal is then demodulated in the lock f_s phase detector and detected in the presence of noise by the lock matched filter. A bias is applied to the lock matched filter to establish a probability of one in lock of $1.5 \times 10^{-2} \pm 25\%$ in the presence of noise alone. When one *in lock* is detected, the search is inhibited, and after two consecutive *in locks* the decoder is enabled for message processing. Additional conditions must also be met in the program control, however, before a command will be recognized.

The command channel phase detector demodulates transmitted message bits with a clocked f_s' reference. The f_s' reference is derived from the PLL coherent $2f_s$ and is reclocked at the beginning of each bit time to obtain proper synchronization with the transmitted data signal. After demodulation, the data bits are detected from the noisy signal by further bandwidth reduction in the command matched filter. Threshold for the detector is defined at a bit error rate of 10^{-5}, and occurs at a composite command signal-to-noise ratio of 16.5 ± 1 dB referred to a 1-Hz noise bandwidth. At bit sync time, the detected bits are serially stored in a data shift register for interrogation by the decoder.

2. Command decoder. A simplified block diagram of the decoder is given in Fig. 35. The function of the decoder is to decode digital data bits from the program control and provide isolated output commands. It consists of 85 universal isolation switches (UISs), a synchronizer module, and a register preset module. The decoding function is implemented within each UIS by an integrated circuit diode and-gate. Depending on the bits

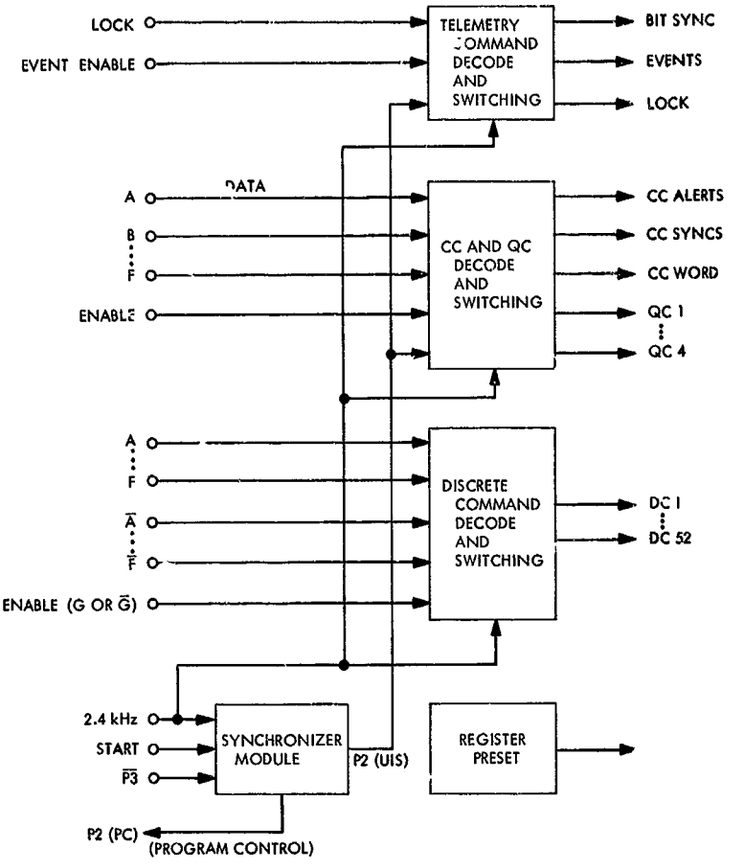


Fig. 35. Decoder block diagram

stored in the data registers, one or more of the UISs is closed upon being enabled by the program control. The synchronizer module synchronizes the UIS enable pulses to the 2.4-kHz power source used by the UIS, thereby controlling the turn-on characteristics of the switch. The register preset inhibits any decoder outputs that could occur during power turn-on.

The command format for the 1969 FCS is given in Fig. 36. Bits 1 through 3 form the word start pattern (110). Bits 4 through 9 are the command subaddress. If a DC subaddress is recognized by the program control, a corresponding set of DC switches is enabled, so that the decoder will activate the UIS corresponding to the DC command address contained in bits 20 through 26. If bits 4 through 9 are not a DC subaddress, bits 10 through 26 are stored in the data registers and the QC and CC UISs are enabled. Thus, either the QC or CC UIS, depending upon the stored address bits 4 through 9, will pass bits 10 through 26 to the specified subsystem.

The 1969 FCS program control is capable of recognizing two DC command subaddresses, although only one DC subaddress is used. Thus, the logic has a built-in expansion capability of 62 additional direct commands. All addresses use one bit for parity check, so that an even number of bit errors would be necessary in order to generate an incorrect command address. However, there is no parity checking of QC magnitude bits, while the CC coded bits are parity checked in the CC&S.

The following three command signals are telemetered to earth:

(1) An indication of the delayed bit sync period which gives an indirect measurement of the detector VCO frequency. This allows the phase-locked loop acquisition characteristics to be predicted.

(2) A binary detector lock signal which indicates whether the command subsystem is capable of detecting and processing command data bits.

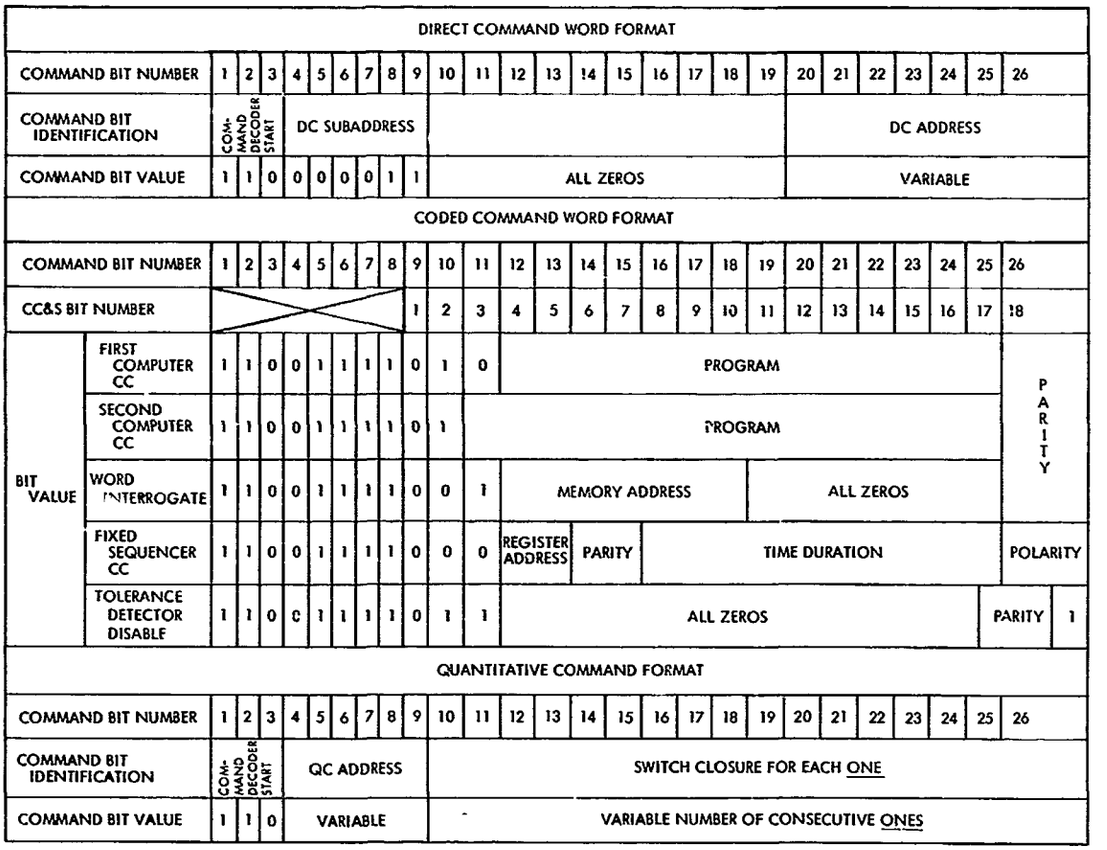


Fig. 36. *Mariner* Mars 1969 command word format

(3) A command event pulse after a subaddress is recognized, and again at the end of each command.

3. Program control. The program control portion of the FCS performs the functions of word-start error checking, subaddress decoding, data processing, and decoder control. A block diagram of the program control is shown in Fig. 37. The program control logic receives decoder enable and timing pulses, along with data bits from the command detector. The logic circuit checks the serial data information for proper format. This information is processed into correct decoder control and data signals if the decoder enable control signal is present and the format checks. The operation of the program control is shown in Fig. 38.

C. Significant Command Unit Problems

1. Cracked solder joints. During early inspection phases of the 1969 FCS units, a number of cracked solder joints were discovered on the spare and the two flight command units. For example, when the spare FCS unit (serial No. A103) was de-sandwiched for closer inspection, over 100 cracked solder joints were found. Admittedly, some of the cracked solder joints may have resulted from stresses created during the opening process. However, it was believed that the solder joints were weaker than usual due to impurities which had flowed into the joints. It was postulated that this had occurred during the wave-soldering process, which caused the solder from the tinned module leads to remelt and flow toward the joints, carrying associated impurities along with it in the process. These impurities mainly included gold which had amalgamated with the solder.

Further investigation revealed that there was no evidence of cracked solder joints on any of the 1969 CC&S subsystems. Since these subsystems had been hand-soldered by the same contractor who had fabricated the FCS units, it was concluded that the wave-soldering

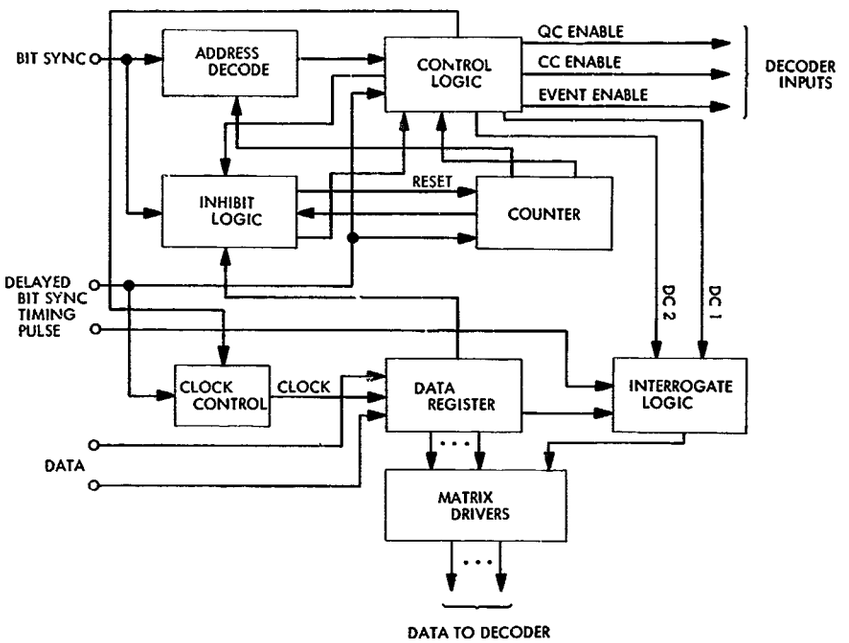


Fig. 37. Program control block diagram

process was perhaps the main contributing factor to the cracked solder joints. During the rework of the two flight units which replaced the RE732J integrated circuits in the UISs with MM732Js (see directly following), new motherboards were used and all joints were hand-soldered. Although no further evidence of cracked FCS solder joints in the flight units has been found since reworking these units, subsequent studies revealed that there had been two problems.

The first was an inherent solder joint weakness at connector wire-pin solder joints because of the difficulty in soldering the joints, which in turn was attributable to the cleaning process prior to the soldering. The second, stresses and cracks in these solder joints caused by insufficient stress relief directly at the connector wire-pins, could have been prevented had the relief been provided to allow for the differences in thermal coefficients of expansion.

2. Integrated circuit failures. A considerable number of open-bond failures of the Signetics RE732J UIS diode array integrated circuits occurred during the earlier subsystem test phases. These failures caused the associated UISs to be activated on wrong command addresses. The primary cause of these failures was due to excessive intermetallic growth ("purple plague") at the gold-to-aluminum bond. The intermetallic growth had been accelerated due to the high temperature exposure for various durations, during the case sealing process. To correct that deficiency on the two flight command units, all UIS diode expander integrated circuits were replaced with MM732Js. The MM732Js are identical to the RE732Js, except for the stricter time and temperature controls and more frequent inspections during the case-sealing process. Therefore, although the possibility of intermetallic growth failure in the two flight units has been reduced, it has not been entirely eliminated by the replacement of the integrated circuits.

A secondary cause of the RE732J failures was found to be due to contamination. This contamination coming from the bonding wire, caused non-conductive aluminum compounds to form at the pads. The source of the contamination was traced to moisture that had been trapped in the lubricant used to extrude the gold wire; the lubricant had not been entirely removed during the cleaning process. Unfortunately, the cause of the contamination failures had not been determined in time to improve the wire cleaning technique for the M732J fabrication. Consequently, the MM732Js presently in the two flight command units, still have the same risk to

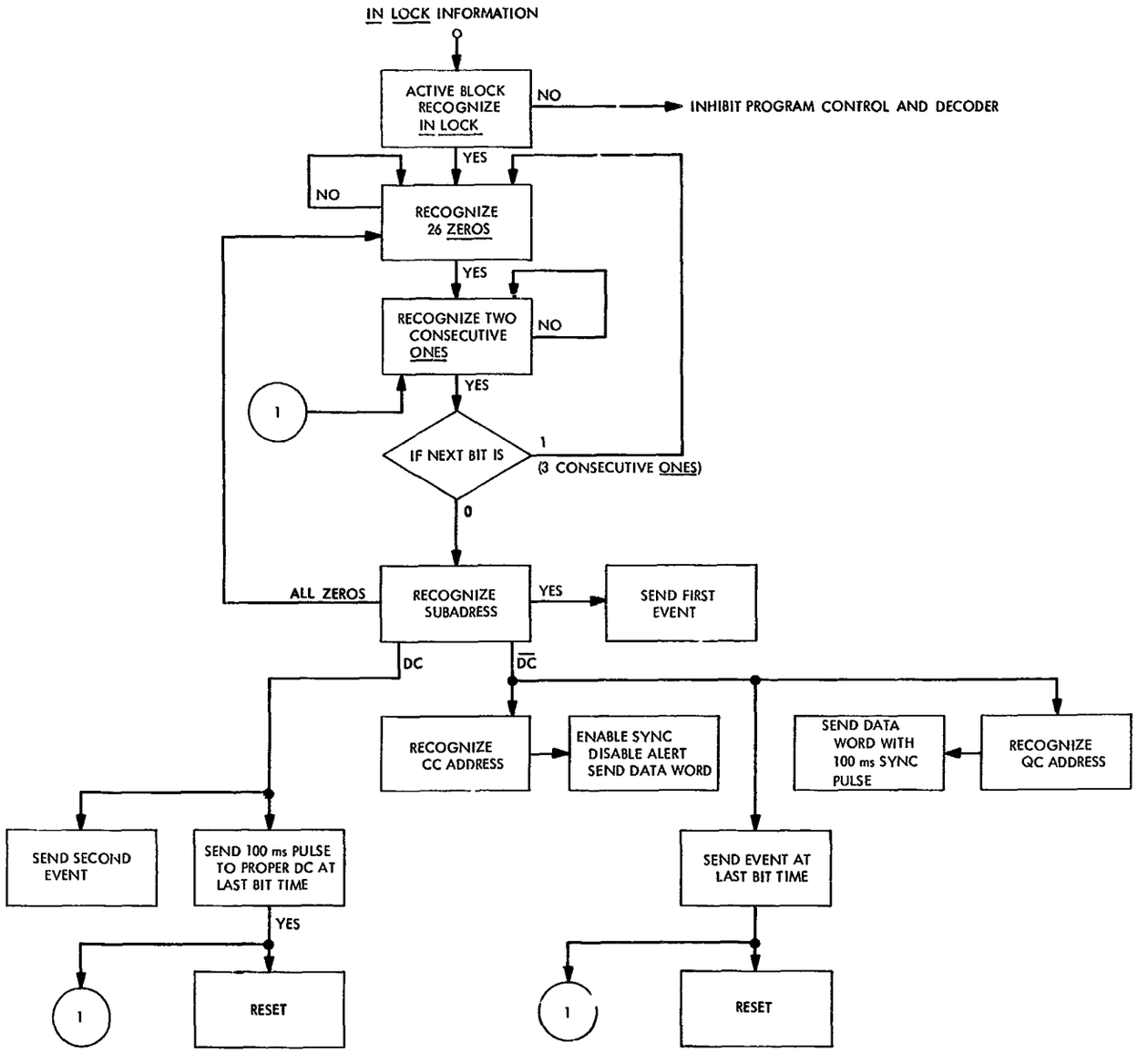


Fig. 38. Program control flow chart

contamination failures as the RE732Js which they replaced, although the risk was considered to be acceptable.

3. Connector problems. Two FCS anomalies occurred due to corroded connector pins. One anomaly occurred while the PTM FCS was mated to the M69-3 spacecraft; the second anomaly occurred with life test serial No. 1 during subsystem life testing. In both instances, intermittent electrical contact of certain pins was caused by a white, powdery deposit on the pin surfaces. Attempts to analyze this substance, however, failed due to an insufficient sample quantity. No other 1969 command unit failures have been attributed to corroded connector pins. Nevertheless, a similar substance was observed and removed from the FCS serial No. A102 harness connector sockets prior to mating with the FCS unit; but once removed, it never recurred.

4. Unexplained losses of command lock. There were two instances when FCS serial No. A104 momentarily lost command lock while in the space simulator. Although this caused no operational difficulty, these cases

are of special interest, since both losses of lock were accompanied by the FCS PN generator skipping states. The FCS would be expected to lose lock if the PN generator had skipped states; however, it could not be positively established why the PN generator had gotten out of sequence in these two instances. The available data did not reveal any unusual events or transients coincident with the two losses of lock.

Subsequent lab tests could induce PN generator skipping by generating large external power transients in the vicinity of the FCS. This phenomenon was repeatable with the EMBB and the PTM FCS units, as well as with the FCS serial No. A104. It is, therefore, possible that the anamolous PN skips, which occurred during the space simulator operation, were caused by transients which were too fast to be detected by the instrumentation used during the system test operations. Since other special tests revealed no component or circuitry deficiencies, FCS serial No. A104 was returned to its spacecraft without corrective action.

D. Test History and Performance

1. Summary of subsystem tests. Functional tests were performed on all of the regular FCS units. Modified tests were performed on the two specially constructed life test models. These tests were always conducted prior to and following thermal vacuum and vibration tests in order that environmentally-induced failures could be identified. The tests were conducted at ambient pressures, while first at +25°C, then at +55°C (+75°C for PTM), followed by 0°C (−20°C for PTM). Bit error rate and VCO tests were also conducted on the units during thermal vacuum environment.

The following FCS functions or characteristics were checked during the functional tests:

(1) Transformer rectifier performance.

(2) Phase-lock loop noise bandwidth.

(3) Phase-lock loop acquisition time.

(4) VCO static frequency.

(5) PN correlation time.

(6) Bit error rate.

(7) Command decoding performance.

(8) Universal isolation switch parameters.

(9) General logic performance.

The PTM FCS was subjected to the following type approval (TA) environmental conditions while in the subsystem configuration in a spacecraft bay IV case:

(1) Duration of 24 h at a control temperature of −20°C while at a pressure of 10^{-5} torr while in a simulated cruise mode.

(2) Duration of 12 days at a control temperature of +75°C while at a pressure of 10^{-5} torr while in a simulated cruise mode.

(3) Sinusoidal vibration of all three axes at frequencies between 5 and 2000 Hz, with a logarithmic sweep at a rate of 1 octave/min. The vibration amplitude levels of these sweeps ranged from 0.75 g rms at the lowest frequency to 13.5 g rms at the highest frequency.

(4) Random vibration of all three axes at a specified shaped spectrum and amplitude resulting in a wideband level of approximately 18.1 g rms.

The flight and spare model command units (serial Nos. A102, A103, and A104) were subjected to the following flight acceptance (FA) environmental conditions while in the subsystem configuration:

(1) Duration of 8 h at a test control temperature of 0°C, and a pressure of 10^{-5} torr while in cruise mode.

(2) Duration of 60 h at a test control temperature of +55°C and a pressure of 10^{-5} torr while in cruise mode.

(3) Sinusoidal vibration of all three axes at frequencies between 5 and 2000 Hz, with a logarithmic sweep at a rate of 3 octaves/min. The vibration amplitude levels during these sweeps ranged from 0.5 g rms at the lowest frequency to 9.0 g rms at the highest frequency.

(4) Random vibration of all three axes at a specified shaped spectrum and amplitude resulting in a wideband level of approximately 10.8 g rms.

During the subsystem tests the FCS subassemblies were affixed to a spacecraft bay IV case. To simulate thermal transfer and vibration characteristics, dummy (FTS) assemblies were also installed in the bay IV case.

2. Typical subsystem tests

a. Phase-locked loop. The phase-lock loop (PLL) bandwidths of all FCS units at a composite command signal-

to-noise ratio of 16.5 ±1 dB/Hz, were within the design limits of 0.4 ±0.1 Hz. The JPL design requirement specifying the detector to completely acquire within a maximum of 12.5 min at a command SNR of 16.5 ±1 dB/Hz was met by all units. This requirement implies that the maximum lockup time for the PLL should not exceed 4 min. Although the PLL acquisition time was normally negligible when the FCS VCO frequency was very near its center value, it would become critical if the VCO frequency were to drift from its specified center value.

b. VCO static frequency offset. During type approval and flight acceptance (TA/FA) tests the FCS VCO static frequency was measured with command modulation off, while applying noise to the FCS input. The measurement of VCO frequency then gave the average VCO frequency while at rest under a simulated system configuration. Another condition which contributes to VCO frequency offset is a noise bias effect. As the RF level into the radio transponder varies from strong signal to command threshold, the noise amplitude to the command subsystem increases due to the radio transponder limiter action. This change in noise amplitude has been observed to cause as much as 0.04% frequency offset in the VCO. In order to reduce this effect when command modulation is off, proper FCS Limiter action must be assured by having a minimum of about 100 mV rms of noise present at the FCS composite signal input. The combined effect of VCO circuit drift, loop filter and phase detector null drifts, and noise bias effect, all contribute less than ±0.05% frequency offset when at the command subsystem threshold. This assures PLL acquisition within the specified time.

c. Bit error tests. One of the primary tests performed on the command units was to determine the bit error rate at various signal-to-noise ratios. The mean SNR of all bit error tests on the two flight and one spare command units, for which the bit error rate was 10^{-5}, was 16.5 dB with 2-sigma limits at +0.95 and −0.3 dB. The bit error tests were performed at 0°C, 25°C, and 55°C at FCS SNRs from 13 to 17.5 dB/Hz.

Earlier in the test program, the bit error rate was determined by dividing the number of errors during a given time period by the total number of bits transmitted during that period. This could be reasonably determined at lower SNRs (viz, 13 dB/Hz) since a sufficient number of errors would occur within a reasonable length of time to permit this calculation. However, as the SNR is increased from the 16.5-dB/Hz region, as long as 45 h could be necessary to confirm that the bit error rate is not greater than 10^{-5} with a confidence level of 80%.

In order to shorten the bit error test time, therefore, it became necessary to use an automated extreme-value theory (EVT) method (Ref. 3). This method considers the amplitude distribution of the command bits before they are quantized. Therefore, the method calculates how close each bit comes to being quantized erroneously, making it possible to determine the probability of bit error without an error actually having to occur during a bit error test.

d. Power margin test. The FCS power margin test was performed on the PTM FCS while it was in its life test environment of ambient pressure and + 55°C. Two criteria were used to establish that the unit was performing to specification while the various power margins were applied:

(1) VCO static frequency offset (average) with 553 mV rms of noise applied to the FCS composite command input.

(2) Bit error rate while the FCS was performing with an applied command signal with an SNR of 15 dB/Hz.

The result of these two test criteria remained within spec under the following simulated spacecraft power conditions:

(1) Power frequency increased by 5% to 2.52 kHz.

(2) Power frequency decreased by 5% to 2.28 kHz.

(3) Power voltage increased by 5% to 52.5 Vrms.

(4) Power voltage decreased by 5% to 47.5 Vrms.

e. Life tests. The PTM FCS successfully underwent a life test at 55°C and ambient pressure for a total of 1,847 h. During the life test, the unit was powered by a 2.4-kHz, 50-Vrms, squarewave power supply with characteristics similar to those of spacecraft power. Since the unit was powered 24 h/day, a specially constructed solid-state current limiter was used to preclude the possibility of overcurrent damage. Periodically, all possible commands were transmitted to the unit by the FCS/OSE, which automatically verified that legitimate commands had been activated (proper universal isolation switch closures) and that improper commands were ignored. Further periodic testing included a check of

all UIS switching parameters. This included saturation-voltage, rise-time, fall-time, and pulse-width when the switches were activated, and leakage-current while the switches were off.

Two special life test units (serial Nos. 1 and 2) were constructed from parts left over from the retrofitting of the two flight command units (serial Nos. A102, and A104). These units were powered for 4,125 and 3,572 h, respectively, without component failure. The detector assemblies on these special units, however, did not have VCOs, making it necessary to simulate the inlock condition while exercising the rest of the FCS circuitry. Therefore, no information was gained on the life test capabilities of the phase-lock loop, or the VCO with these units. Otherwise, the test procedures for these special units were similar to those used while life testing the PTM.

VII. Flight Telemetry Subsystem

The *Mariner* Mars 1969 flight telemetry subsystem (FTS) performs the data conditioning, multiplexing, encoding, and modulation of spacecraft engineering parameters. In addition the FTS performs modulation and block coding of science data for transmission to earth. It does not perform radio transmission functions, or scientific instrument data-conditioning or data-storage functions.

The basic functions, and the operation of the commutated engineering channel and alternative science channels are given in Fig. 39.

The original design requirements and constraints for the FTS can be summarized as follows:

(1) Use as much of the *Mariner* Mars 1964 telemetry system design as will meet the mission requirements.

(2) Design for 100 analog data channels to the multiplexer.

(3) Design for 15 digital data channels to the multiplexer.

(4) Provide for counting pulses, indicating discrete events and counting time pulses between events. The outputs of these counters are to be on the digital channels.

(5) Digitize analog information.

(6) Accept digital data from other spacecraft subsystems.

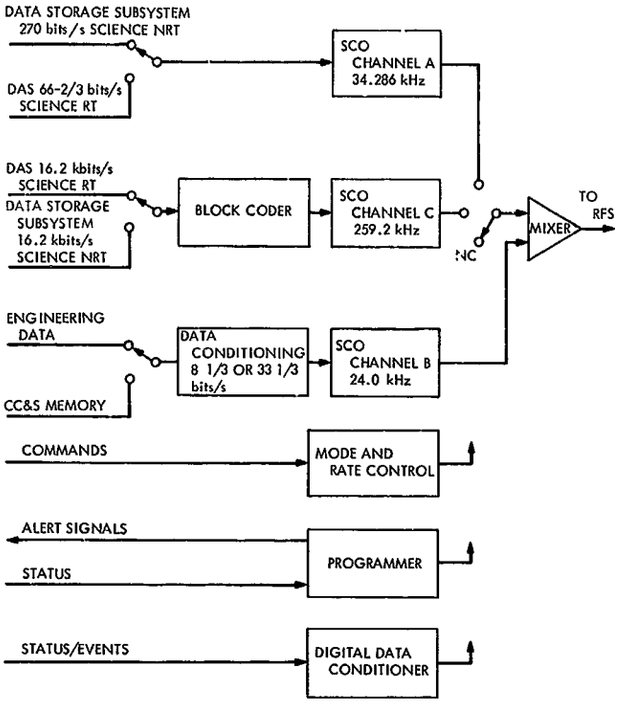


Fig. 39. *Mariner* Mars 1969 FTS simplified block diagram

(7) Provide for multiple data rates and data modes assuming a normal data rate of 33⅓ bits/s at planetary encounter, and 8⅓ bits/s backup for maneuvers, low-gain antenna, and post encounter.

(8) Provide for transmitting word synchronization information along with the data; bit sync is to be regenerated on the ground.

As the design of the spacecraft evolved additional requirements were placed upon the FTS which led to its final configuration. These additional requirements were:

(1) The addition of a block coding data channel, as an engineering experiment, to handle planetary encounter science data at 16.2 kHz.

(2) A telemetry subcarrier channel to handle the high rate block coded science data.

(3) A telemetry subcarrier to handle low rate science data, 66⅔ or 270 bits/s. The simplified block diagram (Fig. 40) shows the basic FTS implementation of the above requirements. Table 15 is a detailed tabulation of the design parameters applicable to the FTS.

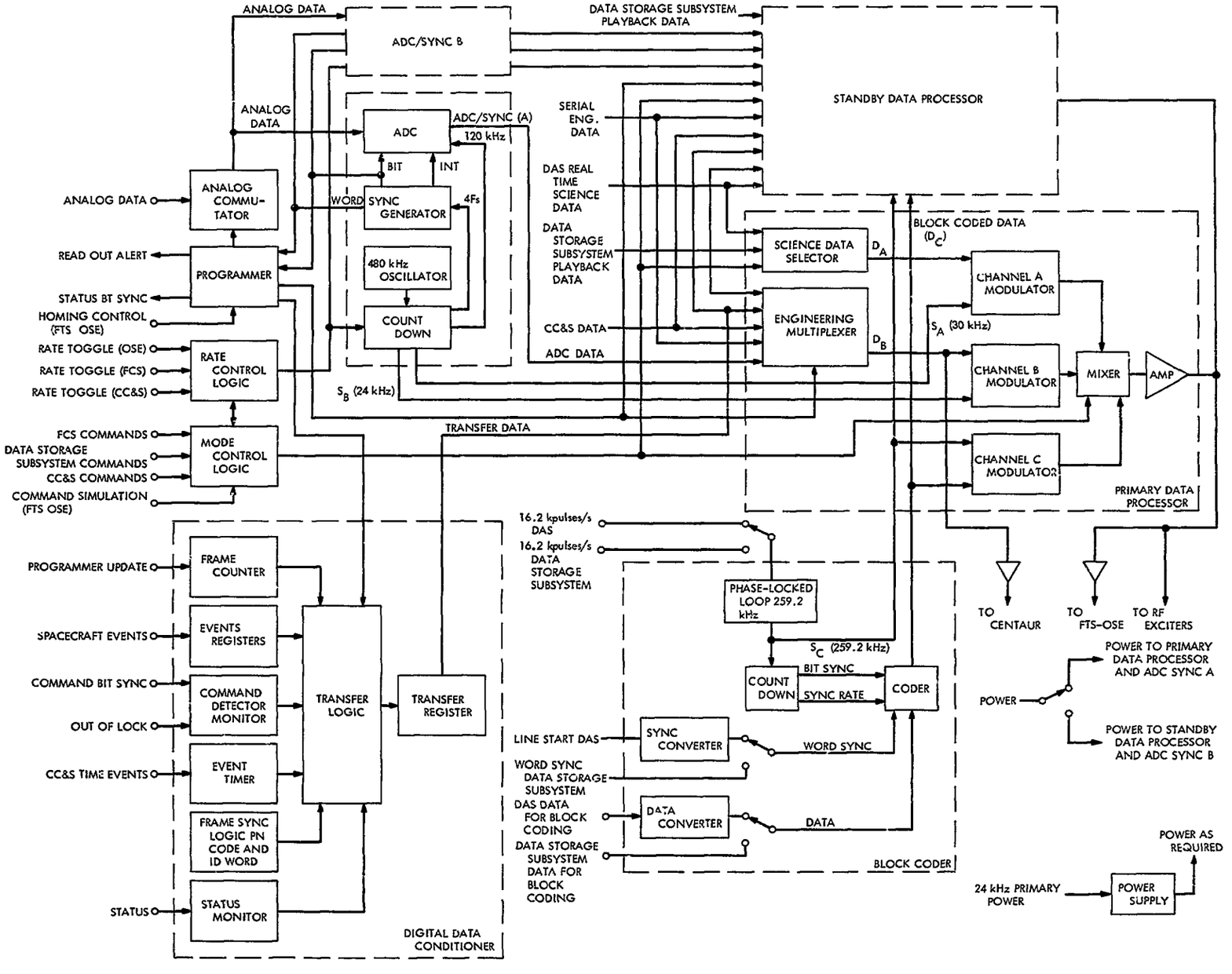


Fig. 40. Flight telemetry subsystem functional block diagram

Table 15. Final design parameters

Function	Parameter
Power	15.50 W
Reliability	0.876
Weight	23.0 lb
Volume	776 in.^{3}
Data handling capabilities	
Engineering data words (data channel B)	94 total
Analog	77
Digital	16
Event registers	2
Frame counter	1
Command detector monitor	1
Event timer	1
Sync words	2
Index words	1
Status word	1
Data storage subsystem	5
Temperature control flux monitor (TCFM)	2
Science data (data channel A)	
DAS	Real-time data
Data storage subsystem	Now real-time data, digital tape recorder
Block-coded data (data channel C)	
DAS	Encounter data
Data storage subsystem	Analog tape recorder data
CC&S memory readout data (data channel B)	33⅓ bits/s
Data modulation channels	3
Data rates	
Engineering or CC&S (D_B)	8⅓, 33⅓ bits/s
Science (D_{A1}), (D_{A2})	66⅔, 270 bits/s
High data rate (D_C)	16.2 kbits/s

Function	Parameter
Data modes	Cruise
	Encounter
	Playback
	Block code
Submodes or special modes	CC&S memory readout mode
Modulation technique	
Cruise	$K_{B1}(D_B \oplus S_B)$
Encounter	$K_{B1}(D_B \oplus S_B) + K_{A1}(D_A \oplus S_A)$
Playback	$K_{B2}(D_B \oplus S_B) + K_{A2}(D_A \oplus S_A)$
Block code	$K_{B2}(D_B \oplus S_B) + K_C\ (D_C \oplus S_C)$
(K_{A1}, K_{A2}, K_{B1}, K_{B2}, K_C are constraints imposed by the modulation angles)	
Modulation angles	
Channel A	$\phi_{A1} = 50.4$ deg
	$\phi_{A2} = 50.4$ deg
Channel B	$\phi_{B1} = 41.0$ deg
	$\phi_{B2} = 11.9$ deg
Channel C	$\phi_C = 65$ deg
Redundancy	Parallel NRTSCI data source lines ADC/timing/data processor
Number of command interfaces	20 total
Flight command subsystem	7
Central computer and sequencer	4
Data storage subsystem	1
Operational (ground) support equipment	8

Commutator sampling characteristics (Fig. 41)	Bit rate, bits/s	
	33⅓	8⅓
Sampling interval		
High deck, 100 series	4.2 s	16.8 s
Medium deck, 200 series	42 s	168 s (2.8 min)
Low deck, 300 series	420 s (7 min)	1680 s (28 min)
Low-low deck, 400 series	840 s (14 min)	3360 s (56 min)
Major frame transmission times		
Time to transmit One frame	840 s 14 min	3360 s 56 min

A. Functional Description

The *Mariner* Mars 1969 flight telemetry subsystem provides three data channels. one for science data, one for engineering data, and one for high rate (block coded) data; and it provides data-rate, data-mode and modulation-index switching.

The science channel (channel A) accepts serial low rate digital science data for transmission to Earth, and biphase-modulates the science data with the subcarrier for this channel.

The engineering channel (channel B) accomplishes the following:

(1) Accepts analog and digital measurement data from the spacecraft.

(2) Accepts and keeps an accumulative count of event pulses from the spacecraft.

(3) Conditions and encodes the engineering data into a 7-bit word format.

(4) Inserts a unique code into the data to provide frame synchronization.

(5) Inserts an index word that will identify subcommutation words during each cycle of high rate commutation and will identify the initiation of computer memory readout.

(6) Biphase modulates the engineering data with the subcarrier for this channel.

The high rate channel (channel C) accomplishes the following: accepts serial digital data from either the science or data storage subsystem for block coding and subsequent transmission to Earth; and biphase modulates the block coded data with the subcarrier for this channel.

1. Element description. A block diagram of the FTS is shown in Fig. 40. The following are detailed requirements of the major physical elements.

a. Commutator. The commutator format is shown in Fig. 41. The 200 deck commutators are stepped once for each cycle of the 100 deck and the 300 and 400 decks are stepped once for each cycle of the 200 decks.

b. Commutator frame synchronization. To establish frame synchronization a 15-bit pseudo-noise code word is provided in the high speed frame. To aid the ground equipment in establishing decommutation, the 15-bit PN code is followed by a 6-bit index word indicating the position of the subcommutation deck or the initiation of a computer memory readout.

c. Digital data conditioner. The digital engineering is routed to the engineering data multiplexer via the transfer register. The transfer register accepts data from the following registers:

Frame counter. The frame counter is a 7-bit binary counter which counts each complete engineering telemetry data frame. It accumulates a count of 100 before resetting to one. Its contents are read out in parallel to the transfer register upon a signal from the programmer.

Event register. The event register consists of four 3-stage binary counters which count spacecraft events. Each counter accumulates eight counts and then spills over. The counters are read out in pairs to the transfer register as directed by the programmer.

Frame synchronization. The frame synchronization logic inserts a 15-bit PN code into the first 15-bit positions of the high rate frame of the commutator. The code inserted is as follows:

MSB LSB

000011101100101

The left hand digit (MSB) is the one which is read out first.

Index word. A 6-bit index word denoting the states of the subcom channels of the commutator is inserted following the 15-bit PN code. This word has 49 states. Forty-eight states identify the sub-frames in the engineering data stream and one state identifies computer memory readout.

Event timer. The event timer is a seven-stage binary counter which measures the time duration of a relay closure to ground received from the central computer and sequencer subsystem. The count is accumulated by gating a reference frequency of word sync divided by two. The count is stored in the counter and is read out in parallel to the transfer register upon direction of the programmer.

Status monitor register. The status monitor register is a 7-bit register which contains information on the spacecraft identification, data mode, and RF subsystem

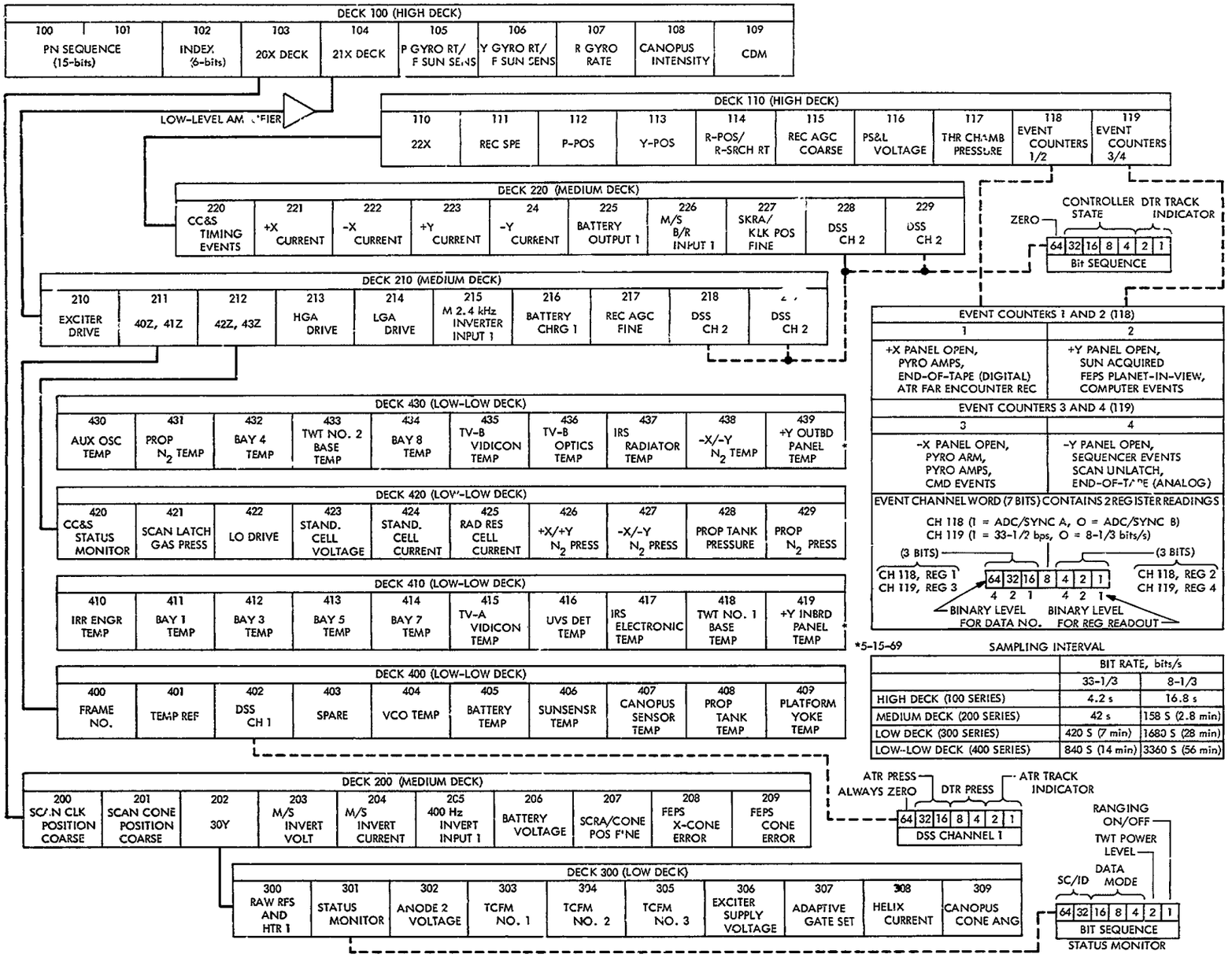


Fig. 41. *Mariner* Mars 1969 commutator diagram

status. The first two stages contain the spacecraft identification, and the third through fifth stages identify the existing data mode. The sixth stage contains the RF power level and the seventh stage indicates RF ranging on/off. The contents of the register are transferred in parallel to the transfer register upon direction by the programmer. Additional FTS status information, viz., engineering channel bit rate and data processor identification, are encoded on the event register channels.

Command detector monitor. The command detector monitor register is a five stage counter which accumulates 12 kHz for one command bit sync interval. One additional stage indicates whether the command detector is in or out of lock. The contents of this register are read out in parallel to the transfer register as directed by the programmer.

Transfer register. The transfer register is a seven stage shift register. The digital data entry is accomplished in parallel. The readout of the register is in a serial form to the engineering data multiplexer. The gating in and shifting out of data is controlled by the programmer.

d. ADC/sync block. The analog-to-digital/sync (ADC/sync) block converts the analog commutator output to 7-bit digital words and also provides the basic timing signals for the FTS. The ADC/sync block is redundant. The following devices make up the ADC/sync block:

Stable 480-kHz oscillator. The basic timing source for the FTS is a 480-kHz crystal controlled oscillator. The oscillator has a frequency stability of $\pm 0.01\%$. The oscillator output drives the ADC/sync countdown circuitry.

Countdown circuitry. The ADC/sync countdown circuitry digitally counts down the 480-kHz oscillator output to obtain the engineering channel subcarrier, science channel subcarrier, ADC clock and the sync generator input frequency. The countdown is controlled by the rate and mode of operation. The sync generator clock is that required by the specific mode of operation.

Sync generator. The sync generator generates the required timing signals for the analog-to-digital conversion and the programmer. The generator generates bit sync pulses for clocking the information bits. There is 1-bit sync pulse per information bit. The generator also generates one word sync pulse for 7-bit sync pulses.

Analog-to-digital converter. The analog to digital converter accepts the analog output of the commutator and converts it into 7-bit binary words. The ADC accepts 0- to 3-V levels from the commutator for digitizing. The ADC receives timing signals from the sync generator and countdown circuitry.

e. Primary/secondary data processor. The primary data processor consists of the engineering multiplexer, science data selector, channel modulators and the mixer amplifier. The data processor is redundant.

Engineering multiplexer and science data selector. The engineering multiplexer and science data selector switch the various data inputs to the modulators as directed by the programmer. The engineering data multiplexer receives inputs from the following four data sources: (1) ADC, (2) CC&S subsystem, (3) transfer register, and (4) serial digital data from data storage subsystem or DAS subsystems. The science data selector receives the following data inputs: (1) data storage subsystem (non-real time), and (2) data automation subsystem (real time).

Modulators. The modulators perform biphase modulation of each data channel with their respective subcarriers as follows:

(1) The engineering modulator modulo-two adds the engineering data D_B with the channel B subcarrier S_B. The result is the following expression: $D_B \oplus S_B$.

(2) The science modulator modulo-two adds the science data selector output D_A (data storage subsystem or DAS) with the channel A subcarrier S_A. The resultant output will be $D_A \oplus S_A$.

(3) The block coding modulator modulo-two adds the block coder output D_C with the subcarrier output S_C. The resultant is expressed as follows: $D_C \oplus S_B$.

Mixers. The mixers add the engineering, science, and high rate channels. The output of the mixers can be expressed as follows:

Spacecraft status	Mixed output
Cruise	$K_{B1}(D_B \oplus S_B)$
Encounter 1	$K_{B1}(D_B \oplus S_B) + K_{A1}(D_A \oplus S_A)$
Playback 1	$K_{B2}(D_B \oplus S_B) + K_{A1}(D_A \oplus S_1)$
Encounter 2 Playback 2	$K_{B2}(D_B \oplus S_B) + K_{C1}(D_C \oplus S_C)$

Quantities K_{11}, K_{B1}, K_{B2} and K_{C1} are constraints determined by the RF modulation angles.

f. Programmer. The programmer controls the state of the commutator, engineering data multiplexer, science data selector, and the digital data processor. The programmer provides timing and alert signals to the above listed blocks and other subsystems in order to generate the correct data format. After receiving the computer submode command, memory readout data shall be selected by the programmer immediately following word 102.

g. Rate-mode logic. The data rate and mode logic control the specific data rates and modes. The rate and mode control is accomplished such that upon loss of power, the FTS will maintain the state commanded prior to power loss. The telemetry modes of operation and available data rates are shown in Table 16.

h. Power supply. The power supply provides all voltages necessary for the FTS operation. The power supply operates from the 2400-Hz spacecraft power.

i. Block coder. The block coder converts each 6 bits of DAS or data storage subsystem 16.2 kbits/s data into a 32-bit biorthogonal comma-free code. The resultant data stream is transmitted at 86.4 ksymbols/s. The block coder is made up of the following devices. See Fig. 42.

Data converter. The data converter converts the DAS pulse (RZ) data into non-return-to-zero (NRZ) form for use by the coder logic.

Phase-locked loop. The phase-locked loop derives a 259.2-kHz square wave from the 16.2-kHz bit sync sent by the DAS or data storage subsystem. The 259.2-kHz signal is phase coherent with the 16.2-kbits/s bit sync. The PLL has a loop bandwidth of 100 Hz and a frequency stability of ±0.01%. The 259.2 kHz is used for the channel C subcarrier.

Coder. The coder converts each 6 bits of data input, (NRZ 16.2 kbits/s data) into a 32-bit bi-orthogonal comma-free code. The symbol rate will be $32/6 \times 16.2 = 86.4$ kHz. The output of the coder is then sent to the channel C modulator. The data output and the 259.2-kHz subcarrier are synchronous, i.e., the respective transitions are less than 0.1 μs apart.

Countdown. The countdown circuitry derives from the PLL the necessary bit sync, word sync and symbol sync required by the coder.

Engineering data readout. Engineering data is formatted such that the most significant bit (MSB) in each 7-bit word is transmitted first.

2. *Interface characteristics*

a. Analog signal inputs

Voltage. Three analog input voltages are accepted by the FTS:

(1) 0 to 3 Vdc

(2) −1.5 to +1.5 Vdc

(3) 0 to 100 mVdc

Impedance. The source impedance required by all analog inputs is less than 10 k and greater than 100 ohms. The input impedance of the FTS during sampling is 250 k or greater. The input impedance exceeds 10 megohms during times when an input line is not sampled.

Filter. The analog channels of the FTS are filtered at the input of the analog-to-digital converter with a single pole, low-pass filter with a 3-dB point at 50 Hz.

b. Digital signals

Serial data input. Digital coded data which are synchronous with the telemetry bit sync are accepted from the data storage subsystem, the temperature control subsystem, and the CC&S.

Readout alert signals. Readout alert signals are supplied by the FTS to the temperature control subsystem, the data storage subsystem, and the CC&S for data readout.

Bit sync output. The bit sync shall be continuously supplied to other spacecraft subsystems for data readout.

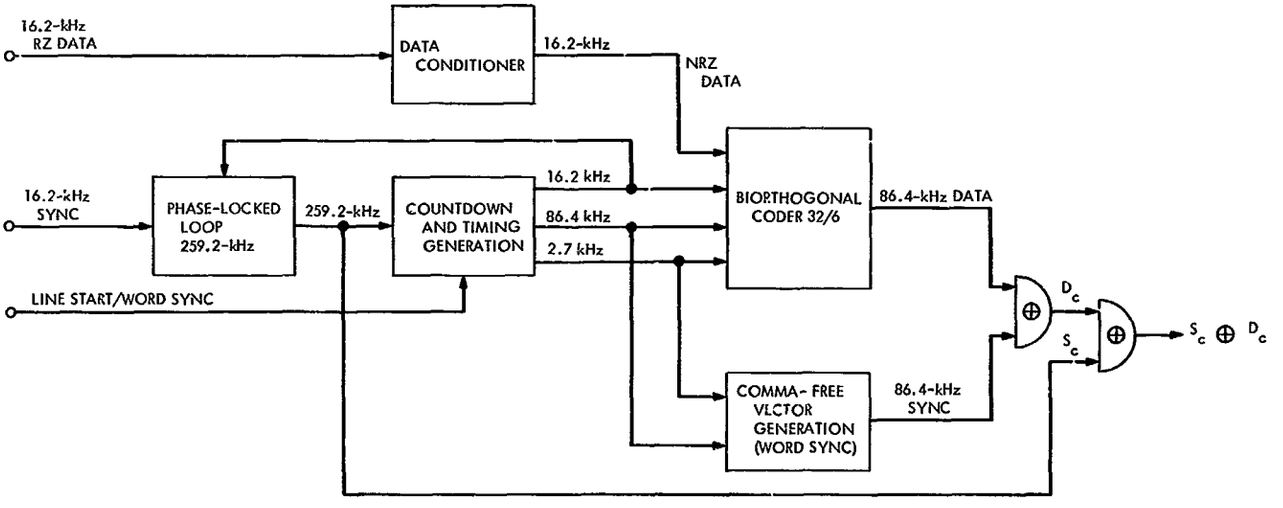
Pulse data inputs, event counters. The event counters accept, on their respective inputs, pulses of a random spacing, and upon interrogation, readout the cumulative count. Pulses are presented to the FTS as switch closures (mechanical or transistor) with the duration of closure at least 3 ms and less than 2 s.

3. *Control signal inputs.* Signals from the computer, flight command subsystem, and data storage switching data modes and rates shall be presented to the FTS as switch closures of at least 3 ms duration.

Table 16. Telemetry modes and data rates

Mode	Science channel (channel A)		Engineering channel (channel B)		High rate channel (channel C)	
	Data	Data rate, bits/s	Data	Data rate, bits/s	Data	Data rate, bits/s
Cruise	—	—	CC&S[a]	8⅓, 33⅓	—	—
Encounter 1	Real time science	66⅔	CC&S[a]	8⅓ 33⅓	—	—
Encounter 2	—	—	CC&S[a]	8⅓ 33⅓	DAS encounter	16.2 kHz[b]
Playback 1	Non-real time science	270	CC&S[a]	8⅓ 33⅓	—	—
Playback 2	—	—	CC&S[a]	8⅓ 33⅓	Direct analog tape recorder	16.2 kHz[b]

[a]Submode = CC&S memory readout; CC&S data substituted for engineering data at existing data rate.
[b]Transmitted symbol rate for 16.2-kHz data rate is 86.4 kHz.



1. EACH 6 bits OF DATA = 32-bit BIORTHOGANAL COMMA-FREE CODE
2. SYMBOL RATE = 32/6 x 16.2 = 86.4 kHz

Fig. 42. *Mariner* Mars 1969 block coder functional block diagram

4. Umbilical functions. The umbilical functions are as follows:

(1) Composite telemetry signal.

(2) Launch mode command.

5. Performance parameters. The accuracy of a measurement as read from the input to the FTS to the analog-to-digital converter output is maintained at ±1% of full scale for all 0-3 and ±1.5-V signals, and ±3% of full scale for 0-100 mV and all temperature measurements. This accuracy is maintained for the mission lifetime requirements and under all specified environmental conditions.

6. Physical characteristics and constraints. The physical characteristics and constraints follow:

(1) The weight of the FTS exclusive of the case and case harness is 21.5 lb.

(2) The 2.4-kHz squarewave power required by the FTS is 15.0 W.

(3) The volume of the FTS is 1000 in.^{3}

B. Design Considerations

Flight telemetry subsystem design studies were performed in 1966, in order to improve the *Mariner* Mars FTS design with respect to: (1) better data handling capabilities, (2) new spacecraft requirements, and (3) improved subsystem reliability. The following recommended conclusions were incorporated into the *Mariner* Mars 1969 FTS, Fig. 40. A detailed tabulation of the design parameters of the FTS is given in Table 15.

1. Integrated circuits. The logic implementation of the previous *Mariner* Mars FTS was done with discrete NAND logic modules. The spacecraft system requirements for 1969 were expanded with respect to previous *Mariner* projects. These requirements increased the functions of the FTS. A packaging study revealed that the FTS could not be mechanized within the allotted 1969 FTS volume. Studies also revealed an FTS power limitation if the *Mariner* NAND logic were used. Concurrent with these investigations, an integrated circuit investigation recommended the use of an integrated circuit logic family. The integrated circuits offered the advantages of a savings in volume, weight, and power, and improved reliability. The logic portions of the FTS gation recommended the use of an integrated circuit were implemented with Texas Instruments, series 51B, resistor-capacitor-transistor, logic.

2. Redundancy. Previous FTS included redundant analog digital converters and PN generators. The 1969 FTS design studies recommended additional redundancy. The changes included the following areas:

a. Redundant data processors. The data processor is used in the FTS for mixing signals which modulate the RF carrier. It was recommended that this area be redundant to improve the overall subsystem reliability.

b. Redundant timing generator. The timing generator reliability could be improved by the addition of a standby local oscillator in the FTS.

3. Subcarrier requirements. Mariner Mars spacecraft prior to 1969 utilized a data processor scheme which transmitted simultaneously one data channel and one synchronization channel. The sync channel consisted of a repeatable 63-symbol PN code. One cycle of the PN code was equivalent to one data word length. Since the timing of the data channel was related to the PN code, the decommutation of the telemetry data channel was done by obtaining bit sync from the sync channel. The 1969 system requirements provided for the use of a bit synchronization technique on earth to decommutate the data channel. This eliminated the need for a spacecraft sync channel. The 1969 FTS data processor is implemented to mix one or two data channels for transmission. Channel B (engineering data) is always transmitted. Channel A (science data) or channel C (block coded science data) can be transmitted simultaneously with channel B by commanding the FTS to the desired mode of data transmission. The telemetry modes of operation and available data rates are shown in Table 16.

4. Analog switches. The 1969 FTS commutator consists of 99 analog switches which route 77 analog voltages to the FTS ADC. The previous *Mariner* spacecraft used Bright switches for analog commutation. The 1969 FTS design studies recommended that a field-effect-transistor switch replace the bright switch. There are many advantages to this design change. The most significant ones include a volume savings, a reliability improvement, and the elimination of the bright switch oscillators. These oscillators generate frequencies near the FTS block coder subcarrier frequency.

5. Timing generator. The FTS timing generator on previous *Mariner* spacecraft consisted of a squarewave operating at a frequency of 2.4 kHz from the spacecraft ac power distribution system. The 1969 reliability studies revealed that the 1969 spacecraft reliability could

be improved by incorporating local, standby redundant crystal oscillators for the FTS timing generator. These oscillators were added to the FTS design. The operating frequency for these oscillators is 480 kHz.

6. Central computer and sequencer memory readout. In order to monitor the CC&S memory, a special mode of operation was provided in the FTS. This mode of operation substituted CC&S memory readout for engineering data on channel B. Upon completion of the CC&S readout, the FTS was commanded back to engineering data readout on channel B. The readout was synchronous with FTS bit sync, e.g., 8⅓ or 33⅓ bits/s.

7. Block coder. A biorthogonal block coder technique of modulation was implemented in the 1969 FTS as an engineering experiment. This data was transmitted on FTS channel C. The block coder (Fig. 42) transforms the science data, which consists of 6-bit words, into coded words, consisting of 32 symbols. Science data operating at 16.2 kbits/s is block coded into 86.4 k symbols/s. This data is transmitted to Earth. The ground decommutation technique compares the 86.4 k symbols/s against the biorthogonal dictionary. From this dictionary, it is possible to reconstruct the 6-bit science data. This technique provides an improvement of 1.8 dB to the telemetry link for high-rate date (e.g., 16.2 kbits/s).

C. Manufacture and Testing

The 1969 FTS hardware was developed and manufactured by Texas Instruments, Inc., Apparatus Division, under a three-phase CPFF/award fee contract. In addition to two flight models, there was a proof-test model and a spare.

1. Subsystem and spacecraft testing. The 1969 FTS PTM was required to pass type approval testing as a subsystem and as part of the PTM spacecraft. All other FTS were subjected to Flight Approval testing on subsystem and spacecraft levels. The FTS successfully passed all TA and FA tests.

2. Special tests. Each FTS underwent special subsystem calibrations to verify proper ADC operations, and to provide highly accurate input/output data.

Special subsystem margin tests were performed on the 1969 FTS PTM to determine design margins of the FTS with respect to input voltage variation and TA temperature extremes.

The compatibility test area (CTA) is a special laboratory at JPL which can perform data handling and data processing in an identical manner as would be done at a DSIF station. During special phases of spacecraft testing, CTA support was used to assure correct telemetry link operation. CTA support was used during spacecraft system test to verify that the FTS output was modulating the radio frequency subsystem carrier within the established tolerances.

D. Telemetry Transducers (Pressure and Temperature)

The transducers for the *Mariner* Mars 1969 spacecraft are essentially the same as those used on all previous *Mariner* Mars spacecraft. These transducers had been used on all the *Mariner* series spacecraft with no flight failures.

1. Pressure transducers. The present series of pressure transducers utilizes a miniature, lightweight, ruggedized pressure-actuated potentiometer, employing a Ni-Span C bourdon tube as the sensing element, which may be used for measuring pressure of noncorrosive liquids or gasses. Eight pressure transducers were used on the *Mariner* Mars 1969 spacecraft i.e., two 4000-psi nitrogen, one 4000-psi propulsion nitrogen, one 500-psi propulsion propellant, one 500-psi TV scan platform, one 300-psi motor chamber, and two 40-psi tape recorder transports).

a. Improvements. A number of modifications made to the pressure transducers during the 1969 program are listed below:

One-piece header. The transducer header and the gas inlet tube were formerly made of two separate pieces and then brazed together. These are now made from one piece of metal by eliminating one welding operation.

Potentiometer wiper arm. The potentiometer wiper arm is now formed from two pieces of metal which are welded together. It was previously made of three or more pieces soldered together. This has reduced the arm complexity and the number of materials required.

Case. The outer case has been made double the former thickness to assure meeting the 300% case burst pressure specification and containment of the system gas.

Welding Change from the tungsten inert gas (TIG) process has produced better welds. The use of the electron beam (EB) welding process has greatly improved the welds because of the increased depth of penetration. Since the case thickness was increased the requirement for 70% minimum weld penetration was more easily satisfied with EB welding. A secondary advantage comes naturally as a by-product of EB welding since it must be performed in a vacuum. The internal area of the transducer is evacuated during the weld process and is thus hermetically sealed.

Column pointer. A new column pointer has been designed to absorb more flexing action. However, the design is still somewhat inadequate from a standpoint of high reliability.

b. Conclusion. Since the pressure transducers, previously used in the *Mariner* series, will no longer be manufactured, it appears necessary to select and qualify a replacement for future spacecraft applications. A survey of all transducer manufacturers and all newer types will be made. A number of transducers will then be selected, environmentally tested, and evaluated.

2. Temperature transducers. The *Mariner* Mars 1969 temperature transducers are the result of a follow-on procurement of transducers developed for earlier *Ranger* and *Mariner* programs. These units have demonstrated a high degree of reliability, giving accurate temperature measurements with no flight failures.

Present temperature transducers being used are manufactured from platinum wire which has a positive temperature coefficient that is quite linear over the required temperature range. Range capability of the transducers is from $-300°F$ to $+300°F$.

There are three basic types of transducers used on the present *Mariner* spacecraft. The first type (solar panel and radio traveling wave tube transducers) is a small, uncased element designed specifically to fit in a very small space. The resistance of the sensing element is approximately 500 ohms at ambient temperature. A platinum wire, used for this resistive element, is wound around a piece of mica. Lead wires are attached and the whole device is covered with a protective coating. The second type transducer is a little larger in size because it is encased in a non-magnetic metal cover which is used for protection of the resistive element and for mounting the element on the spacecraft by the use of screws. Resistance of this type is the same as for type 1. The third type is the same in configuration as type 2, but the resistance value is reduced to 125 ohms. Four of these elements are attached in series and used in an averaging measurement in each of the spacecraft bays. The equivalent resistance of these four transducers adds up to 500 ohms; therefore, it is the same as one of the other type transducers and is treated as one output and measurement.

VIII. Data Storage Subsystem

A. Subsystem Functional Requirements

The purpose of the data storage subsystem, Fig. 43, was to provide buffering between the high rate at which data is acquired by the TV and other scientific instruments, and the lower rate at which these data could be returned to earth. The storage requirement was 1.8×10^8 bits to be recorded at data rates compatible with the TV and data automation subsystems and reproduced at rates compatible with the spacecraft flight telemetry subsystem.

B. Subsystem Design

1. Mechanization. Because of the requirement to use, wherever possible, designs with minimum change from the *Mariner* Mars 1964 hardware designs, it was decided to utilize two magnetic tape transports similar to those used on *Mariner* Mars 1964 to implement the data storage requirement. It was possible, by using the previously proven digital data storage techniques, to only store approximately 2.3×10^7 bits on each machine. A scheme was proposed, by the space sciences division, and subsequently accepted to record data on one of the tape transports in the analog mode, whereby information would be stored as an amplitude-modulated sinewave. Upon playback, each positive peak of the reproduced amplitude modulated sinewave would be digitized to 6 bits. Using conservative packing densities would allow storing approximately 2.62×10^7 cycles or 1.57×10^8 equivalent bits on the analog recorder. This scheme obviously reproduces data with a much higher error rate than does the digital record/reproduce process. The two transports have a combined capacity of the required 1.8×10^8 bits.

The data storage subsystem recorded data from the TV subsystem, which was in the form of an amplitude-modulated sinewave, with a carrier frequency of 18.9 kHz. The analog tape recorder (ATR) played this data back through an analog to digital converter (ADC), which converted each positive peak of the AM signal

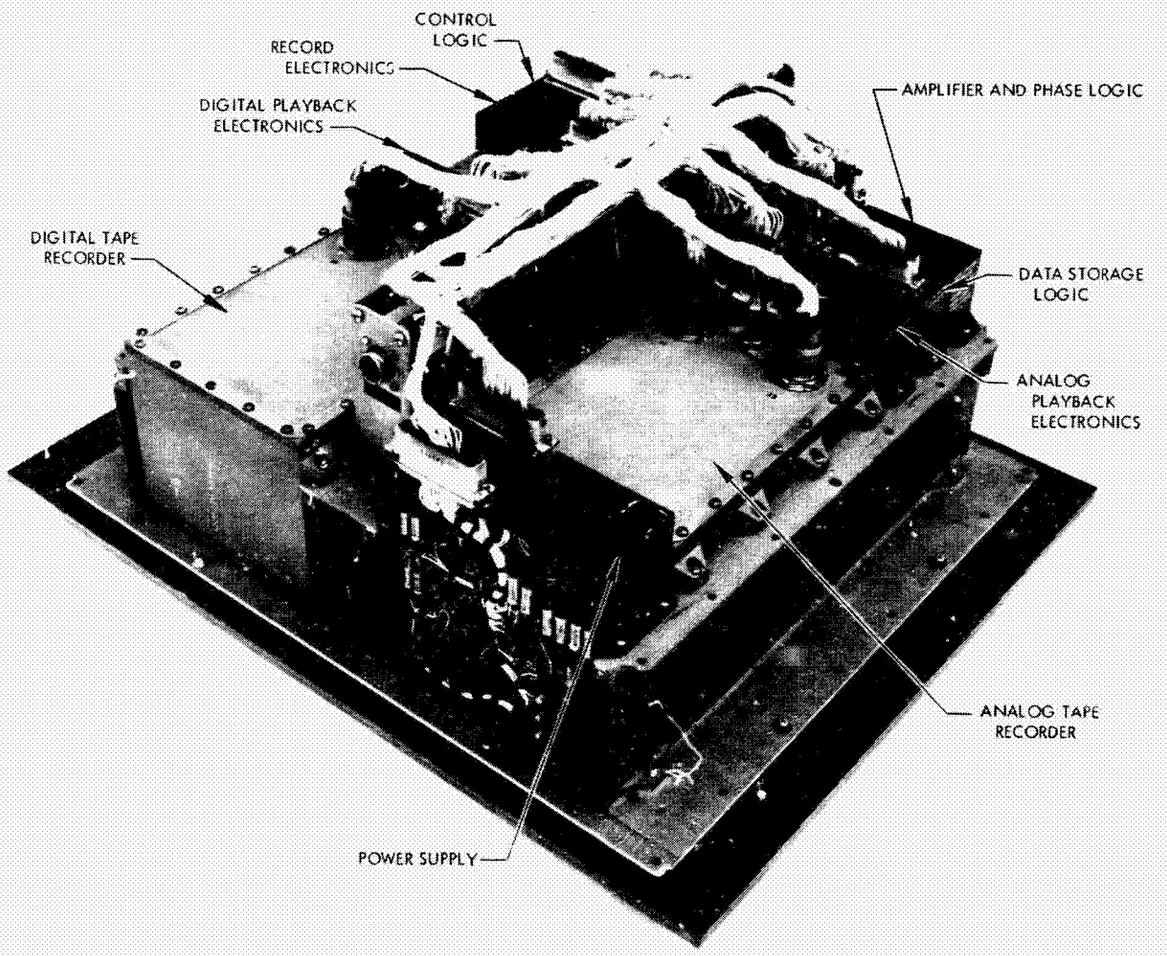


Fig. 43. Data storage subsystem and components

into a 6-bit word. The output rate from the ADC was at 16.2 kbits/s. Digital data from the data automation subsystem was recorded on the digital tape recorder (DTR) at a rate of 16.2 kbits/s. It was played back at a rate of 270 bits/s. The ATR could either play back through the ADC into the flight telemetry subsystem at 16.2 kbits/s, or it could playback through the ADC for recording on the DTR, after which it was played back from the DTR at 270 bits/s.

2. *Analog tape recorder error requirement.* The accuracy requirement on the ATR was developed from the characteristics of the recovered TV information. Given that each reproduced cycle of analog data is digitized to 6 bits, or 64 quantizing levels, the accuracy parameter was defined as the average of the rms deviation of a group of seven adjacent samples to a best-fit straight line through the set of seven samples, averaged over a large number of non-overlapping sets of seven adjacent data samples. The value of this parameter was set at 0.5 of a quantizing interval, as a goal. A more detailed discussion of this accuracy parameter can be found in Ref. 4.

3. *Digital tape recorder error requirement.* The error requirement on the digital record/reproduce function was that the digital data stored on the DTR should be reproduced with an error rate not to exceed one error in 10^5 bits, as measured at the output of the data storage subsystem.

4. *Detail design.* The basic components of the data storage subsystem are shown in Fig. 44. These components are the ATR, DTR, and ADC, the controller and the power conditioner. A detailed block diagram of the subsystem is shown in Fig. 45.

Both tape transports record data sequentially on four tracks. Each record head is driven by its own record amplifier, and each reproduce-head drives its own reproduce preamplifier. The analog data is mixed with a 518.4-kHz bias signal, and recorded directly on the magnetic tape. The record and playback motors are the hysteresis-synchronous type. In the record mode, the motor is driven from a stable frequency source which is counted down from the crystal-controlled basic

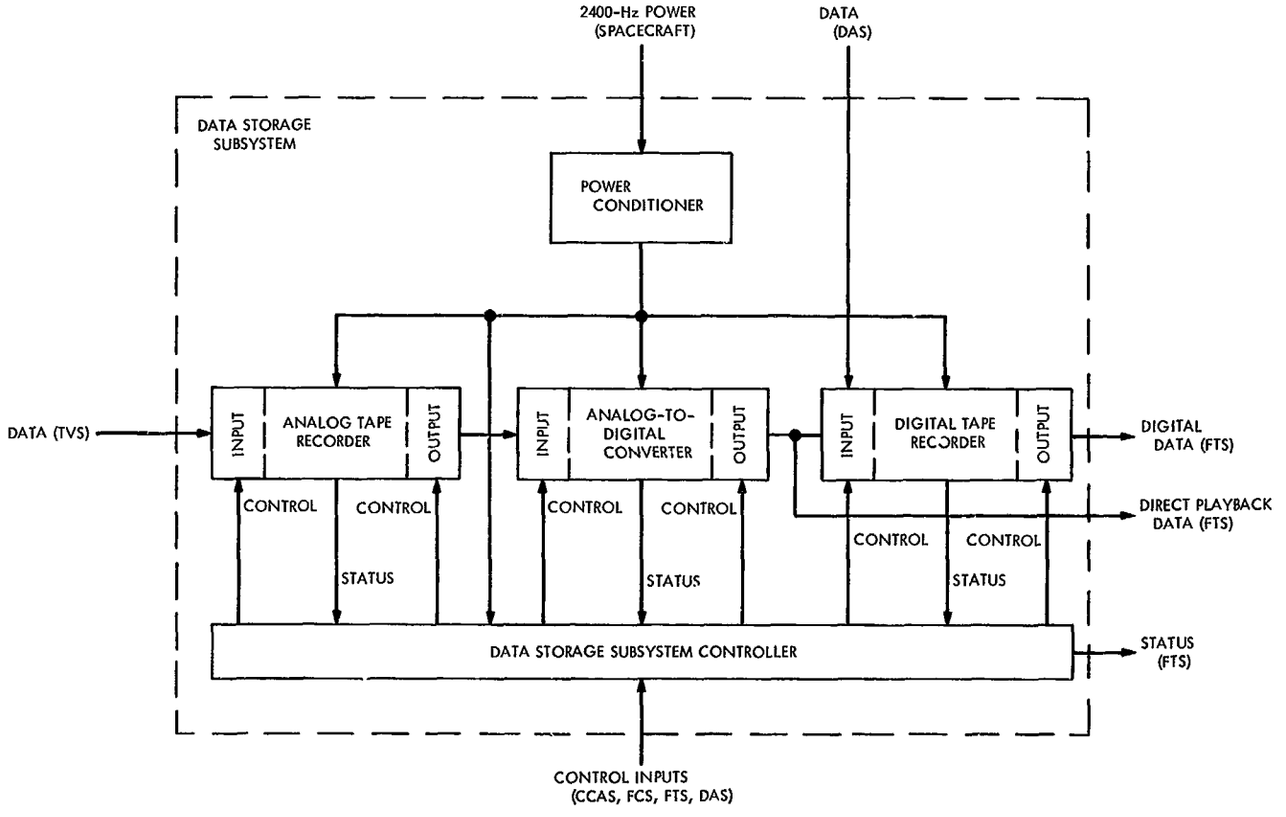


Fig. 44. Data storage subsystem basic block diagram

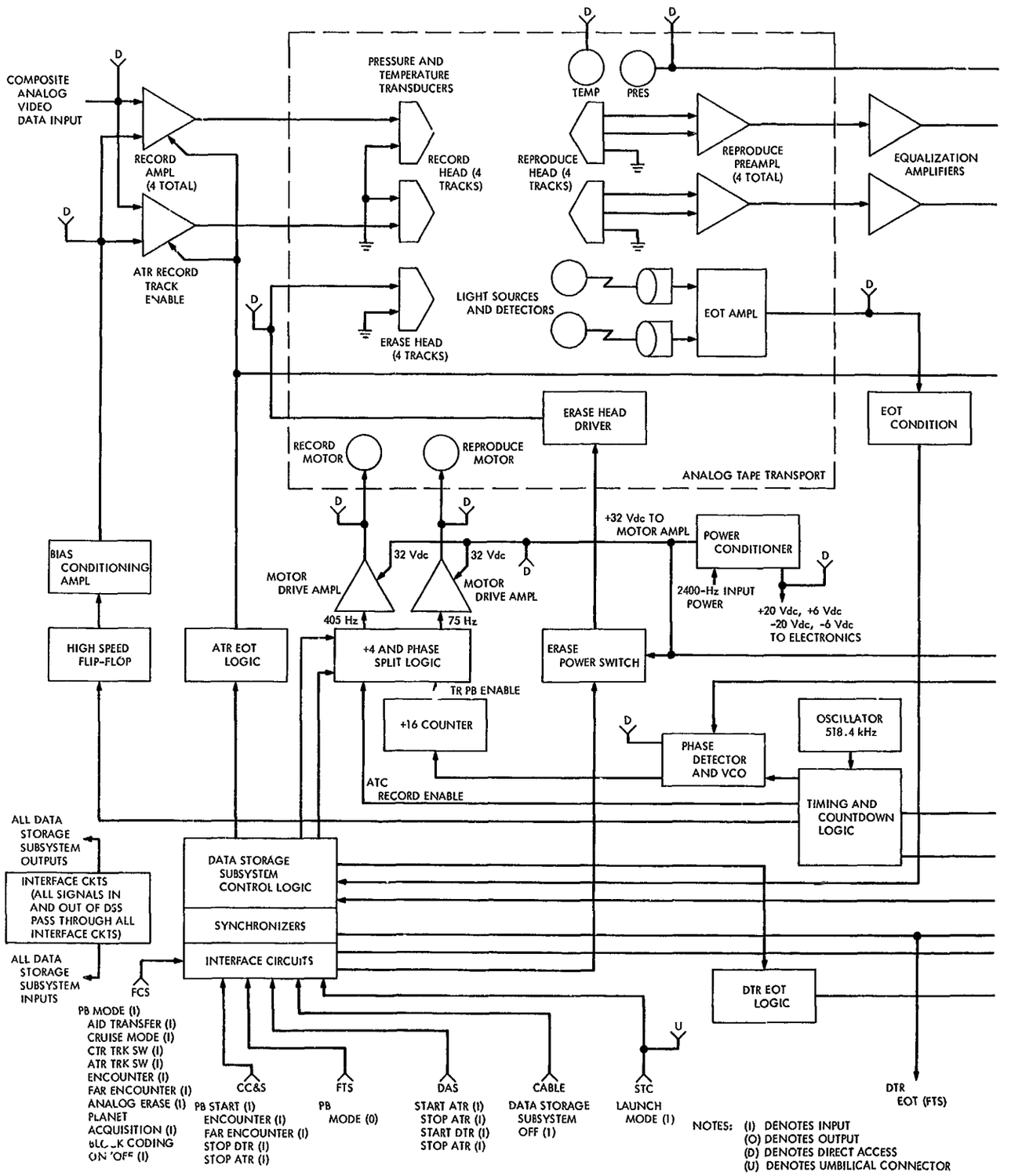


Fig. 45. Data storage subsystem detailed block diagram

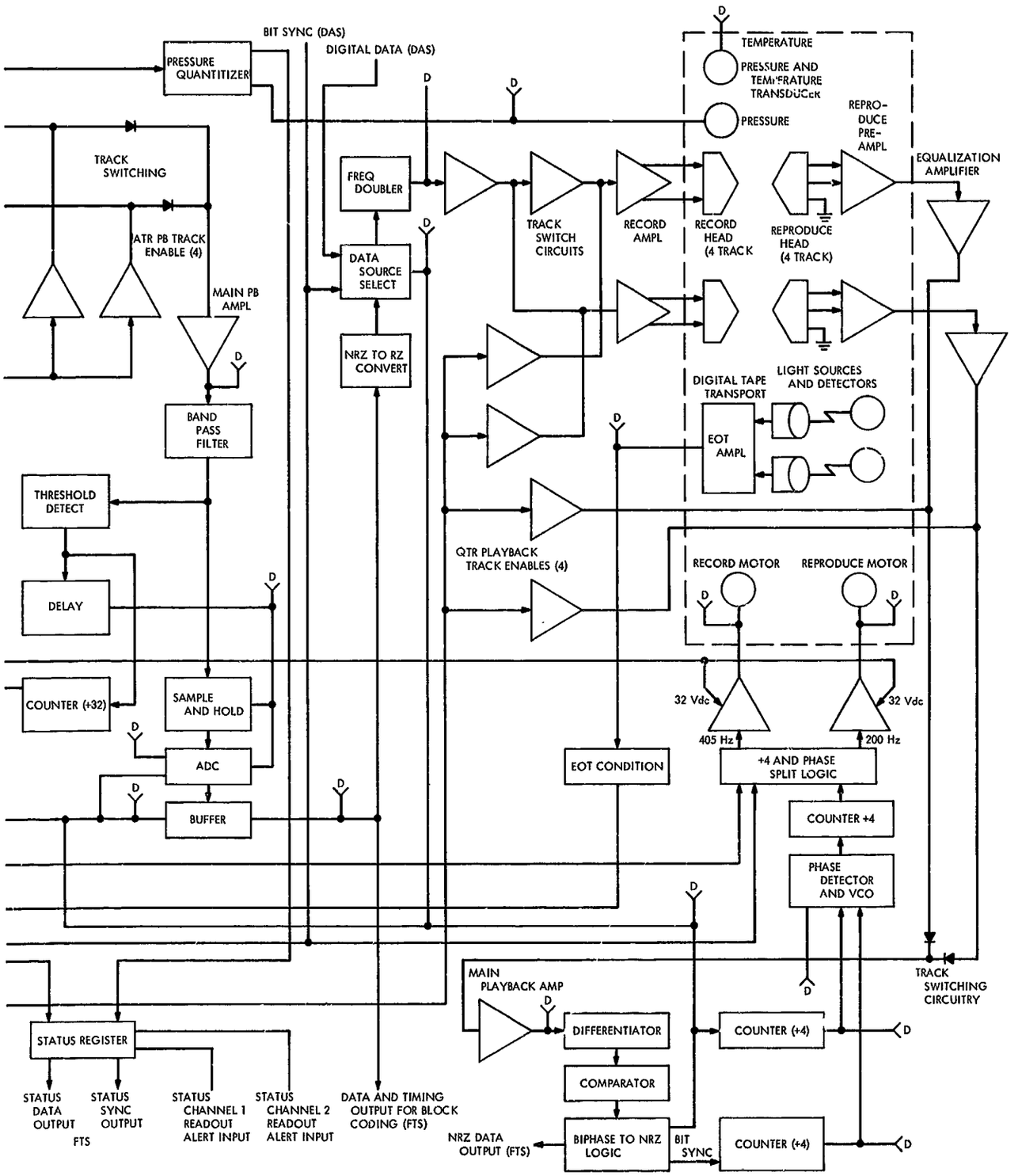

BIT SYNC (DAS)
DIGITAL DATA (DAS)
PRESSURE QUANTITIZER
TRACK SWITCHING
ATR PB TRACK ENABLE (4)
MAIN PB AMPL
BAND PASS FILTER
THRESHOLD DETECT
DELAY
COUNTER (+32)
SAMPLE AND HOLD
ADC
BUFFER
FREQ DOUBLER
DATA SOURCE SELECT
NRZ TO RZ CONVERT
TRACK SWITCH CIRCUITS
RECORD AMPL
RECORD HEAD (4 TRACK
REPRODUCE HEAD (4 TRACK)
REPRO-DUCE PRE-AMPL
EQUALIZATION AMPLIFIER
TEMPERATURE
PRESSURE AND TEMPERATURE TRANSDUCER
PRESSURE
DIGITAL TAPE TRANSPORT
LIGHT SOURCES AND DETECTORS
EOT AMPL
QTR PLAYBACK TRACK ENABLES (4)
RECORD MOTOR
REPRODUCE MOTOR
32 Vdc
32 Vdc
405 Hz
200 Hz
EOT CONDITION
+4 AND PHASE SPLIT LOGIC
COUNTER +4
PHASE DETECTOR AND VCO
TRACK SWITCHING CIRCUITRY
MAIN PLAYBACK AMP
DIFFERENTIATOR
COMPARATOR
BIPHASE TO NRZ LOGIC
BIT SYNC
COUNTER (+4)
COUNTER (+4)
NRZ DATA OUTPUT (FTS)
STATUS REGISTER
STATUS DATA OUTPUT FTS
STATUS SYNC OUTPUT
STATUS CHANNEL 1 READOUT ALERT INPUT
STATUS CHANNEL 2 READOUT ALERT INPUT
DATA AND TIMING OUTPUT FOR BLOCK CODING (FTS)
D

Fig. 45. (contd)

Table 17. Analog record and playback characteristics

Parameter	Performance
Recording method	Direct record
Input bias	259.2-kHz square wave
Data input rate (recording rate)	18.9-kHz AM sine wave
Playback rate	2.7 kHz
Capacity	2.6×10^7 carrier cycles (1.57×10^8 equivalent digital bits)
Accuracy	1.0 quantatizing level rms[a] in one tape pass
Tape dimensions	365-ft endless loop, ¼ in. wide
Number of tracks	Four
Record tape speed	12 in./s
Playback tape speed	1.71 in./s
Tape packing density	1580 cycles/in. track
Volume	431 in.^{3}
Analog record electronics	
Temperature range	−20°C to +85°C
Power supply variation (voltage)	±0.2 dB maximum
Frequency range	8.5 to 30 kHz
Gain stability (with temperature and power variation)	±0.5 dB maximum
Signal-to-noise ratio (with respect to the maximum unmodulated carrier level)	25 dB minimum
Bias electronics	
Frequency	259.2 kHz
Amplitude stability	±0.25 dB maximum
Total rms even-harmonic distortion	<1%
Analog playback electronics	
Temperature range	−20°C to +85°C
Power supply variation (voltage)	±0.2 dB maximum
Frequency range	1.2 to 4.3 kHz
Gain stability (with temperature and power variation)	±0.5 dB maximum
Phase deviation from linear phase response	±20 deg maximum
Signal-to-noise ratio (with respect to the maximum unmodulated carrier level)	25 dB minimum

[a]The error E is determined by the equation:

$$E = \frac{1}{N}\sum_{j=1}^{N}\left(\frac{1}{7}\sum_{i=7j-6}^{7j} E_i^2\right)^{1/2}$$

where E_i is the deviation in quantatizing units for the ith picture unit from the best-fit straight line over the seven picture units being considered under each group number j. There are a total of N groups.

timing oscillator in the subsystem. Analog data is recovered from the magnetic tape by the head, through the preamplifiers, equalization amplifiers, and the main playback amplifier. A phase-locked loop is locked to the reproduce carrier frequency, and develops a timing pulse which is in phase with the peak of the reproduced wave. This timing pulse is used to sample the amplitude modulated wave at the peak and to cause the ADC to digitize the sampled value. This timing pulse is also counted down, and a second phase-locked loop is locked to it which produces a drive signal for the reproduce motor in order that the output data rate is closely controlled at the 16.2-kbps rate. Track switching in the record/reproduce

Table 18. Digital record and playback characteristics

Parameter	Performance
Recording method	Saturation record
Data input rate	16.2 kbits/s
Data input form	Frequency-doubled digital code form
Output rate	270 bits/s
Capacity	2.3×10^7 bits
Accuracy	Maximum of 1-bit error in 10^5 bits (over one tape pass)
Tape dimensions	365-ft endless loop, ¼-in. wide
Number of tracks	Four
Record tape speed	12 in./s
Playback tape speed	0.2 in./s
Tape packing density	1350 bits/in. track
Volume	481 in.^{3}
Digital record electronics	
Temperature range	−20°C to +85°C
Power supply variation (voltage)	±0.2 dB maximum
Input data form	NRZ digital binary bits
Input data frequency	16.2 kbits/s
Digital playback electronics:	
Temperature range	−20°C to +85°C
Power supply variation (voltage)	±0.2 dB maximum
Frequency range	135 to 540 Hz
Gain stability (with temperature and power variation)	±0.5 dB maximum
Phase deviation (from linear phase response)	±20 deg maximum
Average error rate	1 in 10^5 bits over one tape pass maximum

circuits is accomplished through the detection of a transparent end-of-tape (EOT) window on the magnetic tape. The EOT detector consists of redundant pairs of a light-emitting diode and a light-sensing transistor, which generates an output signal when the transparent window moves between the light emitter and light sensor.

5. Technical characteristics. Technical characteristics of the data storage subsystem are shown in Tables 17–21 and Figs. 41–48.

The data storage subsystem has 6 basic modes of operation and has a capability of several submodes as listed in Table 21. Figure 49 is the state diagram for the data storage subsystem, showing the paths for switching modes and the command input required to make the mode change.

The analog and digital transports are essentially similar in construction. In the analog tape transport, the tape is held firmly against both capstans and the head assembly by a pressure belt guided by four crowned pulleys. The downstream capstan rotates at a slightly greater velocity (0.5% differential) than the upstream capstan, causing the tape to be tensioned against the magnetic heads to insure good tape to head contact. The head assembly consists of three magnetic heads mounted on a precision plate. The order of mounting of the tape of the magnetic heads as seen by the tape is: first, the record head, second, the erase head, and third, the playback head. The electronics signal module houses the preamplifiers which are required to be physically and electrically close to the heads to minimize noise pickup. The erase head driver provides the proper signal to the erase head to effect magnetic tape erasure when required.

Table 19. Transport motor and driver characteristics

Parameter	Performance
Motor types	Hysteresis-synchronous
Frequency of record-motor drive	405 Hz, nominal
Frequency of reproduce-motor drive	
Analog	76 Hz, nominal
Digital	202.5 Hz, nominal
Type of motor control	Servo loop
Reproduce motor open-loop cumulative flutter	5.0% peak-to-peak cumulative flutter[a]

[a]Peak-to-peak cumulative flutter is measured using procedures prescribed in IRIG Publication 106-66. The reproduce motor servo loop does not cause the value of the cumulative flutter to increase over the open-loop value.

Table 20. Analog-to-digital converter characteristics

Parameter	Performance
Temperature range	−20°C to +85°C
Encoding technique	Successive approximation
Number of bits	Six
Input level	0.25 to 2.50 V
Input frequency	2.7 kHz
Digitizing time	54.2μs
Digitizing frequency	129.6 kHz
Quantum level (1 digital bit)	50 mV
Encoding accuracy	±0.5 bit (±25 mV)
Bit rate From buffer	16.2 kbits/s
Output format From buffer	Serial NRZ binary code (most significant bit first)

Table 21. Power supply characteristics

Parameter	Performance
Power conditioning electronics	
Input power from spacecraft	100-V peak-to-peak square wave
Input power frequency	2.4 kHz
Output power levels (dc)	
+6 V and −6 V	Rectifier filtered
+20 V and −20 V	Rectifier filtered and regulated
+32 V	Rectifier filtered
Surge (peak) power-maximum percent of maximum average power (at 2400 Hz)	150%
Maximum average power consumption, W (at 2400 Hz)	
Launch mode	21.0
Cruise mode	
Power off submode	0.0
Ready submode	18.0
Record mode	
Far-encounter submode	18.0
Near-encounter submode	
Preterminator	23.0
Post-terminator	18.0
Playback mode	
Playback 1 submode	18.0
Playback 2 submode	19.0
Transfer mode	21.0
Erase mode	22.0

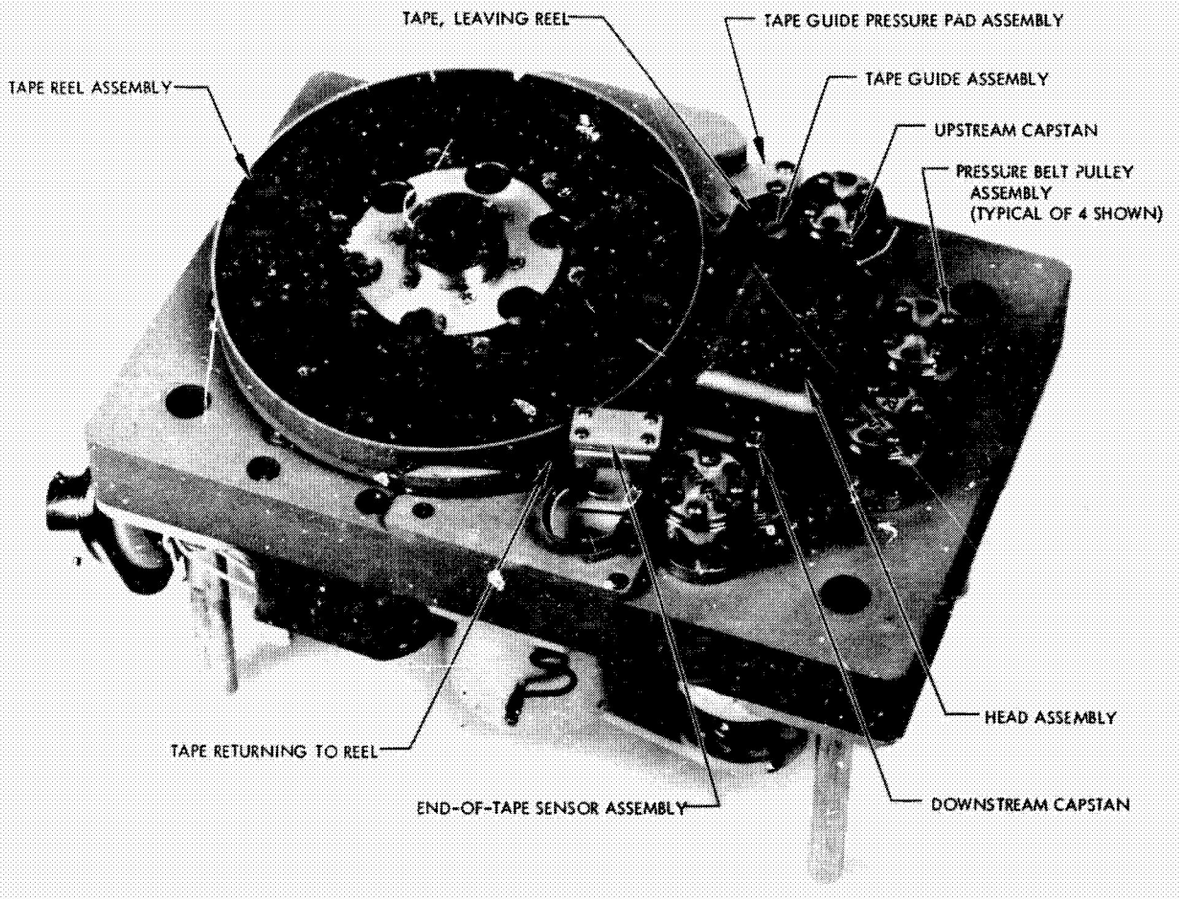


Fig. 46. Digital tape transport, tape side

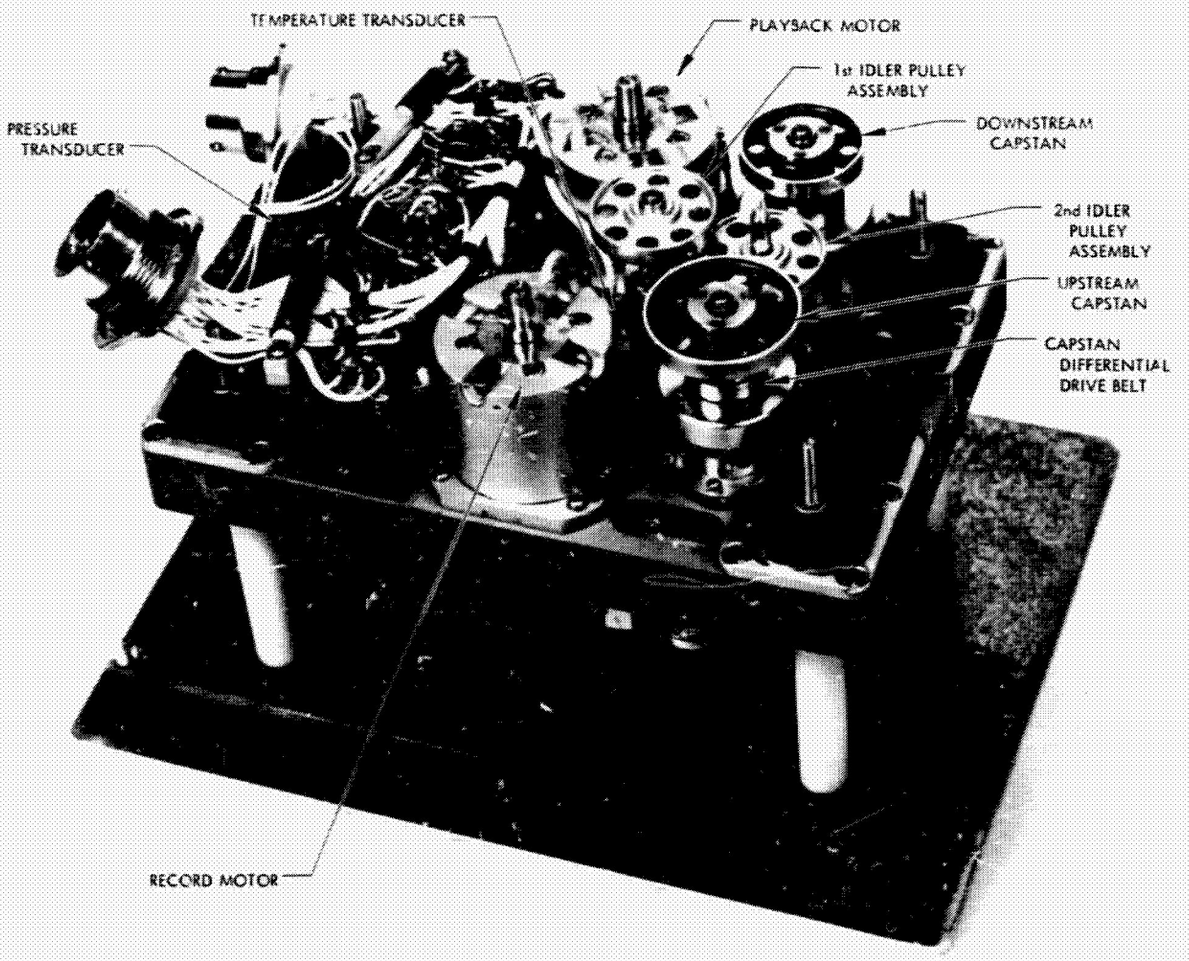


Fig. 47. Digital tape transport, pulley side

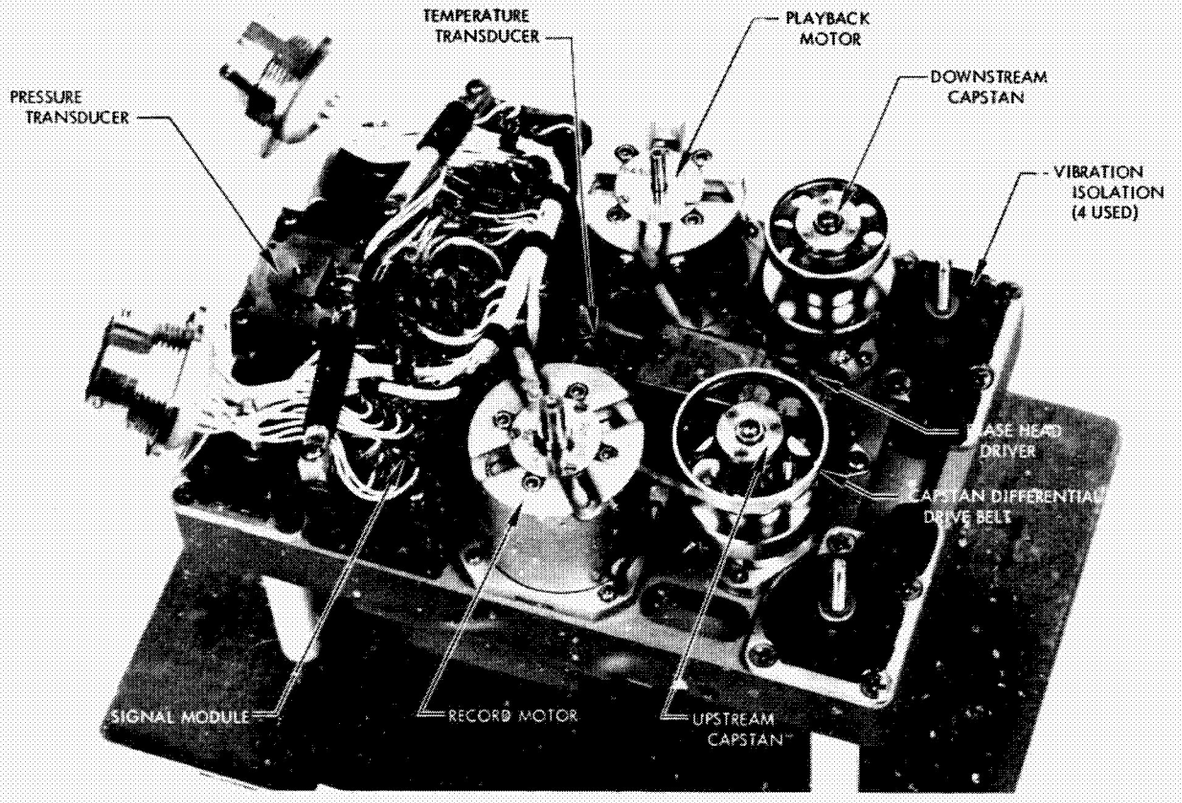


Fig. 48. Analog transport

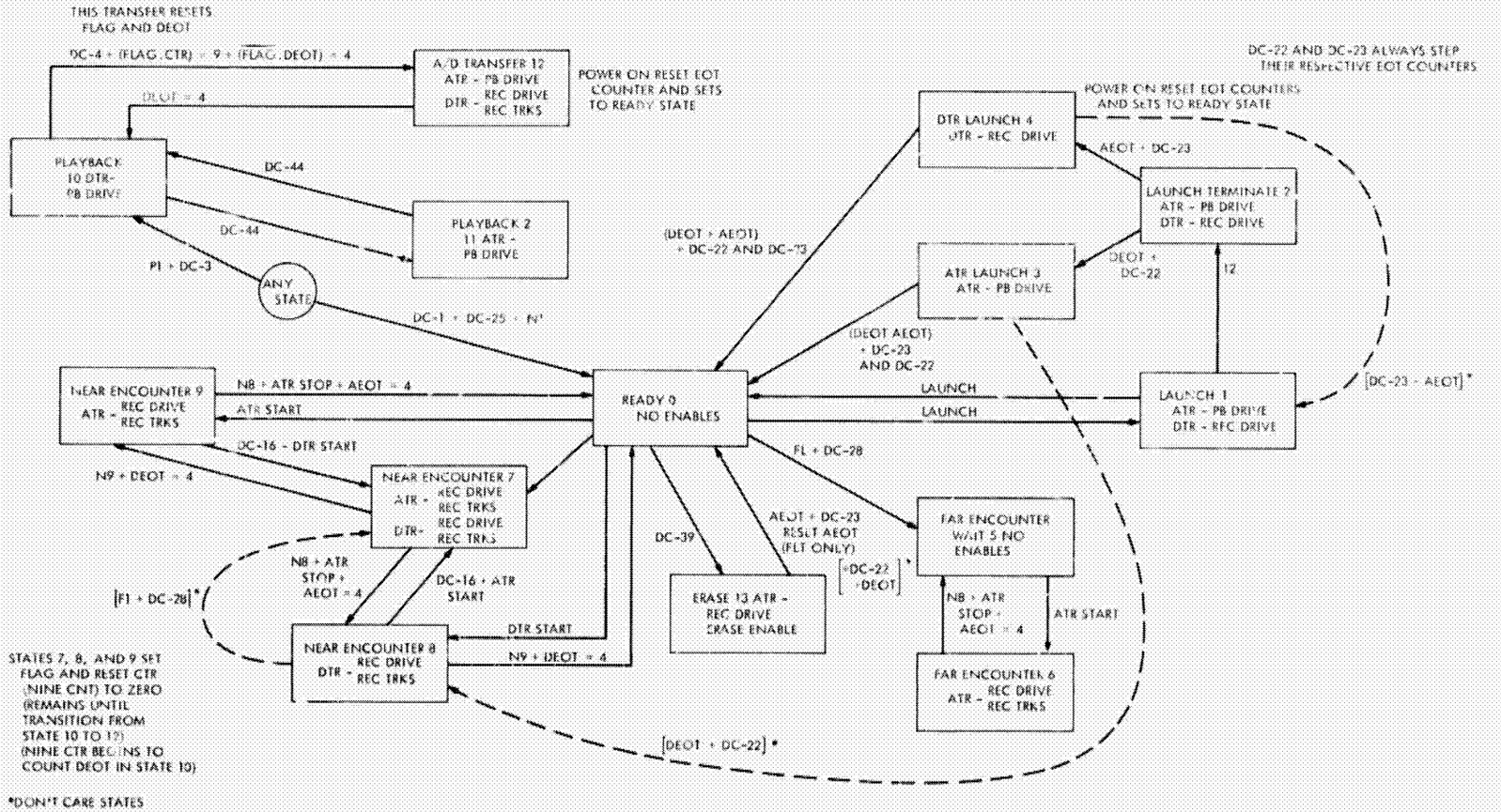


Fig. 49. Data storage subsystem state diagram

The DTR requires two additional stages of speed reduction than does the ATR, necessitating the additional pulley assemblies. Preamplifiers are also located within the transport case, but no erase head nor erase head driver electronics are required, since the digital recorder employs saturation recording.

Both transports are pressurized to 22 psia with a 90% argon, 10% helium gas mixture. Both transport decks are mounted on vibration isolators for protection against adverse shock and vibration inputs during the launch and pyrotechnic firing phases of the mission.

6. Electronic circuit packaging. The data storage subsystem electronics utilizes both discrete components and integrated circuits. The discrete component circuitry is packaged in soldered cordwood modules with some discrete components mounted directly onto the printed circuit interconnection boards. The encapsulated cordwood modules are likewise mounted on the planar interconnection boards. Integrated circuits are packaged in flat, stick-type module assemblies developed by JPL. Figure 50 shows a typical hybrid subassembly. Five of the seven subchassis are hybrid, each containing one to eleven stick subassemblies. The subsystem contains a total of 25 integrated circuit stick subassemblies, all of a different type. It contains a total of 76 soldered cordwood modules of 35 different types.

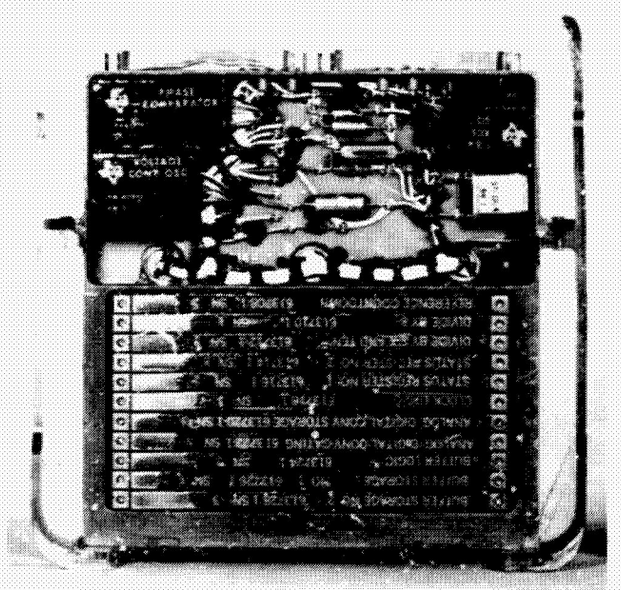


Fig. 50. Hybrid subchassis

7. Design evolution. The *Mariner* Mars 1969 data storage subsystem evolved from designs used on *Mariner IV*. The tape transports are very similar to the *Mariner IV* tape transport, with changes required to implement the required record and playback speeds, the addition of the erase head on the analog transport, and the configuration of the pressure belt which holds the magnetic tape against the heads and the two capstans. The electronic design used circuits which, wherever possible, were developed on the previous programs, and the electronic packaging techniques used on the *Mariner IV* program. Integrated circuits were used for the first time on JPL data storage programs to implement the digital functions.

Several design studies (Refs. 5 and 6) were accomplished during the early part of the program, the results of which contributed to the initial design of the subsystem.

C. Problem Areas

Many problems came to light during the course of this program, some relatively minor, and accepted without changing the design, and others of a more serious nature, requiring hardware changes or procedure changes.

1. False sample pulses generated for ATR output digitization. Difficulties in data retrieval presented a problem with the ATR during spacecraft testing. It was discovered that the ATR would add and/or delete 6-bit digital words along with increased tape flutter during ATR playback. The sample pulse for digitizing the analog signal peak was derived by detecting zero crossings of the analog signal. The output of the zero crossing detector also served as the input to the tape speed servo which controlled the speed of the analog transport.

Noise on the playback signal and signal dropouts due to magnetic tape imperfections caused extra outputs from the zero crossing detector or, in some cases, no output from the zero crossing detector. This caused either extra sample pulses or deleted sample pulses, which resulted in the added or deleted words in the output data stream. These erroneous outputs also caused the flutter of the transport to increase because of the erroneous inputs to the tape speed control servo.

The zero crossing detector was replaced with a phase lock loop tracking filter. The oscillator in the phase lock loop was phase locked to the playback signal from the ATR and provided a stable sample pulse for the sample

and hold circuit and a stable reference for the tape speed control servo. The circuit maintained a stable timing signal in the presence of a noisy input and signal dropouts. The physical modification was fairly simple in that it required the replacement of two modules on a subchassis with two new modules.

2. ***Signal dropouts.*** Early test results from the analog tape recorder indicated poor tape guiding across the heads and poor head-to-tape contact. This was made evident by the reproduction of pictures recorded on the ATR. The two effects of the problem were: first, a dark band appeared across the picture, illustrating poor tape guiding across the head, whereby the tape shifts position for a relatively long period of time while passing over the head, thus causing a gross change in output signal, due to less flux intercepted by the head during the time the tape has shifted position on the playback head; second, dark streaks were illustrating the effect of signal dropouts, whereby the output signal drops in amplitude for a short period of time involving relatively few cycles of playback signal. A design change was made which significantly increased the quality of reproduced signal by changing from the dual pressure belt design to the single pressure belt design. The dual pressure belt configuration utilizes a separate belt to apply pressure to the tape as it passes over each capstan. The differential capstan speed causes tension in the tape as it passes over the magnetic heads. The single pressure belt configuration utilizes a single pressure belt which continuously contacts the magnetic tape from the upstream capstan, across the heads to the downstream capstan. This configuration supplies greater pressure to the tape as it passes over the heads, not only from the tension in the tape, due to the differential capstan speeds, but from the tension in the pressure belt as the belt and the tape pass over the heads while in intimate contact with each other.

Tests were conducted using a single pressure belt of various widths. The single belt configuration significantly reduced high frequency flutter and signal dropouts during playback. The playback signal also displayed uniform track-to-track signal amplitude and constant signal output amplitude. In addition, the overall signal output was increased. Several mechanical advantages resulted with the use of one pressure belt that improved the electrical performance. Tape wobble, lateral tape movement, and rundown time were greatly reduced. Greater tape pressure across the heads improved tape-to-head contact. The increase in tape pressure caused the aforementioned increase in reproduced signal amplitude on all tracks. Since a more uniform stress distribution along the length of the single pressure belt existed, belt relaxation was also made uniform. Less belt tension was required, due to increased wrap angle around the capstan.

There were several disadvantages in using a single pressure belt. Head life and tape life were reduced because of increased tape pressure on the heads. There was an increase in the number of bending stress cycles per tape pass to which the belt was subjected, compared to using a dual belt drive. A larger wobble component due to the longer length also existed.

The single pressure belt configuration was elected to be used in place of the dual belt drive system, since all test results indicated that a substantial improvement in performance was obtainable with a single belt. Increased wear on the tape and heads was judged to be acceptable, due to the relatively low number of tape passes which the transport would experience during the mission.

It then became obvious that the predominant cause of picture degradation was caused by signal dropouts. A drop-out requirement was developed, using measured performance as a guide, which stated that the tape transports as delivered by the contractor should exhibit less than one dropout in 10^4 cycles, measured over one complete track length, where a signal dropout was defined as a signal cycle dropping below 50% of the average playback amplitude. This works out to be 680 dropouts per track. In most cases, the contractor was just able to deliver the transports within this requirement.

After the tape transports had been tested for a few hours, it was observed that the dropout rate increased. After reproducing pictures played back from the data storage subsystem on the spacecraft during SAF testing, it became evident that the signal quality was degraded by the signal dropouts and would have to be improved. The first solution was to simply replace the tape on the tape transports. This resulted in an improvement initially; however, the system soon degraded to an unacceptable condition. Microscopic examination of magnetic tape samples taken from tape packs showed that the oxide surface finish of the tape was excessively rough. Examination of the tape transports after considerable test time showed excessive contamination of the record, playback and erase heads. This contamination resulted from both oxide and graphite (tape lubricant). However, simply replacing the magnetic tape and cleaning the heads did not correct the problem.

As several hundred tape passes had accumulated on each tape transport at this stage of the test program, the magnetic heads had worn considerably by the action of running of the magnetic tape over the heads. Figure 51 shows a closeup photo of a quite severely worn head, with tape lubricant (graphite) build-up on the head. The profile of the wear pattern takes the form of essentially a channel which has been worn into the head surface by the tape. The "rippled" pattern is caused by different wear rates of the head materials. When a new tape was installed, the new tape would not ride stably within the old wear channel in most cases, due to width variations of the new tape. It was then decided that the heads should be resurfaced to the original head profile. It was hoped that this would not have to be done because of the difficulty of removing the head assembly, and because of time constraints.

Testing the transports with resurfaced heads showed a slight increase in quality marked by reduced signal dropouts, and an increase in overall signal output amplitude. Continued investigation of the signal dropout problem led to experimentation of using tape which had first been conditioned. This conditioning process consisted of running the oxide side of the tape over a sharp blade followed by running the tape over rolls of specially made wiping paper, in a modified commercial magnetic tape cleaning machine. Specifically, the tape was pulled under capstan control at a speed of 9.2-in./s. and made to pass over the razor blade fixture and the two cleaning tapes. Passing of the magnetic tape over the blade caused sufficient oxide to be scraped off the tape to reduce the roughness and produce a smooth oxide finish. Loose oxide due to the scraping process was removed from the magnetic tape by cleaning both sides of the tape by the cleaning paper. The cleaning paper is composed of long cellulose fibers, softly woven, which have been treated with a small amount of silicone oil. Reproduced signal quality was greatly improved through the use of this tape conditioning process.

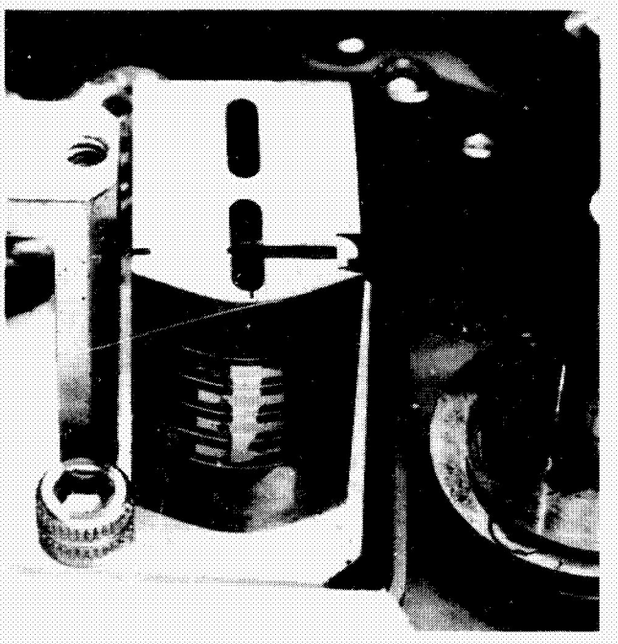


Fig. 51. Magnetic head showing wear

It was then decided to refurbish each flight data storage subsystem just prior to the last spacecraft system test. The refurbishment for the tape transports consisted of removing the head assembly, and returning them to the head manufacturer for the head resurfacing. The resurfacing consisted of hand-lapping the head faces using the same procedure as used in the manufacture of new heads. The resurfaced heads were then reinstalled on the tape transports. New magnetic tape was installed, after being conditioned as previously described.

When the analog recorders were removed from the spacecraft and tested in the lab, they typically showed signal dropout rates on the order of 2,000-3,000 dropouts per track. Following the refurbishment process, the dropout rates ranged from zero to 182 dropouts per track. The average of all the tracks on all three flight systems was 52.

Another problem which occurred after the transport refurbishment process was that the output signal amplitude from the analog tape transports increased as a function of tape passes such that at launch, after the transports had accumulated about 200 tape passes since the refurbishment, the output signal levels had increased typically from 5% to 15%. This was assumed to be caused by the wear-in process of the new tape on the newly resurfaced heads, so that initially the head-to-tape contact improved during this initial wear-in process. On the two subsystems which were used on the flight spacecraft, this effect was not corrected, but instead, accounted for during the last calibration procedure on the TV-data storage subsystems. On the flight spare subsystem, this increase was more noticeable so the gain of the playback amplifiers was reduced to bring the output signal amplitude down to the desired level. This problem was also confirmed by life tests performed on the prototype DSS. It was found in these tests that the output level increased to a maximum of approximately

25% until about 250 tape passes had been accumulated, after which the output level stabilized.

3. Drive belt failures. In early 1968, at the contractor facility, three failures occurred in the capstan drive transmission system. The failure mode was that the seamless Mylar belt connecting the record motor shaft and the first idler pulley of the digital tape transport came off the pulleys. The motor shaft is flat, whereas the idler pulley is crowned, which provides guidance for the belt.

A study program was conducted to try to determine the cause of failure. A transport was tested over temperature range of 0–55°C, using various belt tensions and start/stop sequences. High speed cinematography was used to record any possible failures and to detect slip between the belt and pulleys. Fairly drastic tests were performed on the transport, such as jamming the pulley to cause the motor to stall. The failure could not be reproduced, even under these abnormal conditions. Only by reducing the belt tension to an abnormally low value, was it possible to cause a belt to come off the pulley. The conclusion drawn from the study was that the initial failure was unique, probably due to an inferior belt. The second and third failure were probably related to the surface treatment of the motor pulleys. No belt failures have occurred since the replacement of the surface-treated motor pulleys with plain, stainless steel pulleys. A more detailed discussion of this problem can be found in Ref. 7.

4. Vibration. During type approval random vibration testing of the PTM data storage subsystem, the instrumentation accelerometers mounted on the data storage subsystem and on the vibration table indicated high-level shocks being generated in the subsystem. After considerable test investigation, the problem was isolated to the tape transports, specifically to the fact that under the TA random vibration inputs, the tape deck, which is mounted on vibration isolators, was deflecting to such an extent as to contact the inside of the transport chassis.

A redesign of the vibration isolation system was initiated. Concurrently, information became available from test results from the dynamic test model spacecraft, which indicated that the TA vibration levels specified for the subsystems were quite conservative, and that they could be reduced. The decision was made to reduced the test levels rather than to replace the vibration isolators with stiffer ones. The subsystem subsequently passed the vibration tests, using the reduced levels.

5. Insufficient digital record current. During acceptance testing on the second flight subsystem, excessive bit error rates were encountered in the DTR. It was found that previously recorded data was not being fully erased by the re-recorded data; i.e., the tape was not being fully saturated. The results of oversaturation, however, is that the high frequency response is degraded. A compromise must be made then, so that the record current is high enough to saturate the tape sufficiently to erase previously recorded tape, while not degrading the high frequency response adversely. It was decided that the record current could be increased somewhat to achieve the desired results. The change was consequently made in all units.

6. Analog tape recorder error. The measured error of the data reproduced from the ATR did not meet the specified requirements established during the design and development phase, which was that the error, as a goal, should be less than 0.5 of a quantizing interval. This goal was not met. Typical values for this parameter obtained on the flight units initially averaged around a value of 1.3 of a quantizing interval.

The method of measuring this parameter was to first, record a constant level sinewave signal on the ATR. Typically, this would be at a chosen value of 3.5 V peak-to-peak. The ATR was then played back through the analog-to-digital converter. The 6-bit digital words representing the peak of each cycle of the playback sinewave were formatted and recorded on IBM compatible tape, using a special data formatter which was constructed for that purpose. The data was then computer-processed, and the error calculated, according to the following equation:

$$\text{Error} = \frac{1}{\left(\frac{N}{7}\right)} \sum_{j=0}^{\left(\frac{N}{7}-1\right)} \left[\frac{1}{7} \sum_{i=7j+1}^{7j+8} n_i^2\right]^{1/2}$$

where n_i is the variation from the level predicted by a linear best fit to the points $7j + 1$ to $7j + 8$. $N/7$ is a large number of non-overlapping sets of 7 adjacent samples being considered.

This definition was developed, based on the fact that every seventh picture element would be recorded on the digital recorder, and thus, known accurately.

Therefore, every seventh sample on the analog recorder would be accurately known, and the error introduced by the analog recorder would be of concern only over groups of seven samples.

Assuming that a large part of this error was caused by noise pickup within the data storage subsystem, an extensive test program was begun to try to locate and eliminate the noise sources. It was found that shielding of the power supply from the ATR, which is physically located adjacent to the power supply, and connecting the signal ground to chassis ground made the most improvement. The flight systems were modified in that a magnetic shield fabricated from Conetic material was bonded to the end of the ATR chassis, so as to shield the transport from the power supply; also, inasmuch as in the spacecraft configuration the circuit ground is ultimately tied to the chassis ground, it was felt that the error performance would improve in the spacecraft configuration.

These two actions essentially eliminated periodic components of the analog recorder playback signal degradation, leaving the random components, due to head-to-tape contact variations and tape surface variations. Prior to the last systems test at JPL, new tape was installed on each tape transport, and the heads were resurfaced. With this final configuration, the average value of the error as calculated for all three flight systems was 1.03.

7. Failure of bias supply at high temperatures. During type approval testing of the PTM data storage subsystem, it was found that at + 70°C, a high-speed flip/flop in the bias supply circuitry would not reliably trigger on the input clock pulse. This problem necessitated a change in the value of one of the capacitors within the flip/flop module.

8. Controller sensitivity. The controller, which controls the various modes in which the data storage subsystem can operate, on occasion, has changed states coincident with large power transients on the spacecraft power distribution system. These state changes have been coincident with such spacecraft events as changeover from the main to standby power and gyro power switching. These problems have been infrequent, and since these spacecraft events would not occur during data storage subsystem operation, no effort was made to make the operation insensitive to these large power input transients.

9. Connector soldering. Considerable difficulty was encountered in soldering connectors to the specified requirements. The problem was that soldered connector cups contained pinholes, porosity, cracks, and granular solder to the extent that connectors were continually reworked or scrapped. The subsequent investigation resulted in the modification of procedures to be used in soldering wires into the connector cups. Satisfactory connections were made with the new procedure.

10. Subchassis printed circuit board blistering. The planar printed circuit interconnection boards, as described in the packaging section of this report, employed terminal pins which were swaged into the printed circuit board. During manufacture, delamination of the circuit board occurred in many instances around the terminals. The problem was due essentially to excess heat applied to the terminal during the pre-tinning of the terminals. The problem was solved by a change in the fabrication procedures.

11. Corrosion of magnesium subchassis. During flight hardware fabrication, three subchassis required rework, due to evidence of corrosion of the magnesium subchassis. The corrosion was first observed after the degreasing process which consists of immersing the subchassis in a solution of a mixture of 70% alcohol and 30% Freon. All subchassis prior to this time were degreased, using a solution which has a lower content of alcohol. The new solution, although allowing a more thorough cleaning, apparently caused the corrosion. A procedure was developed which inhibited the corrosion and protected the existing corrosion from further chemical action.

D. Test History and Performance

1. Environmental testing. Type approval testing was performed on the PTM data storage subsystem according to project requirements, except that the high temperature limit was reduced from 75°C to 70°C, and the random vibration levels were reduced because of the problem discussed elsewhere in this volume. Flight acceptance testing was performed on the three flight subsystems, according to project requirements, except that the random vibration levels were also reduced. All subsystems successfully passed the TA and FA tests.

2. Performance testing

a. Signal dropouts. Several tests were performed on each data storage subsystem to measure its performance, and to determine various characteristics. For the ATR,

Table 22. Analog tape recorder performance

Track	*Mariner VI* data storage subsystem (serial No. 2)				*Mariner VII* data storage subsystem (serial No. 4)			
	1	2	3	4	1	2	3	4
Signal dropouts	62	3	6	38	182	0	0	123
Analog error, DN	1.0188	1.0564	1.1038	1.0195	1.0384	1.0009	1.0069	1.0374

the most useful test was the measurement of signal dropouts, since it was found that the signal dropout performance was indicative of the other performance parameters. The test consisted of first recording a constant level sinewave signal on all four tracks of the ATR. The signal was played back and examined in two ways. First, the analog reproduced signal was routed from the main playback amplifier through a counting circuit, which counted all signal cycles below an adjustable threshold, usually set at 50% of the average playback amplitude. This dropout count was used to measure the effectiveness of the tape-to-head interface with the objective of achieving the lowest possible count. Dropout counts were finally obtained as shown in Table 22, as compared to 2,000 to 3,000 dropouts per track before the tape replacement and head resurfacing.

The digitized output from the ATR was also recorded on magnetic tape on IBM 7-track format. The image processing laboratory of the space sciences division computer-processed this data, and produced printouts which plotted dropout depth versus width. This data was interesting and useful in learning the characteristics of the dropout distribution. This data was analyzed and reported briefly in Ref. 8. Further analysis is being performed on this data and will be reported on in a future JPL report.

b. ATR error measurement. The IBM formatted data, which was obtained from the playback of the constant amplitude recordings was used to calculate the error values, as shown in Table 22.

c. Static transfer function and lincarity. Recordings were made on the ATR of several different sinewave signal amplitudes. The signals were played back through the analog-to-digital converter, and the output digital data was recorded on the IBM formatted tape. The data was computer-processed to produce histograms of the output from the analog tape recorder analog-to-digital converter for each input signal amplitude. This data yielded the DC transfer function and linearity characteristics of the subsystem. A typical output histogram for a recorded input amplitude of 3.5 V, peak-to-peak, is shown in Fig. 52. It is observed that the analog recorder reproduces a constant level recorded signal with a considerable degree of inaccuracy. This output noise is due primarily to the dynamic head-to-tape spacing variations during playback. These spacing variations are due to tape surface roughness, debris on the tape and heads from loose oxide and tape lubricant, and tension variations in the tape and pressure belt.

d. Dynamic transfer function. The dynamic or modulation transfer function of the ATR was measured for each subsystem. A carrier signal amplitude modulated with various modulation frequencies was recorded on the

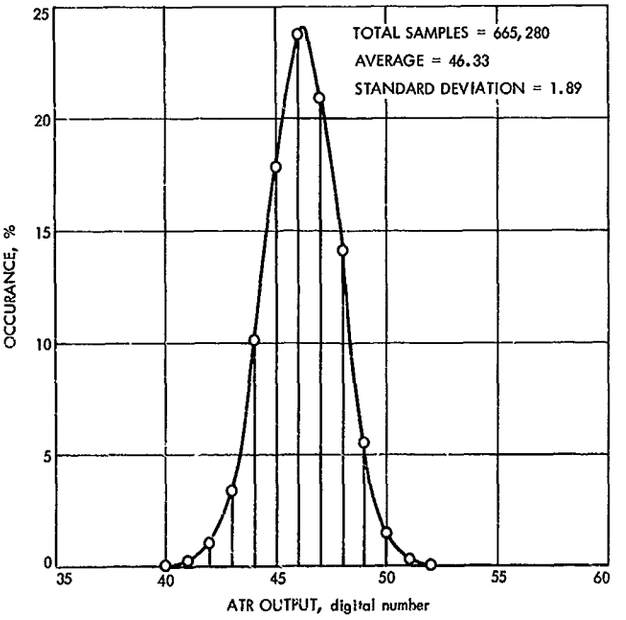


Fig. 52. Analog tape recorder output histogram for 3.5 V peak-to-peak input

ATR. These signals were played back and formatted on computer tape as for the previously described tests. The data was processed to yield histograms and rms power spectrums of the output signal to determine the dynamic response of the subsystem.

e. Bit error performance. The bit error rate was measured on each digital tape recorder. This was done by recording a digital sequence on the DTR, and playing it back, comparing the reproduced sequence with the recorded sequence, and counting each bit which was in error. Provisions were implemented to uniquely locate the position on the tape where errors were made. The bit error rate for each DTR was less than the required one bit error in 10^5 bits.

E. Procurement History

The phase I contract covered design studies, detailed design of the data storage subsystem and associated operational support equipment, fabrication of breadboards the prototype subsystem, and one set of OSE, procurement of parts for the subsequent fabrication of the flight units, and operations support at JPL. The contract was executed on September 23, 1966 with essential completion in February 1968.

The follow-on phase II contract was executed on October 25, 1967 with completion in November 1969. This contract covered the fabrication of one proof test model and three flight model data storage subsystems, three sets of operational support equipment and operation support at JPL. A separate contract was let for the remainder of the support personnel requirements from December 1968 through August 1969.

The data storage subsystem contracts were let to Texas Instruments, Inc., Government Products Division, Dallas, Texas. Texas Instruments (TI) let subcontracts to Lockheed Electronics Co. (LEC), Industrial Technology Division, Plainfield, New Jersey for the tape transports.

F. Evaluation of Design

The endless-loop configuration for handling tape which was utilized in the *Mariner* Mars 1969 design, resulted in a compact, reliable tape transport capable of handling tape lengths of less than 370 ft. Although the subsystem performed well in prelaunch tests and passed all environmental tests, the design did exhibit several weaknesses in the analog portion which should be avoided in future designs. The major one which appeared in several ways, was the concept of using the analog record-reproduce process to store information carried in the amplitude of the recorded signal. Information stored in this manner is degraded by the dynamic behavior of the head-to-tape interface. Since the amplitude of the signal, as reproduced from magnetic tape, is directly dependent on the spacing between the tape surface and the head gap, both during the record and reproduce process, the reproduced signal is degraded by the effects of tape imperfections, debris on the tape caused mainly by loose oxide and tape lubricant, head wear, tape guidance variations, tape thickness variations, and tape tension variations. The use of the endless-loop tape transport for the analog recorder aggravated the problem because the lubricant required on the tape added to the debris problem in the tape-head interface. Also, the maintenance of adequate tape-to-head contact in the analog recorder required high contact pressure which caused rapid head wear.

The electronics design was very satisfactory, and caused no further problems after the installation of the phase-lock-loop, which locked an oscillator to the reproduced analog signal, thus providing accurately timed pulses for the sampling and digitizing of the reproduced analog signal.

Although the analog record technique allowed the storage of more data (at a high reproduced error, however) than could have been stored digitally on the same length of tape, this method should be avoided on all future missions because of the problems encountered on the 1969 program. Any information to be transmitted from the spacecraft should be converted into a digital format as early as possible in the information channel.

References

1. Tausworthe, R. C., *Theory and Practical Design of Phase-Locked Receivers,* Vol. I, Technical Report 32-819, p. 16. Jet Propulsion Laboratory, Pasadena, Calif., Feb. 15, 1966.
2. *Mariner-Mars 1969 Flight Command Subsystem and Operational Support Equipment,* Final Engineering Report, pp. 2–10, JPL Contract 951700. Motorola, Inc., Military Electronics Division, Aerospace Center, Scottsdale, Ariz., Sept. 1, 1967.
3. Ashlock, J. C., and Lurie, S. M., *On the Application of Extreme-Value Statistics to Command Oriented Problems,* Technical Report 32-1025. Jet Propulsion Laboratory, Pasadena, Calif., Oct. 15, 1966.
4. *Flight Projects,* Space Programs Summary 37-50, Vol. I, pp. 73–79. Jet Propulsion Laboratory, Pasadena, Calif., Mar. 31, 1968.
5. *Final Report of Design Studies for Mariner Mars 1969 Program,* Texas Instruments Document, U15-817242-15F, Mar. 23, 1967.
6. *Mariner '69 DSS Detail Design Review, DSS Subsystem Design,* Texas Instruments Document 43-817200-43, July 14, 1967.
7. *Flight Projects,* Space Programs Summary 37-57, Vol. I, pp. 22 and 23. Jet Propulsion Laboratory, Pasadena, Calif., May 31, 1969.
8. Van Keuren, W., *An Examination of Dropouts Occurring in the Magnetic Reproduction Process,* Audio-Engineering Society Preprint No. 656 (H-5), Audio-Engineering Society, New York, Apr. 28, 1969.

PRECEDING PAGE BLANK NOT FILMED

Guidance and Control

I. Central Computer and Sequencer

A. Introduction

The *Mariner* Mars 1969 central computer and sequencer (CC&S), an electronic subsystem of the *Mariner* Mars 1969 spacecraft, was a new design blending results from (1) *Voyager*[1] CC&S studies, (2) *Mariner*[2] Mars 1966 CC&S studies, and (3) advanced development efforts in the areas of component selection and circuit design. Electrical design, piecepart component procurement, and subsystem environmental tests were conducted by JPL. The efforts of packaging design, documentation, fabrication, and functional/temperature tests were subcontracted.

B. JPL Electrical Design

The CC&S was designed to provide timing and sequencing functions (Fig. 1); key features of the new design included:

(1) Organization into a special purpose, programmable computer providing much greater sequencing and input/output flexibility than achieved in previous designs.

(2) Inclusion of internal redundancy for controlling trajectory correction maneuvers in order to assure that no single failure mode within the subsystem would be mission catastrophic.

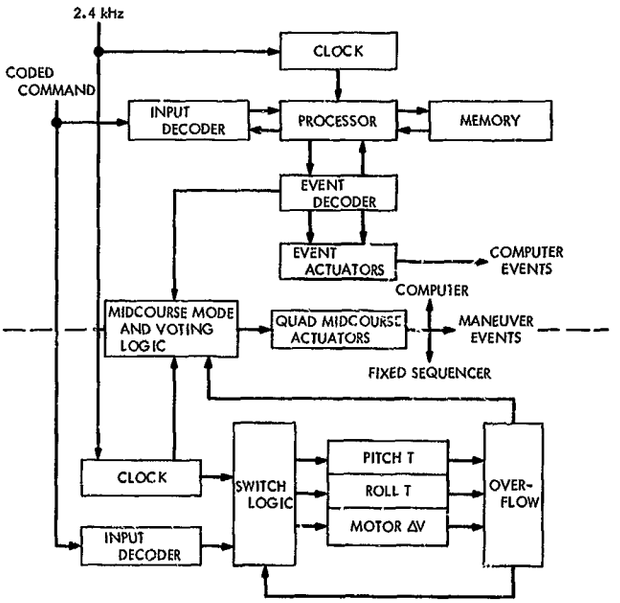


Fig. 1. Functional block diagram of computer and sequencer

[1]*Voyager* was an advanced project with a Mars-orbit-and-lander mission which was cancelled. The CC&S developments supporting this project occurred in 1964-1965.

[2]*Mariner* Mars 1966 was a Mars flyby proposal predicated on very modest changes to the then-current *Mariner* Mars 1964 design. It did not proceed beyond early design and development stages.

(3) A thorough program of component selection and application of worst case circuit design techniques.

The computer design was patterned after *Voyager* CC&S studies insofar as instruction repertoire and sequencing flexibility is concerned. This choice assured a design with more than adequate capability for a Mars flyby and with basic capability and expandability to support follow-on Mars orbiter and orbiter-lander programs. Memory capacity and input/output functions were purposely limited in the *Mariner* Mars 1969 program to conserve power, weight, volume, and cost. The design was such, however, that it was prepared for efficient, reliable expansion. It should be emphasized that the original design limits were set to assure some 30% excesses in both memory capacity and output functions. The flexibility offered by the computer and actuator decoding scheme, however, offered new tradeoffs to the later phases of mission design. As a result, the CC&S functions were rapidly expanded until the capacities of memory and actuators were saturated. It is felt this flexibility and its use in *Mariner* Mars 1969 completely justified the development of the computer oriented CC&S.

The CC&S output events, excepting maneuver events, could easily be mechanized with ground command backups to provide parallel path redundancy. Since ground command access cannot be guaranteed during maneuvers, it was necessary to provide internal backup in order to meet the constraint that no single failure mode would be mission catastrophic. A fixed sequencer tailored after the *Mariner* Mars 1966 CC&S design was introduced to provide an alternate maneuver control path. Furthermore, the availability of the redundant fixed sequencer and the inherent computer flexibility opened the door to establishment of the tandem maneuver mode which evolved into the prime mode utilized in both *Mariner VI* and *VII* spacecraft. In this mode, the computer checked both pitch and roll polarity and duration and the motor burn start time as issued by the fixed sequencer. If an error had occurred due to a permanent or transient failure or via a command load error, the maneuver would have automatically aborted prior to motor burn. The computer was also mechanized to provide a backup motor burn shutoff to prevent against a potentially catastrophic overburn of the motor. In addition to the tandem mode, the computer only or sequencer only modes would have been selectable by ground command in the event a permanent failure had occurred in either path.

In selecting piece part components for the new CC&S, the maximum amount of conservatism possible was applied, but some compromises obviously had to be made in order to meet reasonable power, weight, volume, and cost goals. The majority of component types were selected from those already fully qualified by JPL parts specialists. For those part types not fully qualified or, as yet, not in a qualification process, specifications and qualification efforts were generated. All parts used in flight hardware were fully screened both visually and electrically and subjected to thermal burn-in. All performance parameters were measured before and after test and the parts were serialized for data correlation.

Based on the solid foundation of initially good components with minimized probability of complete parameter failure, circuit design philosophy was directed to establishing the widest reasonable dynamic operating range to protect against transient or end-of-life degradation failures. Experience with the type of components and circuits in question lead to design of circuits which would operate through ±20% voltage variation from −20 to +75°C with parameter values deteriorated to 10,000-h end-of-life values. The major design accomplishment was in the area of magnetic logic, and a fully analytical design was established.

A breadboard of the electrical design was constructed by JPL. This breadboard was tested using special diagnostic programs exercising and monitoring all input/output functions and all internal operation modes. Verification of the electrical design performance within ±20% voltage margins and from −20 to +75°C was accomplished prior to release for subcontracting.

C. Functional Description

1. Computer. Approximately 80% of the total CC&S subsystem was organized into a computer which may be classified as a stored-program serial-operating special-purpose digital machine. The design, as implemented, was an outgrowth of *Voyager* studies tailored to state-of-the-art techniques available within schedule and resources to support the *Mariner* Mars 1969 mission. The computer, utilizing a prelaunch stored program which was inflight variable, could generate all required CC&S mission functions for *Mariner* Mars 1969. The computer, as shown in Fig. 2, consisted of the following basic elements presented in the order by which they will be defined:

(1) Input decoder.

(2) Clock.

(3) Processor.

(4) Memory.

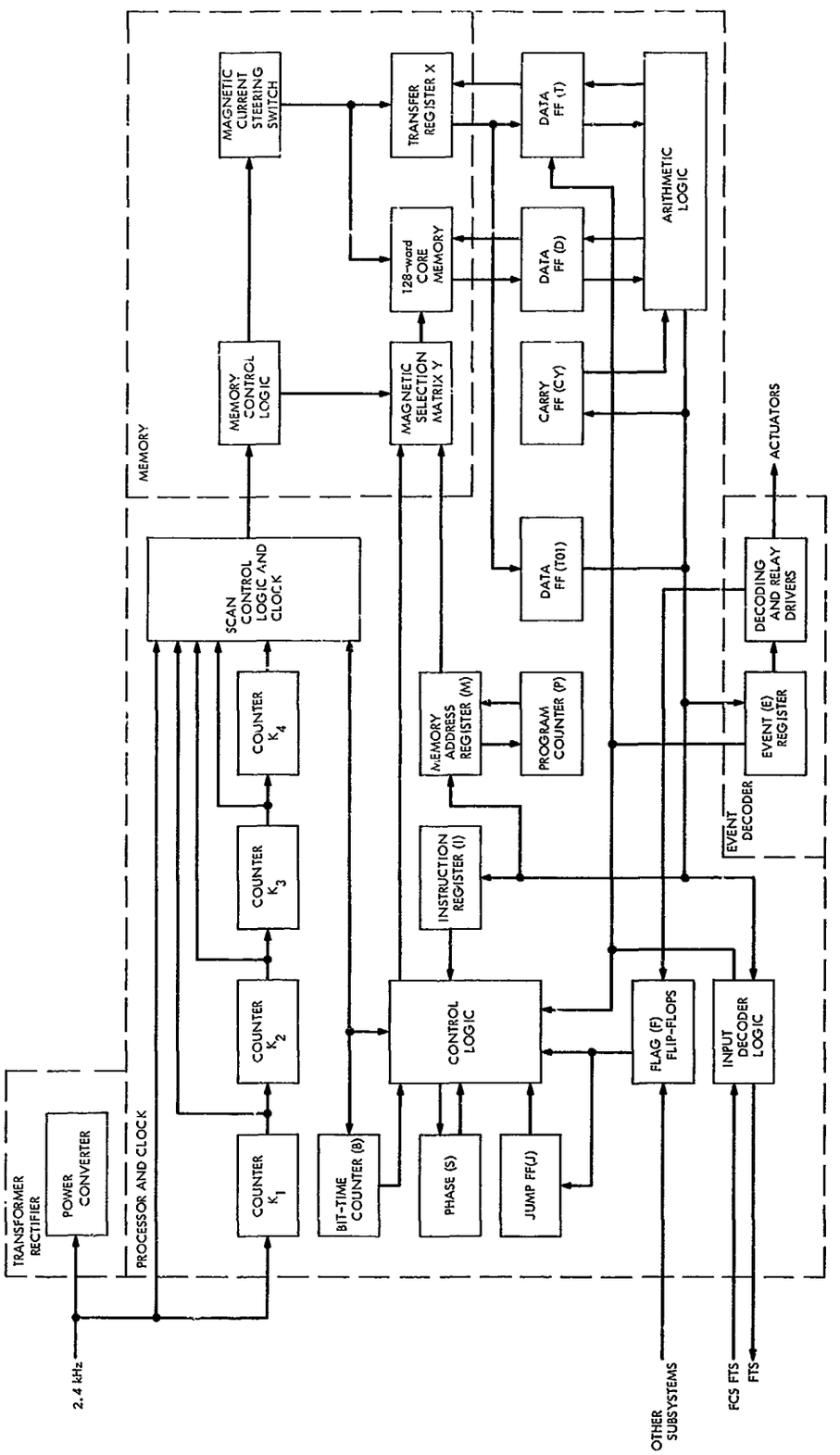


Fig. 2. Block diagram of computer

(5) Event decoder.

(6) Volatility protection.

(7) Power conversion.

a. Computer input decoder. The computer input decoder had the primary function of receiving inflight coded commands (CCs) from the flight command subsystem (FCS) and routing the contained data into the computer memory. Secondary functions included controlling inflight readout of the computer memory via the flight telemetry subsystem (FTS) and prelaunch memory loading and readout via the CC&S-operational support equipment (OSE) as well as direct decoding capability for CC commands. The reception and routing of CC words, for memory loading and readouts, was done in a real-time mode in that normal timekeeping routines were temporarily interrupted in the computer. Such command loading was thus restricted to intervals when the CC&S was in cruise mode (1-h operation cycles) unless time losses or subsequent reprogramming could be tolerated. This loading restriction saved considerable circuitry within the CC&S at essentially no penalty to the spacecraft, since all loading cycles would have normally occurred during intervals when the CC&S was in cruise mode. A timed interlock was provided in the input decoder to return the computer to real-time operation should the CC word be interrupted before completion.

b. Computer clock. The computer clock served as the source of reference signals required by the processor and the memory. It accepted a 2.4-kHz reference frequency and divided it down to provide the following: (1) signals required by the processor scan control, (2) the read/write digit pulse rate for the memory, (3) the time base for counting down the motor burn duration, and (4) a pulse every hour to the attitude control subsystem (ACS), referred to as the Canopus gate cyclic.

c. Computer processor. The processor contained facilities for addressing, fetching, and storing of binary information in the memory, sequencing of instructions stored in memory, arithmetic and time-dependent processing of memory information, and controlling the initiation of relay actuations. The data cycles executed by the processor were, of course, directly related to the information as fetched from the memory. The processor was initiated via the scan control logic (in the control logic block of Fig. 2) during each hour pulse or during each minute pulse if the minute toggle had been set, or during each second pulse if the second toggle had been set. The processor also started during external interrupts such as power turn on, the loading of memory word from the FCS, etc. Any external interrupts would set the second toggle. The scan control logic was essentially a hardwire executive in the processor.

The internal CC&S instruction word format consisted of 22 bits divided into 4 bits of operation code and 2 address codes of 9 bits each called A and B.

The internal CC&S time/event address word format consisted of 22 bits, 13 bits of time magnitude, and 9 bits of event address.

The internal CC&S data format was 22 bits.

d. Computer memory. The memory provided ferrite core storage and associated input/output circuitry for the computer program. Storage capacity was 128 words of 22 bits each. Words could be randomly addressed, but bits had to be sequentially read from each word. Readout of each bit was destructive and required restoration of the stored state with each bit readout cycle. A special one-word storage register (referred to as the X or transfer register) was included and addressed and read in parallel with each and every one of the 128 main memory words.

e. Computer event decoder. The event decoder converted event address information furnished by the processor into relay actuations. A partial decoding matrix capable of decoding 72 discrete states from a 9-bit address had been mechanized so that from one to three of these discrete states in certain restricted combinations could be simultaneously selected.

f. Computer volatility protection. To help assure the ability of the computer to function from launch to the end of mission without reliance on ground command and to minimize the possibility of computer interference due to abnormal performance during mission critical functions, it was mandatory to protect program storage to the maximum extent practicable. The following factors were used in the development of the CC&S: minimizing, by program, the intervals during which the CC&S was volatile to excessive power transients (greater than 20%) or power dropout, and to sense such transients so that, should they occur when program was volatile, operation would be automatically stopped until the program could be analyzed and corrected by ground command as necessary. Studies of typical mission profiles and CC&S related programs indicated the program was volatile about 0.003% of the mission time. This, of course, occurred when the processor was scanning the memory storage and was exe-

cuting instruction cycles dependent on data contained in semi-conductor circuitry. It was a near certainty that excessive transients or power dropout during scan would have destroyed large quantities of program data which would have forced the computer into an uncontrolled performance mode. A power monitor (tolerance detector) was provided in the CC&S design which detected all transients in excess of 2-μs duration and -20% amplitude variance from normal input power.

g. Computer power converter. The computer power converter consisted of transformers, rectifiers, surge suppression chokes and switching circuitry, and pulse power storage capacitors. All dc power was converted from 2.4-kHz spacecraft power without secondary regulation. Turn-on surge protection within 150% overload was accomplished by chokes in the +4 Vdc and −4 Vdc supplies. Relay resistance stepdown was provided in the +80 Vdc and +28 Vdc supplies. Pulsed power storage was provided to handle peak loads of relay switching without reflection into the primary winding.

2. *Fixed sequencer mechanization.* The fixed sequencer, as shown in Fig. 3, provided redundant maneuver capability within the CC&S. The computer and sequencer were electrically independent except at their output interface where voting on the output function was performed with quad redundancy. Thus, maneuver operations were protected from single component failures. Prior to the start of a fixed sequencer maneuver, the duration values for spacecraft pitch, roll, and motor burn had to be received via ground command. Subsequent receipt of the DC27/DC29 command immediately started the maneuver by removing the maneuver clamp which activated the counter. Then, 4096 s after receipt of DC27/DC29, the counter overflowed and started the pitch turn for the duration stored. After completion of pitch, a fixed interval of 512 s was counted which, at its conclusion, started roll for the stored duration. After completion of roll, another 512 s was counted before starting motor burn for the stored duration. Following 512 s after motor burn completion, a reacquire signal was issued returning the attitude control subsystem to the cruise mode. Pitch and roll

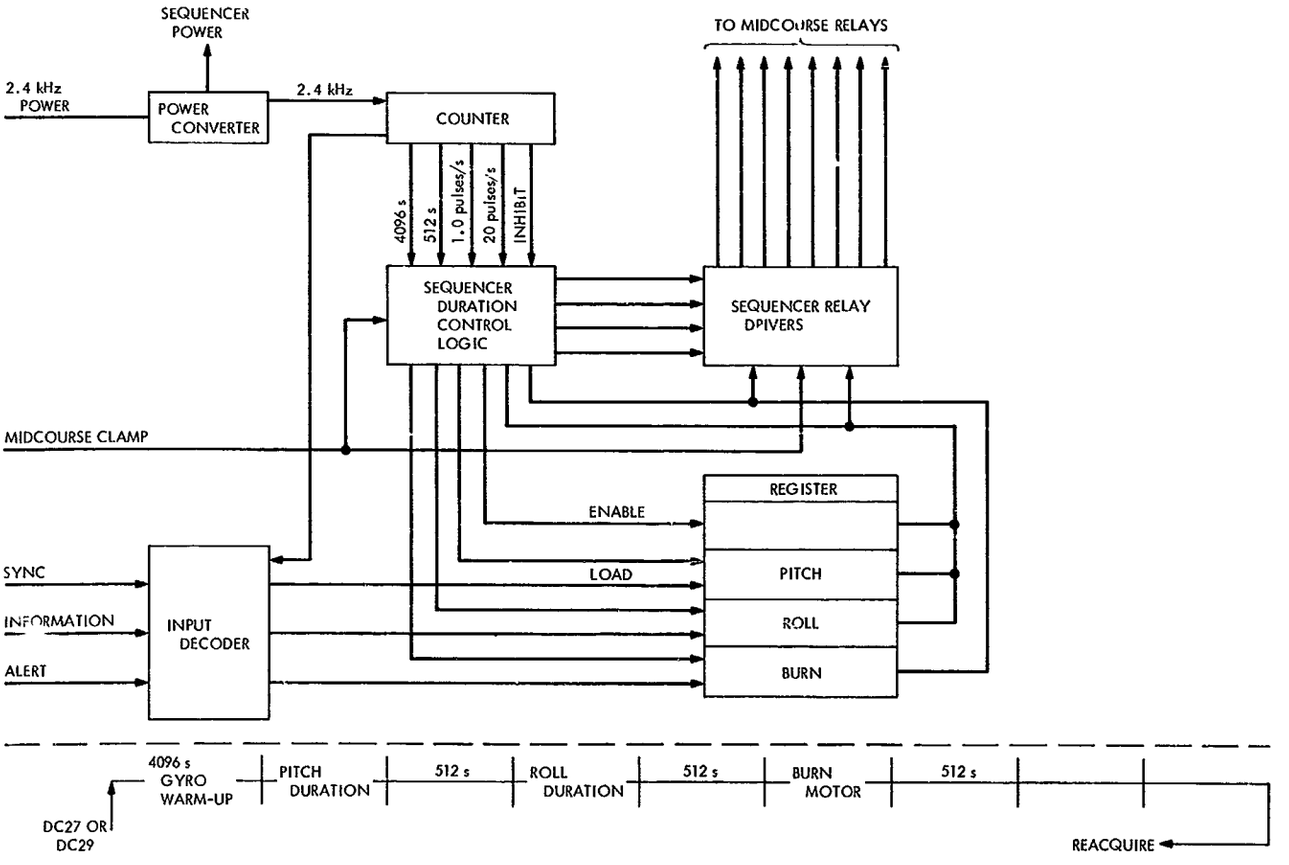


Fig. 3. Block diagram of fixed sequencer

durations were counted down at a 1-pulse/s rate and had values of from 1 to 2047 s. The motor burn duration was counted down at a 20-pulses/s rate and had values from 1 to 2047 counts. An abort of the maneuver via DC-13 immediately reset the fixed sequencer and allowed a second fixed sequencer maneuver to be executed following establishment of the proper roll, pitch, roll, and motor burn durations. The fixed sequencer consisted of the following functional units:

(1) Input decoder.

(2) Counter.

(3) Duration control logic.

(4) Storage registers.

(5) Relay drivers.

(6) Power conversion.

a. Sequencer input decoder. The input decoder provided the following functions: selected sequencer load words from CC command words, transferred appropriate sections of the word to the proper magnetic shift register for storage, checked the load word for proper parity, and stored pitch and roll polarity until needed in executing the maneuver.

b. Sequencer counter. It was the function of the sequencer counter to provide those timing signals necessary to perform a fixed sequence midcourse maneuver. To this end the counter accepted a 2.4-kHz input reference frequency and divided it down to provide signals to operate the turn registers (motor burn duration was provided by counting accelerometer pulses), provided a fixed delay between maneuver events, and provided the initial delay period required for gyro warmup.

c. Sequencer duration control logic. The heart of the duration control logic was a magnetic core stepping switch which controlled the counter gating noted in the previous section, controlled turn-on of pitch, roll, and motor burn registers in the count mode, and controlled initiation of fixed time event relay drivers to activate maneuver events.

d. Sequencer storage registers. The sequencer storage registers used to store and execute maneuver turn and motor burn durations were magnetic core shift registers of 11 bits each. Each register was provided with exclusive OR logic feedback from the ninth and eleventh stages to give counts ranging from 1 to 2047 for duration timing. It must be noted that the count cycle was not binary and was best determined by referring to tables listing each sequential discrete state.

e. Sequencer relay drivers. Included in the fixed sequencer were relay drivers and a sink driver that provided pulsed continuity. These drivers were independent of the computer in order to guarantee that a single component failure in the relay drivers would not affect the ability of the computer to actuate maneuver event relays.

f. Sequencer power conversion. Power conversion for the sequencer was relatively simple in comparison to that required by the computer since only two voltages, +4 Vdc and +28 Vdc, were needed. These dc voltages were turn-on surge limited, had no regulation, and were dc isolated from the spacecraft 2.4-kHz input power by their transformer-full-wave rectifier generation system.

D. Subcontracting

Motorola's Government Electronics Division was selected to develop the packaging design, to fabricate, and to conduct functional/temperature tests of CC&S subsystems. Magnetic logic elements, which required highly specialized techniques, were contracted directly by JPL to the Data Science Corporation and to Electronic Memories Inc. The latter items were furnished along with all piece part electronic components to Motorola as government-furnished equipment.

E. Fabrication and Functional/Temperature Tests

The initial fabrication and functional/temperature testing effort included fabrication and test of the 119 welded cordword (CW) and 34 welded integrated circuit (IC) modules per CC&S subsystem. A total of 106 of the CW and 32 of the IC modules were fabricated by Motorola. Two IC modules in the JPL "IC stick" package were manufactured by Wems, Inc. A total of 12 modules containing magnetic logic was manufactured by the Data Science Corporation while the memory plane module was fabricated by Electronics Memories, Inc. Testing at the module level was limited to room temperature functional tests at Motorola. Modules built by the other vendors were tested to ±20% voltage margins from −20 to +75°C before delivery to Motorola.

After completion of module build and test, modules were next assembled onto printed circuit boards. Each circuit board assembly was tested to ±20% voltage margins from −20 to+75°C. The memory subassembly was tested as a completed unit to these margins both before and after conformal coating.

After circuit board assembly, the subsystem was placed into a special test fixture which did not require conformal coating or assembly of boards into the subassembly frames. After passing ±20% voltage margins from −20 to +75°C, conformal coating and final assembly into the flight subassembly frames took place. The voltage/temperature margin tests were then repeated; after passing these tests the subsystem was delivered to JPL.

The JPL problem/failure report (PFR) system was initiated with the turn-on of power at the module level. A total of 115 PFRs were written during the functional test cycle, of which over 90% were related to PTM activities. A breakdown of these PFRs is as follows:

Problem	No. of problems
Number of manufacturing problems, such as poor welds, solder joints, components backwards, etc.	18
Total materials problems, such as gold flaking, discoloration, etc.	23
Incidences of errors in manufacturing documents, such as circuit board layout errors, parts kitting errors, etc.	11
Number of errors in test sets or procedures	24
Total design errors	23
Number of faulty piecepart components	16
Total number of PFR's	115

Manufacturing-related problems uncovered in electrical test, a total of 52, were felt to be very low considering that some 480 modules, 80 circuit board assemblies, and 4 subsystems were tested. Test-set-associated errors were attributed to the fact that the test sets and procedures were in very rough form during the prototype cycle and were not thoroughly debugged until the PTM cycle. Design problems were all directed toward areas which were modified between the prototype and PTM cycles. The most serious design problem, associated with 11 of the PFRs, was related to the use of 2N2891 transistors. These devices were procured under the flight buy were not the "same" as the identically numbered devices used on the prototype. A close examination of the device parameters showed that the manufacturer had altered the device internally so that switching times had greatly increased and high-voltage breakdown had decreased.

The increased switching speeds led to severe switching transients in the fixed sequencer while the lowered breakdown voltage caused failure of current-driver transistors in the memory. The fixed-sequencer circuitry was partially redesigned and the circuit board layout altered to accommodate the 2N2891 problem. A new transistor with higher breakdown voltage was required to solve the memory problem and, fortunately, screened SDT5505 units were available from parts engineering. These problems accounted for at least a one-month delay in PTM delivery, as well as requiring considerable rework of the PTM hardware.

Of the 16 piece part component failures, those related to ICs presented a major problem to which no completely satisfactory solution was obtainable. The total IC failures in the initial test cycles at Motorola were 10, which were broken down as follows: 7 failures due to corroded bonds caused by the presence of a chlorine contaminant, 1 failure due to excessive Au-Al-Si compound (purple plague), and 2 failures due to metalization-shorts. Motorola's fabrication cycle was carefully studied as a potential source for contaminants leading to the corroded bonds. None of the operations conducted at Motorola could be related to the contaminant source. It was determined much later that the contaminant was a residual lubricant on the lead wire used internal to the IC. It was not known whether or not the high incidence of corroded-bond failures would continue, and it was hoped the problem would be characterized by all contaminated bonds failing early in the test cycle. Since this could not be relied upon, however, spare ICs were purchased, and a spare set of IC modules were manufactured and life-tested for emergency use. The ICs used in this rebuild were purchased to the specification used by the Data Automation Subsystem which had yielded a superior part as compared to the standard JPL specification used for CC&S procurements. It must be emphasized that at the time of this rebuy the source of the contaminant had not been found.

F. Subsystem Environmental and Life Testing

Subsystem environmental tests in accordance with project requirements were conducted by JPL. The PTM CC&S had TA level vibration and temperature/vacuum tests conducted prior to spacecraft assembly facility (SAF) delivery. The TA level static acceleration tests were conducted on the PTM after release from SAF at the end of the PTM spacecraft test cycle. Flight CC&S subsystems received FA level vibration and temperature/vacuum testing. Voltage/temperature margin tests were conducted before and after each environmental test cycle to assure no performance degradation resulted.

Due to the IC failures, a life-test cycle of about 500 h was established for each flight CC&S. This test was conducted at 75°C to help force out any potential bond failures. This life-test cycle preceded the environmental tests so that any partially corroded bonds could be broken loose as a result of being subjected to the FA vibration test.

Table 1. Summary of PFR's

Date	PFR No.	Subsystem serial no.	Failure
Jan. 1, 1968	201903	PTM/A100	Memory sense amplifier marginal at −20°C due to impedance mismatch
Feb. 20, 1968	106830	PTM/A100	IC failure (300 h) prior to TA due to contaminants and purple plague
Mar. 8, 1968	201206	PTM/A100	IC failure (575 h) during thermal-vacuum due to purple plaque
May 24, 1968	106816	FLT/A101	IC failure (500 h) at end of life test due to purple plague
May 28, 1968	204847	FLT/A101	IC failure (520 h) at end of life test due to purple plague
May 31, 1968	201243	FLT/A101	Suspected environmental facility noise causing false set indication on spare actuator
Jun. 15, 1968	201247	FLT/A102	Faulty performance of a nonflight function observed after 368 h operation. Suspect cause is a faulty connection
Jun. 25, 1968	201261	FLT/A102	Vibration overtest
Jun. 25, 1968	201271	FLT/A102	Vibration overtest
Jul. 8, 1968	201606	FLT/A103	IC failure (80 h) during life test due to purple plague
Jul. 15, 1968	201607	FLT/A103	IC failure (350 h) during life test due to purple plague
Jul. 25, 1968	201283	FLT/A103	IC failure (454 h) during therm.-vac. due to purple plague
Aug. 5, 1968	201608	FLT/A102	IC failure (633 h) after FA due to purple plague
Sep. 5, 1968	201609	FLT/A102	While repairing IC noted in 201608, problem in backup circuit found with suspected cause a faulty connection
Sep. 5, 1968	201611	FLT/A102	Wrong value resistors found to be installed making special test interface inoperable

During the life-test environmental test cycle, 15 problems leading to PFRs occurred. The associated PFRs are summarized in Table 1. Testing to the time of SAF delivery indicated that the chlorine contaminant problem was primarily an early-life failure mode and unlikely to continue. As noted from Table 1, however, 8 failures occurred attributable to excessive Au-Al-Si intermetallics (purple plague). The plague failures at this time were of major concern with the only hope being centered on the possibility that the life-testing had forced out all failure-prone bonds.

Table 2 lists pertinent information on the PTM and flight subsystem at the time of SAF delivery.

G. Prelaunch Performance on the Spacecraft

The period from delivery to SAF to the launch of *Mariner VI* on Feb. 24, 1969 and *Mariner VII* on Mar. 28, 1969 covered some 5200 h of operation on the four CC&S subsystems. This time period involved about 1600 h of PTM operation and 1200 h of operation on each of the three flight subsystems. During this period, no integrated circuit failures occurred. This indicated the previous failures might have fallen into a class of early life failures and that a reasonable probability of mission survival existed.

No attempt was made to summarize the number of sequences, actuators or other functions which the CC&S controlled during this period. Attention was focused, instead, on problem areas of the 35 PFRs since they served as a beneficial input to follow-on programs using the *Mariner* Mars 1969 CC&S design.

Table 2. Flight subsystem and PTM data

Subsystem	Date to SAF	Operating time, h	Power, W[a,b]	Weight, lb[c]
PTM A100	Mar. 15, 1968	515	18.0	19.9
FLT A101	Jun. 6, 1968	620	18.3	20.2
FLT A102	Jun. 26, 1968	500	18.1	20.2
FLT A103	Aug. 7, 1968	627	18.2	20.3

[a] 2.4 kHZ, 50 V rms power.

[b] 12 W additional power used until spacecraft-*Centaur* separation to hold actuators reset.

[c] Typical total weight of the four subassemblies, in lb, is as follows:
Power supply (2005A1); 4.89
Timing control (2005A2); 6.37
Event control (2005A3); 6.55
Memory (2005A4); 2.48

The nine design problems and their related PFRs are listed in Table 3. As noted, 6 of the PFRs required engineering change requests (ECR's) and associated hardware changes while 2 were overcome by program and procedure.

The nine problems related to unexpected performance modes are listed in Table 4. As noted from this table, the PFR's relate to conditions that existed in the design and whose documentation had been a valuable reminder to SPAC operations.

Five PFRs were related to the noise sensitivity of the CC&S-OSE sync buffer. This problem was eventually traced to ground noise generated between OSE complex and spacecraft and inserted through the sync buffer into the CC&S load/verify logic. A capacitor filter was installed which solved the problem.

Five PFRs, related to procedural problems were caused as follows: (1) by CC loading a memory word under active program control, (2) by wrong value ranges of dc voltages in SAF measurement procedure, (3) by initiating a DC-2 dump after programming for a computer-only maneuver and then failing to reload memory word 19 as required, (4) by failure to issue DC-33 after power chain switchover, and (5) by failure to send DC-33 after power chain switchover.

The seven PFRs related to non-recurrent, unresolved anomalies are listed in Table 5. The short motor burn PFR was of major concern, but would not have been catastrophic in flight; the first four PFRs were not of major

Table 3. Spacecraft test CC&S design problems

PFR	Date	Problem description
202470	Mar. 20, 1968	Attitude control (ACS) power input low side had 5-Ω short to CC&S signal ground due to printed circuit board layout error; corrected by ECR 12081
202492	Mar. 28, 1968	
202495	Mar. 28, 1968	
202477	Mar. 21, 1968	Logic error causing tandem maneuver to abort if computer issued an actuator with address codes including B1, B2, C1, C2, C3, $\overline{D1}$ during the maneuver (programming constraint avoided reoccurrence)
202498	Apr. 1, 1968	Logic noise during ACS power chain switchover falsely set CC-5 relay on first switchover which subsequently caused DC-30 inhibit on second switchover; correction was procedural requiring DC-33 between switchovers.
202695	Jul. 2, 1968	A time race condition existed in the tandem abort logic which had a 0.02% chance of an abort within 1 ms after motor burn start; logic corrected per ECR 12168
203736	Aug. 12, 1968	Protective clamp on memory read/write logic prematurely released on power chain switchovers causing bits to be dropped; corrected by ECR 12682
203767	Sep. 3, 1968	
202988	Nov. 14, 1968	Fuse subassembly designed with poor physical tolerances; redesigned per ECR 12820

Table 4. Unexpected performance modes

PFR	Date	Problem description
202478	Mar. 21, 1968	No event counter No. 4 event at M1; this was not included in the design since other telemetry channels verify the event
202607	May 6, 1968	No event counter No. 4 event at $\overline{M1}$, $\overline{M2}$ (reacquire); this may or may not occur due to timing but was not corrected since other telemetry channels verify the event
202636	May 19, 1968	Tandem abort if power chain switchover occurs after CC loading. Turn polarity is lost during switchover and causes abort. This was not prevented in the design since it was felt unsafe to do maneuver without parameter reload if such a situation occurred
202671	Jun. 20, 1968	If power chain switchover occurs in launch countdown, operate verify function is set. This is abnormal procedure and not provided for in design
202886	Aug. 13, 1968	Two-V drop in CC data line during the 100-ms CC sync pulse interval; this was due to drop across dc voltage filter and did not affect the interface
202980	Oct. 15, 1968	If a CC-2 with format equivalent to a CC-5 is sent, 4 min or more after a CC-1, the CC-2 will behave as a CC-5; this is per design and must be avoided procedurally
203907	Jan. 13, 1969	False DC-9 flag with breakout box in ring harness; interface not designed for this type of interference
203871	Jan. 22, 1969	Due to asynchronous clocks, there is a small probability of tandem abort if 1-s pitch or roll turns are attempted; avoided by turn adjustment or alternate sequence selection
204113	Mar. 7, 1969	Memory bit 7, address 0 lost due to power chain switchover between a CC-1 and CC-2; normal since CC&S is in scan mode at this time, and would go into DC-30 mode in flight

Table 5. Non-recurrent unresolved problems

PFR	Date	Problem description
202624	May 19, 1968	Logic inhibit controlled by power monitor didn't reset after power off/on cycle. Never repeated but suspected cause was abnormal off/on voltage waveforms. DC-30 would clear this problem in flight
202647	Jun. 5, 1968	Computer input decoder apparently turned on in interlock mode. Procedure wrong to establish how and problem never repeated. Automatic 5-min reset or CC1/2 load would cure such a problem in flight
202841	Jun. 12, 1968	Interlock between CC&S and CC&S OSE occurred such that OSE could not manually initiate actuators; problem never repeated but appears unrelated to flight interface
203761	Aug. 29, 1968	Problem very similar to PFR 202980 in Table 4, but some discrepancies in observed data didn't allow resolution; most probably a data observation problem
203906	Jan. 9, 1969	CC&S A101 issued early motor shutoff in fixed sequencer mode at AFETR. Loaded burn time appeared normal but test complex was being subjected to numerous noise transients by science calibration device. Extensive CC&S analysis and test could not establish cause. A101 CC&S on *Mariner VII* performed maneuver perfectly
203952 203956	Mar. 20, 1969 Mar. 19, 1969	Several CC&S words failed to load and verify on launch pad. New symptoms plus failure of problems to repeat led to removal of A102 from *Mariner VII*

concern. The last two PFRs in Table 5 provided the most significant results in that they caused removal of a CC&S from the spacecraft on the launch pad. Extensive testing subsequent to removal convinced CC&S personnel that the A102 subsystem was normal and that somehow the interface was disturbed by on-going launch vehicle/blockhouse operations. Efforts are under way on *Mariner* Mars 1971 to reduce the criticality of this interface significantly reducing its impact on spacecraft operations.

As a result of prelaunch testing on the spacecraft, CC&S personnel were confident that no problems existed in the new design which would jeopardize flight performance. Problems that remained uncorrected were strictly ground interface oriented with the exception of the integrated circuit problems discussed earlier. The 5200 h of failure-free spacecraft testing, however, provided hope that the subsystems would survive the mission interval.

H. Software Design

The *Mariner* Mars 1969 program represents the first time software design had been a major CC&S effort. The establishment of software design ground rules was exceedingly difficult due to problems; e.g., inexperience with performance of the new design, inadequate memory capacity, lack of visibility into modes of interaction with the spacecraft and spacecraft operational tests, lack of early definition of encounter sequences, and lack of knowledge associated with how to interface with spacecraft performance and analysis and command (SPAC) operations in flight.

A significant weakness caused by the length of time for program design was that flight-structured programs were not available until the terminal phases of spacecraft testing. It would have been more desirable to structure all spacecraft testing around the final mission sequences. There was, however, an alternate program verification technique established by software simulation of the CC&S. All launch programs were exercised through the simulation and resultant mission sequences carefully reviewed and approved. These launch programs in the form of punched paper tape were certified against a required approval cycle by quality assurance (QA), sealed, and then placed in bonded stores until removed for insertion into the CC&S on launch day.

It was recognized that the program placed in the CC&S at launch would require updating and very possibly major reprogramming in flight to support anomalies or changes in mission objectives. The software package was designed as the hub around which SPAC would center all program change activity. As planned, all updates to existing sequences required software simulation and any new programmed sequences required both software verification and verification on the PTM or flight spare spacecraft. After initiation of program changes, the contents of the CC&S memory were read out through telemetry and compared with a memory map as the final approval of the change cycle.

II. Attitude Control Subsystem

A. Purpose and General Description

The function of the attitude control subsystem was to orient the spacecraft to a preselected set of celestial references, after separation from the injection vehicle, and to maintain that orientation throughout the cruise and planetary encounter phases of the mission.

The attitude control subsystem also was required to be able to reposition the spacecraft to any given orientation in space for purposes of the midcourse maneuver. This temporary spacecraft attitude was maintained by the autopilot during the firing of the propulsion subsystem.

At the conclusion of the midcourse maneuver sequence, the attitude control subsystem automatically reoriented the spacecraft to its cruise references; the subsystem had the capability of automatic reacquisition of these references if attitude control was lost due to a noncatastrophic disturbance.

The attitude control subsystem was functionally composed of the attitude control electronics, the cruise and acquisition Sun sensors, the Sun gate, the Canopus tracker, the gyro control assembly, two reaction control assemblies, and the thrust vector control assembly.

The contractor for the attitude control (ACS) and scan control (SCAN) subsystems was Honeywell, Inc. The work was done under JPL Contract No. 951701 at JPL, the Honeywell facilities in Minneapolis and Boston, and ETR.

Five sets of ACS and SCAN subsystems were built and tested. These included production prototype, proof test model (PTM), and three flight sets of subsystems.

The assemblies built and tested at the Honeywell facilities in Minneapolis were the attitude control electronics, gyro control subassembly, Sun sensors, Sun gate, thrust vector control assembly, reaction control assemblies, scan actuators, and scan electronics.

The Honeywell Radiation Center facilities in Boston fabricated and tested the Canopus tracker, the far-encounter planet sensor and the narrow-angle Mars gate subassemblies.

The spacecraft was controlled about its pitch, yaw, and roll axes. The spacecraft roll axis was oriented along the spacecraft Sun line; attitude control pitch and yaw was referenced to the Sun. The spacecraft roll position was referenced to Canopus.

After the spacecraft has been injected onto its heliocentric trajectory, it established the three-axis cruise orientation. This process began when attitude control logic power was switched on by the pyro arming switch at separation. Angular position errors about the pitch and yaw axes were sensed by the Sun sensors. Rotation rates about all three axes were sensed by three single-degree-of-freedom gyroscopes. Both rate and position errors were used as inputs to switching amplifiers which switched power to solenoid valves when the sum of the inputs exceeded a certain deadband value.

Opening a solenoid valve permitted dry nitrogen at low pressure to flow through a small nozzle located at the end of a solar panel. Thus, torques were applied to the spacecraft so that the pitch and yaw rate and position errors were reduced to limit cycle valves. When the combined pitch and yaw error (cone angle) was reduced to about 5 deg, the Sun gate issued a Sun-acquired signal. The Canopus tracker was energized by CC&S event L2 and, if the Sun had been acquired in pitch and yaw, the Canopus search and acquisition phase would begin. The spacecraft roll rate was increased initially to the "search" level (nominally −3.5 mr/s) by the roll search signal from the Canopus tracker. Roll angular position error was sensed when a body with sufficient brightness to stimulate the acquisition logic entered the field-of-view of the Canopus tracker. The roll rate and position error were then reduced to limit cycle values and the three-axis cruise orientation was established. The gyros were then turned off and rate damping was provided by a derived rate signal, which was generated from the gas jet control signals and fed back to the switching amplifier input.

1. Attitude control electronics. The attitude control electronics package housed the logic and power switching functions, the switching amplifiers, the pitch, yaw, and roll attitude control channel electronics, the telemetry buffers for the subsystem, the autopilot electronics, and the power supplies for the subsystem. It utilized welded cordwood module construction with a multilayer matrix board performing the module and connector interconnect functions.

2. The Canopus tracker. The Canopus tracker was a new design for *Mariner* Mars 1969. Its objective was to demonstrate the automatic acquisition of Canopus only. It consisted of an image dissector tube, a Sun shutter, and associated electronics for signal processing and logic functions. Light input to the image dissector's photocathode was converted to an output roll error signal for spacecraft roll attitude control and an intensity signal.

3. Rate mode for gyros. Three single-degree-of-freedom gyros provided rate error signals to the pitch, yaw, and roll attitude control loops. During the launch the gyros were powered to maximize the probability of their surviving the launch environment. The gyro switch control had a 180-s delay in turning off, allowing part of the roll

rate to be damped to cruise values when the Canopus tracker acquired a star and switched off the signal to the gyros.

When used during acquisition, all gyros had an output to the switching amplifiers that was proportional to the sensed spacecraft angular rate. The gyros were turned off after Canopus has been acquired and were not used during cruise.

4. Switching amplifiers, derived rate, and the reaction control assembly. The switching amplifiers used the position and rate error signals during acquisition to control gas valve actuators. The switching amplifiers began operation when the attitude control logic power was switched on at separation. The input-output characteristics of the switching amplifier power switch is shown in Fig. 4.

The deadband was provided so that the gas jets would not be on continuously. The amplifiers had a minimum on-time characteristic (20 ms) which controlled the size of the nominal limit cycle. The gas valve actuators opened the valves to the gas jets which released N_2 gas. The reaction control assembly consisted of two independent gas supplies, regulators, and sets of jets, providing block redundancy for the attitude control functions.

Since the gyros were switched off after Canopus acquisition, their rate error signal was not available to the switching amplifiers during cruise mode. Rate control was provided by the derived rate feedback signal around the switching amplifier. The behavior in the phase plane is shown in Fig. 5.

The switching line without derived rate was vertical. When the switching amplifier power switch activated the gas jets, the derived rate compensation essentially integrated this signal and fed it back to the input. Due to the sign inversion in the switching amplifier, the feedback signal was opposite in polarity to the position error input. Therefore, the switching amplifier would turn off sooner with the feedback than it would without it; thus, damping was introduced into the control loops.

5. Maneuver functions. Injection guidance errors caused the actual trajectory of the spacecraft to differ from the nominal trajectory. In addition, the nominal trajectory was biased at launch to satisfy planetary quarantine constraints. Therefore, a midcourse maneuver was required to correct the trajectory. *Mariner* Mars 1969 spacecraft were capable of performing two midcourse maneuvers.

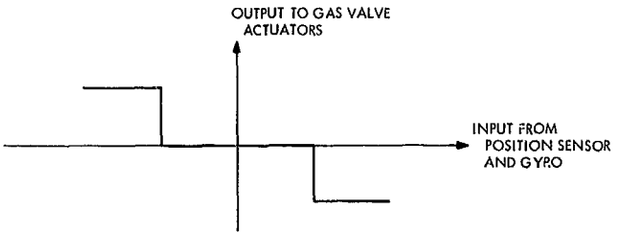


Fig. 4. Switching amplifier characteristics

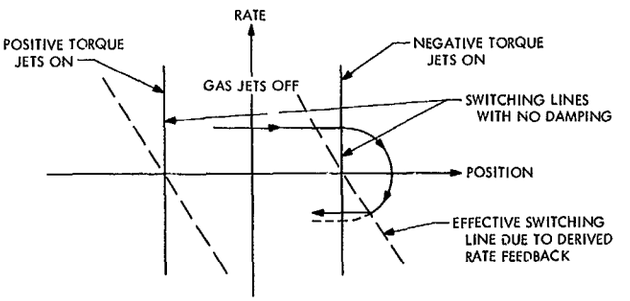


Fig. 5. Derived rate damping in the phase plane

The function of the attitude control subsystem during the midcourse maneuver mode was to orient the thrust vector of a body-fixed rocket motor to some predetermined direction in space. To do this, the spacecraft performed a pitch and roll turn in sequence as commanded by the CC&S. This orientation was maintained during motor burn by control of the thrust vector by the autopilot. After the maneuver, the spacecraft returned to the cruise orientation.

6. Gyros rate and position mode. For a tandem maneuver, the gyros warmed up for 4096 s after the midcourse sequence was initiated by CC&S command M1. The CC&S command M2 then switched power off to all the Sun sensors, turned on the autopilot power, and switched capacitors in the feedback loop of all three gyros. These capacitors integrated the sensed rate to give a position error signal. The gyros thus provided rate plus position error signals to the switching amplifiers for the remainder of the maneuver.

The pitch turn began with the M4 event which occurred simultaneously with M2. The turn was accomplished by switching a constant current from the command current generator into the gyro torquer. The CC&S polarity command M3 controlled an attitude control relay that selected the proper polarity current. When the current was first applied to the torquer, the gyro responded and an error

signal was output to the switching amplifier. The gas jets fired until the resulting spacecraft rate nulled the torquer signal. The spacecraft then continued to turn at this constant rate as long as the current was applied. After the period of time specified by the stored pitch turn duration, the CC&S switched off this current. Since the torquer signal due to the command current was no longer present to null the sensed rate, the gas jets operated to reduce the pitch rate and position errors to small limit cycle excursions about the new pitch position. The roll turn was initiated by CC&S event M5 and was performed in a similar manner to the pitch turn. The new pitch and roll positions were maintained for the remainder of the maneuver.

The maneuver sequence was terminated when the CC&S M1 and M2 relays were reset. The gyros remained on, however, since the Canopus tracker acquisition signal was off. When M2 was reset, Sun sensor power was again applied and normal Sun acquisition began. When Sun acquisition was complete, Canopus acquisition began. The gyros turned off 180 s after the Canopus tracker acquired a star.

7. Roll one shots. The roll one shots were emergency circuits controlled by commands DC-16 and DC-21. If the Canopus tracker were to fail, the roll position could be controlled by switching the capacitor into the roll gyro feedback loop by using DC-18. Vernier control could be obtained by using the roll one shots. The +2¼-deg one shots, triggered by subsequent DC-18's, switched a negative command current into the roll gyro torquer for a time equivalent to a +2¼-deg roll turn (approximately 12.5 s). The 2¼-deg one shot, triggered by DC-21, would switch a positive command current into the roll gyro torquer for a time equivalent to a −2¼-deg roll turn. The spacecraft would not perform the −2¼-deg roll turn unless the capacitor had previously been switched into the gyro loop by DC-18.

8. Autopilot. The midcourse autopilot was used to control the attitude of the spacecraft during midcourse motor burn. This control was accomplished by continuous adjustment of the angular positions of four jet vanes mounted at the down-stream end of the midcourse motor nozzle.

Since the motor was not mounted along the spacecraft body axes, the motion of each jet vane was controlled by a combination of signals from the three gyros.

Each jet vane had its own separate control system, consisting of an autopilot amplifier, a jet vane actuator, and a feedback loop. Power to the autopilot was provided by the main 2.4 kHz inverter and was switched on by the CC&S M2 command. The three gyro signals and the feedback signal were summed in different ratios at the input to each amplifier, deflecting each jet vane so that the motor thrust vector was oriented in the direction required to null the gyro error signals.

B. Considerations, Simulation, and Testing in the Redesign of the *Mariner* Mars 1964 Attitude Control Subsystem for *Mariner* Mars 1969

The attitude control subsystem requirements of the *Mariner* Mars 1969 spacecraft were very similar to those of the *Mariner* Mars 1964 spacecraft. However, as guidelines for redesigning the subsystem for use on the *Mariner* Mars 1969 spacecraft, it was decided to: (1) substitute improved parts if available and re-evaluate part stress levels to improve reliability, (2) redesign the Canopus tracker to increase the probability of performing automatic roll acquisitions, and (3) incorporate into the Canopus tracker the capability for particle rejection to preclude the possibility of recurring loss of roll reference caused by bright particles in the Canopus tracker field-of-view.

The final gyro mixing matrix, which was the only item changed for the auto-pilot subsystem was established when final values for the spacecraft moments of inertia, center-of-gravity location, and motor thrust angle became available.

1. Pitch and yaw control. The derived rate parameters were re-evaluated using the results of a parametric study. While the *Mariner* Mars 1964 parameters were selected for maximum noise rejection, the *Mariner* Mars 1969 parameters were selected to optimize the spacecraft's ability to recover from disturbing torques. This is a significant change, since it was planned for the *Mariner* Mars 1969 infrared spectrometer subsystem to vent coolant gases during the encounter phases. A comparison of the steady-state position errors for the *Mariner* Mars 1964 and *Mariner* Mars 1969 parameters are given in Fig. 6.

a. Sun sensor scale factor. The Sun sensor scale factor was reduced from 16 to 10.2 V/deg to allow the Sun sensors to operate at a lower excitation voltage and thereby significantly improve their reliability.

b. Position deadbands. The pitch and yaw axis position deadbands were reduced from ±8 to ±4 mrad to reduce the initial position errors for the midcourse maneuver turns.

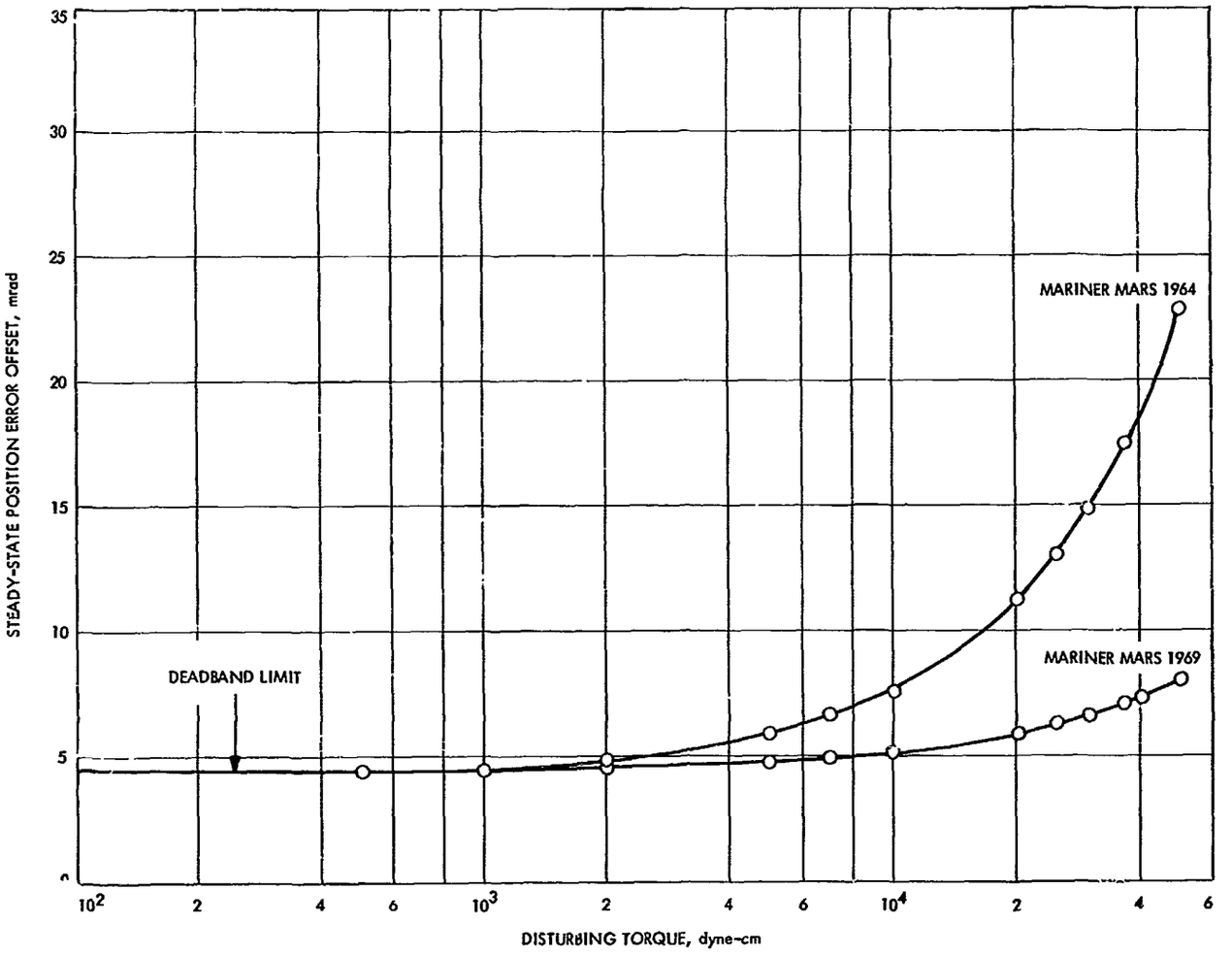


Fig. 6. Steady-state position error offset vs spacecraft disturbing torque

c. Sun gate logic. The Sun gate logic was modified so that a loss of Sun acquisition would directly result in the initiation of a Sun re-acquisition phase. The *Mariner* Mars 1964 logic depended on removing the power from the Canopus tracker to initiate a re-acquisition phase.

2. Roll control. The changes to the roll axis control logic ... of far more significance and scope th... those to the pitch and yaw axis control logic. The most significant chang... was the re-design of the Canopus tracker. The roll con... ol logic was redesigned, and the roll derived rate parameters were optimized. The changes to the roll logic are shown in Fig. 7. The general changes to the roll control syste... were as follows: The new Canopus tracker desig... utilized an instantaneous field-of-view set by the tube aperture of 1 deg, which was electrically scanned to establish a scanned field-of-view of 3 deg. The scanned field-of-view was electronically gimballed to obtain a total field-of-view of 9 deg, roll, and 11 deg, cone. The roll error was generated by observing the position of the scanned field-of-view and the center of the total field-of-view. The scanned field-of-view concept resulted in improved signal-to-noise performance and allowed a larger total field-of-view.

For acquisitions, whether resulting from no star being in the field-of-view or from a logic command, the scanned field-of-view was biased up against the clockwise edge of the total field-of-view with the following results:

(1) A saturated roll error signal was generated whenever the sensor did not have a star in its total field-of-view. The addition of this signal, which was then

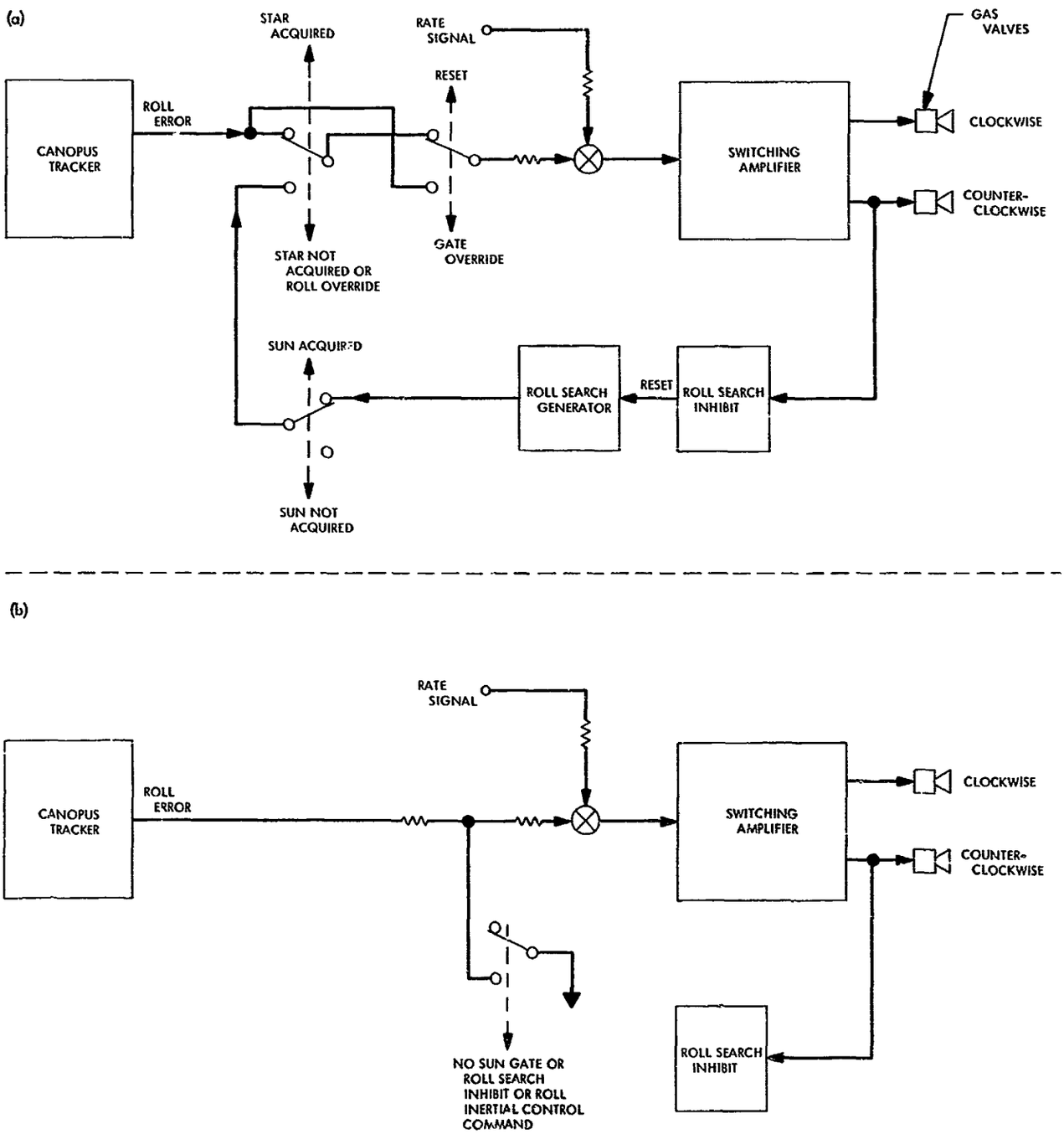


Fig. 7. Roll control logic diagram: (a) *Mariner* Mars 1964, (b) *Mariner* Mars 1969

used as the roll search generator, allowed the deletion of the *Mariner* Mars 1964 roll search generator and simplification of the signal switching.

(2) Reflection problems within the Canopus tracker lens and baffle assembly were eliminated. This deletion of out-of-phase reflection signals during the acquisitions allowed the deletion of the polarity checking circuitry of the *Mariner* Mars 1964 acquisition logic.

To increase the probability of having an automatic roll acquisition, a scheme utilizing star rejection for both high- and low-intensity levels had been implemented. The tracker was mechanized with both a high- and low-intensity gate, such that only objects whose brightness was above the low-gate level and below the high-gate level could be acquired.

The gate setting had been made adjustable in three increments to allow for uncertainties in the calibration of the low intensity gate. The stepping from one level to the next was cyclic; thus, after the circuit had been stepped to the lowest intensity setting, the next command stepped it to the highest. During the actual flight sequence it was expected that the first intensity level would result in the acquisition of Canopus. However, if due to some unforeseen error the star Canopus did not exceed the first low-gate intensity level, the central computer and sequencer cyclic pulse would step the gate to the next level after a minimum of one revolution of roll search. The gate could also be stepped by direct command. The gate settings, normalized to the intensity of Canopus, were 0.7, 0.35, and 0.15 for the first, second, and third gates, respectively. The high-gate level was fixed at approximately 4.0 times Canopus. Thus, in the normal case, only objects between 0.7 and 4.0 times Canopus in intensity could be acquired. Normally, only Canopus and Sirius fall in this range.

To reduce the probability of having a bright fast-moving particle cause the control system to reject a star after acquisition, the following changes were made:

(1) The high intensity gate limit was deleted after acquisition.

(2) A flyback and sweep function along with a time delay was built into the Canopus tracker logic. This allowed a particle to drift through the total field-of-view without causing the spacecraft to go into a roll search until the flyback and sweep function had swept the total field-of-view for the star.

3. Simulation and testing. Both digital computer simulations and breadboard testing were utilized to verify system compatibility and performance. Breadboard models of the Canopus tracker, roll control logic, derived rate networks, switching amplifier, and gyro were assembled into a system and tested in the celestarium. The tests utilized a single axis table, simulated stars of various intensities, bright Mars and Earth disks, and bright particle simulators. The capability of the system to recover from the effects of external torques and bright particles was verified, as was its capability to acquire a star of Canopus intensity through a search of a bright Earth.

A series of special tests was performed with the attitude control subsystem to experimentally verify the compatibility of the derived rate system. The tests were categorized into two parts: (1) verification and study of closed loop system acquisitions, and (2) determination of the capture threshold of the system when in derived rate limit cycle control and subjected to acceleration disturbances.

The verification results are depicted in Fig. 8, and are summarized as follows:

Roll error scale factor: -3.75 V/deg, specification -3.4 to -4.6 V/deg

Saturated roll error: -13 V, specification -12 to -14 V

Acquisition gate:

$$ON_{ccw} = +5.2 \text{ deg roll}$$

$$OFF_{ccw} = -6.8 \text{ deg roll}$$

$$OFF_{cw} = +7.7 \text{ deg roll}$$

A derived rate acquisition with the gyro inhibited (DC-40) and the Canopus tracker brightness gate logic inhibited (DC-15) is shown in Fig. 9. The figure indicates the maximum angular displacement in roll from which a star can be acquired with a full gas system while on derived rate feedback. The limiting factor in establishing the limit is the length of time that the ccw roll valve is on. If the ccw roll valve is on in excess of 30 s, the roll search inhibit circuit actuates and disables the roll error (position) input to the roll switching amplifier. The roll search inhibit circuit can be reset with a roll override command (DC-21).

The capture threshold of the *Mariner* Mars 1969 system was much higher than that of previously flown derived rate attitude control systems. The capture threshold of

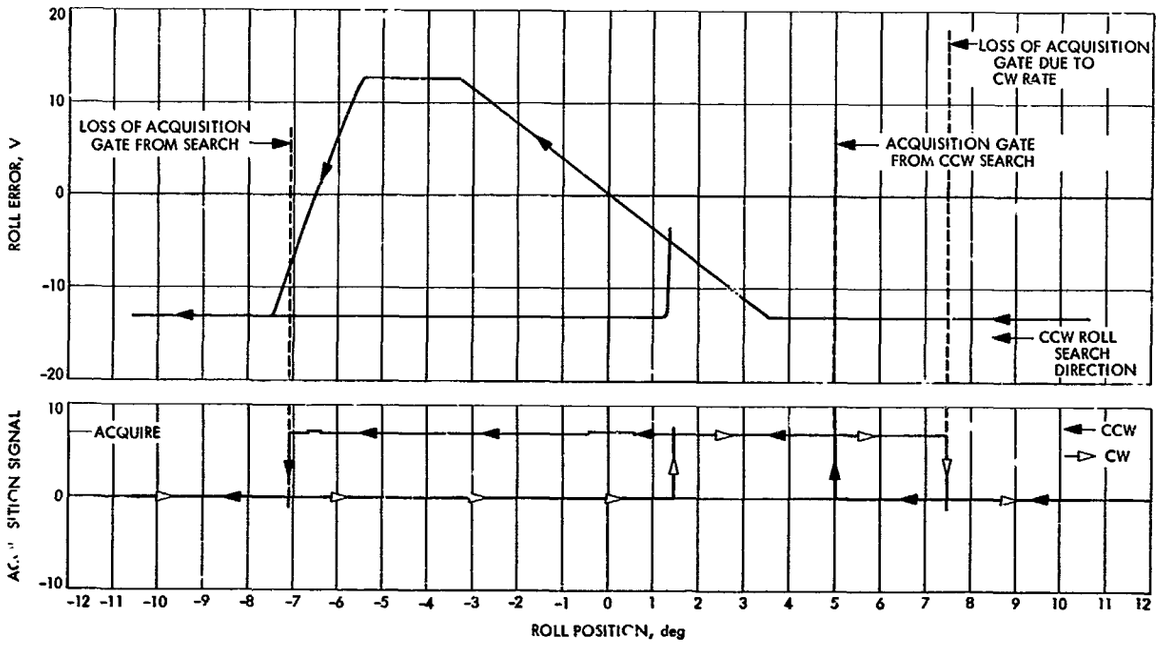


Fig. 8. Canopus tracker characteristics

these systems is shown (the results are for a complete system; i.e., two reaction control assemblies).

System	Capture threshold, deg/s	Acceleration constant, mrad/s²
Mariner Mars 1969	0.50	0.450
Mariner Mars 1964	0.28	0.450
Ranger Block III	0.30	0.60

The limiting factors in establishing the capture threshold were primarily that the ccw roll valve on time shall not exceed 30 s, and that the star shall not exceed the acquisition gate limits during the transient re-acquisition.

The following special tests were conducted successfully in support of this study:

(1) Acquisitions with a bright Earth passing through the field-of-view before Canopus acquisition.

(2) Sun shutter operation.

(3) Acquisition of stars with varying intensity levels to verify operation of the intensity gate limits.

(4) Effect of the system of bright particles. (Generally these bright particles move quite rapidly so that the spacecraft cannot track them. The system operated in a manner such that the control system tried to follow the particle, lost the particle, initiated a Canopus tracker flyback and sweep that re-acquired the star.)

(5) Roll error offset when in the Mars encounter geometry. A special test to observe the effect of a bright Mars disk on the roll error null offset was conducted. With the system locked on Canopus, a 100 ft-cd Mars disk was brought within 23 deg (both cw and ccw roll displacements) of Canopus with minor null offsets (increase of approximately 100 mV).

C. Attitude Control Electronics

1. Functions and subassemblies. The following briefly summarizes the functional operations and the subassemblies of the attitude control electonics (ACE).

a. Attitude control power distribution. The ACE was supplied 50 Vrms, 2.4 kHz square wave primary power by the spacecraft power subsystem. This primary power was distributed by the ACE to the Canopus tracker, the Sun detector, switching amplifier, preamplifiers and power switches, and the ACE transformer-rectifier (T/R). The ACE also controlled the application of primary power to

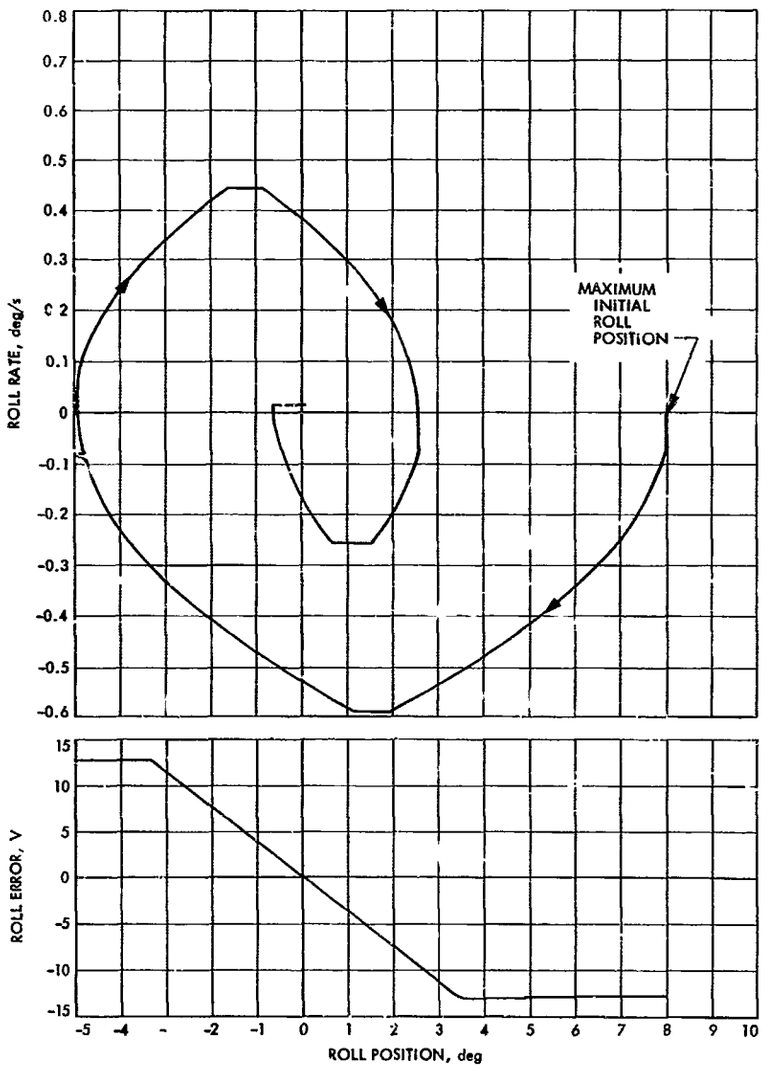


Fig. 9. Canopus acquisition with derived-rate feedback (full gas system)

the gyro control assembly (GCA) T/R and Autopilot T/R and 27.2 Vrms, 400 Hz quasi-square wave power to the GCA gyro spin motors. A GYROS ON command from the ACE to the power subsystem caused a relay closure in the power subsystem.

The ACE T/R generated ±26 Vdc power and distributed it within the ACE in both switched and unswitched form. Unswitched 26 Vdc power was supplied to the power amplifiers, the Sun gate, the gyro switch control, and the logic relay coils. Switched power was supplied to the switching amplifier pre-amplifiers, the Sun sensors, the roll search inhibit logic, and other electronic and logic functions.

The autopilot T/R output was enabled by the all-axis inertial command (CC&S M-2) and supplied ±32 V power to the autopilot electronics (and, thus, to the thrust vector control assembly) and ±26 V power to the jet vane actuator feedback potentiometers.

b. Attitude control and switching logic. The ACE switching logic used commands from CC&S and output states of Sun gate, roll search inhibit circuit, and Canopus tracker acquisition signal to command power on/off states of the attitude control subsystem and control signal switching for the various logical states of the subsystem.

c. Autopilot control electronics. The autopilot mix resistor matrix transformed spacecraft coordinate rate and position information into equivalent information in the autopilot coordinates. The jet vane actuator control amplifiers were also located in the ACE.

d. Reaction control assembly driving electronics. Reaction control system electronics elements included in the ACE were:

(1) The pitch, yaw, and roll switching amplifiers provided power to drive the solenoid operated valves of the reaction control assembly.

(2) The derived rate circuits which provided a rate control feedback signal to the switching amplifiers.

(3) The roll search inhibit circuit that limited the on time of the negative roll jets to limit the roll rates which the spacecraft would attain in the event of a roll search voltage "hard-over" failure.

2. Modifications for Mariner Mars 1969. The design and function of the *Mariner* Mars 1969 ACE was basically the same as that of the *Mariner* Mars 1964 ACE with a relatively small number of changes. The derived rate parameters for *Mariner* Mars 1969 were selected to optimize recovery from disturbing torques rather than for noise rejection as in *Mariner* Mars 1964. The new derived rate design reduced steady-state error offset as a function of disturbing torque, accomodated the new Sun sensor and Canopus tracker scale factors, and permitted replacement of wet slug capacitors with Hi-Rel 350D-type capacitors.

The cruise Sun sensor scale factor was reduced from 16 to 10.2 V/deg. This allowed reduction of the Sun excitation voltage from 16 to 12.4 V to reduce power dissipation in the photodetectors and thus improve their reliability.

The pitch and yaw axis position dead bands were reduced from ±8 to ±4 mrad.

The Sun gate logic was modified so that a loss of Sun acquisition would directly result in the initiation of a Sun re-acquisition phase.

Gate step control logic was added to the system to control the inputs to the Canopus gate step by admitting or inhibiting CC&S, Y2 or FCS DC-12 commands to step the adaptive gate.

An unconditional gyros off command was added to the gyro switch logic to provide the capability of turning the gyros off at any time in any logical state.

The requirement for a roll error polarity check prior to enabling an acquisition to the ACE was deleted from the Canopus and Sun gate logic. A DC-21 signal to the Canopus tracker was added to the logic.

The new Canopus tracker design resulted in a simplification of the roll control loop, Fig. 7, and the deletion of the roll search generator from the roll search inhibit logic. The magnetometer spin generator was also removed.

New components were used in the *Mariner* Mars 1969 ACE where direct substitution would replace components of lesser quality or reliability used in *Mariner* Mars 1964, or where formerly used components were no longer available, or, finally, where significantly superior new parts were available.

3. Physical configuration. The ACE physical configuration is shown in Fig. 10. The 34 welded encapsulated modules of the ACE were mounted in a chassis machined from a single block of magnesium. The chassis was divided into two compartments by a partition which was an integral part of the chassis structure.

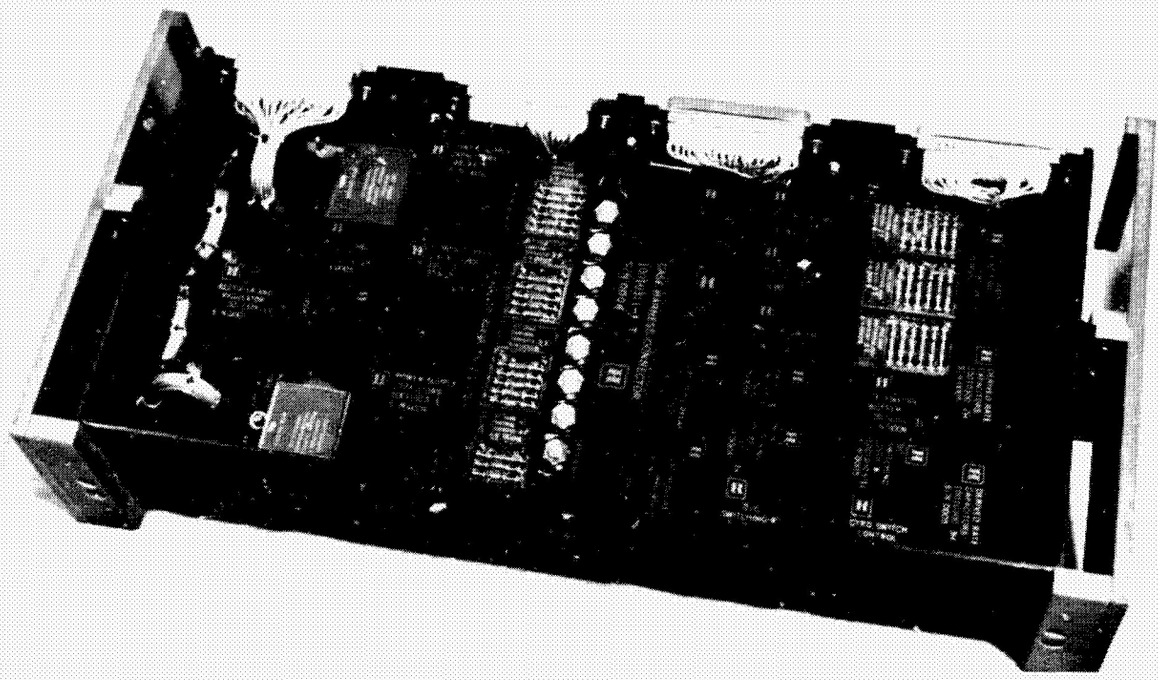


Fig. 10. Attitude control electronics

4. Testing. The TA, FA, and SAF testing are described below.

a. TA and FA testing. The ACE was subjected to environmental tests in combination with the gyro control assembly. During pre-environmental and post-environmental functional testing, the two subassemblies were subjected to individual and combined tests.

Following the vertical axis sinusoidal TA vibration test on the S/N 0002 ACE the normally-open contacts on relay K6 would not close when the relay coil was energized.

The relay module was replaced and the proof test model ACE then successfully completed TA thermal vacuum and vibration tests. Subsequent failure analysis of the relay which malfunctioned indicated that the failure was probably caused by contaminants lodged between the leaf spring and the armature of the relay.

A relay malfunction also occurred during functional tests after FA sinusoidal vibration tests of S/N 0004 ACE. The relay module was replaced, and thermal vacuum and vibration testing of the subsystem was completed.

The relay failure in this case was caused by inadequate staking of the relay armature to its shaft.

Finally, S/N 0003 and S/N 0005 ACE completed FA testing without incident.

b. SAF testing. Modifications of the ACE were made as a result of problems found during spacecraft level testing. The telemetry buffers for channels 105, 106, and 114 were re-scaled to limit telemetry signals to ±4 V. The previous buffer scaling had resulted in signal values to the FTS, exceeding the specified maximum voltages.

The gyro event signal line was removed after it was found that multiple FTS counter one events occurred at gyro turn off; this was due to a circuit design problem that could not be remedied without a major circuit redesign. A counter one event should have occurred only during gyro turn-on.

Canopus tracker power on logic was changed to allow the tracker turn-on time to be controlled by CC&S command L2 rather than L4. This change separated ACS and Canopus tracker turn-on so that Canopus tracker turn-on time could be delayed to avoid danger of high-voltage

corona arcing in the tracker due to insufficient venting of atmospheric gas from the spacecraft prior to turn-on.

D. Sun Sensors and Sun Gate

A flight set of sensors for the *Mariner* Mars 1969 mission included four acquisition sensor assemblies, two cruise sensor assemblies, and one Sun gate assembly. The maximum total power required was 0.3 W. This power level, which was dissipated in the detectors, was dependent on the solar intensity and decreased to approximately 0.2 W at Mars encounter. The weight of the Sun sensor set was 0.8 lb. It was expected that the pointing accuracy of the sensors would be well within a tolerance of ±1.4 mrad. Design and fabrication are described below.

1. Acquisition and cruise Sun sensors. The initial design of the cruise Sun sensor assemblies were the same as for the *Mariner* Mars 1964 design (Ref. 1), except that a modification was made to incorporate a new photodetector. This detector configuration, which was housed in a TO-5 size transistor case having a window to admit light, was used for all *Mariner* Mars 1969 Sun sensors. Two cruise sensors, as shown at the right and left end of the front row of the sensors in Fig. 11, were used. The sensors were mounted on pedestals extending upward from bays IV and VIII of the spacecraft octagon structure. Each cruise sensor assembly contained two acquisition detectors as well as two cruise detectors. The cruise detectors were located nearest to the base plane.

The cruise detector excitation voltage was reduced from the 16 V used in *Mariner* Mars 1964 to 12.4 V to reduce the power dissipation and, consequently, to improve the reliability of the photodetectors.

Four acquisition sensor assemblies, containing two detectors each, mounted in bays I, III, V, and VII, on the lower ring of the octagon structure, were required, compared to two for *Mariner* Mars 1964 because of the more severe field-of-view constraints imposed by the size and configuration of the scan platform. The acquisition sensors are shown in the back row of Fig. 11. TA vibration testing on the proof test model Sun sensor assemblies disclosed that the detectors would crack at the solder joint between the cell and the lead to the case.

Two design modifications were made as a result of the vibration-induced detector failures. First, a resilient detector mount was designed to reduce the high g levels imposed on the detector assembly by virtue of damping

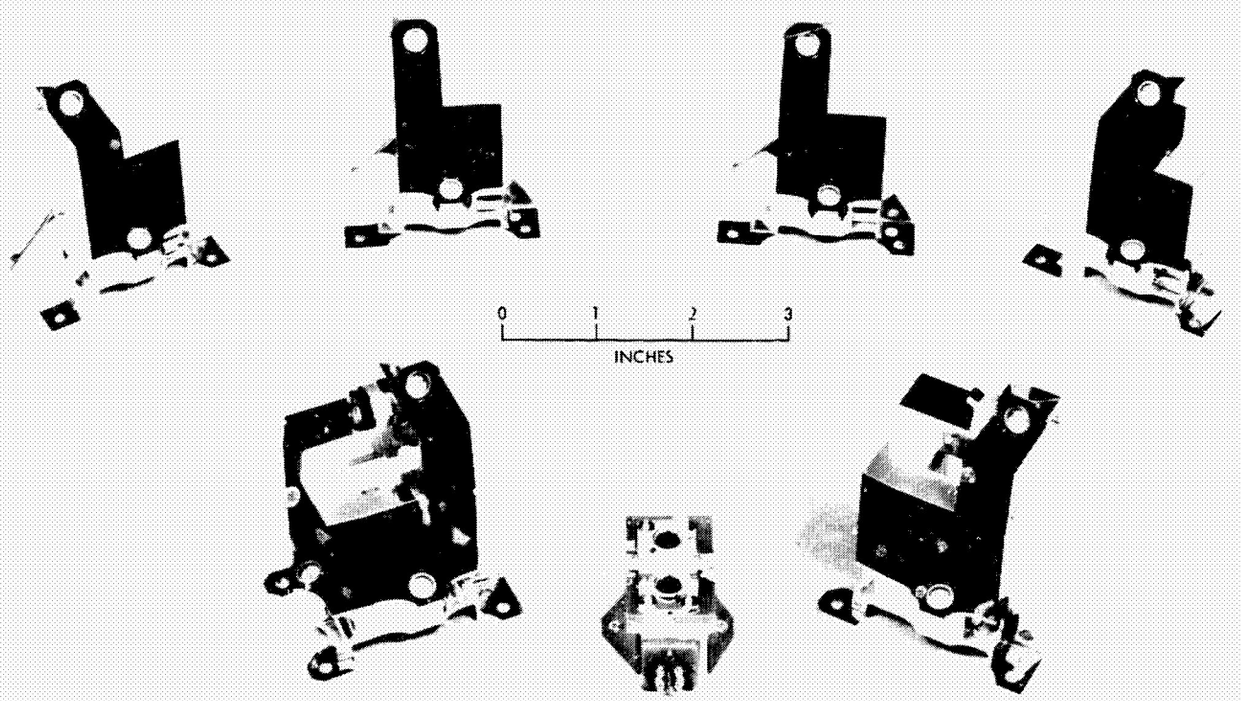


Fig. 11. *Mariner* Mars 1969 sensors

qualities. Second, a design modification was made in the photodetector to increase its vibration resistance.

The configuration of the resilient photodetector mount design is shown by Fig. 12. The isolation washers were made of silicon rubber having a Shore durometer hardness of 35. A small amount of compression (5 to 15%) was used to encourage sliding motion between the isolation washers and the contacting metal parts under vibration conditions. This was done to allow conversion of the kinetic energy to heat through the associated friction.

No failures were experienced when the engineering prototype sensors with the resilient mount design incorporated were evaluated at TA vibration levels or at 160% of the TA levels. The PTM sensors were then modified to incorporate the resilient mount in preparation for the continuation of formal type approval testing.

The screening of the ruggedized detectors was completed in time to incorporate them into all flight sensors subsequent to the PTM sensors. One out-of-tolerance null condition was experienced on the first set of flight sensors, during the post-environmental functional test. The null offset at 0 deg was 68″ compared to the original tolerance of ±54″ of arc. It was found that a null offset could be caused by depressing the detector assembly toward one side of the resilient mount. This indicated that vibration or thermal stresses could change the null by altering the "at rest" position of the detector assembly relative to the sensor shadow edges. The tolerance of 54 arc″ represents a shift in detector position of 0.00066 in.

The sensor assembly was re-worked by lapping the mounting feet to change slightly the mounting plane relative to the shadow edges and detector position. The flight acceptance test was re-run and the post-environmental test revealed "in tolerance" conditions. Another anomaly appeared after TA thermal shock testing.

The post-environmental functional tests revealed that the pitch null was 70 arc″ compared to the 54″ tolerance. It was decided to repeat this test with closer controls to prevent an inadvertent side force on one of the detectors, which could cause a null offset.

The thermal shock test was repeated after the out-of-tolerance null was corrected by reworking the sensor. The post environmental functional test revealed a pitch null offset of 107″ and a yaw offset of 112″. These results indicate that thermal shock can induce thermal stresses which cause the detectors to come to rest at a different position within the resilient mount after testing. A decision was made to change the null tolerance from ±54″ of arc to ±1.4 mrad or 4.8′ of arc, after careful evaluation of the impact of this increased tolerance on the midcourse maneuver accuracy requirements.

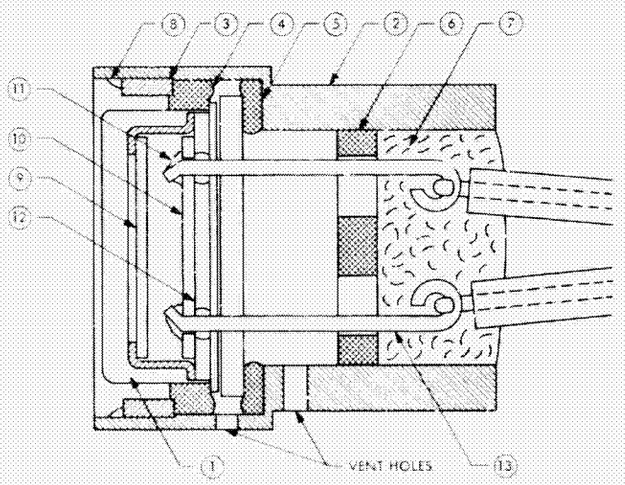


Fig. 12. Resilient photoconductor photocell assembly

2. Sun gate. The *Mariner* Mars 1964 Sun gate design was modified to incorporate the same detector used in the acquisition and cruise Sun sensors. In addition, the mounting surface was made perpendicular to the optical axis instead of parallel. This was done to allow the gate to mount on the same pedestal surface as the bay IV cruise sensor assembly. This resulted in a simplification of the pedestal design.

The Sun gate is shown in Fig. 11. Initial functional tests revealed that additional baffling was needed to prevent stray light from reducing the resistance at angles greater than 5 deg. The needed baffling was accomplished by the addition of a black paint pattern on the face of the detector assembly window. This pattern provided a transparent aperture parallel to and 0.008-in. wider than the detector sensitive strip.

Although no failures were encountered during the environmental testing of the Sun gate, the resilient detector mount and ruggedized detectors were incorporated to ensure against possible failures.

E. Canopus Tracker

A description of the *Mariner IV* star sensor mechanization testing and performance is given in Ref. 1 (pp. 229–249). A description of the *Mariner V* star sensor design changes, testing, and performance is given in Ref. 2.

1. New design requirements. A number of considerations led to a substantial redesign of the Canopus tracker (Fig. 13) for the *Mariner* Mars 1969 mission. An increase in spacecraft roll search rate was desirable, to decrease the roll period from 1 h to 30 min. In order to provide the wider roll error transfer function needed, an internal roll control loop was closed with the roll deflection plates of the image dissector. This yielded a roll error transfer function with excellent linearity over an angular control range nearly three times the previous width.

A design criteria of automatic spacecraft operation with minimum reliance on ground commands was adopted. For the acquisition sequence, this required that the tracker distinguish between Canopus and other celestial bodies, with manual map-matching retained only as a back-up. In the cruise mode, automatic operation required that the tracker automatically handle the more probable anomalous events with minimum disturbance to the spacecraft. These possible events included release of dust particles from the spacecraft into the tracker field of view and a long term variation in image dissector sensitivity.

Finally, the field-of-view cone angle position sequence was modified to follow the Canopus cone angle function beyond encounter in response to the on-board central computer and sequencer step commands.

The estimates of the launch vibration environment were very substantially higher than for the *Mariner IV* and *V* spacecraft due to a change in the injection vehicle from an *Agena* to a *Centaur*. This necessitated a general strengthening of the star tracker structures and redesign of several which were completely inadequate.

In addition to the technical, project policy, and environmental factors, a significant amount of redesign was undertaken because of the obsolescence of some electronic parts previously used, and the availability of more reliable new types such as integrated circuits.



Fig. 13. Canopus tracker

2. Functional characteristics. Figure 14 presents a functional block diagram of the star tracker. Figure 15 illustrates the tracker field-of-view, shown projected forward through the optics. The field-of-view was deflected electronically within the limits indicated. Cone angle gimballing was done in five discrete steps according to a pre-set program in the spacecraft CC&S to assure optimum overlap of the Canopus cone angle position at all times. Figure 16 illustrates the first five cone angle fields-of-view, labelled C1 through C5 and typical cone angle update times. A complete cycle was C1, C2, C3, C4, C5, C2, C1. The separate traces indicated the spread in Canopus cone angle for several possible launch dates.

The stray light baffle was large (approximately 12 x 7 x 5 in.) compared with the one used for the *Mariner V* star sensor and reflects the emphasis placed on decoupling the tracker from bright objects outside the field-of-view. It was fabricated of 0.005-in. stainless-steel sheet pieces which were formed and riveted. Weight was about 1.45 lb. All internal surfaces were finished flat black with 3-M Black Velvet epoxy paint. The baffle plate edges were machine cut to a knife edge to reduce edge scattering.

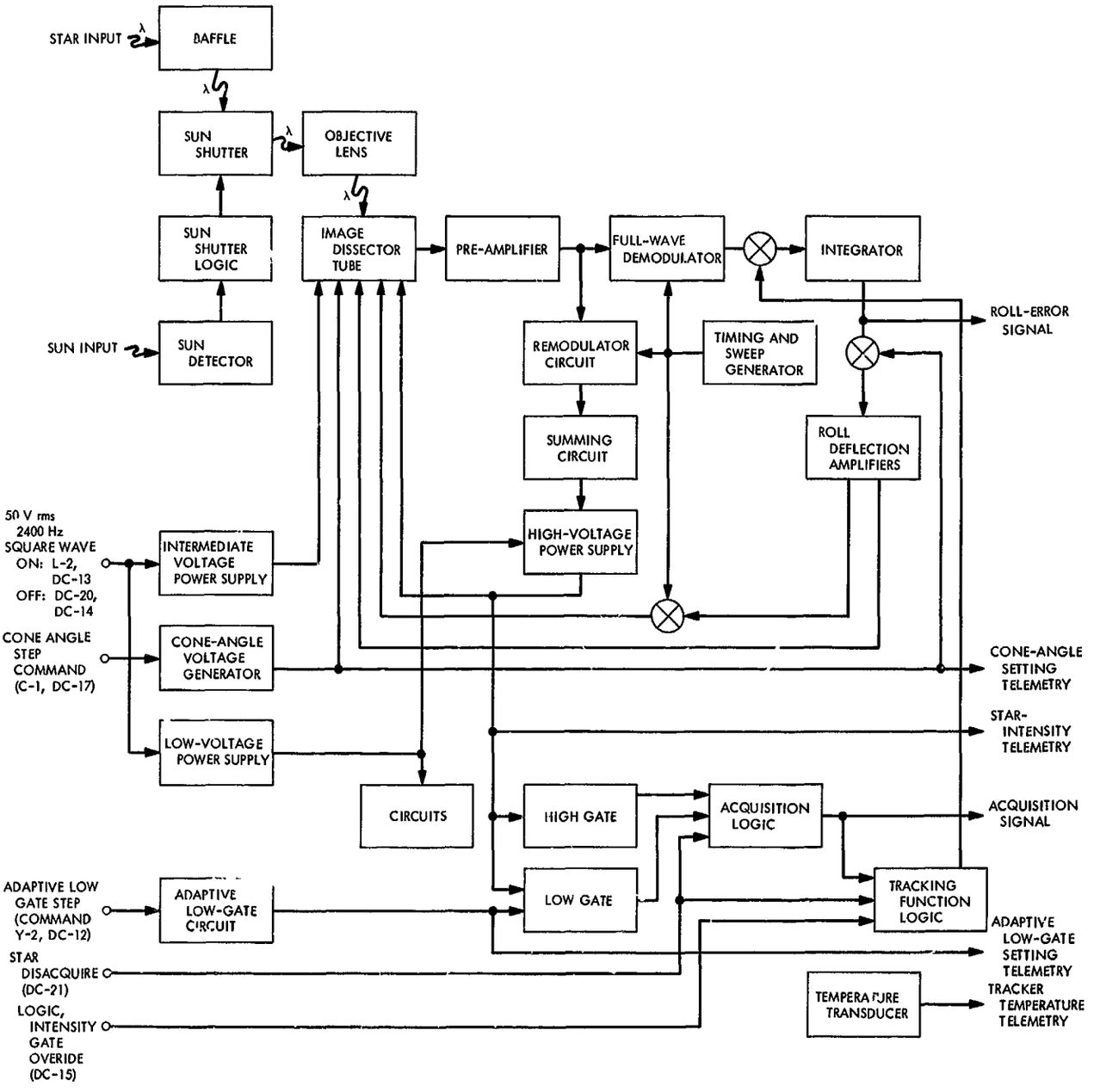


Fig. 14. Star tracker block diagram

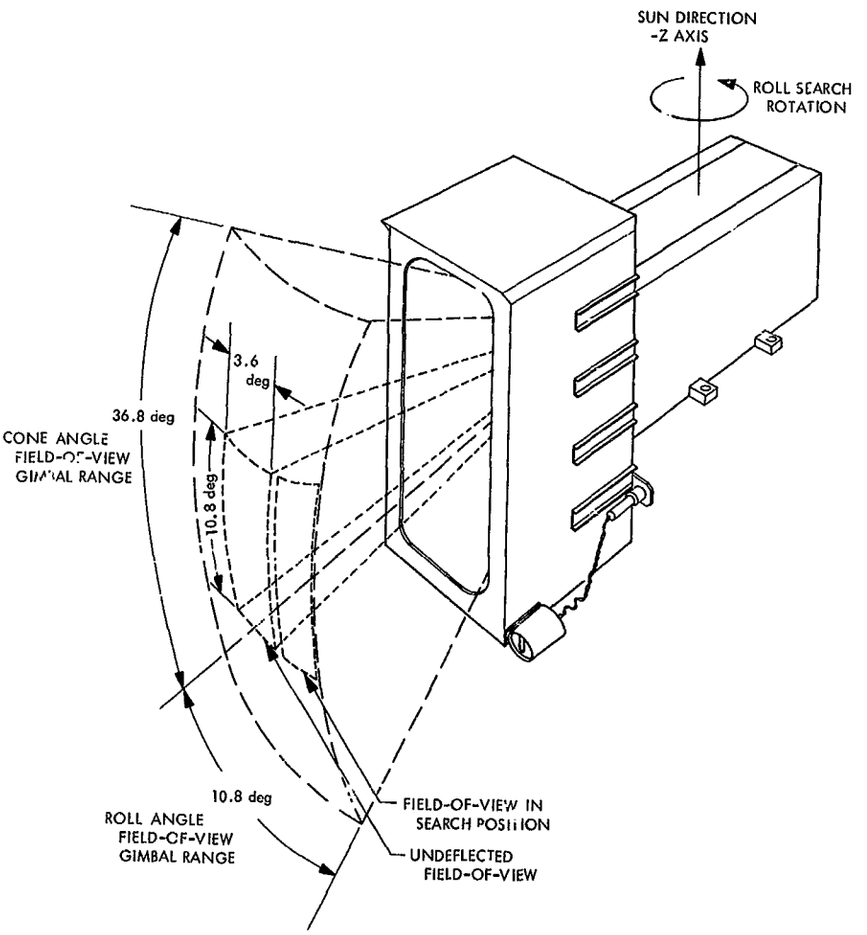


Fig. 15. Star tracker FOV geometry

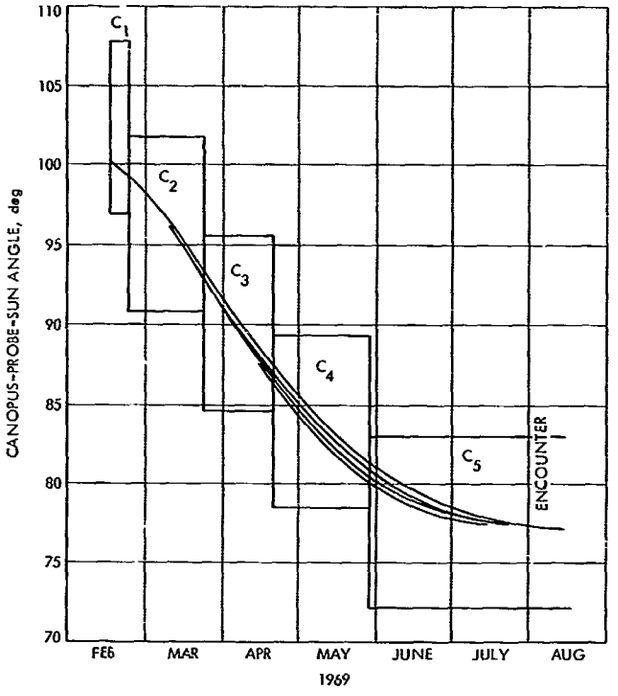


Fig. 16. Star tracker FOV coverage and Canopus-probe-Sun angle

The *Mariner V* lens assembly was a four element flat-field system intended for use with a fibre-optic image dissector face plate which would transfer the flat image to the necessarily curved photocathode surface. For the *Mariner* Mars 1969 program, the image dissector faceplate was clear glass and the lens nearest the faceplate had been designed to have a sagittal image plane backward-curving to match the photocathode surface. The new lens assembly was a three element design, with the objective of fused silica to provide some radiation shielding for the inner elements.

The Sun shutter was located between the objective lens and the inner baffle. The shutter was of the *Mariner V* design, modified to provide a reduced stroke angle with a longer blade. This design proved very reliable. A life-test unit was cycled steadily at the rate of 1 million actuations per month for over four years.

The image dissector was basically the same design as evolved for the *Mariner IV* and *V* missions with some improvements in electron imaging and elimination of the fibre-optic faceplate.

The electronic circuit components were packaged on four circuit boards lying along the two sides and the top and bottom of the tracker. Three of the four were single-sided boards and the two side boards were bonded directly to an inner housing bulkhead. The power supply board, mounted on stand-offs in the bottom cavity was double sided, with high-voltage components isolated to one side. All "canned" components were mounted upside down to the board with leads fanned out to surrounding terminals for ready inspection and accessibility. Flat pack logic elements were mounted into JPL-designed flat pack modules and the modules were bonded to the boards. All circuit boards were conformally coated.

3. Calibration and test. Determination of the star tracker's response to star illumination levels was accomplished with a laboratory simulator. A standard Canopus simulation, for which the significant elements had been calibrated by the National Bureau of Standards, is maintained in the JPL Celestarium. Reproducibility of the standard is thought to be within several percent and the absolute integrated value appears to be correct within 10%.

Tests were individually made of each tracker's stray light response since the required discrimination ratio was so high. Earth illumination at initial acquisition, for example, was typically 2×10^7 as intense as Canopus, and sunlight was 2×10^{10} as intense. Typical measured rejection ratios are illustrated in Fig. 17 with *Mariner IV* and *V* values plotted for comparison. Roll angle response is plotted on one side and cone angle response on the other. The *Mariner IV* sensor and the *Mariner* Mars 1969 tracker data were conservative, since the tests were conducted in air. The *Mariner V* sensor data were taken in vacuum.

Since the illuminated Earth crescent could be expected to pass through the tracker field-of-view during roll search at acquisition for some launch dates, a series of tests was run to verify tracker performance. The tests showed that the high stray-light rejection function and the acquisition logic were able to discriminate against the Earth for all cases except where the Earth passed very near the boresight of the instrument. Weak multiple reflections in the lens elements provided a variety of star-like images causing an unstable acquisition.

Although magnetic constraints were not imposed on the *Mariner* Mars 1969 spacecraft as a whole, a significant amount of effort was expended controlling the effects of magnetic fields on the tracker. The electron image of an unshielded tube is deflected an equivalent 3 deg by a worst-orientation Earth-level magnetic field, or about 0.4 gauss. The cylinder of magnetic shielding material previously used about the image dissector was thickened and

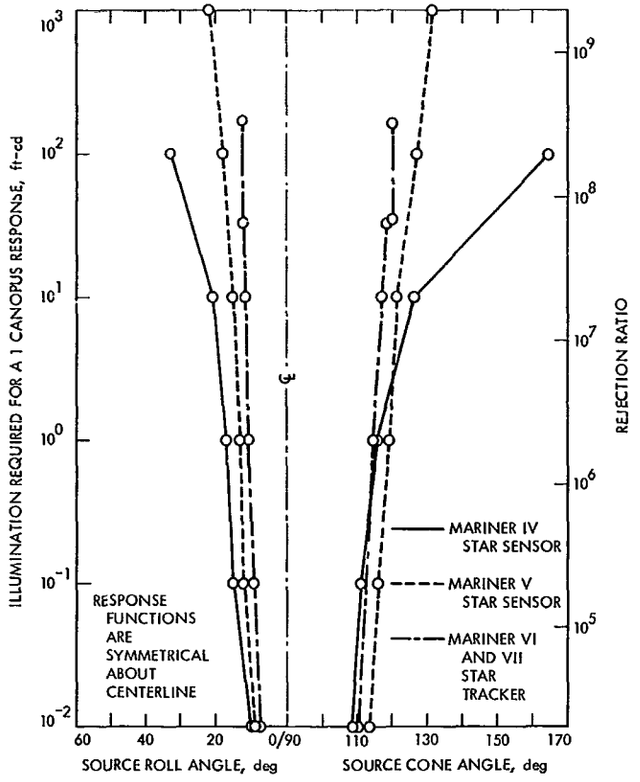


Fig. 17. Star tracker strong light response functions

extended forward of the photocathode by one diameter to become the major member of the mounting structure. This provided axial and transverse attenuation of about 25:1; however, this was still inadequate to allow null-direction testing in the Earth's field. Magnetic shield boxes were used around the trackers during test to establish the true null pointing direction. Care was taken to protect the trackers from intense transient magnetic events and degaussing procedures were developed to erase the effects of such exposures. A substantial number of magnetic events were encountered necessitating degaussing despite the care taken. The spacecraft were surveyed at the tracker's location, but no significant fields were recorded.

Canopus tracker S/N 001 successfully passed TA tests after some structural strengthening of the thin outer walls of the baffle. A wrinkling of the 0.005 stainless steel wall was noted during TA vibration. Some tracker performance problems were found during high-temperature thermal vacuum testing at 125°F. Detailed changes in tracker electrical circuits were made to correct these problems.

Trackers S/N 003, 004, and 005 successfully completed FA tests. The image dissector tube of tracker S/N 005 was replaced due to performance degradation during vibration testing. The tracker was subjected to complete FA level vibration testing following replacement of the image dissector tube.

F. Gyro Control Subassembly

The *Mariner* Mars 1969 gyro control assembly consisted of three miniature floated, rate-integrating gyros and associated gyro loop control electronics, logic, power supplies and special-purpose circuits. The major change from the *Mariner IV* design was in the power supply section. A separate rectifier module was added to the power supply for the purpose of reducing the ripple on the precision command current and to make the positive and negative circuits more nearly equal.

Other changes included the addition of a capacitor to the dc amplifiers and the deletion of a capacitor from the ac amplifier to reduce noise and improve stability. In addition, many component types were changed to use new, improved, and more reliable components.

Gyro testing typically involved an average of 15 runs of heading testing data, 4 runs of tumble testing, and one run of random drift tests before the gyro was committed for use in a flight system. These tests produced values for command rate scale factor, acceleration insensitive drift, and acceleration sensitive drift. Additional heading tests were run after installation into the gyro subassembly.

The electronic subassembly was checked by the contractor at several stages of assembly. Each module was tested at 0, 25, and 70°C, before and after encapsulation and after the modules were attached to the subchassis.

The integrating capacitors of the capacitor subassembly were tested for capacity and current leakage. Repeated current leakage tests were made after assembly of the capacitor bank in an effort to detect any trends that existed. No change in performance was noted.

After all three subassemblies passed their individual tests, they were brought together for assembly level tests. Tests were for the same parameters mentioned above as well as cogging tests and commanded turn rate tests using a servo table. In addition, voltage heading tests, rate scale factor tests, position scale factor tests, and incremental roll angle tests were run. The gyro control subassembly was subjected to all environmental tests, such as vibration and

thermal vacuum, while in the same spacecraft case structure as the ACE subassembly, in order to obtain conditions similar to the actual flight environments.

After passing all the tests at the contractor's facility, the gyro control subassembly was hand carried to JPL and given a somewhat abbreviated series of confirmation tests. It was then delivered to the spacecraft assembly facility for final visual and mechanical inspection and installed in the spacecraft. Prior to shipment of the spacecraft to the AFETR, the gyro control subassembly was removed and the confirmation tests repeated in the inertial sensors laboratory. The gyro control subassembly was hand carried to AFETR where a final abbreviated test was performed before it was installed in the spacecraft for the last time.

As a result of individual gyro tests, three gyros were rejected to the vendor for performance outside specification limits. Of these three, two were returned to the program after rework. The malfunction could not be confirmed by the vendor in one case, and this unit was set aside for use in non-flight tests. Of the 15 gyros committed to use in the gyro control subassemblies, all passed all subsequent tests satisfactorily.

The gyro control subassembly passed the TA tests satisfactorily, and the TA unit was placed on high-temperature life test. It ran for more than 5,000 h and continued operating within specification limits.

G. Thrust Vector Control Assembly

The thrust vector control was an assembly of four jet vanes and their drive actuators mounted on a ring as shown in Fig. 18. The assembly was mounted on the exhaust nozzle of the propulsion subsystem (PS) motor.

During the motor burn portion of the midcourse maneuver, the autopilot processed the three gyro "rate-plus-position" outputs, transforming those error signals into appropriate deflection commands to the four jet vane actuators. Each actuator controlled the position of a vane in the exhaust of the PS motor. The vanes then generated, as a function of their position, corrective torques to maintain the desired spacecraft attitude during motor burn.

The actuators were limited angle dc torquers each requiring 60 mA of current at 12 Vdc to generate 2 oz-in. of torque. Each actuator weighed 0.75 lb. The actuator contained an infinite resolution potentiometer which provided vane position control feedback. Actuator position stops were set at ±25 deg.

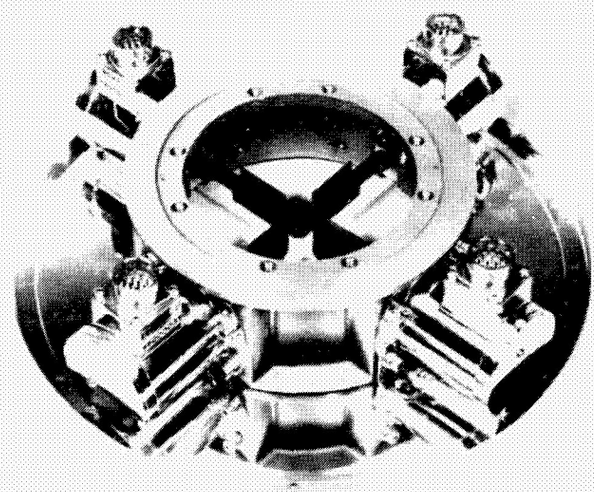


Fig. 18. Thrust vector control assembly

1. Design modifications. Thrust vector control subsystems of basically the same design had been used on all *Ranger* and *Mariner* spacecraft. The *Mariner* Mars 1969 thrust vector control assembly had a modified vane (Figs 18 and 19) and the inside diameter of the portion of the ring in which the vanes were located was 1-in. larger than the rings of *Mariner* Mars 1964.

These design modifications were based on the results of a number of tests conducted at the Edwards Test Station. A *Mariner* motor was mounted on a six degrees-of-freedom test stand to permit measuring side forces during motor firing with deflected jet vanes.

The tests showed that extraneous side forces resulting from aerodynamic shock waves generated at the leading edges of the vanes were acting on the ring in an outward direction along the axis of rotation of the vanes. It was determined that increasing the diameter of the ring resulted in a reduction of the side forces.

Removal of the thermal shields from the vanes did not aid in reduction of the side forces, but did result in lower temperatures at the actuator shaft and mounting areas during motor burn. This temperature reduction was the result of less turbulent flow with the thermal shields removed from the vanes.

2. FA and TA tests. During TA testing, it was found that the jet vane actuator torque gain was below the specified value. This low-torque output was determined to be a

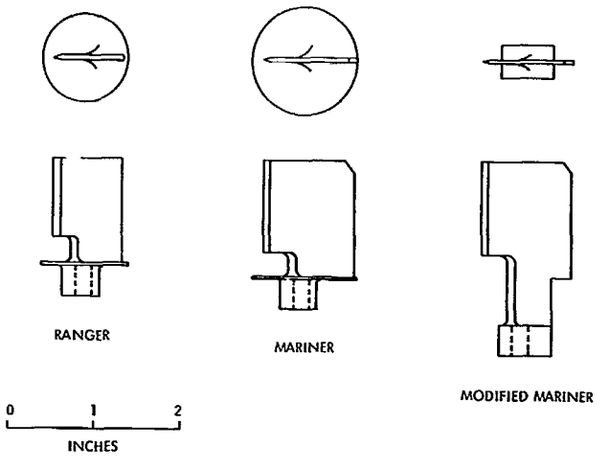


Fig. 19. Jet vane configurations (full scale)

characteristic of the actuators due to their magnets being stabilized at a current of 145 mA. This difficulty was corrected by rework of the actuators by stabilizing their magnets at a current of 130 mA.

Detents in the potentiometer elements of the actuator occurred during TA vibration tests due to wiper bounce against the elements. Measurements of vibration transmissibility to the thrust vector control (TVC) during motor firing tests at Edwards Test Station indicated that the vibration specification levels for the TVC should be changed from Class I to Class II. The actuators were rebuilt and successfully passed testing to the lower vibration level requirements.

Detenting of the potentiometer elements also occurred during the 375°F thermal soak required after completion of the thermal vacuum testing.

The high-temperature soak requirement was eliminated from the test requirements when temperature measurements, during motor burn tests, showed that as a result of the mounting ring and vane redesign, the temperatures at the actuators during motor burn were much lower than with the previous design. Subsequent high-temperature testing of the actuators was limited to the high-temperature requirements of the thermal vacuum test.

The PTM TVC did not complete TA testing at the contractors facility. The TA testing of the unit was completed at JPL after rework of the actuators and reassembly of the unit. The three flight TVC units successfully completed FA testing.

H. Reaction Control Assembly

The *Mariner* Mars 1969 reaction control assembly was basically the same in overall design and function as the gas system for *Mariner* Mars 1964. A description of that system, its major subassemblies and components, fabrication procedures, and leak test procedures is given in Ref. 1 (pp. 255–261).

1. Design modifications. The modifications of the *Mariner* Mars 1964 gas system for *Mariner* Mars 1969 are described below.

a. Relocation of the high-pressure assemblies. On the *Mariner* Mars 1964 and *Mariner* Venus 1967 spacecraft the high pressure assemblies of the reaction control assemblies were mounted on a secondary structure internal to the spacecraft octagon structure. The enlarged scan platform design of *Mariner* Mars 1969 required that the mounting location of the high pressure assemblies be changed to the top surface of spacecraft bus. The relocation resulted in a redesign of the high pressure assembly configuration. The new design configuration is shown in Fig. 20.

The pressure vessel was mounted on an equipment support ring. A spider strap arrangement held the vessel in a cushioned spherical seat in the support ring.

The reaction control assembly mounted on its handling and shipping frame is shown in Fig. 21. Transfer of the reaction control assembly from the handling frame onto the spacecraft was facilitated by brackets on the handling frame which held the two parts of the frame (the stub panels) that supported the gas jet valve assemblies and tubing rigidly in a vertical position; i.e., corresponding to the "stowed" position of the spacecraft solar panels. The brackets also provided support to the high pressure equipment support assembly from its top. Thus, the entire reaction control assembly, still attached to the stub panels and brackets of the handling frame, could be lifted from the handling frame base and mounted in position on the top surface of the spacecraft bus.

The stub panels served as support structures for the gas valve assemblies and tubing when the solar panels were not mounted on the spacecraft.

b. Thrust valve modification. The solenoid-operated gas valves for *Mariner* Mars 1969 were basically the valves used on *Mariner* Mars 1964 as modified for *Mariner* Venus 1967 to increase the performance of the valve at high temperatures. The thrust valve redesign for *Mariner*

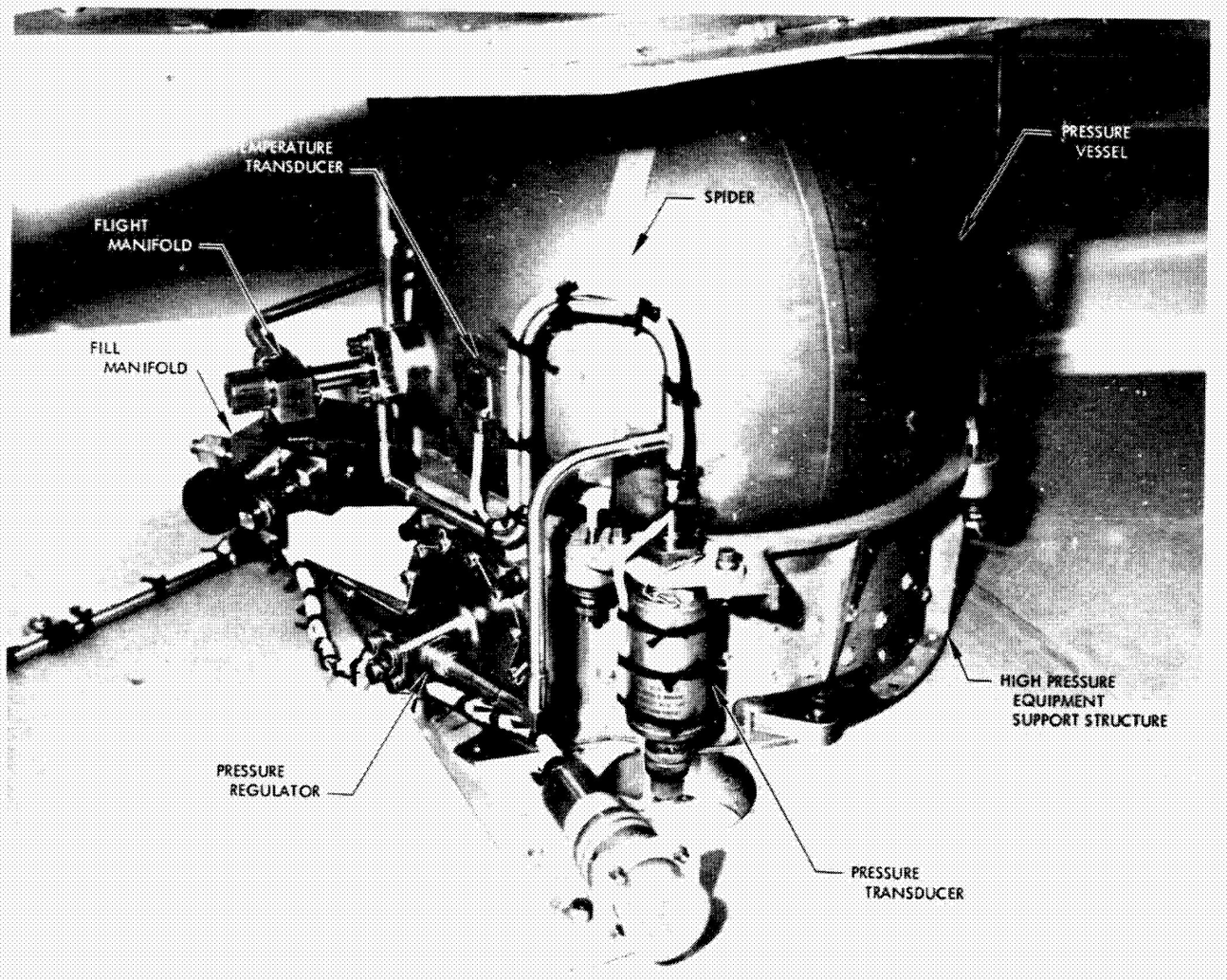


Fig. 20. High-pressure equipment support assembly

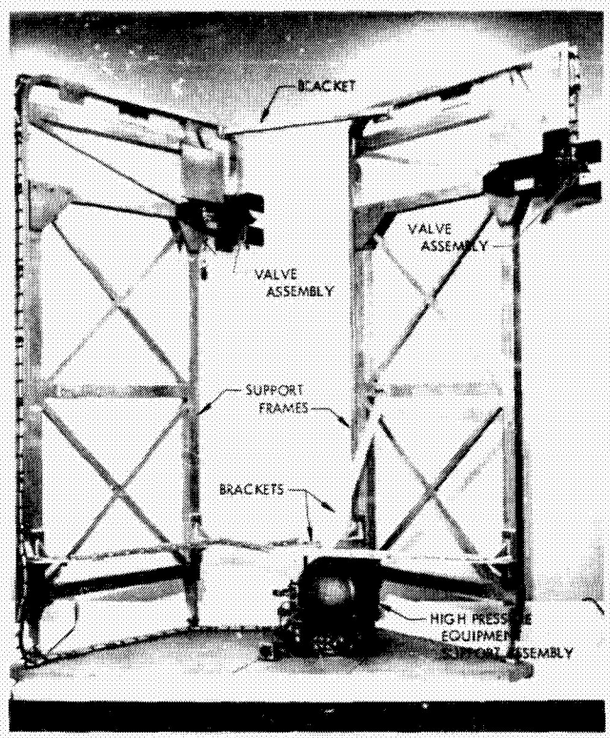


Fig. 21. Reaction control assembly mounted on shipping and handling frame

Mars 1969 concentrated on retaining the high- and low-temperature performance characteristics achieved by the *Mariner* Venus 1967 modifications.

The main area of concern was the elimination of the tantalum shim that had been inserted between the clapper and coil housing of the valve in the *Mariner* Venus 1967 modifications. The addition of this extra moving part created a potential source of contamination within the thrust valve. The design goal was to eliminate the shim without degradation of the valve performance. This was accomplished by machining a 1-mil groove into the head of the clapper (Fig. 22). This groove, located in the path of the magnetic flux, created a secondary air gap thereby minimizing the effects of residual magnetism.

c. Removal of solar vane mounting lugs. The solar pressure control system of *Mariner* Mars 1964 was removed from *Mariner* Venus 1967 by dismounting the actuators and the solar vanes from their mounting bosses on the gas valve manifolds. These mounting bosses were removed from the valve manifolds in the *Mariner* Mars 1969 redesign.

d. Improved gas nozzle sizing procedures. One of the major areas of concern in building an attitude control gas system was the proper sizing of the gas nozzles to meet spacecraft control torque requirements. On past *Mariner* and *Ranger* missions, this sizing had been done primarily by hand calculations and trial-and-error machining. For *Mariner* Mars 1969, and future use, a computer program was generated that predicted the correct nozzle geometry. Test apparatus and procedures were developed to measure steady-state thrust levels under simulated flight conditions. *Mariner* Mars 1969 ACS thrust requirements based on zero cross-coupling are listed below.

Control axis	Moment of inertia, slug ft^2	Desired control acceleration, rad s^{-2}	Moment arm, in.	Calculated required thrust, lbf
Pitch	$I_{XX} = 129.31$	2.25×10^{-5}	111.7	3.13×10^{-3}
Yaw	$I_{YY} = 131.92$	2.25×10^{-5}	111.7	3.19×10^{-3}
Roll	$I_{ZZ} = 209.60$	2.25×10^{-5}	101.2	5.43×10^{-3}

The computer program calculated the steady-state thrust level produced, taking into account the nozzle thrust losses for a given set of input conditions. The relevant initial conditions, based on *Mariner* Mars 1969 requirements, as used in this analysis, are listed in Table 6. The listed area ratio and exit half-angle, although not optimum (less by 1–2%), were established in this case so that previous nozzle tooling and blueprints could be used. Based on the listed initial conditions, the computer program was set up to output a curve of nozzle throat diameter vs thrust; all other relevant parameters were fixed. This curve was then used to pick the proper diameters to meet the flight thrust requirements. Test nozzles, identical to flight nozzles, were then fabricated for test.

Table 6. Initial conditions for nozzle sizing computer program

Parameter	Value
Valve discharge coefficient	0.3478
Valve ball travel, in.	0.006
Ambient temperature, °C	25
Valve ball diameter, in.	0.188
Valve seat diameter, in.	0.132
Nozzle geometric area ratio	250
Nozzle exit geometry half-angle, deg.	25
Ratio of specific heats (nitrogen)	1.4
Nitrogen gas constant, ft-lbf/lbm-°R	55.16
Ambient pressure, psia	0
Valve inlet pressure, psia	15.0
Nozzle throat diameter, in.	Variable: 0.010–0.020

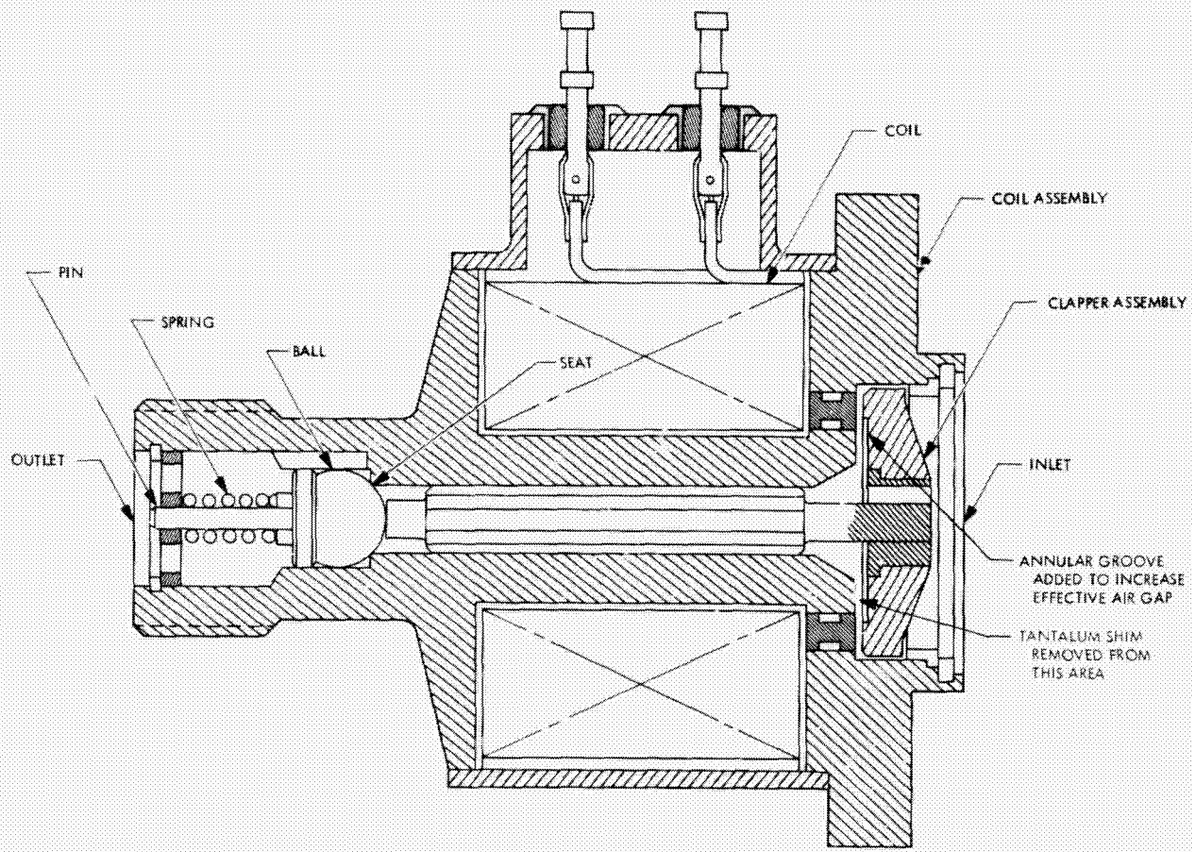


Fig. 22. Section view of *Mariner* Mars 1969 valve

Sili-gel molds were made of the fabricated test nozzles. These molds were inspected in an optical comparator to assure that nozzle internal geometry was identical to the print callouts and computer input data. The nozzles were then tested for steady-state thrust level. The test set-up was a vertical cantilever beam, also used as the gas feed line, pinned at the top. The valve and manifold were mounted at the bottom and at right angles to the beam (Fig. 23). Displacement of the beam was measured by a differential transformer pickoff and recorded on a strip chart recorder. Mercury pot damping had also been added. A hanging steel ball was used for calibration. The tests were run in a vacuum chamber (10^{-6} torr) and every attempt was made to duplicate flight conditions. The results of these tests were in good agreement with the computer generated data.

Based on the accuracy of machining and computer predictions, it was concluded that the pitch and yaw thrust requirements could be taken to be identical. The computer run and test data indicated agreement within 5%, which was considered to be of sufficient accuracy since all the data were obtained for an inlet pressure of 15.0 lb/in^2, and the reaction control assemblies pressure regulation band was 15.0 $\pm$1.2 lb in^2.

2. Tests. The configuration of the reaction control assemblies made environmental testing at an assembly level impractical. Environmental qualification tests were, therefore, conducted on functional assembly levels. The functional subassemblies subjected to vibration and thermal vacuum testing were the high-pressure assembly and the pitch and roll–yaw valve assemblies.

After completion of testing of the separate assemblies, the units were returned to the clean room for installation on a support fixture and welding to the low-pressure tubing.

a. TA tests. During the first axis of sinusoidal vibration of PTM high-pressure assembly S/N 0007, failures of the high-pressure assembly support structure occurred. The

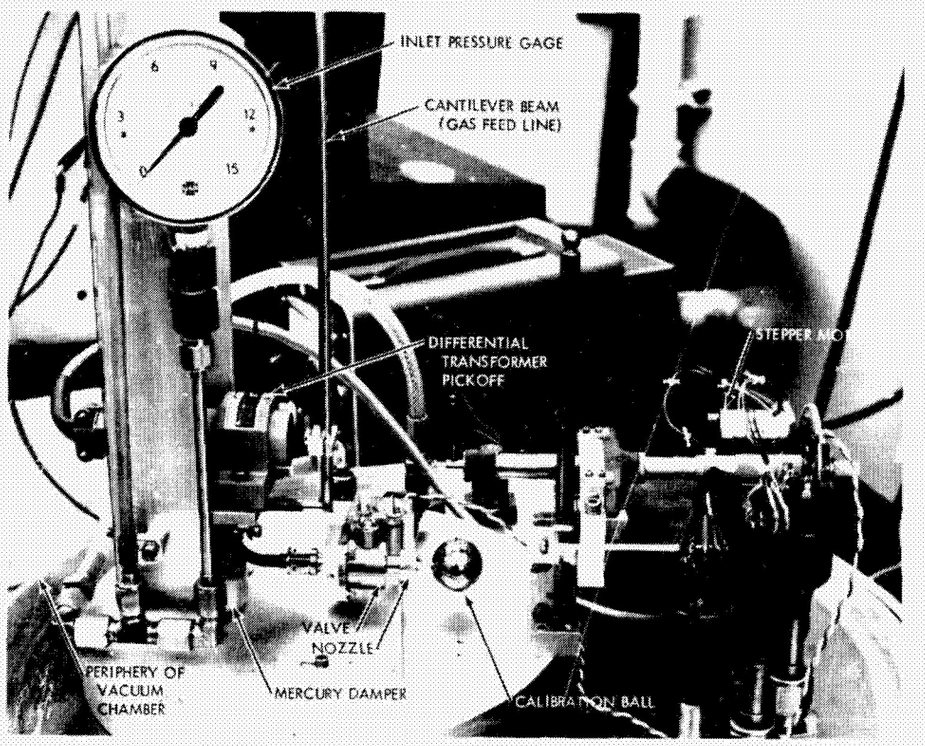


Fig. 23. Thrust measurement stand for nozzle sizing

structure was found to be cracked in two places near its mounting feet. The support was modified by designing a reenforcement ring structure which was riveted to the original support structure.

The PTM units and all flight high-pressure assemblies were fitted with the new support structure. No support structure vibration failures occurred in subsequent TA and FA testing.

The SN 0007 PTM unit completed TA vibration tests. It was delivered to JPL at JPL's request without being subjected to thermal vacuum tests.

The SN 0006 PTM unit failed to pass TA testing due to contamination problems. It was disassembled for failure analysis. The production prototype system was delivered to JPL as the second PTM system.

b. FA tests. All six flight reaction control half-systems successfully passed FA tests.

c. Quantitative leak tests. Quantitative leak tests of the reaction control assemblies were made by the contractor before delivery of the assemblies to JPL.

After delivery of the reaction control assemblies to JPL, each half-system was subjected to quantitative leak tests before delivery to SAF, after spacecraft system test, and at AFETR prior to launch.

Before and after each quantitative leak test, the regulators and thrust valves of each system were checked for internal leakage.

Regulator and valve replacements were made as a result of testing at JPL. One valve and a valve seal replacement were made at AFETR. The results of the final quantitative leak tests made at AFETR prior to launch are shown in Table 7. Valve and regulator leak rates were

Table 7. Quantitative leak test results

Reaction control assembly	Leak rate, cm^3/h
Spacecraft MM69-2	
S/N 0005	10.55
S/N 0004	11.05
Spacecraft MM69-3	
S/N 0006	19.65
S/N 0007	9.22

within specifications. Maximum specified total leak rate for a reaction control assembly was 30 cm^3/h. Maximum specified leak rate for individual valves and for the regulator was 3 cm^3/h.

III. Scan Control Subsystem

A. Purpose and General Description

The function of the scan control subsystem was to provide precision angular control of the two-degree-of-freedom (clock and cone axes) gimballed support structure or "platform" upon which the planet oriented sensors and science instruments were mounted. The scan control subsystem consisted of the planet tracking and acquisition sensors and the control electronics and servos.

The contractor for the ACS and the scan control (SCAN) subsystem was Honeywell, Inc. The work was done under JPL Contract No. 951701 at JPL. Honeywell facilities in Minneapolis and Boston, and AFETR.

Five sets of SCAN and ACS subsystems were built and tested. These included production prototype, proof test model (PTM), and three flight sets of subsystems.

The subsystems built and tested at the Honeywell facilities in Minneapolis were the ACE, gyro control subassembly, Sun sensors, Sun gate, thrust vector control assembly, attitude control gas systems, scan actuators, and scan electronics.

The Honeywell Radiation Center Facilities in Boston fabricated and tested the Canopus tracker, the far-encounter planet sensor, and the narrow-angle Mars gate subassemblies.

The scan control subsystem operated in three principal modes: far encounter, near encounter, and cruise. In the far-encounter mode, the FEPS was used to effect closed loop tracking of the planet center of brightness. In the near-encounter mode, the platform was sequenced through

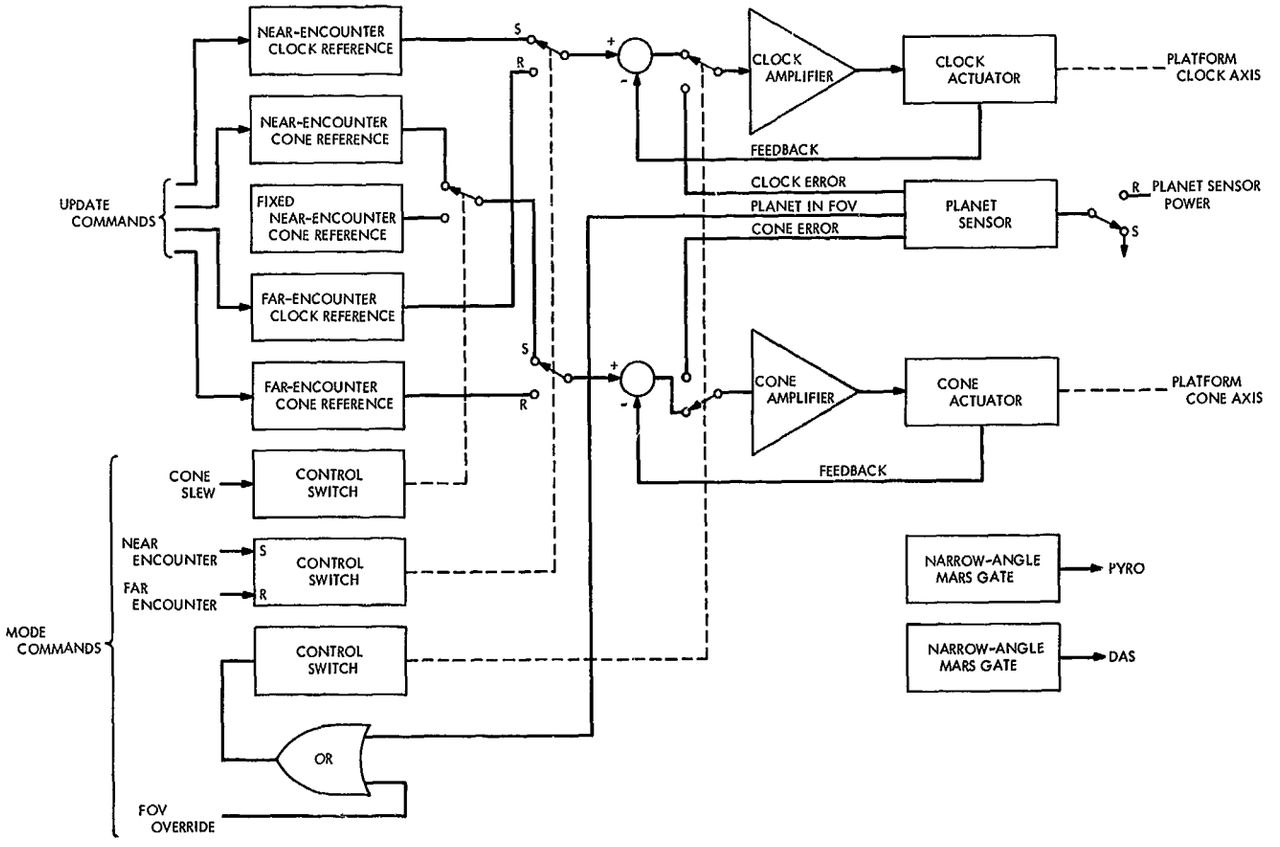


Fig. 24. Scan control system functional block diagram

a series of pointing directions. These pointing directions were fixed angles with respect to the spacecraft structure. They were selected on the launch pad but could be updated in flight and during the near-encounter sequence by quantitative radio commands and CC&S commands. In the cruise mode, the scan control subsystem, with the encounter power off, held the platform stationary in a selected direction. A scan control system functional block diagram is shown in Fig. 24.

1. Scan platform coordinate system. The scan platform coordinate system was a set of right-hand cartesian unit vectors **L**, **M**, **N** fixed to the scan platform and used to define the relative pointing directions of the platform sensors and instruments. This coordinate system is defined in Fig. 25. The **L** vector was the FEPS optical axis and defined the pointing direction of the scan platform. The **N** vector was formed from the cross product of the **L** vector and spacecraft Z axis ($\mathbf{N} = \mathbf{L} \times \mathbf{Z}$). The **M** vector was formed from the cross product of the **N** and **L** vectors ($\mathbf{M} = \mathbf{N} \times \mathbf{L}$). Instrument pointing direction **P** (optical line-of-sight), was specified by the offset with respect to the scan platform pointing direction **L**. The angle from the **L** vector to the $\mathbf{P}_{LM}$ vector (projection of **P** vector onto the **LM** plane) defined the cone offset angle. The cross cone offset angle was defined as the angle from the $\mathbf{P}_{LM}$ vector to the **P** vector. The sign convention used for Fig. 25 is defined as:

(1) The positive cone offset angle is in the direction of increasing cone angle,

(2) The positive cross cone offset angle is in the direction of increasing clock angle.

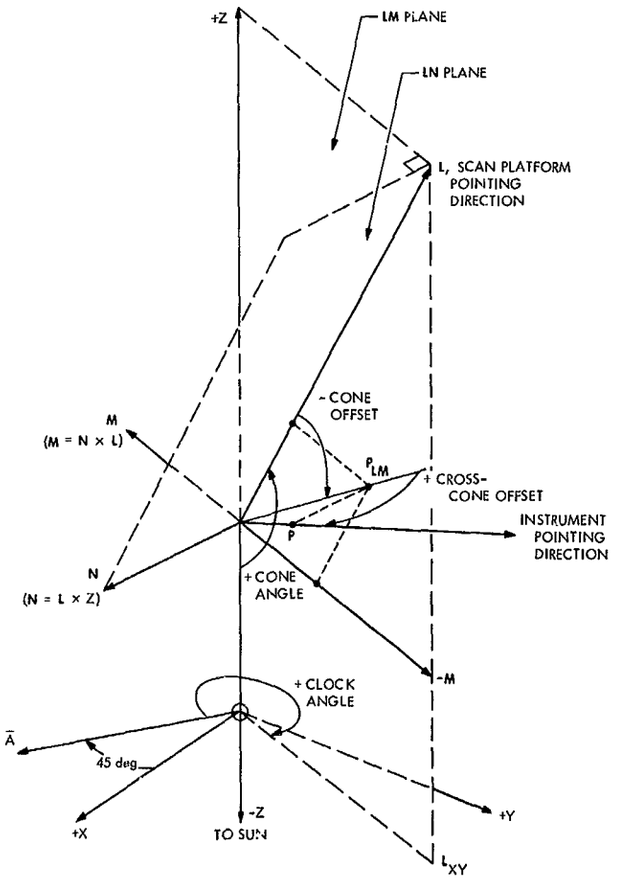


Fig. 25. Scan platform coordinate system

The FEPS, one narrow-angle Mars gate (NAMG-2), TV, and infrared radiometer (IRR) were boresighted parallel to the scan platform pointing direction; no offset was required. The IRS was offset in order to observe the atmosphere of Mars while the TV crossed the bright limb and the tape recorders began storing data. The ultra-violet spectrometer was offset in order to begin observations above the surface of Mars when the tape recorders started. The NAMG-1 was offset in order to initiate IRS cooling before NAMG-2 starts the near encounter sequence.

2. Scan subsystem power. The scan subsystem power supply consisted of a continuous supply and an encounter supply. The continuous power supply was energized from the 2.4 kHz main inverter. This power was transformed and rectified to obtain 5 V and 28 Vdc power. The 5 Vdc power was supplied to the scan control logic and position sensing potentiometers. The 28 Vdc power was supplied to relay coils and stepping motors.

The encounter power supply was energized from the 2.4 kHz main inverter and 400-Hz single phase inverter. These power sources were routed through a relay in the power subsystem which was energized by DC-25 or CC&S-N1. Encounter power was turned off by DC-3, DC-1, CC&S-N5 or CC&S-P1. The 2.4-kHz power was transformed, rectified, and filtered to obtain ±15 Vdc power. The ±15 Vdc power was supplied to the FEPS and scan actuator control amplifiers. A separate winding on the 2.4 kHz encounter power transformer supplied a 2.4-kHz reference frequency to the FEPS. The 400-Hz single-phase encounter power was used to drive the reference winding of the scan platform servo motors; the 400 Hz for the control winding was developed from the 2.4 kHz power supplied to the scan actuator servo control amplifiers.

3. Operating modes. At power turn-on the +5 Vdc power caused a one-shot circuit to generate a nominal 10-ms ground level reset signal. This signal reset the scan control relays in the near-encounter position. In the cruise mode, encounter power was de-energized and the scan actuators could not move the scan platform.

Four reference potentiometers contained the nominal clock and cone angles for the start of both the far- and near-encounter sequences. Each potentiometer was a voltage divider circuit which generated a voltage proportional to the shaft angular position. An additional four potentiometers, directly coupled to each reference potentiometer, provided OSE and FTS monitor voltages. The reference potentiometers were coupled through a gear train to four stepper motors. One revolution of a stepper motor turned the reference potentiometer the equivalent of one degree of scan platform movement. The near-encounter stepper motors (cone and clock) were normally energized by the 28-Vdc continuous power. However, on the launch pad a relay which could be energized by the launch complex equipment switched the 28-Vdc power to the far encounter stepper motors. The far-encounter reference potentiometers could not be up-dated in flight.

At launch, the scan platform was in the stowed position. After the midcourse maneuver, CC&S event C5 or DC-45 signaled pyro to unlach the scan platform.

The far-encounter sequence began with CC&S event N1 which turned on the encounter power. The scan control logic relays were energized in the near-encounter mode. The voltages from the cone and clock reference potentiometers were compared with the voltages from feedback potentiometers which were linked directly to the scan platform cone and clock gimbals. An error voltage was developed which drove the platform at a rate of approximately 1.3 deg/s in cone and clock until the feedback potentiometers were nulled by the reference potentiometers.

The CC&S event F1 switched the scan control logic to the far-encounter mode. This event was backed up by DC-28. The FEPS was energized through a relay. Relays selected the far-encounter reference potentiometers and the scan platform moved to the far-encounter position. When the planet appeared in the field-of-view of the FEPS a planet in field-of-view (PIFOV) signal energized a relay which selected the FEPS control. This signal was backed up by DC-35 which energized the same relay by setting the FEPS control flip-flop. The scan platform moved to null the FEPS cone and cross-cone error signals slaving the scan platform to the planet center-of-brightness.

The near-encounter mode of operation was initiated by CC&S event N1 or DC-25. Power was removed from the FEPS. The near-encounter reference potentiometers were then selected. The FEPS PIFOV signal was inhibited which transferred control from the FEPS to the reference potentiometers. The scan platform moved back to the near-encounter position. The CC&S event N6 enabled NAMG-1 and NAMG-2. When the planet attained sufficient brightness, NAMG-1 initiated the start of IRS cooldown. This was followed by NAMG-2 which started the near-encounter sequence. During the near-encounter sequence, the CC&S sent a variable length pulse train which updated the near-encounter reference potentiometers. The scan platform was slaved to these reference potentiometers and moved in clock and cone. The CC&S event N4 switched near-encounter cone angle control from the reference potentiometer to a fixed voltage divider circuit. This circuit provided the reference for the scan platform final cone angle position.

B. Planet Tracking and Acquisition Sensors

1. Far-encounter planet sensor. The FEPS provided two-axes pointing signals to the scan control subsystem to direct the scan platform at the center of the illuminated portion of the planet during the far-encounter phase of the mission. The two pointing (error) signals were proportional to the displacement between the center of the illuminated portion of Mars and the FEPS optical axis.

a. Operational description. Light from Mars entered the objective lens of the FEPS and was focused on detectors in two different locations by means of a beam-splitting mirror. Each of the two silicon photovoltaic detectors was a dual unit consisting of two half cells. The half cells were sequentially connected to a single amplifier by a multiplex, time-shared, modulator so that a simple radiometric balance was obtained in each control axis when the FEPS was properly pointed at the radiometric centroid of Mars. The tracking transfer function was 10 V/deg over tracking error angles of ±1 deg. A saturated output was maintained out to ±5 deg.

Automatic gain control (AGC) was provided by means of pulse-width modulation of the samples from the detector half cells. The AGC was required because the planet diameter changed from 0.285 to 1.40 deg during the far-encounter phase as the spacecraft approached Mars. The change in the FEPS illuminance could be as much as

Table 8. Nominal FEPS parameters

Parameter	Description	Parameter	Description
Error signals		**PIFOV signal**	
Signal type	DC analog	Signal type	DC digital
Error output	Two axis	Signal magnitudes	4.6 ±0.5 V (PIFOV)
Total range (saturated)	±5 deg		−0.5 ±0.5 V (no PIFOV)
Linear range	±1 deg	Output impedance	5 kΩ
Linearity	0.3 V/deg	Time delay (turn off)	1 s
Scale factor	10 V/deg ±30%		
AGC range	25:1		
Frequency response (−3 dB)	10 Hz	**Miscellaneous**	
Phase shift	6 deg at 1 Hz		
Output impedance	1 kΩ	Power consumption	0.75 W
Threshold and resolution	0.01 deg	Weight	3.3 lb
Accuracy	0.2 deg	Volume	75 in.^{3}
Channel separation[a]	43 dB		
Mounting alignment (around LOS)	0.4 deg		

[a]Corresponds to an orthogonality of 0.4 deg

24.2:1. The AGC signal was derived from the sum of the four half-cells' outputs.

A PIFOV signal was derived from the AGC signal to act as a threshold indication that the FEPS was functioning and that the error signals were available for controlling the scan platform servo system. The error signals were conventional phase-reversing dc signals, and the PIFOV signal was a level change from 0 to approximately 4.6 V. There were no moving parts in the FEPS. Both 2400 Hz square wave power and 15 Vdc power were used.

Table 8 provides a listing of the nominal FEPS parameters. A simplified schematic of the FEPS, consisting of lens, beam splitter, detectors and processing electronics, is shown in Fig. 26.

b. Electro-optical description. The FEPS configuration is shown in Fig. 27 and an exploded view is shown in Fig. 28. The unit had an approximate 12-in. overall length and 3-in. diam. The exploded view in Fig. 28 shows the major subassemblies of the FEPS. The heart of the sensor was the beam splitter and detector assembly. This assembly housed both silicon detectors and the polka-dot beam splitter. The beam splitter slid into the main housing and was positioned with respect to the lens (focus) by means of a threaded rod connected to the main housing. Built into the beam splitter housing were the translational and rotational adjustment devices for the silicon detectors. By providing translational and rotational adjustment of the detectors with respect to the boresight axis of the sensor, the detector bisecting line could be made to fall exactly on the optical axis and, thereby, greatly reduce null error and increase overall pointing accuracy.

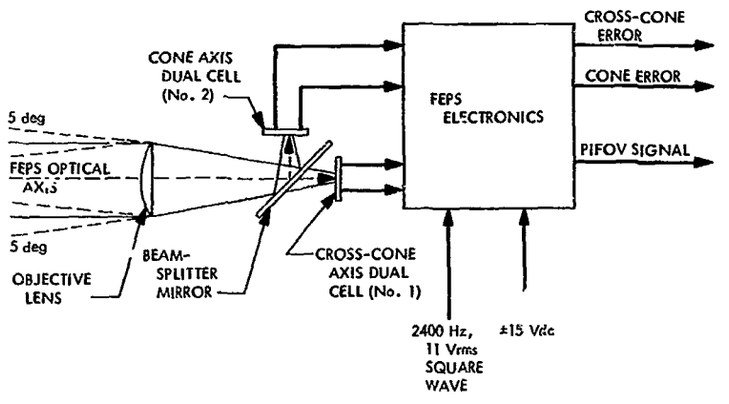


Fig. 26. FEPS simplified schematic

c. Detectors. There were two detectors per FEPS; the detectors were circular photovoltaic silicon cells with an approximate 0.6-in. diam. The detector diameter and lens effective focal length (EFL) combined to define the FEPS field-of-view, which was a 10-deg circular cone. The dual feature of the detector was obtained by producing a mesa-etched border and dividing line; this delineated the active cell areas and provided a common anode. The cathode leads were soldered to an electroless nickel solderable area deposited around the detector periphery.

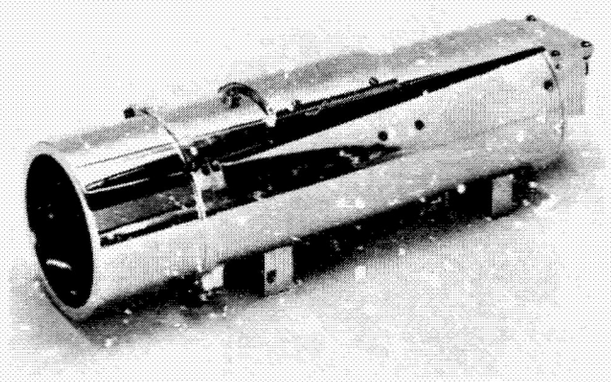


Fig. 27. FEPS mechanical configuration

The silicon detector was fabricated from N on P, 10-Ω-cm material; this material had high-radiation resistance and the desired performance characteristics at low-light levels. The diffusion depth was chosen for maximum voltage output rather than maximum power output as required for solar cells.

d. Objective lens. The objective lens was plano-convex with a 3.5-in. EFL and a 2.0-in. effective diameter. The lens was fabricated from fused quartz and coated with an anti-reflection coating of magnesium fluoride.

e. Beam splitter. A high-efficiency beam splitter, angled at 45 deg to the optical axis, was located immediately behind the objective lens. This beam splitter consisted of a 0.062-in. fused quartz plate with a polka-dot mirror surface. The polka-dots were vacuum-deposited aluminum and acted as individual mirrors. Each dot had a 0.049-in.

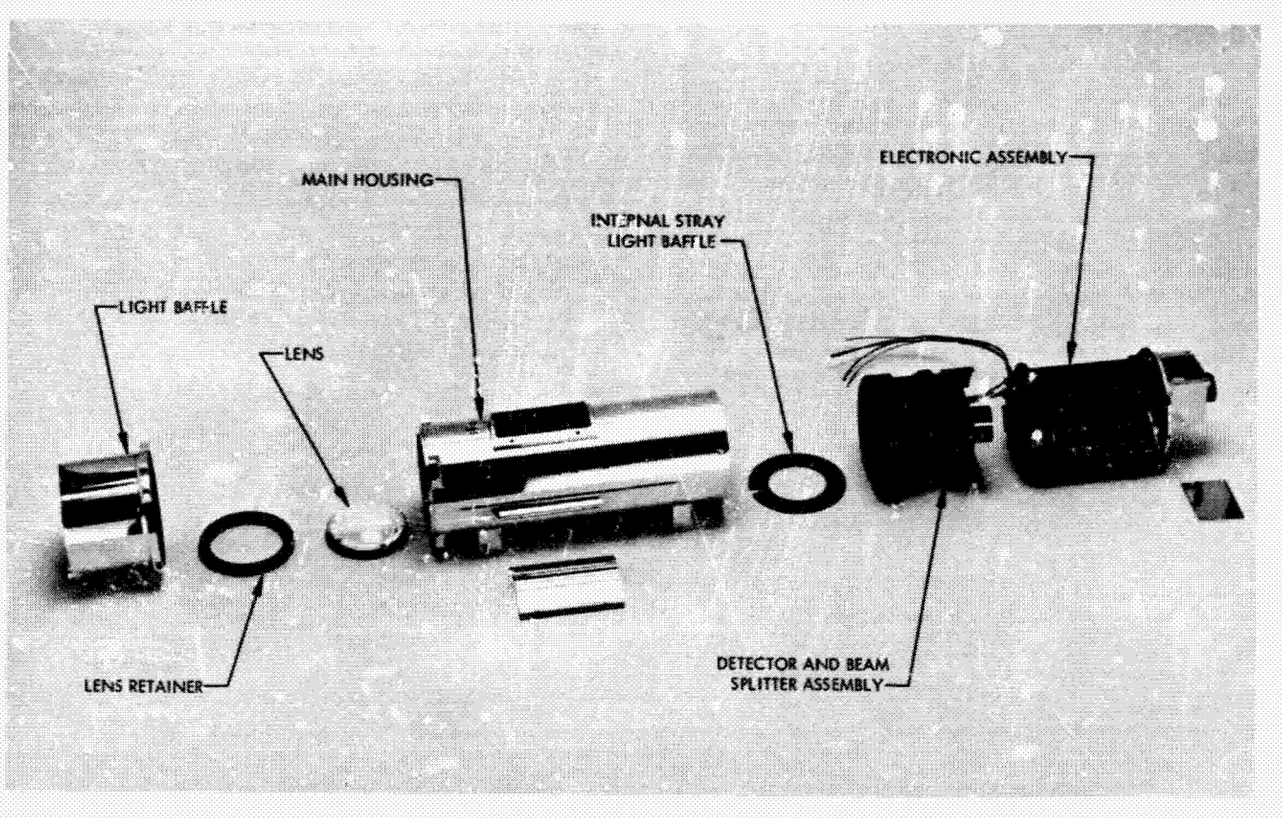


Fig. 28. FEPS subassemblies

diam and was deposited in a rectangular grid pattern. The ratio of reflecting area to transmitting area was adjusted to evenly divide the radiant energy between the two detectors. Both surfaces of the beam splitter were coated with an anti-reflective coating of magnesium fluoride to minimize reflective losses.

f. Electronics operation. The complete FEPS electronic block diagram is presented in Fig. 29. A very general description of FEPS circuit operation follows.

The FEPS electronics sampled a complete set of detector output voltages 600 times/s. The amplitude of each sample was analogous to the irradiation of the corresponding sector. The automatic gain control (AGC) was accomplished by reducing the width of the sampled pulses. The 2400 pulses/s pulse train was then ac amplified and distributed to three demodulator circuits. One demodulator operated synchronously at the 2400-Hz rate to generate an AGC voltage. A low-pass filter removed the ripple component giving a voltage that was an analog of the total irradiance within the FOV. This voltage then went to a pulse-width modulator that established the width of the sampling pulses.

The amplified signal was also fed to two identical demodulator/output amplifier circuits. The demodulator in each was driven by the same logic that sampled the detector voltages. The demodulation generated a voltage proportional to the difference in the areas of corresponding pairs of pulses. This voltage was then dc amplified and filtered by the output amplifier. This amplifier was connected to operate as a filter with a break frequency of approximately 14 Hz. The smoothed output voltage was an analog of the angular error and had a tracking transfer function of approximately 10 V/deg.

g. Sensor performance. All of the original design parameters were met or exceeded by the FEPS flight units. Following the completion of the last unit, the far encounter flight sequence was changed. The original dynamic range of operation was from encounter E minus 48 h ($E - 48$ h) to $E - 12$ h, and the FEPS was designed for this range. A series of tests was performed to determine the FEPS operating characteristics with respect to an extended range of operation of $E - 76$ to $E - 4.5$ h. It was shown that satisfactory operation of the FEPS could be obtained from $E - 76$ to $E - 7$ h for all three flight units. Two of the flight units could also perform satisfactorily down to $E - 4.5$ h, which met the desired performance. Although the sensor was not designed to meet the accuracy requirements at $E - 4.5$ h, it functioned with sufficient accuracy to orient the scan platform to the planet and allow satisfactory television picture coverage.

i. Test procedures and results

Functional tests. All FEPS units underwent a complete series of functional tests to verify compliance with the design requirements. The following specific functional tests were performed:

(1) Transfer curve characteristics.

(2) Orthogonality.

(3) Mounting alignment.

(4) PIFOV signal characteristics.

(5) PIFOV threshold.

(6) Resolution.

(7) Accuracy.

(8) Bandwidth measurement.

(9) Voltage and frequency margin.

The results of these tests showed that all the FEPS units met or exceeded the design requirements.

Extended operation testing and results. The original *Mariner* Mars 1969 design requirements of the FEPS required the device to point to the center of illumination of Mars within an accuracy of 0.2 deg (0.14 deg per axis). The nominal dynamic range of operation must extend from $E - 48$ h to $E - 12$ h. A third requirement defined the scale factor of the output transfer function as 10 V/deg ±30%. Functional test data for the flight sensors S/N 003, S/N 004, and S/N 005 showed that the requirements were met by all three sensors.

Testing was also conducted to provide data on the operational performance of the FEPS over a far-encounter sequence dynamic range from $E - 76$ h to $E - 4$ h.

Extended operation test conclusions. The results of the extended operation tests showed that the three flight-model planet sensors operated satisfactorily from $E - 78$ h to $E - 7.5$ h. The desired null pointing accuracy of 0.2 deg was met only by S/N 004. Both S/N 003 and S/N 005 had somewhat larger errors at these extended operating ranges, although the largest error seen was 0.25 deg. The scale factors decreased at far and near extremes because of the lack of dynamic range of the internal AGC system of the planet sensor, but this decrease only had second-order effects on null pointing accuracy.

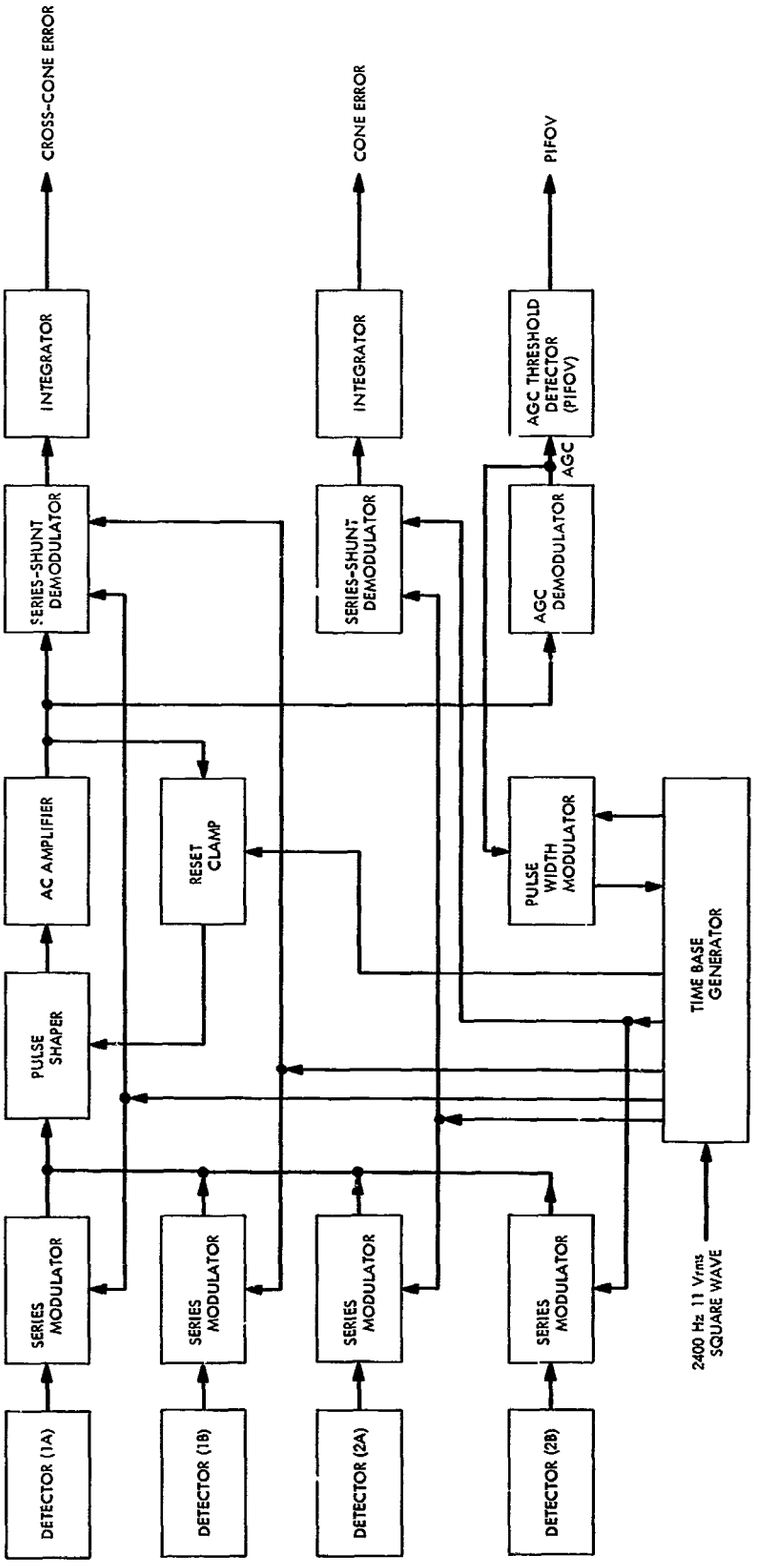


Fig. 29. FEPS electronics block diagram

For operation between $E-7$ h and $E-4$ h the FEPS exhibited null errors greater than 0.2 deg and highly degraded scale factors. The planet sensor S/N 003, because of electronic saturation, could not operate closer than $E-7$ h.

j. Environmental tests

TA tests. The PTM planet sensor S/N 002 was subjected to TA testing. The engineering prototype fabricated at JPL had previously been successfully tested to TA levels of pyro shock and acoustic irradiation. The only failures in the TA environmental test were those that occurred during thermal vacuum testing.

The PTM unit was successfully calibrated with the knowledge gained from the previous unit. However, when the unit was subjected to low temperature during TA testing, the PIFOV circuit gave a PIFOV signal with no applied stimulus. This problem was solved by a redesign of the AGC circuit (component value changes and zener diode addition) that consequently resulted in satisfactory operation in all temperature ranges.

When the unit was replaced in the TA testing, it again failed; this time, when tested under high temperature. The cause of the failure was subsequently determined to be a silicon detector problem. The failure was not due to a particular failure of the detector, but rather to a difference in temperature coefficients between the two detectors. At elevated temperature, the outputs of the two detectors were separated by a voltage whose magnitude was too great for the processing electronics to handle. When the detector pair was replaced with a pair having matched temperature characteristics, the unit performed satisfactorily. The detector problem was prevented from occurring in the flight units by choosing detector pairs with satisfactory temperature characteristics.

No mechanical failures of any sort occurred during any TA test.

FA tests. The three flight model planet sensors were subject to FA levels of thermal vacuum tests and sinusoidal and random vibration tests; no failures or anomalies occurred.

Life test. The PTM planet sensor S/N 002 was installed in a life test configuration on Oct. 18, 1968. The unit was operated at ambient temperature and pressure for a period of nine months, during which time it remained in a POWER ON condition with no optical input. At specified monthly periods the unit underwent a series of margin tests using an operational support test hood as the optical stimulus.

Testing to June 1, 1969 showed no operational degradation or anomalies.

k. Conclusions. All of the original design requirements of the FEPS were met or exceeded. Detailed tests were conducted on each flight model planet sensor to establish individual operating characteristics for revising the encounter sequence by enlarging the required dynamic range of the FEPS operation. These tests showed that satisfactory operation of the FEPS was anticipated as close as $E-4$ h 25 min, rather than at the original design requirement of $E-12$ h.

2. Narrow-angle Mars gates. Preparation for the near-encounter phase of the mission was initiated by a NAMG-1, which provided an acquisition signal to the pyro subsystem to initiate infrared spectrometer cooldown. The actual near-encounter sequence was started by an acquisition signal from the NAMG-2 which started the TV picture and recording sequence. A ground command backup was available for both NAMG-1 and NAMG-2 signals.

The design of NAMG-1 and NAMG-2 were identical in design and followed very closely the design of *Mariner* Mars 1964 except for the addition of a rear connector (Fig. 5). The design evolution of that *Mariner* Mars 1964 unit is discussed in Ref. 1.

a. Simulator tests. Since the actual operating conditions were inaccessible, the testing program for the NAMG's used two different simulators. Simulator I was a large, well collimated, well calibrated source used as the primary reference. It provided a 0.5 deg diam planet that was corrected to approximately 3500°K color temperature to match Mars, and was variable in intensity over the range of interest. Simulator II was a very small, uncollimated, and portable source that could be used under confined conditions and during environmental tests. The color temperature was uncontrolled and the intensity was calibrated against Simulator I.

b. TA and FA tests. No difficulty was encountered during TA testing; FA tests were performed without incident on the six flight units.

c. Life test. Since the design of the *Mariner* Mars 1969 NAMG was nearly identical with the design of the *Mariner* Mars 1964 NAMG, which successfully passed

its life test, no life test was conducted on the *Mariner* Mars 1969 NAMG.

C. Scan Control Electronics and Servos

1. Angular reference assembly. The angular reference assembly consisted of four stepper-motor gear-train potentiometer subassemblies, circuits, and switching logic necessary to actuate the stepper motors, and a voltage divider network. The four stepper motor subassemblies were used as variable storage elements for platform pointing angles; near-encounter clock, far-encounter clock, near-encounter cone, and far-encounter cone pointing angles were stored. Additionally, the voltage divider network provided an output voltage representing a second, fixed near-encounter cone pointing angle. The electronic circuits and switching logic included as part of the angular reference assembly provided the drive signals required to move the stepper motor subassemblies to comply with the angular command inputs.

a. Pulse-sum-to-analog converters. Four stepper-motor gear-train potentiometer subassemblies, more correctly called pulse-sum-to-analog converters, were used in the angular reference assembly. The four subassemblies were identical. A block diagram representation is shown in Fig. 30.

Potentiometer 1 of Fig. 30 was used to provide the reference input to the scan platform servos. This potentiometer was identical to the potentiometers used in the platform actuators for position feedback. The commanded platform angle was, therefore, proportional to the position of this potentiometer. The resistive element in these potentiometers was a plastic film which provided high resolution. This type of potentiometer was chosen for its low noise characteristics.

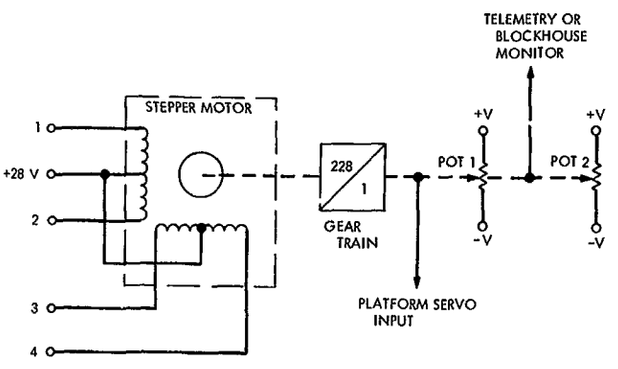


Fig. 30. Pulse-sum-to-analog converter block diagram

Potentiometer 2 in Fig. 30 was used to monitor the angular position stored in the assembly. The monitoring was accomplished through telemetry channels on the near-encounter clock and cone angles and through blockhouse monitor lines on the far-encounter clock and cone angles. The stored near-encounter angles could be updated during flight while stored far-encounter angles could be changed only before launch.

The stepper motor was a 28 V, size 8 device which moved 90 deg per step. Sequential grounding of pins 4, 2, 3 and 1 in Fig. 30 could cause clockwise motor rotation and sequential grounding of pins 3, 2, 4 and 1 would cause counter-clockwise motor rotation.

Since the stepper motor required sequential energizing of four windings to rotate in a specific direction, it was decided to operate the stepper motor subassemblies so that they would always rotate a multiple of 360 deg (either clockwise or counter-clockwise) and stop in a single, unique, rest position. The gear train was then selected to provide a scale factor of 1 deg of gimbal rotation for 360 deg of stepper motor rotation. Since both actuator feedback potentiometers were geared at a ratio of 1.58:1 compared to the platform axes, the desired scale factor required a reduction of about 228:1 between the stepper motor and the potentiometer.

Alternately, it would have been possible to operate the stepper motors so that the required gimbal motion resolution of 1 deg was represented by either 90 or 180 deg of stepper motor rotation. These modes of operation, however, would necessitate building a memory of the stepper motor rotor orientation into the drive electronics so the proper winding could be selected to execute any given command. The mechanization of such a memory, which would have to operate over power transients, was judged undesirable.

b. Stepper motor drive electronics. The stepper motor drive electronics contained the logic and switching circuits necessary to interfa e between the angular command lines and the stepper motor subassemblies. The functional requirements fulfilled by these command lines are provided below:

(1) The stored near-encounter clock angle must be capable of being changed during flight through commands from either CC&S or FCS.

(2) The stored near-encounter cone angle must be capable of being changed during flight through commands issued by the FCS.

(3) All angles stored on the stepper-motor driven subassemblies shall be capable of being changed and monitored for proper operation while on the launch pad.

The angular commands were sent as pulse trains. Each pulse commanded an incremental change of one degree in the stored platform pointing direction. The stepper motors were operated so that a 360-deg rotation represented a 1-deg change in the stored pointing direction. Hence, since the stepper motors move in 90-deg steps for each winding actuation, a sequence of four stepper motor winding actuations was necessary for each input command pulse.

2. Mode control electronics. The scan control system mode control electronics contained all the logic and switching functions necessary to implement the various operating modes and conditions of the system. The mode control electronics accepted a total of seven command signals from other subsystems and three logic control or switching functions generated within the scan control system.

The mode control electronics implemented the following switching and control functions:

(1) Upon receipt of a near-encounter mode command, CC&S-N1 or DC-25, the near-encounter clock and cone reference angles were connected to the inputs of the scan platform servos.

(2) Upon receipt of a cone slew command, CC&S-N4 or DC-41, and while in the near-encounter mode, the cone servo input was transferred to the fixed near-encounter cone reference angle and a relay closure, the automatic aperture control reset (AAC), was provided to the TV system.

(3) Upon receipt of a far-encounter mode command, CC&S-F1 or DC-28, the far-encounter clock and cone reference angles were connected to the inputs of the scan platform servos, and power was applied to the planet sensor.

(4) Upon receipt of either a PIFOV signal (from the planet sensor) or a FOV override command (DC-35), a relay signal which was used to transfer the scan platform servo inputs from the far-encounter angular references to the planet sensor was provided. Coincident with the transfer from angular reference to planet sensor, a one-shot output was transmitted to telemetry event recording channel.

(5) When the encounter power was applied to the scan control system, nominally coincident with CC&S-N1, two telemetry lines were transferred from the near encounter angular references to the platform position fine resolution potentiometers.

The scan control system mode and switching inputs are listed in Table 9.

Table 9. Scan control system mode and switching inputs

Command	Command Function
Inputs from other systems	
CC&S N1	Primary near-encounter mode command
CC&S F1	Primary far-encounter mode command
CC&S N4	Primary near-encounter cone slew command
DC-25	Backup near-encounter mode command
DC-28	Backup far-encounter mode command
DC-41	Backup near-encounter cone slew command
DC-35	Backup up automatic PIFOV switching
Internally generated switching controls	
PIFOV	Switches platform servos between planet sensor and angular references
Continuous power ON	Used to generate reset pulse to control subsystem logic initial conditions
Encounter power ON	Used to switch two telemetry lines from near-encounter angular references to platform multi-speed position readout

3. Scan platform servos. The scan platform servos contained the control elements necessary to provide two axes control of the scan platform. The servos included platform drive actuators and servo electronics for both the clock and the cone axes.

a. Scan drive actuators. The scan drive actuators provided the controlled rotary motion of the scan platform structure which mounted the science instruments. The actuator consisted of a size 11 two-phase servo motor, reduction gearing, including a worm gear stage to prevent back-driving, and a slip clutch (Fig. 31) to provide overload protection during ground handling and testing. A control signal was provided by an output position feedback potentiometer. Two additional potentiometers provided coarse and fine output shaft position angle telemetry data. Figure 32 shows a schematic diagram of the scan actuator. These elements were contained within a sealed pressurized enclosure of polished aluminum (Figs. 33 and 34). The gas used for pressurization was a mixture of 90% nitrogen and 10% helium. The helium trace made

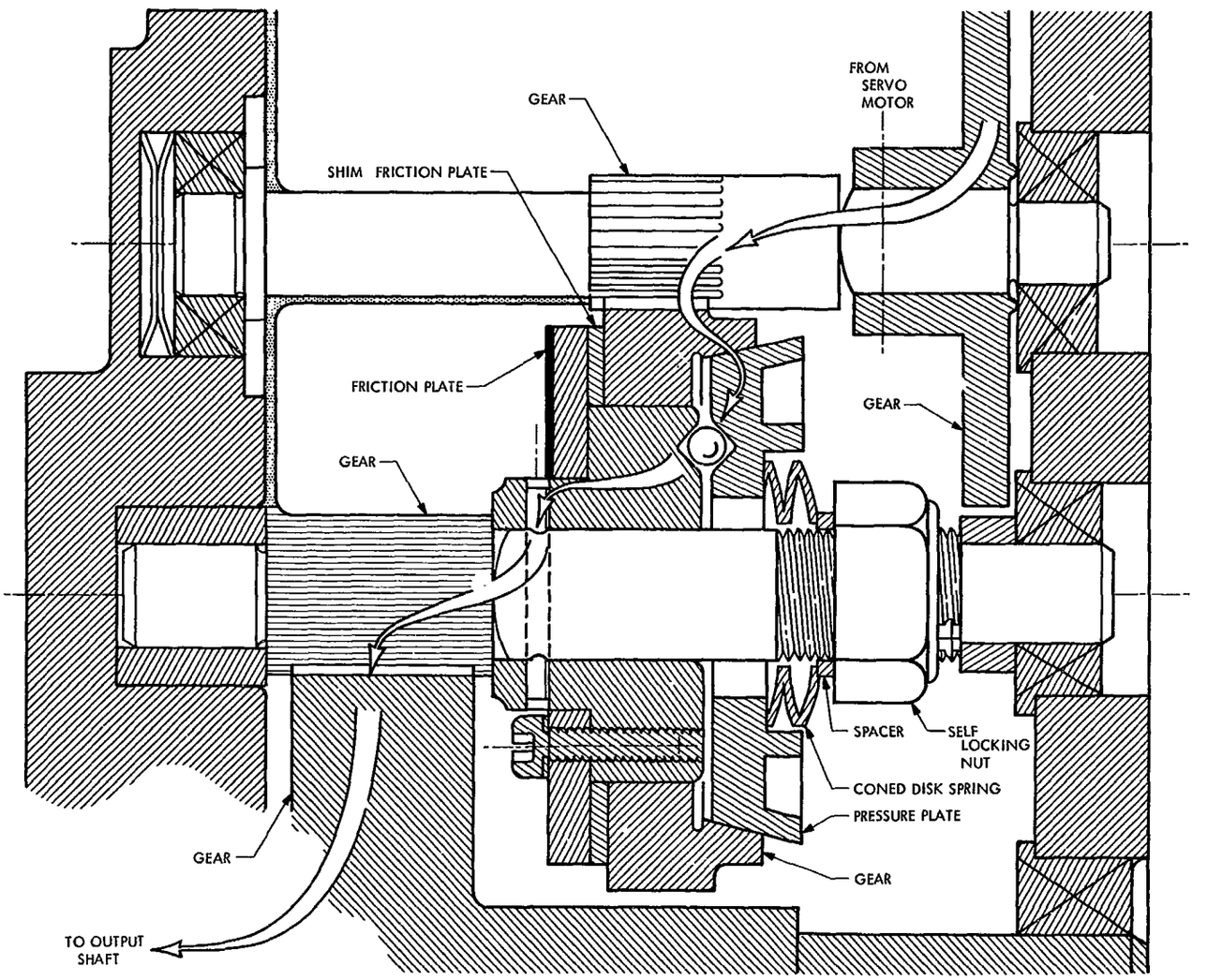


Fig. 31. Scan actuator clutch assembly

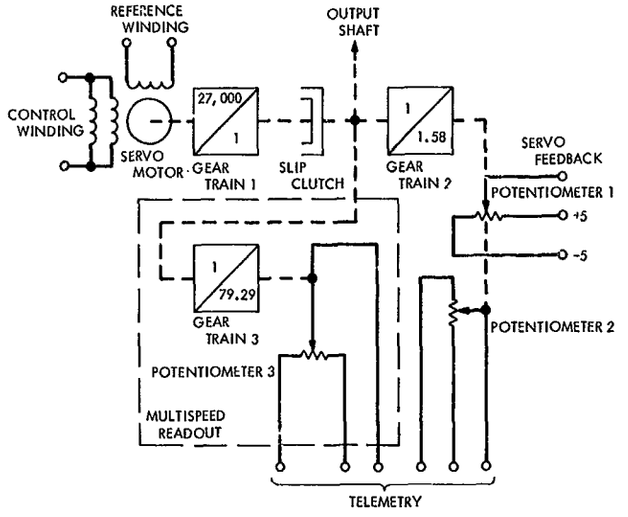


Fig. 32. Scan platform actuator subassembly schematic

it possible to measure the actuator housing leak rate with a mass spectrometer leak detector. A resistance heater was mounted in the actuator to prevent damage during the cruise mode due to low temperature. A box-mounting hermetically-sealed electrical connector mounted on the side of the actuator enclosure provided for electrical inputs and outputs. The actuator's rotary motion was coupled to the scan platform through a crank arm which was keyed and clamped to the actuator output shaft. The arm engaged forks in the platform shaft. The crank arm was not considered a part of the actuator.

The actuators were fitted with mechanical stops which limitted the output shaft rotation to approximately 300 deg.. The function of the stop was to preserve the potentiometer phasing which would be lost if the actuator made more than one full turn, since there was a non-integral gear ratio in the potentiometer drive gearing. The actuator weighed 3.91 lb and was 6-in. long and had a 4-in. diam.

b. Performance characteristics. Average performance measurements of the 10 actuators, along with the predicted performance levels, are presented in Table 10.

The slewing capability of the actuator in deg/s while driving a load is shown on Fig. 35. In the zero-g environment of space flight, the torque load on the actuator while driving the scan platform was expected to be on the order of 20 in.-lb. The efficiency of the actuator gear train was measured to be 41.4%.

Table 10. Scan actuator performance parameters

Parameter	Value		
	Specified	Predicted from design analysis	Test results
Starting voltage, max Vrms	1.5	<1.0	0.3
No-load slewing speed, deg/s	>1.3	1.4	1.4
Clutch slip torque, lb-in.	200-550	200-550	300
Gear train backlash, arc min	<30	13.7	15
Mechanical stiffness, ft-lb/rad	20,000-30,000	30,000	20,000
Static efficiency, %	<50	41.4	41.2

c. Scan actuator testing. The two PTM and six flight scan actuators successfully completed TA and FA testing. A malfunction of a potentiometer in PTM scan actuator S/N 003 was observed during room temperature functional testing after the high-temperature portion of the TA thermal vacuum test. The unit was replaced and TA testing of the unit continued.

Subsequent investigation of the cause of this potentiometer failure and a similar failure of the same type component in the scan electronics was made. It was determined that the design and construction of the potentiometer provided poor reliability of the electrical contact between the resistive element and the end terminals.

All six flight scan actuators were later retrofitted with equivalent, but more reliable, potentiometers from another manufacturer.

d. Scan electronics subsystem tests

Scan control subsystem integration tests. A subsystem integration test was performed using engineering prototype scan electronics and FEPS, production prototype clock and cone actuators, and a mockup platform with one-degree-of-freedom (clock) and bearings and structural characteristics simulating the expected flight configuration parameters. The equipment setup for the tests is shown in Fig. 36.

The first test series, conducted in the normal laboratory environment, corresponded to the near-encounter flight sequence; the control loop was not closed around the FEPS. In this series the positional feedback loop was closed around the actuators, the dynamic performance was evaluated, the reference voltage updating sequence was exercised, and the backup command system was exercised.

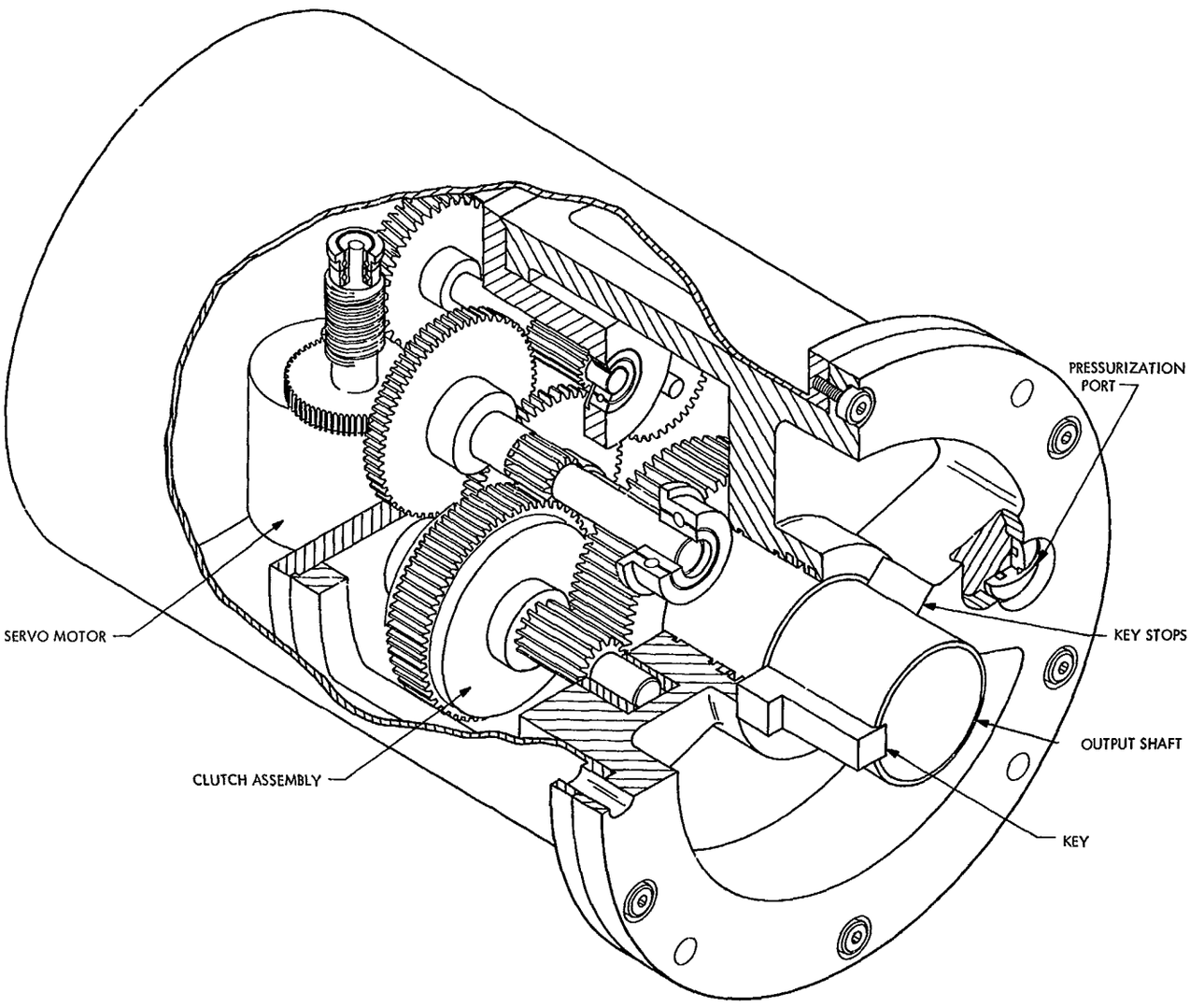


Fig. 33. Scan actuator for *Mariner* Mars 1969: front view



Fig. 34. Scan actuator in sealed enclosure

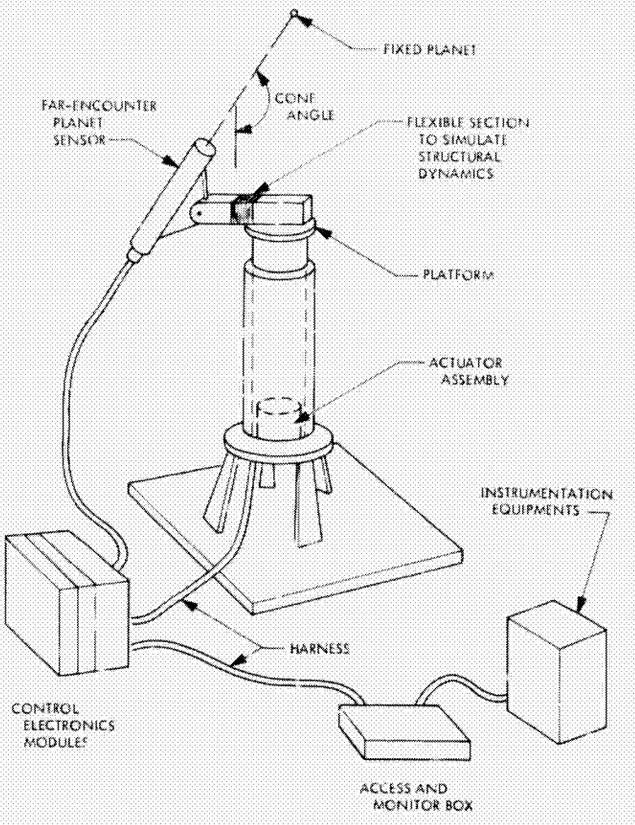


Fig. 36. Test setup

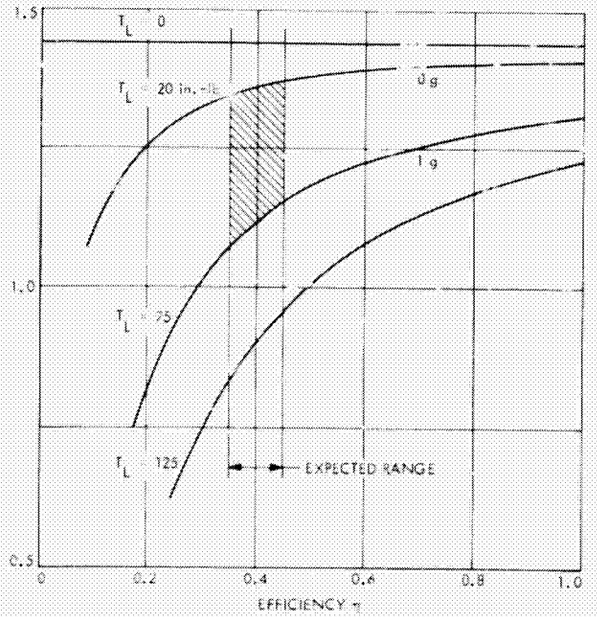


Fig. 35. Actuator slewing performance

In the second series, simulation of far encounter was undertaken in the celestarium with the FEPS control loop closed. In these operations, the drive and structural characteristics were of great importance; interchangeable coupling rods were used in the FEPS mount to provide for controlled variation of structural resonance, and the bearings and other mockup platform elements were chosen to resemble flight configuration.

In the celestarium, an illuminated object simulating the Mars optical properties was used. The Mars simulator was rail-mounted and with the test object mounted in the center of the celestarium, the simulator could be driven in both the cone and clock axes.

The test configuration differed from the actual system operation only insofar as the FEPS was not operated around its null output. The availability of the FEPS transfer characteristics up to several degrees away from null and the high degree of linearity of the FEPS for the operating range warranted this deviation.

A servo analyzer with very low-frequency function generation capabilities was used to evaluate the system bandwidth, the deadband, the subsystem scale factors and other information.

The actuator position was monitored on the available fine telemetry potentiometer. For the purpose of these tests, the voltage on the telemetry potentiometers was adjusted to yield a 1 deg/V scale factor on the fine potentiometer output.

Problems, observations and design changes resulting from the test series are summarized in the following paragraphs:

It was found that a potential race problem existed in the logic design of the circuitry. The logic was modified to eliminate the problem. When it was found that some power switching lines were routed under noise sensitive one-shot integrated circuits causing spurious firing of these units, the wires were rerouted to correct this situation.

Turning on the encounter power caused the stepper motors to increment 1 deg due to coupling of the turn-on transient into the stepper motor electronics. This was corrected by changing the reset pulse to the counter flip-flops from a once-generated pulse at power turn-on to an internally generated pulse available at each step actuation. These changes to the stepper motor drive electronics did not include the addition of any components and were confined to minor changes in the printed circuit board layout.

The servo amplifier engineering prototype showed some small amplitude oscillations when driven into saturation in what was its normal operating mode during slewing. This was corrected by changing the local compensation around a μA709 operational amplifier and modifying the compensation around the overall power amplifier. It was also necessary to add two decoupling capacitors on the board to the ± 15 V supply. To improve amplifier output at saturation, resistor values were changed to allow harder drive.

The tantalum-foil phase-shift capacitors for the actuator servo-motor reference winding were found to be running warm; they had a high power factor. Metallized polycarbonate capacitors were substituted, necessitating an installation change because of the larger size of the new components.

Several switching circuits were found to be biased with insufficient tolerance to accommodate worst-case circuit conditions. A failure in the switching circuitry was encountered during the tests. The circuits were modified to allow for operation under worst-case circuit condition.

Ripple on the -15 V line, brought from the electronics into the FEPS, caused a burst of pulses, in lieu of one, to appear on the PIFOV line. This caused the relay to chatter, transferring servo control from the reference potentiometers to the FEPS. Corrective action was taken by modifying the FEPS circuitry to include a zener diode where a stable reference voltage was required.

Two inductance capacitance filter capacitors on the scan electronics ± 15 V supply were doubled in value, thus lowering the supply voltage ripple during actuator slew by a factor of one-half.

When the actuators were used in conjunction with the scan subsystem in the far-encounter mode, the FEPS error voltage could drive them into a "forbidden" region from which they could not be extricated through the use of commands or resetting the reference potentiometers. This forbidden zone existed because the mechanical stops of the actuator were outside the electrical range of the feedback potentiometer. The actuators could be driven back to their normal operating range by putting the system into the far-encounter mode and driving the actuators through the FEPS. This problem could not occur in flight configuration (actuators coupled to platform) because the platform had its own mechanical stops to limit its range of travel.

TA tests. During the high-temperature thermal vacuum tests, the near-encounter cone-angle reference pot exhibited random drifting. This condition was not observed during the low-temperature portion of the test, nor did it occur during the room temperature test following thermal vacuum. The pot was stable all the way through the vibration tests. At the conclusion of the TA program, failure analysis testing was conducted. During this test, the suspect pot was again subjected to the high-temperature environment. The drifting was also noted during the test. The near-encounter cone-angle reference potentiometer in the servo amplifiers and stepper motors subassembly, S/N 2 was replaced.

Following the replacement of the near-encounter cone-angle reference pot, the scan control electronics was subjected to the following retests: pre-vibration performance tests, one-axis random vibration, post-vibration performance tests, helium leak test, limited visual examination,

thermal vacuum low- and high-temperature test, and a post-environmental test.

The device satisfactorily met all of the requirements of the retest in accordance with the detailed test procedures with the exception of the random vibration spectrum, which was not attained. This was done with the cognizance and approval of JPL vibration personnel.

FA tests. The three flight model scan electronics subsystems successfully passed all of the flight acceptance level thermal vacuum tests and sinusoidal random vibration tests.

Potentiometer retrofit. Extensive investigations of the cause of the malfunction of the cone angle reference potentiometer during TA testing, and of a similar malfunction of the same model component in the PTM scan actuator at a later date, was conducted. The results of the investigations indicated that the design and construction of the contact area between the resistive element and the end terminals of the potentiometer resulted in poor contact reliability characteristics.

All of the near- and far-encounter potentiometers in the three flight scan electronics subsystems were later replaced by an equivalent but, more reliable, potentiometer from a different manufacturer.

Life test. An abbreviated life test of 1290-h duration was run on the PTM scan electronics. The test was terminated in order to make the unit available to the SAF.

The first 500 h of the test were run at ambient temperature and pressure. During the remainder of the test the pressure was ambient and the temperature was 55°C.

A failure of a signetics SE160G one-shot component was observed in the scan logic subassembly about four days before the end of the life test period.

The cause of failure was not conclusively established. The parts failure analysis report on the component indicated that high leakage caused by contaminants entering through a cracked case as the most likely cause of failure. After replacement of the component and successful functional testing, the unit was returned to the SAF for spacecraft system level testing activities.

Scan telemetry calibration tests in the SAF. Scan platform telemetry calibration tests were performed in SAF on the MM69-2, MM69-3, and MM69-4 spacecraft.

e. Test procedure. The scan calibration was performed per JPL procedures. In summary, measurements were taken of the mechanical position of the spacecraft and platform and of the electrical output of the two scan actuator fine- and coarse-telemetry pots at several cone-clock positions on the near- and far-encounter operating ranges of the platform. An inclinometer and theodolite were used for the mechanical measurements, a voltmeter and the spacecraft FTS for the electrical measurements.

The mechanical measurements taken on the spacecraft were two inclinometer measurements of (1) the inclination of the Z-axis to the horizontal, and (2) the rotation of the spacecraft about the Z-axis, taken with the inclinometer axis parallel to the Z-axis. If the platform were kept horizontal, these would be linearly related to the platform cone and clock angles, respectively, with respect to the spacecraft. The clock angle measurement accuracy decreased as the spacecraft Z-axis approached a vertical position. No measurement was taken of the spacecraft rotation about the vertical, hence the spacecraft position was not completely known.

Mechanical measurements of the platform were (1) the level of the N-axis (cone gimbal axis) by inclinometer, (2) elevation, and (3) azimuth of the platform L-axis (reference mirror normal) by an auto-collimating theodolite.

Electrical measurements of telemetry pot excitation and output were taken by a digital voltmeter through breakout boxes and as data number readouts from the FTS.

During the testing it was found that the repeatability of the test data was improved by applying positive torques about the platform clock and cone axes by means of the scan drive actuators. This application of torque tended to keep platform mechanical backlash and deformation at one side of their dead zone during a series of measurements.

f. Test results. The calibration tests and data reductions indicated a typical 1σ calibration error per axis of about 0.12 deg.

IV. Power Subsystem

A. Introduction

Mariner Mars 1969 was modified to a more sophisticated spacecraft than past *Mariners* requiring 83% more power at Mars than *Mariner* Mars 1964, and 47% more

power than *Mariner* Venus 67 at Venus. A large part of the increased power demands for *Mariner* Mars 1969 were due to its scientific instrument package, and for a heater complement to provide proper temperature ambients for instruments. *Mariner* Mars 1964 required no heaters, *Mariner* Venus 67 had one 3 W heater for its magnetometer, while the *Mariner* Mars 1969 heater loads totaled 90 W, 23 W of which were not capable of being turned off. Table 11 compares *Mariner* power subsystem features of several programs.

Table 11. *Mariner* power systems

Systems	*Mariner IV*	*Mariner V*	*Mariner VI, VII*
Solar panel sections	16	12	24
Solar cells	1 × 2 cm P/N	1 × 2 cm P/N	2 × 2 cm N/P
Cover glass	6 mil	6 mil	20 mil
Primary system voltage	25–50 Vdc	25–50 Vdc	25–50 Vdc
Booster regulator output voltage	52 Vdc	52 Vdc	56 Vdc
Booster regulator output power	150 W	150 W	250 W
2.4-kHz voltage	50 Vrms	50 Vrms	50 Vrms
2.4-kHz peak output power	80 W	105 W	200 W
Spacecraft heaters	none	3 W	90 W
Peak steady-state spacecraft power at planet	204 W	184 W	363 W

A larger power demand was one reason for much *Mariner* Mars 1969 power subsystem design modification; switching logic sophistication was another, and a third was modification to withstand the more severe vibration environment imparted by the *Atlas-Centaur* launch vehicle that was used on the *Mariner* program for the first time.

B. Power Subsystem Design and Functional Description

The *Mariner* Mars 1969 power subsystem was designed to support the electrical power requirements of the spacecraft in the various mission phases shown in the power profile of Fig. 37.

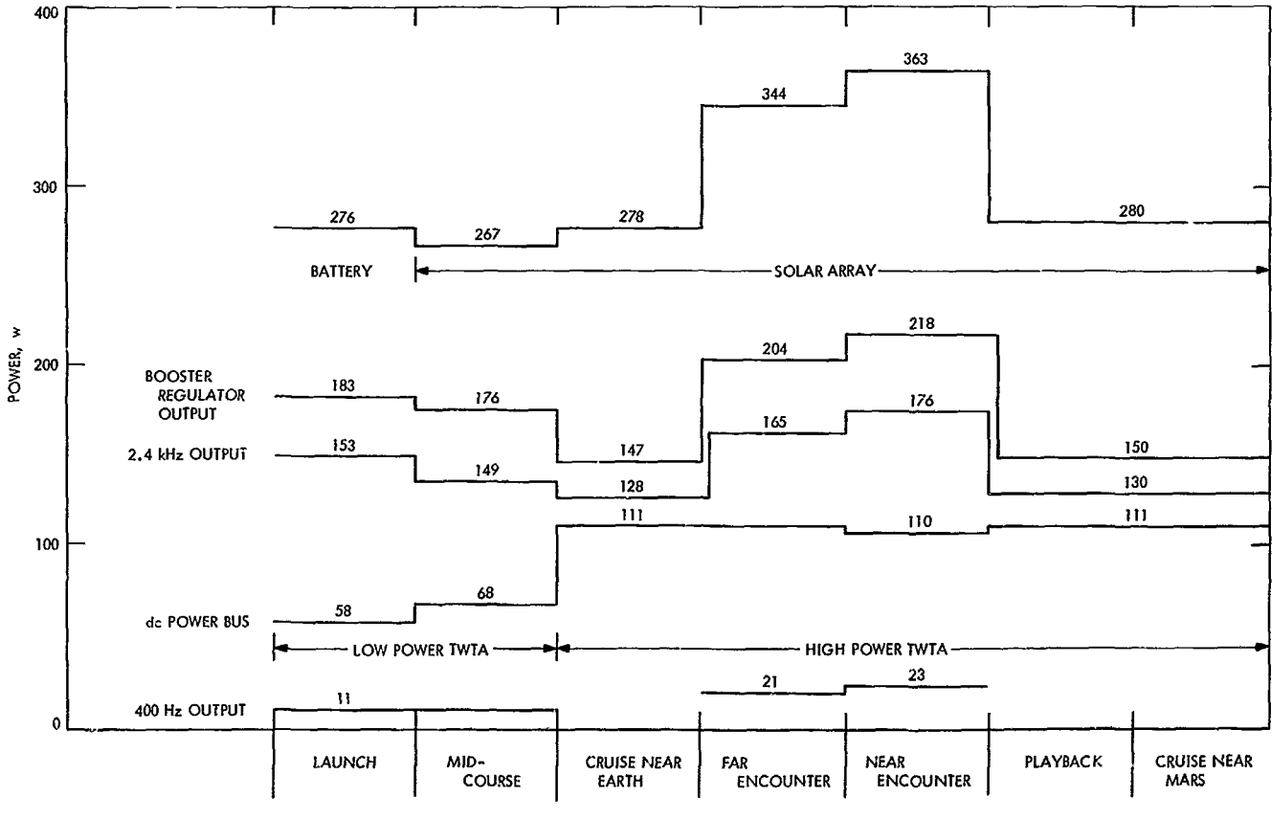
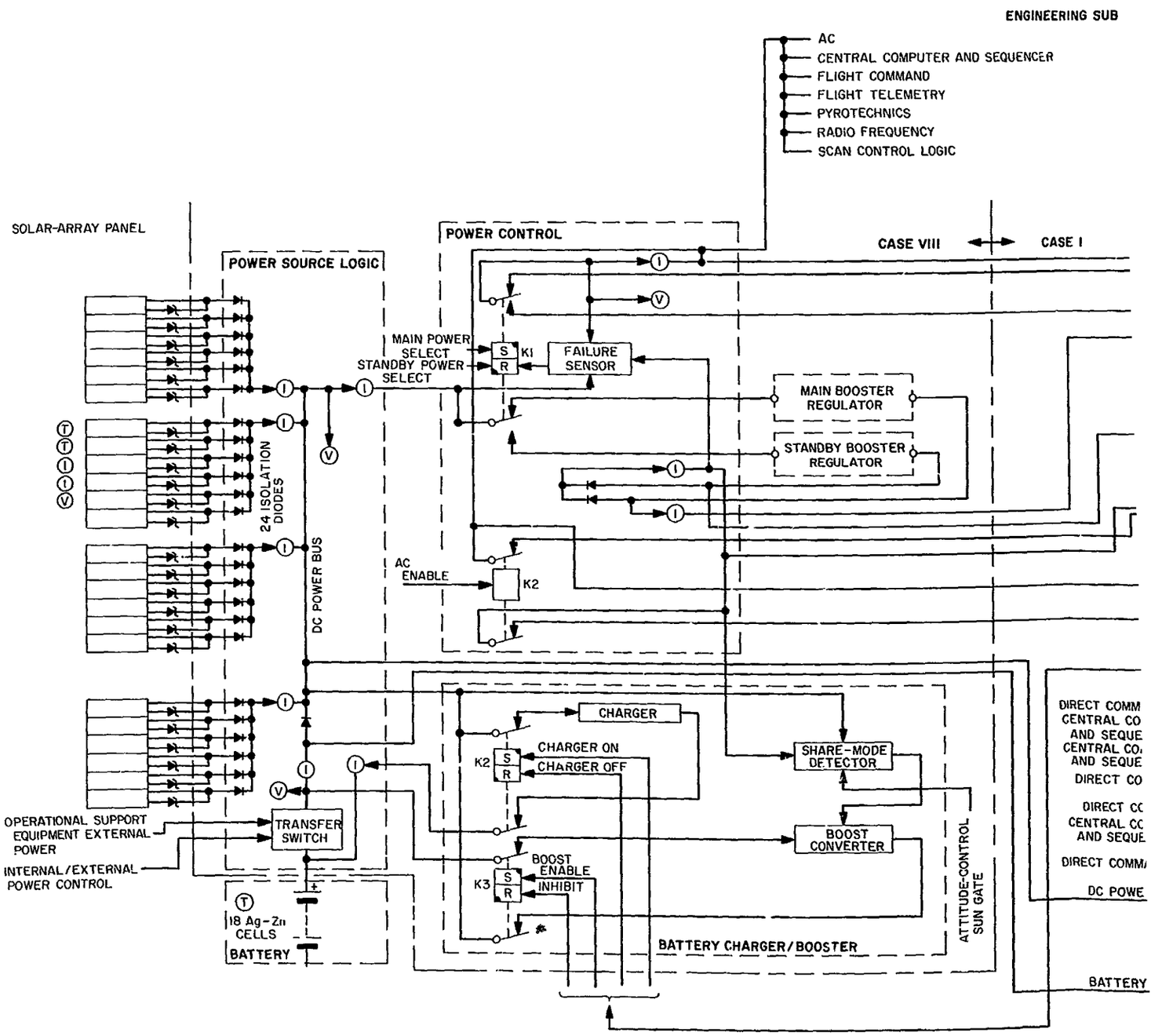


Fig. 37. *Mariner* Mars 1969 power profile



FOLDOUT FRAME

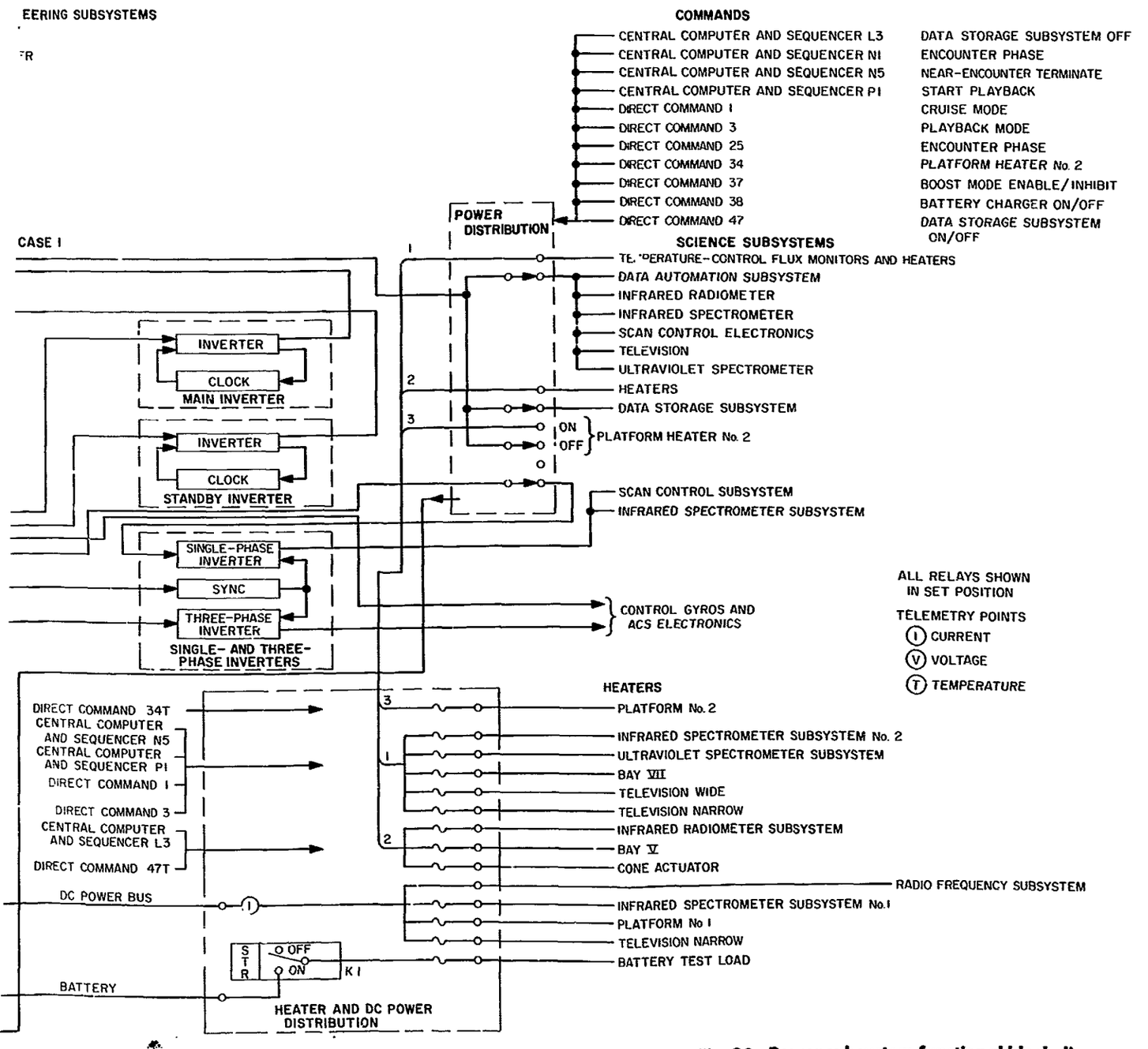


Fig. 38. Power subsystem functional block diagram

FOLDOUT FRAME 2

PRECEDING PAGE BLANK NOT FILMED

The primary source of electrical power for the spacecraft was energy converted from sunlight by four identical solar panels that comprised the solar array. The combined substrate structure area was 83 ft². Each of the four solar panel assemblies were stowed in a plane parallel to the thrust axis of the launch vehicle; pyrotechnic devices on command released the panels that were spring loaded to deploy 90 deg to lock into a position perpendicular to the spacecraft roll axis (see page 84). Automatic spacecraft attitude control maintains the solar array within 5 deg normal to the Sun vector, unless deliberately maneuvered from the Sun as during maneuver for trajectory correction.

An 18-cell sealed silver-zinc alkaline rechargeable battery was the source of spacecraft power during the launch sequence prior to Sun acquisition. The battery was also available as an auxiliary power source should the spacecraft electrical power demand exceed the solar array output power, was maintained fully charged throughout the mission in the event of need. It connected to the dc power bus via an isolating diode (Fig. 38) that was back biased by the solar array operating voltage which normally exceeded the nominal 33-V open circuit voltage of the battery. The dc power bus potential decreased with increased loads that required more current. The battery automatically contributed current to the bus to supplement that of the array, should a load have caused the bus potential to decline below that of the battery to forward bias the battery isolating diode.

About one-third of the spacecraft electrical power was utilized directly from the raw power dc power bus at 25–50 Vdc. A booster regulator boosted and regulated the remaining power bus output to 56 Vdc ±1%. This pulse width modulated switching regulator indirectly supported the spacecraft electrical power requirements, except for users of unregulated dc power. Because the booster regulator was not designed to regulate properly when the input voltage exceeded its output voltage, zener diodes clamped the array output to nominally 50 Vdc. Higher array potentials were reached when the array operated cold after emerging from the Earth shadow in the launch sequence, or after an attitude maneuver requiring off Sun array operation, and during post encounter periods when the spacecraft receded sufficiently from the Sun.

The regulated dc output of the booster regulator was converted to 100 V peak-to-peak square wave, 50 Vrms +2, −3%, in an inverter that provided the main power for the spacecraft. As in earlier *Mariner* programs, users conditioned the square wave power to suit their needs. The frequency reference for the spacecraft was the frequency output of the inverter at 2.4 kHz ±0.01% used to time the spacecraft events.

The regulated output of the booster regulator was also converted to 400 Hz in a three-phase inverter that delivered quasi square wave power to the gyroscope spin motors, and to 400-Hz power in a single-phase inverter whose square wave output at 28 Vrms powered the infrared spectrometer motor and the motors that oriented the science scan platform. Both 400-Hz inverters were synchronized by the 2.4 kHz inverter, and had the same nominal frequency tolerance of ±0.01%. Three-phase power was ON during the mission only when the gyros operated; the single-phase power was ON initially at Mars encounter and during post-encounter operation whenever scan platform slews or science instruments were required.

1. Solar array. Each *Mariner* Mars 1969 solar panel substrate was 35.5 in. by 84.3 in., an area of 20.8 ft². A total of 4,368 solar cells were bonded to each of the four solar panels and were insulated from the substrate structure by a dielectric consisting of Epon 956 epoxy adhesive impregnated sheet fiberglass. There were 78 solar cells connected in series in the solar array which were designed to obtain adequate dc power bus potential levels to recharge the battery in the near-Earth space environment. The worst case array design parameter near Earth was the array temperature at 75°C, with 145-mW/cm² Sun intensity. There were 224 cells connected in parallel on the array designed to support the spacecraft electric power requirements at Mars where the worst case design parameter was the array temperature at 17°C, at 69-mW/cm² Sun intensity.

There were six submodule circuits or sections on each solar panel, each section of which was wired to the dc power bus through an isolating diode. The solar panel sections were divided such that 4 had circuits with 9 parallel cells, and 2 sections had 10 parallel cells (Fig. 39). The overall series-parallel circuit was one of several that permitted the maximum number of solar cells to be mounted.

2. Solar cells. Mariner Mars 1969 used 2 × 2-cm N-on-P solar cells for the first time on *Mariner* flights. These cells had a nominally 1 to 3-Ω-cm base resistivity, were 18 mils thick, and had silver-over-titanium vacuum deposited contacts that are solder coated. The cell material is phosphorous-diffused boron-doped silicon. The output of the average bare solar cell used on *Mariner* Mars 1969

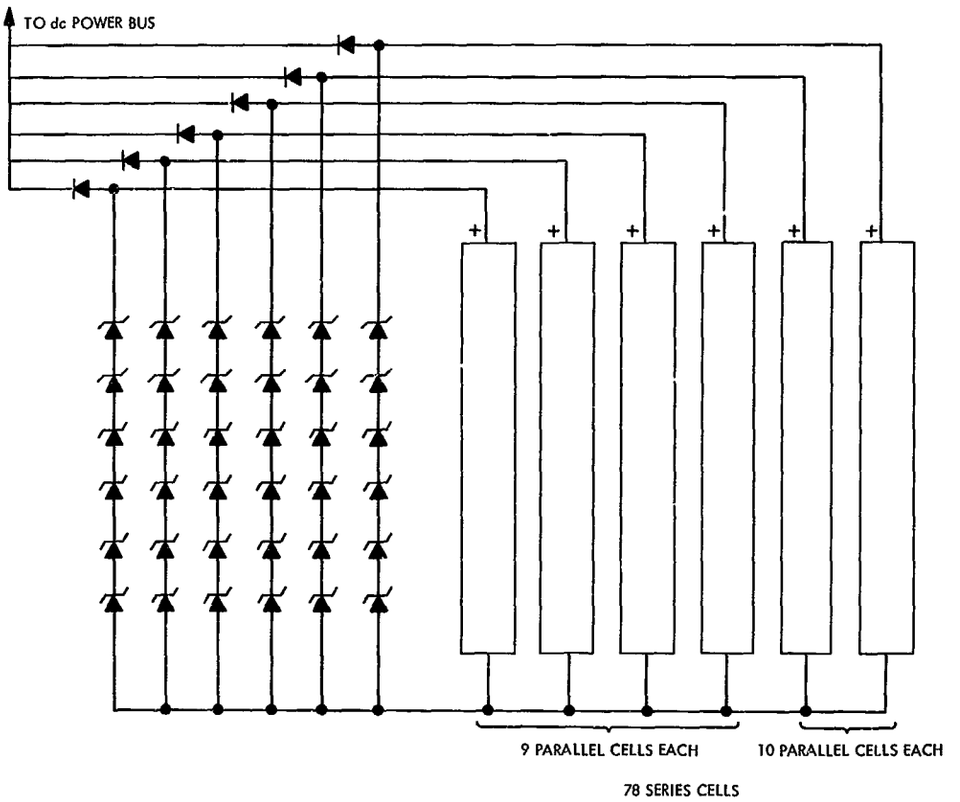


Fig. 39. Solar panel circuit configuration

solar panels was 59 mW of electrical power when illuminated at 140 mW/cm² simulated space sunlight, at 28°C cell temperature, about 11% efficient. Typical bare cell performance characteristics are shown in Fig. 40.

3. Submodules. The solar cells were assembled into 4- and 5-cell submodules that were the building blocks of the 9- and 10-cell submodule circuits. Tunnel oven soldering techniques that were employed in previous *Mariner* programs were again used in *Mariner* Mars 1969 to assemble the solar cells to submodules with the use of tinned kovar bus material. This submodule design reduced thermal stress in the interface between the solar-cell silicon-wafer surface, and the various metals associated with the cell or submodule. The stresses were also associated with divergent coefficients of thermal expansion of various solar panel materials. Bus bars of different designs and materials were fabricated and tested before final design acceptance.

4. Cover glass. Mariner Mars 1969 solar cell cover-glass was 20-mils thick and made of 7094 fused silica to reduce cell radiation damage; it replaced 6-mil 0211 Corning microsheet used on former *Mariner* missions. The new cover glass increased the solar array weight 12 lb. The

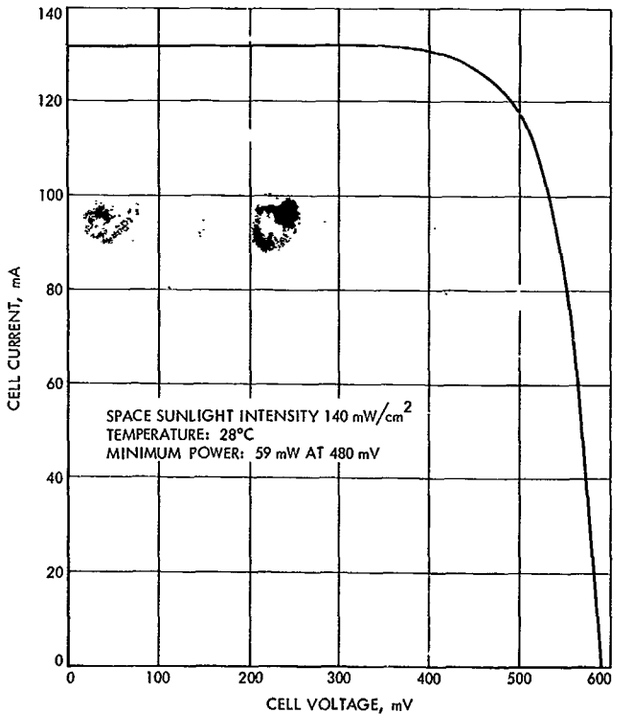


Fig. 40. Bare solar cell characteristics

cover glass was bonded to the surface of the solar cells in the submodule assembly prior to mounting the submodules upon the substrate. The submodules were then electrically tested, and classified for allocation in the submodule circuits.

The 20-mil cover-glass was used for solar cell radiation protection because the *Mariner* Mars 1969 mission occurred during a period of maximum solar activity. The maximum integrated flux expected during the *Mariner* Mars 1969 mission period of 5.5 mo was 4.4×10^9 protons/cm² having energy greater than 30 MeV. It was estimated with 80% probability that the *Mariner* Mars 1969 array power loss due to radiation degradation would not exceed 17% in this radiative environment; this compared to 22% with the use of the 6-mil microsheet.

5. Solar panel diodes. Figure 39 shows the electrical configuration for the zener diode shunt regulator. Each of the 6 submodule sections were shunted by 6-series connected zeners limiting each section and the array at approximately 50 V. The zener diodes had a voltage temperature coefficient of 2.99 mV/°C. The zener diodes were stud mounted to spars on the rear of the panels facing deep space and provided a maximum heat sink for worst case 10.5 W per diode dissipation when the device limited. There were 36 diodes per panel and 144 for the array.

Figure 39 also shows the manner in which the isolation diodes were connected in each submodule circuit. The isolation diodes were located in the power source logic module of the power conditioning equipment.

6. Standard cell transducers. As with previous *Mariner* programs, *Mariner* Mars 1969 solar panels had three solar cell transducers to provide telemetered engineering data. The cells were 1×2 cm because of mounting area limitations, but were otherwise typical of those used for the array, including cover-glass and adhesive. The solar panel mounting location of these transducers is shown in Fig. 41.

Precision resistor loads were selected to measure the short circuit current of two cells and the open circuit voltage of the third, and to provide proper input to the spacecraft telemetry system. On *Mariner* Mars 1969, the resistive loads were not remotely located, but were tested with the transducers as an integral part of the assembly board as shown in Fig. 42; the resistive network is shown encapsulated with RTV-40 to prevent UV damage. The pictured unit was tested on a balloon flown at high altitude and was used on *Mariner VI*. The short circuit of one

Fig. 41. Transducers mounting location on solar panel

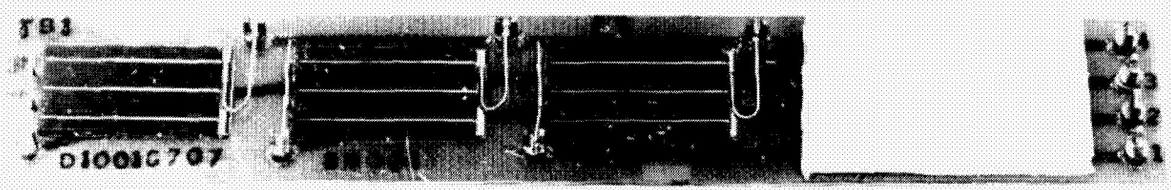


Fig. 42. Solar array transducer assembly board

cell that was monitored had been degraded by about 50% by electron bombardment of 1×10^{15} electrons/cm^2 at 1 MeV, and was rendered relatively insensitive to further radiation damage.

7. Solar panel temperature transducers. Two Trans-Sonics T-4242 temperature transducers were mounted on the underside of the solar panels to monitor the inboard and outboard solar panel temperatures; however, only the +Y solar panel temperatures were telemetered during the mission. These transducer units were used on previous *Mariner* solar arrays, and were again selected for *Mariner* Mars 1969. The transducer mounting locations are shown in Fig. 42 as telemetry channel 419, the inboard, and telemetry channel 439, the outboard solar panel temperatures. The Iso-Voc transducer telemetry provided additional temperature information that was correlative to the panel temperature transducer data.

8. Substrate. The *Mariner* Mars 1969 solar panel substrate structure was longer than that used for the *Mariner* Venus 67 program; construction details, however, are similar. The *Mariner* Mars 69 utilized a 5-mil aluminum skin surface that was bonded to 5-mil lateral aluminum corrugations. Flanged lightening holes were again used in the corrugations and spar units to minimize weight and improve the heat radiative capability from the rear of the panel. The back surface of the *Mariner* Mars 1969 solar panels were coated white with a paint having similar high-thermal emissivity properties to the black paint used in previous *Mariner* programs. However, the white paint had a much lower thermal absorptivity coefficient that minimized the array temperature increase due to expected aerodynamic heating during the launch phase with the *Atlas-Centaur* booster.

9. Wiring. As with previous *Mariner* solar panels, a submodule circuit configuration was chosen to position adjacent current paths to flow in opposite directions. In this manner, magnetic fields generated by solar cell currents would tend to cancel.

C. Array Performance

Mariner solar arrays were tested at Table Mountain, California. The current voltage characteristics of each solar panel section was measured at known temperatures, and the performance characteristics of solar cell standards were obtained simultaneously. Extrapolation to space conditions were then made of Table Mountain performance data of the solar panel sections using data obtained from the standards and the following equations:

$$I_2 = I_1 + Isc_1\left(\frac{x_2}{x_1} - 1\right) + \alpha(T_2 - T_1)$$

$$V_2 = V_1 - \beta(T_2 - T_1) - IR_s$$

$$I = Isc_1\left(\frac{x_2}{x_1} - 1\right) + \alpha(T_2 - T_1)$$

where:

α = *Isc* correction factor

β = *Voc* correction factor

I_1 = reference current coordinate

V_1 = reference voltage coordinate

Isc_1 = short-circuit current of the reference data

I_2 = extrapolated current coordinate

V_2 = extrapolated voltage coordinate

x_1 = reference incident solar intensity

x_2 = equivalent solar intensity to be investigated

T_1 = reference cell temperature

T_2 = cell temperature to be investigated

R_s = panel effective series resistance

1. Tests.

a. Special tests. Sample panels were assembled and tested in environmental conditions that were more severe than those required to pass TA levels. Various candidate submodules were fashioned and connected into sample solar panel circuitry to test for final selection of materials, designs, and fabrication techniques.

b. Solar panel tests. The final design selection was tested once again, this time as a TA solar panel in a full solar panel configuration. Qualification tests included temperature-humidity, vibration, thermal-vacuum, thermal-shock, and acoustic. Performance tests at Table Mountain were repeated after each TA environmental test, and the TA solar panel qualified after each.

c. Flight acceptance tests. Each of 10 flight panels was flight accepted after tests in thermal-vacuum, single panel vibration, and spacecraft vibration. *Mariner VI* was assigned solar panels serial numbers 003, 004, 006, and 007; and *Mariner VII*, 005, 008, 009, and 011. The minimum expected solar array performance of both spacecraft is tabulated in Table 12. Serial number 010 and 012 were designated flight solar panel spares. The predicted solar array output performance of *Mariner VI* and *Mariner VII* were virtually the same based upon ground tests of the individual solar panels. Predicted *Mariner* Mars 1969 nominal solar array performance during various mission phases is shown in Fig. 43.

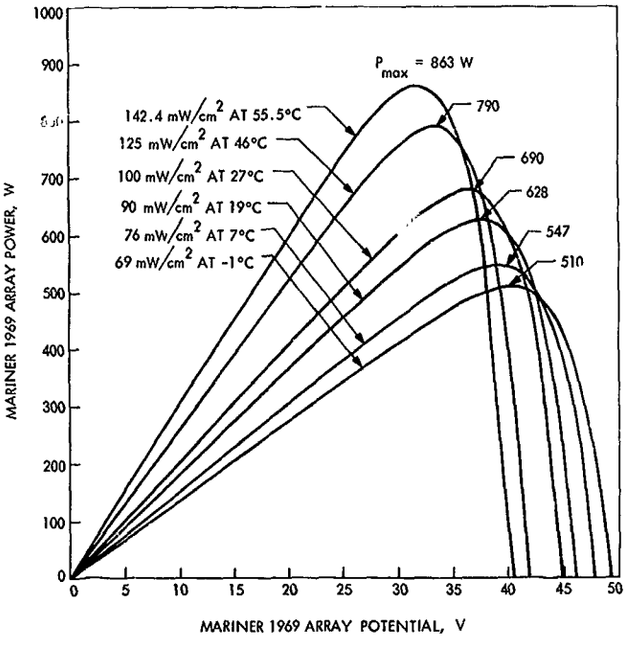


Fig. 43. *Mariner* Mars 1969 nominal solar array performance characteristics

Solar array development. The following are areas of *Mariner* Mars 1969 solar array development that required special attention.

a. Contact delamination. Initial production lots of solar cells exhibited contacts that cracked and delaminated from back surfaces in temperature cycling at 25°C/min that approximated rates which could be expected during the mission. Uneven solder thickness on the P surface of the cells that was particularly heavy near the edges contributed to differential thermal expansion between the silicon cell and the solder. Subsequent solar cell lots were manufactured with new techniques to obtain solder coatings that were thin and uniform in thickness; these withstood thermal cycling with no further contact problems.

b. Low-energy proton damage. As a result of an *Advanced Technology Satellite* experiment (Ref. 3), solar cell power loss was reported and attributed to low-energy

Table 12. Minimum flight solar panel and array performance summary[a]

Array temp, °C	Solcr intensity, mW/cm²	*Mariner VI* array	Panel 003	Panel 004	Panel 005	Panel 006
60	145	799 W at 28.8 V	197 W at 29.0 V	196 W at 29.0 V	197 W at 28.9 V	199 W at 29.0 V
28	100	635 W at 35.5 V	157 W at 33.9 V	155 W at 33.6 V	155 W at 33.6 V	158 W at 33.8 V
2	69	461 W at 37.7 V	114 W at 37.6 V	112 W at 37.0 V	113 W at 37.1 V	110 W at 37.2 V
		Mariner VII array	Panel 007	Panel 008	Panel 009	Panel 011
60	145	786 W at 28.8 V	197 W at 28.7 V	195 W at 28.6 V	199 W at 29.0 V	195 W at 28.9 V
28	100	620 W at 33.5 V	156 W at 33.5 V	154 W at 33.5 V	156 W at 33.3 V	154 W at 33.6 V
2	69	452 W at 37.7 V	113 W at 37.2 V	112 W at 37.1 V	116 W at 37.4 V	112 W at 37.2 V

[a]Data includes 2% solar intensity and 15°C array temperature uncertainties

proton damage to exposed cell areas not completely shielded by the solar cell cover glass. A subsequent study at NASA/Ames Research Center verified serious cell power loss with but 1 to 2% of the cell area exposed to proton radiation at energy levels between 0.2 to 1.0 MeV, with fluxes between 1.3×10^{12} and 2.2×10^{13} protons/cm^2. It was estimated that *Mariner* Mars 1969 spacecraft could encounter proton fluxes of this magnitude with a single proton flare event, and that up to 23% power loss could occur based upon subsequent independent tests. The NASA/Ames Research Center study also verified that the RTV-602 used as the cover glass adhesive provided adequate protection against the low-energy proton damage. Subsequent browning of the silicone adhesive that was unprotected by cover glass was expected to cause 10% of the power loss contributed by degraded exposed silicon surface of the same area, or about 2% degradation of the total solar array output. Accordingly, this material was applied to all areas of the array that may have had small exposed silicon areas due to glass misalignment in assembly

3. *Solar array problem failure reports.* The PFR system was initiated for the solar panel at the first solar panel electrical test.

A discussion of the more important pre-launch solar panel PFRs follows:

a. PFR 200611. Regarding the zener diode anodize coating, an anodize coating on nuts to fasten the zener diode to the solar spars prevented electrical contact to the solar panel structure. The anodize coating was removed from all zener diode stud mounting nuts.

b. PFR 200646. Flight solar panels S/N 003, 004, 005, and 006 did not meet minimum specification power conversion requirements. Causes for the problem were:

(1) Spectral response variation among cells supplied by the manufacturer affected true cell performance characteristics utilized to allocate cells to submodules, and submodules to circuits.

(2) Series resistance variation among solar panels.

Test standardization was modified between the cell manufacturer and solar panel manufacturer.

c. PFR 200650. The S/N 010 solar panel was thermally stressed to environmental test. During the FA thermal vacuum test of flight panel 010 in a 7×14 ft chamber, one section of the light bank failed for 15 min and caused a thermal gradient across the panel. The lowest temperature was 22°F; the highest was 188°F, for a gradient of 166°F. Specifications permitted a maximum 45°F thermal gradient. The solar panel was allocated as a flight spare although there was no evidence of physical damage; nominal electrical performance data was obtained after the event. Stress analyses also indicated that the S/N 010 solar panel was not mechanically overstressed.

d. PFR 204353. Regarding intermittent output temperature transducer, telemetry channel 439 was found to be intermittent at the lead junction to the transducer element of S/N 004 solar panel. Since transducer replacement could damage the solar panel structure, the solar panel was allocated to a position on *Mariner VI* other than +Y. Only the +Y solar panel transducers were telemetered during flight.

D. Battery

1. Electrical characteristics. The prime requirement of the *Mariner* battery was to support spacecraft electric power requirements prior to launch and up to the time the solar array was Sun oriented. It was also sized to provide spacecraft power should the spacecraft attitude adjustment for midcourse trajectory correction require the solar array to partially or totally occult the Sun. Functional requirements specified a minimum battery capacity of 1200 W-h near Earth to serve as a power source for the spacecraft, and 900 W-h near Mars to serve as a power source backup to the solar array at the planet's encounter. Battery energy contribution was not expected during a nominal encounter sequence.

Worst case analyses with limited battery recharge in the time interval between Sun acquisition and a worst-case maneuver, indicated that the electrical design of the silver-zinc battery used in previous *Mariner* missions fulfilled the design requirements for *Mariner* Mars 1969.

A worst case analysis was again performed, Fig. 44, using performance data from initial tests of the *Mariner* Mars 1969 batteries, and the load levels of the then future *Mariner VI* spacecraft during its first ground tests. Initial *Mariner* Mars 1969 battery data suggested that a normally operating battery should provide a minimum of 1323 W-h; this capacity was used for the study. Typical and worst-case launch and flight operation parameters were selected as shown in Table 13. These were based upon estimated prelaunch internal hold intervals when the spacecraft drew upon the energy of the battery for electric power, the worst-case launch dates that required the greatest battery

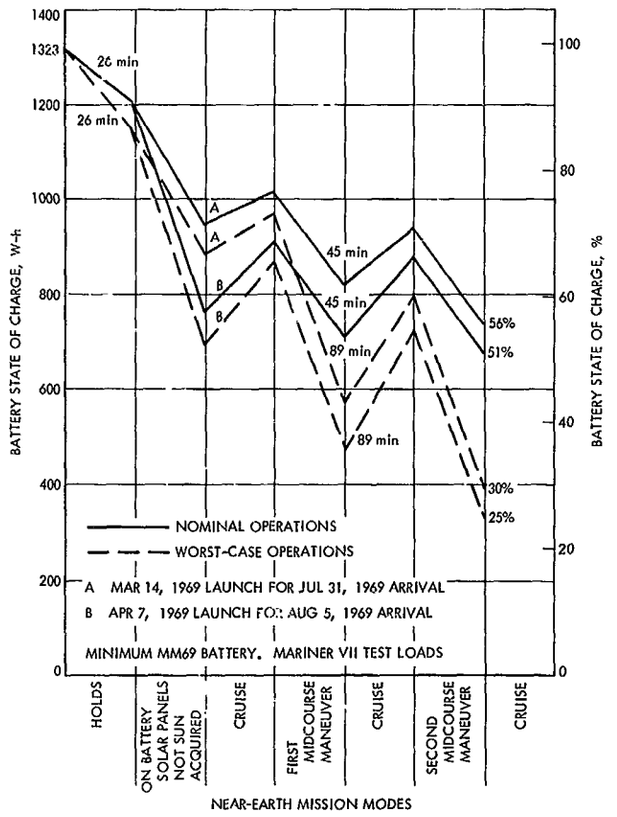


Fig. 44. *Mariner* Mars 1969 battery performance

support prior to solar array Sun acquisition, and worst-angle attitude adjustment off the Sun for midcourse trajectory correction that occults the solar array. Two worst case midcourse trajectory corrections were postulated. The dates are worst case *Mariner VI* launch for a Jul. 31, 1969 planet encounter, and *Mariner VII* for an Aug. 5, 1969 encounter.

The analysis in Fig. 44 indicates the *Mariner* Mars 1969 battery of the minimum expected capacity could sustain a worst-case series of events during the near-Earth portion of the mission, and retain an acceptable 25% state of charge.

Table 13. Operational parameters for worst-case analysis for electrical support of *Mariner* Mars 1969 battery

Parameter	Typical	Worst case
Prelaunch spacecraft battery support, min	26	40
Launch to Sun acquisition battery support, min	57	98
Midcourse maneuver battery support, if solar array was Sun-occult, min	45	89

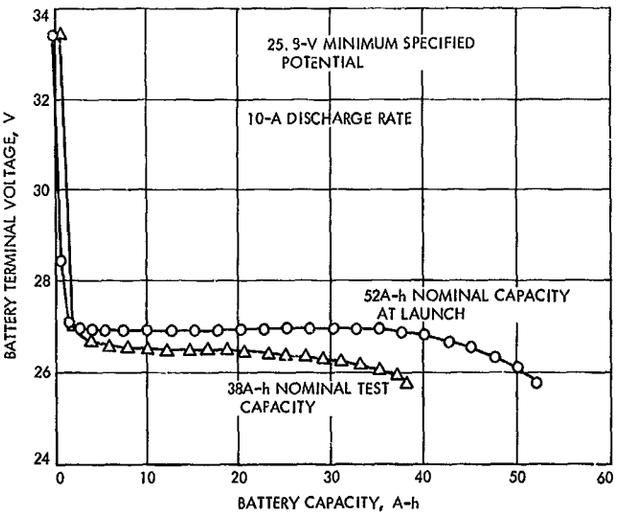


Fig. 45. Battery discharge characteristics

Nominal *Mariner* Mars 1969 battery discharge characteristics at a 10-A rate are shown in Fig. 45. The more frequent battery cycling associated with ground tests caused discharge characteristics at decreased capacity and potential.

2. Mechanical considerations.

a. Vibration. Vibration battery stresses became more severe with each *Mariner* Program. Surveys on *Mariner* batteries and battery cells indicated that the most severe portion of the *Mariner* Mars 1969 TA vibration qualification would be the 13.5 *g* required in the 600- to 2000-Hz range, the most sensitive cell to vibrations at this level was battery cell 14. This cell was in the center of the upper row of cells, as shown in Fig. 46.

Modifications were made both internal to the battery cell and to the battery chassis in order to obtain a battery with adequate mechanical margin beyond the TA requirements.

Increased vibration resistance of the *Mariner* battery at the cell level was investigated in an advanced development program. *Mariner* cells of the old design were more resistant to vibration damage when fabricated with a new plate lock design adapted for *Mariner* Mars 1969. The modifications were:

(1) Wire lead stress relief. A stress relief bend was introduced into the battery cell plate wire lead to reduce wire fracture during vibration, and is seen in Fig. 47. The annealed silver wire leads that were subject to rapid work hardening were also rerouted.

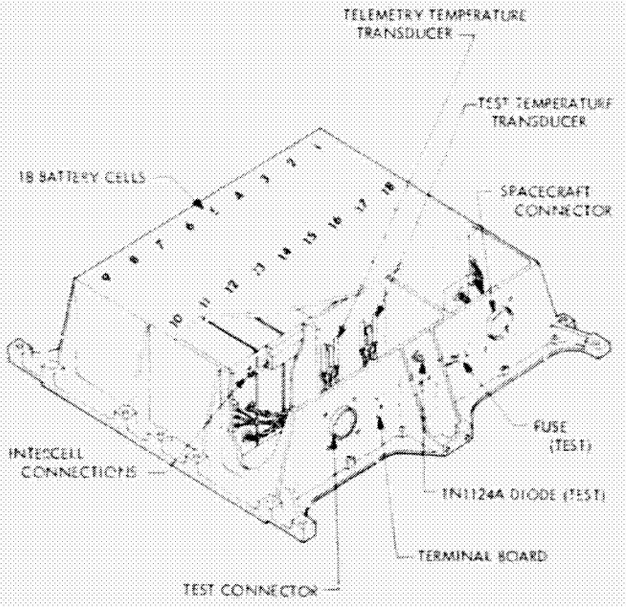


Fig. 46. Battery configuration

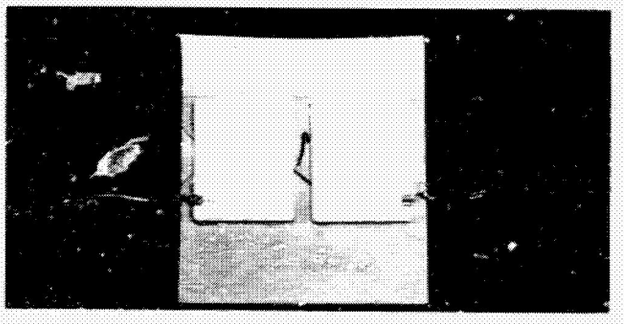


Fig. 47. Battery cell stress relief bend

(2) Plate Lock. An epoxy resin, Bondmaster 639/CH2, was used to immobilize the battery cell plate pack at the bottom corners of the Cycolac container, a jar (Fig. 48). The corner bond, restricted plate pack movement during vibration.

(3) Damping. A visoelastic polyurethane, Solithane 113 300, was substituted for the rigid Epon 815 formerly used to immobilize the upper row assembly (Fig. 49) into the battery chassis. The polyurethane was used to improve battery vibration damping. The row assembly consisted of three monoblocks, three cells to a monoblock.

(4) Chassis. The battery chassis was reinforced with extra webs to limit chassis flexing during vibration and to reduce damaging resonances.

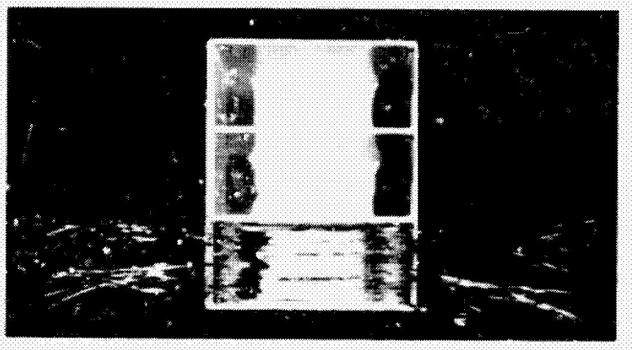


Fig. 48. Battery cell plate back container

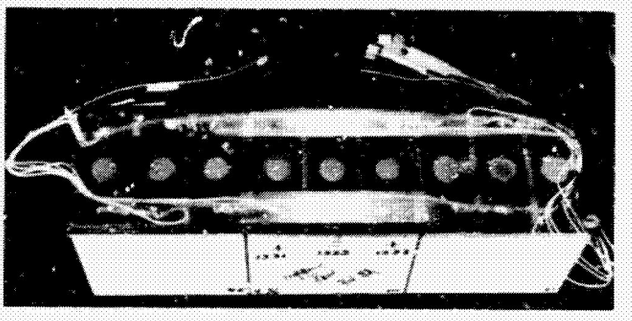


Fig. 49. Upper row assembly

A prototype *Mariner* Mars 1969 battery was used to test two of the modifications; the polyurethane damping and chassis modifications. A tri-axial accelerometer was mounted close to the top center of cell 14 of a *Mariner* Mars 1964 battery used as a control, and upon the *Mariner* Mars 1969 prototype. The *Mariner* Mars 1964 vibration fixture was used. The vibration input was 13.5 *g*, sinusoidal, 600 to 2000 Hz swept at 1 octave/min. The reduction of damaging resonances, particularly during vibration in the Z-axis of the battery where peak levels that cross-couple into the X-axis were recorded at 250 *g* for the *Mariner* Mars 1964 battery, were reduced to 22 *g* for the *Mariner* Mars 1969 prototype.

In order to determine a baseline comparison for the new battery mechanical design, a *Mariner* Mars 1964 battery that was still in good condition, was vibrated at *Mariner* Mars 1969 TA levels. The battery withstood the vibration in the Z- and Y-axes, but catastrophically failed 30 s into the 1-min random noise run in the X-axis, where the cell plates vibrate edge-to-edge, parallel to the electrode working surface. Large current and voltage excursions occurred, with some cell potentials declining to near zero. After the test, electrical measurements indicated 16

of the 18 cells had lead wire fracture. The frictional forces holding the plates in the old design were exceeded by the vibration induced forces at the *Mariner* Mars 1969 TA vibration levels, and caused sufficient plate translation to sever wires. The unrestrained plate pack appeared incapable of meeting of *Mariner* Mars 1969 TA test requirements.

Four *Mariner* Mars 1969 batteries fabricated for TA testing were of two types; two with restrained plate packs, and two unrestrained. The battery chassis, materials, and fabrication techniques in other respects were of the new design for all the TA batteries.

Battery S/N 104, of the unrestrained plate pack design, successfully completed both sinusoidal and random noise vibration tests in the X- and Y-axes, but failed the random noise test in the Z-axis. To probe the feasibility that the vibration runs in the X- and Y-axes may have caused coupling forces in the Z-axis to have weakened the battery, S/N 103 was vibrated first in the Z-axis. The S/N 102 was also a *Mariner* Mars 1969 design with unrestrained plate packs; it also failed the Z-axis random noise test. Data reduction on S/N 103 and 104 indicated that the modes of failure were plate pack movement. Positive plates shorted against negative lead wires, and plate lead wires broke.

The S/N 101 and 102 TA batteries with restrained plate packs passed the TA vibration tests with no observed defects or anomalies; this design was adopted for *Mariner* Mars 1969. A total of 19 batteries were fabricated for use in spacecraft tests, life tests, and as flight and flight spare batteries.

Modifications increased the battery weight by 2.5 lb, exclusive of the battery chassis whose weight increase was 0.7 lb. The modified battery cell met TA vibration levels without failure, and survived peak g levels of 60 g, whereas the former *Mariner* cell design began to fail at peak levels of 20 g. Peak-to-peak battery terminal voltage variation was less than 1 mV during the highest *Mariner* Mars 1969 TA vibration input levels of 10.8 grms random noise for 20 s. These data were obtained from three different batteries of *Mariner* Mars 1969 design; the batteries were vibrated in each orthogonal axis as they discharged at 273 W in launch mode simulation. Battery terminal voltage variation is a function of current density fluctuation related to battery plate movement during vibration.

b. Internal pressure. Environmental tests on charged *Mariner* Mars 1969 cells indicated that the internal pressure on open circuited stand at temperatures between 120 and 140°F was higher than expected. This pressure was found to be caused by reactions between the charged negative electrodes and the material used to inhibit plate pack displacement during vibration. The TA requirement called for a 140°F, 12-day stand and discharge, the same requirement used on the *Mariner* Mars 1964 Program. A cell leak developed after 10 days and the test was terminated. Using the predicted flight temperatures and TA margins, a temperature of 120°F was considered more realistic. In addition, the single discharge was changed to 3 discharges, simulating worst-case launch and 2 maneuvers on a real-time sequencing over the 12-day period at 120°F. The epoxy cure procedure was also modified, and the *Mariner* Mars 1969 TA battery qualified with no further problems with regard to internal pressure.

c. New materials. Fabrication of the *Mariner* Mars 1969 TA batteries also used new materials selected to improve the reliability of the cell, and which had been investigated by an advanced development program and utilized by other flight programs. The new materials were:

(1) Plate wrap. The nylon-dynel plate wrap used in previous *Mariner* programs indicated increased solubility in KOH at high temperatures. This caused the sterilizable battery program to substitute polypropylene wraps, since one of the by-products of the nylon-KOH reaction is ammonia which is reactive with silver. Because high temperatures were used as accelerated life test for batteries, the change was also made for *Mariner* Mars 1969.

(2) Insulation. Heat shrinkable polyolefin tubing replaced the Teflon tubing used as insulation on the plate lead wires. The new tubing provided additional mechanical strength to the wire leads and facilitated assembly.

(3) Storage cell potting. The battery cell sealing potting material was changed from Epon 815 to Bondmaster 639 to provide improved adhesion to the Cycolac cell wall. Previous to the introduction of this material to the *Mariner* program, the superior bonding characteristics had been noted in the *Surveyor* batteries for more than a year.

(4) Storage cell sealing. Electric Storage Battery, the manufacturers of the *Mariner* batteries, developed a new and proprietary cement for sealing the Cycolac cells used on the *Mariner* Mars 1969 units.

d. X-ray inspection. Concurrent with the fabrication of the batteries designated for test use, an extensive X-ray

radiography program was inaugurated on test and production cells to improve and maintain hardware quality. There were a number of battery fabrication steps that must be performed in the blind without adequate subsequent inspection. After the *Mariner* monoblock was manufactured (Fig. 50), inspection was impossible for plate alignment, lead wire dress, and possible voids in potting material. Fabrication techniques were modified when the X-ray inspection program revealed manufacturing problems in these areas. Monoblocks for flight and flight spare batteries were X-rayed and screened for the best quality hardware.

3. ***Flight acceptance tests.*** All *Mariner* Mars 1969 batteries passed FA tests, with no defects or anomalies. Flight battery S/N 117 was installed on *Mariner VI* on Jan. 28, 1969, S/N 118 on *Mariner VII* on Feb. 13, 1969.

Batteries chosen for flight were held in cold storage and mounted into the spacecraft only when the spacecraft was ready to be mated to the *Centaur* booster. Minimum ground vibration tests limited the flight battery component stress, and minimum ground electrical tests conserved cyclic capability for the mission. The flight batteries were identical in design to those that passed environmental tests as components and system tests upon spacecraft. With this procedure, the *Mariner VI* and *VII* spacecraft were provided batteries that were in peak electrical and mechanical condition.

The flight batteries were electrically tested on both spacecraft the week before launch. A battery charge sequence was performed on both spacecraft the day before launch. The prelaunch charge profiles of both batteries are shown in Fig. 51; they differ slightly because of nominal small battery internal impedance variation.

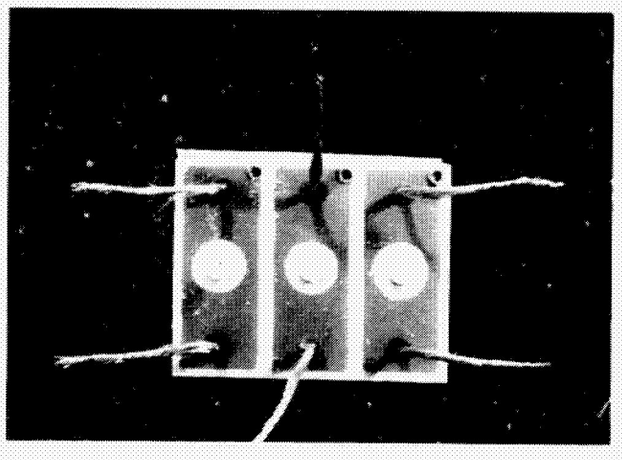


Fig. 50. Three-cell battery monoblock

4. Voltage regulation and battery test load. The internal resistance of a fully charged silver-zinc battery gradually increases as it stands open circuit. Positive battery plate surfaces gradually form a coating, which causes increased internal impedance and impairs transient load voltage regulation. Tests have shown that an open circuited fully charged *Mariner* battery at 33.4 V, having an internal impedance of 0.5 Ω or higher, will undergo a voltage decline of 19.5 V after the application of a 5 to 10 A load. The potential drop lasts for just 40 ms after which the battery recovers to 24 V. In less than 2 s, the potential reaches 26 V. The internal impedance of a typical fully charged *Mariner* 1969 battery was 0.020 Ω. After an open circuit stand of 6 mo, at 75°F, the impedance increased to about 2.0 Ω.

Much of the spacecraft power switching occurred at Mars encounter, where many relays were activated and subsystems were turned on and others off, after months in the cruise state. It was desirable to have a fully charged battery with optimum voltage regulation capability to reduce to a minimum the affect upon the spacecraft of an electrical fault at this critical time in the mission.

Tests indicated that a battery discharge sequence of about 8 to 10 h on the 15-W battery test load, then battery recharge, conditioned the unit to accept a sudden transient load with acceptable voltage regulation. The advantage of conditioning was seen in one such test when a fully

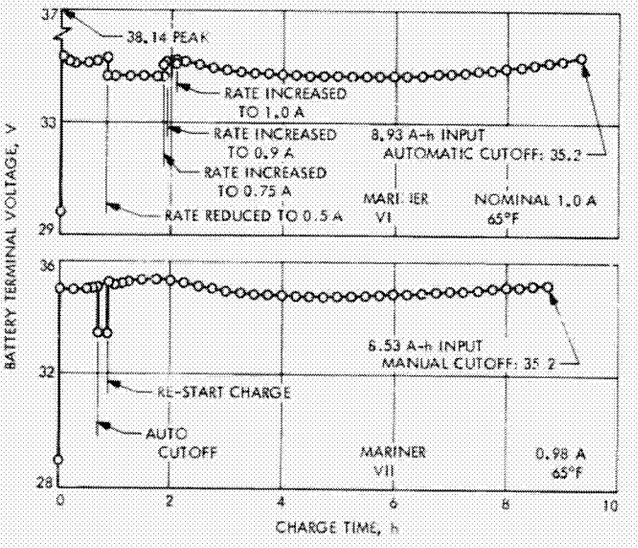


Fig. 51. Prelaunch charge profiles

charged *Mariner* Mars 1969 battery remained open circuited for 67 days before a conditioning sequence and was tested 48 h after the conditioning. The voltage declined from 33.3 V to a minimum of 26.5 V after the sudden application of a 312-W load. After the battery isolation diode potential drop, this was seen as 25.5 V on the dc power bus where a minimum potential of 23 V was necessary to maintain the booster regulator in regulation.

E. Power Conditioning Equipment

The *Mariner* Mars 1969 power conditioning equipment (PCE) contained 10 modules distributed in spacecraft bays I and VIII. The total weight of the PCE was about 50 lb. The modules in each bay are listed in Table 14.

Table 14. Power conditioning units

Bay VIII	Bay I
Power source logic	Power distribution
Main booster regulator	Main 2.4-Hz inverter
Standby booster regulator	Standby 2.4-kHz inverter
Power control	Single and three phase 400-Hz inverter
Battery charger/booster	Heater and dc power distribution

1. Power chains. The *Mariner* Mars 1969 power system contained redundant power chains each having a booster regulator and a 2.4-kHz inverter. Automatic switching to the standby power chain occurred upon a failure in the main chain sensed by the failure sensor located in the power control module. The failure was sensed as an out-of-tolerance voltage when (1) the booster regulator output voltage to the 400-Hz inverter was sensed to deviate from a nominal 53.2 to 58.8-V range, and (2) the frequency of the 2.4-kHz power deviated from a nominal 2.25 to 2.55-Hz range. Should the out-of-tolerance condition have persisted for nominally 1.5 s, the power control relay in the power control module would transfer the power subsystem to the standby power chain, and the main power chain would be isolated from the spacecraft circuitry. This transfer was not controlled by ground command in either direction and was permanent during a mission.

2. Bay VIII modules.

a. Power source logic module. All spacecraft electrical power was supplied through the power source logic module generated from the solar array, battery, or an external source. This unit housed the motor-driven switch that transferred spacecraft power from an external source to the battery. The unit also contained the solar array and battery isolation diodes.

b. Booster regulators. The booster regulator circuit design was modified to provide regulated dc at 56 Vdc ±1%, rather than at 52 Vdc ±1% as on previous *Mariners*. The change improved loop stability when the solar array voltage rose to zener cutoff at about 50 V. The load capacity of the unit was increased from 150 to 250 W and its efficiency was improved from 72 to 92%. The device supplied the major regulated dc power requirements of the power subsystem only. Both the main and standby units were identical.

c. Power control. The power control module contained the failure sense circuit to detect out-of-tolerance conditions in the main power chain, and the power control relay to switch the main power chain to a redundant standby power chain should a failure be sensed. AC square wave power at 2.4 kHz was supplied directly from this module to the seven spacecraft subsystems. This power distribution was continuous and was not controlled by spacecraft commands.

d. Battery charger/booster. The *Mariner* Mars 1969 battery charger was a current limited series-regulator and was powered by the dc power bus to provide charge current to the battery when the solar array was Sun oriented. The unit was turned on or off by ground command. The charge rate was a function of the potential at the dc power bus and at the battery terminals. The rate varied from maximum at 650 mA when the charger output voltage limited at 34.6 V, to trickle at about 10 mA. Charger characteristics are shown in Fig. 52.

Share mode detector. It was feasible that at a given time the *Mariner* Mars 1969 solar array could support the spacecraft steady-state load when a sudden power transient would drive the array operating point to the battery

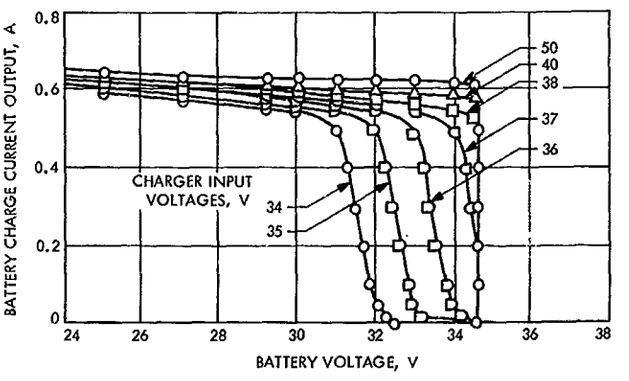


Fig. 52. Battery charger characteristics

potential to force the battery to share the load with the array. The share condition is a stable array operating point that requires continued but unnecessary battery energy contribution after the transient decay. The share mode detector circuit in this module activates a power relay to connect battery power to the boost converter circuit under the following conditions:

(1) A command relay must be enabled for operation, and had been at launch for *Mariner VI* and *VII*. The −Y solar panel current, telemetry channel 224, was used to monitor the status of the relay by having abnormal panel current readings signal relay reset; other telemetry indications easily verified nominal panel operation. Operation of this relay was controlled by ground command.

(2) The share mode detector circuit was inoperative whenever the solar array was not confirmed as Sun oriented by the Sun gate signal from attitude control.

(3) The power relay connects the battery to the boost converter circuit should the dc power bus potential drop to 31.5 ±1.5 V, and the conditions above exist.

(4) The power relay disconnects the battery from the boost converter circuit when the dc power bus potential rises above 33.2 V.

Boost converter. The boost converter circuit was also located in the battery charger/booster module, and was a two transistor dc-dc converter that drew energy from the battery to provide power pulses to the dc power bus. The pulse appeared as another energy source to the dc power bus, in addition to that of the array and battery. Its design was to relocate the operating point beyond maximum power to the other stable operating point on the constant voltage portion of the array characteristics. At this point, the array alone supported the steady-state spacecraft load if the fault cleared. This condition was sensed when the dc power bus rose above 33.2 Vdc, at which potential the boost operation was inhibited. The pulses were nominally 0.6 s in duration with a 7.5-s repetition rate, and would provide a minimum output of 4.5 A at a 25.8-V battery potential. The pulse width and repetition rate were determined by the share mode detector circuit that switched the boost converter input power on and off.

3. Bay I modules.

a. Power distribution. Commands controlling spacecraft power distribution were issued to the power distribution module in the power subsystem. This unit distributed ac power by the flight command subsystem for ground commands, or from the CC&S for time-sequenced commands stored on the spacecraft.

b. The 2.4-kHz inverters. The main inverter used on *Mariner* Mars 1969 converted dc regulated power to a 2.4-kHz square wave source at 50 Vrms as the main power for the spacecraft, as in previous *Mariner* designs. The design of the 2.4-kHz inverter was modified to support larger loads. Integrated circuits were used in the *Mariner* Program for the first time in these inverters.

The frequency of the 2.4-kHz power bus was converted by the CC&S to 2.4-kHz clock pulses that time spacecraft events. Pulses from the CC&S synchronized the 2.4-kHz inverter in former *Mariner* designs, and the FTS also previously utilized its own monitor oscillator for synchronization.

c. The 400-Hz inverters. The input to the 400-Hz inverters was regulated power at 55.2 Vdc from the booster regulator output.

Three phase. The three-phase unit provided three phase quasi-square wave output voltage at 27.2 Vrms ±5% line-to-line at 400 Hz to drive the gyro spin motors in the attitude control subsystem. The 2.4-kHz bus synchronized a divide-by-six integrated circuit countdown circuit to 400 Hz to each of the three phases of the inverter. Output transistors drove each primary winding leg of the delta-connected output transformer, and each phase was driven by a push-pull stage through a coupling transformer.

Single phase. The single-phase 400-Hz inverter provided square wave power at 28 Vrms to the scan platform motors and the infrared spectrometer motor. The output stage of the bridge inverter was driven by a push-push driver controlled by the phase A output of the three-phase integrated circuit counter.

Heater and dc power distribution. This module contained the fuses for the ac and dc heaters on the spacecraft. It also contained the relay that toggled the battery test load on and off by ground command.

4. Heaters. Mariner Mars 1969 provided a stable temperature ambient for its science instruments with the use of 9 ac heaters totalling 67 W, and 3 dc heaters at about 23 W. Most heaters were on when the spacecraft was initially powered. The ac heaters automatically turned off when the science instruments were switched on at Mars encounter. One 7.5 W ac heater, platform heater 2, was

activated by ground command when needed, and was nominally off.

5. Power subsystem telemetry. *Mariner* Mars 1969 power subsystem telemetry transducers were located in a number of modules: nine in 4A8, four in 4A11, and one in 4A19; there were five monitored from the +Y solar panel and one on the battery.

6. Power conditioning equipment (PCE) PFRs. The PFR system was initiated for the PCE at the initial power test for the modules.

a. Design affected by PCE PFRs. The 307.2-kHz crystal used in the 2.4-kHz inverters performed erratically during TA vibration. X-rays indicated the quartz blank to be mounted off center in a poorly designed support. These crystals were replaced by a more rugged crystal mounting design. The crystal case mounting in the inverter modules was also modified and dampened. No further problems occurred after component replacement and modifications.

The motorized switch transferred the spacecraft power from an external source to the battery without command during TA vibration. Data indicated that the switch transferred at frequencies between 1200 and 1600 Hz at a 25 *g* peak input to the vibration test fixtures imparting a peak of 50 *g*'s at the switch case. Several modifications, listed below, solved the problem:

(1) A more rugged M-566-5G switch replaced the model M-566-3E unit; the new switch motor had five times the braking torque characteristics of the previous unit.

(2) Vibration characteristics of the switch case was dampened with the use of Solithane mounting pads.

(3) The switch harness was redressed to improve switch case dampening characteristics. Solithane was used for the wire bond.

The output frequency of the 2.4-kHz inverter provided the master clock for the spacecraft as it operated at 2400 Hz ±0.24 Hz. Frequency variations on the prototype unit were obtained at submultiples of 2.4 kHz in tests at room ambient and at 0°C.

The frequency drift was caused by noise from the module chassis that was capacitively coupled into the crystal oscillator circuit. The capacitance developed between the chassis plane and the printed circuit board plane. Chassis noise was due to electromagnetic interference coupling of the inverter output stage that caused a noise from the 56 Vdc input voltage return to the chassis. The inverter output frequency drift was eliminated within a temperature range of −20 to +90°C with the introduction of the following:

(1) A ground plane between the chassis and the printed circuit board.

(2) The introduction of a zener diode to reduce the output impedance of the crystal oscillator buffer.

(3) Additions of noise suppression circuitry.

A base-to-emitter resistor was added to improve noise immunity and temperature stability of the single-phase 400-Hz interverter.

b. PFR's closed as mission risk An integrated circuit (IC) failure in the PTM of the 2.4-kHz inverter occurred in the frequency synchronizing circuit. A similar failure during the mission would have caused automatic switching to the redundant power chain. The SE 124 K integrated circuit device was found to have an hermetic seal leak, and had two open bonds due to a chlorine derived contaminant. All IC's designated for flight hardware were electrically rechecked and their hermetic seal again tested. Flight modules with IC's were given "burn in" tests for periods of 300 to 500 h, as long as delivery schedules permitted. There were no other IC failures in the power subsystem.

F. Power Subsystem Investigations

1. Power margins and encounter power transients. Worst case user power levels that totalled 388 W, with low-power travel wave tube amplifier operating, exceeded the solar array worst-case power conversion capability at Mars encounter. The worst-case design minimum power output of the solar array at encounter was 374 W, after the consequences of a maximum postulated proton solar flare. However, measured encounter mode spacecraft loads in ground tests were significantly less than the worst-case estimates. For *Mariner VI* the measured encounter load in test was 328 W; for *Mariner VII*, 332 W; and for the flight spare, 328 W. However, there was still some concern due to science "turn on" power transients at Mars encounter which, coupled with the steady-state load, could exceed array capabilities. Accordingly, sunlight tests were performed with *Mariner* Mars 1964 solar panels configured to simulate the expected *Mariner* Mars 1969 solar panel performance at Mars, and the *Mariner* Mars 1969 prototype power conditioning equipment. The tests demonstrated that spacecraft loads would not exceed the power

output of the worse-case array, either in steady state or because of the transient.

2. *Near-Earth battery charging.* Analysis showed that the *Mariner* Mars 1969 solar array operating near earth at worse case 75°C temperatures, would not provide dc power bus potential levels high enough to support full battery recharge after launch. Partial recharge, below the battery charger limiting potential of 34.6 V, was shown to be capable of supporting the spacecraft in worst-case launch conditions.

V. Approach Guidance

Approach guidance was a technique utilizing on-board instruments to increase accuracy of trajectory prediction during a period of several days prior to planet encounter, and subsequently utilized during this period for guidance purposes in trajectory alteration. Advantages of approach guidance included more exact control of orbit insertion or descent to planetary surface, as well as attainment of a closely-controlled trajectory for single or sequenced flyby of one or more planets.

Pointing angles to the planet were measured in a spacecraft-fixed coordinate system by an optical tracker; these angular measurements, after correction for attitude control limit-cycle motion, were used to estimate trajectory parameters. Processing of the optical measurements for orbit estimation could have been achieved either by ground-based software or by an on-board computer which would eliminate the requirement for telemetry and ground processing as a series part of the guidance process. The latter method would have been particularly useful on flights where large operational time lags were involved, or where multiple-spacecraft missions would result in heavy loading of the Deep Space Network.

A. Preliminary Design Study

A preliminary design study for an approach guidance engineering experiment to demonstrate the flight feasibility of a spacecraft-based optical approach guidance system aboard the *Mariner* Mars 1969 spacecraft (Ref. 4) was made in 1967 by Electro-Optical Systems, Inc. (Ref. 5) under contract for JPL.

The main elements evolved in the proposed approach guidance engineering experiment consisted of:

(1) The approach guidance subsystem (AGS), a null-seeking-type planet tracker making angular measurements with respect to spacecraft coordinates of the direction to the target planet.

(2) The Sun sensor and star sensor which made angular measurements of the Sun and the star Canopus to establish the spacecraft coordinates with respect to the celestial references.

(3) The telecommunications subsystem linking the spacecraft to Earth and transmitting and receiving information to and from the ground-based data processing subsystem.

(4) The data processing subsystem which performed (1) estimates of position and velocity of the spacecraft from the approach guidance data, and (2) maneuver computation (a spacecraft velocity change and time of execution is computed from the estimated parameters in order to prepare for a trajectory correction).

(5) The corrective maneuver execution system, not a part of the assumed *Mariner* Mars 1969 mission.

The Sun sensors, Canopus sensors, and telemetry system (*Mariner* Mars 1969 hardware required for the approach guidance engineering experiment) were being used for spacecraft attitude control and, therefore, were similar to those previously developed for *Mariner IV*. The major hardware developed was the planet tracker (AGS).

The planet tracker functioned as follows: An image of a target planet was produced by a 24-in. focal length optical system. The image was centered on the photocathode of an electrostatic image dissector tube by angular displacements in the field-of-view which resulted from counter-rotation of two pairs of prisms. The electronic image produced in the image dissector tube was scanned in such a way that the illuminated planet limb geometry was electronically measured, and orthogonal error signals produced by the scan controlled the prism pairs in such a way as to position the center of the planet image at the center of the photocathode.

Digital encoders recorded the positions of the prism pairs directly and monitored the changes in prism position required for changes in pointing angle to the planet. Ten bits of encoder data for each prism pair defined the prism positions to a minimum (center-of-field) resolution of 55″ arc/bit, for a field-of-view 10-deg square. A digital converter was used to transform the 10-bit encoder words into a format of 7-bit words compatible with spacecraft telemetry. The AGS hardware block diagram (Ref. 6), shown in Fig. 53, represented the proposed system layout containing both linear and nonlinear blocks. From the input block

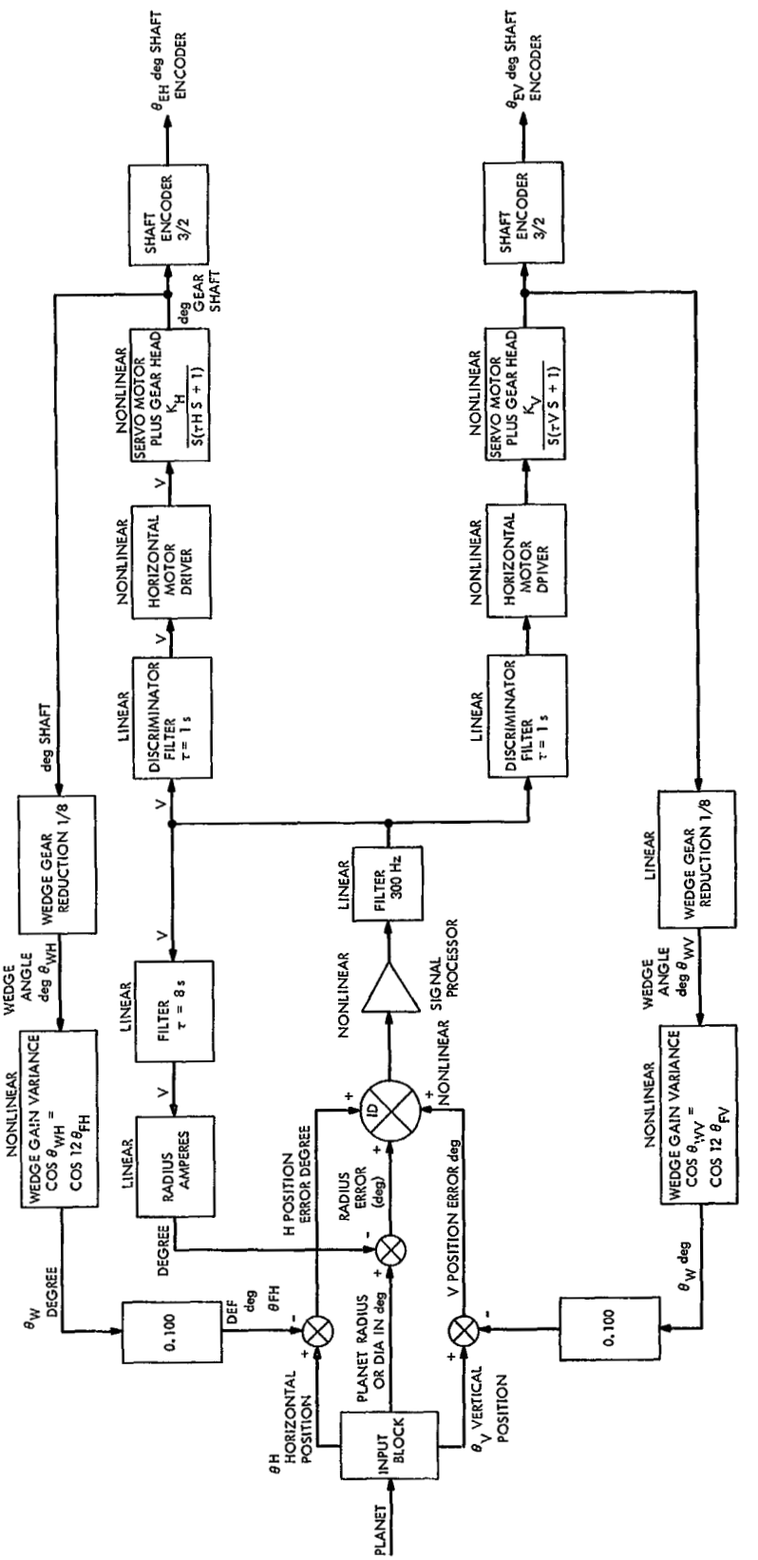


Fig. 53. Hardware components for AGS

(mathematical time representation of planet position) the horizontal, vertical, and radius information entered the error summing modes. These error signals were applied to the image dissector tube. The net signal was then processed and applied to a linear 300-Hz filter where the signal was applied to three channels: radius, horizontal, and vertical. The radius channel was a linear loop containing an eight-second time constant, single pole filter and an amplifier. The other two loops, vertical and horizontal, were identical.

A planet tracker was built (Ref. 7), and data interfaces were established between the telemetry data stream in the SFOF and the optical data pre-processing software in the spacecraft performance analysis and command area. A draft description of a computer program for implementing each data interface was written. Equations were derived and documented that related the planet tracker measurements to the spacecraft trajectory parameters and to measurement errors. Orbit determination accuracy studies were performed to define measurement system accuracy requirements.

To perform detailed studies of the measurement system and to provide test data for evaluating the software, an IBM 7094 digital computer program to simulate the optical measurement telemetry data was developed (Ref. 8). The contract for program development began in June 1967 and was completed in December 1967.

B. Study and Utilization of Existing On-Board Optical Data Sources

With the deletion (Ref. 7) of the planet tracker from the mission, as a result of budget constraints, a study was initiated to evaluate existing on-board sources of optical data that could be used for orbit determination.

These sources include the far-encounter planet sensor, the scan platform, the attitude-control celestial sensors, and the science TV system. Sufficient accuracy could be obtained using data accumulated over a 24-h period.

Studies have also shown the usefulness of TV data in the orbit determination process when Mars is in a TV frame. The value of the TV data is greatly increased if a star is visible in the TV frame along with Mars. A star of 3.64 magnitude had a high probability of being in the TV field-of-view for trajectories having a launch date before March and an arrival date between July 31 and Aug. 15, 1969.

C. Off-Line Software System

Since sufficient accuracies of optical data were available through accumulation over periods of time, an off-line software system was developed to process the data for orbit estimation. A block diagram of the off-line software system is shown in Fig. 54. This software system was

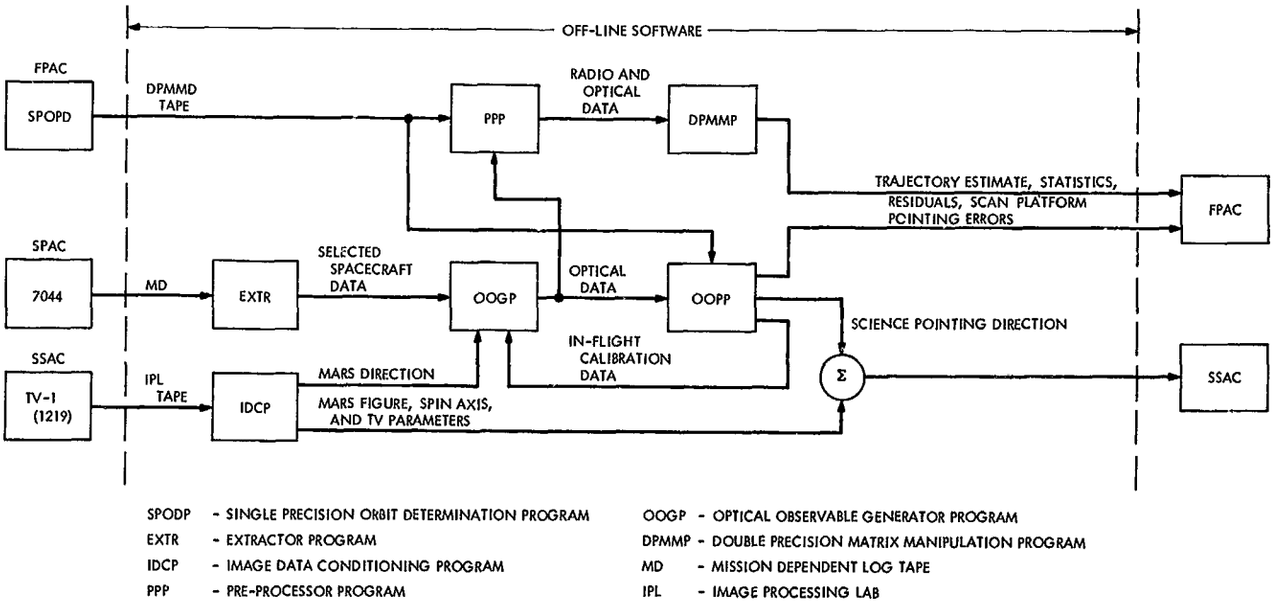


Fig. 54. Data interfaces

coded for the IBM-7094 DCOS and the UNIVAC-1108, and did not require support from the MOS computers. A description of the individual programs follows.

The extractor program (EXTR) used, as input, the mission dependent (MD) log tape. The program picked out from each 100 deck telemetry frame those channels which contained attitude control or scan subsystem angle data, and added channel numbers and status flags. The program then wrote a tape containing these data and frame time.

The image data conditioning program (IDCP) used, as input, an Image Processing Laboratory formatted tape. The TV coordinates (line and pixel number) of Mars lit limb, stars, and satellites were determined and then corrected for geometric distortion. The corrected lit limb data was used to estimate Mars direction, figure, and spin axis. The TV parameters, such as principal point and focal length, could be included in the estimation process.

The optical observable generator program (OOGP) used, as input, the EXTR output tape, spacecraft calibration data, and planet direction from the IDCP. A subset of these data (several options were available) was used to calculate the planet clock and cone angles (α, β) and their noise covariance matrix. These (α, β) data points were then smoothed and filtered over specified time spans to yield one equivalent data point per time span. These equivalent data points, their noise covariance and data, needed for the partial derivatives in the OOPP, were written on a tape and/or cards.

The optical observable processor program (OOPP) used, as input, the output tape of OOGP, the DPMMP tape containing trajectory information, and *a priori* values and covariance matrix of the parameters to be estimated. These parameters included trajectory parameters and optical observable biases and drifts. The program estimated these parameters over a specified time span and output the estimate and its covariance. *A priori* data on trajectory parameters were from radio tracking estimates. Estimating the optical observable biases and drifts constituted an in-flight pointing calibration of the scan platform.

Another set of software, using a different numerical method, was also used to process the OOGP output tape.

The pre-processor program (PPP) used, as input, the OOGP output tape and the DPMMP tape. The program performed various computations such as the calculation of the cone and clock angles of the scan platform, partial derivatives of the cone and clock angles with respect to the estimated parameters, and the linear differential corrections to the cone and clock angles due to biases. The program took the values of these computations and added them to the records of the DPMMP tape.

The double precision matrix manipulation program (DPMMP) used, as input, the DPMMP tape modified by the pre-processor program. The program solved the normal equations in addition to performing various other computations. Its output were the corrections to the spacecraft orbit, B-plane statistics, and residual plots.

References

1. *Mariner Mars 1964 Project Report: Mission and Spacecraft Development. Volume I. From Project Inception Through Midcourse Maneuver,* Technical Report 32-740. Jet Propulsion Laboratory, Pasadena, Calif., Mar. 1, 1965.
2. The Planetary–Interplanetary Program, Space Programs Summary 37-45, Vol. II. Jet Propulsion Laboratory, Pasadena, Calif., May 31, 1967, pp. 26–39 (Confidential).
3. Brown, W. D., *ATS Power Subsystem Radiation Effects Study, Phase I,* Final Report SSD 80089R. Hughes Aircraft Co., Culver City, Calif., Feb. 1968.
4. *Supporting Research and Advanced Development,* Space Programs Summary 37-42, Vol. IV, pp. 48–49. Jet Propulsion Laboratory, Pasadena, Calif., Dec. 31, 1966, pp. 48–49.

References (contd)

5. *AGS Final Report,* EOS 7149-FR, Electro-Optical Systems, Inc., Pasadena, Calif., Feb. 23, 1969.

6. *Servo Analysis, AGS Final Report,* EOS 7149-SFR. Electro-Optical Systems, Inc., Pasadena, Calif., Jun. 5, 1968.

7. *Supporting Research and Advanced Development,* Space Programs Summary 37-51, Vol. III, pp. 50–51. Jet Propulsion Laboratory, Pasadena, Calif., Jun. 30, 1968.

8. Supporting Research and Advanced Development, Space Programs Summary 37-50, Vol. III, p. 104. Jet Propulsion Laboratory, Pasadena, Calif., Apr. 30, 1968.

Propulsion and Pyrotechnic Subsystems

I. *Mariner* Mars 1969 Propulsion Subsystem

A. Introduction

The function of the *Mariner* Mars 1969 propulsion subsystem was to remove or reduce launch injection dispersion errors and biases so that a Mars flyby with the desired small miss distance could be reasonably assured. To accomplish this function, a 50-lbf vacuum thrust propulsion subsystem employing anhydrous hydrazine as a liquid monopropellant was developed (Fig. 1). As shown in the schematic diagram in Fig. 2, high-pressure nitrogen gas was regulated to 308 psia to force propellant from the storage tank to the rocket engine. Start and stop of the propellant and the pressurant flows was accomplished by multiple explosive valves. The propellant storage tank contained a butyl rubber bladder for positive expulsion in a gravity-free environment. The rocket engine contained Shell 405 (Shell Development Co.) catalyst for spontaneous ignition and sustained decomposition of the hydrazine. The thrust vector control assembly (TVCA), utilizing four jet vanes located in the exit plane of the nozzle, provided pitch, yaw, and roll control of the spacecraft during engine operation.

Design and development of the subsystem was conducted at JPL. Fabrication and component type approval (TA) and flight acceptance (FA) testing was accomplished by the Power Systems Division of TRW Systems Group (Ref. 1). Type approval testing of the subsystem was done at JPL. Support of the spacecraft system test, launch operations, and mission operations was provided by JPL.

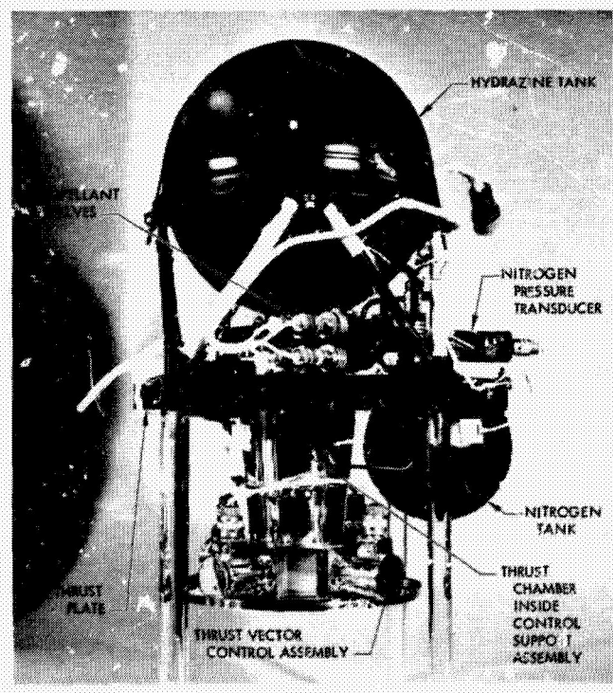


Fig. 1. Propulsion subsystem

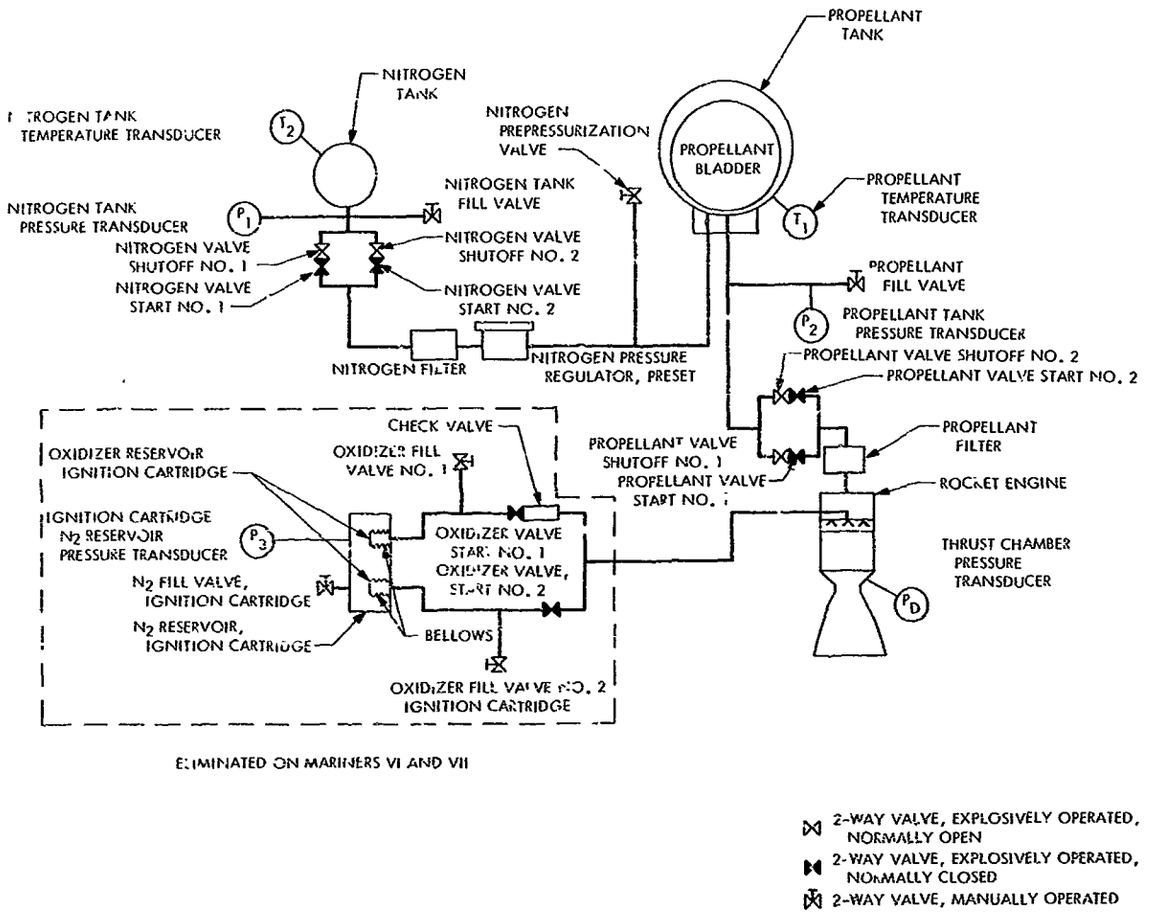


Fig. 2. Propulsion subsystem schematic

The *Mariner* Mars 1969 subsystem is an outgrowth of the *Mariner* Mars 1964 and *Mariner* Venus 67 propulsion subsystems. A major change from the *Mariner* Mars 1964 system was the incorporation of the Shell 405 spontaneous catalyst in the rocket engine. This eliminated the requirement for the nitrogen tetroxide start system employed on the earlier subsystems. In the *Mariner* Mars 1964 system, initiation of hydrazine decomposition was accomplished by injecting nitrogen tetroxide into the rocket engine simultaneously with the initial injection of hydrazine. The ensuing hypergolic reaction heated the catalyst bed to a temperature sufficient to maintain decomposition of the hydrazine. Elimination of this oxidizer start system (shown boxed in Fig. 2) removed eight major components from the propulsion system.

The only other major design change was in the configuration of the thrust plate, the main structural member to which all of the subsystem components are mounted. Here, the number of subsystem attach points to the spacecraft were reduced from four to three and the rocket engine location was shifted 2 in. because of relocation of the spacecraft CG. The 2-in. shift in the rocket engine also aligned the thrust axis with the center of the propellant tank, which minimized the effects of shifting CG during rocket engine firing.

To meet the *Mariner* Mars 1969 requirements for maximum mission reliability and long-term storage in deep space, the following key features were incorporated in the propulsion subsystem design:

(1) Gaseous nitrogen was chosen as the pressurant in lieu of gaseous helium to minimize gas leakage potential.

(2) Welded and brazed tubing and fittings were used wherever possible.

(3) In places where mechanical joints were required to facilitate component removal and replacement, all metal seals (aluminum crush gaskets) were chosen in place of any elastomeric seals.

(4) Highly reliable squib-actuated valves were chosen for system startup and shutdown.

(5) Squib-actuated valves are used to isolate the high pressure nitrogen from the propellant tank during the cruise phase. This removes the requirements for a heavy walled propellant tank or for complete regulator lockup during the long space storage.

The propulsion subsystem was designed for a maximum allowable weight of 47.0 lbm when fully loaded with propellant and pressurant. A summary of the subsystem nominal performance parameters is presented in Table 1, and the nominal operating pressures and temperatures are shown in Table 2.

B. Propulsion Subsystem Components

Overall subsystem performance was primarily dependent upon the performance and interactions of the subsystem components. In this section, a description is presented of the changes from the *Mariner* Mars 1964 designs; in addition, FA and TA tests of the components are discussed.

Table 1. Nominal performance summary

Parameter	Performance
Velocity increment (ΔV) capability	58.5 m/s
Burn time capability at launch	97 s
Maximum thrust vector deflection compatibility, 2 jet vanes deflected 25 deg	±5.0 deg
Number of ignitions possible	2
Operating temperature range	+35 to +90°F
Propellant	Anhydrous hydrazine
Vacuum thrust, without jet vanes	51.3 lbf
Vacuum thrust, 4 jet vanes deflected 10 deg	50.7 lbf
Stagnation chamber pressure	198 psia
Throat area at ambient temperature	0.15 in.^{2}
Nozzle expansion area ratio	44:1
Vacuum thrust coefficient, without jet vanes	1.71
Propellant flowrate	0.222 lbm/s
Characteristic exhaust velocity	4349 ft/s
Vacuum specific impulse, without jet vanes	231.1 lbf-s/lbm
Vacuum specific impulse, 4 jet vanes deflected 10 deg	228.5 lbf-s/lbm
Uncertainty in rocket engine pointing accuracy	2.5 mrad max

1. Rocket engine. A sectional view of the 50-lbf thrust monopropellant engine is shown in Fig. 3. The injector

Table 2. Nominal pressures and temperatures

Function	Pressure, psia	Temperature, °F
Nitrogen reservoir, at first ignition	3015	70
Propellant tank, at launch	280	70
Propellant tank, operating	308	70
Injector inlet, operating	295	70
Thrust chamber, operating	198	1800

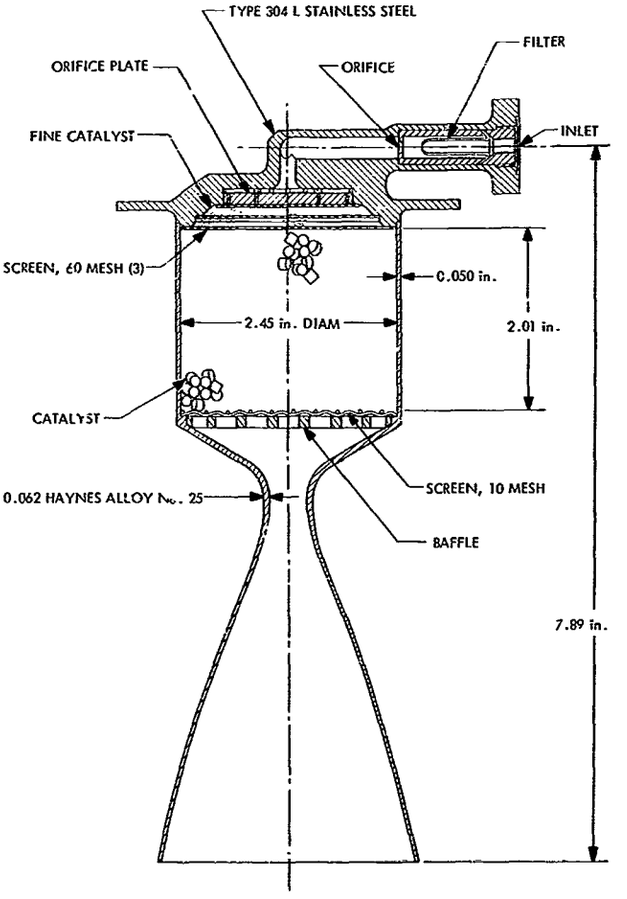


Fig. 3. Section view of *Mariner* Mars 1969 engine

was a showerhead type with two layers of 20 30 fine mesh Shell 405 spontaneous catalyst packed against the injector face. The two layers were retained by three 60 mesh screens. The remainder of the catalyst bed consisted of a uniform mixture of 75% by weight Shell 405 and 25% JPL Type HA3 ⅛ in. cylindrical catalyst pellets.

a. Spontaneous catalyst change. The incorporation of a spontaneous catalyst engine into the *Mariner* Mars 1969 propulsion subsystem was accomplished after a careful comparison of the merits of the existing *Mariner C* design with those of a spontaneous catalyst design.

By changing to the spontaneous engine a lighter, simpler, and more reliable propulsion subsystem could be designed. The number of potential leak paths was reduced from 18 on *Mariner C* to 10 on *Mariner* Mars 1969. In addition, the elimination of the oxidizer start system resulted in a weight savings of 4.6 lbm.

b. Spontaneous catalyst test program. The initial designs of the spontaneous catalyst rocket engine were tested in heavyweight hardware. After confirmation of an acceptable design, two engines essentially conforming to the *Mariner* Mars 1969 flight design were fabricated and subjected to a prequalification test program at JPL (Ref. 2).

Each engine was initially calibration test fired. Engine 1 then went through a series of firings in a vacuum environment, to obtain performance data. Engine 2 was subjected to TA level vibration and acceleration tests. These tests were followed by a post-environmental calibration test firing and then a high-chamber pressure firing (at 1.25 times operating chamber pressure).

The prequalification test program is outlined in Table 3. The test results are given in Table 4. As anticipated, the measured specific impulse was approximately 2.5% lower than the previous nonspontaneous design engine of the *Mariner C* type.

Oscillographic records indicated acceptably smooth chamber pressure with satisfactory start and shutdown transients.

Post-environmental test performance of engine 2 appeared nominal, except for an increased roughness. The average peak-to-peak values in chamber pressure during the post-environmental firing were ±12 psi, as compared to the ±5.6 psi obtained during the calibration firing. This roughness was still acceptable.

These results indicated that the new engine design would adequately perform the *Mariner* Mars 1969 mission. It was concluded, however, that the design appeared to be life limited, since chamber pressure roughness values increase progressively after repeated operations. This limitation did not impose any restrictions upon its use for the relatively short burns required by the *Mariner* Mars 1969 mission.

Table 3. Rocket engine prequalification test program

Engine 1 assembly	Engine 2 assembly
Calibration firing	Calibration firing
Vacuum ignition firings at Edwards Test Station	TA sinusoidal vibration
	TA random vibration
	Static acceleration
	Post-environmental firing
	High-chamber pressure firing

Table 4. Prequalification engine firing test results

Test	Engine	Duration, s	Chamber pressure, psia	Flow rate, lbm/s	Specific impulse, s	Roughness, psi (peak-to-peak)
Calibration	2	30	182	0.207		5.6
Post-environmental	2	100	180	0.203		12.0
High-pressure	2	200	242	0.271		8.4
Calibration	1	30	186	0.206		4.0
Vacuum 1	1	60	188	0.217	228.7	10.5
Vacuum 2	1	20	188	0.218	228.5	12.3
Vacuum 3	1	60	188	0.216	229.7	12.3
Vacuum 4	1	20	190	0.217	230.0	14.3

c. Flight acceptance testing. The FA test sequence for the spontaneous catalyst engine consisted of the following tests: injector water flow, engine assembly proof and leak, vibration (sinusoidal and random), leak check, and engine performance acceptance. During injector water flow tests, the injector assembly was trimmed to the desired pressure drop by installation of a trim orifice in the injector inlet. The engine performance acceptance test consisted of two 30-s vacuum firings. The acceptance criteria for the engine was 50.71 ±2.5-lbf thrust at an injector inlet pressure of 295 psia. Following acceptance firings, the engine was given a final leak check.

d. Type approval testing. One rocket engine, after completion of flight acceptance testing was subjected to the following type approval tests: humidity exposure, static acceleration, sinusoidal vibration, random vibration, leak tests, and performance evaluation including extended duration firings.

The TA engine S/N002 successfully passed all the FA and TA environmental and hot firing tests accumulating 419 s of total firing time.

2. Pressure regulator. The pressure regulator maintained the propellant tank pressure at 308 ±3 psia at a nominal flowrate of 0.006 lbm/s of GN_2. The position of the nitrogen pressure regulator on the *Mariner* Mars 1969 subsystem thrust plate was rotated 90 deg from the *Mariner* Mars 1964 installation. This change, shown in Fig. 4, allowed the regulator to be recessed into the thrust plate and, thus, eliminated the need for the mounting screw inserted into the regulator spring housing which could cause distortion and binding of the spring package.

a. Flight acceptance testing. The regulator, following final assembly and spring package adjustment, was subjected to proof and leak tests followed by a series of flow and lockup tests. The regulator was then subjected to FA vibration tests and additional flow tests. Following the flow tests, the regulator was flow tested at temperatures of 32 and 131°F. Finally, a series of characterization tests were conducted with a simulated subsystem (water calibration system) with regulated nitrogen expelling water from a full sized propellant tank under vacuum conditions. The regulator was then subjected to final flow and leak tests.

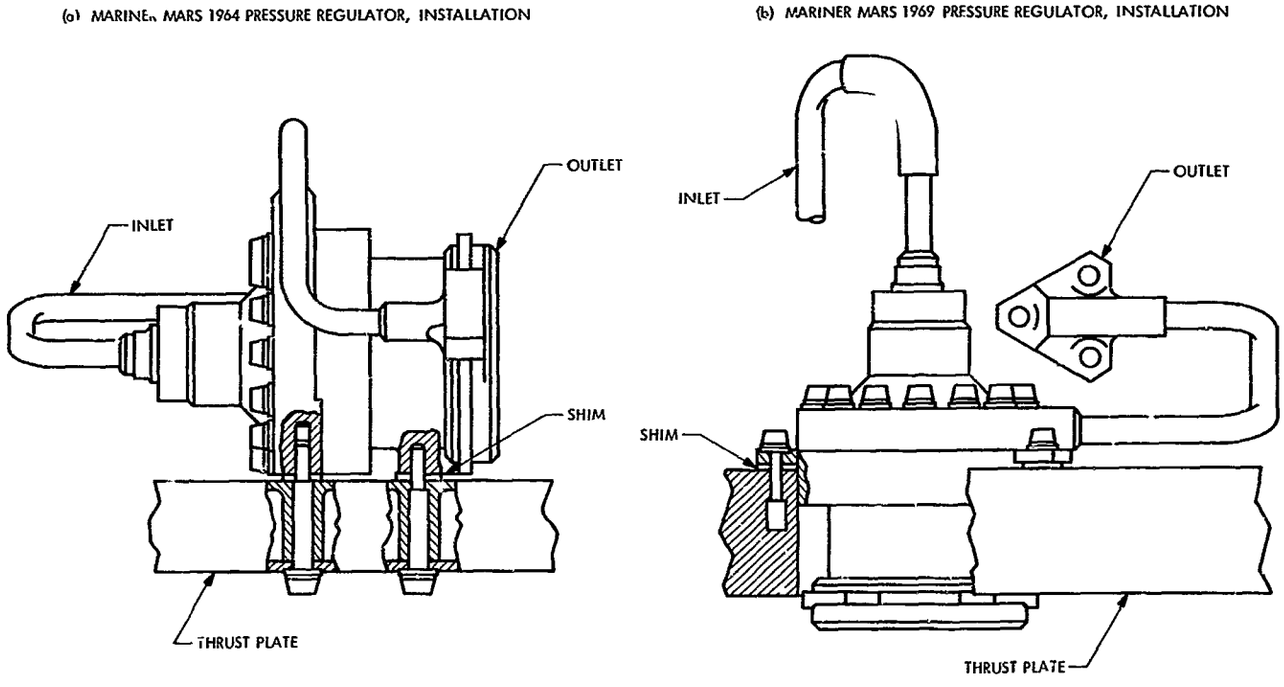


Fig. 4. Regulator mounting comparisons

b. Type approval testing. Because the regulator was identical to that used on *Mariner* Mars 1964, it was decided that a TA test was not required. Problems that developed during subsystem TA testing are described in Subsections C and D-1.

3. *Nitrogen and propellant valves.*

a. Description. The propulsion subsystem employed two sets of squib-actuated valves to control the rocket engine firing. Each valve assembly consisted of two parallel legs of one normally open and one normally closed valve in series. Each leg provided the capability for a single startup and shutdown. The nitrogen valve controlled the flow of high-pressure nitrogen to the pneumatic regulator, while the propellant valve controlled the flow of hydrazine from the bladdered propellant tank to the rocket engine.

Both of these valves were nearly identical to the *Mariner* Mars 1964 configuration with the exception of the inlet and outlet tubes that were rerouted to accommodate component layout modifications as part of the design change for the engine relocation. A comparison of the manifolding on the *Mariner* Mars 1969 and *Mariner* Mars 1964 valves is shown in Fig. 5. The T joint incorporated in the *Mariner* Mars 1969 design appeared to be simpler to manufacture and assemble than the Y joint manifold employed in the *Mariner* Mars 1964 design. However, this change later produced some problems with the valves as discussed in Subsection C.

The selection of adequate criteria for the design and acceptance of valve braze joints evolved into an extensive test program. A cutaway of a nitrogen valve, Fig. 6, showed some of the braze joints in question. The original procurement drawing specified that braze acceptance should be based on "80% or more of faying surfaces joined by braze material." It was found, however, after comparison of sectioned braze samples with X-rays of final brazed valves, that there really was no accurate nondestructive method of measuring the extent of the braze flow in the various joints because of the material thickness and intricate shape of the valve bodies. It was then decided to abandon radiographic measurement of the braze flow as an acceptance criterion and to use a helium proof and leak test instead.

b. Squib firing tests. Since the squib actuated nitrogen and propellant valves used in the propulsion subsystems were of a one-shot design, no operational ground testing was possible prior to launch to verify flight readiness. Therefore, to qualify the valves for flight use, two randomly selected valves of each configuration were subjected to a series of squib firing tests for demonstration of acceptable (predicted) valve operation.

The tests were conducted in two series. The tests consisted of installing the valve in a flow system that was pressurized to simulate actual conditions; i.e., nitrogen for the N_2 valve and water for the propellant. Data recorded during the tests were: firing shock acceleration, firing current, and inlet and outlet pressures for determination of valve open flow pressure drop.

The first test valves were exposed first to low temperatures (14°F for the N_2 valve, 37°F for the propellant valve) for a test of one leg and an elevated temperature

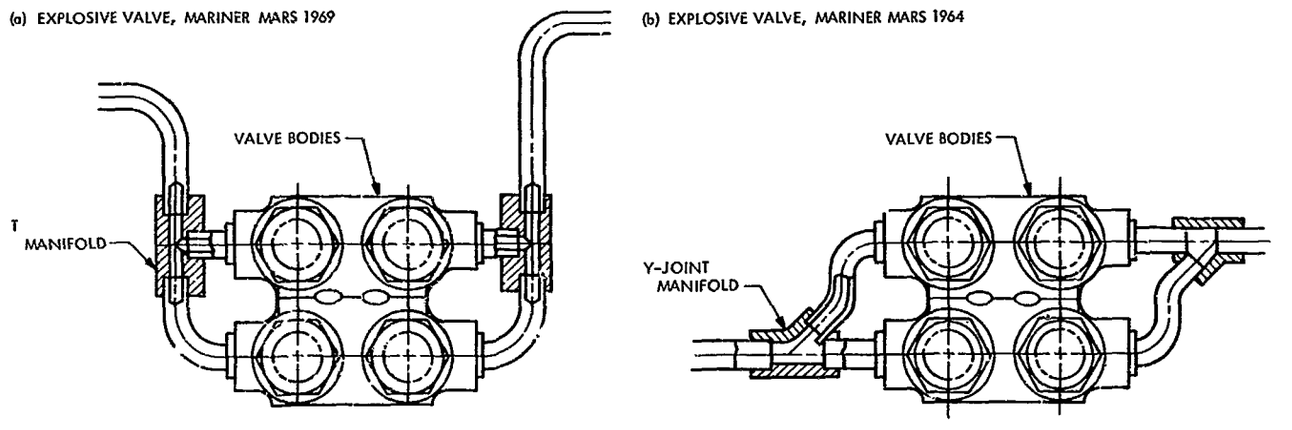


Fig. 5. Explosive valve manifold comparisons

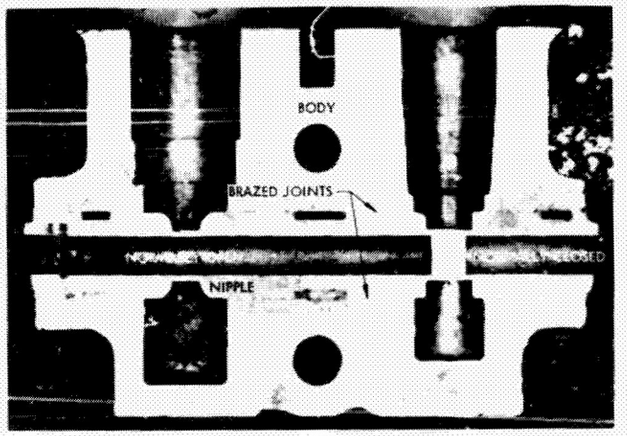


Fig. 6. Sectioned N_2 valve showing brazed joints

(167°F for both valves) for the other leg of the same valve. The second valve lot series were test fired at ambient temperature only. All valves operated as predicted and successfully passed proof and leak following these firing tests.

4. Pressure transducers. Pressure instrumentation was necessary to determine the status of the subsystem (leak tightness and amount of hydrazine decomposition, Subsection B-5), to determine the initial conditions for the timed burn prediction, and to measure the performance of the engine during the trajectory correction burn. The *Mariner* Mars 1969 transducers were identical to those used on *Mariner C* with one exception. The nitrogen pressure transducer required a thicker case wall to meet the AFETR range safety requirement that the burst pressure be four times the maximum operating pressure. The other two transducers could meet this requirement without modification.

a. Flight acceptance testing. The FA test sequence for pressure transducers consisted of calibration, vibration (sinusoidal and random), proof, leak, and calibration.

b. Type approval testing. The TA tests conducted on one of each of the three pressure transducers consisted of first the FA sequence followed by TA sinusoidal vibration, random vibration, leak check, calibration, and a burst test.

During burst testing, the nitrogen unit failed at less than the design requirement. Two-thirds of the end closure weld seam separated at 10,950 psig, or 2,410 psig below the minimum value. An investigation of the failed end closure revealed an inadequate depth of penetration

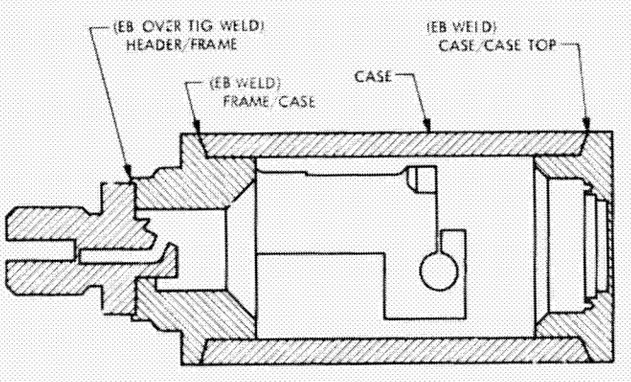


Fig. 7. Cross-section of N_2 pressure transducer

of the tungsten inert gas (TIG) weld. A proposed fix to the problem was to use electron beam (EB) welding for the case closure welds (Fig. 7). Two sample cases with closures welded by the EB process burst well above the minimum design requirement (Table 5). On the basis of these successful test results, all nitrogen transducers were submitted to rework. All reworked units successfully passed FA testing.

5. Propellant tank bladder.

a. Description. A butyl rubber bladder inside the propellant tank restrained the hydrazine over the tank outlet during flight in the zero-g environment.

b. Bladder storage tests. Two propellant tank assemblies were placed in long-term storage to determine the effects of temperature upon the rate of propellant decomposition. Propellant tank pressure rise was observed during earlier *Mariner* missions and is the result of a slight incompatibility of the butyl rubber bladder and the hydrazine propellant. *Mariner* Mars 1969 bladders molded from two separate batches of rubber stock were tested to determine the effects of processing and material variations upon the tank pressure rise rate. The tanks were filled with 21.5 lbm of hydrazine and pressurized to 280 psia at 70°F—these being the launch conditions. Temperature was then increased to 100°F to

Table 5. Transducer case burst pressure

Transducer	Minimum burst, psig	Actual burst, psig
Chamber pressure	1,200	4,920
Propellant pressure	1,640	4,250
Nitrogen pressure	13,360	10,950
Nitrogen pressure reworked		18,400

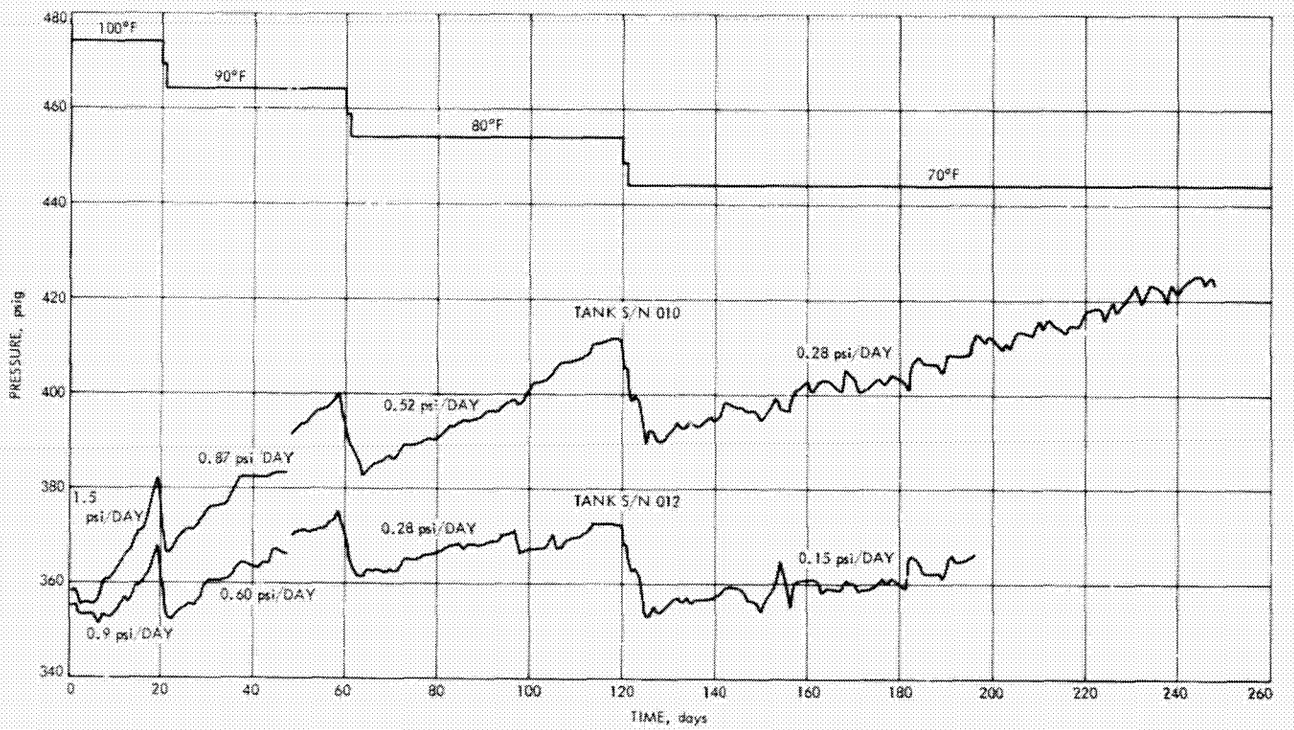


Fig. 8. Propellant tank storage test history

begin the storage test. As shown in Fig. 8, temperatures between 100 and 70°F were investigated over a period of 6 mo for one tank and 8 mo for the other. Pressure rise rates differed by nearly a factor of two between the bladders, typical of similar tests performed in the past. The rates of pressure rise at 70°F were similar to those observed on *Mariner IV* and *V*.

At the completion of these tests, the pressurant gas, propellant, and the gases dissolved in the propellant were analyzed. The pressurant gas contained small amounts of ammonia which had diffused through the bladder. Hydrazine diffusion was negligible. The hydrazine was found to contain less than 1% dissolved ammonia. There was no visual evidence of degradation of either bladder.

6. Pressurant and propellant tanks. Both the nitrogen tank and propellant tank consisted of two 6AL-4V titanium alloy forged and machined hemispheres with a single girth weld.

The FA testing of the flight tanks consisted of inspection (mechanical and radiographic), measurement of weight and volume, proof pressure test (hydrostatic) at ambient temperature, and proof (hydrostatic) at low temperature with liquid N_2 followed by cleaning and packaging.

The TA tests for both the nitrogen and propellant tanks, consisted of measuring the bulk yield and burst pressures for three tanks of each type. Although all test tanks burst at pressures well above their minimum design requirements, the propellant tank data scatter exceeded the allowable 5% between tanks. Because of this condition, the maximum allowable working pressure was downgraded to 390 psig at 70°F and 375 psig at 125°F, a reduction of approximately 20 psi in both cases. This change maintained the man-rated safety factor at the specified value of 2.2 times the maximum operating pressure.

7. Thrust plate and mounting hardware. The change of the *Mariner* Mars 1969 spacecraft CG with respect to that of *Mariner* Mars 1964 necessitated a 2-in. shift in the position of the engine on the thrust plate. This produced a redesign of the thrust plate and a relocation of components and their interconnecting tubing. The *Mariner C* thrust plate design consisted of a dip brazed aluminum box. Although this design provided an optimum strength-to-weight ratio, it was difficult to braze.

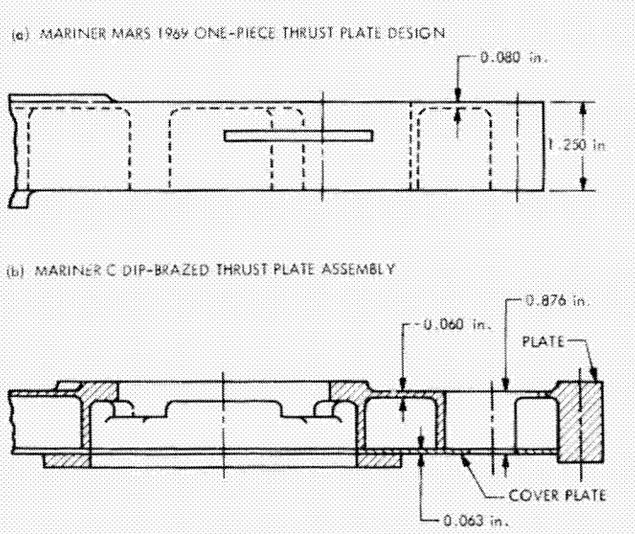


Fig. 9. Thrust plate design comparisons

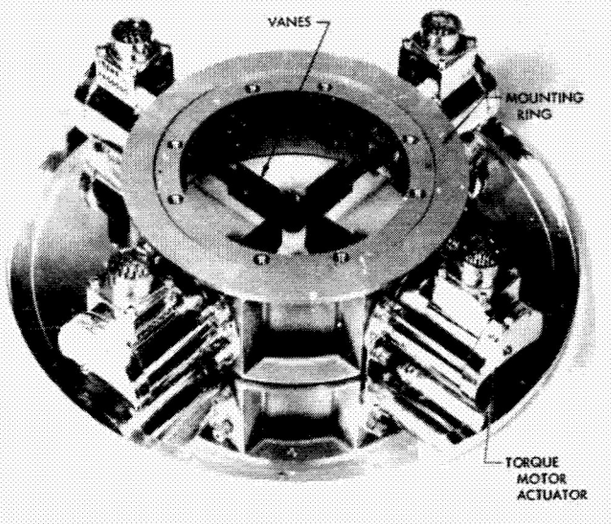


Fig. 10. Thrust vector control assembly

Therefore, for the *Mariner* Mars 1969 thrust plate, it was decided to employ a one-piece machining. Cross sections of these two designs are compared in Fig. 9.

Two *Mariner* Mars 1969 propulsion subsystems were structurally tested for design verification of the new one-piece thrust plate and the three-point spacecraft attachment. The first of these units to be tested was the dynamic/development test model (DTM). This unit was structurally evaluated during subsystem modal tests, DTM spacecraft vibration testing, and finally during the propulsion vibration test fixture qualification. Both the DTM spacecraft and fixture qualification testing involved vibration levels equal to or greater than the TA levels. In addition, because of the fixture problems many more vibration runs were conducted than originally planned. The second unit was the propulsion PTM unit and was structurally evaluated during the propulsion TA three-axis vibration done prior to the hot firing sequence.

No problems were encountered with this new thrust plate design during any of the testing, thus demonstrating an acceptable replacement for the earlier *Mariner* design.

8. Thrust vector control assembly (TVCA). Spacecraft attitude during the rocket engine firing was maintained by the thrust vector control assembly shown in Fig. 10.

During the midcourse correction maneuver on the *Mariner* Venus 67 spacecraft, an anomaly occurred in the TVCA and autopilot system (Ref. 3). Testing showed that high side forces were generated on the TVCA actuator ring and jet vane thermal shield when the jet vanes were deflected to large angles (25 deg). These forces were caused by the high pressure behind the shock wave extending from the leading edge of the jet vane. The problem was alleviated for *Mariner* Mars 1969 by deleting the vane thermal shield and increasing the diameter of the actuator ring by 1 in. to reduce both the forces and the thermal input. The vane shaft was lengthened 0.5 in. to maintain the jet vane within the rocket engine exhaust.

C. Subsystem Type Approval Testing

The *Mariner* Mars 1969 subsystem TA environmental testing was conducted with an "all-up" flight type unit which was assembled from components that had previously passed all the required FA tests and were representative of the flight hardware. This test unit was built for the spacecraft PTM and when tested, essentially duplicated the "as launched" configuration; i.e. the TA tests were conducted with:

(1) Live squibs installed in the explosive valves.

(2) Propellant tank and bladder containing 21.5 lbm of anhydrous hydrazine.

(3) Nitrogen and propellant tanks fully pressurized to launch level with gaseous nitrogen.

(4) TVCA installed.

The TA environmental testing consisted of subjecting the PTM to three orthogonal axes of both sine sweep and random vibration followed by two vacuum hot fire tests of 60 and 30 s duration to verify satisfactory system performance.

A vibration test fixture was designed and built to accept the new *Mariner* Mars 1969 propulsion configuration. This fixture was tested and qualified at the JPL/Edwards Test Station vibration facility with the *Mariner* Mars 1969 propulsion DTM unit (dummy hardware simulating only weight and center of gravity). The fixture exhibited excessive amplification factors at several frequencies. Fixture rework done to alleviate the problem was not completely successful in eliminating these excessive amplifications. Since the fixture was only to be used for TA testing and since little time remained for additional rework, it was decided to reduce the input vibration level at the critical frequencies to compensate for the fixture induced amplification.

Despite the fairly severe input vibration levels and the fixture problem, no significant problems or changes could be detected in the PTM either during or after vibration. However, at the time of final checkout, prior to the vacuum firing tests, the flight chamber pressure transducer was found to be electrically inoperative. As an expedient fix, the metal tube connecting the transducer to the engine was severed and two other transducers were spliced in to monitor P_c during the hot firing tests.

The first hot fire test was successfully initiated and terminated at the end of the planned 60-s duration. The test data indicated that the rocket engine had achieved only 40% of rated thrust. All other system components, however, appeared to have functioned nominally. Post-test tear down and inspection showed that the low-thrust failure resulted from clogging of the engine inlet filter by contaminants from the propellant valve. It was determined that successful removal of this contamination required both a change in the valve hardware and in cleaning procedures. In addition, the filtration rating of the engine inlet filter was decreased from 40 to 150 μm. These corrections were evaluated and successfully demonstrated in several component and engine firing tests before being incorporated into the PTM and *Mariner* Mars 1969 flight designs.

The PTM was returned to TRW for rework consisting of installation of new explosive valves, chamber pressure transducer, 150-μm engine filter, and a system proof and leak test. It was then returned to the JPL/Edwards Test Station for hot firing retest. However, before the hot fire tests, the loaded and pressurized PTM was subjected to a one-axis TA level random vibration test as a proof of workmanship.

Four weeks after the initial unsatisfactory hot fire test, the PTM completed the two required burns without propellant flow clogging, which demonstrated the aptness of both the design modification and the hardware rework. The test data from both hot fire test series are summarized in Table 6.

Two new problems occurred during the retest; the jet vanes changed position during the firings producing an unknown amount of drag, and the regulator outlet pressure limit cycled during the second burn. The thrust data were corrected by using an assumed drag value based on computed vane deflection angles which were derived from the measured side thrusts during the test. The second problem, the regulator limit cycling, appeared to be a result of the time constant of the gas system being greater than that of the regulator spring package and is discussed in Subsection D. Based on a study by the JPL flight path analysis group, it was determined that it would be unlikely that the conditions needed to induce the limit cycling would be reached in a nominal mission. Therefore, it was decided that regulator redesign would not be worthwhile.

Table 6. Test results, PTM firings

Test data	Run No. Dd 260	Run No. Dd 270	Run No. Dd 271
Date	2-23-68	3-22-68	3-22-68
Test duration, s	60.497	60.010	30.500
Data taken at time slice	60.247	59.730	30 240
Propellant flowrate, lbm/s[a]		0.2247	
Vacuum thrust, lbf	16.67	51.58[c]	51.39
Chamber pressure, psia	64.56	199.6	197.2
Characteristic velocity, ft/s[b]		4381	
Specific impulse, lbf-sec/lbm		229.6	
Thrust coefficient,[b]	1.684	1.686	1.700
Propellant temperature, °F	75.6	65.4	72.4

[a]Propellant flowrate is the total weight of propellant used divided by the test duration.

[b]Throat temperature assumed = 1650°F, hot throat area = 0.1533 in^2.

[c]Measured thrust data plus 1.20 lbf vane drag (assumed).

The chamber pressure transducer failure noted earlier, was found to be caused by local vibration inputs in excess of the design capability. Similar units successfully passed component TA vibration, PTM spacecraft TA vibration testing, and other flight propulsion subsystem testing without failure. Therefore, the P_c transducer design was considered to be acceptable for *Mariner* Mars 1969 flight without modification.

D. Summary of Problems

The *Mariner* Mars 1969 propulsion subsystem was charged with 34 problem failure reports (PFR's). These PFR's have been catalogued by component or type of failure and are listed by PFR number and date of occurrence in Table 7. A brief description is included along with a callout of the section in which more detail appears. Major problems not discussed elsewhere are covered in this section.

1. Regulator. The major problem inherent in the design of the regulator is the tendency toward limit cycling; i.e., oscillation of the outlet pressure instead of maintaining the nominal regulated pressure. The first *Mariner* Mars 1969 occurrence of limit cycling was during the PTM subsystem TA test on Mar. 23, 1968. After a 60-s first burn, the regulator during the second burn went into a limit cycle mode where the outlet pressure oscillated between 271 and 313 psia. At the start of the second burn, the propellant tank pressure was at 304 psia and during the 30-s test the regulator pressure oscillated through two cycles.

After completion of the subsystem TA tests, the regulator was removed from the PTM subsystem for failure analysis testing in the water flow calibration system. This testing could not reproduce the limit cycling condition of the TA test, but it did trigger a blowdown anomaly originally seen during some second-burn simulations during the *Mariner* Venus 67 Program. Analyses indicated that the blowdown cycle and the limit cycling were related phenomenon which could be triggered when the time constant of the gas system was greater than that of the regulator spring package.

Much later, during testing conducted to provide additional data for the burn time estimation computation, a regulator limit-cycled on the first burn with the propellant tank pressure oscillating between 270 and 325 psia for 9 cycles during the 65-s burn. This test system, although not a flight system, utilized flight hardware; the regulator had been on the flight spare subsystem and had been removed during the rework of the N_2 welded assemblies.

After the first burn limit cycling episode, the regulator was removed from the test system and installed initially in the water calibration system, then later in the gas flow bench which had been used for the component-level regulator calibration testing. This time it was possible to reproduce the anomalous regulator behavior. The results of the testing indicated that increased filter ΔP was not the primary cause of cycling, but a high ΔP could aggravate the condition if it already existed.

The Belleville spring package was the most logical suspect for the primary cause of cycling. A check of the force-deflection curve of the spring package of the offending regulator did not indicate anything grossly out of the ordinary except that the slope of the curve was slightly steeper than that for most of the other regulators and much steeper than that for typical *Mariner* Mars 1964 regulators. An extensive review of the assembly and FA test data showed that this regulator had been rebuilt because of inadequate performance at low temperature. During the rebuild process, the regulator housing was remachined and the spring guides were replaced to increase the housing to spring package clearance. In addition, five springs of the original package were replaced during the rework and one was eliminated.

The only anomalous behavior found in the FA test results occurred in the second burn of a two burn (60–30 s duration) water calibration test. In this test the regulated pressure had changed in a series of small steps (stair-stepping effect) rather than in a smooth sweep as seen in the other regulators. Because of the later and thorough review of the data on all regulators, including *Mariner* Mars 1964 and *Mariner* Venus 67 regulators, such stair-stepping behavior effect is believed to be an indication of an incipient regulator instability which was not known during the earlier FA test program. Since the flight systems were already at the AFETR for launch, another review of the FA test data for the flight regulators was conducted along with a review and comparison of the cycling regulator data. The conclusion of this review was that the regulators on the three flight systems had a very low probability of limit cycling on the first burn Therefore, it was recommended to the *Mariner* Project that the flight regulators not be removed from the spacecraft for change out or additional testing.

Table 7. Problem failure summary

PFR No.	Date of occurrence	Description and corrective action	Section for details
		Regulator	
200521	Dec. 14, 1967	Failed internal leak test after weldup. Assembly procedure changed to test prior to weld. Regulator assigned to PTM.	
200530	Dec. 18, 1967	Outlet pressure exceeded 308 ±3 psi in start test. Procedure corrected to simulate flight conditions.	
200531	Mar. 22, 1968	Outlet pressure limit cycled during PTM second burn; this was a function of tank ullage and N_2 tank pressure. Conditions unlikely to occur in flight.	C
200997	Jan. 10, 1969	Outlet pressure limit cycled during first burn on test subsystem. Cause of problem not fully understood. Comparison of FA test data showed flight regulators probably would not cycle.	D-1
200534	Apr. 11, 1968	Outlet pressure was 322 psia instead of 308 ±5 psig in low-temperature FA test. Spring housing tapered. Housing remachined and spring guides replaced.	
200546	May 13, 1968	Particles from regulator inlet filter scored ball and seat preventing lockup. New deburring technique developed.	
		Pressure Transducer	
200511	Feb. 20, 1968	N_2 transducer case failed burst test. Inadequate weld penetration. Cases were rewelded using EB welding techniques.	B-4-b
200517	Nov. 8, 1967	The Pc transducer overpressured changing calibration; the unit was repaired. Maximum pressure levels were etched on transducer cases to prevent mistakes.	
200522	Dec. 8, 1967	Glass insulator cracked reducing insulation resistance. Soldering temperature reduced and post soldering inspection increased. Unit scrapped.	
200533	Apr. 9, 1968	Output voltage ratio inadequate because of pinhole leak in bourdon tube. Leak repaired.	
200541	Apr. 12, 1968	Potentiometer coils burned out in two N_2 transducers because of current >10 mA applied during checkout. A microamp circuit was fabricated for transducer checkout. Both circuits were repaired.	
200548	Jun. 3, 1968	Joint between inlet tubing and header of N_2 transducer leaked. Joint 65% void of braze material. Joints on all transducers checked.	
		Valves	
200509	Jan. 26, 1968	Three metal chips caused a restriction in the flow bench during lot acceptance test. Believed to be from flow bench and not from valve.	
200526	Feb. 23, 1968	Contamination from valve caught in engine filter causing low thrust (⅓ nominal) during first PTM test. Contamination was the result of poor post-dip brazing cleaning and poor access to blind passages. Drilled access holes and employed acid cleaning.	C
200535	Apr. 13, 1968	Leak between inlet line and T on N_2 valve. Tubing had been bent, possibly failing braze joint, or may have been poor braze joint. Unit repaired.	
200542 200543	Apr. 30, 1968 Apr. 30, 1968	Threads stripped out of aluminum flanges of two propellant valves. Steel inserts were installed and procedure changed to aid assembly.	
200550 200976	Jun. 20, 1968 Jul. 8, 1968	Rams from two N_2 valves ejected during proof and leak tests because of leakage from flow passages. Leaks result of poor braze and poor post-braze cleaning. Inspected all valves carefully and selected best for flight.	D-3
200994	Nov. 1, 1968	Leak at joint between inlet tube and Tee of propellant valve. Valve previously rejected for excessive corrosion and was to be used for test only. Valve scrapped.	

Table 7 (contd)

PFR No.	Date of occurrence	Description and corrective action	Section for details
		Vibration testing	
200518	Dec. 14, 1967	Regulator FA vibration test out of spec. Operator error. No damage to regulator.	
200523 200525	Jan. 25, 1968 Jan. 25, 1968	Vibration levels out of spec during FA test of a N_2 and a P_c transducer. Operator error. No damage to units.	
200536	Feb. 20, 1968	PTM subsystem received excessive vibration accelerations during TA test because of severe crosstalk and resonances in test fixture. No damage to subsystem except to P_c transducer (see below).	C
200537	Feb. 22, 1968	P_c transducer failed during TA vibration of PTM subsystem. Transducer saw up to 50-*g* peak (design level was 13.5 *g*). Acceleration checked during spacecraft TA test and found lower than specified levels. Thus, design was considered adequate.	C
200549	May 4, 1968	Vibration levels out of spec during FA test of P_c and propellant pressure transducer. Operator error and improper fixture bolt torque. Operator and QA representative reprimanded. No damage to units.	
		Miscellaneous	
200501	Oct. 9, 1967	Propellant tank burst test data scatter 7% instead of $<5\%$. Maximum working pressure reduced from 400 psia to 375 psia at 125°F.	B-6
200508	Jan. 10, 1968	Test stand filter failed during regulator FA testing. Filter element installed backwards. Procedures changed to have QA cognizance of assembly and installation of filters.	
200510	Jan. 2, 1968	Force-deflection curve of Belleville spring package changed with cycling. Springs maintain tie down of tanks. Method for adjusting preload on tanks modified.	
200540	Mar. 22, 1968	Vacuum test stand steam system backflowed 7 s after PTM firing because of leak between 2 flanges. Flange bolts tightened and periodically checked. No damage to subsystem or thrust stand.	
200544 200547	May 4, 1968 Jun. 1, 1968	N_2 tank-manifold flange joint leaked at 5400 psi proof pressure. Design did not permit testing to 5400 psi. Proof pressure reduced to 4000 psi, and aluminum crush gaskets deoxidized in Aldox Type W solution.	
200989	Jun. 19, 1968	Flight subsystem in container dropped 15 in. from forklift. No apparent damage to subsystem. Reassigned as spare because no way to check regulator.	D-2
203781	Sep. 20, 1968	Subsystem pyrotechnic harness was too long and rubbed on another subsystem in spacecraft. Harness repositioned to prevent wearing of insulation.	

2. Subsystem drop. While transporting S/N 002 propulsion subsystem from the JPL receiving dock to the liquid propulsion test area, the unit in its shipping container fell from the fork lift 15 in. to the asphalt roadway. After this accident the subsystem was given a thorough visual inspection. Also leak tests and pressure transducer calibrations were accomplished. No leaks were found and the transducer calibrations had not changed. Because of the welded, no-bolted-interfaces of the nitrogen system, it was not possible to check the performance of the pneumatic regulator. Since the *Mariner* Mars 1964 subsystem had successfully passed drop tests, it was assumed that the regulator was not damaged. However, since the regulator could not be checked without removal from the welded system, this propulsion unit was reassigned to the spare spacecraft as a precautionary move. Later, the regulator was removed when the nitrogen valves were replaced.

3. Nitrogen valve. Late in the program, a nitrogen valve was subjected to a burst test for the purpose of establishing the basis for obtaining an AFETR range safety waiver to the requirement that tubing and manifolds have an ultimate burst-to-working pressure safety factor of four times. Since the valve was so similar to the *Mariner* Mars 1964 valve, it had been decided not to change the tubing to avoid affecting the operating characteristics of the valve. Previously, the *Mariner* Mars 1964 valve had demonstrated a tubing safety factor greater than three. In the *Mariner* Mars 1969 burst test the tubing failed at a hydrostatic pressure of only 8000 psi; i.e., 2.4 times the maximum operating pressure of 3300 psi. An evaluation of the low-burst pressure (greater than 11,000 psi had been expected) found that the heat treat condition of the aluminum 6061 tubing was apparently at a T-4 condition instead of the specified T-6.

Just prior to starting the hydrostatic burst testing, one N_2 valve ejected a ram from the No. 1 squib port during final proof and leak testing. A second N_2 valve then exhibited the same kind of failure a week after starting the burst testing. During failure analysis, it was determined that one of these N_2 valves had not been cleaned by the braze vendor immediately after the dip brazing operation. Electron microscope examination of the leak area showed excessive corrosion pitting of the tube within the squib port. The second leak failure resulted from insufficient braze material in the nipple-body joint. Post-leak visual inspections showed poor or nonexistent braze fillets at the joints; the valve should have been rejected during the original receiving inspection.

Because of the reduced burst strength data and the two leak failures, it was decided to replace all of the N_2 valves on the three flight subsystems. All available valves including spares and the valves removed from the flight subsystems were thoroughly inspected for corrosion pits in all tubing and the quality of all braze fillets. By this means, the four best valves were selected for rework. The external tubing was removed from the valves. The valves were recleaned and heavier walled tubing was welded into the T manifolds. The valves were then heat treated to the T-6 condition, and, finally, three valves were welded into the nitrogen system welded assemblies (which included a regulator, N_2 tank manifold and pressure transducer) with extensive use of weld chill blocks to minimize heat treat changes. A burst test weldment was made up using the fourth valve and a spare N_2 tank manifold. The test valve and manifold assembly were reworked in the same manner and at the same time as the flight hardware. The test assembly was hydrostatically pressurized to 11,400 psig at which point the N_2 manifold outlet tube burst. This indicated that the reworked welded assembly has a safety factor of 3.4 for a maximum tank presure of 3300 psig at 125°F. Though this safety factor was below the AFETR 4:1 requirement, a waiver to permit its use was granted since the tank temperature would not exceed 90°F during loading and ground testing and, by virtue of its location within the spacecraft, the tubing is protected from accidental damage. Upon completion of assembly and proof and leak testing, the flight nitrogen system welded assemblies were shipped to AFETR where they were installed on the flight propulsion subsystems.

4. Propellant valve. Because of the leakage failures in the N_2 valves described above and failure of a propellant valve, all propellant valves including four new valves were also inspected for corrosion pits and the quality of all braze joints. The four best valves (three flight and one spare) were reworked; this included recleaning, welding in a new inlet tube, and reheat treating. Then the valves were proof pressure checked with helium to 1600 psi, four times the maximum operating pressure, to assure that all the brazed and welded joints had been satisfactorily processed. The valves were immersed in alcohol to aid in leak detection. The pressure was increased to 1600 psi three times. The 1600 psia was held 1 h during the last cycle. No leakage from the squib ports or from any of the brazed or welded joints was

noted. The valves were installed along with the nitrogen assemblies at AFETR.

E. System Test

Propulsion involvement in the spacecraft system test activity was limited since it was not possible to perform a hot firing during system test. During much of the system testing on the PTM and flight spacecraft, the PTM propulsion subsystem was used. In all testing except the PTM pyro shock test, squib simulators containing 1-Ω resistors were installed to provide a termination for the pyrotechnic subsystem. Both the pressurant and propellant tanks were pressurized to 50 psig for a readout check through the spacecraft telemetry subsystem.

For the PTM pyro shock test, live squibs were installed in test valves mounted on the PTM subsystem. Data on the shock levels felt throughout the spacecraft were determined during squib actuation of the valves. The results of this testing verified that there were no problems resulting from the propulsion valve actuation within the subsystem or spacecraft.

The PTM propulsion subsystem was also used for checkout of the FTS data display from the pressure transducers. In this test, the nitrogen tank and the propellant tank were separately pressurized over a range of pressure. The output of the FTS was compared with that shown on a high-resolution pressure gauge. The data deviated considerably. A post-test investigation showed that there had been a design modification made to the FTS to make the pressure transducer 0 to 3-v analog-signal compatible with the 0 to 100-mV range required by the FTS for the two tank pressure channels. This modification consisted of adding voltage divider networks which, in turn, had the effect of changing the curve of pressure-FTS signal from a linear to a second order curve. After the effect of this voltage divider network was incorporated into the FTS output computations, a checkout test was rerun on the PTM. The FTS output agreed with the recomputed curves.

During FA vibration testing of the flight spacecraft, the PTM propulsion subsystem was used in place of the flight propulsion units. To simulate dynamic mass effects and for reasons of safety, the PTM propellant tank was filled with water rather than hydrazine. The flight units were not vibrated because of concern that the water could not be totally removed and any residual may affect the performance of the rocket engine and the reproducibility of the timed burn. After the vibration testing the PTM unit was removed and the flight propulsion subsystem reinstalled in the spacecraft for the solar thermal vacuum testing.

F. AFETR Operations

The propulsion operations at the AFETR began in mid-December 1968. The initial efforts were preparing the propellant loading and instrumentation buildings (PLB) at the explosive safe area (ESA) for subsystem loading operations, obtaining range safety approval of the pressurization and propellant loading procedures and equipment, and preparing the PTM propulsion system for installation in the spare spacecraft M69-4.

The PTM propulsion unit was received at AFETR loaded with water. After an inspection the squibs were installed and the unit was pressurized to 50% of the flight pressures. The PTM was then installed in the M69-4 spacecraft for the match mate, J-FACT, and EMI testing with both launch vehicles.

The flight propulsion units were received at the PLB following an abbreviated post-shipment spacecraft system test at the Hangar AO facility. The primary purpose of this system test was to assure that the jet vane actuators performed normally with the attitude control subsystem. At the PLB, each flight unit went through a rebuild cycle for replacement of the N_2 system welded assembly and the propellant valve. After each unit was rebuilt it was then proof and leak tested, squibs installed, filled with propellant, and pressurized. The propellant tank was pressurized to approximately 265 psig at 70°F using nitrogen gas. The high-pressure nitrogen system was then pressurized with GN_2 to 3000 psig at 70°F.

With the completion of the propellant fill and pressurization, the propulsion subsystems were installed in their shipping containers and moved to separate storage areas. During this storage period the subsystems were monitored via the flight transducers for indications of leakage. Pressure and temperature readings were obtained twice daily from both the propellant tank and the nitrogen tank. This monitoring continued until the units were installed in the flight spacecraft prior to launch. Subsystems S/N 003 and S/N 001 were installed in *Mariner F* and *G*, respectively. The remaining subsystem S/N 002, was offloaded after the launch of the last spacecraft and returned to Pasadena.

II. *Mariner* Mars 1969 Pyrotechnic Subsystem

A. Functional Description

The *Mariner* Mars 1969 pyrotechnic (pyro) subsystem was involved in the performance of the following in-flight events:

(1) Spacecraft separation.

(2) Solar panel deployment and scan platform unlatching.

(3) Propulsion thrust initiation and termination.

(4) Infrared spectrometer (IRS) cooldown and motor start.

The pyro subsystem, shown in Fig. 11, was logically similar to that of previous *Ranger* and *Mariner* series in that pyro devices were initiated (fired) redundantly. The planned inflight sequence of pyro-related events is presented in Table 8.

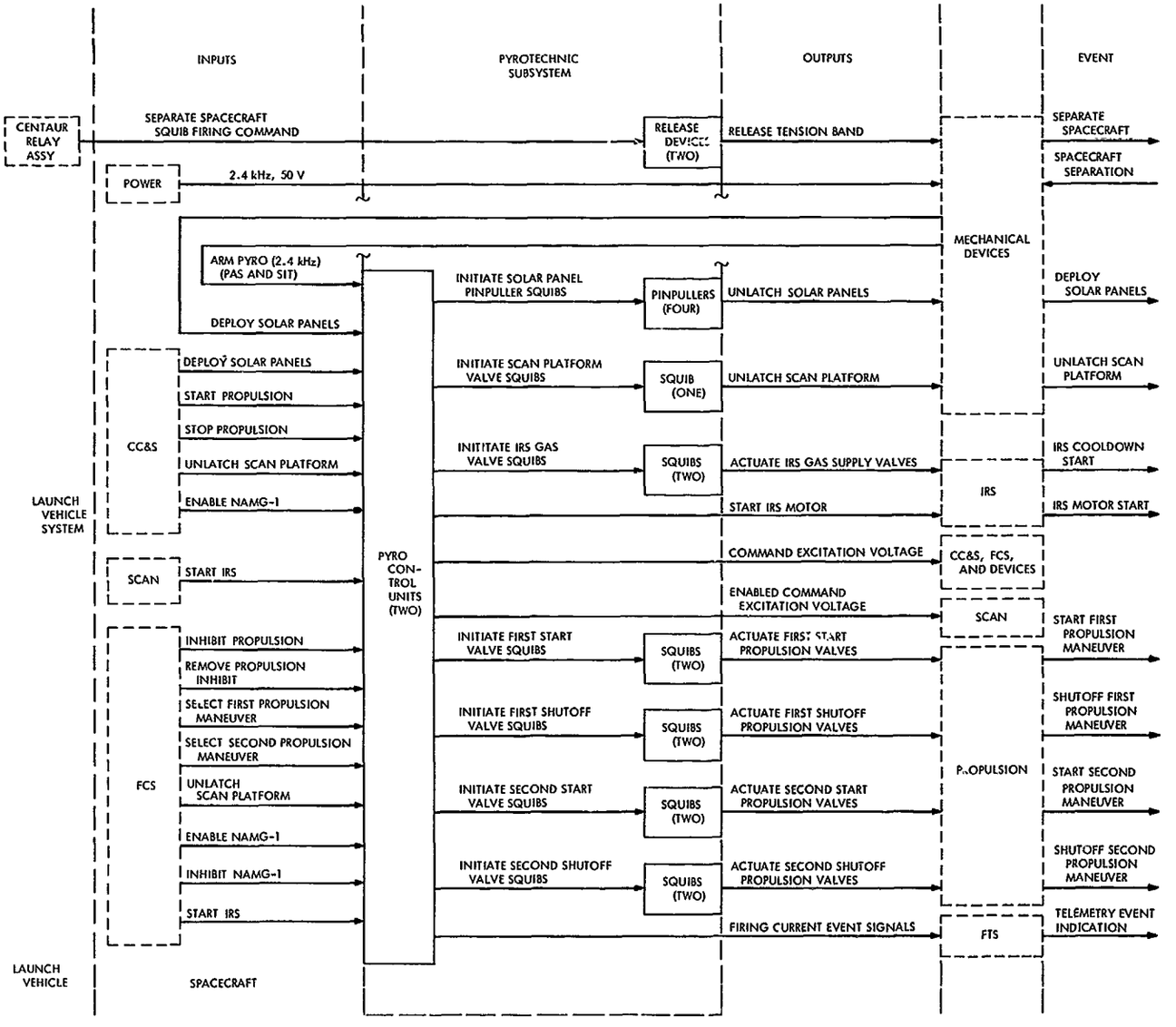


Fig. 11. Functional block diagram of the pyrotechnic subsystem

Table 8. Pyrotechnic subsystem functions

Event	Source	Pyro function	Number and type of device	Total number of squibs	Total number of bridgewires	Telemetry outputs from pyro	Comments
Spacecraft separation	Launch vehicle	Release tension band	Two mechanically redundant release devices. Each device utilized two redundant squibs.	4	4	None	Firing circuit of launch vehicle supplied initiation current to squibs upon command which was generated within launch vehicle.
Arm pyrotechnics	Devices pyrotechnic arming switch (PAS)	Charge energy-storage capacitors and supply command-excitation voltage	Capacitor banks in each of the two redundant spacecraft pyro control units are charged. Both units supply command-excitation voltage.			None from pyro (outputs from mechanical device subsystem)	2.4 kHz, 50V power routed from power subsystem to both pyro control units through PAS arming switch which actuated at spacecraft separation.
							Pyro control unit (PCU) internal reset to ensure inhibiting IRS circuit.
	Devices separation initiated timer (SIT)	Same as above, if required					Backup to above. Same as above, except thru SIT.
Deploy solar panels	Devices SIT	Unlatch solar panels	Four pinpullers.[a]	8	8	Firing current event indication to: (a) event counter 1 (b) event counter 3	Command from devices to pyro will not occur sooner than 1.5 min after pyro arming. Each PCU initiates one squib of each pinpuller.
	CC&S	Same as above, if required				None expected[b]	Backup to above.
Transfer to first propulsion maneuver position	Flight command subsystem (FCS)	Transfer control circuits to first maneuver position				None	Pyro in first maneuver position at launch.

[a]Each pinpuller utilizes two redundant, single-bridgewire squibs.

[b]SIT (T2) command expected to initiate event. If SIT did not initiate event, then event counters 1 and 3 indications expected. If SIT did initiate event, then outputs could occur on event counters 1 and/or 3 if there were post-fire squib shorts.

Table 8 (contd)

Event	Source	Pyro function	Number and type of device	Total number of squibs	Total number of bridge-wires	Telemetry outputs from pyro	Comments
Remove propulsion inhibit	FCS	Enable pyro control units to operate upon subsequent CC&S commands for start and stop of propulsion				None	Pyro in enabled condition at launch.
Start first propulsion maneuver	CC&S	Actuate propulsion first start valves	Two normally-closed valves.[c]	2	4	Firing current event indication to: (a) event counter 1 (b) event counter 3	Each PCU initiates one bridgewire of each squib.
Shutoff first propulsion maneuver	CC&S	Actuate propulsion first shutoff valves	Two normally-open valves.	2	4	Firing current event indication to: (a) event counter 1 (b) event counter 3	Each PCU initiates one bridgewire of each squib.
Transfer to second propulsion maneuver position	FCS	Transfer control circuits to second maneuver position				None	Required for second maneuver.
Start second propulsion maneuver	CC&S	Actuate propulsion second start valves	Two normally-closed valves.	2	4	Firing current event indication to: (a) event counter 1 (b) event counter 3	Each PCU initiates one bridgewire of each squib.
Shutoff second propulsion maneuver	CC&S	Actuate propulsion second shutoff valves	Two normally-open valves.	2	4	Firing current event indication to: (a) event counter 1 (b) event counter 3	Each PCU initiates one bridgewire of each squib.
Inhibit propulsion	FCS	Inhibit pyro control units to prevent response to subsequent CC&S command for start and stop of propulsion				None	Optional command.
Unlatch scan platform	CC&S	Unlatch scan platform	One normally-closed valve.	1	2	Firing current event indication to: (a) event counter 1 (b) event counter 3	Each PCU initiates one bridgewire of the squib.
	FCS	Same as above, if required				[d]Firing current event indication, event counter 1	Backup to above.

[c]Each valve utilizes one dual-bridgewire squib.

Table 8 (contd)

Event	Source	Pyro function	Number and type of device	Total number of squibs	Total number of bridge-wires	Telemetry outputs from pyro	Comments
Enable narrow-angle Mars gate (NAMG-1)	CC&S	Enables Pyro Control unit to apply excitation to NAMG-1 and IRS start circuits				None	
	FCS	Same as above, if required				None	Backup to above.
Start IRS	SCAN	Actuate IRS gas valves and supply IRS motor start signal	Two normally-closed valves.	2	4	Firing current event indication to: (a) event counter 1 (b) event counter 3	
	FCS	Same as above, if required				[d]Firing current event indication, event counter 1	Backup to above.
Inhibit NAMG-1	FCS	Removes PCU excitation from NAMG-1 and IRS start circuits				None	Pyro in inhibited condition at launch.

[d]For FCS commands; if given FCS command is used as the prime command for an event, then event indication is only expected in event counter 1 because the FCS command indication on event counter 3 masks the pyro event.

B. Hardware Design, Development, and Test

1. Pyro control units. The design of the *Mariner* Mars 1969 pyro control units (PCU) was based on the preceding *Mariner-C* design, which was the authorized baseline configuration. Changes were made in the baseline design to satisfy differences in functional requirements, to improve inherent reliability, to increase performance margins, and to reduce cost.

The responsibility for the design, development, and testing of the pyro subsystem electronics was subcontracted to Electro-Optical Systems, Inc., Pasadena, California.

The major functional and detail changes from the *Mariner-C* baseline design consisted of the following:

(1) Incorporation of the IRS cooldown and motor start function.

(2) Change in the mechanization detail of the maneuver inhibit function for the propulsion start event.

(3) Addition of unijunction transistor driver circuits for triggering of the SCR squib firing output switches.

(4) Addition of fuses in the power transformer primary to provide short-circuit protection for the 2.4 kHz inverter.

Two of the changes presented above resulted in the majority of the problems which were subsequently experienced in development and testing; these items were the IRS cooldown and motor start function and the protective fusing.

The problems in the IRS interface area occurred because requirements were defined relatively late in the program; as a result, the circuit design had to be hastily completed to meet the hardware schedules. In addition, because of delay, the parts were not procured in a manner that would ensure acceptable quality. There was an unusually high incidence of problems associated with the particular relay type used in the circuit. The problems were primarily lead breakage plus one case of relay anomaly caused by internal contamination. The latter problem was found in only one relay; several other relays from the same lot were opened and inspected for contamination, and all relays were cycled and checked for

time delay. It was concluded that the relays designated for flight were most likely not contaminated. This problem pointed up the need for precanning inspection as well as ultra cleanliness. The lead breakage showed up during installation and appeared to be a combination of misinstallation of the transipad and hydrogen embrittlement of the wire which made the leads very susceptible to mishandling failures. Relays which had been installed properly and conformally coated did successfully pass TA vibration testing. The relays in the subsequent flight PCU were installed with care.

A problem associated with the protective fusing was identified, somewhat by accident, early in the test program on the PTM spacecraft. The configuration of the wiring between the power and pyro subsystems was such that only one of the two parallel fuses in each PCU was connected. The improper wiring resulted from the fact that the flight-type PAS and SIT switches were not installed on the spacecraft, and the simulators for these devices were incorrectly configured because of the absence of correct definitive documentation. Additional testing and analysis of the PCU's showed that the rating of a single fuse was not compatible with the maximum peak current level which could occur as a result of inrush magnetization current to the 2.4-kHz power transformer in the PCU. To provide a margin of safety in the event another miswiring or a wiring failure occurred, a resistor was added in series with the transformer primary and the fuses, such that the current-time firing characteristics of a single fuse would not be exceeded. After this design change was implemented, an extensive test program was conducted on the PTM PCU and the flight PCU to demonstrate acceptable reliability and confidence levels.

The fact that the fuse problem had not been uncovered earlier during bench testing of the PCU was attributed primarily to the fact that no consideration had been given to this potential failure mode. All testing had been conducted with the flight-design parallel fuse configuration. Furthermore, as it was subsequently learned, the 2.4-kHz power supply used in the pyro lab test set (LTS) did not adequately simulate the spacecraft 2.4 kHz inverter. The LTS supply had a relatively high-dynamic output impedance, such that the peak output current was limited to a value which would not have blown the single fuse had such a test been performed. The cyclic turn-on demonstration testing, conducted after the PCU redesign, was performed using a prototype of the flight 2.4-kHz inverter and was done separately through each of the parallel fuses in the PCU.

The mechanical design of the PCU is shown in Fig. 12. There were two subassemblies, each redundant to the other. Each subassembly was packaged in a standard 6 by 6 in. chassis which was 3½-in. deep. In general, planar packaging techniques were utilized; however, to a limited degree, similar circuits were packaged in modular form. It was decided that welded connections would not be introduced into the *Mariner* Mars 1969 PCU module design.

Discrete components were used in all applications. The use of integrated circuits was not considered, since the weight and volume of the PCU was controlled primarily by the energy-storage capacitors. Furthermore, there was no system requirement to reduce the weight below that value which had initially been estimated.

2. Release device. The release devices used on the *Mariner* Mars 1969 spacecraft were of essentially the same design as the devices previously utilized on the *Mariner IV* and *V* spacecraft.

For the *Mariner* Mars 1969 program a field joint was introduced below the separation plane thereby placing cognizance of the complete separation mechanism with JPL. The V-band assembly, including the two release devices, was therefore procured, assembled, and flight qualified by JPL for the *Mariner* Mars 1969 Program.

Early in the *Mariner* Mars 1969 Program, a small quantity of release assemblies were procured from the Holex Company for preliminary evaluation of the devices and squibs at JPL. After completion of the test program, a purchase order was placed with the Holex Company for one flight lot of release devices and squibs.

Only minor changes to the basic design of the device were found to be necessary during fabrication and testing of the flight devices at the Holex Company. The changes were essentially an increase in quality control during manufacture, a decrease in dimensional tolerances of the detail parts, the addition of a thin mylar disk to act as a heat shield in front of the beryllium copper diaphragm, and additional vacuum processed epoxy under the fixed bolt end, to prevent blowby of the hot gases.

a. Testing. Upon receipt of the flight hardware at JPL, a large sample of the devices and squibs were formally TA tested to verify structural integrity and reliable device actuation under the worst-case flight environmental and functional conditions. The remaining devices and squibs were then FA tested and designated as flight equipment.

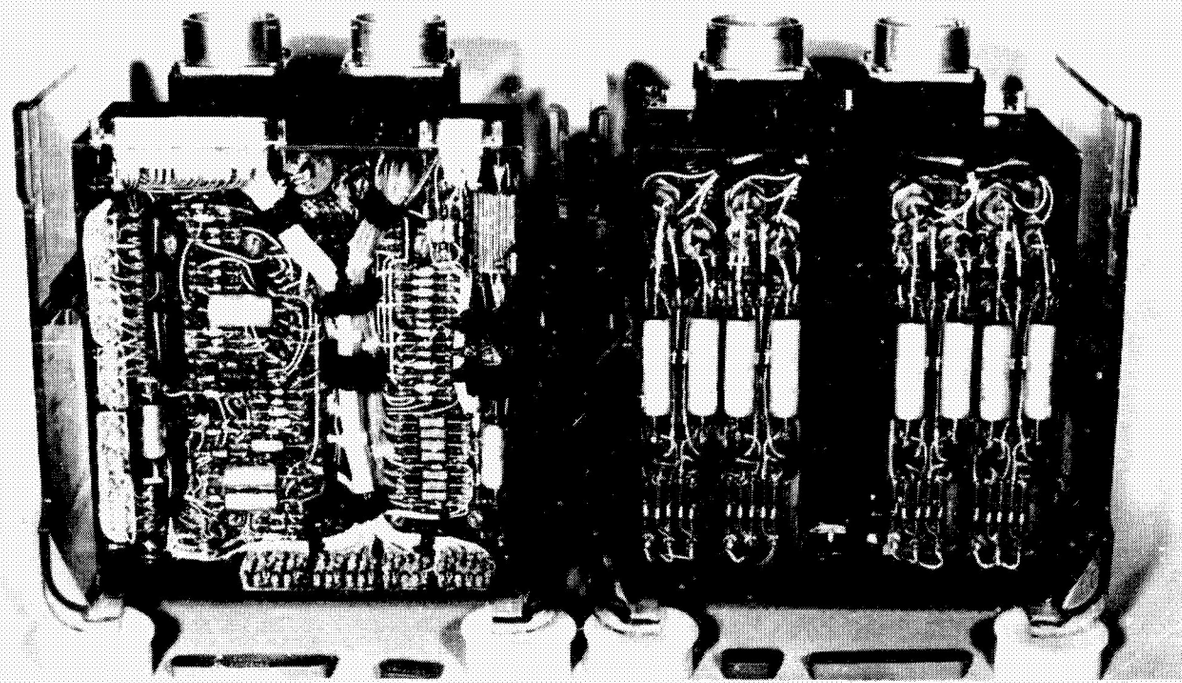


Fig. 12. Pyrotechnic control units

In addition, system pyro shock test actuations were accomplished on the completely assembled PTM and two flight spacecraft. Approximately 24 devices were also tested as part of the V-band assemblies in support of tip-off rate studies. The results of all component and subassembly testing were generally satisfactory.

b. Problems. Three problems which required design fixes or imposed constraints on the use of the device, occurred during fabrication and testing of the flight lot hardware. These problems were (1) creep of the shear washer, (2) failure of the release bolt, and (3) squib gas blowby.

The basic design permitted shear/tensile loads on the internal shear washer in excess of its yield strength. This resulted in coining of the shear washer at tensile loads less than the flight tension requirements. Although the device was reported to have a 4800-lb structural capability, yielding (creep) of the internal washer occurred at approximately 2000-lb tension.

After being loaded to 2500-lb tension, it was observed that the device tension would drop to approximately 2200 lb and several additional tensionings were necessary before flight usage. To preclude possible degrading effects on reliable device actuation, TRW and Holex recommended not structurally proof-loading the device prior to flight. The devices were, therefore, FA tested and then delivered to AFETR for flight in an unproofed condition.

During prelaunch operations at AFETR, the PTM spacecraft was mated to the adapter with two flight release devices at 2500-lb tension. After approximately 16 h of tension, one of the release devices failed in tension and released the V-band assembly. The failure was a fracture of the stud head of the release bolt from the stud shank. The cause of the failure was attributed to a combination of (1) hydrogen embrittlement of the 4140 bolt material which occurred during the cadmium plating/pickling process, and (2) a high-stress concentration because of the minimal fillet radius (0.005 in.) between the stud head and shank. A design fix was incorporated to increase the fillet radius to the range 0.010 to 0.015 in. In addition, the pickling process prior to cadmium plating the bolts was eliminated and replaced with vapor honing. After cadmium plating, the bolts were immediately (within 7 min) subjected to hydrogen embrittlement relieve for 24 h at 400°F. The new bolts were subjected to a proofloading of 3750 lb for 24 h.

The new bolts were fabricated, tested, accepted, and delivered to AFETR within two weeks.

During component and system development testing, the device periodically leaked squib gases. The leakage occurred at both the fixed stud end and around the diaphragm at the released stud end. The leakage at the fixed end was eliminated by adding a high-temperature vacuum-cured epoxy over the original epoxy joint. Any voids in the original epoxy were opened to permit complete filling of the joint. Also the TA maximum temperature was reduced from 167 to 131°F which was compatible with the *Mariner* Mars 1969 requirements. The 167°F was a design goal. The leakage at the release end was determined to be from cracks in the sealing diaphragm caused by the impact of hot molten particles (solder or propellant) from the squibs. It was noted, by the vendor, that this type of failure had occurred on their larger device. The correction was to add a 0.003-in. disk of Mylar on the gas side of the diaphragm and liberal amounts of high-vacuum grease. The Mylar disk and grease provided a heat shield (ablative film) between the diaphragm and the hot particles. This change was incorporated into the *Mariner* Mars 1969 device. No further leakage was seen from either end of the device.

3. Pinpullers. The pinpuller used on the *Mariner* Mars 1969 program was essentially the same design as that used on the previous *Mariner IV* and *V*. For the *Mariner IV* and *V* spacecraft, the pinpuller squibs were the ½-A ¼-W no-fire variety. A new pinpuller squib was required to meet the 1 A/1 W no-fire requirement of the *Mariner* Mars 1969 program. Early in the program, several different types of candidate 1 A/1 W no fire squibs were procured for evaluation testing. It was determined that the single bridgewire *Apollo* standard initiator squib was compatible with the safety and reliability requirements of the *Mariner* Mars 1969 pinpuller application. Only minimal design changes were made to the pinpuller mechanical body assembly.

a. Testing. Nondestructive testing was conducted on the pinpuller body assembly, the monitor connector, and the squibs at the vendors' facilities prior to acceptance by JPL. Upon receipt of the hardware at JPL, the units were inspected and a large portion of the lot was selected for the destructive TA test program. Type approval testing was conducted in two phases, testing of the squibs and testing of the completely assembled pinpuller. Worst-case conditions of environments and configurations were used to demonstrate the structural integrity and actuation reliability of the assembly. The remaining units were designated as flight equipment and were FA tested prior to delivery for systems test or flight usage. Four flight lot pinpullers were used during pyro shock tests on the PTM spacecraft.

The results of component level and systems level testing were generally acceptable; however, a problem with a loose insulator-contact was uncovered on one pinpuller during TA testing; a shear pin failure occurred on one pinpuller during handling and installation prior to a pyro shock test.

b. Problems. The loose insulator-contact of the monitor connector raised two areas of concern. First, it would inhibit the stroke of the pin and prevent deployment of the solar panels and, secondly, it would short across the monitor connector giving a false indication of pin retraction on the launch pad (a launch abort indication). Actuation tests were performed with a loose insulator-connector in various positions in the bore. In all tests the pin retracted farther than the specified value indicating that the pinpuller would correctly perform even in the failed condition. All the insulator-connectors were inspected to see if they were correctly epoxied into the piston. It was believed that the third lot of pinpullers had the best bond based on the color of the epoxy joint. Other than this visual qualitative criteria, there were no new nondestructive tests which could identify potentially weak joints. Because of the situation described, the flight pinpullers were selected from the third lot and were x-rayed at AFETR immediately prior to installation on the spacecraft to assure that the insulator-contacts were not loose.

The aforementioned shear pin failure was most probably a mishandling problem which occurred during installation on the spacecraft. The AFETR X-rays, taken for insulator-contact problem, also showed the integrity of the shear pin. The spacecraft technicians were cautioned to use care when handling the pinpullers; in addition, pyrotechnic personnel were instructed to be present during future pinpuller installations.

4. Valve squibs. The *Mariner* Mars 1969 propulsion system used explosively actuated valves to start and to stop the rocket engine. The valves were to be of the same design as used in the *Mariner* Mars 1964 and *Mariner* Venus 67 spacecraft. Squibs identical to those used on *Mariner* Mars 1964 were procured to preclude the necessity of repeating a valve qualification program.

The contract for procurement of the *Mariner* Mars 1969 valve squibs was let to the Hi-Shear Corporation. No changes were allowed from the production base line drawings used on the *Mariner* Mars 1964 squibs. Because of the problems in the *Mariner* Mars 1964 in obtaining acceptable pin-headers, a contingency fund was incorporated for purchase of additional ceramic pin-headers for the squib if the initial lot of headers were not sufficient. Most of this fund was expended to obtain pin-headers.

The only major problem in the procurement of the valve squib was in obtaining satisfactory pin-headers. The pin-headers consisted of an alumina ceramic plug in which four iron-nickel-cobalt pins were brazed. This assembly acted as the electrical connector insert, had the mechanical strength to withstand the squib firing pressure, and provided a heat sink for no-fire current tests. It was required to maintain its mechanical integrity after firing to prevent leakage of propellant gases and the consequent blowoff of the connector which could destroy other hardware. Because of this potential failure mode for both *Mariner* Mars 1964 and *Mariner* Mars 1969 Projects, JPL set high standards for leak tightness and braze joint filling on these headers. As a result, the yield of acceptable parts was low, though improved manufacturing techniques increased the yield from 4% for *Mariner* Mars 1964 to 12–15% on *Mariner* Mars 1969.

C. System Testing and Prelaunch Operations

It was interesting, and somewhat discomforting, to note that the two most critical problems of the *Mariner* Mars 1969 pyro subsystem were identified during the system-level test program. Either of the two problems, which were entirely unrelated, could have resulted in a mission catastrophe.

The first problem of interest was that associated with inrush magnetization current of the PCU power transformer and the consequent blowing of the protective fuses in the PCU. The failure occurred early in the system test program of the PTM spacecraft when the prototype PCU was aboard. There was a discrepancy in the electrical configuration of the spacecraft at the time, which allowed the problem to be identified. It was shown in subsequent test and analyses that for a normal flight configuration the failure most likely would not have occurred; however, there would have existed an unknown marginal condition. It was subsequently determined in the investigation that the reasons the problem was not discovered in subsystem testing (and probably would not have been discovered) was the fact that there were no tests designed to uncover the failure mode and the characteristics of the spacecraft power subsystem 2.4-kHz inverter was not adequately simulated in the pyro laboratory test set.

The second problem of interest was that of the mechanical failure of the V-band release device during a test period on the *M69-4* spacecraft. This potential failure had not been identified during subsystem testing. As discussed previously, design deficiencies were identified after the failure had occurred; however, a reasonably rigorous subsystem test program had previously failed to identify a problem or marginal condition. It may well be that in the subsystem test program, consideration was not given to the possible affects of imposed loads which may result in the field assembly process, and which had not been planned for in the design of the device.

Two other problems of interest uncovered during the system test program were of lesser potential consequence than those discussed above.

During the pyro shock test performed on the spacecraft, it was determined that the command event indications from the FCS masked the pyro channel B firing event indication to the FTS, since both the FCS indications and the pyro indication outputted to the same event counter in the FTS. Thus, during a commanded pyro event there would be no assurance that PCU-B had operated properly. Because of the redundancy in the pyro subsystem, it was decided not to change the event counters.

During the final assembly of the *M69-4* spacecraft at the explosive safe facility, it was found that the energy-storage capacitor banks of the PCU were charged to a small degree when spacecraft power was turned on, even though the pyro arming switches were in the "safe" mode. The observed charge, on the order of 1V, or less, was determined by analysis to not represent a potential safety hazard; however, the situation did introduce certain possible interface problems with AFETR range safety. The JPL electromagnetic compatibility group evaluated the situation and postulated a reasonable cause and corrective action for the condition. By analysis, the problem was concluded to be caused by the effect of capacitative coupling in the wiring running between the spacecraft 2.4-kHz inverter, the pyro arming switches (PAS and SIT), and the PCU. The analytic conclusion was confirmed by test. The recommended correction action consisted of the rerouting of certain of the existing cabling and the selective addition of shielding. This corrective action was not feasible for the *Mariner* Mars 1969

Program, but was subsequently incorporated into a future program. For the subsequent *Mariner* Mars 1969 flight spacecraft, the applicable AFETR prelaunch test procedure was revised to specify the expected partial charge condition, rather than a no-voltage condition. The procedure revision was approved by AFETR range safety.

D. Recommendations

Several major deficiencies in subsystem functional design and spacecraft system implementation are listed below. While some of these problems were passed on from previous projects as established practice, it is recommended that future missions carefully re-examine the risks inherent in all areas discussed.

(1) The mechanization of the solar panel unlatch event was such that all four pinpullers had to actuate to effect deployment of the four solar panels. Failure of any single pinpuller would prevent two adjacent panels from deploying, a result which would be mission catastrophic.

(2) Squib-operated valves in the propulsion subsystem, the scan platform latch, and the IRS were all dependent on successful operation of a single squib to perform intended functions. Consequences of a single squib failure ranged from loss of some science data in the case of the IRS and scan latch valves to possible catastrophic mission failure in the case of any of the propulsion valves.

(3) The NAMG-1 command output was not a simple switch closure. There was an undesirably high-degree of interaction between the NAMG-1 and the PCU circuitry.

(4) The maneuver inhibit command (DC-13) affected not only pyro but also the CC&S and attitude control subsystems. It was desired to keep Pyro in the maneuver-inhibit state except during midcourse maneuvers to protect against a possible SCR failure by shorting which would initiate an undesired start of the propulsion engine.

(5) Insufficient diagnostic telemetry was available to the pyro subsystem. Relay positions associated with propulsion maneuver position, propulsion inhibit/enable, and IRS inhibit/enable were not monitored by telemetry. The meager telemetry data available was further reduced by masking of one of the two "pyro amps" event channel indications by one of the direct command event channel indications.

(6) The minimum time between pyro arming by the SIT switch and the solar panel deployment command from the SIT did not allow a reasonably conservative capacitor bank charging duration to be employed.

(7) The cabling associated with the pyro safe/arm switches was mechanized such that the capacitors received a small voltage, even though the system was nominally turned off in the safe mode.

(8) The ability to analyze PCU performance was compromised by the limited accuracy of the current amplitude and time data obtained from the pyro OSE oscillograph.

(9) There was only one system-level test in which all the pyro devices were actuated; this was the pyro shock test conducted on the PTM spacecraft. The flight PCU were launched without actually having fired a full complement of live squibs (there were some firings of the IRS gas system squibs during space simulator testing of the flight spacecraft).

References

1. Sackheim, R. L., and Boyd, B. R., *Mariner Mars 1969 Propulsion Subsystem Functional Description and Program History*, Report MM.4701.68-043. TRW Systems Group, Redondo Beach, Calif., Sept. 26, 1968.

2. *Flight Projects*, Space Programs Summary 37-49, Vol. I. Jet Propulsion Laboratory, Pasadena, Calif., Jan. 31, 1968.

3. *Mariner Venus 67 Final Project Report: Vol. II. Midcourse Maneuver Through End of Mission*, Technical Report 32-1203, pp. 336-345. Jet Propulsion Laboratory, Pasadena, Calif., May 1, 1969.

PRECEDING PAGE BLANK NOT FILMED

Environmental Test Program

I. Introduction

Prior to launch of the *Mariner* Mars 1969 spacecraft, the spacecraft and component subsystems were subjected to an extensive environmental test program. The program was intended to:

(1) Provide design verification and certification of acceptability for flight of the spacecraft and its subsystems in the mission environments.

(2) Provide a high degree of confidence in the ability of the spacecraft to perform satisfactorily in the mission environments.

The importance of an environmental test program which would provide the necessary design verification and confidence was imperative due to the very nature of the *Mariner* Mars 1969 spacecraft missions. Since there was not a flight test program and the available launch window was limited, the environmental test program was required to be sufficiently broad and thorough so as to encompass all mission environments and allow for an assessment of their impact on the spacecraft and subsystems during both ground and flight operations.

The conduct of an environmental test program which would meet project requirements has been demonstrated in the past. Both the *Mariner* Mars 1964 *(Mariner IV)* and *Mariner* Venus 67 *(Mariner V)* projects implemented environmental test programs similar to that of *Mariner* Mars 1969. The success of these two missions can be related to the adequacy of their environmental programs.

The *Mariner* Mars 1969 project provided new challenges to the environmental test program. The complexity, physical size, and sophistication of the science payload in conjunction with the utilization of state-of-the-art techniques in the electrical and mechanical design of the spacecraft required that the environmental test program be capable of yielding the desired confidence. In selected areas, it was required that innovations to the test program philosophy be made to assure compliance with the program requirements.

The environmental test program philosophy evolved at JPL has been to:

(1) Demonstrate the design adequacy by requiring successful type approval (TA) tests of flight-quality subsystems and a flight-quality system.

Table 1. Summary of TA and FA subsystem environmental test requirements

Test environment	TA requirements	FA requirements
Package drop	Height variable to weight	N/A
Transportation vibration	1.3 g pk, 2.5–35 Hz 3.0 g pk, 35–48 Hz 5.0 g pk, 48–500 Hz	N/A
Explosion proof	Fuel and air during assembly operation	N/A
Humidity	75% RH, variable temperature	N/A
Static acceleration	±9 g, 3 axes, 5 min (6 tests)	N/A
Shock	5–200 g, 0.7 ±0.2 ms terminal peak, sawtooth pulses, 3 axes (15 tests)	N/A
Acoustic	Shaped spectra, 148-dB wide-band, 60 s	N/A
Vibration sine wave (bus assemblies)	0.75 g rms, 5–30 Hz 7.5 g rms, 30–250 Hz 4.5 g rms, 250–600 Hz 13.5 g rms, 600–2000 Hz } 1 oct/min	0.5 g rms, 5–30 Hz 5.0 g rms, 30–250 Hz 3.0 g rms, 250–600 Hz 9.0 g rms, 600–2000 Hz } 3 oct/min (3 axes)
Sine wave[a] (scan platform assemblies)	0.75 g rms, 5–30 Hz 15.0 g rms, 30–200 Hz 9.0 g rms, 200–1000 Hz 6.0 g rms, 1000–2000 Hz } 1 oct/min (3 axes)	0.5 g rms, 5–30 Hz 10.0 g rms, 30–200 Hz 6.0 g rms, 200–1000 Hz 4.0 g rms, 1000–2000 Hz } 3 oct/min (3 axes)
Sine wave (top of bus assemblies)	0.75 g rms, 5–30 Hz 7.5 g rms, 30–200 Hz 9.0 g rms, 200–1000 Hz 6.0 g rms, 1000–2000 Hz } 1 oct/min (3 axes)	0.5 g rms, 5–30 Hz 5.0 g rms, 30–200 Hz 6.0 g rms, 200–1000 Hz 4.0 g rms, 1000–2000 Hz } 3 oct/min (3 axes)
Random vibration (all assemblies)	Shaped spectra, 18.1 g rms, 3 axes, 60 s	Shaped spectra, 10.8 g rms, 3 axes, 20 s
Thermal/vacuum heat exchanger[b]	−20°C (−4°F), 24 h +75°C (+167°F), 12 days 10^{-5} torr (average pressure rate = 15 torr/s)	0°C (+32°F), 8 h +55°C (+131°F), 60 h 10^{-5} torr (average pressure rate = 15 torr/s)
Radiative[c]	-20°C (−4°F), 24 h +75°C (+167°F), 12 days 10^{-5} torr (average pressure rate = 15 torr/s)	0°C (+32°F), 8 h +55°C (+131°F), 60 h 10^{-5} torr (average pressure rate = 15 torr/s)
Thermal shock[c] (external assemblies only)	+75°C (167°F) to −46°C (−50°F) 10^{-5} torr	N/A
Electron radiation	Variable flux and energy	N/A
Proton radiation	Variable flux and energy	N/A

[a]Except for science payload.
[b]Except for external assemblies.
[c]Except for antennas, solar panels, and other selected assemblies.

(2) Perform flight acceptance (FA) tests on flight and spare subsystems and systems to give assurance that they are representative of the design verified by the TA tests and to identify workmanship and manufacturing flaws.

The test requirements were based on the established JPL policy of setting FA test levels at the 95% values of the flight environment and TA at a more severe level, in excess of the 99% value, to the degree that such a definition of the environment is possible. Subsystem TA tests provide for the design verification for all mission environments of significance, including those experienced prior to and following system integration.

In accordance with the *Mariner* Mars 1969 project policies and requirements, the JPL environmental requirements section established the spacecraft system environmental requirements. These requirements are specified in the system and subsystem general environmental specifications for TA and FA testing of the spacecraft and its component subsystems.

Table 1 summarizes the TA and FA subsystem test requirements. The electrical and mechanical design, function, operational modes, and special characteristics of each subsystem were evaluated with respect to each TA environmental test. Only those TA tests which were of significance and which would provide for the maximum assessment of equipment environmental compatibility were required for the individual subsystems. In addition to the above parameters, the environmental test histories of all *Mariner IV* and *Mariner V* assemblies were reviewed, in conjunction with changes incorporated for *Mariner* Mars 1969, to eliminate tests for which previous design verification was valid. All FA subsystems were required to complete the vibration and thermal/vacuum tests. The required subsystem environmental tests for all spacecraft equipment were defined in an environmental test configuration list.

A summary of the TA and FA system level environmental tests and test parameters is tabulated in Table 2. The proof test model (PTM) spacecraft was subjected

Table 2. Summary of TA and FA system environmental test requirements

Test environment	TA requirements	FA requirements
Acoustic	Shaped spectra, 148-dB wide-band sound pressure level (SPL), 60-s duration	N/A
Shock	V-band firing, solar panel pinpuller firings, propulsion subsystem valve firings, scan platform release firing, IRS explosive valve firing	
Vibration sinusoidal	Roll axis 0.75 g rms, 5–120 Hz 12 dB/oct from 120 to 500 Hz 13.5 g rms, 500–2000 Hz } 1 oct/min Lateral axes (two) 0.5 g rms, 5–50 Hz, 0.75 g rms, 50–250 Hz } 1 oct/min	Roll axis 0.50 g rms, 5–120 Hz 12 dB/oct from 120 to 500 Hz 9.0 g rms, 500–1900 Hz } 3 oct/min Lateral axes (two) 0.35 g rms, 5–50 Hz 0.50 g rms, 50–250 Hz } 3 oct/min
Random	Roll axis and two lateral axes Shaped spectra: 7.0 g rms overall, 0.0225 g^2/Hz from 100 to 225 Hz, 0.063 g^2/Hz from 350 to 750 Hz, 6-dB/oct rolloff below 100 Hz, 12-dB/oct rolloff above 750 Hz, 60 s each axis	Roll axis Shaped spectra: 4.2 g rms overall, 0.008 g^2/Hz from 100 to 225 Hz, 0.0225 g^2/Hz from 350 to 750 Hz, 6-dB/oct rolloff below 100 Hz, 12-dB/oct rolloff above 750 Hz, 20-s duration Lateral axes (two) Shaped Spectra: 2.8 g rms overall, 0.00355 g^2/Hz from 100 to 225 Hz, 0.010 g^2/Hz from 350 to 750 Hz, 6-dB/oct rolloff below 100 Hz, 12-dB/oct rolloff above 750 Hz, 20 s each axis

Table 2 (contd)

Test environment	TA requirements	FA requirements
Torsional	2.25 pk rad/s², 5–20 Hz 7.5 pk rad/s², 20–50 Hz 15.0 pk rad/s², 50–150 Hz } 1 oct/min	N/A
Launch pressure profile	Atmospheric pressure to 1% atmospheric in 65 s or less; pressure rate spike, 108–124 torr/sec in less than 10 s	N/A
Space simulator	350-h minimum at 1×10^{-5} torr or less, −290°F or less chamber shroud temperature; angle of incident solar radiation within 3 deg of roll axis of spacecraft	200-h minimum at 1×10^{-5} torr or less, +290°F or less chamber shroud temperature; angle of incident solar radiation within 3 deg of roll axis of spacecraft
Phase I: Mission test	250 h	150–200 h
Phase II: Flight mode test	100-h min thermal steady-state with variable solar intensities[a] of 65 to about 143 W/ft²	50–100 h variable solar intensities[b] of 65 to 130 W/ft²
Electromagnetic interference RF simulation	Spacecraft subjected to RF generated by the *Atlas/Centaur* and AFETR from liftoff minus 2 min through injection plus 4 min	Spacecraft subjected to RF generated by the *Atlas/Centaur* and AFETR from liftoff minus 2 min through injection plus 4 min
Umbilical/ separation connector transients	Spacecraft umbilical and separation connector lines subjected to induced voltage pulses, positive and negative	N/A
S-band noise	Radiated S-band noise monitored and measured	Radiated S-band noise monitored and measured
Spectrum signature	Spacecraft radiated RF noise measured from 30 Hz to 10 GHz with spacecraft operating in near encounter mode	N/A

[a]The upper and lower resultant temperatures cannot exceed the assembly level TA upper and lower limits of solar-exposed items such as antennas, sensors and temperature control flux model

[b]The upper and lower resultant temperatures cannot exceed the assembly level FA upper and lower limits.

to each of the TA tests; each of the three flight spacecraft was subjected to the FA tests. In addition to the formal TA and FA system level environmental tests, dynamic and thermal/vacuum testing was performed on the structural analysis model, developmental test model (DTM), and temperature control model (TCM) spacecraft to assure design adequacy in selected critical areas.

The PTM environmental tests provided for design verification of the spacecraft in the most critical environments and those which are primarily related to the interactions of spacecraft subsystems. In addition, the PTM spacecraft testing demonstrated that the test procedures and implementation techniques were in accordance with the test requirement and reduced the potential risk to flight spacecraft.

II. Subsystem Testing Summary

A. Type Approval Testing

Figures 1 and 2 provide a summary of the subsystem TA environmental testing. The testing is categorized by major subsystem (Table 3) in terms of numbers of tests and failures both in total and in selected environments.

The vibration and thermal/vacuum test results are emphasized because of the critical nature of these environments. The results of past programs has indicated that, of all environmental tests, vibration and thermal/vacuum are the most informative in the subsystem test program. The successful completion of these tests by an assembly is indicative that other TA and FA tests will result in a minimum number of failures.

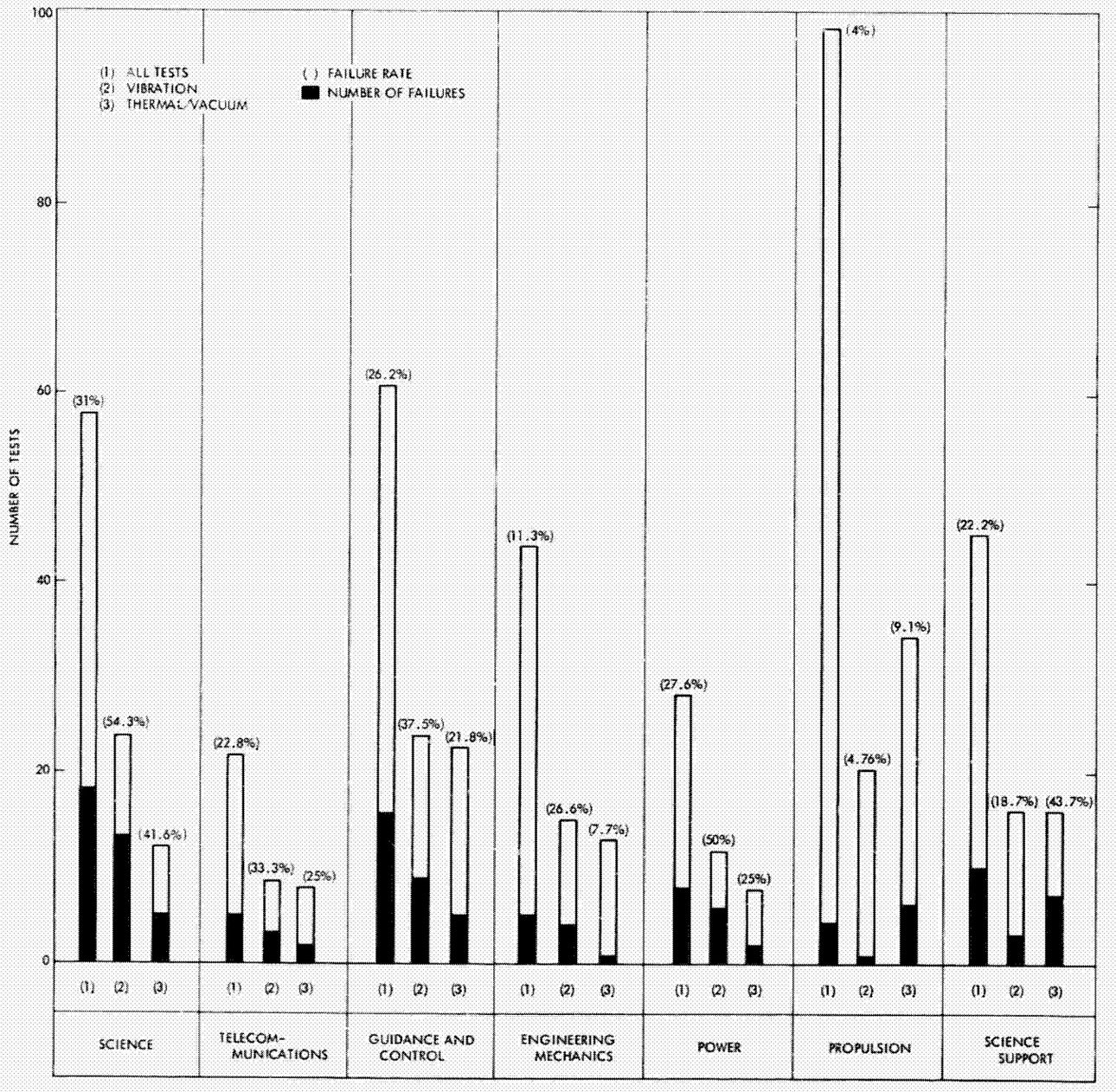


Fig. 1. Summary of TA environmental testing by major subsystem

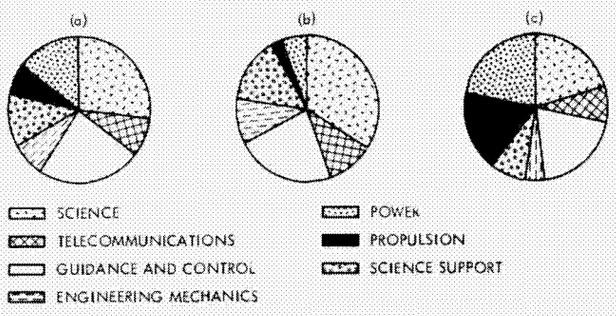


Fig. 2. Failure distribution by major subsystem for (a) all TA environmental tests, (b) TA vibration, and (c) TA thermal/vacuum

The failure rates indicated are based on actual failures of the assembly being tested and do not reflect operational support equipment (OSE), operator, or test equipment failures, etc. The failures comprise design, part, or workmanship failures of the assembly which were detected during or following the environmental tests.

During the TA test program, 128 tests other than thermal/vacuum and vibration were performed. Two system failures occurred during these 128 tests; both occurred during TA thermal shock testing. Therefore, subsystem failure rates are primarily associated with vibration and thermal/vacuum testing.

Table 3. Spacecraft equipment grouping by major subsystem

Science Support	**Science**
Data automation	Television
Data storage	Infrared spectrometer
Scan control and actuators	Infrared radiometer
Narrow-angle Mars gate	Ultraviolet spectrometer
Far-encounter planet sensor	**Telecommunications**
TV stimulus	Radio
Propulsion	Flight telemetry
Pyrotechnic control	Flight command
Pinpullers	Antenna
Release devices	**Power**
Propulsion (postinjection propulsion system)	Battery
Propulsion components (valves, regulator, etc.)	Solar panels
Scan unlatch valves	Power regulator
Engineering Mechanics	Power conversion
Dampers	**Guidance and Control**
Louvers	Central computer and sequencer
Pyrotechnic arming switch	Attitude control and gyro
Separation initiate timer	Attitude control gas equipment
Temperature control flux monitor	Sun sensors
	Canopus sensor
	Thrust vector control
	Sun gates

Except for those assemblies listed under the propulsion subsystem, the equipment subjected to the TA tests comprised complete flight assemblies. The propulsion testing included the TA testing of squibs, valves, and PIPS components, design adequacy being verified on a sample basis. From a given manufacturing lot, several of the components were subjected to tests, thereby qualifying all similar units.

Because of assembly modification, failures during other phases of environmental testing, or rework of the subsystems, selected equipment was retested to assure the validity of the initial testing and the verification and compatibility of any changes.

B. Flight Acceptance Testing

A summary of the subsystem FA testing is shown in Figs. 3 and 4. The subsystem FA tests consisted of vibration and thermal/vacuum. Each of the flight assemblies was subjected to these tests. In general, there were three flight subsystems. The total number of FA tests includes any requalification tests performed.

According to the environmental test program philosophy, the only failures which should occur during FA testing are those associated with workmanship or piece-parts. This was not the case; failures other than those in workmanship or parts did occur during the FA testing. These failures were attributed to scheduling problems of the PTM and flight spacecraft.

C. Comparison of TA/FA Testing

In evaluating the effectiveness of the subsystem environmental test program, conclusions may be drawn from:

(1) A comparison of the TA/FA testing and test failure rate.

(2) A comparison of the problems detected during TA/FA testing.

(3) A comparison of the types of problems encountered during testing.

Table 4 provides an overall summary of all TA and FA environmental testing and the failure rates for each

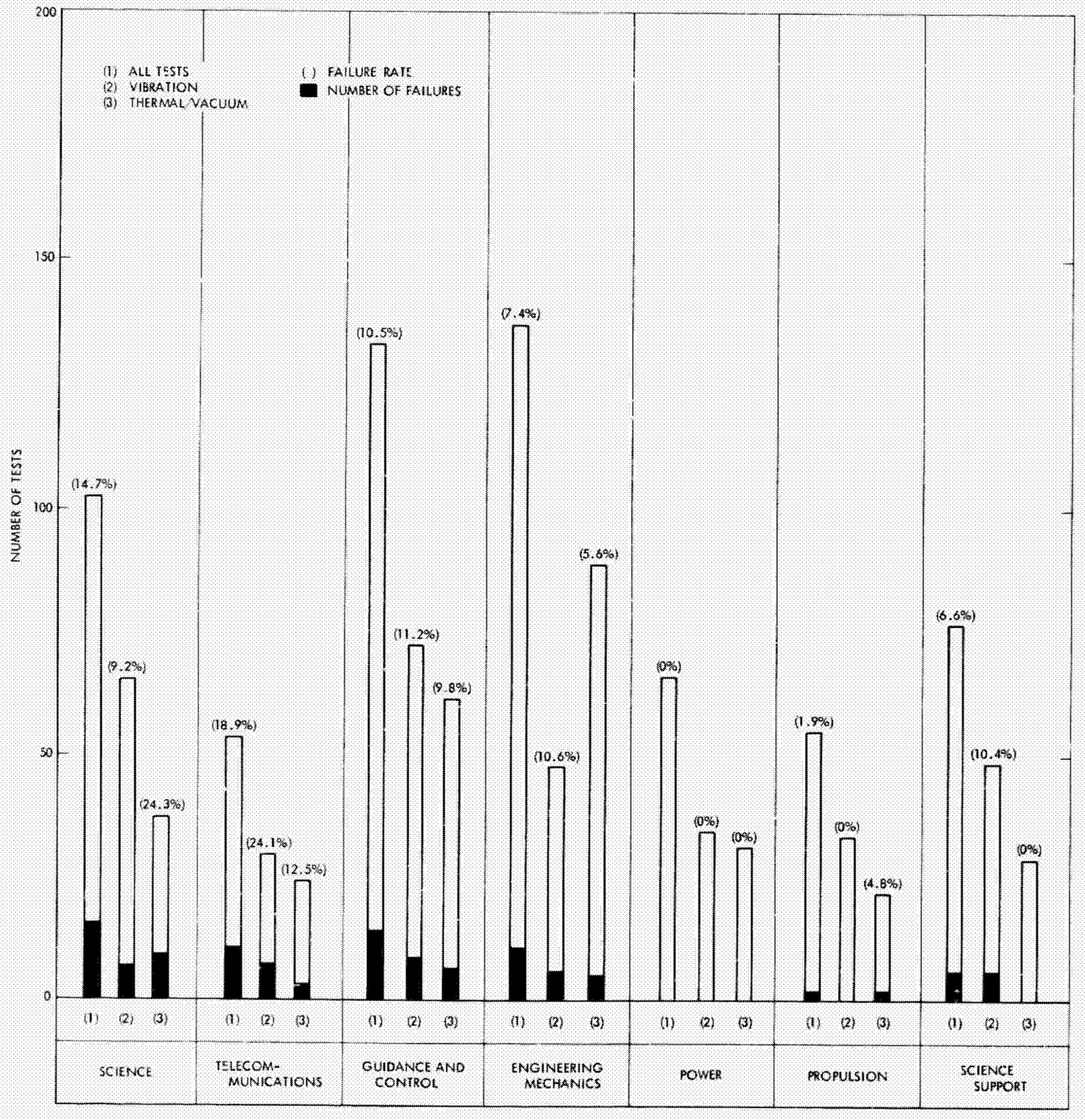


Fig 3. Summary of FA environmental testing by major subsystem

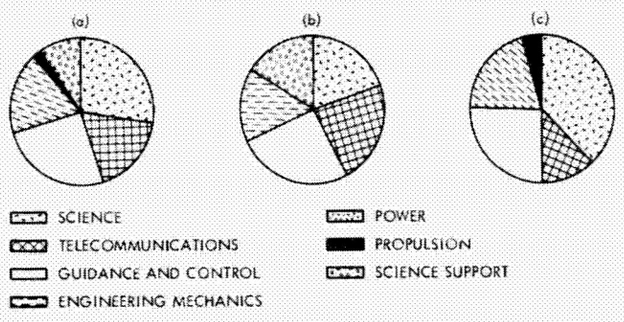


Fig. 4. Failure distribution by major subsystem for (a) all FA environmental tests, (b) FA vibration, and (c) FA thermal/vacuum

test. With the exception of the science subsystems and several other particular items, most of the equipment was subjected only to TA and FA vibration and thermal/vacuum testing. The design adequacy demonstrated during the 1964 and 1967 *Mariner* environmental test programs and the use of similar equipment for the 1969 program permitted the elimination of many tests. In addition, the system-level pyrotechnic shock and acoustic tests provided adequate testing of the bus equipment, obviating the need for separate TA tests at the assembly level.

Figure 5 compares the number of problems encountered during both TA and FA testing. Figure 6 categorizes the problems by type (design, part, workmanship, etc.). If, in practice, the TA testing program was nearly

Table 4. Subsystem environmental test summary

Environment	Number of tests	Number of test failures	Failure rate, %
FA tests			
Vibration	328	31	9.4
Thermal/vacuum	291	24	8.3
TA tests			
Vibration	121	39	32.2
Thermal/vacuum	113	25	22.1
Thermal shock	27	2	7.7
Humidity	30	0	0
Static acceleration	29	0	0
Explosive atmosphere	6	0	0
Bench handling	6	0	0
Transportation vibration	5	0	0
Pyrotechnic shock	12	0	0
Acoustic	13	0	0
Totals			
TA tests	362	66	18.3
FA tests	619	55	8.9

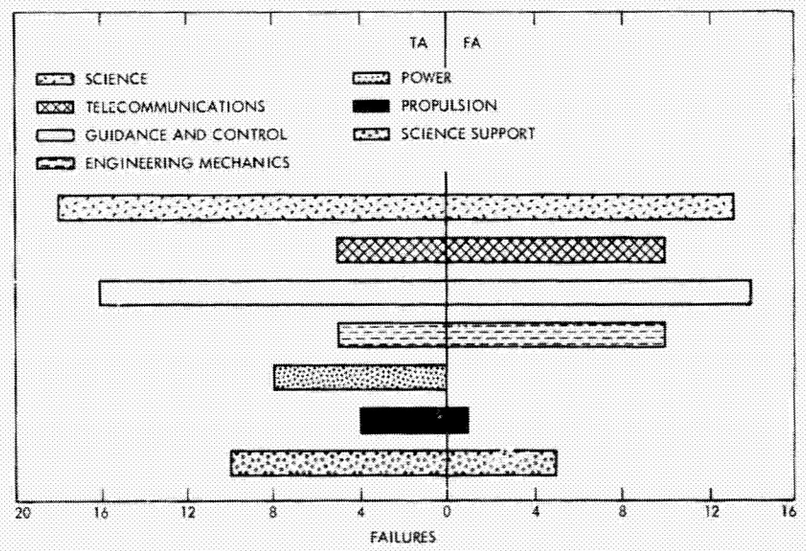


Fig. 5. Comparison between TA and FA environmental test failures

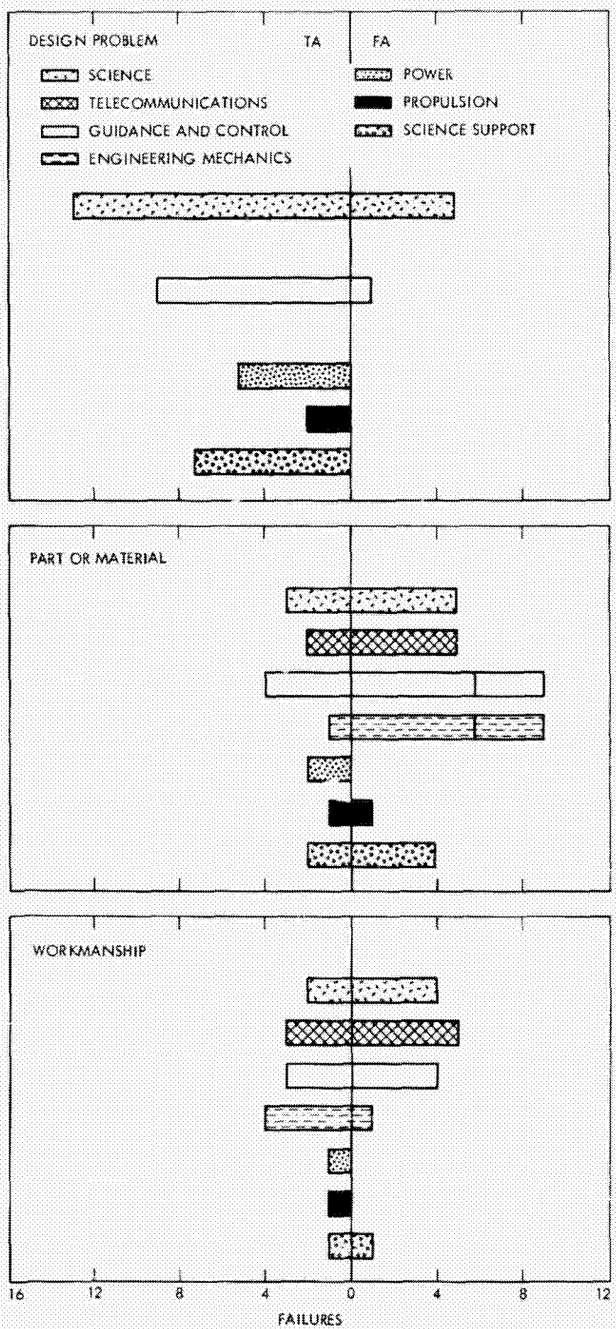


Fig. 6. TA/FA failure distribution

perfect in its intent to provide design verification, the number of problems which occur during FA testing should be minimized. As can be seen from Fig. 6, this was not the case; subsystems experienced design failures during FA testing.

When the *Mariner* Mars 1969 environmental program was developed, it was predicated upon the availability of five sets of spacecraft hardware assemblies: type approval (TA), proof test model (PTM), and flight equipment (three sets). The TA assembly was to be exposed to the TA and life tests. The PTM assembly was to be subjected to the FA tests and then integrated with the PTM spacecraft for the system-level tests. Owing to budget and schedule constraints, the PTM assemblies were deleted. The TA assemblies performed the function of the PTM in addition to the normal TA function. The effect of this was that some subsystems, science in particular, did not complete the TA vibration and thermal/vacuum tests prior to integration with the PTM spacecraft, which resulted in flight equipment being subjected to FA testing without having completed the TA tests or having demonstrated design adequacy.

The science equipment was of a new design which had no test history, whereas most of the other spacecraft components employed a design similar to the *Mariner* 1964/1967 programs. This factor together with the types of failures which did occur emphasizes the necessity of performing the TA tests at the earliest possible date on equipment which is of a new design.

The failure rates experienced during the *Mariner* Mars 1969 TA and FA environmental test program were consistent with past projects. The TA/FA failure ratio of 3 or 4 to 1 had been observed on previous *Mariner* and other NASA spacecraft programs. In general, the same subsystems (science) in each of the programs were the major contributors to the failures.

III. System-Level Environmental Testing

System-level environmental testing provides the only opportunity for an evaluation of spacecraft performance under conditions similar to those to be encountered during the mission. This is of major importance since the thermal/dynamic/electrical interactions of the spacecraft assemblies cannot be realistically simulated on the individual subsystems.

Mariner Mars 1969 system-level environmental testing consisted of TA testing the PTM spacecraft for design verification and FA testing each flight spacecraft to assure flight acceptability. As is the case in subsystem testing, TA levels were greater than those expected during the mission, whereas FA levels were equal to the maximum predicted.

A summary of the significant problems encountered during system-level environmental testing is shown in Table 5 (PTM spacecraft) and Table 6 (flight spacecraft). Also, the resolution for each problem is indicated. It should be noted that several problems which occurred during the PTM testing reoccurred during the flight spacecraft tests; the final verification of the design modifications was completed by performing subsystem testing.

Table 5. Significant PTM spacecraft environmental test problems

Problem	Environment	Resolution
UVS motor stalled[a]	Thermal/ vacuum	Redesign: gears/ bearings
TV shutter failed[a]	Thermal/ vacuum	Redesign: shutter
TV camera cover failed[a]	Thermal/ vacuum	Redesign: microswitch position
IRS channel 2 failed[a]	Thermal/ vacuum	Redesign: detector mounting
IRS cryostat plugged[a]	Thermal/ vacuum	Modified manufacturing procedures to eliminate contamination
Stepping of IRR motor interfered with TV-A	Thermal/ vacuum	Redesign: added magnetic shield
Scan platform unlatch valve leaks[a]	Thermal/ vacuum	Redesign: provided for proper loading
Analog tape recorder switched tracks	Shock	Cause unknown: unit was subjected to TA shock test and passed
Scan platform driven to wrong position	Thermal/ vacuum	Redesign: added mechanical stops

[a]Detectable during subsystem test.

In reviewing the failures which did occur during the system testing, it is evident that most of the system problems were associated with those subsystems which had experienced problems during subsystem testing. Once again, this points up the need for a comprehensive subsystem test program if system level problems are to be minimized. Problems which occurred at the system level but could have been detected with adequate subsystem testing are indicated.

For each of the system level tests, it was desired that the spacecraft configuration be as similar as possible to the launch configuration. It was recognized during the initial tests that this would not always be possible. As more information concerning the design and functional characteristics of the spacecraft components was obtained, it became necessary to modify some of the assemblies. In some cases, modifications could not be made in time to meet the system test schedule. Tables 7 and 8 provide summaries of PTM and flight spacecraft environmental test configuration discrepancies. Even though these discrepancies did affect the objectives of the spacecraft tests, the comprehensive subsystem and system tests on all of the spacecraft greatly reduced the effect of these discrepancies.

The following paragraphs briefly discuss the system-level environmental tests and the results of each.

Table 6. Significant flight spacecraft environmental test problems

Spacecraft	Problem	Environment	Resolution
M69-2	IRS gas leak[a]	Thermal/vacuum	Redesign: used two gaskets
M69-2 M69-4	Data storage subsystem tape problem	Thermal/vacuum	Retrofitted the tape and modified tape heads
M69-2 M69-3 M69-4	Radio susceptible to L/V RF sources	RF simulation	Testing at AFETR showed that this condition would not exist at launch
M69-3	IRS motor stalled[a]	Thermal/vacuum	Redesign: gears
M69-3 M69-4	IRS cryostat plugged[a]	Thermal/vacuum	Modified manufacture procedures to eliminate contamination
M69-2	TV "B" video incorrect[a]	Thermal/vacuum	Redesign: deleted dark current circuit

[a]Detectable during subsystem test.

Table 7. PTM spacecraft environmental test configuration discrepancies

Subsystem	Configuration discrepancy		Test environment
	Major	Minor	
Television	Shutters, cover, heaters, EMI shield, and circuit modifications not incorporated		All tests
Infrared spectrometer	H2 vessel and squibs nonflight; motor change not incorporated		All tests
Data storage	Prototype motor drive amplifiers and digital transport		Vibration, Pyrotechnic, RFI
Attitude control gas system		Prototype 1/2 system	All tests
Pyrotechnic arming switch		Prototype	Thermal/vacuum, vibration
AC electronics		Prototype	Thermal/vacuum part 1
Far-encounter planet encounter		Prototype	Thermal/vacuum part 1
Ultraviolet spectrometer	Motor bearings nonflight		All tests
Thermal control flux model		M69-2 harness and interconnecting harness	All tests
Scan electronics		M69-2 scan harness	Thermal/vacuum
Scan actuators		Units reversed	All tests

Table 8. Flight spacecraft environmental test configuration discrepancies

Subsystem	Discrepancy	Test environment
M69-2		
TV	EMI shield, shutter, and electronic modifications not incorporated	All tests
DSS	PTM digital tape transport not in flight configuration	Thermal/vacuum phase II, vibration, pyrotechnic
IRS	Motor change not incorporated	All tests
	Gas system bottles not in flight configuration	Thermal/vacuum phase I
M69-3		
IRS	Motor change not incorporated	All tests
TV	Electronic modifications not incorporated; EMI shield used in phase II thermal/vacuum only	Thermal/vacuum
M69-4		
IRS	Motor change not incorporated	Vibration, pyrotechnic
TV	DTM TVS (dummy)	Thermal/vacuum

A. Dynamic Tests

The dynamic tests were performed to assure integrity of the spacecraft when subject to the environmental stimulus existing during the launch phase of the mission. The dynamic testing consisted of vibration, acoustic, and pyrotechnic shock and was performed in accordance with the parameters summarized in Table 2 and in the PTM and flight spacecraft system environmental test specifications.

B. Random Vibration Tests

The PTM and each of the three flight spacecraft were exposed to the random vibration tests indicated in Table 2. A comparison of the specified and actual wideband random vibration levels is shown in Table 9.

The *Mariner* Mars 1969 program employed several innovations in the testing methods which provided added assurance that the simulation would be as close as possible to that existing at launch. It was required that the spacecraft be tested on at least its own flight adapter and that vibration levels be controlled by using the average mean square spectrum of eight accelerometers mounted in selected orientations at the spacecraft separation plane. Both of these innovations were refined

Table 9. Spacecraft random vibration test levels[a]

Axis of test	Specified test level		Actual test level[a]			
			Type approval	Flight acceptance		
	TA	FA	M69-1	M69-2	M69-3	M69-4
Roll axis (Z)	7.0	4.2	6.8	4.41	4.28	4.36
Lateral axis (XY)	7.0	2.8	5.7	2.80	2.93	2.86
Lateral axis (XY-bay VIII)	7.0	2.8	5.2	2.86	3.13	2.93

[a]Specified and actual test levels are in wide-band g rms. The spectrum of both the TA and FA is as indicated in Table 2.

during the structural analysis model and developmental test model (DTM) testing programs to provide the optimum test configuration and implementation.

As can be seen in Table 9, the actual lateral axes wide-band levels of 7.0 g rms for the PTM spacecraft were not realized. During initial testing of the DTM spacecraft, several problems occurred which indicated that this condition would exist. Modifications could, however, be implemented to eliminate the problem areas. Subsequent testing of the PTM spacecraft indicated that the problems had not been corrected and that excessive high-frequency (above 1500 Hz) and insufficient low-frequency (50–300 Hz) energy resulted in a failure to achieve the desired levels.

The energy at the high frequencies was produced by the high-frequency content of some vibration distortion in the lower frequencies. The system equalizer was completely depressed at the higher frequencies; the high frequency could not be reduced further without depressing the lower frequencies. Based on the results of the PTM test, the lateral axes random vibration wide-band levels were reduced to reflect the presence of the above conditions. The resulting lateral axes tests were considered to be less severe than desired, but in an evaluation of the overall dynamic test program they were considered acceptable for flight certification.

During the vibration test program, no significant failures or degradations of the spacecraft were detected. Those minor problems which did occur were nonrepeatable and did not present a risk to the success of the mission.

In all cases, the PTM test parameters enveloped those of the flight spacecraft. The TA/FA test margins desired for design verification were maintained.

C. Sinusoidal Vibration Tests

The PTM and each of the three flight spacecraft were subjected to the sinusoidal vibration tests (Table 2). The test techniques and test methods, use of flight adapters and multiple control accelerometers were similar to those used for random vibration testing. No significant spacecraft problems occurred during any of the testing.

The vibration levels were as indicated in Table 2, with several exceptions. During all axes of testing on all spacecraft, the vibration level exceeded the 10% tolerance in narrow frequency bands between 50–100 Hz and 200–300 Hz (Fig. 7).

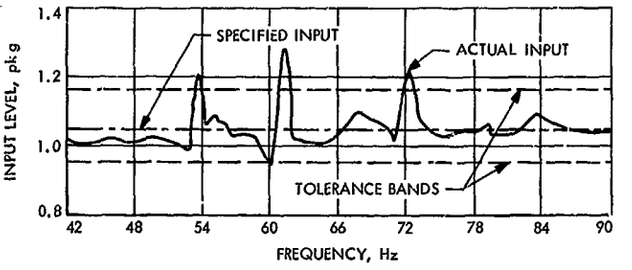


Fig. 7. Out-of-tolerance condition during spacecraft sinusoidal vibration test (PTM data shown)

The low-frequency out-of-tolerance conditions were determined to be related to structural resonances of the spacecraft which were so narrow in bandwidth that the test controller could not respond. The narrow-band nature of these resonances and the degree to which they were out of tolerance were considered acceptable. During testing, the desired TA/FA test margin was maintained over the entire frequency range.

The high-frequency (200–300 Hz) out-of-tolerance condition also occurred during testing of all spacecraft. Analysis of the vibration data indicated that the condition was due to distortion of the input or high-frequency energy. Therefore, the out-of-tolerance condition was not considered either excessive or potentially degrading to the spacecraft.

D. Acoustic Tests

The PTM spacecraft in the launch configuration was exposed to a reverberant acoustic field. The field was

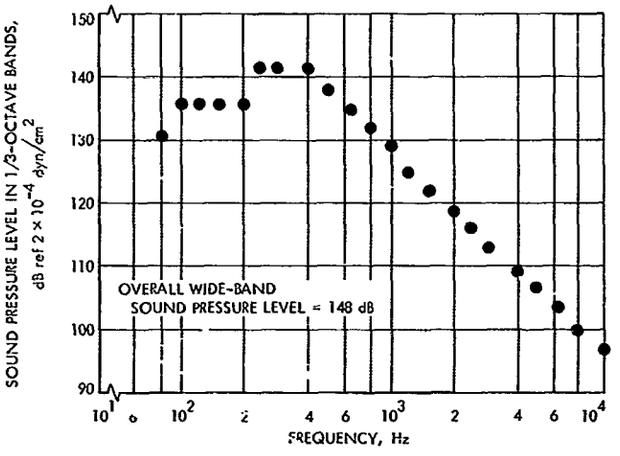


Fig. 8. *Mariner* Mars 1969 PTM spacecraft acoustic test—sound pressure levels

wide-band gaussian noise with a shaped spectrum as indicated in Fig. 8. The exposure lasted 60 s, with a total wide-band sound pressure level of 148 dB.

The spacecraft was operated in the launch mode during the tests; prior to and following the test a system verification test was performed. The spacecraft operated properly with no anomalies or degradation noted.

E. Shock Tests

The PTM and each of the three flight spacecraft were subjected to a shock test during which the spacecraft pyrotechnic devices were actuated to produce the environment. (The shock environment generated by the *Atlas/Centaur* is simulated during the spacecraft sinusoidal vibration test.) During the PTM test, all spacecraft devices were actuated; flight spacecraft tests consisted of V-band firing only. The following devices were actuated during the testing:

(1) Spacecraft V-band release.

(2) Solar panel deploy.

(3) Propulsion.

(4) Scan unlatch.

(5) IRS cooldown.

For the PTM test, the V-band and the propulsion devices were fired twice, resulting in a total of seven actuations. Data derived from the PTM testing indicated that the shocks resulting from the V-band and IRS actuations are the major sources of the shock environment. The flight units were subjected to the formal V-band test; then during the space simulator tests the IRS valves were actuated.

The anomalies noted during the initial PTM pyrotechnic shock test were resolved as indicated in Table 6. During the flight spacecraft pyrotechnic shock testing, no anomalies occurred.

F. Torsional Vibration Tests

The torsional vibration test was not performed on any spacecraft. The results of the DTM, structural analysis model, and PTM sinusoidal vibration tests demonstrated that the lateral axes tests produced a response in the spacecraft greater than that which would be experienced during the normal torsional test.

G. Space Simulator Tests

Each of the spacecraft was exposed to a thermal/vacuum test wherein the space environment was simulated. Each of the tests was conducted in two phases. Phase I of the test was performed to qualify/verify the functional integrity of the spacecraft while in a thermal/vacuum environment. No solar simulation was required; liquid nitrogen cold walls were used as a heat sink to provide adequate heat dissipation for the spacecraft. To assure maximum information on each of the subsystems in this environment, there was no constraint on the spacecraft/OSE cabling configuration. Phase II of the test was similar to Phase I except that solar simulation (0–130 W/ft^2) was provided, and the spacecraft/OSE cabling was held to a minimum. This phase allowed for an evaluation of spacecraft functional performance and characteristics in an environment and a data base very similar to those which would be encountered during the mission.

During both phases of the test, spacecraft performance was evaluated in the launch, cruise, midcourse correction, Mars cruise, encounter, and playback modes of operation. An attempt was made to assure that in each mode the spacecraft was conditioned as to power dissipation to provide maximum information on the thermal performance of individual subsystems and spacecraft system.

Table 10 shows the amount of time each spacecraft was in the simulated environment. The additional time which the flight spacecraft were in the environment was used effectively to evaluate various modes of operation

Table 10. Spacecraft solar simulator test time

Test	Test time, h			
	M69-1	M69-2	M69-3	M69-4
Phase I[a]	260	260	245	245
Phase II[b]	148	142	255	211
Total[c]	408	402	500	456

[a]Specified duration of 250 h for PTM and 150–200 h for flight spacecraft.

[b]Specified duration of 100 h minimum for PTM and 50–100 h for flight spacecraft.

[c]Specified duration of 350 h minimum for PTM and 200 h for flight spacecraft.

and the performance of additional tests (e.g., IRS cooldown).

The significant problems encountered during the thermal/vacuum tests are indicated in Tables 5 and 6. It should be noted that those problems encountered during testing of the flight spacecraft (Table 6) did not represent a first occurrence. The IRS and data storage subsystem problems had been encountered previously during subsystem and PTM spacecraft testing.

H. Launch Pressure Profile Tests

A launch pressure profile test was initially desired for the PTM spacecraft. Owing to cost and schedule considerations, it was deleted. In lieu of the formal PTM spacecraft test, the flight configuration thermal blankets were subjected to an extensive launch pressure profile test to assure the design adequacy and allow for an assessment of their response to this condition.

I. RF Simulation Tests

The *Mariner* 1969 spacecraft was subjected to an RF simulation test. Each of the spacecraft was radiated with RF sources at power levels similar to that expected at launch (Table 11). It was determined that the spacecraft telemetry channels 210, 213, and 214 were degraded by *Centaur* telemetry and C-band sources (Tables 5 and 6). Owing to the problems associated with simulation and questions relative to near-field vs far-field power density calculations, the prelaunch EMI/RFI test at AFETR was used as the final verification that the RF sources would not affect the spacecraft. During these tests at AFETR, no degradation was noted.

Table 11. RF simulated test frequencies and power densities

Source simulated	Frequency, MHz	Modulation	Power density,[a] W/m²	
			Average	Peak
Atlas/*Centaur*				
Centaur telemetry 1	225.7	PAM/FM/FM	4.3	N/A
Atlas telemetry	229.9	PAM/FM/FM	9.8×10^{-3}	N/A
Centaur telemetry 2	259.7	PAM/FM/FM	4.3	N/A
Centaur transponder	5765	Pulse	28.8×10^{-3}	60.5
AMR				
Command destruct	414	CW	150×10^{-6}	N/A
AN/FPS-16 radar	5690	Pulse	38.9×10^{-3}	486
AN/FPQ-6 radar	5690	Pulse	20.9×10^{-3}	131
AN/TPQ-18 radar	5690	Pulse	43.4×10^{-3}	584

[a]Power density at spacecraft separation plane (includes a 6-dB margin for simulation tests).

J. EMI Umbilical Transient Tests

The umbilical transient test was performed (PTM only) to examine the potential reaction of the spacecraft umbilical and separation functions as the result of noise or large signals that might exist on adjacent conductors at the launch complex. The test consisted of inducing a known signal into each of the umbilical lines through the use of a capacitive and inductive coupling network. Analysis of data following the test indicated that the spacecraft met the desired requirements and that there would be no degradation in spacecraft performance during launch activities as a result of induced noise on the umbilical lines.

K. EMI S-Band Noise Measurement

During system testing of each of the spacecraft, the S-band transponder receiver and image frequencies were

monitored for possible interfering signals. These frequencies were monitored with equipment which had a sensitivity similar to that of the flight transponder. This provided for a determination of possible degradation in spacecraft performance due to spacecraft generated noise. No significant spacecraft noise was detected at these frequencies; therefore, no degradation to the telecommunications receiver could be expected.

L. RF Spectrum Signature Tests

The RF spectrum signature test was performed on the PTM spacecraft (M69-1) to obtain measurements of the radiated RF noise spectrum generated by the spacecraft in its expected noisiest operating mode. The spectrum signature was compared with that obtained during the *Mariner* Mars 1964 program to isolate RF sources which could have the potential of creating interference. The amplitudes of noise in all frequency ranges were similar to those of 1964, except in the region of 1–5 GHz, where the 1969 spacecraft had considerably fewer signals.

IV. Comparison of *Mariner* Mars 1964, *Mariner* Venus 67, and *Mariner* Mars 1969 Subsystem Testing

A comparison of subsystem vibration and thermal/vacuum testing for the *Mariner* 1964, 1967, and 1969 projects is shown in Table 12. It should be noted that the 1967 test program was relatively limited.

Many of the *Mariner* Venus 67 subsystems were spare *Mariner* Mars 1964 units and required only a nominal reverification.

The vibration testing as indicated for the 1964 program included sine and random vibration tests, each tabulated separately. The 1969 data reflects this as being one test. Therefore, the total number of tests for 1964 is approximately equal to 1969. The number of failures for both projects fall into the same range (*Mariner* 1969 had 39 TA and 31 FA while *Mariner* 1964 had 30 TA and 26 FA failures). The similarity in basic design of spacecraft would tend to indicate that the number of vibration-related failures for 1969 should be much less than 1964. In reviewing the failures and the contributing subsystems, it is noted that the failures were associated primarily with units of a new design, with no or limited test history (this was particularly true for the science subsystems). The numerical results are indicative of the review which must be performed on all units of a new design to assure adequacy in the dynamic environments and to reduce the failure potential.

The failure rates for the thermal/vacuum testing for all three projects were nearly equal. The number of subsystems tested during both the 1964 and 1969 programs was approximately the same. The effect of the thermal/vacuum environment can, in many cases, be more adequately evaluated prior to test. This, in conjunction with the thermal characteristics of the spacecraft and the adequacy of the thermal control subsystem, allowed for the use of analytical techniques in the early design stage to assure compliance with the requirements. This then eliminated many of the thermal design problems and was reflected in the 1969 test results. Most FA problems were associated with part failures. In most cases, these failures could not be related to the environmental stimulus; rather they were associated with the normal failure rate of the components. (Four of the FA part failures which occurred during testing of the TVS were later judged to have been OSE-associated.)

The failures during TA thermal/vacuum testing were divided between design and part. In general, the design problems were related to pressurized components which leaked when subjected to low vacuum conditions. This was not a new problem, but one which had also occurred during the 1964 program.

Table 12. Summary of *Mariner* project subsystem test results

Project	Vibration test						Thermal/vacuum test					
	Number of tests		Number of failures		Failure rate, %		Number of tests		Number of failures		Failure rate, %	
	TA	FA	TA	FA	TA	FA	TA	FA	TA	FA	TA	FA
Mariner Mars 1964	224	538	30	26	13.4	4.8	95	310	19	28	20	9
Mariner Venus 67	21	118	4	7	19	5.9	22	83	7	6	31.9	7.2
Mariner Venus 1969	121	328	39	31	32.2	9.4	113	291	25	24	22.1	8.3

In comparing the various programs, some very informative conclusions can be made if the progress of the testing vs the required time of delivery to the spacecraft assembly facility (SAF) is plotted. As is shown in Fig. 9, the various projects have tended to follow similar trends. Extrapolating the trends of earlier projects allows for a determination of the expected spacecraft configuration for the major system-level tests. This is significant in that the expected status is known two to three months prior to such tests as vibration or solar/thermal/vacuum. This allows for an early evaluation of the expected late subsystems and for the development of work-around plans such as hardware changeouts or rescheduling. This minimizes the overall impact on the spacecraft testing and provides maximum use of spacecraft components which have demonstrated design adequacy.

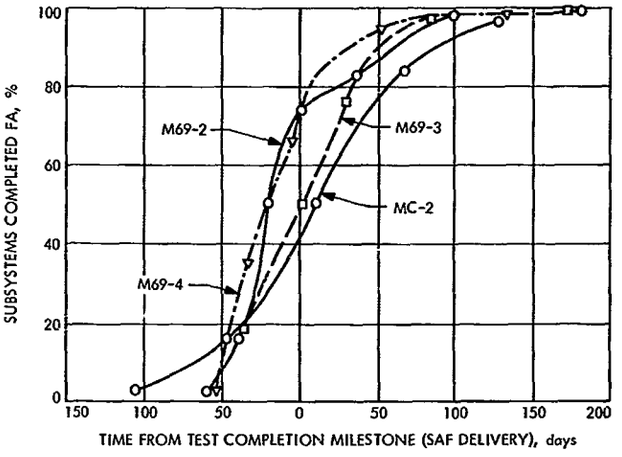


Fig. 9. *Mariner* Mars 1964 and 1969 completion history (referenced to test completion milestones, SAF delivery)

V. Comparison of *Mariner* Mars 1964, *Mariner* Venus 67, and *Mariner* Mars 1969 System Test Levels

A. Random Vibration Tests

The 1964 and 1967 random vibration requirements are indicated on Fig. 10. The overall FA level was 10.7 *g* rms as compared to 4.2 *g* rms for 1969. The 1967 requirement was only slightly modified from 1964 to a level of 9.7 *g* rms.

It should be noted that the 1969 requirement was specified at the spacecraft feet, whereas the 1967 requirement was specified at the test fixture, which was removed approximately 8 in. through the *Mariner* Venus 67 adapter.

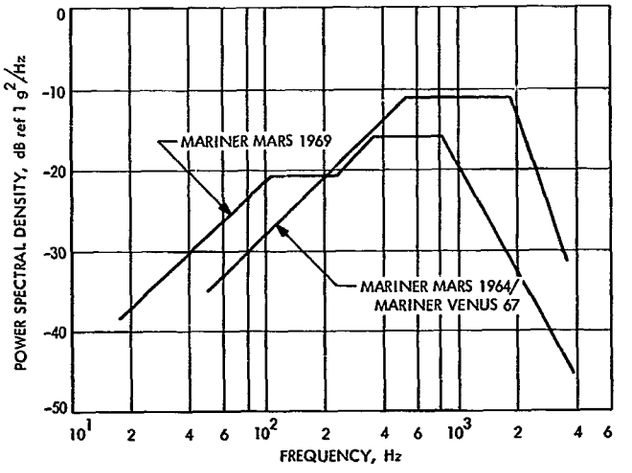


Fig. 10. *Mariner* Mars 1964/1969 FA random vibration level comparison

Although 1967 test levels appear significantly higher, the environment induced into the bus was comparable for the two spacecraft.

B. Sine Vibration Tests

Figures 11 and 12 compare the system sine test requirements for the 1964, 1967, and 1969 programs. Two events in the 1969 environment contributed significant excitation in the 600-Hz frequency range. These were the *Centaur* insulation panel jettison and the *Atlas/Centaur* separation. Thus the 1969 test requirements were somewhat more severe in this frequency range than in previous *Mariner* programs.

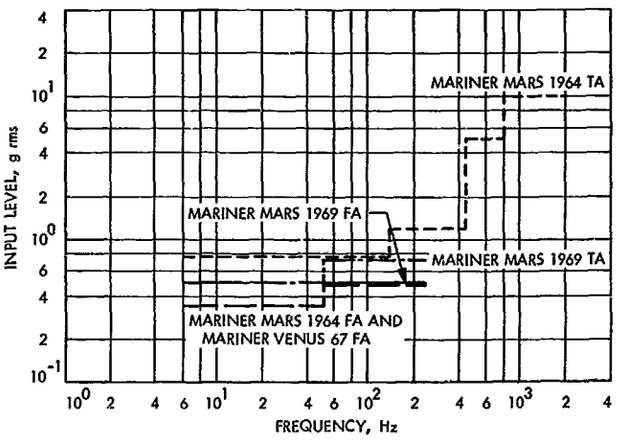


Fig. 11. Comparison of lateral sine vibration test requirements: *Mariner* Mars 1964/*Mariner* Venus 67/*Mariner* Mars 1969

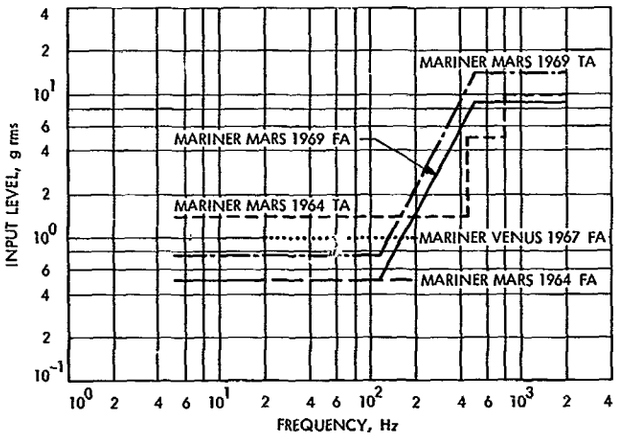


Fig. 12. Comparison of roll axis sine vibration test requirements: *Mariner* Mars 1964/*Mariner* Venus 67/ *Mariner* Mars 1969

C. Acoustic Tests

The PTM acoustic test requirements for 1964 and 1969 are shown in Fig. 13. There was no FA acoustic test requirement. The higher levels in 1969 reflect the higher acoustic field at liftoff inside the *Centaur* shroud.

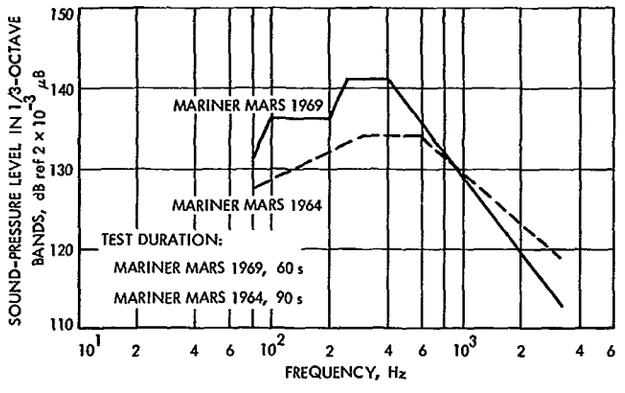


Fig. 13. Comparison of acoustic test requirements: *Mariner* Mars 1964/1969

D. Thermal/Vacuum Tests

Tables 13 and 14 show a comparison of the TA and FA test levels required during systems testing of the *Mariner* Mars 1964, *Mariner* Venus 67 and *Mariner* Mars 1969 spacecraft. It should be noted that *Mariner* Venus 67 was towards the Sun; hence some of the test levels were higher.

E. Solar Simulation Tests

Tables 13 and 14 provide a comparison among the 1964/1967/1969 system-level solar simulation tests. The 1967 testing differed somewhat because of the degree of solar simulation required in order to reflect the Venus mission.

VI. Test Implementation

The following paragraphs briefly describe the test techniques, problem/failure reports, and general problems associated with the environmental tests conducted at JPL on *Mariner* Mars 1969 subsystems and systems. Most of the induced environments, or dynamic testing, and the natural environments, or thermal/vacuum testing was performed in the environmental and dynamics testing laboratory (EDTL). In general, facilities other than the EDTL were used to meet special requirements for environmental testing. For example, hazardous hardware such as the propulsion subsystem was tested at the JPL facility at the Edwards Test Station, and all acoustic tests were performed in building 82.

A. Subsystem Testing

Most environmental testing performed at JPL was on formally controlled subsystems (pyrotechnic control, TV, etc.) or on development assemblies (relays, switches, camera lens, etc.). Spacecraft tests, although much more complex and time-consuming than individual subsystem tests, were limited in number and consequently had less impact on the test facility schedules. The summary in Table 15 shows a breakdown by category and test type of all *Mariner* Mars 1969 subsystems and assembly testing performed at JPL. This table includes development tests and retests of type approval and flight acceptance hardware. It should be noted that Table 15 does not reflect the extensive vacuum test support provided by EDTL at Cape Kennedy for IR spectrometer calibration and in Building 168 for the TV subsystem.

Of the total of 52 spacecraft subsystems, approximately 50% were subjected to development, type approval, and flight acceptance tests at JPL and are included in the summary in Table 14. The other subsystems were tested by approved contractors.

At the subsystem test level, there were 57 problem/failure reports (PFRs) written which were associated with test implementation at JPL. The majority of the

Table 13. Comparison of *Mariner* project PTM system thermal/vacuum tests

Parameter	*Mariner* Mars 1969[a]	*Mariner* Venus 67[a]	*Mariner* Mars 1964[a]
	Test requirements		
Total test duration	300-h min	250-h min	250-h min
Chamber pressure	1×10^{-5} torr or less	Less than 1×10^{-5} mm Hg	1×10^{-5} mm Hg or less
Shroud temperature	−290°F or less	Effective heat sink temp of less than −250°F	Less than −300°F
Phase I: Mission test			
Test duration	250 h	212.5 h	250 h
Solar simulation		Variable intensities	Variable intensities
Mission modes	Launch: Max chamber pumpdown	Launch: *Atlas/Agena* pressure profile (0)	Pumpdown: *Atlas/Agena* pressure profile
	Earth cruise[b]	Earth cruise (126)	Earth cruise[c] (134)
	Midcourse/shadow[c]	Midcourse[c] (0)	Midcourse[c] (134)
	Mars cruise[d]	Venus cruise[c] (248)	Mars cruise[c] (51)
	Encounter[c]	Encounter[c] (248)	Encounter[c] (51)
	Playback[c]	Playback[c] (263)	Playback[c] (51)
	TA high temp: Simulate assembly high-temp levels	Encounter[e] (275)	
	TA Low temp: Simulate assembly low-temp levels	Playback[e] (290)	
Phase II: Flight mode test			
Test duration	100-h min		133.5 h
Solar simulation	Variable intensities	Variable intensities	Variable intensities
Mission modes	Launch: Max chamber pumpdown (0)	Launch: *Atlas/Agena* profile	Pumpdown-*Atlas/Agena* pressure profile
	Earth cruise[c] (~143)	Earth cruise[d] (100/126)	Earth cruise[c] (134)
	Midcourse/shadow[c] (130/0)		Midcourse[c] (134/0)
	Mars cruise[c] (65)	Venus cruise[c] (248/290)	Mars cruise[c] (51)
	Encounter[c] (65)	—	Encounter[c] (51)
	Playback[c] (65)		Playback[c] (51)
	—		Louvers closed[d] (30)
Special modes: Spacecraft configuration	Minimum OSE cables —	Minimum OSE cables	Minimum OSE Cables

[a]Numbers in parentheses represent solar intensity in W/ft.^{2}

[b]High-power spacecraft mode.

[c]Normal spacecraft mode.

[d]Low-power spacecraft mode.

[e]High solar intensities.

Table 14. Comparison of *Mariner* project FA system thermal/vacuum tests

Parameter	*Mariner* Mars 1969	*Mariner* Venus 67	*Mariner* Mars 1964
	Test requirements		
Total test duration	200-h min	250-h min	250-h min
Chamber pressure	1×10^{-5} torr or less	Less than 1×10^{-5} mm Hg	1×10^{-5} mm Hg or less
Shroud temperature	−290°F or less	Effective heat sink temp of less than −250°F	Less than −300°F
Phase I: Mission test:			
Test duration	150–200 h	212.5 h	250 h
Solar simulation		Variable intensities	Variable intensities
Mission modes	Launch: Max chamber pumpdown	Launch: *Atlas/Agena* pressure profile	Pumpdown: *Atlas/Agena* pressure profile
	Earth cruise[b]	Earth cruise[c] (126)	Earth cruise[c] (134)
	Midcourse/shadow[c]	Midcourse[c] (0)	Midcourse[c] (134)
	Mars cruise[d]	Venus cruise (248)	Mars cruise[c] (51)
	Encounter[c]	Encounter[c] (248)	Encounter[c] (51)
	Playback[c]	Playback[c] (263)	Playback[c] (51)
Special modes		Encounter[e] (275)	
		Playback[e] (290)	
Phase II: Flight mode test			
Test duration	50–100 h		133.5 h
Solar simulation	Variable intensities	Variable intensities	Variable intensities
Mission modes	Launch: Max chamber pumpdown (0)	Launch: *Atlas/Agena* pressure profile	Pumpdown: *Atlas/Agena* pressure profile
	Earth cruise[b] (130)	Earth cruise[d] (248/126)	Earth cruise[c] (134)
	Midcourse/shadow[c] (130/0)	Venus cruise[c] (248-290)	Midcourse[c] (134/0)
	Mars cruise[c] (65)		Mars cruise[c] (51)
	Encounter[c] (65)		Encounter[c] (51)
	Playback[c] (65)		Playback[c] (51)
	—	—	Louvers closed[d] (30)
Special modes: Spacecraft configuration	Minimum OSE cables —	Minimum OSE cables —	Minimum OSE cables

[a]Numbers in parentheses represent solar intensity in W/ft^2.

[b]High-power spacecraft mode.

[c]Normal spacecraft mode.

[d]Low-power spacecraft mode.

[e]High solar intensities.

Table 15. Summary of *Mariner* Mars 1969 tests at JPL

Test type	Environment							
	Vibration	Shock	Centrifuge	Vacuum	Temperature	Acoustic	Explosive atmosphere	Totals
Development	157	24	2	116	24	5		328
Type approval	83	11	23	44	20	14	6	201
Flight acceptance	160			104				264
Life tests				6				6
Totals	400	35	25	270	44	19	6	799

PFRs were for minor or temporary out-of-tolerance conditions, and all were classified as noncritical. Approximately 40% of the PFRs were related to vibration testing of case subsystems. The problems encountered were, in most instances, traced to system resonances that were characteristic of the hardware/fixture combination.

B. System Testing

A summary of the various *Mariner* Mars 1969 spacecraft (system) tests performed by EDTL is shown in Table 16.

The program of spacecraft testing began with vibration evaluation tests on the structural analysis model, and was followed by more extensive evaluation (acoustic and vibration) tests on the DTM.

The formal test program began with the tests on the PTM and concluded with flight acceptance tests on the three flight systems (M69-2, M69-3, and M69-4). The spacecraft safety provisions were greatly enhanced for formal vibration testing by the addition of humidity control in the test area, use of a portable, laminar-flow cleanout tent around the spacecraft, and generation of a combined operations plan which defined specific responsibilities for all personnel concerned with the operation and implementation of the tests. Figure 14 shows the solar simulator test configuration. A summary of the test conduct and test implementation problems on PTM and flight spacecraft follows:

Table 16. Spacecraft system tests at JPL

Spacecraft	Vibration	Acoustics	Solar/thermal/vacuum
Temp control flux monitor			X
Structural analysis model	X		
Dynamic test model	X	X	
PTM (M69-1)	X	X	X
Flight (M69-2)	X		X
Flight (M69-3)	X		X
Flight spare (M69-4)	X		X

1. Proof test model (M69-1). The PTM vibration test was completed on June 7, 1968. There were three major problem areas attributed to procedural errors. For the Z-axis random noise tests, the control accelerometers were not reoriented per test procedure direction. The second problem occurred because of clipping and subsequent wave distortion of the control signals. A new 3-sigma clipper was installed in the amplifier system primarily for the random noise test. During the sine run, a high servo output signal overdrove a line amplifier in the clipper. The 3-sigma clipper was adjusted to the sine conditions and then worked properly. The third problem was due to improper damping in a spectral density voltmeter readout. This erroneous readout was caught immediately during the level verification with other instruments. This meter response was too slow for the rapidly changing signals of the spacecraft tests. A total of six PFRs was generated during the PTM vibration test to cover the above and other minor anomalies and all were classified as noncritical.

The PTM acoustic test was completed on June 13, 1968. One minor procedural error occurred during the calibration runs, but data analysis showed that the error

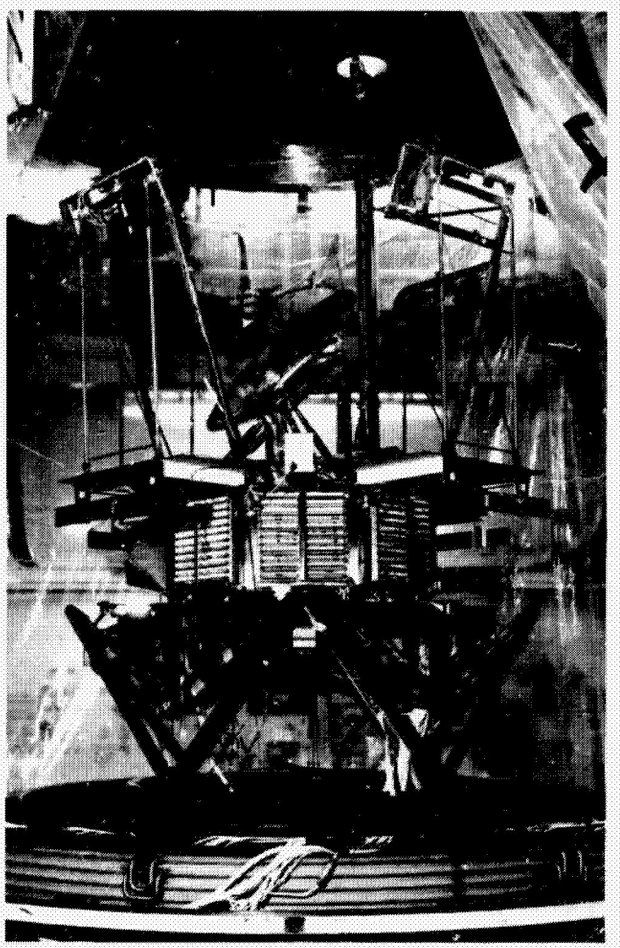


Fig. 14. Spacecraft solar simulator test configuration

had an insignificant effect on the desired acoustic spectrum. One PFR was issued to cover the anomaly; it was classified as noncritical.

The PTM solar simulator testing started on April 27, 1968, and was completed on May 20, 1968. No significant test implementation problems occurred. A problem associated with the gyro response to vacuum pump vibration was corrected by a procedural change. As with some of the flight spacecraft testing, occasional facility power outages did not degrade the spacecraft or the implementation of the tests.

2. Flight spacecraft M69-2. Vibration testing of the M69-2 spacecraft was concluded satisfactorily on September 26, 1968, without any significant problems. No PFRs were issued.

3. Flight spacecraft M69-3. Vibration testing of the M69-3 spacecraft was completed successfully on November 1, 1968. No significant problems were observed during the test, and no PFRs were issued.

Solar simulator testing of M69-3 started on September 23, 1968, and was completed on October 18, 1968. No significant test implementation problems occurred.

4. Flight spacecraft M69-4. Vibration testing of the M69-4 spacecraft was completed on October 19, 1968. One anomaly occurred during run 9 (*X*-axis random exposure). During run 9, equalization verification (less than the required 2.0 g rms), an adjustment to the slide wire for the equalization filter 25 was made. This adjustment caused a loss of continuity in the servo control for filter 25 (625-Hz center frequency), and the input exceeded the set level by approximately 15 dB. This parameter was, however, being monitored, and the test was aborted immediately (1–2 s). Once the slide wires were cleaned, the test was continued without further difficulties. This anomaly was documented with a PFR which was classified noncritical.

Solar simulator testing of M69-4 started on October 31, 1968, and was completed on November 22, 1968. No significant test implementation problems occurred.

C. General Test Problem Areas

The purpose of this section is to provide a well-documented record of the test obstacles encountered, so that the experience gained from the *Mariner* Mars 1969 program will be available in planning future programs. No attempt has been made in this report to classify problems in order of magnitude, because a satisfactory solution to all obstacles is a primary EDTL goal, and the reader's personal interest or involvement will dictate an order of importance. The types of problems encountered are summarized below.

Dynamic test fixture problems were encountered primarily in testing case (class I) equipment. These case fixtures had been designed to test louver assemblies with the case electronics on earlier *Mariner* programs. The *Mariner* Mars 1969 project did not test case electronics with louver assemblies attached underneath. As a result, the fixtures used at JPL, as well as contractors' fixtures, were not optimized for minimized height and maximum structural strength. An example of one of the more severe

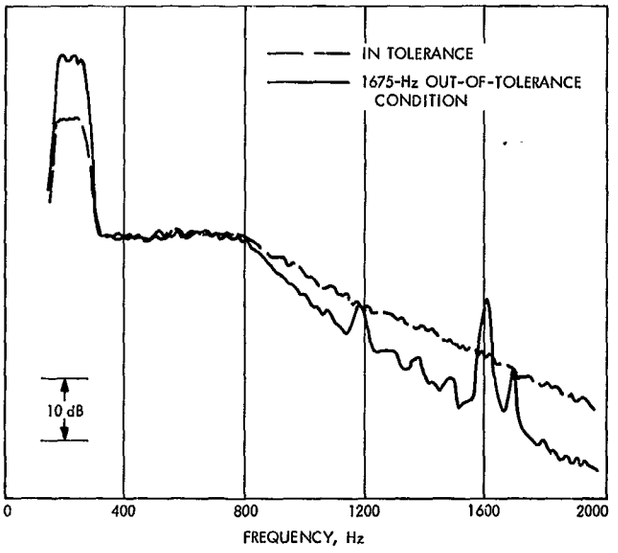


Fig. 15. Typical subsystem random vibration equalization

out-of-tolerance (equalization) random tests is illustrated in Fig. 15. As mentioned previously, a large percentage of the EDTL PFRs were written against hardware tested in these fixtures. These PFRs were either for out-of-tolerance conditions or fixture/hardware resonances which actuated the vibration safety equipment and produced test aborts.

VII. Conclusions

The *Mariner* Mars 1969 environmental test program achieved the project requirements of design verification and flight acceptability of the spacecraft and component subsystems. The problems which occurred during the course of the project were resolved to a sufficient degree that the effect on the program was considered minor. The following paragraphs discuss subsystem and system environmental test program compliance with project requirements.

A. Subsystem Testing

Subsystem testing was completed successfully except for one subsystem (IRS). The elimination of separate TA and PTM assemblies resulted in fewer tests than initially desired. Yet this action precipitated a detailed review of the test requirements for the individual subsystems to eliminate those tests for which prior *Mariner* projects design verification was still valid. In addition, the use of system-level tests to assess the compatibility of a majority of the subsystems in the acoustic and pyrotechnic shock environments proved to be very successful.

The major impact on the environmental test program was the elimination of separate assemblies and the resulting problems associated with the test status of assemblies at the time of delivery to the PTM spacecraft. Certain assemblies, primarily science, were delivered to the PTM spacecraft without having completed the TA test program. In some instances no successful TA testing of any type had been completed. For the total TA test program this may not have been significant; yet the fact that assemblies had not completed vibration and/or thermal/vacuum testing was considered to be a degradation to the PTM spacecraft testing and the FA subsystem and system tests. Most of the failures which occurred during the PTM spacecraft tests (primarily thermal/vacuum) and the FA subsystem tests were failures which should have been and were detectable during the TA subsystem testing.

Owing to the elimination of the separate TA and PTM assemblies, the formal life test program as initially required was greatly reduced. The scheduled use of the TA/PTM equipment in support of PTM system testing, flight spacecraft testing, and the completion of the TA test program precluded formal extended-duration life testing. Instead, the assemblies were subjected to the maximum life test consistent with other use of the units.

B. System Testing

The PTM and flight spacecraft environmental testing was completed successfully and consistent with project requirements. The extended duration test in the thermal/vacuum environment to which each of the spacecraft was exposed provided added confidence in the adequacy of design and allowed for additional evaluation of spacecraft capabilities and problem areas. The success of the dynamic test program was reflected in the minimum number of failures in these environments. Problems in testing due to facility limitations resulted in lower lateral axes random vibration levels than desired. Yet the overall performance of the spacecraft during dynamic testing removed any doubts as to flight acceptability.

As stated above, the effect on the system testing due to incomplete TA subsystem testing resulted in some delays and unknowns due to the configuration of the

spacecraft. These problems occurred primarily in the thermal/vacuum environment. Owing to the implementation of this environmental stimulus, test time was lost because of problems which should have been resolved through adequate subsystem testing.

VIII. Recommendations

In reviewing the results of the *Mariner* Mars 1969 environmental test program it was seen that certain areas were susceptible of improvement and that the implementation of a similar program for future projects could be made more effective. The following recommendations are presented for consideration and possible implementation:

1. Primary emphasis should be placed on assemblies of a new design (science assemblies in particular) during the early developmental and TA test program to assure that an adequate assessment of the design is achieved and that it is in the optimum configuration for system-level testing. The environmental requirements engineer and project management should stress the design verification program and its implementation to cognizant personnel.

2. A thorough review should be made of the design maturity and past test history of all assemblies prior to the generation of the test configuration document to assure that the capabilities and limitations of the equipment are accurately reflected in the required tests. The performance of this task at the earliest possible time will allow for a more exact definition of test program scope to concerned personnel.

3. More emphasis and stress should be applied to assure that subsystem TA vibration and thermal/vacuum tests are completed prior to the PTM and FA testing. Failure to do this results in flight equipment being subjected to a design verification rather than an acceptance test, with the potential degradation not being known.

4. The TA/FA test margins should be continuously evaluated such that the intent (design verification) is maintained and not degraded by ground operations (vibration, shock, etc.) which can expose flight equipment to potentially degrading environments.

5. Additional emphasis should be placed on the electromagnetic compatibility program and its function during the early stages of spacecraft design and development. The electromagnetic interference problems occurring during and following spacecraft integration should be minimized. This will reduce schedule difficulties resulting from investigation/correction of these problems at the system level.

6. The RF simulation requirements and method of simulation should be continuously reviewed to reflect all sources at launch and the simulation of the sources in the optimum fashion. In addition, the RF simulation test should be performed with the spacecraft operated in the maximum number of modes. During launch, most subsystems are not operating, but prelaunch testing does include operation of all subsystems. During these periods, AFETR RF sources could create problems.

7. The philosophy of life testing should be reviewed and methods developed so that useful data can be acquired at the earliest time. The different life modes associated with electrical and mechanical equipment should be recognized and reflected in life-test requirements.

8. Test fixtures used for dynamic and thermal testing of subsystems should have the necessary qualifications prior to any TA testing. Therefore, dynamic thermal mockups of the assemblies to be tested should be provided at the earliest possible time. Additionally, the development of test fixtures which have dynamic characteristics that simulate those existing on the spacecraft would eliminate the use of rigid fixtures and the problems associated with unrealistic responses at resonance frequencies. This would be a major advancement and allow for a more adequate dynamic test program and increased confidence in the results.

9. During the *Mariner* Mars 1969 test program, as in past programs, certain types of components and processes were determined to be more vulnerable to the launch and space environment. These components require added attention during the design phase and continuous evaluation during test. Examples of these components and the special handling required are:

(1) Vacuum tubes (vidicons, image dissectors, and photomultipliers) require mounting to assure that the dynamic environment will not cause internal damage or mechanical motion which affects optical characteristics.

(2) Relays should be installed with an orientation which is insensitive to the dynamic environment to assure that change of state and chatter do not occur. During dynamic testing, the operation of the devices should be monitored.

(3) Preliminary evaluation should be made of the magnetic characteristics of each unit to assure that it is not highly sensitive and will not generate magnetic fields which could degrade its own performance or that of adjacent equipment. This evaluation should also be performed for OSE and test equipment (e.g., Canopus sensor, vibration equipment).

(4) Those OSE components which are subjected to an environmental stimulus should be qualified to operate properly in that environment without the potential of contributing to spacecraft degradation (e.g., TV stimulus failure in the simulator resulted in contamination of the spacecraft).

System Test and Prelaunch Operations

I. Test and Operations Planning

The *Mariner* Mars 1969 spacecraft were conceptually more like hand-built R&D models than like production models commonly produced in the aerospace industry. An integrated test program was developed to effectively demonstrate the ability of these R&D-type spacecraft to meet their mission objectives. The test program had to consider (1) the relative complexity of the spacecraft, (2) the nature of the environments in which the spacecraft had to operate, and (3) the restraints imposed by launch schedules.

Because the 1969 Mars mission required thousands of hours of operation in the space environment, it was necessary to develop consistent and reliable methods of demonstrating spacecraft performance. Verification of spacecraft system design by formal testing and performance evaluation was accomplished as a normal step in the spacecraft development effort.

Preflight spacecraft testing was based on an integrated, comprehensive program designed to show, with a high degree of confidence, that each spacecraft would meet its flight mission objectives. The integrated test program consisted of three major elements:

(1) *Component test.* Component selection and test operations were performed at JPL and at hardware vendors using standard quality-control techniques such as parts screening, stress testing, serialization, parameter trend analysis, and test history evaluation.

(2) *Subsystem test.* Subsystem testing included all testing performed below the system level, e.g., breadboard and prototype tests, subsystem environmental tests, life tests, detailed functional tests, laboratory-type calibrations, and margin tests.

(3) *System test and launch operations.* System operations began with the inspection, certification, and assembly of subsystems into a complete spacecraft system; included the performance of subsystem integration tests, special tests, environmental tests, interface tests, and special tests; and concluded with launch operations at AFETR and postlaunch flight-support testing at JPL.

Each of the test phases was designed to minimize incipient failures and to reduce the number of problems occurring during system-level integration and acceptance testing. Applicable tests performed at the subsystem level and below were repeated as required during system-level testing. In each case, the testing was designed to realize the maximum benefit from the efforts expended at each test level. Emphasis throughout the program was placed on satisfactory hardware performance, especially under simulated launch and space environments. Functional, environmental, and operating margin tests were required for all hardware delivered for system-level integration.

A. JPL Operations Objectives and Requirements

About 10 mo were allocated to the JPL operations schedule (Fig. 1) for spacecraft design qualification and flight-acceptance (FA) testing. About 5 mo of design qualification using the PTM spacecraft preceded the FA testing of the flight spacecraft. The JPL operations were the result of careful analysis of test program objectives, priorities, and available time.

1. Prooftest model spacecraft objectives and requirements. The PTM spacecraft (M69-1) was used for spacecraft design verification. It was subjected to a variety of tests, many of which were conducted under more severe conditions than would normally be expected in flight, e.g., type-approval (TA) tests, in order to verify and perform a confidence-check of spacecraft design and performance. In general, when PTM testing revealed the need for a design change, the change was incorporated and tested on the PTM before incorporation on the flight spacecraft.

a. Objectives. The primary objective of PTM testing was to verify spacecraft design and thereby determine the degree to which the assembled spacecraft met its design criteria. Supplementary objectives that needed to be fulfilled in order to attain the primary objective are shown in Table 1.

b. Test plan. The test plan for the *Mariner* 1969 PTM was intended to provide efficient use of the schedule time in order to yield the maximum possible knowledge of spacecraft performance. As a result, the test plan schedule gave precedence to the following types of tests:

(1) Tests which were likely to reveal design deficiencies requiring lead-time for investigation, rework, and retest.

Table 1. PTM supplementary test objectives

Type of objective	Detailed objective
Interface compatibility and system performance	To verify that each subsystem, while operating on the spacecraft, met the requirements of its functional requirement and design requirement
	To verify that all analog, digital, and power signals from subsystem to subsystem were within tolerance and remained so throughout the test program
	To demonstrate that the spacecraft would perform all "logic functions" in all appropriate operational modes
	To verify that the interface circuits met the design requirements for grounding and isolation
	To demonstrate the operational capability of all spacecraft-to-earth data links and earth-to-spacecraft command links
Parameter variation and failure mode	To demonstrate the ability of backup circuits and redundant paths to correct for failures in primary functions
	To verify that backup circuitry or redundant paths, when in their quiescent modes, did not interfere with the proper operation of the primary circuitry
	To determine the effect on the spacecraft system of certain selected failure modes and develop possible corrective procedures
	To evaluate system performance characteristics during a planned series of parameter variations at extremes of tolerance
Environmental performance	To demonstrate that the spacecraft system would perform to specification during and after having been subjected to environments in excess of those expected during prelaunch, boost, and injection
	To demonstrate spacecraft system operability when subjected to a simulated space environment where temperature levels exceed those expected during a nominal mission
Miscellaneous	To verify spacecraft failure protection logic; to determine failure rates within the time available; to develop and verify system test procedures; to develop and train personnel

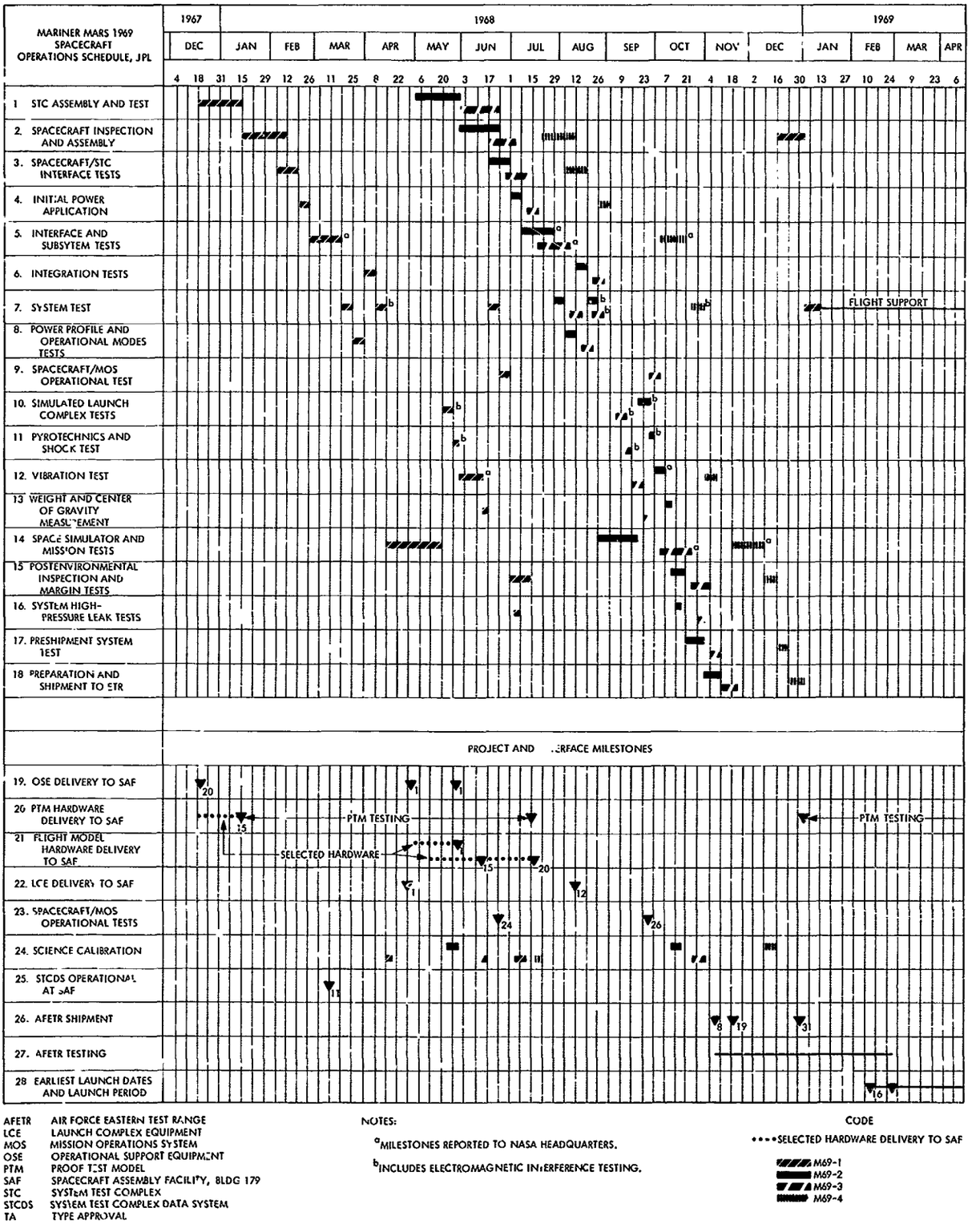


Fig. 1. Typical JPL *Mariner* Mars 1969 operations schedule

(2) Tests which provided data that allowed for an evaluation of the overall spacecraft design.

(3) Tests upon which other tests were dependent.

Secondary considerations used to determine test priorities were:

(1) A greater portion of the allotted test time would be given to those spacecraft elements which were new in concept (e.g., CC&S) and had no previous flight experience.

(2) Emphasis would be given those tests which required a spacecraft environment, as opposed to those which could be performed off the spacecraft.

c. Schedule, order of priority. The JPL operations schedule (Fig. 1) was based on the considerations outlined above. When conflicts regarding the use of the *Mariner* 1969 PTM arose, the order of priority shown in Table 2 was used.

Table 2. PTM test priorities

Priority	Test type
First	PTM tests which permitted detailed examination, evaluation, and verification of the adequacy with which the spacecraft met design specifications
Second	PTM tests which permitted examination of problems that occurred during flight spacecraft tests where exploratory testing with troubleshooting might have damaged the flight spacecraft
Third	PTM tests which were necessary for establishing spacecraft operational characteristics and compatibility with that ground equipment necessary for performing the mission
Fourth	PTM tests which permitted early establishment of launch vehicle interface compatibilities
Fifth	PTM tests which provided a basis for generation and acceptance of procedures and check sheets for qualifying flight spacecraft
Sixth	PTM tests which provided system qualification for flight spares
Seventh	PTM tests which provided training of personnel

2. Flight spacecraft objectives and requirements. The primary objective of the flight spacecraft test plan was to provide two fully qualified, flight-accepted spacecraft for the first day of the 1969 Mars launch period. To meet the primary objective, the apportionment of the total JPL assembly and test time (approx 5 mo) was based on the following considerations:

(1) The testing was not for design verification, as it had been for the PTM spacecraft, but rather for verification of normal equipment operation. The testing was primarily concerned with acceptance; the test data obtained from the PTM spacecraft was used as a standard against which to check flight spacecraft performance.

(2) The flight spacecraft acceptance criteria were: (a) The spacecraft had to operate for a minimum of 250 h in a simulated space environment without major failures. (The flight spacecraft were scheduled for 400 h in the space simulator.) A major failure was defined as one that would prevent the successful completion of the mission; e.g., a power failure would be considered major, whereas a temperature transducer failure would be considered minor. (b) The spacecraft would be shipped to AFETR only upon successful completion of the preshipment system test at JPL. A successful system test was defined as one in which no major failure occurred.

(3) The flight system spares were qualified in a system environment on the flight spare spacecraft (M69-4) or the PTM before incorporation on the flight spacecraft. The minimum system qualification time for any subsystem was 100 h.[1]

(4) Because of the limited number of flight spares, the same methodic and careful initial power application and subsystem interface test was performed on the flight spacecraft as was performed on the PTM spacecraft.

(5) Since only one spacecraft, the PTM, was tested before the flight spacecraft were tested, verification tests were performed on all subsystems to ensure that their outputs were within specification and compared closely to those of the PTM spacecraft; e.g., a parameter variation test was performed on the flight spacecraft, and the overall effects were studied and compared with the results obtained from the PTM spacecraft test.

(6) The environmental tests, both vibration and space simulation, were scheduled to be performed as close to the shipping time as possible. The object was to give maximum assurance that the equipment that would be committed to the mission was used to meet the qualifications stated in (1) above.

[1]Total test time (subsystem and system) was 400 h minimum.

(7) The testing had to ensure compatibility of the spacecraft and all other elements utilized in the 1969 Mars mission. Spacecraft data were made available to the MOS and DSN upon request. Compatibility tests between the spacecraft, launch complex equipment (LCE), *Centaur* shroud and adapter, and supporting personnel were performed at various times during the overall test program. The test plan was designed to allow sufficient time for correction of any incompatibilities.

The test plan recognized the importance of the PTM spacecraft in establishing the standards and procedures that would be used to qualify the flight spacecraft. Therefore, the amount of time that was spent on various phases of the flight spacecraft test plan was, in general, less than that used for the PTM spacecraft.

In general, the flight spacecraft test sequence followed the same pattern as the PTM spacecraft. However, unlike the PTM spacecraft, where one objective was to become acquainted with the overall system behavior as early as possible, the flight spacecraft were required to successfully pass each test in the sequence before advancing to the next test in the sequence. The flight spacecraft ordinarily were not used for detailed troubleshooting as was the PTM spacecraft, but rather the problems were transferred to the PTM spacecraft or flight spare spacecraft when possible. Exploratory testing that required special test setups ordinarily was not permitted on the flight spacecraft.

If the problem was peculiar to the flight spacecraft and could not be examined on the PTM or flight spare spacecraft or in the subsystem laboratories, the problem was necessarily investigated in its own spacecraft environment. When this was the case, the cognizant engineer and quality assurance personnel monitored the test to decrease the possibility of equipment damage.

B. AFETR Operations Objectives and Requirements

The primary objectives of spacecraft operations at AFETR were:

(1) To evaluate the spacecraft performance after shipment from JPL.

(2) To participate in combined system tests that would demonstrate spacecraft compatibility with the Deep Space Network, launch vehicle, launch complex, and range facilities.

(3) To prepare and deliver two flight-qualified spacecraft for each launch opportunity.

Test operations at AFETR were designed to minimize spacecraft activities to those operations required to demonstrate launch environment compatibility and to complete spacecraft launch preparations.

Functional test and calibration activities were restricted to activities that could be performed without removal of flight hardware from the spacecraft or the demating of flight connectors. Equipment shipped to AFETR on the spacecraft was removed only to complete hazardous flight preparations (e.g., propulsion subsystem fueling) and, when necessary, to replace the hardware with flight-qualified provisioned spares.

The AFETR test program and schedule (Fig. 2) was developed subject to the following constraints:

(1) Two sets of operational support equipment (OSE) and two test teams were used for spacecraft test activities at AFETR.

(2) Two spacecraft had to be ready to support each launch date.

(3) Scheduled work during weekends and the holiday periods had to be held to a minimum.

(4) The earliest launch readiness dates were February 16, 1969, for the first spacecraft and March 1, 1969, for the second spacecraft.

(5) There was a 10-day minimum interval between launches.

The test program originally consisted of two distinct phases for each flight spacecraft: (1) the initial phase, and (2) the preflight phase.

In the initial phase, the test sequences were designed to evaluate procedures, train personnel, and demonstrate spacecraft and LCE compatibility with the launch complex environment and interfacing system hardware.

Following the completion of initial phase operations, the flight spacecraft was to be demated from its launch vehicle and returned to its hangar for preflight preparation. The preflight-phase operations were limited to activities required for spacecraft launch. Each preflight test utilized data obtained during similar operations at AFETR and JPL. The spacecraft system was committed to launch when test results showed that spacecraft performance would meet the mission objectives.

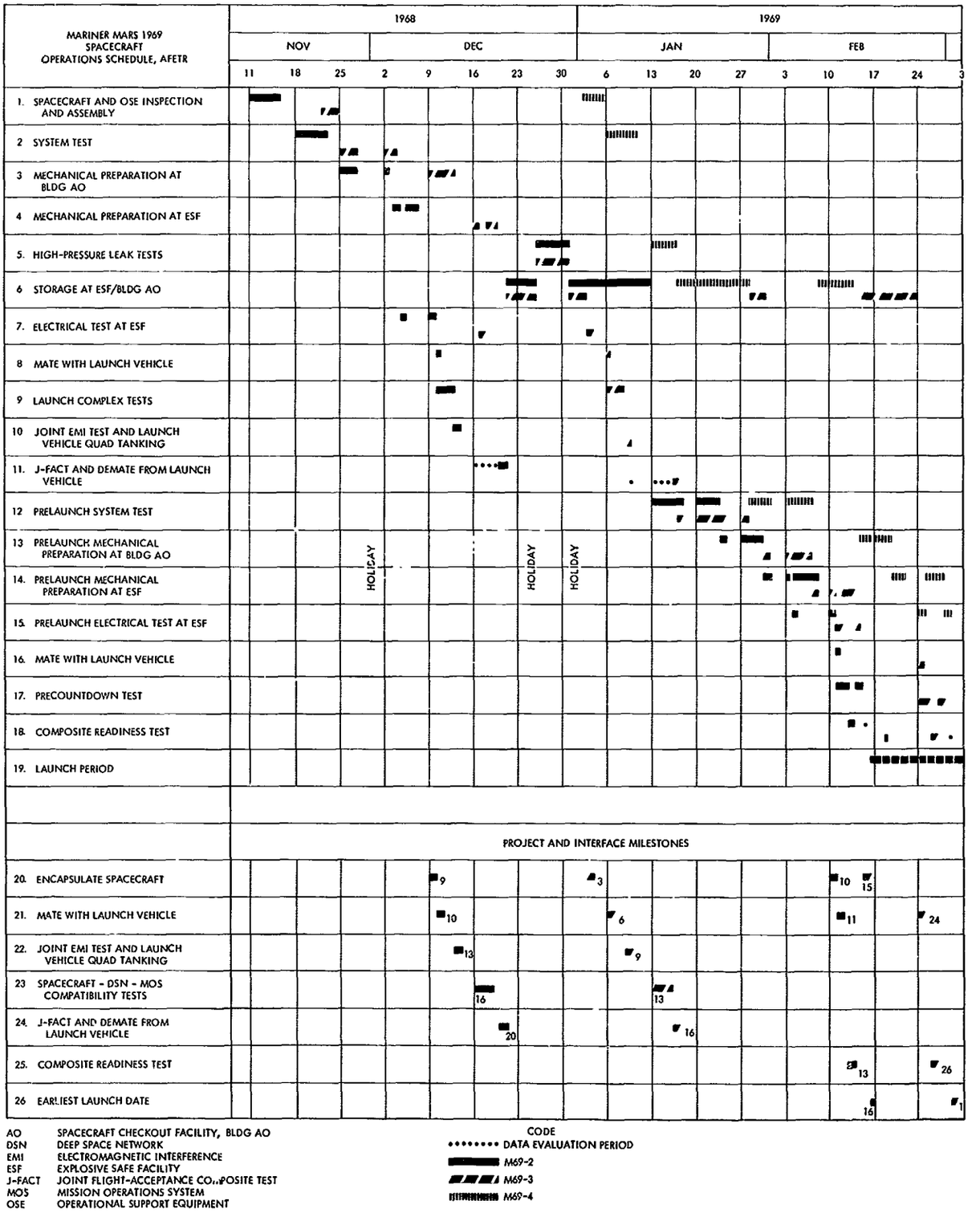


Fig. 2. Typical AFETR *Mariner* Mars 1969 operations schedule

During the flight spacecraft test program at JPL it became obvious that it would be desirable to lengthen the JPL test period if some method could be found for reducing the test period at AFETR without compromising the AFETR test objectives. The method chosen was to use the flight spare spacecraft (M69-4) to perform the initial operations for both flight spacecraft, thus compressing AFETR time requirements by about 6 wk.

C. Test Team Organization

The JPL Systems Test and Launch Operations Section organization for *Mariner* 1969 spacecraft test and launch operations is shown in Fig. 3. Within the section, three test teams and three support groups reported directly to the operations manager. On-call support was available to the operations manager from the technical divisions and the project office whenever specific conditions required such support.

Each test team consisted of a system test director, assistant test director, five system engineers, and a system test technician. Each team was responsible for system-level supervision of the assembly, test, and (flight spacecraft) launch of *Mariner* 1969 spacecraft. Test team responsibilities included system assembly and test procedure development, test data management and analysis, problem identification, subsystem performance evaluation in the spacecraft system, and preparation of test records and reports. The test team nucleus was in turn supported by from 25 to 30 engineers and technicians from the technical divisions representing all spacecraft subsystems.

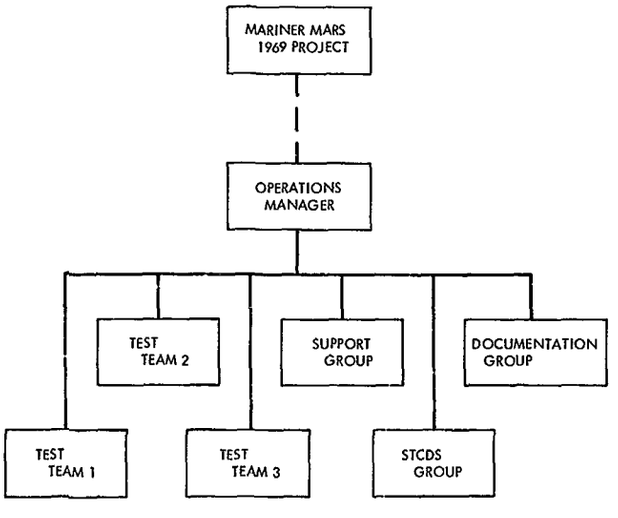


Fig. 3. Systems Test and Launch Operations Section organization

II. Spacecraft Operations

A. Introduction

Table 3 shows the dates of testing and operations of the four spacecraft (M69-1, -2, -3, and -4) from assembly to flight support or AFETR testing. The date shown in the table indicates either the start date of the operation or the inclusive dates.

The tests and operations that were common for all four spacecraft are briefly discussed; the individual operations for specific spacecraft as well as the operations for flight support or after delivery to AFETR are presented with each spacecraft discussion.

1. Subsystem tests. Following verification of the subsystem interfaces, a detailed subsystem test was conducted to (1) provide a detailed evaluation of subsystem performance during operation on spacecraft power, and (2) allow a preliminary determination of any possible effects the subsystem may have had on the system environment.

2. System test. The first system test, which was conducted at the SAF, served to verify the functional performance of the spacecraft as an integrated system within the constraints imposed by the test equipment and the earth-based environment.

3. Preliminary telemetry calibration, scan-control subsystem. A telemetry calibration was performed to enable a cursory calibration of scan control telemetry DNs relative to the physical position of the spacecraft scan platform for various sets of far- and near-encounter pointing directions. In addition, the test provided a demonstration of scan-control subsystem performance, including far-encounter planet sensor control and scan actuator clutch operation.

4. Space simulation test part I. The purpose of part I of the space simulation test was to demonstrate long-term (at least 250 h) spacecraft functional performance while operating in a simulated space environment created in the JPL 10-ft space simulator. During part I, the spacecraft was operated through all nominal modes several times while data were compiled for analysis. The nominal simulated space environment was a pressure of less than 5×10^{-5} torr and a cold wall temperature of about $-300°F$.

Table 3. Spacecraft operations

Operation	Operation date (1968–1969)			
	M69-1	M69-2	M69-3	M69-4
Assembly	1/17–4/17	5/22–7/26	7/18–8/28	8/12–10/2
Power subsystem test	1/29	6/6	–	8/10–8/20
Initial power application and system interface tests[a]	1/30–2/9	7/7–7/26	7/27–8/28	8/21–9/23
Subsystem tests[a]	1/31	7/8	7/1–8/7	8/22–9/23
System test 1	3/20–3/28	7/26–8/1	8/28–9/4	9/23–10/3
System test 2	4/10–4/18	10/8–10/16	11/7–11/13	11/26–12/6
Preliminary scan control subsystem telemetry calibration	4/18	–	8/19–8/23	9/9
Space simulation testing preparation	4/19–4/26	8/17–8/23	9/12–9/23	10/25–10/31
Space simulation test, part I	4/26–5/10	8/23–9/3	9/23–10/4	10/3–11/10
Space simulation test, part II	5/13–5/20	9/14–9/17	10/7–10/17	11/10–11/13
Vibration test	6/3–6/7	9/24–9/26	10/31	10/17–10/19
Pyrotechnic shock test	7/12	9/26	11/1	–
Weight and CG measurement and propulsion subsystem alignment	7/14–7/15	9/27–9/30	10/21–10/22	10/7–10/10
Simulated precountdown	7/21	10/3	10/26	10/24
Simulated countdown	7/24	–	10/28	10/23
System test 3	7/1–7/9	11/15–11/26	12/5–12/20	–
Scan platform instrument alignment verification	7/31	10/23, 1/15	9/6, 11/5	10/15, 10/21
Scan control subsystem telemetry calibration	8/5	10/24, 11/11	12/2	–
Cleaning and disassembly	8/6–8/10	11/4–11/8	11/13–11/20	11/22–11/23
Reassembly	12/6–1/6	11/8	11/21–11/27	11/23–11/26
System test 4	1/17–1/24	1/8–1/17	1/16–1/23	–
Shipment to AFETR	–	12/17–12/21	1/2–1/5	12/17–12/21

[a]The duration of interface and subsystem testing was dependent upon the availability of other subsystems and the number and complexity of the interfaces involved.

5. Space simulation test part II. Spacecraft preparation for part II of the space simulation test included the removal of externally mounted test equipment, stimuli, test cables, and other hardware that would interfere with the compilation of good data for temperature control subsystem performance evaluation.

The space simulation test, part II, was developed to verify spacecraft temperature control design. In addition, spacecraft temperature control margins were verified by operating the spacecraft in hot and cold temperature configurations. Following completion of part II, a system verification test was performed to ascertain that the spacecraft had not been degraded by the thermal environment.

6. Vibration test. The vibration test was performed to verify that the spacecraft would operate satisfactorily during and after exposure to vibration levels based on the expected environment from the *Atlas* and *Centaur* launch vehicles during the boost phase. The spacecraft was vibrated in three different axes: (1) the Z axis, (2) the *X* axis (vibration equipment attached to bay I), and (3) an *X-Y* axis (vibration equipment attached to bay VIII). Following vibration in each axis, a brief test was performed to verify that spacecraft performance had not been degraded.

7. Pyrotechnic shock test. A pyrotechnic shock test was performed on the PTM spacecraft to (1) evaluate spacecraft operation during the detonation of pyrotech-

nic devices, (2) determine the nature of pyrotechnic shocks by measurement with accelerometers, and (3) demonstrate spacecraft pyrotechnic compatibility with the electromagnetic interference sources encountered on the launch complex at AFETR.

8. Simulated precountdown. The purpose of the launch precountdown was to perform the most detailed spacecraft verification permitted within the limits of the launch configuration and the launch complex equipment (LCE).

9. Simulated countdown. A simulated countdown was performed on the PTM spacecraft using the LCE and system test complex. The purpose of the simulated countdown was to provide training for personnel taking part in the spacecraft launch operations at AFETR and to develop an optimum sequence for conditioning the spacecraft for launch and taking engineering measurements that would aid in postlaunch acquisition and spacecraft performance analysis.

10. Scan platform instrument alignment verification. During the alignment of the scan platform instruments, the lines-of-sight of all planetary instruments mounted on the platform were measured with respect to the others and to a reference plane on the scan platform.

11. Scan control subsystem telemetry calibration. A scan control subsystem telemetry calibration was conducted to provide accurate data concerning the correlation between the telemetered scan platform position data and the actual position of the scan platform clock and cone axes.

12. Cleaning, disassembly, and reassembly. Spacecraft cleaning and disassembly were performed by means of the usual cleaning methods utilized on the spacecraft temperature control surfaces. In addition, a new ultrasonic procedure was tried experimentally. Selected spacecraft subsystems were removed and returned to the subsystem laboratories for additional testing. The remainder of the spacecraft was placed in bonded storage in the SAF pit, where it remained until reassembly.

As equipment was returned from subsystem laboratories to the SAF, it was cleaned and reassembled on the spacecraft bus. All cleaning and assembly were performed in specially prepared clean rooms in the SAF high-bay area.

B. Spacecraft M69-1 Operations

The operations conducted with spacecraft M69-1 are shown in Table 3, except for the following individual operations and flight support functions.

1. Power transient survey. A power transient survey was performed on March 28 and 29 to obtain oscilloscope pictures and oscillograph recordings of the power transients produced during the turn-on of the spacecraft subsystems. A secondary objective was to verify that the transients produced were insufficient to cause the spacecraft battery and spacecraft solar panel supplies to go into a sharing mode, even when the total spacecraft power load was at or near maximum. Spacecraft power transients did not cause transfer to the sharing mode.

2. Spacecraft telemetry channel calibration. In early April, spacecraft telemetry channel calibrations were verified and, when necessary, corrected. During the end-to-end calibrations, data were obtained that allowed verification of computer-derived curves describing the relationship between the data numbers (DNs) telemetered by the flight telemetry subsystem and the engineering parameter (e.g., voltage, temperature, or pressure) being transduced on the spacecraft.

3. Power profile determination. Power profile data were obtained in April to determine the power dissipation of each spacecraft subsystem in each of its pertinent steady-state electrical modes of operation. These data were used primarily in the development of a spacecraft heat-source profile for performance analysis of the spacecraft temperature-control subsystem.

4. Acoustic test. An acoustic test was performed on June 10 in the acoustic chamber. The purpose of the acoustic test was to evaluate the performance of the PTM spacecraft during exposure to type-approval acoustic levels based on the expected environment from the *Atlas/Centaur* at liftoff. No spacecraft problems were observed during the test. A spacecraft verification test was satisfactorily completed following the acoustic test.

5. Weight and center-of-gravity measurement and propulsion subsystem alignment. Spacecraft M69-1 weight was 835.9 lb. The measured center of gravity location in spacecraft coordinates was $X = +0.456$ in., $Y = +0.473$ in., and $Z = -9.034$ in. The alignment error after adjustment of the propulsion subsystem thrust axis was 0.019 in.

6. Spacecraft–DSIF interface compatibility tests. A series of preliminary compatibility tests was held between the M69-1 spacecraft and Compatibility Test Area 21 of the DSIF during the period July 10–17. The purpose of the tests was to establish the degree to which the telecommunications portions of the spacecraft and DSIF designs met the requirements of the *Mariner* Mars 1969 project and to establish the design compatibility between a preliminary version of the DSIF telemetry and command processor operational software and the spacecraft data stream.

7. Power transient survey. A power transient survey was performed on July 18 to obtain oscilloscope pictures and oscillograph recordings of the power transients produced during the turn-on of spacecraft subsystems. A secondary objective was to verify that the transients produced were insufficient to cause the spacecraft battery and spacecraft solar panel supplies to go into a sharing mode, even when the total spacecraft power load was at or near maximum.

8. Free mode test. A free mode test was held on July 19 to (1) demonstrate the correct operation of the spacecraft on solar power, (2) verify the functional integrity of the spacecraft in the absence of any support equipment electrical connections, and (3) verify that the system test complex and associated cabling did not affect spacecraft data readouts. To meet the test objectives, the spacecraft solar panels were installed in protective boxes, placed outside the test facility, and oriented toward the sun (Fig. 4). The electrical power produced by the solar panels was used to operate the spacecraft, which was located inside the facility on its low-level positioner. Data analysis was performed via the telemetry link.

9. Parameter variation tests. During the periods July 22–23 and 29–30, parameter variation tests were performed on the M69-1 spacecraft. The purpose of the tests was to vary selected spacecraft parameters above and below the nominal operating range to evaluate spacecraft system performance margins and subsystem interactions under specific tolerance variations.

10. Television subsystem calibration. Television subsystem calibration was verified on July 25 and 26. The verification included all elements of the television picture-taking system.



Fig. 4. Solar panels in protective containers outside SAF during free mode test

11. Transient test. The umbilical and in-flight separation connector transient test was conducted on August 2; the spacecraft was operated in the launch mode while specific transients were introduced into each separation connector function. In addition, each connector wire was grounded to the chassis in a separate test. Spacecraft performance was monitored to verify that the transients and grounding produced no deleterious effects.

12. Power subsystem test. A power subsystem test was performed January 6–9, 1969, to verify proper operation of the spacecraft power subsystem before applying spacecraft power to other subsystems of the newly reassembled spacecraft. Initial power application to spacecraft subsystems began January 10, 1969, and continued through early January as additional subsystems were installed. The objective of the initial power application procedure was to safely apply spacecraft power to the newly reassembled spacecraft.

13. Mission Operations System support. Spacecraft M69-1 was used in support of Mission Operations System (MOS) operations during the period January 21–28.

The spacecraft was used as an aid in verifying the operational readiness of the various elements of the MOS to support *Mariner* Mars 1969 launch and flight operations.

14. SPAC training tests. A spacecraft performance analysis and command (SPAC) group training test was conducted January 23 and February 4, 6, and 17. The purpose of the exercise was to simulate launch and trajectory-correction maneuver operations and introduce controlled anomalies requiring corrective command action by SPAC.

15. Special tests. A series of special tests was performed from the end of January through February to determine the source of or explanation for minor anomalies.

16. MOS demonstration tests. On February 10–13 an MOS demonstration test was performed. The purpose of the four-part test was to demonstrate the readiness of all elements of the MOS to support spacecraft M69-3 launch and trajectory-correction maneuver operations. The trajectory-correction maneuver was aborted several seconds before the start of motor burn by SPAC. The data available to SPAC indicated that low-gain antenna drive and several other channels were sufficiently erratic to require that the maneuver be aborted. Spacecraft telemetry and hardline data available on the STC in the SAF were normal.

17. Mariner Mars 1971 scan platform vibration tests. A scan platform vibration test was performed on the *Mariner* 1969 PTM spacecraft in support of the *Mariner* Mars 1971 project. During the test the spacecraft was operated in about 15 different states, and the vibration associated with each state was recorded on magnetic tape.

18. Support of spacecraft M69-3 launch operations. On February 24, the PTM spacecraft was operated in parallel with spacecraft M69-3 from $T - 90$ min in the countdown through Canopus acquisition.

19. Support of Mariner VI trajectory-correction maneuver. A CC&S tandem-mode trajectory-correction maneuver was performed on spacecraft M69-1 to verify the SPAC COMGEN tapes (see Mission Operations System, Section IV-D) to be used for the *Mariner VI* maneuver. The maneuver parameters used were: ccw pitch duration = 131.04 s, cw roll duration = 453.18 s, motor burn duration = 5.4 s.

C. Spacecraft M69-2 Operations

Operations conducted with spacecraft 1969-2 are shown in Table 3 and Figs. 1 and 2. The order of testing differed somewhat from that employed with M69-1. Operations at JPL were generally as described in Section II-A above, except that the order of testing was fitted to the availability of facilities.

1. Weight and center-of-gravity measurement. Spacecraft M69-2 weight, center-of-gravity location, and the required adjustment to the propulsion subsystem thrust axis were measured from September 27 to 30. Spacecraft launch weight was 845.2 lb. The measured center-of-gravity location in spacecraft coordinates was $\mathbf{X} = +0.188$ in., $\mathbf{Y} = +0.541$ in., and $\mathbf{Z} = -9.047$ in. The alignment error after adjustment of the propulsion subsystem thrust axis was 0.032 in.

2. Shipment to AFETR. Preparation for shipment of the spacecraft to AFETR began after completion of system test 3 in late November and continued through the first half of December. Preparation included the removal of certain delicate hardware (e.g., gyroscopes) for separate shipment by aircraft.

The spacecraft left JPL on December 17 in an escorted convoy of four air-ride electronics moving vans and arrived at AFETR on December 21. Following arrival at AFETR Building AO, a careful visual inspection of the spacecraft was performed. The spacecraft was then installed on its low-level positioner in the Building AO high-bay and stored until the start of mechanical operations.

On January 6, 1969 the interface compatibility of the M69-2 spacecraft and STC 2 in AFETR Building AO was verified.

System test 4 (AFETR system test 1) was conducted January 8–17. The purpose of the test was to verify the functional performance of the spacecraft as an integrated system within the constraints imposed by test equipment and the earth-based environment. During the test, the spacecraft was operated in all major modes of the nominal flight sequence. In preparation for the system test, the television subsystem/data storage subsystem interface was verified using data from a television simulator. During the system test a fixed sequencer trajectory-correction maneuver was performed in which the motor burn time was of the wrong duration. Troubleshooting showed that either the flight command subsystem or central computer and sequencer subsystem

was at fault. Attempts to duplicate the problem were unsuccessful. In conjunction with system test 4, a scan platform instrument alignment verification was performed January 15–16.

3. Compatibility verification. On January 17, the functional and operational compatibility of the interfacing elements of the spacecraft, Mission Operations System, and Deep Space Network systems was verified.

4. Attitude control leak test. Spacecraft M69-2 was moved to the AFETR Explosive Safe Facility (ESF) on the morning of January 18. An attitude control leak test was performed January 18–22 to verify the ability of the attitude control subsystem pressure vessels to maintain flight pressure and to measure nitrogen leak rates.

5. Decision to launch M69-3 instead of M69-2. On January 22 a decision was reached to substitute the M69-3 spacecraft for the M69-2 spacecraft for the February 24 launch opportunity. The decision was based on problems encountered with several M69-2 subsystems during the fourth system test, notably the problem of the incorrect fixed sequencer motor burn duration during a simulated trajectory-correction maneuver.

6. Equipment changeout and interface reverification. After the decision was reached to substitute M69-3 for M69-2, the period January 23–February 6 became available for changeout of spacecraft subsystems that had demonstrated performance anomalies during the system test. In addition, certain equipment preferred for use on the February 24 launch (e.g., the far-encounter planet sensor and the IRS) was removed from M69-2 and installed on M69-3. As equipment was returned from subsystem laboratories and installed on the spacecraft, every function passing through every connector that had been demated was reverified.

An abbreviated system test was performed February 10–12 to demonstrate the functional performance of the new equipment within the spacecraft system environment. During the test, the new subsystems were operated in the major elements of the nominal flight sequence.

7. Final Building AO electrical and mechanical operations. Final preparation of the spacecraft for launch was performed in Building AO February 13–17. Preparations included installation and flow-testing of the attitude-control flight gas nozzles, sun sensor and gas-jet phasing verification, installation of the flight battery, solar panel deployment tests, verification of proper scan platform motion in response to ground commands, and stowing of the scan platform in its launch position. The measured spacecraft weight during final preparation was 848.48 lb.

8. ESF electrical and mechanical operations. Spacecraft M69-2 was moved to the ESF February 18 for final launch preparation. During the period February 18–22, the propulsion subsystem and flight pyrotechnics were installed, high-pressure gas vessels were pressurized, final electrical tests were performed (e.g., autopilot and jet vane phasing verification), and the spacecraft was mated to its adapter and encapsulated in the *Centaur* nose fairing (Fig. 5). Precountdown tests were conducted before and after encapsulation to verify spacecraft performance. Spacecraft M69-2 remained encapsulated and under gaseous dry nitrogen purge in ESF during the period February 23 through March 9, 1969.

A special precountdown test and additional special tests required to verify spacecraft launch readiness were performed at ESF March 10 and 11. The spacecraft was then placed in storage awaiting shipment to Launch Complex 36A.

9. Mate with launch vehicle. On March 17, spacecraft M69-2 was moved to Launch Complex 36A and mated to the *Atlas/Centaur* launch vehicle AC-19. An on-pad verification test and precountdown were performed to verify spacecraft compatibility with the launch environment.

10. Practice countdown. A practice countdown was performed March 18 to provide final verification of certain discrete changes to the procedure required by the M69-2 radio configuration at launch.

11. Countdown during launch vehicle EMI/RFI test. A practice countdown was performed March 19 in parallel with a launch vehicle electromechanical interference/radio frequency interference (EMI/RFI) test. Spacecraft telemetry was monitored to verify that the EMI/RFI environment had no effect on data readout.

12. Precountdown test. During a precountdown test performed March 20, anomalous CC&S and IRR performance was observed. Extensive special testing on March 21 and 22 failed to prove conclusively that the

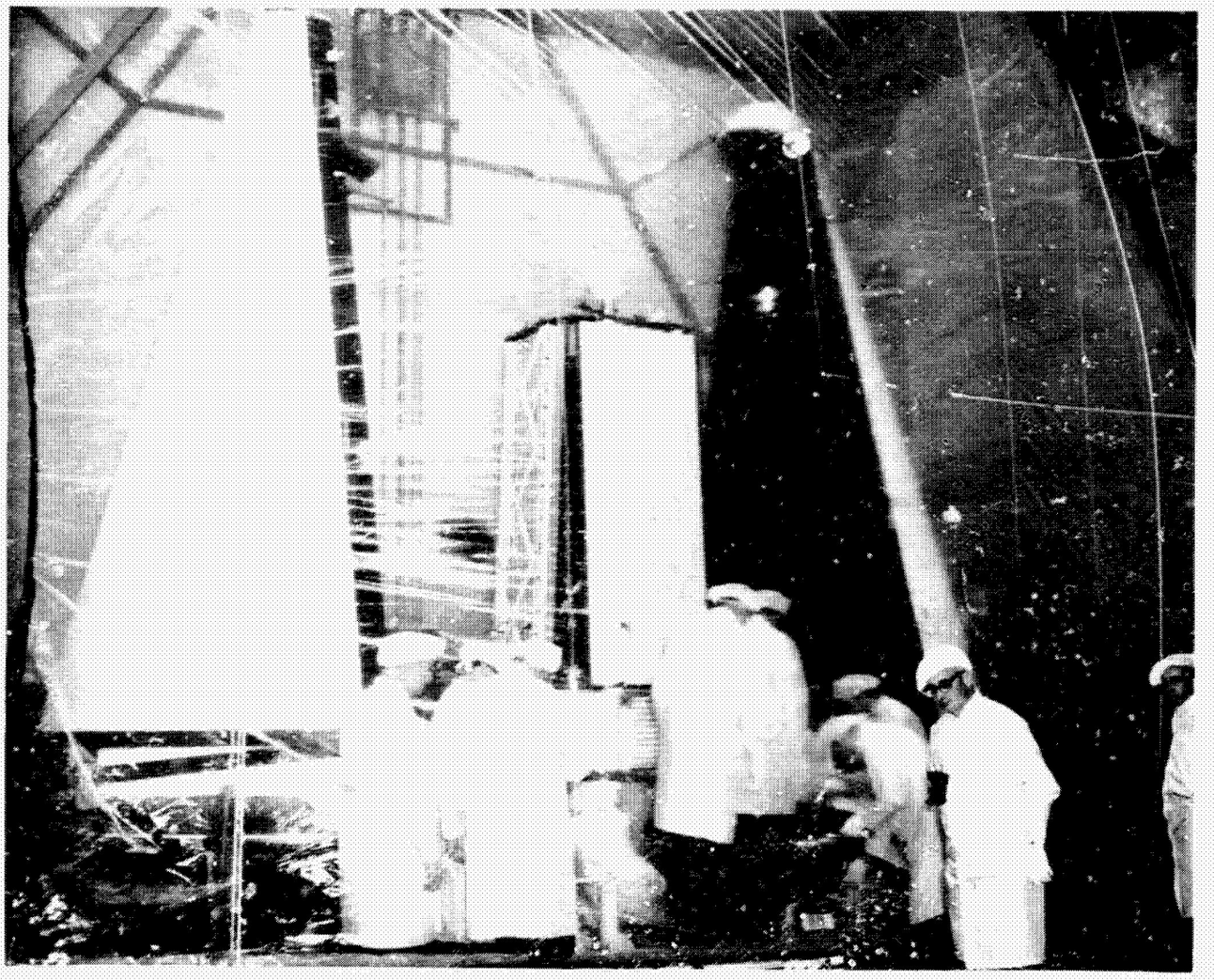


Fig. 5. Encapsulation of spacecraft in Centaur shroud at ESF

subsystems involved were flightworthy. Consequently, the spacecraft was demated from launch vehicle AC-19 on the evening of March 22 and returned to ESF for de-encapsulation. Following removal of the propulsion subsystem, the spacecraft was taken to Building AO for replacement of the CC&S and IRR.

13. Interface reverification. After changeout of the CC&S and IRR, all affected interfaces were reverified; i.e., each signal passing through each connector that was demated during the changeout was individually reverified. In the early morning hours of March 24, the spacecraft was returned to ESF for mate with its spacecraft adapter and re-encapsulation. Launch readiness was then verified by a special postencapsulation test.

14. Mate with launch vehicle. Spacecraft M69-2 was moved to Launch Complex 36A and remated to the *Atlas/Centaur* launch vehicle AC-19 on March 25.

15. Precountdown. The launch precountdown was performed March 25 to provide a final detailed verification of spacecraft launch readiness. The precountdown included a careful examination of science subsystem instrument performance.

16. Countdown. The spacecraft M69-2 launch countdown was performed March 27. The spacecraft portion of the countdown went smoothly, terminating with the launch of spacecraft M69-2 (*Mariner VII*) at 22:22:01.198

GMT. The launch occurred 47 min into the launch window because of a hold caused by a *Centaur* guidance acquisition problem.

D. Spacecraft M69-3 Operations

Operations conducted with spacecraft M69-3 are shown in Table 3 and Figs. 1 and 2. The order of testing differed somewhat from that employed with M69-1. Operations at JPL were generally as described in Section II-A, except that the order of testing was fitted to facility availability.

*1. **Center-of-gravity measurement.*** The measured center-of-gravity location in spacecraft coordinates was found to be: **X** = +0.130 in., **Y** = +0.522 in., and **Z** = −8.995 in. Figure 6 shows the measurement in process.

*2. **Shipment to AFETR.*** Preparation for shipment of the spacecraft to AFETR continued through the remainder of December. Certain delicate equipment was removed from the spacecraft for separate shipment. Spacecraft M69-3 left JPL January 2 in an escorted convoy of three air-ride electronics moving vans and arrived at AFETR on January 5. Following arrival at AFETR Building AO, a careful visual inspection of the spacecraft was performed. The spacecraft was installed on its low-level positioner in the Building AO high-bay.

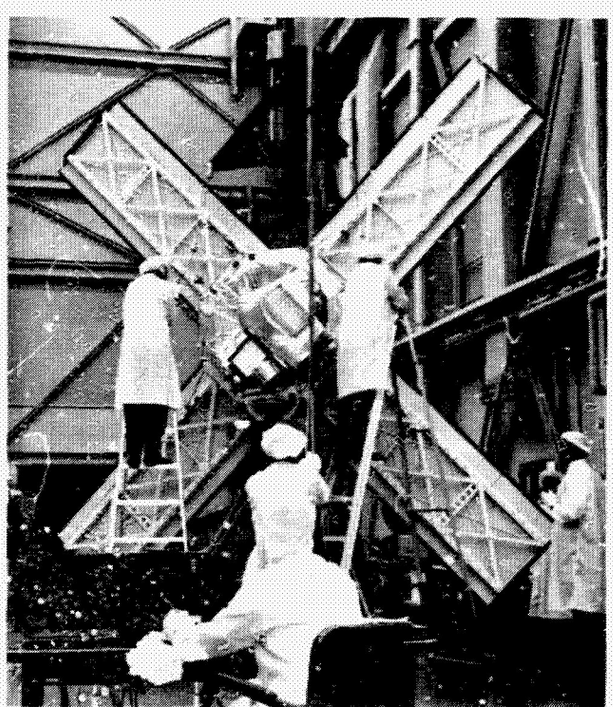


Fig. 6. Spacecraft weight and center-of-gravity measurement

During the period January 7–10 spacecraft M69-3 was assembled to the system test configuration. Several verification tests were performed January 13–15 to demonstrate the compatibility of spacecraft M69-3 with STC 2 and DSS 71, the Cape DSN station. In addition the television/data storage subsystem interface was verified using television subsystem simulator data.

*3. **System test 4.*** During the period January 16–23, spacecraft M69-3 system test 4 (AFETR system test 1) was conducted to verify the functional performance of the spacecraft as an integrated system. All major parts of the nominal flight sequence were tested, including several types of encounter sequences and trajectory-correction maneuvers. Because of the decision on January 22 to substitute M69-3 for M69-2 during the February 24 launch opportunity, system testing of M69-3 was accelerated through the use of two-shift operations.

*4. **Scan platform instrument alignment verification.*** Scan platform instrument alignments were reverified on spacecraft M69-3 on January 17, 20, and 23. The line-of-sight of each planetary instrument was measured.

*5. **Attitude control leak test.*** The spacecraft was moved to the ESF January 24. The attitude control leak test was performed January 24–27.

*6. **Final Building AO electrical and mechanical operations.*** Final preparation of the spacecraft for launch was performed in Building AO January 28–February 3. Preparations included installation and flow-testing of the attitude-control flight gas nozzles, sun sensor and gas-jet phasing verification, installation of the flight battery, solar panel deployment tests, verification of proper scan platform motion in response to ground commands, stowing of the scan platform in its launch position, and measurement of spacecraft weight and X-Y plane center of gravity. Measured spacecraft weight was 850.31 lb; the measured spacecraft CG location was **X** = +0.14 in., **Y** = +0.57 in., and **Z** = −13.92 in.

*7. **ESF electrical and mechanical operations.*** Spacecraft M69-3 was moved to the ESF February 4. Prelaunch preparations performed at the ESF February 4–11 included installation of the propulsion subsystem (Fig. 7) and flight pyrotechnics, pressurization of high-pressure gas vessels, performance of final electrical verification

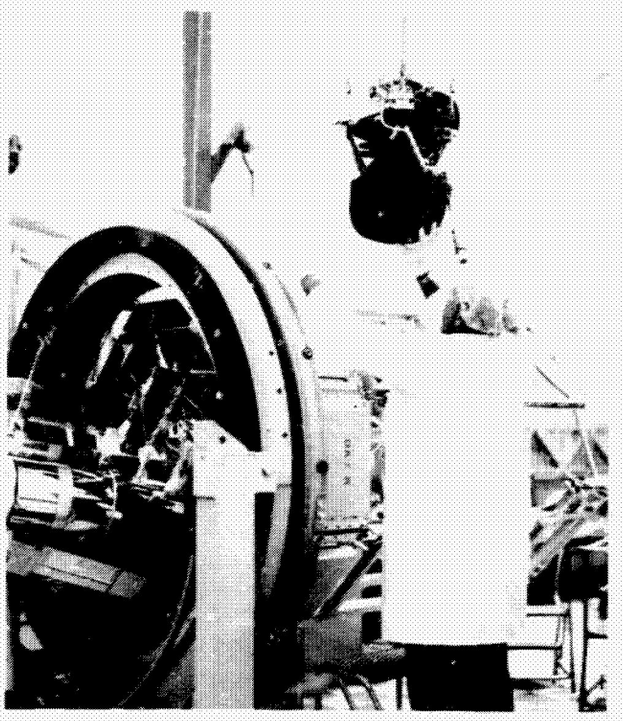


Fig. 7. Installing propulsion system in spacecraft at ESF

(e.g., in-flight accelerometer calibration), mating of the spacecraft with its adapter, encapsulation of the spacecraft in the *Centaur* nose fairing, and the performance of pre- and postencapsulation precountdown tests.

8. Mate with launch vehicle. On February 12, spacecraft M69-3 was moved to Launch Complex 36A and mated to the *Atlas/Centaur* launch vehicle AC-19. An on-pad verification was performed to demonstrate spacecraft compatibility with launch complex equipment and the launch complex environment.

9. Precountdown test. A precountdown test was performed February 13. The purpose of the precountdown was to perform the most detailed spacecraft verification permitted within the limits of the launch configuration and the launch complex equipment. No significant problems were encountered during the precountdown.

10. Countdown during launch vehicle EMI/RFI test. A launch countdown test was performed February 14 to provide additional training for personnel who would be involved in the actual launch of M69-3 and to verify the countdown procedure that would be used. The countdown was performed in conjunction with an EMI/RFI test performed by launch vehicle personnel. Spacecraft telemetry was carefully monitored to verify that the EMI/RFI environment had no effect on data readouts. Shortly after completion of the test, the AC-19 launch vehicle suffered major damage due to loss of the pressure used to maintain structural rigidity. The spacecraft was demated from the launch vehicle, returned to the ESF, and de-encapsulated in preparation for a thorough investigation of spacecraft condition.

11. Spacecraft verification test. A comprehensive verification of all subsystems that might have been affected by the motion imparted to the spacecraft when AC-19 temporarily lost pressure was performed February 15–16. No anomalies were observed. The spacecraft was re-encapsulated in the *Centaur* nose fairing February 17, and an abbreviated precountdown was performed to verify spacecraft functional performance.

12. Mate with launch vehicle. Spacecraft M69-3 was moved to Launch Complex 36B on February 18 and mated with the *Atlas/Centaur* launch vehicle AC-20. An on-pad verification based upon the precountdown test was performed to demonstrate spacecraft compatibility with the launch vehicle and the launch complex environment.

13. Countdown during operational readiness test. A practice countdown was performed in conjunction with the Mission Operations System final operational readiness test on February 19. Based on data obtained during the practice countdown, the launch countdown procedure was finalized.

14. Precountdown. The launch precountdown was performed February 20-21. The precountdown provided a final detailed spacecraft verification before launch and included careful examination of science subsystem instruments.

15. Countdown. The spacecraft M69-3 launch countdown was performed February 24. The spacecraft portion of the countdown (Fig. 8) went smoothly, terminating with the launch of spacecraft M69-3 (*Mariner VI*) at 01:29:02:013 GMT, February 25. The launch occurred 15 min into the launch window because of holds caused by a launch vehicle guidance system problem.

E. Spacecraft M69-4 Operations

Operations conducted with spacecraft M69-4 are shown in Table 3 and Figs. 1 and 2. The order of testing

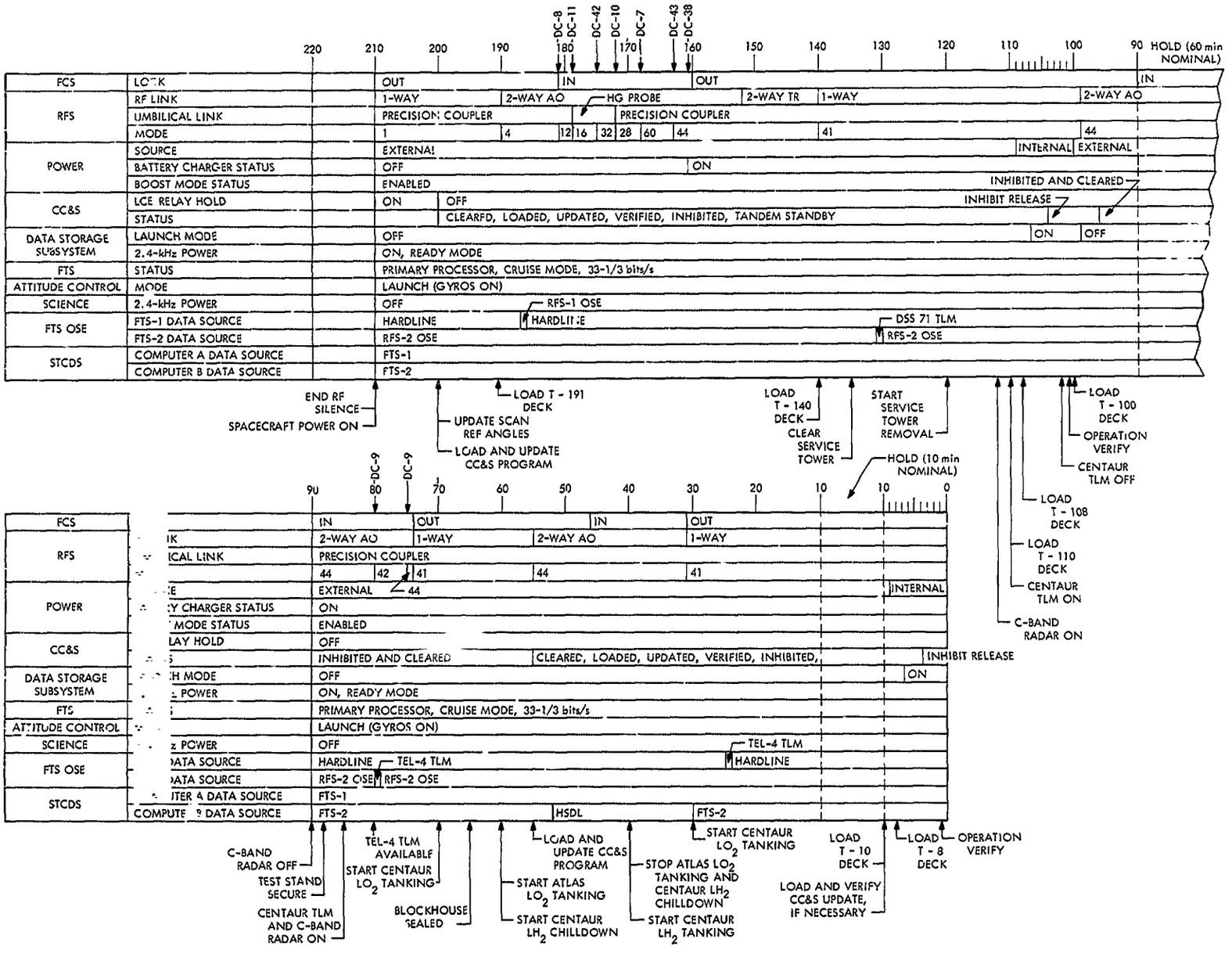


Fig. 8. Spacecraft M69-3 countdown

differed somewhat from that employed with M69-1. Operations at JPL were generally as described in Section II-A, except that the order of testing was fitted to facility availability.

1. Weight and center-of-gravity measurement. Spacecraft M69-4 weight and center-of-gravity parameters were measured during the period October 7–10. The measured center-of-gravity location in spacecraft coordinates was found to be $\mathbf{X} = +0.213$ in., $\mathbf{Y} = +0.540$ in., and $\mathbf{Z} = -8.992$ in. The alignment error after adjustment of the propulsion subsystem rocket engine undeflected thrust axis was 0.054 in. Spacecraft launch weight, less adapter, was 846.3 lb.

2. Shipment to AFETR. Spacecraft M69-4 was readied for shipment to AFETR on December 9–16. The spacecraft left JPL on December 17 in an escorted convoy of four air-ride electronics moving vans. (Spacecraft M69-2 was shipped in the same convoy.) The convoy arrived at AFETR on December 21. After arrival at the AFETR ESF, a careful visual inspection of the spacecraft was performed. The spacecraft was then installed on its low-level positioner inside a portable laminar downflow clean room.

3. ESF electrical and mechanical operations. From December 23, 1968, through January 8, 1969, spacecraft M69-4 was prepared at the ESF for launch pad testing. Operations included installation of the propulsion subsystem (filled with water instead of propellant) and flight pyrotechnics (except for adapter V-band), pressurization of high-pressure gas vessels to one-half of their flight pressures (except IRS gas tanks which were at flight pressure to test on-pad monitoring instrumentation), mating of the spacecraft with its launch vehicle adapter, encapsulation of the spacecraft in the *Centaur* nose fairing, and performance of pre- and postencapsulation precountdown exercises. The flight spare spacecraft (M69-4) was used for the initial period of on-pad testing with the launch vehicle to minimize the exposure of flight spacecraft to the relatively unknown launch pad environment and to provide additional time for detailed examination of the flight spacecraft at AFETR prior to their commitment to launch.

4. Launch Complex 36A operations. Spacecraft M69-4 was moved from the ESF to Launch Complex 36A early in the morning of January 9, where it was mated to the *Atlas/Centaur* launch vehicle AC-19. Following initial launch pad checkout, a precountdown exercise was performed January 9–10 to verify spacecraft performance in the launch complex environment. Countdown exercises were performed January 14 and 15 to develop the procedures that would be used for launch of the flight spacecraft and determine the effects of the launch complex environment, particularly electromagnetic interference, on spacecraft launch operations. During the countdown on January 15 held in conjunction with the launch vehicle flight control and propellant tanking integrated test, a problem was encountered in loading the CC&S memory from the LCE in the blockhouse. A countdown exercise was again performed January 21 in conjunction with the launch vehicle flight-acceptance composite test.

5. Launch Complex 36B operations. The spacecraft was removed from AC-19 on Pad 36A and installed on the *Atlas/Centaur* AC-20 on Launch Complex 36B on January 22. Pad 36B operations included a spacecraft/launch complex compatibility test January 22, a precountdown on January 23, and a spacecraft countdown in conjunction with a launch vehicle flight-acceptance composite test on January 24. During the spacecraft countdown, the spacecraft was irradiated by AFETR electromagnetic interference sources that would be operating during the actual launch. No anomalous spacecraft performance was observed.

6. Attitude control leak test. The spacecraft was returned to the ESF January 24 following the completion of Pad 36B operations. An attitude-control leak test was performed January 25–29 to verify the flightworthiness of the M69-4 gas systems and to measure their leakage rates.

7. Disassembly and inspection. The spacecraft was moved to Building AO January 29, 1969. During the period January 30 to February 14, the spacecraft was completely disassembled and equipment was inspected for physical damage and cleaned.

8. Reassembly. Spacecraft M69-4 was reassembled to the system test configuration February 17–19. A brief electrical checkout February 20 verified the operational readiness of the spacecraft. The spacecraft remained in the system test configuration February 21–26 in support of M69-3 launch and flight operations.

Test Support Equipment

I. Operational Support Equipment

Spacecraft subsystem and system-level functional testing was supported by special equipment which was in large part modified and updated from that used in a similar way on previous projects. It included subsystem operational support equipment (OSE), provided under the cognizance of the technical divisions and sections responsible for the corresponding flight hardware, and data systems provided by the systems division. Integration into system test complexes and into launch complex equipment, and application of the equipment in system testing was under the cognizance of the project engineering division.

Generally speaking, the role of OSE was to provide power and stimuli (including command effects) to the subsystem, and to obtain data and other output from it. The interfaces with other subsystems were to be simulated, providing for operation of the subsystem as if it were on the spacecraft, under various conditions and states. When the spacecraft was assembled, the OSE could be supplanted in these interfaces by the real interfacing subsystems. Conditions such as power and signal level were variable, to provide for margin testing. The role of the data systems was to integrate the data streams in test, and to condition and select data as appropriate in the manner of the telemetry data system developed for flight operations.

A. Radio Frequency Subsystem Operational Support Equipment

The *Mariner* Mars 1969 radio frequency subsystem operational support equipment (OSE) consists of (1) the system test complex equipment (STCE) for support of spacecraft system tests, and the bench checkout equipment which is equivalent to the STCE; and (2) the launch complex equipment (LCE) for spacecraft launch configuration test support. The main components of the radio frequency subsystem OSE, shown in Fig. 1, are the test transmitter, receiver, converter, signal conditioner and mode control, interface switches, and test equipment.

The *Mariner* Mars 1969 system test complex equipment is an improved and almost completely redesigned version of the *Mariner* Mars 1964 design. It uses DSIF modules

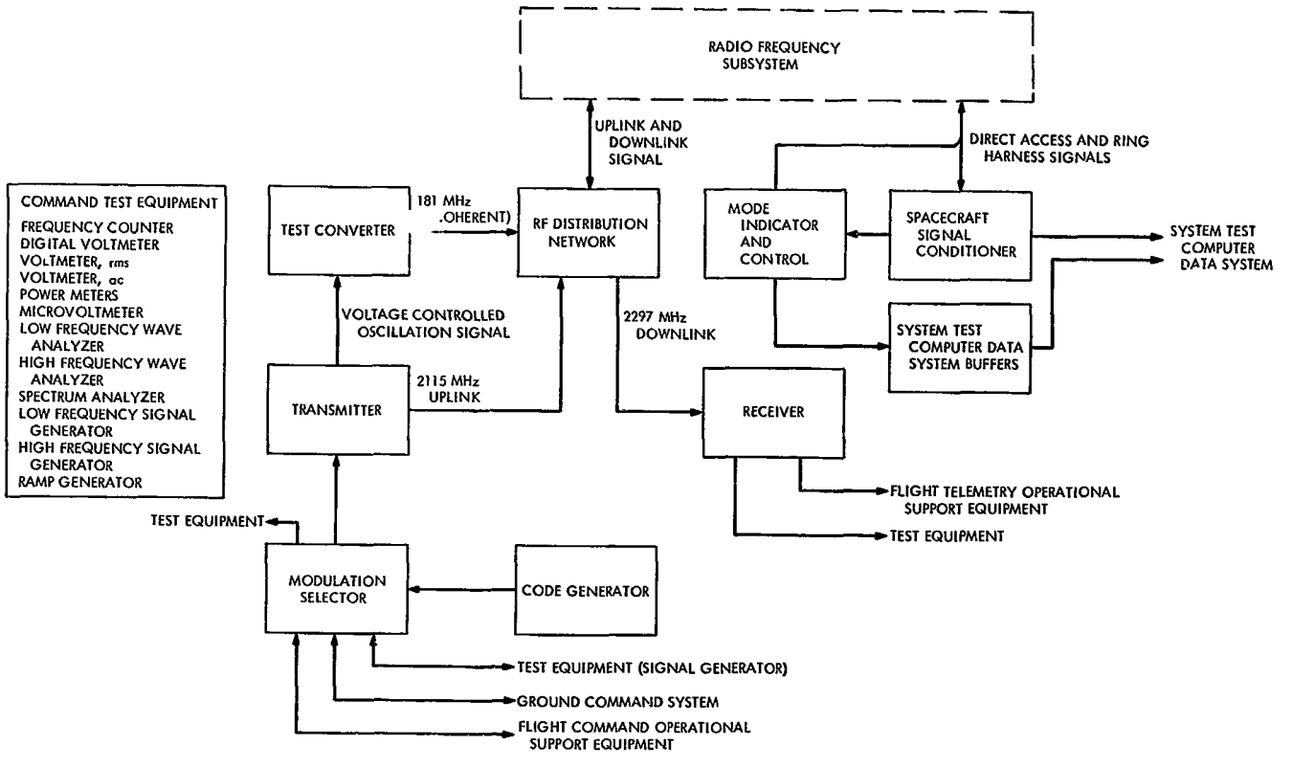


Fig. 1. Radio frequency subsystem operational support equipment

in the receiver and transmitter, providing maximum interfacing with DSIF components as well as the reliability of a proven design, and the ability to use existing calibration facilities and documentation. Some of the improvements in the design are the following:

(1) Elimination of transmitter leakage and receiver susceptibility problems.

(2) Improvement of attenuator setability.

(3) Improvement of transmitter frequency tunability.

(4) Addition of monitoring of the operational support equipment frequency counter by the system test computer data system (STCDS).

(5) Furnishing of analog signals to the STCDS without noise pickup or ground current problems.

In general, the operational support equipment is of advanced design. However, a large number of problems were experienced because of poor workmanship. Many of these problems were corrected during the course of the program.

The following recommendations are made for future programs:

(1) Improved operator training so that problems are recognized and solved correctly and promptly.

(2) A ready means of checking the spacecraft signal conditioner.

(3) Front panel access to the radio frequency subsystem direct access and telemetry functions.

(4) Improved switches for selecting functions and operating modes, capable of switching extremely low currents reliably.

(5) Digital isolation modules replaced with a type more stable under support equipment operating conditions.

(6) Determination and correction of the source of the OSE transmitter/receiver phase jitter which prevents accurate measurement of radio frequency subsystem phase jitter.

(7) Improvement in the operation of the ramp generator which tunes the voltage-controlled oscillator

to provide a semi-automatic means of performing radio frequency subsystem measurements.

(8) Front panel test points for OSE power supply voltages.

(9) Correction of frequent indicator bulb failures.

The launch complex equipment of the radio frequency subsystem supports-system level testing of the subsystem when the spacecraft is in the launch configuration. Essential launch complex equipment components shown in the block diagram (Fig. 2) are the S-band transmitter, RF power meter and monitor recorder, frequency counter, RF coaxial lines, umbilical tower RF junction box, and RF link antennas.

B. Flight Command Subsystem Operational Support Equipment

1. Introduction. The operational support equipment for the *Mariner* Mars 1969 flight command subsystem (FCS) consisted of four double-rack consoles, four bench test fixtures, and one auxiliary console. The equipment can be used to test the FCS flight command subsystem either as an integrated unit, or as separate functional elements. The support equipment program generates all commands and signals that can be programmed, including power used by the flight command subsystem, and receives, decodes, and monitors the outputs from the subsystem. It also displays signal outputs and provides a printout of error data. A block diagram for these operations is shown in Fig. 3.

2. Test capabilities. The following paragraphs describe four OSE test configurations.

a. Bench tests. The flight command subsystem is plugged into the bench test fixture chassis and is controlled by signals generated by the operational support equipment. This configuration may be used during both vacuum and ambient pressure in-place testing, but is not

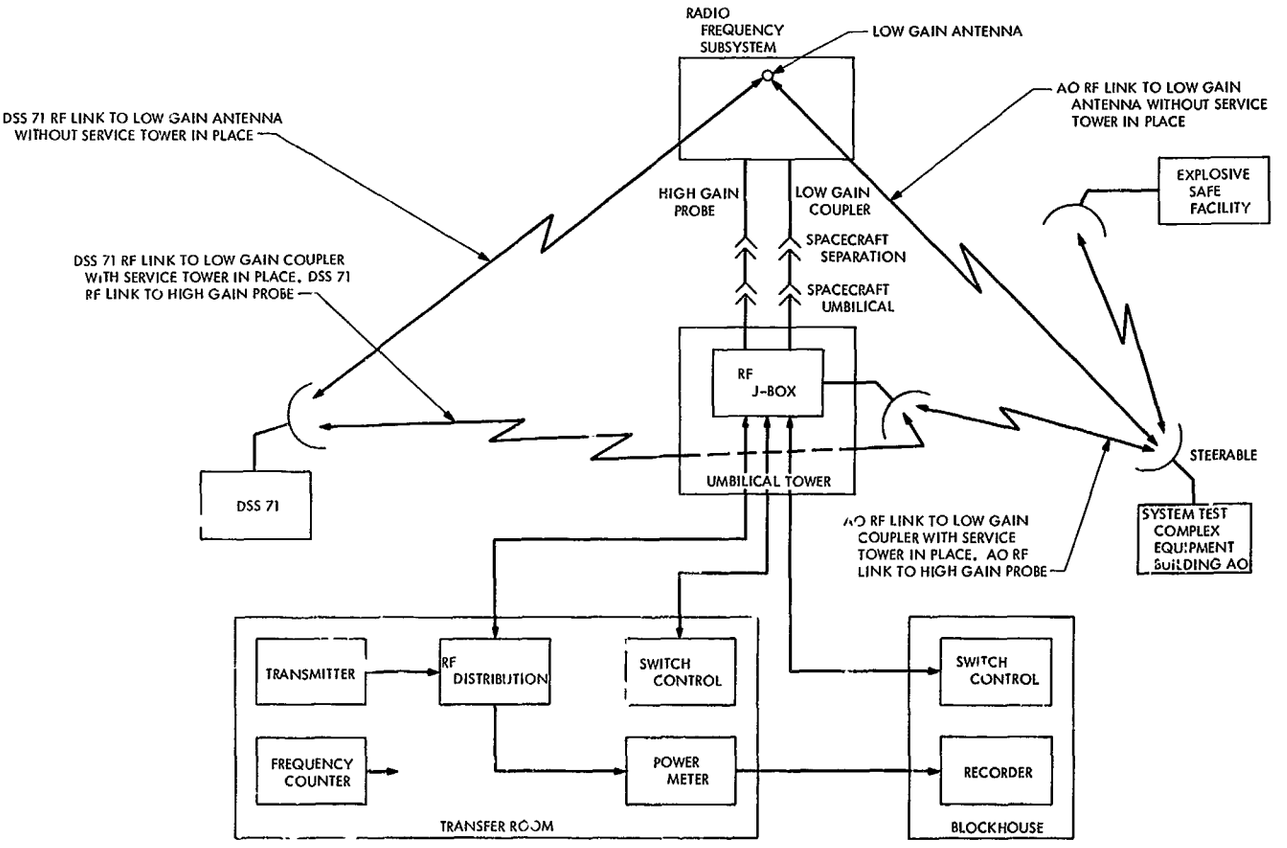


Fig. 2. Launch complex equipment

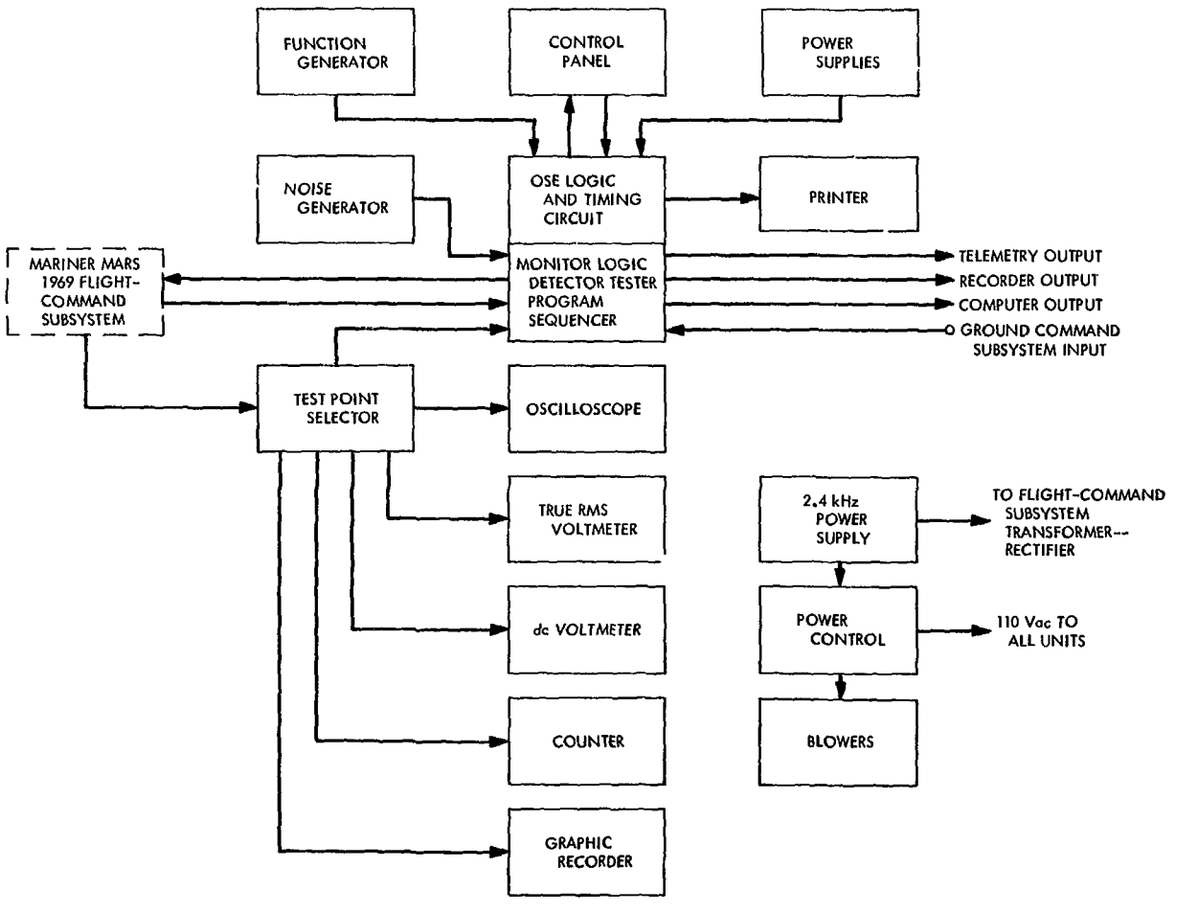


Fig. 3. Flight command subsystem operational support equipment

suitable for vibration excursions. Eight types of bench tests can be performed on the FCS:

(1) Tests of the decoder at normal bit rate with the detector connected.

(2) Tests of the decoder at four times the normal bit rate with the detector bypassed.

(3) Tests of the detector.

(4) Detector correlation.

(5) Detector bandwidth.

(6) Word start error.

(7) Bit error.

(8) Troubleshooting.

b. Data logging test. The flight command subsystem is plugged into the bench test fixture chassis or the functional element test drawer, which is connected to the data logging input of the auxiliary console. The prime purpose of the auxiliary console is to automatically measure five parameters of the FCS universal isolation switches. Data logging is controlled by a program sequence generated in the operational support equipment or in the data logger. Parameters measured in this configuration are (1) leakage current, (2) crest time, (3) rise time, (4) fall time, and (5) saturation voltage. The values of these parameters are printed on the digital recorder permitting non-real-time evaluation. Leakage-current and crest-time measurements are made with a minimum load, while the rise-time, fall-time, and saturation-voltage measurements are made with a maximum load.

c. Spacecraft assembly facility test. This mode is used for system testing of the flight command subsystem, except that the commands are generated by the operational support equipment instead of the read/write verify

(RWV) equipment. Since the OSE does not have a verify cycle, commands may be executed faster than with the RWV. Thus system test time can be greatly reduced.

3. Modification program. The basic FCS OSE built for *Mariner* Mars 1964 was subsequently modified for *Mariner* Venus 67 and further modified for *Mariner* Mars 1969. In general, the test philosophy developed for *Mariner* Mars 1964 support equipment remained the same for *Mariner* Mars 1969. Major improvements included the following:

(1) Replacement of obsolete or worn-out test equipment.

(2) Replacement of cordwood logic modules with integrated circuits.

(3) Rewiring of power distribution circuits, control panels, and test point selector panels.

(4) Logic changes to accommodate expansion of commands, command format changes, and improvement of displays.

4. Performance. Although the basic performance of the *Mariner* Mars 1969 FCS operational support equipment was satisfactory, the following two problems caused the most trouble:

(1) False error printouts from environmental transients. Although this problem was greatly reduced by shunting each signal input with a 0.01-μf capacitor, occasional false printouts still occurred during system testing.

(2) Excessive failures of the Motorola MC830P-series dual in-line plastic-encapsulated integrated circuits, partly from inadequate cooling. These failures were usually difficult to isolate because they tended to be intermittent.

C. Flight Telemetry Subsystem Operational Support Equipment

The flight telemetry subsystem operational support equipment provides subsystem and system test functions. Subsystem testing of the flight telemetry subsystem includes acceptance testing, type approval testing, and flight approval testing. To verify proper operation and environmental tolerance these tests are performed before the FTS is installed on the spacecraft. Once the FTS is onboard, the OSE then provides system test support by monitoring subsystem performance. In the system test configuration the FTS operational support equipment has an additional requirement of recording test complex signals for later analysis in the event of an anomalous spacecraft operation.

The equipment for subsystem tests and system tests is identical except for the rack, in the system test equipment, for recording the required signals. This rack, called the tape recorder/time console equipment, is housed in a two-bay console designated as the monitor and control console and is used as an interface with the FTS in either test function.

To perform subsystem testing, analog, digital, and command simulators are built into the OSE. The analog simulator contains 3-V, $\pm$1.5-V, and 100-mV regulated power supplies, voltage dividers, and source impedances. Pressure and temperature channels are simulated by the use of variable resistors. Each FTS analog channel is calibrated by varying the input voltage (or resistance) and noting the encoded pulse code modulated output data value. The digital data simulated is of two types: serial and parallel (event). The command simulator is used to exercise every operating mode of the flight telemetry subsystem.

The high-rate data generator and display is used to test the block-coded data channel. A 6-bit data word and its corresponding 32-bit block-coded word is generated. The 6-bit word is serially shifted into the FTS and the resulting block-coded word is compared with the operational support equipment generated block-coded word. A word-for-word comparison is made until an error is detected, then the erroneous blocked word from the FTS is displayed.

To verify proper operation of the support equipment operation a composite telemetry signal simulator is included in the equipment. This equipment generates a telemetry signal with the same characteristics as the signal received from the flight telemetry subsystem. Each detector and bit synchronized, as well as the decommutator, is operationally verified. Engineering and CC&S data are simulated by generating the high-rate deck data which is three words of PN synchronization and the index word followed by a selectable 7-bit word repeated 17 times. When CC&S data are transmitted, the PN synchronization is followed by the special CC&S index word followed by alternating *ones* and *zeros*. Science data is simulated by an alternating data stream of *ones* and

zeros. The high-rate data is simulated with a fixed (selectable by 32 switches) 32-bit word.

The design of the monitor and control console incorporated integrated circuits for all logic implementation and extensive use was made of linear integrated circuits in analog circuits. The *Mariner* Mars 1969 flight telemetry subsystem OSE was advanced over the *Mariner* Mars 1964 and the *Mariner* Venus 67 OSE, where discrete components were used throughout.

D. Data Storage Subsystem Operational Support Equipment

The purpose of the operational support equipment was to provide test and monitor support during subsystem and system level tests. During the subsystem level tests, the OSE supported the manufacturing and subsystem acceptance tests, providing control signals, reference signals, signal processing, power, and status signal monitoring capabilities. During system level tests, the OSE was used primarily for status signal monitoring. Figure 4 depicts the OSE as comprising eight functional blocks.

Ancillary test equipment consisted of commercial equipment required to support the main data storage subsystem tests and for subsystem–OSE interface tests performed during the initial manufacturing tests. The commercial equipment consisted of a counter, oscilloscope, oscillograph, digital voltmeter, discriminator, rms voltmeter, printer, and amplifiers.

1. Subsystem tests performed on the data storage subsystem.

a. Data storage subsystem test mode. In the data storage subsystem test mode, the OSE generates, monitors, and processes the signals required for the following subsystem test submodes:

(1) In the analog tape recorder record mode, the OSE generates a manually initiated control signal to activate the analog tape recorder record motor of the data storage subsystem. The OSE will generate a manually selectable continuous wave reference video signal for recording on a manually selected analog tape recorder track. An additional submode allows the generation of complex modulated carriers for recording on the analog tape recorder.

(2) In the analog tape recorder playback test mode, the OSE generates a manually initiated control signal to start/stop the recorder playback motor. Also in this test mode, the OSE clocks the digitized video signal for use in the data formatter. Output data from the recorder can be recorded in analog fashion on the oscillograph, or the digitized output can be recorded on the data formatter.

(3) In the digital tape recorder record test mode, the OSE generates a manually initiated control signal to start/stop the recorder record motor. The OSE also generates a manually selected repeating six-bit code that can be recorded on the digital tape recorder through the science data input. This digital data can also be derived from a pseudo-noise (PN) code generator in the OSE digital test section.

(4) In the digital tape recorder playback test mode, the OSE generates a manually initiated control signal to start/stop the recorder playback motor and monitors the recorder playback signal. A bit error test is performed on the serial data as it is received from the data storage subsystem. The OSE will lock onto a special sync word recorded on the digital tape recorder during the *record* mode. After it has locked onto the sync word, the OSE digital test section compares each received bit against a reference bit that has been regenerated by the OSE during the in-sync condition. If a bit error is detected, the OSE printer will print out the received and simulated data in an octal code.

b. Digital tape recorder test mode. The digital tape recorder test mode is a special mode for testing a digital tape transport external to the data storage subsystem. A digital tape recorder/analog tape recorder interface test box containing special record amplifiers necessary for interfacing the digital recorder to the OSE is used. Since the digital recorder is separate from the subsystem in this test mode, the test operation is concerned with just those parameters pertaining to the digital recorder performance. For problems in the performance of the digital tape recorder, this test mode is used as a diagnostic tool.

c. Analog tape recorder test mode. The analog tape recorder test mode is similar to the digital recorder test mode and uses the same interface test box. Analog input signals to the analog recorder are generated and controlled by the OSE as if the analog recorder were an integrated part of the data storage subsystem. Since the subsystem analog-to-digital converter is not used during the analog recorder test, the recorder test mode does not

provide for testing with the data formatter but is used only when analog recorder problems need to be diagnosed in a configuration separate from the data storage subsystem.

2. Self-test mode. In the operational support equipment self-test mode, the digital test section is tested functionally and operationally. The digital test section functional block, such as the input register, frame counters, word counter, word rate clock generator, and other clock signals are operationally tested in an automatic or manual test condition. The bit error check logic, error buffer logic, and printer are tested during this mode.

3. Configuration. The operational support equipment was used in two test configurations, lab and environmental testing with the data storage subsystem only, and operational testing with the spacecraft. The test requirements for these two configurations were different and required modifications to the respective OSE units assigned to support these two activities. The OSE sets, as delivered by the contractor, were identical. It was found that the set to support subsystem testing could be made more versatile with some moderate modifications. Accordingly, modifications were made to increase the signal recording capability of the oscillograph and to permanently connect some monitored signals to the oscillograph, and the flutter measurement was improved by a dc response, programmable FM discriminator.

The OSE used for spacecraft testing did not monitor as many signals, or perform detailed subsystem tests in the Spacecraft Assembly Facility, so these units were not used to their capability. However, some modifications were necessary for the facility OSE to provide for interfacing some signals with other OSE units in the test complex, which were not originally planned.

E. Central Computer and Sequencer Subsystem Operational Support Equipment

This section describes the evolution, functions, and design characteristics of the operational support equipment that was developed to support testing of the *Mariner* Mars 1969 central computer and sequencer. Included also are the CC&S system test and launch operations activity for *Mariner* Mars 1969, and other associated information.

1. Design evolution. The *Mariner* Mars 1964 CC&S operational support equipment, which was later modified for use in the *Mariner* Venus 67 project, was designed as special purpose equipment to test a fixed-sequencer type of CC&S. A single test set design was used for testing the CC&S in all test locations (laboratory testing, system testing, or launch operations). Laboratory testing of the CC&S required that the OSE be able to automatically stimulate and monitor the fixed sequence of the CC&S. Because the fixed CC&S sequence is hard-wired, the OSE automatic sequence is also fixed and hard-wired.

The *Mariner* 66 CC&S OSE employed a punched paper tape as a source of instructions for automatically controlling and monitoring the CC&S. The tape control concept proved to have significant advantages over previous designs because of the relative ease of changing automatic test sequences and the elimination of human errors in monitoring CC&S performance.

The *Mariner* Mars 1969 CC&S OSE design used the *Mariner* 1966 design as a starting point, and incorporated features peculiar to the *Mariner* Mars 1969 design, as well as design refinements based on *Mariner* 1966 OSE history.

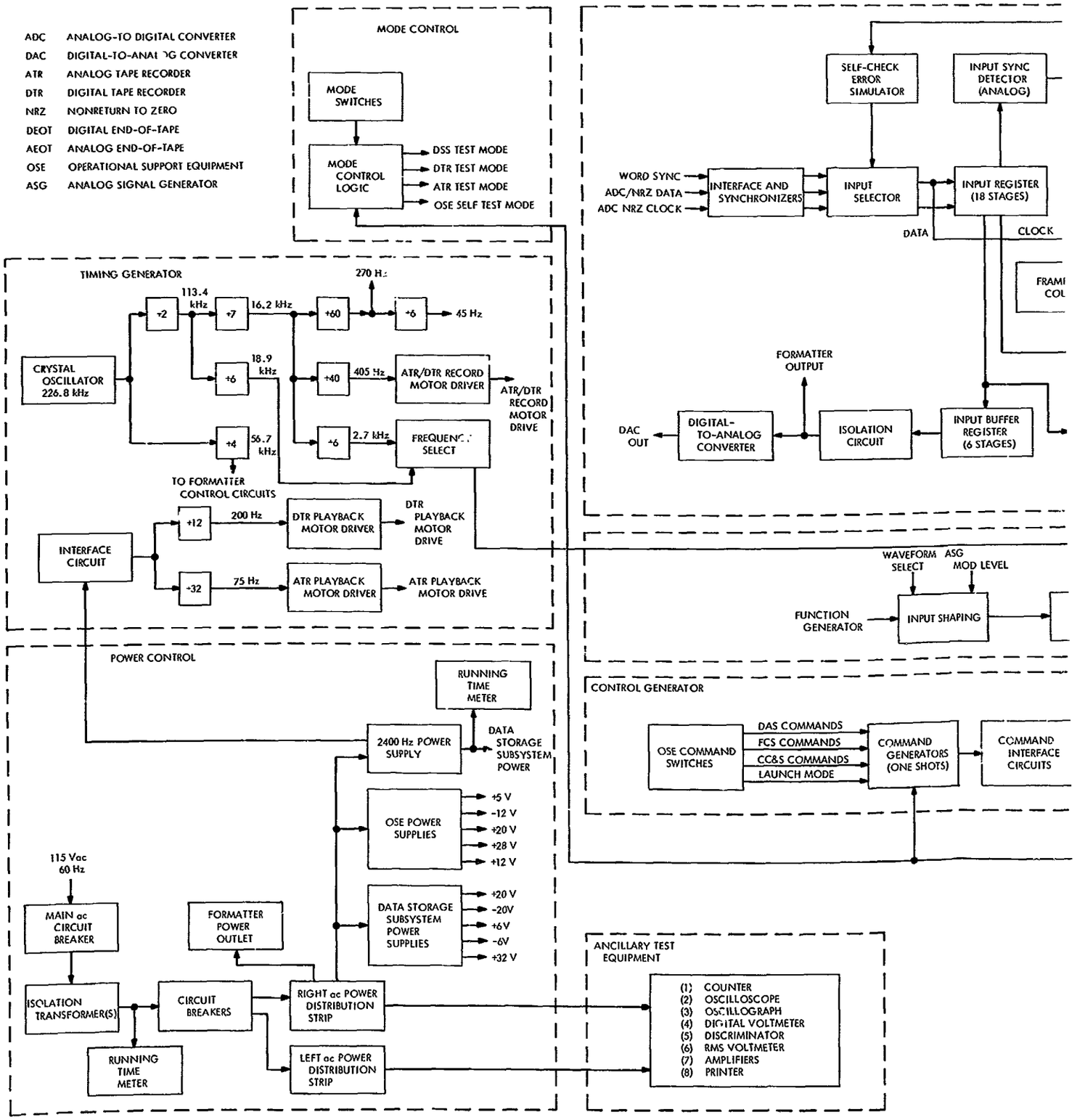
To verify the OSE concepts, a developmental model of the OSE was fabricated and tested. Subsequently a contract was awarded to manufacture six sets of OSE, including a prototype. The first set of OSE (prototype) was delivered to JPL on May 15, 1967, and was used for laboratory testing of the *Mariner* Mars 1969 prototype CC&S.

2. Functional description.

A functional diagram of the 1969 OSE is shown in Fig. 5.

a. Central computer and sequencer tests. The CC&S OSE performs tests necessary to assure a functionally qualified CC&S. The system test set has the capability of testing the CC&S in the laboratory, at the spacecraft assembly area, and at the launch site.

Subsystem test (laboratory). When testing at the subsystem level, the OSE provides the CC&S with power and commands normally supplied by other spacecraft subsystems. All CC&S functions can be manually operated by OSE front panel controls, and the CC&S events and outputs are monitored by OSE front panel indicators.



FOLDOUT FRAME

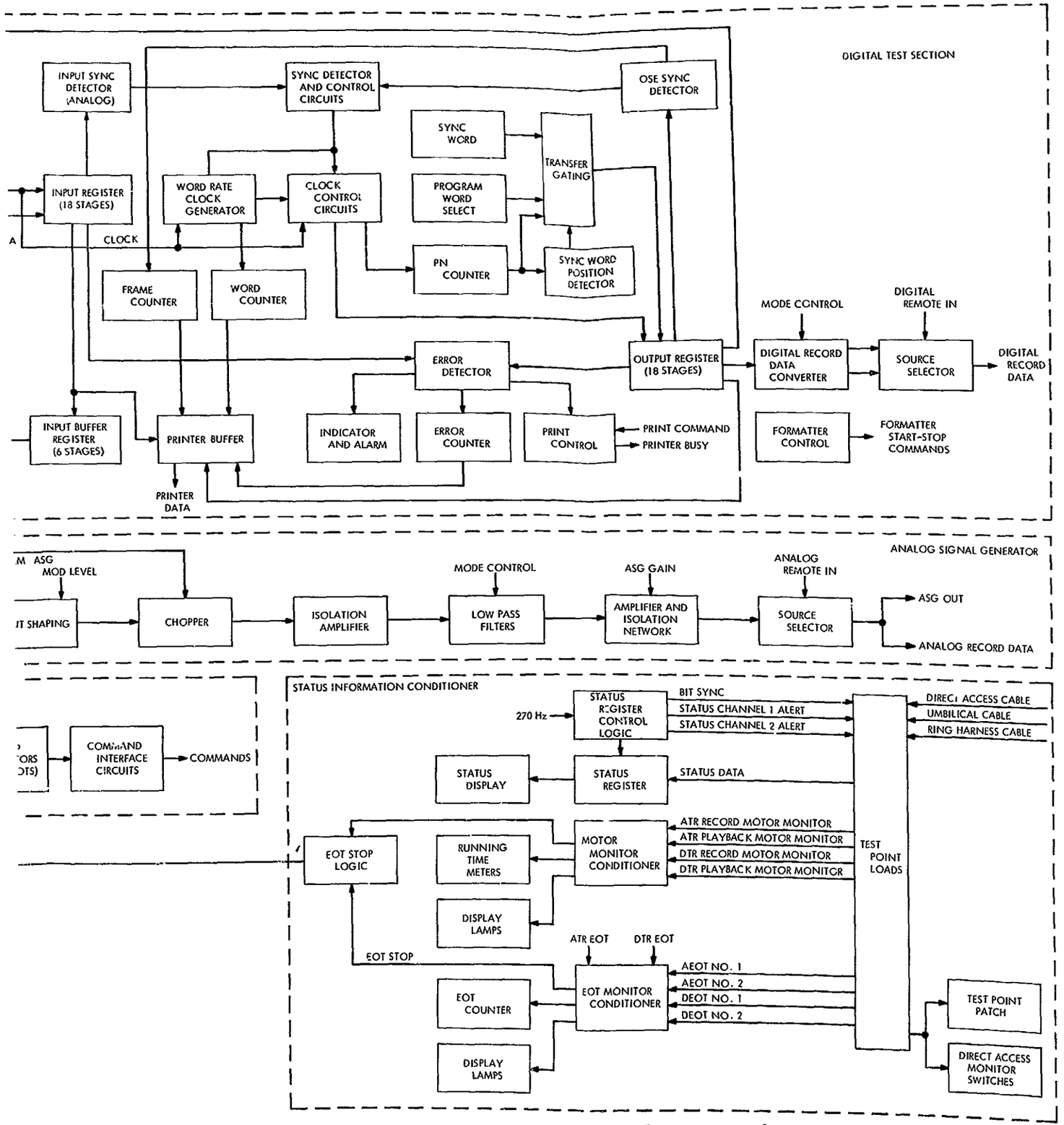


Fig. 4. Data storage subsystem operational support equipment

FOLDOUT FRAME

PRECEDING PAGE BLANK NOT FILMED

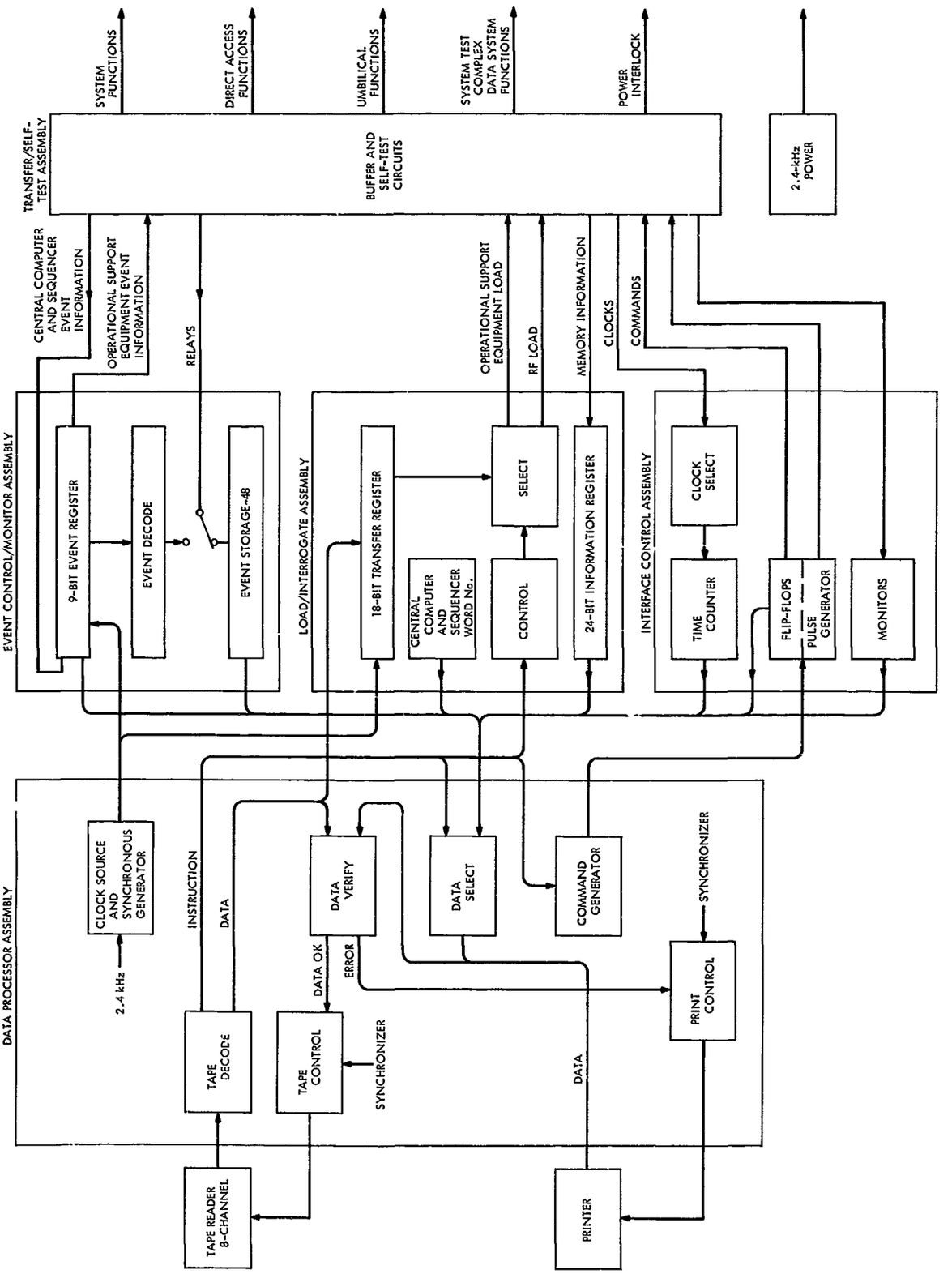


Fig. 5. Central computer and sequencer operational support equipment

To reduce operator effort, test time, and the possibility of human error, an automatic checkout test mode is also provided. The commands and information necessary to stimulate and to monitor the CC&S through a test sequence are programmed on a punched paper tape. If an error in the operation occurs a printer prints a paper record of the CC&S time and the status of the CC&S output lines at this time. The OSE printer can also be operated in a mode where all changes of state on CC&S output lines are recorded.

To test the CC&S operational sequence completely, the OSE also tests the CC&S launch sequence during subsystem testing. Thus, the OSE is able to test the CC&S subsystem in all operating modes.

b. System test. During system test, the OSE basically performs two functions:

(1) Loads the CC&S stored program, and interrogates the CC&S to verify that no loading error has occurred.

(2) Performs a monitoring function. The CC&S is cabled into the spacecraft system and the OSE is connected to it by the direct access and umbilical connectors. The CC&S power is provided by the spacecraft, and commands to the CC&S are sent through the spacecraft command subsystem. The OSE, however, is capable of controlling the CC&S relays by means of the direct access connections.

To decrease test time, controls are provided from the OSE to speed up the CC&S clocks by a factor of 20. A preset counter in the OSE is used to control the duration of each speed-up cycle. An interlock to the power subsystem is provided so that certain initial conditions in the CC&S must be satisfied before power can be applied to the spacecraft.

c. Launch operations. During the countdown sequence at the launch complex, a simplified system test set is used to test and prepare the CC&S for launch. The simplified OSE performs the following functions:

(1) Loads the CC&S stored program, and interrogates the CC&S to verify that no loading errors or memory transients have occurred.

(2) Electrically holds all CC&S relays in the reset or safe position.

(3) Inhibits CC&S counter operation.

(4) Clears CC&S counters.

(5) After the application of spacecraft power and the release of inhibit, provides a go/no-go lamp indicating that the CC&S is operating properly.

(6) Provides CC&S program update status with OSE panel indicators.

d. Self-test. An OSE self-test assembly is provided as an integral part of the OSE to verify that the test set is functioning correctly. In the self-test mode, a control switch in the transfer assembly switches the interface lines from the CC&S to the OSE self-test assembly, permitting the self-test to be performed without physically disconnecting the CC&S from the OSE.

3. System test and launch operations. The *Mariner* Mars 1969 CC&S system test and launch operations team consisted of two data analysts and three OSE operators, one analyst and two operators from the manufacturer, and the others from JPL. The test and launch procedures were different from the *Mariner* Mars 1964 and *Mariner* Venus 67 in that the CC&S was now a memory-oriented computer type of machine and quite flexible. Test programs (tapes) had to be generated to test the spacecraft through various flight sequences. Before launch, a complete flight program had to be loaded into the CC&S memory from the OSE and verified, although inflight program changes are possible.

Test tapes were generated from two sources: (1) system test tapes and other special tapes made with the IBM 1620 and with a specially procured tally corporation tape punch machine; and (2) launch and launch test tapes generated by the program COMGEN. Several significant problems were encountered during system test and launch operations, mostly in the CC&S memory load/verify mechanism:

(1) During the early phases of testing at the spacecraft assembly area, considerable numbers of CC&S memory load/verify errors were experienced. The problem was finally traced to the sync input buffer in the CC&S; however, in order to further improve and protect the interface, a conditioning circuit for the sync signal was installed in the umbilical junction box.

(2) OSE tape reader failed on two occasions with a broken clutch assembly. Experience with the tape reader indicated that factory preventive maintenance should be performed regularly.

(3) During launch complex testing at the AFETR with the M69-4 spacecraft, a number of CC&S memory load/verify errors again appeared. Extensive investigation revealed a design deficiency in the OSE tape reader mechanization. Dry circuit operation and contact bounce was discovered as the cause of the problem. Modifications were made to filter the contact bounce and increase contact operating current. Why this problem did not appear sooner can only be explained by the change in environment (blockhouse) where some contaminate in the air affected the tape reader contacts and its operation.

(4) During final preparation for the *Mariner G* launch, several more memory load/verify errors appeared that could not be explained or localized to the flight equipment or to the OSE. The CC&S was therefore removed and replaced with the spare unit.

(5) During *Mariner F* prelaunch activities an integrated circuit component failure caused extraneous illumination of OSE indicators. Analysis by the parts failure group revealed an excessive amount of intermetallic interaction ("purple plague") caused component failure.

F. Attitude Control and Scan Control Operational Support Equipment

During the course of the *Mariner* Mars 1969 program a large variety of support equipment was designed and built to test the attitude control and scan control flight equipment. This equipment can be separated into two distinct groups: (1) laboratory or subsystem level test equipment, and (2) spacecraft of system-level test equipment. The system-level test set (STS) and the launch control equipment are described and explained in the following paragraphs. The attitude control and scan test set consists of three 6-ft standard 19-in. racks of equipment plus peripheral hardware interconnected through junction boxes and cables (Figs. 6 and 7). The launch control equipment contained three chassis identical to

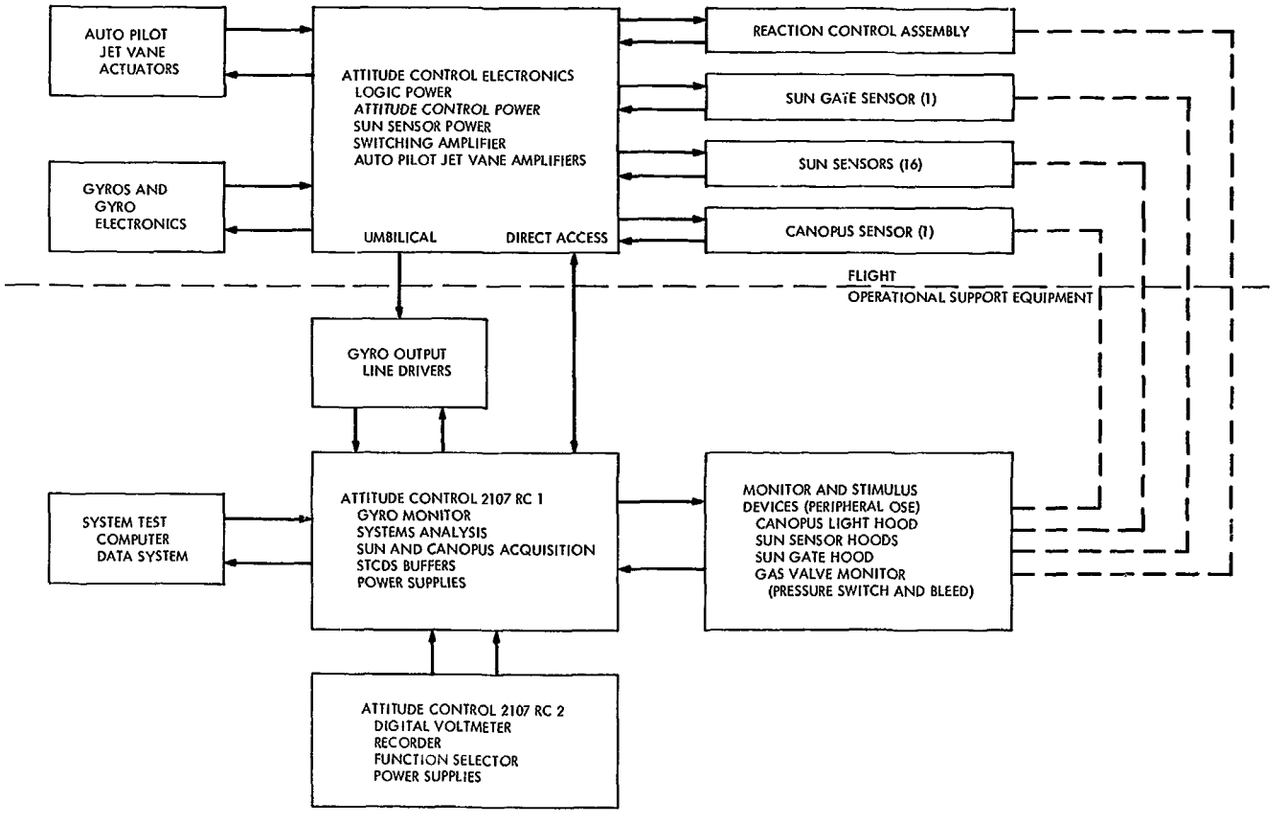


Fig. 6. Flight/test equipment interface: attitude control subsystem

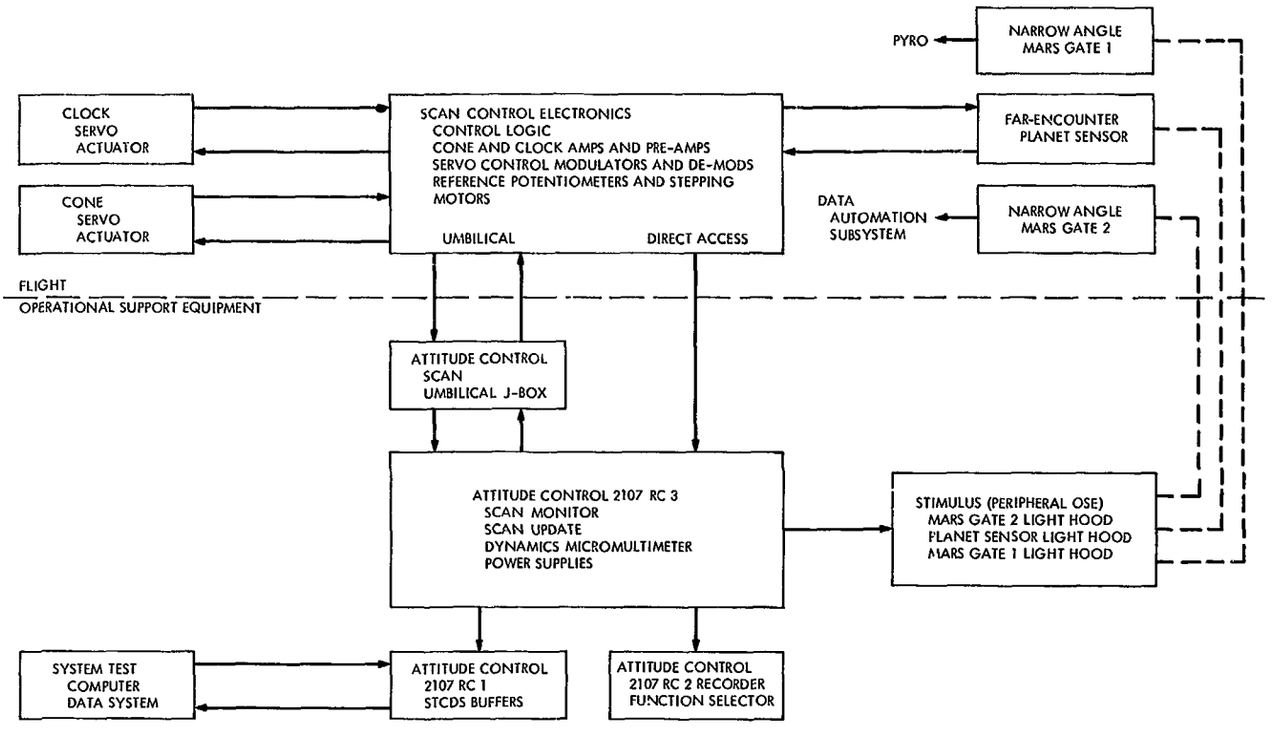


Fig. 7. Flight/test equipment interface: scan subsystem

units located in the system test set but installed in the block house racks along with power and the CC&S.

Individual pieces of equipment were used to fill and test the reaction control assembly (gas system) such as Lo-Boy (nitrogen gas booster pump), portable gas charging system, calibration gauges, leak test consoles, dew point measurement units, and the pneumatic control console (used only at the AFETR).

1. Functional description.

a. Systems test set. The systems test set consisted mainly of three 6-ft racks that were placed side-by-side in the system test complex. The controls and test points necessary to check out the attitude control and scan flight equipment in a system environment were located within these racks and included access points for applying stimuli and monitoring the gyros, the autopilot jet vanes, gas jet activity, recycling characteristics of the gyro position capacitors, derived rate performance, and sensor (sun sensors, sun gate, Canopus sensor, far-encounter planet sensor), and narrow angle Mars gates (NAMG-1,2), characteristics. Also included in the system test set was provision for self-testing.

b. Auxiliary equipment. Several pieces of auxiliary equipment were built to support the test program, which were not part of the daily system test routine but were occasionally required. These included dummy load boxes, actuator drive box, and Mars simulator.

c. Mars simulator. Midway through the test program it was decided to verify that the far-encounter planet sensor/scan platform combination could track a moving object of planet size and brightness. The Mars simulator, as shown in Fig. 8, was built to accomplish this verification. A bank of lights behind a translucent screen inside the box provide a uniformly illuminated source. The iris on the front of the box was adjustable for diameter and the center of the iris could be moved outward from the center of rotation. Therefore, the size of the simulated planet, amount of circular movement, speed of movement, and simulated brightness were all variable. This box was backed up by a heavy-duty power supply for the light bank, another supply for the drive motor, and an eight-channel recorder.

2. Launch complex equipment.

The attitude complex and scan part of the launch control equipment consisted

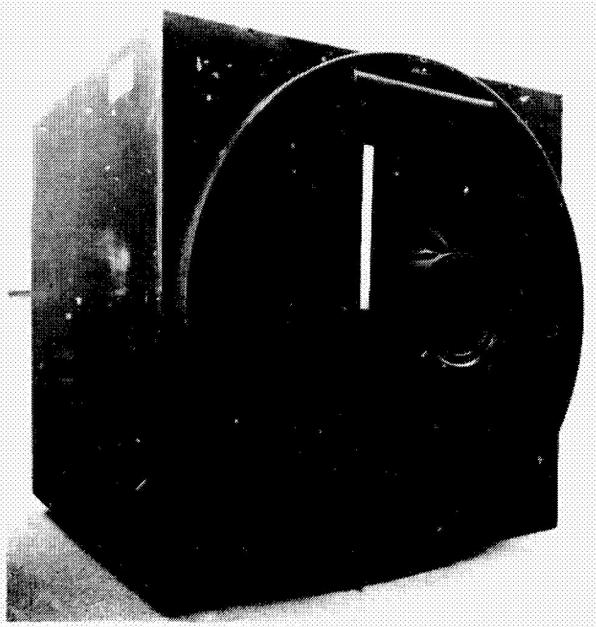


Fig. 8. Mars simulator

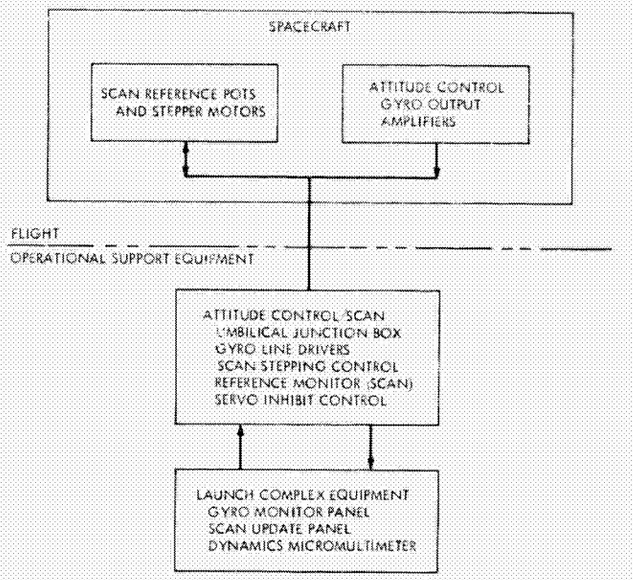


Fig. 9. Flight/launch complex equipment interface: attitude control and scan subsystem

of three panels identical to units located in the systems test set. A fourth unit, attitude control and scan umbilical J-box, was installed in the umbilical tower junction box located near the top of the umbilical tower. The configuration of the launch control equipment and the spacecraft is shown in Fig. 9.

At the AFETR a pseudo launch control equipment (LCE) was set up in a trailer just outside the spacecraft assembly building in the explosive safe facility with the purpose of providing launch complex capability to turn on the spacecraft and perform a complete pre-countdown procedure. This setup was also used at Pasadena in the vibration test.

The attitude control and Scan equipment in the pseudo LCE was the same type of equipment discussed in the section on launch complex equipment. At Pasadena the panels were actual LCE-built panels but at the AFETR the panels were taken out of a system test set and installed in the pseudo LCE.

One extra panel was designed and built for the pseudo LCE at the AFETR that provided the stimulus and control circuitry to turn on the autopilot and excite the jet vane amplifiers through direct access. That test was performed after the final installation of the midcourse motor and jet vane ring.

3. Production and test history. The basic design of the present attitude control OSE was begun on the *Mariner* Mars 1964 program. Three system test sets were built, two racks plus peripheral equipment each. Two of the three sets were modified (20%) to support the *Mariner* Venus 67 program. The peripheral equipment changed very little except for a newly designed Canopus hood.

For the *Mariner* Mars 1969 test program some major changes were required. The two sets of *Mariner* Venus 67 OSE and the one *Mariner* Mars 1964 set were extensively modified (70%) and a new rack was required to support the scan system, as well as new laboratory test sets and launch complex sets. The contract to accomplish the task was awarded and design of the new equipment and drawing changes for modification was performed at JPL by the contract engineers. One system test set and one attitude and control and one scan laboratory test set were built at JPL. The remainder of the hardware the optical part (sun sensor hoods, Canopus hoods, etc.) was built at the contractor's facility. The Canopus hood used on *Mariner* Venus 67 was modified for *Mariner* Mars 1969. The sun sensor hoods and sun gate hoods were manufactured new because of dimensional changes but remained similar in appearance to the *Mariners* Venus 67 and Mars 1964 configurations. Slight modification to the nitrogen gas handling and leak test equipment, and acquisition of certain *Surveyor* program equipment for

gas handling, was performed in-house by the OSE cognizant engineer.

The first system test set was delivered to the spacecraft assembly facility in February 1968. The other two system test set assemblies were delivered later. The M69-1 spacecraft was the first one to be checked with the system test set. When the 69-1 spacecraft was moved to the space simulator the system test set was moved to the same building where it remained to support the other *Mariner* 1969 spacecraft space simulator testing. Soon there were three system test complexes in operation, two at the spacecraft assembly facility and one at the environmental test laboratory. To support the M69-1 in the vibration test, the pseudo LCE was set up in the building near the vibration fixture. Chassis from the system test set were used for the attitude control and scan portion. The pseudo LCE was later replaced by one of the actual LCE assemblies. The pseudo LCE accompanied the M69-1 through the audio noise test, and the pyro shock test.

The system test set near the space simulator was the first to be moved to the AFETR where it was set up in a system test complex in building AO. This complex was mostly concerned with testing in the adjoining high-bay but the ground telemetry, ground command, and radio frequency gear were used as backup on pad testing. Another complex was set up to support testing at the explosive safe facility and the launch pad. The OSE on this complex consisted of the radio frequency, the ground command, and the ground telemetry racks plus the computer data input system. The two sets of LCE assemblies were installed at the launch complex-36 block house and the pseudo LCE was in a trailer in the explosive safe facility. At that time, one system test set was still in Pasadena for M69-1 support, one at the AFETR on the system test complex, and one at the AFETR with certain chassis installed in the pseudo launch complex equipment.

4. Test and developmental problems. In the *Mariner* Mars 1969 test program four problems stood out in the OSE test history and development. First, the Zeltex amplifiers, both in the attitude control and scan umbilical J-box and the system test set, exhibited erratic behavior not verified in the laboratory. The suspected cause was wear on the thin gold plating on the connector pins exposed metal that corroded and turned black. The result was a poor connection combined with very low current (dry circuit) levels. The amplifiers in the attitude control and scan umbilical J-box were modified and hardwired into the box harness to eliminate the connector.

Second, the computer interface to the low-speed analog unit was never successfully obtained. Running long lines of analog signals, insufficient isolation, and lack of spacecraft test time all combined to spell doom for the low-speed analog unit. The equipment was removed from the test complex about two-thirds of the way through the test program.

Third, three returns were brought back to the system test system. One was the scan return, one was the attitude control return, and another was the gyro return. These returns should have been isolated by at least two to three megohms but instead were down to 50 k to 100 kΩ because the buffer amplifiers were all powered by the same two power supplies. There should have been a set of amplifiers/power supplies for scan, a set for the attitude control direct access signals, and another set for the gyro signals.

Fourth, a design change in the sun gate resulted in a drop in sensitivity. The sun gate stimulus originally provided was then not bright enough to be able to achieve a sun acquisition with either cell but only with both cells illuminated. A new hood was designed consisting of two quartz iodine lamps and collimating lenses. The heat problems, both in free air and in the vacuum chamber, took a long time to solve and the new design was never used on the *Mariner* Mars 1969 test program.

A few minor problems were encountered and corrected as follows:

(1) The attitude control J-boxes were units that were modified from the *Mariner* Venus 67 program and contained many wires now labeled *spare*. One of these wires caused an extra return to the system test set, which effectively tied the 28-V supply to the 30-V supply when a stimulus push button was activated. A engineering change request was generated to remove all spare wires from the J-box.

(2) Another problem with the J-box resulted when the pressure switch return was incorrectly used for the sun gate stimulus return. A wire in the cable for sun gate stimulus return and a jumper wire in the J-box was moved by change request.

(3) One of the three J-boxes was miswired on the acquisition sun sensor stimulus, resulting in transposition of certain pitch and yaw stimuli. The box was reworked per print.

(4) An interference problem came to light when the spacecraft was installed in the space simulator. The connector on one of the acquisition sun sensor hoods interfered with the stimulus of the ultraviolet spectrometer with the platform in the stowed position. A change request was initiated to turn the connector on the sun sensor hood to provide the necessary clearance.

(5) Because of the high input impedance of the amplifiers in the attitude and control and scan umbilical J-box, some capacitors were added to reject pickup noise.

(6) When one of the amplifiers in the attitude control and scan umbilical J-box failed (not reproduced in the Laboratory) during a space simulator test, the data indicated that it fed voltage back into the gyro monitor line and caused gas jets to actuate. A modification was made to the J-box to add resistors in the feedback and input lines so that if the amplifier were to saturate, the resistors would limit current flow back to the spacecraft.

G. Power Subsystem Operational Support Equipment

The power operational support equipment was developed to test the *Mariner* Mars 1969 flight power subsystem (FPS) when in the case I and case VIII configurations in the laboratory, at the spacecraft assembly facility, and at the AFETR. The power support equipment was originally fabricated for similar testing of the *Mariner* Mars 1964 flight power subsystem, modified to test the *Mariner* Venus 67 flight power subsystem, and subsequently modified to test the *Mariner* Mars 1969 flight power subsystem. This section describes the evolution, design changes, and equipment of the *Mariner* Mars 1969 power OSE.

1. Design evolution. The OSE was designed and newly fabricated to test the *Mariner* Mars 1964 flight power subsystem, which consisted of the power conditioning equipment (cases I and VIII) and the battery. The support equipment was designed in three configurations: (1) the laboratory test set, (2) the system test set, and (3) the launch complex set.

The laboratory test set is made up of a system test set plus a laboratory adapter rack and was designed to power, control, and monitor the power-conditioning equipment when assembled in its two cases and operating either separately or together.

The system test set and each assembly was designed to provide the necessary power, control, and monitoring functions to support the flight power subsystem during spacecraft test operations at the spacecraft assembly facility for initial power application, power subsystem evaluation, and spacecraft system testing. It was also used as part of the laboratory test set at the spacecraft environmental test facility.

The launch complex set was designed to provide the power, control, and monitoring required during launch operations. The launch complex set consisted of a control panel assembly within the blockhouse, a rack of equipment in the launch pad area, and the ac–dc conditioner mounted in a junction box in the umbilical tower.

The support equipment was modified for *Mariner* Venus 67 and again for *Mariner* Mars 1969. Fund limitations permitted only about 60% of the proposed changes for updating and improving the power OSE. Briefly, these changes or improvements included the following:

(1) Changing Zener diodes in over-voltage protection circuits to the *Mariner* Mars 1969 voltage levels.

(2) Replacing the tolerance detectors and their power supplies for the booster regulators with those having a 60 Vdc maximum sensing level.

(3) Adding several inhibit and interlock circuits to prevent improper and unsafe power subsystem operation.

(4) Adding circuit cards for the 4A17 inverter monitor.

(5) Connecting the A and B portions of the dual power-source/simulator assembly in parallel with diodes.

(6) Adding a 2.4 kHz buffer amplifier in the ac-dc conditioner assembly.

(7) Adding system test computer data system (STCDS) buffer amplifiers and signal conditioning circuits.

(8) Adding a power-synchronization free-run test command circuit, a sun-gate command circuit, and a battery charger test command circuit in the test monitor assembly. Modifying the booster regulator sensing test command circuits the power distribution test command circuits, and replacing the dummy load resistors where required in the test monitor assembly.

(9) Dividing the control panel of the laboratory adapter control into separate control assemblies for cases I and VIII, changing the adapter control display lights from ac to dc power, replacing all laboratory test setup external cables, and adding circuits and test equipment to test the synchronizer oscillator.

(10) Modifying the flight power subsystem simulator equipment rack to *Mariner* Mars 1969 operational support equipment requirements.

(11) Modifying the solar panel simulator supplies (dual power-source/simulator assembly) and the solar panel substitution J-boxes for the six-section *Mariner* Mars 1969 solar panel configuration.

(12) Increasing the voltage capability of the kinetic switch power supply.

2. Design changes. Though many design changes and improvements were made to the OSE, generally, they required only moderate modifications. Most of the changes were required by changes in load levels and voltage levels, addition or deletion of command circuits and monitoring circuits, requirements for more accurate measurements and better buffer amplifiers, and replacement of worn or obsolete equipment. More extensive changes were made in the laboratory adapter rack and the flight power subsystem simulator.

Two typical support equipment changes that indicate the complexity of the changes were the addition of a frequency counter in the system test set to measure the power synchronizer oscillator frequency, and the paralleling of support equipment power supplies to increase the capability for supplying adequate power to the flight power subsystem.

The relocation of the spacecraft frequency synchronization oscillator from the *Mariner* Venus 67 CC&S

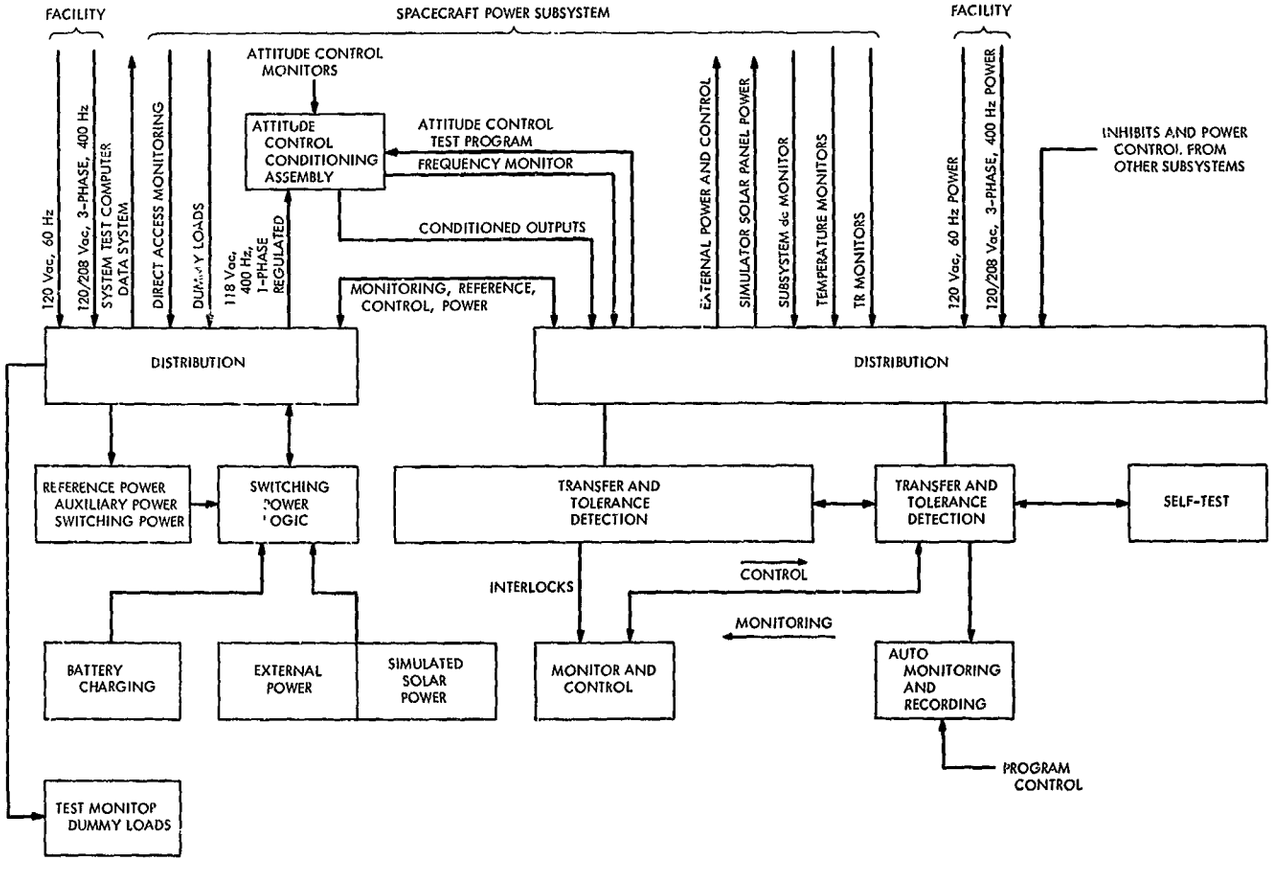


Fig. 10. Power operational support equipment: system test

subsystem to the *Mariner* Mars 1969 power subsystem shifted the requirement for the measurement of this frequency from the CC&S support equipment to the power support equipment. This was accomplished with the addition of the digital counter in the power support equipment system test set and the interconnections and modifications of all control and test circuits related to the measurements.

The kinetic switch, used to switch the spacecraft from external to internal power, is a make-before-break-type switch that briefly connects the battery and the spacecraft power switch and logic output in parallel. Current limiting was encountered in the external power supply when spacecraft power was switched from internal (battery) to external power. The power switch and logic output voltage dropped from 25 to 19 V for 0.3 s before going to 40 V because of this limiting, and showed an out-of-tolerance condition during the 0.3-s interval. By connecting a second power supply in parallel through diodes with the existing supply this condition was corrected and the OSE supply capability was increased from 12 to 24 A. Procedural changes were also made for a smooth power switchover from internal to external power.

The design modifications just discussed have only slightly changed the external appearance and functional operation of the support equipment. Functional block diagrams of the system test set and the launch complex set are shown in Figs. 10 and 11, respectively.

3. *System testing and launch operations.*

a. Pasadena operations. The test sequence at Pasadena was divided into two phases: five months of design qualification testing of the proof test model spacecraft, followed by five months of flight acceptance testing of spacecraft M69-2, -3, and -4. System test complex 1 was used at the 10-ft space simulator; system test complexes 2 and 3 and launch complex set 1 were located in the spacecraft assembly facility. Launch complex set 2 was located in the environmental laboratory.

b. Air Force Eastern Test Range operations. Test operations at the AFETR were reduced to a three-month period as a result of extending the space simulator testing at Pasadena from 400 h to 500 h for the flight spacecraft. Two test teams checked out the flight spacecraft during

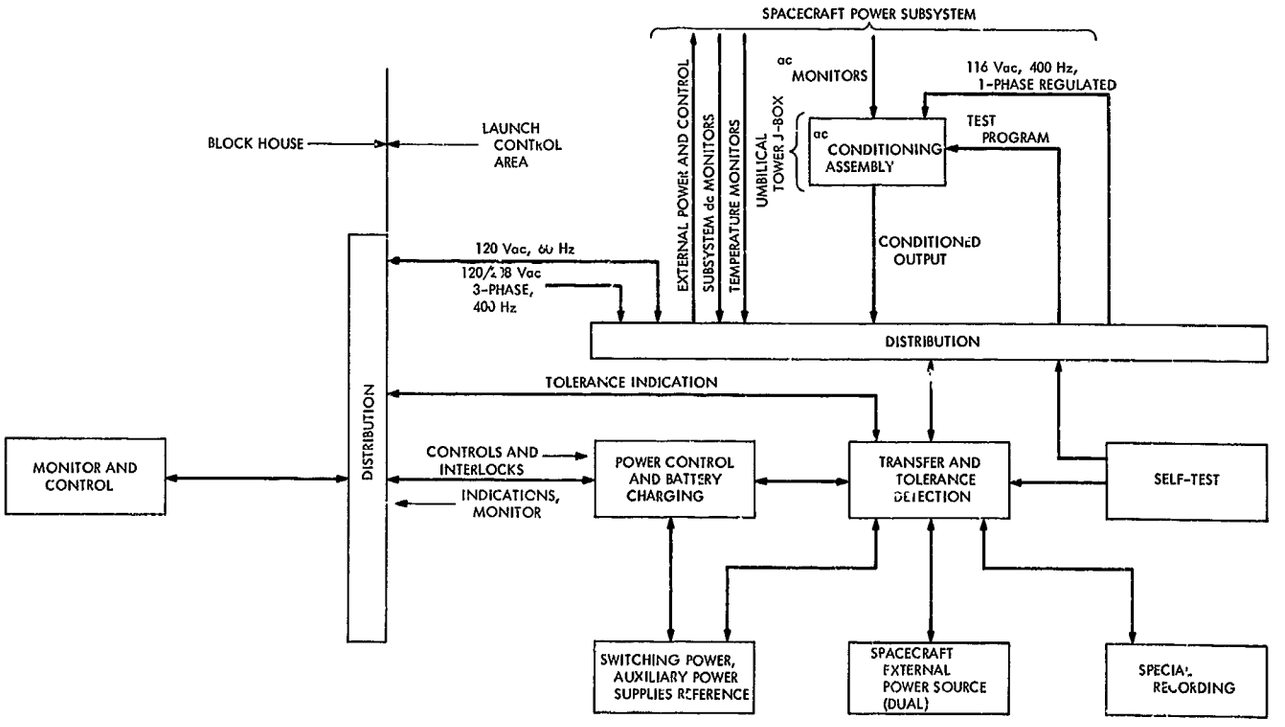


Fig. 11. Power operational support equipment: launch complex

this period. An additional test team was required during the first month's operations to support checkout of launch pad 36A and 36B with the flight spare spacecraft.

Two system test complexes were used at the AFETR; one remained at Pasadena to support problem investigation with the proof test model spacecraft.

c. Summary of major problems. Operating the external power supply extremely close to its current limit resulted in periodic cases of limiting. Once the primary system voltage momentarily dropped to 19 V during transfer from internal battery power (27 V) to external power (40 V). Limiting was due to the supply picking up the spacecraft load, charging the booster/regulator filter capacitors, and attempting to charge the battery during the make-before-break part of kinetics switch transfer. The transient condition was readily duplicated in the laboratory by using breadboard subassemblies.

In other instances, when transferring from internal to external power at very high power levels, limiting occurred from which the power supply was unable to recover. This mode of operation invariably resulted in automatic switching to the standby power chain, where the limiting continued. A change request was generated to add the necessary circuitry for providing dual power supply capability, thus doubling the current capacity of the ground power supply.

The umbilical lines checker was designed without provision for simulating the spacecraft load on the external power supply. This problem was circumvented by providing a 10-Ω load resistor which connected into the system at the power OSE. The physical separation of the load resistor from the umbilical lines checker resulted in turning on M69-2 at a very low voltage, however. This was caused by applying power to the spacecraft after the lines checker removal but with the load resistor still in the circuit. The resistor was effectively in series with the external supply lines, resulting in 11 V at the booster/regulator input, 14 V below specification. The output of the 2.4 kHz inverter was estimated as reduced by 70% in amplitude with frequency variations as low as 600 Hz.

All subsystems subjected to the degraded inverter output were analyzed for possible overstressing of components. A complete analysis of the power subsystem reaction to an 11-V input was performed. No instance of component overstress was indicated by analyses.

H. Temperature Control Flux Monitor Subsystem Operational Support Equipment

The primary function of the temperature control flux monitor (TCFM) operational support equipment was to support subsystem and system testing of the TCFM flight equipment. Four OSE test sets were constructed. Three of the test sets were designed specifically for system-level testing; the fourth set specifically for laboratory subsystem testing. The criteria used for the design of the system level test sets were (1) to provide for monitoring the TCFM outputs, and (2) to provide the ability to distinguish, in the event of abnormal TCFM operation, whether such operation is in the flux monitor or in interfacing subsystems.

The primary function of the subsystem OSE is to monitor and record the cone power, control loop error of the cone-guard servo, and the guard set point temperature. A number of ancillary functions are also performed that include (1) 2.4 kHz, 50 VRMS power supply, (2) a controlled source of visible radiation, (3) external heater power to an adaptive transducer cover for operation in air, (4) a safety interlock to ensure reduced temperature operation in air.

Figure 12 is a functional block diagram of subsystem test OSE. As shown, cone power and loop error can be monitored in two ways. The primary method is the direct access interface which receives the data in a fourteen-bit shift register each time the flux monitor updates (every 213 ms), or at 2^N ($N = 0$ to 9) multiples of each update as determined by the interval control setting.

The second method is through the telemetry interrogate circuits. These circuits duplicate the flight telemetry subsystem interface in that they simulate the flight telemetry subsystem bit sync pulses alert pulses. This function is used mainly to ensure the proper operation of the TCFM telemetry interface. The data rate of telemetry interrogate function can be controlled at 8⅓ bits/s and 33⅓ bits/s.

The measurement of guard temperature can be accomplished also by two methods. The first method monitors the TCFM normal output to telemetry The output is an analog voltage representing a deviation from set point. Full scale is ±1.5 V corresponding to ±0.5°C from flight temperature set point. The second method is a direct calibration of guard temperature set point in which instance a platinum resistance thermometer is located in the guard to be monitored.

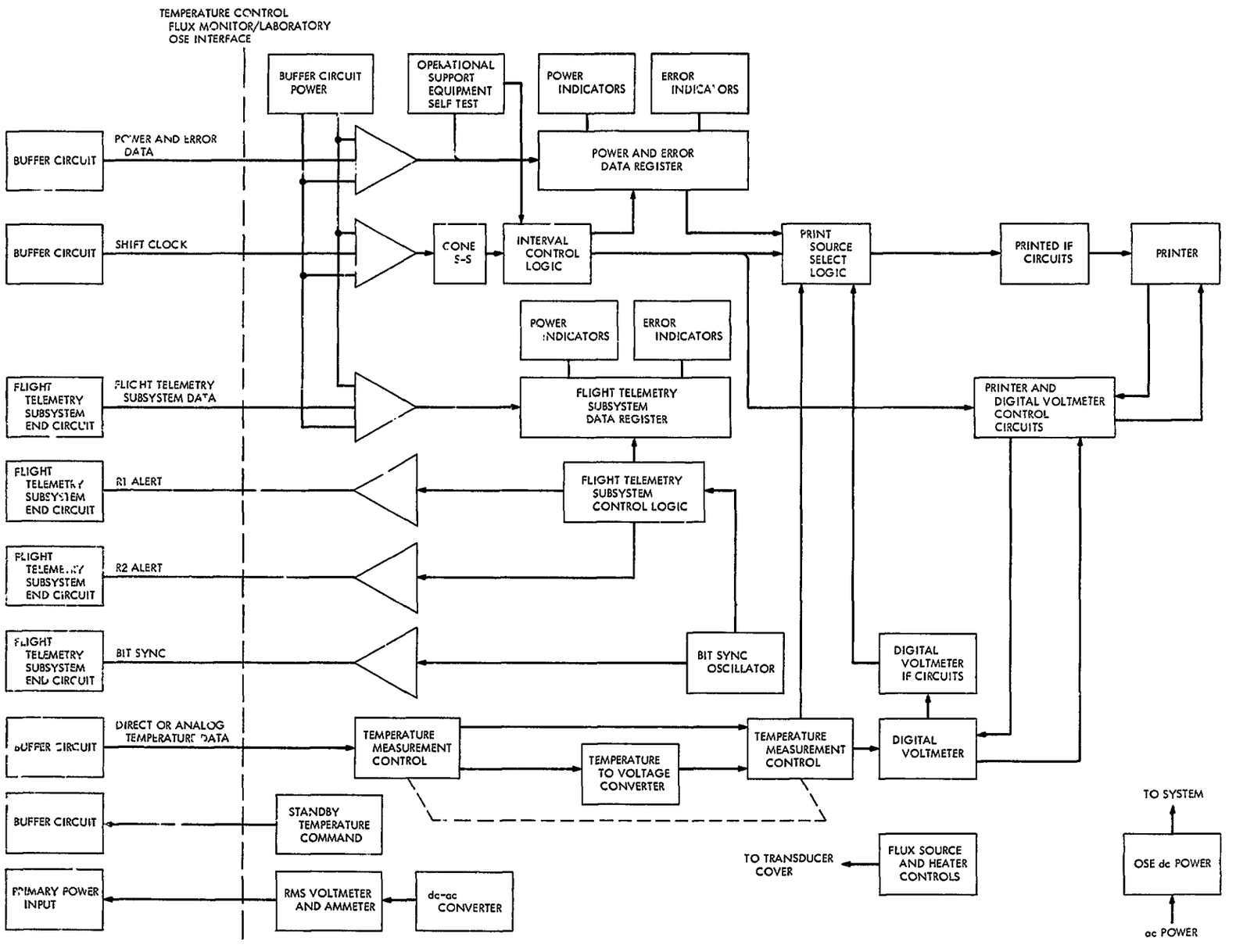


Fig. 12. Temperature control flux monitor operational support equipment: laboratory test

Cone power and loop error is displayed by lights located on the front panel. Guard temperature is displayed on a digital voltmeter. Permanent recording of cone power, loop error, and guard temperature is accomplished with a digital printer. The system-level OSE is functionally identical to the subsystem OSE but for four exceptions: (1) it is significantly more compact, occupying about one-fifth the space of the subsystem OSE, (2) it has the added ability to interface with the system test computer, (3) it does not use a digital voltmeter but, rather, an analog meter for guard temperature measurement, and (4) it does not have a printer since the system test computer does the recording. The system test computer compares OSE received data against telemetry data as an insurance of proper operation of both the telemetry and OSE data links. In system test the OSE receives data through direct access circuits. The system level OSE can also be used for subsystem testing if necessary.

I. Pyrotechnic Subsystem Operational Support Equipment

The operational support equipment for the pyrotechnic subsystem was required to support the qualification testing of the pyrotechnic flight electronic equipment at the subsystem level and to support the checkout and verification testing of the pyrotechnic subsystem during system-

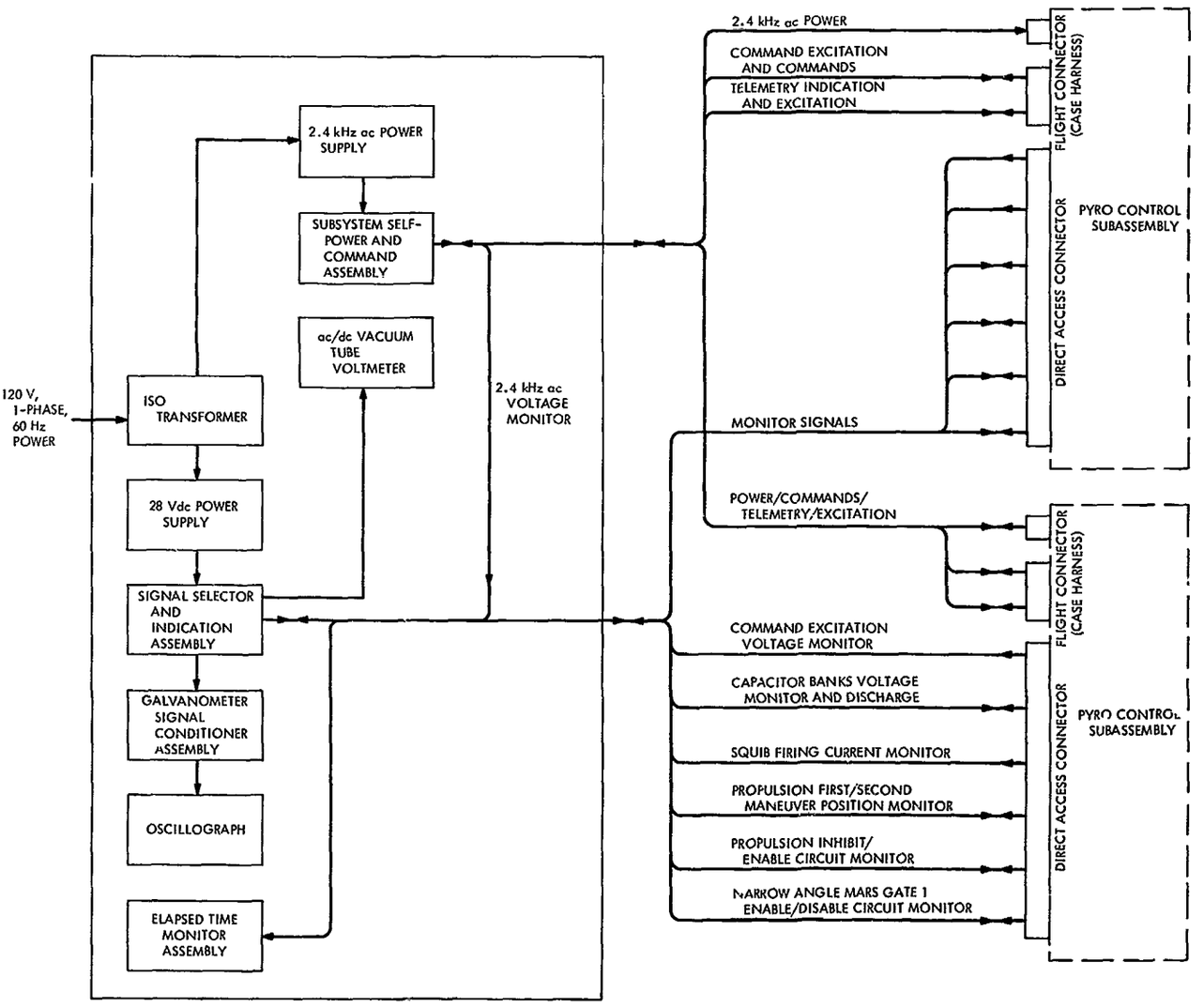


Fig. 13. Pyrotechnic operational support equipment: laboratory test

level testing, spacecraft assembly operations, on-pad testing, and launch countdown sequence. The pyrotechnic equipment is described in the following paragraphs.

1. Laboratory test set. The laboratory test set console supported bench checkout and environmental testing of the pyro control units. A functional block diagram of the test set is shown in Fig. 13. The laboratory test set was manually operated to apply power and command stimuli to the pyrotechnic control units and to monitor and measure the response of the units by means of visual indicators such as lights, meters, and an oscillograph recorder.

2. System test set. The system test console verified the performance of the pyrotechnic control units during system level testing (including environmental testing such as vibration and thermal/vacuum). The system test set provided power and monitoring functions for the pyro control units. A functional block diagram of the system test set is shown in Fig. 14.

3. Field test kit. The field test kit assembly was used for checkout of the pyro control units and electroexplosive devices during system-level testing and prelaunch assembly operations at the AFETR explosive safe facility. A functional block diagram of the field test kit is shown in Fig. 15. The field test kit was manually operated and monitored the condition of the pyro control units and the electroexplosive devices (including the V-band release devices) during spacecraft assembly and pyro subsystem

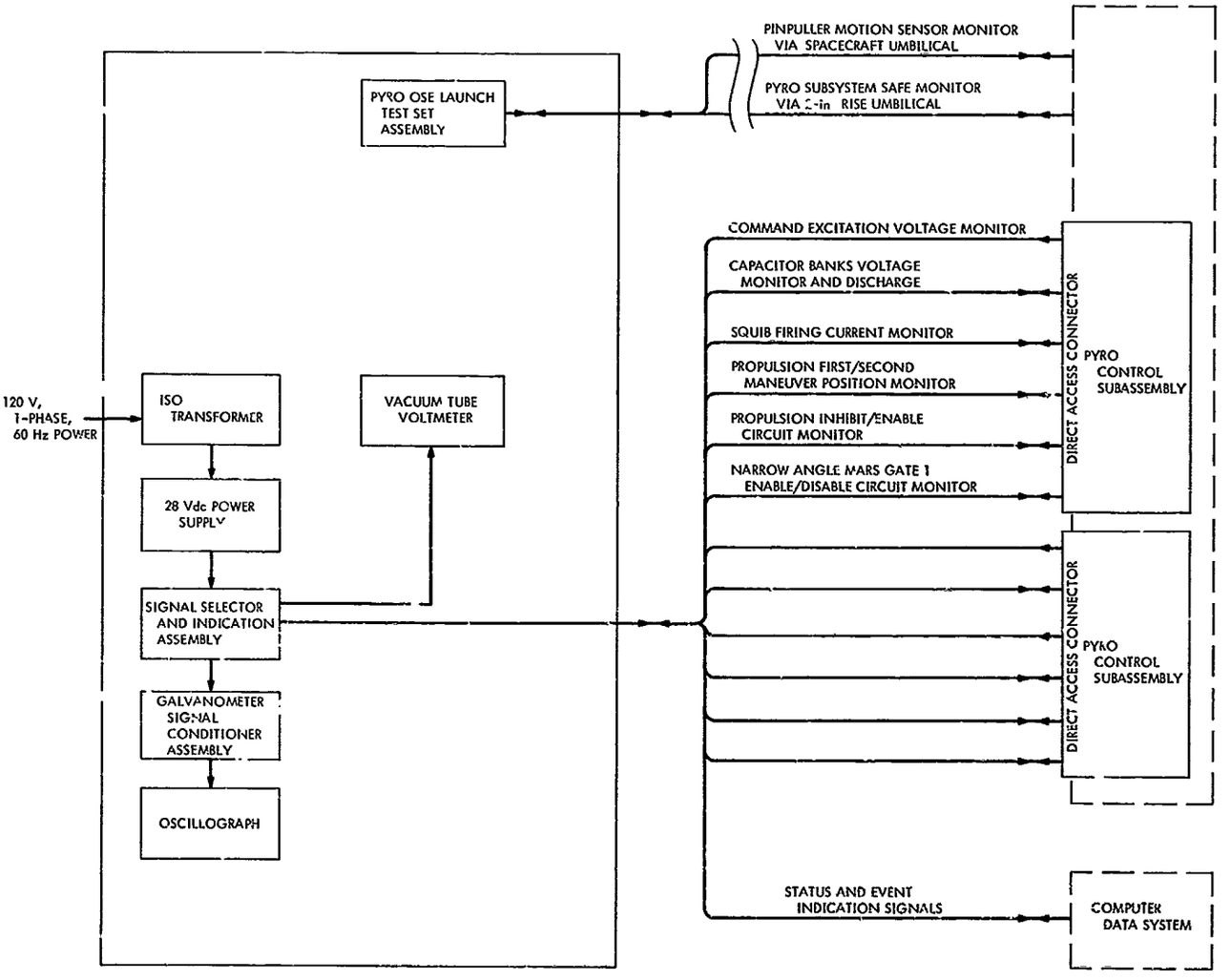


Fig. 14. Pyrotechnic operational support equipment: system test

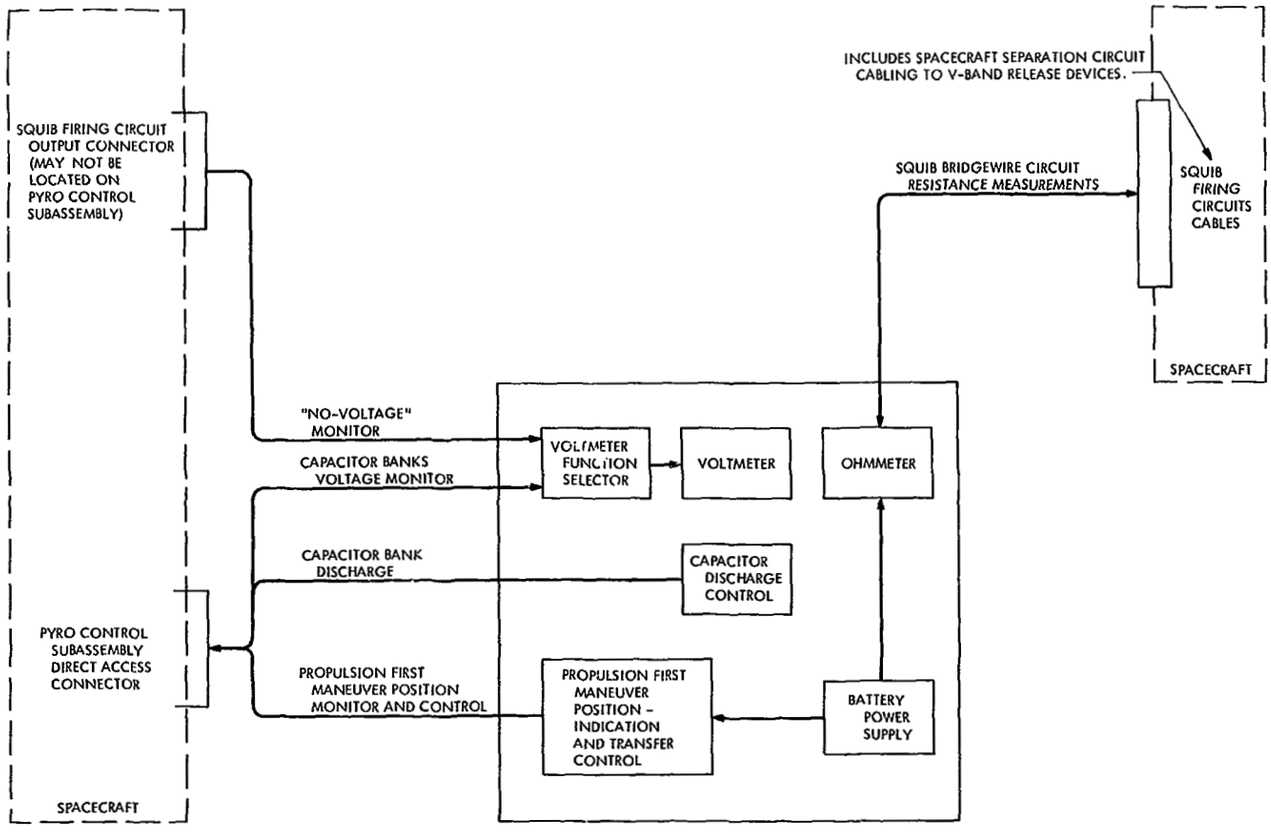


Fig. 15. Pyrotechnic operational support equipment: field test

checkout at the explosive safe facility. The field test kit was compatible with the requirements of the AFETR relating to the checkout of hazardous devices.

4. Launch complex equipment. The launch complex equipment verified the performance of the pyro subsystem and the safe and arm function during prelaunch countdown. A functional block diagram of the launch complex equipment is shown in Fig. 14. The launch complex equipment had no controls, but provided indication of pyrotechnic subsystem Go/No Go condition to establish hold criteria.

5. Squib simulators. The squib simulators supported testing of the pyrotechnic control units at the subsystem and system level.

6. Problems. The only major problem associated with the operational support equipment was with the oscillograph readout of the squib firing pulse. An analysis of the capability of the pyro control unit to reliably initiate squibs under worst-case conditions indicated that there was a sufficient design margin in the unit. However, the method of demonstrating this capability by test was deficient and difficult. The accuracy of both current amplitude and time data obtained with the pyrotechnic support equipment oscillograph was never determined. A cursory analysis of the situation indicated that the inherent instrumentation error was reasonably large compared to the design margin. Compounding the problem was the potential for relatively large operator error in data reduction, particularly considering the tedious process employed.

J. Science Subsystem Operational Support Equipment

1. Science testing objectives and requirements. The science operational support equipment is that nonflight hardware that is used to verify the performance of the spacecraft science payload in real time. The science support equipment does not contain the capability for detailed processing and timing checks, nor does it provide

a detailed calibration printout of the data. These functions are performed by the system test complex data system. The objectives and requirements that were established for the science operational support equipment are as follows:

(1) Verification of the functional operation of the science payload, including the data automation, television, infrared spectrometer, infrared radiometer, and ultraviolet spectrometer subsystems.

(2) Provide basic troubleshooting equipment which will allow problem isolation to the subsystem level without removal of subsystems or alteration of the test configuration.

(3) Acquire for recording and processing by the STCDS, all science data required for post test subsystem performance analysis.

(4) Verification of the functional interfaces between the science payload and other spacecraft subsystems.

(5) Provide control and power for stimuli which, as nearly as possible, simulate flight conditions and exercise the science instruments through all modes of operation.

(6) Provide external power and signals required for operation of the science payload independent of the spacecraft.

2. Description. One complete set of science OSE consists of six standard 72-in. *Mariner* primary equipment consoles, two 48-in. remote display equipment consoles, cabling, and one STCDS line printer.

One set of remote display equipment console was fabricated after the start of the testing program to provide a real-time plotting display in the science analysis area. The remote display console was connected to whichever system test complex was being used for systems testing or, in the case of simultaneous tests, whichever test had priority.

Two STCDS line printers for the OSE were provided and assigned to the complexes according to proposed use and the testing schedule of a particular complex.

A single 48-in. equipment console known as the video simulator was fabricated midway through the testing program to provide a video calibration source for the spacecraft tape recorder and the science OSE.

The primary support equipment consoles use approximately 6 kVA of 120 V, 60 Hz power. The weight of the six primary consoles is approximately 500 lb.

a. General block diagram description. The basic purpose of the science OSE was to acquire, process, and display science functions. In addition, certain external stimuli and signals were provided to allow a complete checkout of the science payload. Support equipment processing and display of data provided periodic verification of subsystem operation in real time. Continuous data monitoring and non-real-time processing was performed by the STCDS. Figure 16 shows a simplified block diagram of the science OSE.

b. Testing configurations. Three main different testing configurations were used during the testing program. Figure 17 shows the normal science system test configuration used during spacecraft systems testing. All direct access cables between the support equipment and science instruments are used for analog and digital data acquisition and stimulus control.

Figure 18 shows the science subsystem test configuration that was used with the mock-up scan platform. This configuration used all of the direct access cables used in the system test configuration and in addition the OSE provided the science payload 2.4 KHz and 400 Hz power required for operations. Certain commands normally generated by CC&S and FCS were initiated by the science OSE. Additional special cabling was used as shown in the diagram.

In Figure 19 is shown the umbilical-only or launch-pad test configuration. Only the 16.2 kbits/s data was acquired by the science OSE in this configuration.

c. Interfaces. The science OSE has a total of 49 interfaces with the data automation subsystem, which include data, synchronization, instrument analog-to-pulse width timing signals, commands, voltage monitors, and TV timing signals.

The interfaces between the science OSE and the instruments primarily involve analog data. There are five interface functions with the television subsystem (TVS), six interface functions with the ultraviolet spectrometer subsystem (UVS), nine interface functions with the infrared spectrometer subsystem (IRS), and three interface functions with the infrared radiometer subsystem (IRR).

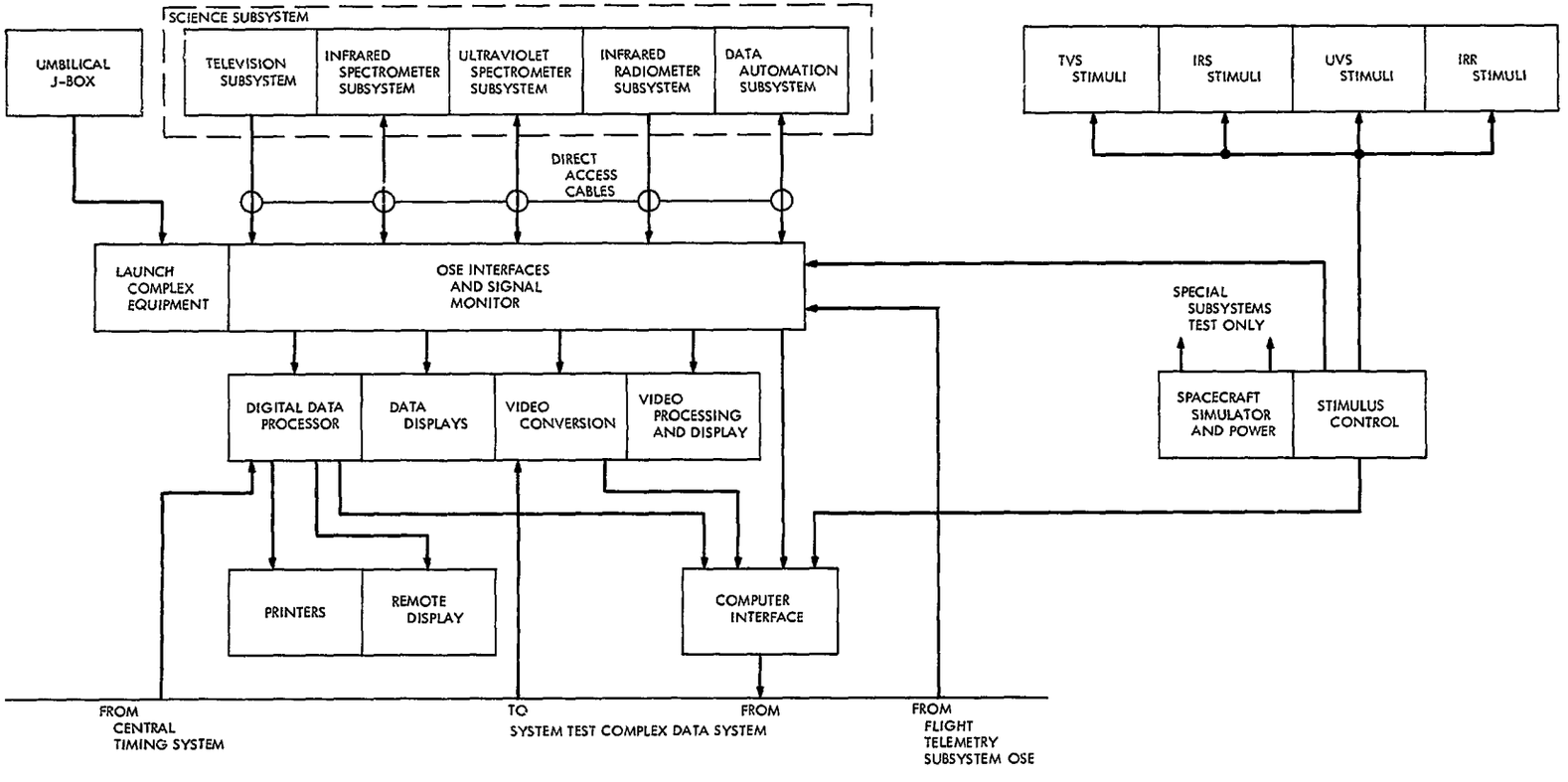


Fig. 16. Science operational support equipment

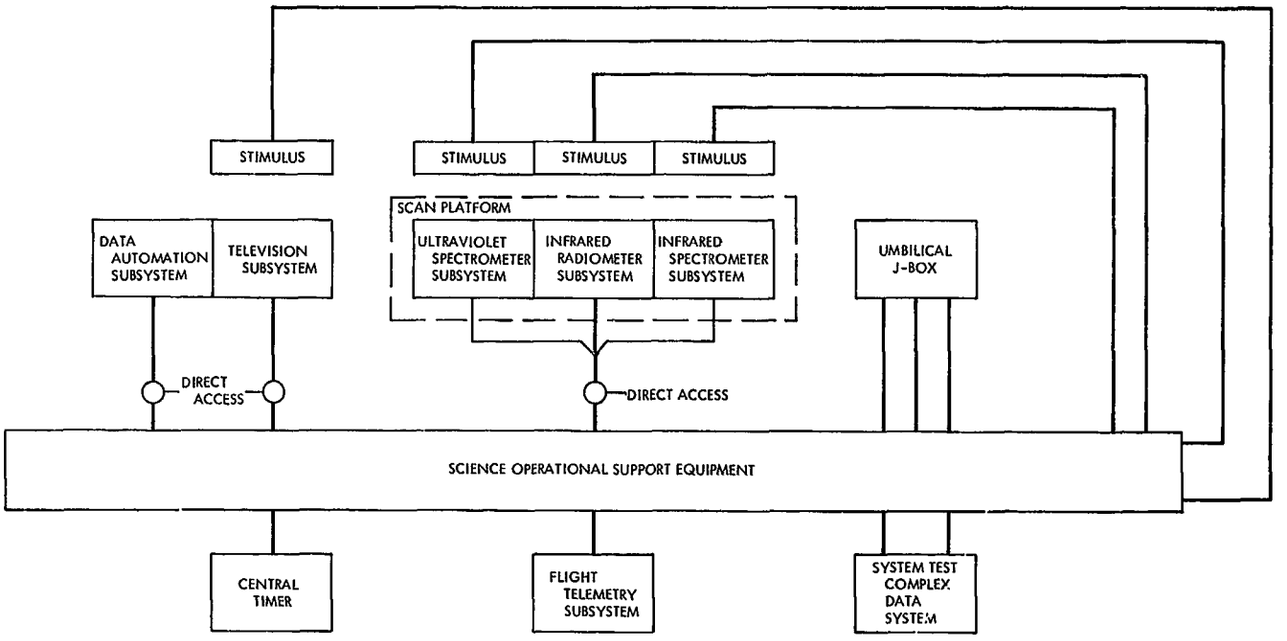


Fig. 17. System test configuration

Four of the interface functions with the infrared spectrometer are used by the OSE to internally stimulate the instrument and two interface functions are used to control the motor. Two of the UVS interface functions are used for internal stimulus.

There are 34 interface functions between the science OSE and the STCDS. These functions include digital data direct from the data automation subsystem, direct commands, OSE status and events, and digitized analog video.

Interfaces exist between the science OSE and the flight telemetry subsystem OSE, the central timing system OSE, and the data storage subsystem OSE. The science OSE receives the digital data from the flight telemetry subsystem as a backup to the data received direct from data automation. The timing signals for time tagging of data are received from the central timing system. The interface with the data storage system was set up to allow the science OSE to perform an analog-to-digital conversion of the data storage data.

Additional interfaces that are used only in the subsystem testing configuration (see Fig. 18) exist between the science OSE and the science payload. External power, commands, and end circuits which are all necessary for subsystem level testing are provided by the science OSE.

3. Design evolution.

a. Improvements over previous programs. The major improvement in the OSE was the elimination of the science isolation box located near the spacecraft on previous programs. It had been necessary on previous programs to have OSE operators near the spacecraft checking inside the iso-box whenever a problem occurred with an instrument. It is now a simple case to check the input side of the OSE input buffer circuits on the 1969 OSE signal monitor chassis. The 1969 science OSE has the capability at the signal monitor panel for monitoring of all signals which input to the OSE. This capability has not existed on previous programs.

The video film recorder design is a significant improvement over the previous OSE film recorder used in the *Mariner* Mars 1964 program. The previous recorder system used a continuous film transport with a single line scan on a modulated cathode ray tube. There were numerous problems with this system and satisfactory recordings were few. The results have been good from the present system in which a full video frame is presented on a monitor and photographed with the film advanced between frames.

An increase in the visual displays of data was made in the present OSE, which has been very useful for quick

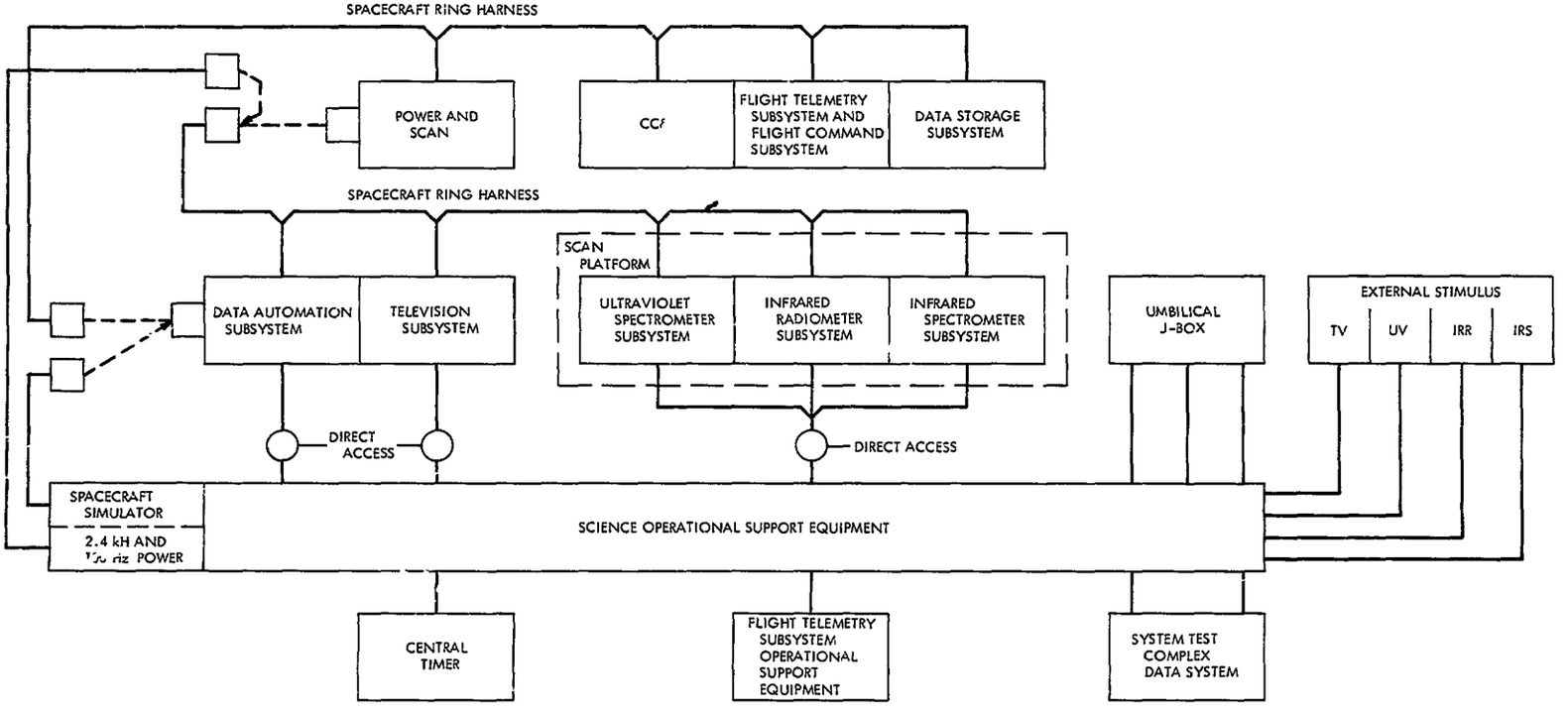


Fig. 18. Subsystem test configuration

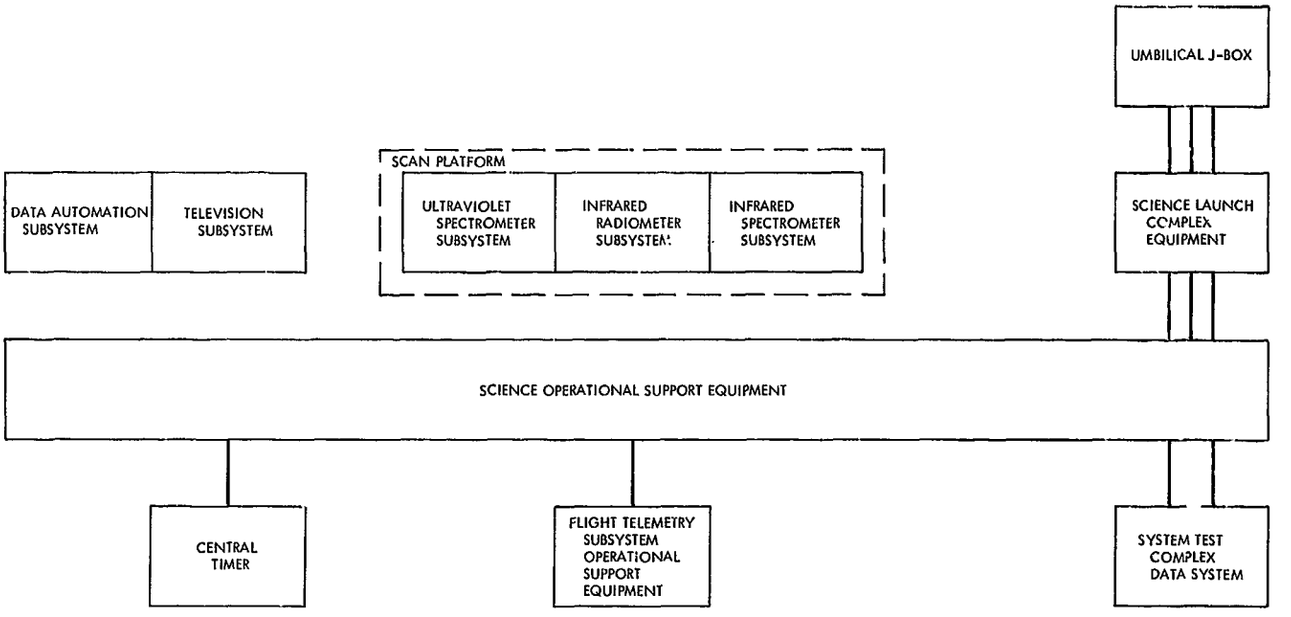


Fig. 19. Launch pad test configuration

determination of science payload status. The data display panel shows the real-time frame count and any two real-time words continuously. The status display panel provides fairly complete status information valuable in determining the present operational mode of the science payload, especially the data automation and television subsystems.

A useful improvement made was the STCDS recording of the data streams on magnetic tape. The perforated paper tape recorder used on the previous programs was prone to failure and consumed considerable operator time for paper changing and maintenance during testing operations.

b. Changes and additions to the OSE. Owing to changing instrument requirements and problems encountered in spacecraft testing, several modifications were performed on the science support equipment. These modifications are listed as follows:

IRS stimulus controller. A change in the external stimulus made necessary a change in the stimulus supply in the OSE. The OSE–IRS internal stimulus controller was modified several times throughout the program also.

IRR stimulus controller. Changes were made in IRR stimulus supply and controller to eliminate data errors and erratic instrument operation which occurred whenever the stimulus power was activated.

UVS stimulus controller. The stimulus unregulated power supplies were replaced with full regulated supplies to eliminate problems which first occurred because of overvoltage and later, insufficient power.

Video processing. The video signal as observed at the input to the OSE analog-to-digital converter was too noisy for reliable conversion. A totally new video processing circuit was added to the OSE, which reduced the noise to an acceptable level.

Spacecraft problems with the television–data storage subsystem combination and deficiencies in the data handling capability of the STCDS brought about hardware additions to the science OSE after the delivery of the first OSE to the spacecraft assembly facility.

STCDS video playback. Because of the problems that had occurred with the television and data storage subsystems during the first series of spacecraft testing, the spacecraft operations personnel saw a need for a quick picture-reproducing capability of the video data played back from the data storage during AFETR operations. To receive the reproduced pictures from JPL would require two to three days. A proposal by the science OSE group to construct a unit which would convert all digital

video data to analog signal for display on the OSE video monitors was accepted by the project.

The interface and conversion circuitry were all constructed into one chassis designated the video playback chassis. The six-bit parallel data is received from the STCDS over the same lines that are used to send the converted composite analog video data to the STCDS from the OSE. The OSE can accept data originally recorded on the analog tape recorder, digital tape recorder, or digital composite analog video from the OSE to STCDS.

Remote display of converted IRS/UVS data. It became apparent after the start of spacecraft testing that the data available in the science analysis area for evaluation of the infrared and ultraviolet instruments was inadequate. The STCDS could not provide the necessary processing of the 16.2 kbits/s digital recorder data to extract the instrument data and present it in an easily discernible form. Since the science OSE already decommutates the instrument data for presentation on the high-speed printer, a proposal was made to the project that the OSE perform a digital-to-analog conversion of the instrument data and plot the analog signals on strip chart recorders in a remote display console located in the science data analysis area. This plan was approved by the project. This addition consisted of two parts: the infrared and the ultraviolet subsystems 16.2 kHz data processor chassis and the remote display console.

Analog tape recorder playback. In March a special test was arranged where the OSE was used as an interface between the spacecraft analog tape recorder data output and the STCDS. The video data at a 2.7 kHz rate was analog-to-digital converted in the science OSE and transmitted to the STCDS.

4. Testing summary.

a. Science subsystem integration. The objectives of science subsystem integration testing before delivery to the spacecraft assembly facility were established as follows:

(1) Initial electrical compatibility test of science subsystems.

(2) Initial electrical compatibility test of science OSE and STCDS.

(3) Initial operational checkout of entire science test support.

(4) Development and verification of computer processing and display.

(5) Development and verification of test procedures.

(6) Initial verification of instrument mechanical alignment techniques and equipment.

The prototype or breadboard instruments were all made available for short periods of time in November and December 1968 for individual interface tests with the OSE. A breadboard or prototype data automation subsystem was used full time. Several problems were encountered with both the instruments and the OSE.

A mock-up spacecraft with a stationary scan platform was constructed for science subsystem testing. The platform and mock-up cabling were used for complete subsystem testing. The test configuration shown in Fig. 18 was used.

The data automation and television subsystems electronic modules were assembled into a bay 7 case and mounted beneath the mock-up platform. The science payload was assembled in a sequential manner (i.e., each instrument was mounted on the mock-up platform and the operation verified before the next instrument was added), and the problems resolved or isolated before the subsystem test was conducted according to the subsystem checkout procedure. Once all the instruments had been assembled on the platform and individual operation verified, two complete subsystem verification tests were performed according to a modified subsystem checkout procedure. The infrared radiometer, ultraviolet, and infrared spectrometer subsystems were removed from the spacecraft mock-up at the end of the second day. The television and data automation subsystems were tested an additional day for further problem investigation.

It was felt that the entire test was very worthwhile and successful. Most of the problems encountered were solved and therefore would not delay testing operations at the spacecraft assembly facility. Many problems had been eliminated in the previous individual instrument interfacing and thus contributed to the successful subsystem test.

The objectives of the subsystem testing were accomplished with the exception of the verification of the STCDS processing and display. Only the interface between the OSE and the STCDS was checked out prior to OSE spacecraft assembly facility delivery. The STCDS

hardware and software were not at all prepared for operation at this time.

Science prototype instruments were used again for interfacing with OSE 2 and OSE 3 before their delivery to the spacecraft assembly facility. Problems encountered were very few, and were minor ones. A full science subsystem integration test was not performed with either OSE 2 or OSE 3 because the instruments could not all be obtained at the same time. Each individual instrument was interfaced with each OSE; however, the problems found and corrected in OSE 1 provided a smooth checkout of OSE 2 and OSE 3.

b. Spacecraft operations. Following subsystem-level integration and verification of flight units and OSE, the equipments were delivered for use in system-level testing and operations.

SAF operations. After delivery to the spacecraft assembly facility, a thorough recheckout of each OSE was performed. The OSE was then verified as ready to support all testing operations. The subsystem test configuration as shown in Fig. 18 was not used again in any spacecraft assembly facility testing after the science instruments were moved to the spacecraft from the mockup. A formal subsystem test procedure was in use during February and March.

A minimum of one complete science subsystem verification test was performed during each systems test. In addition, whenever an instrument was initially interfaced aboard the spacecraft or replaced, a verification test on that instrument was performed. It was decided early in the program that an operator would always be on station whenever spacecraft power was on, whether science power was on or not. An inadvertent science power turn-on occurred once during all of the testing.

A check was performed on the engineering data from each instrument each time that science power was turned on for any reason. The data values checked were recorded on special data sheets kept with the OSE for performance evaluation. In addition, the analog data from each instrument, when available, was continuously displayed on either the visicorder or oscilloscope. It was during these normal operations that many of the science instrument problems were discovered.

Requirements for obtaining television subsystem data were increased during the later systems testing. Single line trace and video monitor photographs were required of each camera frame recorded on the analog tape recorder for comparison with the playback data. The alignment of the TV stimulus also became more critical.

In addition to the regular systems tests and the troubleshooting tests, television subsystem calibration verification tests were performed aboard each spacecraft except the M69-4. Scan platform alignment operations were conducted that required special assistance from the OSE personnel in checking the alignment of the TV cameras.

The STCDS support, though improved over the support received during the first systems test, was still not considered entirely satisfactory during much of the testing operations at the assembly facility. Many parts of science operations were performed without STCDS data processing or handling. The science OSE was designed with STCDS use as a firm requirement. Constraints were placed on the OSE design by the project that limited the amount of data processing that could be performed in the OSE. Support by the STCDS and use of an STCDS line printer were considered a necessary tool to adequately test and analyze the performance of the science payload. After the move of the STCDS and data input system and printers to building 248, operations on system test complex 2 were difficult because of the lack of an STCDS printer.

Building 248 operations. On April 18, 1968, OSE 1 was moved from the assembly facility to building 248 to support spacecraft operations in the space simulator, and remained at building 248 till November for support of the space simulation testing of the four spacecraft.

AFETR operations. The OSE 1 and 2 were shipped to Florida to support the AFETR operations. The video display and processing section of OSE 3 was exchanged with number 1 because of better performance during SAF operations at the spacecraft assembly facility. The two video playback chassis and the remote display console were also shipped to AFETR leaving OSE 3 at the spacecraft assembly facility with the least capability.

Four separate systems tests were performed on the three spacecraft at AFETR with two separate tests performed on spacecraft M69-2. The STCDS support was improved and very few tests were performed without STCDS data processing and recording.

Three separate television subsystem calibration verification tests were performed on the M69-2 and M69-3 spacecraft. A second calibration verification test had to be re-run because the data received was not consistent with previous tests. The exchange of the subsystem on the M69-2 spacecraft also brought about an extra scan platform alignment operation. Three alignment operations were performed. All of the system tests, television subsystem calibration verification tests, video simulator recordings, scan platform alignment operations, and all other special testing with a spacecraft in building AO were conducted with OSE 2.

Testing operations with OSE 1 consisted of launch pad tests and explosive safe facility operations. Only the 16.2 kbits/s umbilical digital recorder data was received at the OSE. After a pre-countdown test was performed a video playback operation with data from the STCDS would be conducted. These playback operations were very successful.

Numerous problems occurred with the science payload during the testing program. A brief summary of the more significant problems in which the science OSE contributed significantly to the solution or the discovery are listed as follows:

TVS-DSS processing problem

TV line dropouts during camera TV-A pictures

UVS motor failure

TV "B" camera shutter light leak

UVS double fiducial pulse

IRR misstepping

TVS video clamping

IRS motor failure

TVS driver amplifiers "locked up". (This particular problem was found to be OSE-induced.)

II. Data Systems for Test Support

Two major digital data processing systems, the system test complex data system and later the UNIVAC 1219 data system were used to support the *Mariner* Mars 1969 Spacecraft System tests. Subsystem level data automation subsystem tests used a PDP-7 computer system for stimulating, and recording the output of the data automation subsystem. Television subsystem calibration data processing, and extensive processing of TV and data storage subsystem data were provided by the UNIVAC 1219 system. Some non-real-time plotting and data listing was provided by the IBM 7094 computing systems.

A. System Test Complex Data System

The *Mariner* Mars 1969 system test complex data system was an extension of the single-computer system used for *Mariner* Venus 67 system test data processing*. The original CDC 3300 leased system was expanded in capability by the addition of 32,000 words of core memory, two input/output channels, a plotter, an alphanumeric cathode ray tube display for the test director, and substitution of line printers for teletype machines. Data acquisition capability was increased to accommodate the high-rate block coded telemetry data and the 113.4 kbits/s digitized analog video from the science OSE, as well as parallel low-rate digital data, principally from the radio subsystem OSE. Table 1 lists the data, rates, and devices providing inputs to the STCDS. The system produced displays of telemetry and hardline data during spacecraft

**Mariner Venus 67 Final Project Report: Volume I. Launch Through Midcourse Maneuver*, Technical Report 32-1203. Jet Propulsion Laboratory, Pasadena, Calif., June 15, 1968.

Table 1. Data acquisition

Data stream	Maximum rate, bits/s	Average rate, bits/s	Input device
Telemetry, science channel	270	270 or 66⅔	TIM[a]
Telemetry, engineering channel	33⅓	33⅓ or 8⅓	TIM
Telemetry, high-rate channel	86.4K	86.4K	TIM
Operational support equipment and spacecraft events/status	1.0K	10	ESM[b]
Data automation subsystem TV	16.2K	16.2K	TIM
Science operational support equipment	4.5K	4.5K	DDM[c]
Analog TV	120K	120K	DDM
Analog hardline, low-speed	120	120	AIM[d]
Analog hardline, high-speed	5.3K	80	AIM
Operational support equipment, digital	1.0K	10	DDM
Central computer and sequencer	120	120	TIM

[a]TIM = telemetry input module.
[b]ESM = events and status module.
[c]DDM = digital data module.
[d]AIM = analog input module.

system tests consisting of messages on multiple line printers indicating changes in the operating condition of the spacecraft and OSE, and magnetic tape records of all acquired data. Printouts of the latest available spacecraft subsystem data were available upon request. The recorded data could be reprocessed by the computer to obtain additional detail, to plot data, or to generate other magnetic tape records in decommutated (frame-synchronized) formats for offline processing. The principal use of these tapes was to provide the combined science format data (972-bit frame) and TV science format data (6804-bit frame) to the image processing laboratory. These tapes, as well as frame-synchronized tapes containing the real-time science 280-bit frames and the engineering 140-bit frames were also used as input data sources from which telemetry simulation data was derived for use in some MOS/TDS training and operational tests. The data system configuration is shown in Fig. 20, including two data input subsystems (DIS A and DIS B) and the display and control equipment located on the system test complexes. More detail on the subsystem elements is shown in Fig. 21.

Data processing requirements of the STCDS were stated in a series of 41 documents called user service requests, which described most of the supplementary data processing requirements beyond those provided by the software operating system and basic decommutation and data distribution programs. Requests by users for various engineering telemetry data processors were approved by the test and operations manager prior to implementation. The science subsystem test requirements, which were planned for development prior to the start of proof test model system testing formed a set of independent requirements. This plan later caused problems because the test requirements for subsystem integration and system-level support differed from those of the test and operations staff, and duplication of software development effort resulted. The STCDS was unable to process data as planned during the science subsystem integration period because the late delivery of the subsystems coincided with the December 1967 to January 1968 period when major modifications and additions were being made to the *Mariner* Venus 67 computer system and data acquisition subsystem.

Considerable difficulty was encountered in providing real-time decommutation and processing of 16.2 kbits/s data automation subsystem hardline data. During the several months required to accommodate this function in the real-time system, non-real-time processing of data recorded on the log tape was required. Non-real-time processing functions required during the remainder of the test program were principally plotting (using the IBM 7094 with its associated GD/C 4020 cathode ray tube plotter, or the STCDS incremental plotter), and block decoding of the 86.4 kbits/s data using the CDC 3300. The latter function required about four times that of real time for accomplishment.

A second computer system and data input subsystem were delivered and checked out during the April to July 1968 period, primarily to provide the capability for simultaneous test of two flight spacecraft, but also to permit testing of one spacecraft while accomplishing non-real-time processing or program development and checkout on the other computer system. From August to December, the system handled the spacecraft assembly facility system tests and environmental test laboratory simulation and vibration tests for a maximum of three spacecraft simultaneously, although only engineering telemetry data was processed for the third spacecraft. The 65,000-word program in one CDC 3300 provided full encounter-type test data acquisition and processing for one spacecraft (or the non-real-time processing of encounter data) plus engineering telemetry decommutation and display from a second spacecraft, complete with printer output and cathode ray tube display.

Only 314 core locations remained unused. Nine major versions of the support program were developed on approximately one month centers. Each succeeding assembly improved some aspect of the performance of the preceding one, and in addition included new capabilities requested by users. Any changes required to correct the operation of a preceding assembly were included in each new assembly to eliminate the "patch" cards previously required at program initialization.

The first of the two computer systems, including input controllers and data input modules, was shipped to the AFETR and set up to support spacecraft test operations late in December 1968. The second system arrived at the AFETR as the first system finished checkout, and both supported tests starting in early January 1969. A modem and error decoder was installed at the AFETR to provide the STCDS with DSIF telemetry data. A software interface was developed to enable handling the raw telemetry stream received from any of the DSIF telemetry and command processors by means of the 2400 bits/s high-speed data line in block-multiplexed form, i.e., containing intermingled blocks of engineering, science, and

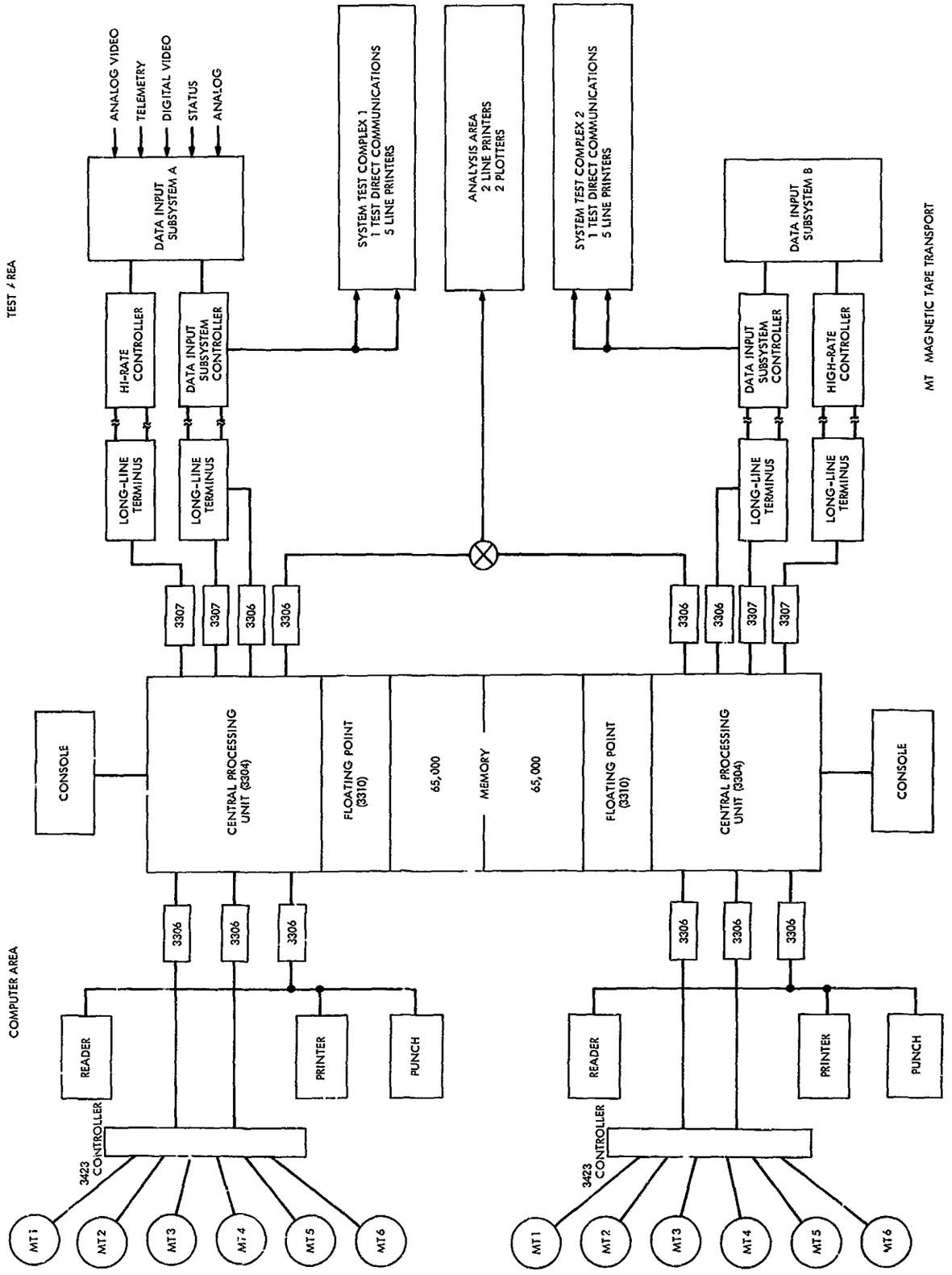


Fig. 20. *Mariner* Mars 1969 system test complex data system

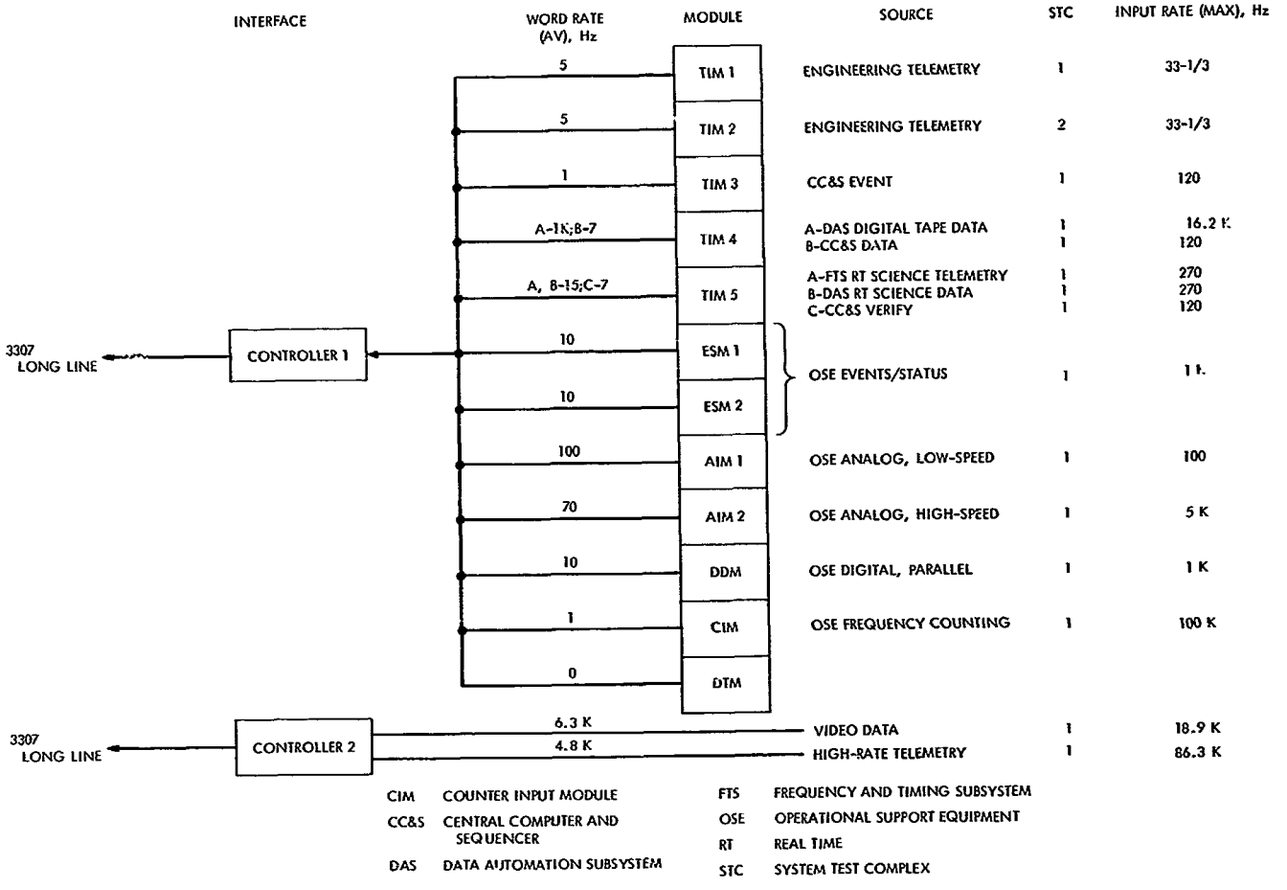


Fig. 21. Data input subsystem

DSIF ground data system status information. This capability was used to permit system test personnel to monitor spacecraft performance during prelaunch MOS tests, launch operations, and midcourse maneuver of *Mariner VI*.

During the launch of *Mariner F* on February 24, both computers processed telemetry received by way of the umbilical connector until liftoff, when the program was reloaded and the systems started processing high-speed data line telemetry. Canopus sensor and gyro data were plotted in real time and, following the establishment of the cruise operation of *Mariner VI*, a number of non-real-time selective tabulation runs were made using recorded data, while single-computer support of cruise continued. Support of the *Mariner G* launch on March 27 was similar to that provided for the *Mariner F* launch except that a large number of event and status-change occurrences at $T - 10$ min caused the prime STCDS program to halt. The backup system operation continued normally, and immediate reloading of the program resulted in a data loss of less than one minute in the prime system. Following postlaunch testing associated with the anomalous CC&S readout which occurred on *Mariner G*, both leased CDC 3300 computer systems were returned to Control Data Corporation on April 4.

A total of 2772 log tapes were recorded by the STCDS during the test history of *Mariner* Mars 1969, some of which were re-used. Most log tapes were retained at JPL until the end of the mission to aid analysis of inflight anomalies or other studies. They were processable by the UNIVAC 1219 system described in the following section. During the first three months of 1969 AFETR operations the two STCDS computer systems were operated a total of 1000 h with a down-time of about 0.4%. About 44% of the support provided was for real-time system testing, and 34% for non-real-time data processing, with the remaining 22% for maintenance, program checkout and development, and administrative functions.

B. UNIVAC 1219 System

The *Mariner* Mars 1964 project used a UNIVAC 1218 computer system to process spacecraft telemetry and OSE hardline data and provide alarm monitoring and data printout in real time. At project conclusion, the system was transferred to the *Surveyor* project and significantly expanded in size and scope by the addition of a second 1218 computer, two 1219 computer systems, and display equipment including printers, plotters, and a cathode ray tube display. The system was used for mission operations as well as system test applications. At the conclusion of *Surveyor* development, a software system was available providing general telemetry decommutation capability, programming for all input/output functions including Dataphone, and alphanumeric displays of selected data tables, as well as plotting capability on the cathode ray tube system. The data system, including software was, therefore, almost immediately applicable to the acquisition and processing of *Mariner* Mars 1969 low-rate engineering and science telemetry.

After a number of iterations on potential uses, a plan for the UNIVAC 1219 system was stated by the project in August 1968. This plan was based on substitution of the JPL-owned UNIVAC system for the second CDC 3300 leased computer system during the post-launch proof test model test-support period without increasing project costs. This plan also provided proof test model test support starting in January 1969 following the shipment of the STCDS to AFETR, providing computer data processing functions which otherwise would have been unavailable until April when the STCDS was to have been returned.

The availability of the UNIVAC system enabled several other project applications; of special interest were the production of TV pictures and UVS/IRS plots in conjunction with the converted *Surveyor* spacecraft TV ground data handling system (TV-1), the TV subsystem calibration data processing effort, and the real-time encounter TV display capability developed after launch.

The initial 1219 system application in July 1968 provided block decoding and frame synchronization of high-rate telemetry in real time, thus enabling quicker disclosure of malfunctions in the TV subsystem, data storage subsystem, or high-rate data encoder and OSE ground demodulation and symbol synchronization functions. The prime frame-synchronized high-rate science data tape was produced by the 1219 system from the data recorded in real time, primarily to provide data to the image processing laboratory. Statistical analysis programs were developed to calculate histograms of data distribution, and the input/output transfer function of the analog data storage subsystem and the high rate telemetry system, which proved invaluable in system test.

During a four-month period starting November 1968, a hardware/software system was developed to read the TV subsystem calibration data which had been recorded in digital form on an FM analog tape recorder. These data were processed to produce master tape records which were in turn processed to provide approximately 1700 output tapes of four different types: (1) full analog video, (2) composite analog video, (3) digital video (every seventh element data), and (4) every 28th element video data. Quick-look pictures of most calibration frames were also produced by the TV-1 system resulting in a very high volume of hard-copy output; approximately 30,000 pictures or 150,000 70mm strip contact prints. This development was excessively time consuming and costly because of the poor quality of the original recorded data and the difficulty in reading digital data reliably from the analog recorded tape. Production of the complete backlog of TV calibration data was not completed until May 1969.

In October, capability was developed to acquire and log the 18.9 kbits/s digitized full analog video from science OSE and the 16.2 kbits/s science data automation subsystem hardline data to supplement the STCDS. Real-time processing capability for commands, CC&S (engineering telemetry) memory dumps, and 16.2 kbits/s or 270 bits/s data in either the 972-bit combined-science format or the 6804-bit TV science format was developed in December 1968 to complete the functions required for proof test model test support.

The primary UNIVAC 1219 system development for encounter was the real-time processing of high-rate TV data. These data were sent to JPL from the DSS 14 high-rate subcarrier demodulator assembly at symbol rate to the correlator at CTA 21, and then transferred to the 1219 computer system by parallel transfers of data characters at a rate equivalent to 16.2 kbits/s. A block diagram of the 1219 TV-1 system for handling the high-rate telemetry is shown in Fig. 22. The video data processing system received the high-rate spacecraft data by way of a special microwave data line installed between the Mars Goldstone station and JPL. The data system successfully displayed pictures in the SFOF on

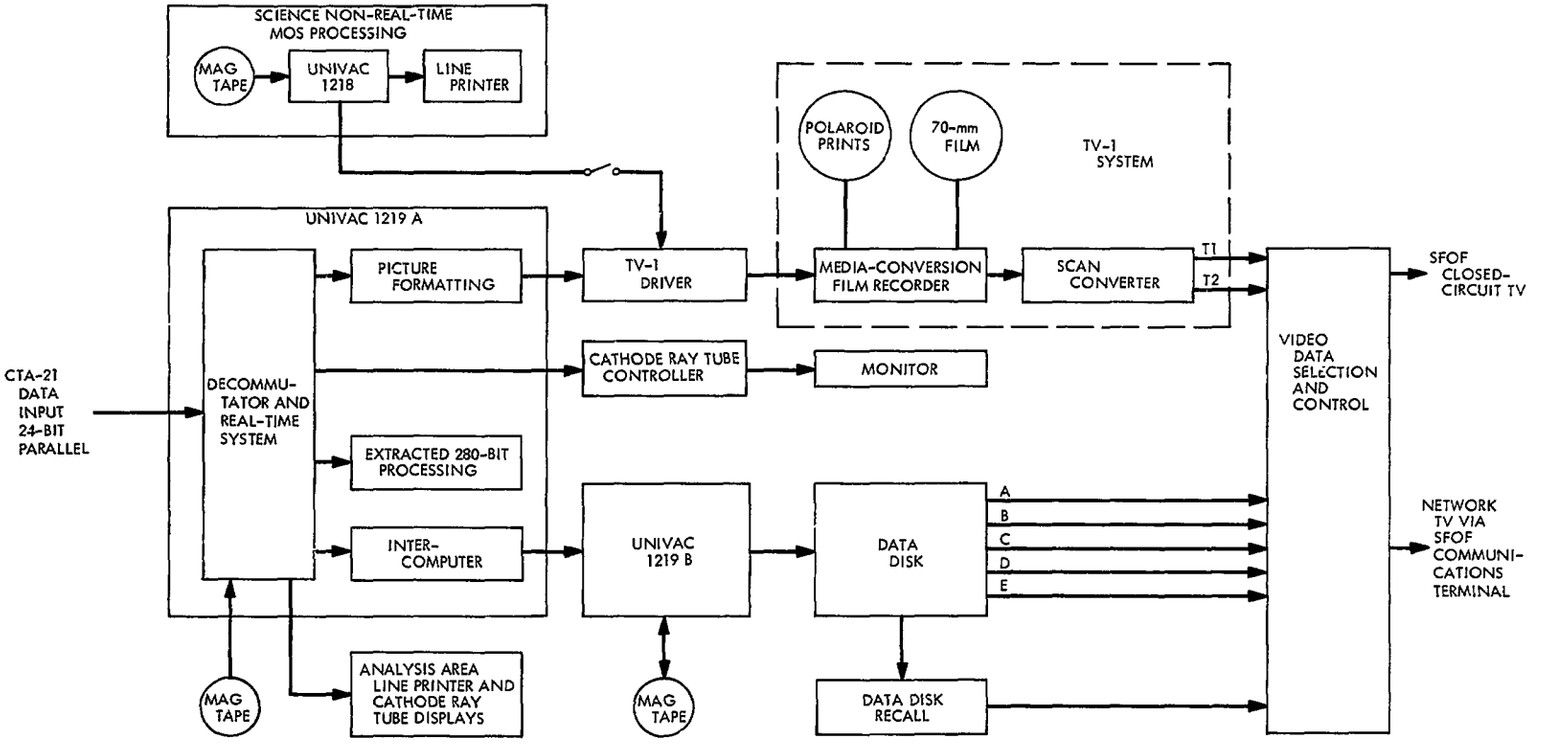


Fig. 22. UNIVAC 1219/TV-1 real-time high-rate telemetry data processing system

the computer complex television system during both the far- and near-encounter phases of *Mariners VI* and *VII* operations. An interface with the broadcast television network was established through the data disk or recall-disk storage devices shown on the block diagram. The UNIVAC 1219 system also established the interface with the real-time hardcopy picture production facility in TV-1, which was used to provide quick-look picture output in the form of strip film, prints, and enlargements to the space science analysis and command team, to the principal investigators, and to the news media and other public information services. Prints and films were exposed using the TV-1 media-conversion film recorder (MCFR), which also contains the digital-to-analog converters to drive the scan converter. The converter permits storing spacecraft video data as it is received, while simultaneously scanning it at line and frame rates compatible with broadcast television. The scan-conversion system functioned effectively as a backup to the data disk system during its occasional periods of difficulty or malfunction.

Development of 972 and 6804 bits/frame telemetry decommutation programs with simplified logic for PN-code frame-synchronization recognition and line count identification was required to obtain sufficient additional machine time for performing the picture formatting and data input/output functions associated with driving TV-1 in either a line-behind or frame-behind mode. The former mode provided line-by-line picture buildup as the data was received in real time, corresponding to the 42 s required for transmission of a picture in the combined science data format. Approximately 5 min were required for picture transmission in the TV science data format, obtained when reproducing the spacecraft analog tape recorder data through the high-rate telemetry system. The frame-behind mode required storage of a complete picture on 1219 digital magnetic tape and the subsequent output of the picture data to TV-1 at maximum data transfer rate, requiring approximately 30 s for a combined science format picture and 70 s for a TV science format picture. Either type of picture was displayed until availability of the next frame, either 42 s or 5 min later. The availability of a dual-channel scan converter allowed alternate viewing of completed pictures on CCTV, or the viewing of the pictures during their buildup.

Television science data was stored on the 72-track data disk at a resolution corresponding to one-half that of the original picture data received from the spacecraft. Data reproduction from the disk occurred without further loss of resolution, or fadeout as encountered in the case of cathode ray tube scan conversion devices. The recorded digital data was continuously reproduced at the 30-Hz interlaced full-frame rate of broadcast TV, as a consequence of the disk speed of 30 rps. The reproduced data at 9-MHz bit rate was converted by high-speed digital-to-analog converters to analog form compatible with TV broadcast requirements. The four data output channels shown (A, B, C, D, Fig. 22) provided for selection of a line-behind or frame-behind data mode, as previously described in connection with the TV-1 scan converter mode of operation. This frame-behind mode also operated from data stored on the 1219B magnetic tape units. Figure 23 illustrates a capability developed to select any of nine coordinate positions within a standard TV frame and enlarge the linear dimensions of the surrounding area by a factor of two (square areas enclosed by solid lines) or four (square areas enclosed by dotted lines). The 2× enlargement has the same resolution as the original picture, since disk storage of full-frame pictures requires reduction of the original 704-line × 934-element picture to one of 352 lines × 467 picture elements. Also shown in Fig. 23 is the identification information generated by the computer and output as a readable display accompanying the picture information. An explanation of this information appears at the right side of the figure. The lower right part of the picture also contains a histogram of the relative frequency of occurrence of picture elements in the 00 to 63 full range of the picture, and a corresponding 0 to 63 gray scale.

A capability was developed to modify received picture data which covered only a limited part of the full range of the system to form a picture with increased contrast. For example, the picture element values with major data distribution in the range 18 to 32, as indicated by the input data histogram, could be transformed so that this range covered the full 00 to 63 output data range of the system. In addition, the relative contrast of light, gray, and dark areas of any pictures could be modified by selection of one of seven different transfer functions relating output data value to input data value. The transfer functions provided are shown in Fig. 24, with the table number in this figure corresponding to that shown as "TT - X" in the picture identification information in Fig. 23. The Table 1 transfer function was used in viewing far-encounter pictures when it was desired to increase contrast in both the dark areas near the limb and terminator (low data numbers) as well as in the light areas at or near the polar cap (high

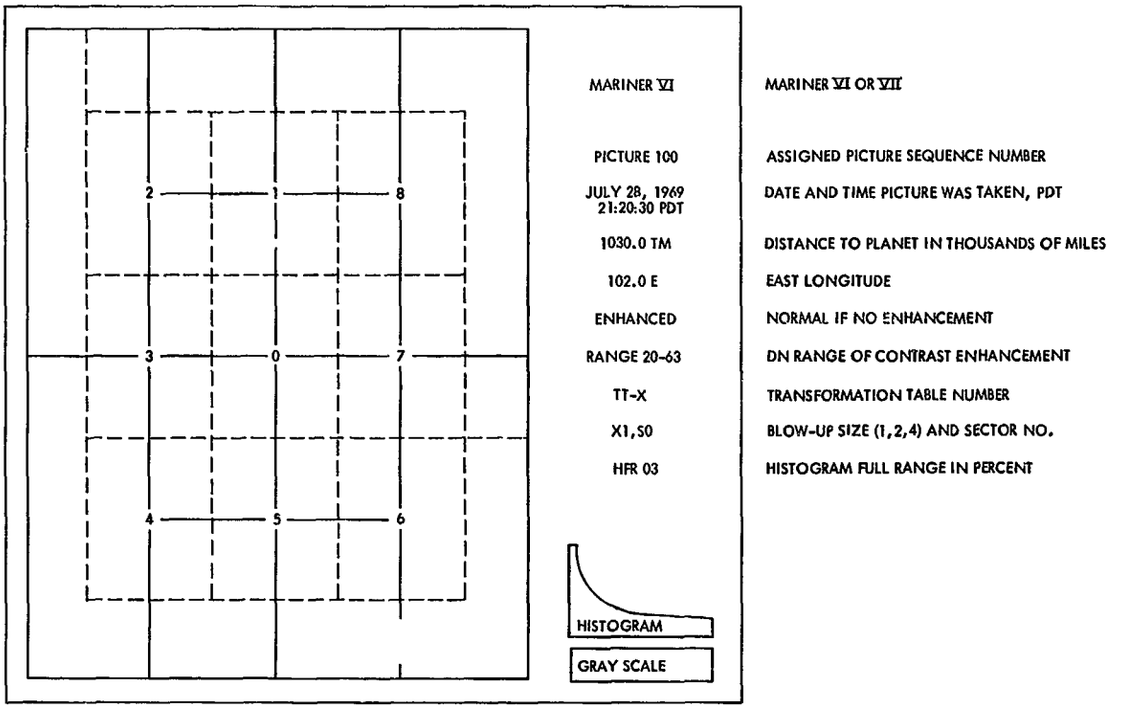


Fig. 23. Television picture enlargement capabilities and picture identification

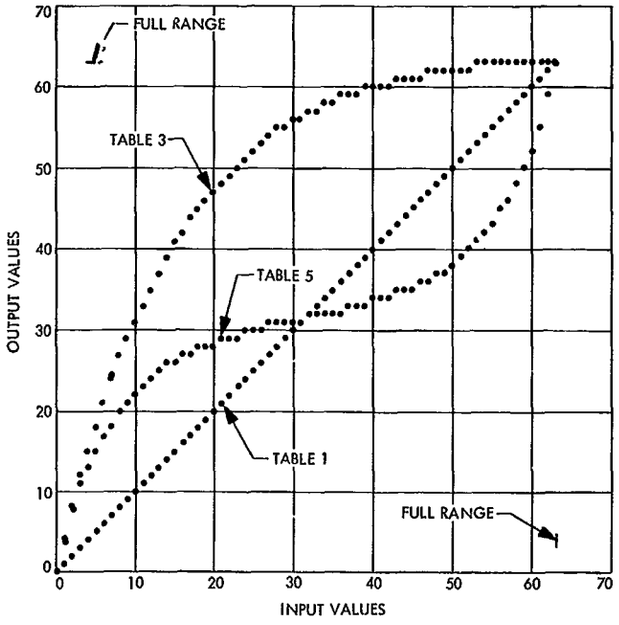


Fig. 24. Typical contrast transformation tables

data numbers). Near-encounter pictures were usually modified by changing only the linear scale range. These capabilities proved valuable for near-real-time evaluation of areas of special interest and examination of areas of low contrast by altering the range or nonlinear representation of the received picture intensity values.

III. Test Support Operations

Test support operations included the assembly and test of the system test complexes and launch complex equipment used for spacecraft system checkout, shipment of support equipment to AFETR, and assembly and test checkout at AFETR. Figure 25 shows the OSE utilization schedule covering the period in which parallel testing of several spacecraft was performed.

Assembly and test of system test complex 1. Assembly and test of STC 1 began December 19, 1967 with the arrival of power and radio OSE at the racks. As subsystem OSE racks were delivered (Table 2), they were installed in the STC area of the new south wing of the spacecraft assembly facility and interfaced with power distribution console 194RC1. Phasing and voltage of the STC 60-Hz and 400-Hz ac power were verified and grounding checks were performed. Figure 26 shows the planned location of OSE on complexes 1 and 2.

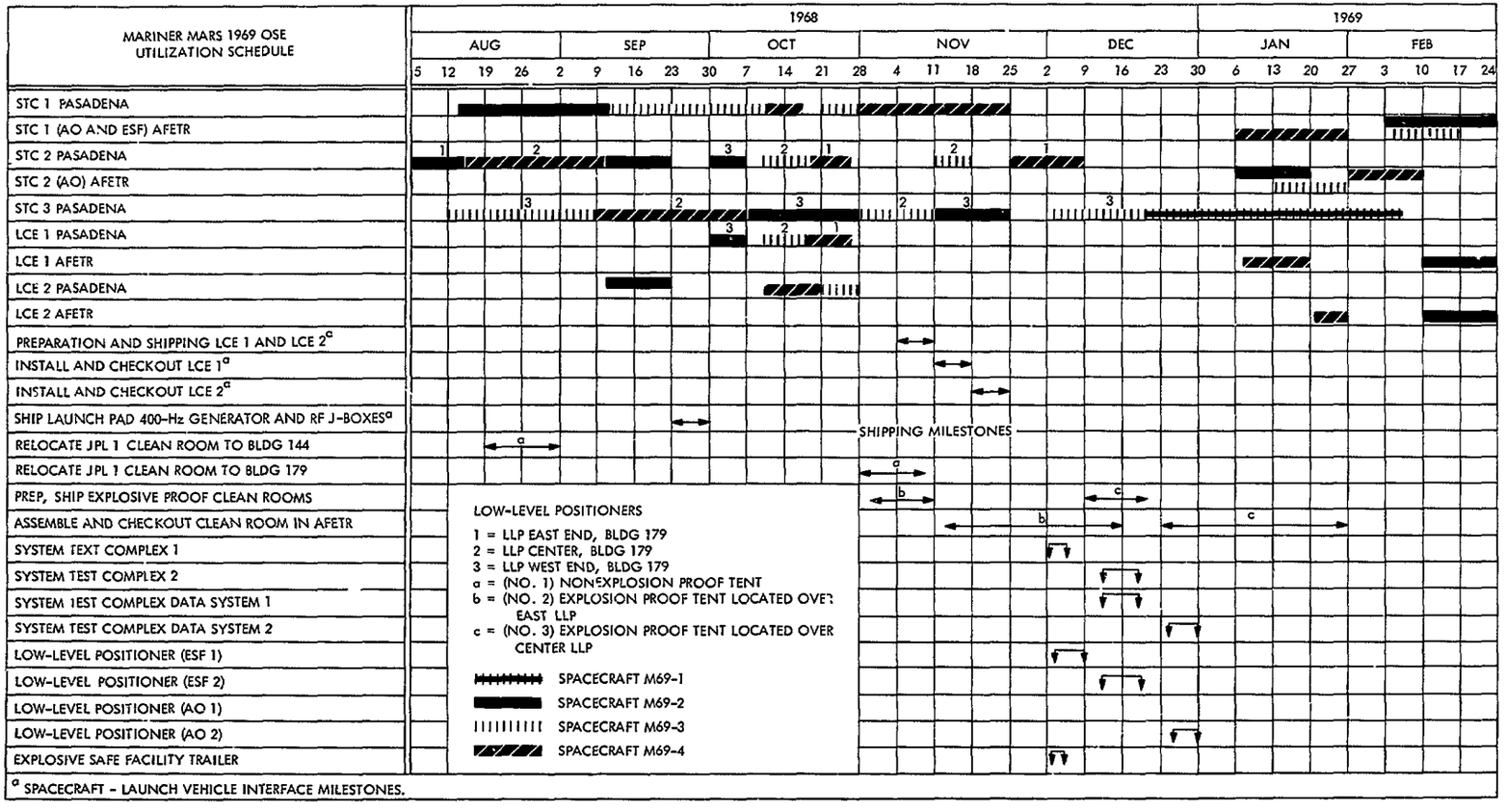


Fig. 25. Operational support equipment utilization schedule

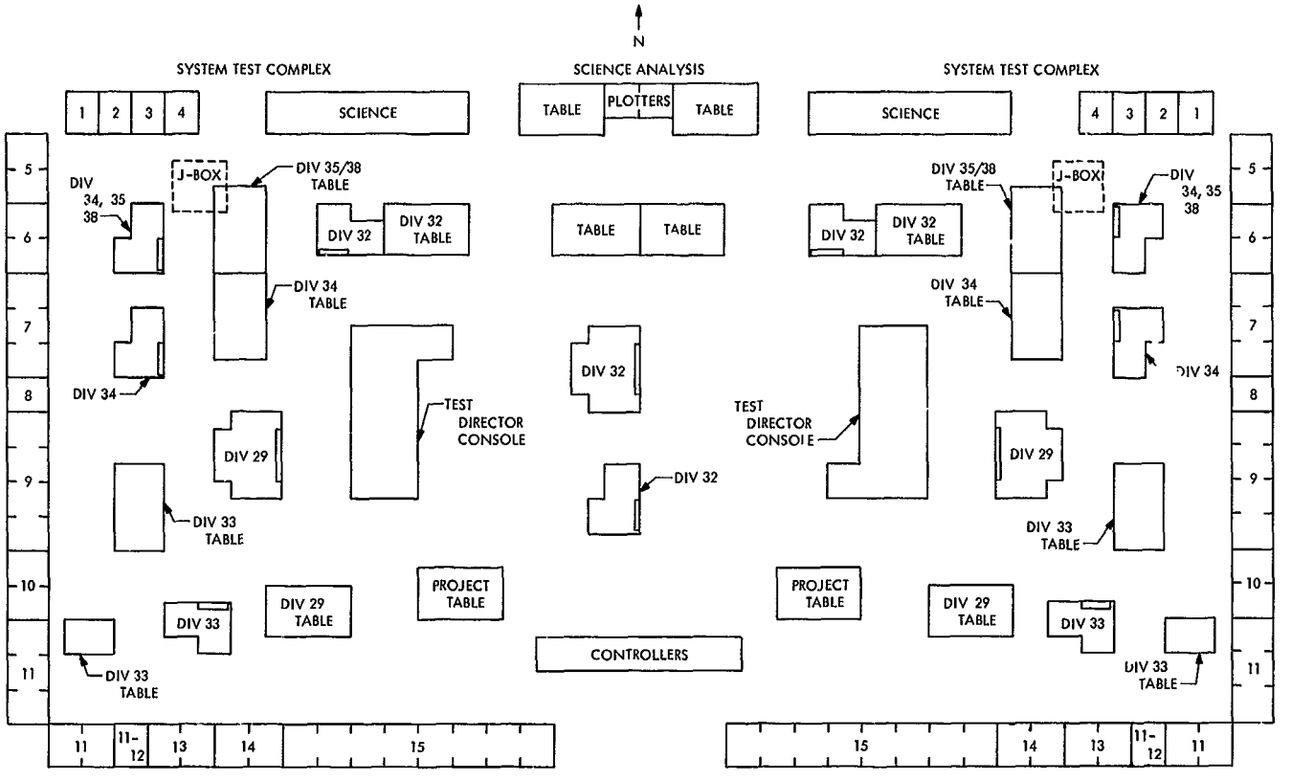


Fig. 26. System test complex configuration in spacecraft assembly facility

Assembly and test of system test complex 2. Following installation of STC 1 in the 10-ft space simulator OSE area, assembly and test of STC 2 began in the spacecraft assembly facility south wing. As OSE were delivered they were installed in the former STC 1 area.

Assembly and test of system test complex 3. Assembly and test of STC 3 began in May 1968 and continued through June as OSE were delivered. The complex was assembled in the west end of the assembly facility OSE area. During the latter part of June, spacecraft M69-1 was used for spacecraft–STC ground integrity verification and other integration activities.

Assembly and test of pseudo launch complex equipment. Because of the late arrival of LCE hardware, a set of pseudo-LCE was fabricated from existing STC 1 OSE during the latter part of May and early June 1968 for use during spacecraft M69 1 vibration, acoustic, and pyrotechnic shock testing. Figure 27 shows the OSE used and the cabling.

Assembly and test of launch complex equipment 1. Assembly and test of launch complex equipment 1 began in May 1968 and continued sporadically as equipment became available. The pacing equipment was the cables connecting the launch complex equipment with the spacecraft. Once the cables became available, final assembly and checkout proceeded smoothly and without difficulty in the east end of the south wing of the assembly facility.

Assembly and test of launch complex equipment 2. Assembly and preliminary checkout of the second set of launch complex equipment was performed in the Environmental and Dynamics Test Laboratory during July and August. The second set was used to support spacecraft vibration and pyrotechnic shock testing.

Table 2. Subsystem operational support equipment delivery to the spacecraft assembly facility

Reference designation	Subsystem OSE	Delivery date		
		STC 1	STC 2	STC 3
2102	Radio frequency	Dec 19, 1967	Mar 27, 1968	May 6, 1968
2103	Flight command	Jan 15, 1968	Jun 25,	Jun 13,
2104	Power	Dec 19,	Apr 8,	Jun 5,
2105	Central computer and sequencer	Dec 23,	May 3,	Jun 5,
2106	Flight telemetry	Jan 15,	Jun 25,	Jun 17,
2107	Attitude control and scan control	Jan 8,	May 3,	Jun 5,
2108	Pyrotechnics	Jan 4,	Mar 27,	Jun 18,
2109	Cabling	Jan 11,	Jun 10,	Jun 20,
2111	Temperature control	Mar 27,	Jun 18,	Jul 24,
2112	Mechanical devices	Mar 27,	Jun 18,	Jul 24,
2116	Data storage	Feb 5,	May 3,	Jun 18,
2120	Science	Jan 2,	Mar 27,	Jun 18,
2190	Data input (STCDS)	Jan 2,	Jun 10,	—
2192	Facility instrumentation	May 3, 1968	Jun 18,	—
2194	Power distribution	Dec 19, 1967	Mar 26,	Jun 5,
2196	Central timing	Jan 29, 1968	May 3,	Jun 5,
2197	Ground command	Jan 4, 1968	Apr 29,	Jun 5,
2198	Central recorder	Jan 22, 1968	May 3, 1968	Jun 5, 1968

Shipment to AFETR. Launch complex equipment sets 1 and 2 were shipped to the AFETR November 7, 1968 and were delivered to the launch complex 36 blockhouse November 11, 1968. The single tractor/trailer used for shipment was not escorted.

Installation and checkout. Installation and checkout of *Mariner* Mars 1969 launch complex equipment and associated cabling was scheduled during the period November 11 to 23, 1968. Although operations started on schedule (Fig. 8), checkout was not completed until early January because of limited access to launch complex 36 caused by slippage in the launch of an *Orbiting Astronomical Observatory.*

Electrical verification of complexes 36A and 36B cabling included (1) loop resistance tests (no end termination), (2) no ground tests (with OSE connected), (3) shield isolation tests (with OSE connected), (4) facility power tests, and (5) operational tests using the complex equipment and the umbilical lines checker.

Shipment of system test complex 1. System test complex 1 from building 248 was shipped December 4, 1968 and was delivered to the AFETR December 9.

Shipment of system test complex 2 and STCDS 1. System test complex 2 (building 179) and STCDS 1 were shipped December 12 and were delivered to the AFETR December 16.

Installation of test of system test complexes 1 and 2. Following their arrival at the AFETR, system test complexes 1 and 2 were installed in the building AO complex area and tested. System test complex and test complex grounding interfaces with the STCDS were verified. All checkout was completed before spacecraft M69-2 power turn-on in January 1969.

Shipment of STCDS 2. System test complex data system 2 and its support equipment were shipped to the AFETR December 26, 1968 in an unescorted convoy. The convoy arrived and was unloaded at building AO on December 30.

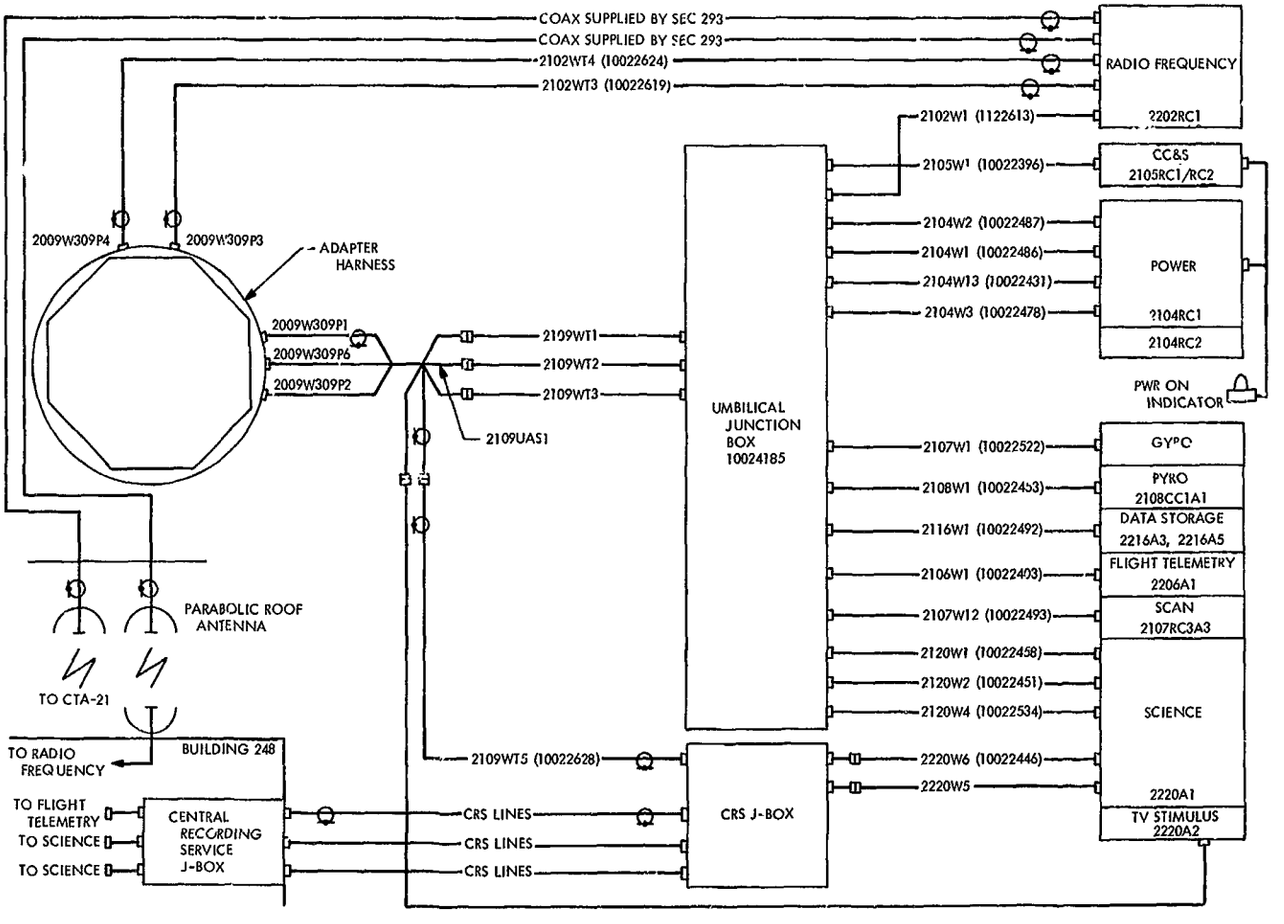


Fig. 27. Pseudo-launch complex equipment used for M69-1 vibration, acoustic, and pyrotechnic shock tests

PRECEDING PAGE BLANK NOT FILMED

Reliability and Quality Assurance

I. Documentation

The reliability and quality assurance programs for *Mariner* Mars 1969 were developed and implemented in response to NASA program level direction. The project approval document provided that the "Jet Propulsion Laboratory and other participating Centers . . . will establish and manage Reliability and Quality Assurance programs within their organizations and at their subcontractors to the degree necessary to satisfy over-all mission and project requirements . . . The status of these programs will be reported either separately or as part of the monthly progress reports."

Task Order RD-59 and Amendments 1 and 4 to NASA Contract NAS 7-100 required that "Particular emphasis shall be given to developing a simple, conservative and test verifiable design, the utilization of redundancy where a sufficient increase in reliability can be demonstrated, and a complete and integrated program of component, subsystem, and system testing to ensure mission success . . . . the Contractor shall establish and manage reliability and quality assurance programs within its organization and at its subcontractors . . . ."

Significant activities of the quality assurance effort included such conditions as (1) vendor surveys in support of source selections, (2) participation in source evaluation boards with assessment of proposer's quality assurance experience, capability, and planned efforts as a criteria for selection, (3) monitoring and inspection of hardware fabrication, assembly, and testing at subsystem contractors, (4) documentation of nonconformities and control of nonconforming hardware, (5) review and approval of data packages accompanying delivered hardware, (6) reviewing, inspection, and certification of all flight hardware delivered to JPL spacecraft assembly facility, (7) control of all flight hardware subsequent to delivery to spacecraft assembly facility, (8) monitoring of spacecraft assembly, test, and preparations for launch at JPL and AFETR. Selected parts of this activity are discussed in a separate quality assurance section.

Reliability assurance activities in support of the project, comprising efforts at subsystem, spacecraft system, and at project level, included (1) application of reliability engineering techniques to support design decisions and tradeoffs during the design development and evaluation

phase, (2) comprehensive review and assessment of parts and materials/processes, (3) failure mode effect reviews, (4) formal reviews of design and hardware, (5) comprehensive functional and environmental testing of hardware, (6) standardization of design practices, (7) monitoring and control of subcontractors and suppliers, (8) problem–failure reporting and corrective action. Selected areas of this activity are discussed in the following section.

II. Reliability Assurance Program

A. Organization

Reliability activities at all levels were implemented under the cognizance of or by the project reliability assurance group reporting to the project manager.

B. Basic Objectives and Guidelines

The basic objective of the *Mariner* Mars 1969 project reliability assurance program was to ensure maximum mission success possible with effective application of limited available resources. Guidelines and areas of emphasis in achieving this objective were stated in the following paragraphs.

(1) Vigorous and effective reliability assurance actions and surveillance in all phases of project activity from initial mission planning through preliminary design, detail design, development tests, fabrication, flight hardware testing, handling and transportation during all phases, final launch preparations, launch operations, and flight operations.

(2) Emphasis upon reliability actions that were most effective in the very early design and development phases. Of equal importance was a test program which effectively supported and complemented the design/development effort. Sources of unreliability were to be identified and analyzed effectively by a planned and monitored set of tests that were based upon consideration of design factors and mission requirements.

(3) The identification and elimination of all sources of unreliability within the limits of effective application of resources as the primary reliability goal of all design, development, and test activity. Residual items of unreliability were to be identified, described, and accompanied with an indication of possible actions required to eliminate the specific sources and a statement of resources required for timely implementation of such actions. This effort and data permitted system and project managements to allocate or reallocate resources as necessary, or to accept identified unreliabilities and direct planning of mission operations accordingly.

(4) The effective and timely use of techniques for reliability predictions, estimates, or apportionments during early design optimization efforts. Numerical goals, apportionments, or predictions developed in *Mariner* Mars 1969 activity, such as total mission probability of success statements, and system, subsystem, component, and parts level reliability goals and apportionments, were not considered as primary criteria that defined the satisfactory accomplishment of the basic reliability requirement for identifying and eliminating sources of unreliability during the design/development phase.

Application of numerical reliabilities or probabilities of success data developed in reliability engineering efforts supporting the design/development activity and mission development were limited to the following:

(a) Providing guidance for specific decisions in design optimization and tradeoffs during subsystem and mission analyses and development.

(b) Providing a basis for selecting the type and scope of reliability actions to be accomplished in the design optimization and unreliability identification and elimination efforts.

(c) Establishing priorities or relative criticality of competing tasks and problems.

(d) Indicating requirements for management attention and efforts.

(e) Providing a basis for allocation and necessary reallocation of resources by systems and project managements.

(5) Emphasis upon a contractor's responsibility for delivering quality hardware that included materials, parts, components, assemblies and services obtained from its subcontractors/suppliers.

(6) Emphasis placed upon early development phase quality activities that would preclude problems during subsequent fabrication, test, and flight operations.

C. Subsystem Reliability Assurance Plans

Each spacecraft subsystem was required to develop for project approval a plan defining activities, responsibilities, and outputs of reliability efforts to be implemented in support of the subsystem design, development, test, fabrication, checkout, and operation of its flight hardware and critical support equipment.

The source evaluation plans were prepared in a uniform format that was specified by project reliability assurance. The content of the plans covered all subsystem reliability efforts of both the subsystem contractor and the JPL cognizant section. The plans were usually published by the subsystem contractor following joint efforts of contractor's project and reliability group, the JPL subsystem cognizant section, and *Mariner* Mars 1969 project reliability assurance.

D. Problem/Failure Reporting

The problem/failure reporting program implemented by the *Mariner* Mars 1969 project provided a closed loop procedure for reporting, analyzing, defining corrective action, and verifying the accomplishment of correction. Project requirements provided for the origination of a report to document all incidents of failure, problem, malfunction, anomalies, and nonstandard or unexpected results. Reports were to be originated by anyone observing what was believed to be an incident or problem within the required scope that involved any item of proof test model, flight, or flight type hardware. Formal reporting was starting with whatever phase of fabrication/assembly/checkout (at JPL, the subsystem contractor or at his suppliers) of electronic hardware resulted in the first application of power to electronic and electromechanical piece parts subsequent to screening or receiving/inspection of such parts; for mechanical assemblies reporting started at the initial functional checkout of assemblies or subassemblies.

Provisions of the program provided very close communication and coordination between subsystem contractor, JPL cognizant engineer, and project reliability assurance.

Table 1 provides a summary of problem/failure reports by total project and by individual subsystem. The data includes both flight hardware and OSE problem/failure reports Figures 1 and 2 indicate the history of problem/failure reports in terms of accumulated total number and frequency per week.

Classification of individual problem/failure reports involved two systems as defined here: one system, employed at initial release of the problem/failure report (PFR), addressed itself to the criticality (*critical* or *noncritical*) of the reported incident; and a second, employed at the time of report close-out, assessed the adequacy of the verification, analysis, and corrective action to confidently preclude an occurrence of the incident during flight operations.

In the critical/noncritical assignment given to problem/failure reports at the time of initial release, *critical* was assigned if the occurrence of the failure or problem in flight would result in the loss or significant degradation of a subsystem or spacecraft function, including redundant and backup functions or elements. Also a *critical* was assigned where available initial data was not adequate to clearly support a noncritical judgement or where factors in the situation indicated some urgency in accomplishing the analysis. Results of analysis and corrective action were reviewed at the time of close-out to modify the critical/noncritical assignment if appropriate.

The second classification, assigned at the close-out of the problem/failure reports, assessed the adequacy of the overall effort and indicated the degree of risk or concern that an occurrence during flight had not been eliminated. The several categories of assignment were:

Closed. In those cases where analysis, corrective action and verification of correction was considered to have determined the cause, defined an acceptable correction that was both implemented and demonstrated to be a correction.

Closed–Unknown. Wherever it was judged that the problem/failure had not been confidently resolved since either the cause had not been determined, or the problem/failure could not be repeated in tests, or checkouts and analysis had not provided positive indication of the cause. *Unknown* also was assigned where resolution of an immediate problem or symptom appeared to be satisfactory, but underlying or undefined secondary causes were considered probable.

Closed–Risk. Where efforts that could be accomplished within constraints did not satisfy all doubts or concerns regarding the effectiveness of the corrective action or where correction was judged to be a symptomatic treatment without ensuring complete correction of the basic cause.

Table 1. Summary of problem/failure reports by subsystem

Subsystem	Total	Pre-Launch			Post-Launch	
		Total	Flight hardware	OSE	*Mariner VI*	*Mariner VII*
Spacecraft System	113	108	95	13	2	3
Structures	44	44	42	2	—	—
Radio	699	684	620	64	7	8
Command	188	186	117	69	1	1
Power	112	108	96	52	2	3
CC&S	204	197	179	18	—	6
Telemetry	147	143	94	49	—	4
Attitude control	619	610	548	62	5	4
Pyrotechnics	54	54	46	8	—	—
Cabling	60	60	28	32	—	—
Propulsion	52	51	48	3	—	1
Temperature control	72	70	69	1	—	2
Mechanical devices	50	49	49	—	1	—
Data storage	163	160	133	27	2	1
Data automation analysis	55	55	46	9	—	—
Scan control	114	114	107	7	—	—
Ultraviolet spectrometer	57	57	54	3	—	—
Television	225	224	221	3	1	—
Infrared spectrometer	118	117	114	3	1	—
Infrared radiometer	31	29	29	—	1	1
Science OSE	28	28	1	27	—	—
Command simulator	1	1	—	1	—	—
Telemetry simulator	11	11	—	11	—	—
Ground command	47	47	—	47	—	—
Central recorder	2	2	—	2	—	—
Environmental test	62	62	1	61	—	—
Spacecraft assembly facility	37	37	35	2	—	—
Environmental instruments	1	1	1	—	—	—
Compatibility test area	1	1	—	1	—	—
STC data system	8	8	1	7	—	—
Environmental requirements	3	2	—	2	1	—
Total	3378	3320	2734	586	24	24

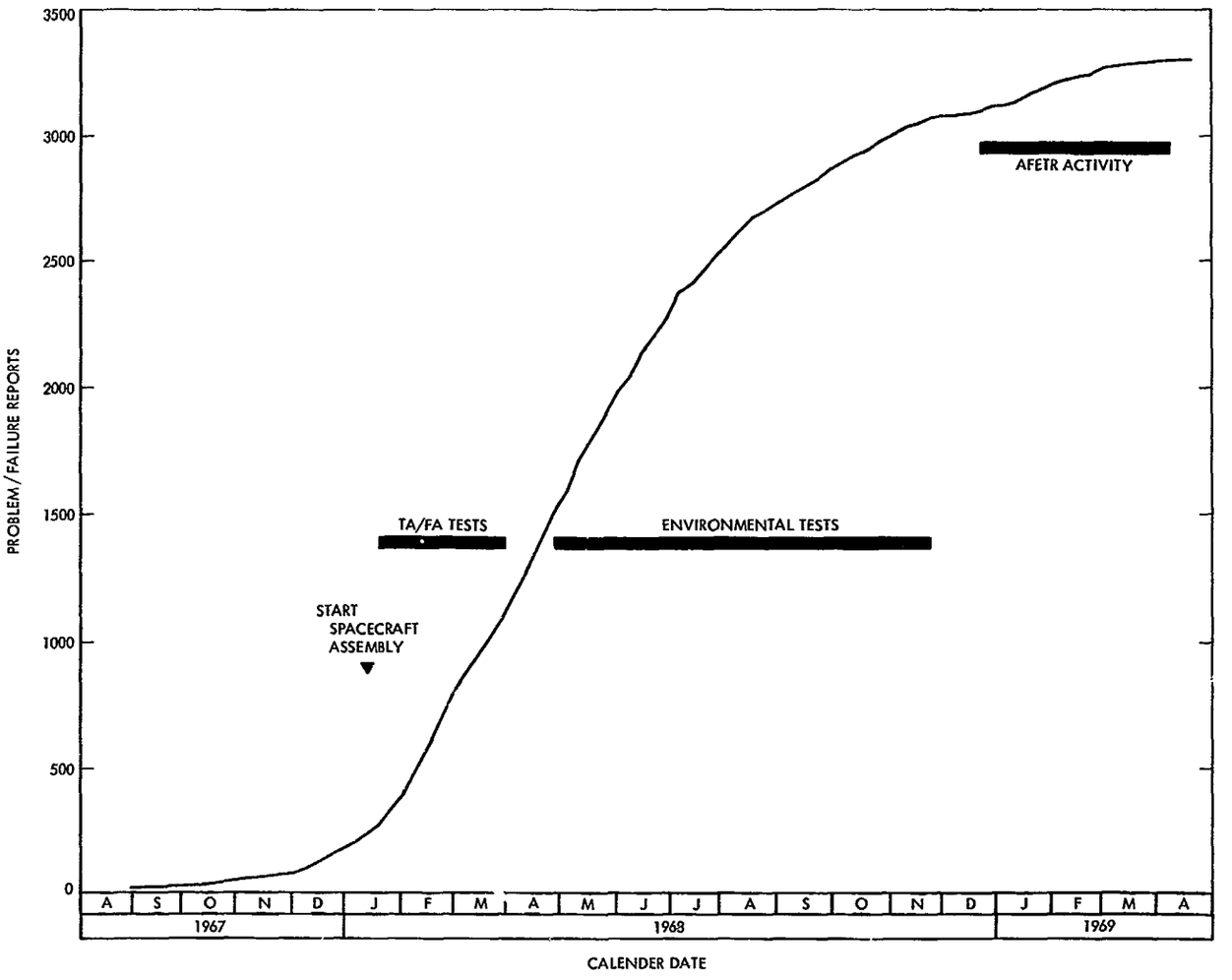


Fig. 1. *Mariner* Mars 1969 total problem/failure reports vs date, Spacecraft System flight hardware, and OSE

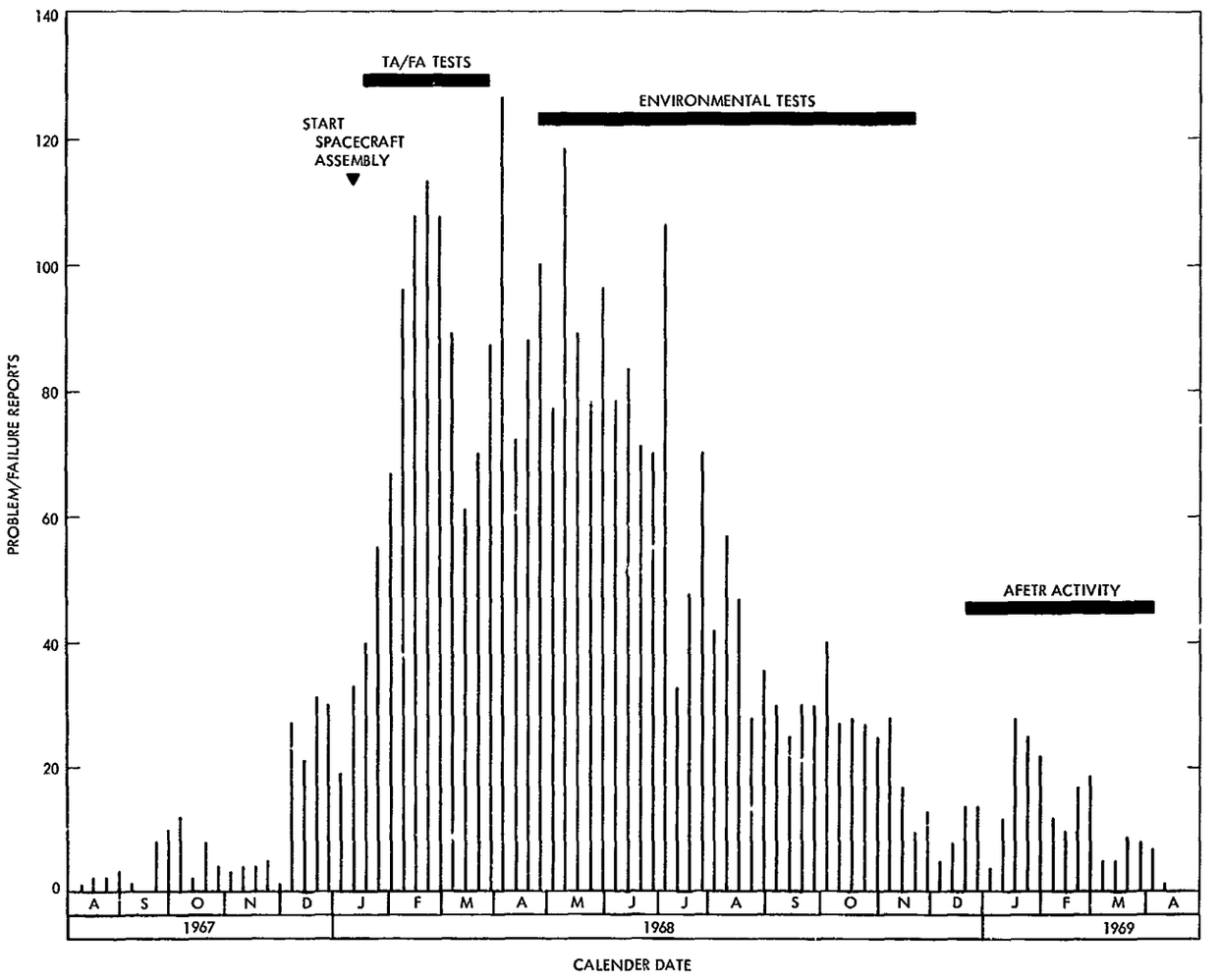


Fig. 2. *Mariner* Mars 1969 problem/failure reports per week vs date, Spacecraft System flight hardware, and operational support equipment

Open-project reliability assurance. Where resolution was considered to be unsatisfactory and further action by subsystem or Spacecraft System was precluded by constraints of time, resources, availability of hardware, or inability to define further effective actions. Where additional worthwhile action could be defined and could be implemented, the problem/failure report was reassigned to the cognizant subsystem pending completion of such activity.

Reports assigned to the *unknown* or *risk* categories comprised a group identified as *notables* (Table 2). Closure review and assignment was accomplished for all problem/failure reports. The closure classification assignment did not attempt to define the criticality to mission operations in the event the problem or failure occurred in flight.

Table 2. Summary of notable problem/failure reports

Subsystem	Closed-Unknown	Closed-Risk
Spacecraft system	10	14
Structures	2	0
Radio	22	47
Command	13	21
Power	6	2
CC&S	26	31
Telemetry	9	2
Attitude control	11	9
Pyrotechnics	2	7
Cabling	1	0
Propulsion	1	9
Temperature control	11	5
Mechanical devices	1	1
Data storage	19	17
Data automation system	5	18
Scan control	1	11
Ultraviolet spectrometer	3	2
Television	9	37
Infrared spectrometer	8	15
Infrared radiometer	5	8
Science OSE	1	0
Ground command	4	0
Radio	6	6
CC&S	1	1
Attitude control	0	7
Data storage	2	0
Infrared spectrometer	0	1
Infrared radiometer spectrometer	0	2
Total	183	278

Problem/failure reports were considered project "open" until

(1) Cognizant subsystem and section completed a verification and analysis of the problem/failure, a determination of corrective action, accomplished the corrective action, and verified that correction had been effective.

(2) Spacecraft System engineering completed a system-oriented review/analysis and follow-up to a concurrence with subsystem's analysis and corrective action.

(3) Project reliability assurance completed a review and follow-up for concurrence with the analysis, the corrective action, and the verification of correction.

The total number of problem/failure reports on the project, a high count compared with that of earlier *Mariner* projects, resulted from a combination of

(1) A comprehensive effort that delivered more effective PFR documentation of items at JPL and all subsystem contractors.

(2) A scope of items requiring and receiving PFR documentation that was significantly broader than for previous projects.

(3) A starting point for documentation that was earlier in the fabrication/assembly/test cycle than for previous projects.

(4) The production and complete system functional and environmental test of four flight-type spacecraft, a proof test model, and three flight-ready items.

E. Electromagnetic interference and Anomalous Performance Incidents

Monitoring of problem/failure reports and correlation of causes during spacecraft operations indicated a continuing and significant frequency of incidents associated with (1) EMI/EMC (electromagnetic interference/electromagnetic compatibility) problems, and (2) incidents of anomalous performance as opposed to performance failures.

The high incidence of EMI items being encountered during system test and checkout became an item of concern. Tables 3 and 4 provide a summary of results from an analysis of all project problem/failure reports. Those reports assigned to the *known* EMI category comprised those incidents where analysis and closeout data established EMI as the cause. A category of *suspected* EMI included those incidents with indications of probable EMI association. Incidents of anomalous performance but without at least some indication of EMI involvement were not included in the *suspected* category; it is likely that a reasonable percentage of the source evaluation anomalous performance incidents involved electromagnetic interference. A review of incidents involving anomalous performance in contrast to performance failures is summarized in Table 5. This study was limited to problem/failure reports written subsequent to the start of spacecraft performance. Individual reports were classified as a problem, failure, or anomaly and defined as follows:

(1) Problems were those incidents occurring not as a termination of performance but as an undesirable condition requiring analysis and correction.

Table 3. Subsystem summary of electromagnetic interference problem/failure reports, preflight and flight

Subsystem	Total	Internal	External	Closure status		
				Closed	Closed–Unknown	Closed–Risk
Spacecraft system	43	33	10	26	2	10
Radio	43 plus 2[a]	23 plus 2[a]	20	24	1 plus 2[a]	16
Command	31	5	26	25	2	4
CC&S	31 plus 1[a]	16	15 plus 1[a]	17	6 plus 1[a]	8
Attitude control	30	18	12	27	3	0
Data storage	30	13	17	24	5	1
Television	30	19	11	27	0	3
Telemetry	22	8	14	17	4	1
Infrared spectrometer	17	14	3	13	4	0
Infrared radiometer	10 plus 2[a]	6	4 plus 2[a]	8	0	2 plus 2[a]
Data automation	8	4	4	2	3	3
Power	8	2	6	7	1	0
Scan control	7	4	3	7	0	0
Science OSE	7	0	7	6	1	0
Ultraviolet spectrometer	5	5	0	4	1	0
Environment	5	0	5	5	0	0
Ground command system	4	0	4	3	1	0
Temperature control	4	4	0	1	3	0
Spacecraft assembly facility	4	2	2	4	0	0
Mechanical devices	2	1	1	2	0	0
STC data system	2	0	2	2	0	0
Pyrotechnics	1	1	0	1	0	0
Cabling	1	1	0	1	0	0
CTA-21	1	0	1	1	0	0

[a]Numbers shown as *plus* are flight electromagnetic interference problem/failure reports.

Table 4. Subsystem summary of electromagnetic pr

Subsystem	Total						Total known				Known internal				
	Total	Internal	External	Closed	Unknown	Risk	Total	Closed	Unknown	Risk	Total	Closed	Unknown	Risk	To
Spacecraft System	43	33	10	26	7	10	30	18	3	9	24	12	3	9	
Radio	45	25	20	24	1	18	32	18	0	14	17	5	0	12	1
Command	31	5	26	25	2	4	18	18	0	0	0	0	0	0	
Power	8	2	6	7	1	0	5	5	0	0	1	1	0	0	
Ground command	4	0	4	3	1	0	3	3	0	0	0	0	0	0	
Telemetry	22	8	14	17	4	1	15	13	1	1	7	5	1	1	
Attitude control	30	18	12	27	3	0	26	26	0	0	16	16	0	0	
Pyrotechnics	1	1	0	1	0	0	0	0	0	0	0	0	0	0	
Cabling	1	1	0	1	0	0	1	1	0	0	1	1	0	0	
Temperature control	4	4	0	1	3	0	4	1	3	0	4	1	3	0	
Mechanical devices	2	1	1	2	0	0	2	2	0	0	1	1	0	0	
Data storage	30	13	17	24	5	1	21	21	0	0	6	6	0	0	1
Data automation	8	4	4	2	3	3	3	2	0	1	1	0	0	1	
Scan	7	4	3	7	0	0	7	7	0	0	4	4	0	0	
Ultraviolet spectrometer	5	5	0	4	1	0	4	4	0	0	4	4	0	0	
Television	30	19	11	27	0	3	17	17	0	0	8	8	0	0	
Infrared spectrometer	17	14	3	13	4	0	12	12	0	0	12	12	0	0	
Infrared radiometer	12	6	6	8	0	4	6	5	0	1	4	4	0	0	
CC&S	32	16	16	17	7	8	21	13	1	7	8	7	0	1	
Environmental	5	0	5	5	0	0	4	4	0	0	0	0	0	0	
Science OSE	7	0	7	6	1	0	5	5	0	0	0	0	0	0	
Spacecraft Assembly Facility	4	2	2	4	0	0	2	2	0	0	1	1	0	0	
STC data system	2	0	2	2	0	0	2	2	0	0	0	0	0	0	
CTA-21	1	0	1	1	0	0	1	1	0	0	0	0	0	0	
Total	351	181	170	254	43	52	241	200	8	33	119	88	7	24	1

FOLDOUT FRAME

omagnetic problem/failure report analysis

rnal		Known external				Total suspect				Suspect internal				Suspect external			
nown	Risk	Total	Closed	Unknown	Risk	Total	Closed	Unknown	Risk	Total	Closed	Unknown	Risk	Total	Closed	Unknown	Risk
3	9	6	6	0	0	13	8	4	1	9	5	4	0	4	3	0	1
0	12	15	13	0	2	13	6	1	4	8	2	3	3	5	4	0	1
0	0	18	18	0	0	13	7	2	4	5	1	0	4	8	6	2	0
0	0	4	4	0	0	3	2	1	0	1	0	1	0	2	2	0	0
0	0	3	3	0	0	1	0	1	0	0	0	0	0	1	0	1	0
1	1	8	8	0	0	7	4	3	0	1	0	1	0	6	4	2	0
0	0	10	10	0	0	4	1	3	0	2	1	1	0	2	0	2	0
0	0	0	0	0	0	1	1	0	0	1	1	0	0	0	0	0	0
0	0	0	0	0	0	0	0	0	0	0	0	0	0	0	0	0	0
3	0	0	0	0	0	0	0	0	0	0	0	0	0	0	0	0	0
0	0	1	1	0	0	0	0	0	0	0	0	0	0	0	0	0	0
0	0	15	15	0	0	9	3	5	1	7	3	3	1	2	0	2	0
0	1	2	2	0	0	5	0	3	2	3	0	1	2	2	0	2	0
0	0	3	3	0	0	0	0	0	0	0	0	0	0	0	0	0	0
0	0	0	0	0	0	1	0	1	0	1	0	1	0	0	0	0	0
0	0	9	9	0	0	13	10	0	3	11	8	0	3	2	2	0	0
0	0	0	0	0	0	5	1	4	0	2	1	1	0	3	0	3	0
0	0	2	1	0	1	6	3	0	3	2	2	0	0	4	1	0	3
0	1	13	6	1	6	11	4	6	1	8	4	3	1	3	0	3	0
0	0	4	4	0	0	1	1	0	0	0	0	0	0	1	1	0	0
0	0	5	5	0	0	2	1	1	0	0	0	0	0	2	1	1	0
0	0	1	1	0	0	2	2	0	0	1	1	0	0	1	1	0	0
0	0	2	2	0	0	0	0	0	0	0	0	0	0	0	0	0	0
0	0	1	1	0	0	0	0	0	0	0	0	0	0	0	0	0	0
7	24	122	112	1	9	110	54	35	19	62	29	18	14	48	25	18	5

FOLDOUT FRAME
2

PRECEDING PAGE BLANK NOT FILMED

PRECEDING PAGE BLANK NOT FILMED

Table 5. Summary of analysis of problem/failure reports and anomalous performances

Flight hardware					
Total reviewed	660 (Post-start of spacecraft assembly)				
Anomalous performance:	514			78%	
Problems	120			18%	
Failures	26			4%	
Distribution by spacecraft					
	69-1	69-2	69-3	69-4	
Anomalous	212	131	110	61	
Problems	52	29	23	16	
Failures	7	9	8	2	
	271	169	141	79	
Probable cause of anomalous performance					
Design			126		24%
EMC[a] (design)			74		15%
Procedure error			70		14%
Configuration error			49		10%
EMI[b] (probable)			52		10%
Manufacturing discrepancy			34		7%
Part/Components			27		5%
Unknown cause			31		6%
EMI (OSE-induced)			14		2%
OSE-induced			3		—
Accidental damage			2		—
Operational support equipment					
Total reviewed			295		
Anomalous performance			242		82%
Problem			41		14%
Failure			12		4%
Probable cause of anomalous performance					
Part/Components			75		25%
Configuration error			43		15%
Design			33		11%
Unknown cause			23		8%
Manufacturing discrepancy			16		5%
Procedure error			17		6%
EMI (probable)			12		4%
EMI (design)			11		4%
EMI (OSE-induced)			11		4%
Accidental damage			1		—

[a]Electromagnetic compatibility.

[b]Electromagnetic interference.

(2) Failures comprised those incidents involving premature terminations, failures to turn on, and performance outside limits of specification requirements.

(3) Anomalies were those incidents involving incorrect response to commands and signals; performance within design specification limits but with undesired or unexpected characteristics such as instability, oscillations, toggling, drifting, etc.; unexpected response or performance such as glitches, spikes, transients.

F. Parts, Materials, and Processes Control

During the *Mariner* Mars 1969 program an effort was made to upgrade the control of parts and materials used in the flight hardware. Specific objectives included closer liaison with design agencies; more knowledge, particularly early in the design phase, of items and specific applications; review of items, applications, and control provisions by JPL parts and materials technical support groups to develop technical assessments in support of cognizant engineers; and increased efforts to influence initial selections or changes to those of more reliability or more general use.

Review and assessment covered combinations of data consisting of (1) parts type, or material, (2) specific applications, and (3) control provisions. This combination was treated as an integral item in the technical assessment made by the discipline support groups, and the assessment was expressed as a classification (class 1, 2, 3, or 4) reflecting the groups' judgment regarding the adequacy of all factors. The combination approach assured the proper application of inherently good items, and the adjustment of controls provisions accordingly.

Determining the optimum tradeoffs between functional performance, reliability, cost, and schedule was the responsibility of the cognizant engineer. Thus the classification system did not establish *approved* and *disapproved* ratings. Although the cognizant engineer was assisted by specialists from the discipline support groups who acted as technical advisors, the final decisions in tradeoff were the responsibility of the cognizant engineer, subject to design review and, in turn, Spacecraft System management review.

Classification and reporting requirements were limited by available resources to electronic and electromechanical parts. In these categories, 929 combinations were

reviewed, representing 602 separate part types with a listed piece part count of 24,515. Class 4 was assigned to 358 of the 929 listed combinations (38%). Table 6 shows that inadequate qualification and evaluation was a reason for the class 4 judgment in 258 of the 358 combinations (71%). Table 7 presents a summary of the estimated parts, by subsystem, and Table 8 presents a breakdown of parts classification.

G. Reliability Recommendations

An appraisal of experience during design, test, and operation of the *Mariner* Mars 1969 spacecraft resulted in the following recommendations for improving the effectiveness of subsystem, system, and project level reliability assurance efforts.

1. Design optimization/evaluation.

(1) Increased application of parts-level failure mode analysis where individual analyses are keyed to single functions of circuits or modules at the piece-parts next assembly level. A series of such single function analyses would combine in a sequence covering individual subsystem functions and thus correlate directly to mission operations functions.

(2) Earlier and more complete acquisition and review of data regarding parts-type selections, functional requirements, and design application factors.

(3) Implementation of an effective EMI/EMC program with emphasis on an early check of designs for potential sources and sensitivities, checkout

Table 6. Summary of class 4 combinations: electronic and electromechanical parts

Subsystem	Combinations listed in documentation	Combinations in class 4	Reason for class 4 status[a]			
			Inferior parts type	Application data not available	Inadequate qualification [illegible] luation data	Controlling documents: provisions inadequate
Structure						
Radio	130	[illegible]	3		60	31
Command	31	6			6	
Power	89	42	2		42	
CC&S	46	16	8	1	7	
Telemetry	58	45		1	17	28
Attitude control	87	15	2		14	
Pyrotechnics	20	1			1	
Cabling	—	—				
Propulsion	—	—				
Temperature control	40	6	2		4	
Mechanical devices	2	0				
Data storage	76	44	1		19	24
Data automation	45	9	1		8	
Scan control	48	15			15	
Ultraviolet spectrometer	58	14			15	
Television	106	34	1		33	
Infrared spectrometer	53	12			12	
Infrared radiometer	37	5	—	—	5	—
Total	929	358	20	2	258	83

[a]No combinations in class 4 due to inferior design application or to unavailable controlling documentation.

tests of breadboards and engineering prototypes, an improved presentation of required [illegible] practices and prohibitions as being more [illegible]ive than a general design performance requirement, and involvement in analysis of early and continuing problem/failure reports indicating electromagnetic interference or anomalous performance.

Early test checkout should be emphasized by not permitting proof test model, type approval, or flight subsystem hardware or assembled spacecraft to be committed for planned periods of EMI survey type of checkouts. With effective early checkout of breadboard and prototype items, and including check of known inter-subsystem interfaces, the normal functional and environmental testing at spacecraft system level would provide ample opportunity to detect remaining system interface related items; the requirement to check the complete spacecraft for compatibility with external environments, such as launch vehicle and pad, is an exception.

2. Parts reliability.

(1) Improved acquisition and review of data regarding control provisions, earlier acquisition, and complete coverage. Specific and more comprehensive definition of requirements in subsystem requirements documents and the contract statement of work and the delivery schedule.

(2) Development and application of standard procedures for failure analysis of parts and for data to be derived during the analysis. Acquisition and

Table 7. Electronic and electromechanical parts: estimated count in complete design

Subsystem	Capacitors	Controlled rectifiers and switches	Crystals	Diodes and rectifiers	Fuses	Inductors	Microcircuits	Photosensitive devices	Resistors	Thermistors	Transformers	Transistors	Motors	Potentiometers	Relays	Switches	Other Devices	Estimated number of parts in complete design
Structure	—	—	—	—	—	—	—	—	—	—	—	—	—	—	—	—	—	—
Radio	744	0	3	385	0	122	4	0	908	2	35	183	0	2	11	0	100	2499
Command	188	0	0	371	0	3	145	0	925	0	86	365	0	0	0	0	—	2083
Power	131	4	2	368	41	7	17	0	421	—	47	77	0	1	9	1	4	1130
CC&S	118	0	0	985	6	75	343	0	897	0	9	329	0	0	119	0	—	2881
Telemetry	495	0	2	442	9	60	583	0	1355	0	20	667	0	0	12	0	—	3645
Attitude control	274	5	0	351	0	2	31	19	738	0	24	138	4	0	25	0	4	1615
Pyrotechnics	96	22	0	54	4	0	0	0	194	0	6	26	0	0	12	0	—	414
Cabling																		0
Temperature control (including TCFM)	71	0	0	95	2	1	120	17	577	0	5	84	0	0	0	0	0	972
Mechanical devices	0	0	0	0	0	0	0	0	6	0	0	0	0	0	0	15	0	21
Data storage	318	0	1	358	1	37	338	8	1466	0	19	418	2	0	0	0	—	2966
Data automation	196	12	2	162	0	2	653	0	402	0	55	107	0	0	0	0	—	1591
Scan control	80	0	0	120	0	4	44	3	216	0	6	61	6	8	10	0	—	558
Ultraviolet spectrometer	218	1	0	125	0	34	32	2	477	5	5	100	1	0	1	0	6	1007
Television	350	0	0	309	0	12	421	0	971	0	6	255		18	0		4	2355
Infrared spectrometer	115	0	0	211	4	0	13	1	413	0	2	118		0		0	0	877
Infrared radiometer	81	0	0	60	2	0	15	0	245	3	1	105	1	0	0	0	0	509
Total	3454	44	10	4396	69	359	2759	50	10,211	10	326	3033	14	29	199	16	118	25,127

Table 8. Subsystem use of acquired parts

Parts type	Data automation system (BAAA)	Analog-to-pulse-width converter (BAAF)	Ultraviolet spectrometer (BAAG)	Pyrotechnics (BAAH)	Infrared spectrometer (BAAI)	Infrared spectrometer (BAAJ)	Television (BAAK)	Central computer and sequencer (BAAL)	Solar panel (BAAM)	Spacecraft power supply (BAAU)	Scan (BAAQ, BAAO, BABG)
A Crystals	6										
B Cores										239	
C Capacitors	447	1,430	3,304	297	987	1,860	5,156	2,517		598	110
D Diodes	1,868	2,170	1,376	270	866	2,245	3,276	11,234	514	671	187
E Controlled rectifiers			22	18							
F Fuses				200	75	107		510		201	
G Transducers										87	
J Connectors								76		4	
K Relays			10	47		15		1,312		28	17
L Chokes	30		309				115	2,488			32
M Miscellaneous			18		18		16			205	
N Thermistors		200	135		75						
P Variable resistors							314			12	46
Q Transistors	47	1,215	1,002	95	1,282	1,588	2,795	3,782		604	96
R *Fixed resistors*	420	3,236	5,013	420	4,534	6,537	19,386	17,341	213	2,28[illegible]	497
S Switches							82				
T Transformers	37	250	21	11		22	88	120			
U Tuning forks											
W Vacuum tubes							4				
Y Microcircuits			406		124	113	4,524	3,615		42	55
Z Special semiconductor											
Total subsystem parts acquired	2,859	8,501	11,586	1,358	7,968	12,487	35,756	42,995	727	4,972	1,040
Total subsystem parts screened	2,101	5,638	10,169	1,080	6,726	11,638	34,427	38,279	722	1,503	158
Percent procured parts screened	76%	66%	87%	79%	84%	93%	96%	89%	99%	30%	15%
Number parts required for subsystem	1,140	804	971	378	519	1,306	2,153	2,881	160	950	552
Total number parts screened[a]	1,914	340	6,472	—	3,796	5,626	25,947	17,527	118	499	—

[a]By Litton, Mid-Continent Labs, and Continental Test Labs.

Table 8 (contd)

TCFM (BAAP)	Mechanical devices (BAAU)	Battery (BAAX)	Attitude control Canopus sensor (BAAW, BAAZ)	Data storage (BAAC)	Backup (BABF)	Quality test (BQAA)	Total acquired parts	Total number parts screened by parts type	Average yield, percent (after JPL final review)	Total number parts[a] by parts type	Parts type
							6				A Crystals
							239				B Cores
1,193			16	30	2,342		20,284	18,694	79%	11,846	C Capacitors
1,460		30	8		2,305	1,564	30,014	27,575	71%	11,139	D Diodes
							40	37	56%		E Controlled rectifiers
90		40			540	280	2,043	1,583	62%		F Fuses
							87	71	7%	42	G Transducers
							80				J Connectors
							1,429	1,306	85%	206	K Relays
15							2,989	2,766	82%	2,333	L Chokes
							264	37	85%		M Miscellaneous
							410	179	88%	153	N Thermistors
							372	353	68%	211	P Variable resistors
998	40		9	115	1,679		15,317	14,295	62%	7,032	Q Transistors
7,330	239		637	21	1,527		69,432	55,787	92%	38,304	R Fixed resistors
							322	305	90%		S Switches
97							646	628	74%	144	T Transformers
											U Tuning forks
							4				W Vacuum tubes
768			8				9,655	9,013	86%	1,609	Y Microcircuits
			196				196	98	79%		Z Special semiconductor
11,948	279	70	874	166	8,393	1,844	153,829		82% overall yield		Total subsystem parts acquired
9,854	269	70	868	166	8,035	1,024		132,727			Total subsystem parts screened
82%	96%	100%	99%	10%	95%	55%			86%		Percent procured parts screened
970	21	2	1,606	2,963	—	—					Number parts required for subsystem
8,096	—	—	—	—	—	—				73,018	Total number parts screened[a]

correlation of parts failure analysis data for all analyses performed by subsystem contractors. Performance of parts failure analyses at JPL in all possible cases.

(3) Acquisition and correlation of screening results from subsystem contractors to allow for identification of repeating problems, poor design features, low yield, rejections associated with design configuration changes/faults, manufacturing defects, or process control problems. Screening data should be submitted immediately upon completion of screening for each lot.

(4) Development of a more detailed set of requirements for parts stress analyses and application parts derating criteria.

(5) Development as a part of the preferred parts list provision for conveying guidance to designers regarding at least a best available (i.e., preferred) part for all functions; necessary restrictions, cautions, and problems should be stated.

(6) Improvement in the efficiency and capability of the JPL parts acquisition, screening, and handling activity. The objective should be maximum practical acquisition of parts for all subsystem and science instruments. Specific efforts should be directed to more efficient procurement processing, effective technical followup/monitoring of suppliers by parts engineering, a control facility for parts receiving, physical inspection, stocking, and delivery to subsystem use.

3. Parts documentation.

Listing review, analysis, and classification of purchased devices similar to procedures intended for these parts.

4. Functional failure mode analysis.

Implementation of a correlated failure mode analysis program oriented to individual functions from circuit/module (piece parts) to mission level. Correlation of problem/failure reports with these analyses would provide maximum assessment of flight hardware and a direct association with flight operations

5. Problem/Failure reporting and analysis.

(1) Increased capability of analyzing and correlating problem/failure reports in terms of cause, phase of activity, technical factors, serialized hardware items, and actual spacecraft configuration.

(2) PFR documentation of all incidents of anomalous performance. This coverage should include incidents where performance is within upper and lower limits of spec requirement, but with dynamic characteristics that are abnormal, undesirable, or not anomalous (i.e., drift, oscillations, toggles, steps, glitches, etc.).

(3) Compliance with requirements to identify in problem/failure reports the hardware item serial number and the accumulated operating time at time of failure. Both items are significant in correlating problem/failure data. Association with hardware serial number is required to provide a summary of PFR incidents correlated with an as-launched spacecraft hardware configuration.

6. Contamination.

Upgrading of spacecraft contamination requirements and procedures for more effective control of this spacecraft characteristic.

7. Test plan correlation.

Review of system test plans and procedures for a comparison with spacecraft and subsystem modes and the results of a correlated failure mode analysis.

III. Quality Assurance Program

The *Mariner* Mars 1969 quality program was based on a series of requirements and activities which take place during the various program phases, all directed toward ensuring maximum mission success. Later sections of this report describe these requirements and outline the basic quality assurance program activities.

A. Organization and Management

Figure 3 illustrates the quality assurance organization. Within the framework of this organizational structure, the quality assurance functions, encompassing management, quality engineering, surveillance, and inspection are performed. A quality assurance representative was assigned to the project to provide quality program planning and to establish the requirements for all quality assurance activities in support of the project. In this role,

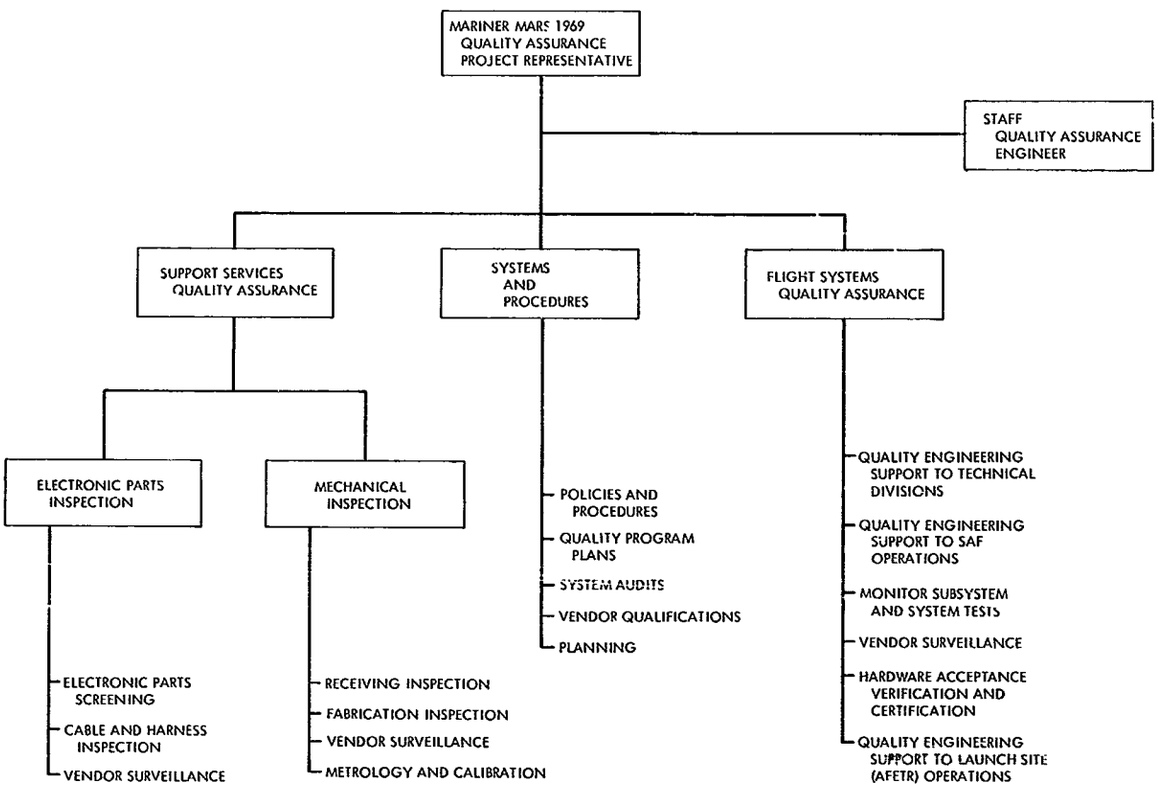


Fig. 3. JPL quality assurance organization, *Mariner* Mars 1969 project

the quality assurance representative was delegated commensurate authority by the manager of the Spacecraft System to accomplish the following:

(1) Develop and implement the quality assurance program at the various project levels responsible for the design, development, fabrication, test, and flight operations.

(2) Establish guidelines for, and approval of, contractor quality assurance plans.

(3) Audit the accomplishment and effectivity of quality assurance program activities, wherever conducted; and notification to the project of such information.

(4) Investigate quality problems and recommendation of quality improvement actions to the Spacecraft System manager and his staff.

(5) Arrange for quality assurance activities requisite to the acceptance and certification of flight configuration hardware and associated support equipment.

(6) Preparation (or review and approval) of quality assurance provisions sections of specifications issued by JPL for use by the *Mariner* Mars 1969 project.

In support of the implementation of these responsibilities, quality assurance engineers were assigned to each spacecraft subsystem on a full-time basis. The quality assurance engineers were responsible for conducting quality activities at JPL and at subsystem contractors, as necessary, to ensure the conformance to project and contractual quality requirements and were also responsible for providing support to the cognizant technical divisions' development and delivery of flight quality hardware.

B. Quality Task Elements

An essential part of the quality assurance program was the identification of all quality functions by task elements. Toward this objective the project quality assurance representative was required by project management to develop a quality assurance program plan and coordinate the development of such subordinate program plans at system, subsystem, or lower levels as considered essential

to accomplishing project requirements. The tasks, activities, and responsibilities defined by the project plan included implementation of appropriate provisions of the NASA quality publication NPC 200-2, the JPL quality policies, and the consideration of conditions and requirements unique to the project. Figure 4 illustrates the origin and areas of implementation of quality documents that governed the *Mariner* Mars 1969 quality program activities. The project plan included, but was not limited to, the following quality task elements and required actions by JPL quality assurance to implement and monitor these tasks.

1. Planning. Initial quality planning was accomplished at JPL with the project quality assurance representative participating in the review and generation of input material to the governing project requirements documents. Included was the establishment of quality requirements for subcontractors and the formalization of the total *Mariner* Mars 1969 quality program policy.

2. Procurement review. Procurement approach required that use be made of industrial support while maintaining adequate control by JPL in both management and engineering areas. Competition by industry was used for all contracts as much as possible, and source evaluation board procedures were used on all contracts over one million dollars. Each procurement initiated by the technical divisions to purchase services and equipment was supported by JPL quality assurance in the following areas of activity:

(1) Membership on source evaluation boards and associated evaluation subcommittees for competitively negotiated major procurements.

(2) Reviewing procurement documentation, i.e., requests for programming, technical statements of work, etc., for inclusion of applicable quality requirements.

(3) Providing technical divisions and procurement with information concerning contractor quality system capabilities derived from previous and current quality survey efforts.

(4) Participating in contract negotiations to interpret and clarify quality requirements, and to analyze contractor cost elements related to quality activity.

3. Control of procurement sources. Project quality assurance prepared and issued procurement control documents which provided subsystem contractors and science instrument investigators with directions for planning, developing, and implementing a quality program. These documents directed the contractors to make maximum use of their existing quality system in complying with the JPL requirements.

To ensure an effective interface with the JPL technical divisions on matters pertaining to quality, it was established that the review and approval of all contractor quality plans would be a joint effort by both JPL quality assurance and the technical divisions. This method proved to be of significant value as it improved communications with the technical divisions, and identified the project quality elements to technically oriented personnel during the design and development phases of the program. Quality representatives from JPL were assigned on a resident or itinerant basis at each contractor facility. The responsibilities and authorities of the representatives included:

(1) Monitoring and auditing contractor's quality assurance activities to assure compliance with the JPL quality assurance plan.

(2) Participating in design reviews of drawings, specifications, and technical documents.

(3) Establishing and performing JPL mandatory hardware inspections at the contractor's facility with contractor inspection procedures and instructions approved by JPL.

(4) Monitoring specific test operations.

(5) Participating in the disposition of all nonconforming material and acting as "government representative" on all material review boards.

(6) Performing final inspection at the contractor's facility before delivery of hardware to JPL.

(7) Verifying the accuracy and completeness of the contractor's end-item data package.

Quality representatives in the field were supported by other elements of the JPL quality organization; i.e., electronic parts inspection, mechanical inspection, systems and procedures, and spacecraft assembly facility quality assurance.

4. Acceptance and test verification. Contractually delegated contractor quality assurance personnel or JPL were required to witness all type approval and flight acceptance assembly and system level environmental tests.

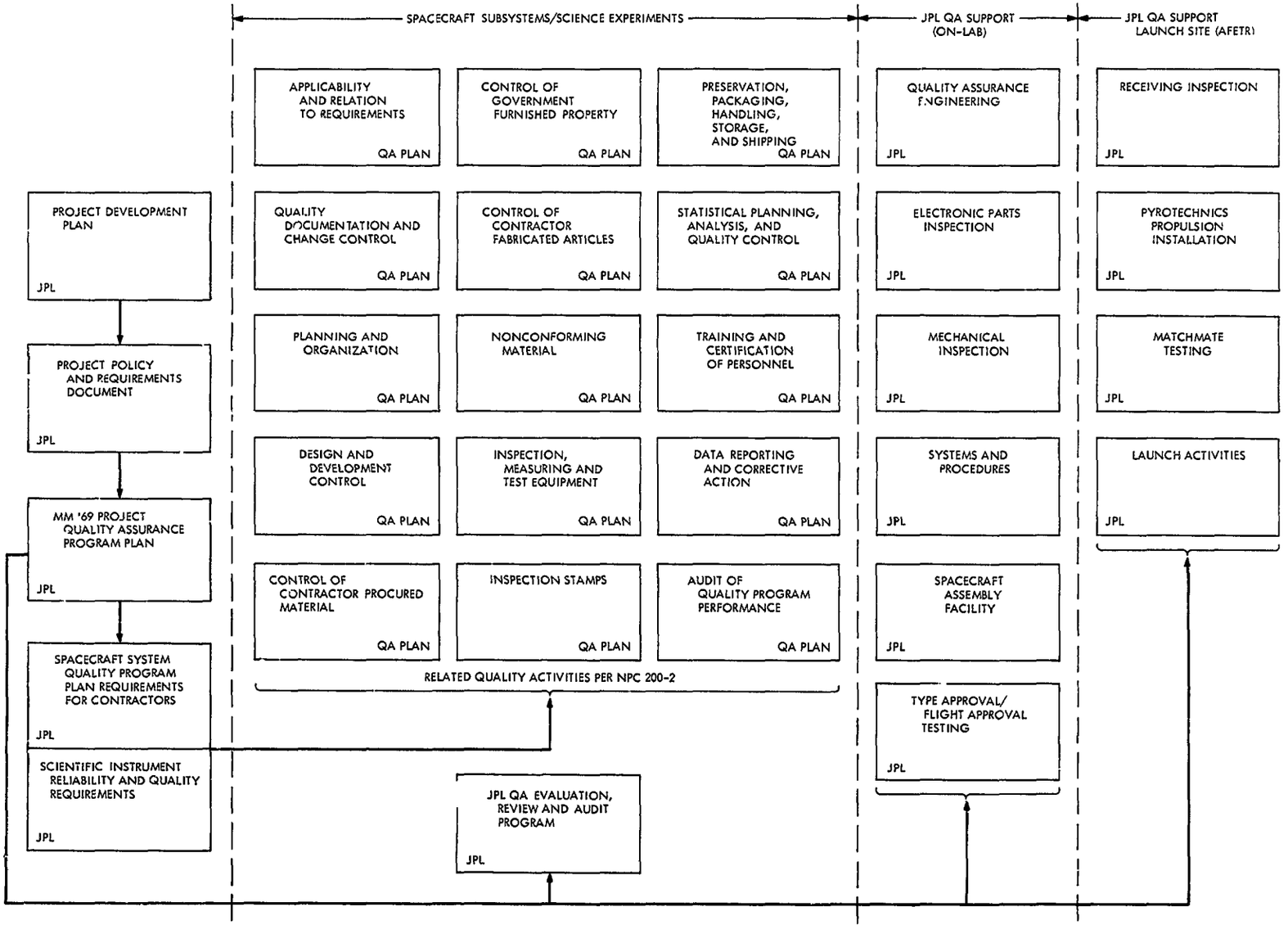


Fig. 4. Origin and implementation areas of governing quality documents, *Mariner* Mars 1969 project

Specific quality activities included verifying (before the start of testing) that all applicable procedures and deviations had been approved; certifying that testing was conducted in accordance with provisions of approved procedures; certifying the completion of all documentation regarding procedure sequence check-off and summary of test results; and re-establishing required quality surveillance of the equipment following completion of testing.

5. Subsystem hardware reviews. Under the direction of project management, hardware reviews were required at the subsystem level on all proof test model and flight hardware as a condition for delivery to the spacecraft assembly facility. These reviews were to provide records reflecting the results of testing, quality control, manufacturing, and logistics operations.

The information required for the hardware reviews included the completion of the *Mariner* Mars 1969 hardware review/certification requirements form (Fig. 5) to serve as the written output of the review and certification of the hardware. In support of the implementation of hardware reviews, JPL quality personnel were responsible for the submittal of support data to the review board, reflecting the complete quality history of the hardware, including inspection status and material review activity.

6. Spacecraft assembly facility. Quality assurance (JPL) supported the spacecraft operations manager by maintaining control of all hardware (flight and operational support equipment) delivered to the spacecraft assembly facility. This was accomplished with the implementation of quality assurance procedures which established requirements for delivery, storage, inspection, documentation, and removal of hardware from the spacecraft assembly facility. Specifically, SAF quality assurance activities and areas of responsibility included the following:

(1) Performing appropriate inspections of all hardware as part of the certification process.

(2) Maintaining a bonded stores within the spacecraft assembly facility.

(3) Monitoring spacecraft buildup and pertinent test operations.

(4) Maintaining a daily log on status o significant activities and buildup configuration of each spacecraft

(5) Reporting and documenting all anomalies, unusual circumstances, and problems.

(6) Surveillance over the packaging and movement of the spacecraft in preparation for delivery to the launch site at the AFETR.

7. Launch site quality assurance. Quality assurance personnel of JPL were assigned to the AFETR to provide proper quality coverage at the launch site. Assigned quality personnel were responsible for performing and properly documenting the inspection and surveillance of spacecraft operations which included equivalent activities performed at the spacecraft assembly facility at JPL.

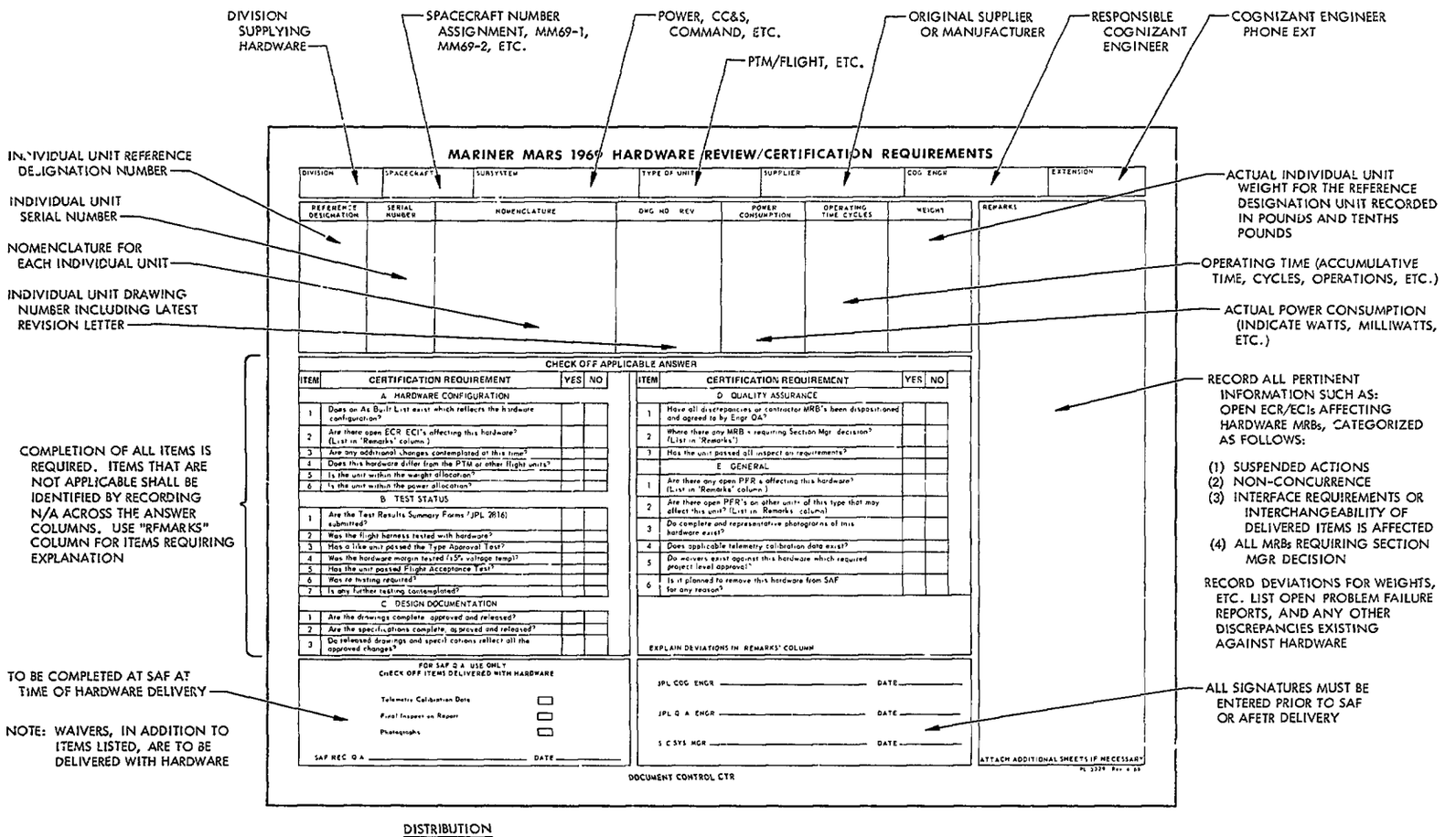
8. Quality performance reporting. The principal method of reporting quality program status to the *Mariner* Mars 1969 project office was by means of the weekly project quality status report. This report, prepared and issued by the project quality assurance representative, consisted of two sections: (1) narrative explanations of significant events accomplished (refer to Fig. 6 for typical report); (2) an itemized listing of significant problems requiring action (refer to Fig. 7 for typical report). Input material to these reports was derived from JPL quality representatives in the field (weekly TWX) and from weekly activity reports of the on-lab quality assurance engineers. This method of reporting proved to be of significant value, as it provided project management with a timely and factual view of contractor performance and identification of existing and potential problems.

C. Problem Areas

The *Mariner* Mars 1969 program was not free of problem areas. During the negotiations phase, significant problems were encountered with the NASA (NPC 200-2) requirement for the submittal of a preliminary quality program plan by the contractor within 45 days after contract award. As a result of this requirement, contractors participating in negotiations were not prepared to present, in sufficient detail, their planned quality actions and related cost elements. In numerous instances, negotiations were concluded without putting into final form the scope of quality activity and without even rough estimates of cost. The consequences of this situation are too numerous to dwell on; however, some of the prominent outgrowth of this problem included (1) inadequate quality participation during design/development phase because of the late statement defining required quality actions, (2) milestones slipped relative to the preparation

INSTRUCTIONS FOR COMPLETION OF MARINER MARS 1969
HARDWARE REVIEW/CERTIFICATION REQUIREMENTS FORM

THIS FORM MUST BE USED TO RECORD PERTINENT INFORMATION
TO CERTIFY HARDWARE DELIVERY TO SAF AND AFETR



DISTRIBUTION

WHITE - DOCUMENT CONTROL CENTER
CANARY - ENGINEERING DATA MANAGEMENT GROUP
BLUE - COGNIZANT ENGINEER
PINK - SPACECRAFT INSPECTION
GREEN - SPACECRAFT SYSTEM MANAGER
GOLDENROD - COGNIZANT QA ENGINEER

Fig. 5. Hardware review/certification requirements

PROJECT
QUALITY STATUS REPORT

TECHNICAL DIVISION	REPORTING PERIOD
33	2-26-68 through 3-1-68
PROGRAM	QUALITY ASSURANCE
Mariner Mars 1969	H. Wilkeyson
DIVISION REPRESENTATIVE	
N. de Groot	

FCS at MOTOROLA

1. The PTM unit has been returned to Motorola for repair as a result of a failure detected during post thermal-vacuum functional test.

2. A meeting was held at Motorola on February 27-28, 1968 at the request of JPL quality assurance and Division 33 management, to discuss the cracked solder joint problems, previously reported, and to obtain corrective action from Motorola.

   Prior to this meeting, cracked solder joints were found in boards of flight units #s 2 and 3. Investigation and analysis to date, per Motorola's evaluation, indicates that the problem was caused by the type of handling fixture utilized in assembly, and the flexibility of the boards. The handling fixture is presently being modified.

   Subsequent to the meeting, flight unit #1 was returned to Motorola, inspected, and found to contain cracked solder joints also. The PTM unit will be inspected to determine its condition.

RFS at PHILCO-FORD

3. The previously reported welded module problem is being resolved. Presently, Philco-Ford is implementing the following controls:

   a. Verification of the Allen Bradley 1/4-W resistor lead material.

   b. Verification of weld schedules by utilizing clippings from MM69 RFS flight components.

   c. Weldability checks will be made for each different type of lead and geometry for each module kit.

   Both JPL and Philco-Ford quality assurance will closely monitor these activities.

DSS at TEXAS INSTRUMENTS

4. Due to the present heavy work schedule, the investigation of the previously reported connector soldering problem has slowed down considerably. Texas Instruments has demonstrated, however, that after a considerable amount of rework and x-raying the connectors are acceptable.

11 JPL 3254 (1-68)

Fig. 6. Narrative explanations of significant events, typical report

Subsystem	Subcontractor	Quality Assurance Engineer
TV Electronics	EOS	

Item	Subject	Description	Action
9 0193 12-15	Qualification Testing of Weld Samples	Formal written approval of the qualification testing of weld samples submitted from ATC through EOS has not been granted Qualification is a requirement of JPL Specification FS 501495, Parallel Gap Resistance Welding. This problem, reported for several weeks, has not been resolved at this time MRB's will be utilized until problem is resolved. Technical Division 32 is aware of the problem	Resolution by Division 35 process personnel is requested. EOS has given verbal approval to ATC based on photo-micrographs of weld samples submitted. However, samples were sectioned in wrong plane not in accordance with specification. Prior to flight fabrication weld qualification will have to be repeated in accordance with JPL Spec FS 501495. Item remains open January 6, 1968. Item remains open January 20, 1968. EOS has formally waived the requirement for ATC to furnish weld samples for qualification based on satisfactory results on the PTM hardware. JPL Quality Assurance does not concur with this decision and strongly requests that weld qualification be accomplished prior to flight hardware fabrication. Item remains open as of January 26, 1968 No resolution as of February 9, 1968.

Fig. 7. Typical itemization of significant problems

of controlling quality procedures and standards, (3) little or no learning curve established during prototype construction. It took considerable and often very tedious post-negotiations to bring about the final statement of contractor quality plans and establish suitable corrective actions where required.

During the fabrication/assembly and test phases of the program, problems were also encountered with contractors supplying hardware which exhibited poor workmanship, lacked proper documentation, or failed to satisfy specific technical requirements. These problems were usually traceable to uncontrolled areas of processing, fabrication and assembly, inadequacies in basic design, or the failure of some contractor to work to established plans. The following discussion identifies significant problem areas associated with the *Mariner* Mars 1969 hardware fabrication and those subsystems affected:

1. Cracked solder joints. Inspection of the solder connections on the flight command subsystem resulted in the detection of cracked solder joints between welded modules and mother boards. Investigation and analysis indicated that the problem was caused by the type of handling fixture used in assembly, flexibility of the boards, and method of soldering. After several weeks of concentrated effort by both contractor and JPL quality assurance engineering, a method of rework was determined and accomplished on all affected flight units. To prevent recurrence of the problem, the contractor made the following changes in fabrication/assembly processes: (1) improved handling fixture to relieve stresses, (2) replaced machine soldering by hand soldering, (3) improved tinning techniques. Inspection of the reworked units showed that the new assembly techniques had eliminated the problem.

2. Cracked integrated circuits. The problem of the cracked integrated circuits associated with the data automation subsystem was detected during a JPL mandatory in-process inspection point. Investigation revealed that the cracks were appearing adjacent to leads and were not visible before or at the time of installation. In looking for possible causes for the cracking, it was found that the vendor supplying cases to the IC manufacturer had changed material just before the *Mariner* Mars 1969 buying had taken place. Further findings resulting from studies of assembly techniques, case material, and mounting configuration identified the case material as the prime contributor to the cracking problem. Hardware delivery schedules ruled out the possibility of a complete new procurement since the integrated circuits were a 26-wk lead-time item.

The decision was made to continue the assembly of the data automation system in parallel with an extensive evaluation and life test program, for the purpose of analyzing effects on functional performance and reliability. During this evaluation, methods were established to more clearly define criteria for acceptance or rejection based on leak testing and microscopic visual examination data. After several thousand hours of life testing, no failures could be attributed to the cracking problem. From the engineering evaluation and analysis, the data automation system was accepted as flight-worthy and was delivered to the spacecraft assembly facility.

3. Workmanship/System discrepancies. During the fabrication and assembly phases of the radio subsystem numerous workmanship discrepancies were identified by resident JPL quality personnel at the contractor location. In addition, weekly quality status reports from resident personnel indicated major quality system deficiencies in the areas of documentation, process controls, personnel training and certification, subcontractor control, and quality management. The detection of quality system deficiencies with "out of control" conditions existing in many areas coupled with the numerous workmanship deficiencies were considered detrimental to product quality. In the opinion of JPL quality assurance, these

conditions made a "tear down" inspection of the radio subsystems a necessity, to verify hardware integrity. As a result of JPL quality insistence, a "tear down" inspection was performed at JPL on all flight radio subsystems which consisted of radio frequency subsystem receivers, exciter power supplies, and T-frame modules. As a result of this inspection, a total of 187 discrepancies were found; of these, 143 were reworked and the remaining 44 were returned for use "as is". Numerous types of discrepancies in workmanship were identified, with the leading types being categorized as follows: (1) missing conformal coating, (2) broken component end seals and leads, (3) inadequate spot-bonding, (4) improper component mounting, (5) cracked solder joints, (6) cracked and chipped components.

Rework consisted of retrofitting, replacing, and inspecting all defective parts—including resistors, diodes, capacitors, wiring, inserts, etc.—, reprocessing of soldering, and adding solithane and stycast. The radio frequency subsystems were requalified by performing selected flight acceptance tests. With the completion of testing, the concern of JPL quality assurance personnel was relieved and the radio subsystems were accepted as flightworthy.

D. Quality Assurance Recommendations

The following is a list of recommendations which should help to alleviate problems associated with the implementation of quality assurance programs:

(1) Each contractor should be required to submit as part of his proposal or bid, a quality program plan in sufficient detail to provide a basis for its negotiation before a contract is awarded.

(2) Project controlling documents relative to quality assurance requirements for subsystem contractors should specify the required quality actions in detail instead of in generalized statements, in order to minimize interpretations and clarifications during negotiations.

(3) Deliverable documentation requirements should be consistent and be those established by project management. These requirements should be mandatory to each contract.

(4) Considerable effort should be taken to establish and document consistent methods and standards relative to process specifications and workmanship criteria which are acceptable to all JPL divisions.



Part 3. Launch and Earth-Based Systems

PRECEDING PAGE BLANK NOT FILMED

Launch Vehicle System

The Launch Vehicle System used on *Mariner* Mars 1969 missions was the *Atlas* (SLV-3C)/*Centaur*, managed by NASA/Lewis Research Center, Cleveland, Ohio. Both the *Atlas* and *Centaur* stages were manufactured under NASA contract by General Dynamics Corporation, Convair Division, San Diego, California.

Atlas/Centaur vehicles AC-19 and AC-20 were essentially the same as the vehicles used on the last three *Surveyor* missions, known as *Surveyors V, VI,* and *VII*, which used AC-13, AC-14, and AC-15, respectively. All these vehicles, starting with AC-13, made use of the *Atlas* booster SLV-3C which incorporated an extended propellant tank length, increased propellant loading, and uprated engines. The net effect of these changes was to improve payload capability.

The SLV-3C *Atlas/Centaur* vehicle with the *Mariner* Mars 1969 spacecraft encapsulated in the nose fairing was 117.3 ft long and weighed about 323,000 lb at liftoff. The basic diameter of the vehicle is a constant 10 ft from the aft end to the base of the conical section of the nose fairing. The configuration of the completely assembled vehicle is illustrated in Fig. 1. Both the *Atlas* first stage and *Centaur* second stage use thin-wall, pressurized, main propellant tank sections of monocoque construction to provide primary structural integrity and support for all vehicle systems. The first and second stages are joined by an interstage adapter section of conventional sheet and stringer design. The clamshell nose fairing is constructed of laminated fiber glass over a fiber glass honeycomb core and attaches to the forward end of the *Centaur* cylindrical tank section.

I. *Atlas* Stage

The first stage of the *Atlas/Centaur* vehicle is a modified version of the *Atlas* used on many previous Air Force and NASA missions such as *Ranger*, *Mariner* Mars 1964, and *Surveyor*. The SLV-3C *Atlas* uses an up-rated Rocketdyne MA-5 propulsion system, which burns RP-1 kerosene and liquid oxygen in each of its engines to provide a total liftoff thrust of approximately 395,000 lb. The individual sea-level thrust ratings of the engines are two booster thrust chambers at 168,000 lb each, one sustainer engine at 58,000 lb, and two vernier engines at 670 lb each. The 51-in. extension of the SLV-3C *Atlas* tank section permits tanking of approximately 20,000 lb of additional propellants.

The *Atlas* can be considered a 1½-stage vehicle because the "booster section," weighing 6000 lb and consisting of the two booster thrust chambers, together with the booster turbopumps and other equipment located in the aft section, is jettisoned after about 2.6 min of flight. The sustainer and vernier engines continue to burn until

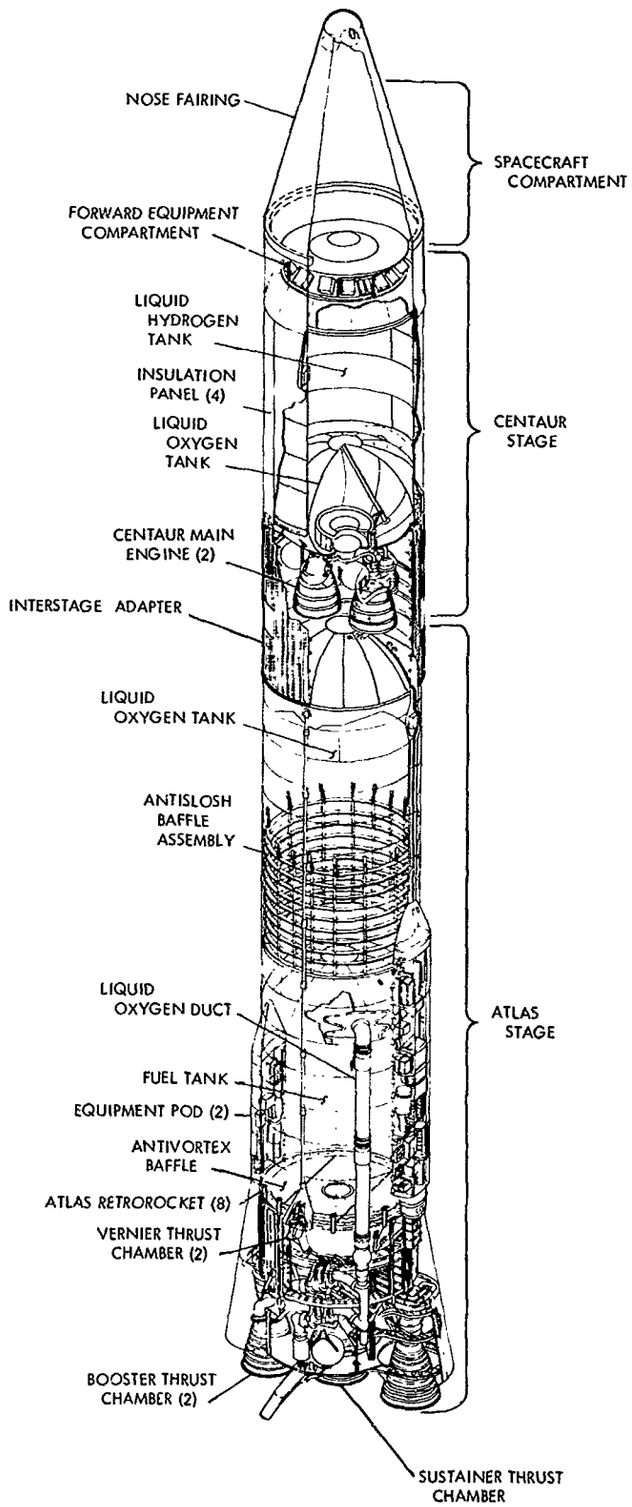


Fig. 1. *Atlas* (SLV-3C)/*Centaur* spacecraft vehicle configuration

propellant depletion. A mercury manometer propellant utilization system is used to control mixture ratio for the purpose of minimizing propellant residuals at *Atlas* sustainer engine cutoff.

Flight control of the first stage is accomplished by the *Atlas* autopilot, which contains displacement gyros for attitude reference, rate gyros for response damping, and a programmer to control flight sequencing until *Atlas/Centaur* separation. After booster jettison, the *Atlas* autopilot also is fed steering commands (including those required for the first of the yaw maneuvers, if appropriate) from the all-inertial guidance set located in the *Centaur* stage. Vehicle attitude and steering control is achieved by the coordinated gimballing of the five thrust chambers in response to autopilot signals.

The AC-19 and AC-20 *Atlas* vehicles each contained a single solid-state telemetry package using 18 Interrange Instrumentation Group IRIG channels (12 continuous, 5 commutated, 1 spare) for transmission of data over a VHF link operating on a frequency of 229.9 MHz. The telemetry link used each of two antennas mounted on opposite sides of the vehicle at the forward ends of the equipment pods. Redundant range-safety command receivers and a single destructor unit were used on the *Atlas* to provide the range safety officer with means for terminating the flight by initiating engine cutoff, or destroying the vehicle, or both. The *Atlas* destruct system is inactive after normal *Atlas/Centaur* staging occurs.

II. *Centaur* Stage

The *Centaur* second stage uses liquid hydrogen/liquid oxygen, high-specific-impulse propellants. The cryogenic propellants require special insulation to be used for the forward, aft, and intermediate bulkheads as well as the cylindrical walls of the tanks. The cylindrical tank section is thermally insulated by four jettisonable insulation panels having built-in fairings to accommodate antennas, conduits, and other tank protrusions. Most of the *Centaur* electronic equipment packages are mounted on the forward tank bulkhead in a compartment which is air-conditioned prior to liftoff.

The *Centaur* is powered by two Pratt & Whitney constant-thrust engines rated at 15,000 lb of thrust each in vacuum. Each engine can be gimballed to provide control in pitch, yaw, and roll. The AC-20 *Centaur* used RL10A-3-3 main engines, which were improved over those used on *Surveyor* direct-ascent flights to provide for opera-

tion at lower net positive suction head and an increased specific impulse nominal rating of 444 s.

A propellant utilization system is used on the *Centaur* stage to achieve minimum residual of one propellant at depletion of the other. The system controls the mixture ratio valves as a continuous function of propellant in the tanks by means of capacitive-type tank probes and an error ratio detector. The nominal oxygen/hydrogen mixture ratio is 5:1 by weight.

The second stage uses a Minneapolis-Honeywell all-inertial guidance system containing a navigation computer which provides vehicle steering commands (including the yaw maneuvers when needed to provide the desired injection azimuth) after jettison of the *Atlas* booster section. For windshear relief during the *Atlas* booster phase, the navigation computer may also be used to generate incremental pitch and yaw corrective signals to supplement the *Atlas* fixed pitch and yaw program. The incremental pitch and yaw programs are selected according to measured wind conditions and fed into the navigational computer before launch. The *Centaur* guidance signals are fed to the *Atlas* autopilot until the *Atlas* sustainer engine cutoff, and to the *Centaur* autopilot after the *Centaur* main engine ignition. During flight, platform gyro drifts are compensated for analytically by the guidance system computer rather than by the application of corrective gyro torquing signals.

The *Centaur* autopilot system provides the primary control functions required for vehicle stabilization during powered flight, execution of guidance system steering commands, and attitude orientation following the powered phase of flight. In addition, the autopilot system employs an electro-mechanical programmer to control the sequence of programmed events during the *Centaur* phase of flight, including a command to fire the four spacecraft separation pyrotechnic devices.

The AC-19 and AC-20 *Centaur* telemetry configuration consisted of 158 measurements each. Mission-oriented and other special instrumentation changes from AC-15 were extensive, requiring the use of two telepaks as follows:

(1) RF 1 (225.7 MHz) using 18 IRIG channels. Twelve channels were continuous (channels 1-7, 10, 13, 14, 16, and 17), and six were commutated (channels 8, 9, 11, 12, 15, and 18).

(2) RF 2 (259.7 MHz) using 8 IRIG channels (channels 11-18), all of which were continuous.

Table 1. *Atlas/Centaur Mariner* Mars 1969 RF systems summary

Vehicle stage	Vehicle system	Subsystem or link	Type of modulation[a]	Radiated power, W	Nominal frequency, MHz
Atlas	Telemetry	RF 1	PAM/FM/FM	3.5	229.9
	Range safety command	Command receivers (2)	FM	—	414
Centaur	Telemetry	RF 1	PAM/FM/FM	4.3	225.7
		RF 2	PAM/FM/FM	4.3	259.7
	Range safety command	Command receivers (2)	FM	—	414
	Tracking	C-band transponder			
		Ground-to-airborne	Pulsed	—	5690
		Airborne-to-ground	Pulsed	1 (av) 500 (peak)	5765
Mariner[b]	Telecommunications (S-band)	Telemetry link	PCM/PSK/PM	10 or 20[c]	
		Tracking link			
		Ground-to-airborne	CW	—	
		Airborne-to-ground	CW	10 or 20[c]	
		Command link	PM	—	

[a]PAM: pulse amplitude modulation
PCM: pulse-code modulation
PSK: phase-shift-keyed
CW: continuous wave
FM: frequency modulation

[b]Individual spacecraft frequencies are as follows:

Spacecraft	Spacecraft to earth (MHz)	Earth to spacecraft (MHz)
Mariner VI	2297.222222	2115.358796
Mariner VII	2296.851852	2115.017747
Proof test model	2298.333333	2116.381944

[c]Two different power levels selectable by command.

Redundant range safety command receivers were used on the *Centaur*, together with shaped-charge destruct units for the second stage. This provided the range safety officer with means for terminating the flight by initiating *Centaur* main engine cutoff and destroying the vehicle. The system could be safed by ground command, which is normally transmitted by the range safety officer when the vehicle has reached orbital energy. Separate spacecraft destruct units were not required by range safety.

A C-band tracking system was contained on the *Centaur*, which included a light-weight transponder, circulator, power divider, and two antennas located under the insulation panels. The C-band radar transponder provided real-time position and velocity data for the range safety instantaneous impact predictor as well as data for early orbit determination and postflight guidance and trajectory analysis. A summary of *Atlas/Centaur Mariner* RF systems is given in Table 1.

III. Launch Vehicle/Spacecraft Interface

The general arrangement of the *Mariner/Centaur* interface is illustrated in Fig. 2. The spacecraft is completely encapsulated within a nose fairing/adapter system in the final assembly bay of the explosive safe facility at the AFETR before being moved to the launch pad. This encapsulation provides protection for the spacecraft from the environment before launch as well as from aerodynamic loads and heating during ascent. An ablative-type coating is applied over the nose fairing and *Centaur* insulation panels to provide added thermal protection.

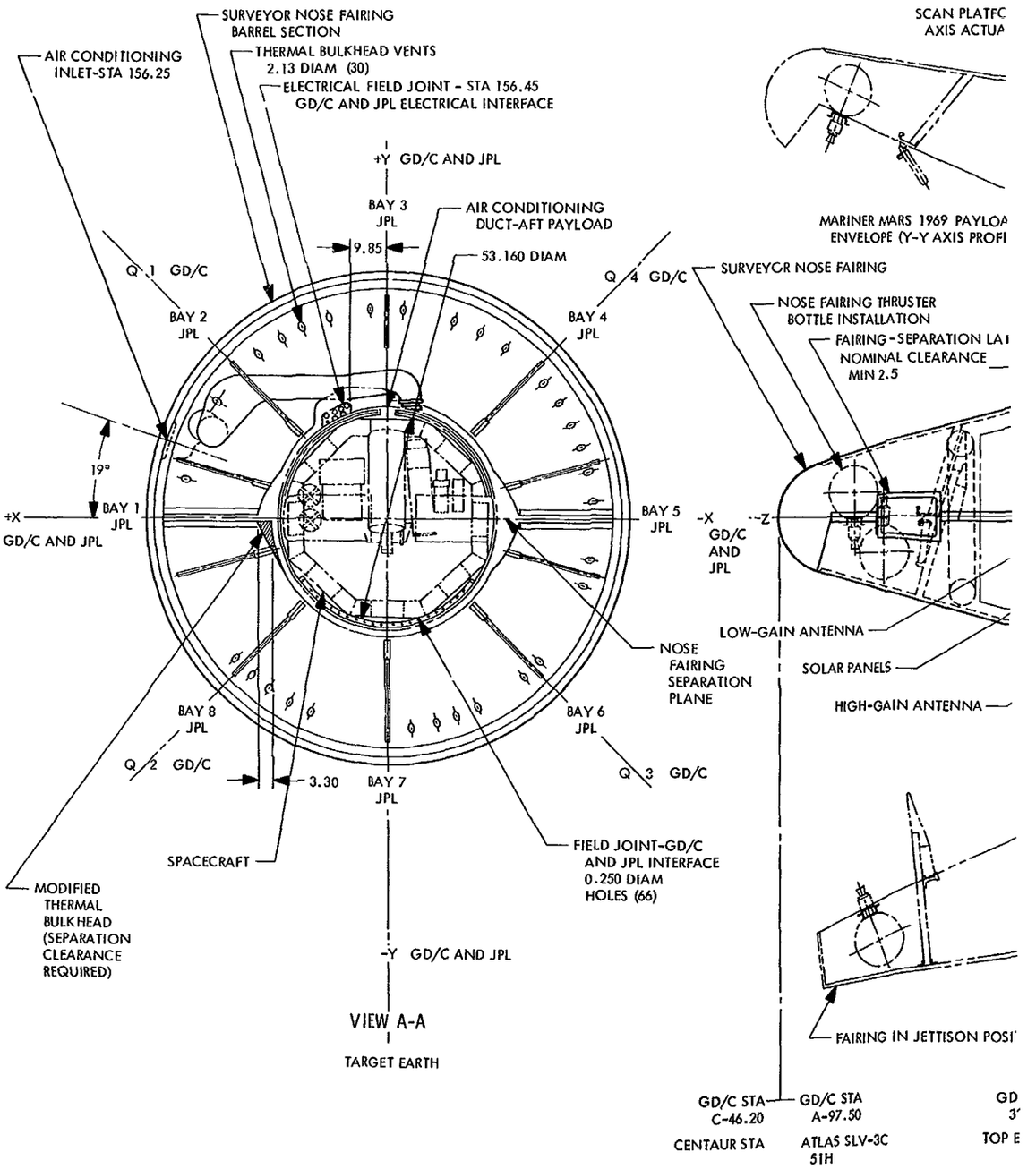
The *Mariner* spacecraft was mated to the *Centaur* vehicle at the field joint, station 156.45. This is the station where the two halves of the spacecraft adapter, the forward half and the aft half, are joined by bolting. The forward half was designed and furnished by JPL, the aft half designed and furnished by General Dynamics/Convair (GD/C). The spacecraft was first attached to the forward half adapter by means of a V-band release mechanism* containing two pyrotechnic release devices each of which has two squib devices. The firing of one release device is sufficient to execute separation. The field joint contains an electrical interface consisting of seven interface connectors and a test connector rigidly mounted on a flange on the forward half of the adapter. These connectors provide for the physical separation of the electrical interfaces according to required characteristics. The electrical interface can be generally classed into RF transmission lines to ground checkout equipment, umbilical cables containing power and signals, flight instrumentation containing spacecraft engineering telemetry and environmental flight data, and pyrotechnic signals. The flight electrical interface consists of circuits for the spacecraft engineering telemetry to the launch vehicle telemetry system, environmental data to the launch vehicle telemetry, and the spacecraft separation pyrotechnic firing current from the launch vehicle relay assembly. There were two high frequency accelerometers located on the spacecraft, one high frequency accelerometer located on the forward half adapter, and six low frequency accelerometers located on the aft half adapter. Information from all accelerometers was transmitted by way of the *Centaur* telemetry system from launch to spacecraft separation. The forward half adapter contained a thermal diaphragm located on the inside of the adapter that provided a thermal seal and prevented contamination from entering the spacecraft compartment.

The nose fairing is an RF-transparent clamshell configuration consisting of four sections fabricated of laminated fiber glass cloth faces and honeycomb fiber glass core material. Two half-cone forward sections are brought together over the spacecraft mounted on the forward adapter. An annular thermal bulkhead between the forward adapter and the base of the conical section completes the encapsulation of the spacecraft.

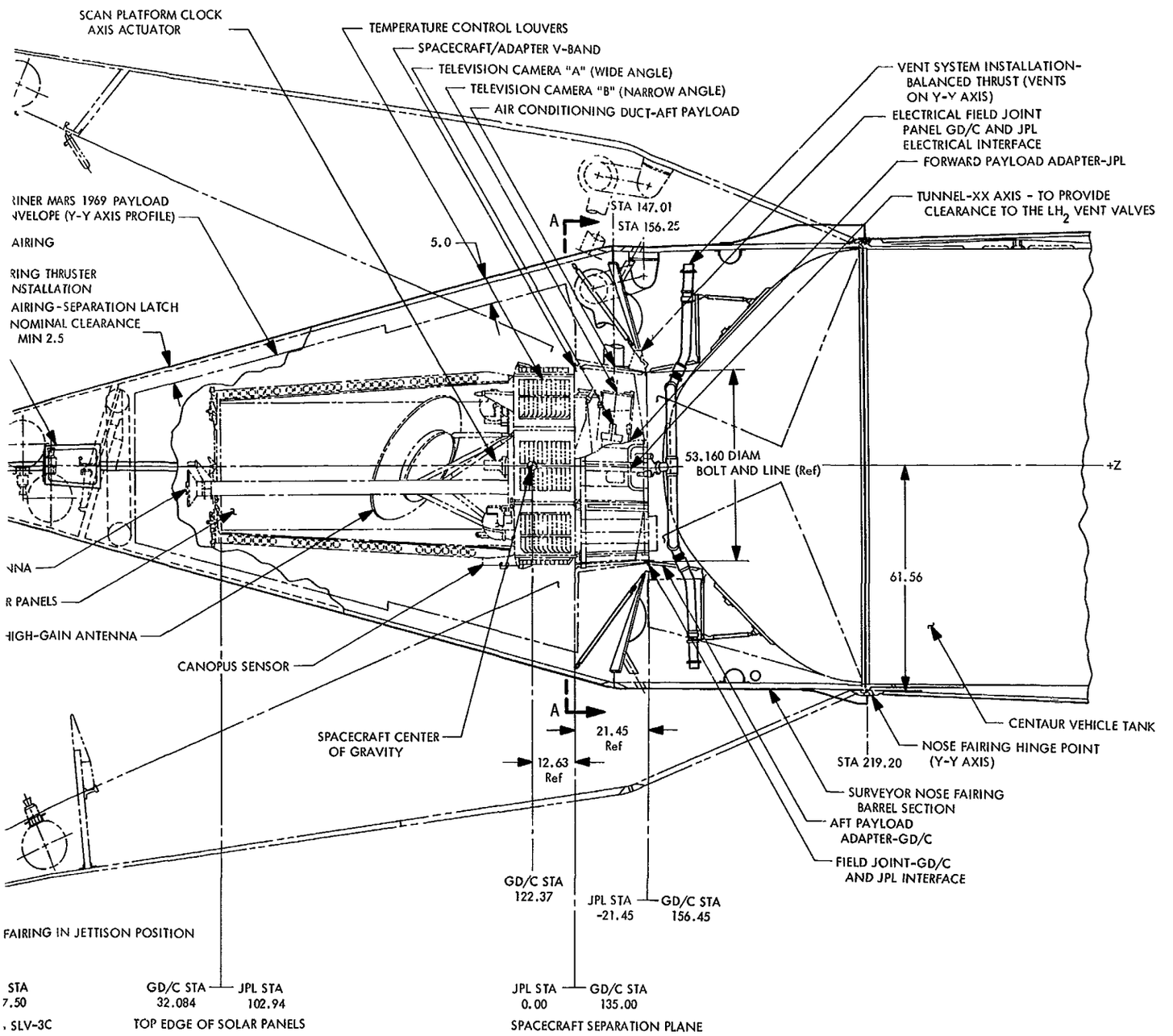
The encapsulated assembly is transported on a ground transport vehicle from the final encapsulation area to the launch pad. During transport the spacecraft cavity within the nose fairing is pressurized with dry nitrogen to preclude entrance of foreign material. At the launch pad the encapsulated assembly is mated to the *Centaur* by the forward adapter section attaching to the aft adapter section on the *Centaur* at the field joint where it is bolted. The conical part of the nose fairing is bolted to the cylindrical part of the fairing, the two halves of which are attached to the forward end of the *Centaur* tank. Doors in the cylindrical sections provide access to the adapter field joint.

Special distribution ducts are incorporated in the nose fairing and thermal bulkhead to provide air conditioning to the spacecraft cavity and forward adapter after encapsulation and until lift-off. Seals are provided at the joints to prevent fairing leakage except through vent holes located in the cylindrical section. The cavity is air conditioned with temperature and humidity controlled air at approximately 1,000 ft^3/min from a ground supply source

Flight Projects, Space Programs Summary 37-53, Vol. I, p. 7. Jet Propulsion Laboratory, Pasadena, Calif., Sept. 30, 1968.



FOLDOUT FRAME 1



ALL MEASUREMENT IN INCHES

Fig. 2. *Mariner/Centaur* interface

FOLDOUT FRAME 2

PRECEDING PAGE BLANK NOT FILMED

up to the time of cryogenic tanking of the *Centaur* stage. At that time the air conditioning system is switched over to provide dry nitrogen conditioning of cavity.

The entire nose fairing is designed for jettison by separation of two clamshell pieces each consisting of a conical and cylindrical section. Four pyrotechnic pin-puller latches are used on each side of the nose fairing to carry the tension loads between the fairing halves. A bolted connection with a flexible, linear-shaped charge for separation transmits loads between the nose fairing and *Centaur* tank. A nitrogen bottle is mounted in each half of the nose fairing near the forward end to supply cold gas jets to force the panels apart. Deflector bulkheads inside the fairing and immediately below the nitrogen jettison bottles are provided to eliminate high pressure gas impingement upon the spacecraft. Hinge fittings are located at the base (aft end) of each fairing half of the cylindrical section on the *Centaur* tank to control jettisoning which occurs under vehicle acceleration of approximately 1 g during the *Atlas* sustainer phase of flight.

Minimum changes from the *Surveyor* configuration were made to the Launch Vehicle System consistent with the peculiar requirements of the Spacecraft System and the mission. The changes were in the following areas:

(1) Nose fairing air conditioning ducts and thermal bulkhead.

(2) *Spacecraft/Centaur* adapter.

(3) *Spacecraft/Centaur* interface electrical harness.

(4) Umbilical cable and landlines between the launch vehicle and the blockhouse.

(5) *Centaur* telemetry channel assignments.

(6) Separation sequence of events.

It was necessary to enlarge the allowable payload envelope within the *Centaur* nose fairing to accommodate the *Mariner* Mars 1969 spacecraft. This was a drawing change only, having no effect on nose fairing hardware. Confidence to make such an enlargement was gained as a result of early *Surveyor/Centaur* dynamics investigations and was confirmed by X-ray photographs of the critical points after the spacecraft was encapsulated within the nose fairing. There were differences between pad 36A and 36B with respect to electromagnetic interference environmental conditions and line loss between the launch vehicle and the launch complex.

Peculiar requirements placed on the Launch Vehicle System were classified in two categories: (1) interface (hardware) design; (2) mission requirements. Hardware requirements were documented and both document and drawing were subject to negotiation and sign-off by JPL and LeRC. They were maintained under strict control. A panel known as *Mariner Mars 1969 Spacecraft/Launch Vehicle Hardware Interface Panel* was established jointly by JPL and LeRC to have responsibility over the technical contents of the interface control document and to insure the timely execution of those requirements. A panel known as *Atlas/Centaur/Mariner Mars 1969 Panel For Trajectories, Performance and Guidance* was established by JPL and LeRC to have responsibility over the mission requirements interface.

A. Hardware Interface Panel

Members of the hardware interface panel, appointed from JPL and LeRC, were under two co-chairmen, one from each organization. Efforts of the panel were directed primarily at the interfaces between the spacecraft and the launch vehicle and between the spacecraft and its operational support equipment and the launch complex. Panel areas of responsibility included environmental requirements and design criteria, mechanical and electrical design requirements, electromagnetic interference, ground support equipment requirements, and development and test requirements.

The hardware interface panel held 17 meetings during the period July 20, 1966 to November 15, 1968, at approximately six-week intervals, at JPL in Pasadena, LeRC in Cleveland, or GD/C in San Diego. It was superseded during launch preparations at Cape Kennedy by the activities of the launch operations working group, which had similar functions and structure and more frequent meetings. Principal functions of the hardware interface panel included the following:

(1) Define and establish the design requirements of the interface.

(2) Define development and qualification test requirements of the interface hardware.

(3) Establish combined system operations planning and scheduling.

(4) Review the spacecraft/launch vehicle interface control document and the interface control drawings.

(5) Expedite the flow of information of detailed design and design criteria across the interface.

(6) Review periodically the status of the combined systems operations schedule and the status of items appearing on the interface working schedule.

(7) Formulate, for project consideration, technical and schedule recommendations for the resolution of incompatibilities or other problems that related to interface design, interface testing, and spacecraft/launch vehicle combined systems operations.

(8) Examine the technical ramifications of proposed new or changed requirements which might affect the interface. Review and submit for approval of the system managers all proposed changes.

(9) Assign action items as required in the coordination of schedule requirements and design efforts.

B. Performance, Trajectories, and Guidance Panel

Appointed personnel from JPL and LeRC were members of the performance, trajectories, and guidance panel; the chairman was from LeRC. The purpose of the panel was to continually review, compile, evaluate, interchange data, and assess the performance, trajectory, launch period, and guidance and control requirements of the *Atlas/Centaur Mariner* Mars 1969 project. In addition, the panel was to pinpoint problems in these areas, determine possible courses of action, and recommend solutions. The panel was responsible to the *Mariner* Mars 1969 project manager and the Launch Vehicle Systems manager to continually review, assess, and interchange data relative to performance, trajectory, launch period, and guidance and control as these items interact within the project and the launch vehicle, and with the spacecraft.

For detailed investigation of specific problem areas, the chairman was responsible for assigning action items to members, including the establishment of ad hoc working groups for assignment in connection with the problems for which more than one agency was involved. Wherever an interface problem was isolated, the chairman recommended the necessary actions to the responsible agencies and the minutes of the meeting served as documentation of the recommendation. Meetings were devoted to the general discussion of problem areas, presentation of information, discussion of results of work assigned to individuals or working groups, and consideration of recommendations to be made to the project manager. The panel met at intervals of 6 to 8 weeks during the period August 17, 1966 to January 23, 1969, at JPL, LeRC, and the AFETR.

IV. Interface Development and Combined Testing

The *Mariner* Mars 1969 spacecraft/launch vehicle interface was defined and controlled by the interface control drawing and the hardware interface control document. The mechanical sheets of the drawing were first released in February 1967, and the electrical sheets were added in October. The provisions of the control document were initially agreed to by the Spacecraft and Launch Vehicle Systems managements on March 27, 1967; occasional revisions and updates to both drawing and document were negotiated as needed.

The principal events of the launch vehicle development, manufacture, and test cycle carried out at General Dynamics/Convair, San Diego until shipment to the launch site are given in Fig. 3. Since the vehicle was operational, development as such was limited to additions and special equipment peculiar to *Mariner* spacecraft, flown on the vehicles or employed as part of the ground support equipment. In addition a series of interface tests and checks were carried out at General Dynamics/Convair and the AFETR.

A. Match/Mate Test

The spacecraft/launch vehicle match/mate test was conducted at General Dynamics/Convair during the period March 11 to March 14, 1968. Test results indicated that all expected clearances between the spacecraft payload adapter assembly and the General Dynamics/Convair nose fairing and *Centaur* forward bulkhead were satisfactory. In addition, it was concluded that the encapsulation ground support equipment was suitable for use in the *Mariner* program upon completion of minor modifications. The encapsulation procedure was found to be basically sound. A number of improvements evolved from the test and were incorporated before being used at the AFETR. Pressurization of the assembled nose fairing proved to be feasible as did the X-ray technique to be used at the AFETR for determining static clearances between the encapsulated spacecraft and the nose fairing.

B. *Centaur/Mariner* Pyrotechnic System Test

Pyrotechnic system tests were conducted at General Dynamics/Convair between March 25 and April 12, 1969. They demonstrated that the requirements for spacecraft separation had been met.

C. Combined Systems Tests

Combined systems tests were completed on AC-19 and AC-20 with the development test model spacecraft at

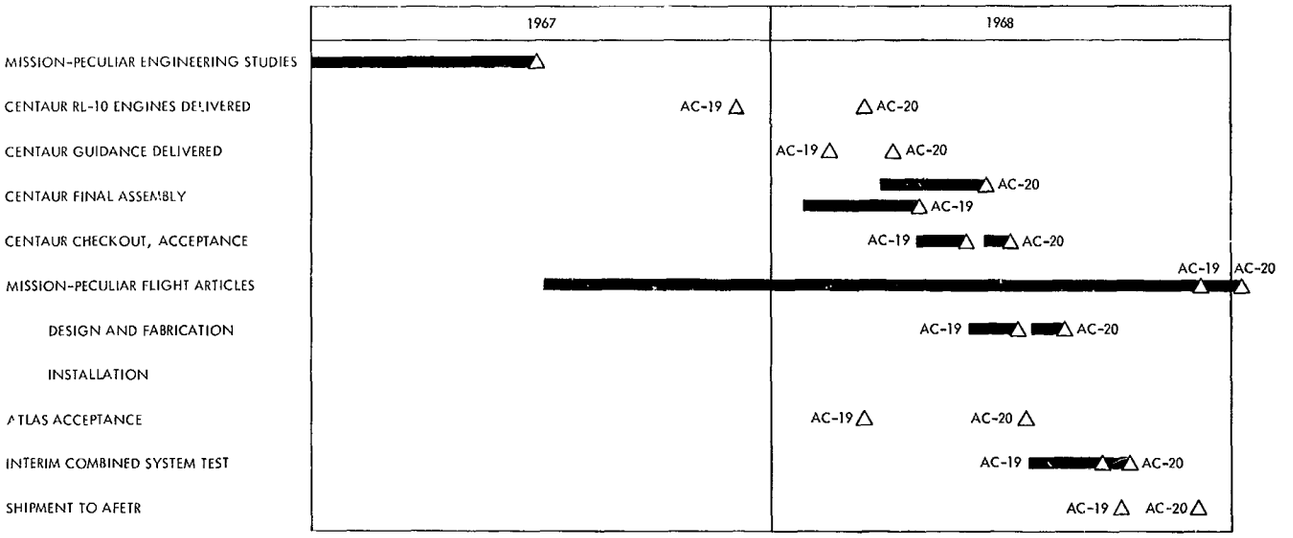


Fig. 3. Launch Vehicle System development, manufacture, and test milestones

General Dynamics/Convair on August 22, 1968 and September 30, 1968, respectively. The purpose of these tests was to demonstrate that the combined space vehicles would operate satisfactorily under simulated flight conditions with no detrimental interference between systems. The test was performed in two parts: (1) the "plugs-in" test, lasting about 26 min, was designed to use maximum control and monitoring capabilities through the umbilical connectors, and (2) the "plugs-out" test, lasting about 26 min, was designed to demonstrate performance independent of the ground support equipment as nearly as practicable. Both vehicles were checked out with the modifications peculiar to the *Mariner* Mars spacecraft and with the forward spacecraft adapter mounted. Electrical signals to and from the spacecraft were simulated and the spacecraft separation was simulated by pulling the umbilical plug at the proper time.

Analysis of telemetry and landline data as well as visual observations of panel indicators during the test indicated a satisfactory composite test with minor irregularities. All anomalies were corrected before the launch date.

D. Joint Flight-Acceptance Composite Test

The AC-19 launch vehicle was shipped to the AFETR October 2, 1968, and the AC-20 on December 2. The launch complex operation support equipment arrived at the AFETR in mid-November 1968, was installed on launch complex 36, and was checked out for system and operational compatibility. The miscellaneous hardware from JPL and LeRC–General Dynamics/Convair was received in mid-November 1968 for use in the quad tanking, Joint Flight-Acceptance Composite Test/(J-FACT), encapsulation, and composite readiness test prelaunch operations and tests. Spacecraft M69-2 and M69-4 arrived December 20, and M69-3 on January 6, 1969.

The J-FACT was conducted for AC-19 on January 21 and for AC-20 on January 24, 1969; spacecraft M69-4 was encapsulated and mated to each launch vehicle in succession, to participate in both tests. The purpose of the test was to verify systems operational compatibility under simulated flight conditions. It included a compressed countdown and simulation of flight events through spacecraft separation and the *Centaur* retromaneuver. In the AC-19 J-FACT a simulated problem was introduced during countdown at $T - 3$ min to verify the ability of the spacecraft to hold and recycle. After resumption of the count a genuine spacecraft hold was called and, after solution of the problem, the countdown proceeded. In the AC-20 test, a C-band beacon anomaly was observed briefly at $T - 35$ min, but no unscheduled holds were called.

The ordnance circuits used squib simulators (in AC-19, the nose-fairing circuits were not used). Range safety command, C-band beacon interrogation, vehicle power, guidance, control, telemetry, mechanical, and hydraulic systems were exercised. All systems operated properly with the following exceptions:

(1) During the AC-19 J-FACT, the umbilical adapter ejected satisfactorily but could not be re-locked after the test; it was replaced.

(2) Noise in low-frequency accelerometers observed in the AC-19 quad tanking test did not recur during AC-19 J-FACT, although spiking occurred; when the *Centaur* went to internal power, the spiking cleared up.

(3) The pneumatic system of a nose-fairing thruster bottle did not operate satisfactorily in the AC-20 test.

(4) The C-band beacon performed irregularly during the AC-20 test.

E. Changes on the AC-19 Schedule

On February 14, following a test for radio-frequency interference, for which the service tower had been removed, and during preparations for continued operations using the service tower, the tanks of *Atlas* 5402 (for AC-19) lost pressure because of a ground-equipment failure. Two platforms of the tower had been deployed, but the sling that normally supports the vehicle from the tower had not been installed. The manual pre-valves were closed by members of the ground crew, restoring tank pressurization and saving the space vehicle. Restrained by the work platforms, it had not toppled; but the *Atlas* skin was damaged and the *Centaur* barrel-section insulation panels were scraped.

The *Atlas* was replaced by vehicle 5105, which arrived at the Cape on February 20; vehicle 5402 was repaired at the factory and launched another mission. The *Centaur* was repaired at the Cape. Launch vehicle AC-19 was reassigned to the second launch, and AC-20 to the first launch; spacecraft M69-3, was transferred to AC-20 after its post-accident checkout. The effect on operations scheduling is shown in Table 2.

The reconstituted AC-19 vehicle repeated the quad tanking test, a vehicle FACT, and an electromagnetic interference/radio-frequency interference series, in addition to the composite readiness test, which is the final combined readiness verification test before the countdown.

F. Final Prelaunch Operations

The composite readiness tests were conducted for AC-20 on February 17 and 22 and for AC-19 on March 18, 1969. The purpose was to verify electrical and RF readiness with minimum system violation.

Noncryogenic propellants were tanked in the launch vehicle two days before scheduled launch (Atlas fuelling

Table 2. Cape operations schedule before and after February 14, 1969

Milestones	Date
Original AC-19 launch vehicle (M69-3)	
Received *Atlas* (5402) at AFETR	1968 Sep 17
Received *Centaur* (16D) at AFETR	Sep 29
Atlas (5402) erected	Oct 3
Centaur (16D) erected	Oct 4
Initial FACT[a]	Nov 11
M69-4 spacecraft encapsulation	1969 Jan 7
M69-4 spacecraft mate, LC-36A[b]	Jan 9
Compatibility test, LC-36A	Jan 9
Quad tanking test (with M69-4)	Jan 14
J-FACT	Jan 21
M69-4 spacecraft demate, LC-36A	Jan 22
Second vehicle FACT (without spacecraft)	Feb 11
M69-3 spacecraft encapsulation	Feb 11
M69-3 spacecraft mate, LC-36A	Feb 11
EMI/RFI tests[b]	Feb 14
AC-19 Launch Vehicle (M69-2)	
M69-3 spacecraft demate	Feb 14
Centaur/Atlas demate	Feb 18
Received *Atlas* (5105) at AFETR	1969 Feb 20
Erected *Atlas* (5105)	Feb 25
Erected *Centaur* (16D)	Feb 26
Quad tanking test	Mar 12
Vehicle FACT	Mar 14
M69 2 spacecraft mate	Mar 17
Composite readiness test	Mar 18
EMI/RFI tests	Mar 19
Launch	Mar 27
AC-20 Launch Vehicle (M69-3 spacecraft)	
Received *Atlas* (5403) at AFETR	1968 Nov 12
Received *Centaur* (17D) at AFETR	Dec 6
Atlas (5403) erected	Dec 11
Centaur (17D) erected	Dec 13
M69-4 spacecraft encapsulation	1969 Jan 8
M69-4 spacecraft mate, LC-36B	Jan 22
Compatibility test, LC-36B	Jan 22
EMI/J-FACT	Jan 24
M69-4 spacecraft demate, LC-36B	Jan 24
Quad tanking test	Feb 6
Vehicle FACT	Feb 11
Combined readiness test (without spacecraft)	Feb 17
M69-3 spacecraft encapsulation	Feb 17
M69-3 spacecraft mate, LC-36B	Feb 18
Vehicle FACT	Feb 21
EMI RFI	Feb 21
Composite readiness test	Feb 22
Launch	Feb 24

[a]Flight acceptance composite test (launch vehicle only).
[b]Launch complex number.
[c]Electromagnetic interference/radio-frequency interference tests.

was delayed one day on AC-20 for guidance-circuit troubleshooting, and cryogenics were tanked on launch day. The countdown proceeded to launch at the first attempt on each vehicle, although difficulties in optical alignment of the *Centaur* inertial guidance caused delays in both cases. Launch was delayed 15 min into the window for *Mariner VI* and 47 min into the window for *Mariner VII* by these problems.

Mission Operations System

I. Introduction

The Mission Operations System was the management organization formally responsible for the design, development, and execution of the *Mariner* Mars 1969 mission operations. The Tracking and Data System (TDS) and the Mission Operations System (MOS) joined in a significant part of the effort. Mission operations, in turn, were defined in the MOS/TDS management documentation as "those activities, before and after launch, which are necessary to obtain and process spacecraft information and commands and related data as required during the period of flight from liftoff to the end of the mission."

A. Origins: 1966

The development of the mission operations for *Mariner* Mars 1969 commenced in the early spring of 1966. The initial tasks were to identify the characteristics and describe the scope of the mission operations, and to formulate a plan to manage the design and development of the mission operations.

The managers of the Mission Operations System and the Tracking and Data System agreed that the design, development, and execution of the mission operations would be a joint effort of the two systems (the management systems of the project). This joint responsibility was approved by the project manager during the late spring of 1966 and incorporated in the charters of each system in the project development plan.

Concurrently, considerable effort was expended by the project office, the Office of Tracking and Data Acquisition, and the technical divisions to formulate a management structure to discharge this responsibility. The work, which extended through the early fall of 1966, resulted in the publication of a memo describing how the system design of the mission operations was to be accomplished and two memos describing how the system design of the software was to be accomplished. This effort culminated with the commencement of the system design in the first meeting of the mission operations design team (MODT) on January 1, 1967, and the publication of the first *Mariner* Mars 1969 management systems' document on February 1, 1967.

B. Management Plan

The purpose of the first MOS/TDS management systems' document was to establish policy and place manage-

ment requirements on all elements of the two management systems and supporting organizations for the development of the *Mariner* Mars 1969 mission operations. Particular emphasis was placed upon attempting to establish a management structure that would possess the flexibility to respond to problems that arose as the design and development efforts progressed, the strength to permit accomplishment of the design on the required schedule and the clarity to encourage understanding and acceptance by the personnel of the MOS and TDS.

The combined resources of the two management systems were divided into three functional, technically oriented systems; and the time period of the mission operations into three, somewhat overlapping phases of activity. The systems (analogous, for mission operations, to subsystems as used in the spacecraft design) were the data system, the software system, and the operations system. The data system included all Earth-based equipment provided by all systems of the project (principally, of course, the Tracking and Data System) for the receipt, handling, transmission, processing, and display of spacecraft data and related data during the mission operations. The software system included all computer programs and associated documentation provided by either management system, or both, for the accomplishment of the mission operations. The operations system included the personnel, plans, and procedures provided by the management systems, that were required for the execution of the mission operations.

The phases of activity were the design, test, and operational phases. The design phase was characterized by intensive activity from project inception to the start of the test phase and lesser activity that followed, in which additional design and development of the technical systems were accomplished. The test phase began with the start of compatibility testing between the spacecraft and the Mission Operations System elements, and included system-level operational testing preceded by training exercises to familiarize personnel of the Mission Operations Systems with equipment and procedures to be used during operations. The operational phase, or Space Flight Operations, ran from final prelaunch operational readiness testing through the end of the mission, during which the Mission Operation System elements and assigned Tracking and Data System elements executed the operational plans developed during the design phase and tested during the test phase.

During the phased program of design, testing, and operations, each system was jointly supported in varying degrees by appropriate resources (hardware, software, or personnel, or all three) of the two management systems of the project.

As was expected, experience identified flaws in the original management document and it was revised on July 1, 1967 when the system level designs of the mission operations had been completed and work on the subsystem level, i.e., the three functional, technically oriented systems, was to commence. It was again revised on September 1, 1968, at the start of the operational testing, to correct errors of omission and commission in the original management structure that had been detected during the design and development phases. A brief chronology of activities, milestones, and phases is given in Fig. 1.

II. System Design

The system design of the mission operations was accomplished by borrowing the techniques used in the Spacecraft System for the system design of the spacecraft. System level functional requirements were developed by the mission operations design team and documented. The system level functional requirements for the mission operations affected and controlled the next level of design, which was accomplished in three separate design teams of one for each functional, technically oriented system. The development of the data system was accomplished in the Deep Space Network (DSN) design team, of the software system in the software design team, and of the operations system in the mission operations design team (which then acted as an operations design team).

A. Mission Operations Design Team

The mission operations design team was formally chartered in December 1966, and held its first meeting on January 10, 1967. Its scope covered the system-level functional design of the mission operations, and the design and plan of the space flight operations and associated operational tests and training exercises.

The evolution of the system-level functional design of the mission operations from the general requirements in the project development plan and specific technical requirements in the Mission Plan and Requirements Document resulted in a set of system-level mission operations functional requirements (MOFR) for the mission operations. These functional requirements formed the basis for the subsequent design of the data, software, and operations systems produced by the design team. Other specific objectives of the team included: (1) development of the

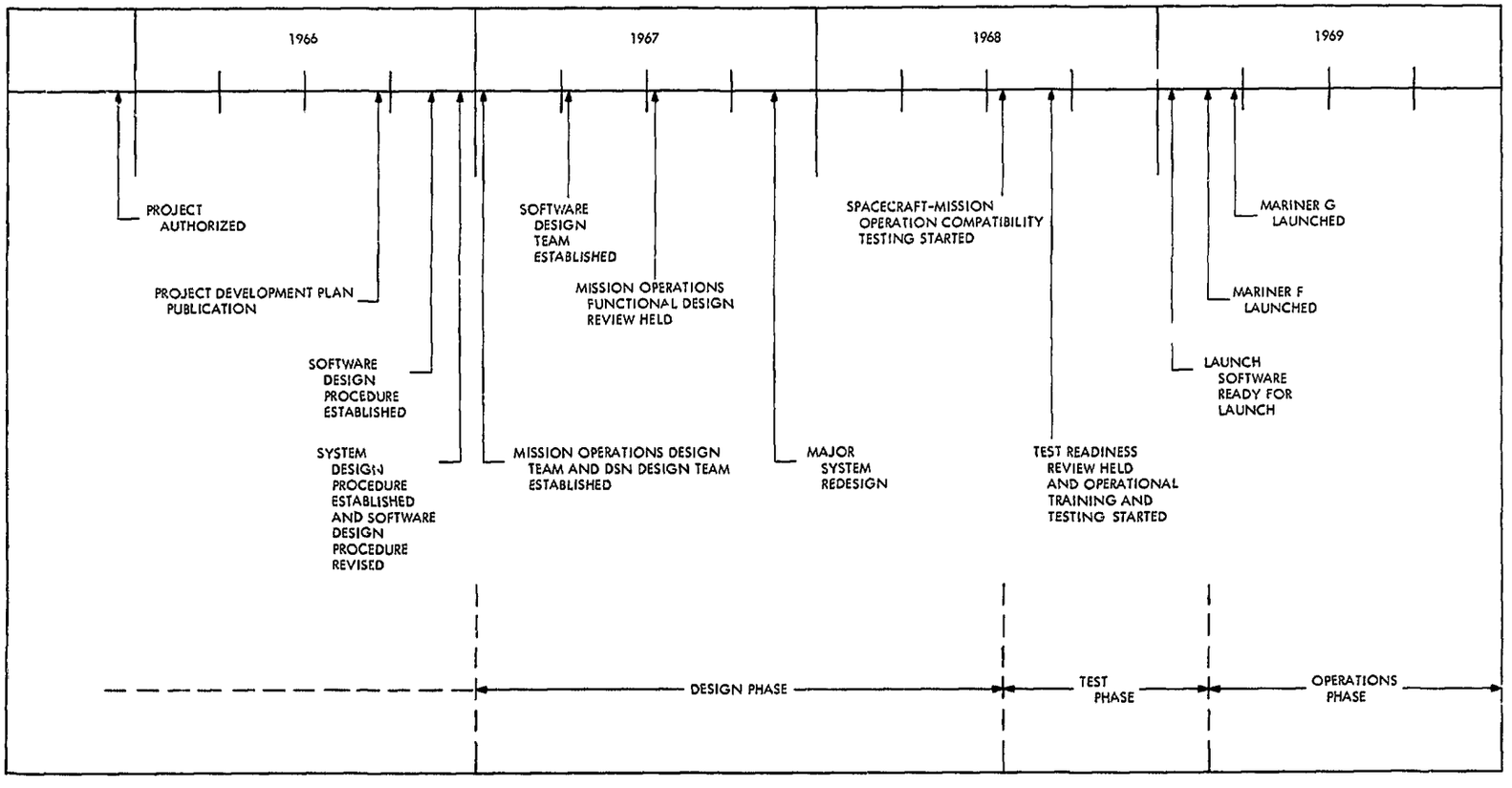


Fig. 1. Chronology of significant events of the *Mariner* Mars 1969 mission operations

spacecraft MOS interface control document, (2) development and publication of the *Mariner* Mars 1969 Space Flight Operations plan, this to be the controlling operational document for use during Space Flight Operations, and (3) development and publication of the training and test plans required for mission operations.

The design team included the following members:

Space Flight Operations Director (SFOD) Chairman

Spacecraft Performance Analysis and Command (SPAC) Director

Flight Path Analysis and Command (FPAC) Director

Space Science Analysis and Command (SSAC) Director

Deep Space Network (DSN) Project Engineer

Simulation Engineer

Software System Engineer

Operations System Engineer

Mission Analysis and Engineering (MA&E) Representative

Technical Division support as requested

One aspect of system design that continued after launch until shortly before encounter was the continuing refinement of the encounter sequence design. Sufficient planning was done before launch to enable sequences to be stored aboard each spacecraft so that minimum mission objectives could be obtained should ground command capability be lost to either spacecraft. This design was accomplished in two stages, the first conducted by the MA&E manager, and the second with emphasis on the operations aspects of the design by the MOS manager. The continuing effort after the launch was conducted by an encounter planning team.

Following the completion of its system design task, the design team became responsible for the operations system (a subsystem of the mission operations). The design organization of the management systems is given in Fig. 2, and a diagram of the design process in Fig. 3

The design of the mission operations was essentially complete with the publication of the functional requirements in early 1968, the Space Flight Operations plan in September 1968, and the training plan and Space Flight Operations test plan in October 1968.

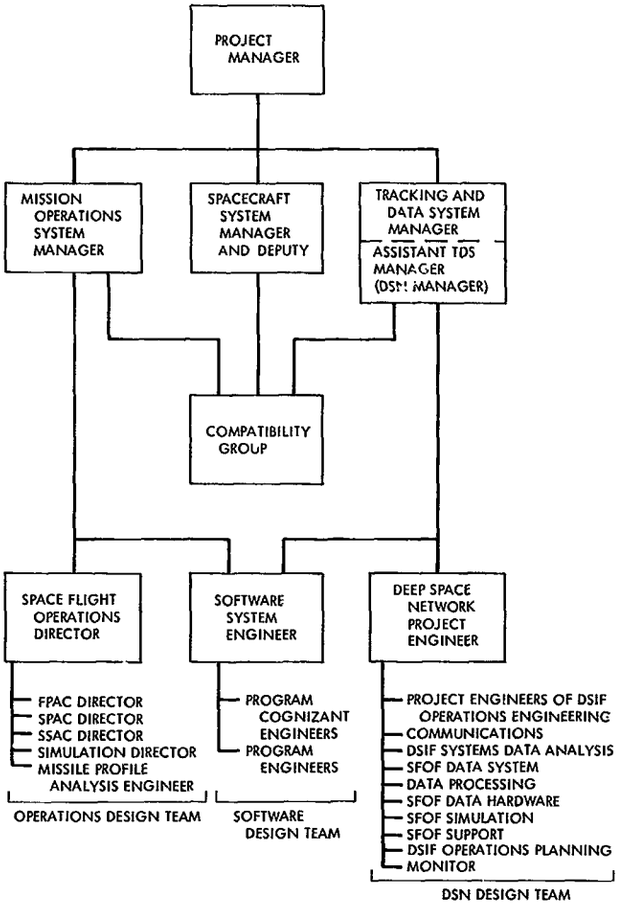


Fig. 2. Mission operations design organization

B. Reviews

Consistent with the project objectives to hold formal reviews of project activities, a series of formal design reviews was conducted of the Mission Operations System to ensure compliance with the mission requirements, to ensure implementation of optimum designs and approaches, to identify problems, and to implement corrective action if required.

The most significant reviews are described in this section.

1. Mission operations functional design review. The functional design review was conducted on July 6 and 7, 1967 before a formal review board under the chairman, the project manager. Its purpose was to review project requirements and to evaluate the design, in depth, to meet these requirements before commencing the implementation and detailed planning phases of mission operations. The review covered all work from the beginning of the

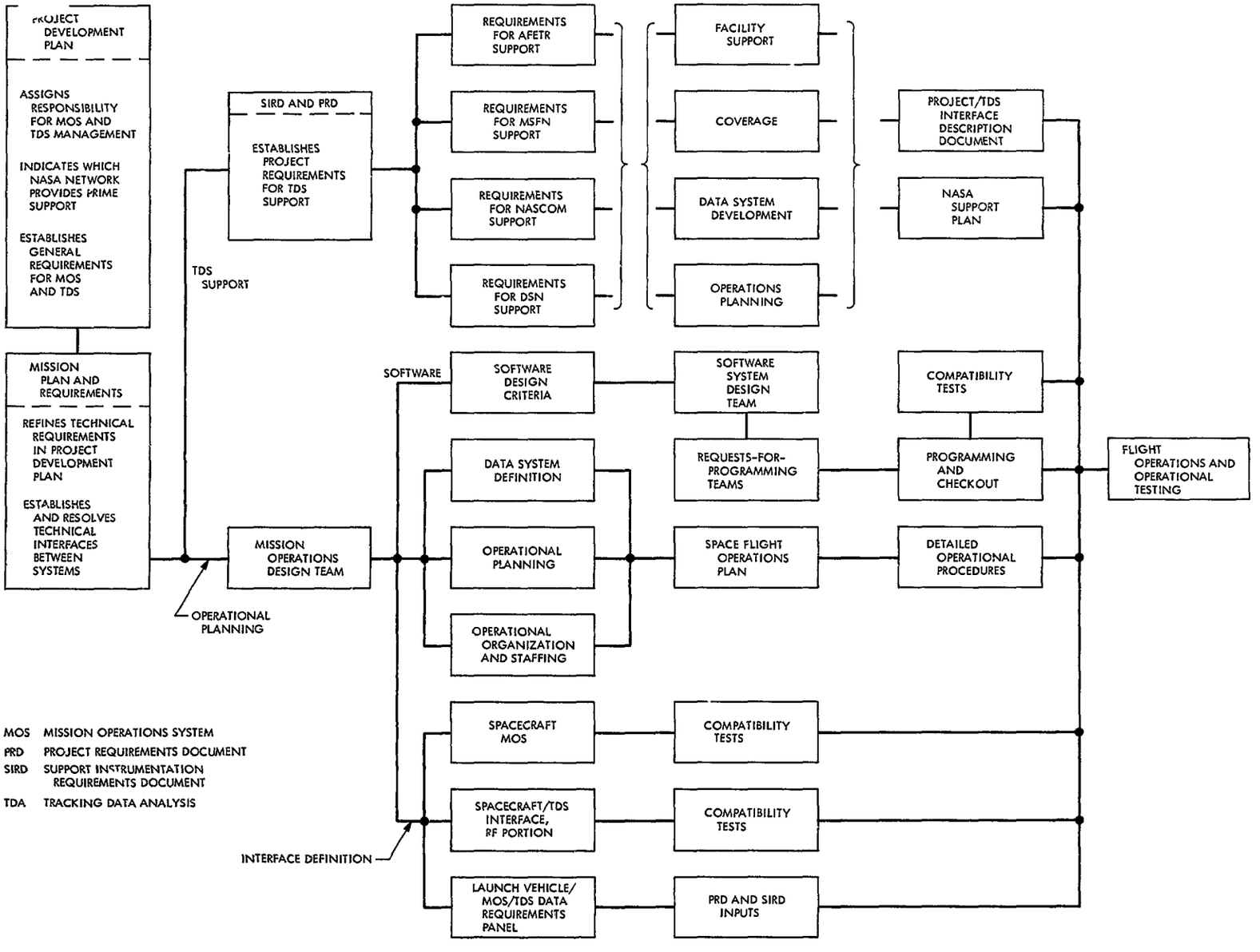


Fig. 3. Mission operations design process

design of the *Mariner* Mars 1969 mission operations by the two management systems.

The three areas of mission operations design examined were the data system, software system, and operations. The presentations were under the direction of the manager of the Mission Operations System. Two general concerns were voiced many times during the Review:

(1) The MOS is a complex system that comprises a very large and complex set of equipment, software, and procedures, and many people, located throughout the world. Thus the design of the mission operations is not simple. The concern is that, unless extreme care is observed, details may be overlooked that could affect the attainment of the mission objectives.

(2) The review was primarily concerned with the *what* and *why* of the MOS. However, so that nothing should be left to chance or verbal agreement, the board also considered formal control procedures, interface agreements with participating systems, agencies, and principal investigators, and formal definition of requirements and commitments so that desired results would be highly probable. The consideration of these matters and others of lesser importance had significant effect on mission operations design and achievement.

2. Mission operations planning review. On May 14, 1968, a mission operations planning review was conducted to present to the project, the mission operations manager, and the other members of the review board, the status of the DSN, the software, and the operations design before the design was completed so that corrective action could be taken if necessary. No serious problems were uncovered during the review. Some of the concerns identified were for (1) intensive training and testing before launch, and (2) software utilization plan and flow chart, suggested because of the large number of software programs requiring input material either from other software programs or from sources that were not a direct part of the operation.

3. Mission operations test readiness review. This review, conducted September 19, 1968, was to present the status of the mission operations training and test plans to a review board for its evaluation. The planning status of operational testing and system-level operational training was presented, and the simulation plans to support this testing and training. The testing and training described in the Space Flight Operations training plan and the Space Flight Operations test plan, the objectives of the individual training exercises and tests, a description of the tests, and the schedule for performing the tests and exercises were all presented to the review board. No problems were identified that prevented the start of training and testing, although the board did voice some concern that (1) the MOS had exceeded the committed resources, because of the total number of tests, and the ability of the SFOF and other support areas to support the ambitious test schedule; and (2) two-spacecraft operations should be more heavily emphasized in the testing.

These and other concerns were evaluated, and modifications were made to the test schedule and the makeup of the individual tests before the test program began.

4. Launch readiness reviews. Mission operations participated in the following launch readiness reviews:

(1) The first, held before the launch of spacecraft F on February 14, 1969 at JPL, Pasadena, was directed to the mission plan, the status of the two management systems, and the readiness of each system to support the first launch. The spacecraft and launch vehicle part of the review were conducted at the Air Force Eastern Test Range (AFETR) on February 3 and 4, 1969 and are discussed in another section of this report. A follow-up to this review was a launch readiness verification meeting held two days before the launch of the first spacecraft. The Mission Operations System part of this review was held by telephone conference between JPL and the project manager at the AFETR. All elements of the Mission Operations System were reported ready to support the launch.

(2) Following the successful launch of *Mariner* VI, was a *Mariner* VI launch-phase review conducted in two parts. The first, on February 25, 1969 at the AFETR, covered the launch vehicle performance, countdown, and range operations. The second, at JPL on March 4, 1969, covered the spacecraft performance, flight path analysis, and launch-related operations of the management systems. The purpose of these reviews was to determine whether any changes or refinements should be made in the procedures or operations before attempting the launch of *Mariner G*. No changes of any significance were recommended by any of the operational elements.

(3) The launch readiness review for *Mariner G* was held on March 20, 1969 at the AFETR with the MOS/TDS participation by means of a telephone conference at JPL. No changes for the launch operations were recommended by the Mission Operations

System and all operational elements reported their readiness to support the launch attempt of *Mariner G*.

5. Encounter sequence design reviews. Two encounter sequence design reviews were conducted before encounter of the first *Mariner* Mars 1969 spacecraft: one on September 13, and the other on November 12, 1968.

The first, a review of the encounter sequence developed under the direction of the MA&E manager was directed to the attainment and satisfaction of the various experiment requirements, and the desires to maximize the science return from the mission. The second, under the direction of the MOS manager was a second iteration with emphasis on the mission operations aspects of the encounter sequence design. The review board chairman for both reviews was the project manager.

The guidelines provided to the encounter sequence planning group by the project manager, following the reviews, resulted in a series of time-line encounter sequences that specified a standard encounter sequence and a conservative encounter sequence be stored into the on-board central computer and sequencer (CC&S) of each spacecraft. The standard sequence was to be performed by the initiation of ground commands for attaining maximum scientific return, and the conservative sequence would enable project objectives to be accomplished even if ground command capability was unavailable.

Refinement of the encounter sequences for both spacecraft continued after launch under the direction of the MA&E manager, and resulted in several iterations of the time-line diagrams and, eventually, in a more ambitious plan for the standard encounter sequence for *Mariner VII*. Science data return far exceeded the original mission objectives because of this planning.

C. Schedule of Mission Operations System Design and Development

Essential milestones of the design and planning documents, the reviews, the test and training periods, and the relevant project and mission events are given in Fig. 4.

III. Data System

The MOS data system included all Earth-based equipment, mission-independent (provided by TDS) and mission-dependent (provided by other project systems), used to receive, handle, transmit, process, and display all spacecraft and related data during mission operations. This equipment was operated, maintained, and tested by TDS elements, and participated as well in various compatibility and readiness tests conducted by the two management systems. System characteristics and development

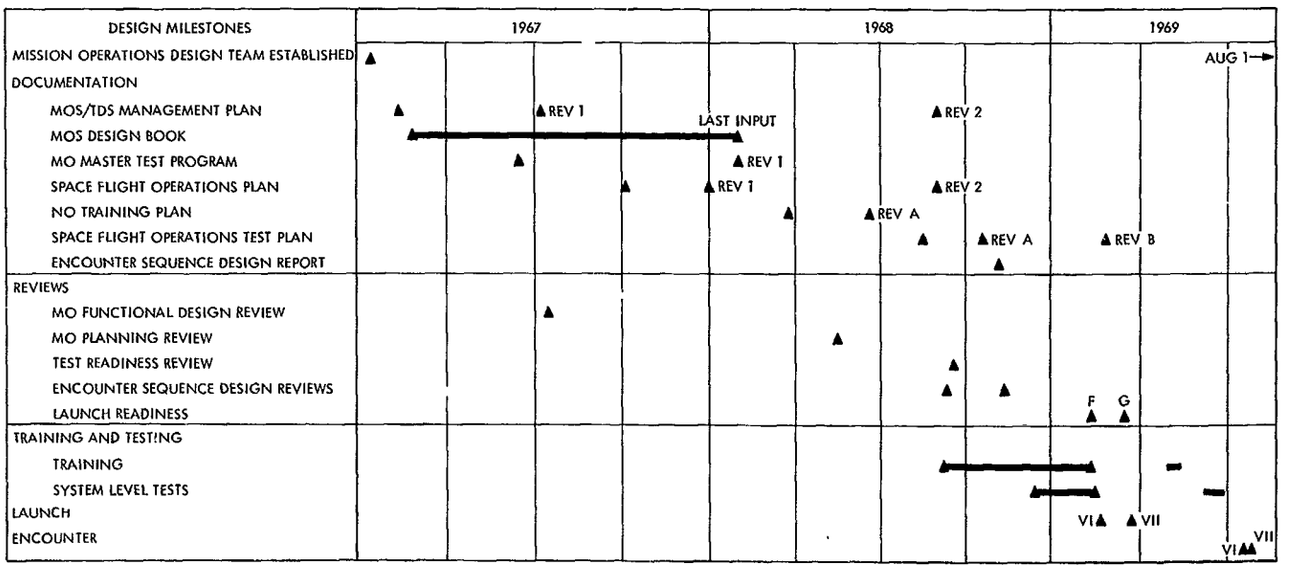


Fig. 4. Design milestones of the *Mariner* Mars 1969 mission operations

are described in the TDS section; however, for reference, some aspects of it are illustrated here.

A. Mission-Independent Equipment

The tracking configuration with the 85-ft DSIF stations, showing the flow of metric data in the Ground Communications Facility (GCF) and Space Flight Operations Facility (SFOF), is given in Fig. 5. The DSN real-time telemetry configuration is shown in Fig. 6. The command configuration is portrayed in Fig. 7.

Each DSIF station contains two separate areas for equipment. One area contains the mission-dependent equipment (MDE), and selection is based on the mission to which the station is assigned.

The other area contains the mission-independent equipment, and consists of the subcarrier demodulator assembly (SDA), the receiver subsystem (RCV), the telemetry command data handling (TCD), and the telemetry computer processor (TCP), and other multiple mission telemetry equipment necessary to perform telemetry functions.

B. Hardware-Based Mission-Dependent Equipment

Certain spacecraft subsystems were designed to be compatible with mission-peculiar ground equipment which, though developed in conjunction with flight equipment became part of the Mission Operations System data system, operated and maintained together with mission-independent equipment by the Tracking and Data System. This ground equipment included the ground telemetry system, modified from previous *Mariner* missions, and the ground command RWV equipment, originally developed for *Ranger* and modified successively for three *Mariner* projects.

1. Ground telemetry system. Mission-dependent equipment, known as the ground telemetry system (GTS), has been used in the mission support area on *Mariners IV* and *V* and the *Mariner* Mars 1969 programs. This system is a backup source of data for SPAC personnel during mission operations in the event of a computer failure in the SFOF. The telemetry system decommutator receives its input from a hardwired computer known as the "green box", which accepts high-speed data line (HSDL) data direct from the telemetry computer processor at the DSIF station after bypassing the SFOF computers. This enables the telemetry system to display information with less delay (the SFOF computers insert about a 20-s delay). The green box provides bit synchronization, word synchronization, data, and time to the telemetry system. The serial data input to the telemetry system is formatted at the green box to always supply normal data (not inverted) to the system decommutator. The time input is generated within the green box and must be manually set at the start of operations in the green box.

The *Mariner* Mars 1969 equipment was acquired by modifying the system previously used on the *Mariner* Venus 67 mission. To be compatible with the *Mariner* Mars 1969 telemetry format, the system underwent appropriate modifications.

Telemetry simulators were built for the DSIF, and were located at the Deep Space Stations in order to provide training to the DSIF station operators on facility equipment operation during the various spacecraft flight modes, and to provide hardware and software verification of the DSIF stations and the telemetry command processor.

2. Ground command subsystem. The original design of the *Mariner* Mars 1969 ground command subsystem, referred to as RWV (read write verify) provided the versatility required to support *Rangers III* through *IX* and all the *Mariner* programs. While the design of the *Mariner* Mars 1969 flight and ground command subsystems was underway, the actual RWV equipment was in service in the *Mariner* Venus 67 configuration.

Therefore, modification kits were designed and fabricated by the subsystem contractor (Motorola, Inc.) for installation at the DSIF sites where the equipments were located. Additional modifications were designed and tested at JPL. An interface working group resolved problems and brought about the transfer of the modified equipment back to the DSIF for operations and maintenance.

The RWV functions were as follows:

(1) To read and display incoming command information and verify through redundancy that it is correct.

(2) To convert the incoming information to a form suitable for transmission to the spacecraft.

(3) To verify through the converted information that the RWV internal circuitry is functioning correctly.

(4) To supply modulation to the transmitter with the converted information, and verify that the modulated signal is correct. If the modulated signal is incorrect, modulation will be coded in a manner that will cause the spacecraft to ignore the command.

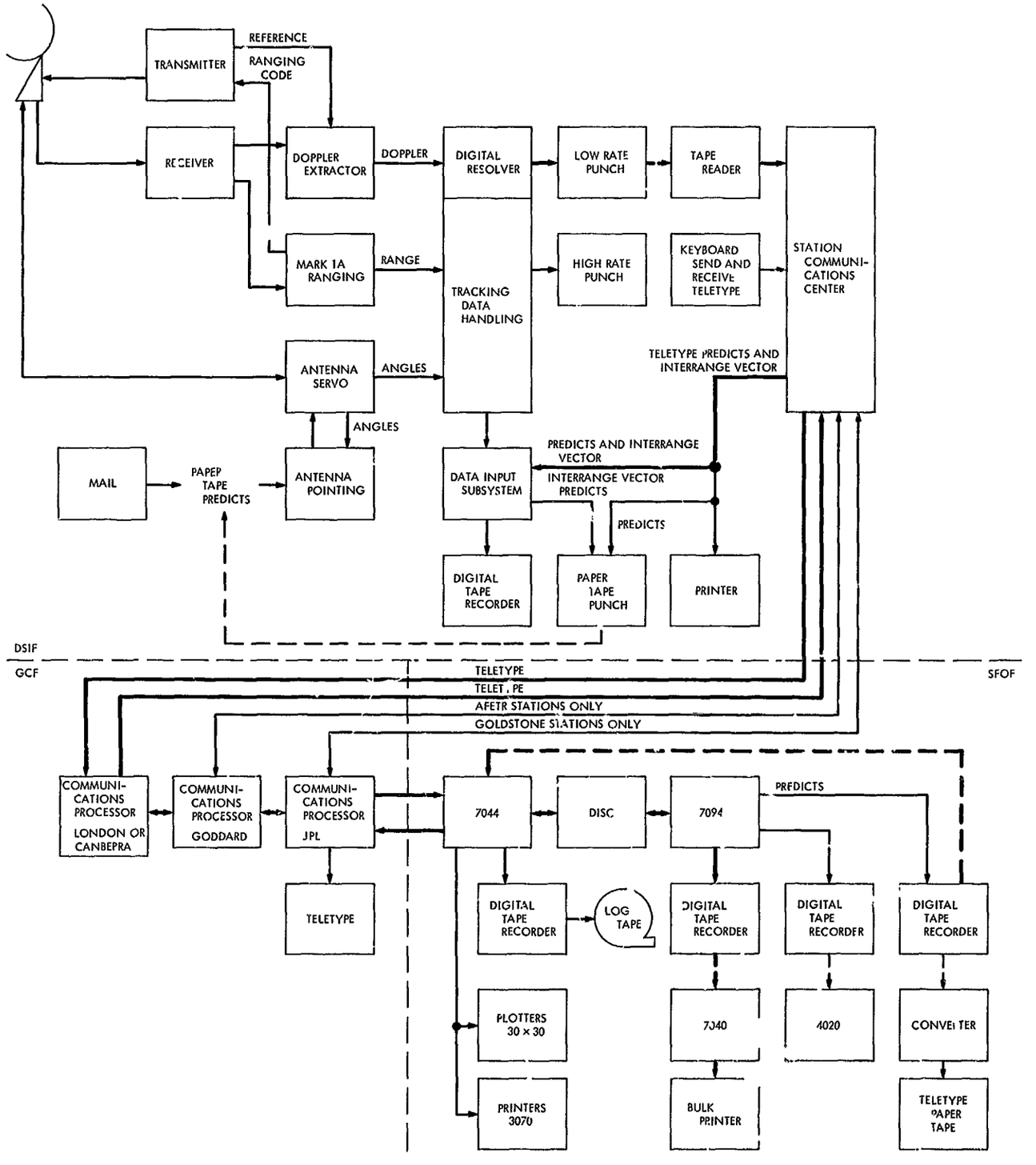
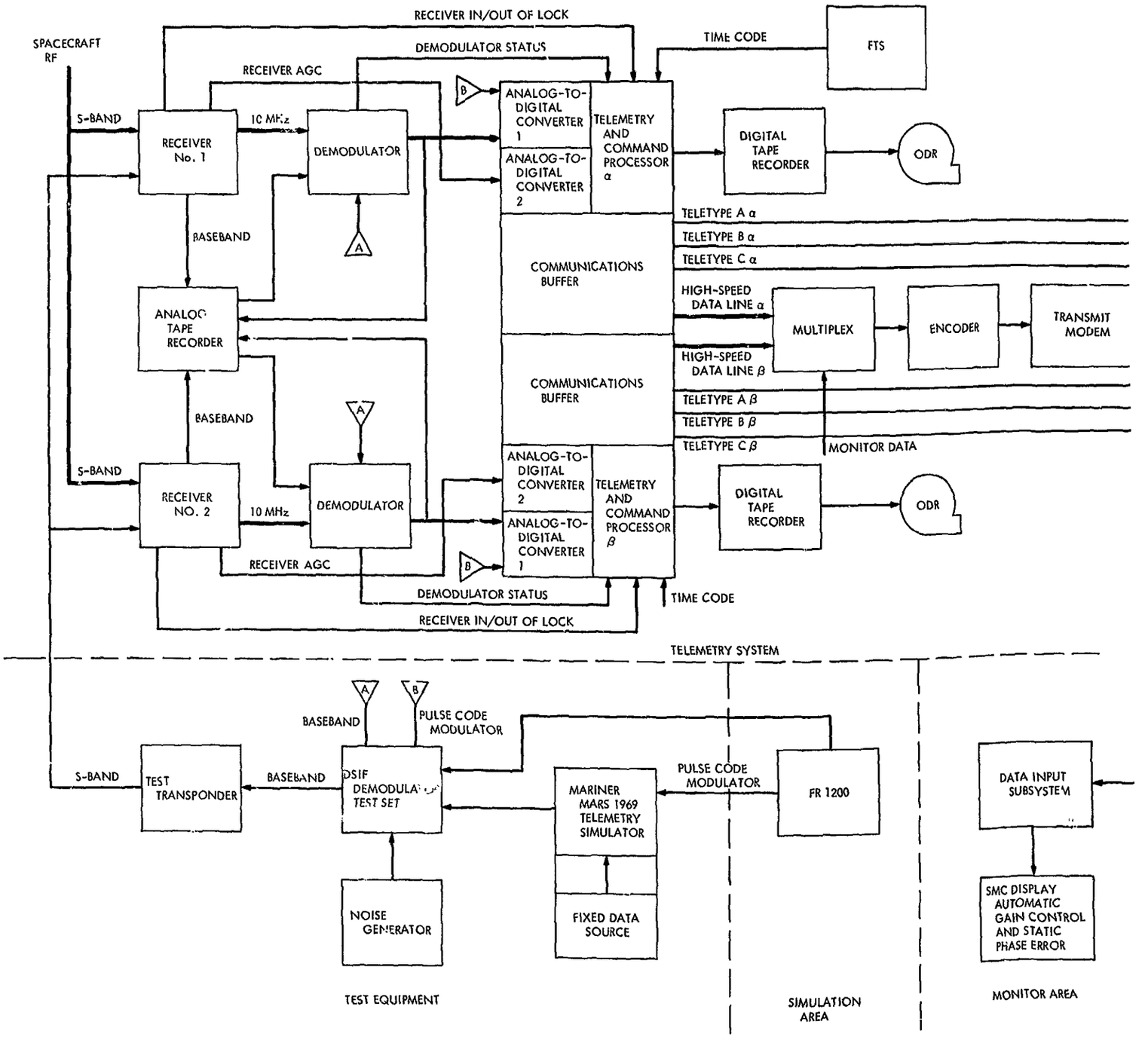


Fig. 5. DSN tracking configuration, 85-ft network



FOLDOUT FRAME

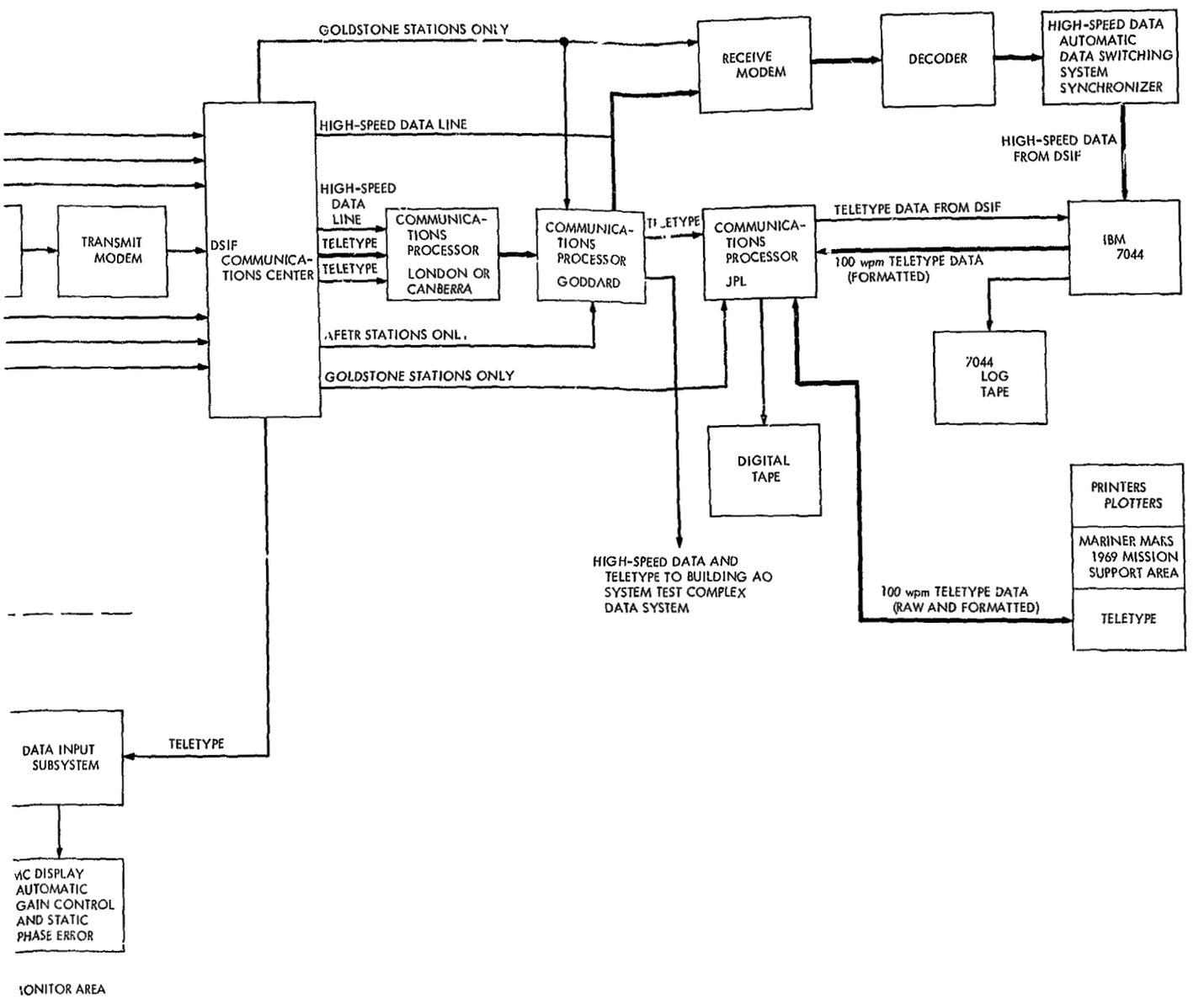


Fig. 6. DSN telemetry configuration

FOLDOUT FRAME 2

PRECEDING PAGE BLANK NOT FILMED

(5) To write by means of a punched paper tape the transmitted signal.

(6) To write on punched paper tape information suitable for transmission to the spacecraft.

(7) To allow command transmission to be initiated, either manually or automatically by an external time source.

(8) To provide an emergency mode of operation that either a power supply failure, or a failure in a noncritical circuit will not prevent command transmission.

IV. Software System

The *Mariner* Mars 1969 software system was defined in the plan of the two management systems (Mission Operations System and Tracking and Data System) as all software for accomplishing the mission operations and the Spacecraft/Mission Operations System compatibility tests, including that provided by the Tracking and Data System. It thus included Tracking and Data System mission-independent software, Mission Operations System mission-dependent software, and the system resulting from the integration of these elements. In an attempt to prevent the separate development of two relatively independent software systems and the difficulties that would then result during the integration period, the responsibility for all software development was assigned to the Mission Operations System.

The TDS software generally was required to operate and monitor the performance of the tracking, telemetry, and command data processing systems. Each TDS/DSN facility (DSIF, GCF, and SFOF) contained mission-independent software in varying degrees. The GCF communications processors, DSIF antenna pointing computers, and SFOF monitoring computer, for example, contained wholly mission-independent software. This type of software undergoes continual evolution as a result of the performance improvements required of the data systems within which it resides, and to a lesser extent as a result of the requirements of the projects which it supports. There was a large amount of mission-independent software in the SFOF IBM 7044 system, since the system was designed to be shared simultaneously by several projects. Also, the input and output functions of receiving data from the GCF and from the SFOF control consoles, of formatting and transmitting data to the GCF and to the SFOF displays, and of writing and reading data on the drum and tape units constituted a large part of the processing load on the system. The DSIF telemetry and command processor software and the SFOF IBM 7094 computer software systems contained relatively less mission-independent software since these computers basically were used to support the sequential operation of mission-dependent programs. The 7094 mission-independent software consisted essentially of an operating system for the project analysis programs, containing all necessary functions for tape, disk, printer, and console input and output functions. The data interface between 7094 and 7044 computers was by means of disk files, although a direct-data connection between computers was used for disk control purposes. Two DSN analysis types of programs were operated in the 7094, the tracking data prediction (PRDX) and the tracking data processor (TDP) programs. The DSIF telemetry and command processor program was actually developed as mission-dependent software, containing some mission-independent functions specified by the tracking system related to software/hardware monitoring and inter-computer data transfers.

Mission-dependent 7094 programs, consisting primarily of some 19 analysis programs required to perform specific mission-oriented tasks, were usually operated separately in a sequence dictated by operational requirements, in either the IBM 7094 computers located in the SFOF or in the scientific computing facility.

Development of software in the UNIVAC 1219 system which contributed to mission operations at encounter is described in Data Systems for Test Support, Section II (see page 496). The use of Mission Operations System programs developed in the 1219 system was minimized as a result of additional capabilities developed in the 7094 high-rate formatter program after launch.

A. Development Process and General Characteristics

The development of software usually was expected to follow the process outlined in the flow plan in Fig. 8, which illustrates the steps leading from initiation of functional requirements for software by the mission operations design team, to a system of programs ready to support initial operational training tests. Not included are the change control procedures which the project Mission Operations System invoked at specific times during the software development or test phase, or later in testing, depending on the type of program and the deployment—i.e., the DSIF or other overseas locations.

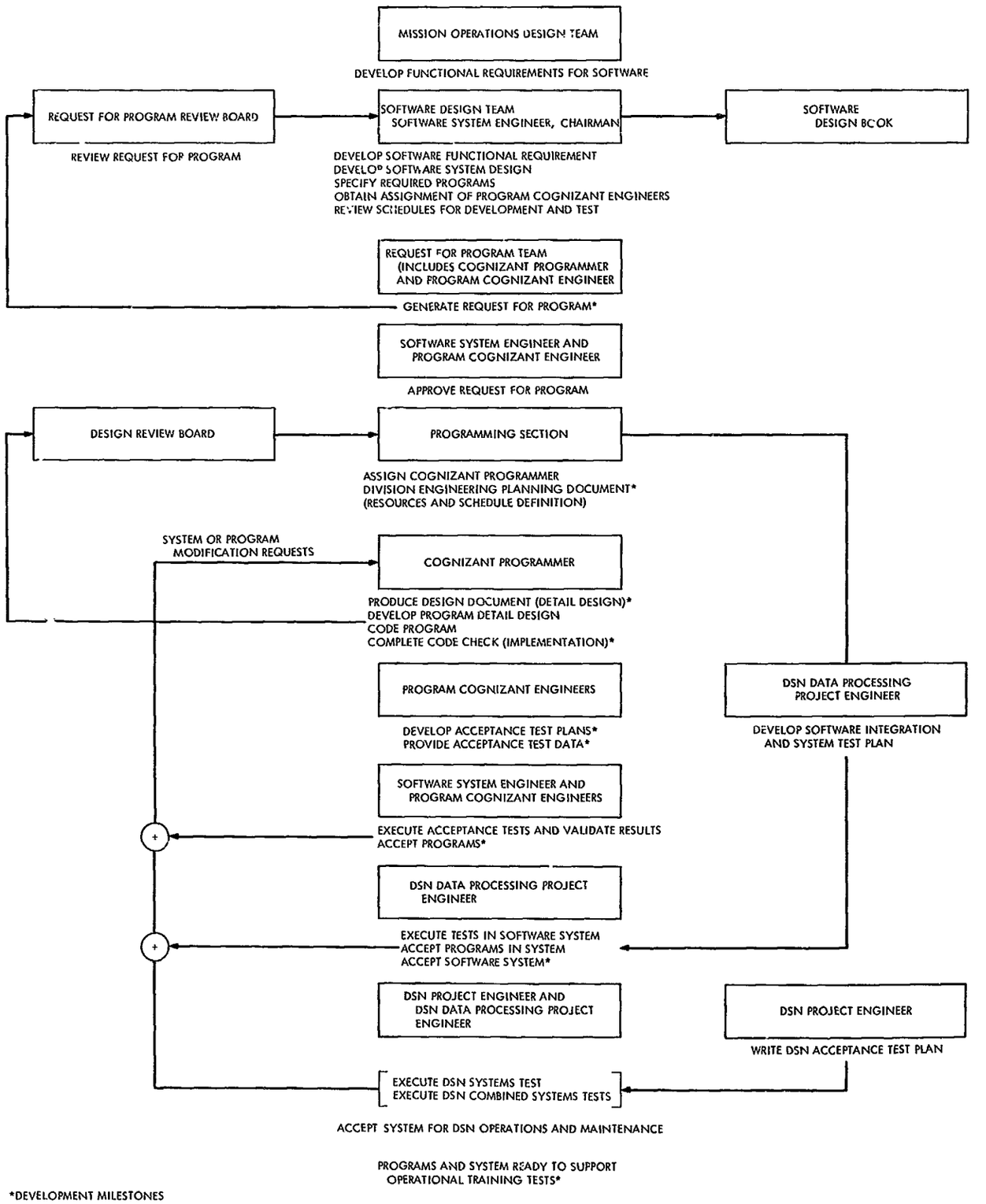


Fig. 8. Flow plan for typical Mission Operations System software development

Functional requirements for mission operations as well as Mission Operations System software were an innovation of the *Mariner* Mars 1969 Mission Operations System. Mission-independent software development generally started with the adoption of a particular benchmark, version, or model of each program, followed by successive adaptations as necessary to accommodate the program to the development of the *Mariner* Mars 1969 data system. Since documentation in the form of functional requirements and requests for programming were not initially required for mission-independent software, difficulties were encountered during the mid-1968 software integration period when certain program capabilities required for operation of the data system were deficient, and the monitor data validation programs were found to interact with the mission-dependent system. Mission Operations System scheduling or rescheduling of milestones was later instituted, but functional requirements and requests for programming were never written for six of the programs listed (see Table 6).

The request for programming document was the most significant and important working document in the software design process. It provided the formal contract between the program cognizant engineer and the programmer/analyst by specifying the detailed requirements for each program. The requirement for the cognizant engineer to produce this document with consulting support by the programmer was a very important and generally successful concept. Significant problems in programming development, execution, and operation were caused for nearly two years whenever the cognizant engineer was identified late in the development process, or was derelict in producing the requests for programming document. When approved, the document was used as the controlling document for the development and implementation of the software. The software change control procedure was used to control changes to the document during the program implementation phase to ensure that the resources assigned were properly used and interfaces with other software and the operating system were correctly maintained, and to provide a basis for developing the software test plan for the program.

The division engineering planning document provided a specification of resources required to accomplish the requested programming task. Its main job was to enable commitment of manpower and machine time to the task on schedule.

The software acceptance test plans described the tests required on each program to qualify it for integration with other programs, and eventually into a system of programs suitable for DSN system-level testing. The system-level tests qualified the system for DSN operations and maintenance, and demonstrated the capability to support operational training. The software tests were designed to provide a repeatable measure of the software transfer function, i.e., given the same input, a consistent environment, and the exercise of test procedure, the output should duplicate the results of previous tests.

The acceptance test requirements functionally specified what was being tested so that the resources required for testing could be identified; the acceptance test data constituted the total data required to accomplish testing, and the acceptance test procedure described the testing and the evaluation criteria for acceptance.

The software schedule reflected the management of and control over the implementation of the software. Each of the 32 programs identified on the schedule had a total of 7 items capable of being scheduled, as indicated in Fig. 8. Major scheduling problems included periods of several months with no milestones, and the failure of cognizant engineers to understand schedule milestones and to meet schedules.

B. Development Structure and Management

The structure of the software development system was intended to reflect the management systems' control over requirements definition, design, development, and testing, while also providing sufficient centralized authority in the programming section to accomplish effective system design and implementation. Key elements of the structure as it was finally conceived were as follows:

(1) The concept of a single MOS/TDS software system.

(2) A software system engineer responsible for all aspects of the development, testing, scheduling, and documentation of this system.

(3) Use of the mission operations design team to derive the functional requirements for software.

(4) A software design team to establish the working-level interface between the software users (in the JPL technical divisions) and the software system engineer representing the implementing section, in all matters relating to functional and detailed requirements, scheduling, and testing.

(5) Assignment of a program cognizant engineer for each program in the system, to act as a member of

the software design team and be responsible for the requests for programming, the acceptance test plan, the requirements, the data, and the final user acceptance test and buyoff.

(6) A software design book, similar to that used by the spacecraft system, containing software functional requirements, requests for programming, and test plans.

(7) A detailed schedule, reviewed weekly and updated monthly, showing dates for completion of requests for programming, design, code check, acceptance test (satisfaction of RFP requirements), and integration (operability in system satisfying all interface requirements in the software system), with appropriate Mission Operations System master schedule constraint points.

(8) Application of formal change control procedures at appropriate times to assure configuration control during spacecraft compatibility tests and Mission Operations System tests.

(9) Formal program design reviews, and software system design reviews included as part of the Mission Operations System design reviews.

(10) A requirement for formal, well documented, acceptance tests.

C. Development History and Resulting Software System

In November 1967 the Mission Operations System manager issued a set of guidelines which significantly impacted the existing tracking, telemetry, and command system design data processing. The guidelines were intended to simplify the configuration of the Mission Operations System, and decrease mission-dependent capabilities somewhat, primarily to reduce the costs of development and operation. The action taken in response to these guidelines will be used to describe the foundation for the software design and development. The DSN NASCOM hardware elements of the original telemetry and command data processing systems are shown in Figs. 5 and 6. The guidelines referred to were as follows:

(1) Do not use the high-speed data transmission capability between the telemetry and command processor, located in the DSIF, and the 7044 processor, located in the SFOF.

(2) Do not use the 7044 processor for any type of telemetry data processing. Accomplish the real-time Mission Operations System telemetry processing previously planned for the 7044 by use of the system test complex data system (see the chapter entitled Data Systems for Test Support in Part 2 of this volume).

(3) Do not use the 7044 processor for command transmission and verification purposes. Remove all command handling and verification functions from the telemetry and command processor.

(4) Use the 7094 processor in a separate configuration for the operation of spacecraft performance analysis and command programs. In this configuration, no connection is established between the 7094 and 7044 computers, and thus no capability exists to control from the spacecraft performance and analysis area in SFOF the 7094 program being executed.

(5) Minimize the number and simplify the capabilities of the 7094 performance analysis and command programs.

(6) Minimize the development of new flight path analysis and command program capability and freeze, i.e., place under immediate change control, most of the programs in their existing configuration.

(7) Reduce the programming effort for data simulation to only that required for program checkout and the provision of "canned" or constant-value data for operational training purposes.

A detailed review of all previously planned capabilities of the data processing system started immediately upon receipt of these guidelines. The functions that had been requested in functional requirements documents, requests for programming documents, and memoranda for performance in the telemetry and command processor and 7044 were reviewed, and each function was assigned a priority category. Detailed reviews of the requirements for 7094 FPAC and SPAC programs were also conducted. The guidelines also specified delaying development of the space science analysis and command non-real-time 7094 programs until fiscal year 1969. Consequently the detailed review of these program requirements was postponed pending completion of requests for programming documents and decisions on encounter science data handling, including the science master data record and experiment data record (extract). As a consequence of the reviews, a somewhat modified data system design evolved, but with most of the hardware and software capabilities that were originally proposed still intact:

(1) High-speed data transmission from the DSIF to SFOF was reinstated as the prime means for transmitting telemetry data from the DSIF to the SFOF, because this data did not pass through any com-

munications processors and was considered quite reliable. The resulting telemetry and command processing functions are listed in Table 1.

(2) The use of the SFOF 7044 as a telemetry processor was continued, primarily because of the need to maintain near-continuous automatic alarm monitoring capability during the long cruise-phase operation of the two-spacecraft mission. Although this capability might have been accommodated in the DSIF telemetry processors, such an arrangement posed logistic problems in transmitting, modifying, and verifying the limits to be used at the DSIF stations. Since the DSN planned in any case to continue using the 7044 for recording teletype tracking data on magnetic tape (or disk file in the 7044/7094 shared mode), for transmitting tracking data predictions, and for monitoring—including tracking pseudoresidual plotting—, the telemetry alarm monitoring function did not require significant additional hardware or operations costs. Once the 7044 mission-dependent function of telemetry decommutation was performed as a prerequisite to alarm monitoring, certain processing and display capabilities of the DSN 7044 mission-independent processor became usable at low cost by modifying parts of the *Mariner* Venus 67 mission-dependent engineering data processor. These additional 7044 processing functions and capabilities are included in Table 2 and Fig. 9.

An important secondary requirement of the 7044 processor was the preparation of frame-synchronized telemetry log tapes for use by offline processors. Engineering quick-look processing was accomplished in RECM, the 7094 engineering records program which accepted these tapes as input and provided tabular lists and GD/C 4020 plot tapes as an output. The frame formatted tapes also provided the means for video data transmission to the JPL image processing laboratory. There was no project requirement for an engineering master data record in an archival sense except during critical mission phases or spacecraft failure modes. Gaps or deficiencies in the data were filled in by retransmitting the telemetry processor log tape original data record from the DSIF, or by processing the tape after receipt at JPL.

The guideline specifying use of the system test complex data system (STCDS) was not applicable following acceptance of the 7044 telemetry processing function. One 7044 computer and its associated mission-independent software system accommodated the telemetry data streams from two missions by using two mission-dependent processors operating in one mission-independent system, thus permitting the processing of data from both *Mariner*

Table 1. Data processing functions of the DSIF telemetry and command processor

Function	Description
Bit synchronization	Determined timing of analog-to-digital converter samples and bit decision sampling of the demodulator output.
Bit detection	Integrated demodulator output samples over bit time interval and made bit decision.
Frame synchronization	Searched for and recognized PN codes defining start of engineering or science data frames.
Decommutation	Separated, identified, and stored science and engineering data words within a frame.
Teletype formatting	Formatted and encoded decommutated data for teletype transmission.
High-speed data line formatting	Formatted raw data bits into data blocks for high-speed data line transmission, including signal-to-noise ratio (SNR)-based parameters. Provided separate data blocks for ground receiver automatic gain control and static phase error data.
Data recording	Produced digital log tape of received data, SNR-based parameters, ground data system status, bit sync status, time identifiers, and automatic gain control and static phase error data.
Operator messages	Provided telemetry command processor system status to operator, allowed program control input by operator.
SNR-base parameters	Calculated demodulator analog signal output sample sums and sum of squares for signal-to-noise ratio (SNR) calculations at SFOF.
Ground data acquisition	Provided ground receiver lock and demodulator lock status to teletype and high-speed data line formatter, automatic gain control and static phase error data to high-speed data line formatter.
Bit synchronization status	Provided loop-lock status of demodulator bit synchronization loop to high-speed data line output.
Status to DSS operators	Provided spacecraft telemetry data to DSS operators; spacecraft automatic gain control, static phase error; command lock, events, and voltage-controlled oscillator offset.
Status to DSN monitor	Provided operational mode, configuration, and synchronizati n status; tape recording status, ADSS bloc' ,tatus, to DSIF digital instrumentation subsystem.
Data playback	Read digital log tape, retransmitted data via high-speed data line to SFOF.
Test mode	Received canned data via demodulator interface, calculated performance statistics.

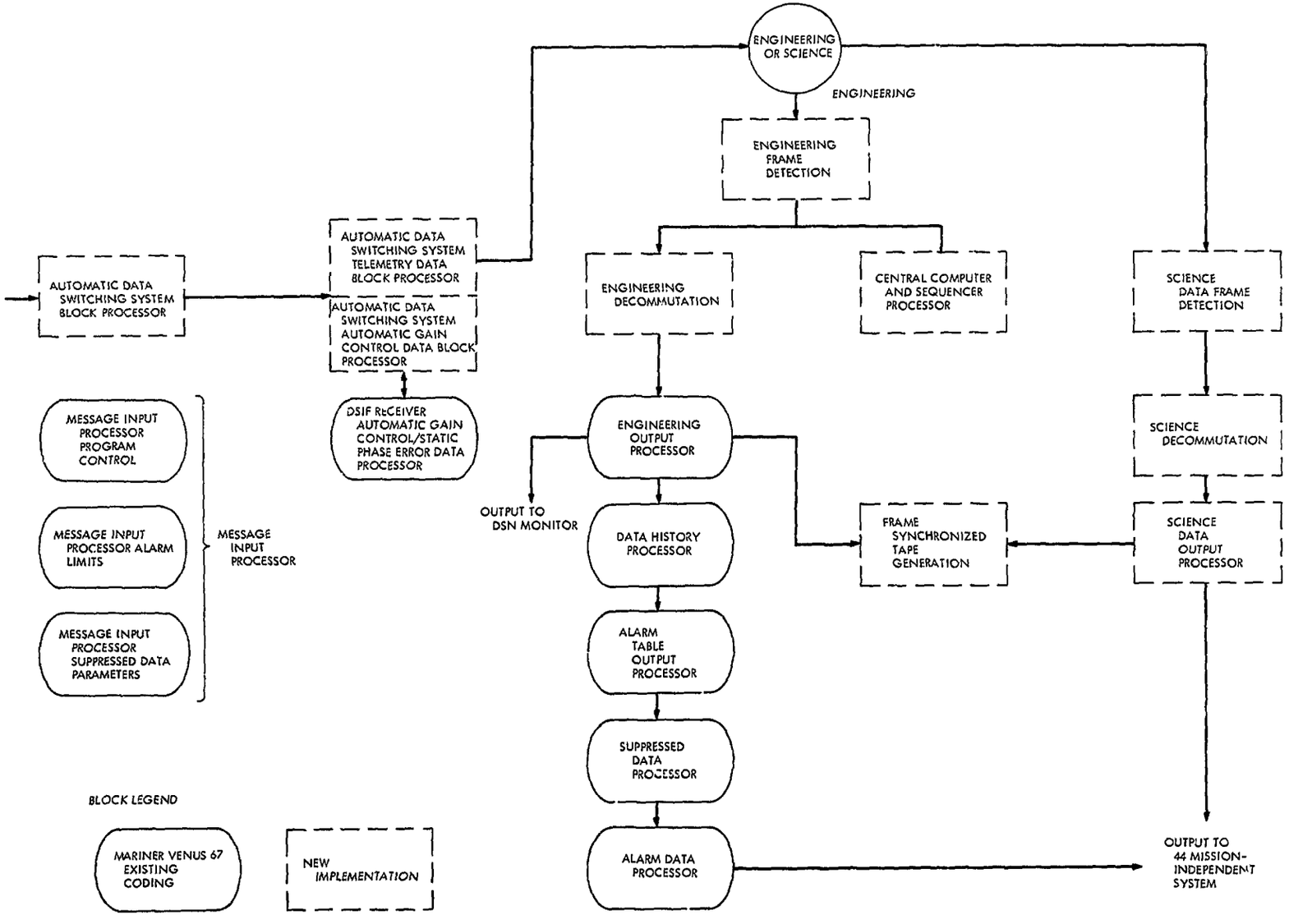


Fig. 9. Mission-dependent program of the 7044 processor

Table 2. Data processing functions of the SFOF 7044 mission-dependent processor

Function[a]	Description
High-speed data line input processor	Received automatic data switching system data blocks, extracted data and time tag, routed to correct processor.
Frame synchronization	Searched for and recognized PN codes defining start of engineering or science data frames.
Decommutation	Separated and identified science and engineering data words within a frame.
Raw data dump	Provided raw binary science data dump to verify correct receipt of science data (during early telemetry processor/7044 tests).
Alarm monitoring	Checked input data samples for violation of upper or lower limit values.
Data suppression	Provided output data only when sample value changed by more than prescribed tolerance.
Data history	Stored total frame of latest available engineering data for demand printout.
Output processor	Provided interface between mission-dependent processors and the mission-independent line print, teletype print, and plotting capabilities of the 7044.
Data recording	Provided frame-synchronized digital tape of received engineering and science data; master data record tape.
Signal-to-noise ratio (SNR) calculation	Received SNR-base parameters from telemetry and command processor, calculated signal-to-noise ratio periodically.
Acquisition system status	Received and processed ground receiver status data received from telemetry and command processor.
Operator messages	Provided for proce ing input messages for program control, and alarm and data suppression limits and tolerances.
Status to DSN monitor	Provided information on mission-dependent processor operation to DSN monitor.

[a]excludes tracking data proce sing, NASCOM functions, and DSN monitoring.

Mars 1969 spacecraft simultaneously. Overlap data, i.e., data from one spacecraft sent from two stations simultaneously, could be recorded by the 7044 mission-independent processor, but only one combined engineering/science data stream per spacecraft could be processed in real time. It was possible to process engineering telemetry received from one station and science telemetry from another, from one spacecraft source.

(3) The configuration for command transmission consisted of perforated-tape teletype transmission equipment in the spacecraft performance analysis area and conventional teletype transmission to the DSIF. Teletype commands were received, printed, and punched at the DSIF ground command subsystem operators position, and no use was made of the 7044 or telemetry processor data systems for commands. The increased time required to prepare commands in the SFOF, send them to the DSIF, and verify the punched commands was accepted by the project.

(4) The planned use of the 7044 for alarm monitoring permitted the use of the available control capabilities of the 7044 including the use of the SPAA control console to communicate (in 7044/7094 shared mode) with the 7094 computer. This allowed control of 7094 SPAC programs, as well as the capability to change 7044 alarm limits, select print, plot formats, etc.

(5) The review of the proposed spacecraft performance analysis programs resulted in development of the programs described in Table 3.

(6) The review of the flight path analysis programs resulted in plans for developing the set of programs listed in Table 4.

(7) The recommendation for minimizing the project-funded simulation effort was adopted, thus reducing the effort planned for the simulation of spacecraft performance, interaction between spacecraft subsystems under simulated failure conditions, etc. Emphasis was placed on the use of PTM spacecraft tests, either directly or by use of recorded test data, to provide data for operational tests and training purposes.

The DSN phase I simulation program provided fixed format telemetry data for data system checkout, but it was supplemented in Phase IA to permit the program to accept real spacecraft data recorded on digital magnetic tape by the STCDS, in order to provide more realistic data for use in operational training tests (see Table 5). Tracking data simulation was provided by SIM 94 and a 6050 program developed and provided by the DSN.

Other programs developed to support *Mariner* Mars 1969 mission operations are listed in Table 5, which also shows the computer or system in which the program operated. All these programs were mission-independent or

Table 3. List of 7094 spacecraft performance analysis and command programs

Title of program	Acronym	Function	Title of program	Acronym	Function
Command generation and validation[a] Assembly Translation CC&S memory processor CC&S simulator Operational support equipment formatter Command formatter Comparator	CMDM or COMGEN	Prepared CC&S programs, generated coded commands, recorded tape data necessary for punching CC&S operational support equipment tapes to support system test, launch operations, and flight operations. Provided flight operations analysis, simulation of sequences, and modification of CC&S memory.	Communications measurements[a]	CMPM	Provided actual performance data for comparing with predictions (CP2M). Used real time telemetry master data record tape from 7044 (spacecraft and DSIF ground system data), CP2M output tape, and predict data cards as input data. Put out prints and plots.
			Automatic gain control calibration[b]	AGCM	Processed DSS data acquisition system pre-pass calibration data to produce look-up tables and plots.
			Star identification[c]	SIPM	Provided data on inflight star sensor performance vs clock angle; listings of acquirable objects from known sensor characteristics and trajectory SAVE tape input.
			Attitude reference[c]	ATRM	Computed spacecraft attitude relative to sun, planets, or selected stars. Provided cone and clock angles of desired celestial objects.
			Sequence-of-events generator[a]	SOEM	Generated time-ordered sequences of events from card input. Provided sort capability by DSS, mission, or "report to or by". Put out prints, plots, or sequences to DSIF by teletype.
Engineering data records[a]	RECM	Accepted frame-synchronized 7044 log tape, and produced tapes for offline listings by 7040 computer and plotting.	High-rate playback data formatter[a]	HRFM	Reformatted for image processing laboratory the combined science format or TV science format data recorded by DSS 14 or CTA-21 high rate systems, or by telemetry processor or 7044 log tapes.
Telecommunications performance prediction[a]	CP2M	Computed predicted telecommunication channel performance from antenna pattern tape, system characteristics, and trajectory SAVE tape data.			

[a]New program.
[b]Existing *Mariner* Venus 67 program.
[c]Modified *Mariner* Venus 67 program.

were developed with DSN funds, with the exception of phase IA simulation.

Not included in this table are a number of preprocessors for SPODP or DPODP which were not developed under control of the software system engineer, although attempts were made to establish configuration control of these small programs during the mission operations application of the DPODP. These seven programs were used to generate and process ionospheric data and compute corresponding corrections to be made to range and doppler data, to calculate a timing polynomial for correcting DSIF station time based on observations received by JPL from U.S. Naval Observatory (USNO), and to calculate a best estimate of the current pole position from USNO-received data for determining DSIF station locations.

D. Spacecraft Subsystem Special Software

Certain programs evolved or were developed from previous projects in connection with special spacecraft needs. These were consistent with the Mission Operations System software system, but were prepared under the cognizance of the hardware subsystem.

1. Central computer and sequencer command generation software system. The command generation program (COMGEN) software system was designed to support the *Mariner* Mars 1969 central computer and sequencer (CC&S) during prelaunch testing, launch, and flight operations (Refs. 1 and 2). This program was to be used to prepare CC&S programs, to generate coded commands, and to generate and record data necessary to punching CC&S operational support equipment (OSE) tapes for support of system testing, launch operations, and flight

Table 4. List of 7094 flight path analysis programs

Title of program	Acronym	Function
Tracking data prediction[a]	PRDX	Computed station view periods, spacecraft position in topocentric DSIF coordinates, best-lock transmitter frequency, doppler shift, and range.
Tracking data processor[a]	TDPM	Wrote master file of tracking data, rejecting data with erroneous format, bad condition code, or out of range.
Orbit data generator[a]	ODGX	Prepared orbit data file from TDPM master file using selection and editing criteria to correct or average the data.
Single-precision orbit determination[a]	ODPM or SPODP	Calculated orbit from ODGX file using weighted least-squares method. Solves for orbital elements, physical constants, encounter statistical errors, etc.
Double-precision orbit determination[a]	DPODP	Similar to SPODP except for double-precision arithmetic calculations.
Midcourse maneuver operations[a]	MOPM	Calculated maneuver capabilities, maneuver values, and commands, subject to mission constraints. Optimized maneuver.
Planetary encounter geometry and science instrumentation sequence and PEGASIS plotting[b]	PEGM or PEGASIS	Computed Mars-centered coordinates of instrument traces, event times such as limb or termination crossings, etc., using assumed approach asymptote and pointing directions.
Injection condition generator[c]	ICGM	Computed injection time, velocity, radius, coordinates, azimuth, using launch time and a polynomial equation.
Trajectory[a]	TRJM	Integrated equations of spacecraft motion from epoch to desired point. Input from ODP, ICG, or nominal values. Provides listings or trajectory SAVE tape output of position, velocity, and DSIF view.
Flyby fine print[a]	FLYM	Calculated details of encounter geometry (angles, times, etc.) and timing of backup commands.

[a]Modified *Mariner* Venus 67 program.
[b]New program.
[c]Modified *Surveyor* program.

Table 5. List of additional *Mariner* Mars 1969 mission operations programs

Title of program	Computer	Program function
Simulation phase I	EMR 6050	Generated engineering and science telemetry and DSN monitor data for system checkout and training.
Phase IA	EMR 6050	Provided telemetry data for training, using spacecraft recorded data source.
Simulation math model	EMR 6050	Provided command-responsive telemetry for operational training.
Tracking data simulation	7094 or EMR 6050	Generated simulated doppler and angle data containing desired noise and bias, formatted to correctly represent DSS data.
Telemetry data validation	7094	Provided summary of quantity and quality of data on original data record of telemetry and command processor.
Tracking data validation	7094	Provided summary of quantity and quality of tracking data in master file of tracking data processor.
DSIF/GCF interface	SDS 910	Received, deblocked, and distributed data contained in high-speed data line blocks to DSIF telemetry simulator.
DSN monitor	CDC 3100	Identified in real time degraded or lost data, using status and alarm inputs from DSIF, GCF, and SFOF.
Monitor criteria data	7094	Generated master file and teletype output of DSIF configuration and performance criteria for input to the DSIF monitor system.

operations. It was also to be used extensively for flight operations analysis and simulation of the spacecraft CC&S computer.

The COMGEN support of launch and flight operations and training support was to consist of verification of the CC&S memory during test, modification of the CC&S memory through the generation of coded commands to be transmitted to the spacecraft, and simulation of the original program and the modified sequences. The simulation capabilities included the CC&S program, switching logic, other subsystem interface interactions, and ground command responses. In conjunction with the coded command generation and the simulation of the sequences, the program was required to generate the necessary teleprinter messages and co mand tapes to be transmitted to the Deep Space Stations.

Post-launch, inflight use of the COMGEN program was to be extensive, and was to serve as an aid to the following activities: (1) preparation of midcourse commands, (2) preparation of special diagnostic and memory modification commands, (3) simulations involving the midcourse phase, and the addition, modification, and subtraction of cruise and encounter events, and (4) evaluation of CC&S memory readouts.

The capability of the COMGEN program to predict the times of occurrence of the events controlled by the CC&S

was very effective and valuable to flight operations analysts and mission engineers. The formatted output of the program was used to follow the sequence of spacecraft events in real time. The program was also used in mission engineering as an aid to the construction, analysis, and validation of sequence of events.

The main operational uses of the COMGEN program were briefly summarized as follows:

Condition	Required operations
Pre-flight	Simulations Launch tapes
Flight Normal	Simulations (as desired) Tandem midcourse coded commands DC-2
Flight Contingency	Simulations (as required) Spurious/missing event Single word dump Addition of event Subtraction of event Computer only midcourse coded commands

The COMGEN program for *Mariner* Mars 1969 consisted of ten subprograms and an executive program which operated under the JPL trajectory monitor system, in the SFOF. Each of these subprograms performed specific operations; various combinations of these subprograms provided vital information which was used in preflight testing and in inflight operations for programming and simulating the *Mariner* Mars 1969 CC&S subsystem. The subprograms were controlled by an executor program which functionally linked the subprograms as shown in Fig. 10. The subprograms were the following:

Assembler
Time conversion
Command formatter
Comparator
Load commands
Memory retrieval
Operational support equipment tape
Print/punch
Simulator
Translator

These subprograms controlled by the executor in conjunction with several common memory areas generated CC&S memories and commands, compared memories, and produced operational support equipment load tapes.

2. *Attitude control supporting software.* The attitude reference program for *Mariner* (ATRM) and the star identification program for *Mariner* (SIPM) were developed to provide necessary preflight, flight, and postflight information in support of the *Mariner* Mars 1969 missions. (Refs. 3 and 4). The ATRM and SIPM programs evolved from similar existing programs used on previous *Mariner* missions that required several modifications and improvements to be compatible with the *Mariner* Mars 1969 spacecraft hardware design, and to provide the type and quantity of data needed for the following circumstances:

(1) Determining the location and characteristics of various celestial bodies and sources of light relative to the spacecraft for use in preflight and inflight analyses.

(2) Assisting in star identification in real time during flight operations.

(3) Postflight processing, analyzing, and performance evaluating.

The ATRM modifications were relatively minor, basically providing additional plotting capabilities for parameters generated by the ATRM. The following information was processed from trajectory input data and provided by this program upon request:

(1) Spacecraft coordinates as a function of time from injection.

(2) Clock and cone angles, Canopus ratios, angular diameters, bolometric fluxes, phase angles, and visual magnitudes for Venus, Earth, Mars, Jupiter, Saturn, and the Moon.

(3) Spacecraft-to-planet distances.

(4) Sun-to-planet distances.

(5) Earth–probe–Earth communications time.

(6) Bodies (stars, planets, and the Moon) in a spacecraft roll window.

(7) Plots of selected parameters from items (2) and (5) such as the following:

(a) Clock angle of any of the planets or the Moon.

(b) Cone angle of any of the planets or the Moon.

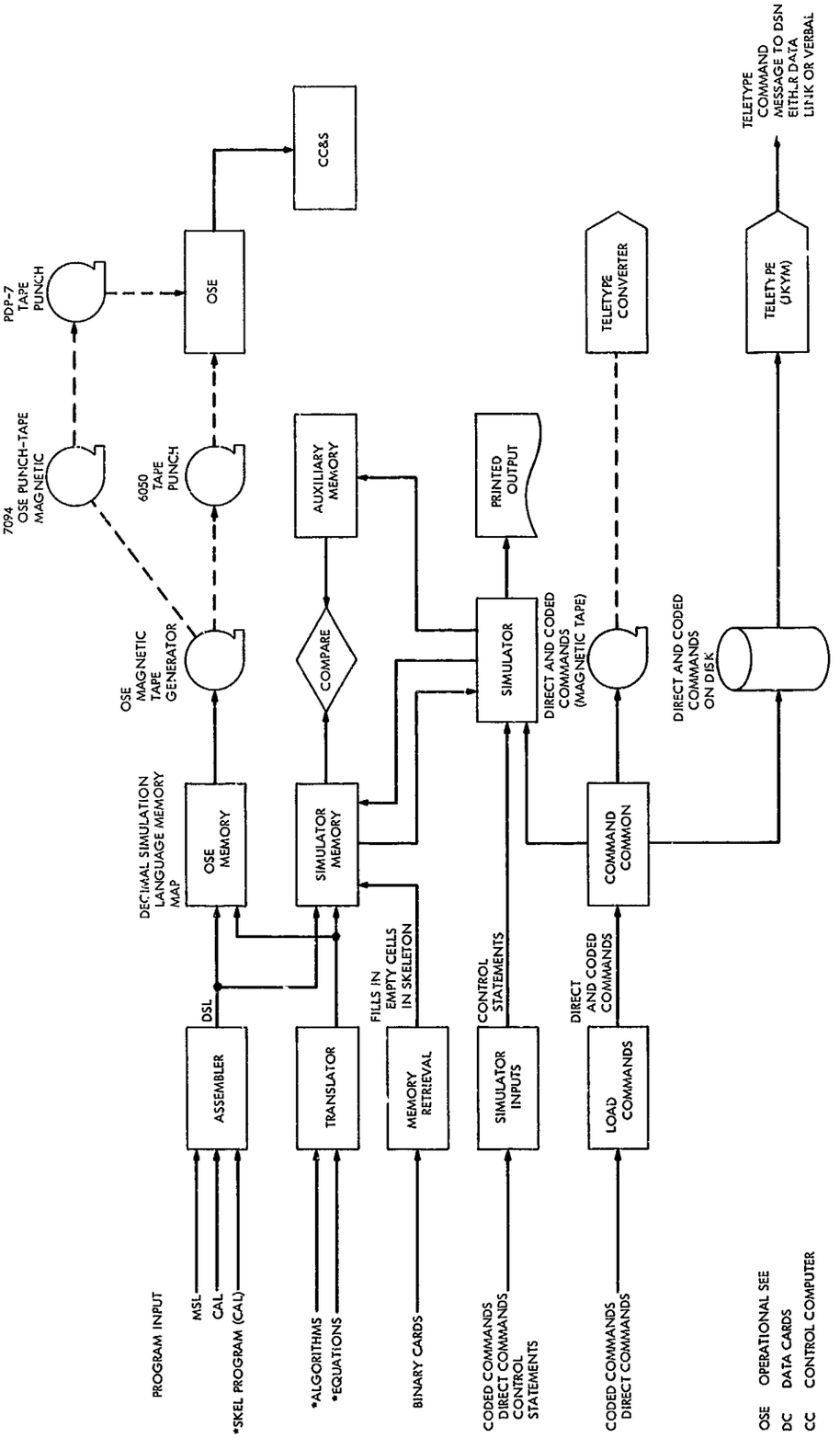


Fig. 10. Diagram of the COMGEN software system

(c) Illumination at the probe due to any of the planets or the Moon.

(d) Canopus ratio of any of the planets or the Moon.

(e) Celestial longitude of the probe.

(f) Celestial latitude of the probe.

(g) Earth–probe–Earth communication time.

(h) Primary–probe–secondary angle.

Major modifications were necessary for the SIPM. Formerly, star identification capabilities were required only during the roll search mode. Logic associated with the *Mariner* Mars 1969 Canopus sensor allowed the receipt of telemetry from the sensor during any spacecraft maneuver. Therefore, it was necessary to provide upon request (1) bodies (stars, planets, and the Moon) in the field-of-view of the Canopus sensor during any or all spacecraft maneuvers; and (2) prediction of the Canopus sensor response (in terms of either voltage output or telemetry data numbers) during any or all spacecraft maneuvers.

The capability of SIPM to provide star maps (simulation of Canopus sensor response as a function of light stimuli, i.e., stars, planets, and background in the field-of-view of the Canopus sensor) during a midcourse maneuver enabled the SIPM to provide information not available from previous programs. First, star maps could be obtained for turns about the pitch axis, where previously star maps could be obtained only for turns about the roll axis. Second, star maps could be obtained for turns about an axis arbitrarily oriented with respect to the sun–probe–canopus coordinate system. This last capability could be particularly important in identifying acquirable objects when and if the spacecraft coordinate axes ever achieved a fixed orientation with respect to the Sun–probe–Canopus coordinate system which was not the nominal orientation. In addition to trajectory input, various Canopus sensor characteristics, the spacecraft configuration (cone angle setting, roll search or maneuver, etc.), and the spacecraft initial attitude were required input.

Program output could be selected by the use of various control options; typical output was the *a priori* star map plot for a planned roll search (or maneuver) as shown in Fig. 11, along with various tabulated printouts of, for example, the following:

(1) Planet data for each turn and each cone angle, consisting of the name, radius, albedo parameter, and phase angle of each of five planets and the Moon.

(2) Name, number, and total effective Canopus ratio of objects in the roll search window.

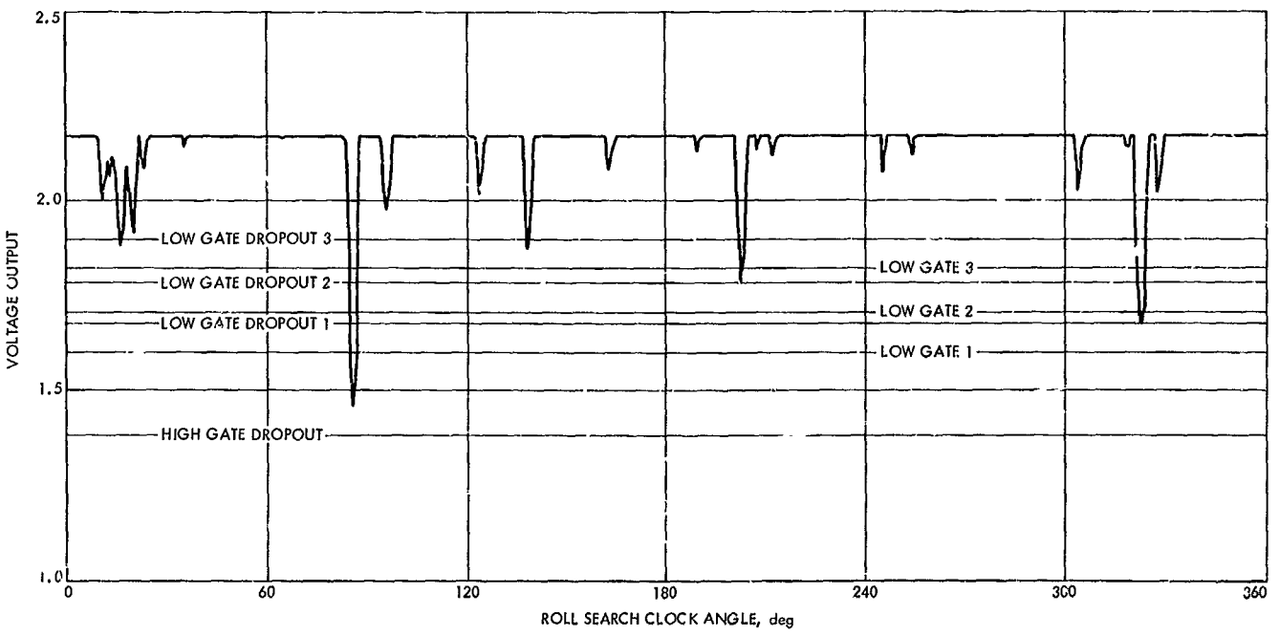


Fig. 11. Typical *a priori* star map generated by the SIPM program

(3) Object, number, pitch turn angle, pitch cone angle, and total effective Canopus ratio of objects in the midcourse pitch turn window.

(4) Object, number, roll turn angle, roll cone angle, and total effective Canopus ratio of objects in the midcourse roll turn window.

3. BUTEC program. Trajectory corrections for the *Mariner* Mars 1969 spacecraft were provided by the propulsion subsystem under control of the central computer and sequencer. A timed engine firing duration was used for impulse control, in differentiation to control by an accelerometer. The timer setting, or burn time, was transmitted to the spacecraft shortly before the maneuver. The specific time was the final product of the orbit prediction that yielded the spacecraft velocity change required to reach the aiming point, and the propulsion subsystem performance prediction that yielded the burn time required to give the desired velocity increment. The predicted time was calculated by the burn time estimation computation computer program, or BUTEC, which is known as PRPLS—for propulsion—in the Mission Operations System software chain.

a. Modification program. The BUTEC program used for the 1969 mission operations was a slightly modified version of that used for 1964 and 1967. The principal modifications and resulting operating improvements were as follows:

(1) A table of instantaneous specific impulse vs time was fed to the computer in place of the previous single value which was determined manually for each run.

(2) All specific impulse values put in to the program were for 70°F propellant. Corrections for other in-flight temperatures were now handled automatically by the program, by using a linear relationship.

(3) The treatment of regulator outlet pressure was broadened to include an initial propellant tank overpressure. Where initial propellant tank pressure was greater than 308 psia, the regulator remained locked up until the blowdown minimum pressure was reached, recovered to the regulator set pressure, and remained there for the rest of the burn unless cycling occurred.

(4) The regulator set pressure was then treated as a linear function of the instantaneous upstream nitrogen pressure instead of as a constant.

In general, these changes were minor, although the regulator improvements mentioned in item (3) necessitated a major restructuring of the program logic flow.

b. Error analysis. Maneuver velocity errors were estimated with a modified version of the BUTEC error analysis developed for *Mariner* Mars 1964. Only two significant changes were made for *Mariner* Mars 1969:

(1) Error sources related to the oxidizer start sequence were eliminated.

(2) Statistical estimates of actual measurement errors for flight analysis test data were used in lieu of analytical estimates of instrumentation capabilities.

In general, experience gained on the *Mariner* Mars 1964 and *Mariner* Venus 67 projects resulted in simplifying the designation of error sources and provided error estimates that more accurately reflected the hardware capabilities.

Table 6 shows the contributing sources to the proportional velocity error. For *Mariner* Mars 1969 a standard deviation of 1.26% was estimated, as compared with the *Mariner C* estimate of 0.74%. Judging from actual performance, the large increase was almost entirely due to the more realistic estimates of instrumentation accuracies.

Table 7 shows the contributing sources to the "resolution", or nonproportional velocity error. The reduction in trapped liquid volume and in catalyst bed volume that the spontaneous catalyst engine allowed resulted in a significant reduction in tailoff impulse as compared with the *Mariner C* estimates. The combined proportional and resolution errors are shown in Fig. 12 for a nominal spacecraft mass of 840 lbm.

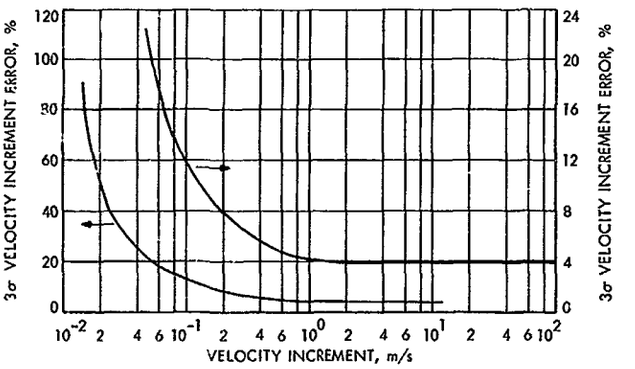


Fig. 12. Three-sigma velocity increment error vs velocity increment for a *Mariner* Mars 1969 840-lbm spacecraft

E. Testing and Change Control

The typical program testing sequence is shown schematically in Fig. 8, including the persons responsible for accomplishing the various phases of testing of both the programs and the software system. In the case of programs such as the DSIF telemetry processor and the SFOF 7044, the cognizant engineer acted as agent in accepting the program for multiple users representing science, engineering, the DSN and, in the case of the processor, the spacecraft system, since the processor bit synchronization algorithm was defined as a spacecraft data system responsibility. This was a very important function performed by the cognizant engineer.

The testing depicted is that required to assure that programs satisfied request for programming and design requirements, operated correctly in their associated systems including the satisfaction of all interface requirements, and were operable by persons not associated with their design or development. Not included is the type of testing required to demonstrate Spacecraft/MOS data systems

Table 6. Proportional velocity error propulsion contribution

Source	Magnitude	Influence coefficient	Conversion	Error (3σ), lbf
Thrust measurement:				
Thrust stand (3σ)[a]	1.0 lbf	1	1	1.0000
Vacuum correction (3σ)[a]	0.025 psi	6.62	1	0.1655
Chamber pressure measurement (3σ)[a]	2.1 psi	0.2681	1	0.5630
Regulator set point (3σ)[a]	10 psi	0.1209	1	1.2090
Regulator spring temperature (uniform)	1.0 psi	0.1209	$\sqrt{3}$	0.2094
Regulator operating uncertainty (uniform)	3.0 psi	0.1209	$\sqrt{3}$	0.6282
Propellant temperature measurement (3σ)[a]	1.3°F	0.000381	1	0.0005
Spacecraft propellant temperature				
Transducer (uniform)	1°F	0.000381	$\sqrt{3}$	0.0007
Telemetry (uniform)	4.5°F	0.000381	$\sqrt{3}$	0.0030
Flow resistance (3σ)	0.05	13.22	1	0.6610
For nominal thrust 50.7 lbf			Sum	4.4403
3σ error = 1.919 lbf or 3.78%			Root sum square	1.9187
1σ error = 0.640 lbf or 1.26%				

[a]Based on TRW instrumentation accuracies. All others are JPL-derived.

Table 7. Resolution velocity error propulsion and pyro contributions

Source	Magnitude	Error (3σ), lbf–s
Timing errors		
Ignition delay (3σ)	0.005 s × 50.7 lbf	0.254
Squib and valve (3σ)	0.001 s × 50.7 lbf • (count twice)[a]	0.102
Tailoff impulse (3σ)		0.758
	Sum	1.114
	Root sum square	0.803
3σ error = 0.803 lbf–s		
1σ error = 0.268 lbf–s		

[a]For start and shutdown.

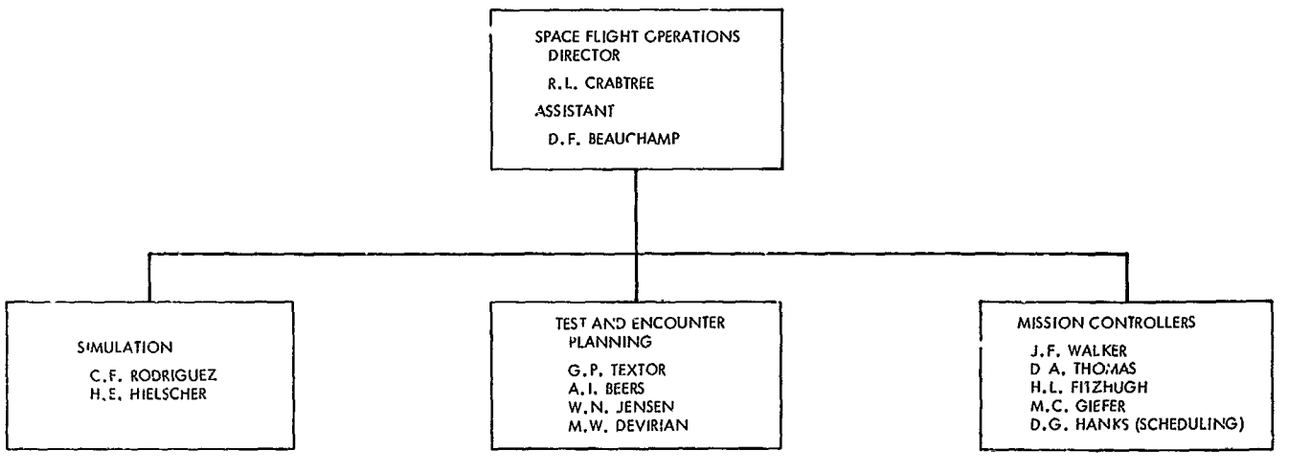


Fig. 13. Mission control team organization

compatibility, for example. However in the event incompatibility was demonstrated in such tests, it was necessary to modify either programs or software system accordingly.

A software change control procedure was defined in the first management document issued by the two management systems in 1966. The procedure was applicable to functional requirements, request for programming documents, and operations manuals as well as to actual program code. Any program or software system that had been accepted for operations or for test purposes such as compatibility demonstration of the spacecraft with the Mission Operations System was never actually changed. The accepted program versions or systems were kept available on tape or in card deck form for later use; meanwhile a new version of the program or system incorporating the approved change was developed for later testing, acceptance, and use.

Changes requested by software users required concurrence of the system engineer, including a review of system compatibility and an approval of resource and schedule requirements prior to implementation. Several weeks before the launch and encounter operational readiness tests, all requested changes also required the approval of the Space Flight Operations director. Disapproved requests could be appealed to the manager of the appropriate management system.

V. Operations System

The design of the operations system was closely related to that of the mission operations, and its history is therefore discussed briefly in Part 1 of this volume (see page 32). The present section provides a functional description of the operations system. It consisted of the mission control team, the SPAC group, the FPAC group, and the SSAC group. The operational organization during space flight operations is described in the following paragraphs.

A. Mission Control Team

The mission control team was the functional mission control organization composed of the Space Flight Operations director, the assistant directors, and several members of the director's staff.

The composition of the team changed with the operational design cycle. Before launch, the team developed test and training plans, simulation design, and preparation of test data packages, and participated in mission operations design activities. After launch, the team assumed the organization shown in Fig. 13, with responsibilities that included the following:

(1) Controlled the conduct of the Space Flight Operations in accordance with the standard sequence of events; controlled and disseminated changes to the standard sequence of events.

(2) Continuously monitored and assessed the use of the DSN facilities assigned to support the project, and recommended changes in the DSN utilization plan to the mission director.

(3) Coordinated the operational activities required to send commands to either spacecraft.

(4) Ensured the correlation between the state of the spacecraft data system and the state of the DSN telemetry software at all times during the mission.

(5) Monitored status of the operational facilities and the spacecraft at all times, and reported such status as required by the SFOD.

(6) Assisted in determining nonstandard spacecraft conditions and was responsible for notifying proper personnel for evaluation of these conditions, determined the necessity for additional data processing, and directed the execution of additional processing for making proper evaluation.

(7) Maintained an operations log.

The mission controllers were operational positions that were staffed on a 24-h-day basis by members of the mission control team. During all phases of the mission, the Space Flight Operations were under the immediate control of the mission controllers, who were delegated the authority of the Space Flight Operations director to perform those operational functions stated in the previous paragraph.

The assistant mission controller was an operational position staffed by a member of the mission control team during mission periods of high activity and, normally, activities of the noncritical spacecraft.

B. Spacecraft Performance Analysis and Command Group

The principal function of the spacecraft performance analysis and command group (SPAC) was the analysis of spacecraft performance at two levels: the subsystem level and the system level, i.e., (1) analysis of performance of each subsystem of the spacecraft, and (2) integration of the

analyses into an interpretation of performance of the spacecraft as a system. The specific functions of the performance analysis group were as follows:

(1) To monitor and analyze the performance of the spacecraft throughout the mission.

(2) To recommend and execute courses of action for optimizing spacecraft performance.

(3) To provide technical information about the spacecraft required by the Space Flight Operations director for the control of the flight operations.

(4) To recognize nonstandard conditions on the spacecraft, recommend to the Space Flight Operations director alternate procedures or sequences, and analyze the effects of such recommendations on mission success.

(5) To evaluate all command actions proposed by other technical analysis groups, as well as those originating within the SPAC group, and recommend future courses of action to the Space Flight Operations director.

(6) To assemble, verify, and generate command messages for all commands to be sent to either spacecraft in support of all technical analysis groups.

The flight spacecraft were designed so that all standard cruise, encounter, and playback events could be initiated and executed automatically by external stimuli or in accordance with a program stored in the CC&S before launch. The design also included provision for changing the stored program after launch by ground command. This capability was to be used to increase the probability of mission success and provide the flexibility for the following:

(1) To assure proper execution of all standard events by planning and carrying out parallel initiation and execution of events; e.g., transmitting direct commands to execute events in parallel with on-board-initiated commands.

(2) To monitor spacecraft performance to detect as early as possible anomalous behavior or operational trends that may presage failures.

(3) To initiate corrective action when failures occur or seem probable.

(4) To plan and execute changes in the stored program according to developments during the flight; e.g., execute a trajectory correction maneuver to remove the injection errors, change bit rates to optimize telemetry reception, modify the encounter sequence, etc.

1. Organization. To accomplish its functions at the system–subsystem levels, and to use the spacecraft capabilities as designed, the SPAC was organized in teams and crews as shown in Fig. 14. The subsystem analyses for both spacecraft were performed by the analysis crew. The system analysis was performed by the *Mariners VI* and *VII* teams for their respective spacecraft. The operational organization of the SPAC, shown in Fig. 15, was designed to support varying levels of activity during the mission and to operate two spacecraft simultaneously.

2. Responsibilities of the SPAC director and deputy. The SPAC director and his deputy were in operational control of all members of the group. The director directed the overall activities of the group in fulfilling its assigned responsibilities, established and controlled the SPAC organization and ensured appropriate staffing, controlled the interfaces between the SPAC and the other elements of the operational organization, and ensured that detailed operating procedures for the SPAC were prepared. He approved all command messages before submitting them to the Space Flight Operations director. In addition, he

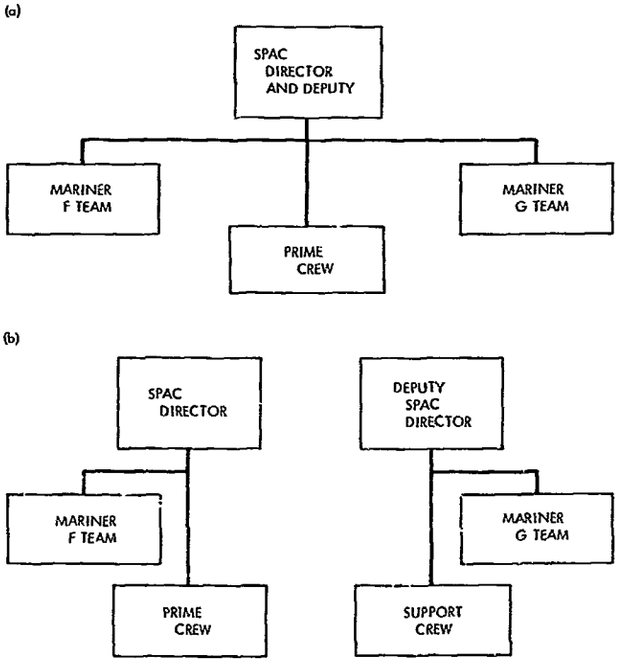


Fig. 14. SPAC organization for one- and two-spacecraft operations: (a) one spacecraft, (b) two spacecraft

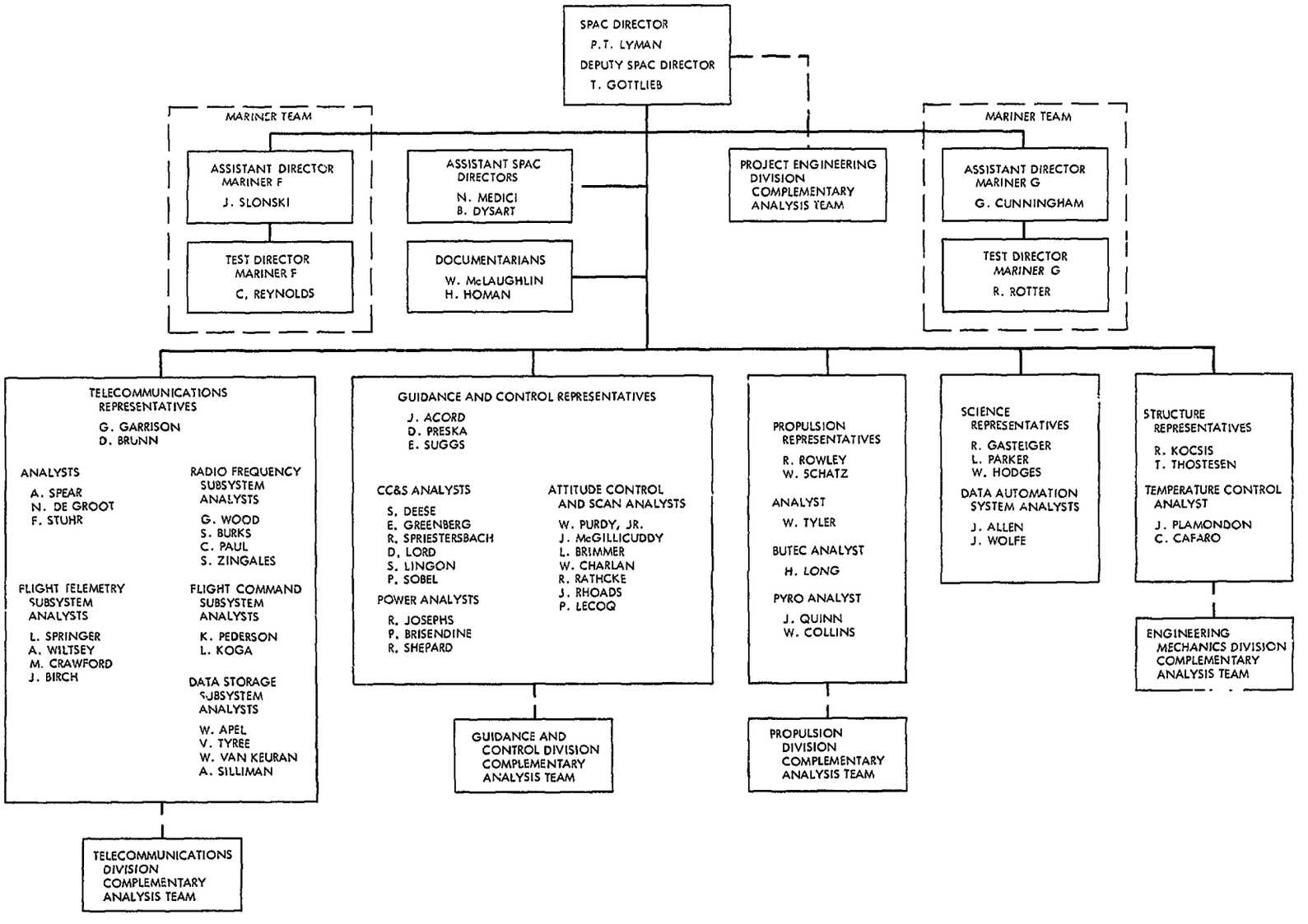


Fig. 15. SPAC organization

maintained and disseminated spacecraft status information, and gathered the designated spacecraft data for post-mission analysis. The deputy director assisted the director and performed the duties of the director in the latter's absence.

3. Role of the spacecraft teams. Each spacecraft team was permanently assigned to a spacecraft (*VI* or *VII*) and included an assistant director, a test director, and a documentarian who maintained a log book and a status summary on the spacecraft. Each team, in addition to analyzing the system performance of its assigned spacecraft, served as the central, authoritative, and comprehensive source of current and historical information about its spacecraft. The assistant SPAC director for the team served as the cognizant engineer for his spacecraft, and maintained constant awareness of its status. This included maintaining the current memory image of the central computer and sequencer spacecraft.

After the launch of his spacecraft, the spacecraft test director joined the spacecraft team as a consultant, contributing the experience gained during the testing of that spacecraft at the spacecraft assembly facility and the AFETR.

4. Role of analysis crews. The subsystem analysts were organized into two crews: the prime crew, consisting of all subsystem analysts (Fig. 15), and the support crew. With the exception of the telecommunications representative, the telecommunications analysts, the CC&S analyst, and the assistant CC&S analysts, the prime crew was duplicated on a man-for-man basis by a support crew. The prime crew functioned during all critical phases and was responsible for both spacecraft throughout the mission.

The support crew provided a second-shift support for the prime crew for those critical events which required extended SPAC operations. In addition, it provided subsystem analysts for a SPAC organization, which can control the second spacecraft if both spacecraft become critical at the same time because of nonstandard performance of either. The standard mission was planned so that critical phases of two spacecraft did not overlap.

Each subsystem analyst had to interpret and provide detailed analysis of the engineering telemetry related to his subsystem, advise the SPAC director of his subsystem status and performance, and analyze the effect on his subsystem of any action proposed by the director. In addition to these general responsibilities, specific analysts had special responsibilities.

The SPAC science representative was a member of that group and responsible to its director, who served throughout the mission as the primary liaison between SPAC and SSAC. He was responsible for the analysis of data related to the science subsystems as contained in the spacecraft engineering telemetry. During periods when the space science analysis area was not staffed, the science representative served as SPAC science instrument analyst. When the area was staffed, he provided the SPAC director with the science instrument engineering status and performance from SSAC. In addition to his SPAC responsibilities, the science representative advised the SSAC director of anomalous conditions or trends as they became apparent in his analysis of the science-related engineering telemetry data.

The data automation subsystem (DAS) controlled the science data and the science instruments on the spacecraft. The subsystem analyst was responsible for analyzing and evaluating the data automation subsystem operation. He prepared and maintained predictions of the occurrence of spacecraft events related to the science instruments, and provided, for the science data team, spacecraft data recorded on display devices of his subsystem. In addition, he informed the SPAC director regarding the data automation subsystem operation of the science instruments in order that the interaction of all spacecraft systems might be properly evaluated; and, in the event of anomalous instrument behavior, he recommended corrective action.

The telecommunications representative performed analysis to determine and predict the RF link performance and advised the SPAC director of its status; he was assisted by the telecommunications analyst. In addition, he recommended to the SPAC director alternate procedures or sequences to overcome degraded performance or to optimize performance; and, when necessary, prepared a diagnosis in conjunction with the DSIF operations project engineer and the analyst of the possible sources of loss of data, with recommendations for appropriate courses of action.

The flight command subsystem analyst prepared all command messages, and calculated the delay between the transmission of a command from the ground command subsystem (RWV) and its execution by the flight command subsystem.

The CC&S subsystem analyst prepared assembly-language CC&S computer programs for the 7094 CC&S assembler (COMGEN), prepared and maintained the standard CC&S sequence used in the 7094 CC&S program

translator (COMGEN), analyzed the response of the 7094 simulation program (COMGEN), and prepared coded commands. When reprogramming of the CC&S or readout of the CC&S memory was planned (for example, in preparation for a maneuver) the analyst was helped by an assistant analyst.

The structure representative provided information to SPAC on the spacecraft configuration and coordinate systems, assisted the temperature control analyst, and maintained expertise in interpreting engineering teletype format of the telemetry and command processor.

The temperature control analyst analyzed the temperature of all parts of the spacecraft, predicted the spacecraft temperature at future points in the mission, and recommended alternate procedures or sequences to optimize the temperature control of the spacecraft.

The burn time estimation/calculation (BUTEC) analyst coordinated with the FPAC during the maneuver calculations, to insure the selection of the proper burn time.

5. Division representatives. In addition to the duties of analysts listed above, each technical division that provided personnel to the SPAC had a division representative who coordinated the activities of the subsystem analysts from his division, ensured adequate staffing, and served as the point of contact with his division's complementary analysis team.

6. Complementary analysis teams. Certain divisions provided complementary analysis teams that supplemented the SPAC. All these teams were under operational control of the appropriate division representative. (The complementary analysis team of the Project Engineering Division was controlled by the SPAC director.) The teams were located in several buildings at JPL in Pasadena (not in the SFOF) and were responsible for supplementing the SPAC team by analysis, interpretation, and evaluation of the performance of the spacecraft during operations.

The teams analyzed in detail the problem areas of proposed alternate sequences as requested by the division representative, provided access to documentation too extensive to be stored in the space performance analysis area, permitted monitoring of the space flight operations by personnel not in the SPAC group, and trained personnel for that group.

7. Spacecraft launch team. At the AFETR, a supplementary SPAC capability was maintained from the launch of each spacecraft through its first midcourse maneuver. The group director decided if and when this capability should be used.

The SPAC operations at Cape Kennedy were performed by selected members of the spacecraft launch team. Specifically, the same people who had been analyzing the spacecraft test data, analyzed the flight data using the same display devices, data formats, and data processing software that were used for test data analysis.

The organization for control and use of the launch team was the same after launch as before except that the spacecraft test director (who functioned as the SPAC director at the Cape after launch) received operational instructions after launch from the SPAC director rather than from the spacecraft operations manager.

The SPAC–Cape liaison operator provided a communication link to the SPAC during this period; before the launch he kept the director informed of the test progress and activities of concern to that group, and after launch he kept the test director informed on SPAC activities. The functional relationships of the SPAC and the spacecraft test team are shown in Figs. 16 and 17.

8. Operational plan. The formation of the SPAC operational organization took place September 13, 1968, when a series of exercises and tests were planned for developing within the organization the following capabilities:

(1) To perform the functions and carry out the responsibilities listed in the previous paragraphs.

(2) To work effectively with the other members of the mission operations.

(3) To understand normal spacecraft operation.

(4) To diagnose anomalous spacecraft behavior.

(5) To simultaneously operate two spacecraft in flight.

The operational mode of the SPAC organization changed slightly with different mission phases. The specifics of each phase are listed in the following paragraphs.

The SPAC organization first conducted actual operations at the time of the launch of the first spacecraft. The pre-launch countdown, conducted by the launch team, was monitored by the organization to provide continuity in the monitoring and controlling of the spacecraft, since the responsibility for monitoring the spacecraft performance shifted from the launch team to the SPAC at the time of lift-off. Lift-off is defined as the point when the 2-in.

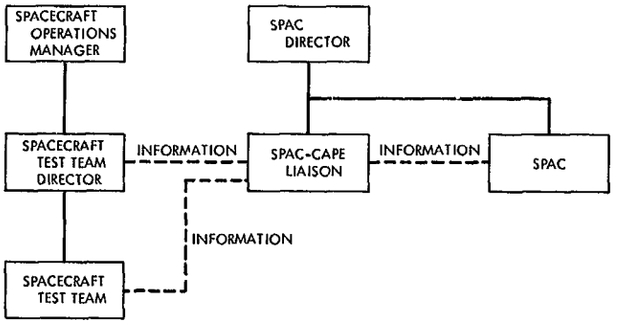


Fig. 16. SPAC–Spacecraft test team prelaunch operational organization

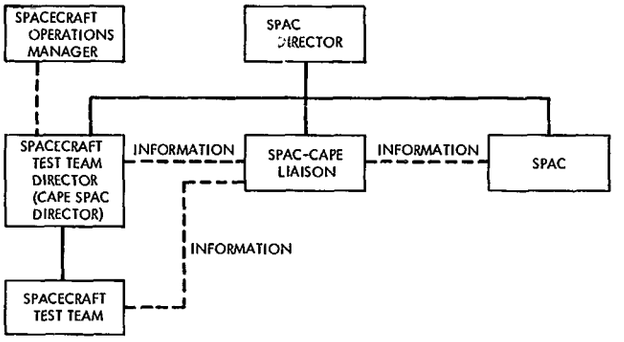


Fig. 17. SPAC-Spacecraft test team postlaunch operational organization

umbilical is dropped from the launch vehicle. The launch team continued to monitor the operation of the spacecraft and advised the SPAC of its evaluation of the performance.

The organization monitored the spacecraft until the spacecraft acquired the Sun and Canopus, all subsystems were switched to the cruise mode, and the spacecraft performance in the cruise mode was sufficiently stabilized to be pronounced normal. At this point the organization converted to cruise mode operation.

Except during the launch, the maneuver, the encounter, and the playback phases, the SPAC organization operated in the cruise mode. In this mode the performance of the spacecraft was monitored by collecting all the telemetry acquired by the DSN during a 24-h period, analyzing the data, and preparing a report that was submitted to the director of flight operations describing the performance of the spacecraft. The data was not analyzed by SPAC in real-time. However, the 7044 computer performed alarm limiting on all spacecraft telemetry which permitted automated surveillance of the spacecraft whenever the DSN could provide telemetry data. Each week a summary report was submitted by SPAC to the Space Flight Operations director. Every six weeks a composite report was submitted covering the entire period.

During the cruise phase of the mission certain events took place on the spacecraft. Whenever events occurred that changed the state of the spacecraft, the SPAC organization changed to an active cruise mode. The spacecraft was monitored in real time, and the change in state analyzed; and when the normal operation of the spacecraft in the new state was verified the SPAC organization returned to its passive cruise mode of operation.

The maneuver phase required extensive coordination with the FPAC team to select the time of execution of the maneuver. The maneuver could be performed in one of three modes by the on-board central computer and sequencer. These were a tandem maneuver, a computer maneuver, or a fixed sequencer maneuver. Depending on the mode of execution of the maneuver, the SPAC team used the COMGEN program to simulate the maneuver and generate the command message for transmission to the Deep Space Station which in turn transmitted the commands to the spacecraft. After completion of the maneuver, the spacecraft was returned to the cruise mode and its normal operation verified. Upon completion of this verification, the SPAC operation returned to the cruise mode of operation.

The encounter phase required the heaviest interaction between the SSAC, the FPAC, and the SPAC organizations. The strategy for this phase of the mission was developed by the encounter planning group. When the strategy was formulated, the SPAC and SSAC organizations combined their monitoring and analysis functions to confirm that the spacecraft was performing normally and the strategy could be carried out as planned.

The SSAC organization provided SPAC with its analysis of the performance of the science subsystems so that the SPAC organization could perform its function of analyzing the overall performance of the spacecraft.

The playback phase was handled somewhat like the cruise phase in that there were periods of active monitoring and control of the spacecraft and other periods of lesser activity when the computer merely kept track of the spacecraft performance. When the playback phase was initiated, the SPAC verified the spacecraft performance in the playback mode in real time. In addition, all events of the playback phase were monitored in real time.

The normal procedure for the two-spacecraft operation was to maintain at least one spacecraft in the cruise mode at all times so that the attention of the SPAC organization could be focused on the spacecraft in a critical or an active mode. However, if both spacecraft needed to be monitored, analyzed, and controlled, the assistant director for that spacecraft and some analysts were used to carry out a holding action to delay the necessity for controlling that spacecraft by the entire SPAC organization. If the holding action could not be maintained until the active spacecraft was switched to a passive mode, the SPAC organization for two-spacecraft operation, consisting of the support crew and the appropriate spacecraft team, was implemented. Control of each spacecraft was performed independently in this case.

C. Flight Path Analysis and Command Group

Operations associated with determination of the orbits, positions, and encounter parameters of the spacecraft were the responsibility of the Flight Path Analysis and Command (FPAC) group. Specific functions included the following:

(1) Determining spacecraft orbit as soon as possible after launch, and obtaining an ephemeris of the spacecraft to provide initial acquisition and prediction data for the DSIF and initial input for a launch vehicle trajectory performance evaluation.

(2) Determining the spacecraft orientation to assist in the evaluation of spacecraft performance.

(3) Obtaining trajectory parameters so that successive blocks of antenna-pointing-angle predictions and other DSN acquisition information can be generated.

(4) Estimating, at any time, the orbit of the spacecraft from available tracking data, with periodically increasing accuracy as additional data is accumulated.

(5) Conducting midcourse studies for evaluating possible trajectory correction alternatives.

(6) Generating required information for correcting the trajectory to achieve the desired aiming point.

(7) Providing information for updating trajectory-dependent spacecraft parameters, and of encounter information for updating the science platform pointing angles.

(8) Generating the information required to evaluate the encounter geometry.

(9) Calculating a post-encounter orbit and the corresponding spacecraft ephemeris.

(10) Establishing the criteria to determine the quality of the tracking data.

The FPAC organization is shown in Fig. 18, and its various elements are described in the following paragraphs.

1. Air Force Eastern Test Range/Real Time Computer Complex. Metric data collected during powered flight were monitored in real time. The data collected between the time of *Centaur* main engine cut-off and spacecraft separation were processed to give the first indication of the orbit achieved. Station predicts were generated as a backup procedure.

2. Orbit determination group. Orbits were fit to the accumulated tracking data. As soon as enough data were received, checks were performed to determine whether data from all stations were consistent. Any systematic errors detected were then investigated to determine corrective action.

Nominal maneuver orbits were computed for maneuver calculations, and a definitive orbit estimate was made as late as possible (in order to use the latest tracking data) for computing the actual maneuver. Post-maneuver orbits were then estimated as sufficient tracking data were collected, and actual maneuver performance was evaluated by comparison with the pre-maneuver orbit.

Near encounter, orbits were estimated in rapid succession with the use of short data arcs (on the order of 5 days of data), in order to observe the spacecraft acceleration, which is sensitive to the exact encounter geometry. With post-encounter data, the actual encounter orbit was estimated very accurately because of the very high sensitivity of the acceleration profile to the spacecraft position near closest approach. The final orbit was then used by the experimenters to evaluate their data.

a. Double precision orbit determination program encounter operations group. The double precision orbit determination program (DPODP) was officially delivered to the *Mariner* project on May 1, 1969. This program had been under development by the JPL precision navigation project for several years, and was needed for taking advantage of the inherent accuracy of the tracking data. In order to use the capabilities of the program, other error sources, which were formerly masked by single precision computational accuracy, had to be reduced. The subgroups to be described were organized for this purpose.

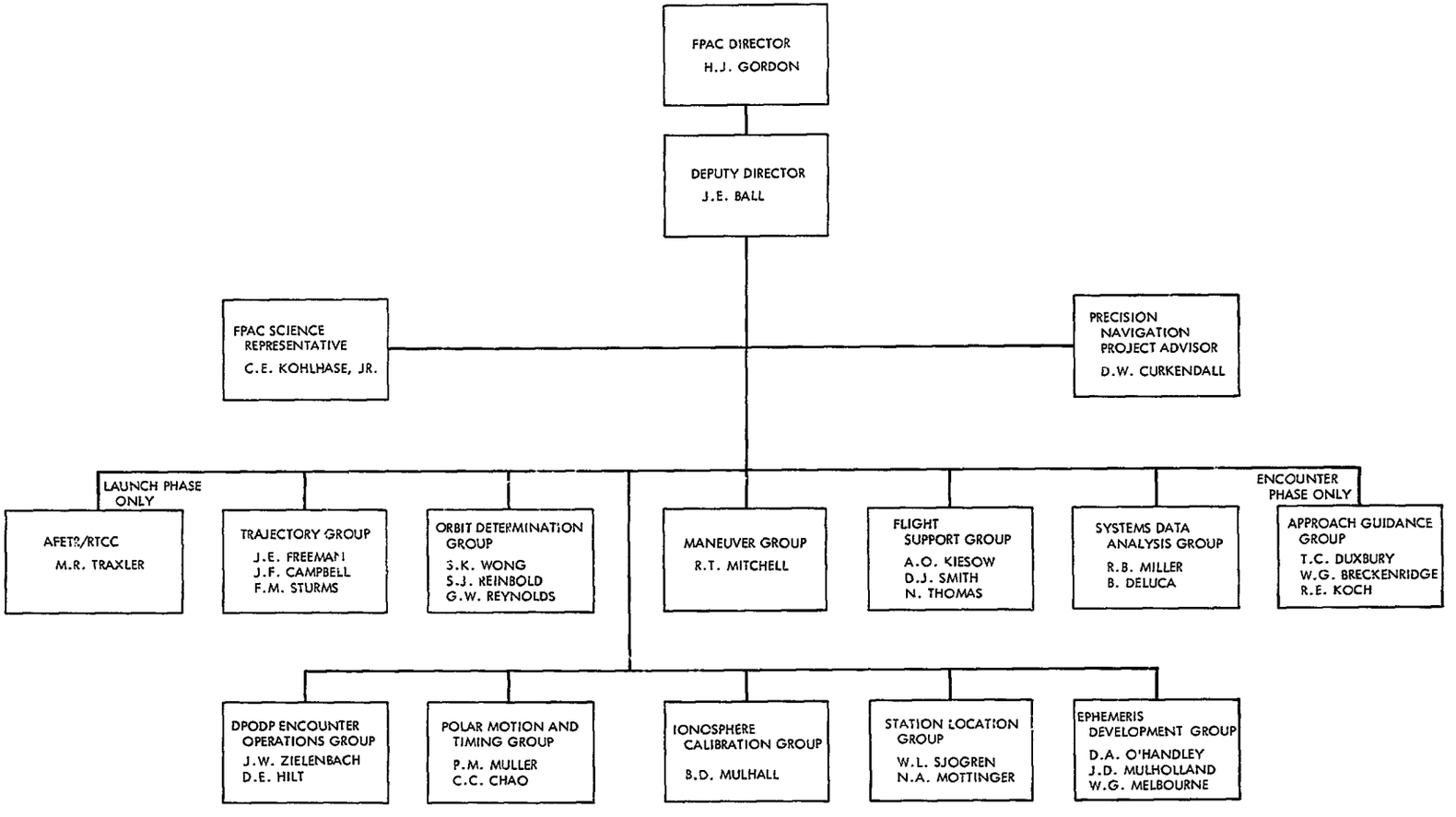


Fig. 18. FPAC operational organization

b. Polar motion and timing group. Daily astronomical observations were processed to determine the position of the Earth's crust relative to the spin axis, and to determine the Earth's spin rate. This enabled daily updating in the difference between universal time (UT) and ephemeris time (ET).

c. Ionosphere calibration group. Radio signals propagating through a plasma of charged particles undergo changes in both phase and group velocity. If not corrected, the effects of the ionosphere can cause an apparent change in path length. Ionosonde and Faraday rotation measurements were made in California, Spain, South Africa, and Australia in order to properly model the ionosphere of the Earth and account for the effect on the spacecraft signal.

d. Station location group. The largest single error source affecting encounter orbit determination accuracy was the knowledge of the positions of the tracking stations relative to the spin axis of the Earth. Data from previous missions were reprocessed by the DPODP to accurately determine positions on the Earth's crust. Observations of polar motion then enabled proper values of latitude, longitude, and distance from the spin axis to be used.

e. Ephemeris development group. Not actually an operational group, the ephemeris development group processed up-to-date Mars radar bounce data together with recent optical observations to supply a Mars ephemeris which was as accurate as possible. Mission planning and actual launch used Development Ephemeris (DE) 40. This was upgraded before performing a maneuver, by DE 69; and this was further upgraded before encounter, by DE 71.

3. Maneuver group. Plots of maneuver capabilities were prepared for making real-time rough estimates of maneuver requirements immediately after launch. When the nominal maneuver orbits were computed, a maneuver study was carried out to determine when the maneuver was to be made so that all constraints were satisfied. After holding a maneuver conference at which all members of the Mission Operations System were represented, the project manager approved a maneuver to be executed. The maneuver parameters were then computed from the latest orbit available and required turns and burn time were given to the SPAC for preparation and to the mission control team for transmission to the spacecraft.

4. Flight support group. The flight support group handled all computer interfaces. They ran all the FPAC programs used in the software system, and were responsible for maintaining the tracking master data files in an up-to-date condition.

5. Systems data analysis group. Nominal predicts were prepared and transmitted to the tracking stations before launch. At $L-24$ h, predicts based on final RF frequency measurements made at Cape Kennedy were transmitted. During the launch countdown, predicts were generated and transmitted whenever a nonscheduled hold occurred. After a good orbit determination was made, a longer set of predicts was generated and transmitted to all the tracking stations.

Incoming tracking data was monitored during all mission phases. Monitoring was accomplished by examining a printed display of the data as it arrives, and by using the pseudo-residual program which computed and plotted the differences between observed and predicted data. During the encounter phase there was close liaison with the occultation experimenter who must have very accurate exit occultation predictions to enable rapid reacquisition of signal.

6. Approach guidance group. Optical data from TV pictures and output of the far-encounter planet sensor accumulated during the far-encounter mission phase was processed as an additional tracking data type, and combined with radio tracking data. This group operated outside of the SFOF environment, and activities were coordinated by the deputy FPAC director.

D. Space Science Analysis and Command Group

The SSAC group is the element of the Space Flight Operations organization that performed those operational functions related to the accomplishment of the scientific objectives of the *Mariner* Mars 1969 mission. The group is organized under the SSAC director into the principal investigators team and the operations and analysis team, as indicated in Fig. 19.

The principal investigators team was composed of a chairman, in the person of the SSAC deputy director, the principal investigators with the participating co investigators for the scientific investigations selected for the *Mariner* Mars 1969 mission, and the FPAC science representative. The principal investigators team conducted flight and trajectory studies and evaluated science and engineering tradeoffs, both as to the constraints and requirements necessary to the accomplishment of the scientific investigations and as related to the performance and environment of the science instruments. During flight

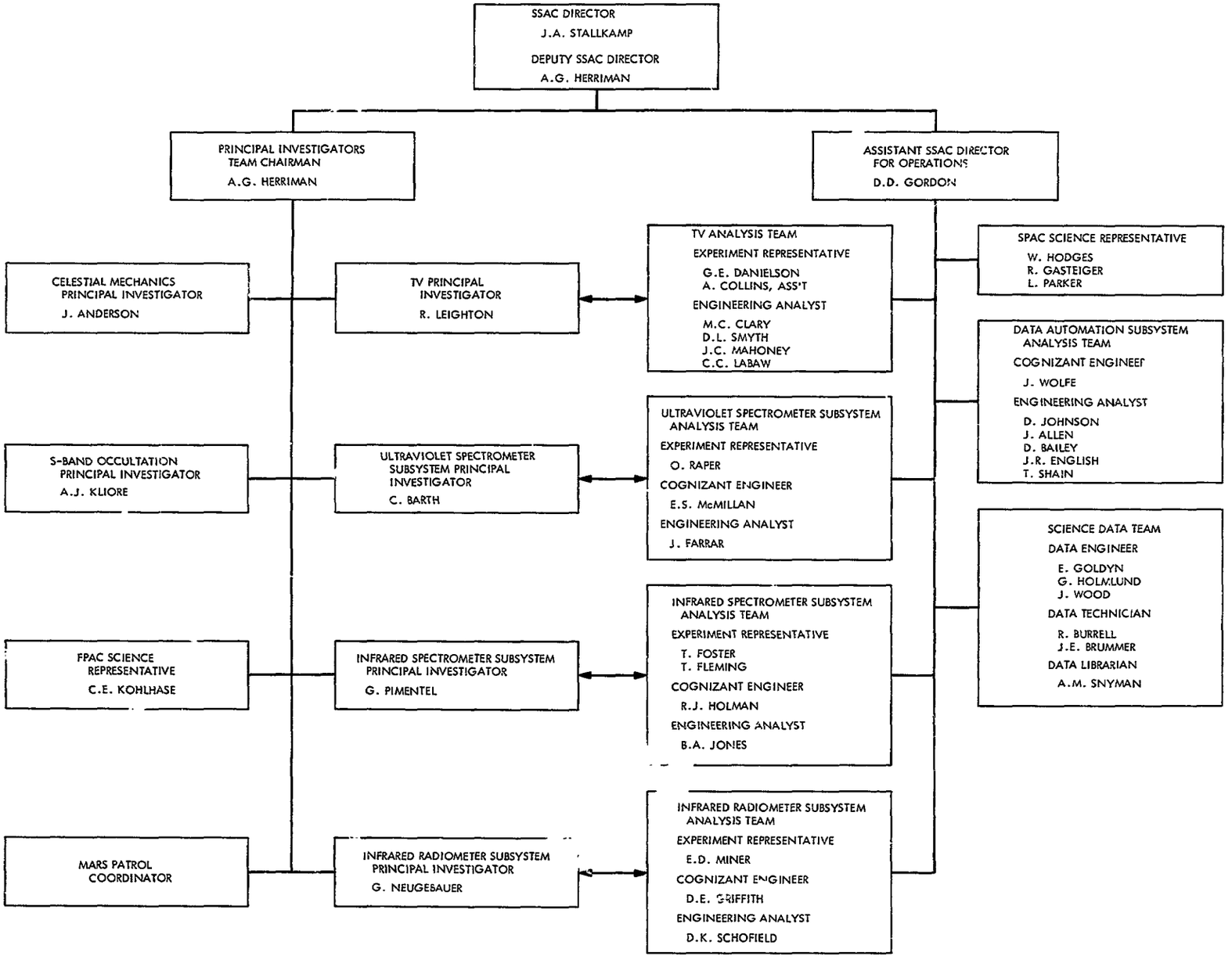


Fig. 19. SSAC operational organization

operations at critical phases of the mission, and as requested, the principal investigators team provided procedural recommendations for the enhancem· ·· ·· ·· the scientific value of the mission.

The operations and analysis team, under the supervision of the SSAC assistant director for operations, included the instrument analysis, the data automation subsystem analysis team, the science data team, and the division space science representative.

Instrument analysis teams, one for each science instrument (IRR, IRS, UVS, and TVS) were composed of the experiment representative and the cognizant engineer in each case. The instrument analysis teams analyzed the science instrument data and evaluated the operation of the science instruments. Each team was available to the principal investigator on a continuous basis for consultation and assistance in his evaluation of the conduct of the science investigation for which he was responsible.

The data automation subsystem analysis team was responsible for analysis and evaluation of the data automation subsystem operation. The subsystem controlled the science data and the science instruments on the spacecraft.

The science data team was responsible for coordinating the display, processing, distribution, and cataloging of all science and science-related data.

The SPAC science representative was responsible for the analysis of data related to the science subsystems as contained in the spacecraft engineering telemetry. He also reported the status of all science subsystems to the SPAC director, who was responsible for the performance of the total spacecraft.

E. Operational Organization

The operational organization that managed and controlled the execution of the *Mariner* Mars 1969 space flight operations is shown in Fig. 20 and described in detail in the Space Flight Operations plan. This chart depicts lines of responsibility, not lines of communication, data flow, or information flow. A brief role statement of each position is indicated in the following paragraphs.

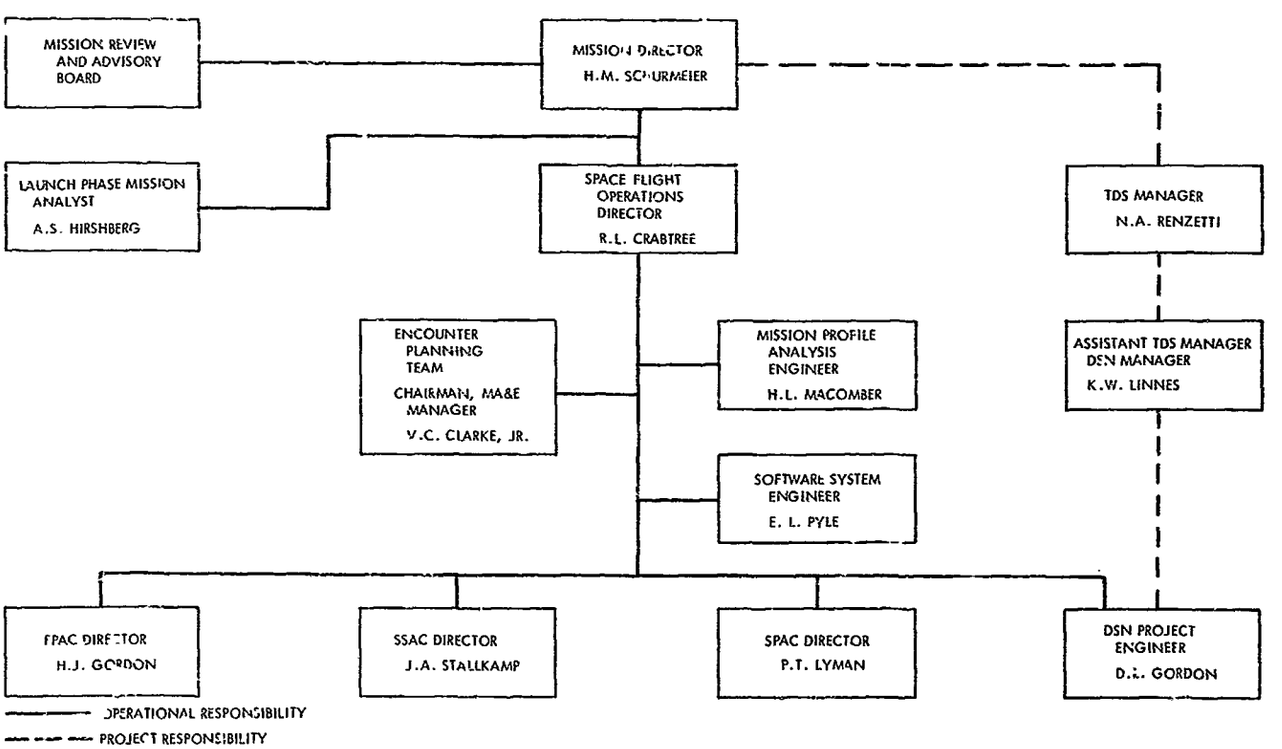


Fig. 20. SFO operational organization

Mission director. The mission director was the project manager and was responsible for overall direction of the mission.

Mission review and advisory board. The mission review and advisory board, established by the mission director, who is also chairman, consisted of the project system managers, other members of the project staff, and other personnel as requested by the mission director, and served to periodically review progress of the mission and review planned operational sequences.

Launch phase mission analyst. The launch phase mission analyst served as a staff engineer to the mission director before the launch at Cape Kennedy and, by assessing the constraints imposed on the launch by the various systems of the project, assisted the mission director in determining acceptable modifications to the launch period and launch window duration. After launch the launch phase mission analyst collected and assessed data from the launch vehicle, spacecraft, and TDS systems, and informed the Space Flight Operations director of significant data available in real time only at Cape Kennedy.

TDS manager. The TDS manager was responsible for the design and readiness of the tracking and data system for the project. Operationally he monitored the condition and performance of system elements and advised the mission director on their application.

Assistant TDS manager. The assistant manager of the TDS was also the DSN manager for the *Mariner* Mars 1969 project and was responsible for formulating the plans and tests required by the DSN to meet the project requirements. He was also responsible for monitoring the DSN performance, and responded to the project requirements requiring changes in the committed resources.

Space Flight Operations director. The Space Flight Operations director assisted in the overall functional design of the mission operations and plans and directed the execution of the Space Flight Operations. The director was delegated the authority of the project manager to direct and place requirements on the technical analysis groups and the DSN during pre-launch testing and during the Space Flight Operations. Before launch the director was accountable to the *Mariner* Mars 1969 manager of the Mission Operations System and after launch to the mission director in the discharge of his responsibilities.

Mission profile analysis engineer. The mission profile analysis engineer serves as a staff engineer to the Space Flight Operations director. His function was to maintain an up-to-date awareness of the status of the mission and assist in the development of the strategy by which the project used the DSN resources.

Software system engineer. The software system engineer advised and assisted the Space Flight Operations director, as required, in determining the optimum software state that assured effective use of the DSN data system resources to meet the mission objectives, particularly during changing mission requirements because of unforeseen events.

Encounter planning team. The encounter planning team was established after the trajectory correction maneuver of the second spacecraft with the MA&E manager as chairman. The operational function of the team was to refine the far- and near-encounter sequences to be executed by each spacecraft and provide to the Space Flight Operations director optimal encounter sequences to attain maximum scientific return consistent with practical considerations and operational risks.

F. Mission Operations Training and Testing

The requirement for a comprehensive test program for the *Mariner* Mars 1969 mission operations was established in the MOS/TDS management plan. The objectives of this test program were as follows:

(1) To ensure operational readiness of all elements of the MOS and TDS required to execute the mission operations.

(2) To demonstrate and verify compatibility between the flight spacecraft and mission operations.

(3) To train MOS and TDS personnel.

The test program was documented in the mission operations master test program document and approved by the managers of the Missions Operations System, the Tracking and Data System, and the Spacecraft System. The master test program established four categories of tests for mission operations—the compatibility, software, training, and system tests. The types of tests in each category, the individual responsible for preparing and conducting the test, and the location of test documentation is shown in Table 8. A list of training and system-level testing and a schedule are shown in Fig. 21.

1. Compatibility tests. The compatibility tests were required by the project to demonstrate compatibility between the spacecraft and mission operations.

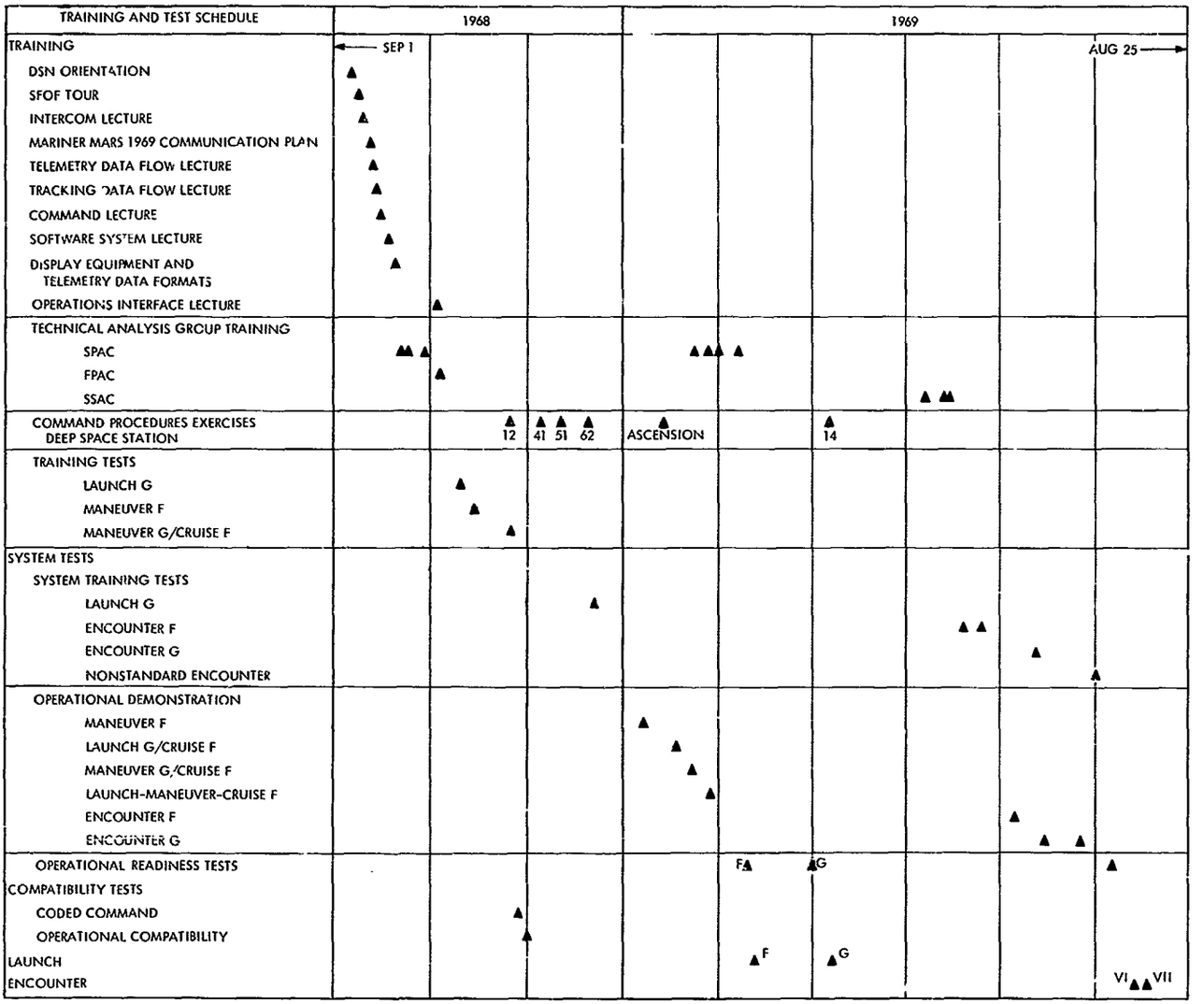


Fig. 21. Mission operations training and test schedule

The spacecraft-coded command data test was conducted on November 18, 1968 using the M69-4 spacecraft. The objectives of the test were to demonstrate that coded commands could be correctly produced by the COMGEN software program and that qualitative commands, coded commands, and direct commands could be correctly transmitted to a flight spacecraft by the DSN command system. The test objectives were met and compatibility was demonstrated.

The second operations system compatibility test was the *Mariner* Mars 1969 operational compatibility test and was conducted on November 20, 21, and 22, 1968, again using M69-4 as the flight spacecraft. The objectives of this three-day test were to demonstrate that the mission operations personnel using the facilities, hardware, software, procedures, and selected parts of the standard encounter sequence of events could operate and control a flight spacecraft. No basic incompatibility was detected during the test. Problems that did occur resulted in improvements in the standard sequence of events and in other procedural areas.

2. *Training.* The objectives of the training tests for mission operations were (1) to familiarize mission operations personnel with the equipments, software, data formats, displays, and facilities to be used during Space Flight Operations; (2) to train mission operations personnel in the execution of mission-dependent operational procedures and sequences; and (3) to train mission operations personnel to operate as an integrated team.

The operations system training exercises started on September 9, 1968 with a series of classroom orientation lectures as shown in Fig. 21.

The next phase of the operations system training, the technical analysis group (TAG) training, was the responsibility of the respective TAG director and had as a general set of objectives (1) to verify TAG internal procedures; (2) to train individual groups to function as a coordinated team; and (3) to establish readiness of the TAG personnel to support system-level testing.

Since most of the FPAC team had operations experience on other missions, the process of developing a smooth functioning team was greatly simplified. Therefore, only one exercise was conducted. During the exercise, minor problems were experienced in computer program initialization, communication network configuration, area configuration, and card reader operation, and the simulated tracking data was somewhat unrealistic. However, the training objectives were met and the problems noted were resolved in subsequent training operations.

Table 8. Training and system-level testing

Test category	Types	Responsibility	Documentation
Compatibility	Spacecraft–DSIF	Spacecraft System manager	Compatibility test plan
	Spacecraft–MOS	Space Flight Operations director	
Software	User acceptance	Software system engineer	Software test plan
	DSN acceptance	DSN project engineer	
	Software system	Software system engineer	
	SFOD acceptance	Space Flight Operations director	
Training	DSN personnel training	DSN project engineer	Mission operations training plan
	MOS/TDS personnel training	Space Flight Operations director and DSN project engineer	
System	TDS verification	DSN project engineer	DSN test plan
	DSN integration	DSN project engineer	
	MOS training	Space Flight Operations director	Space flight operations test plan
	MOS demonstration	Space Flight Operations director	
	Operational readiness	Space Flight Operations director	

The SPAC training of the technical analysis group was conducted in a series of seven exercises performed on the schedule shown in Fig. 21. The first two training exercises were for internal SPAC function verification, and the third was a two-day monitor exercise of a flight spacecraft system test.

Before the launch of the first flight spacecraft and after the availability of the proof test model spacecraft for mission operations testing in January 1969, the SPAC participated in a series of four training exercises to further its proficiency in the analysis of nonstandard spacecraft performance.

The SSAC training of the technical analysis group was not performed until the launch and maneuver phases of both flight spacecraft were complete. This was done because of a project decision not to establish the SSAC organization until May 1, 1969, primarily because of budgetary reasons. Shortly after SSAC was established, a series of three training exercises were accomplished. Minor changes in area configuration, data formats, and in SSAC

procedures were initiated as a result of the training exercises and SSAC was declared ready to support the encounter system-level testing.

a. Command procedures exercises. These tests were the first project-directed training activities with the Deep Space Stations and were performed soon after the stations were declared operational by the DSN. In addition to standard command procedures, nonstandard and command abort procedures were exercised. The results of most of these exercises were satisfactory; however, in the instances where procedural problems or lack of understanding was indicated, portions of the test were repeated.

b. Training tests. These tests, the last in the training series, involved mission control, SPAC, FPAC, and DSN Space Flight Operations facility personnel and were the final training exercises prior to involvement of all other DSN systems. The elements not involved in these exercises were the Deep Space Stations, and telemetry, command, and ground systems external to the SFOF.

The most significant problems identified during these tests were errors and omissions in the standard sequence of events, minor software deficiencies, minor hardware problems, and area configuration problems. No problems significant enough to impact the start of system-level testing were discovered and all test objectives were accomplished.

3. *System tests.* The system tests performed for the Mission Operations System were as follows:

(1) To develop and demonstrate teamwork between the operating groups.

(2) To refine the operating procedures and sequence of events to be used during Space Flight Operations.

(3) To demonstrate the capability of all operating groups to execute the Space Flight Operations in accordance with the Space Flight Operations Plan during standard and selected nonstandard operations.

(4) To demonstrate the overall readiness of all elements of the MOS and TDS to support the Space Flight Operations.

a. System training tests. The launch G system training test was, in addition to the mission control personnel located in the SFOF, the first to involve other system elements. Support was provided by the near-Earth elements at the AFETR, including building AO and the RTCC, DSS 71, DSS 51, and DSS 62. During the test there were minor data processing problems, an RWV unit problem at DSS 51, a high-speed data transmission problem, and a predicts transmission problem. These problems resulted in changes to procedures and some modification to the launch sequence of events.

The remaining system training tests were conducted after launch in preparation for the encounter phase of the mission. These consisted of two encounter F tests, an encounter G test, and two nonstandard encounter tests. Test objectives for the encounter training tests had an additional emphasis on refinement of the encounter sequence of events and the encounter data system configuration. During the three encounter tests no significant difficulties were experienced, and confidence was established in the sequences planned for the complex encounter period.

The last training tests in the program were the two nonstandard encounter tests. These were simulated failures of the spacecraft CC&S and scan platform. The selection of these two failures was made because of the high command concentration that would be required in the unlikely event they would fail during the near encounter period. The performance of SPAC, FPAC, and SSAC and the response of the DSN to the highly nonstandard command activity was an indication that the mission operations personnel were ready to support the important encounter phase of the mission.

b. Operational demonstration tests. Four operational demonstration tests were performed before the launch of *Mariner F*: (1) maneuver F, (2) launch G/cruise F, (3) maneuver G/cruise F, and (4) launch/maneuver/cruise F. In general, the tests were structured to be progressively more difficult with anomalies induced so that the previous objectives could be demonstrated. The last test in the sequence was a three-day continuous operation in which staffing plans for the mission were demonstrated by all technical analysis groups, mission control, and the DSN. At the end of this test series, the mission operations organization was ready to support the launch of *Mariner F*.

Before the encounter operations, two encounter operational demonstration tests were performed: the first for *Mariner VI*, the second for *Mariner VII*. The readiness of mission operations personnel was demonstrated in these tests to support the encounter phase of the mission.

c. Operational readiness tests. The operational readiness tests were to demonstrate that all committed elements of the Mission Operations System and the Tracking and Data

System were operational and ready to support the launch, acquisition, and maneuver phases of the mission, and the encounter phase of the mission.

The readiness test for *Mariner F* was divided into two parts, the first covering the period from launch minus 6 h to launch plus 4 h, and the second from maneuver minus 3 h to maneuver plus 3 h. The flight spacecraft located on the launch pad at the AFETR was used as the data source for the countdown part of the test and simulated data was used after $T = 0$ and during the maneuver phase. No problems of significance arose and the Mission Operations System was ready to support the actual launch of *Mariner F*.

The objectives of the readiness tests for *Mariner G* were changed from those of *Mariner F* in that only the launch and acquisition phases of the mission were checked in the test. This was done because the DSN elements in the maneuver were actively engaged in tracking and commanding *Mariner VI* as required and were, therefore, ready to support a maneuver. No problems arose in the countdown with the flight spacecraft *Mariner G* or with the other MOS or DSN elements needed to support the launch attempt.

The final test for the mission was a three-day readiness test before the encounter of *Mariner VI*. The first two days of the test had the specific objectives of demonstrating that all hardware, software, and procedures which were to be used to gather, coordinate, process, distribute, display, and evaluate the *Mariner* science and engineering data during the encounter period, together with encounter inter-TAG coordination, decision making, and commanding procedures were ready to support encounter operations. The third day of the test was to demonstrate the readiness of the ground data system to process and display data during the encounter and playback phases of the mission. No difficulty was experienced.

The first test used the *Mariner VI* encounter sequence, and the second test the *Mariner VII* encounter sequence. All elements of the project were declared ready to support encounter operations.

4. Simulation system. The *Mariner* Mars 1969 simulation system was established and defined on June 1, 1967 by the Mission Operations System manager and the Systems Division manager. The simulation system is defined as the software and data system configuration that was to be used to generate and process simulated spacecraft telemetry data, related trajectory data, and Deep Space Station data for checking out the software and data systems training personnel, conducting operational tests, and diagnosing data and software system problems during the space flight operations.

Also, at this time, the *Mariner* Mars 1969 simulation design team was established by the same managers. The objective of the team was to identify and define a simulation system configuration and to develop software so that the DSN could develop a system to generate and process the required data.

Software programs developed by the simulation design team were identified as phase I, phase IA, and phase II ASI 6050 programs. Phase I programs were used primarily as static telemetry test data patterns to verify software and data system designs. Phase IA was a refinement in the program and used to some extent real spacecraft data derived from magnetic tape recording of spacecraft system testing. Phase IA was the simulation program that was used to support much of the operations system training and a large part of the system-level tests. The phase II program was designed to overcome some of the deficiencies observed during the use of phases I and IA. The program made extensive use of a spacecraft math model and was automatically responsive to ground commands but, because of the late development, was used only during the last few system-level tests before the launch.

5. Conclusions. The training and test program used in preparing mission operations personnel for the Space Flight Operations of the complex *Mariner* Mars 1969 mission was very successful. This was evidenced by the state of readiness demonstrated before the launch and also by the way in which many nonstandard and unplanned-for events were handled after launch up to and including encounter operations. The following observations are made about ways in which the program could possibly have been improved.

The number of tests for training and testing the mission operations personnel as a team was considered about the correct quantity. However, this number of tests to some extent competed with the technical analysis group training and all system-level testing occurred in the two-and-a-half months before the launch of the first spacecraft. The tests, therefore, were conducted on a schedule that prevented problems in software, hardware, and procedures from being corrected before the next scheduled test would take place. Fortunately, the problems were never serious enough to prevent meeting the test objectives. Opening this period of system-level testing to start four months before launch, and not increasing the number of tests, would relieve this problem.

Improvement could also be made in simulation. Command-responsive spacecraft engineering and science telemetry and the tracking data to follow would make the tests more realistic and result in a more qualified team of personnel before launch. Late in the test program, this was achieved somewhat in the telemetry simulation but responsive tracking data when involving the Deep Space Stations was never entirely satisfactory.

Minor problems which more time and money would solve and would give a higher confidence level to in meeting mission uncertainties, are the following:

(1) More formal nonstandard procedures should be developed for mission control, the technical analysis groups and the DSN.

(2) Formation of an SSAC group before the launch rather than after would reduce the risk that some area of the encounter operations procedures would be overlooked and would be difficult to correct.

(3) To some extent SPAC personnel were shared between spacecraft subsystem problem analysis and training and testing for mission operations. This is always a problem as the best, most knowledgeable people are desired in both areas.

(4) One-shift capability of FPAC personnel would put a severe handicap on preparation of maneuver and encounter operations in the event of illness or accident. Some backup should be provided during critical mission phases. This also applies to key people in SPAC, SSAC, and mission control.

References

1. *Flight Projects,* Space Programs Summary 37-53, Vol. I, p. 33. Jet Propulsion Laboratory, Pasadena, Calif., Sept. 30, 1968.
2. *Flight Projects,* Space Programs Summary 37-58, Vol. I. Jet Propulsion Laboratory, Pasadena, Calif., July 31, 1969.
3. *Flight Projects,* Space Programs Summary 37-51, Vol. I, p. 13. Jet Propulsion Laboratory, Pasadena, Calif., May 31, 1968.
4. *Flight Projects,* Space Programs Summary 37-56, Vol. I, pp. 17 and 18. Jet Propulsion Laboratory, Pasadena, Calif., May 31, 1969.

Tracking and Data System

I. Introduction

Provision and maintenance of the Earth-based tracking, telemetry, and command stations, the ground communications, and the operational facilities for the *Mariner* Mars 1969 mission were the responsibility of the Tracking and Data System, assigned to the JPL office of Tracking and Data Acquisition. During the conduct of mission operations, these facilities were to be operated or occupied, or both, by the mission operations organization, under the direction of the mission director (project manager) and space flight director, as described in Mission Operations System, Part 3.

The manager of the Tracking and Data System, appointed by the office of Tracking and Data Acquisition to the project, together with the manager of the Deep Space Network, who served as his assistant, were responsible for planning, developing, negotiating, and committing elements of the Air Force Eastern Test Range, the Manned Space Flight Network, the NASA Communications System, and the Deep Space Network to support the near-Earth and space-flight phases of the mission operations. A DSN design team headed by the DSN project engineer formulated the DSN configuration and other aspects of mission support, and the Tracking and Data System participated jointly with the Mission Operations System in the design of the mission operations.

Mission operations, essentially the joint product of the MOS and TDS design, development, and test efforts, consists of a data system, a software system, and an operations system, the last two of which are also described under mission operations. The data system includes all Earth-based equipment provided by all project systems for the receipt, handling, transmission, processing, and display of spacecraft data and related data during the conduct of mission operations. Except for relatively small amounts of mission-dependent equipment supplied by project elements, all equipment is provided and operated by the DSN and, during the near-Earth phase, by the AFETR and the MSFN. Mission-dependent equipment is operated and maintained by the DSN after acceptance.

The Tracking and Data System support required by the project was formulated in a support instrumentation requirements document (SIRD) for NASA facilities, and a program requirements document (PRD) for Department of Defense facilities (through AFETR). The NASA support plan described the DSN, the NASCOM, and the MSFN support.

II. Description of the Tracking and Data System

The TDS was composed of the facilities and resources of four major support agencies:

Air Force Eastern Test Range. The U.S. Air Force, through the Air Force Systems Command and the National Range Division, manages the Air Force Eastern Test Range (AFETR) for the Department of Defense. As the lead range for *Mariner* Mars 1969, the AFETR arranged the required worldwide support from Department of Defense resources. The AFETR provided prelaunch, launch, and near-Earth tracking and data acquisition support for *Mariners VI* and *VII*.

Manned Space Flight Network. Operated for NASA by the Goddard Space Flight Center, the Manned Space Flight Network provided near-Earth tracking and data acquisition support for *Mariners VI* and *VII*.

NASA Communications System. The NASA Communications System (NASCOM), operated for NASA by the Goddard Space Flight Center, provided ground communications circuits required for support of *Mariners VI* and *VII*.

Deep Space Network. The Deep Space Network (DSN), operated for NASA by Jet Propulsion Laboratory, provided mission support in the areas of deep space tracking, metric and telemetry data acquisition, commands, and operational control.

The organization developed to manage TDS activities for the *Mariner* Mars 1969 project is shown in Fig. 1. Personnel in TDS activities had the following responsibilities:

Associate administrator for Tracking and Data Acquisition. The associate administrator for Tracking and Data Acquisition at NASA Headquarters designated the Jet Propulsion Laboratory as the Tracking and Data Acquisition support center for *Mariner* Mars 1969.

TDS manager. A tracking and data system manager was appointed by JPL, whose primary responsibility was to match the tracking and data acquisition requirements of the project with the capabilities of the TDS facilities which provide support. His task was to organize and direct all cognizant agencies in accomplishing the evaluation, planning, and implementation of TDS capabilities to support the mission.

TDS assistant manager. The assistant manager of the TDS, who also served as the DSN manager, was directly assigned to the TDS manager. He was responsible for the planning and implementation of DSN support and, in addition, acted for the TDS manager in the latter's absence.

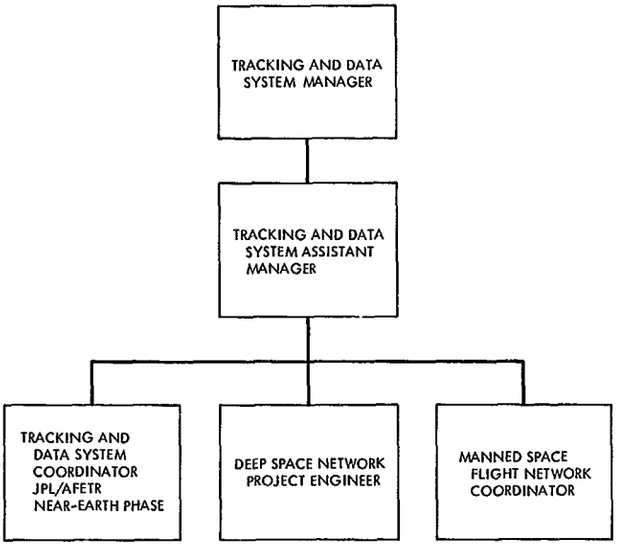


Fig. 1. Tracking and data system organization for *Mariner* Mars 1969

TDS coordinator for the near-Earth phase. The TDS coordinator for the near-Earth phase was a representative of the JPL/AFETR field station at Cape Kennedy. He was responsible for integrating AFETR, MSFN, and DSN plans, testing, and operations as needed to verify the TDS near-Earth phase.

MSFN coordinator. An MSFN coordinator from the Goddard Space Flight Center was the central point of contact between MSFN elements and other interfacing agencies. He was responsible for MSFN planning support and for assuring that compatible interfaces were established to make the MSFN function an integral part of the TDS in meeting project requirements. He represented the MSFN at TDS meetings and at project meetings.

AFETR program management officer. The AFETR program management officer was the single point of contact between AFETR elements and other interfacing agencies. He was responsible for AFETR planning support and for assuring that compatible interfaces were established to make the AFETR function as an integral part of the TDS in meeting project requirements. He represented the AFETR at TDS meetings and at project meetings.

DSN project engineer. The DSN project engineer coordinated all DSN systems and subsystems, working with representatives from numerous technical sections at the Laboratory. He ensured that all systems interfaced in a compatible and timely fashion. He was responsible to both the DSN and the *Mariner* Mars 1969 project for matching the requirements of the project to the capability and commitments of the DSN. He also served as the chairman of the DSN/*Mariner* Mars 1969 planning and operations team.

DSN facility project engineers. Facility project engineers of the DSN, assigned technically to the DSN project engineer, were responsible for interface engineering and operations planning before launch. Interface engineering included the system-to-system integration and testing of hardware and software. Operations planning included the design and preparation of the operational support to be supplied to the project by the DSN. During prelaunch testing and during the flight, the DSN facility project engineers had operational assignments in support of the operational elements of the TDS.

The DSN planning and operations team for the *Mariner* Mars 1969 project met once a week under the chairmanship of the DSN project engineer for the purpose of controlling and directing the interface engineering and operations planning. The facility project engineers comprising the team are shown in Figure 2.

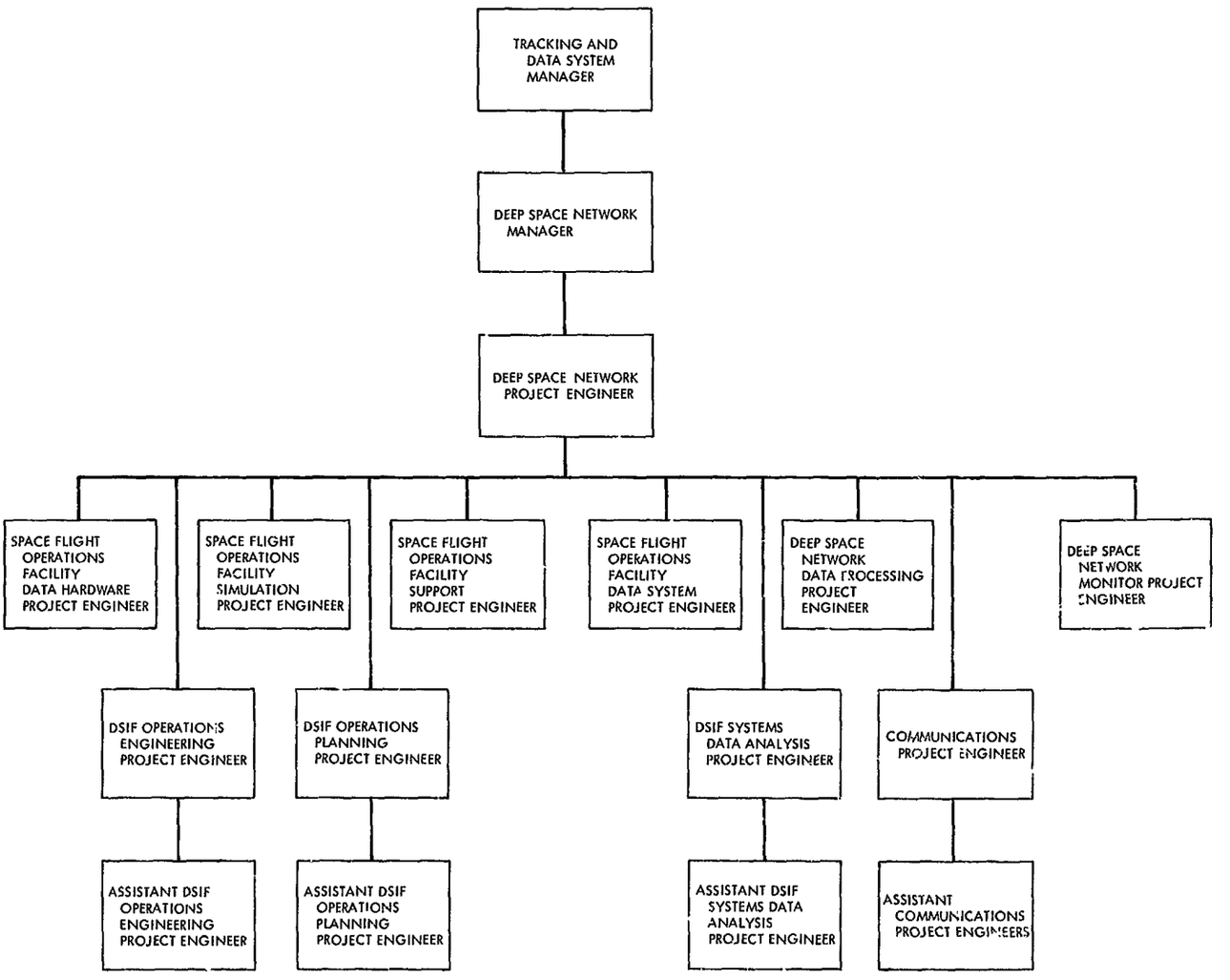


Fig. 2. Deep Space Network project engineering organization for *Mariner* Mars 1969

III. Flight Project Support Instrumentation Requirements

Tracking and data acquisition is defined as the acquisition, transmission, and processing of information which enables the determination of space vehicle position, velocity, direction, system and subsystem performance, and experiment measurements, all with respect to a common time base. The *Mariner* Mars 1969 project tracking and data acquisition requirements which the TDS was assigned to support are presented in this section.

Requirements were identified as occurring in either the near-Earth or deep space phases of the mission, and were grouped according to type: metric (tracking), telemetry, data transmission, communications, and data processing. The near-Earth phase began with prelaunch activities and continued through launch to continuous DSN view. At this point, the deep space phase began and continued to the end of the mission.

A. Near-Earth Phase Requirements

The project required the TDS to support a launch period each day from February 23 to April 8, 1969, with a daily launch window of one hour.

The powered flight trajectory mode was to be direct ascent (i.e., nearly continuous thrusting by the launch vehicle from launch to injection) and was to include one or two yaw maneuvers to achieve required high orbital inclinations without violating range safety restrictions. Launch azimuths for planar trajectories (i.e., trajectories without yaw maneuvers) were between 80 and 108 deg east of north. Trajectories requiring yaw maneuvers had an initial launch azimuth of 108 deg east of north.

Coverage problems of the TDS for the *Mariner* Mars 1969 project were less severe than for previous *Mariner* projects. The use of the direct ascent mode caused injection and *Centaur*/spacecraft separation events to occur well uprange, in the vicinity of Antigua Island, rather than near the African coast as happened with three previous *Mariner* missions. Since the area from Cape Kennedy past Antigua is one of concentration of AFETR/MSFN resources, coverage of launch through *Centaur*/spacecraft separation was easier than in the past.

Data acquisition requirements for the near-Earth phase were of the following: launch vehicle telemetry, launch vehicle metric data, spacecraft telemetry, and spacecraft metric data. The requirements anticipated use of very high frequency links for launch vehicle telemetry, C-band radar tracking for launch vehicle metric data, S-band reception for spacecraft telemetry and metric data, and very high frequency links for certain selected spacecraft telemetry channels through the launch vehicle telemetry system.

B. Deep Space Phase Requirements

1. Deep space phase coverage. Project requirements for TDS support during the deep space phase were divided according to mission intervals as shown in Table 1. Coverage of basically two types was required. Continuous coverage was required during launch, trajectory correction, and encounter operations. During cruise, the requirement was for telemetry data often enough to detect any spacecraft problems and take corrective action. Two consecutive spacecraft telemetry commutator cycles were stated as an adequate amount of information provided these operations were separated by a time slightly less than the spacecraft battery life. Since only engineering data was to be transmitted during cruise, observation periods of at least 28 min at 33⅓ bits/s or 112 min at 8⅓ bits/s were required, separated by not less than 5.6 h; 5.6 h is the closest multiple of a commutator cycle to the 6-h battery life restriction.

Metric data during cruise was required no less often than once every four days with the restriction that it must be derived from a complete horizon-to-horizon pass with no more than 20% of the data missing. One pass every 2 wk per spacecraft from the station equipped with the 210-ft antenna (DSS 14) was desired to meet a secondary objective: improvement of trajectory determination by the inclusion of ranging data obtained from research and development ranging equipment. Overall telecommunications performance did not predict acquisition of data from the operational Mark I ranging equipment at the 85-ft antenna stations much beyond 800,000 km, certainly not to planetary distances. Metric data were required for determination of the spacecraft trajectory and the required trajectory corrections. The required accuracies for metric data are listed in Tables 2 and 3.

2. Data acquisition and handling. Metric data requirements included angle data during the initial phase of the mission, but omitted this requirement later; range in two-way doppler was required throughout all phases. The data was required in real-time, except that the one-sample-per-second rate, during critical phases, was displayed on printers and plotters in the SFOF and recorded on magnetic tape. During cruise, or noncritical phases, requirements for metric data were that it be recorded on magnetic

Table 1. Deep space phase tracking and telemetry coverage requirements

Mission interval	Metric data required		Telemetry coverage required	Remarks
	Type	Sample rate		
First acquisition to launch plus 3 h	Range Doppler (2-way) Angles	Continuous at 1 sample/min 1 sample/10 s	Continuous	
Launch plus 3 h to midcourse maneuver plus 5 days	Range Doppler	Continuous at 1 sample/15 min 1 sample/min	Continuous	Mark I ranging expected only to about lunar distance. Assumes R&D ranging thereafter at 210-ft antenna only; one pass every 2 wk per spacecraft desired to meet secondary objective.
Cruise	Range Doppler	To be specified during operations 1 sample/min	Two complete spacecraft commutator cycles separated by no more than 5.6 h	Metric data requirement for one complete horizon-to-horizon pass every four days, separated by not more than 90 h. No single station shall be used for more than three consecutive passes. At 8⅓ bits/s, two commutator cycles are of 112-min duration; at 33½ bits/s, 28-min.
Second midcourse maneuver minus 10 days to plus 5 days	Range Doppler	Continuous at 1 sample/15 min 1 sample/min (1 sample/s during maneuver)	Continuous	May not be performed.
Encounter				
$E-14$ days to $E-1$ day	Range	1 sample/15 min	Continuous —	Mission design assumes three 85-ft antennas and one 210-ft antenna for standard operations and plans to take advantage of any additional support that may become available.
$E+1$ day to $E+10$ days	Doppler	1 sample/min		
$E-1$ day to $E-2$ h Exit occultation $+1$ h to $E+1$ day	Range Doppler	1 sample/min 1 sample/min	(8⅓ or 33⅓ bits/s and 66⅔ or 270 or 16,200 bits/s	
IRS[a] gas jetting -30 min to occultation Exit occultation $+20$ min to exit occultation $+1$ h	Range Doppler	1 sample/s 1 sample/s		1 sample/s data required in real time.

[a]Infrared spectrometer subsystem.

Table 2. Doppler and angle data accuracy requirements

Data accuracy	Correlation width T, min	2σ noise[a]		
		Two-way doppler, Hz[b]	Three-way doppler, Hz[b]	Angles, deg
To support primary mission objectives	$T < 10$ min	0.01	0.01	0.05
	$T \geq 10$ min	0.01	0.01[c]	0.2
To support secondary mission objectives	$T < 10$ min	0.005	0.005	0.01
	$T \geq 10$ min	0.005	0.005[c]	0.06

[a]All 1σ standard deviations are for tracking data taken above 5 deg local elevation.

[b]Based on 1 sample/min.

[c]Deviation from a constant bias; bias < 0.01 Hz for primary mission objectives and < 0.003 Hz for secondary mission objectives, throughout the pass.

Table 3. Ranging data accuracy requirements

Characteristic	Particular case	To support primary mission requirements noise (1σ)	To support secondary mission requirements noise (1σ)
Stability	Sample period		
	10^2 s	0.7 ns[a] — 0.1 m	0.3 ns
	10^4 s	5 ns — 0.8 m	1 ns
	10^5 s (1–2 days)	40 ns — 6 m	8 ns
Absolute accuracy	Signal-to-noise ratio		
	Strong	100 ns — 15 m	10 ns
	Weak	300 ns — 45 m	200 ns

[a]1 nanosecond (ns) $= 10^{-9}$ s $= 0.15$ meters (m).

tape and be immediately available if needed. All tracking data received in the SFOF in real time had to be displayed on teletype printers. Requirements for telemetry data were processing and recording in the IBM 7044–7094 computer string for display in the flight operations facility (Fig. 3). At each tracking station, requirements for telemetry data were processing in the telemetry and command processor for local display of selected spacecraft parameters and for preparation of the data for transmission to the SFOF. The requirement for the digital output of the processor was that it be recorded.

Since it appeared that *Mariner* Mars 1969 project would be the first with a high probability of two spacecraft successfully launched, the project agreed to schedule operations of the two spacecraft so that when one was in a critical phase, the other would be in a quiescent state. The intent was to scale the requirement to stay within the capability of the 7044 redesign to handle two missions or data streams simultaneously in one 7044–7094 computer string. The project was aware that DSN resources would permit the operation of but two such strings so that scaling the requirement in this manner permitted achieving the project goal of having block redundancy in major parts of the data system during mission operations.

An additional requirement was a capability to operate a double precision orbit determination program (DPODP) with the use of a 7040–7094 direct couple arrangement to be provided on a research and development basis, i.e., no backup.

3. Ground command requirements. Starting at approximately launch plus 1 h, command capability was required during any phase of the mission. The command system required use of read-write-verify (RWV) equipment provided by the spacecraft system and maintained and operated by the DSN. The project assumed the commands would be sent with the 10-kW transmitter capability at the 85-ft antenna stations. The project also required backup command capability from the 20-kW transmitter and the 210-ft antenna from 30 days before encounter through completion of playback in the event of nonstandard spacecraft performance.

4. Simulation. The DSN was required to provide a simulation capability which the project assumed was to be provided by the DSN simulation data conversion center, a primary element of which was an ASI 6050 computer. The center was required for the generation of simulated spacecraft telemetry and metric data during computer program testing and mission operations testing.

By means of mission operational function requirements, the project required that the capability exist to simulate simultaneously two operating spacecraft in the cruise

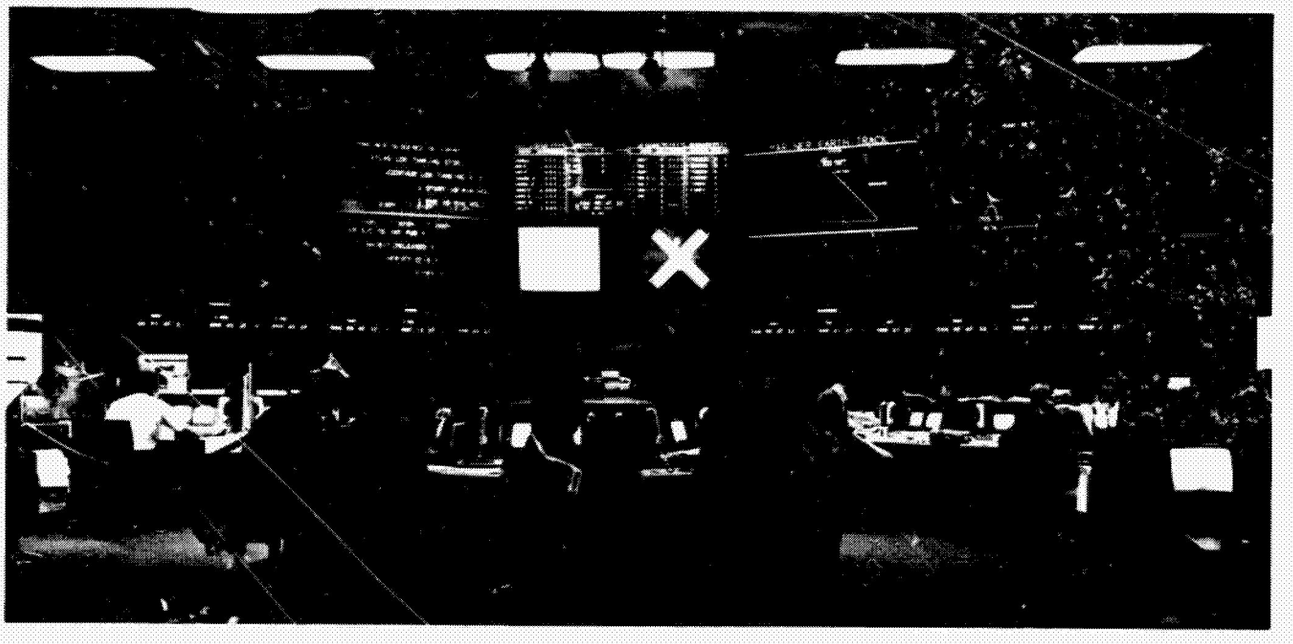


Fig. 3. IBM 7044–7094 computer string in the Space Flight Operations Facility

mode as well as one in the cruise mode and the other in a critical phase such as launch, maneuver, encounter, or nonstandard condition. A requirement of the simulation system was the capability required to be capable of inserting simulated data at various points in the data system including each prime tracking station.

5. Mission support area. The project requested a total of 7,750 ft² of space in the Space Flight Operations Facility in which to conduct mission operations. Separate rooms were requested for the functions of project management, mission control, flight path analysis, spacecraft performance analysis, space science analysis, and conference. A

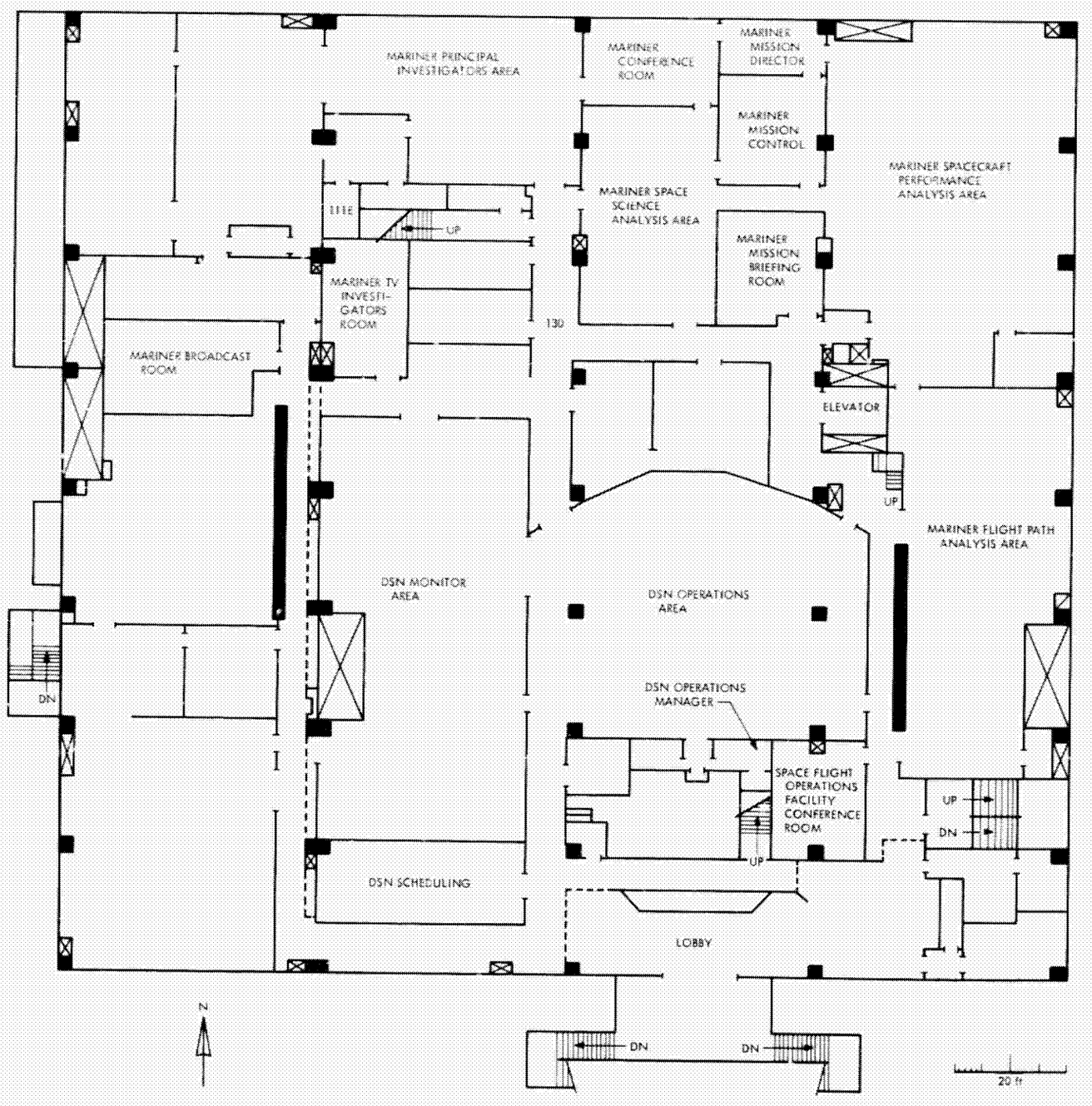


Fig. 4. Working area in the Space Flight Operations Facility

plan of these areas together with the DSN working areas, all located on the first floor of the SFOF, is given in Fig. 4.

Assistance was also required in interfacing with and providing data to complementary analysis team areas outside the SFOF. All areas were located in other buildings at JPL.

6. Compatibility testing. Support from the TDS facility was required to design, plan, and conduct radio frequency and data compatibility tests between the spacecraft and TDS facilities. The project based this requirement on the assumed availability of a DSN compatibility test area (CTA-21) at JPL. This capability was required to perform telecommunications subsystem tests and computer program checkout.

IV. Tracking and Data System Configuration and Operations Plan

Activities of the tracking and data system in support of mission operations design were conducted as outlined in Section I, by the system manager, the DSN manager, and the DSN project engineer, and supported by the DSN design team and the near-Earth phase coordinator. Results of such activities were documented in a comprehensive set of plans which, together with their accompanying schedules, were coordinated with similar activities and plans in the design of Space Flight Operations and the software system.

The principal elements of the TDS planning are set forth in a NASA support plan, a DSN operation plan for the *Mariner* Mars 1969 project, a DSN test plan for the *Mariner* Mars 1969 project, and a near-Earth phase operations plan for the *Mariner* Mars 1969 project. Additional provisions of the plan included interface descriptions between the deep space and near-Earth phases of the TDS with the spacecraft and mission operations systems and compatibility test plans for testing the interface design. Support from the Ascension Island station by the Manned Space Flight Network was covered separately by an MSFN operations plan for *Mariner* Mars 1969.

The NASA plan states the general capabilities to be supplied by the TDS, in response to the project requirements stated in the SIRD. The tracking stations planned for support of *Mariner* Mars 1969 in the near-Earth and deep space phases are shown in Tables 4, 5, and 6. The site of DSS 51, a typical 85-ft station, is shown in Fig. 5; the 210-ft advanced antenna system at DSS 14 is shown in Fig. 6.

The southerly declination of Mars during this mission resulted in a very southerly departure asymptote for the spacecraft for launches early in the opportunity. Figures 7 and 8 show how spacecraft at the southerly declinations

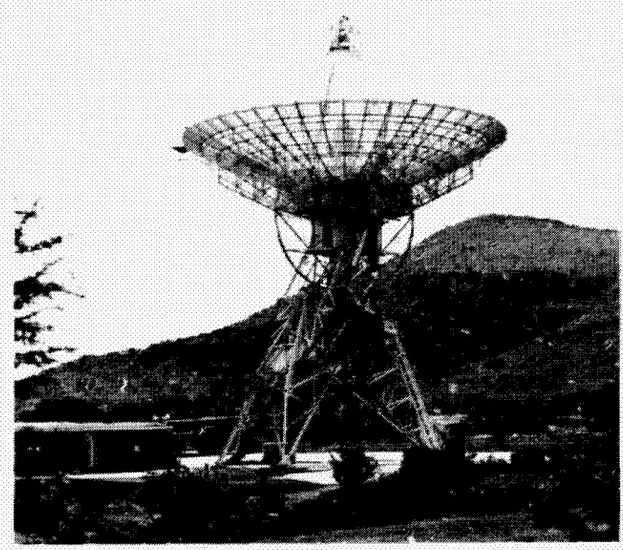


Fig. 5. Deep Space Station 51, near Johannesburg, South Africa

Table 4. Supporting stations in near-Earth phase, DSN and MSFN

Location	Instrumentation	Agency	Use	Remarks
Cape Kennedy	S-band telemetry and command	DSN	Spacecraft/DSN, compatibility test, spacecraft checkout, telemetry reception in early launch phase, and processing of AFETR telemetry	DSS 71, 4-ft manually aimed antenna
Ascension Island	S-band tracking and telemetry	MSFN	Spacecraft tracking and telemetry	30-foot X/Y antenna

Table 5. Supporting stations in near-earth phase, AFETR

Location	Instrumentation	Use	Remarks
Cape Kennedy	C-band radar	Launch vehicle tracking	AFETR Station 1.16: FPS-16, monopulse, 12-ft antenna, 1.0 MW peak power
Merritt Island	C-band radar	Launch vehicle tracking	AFETR Station 19.18: TDQ-18, monopulse, 29-ft antenna, 2.5 MW peak power
	S-band telemetry	Spacecraft telemetry	Tel-4: TAA-3, 33-ft antenna
	P-band telemetry		Tel-4: TAA-2A, 85-ft antenna
Patrick Air Force Base	C-band radar	Metric data and range safety	PAFB Station 0.18: FPQ-6, monopulse, 29-ft antenna, 2.5 MW peak power
Grand Bahama Island			AFETR Station 3:
	C-band radar	Launch vehicle tracking	FPS-16 and TPQ-18
	S-band telemetry	Spacecraft telemetry	TAA-3, 33-ft antenna
	P-band telemetry	Spacecraft and launch Vehicle telemetry	TAA-2A, 85-ft antenna
Grand Turk			AFETR Station 7:
	C-band radar	Launch vehicle tracking	TPQ-18
	S-band telemetry	Spacecraft telemetry	TAA-3
Antigua			AFETR Station 9:
	C-band radar	Launch vehicle tracking	FPQ-6
	S-band telemetry	Spacecraft telemetry	TAA-3
	P-band telemetry	Spacecraft and launch Vehicle telemetry	TLM-18
Ascension			AFETR Station 12:
	C-band radar	Centaur vehicle tracking	TPQ-18 and FPS-16
	S-band telemetry	Spacecraft telemetry	TAA-3
	P-band telemetry	Spacecraft and launch Vehicle telemetry	TLM-18
Pretoria	C-band telemetry	Centaur vehicle tracking	MPS-16
	S-band telemetry	Spacecraft telemetry	4-ft antenna
	P-band telemetry	Spacecraft and launch Vehicle telemetry	
Ship (metric)	C-band radar	Launch vehicle tracking	FPS-16
	S-band telemetry	Spacecraft telemetry	TAA-5-16
	P-band telemetry	Spacecraft and launch Vehicle telemetry	Rantec
Ship/Aircraft	S-band telemetry	Spacecraft telemetry	TAA-5-24 (ships only)
	P-band telemetry	Spacecraft and launch Vehicle telemetry	TAA-1 (ships); NKC 135 aircraft, 7-ft antenna
Trinidad	UHF radar	Centaur vehicle tracking	

Table 6. Instrumentation summary chart, deep space phase

Location	Instrumentation	Use	Remarks
Goldstone, California	S-band tracking, telemetry, and command	Spacecraft tracking, telemetry, and command	DSS 12, 85-ft equatorial antenna
	S-band tracking, telemetry, and command	Spacecraft tracking, telemetry, and command	DSS 14, 210-ft az/el antenna
Woomera, Australia	S-band tracking, telemetry, and command	Spacecraft tracking, telemetry, and command	DSS 41, 85-ft equatorial antenna
	S-band tracking, telemetry, and command	Spacecraft tracking, telemetry, and command	DSS 42, 85-ft equatorial antenna[a]
Madrid, Spain	S-band tracking, telemetry, and command	Spacecraft tracking, telemetry, and command	DSS 61, 85-ft equatorial antenna[a]
	S-band tracking, telemetry, and command	Spacecraft tracking, telemetry, and command	DSS 62, 85-ft equatorial antenna
Ascension Island	S-band tracking, telemetry, and command	Spacecraft tracking, telemetry, and command	MSFN, 30-ft X/Y antenna
Pasadena, California	Data processing and communications	Mission operations and DSN control	Space Flight Operations Facility
Johannesburg	S-band tracking, telemetry, and command	Spacecraft tracking, telemetry, and command	DSS 51, 85-ft equatorial antenna

[a]Deep Space Stations 42 and 61 were not available for meeting basic requirements since they were included in the planned support of other projects with uniform schedules. When not used for other projects, these stations could be used by the DSN to provide backup or additional coverage.

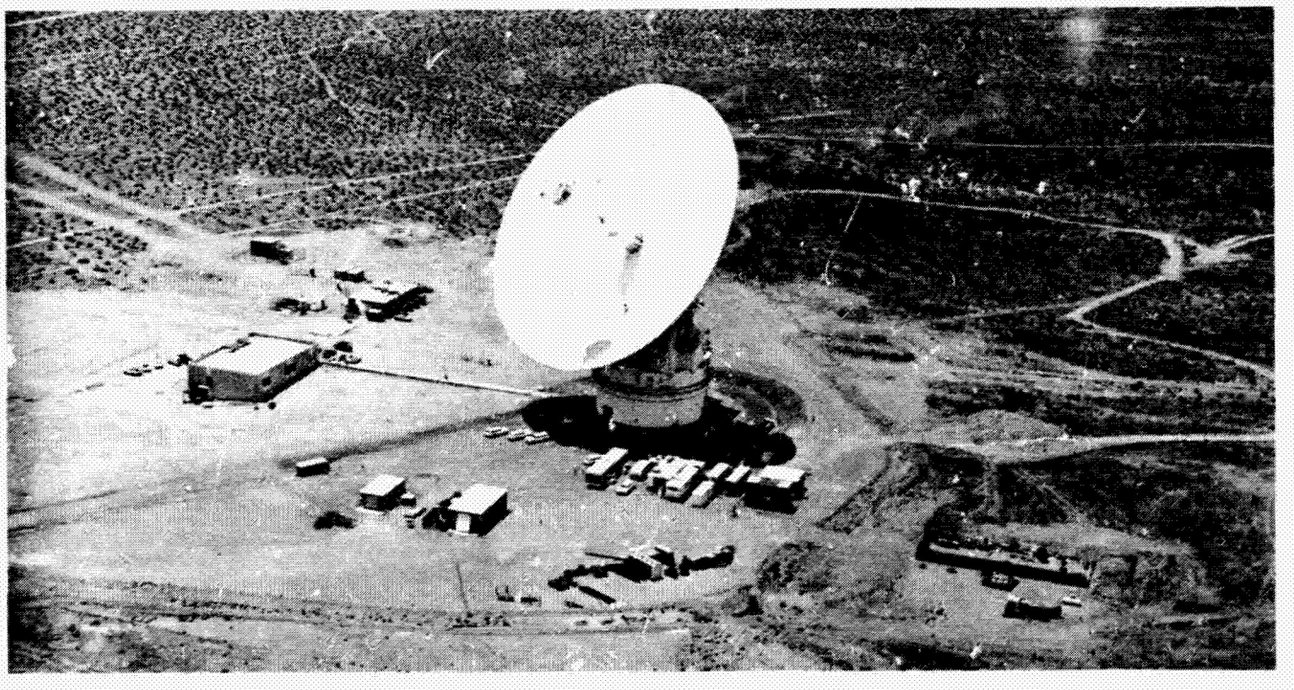


Fig. 6. Deep Space Station 14, the 210-ft diam Mars site, Goldstone, California

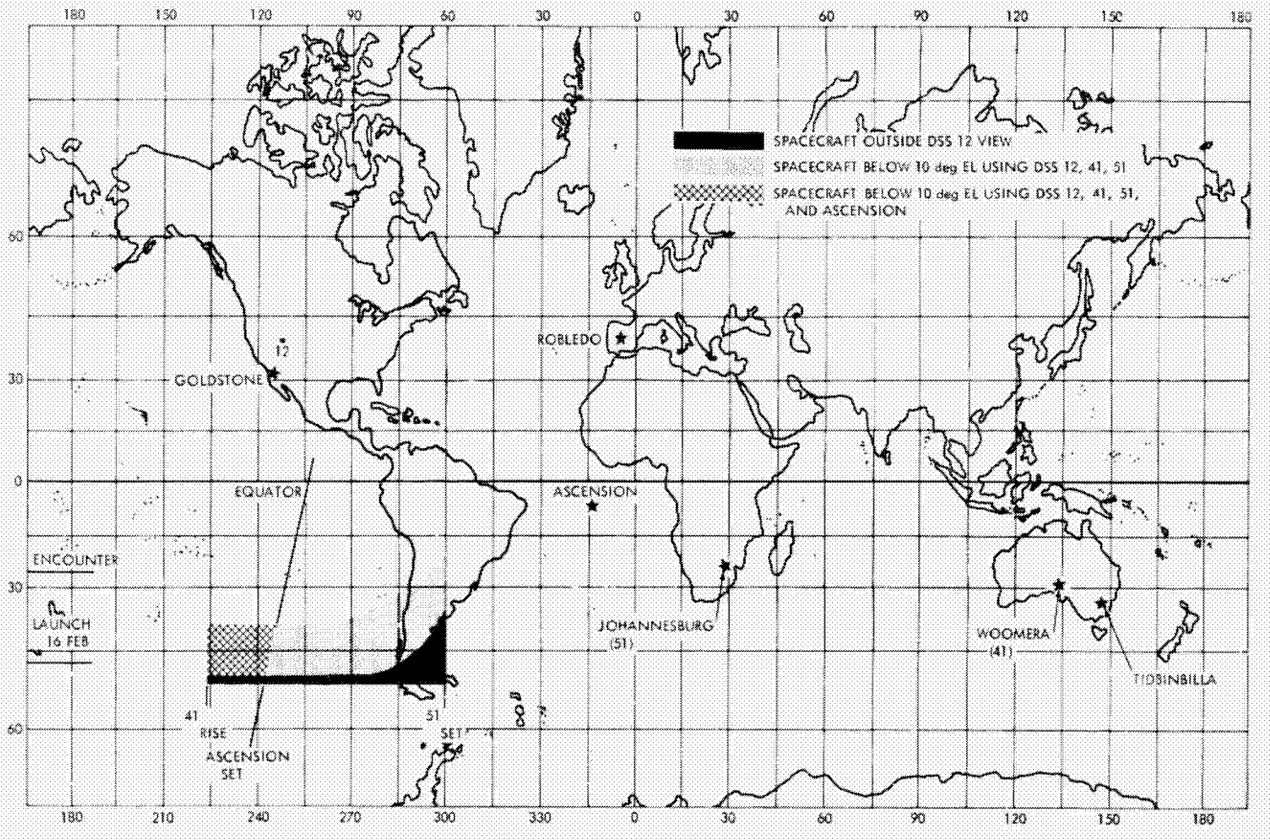


Fig. 7. Regions of degraded coverage with DSS 51

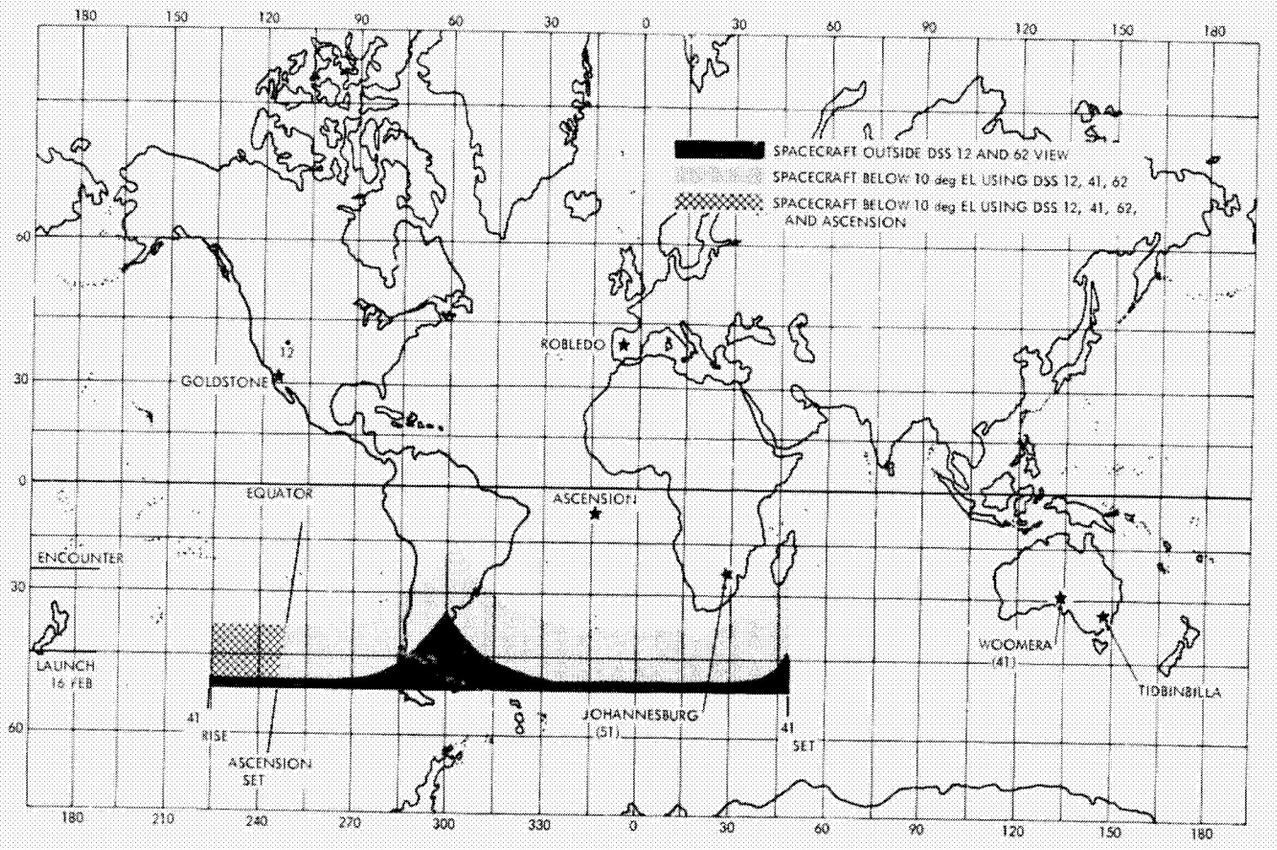


Fig. 8. Regions of degraded coverage without DSS 51

would receive somewhat degraded tracking from stations in the Northern Hemisphere. Such degradation was expected only during the first part of the *Mariner VI* flight.

Ground communications planned in the near-Earth and deep space phases are shown in Figs. 9 and 10, respectively. The numbers and types of circuits are generally consistent with those provided for previous projects.

Space available in the Space Flight Operations Facility for mission operations was 6,890 ft², compared with the 7,500 ft² requested by the project. A number of detailed requirements could not be met by the operational systems of the DSN. In some cases, research and development equipment was provided for limited periods of time on an experimental basis. The primary requirement for timing synchronization to within ±2 ms could be met. However, the secondary requirement for synchronization to within ±20 μs could be met only by use of the experimental, X-band, moon-bounce system. Ranging beyond lunar distances was not possible with the Mark I radar with which all stations were equipped. Experimental planetary ranging was provided at the 210-ft antenna station (DSS 14) at Goldstone, California. Continuous 24-h coverage of two spacecraft during critical phases could not be provided because of loading problems in the network. One subnet of three 85-ft-antenna stations was required to support the *Apollo* project shortly before *Mariner* encounter. *Pioneer* project had several spacecraft also requiring use of the network.

The Ascension Island station of the MSFN (Fig. 11) was committed to provide acquisition of metric and telemetry data and a command capability before initial acquisition by the DSN. It was expected that this station would continue to be able to track for a number of hours during the first pass.

The central processing system committed in the flight operations facility was a computer string composed of an IBM 7044, disc file, and IBM 7094. The string was committed in what was called the redesign mode to indicate the designed capability to handle two data streams in one string. A second string was provided for backup during critical phases. Since the string was not designed to handle the double precision orbit determination program (DPODP), the capability was also provided for an IBM 7040 and IBM 7094 to operate in a direct couple operating system mode.

The development of the operational organization for DSN *Mariner* Mars 1969 support was predicated on two assumptions: first, that the facility level operational organization was thoroughly experienced through support of many projects and, second, that the coordinator of interfacility operations and multi-project support was not a

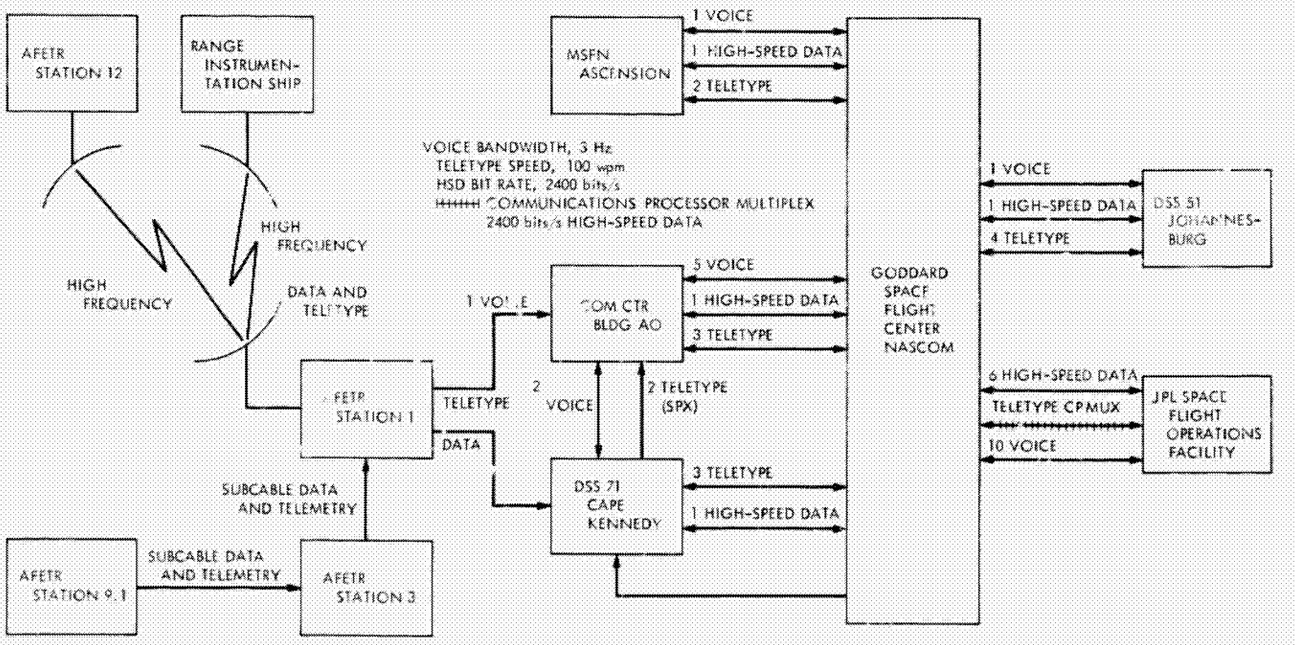


Fig. 9. Ground communications, near-Earth phase

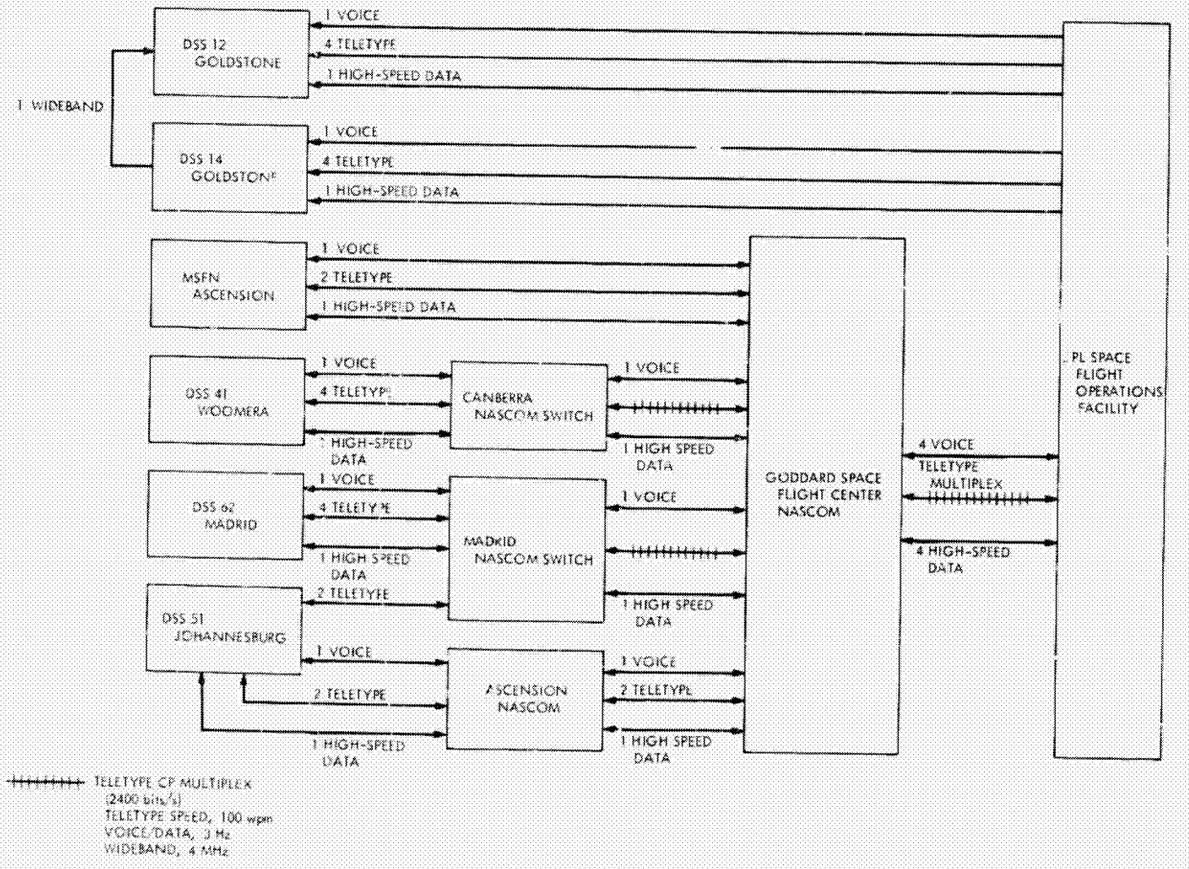


Fig. 10. Ground communications, deep space phase

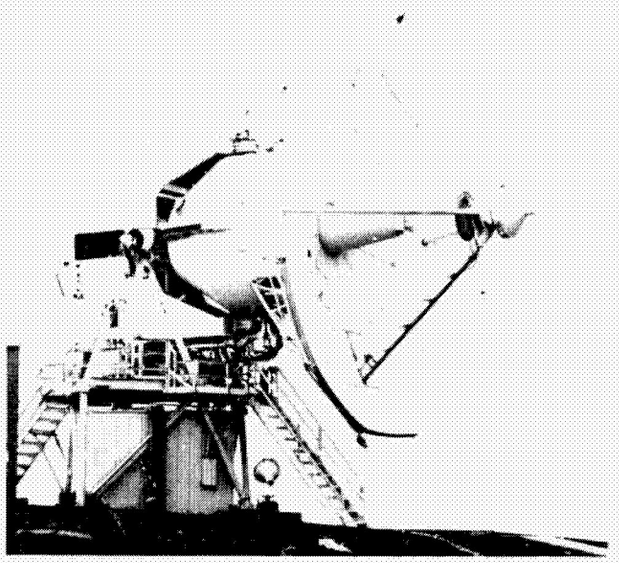


Fig. 11. Manned Space Flight Network, the 30-ft station at Ascension Island

logical point for the DSN to interface with the *Mariner* Mars 1969 Mission Operations System. This led to the formulation of the operational position, DSN operations director for *Mariner* Mars 1969. The interface with the Mission Operations System was defined as being between the operations director and the Space Flight Operations director. With this interface established, the first level of operational organization was defined as shown in Fig. 12. The duties of the operations director were as follows:

(1) To receive direction from the Space Flight Operations director and translate the requests into appropriate instructions for the three DSN facilities.

(2) To receive status reports from the facilities and relay these to the Space Flight Operations director or his designee.

(3) To designate a coordinator from the facility representatives for all tasks requiring interfacility coordination; then monitor the execution of the delegated tasks.

(4) To hold briefings as required to provide information relating the actual sequence to the planned sequence.

The next task was to define the working relationship between the operational team and an advisory group, consisting of individuals from the DSN interface design team for *Mariner* Mars 1969. The advisory group provided

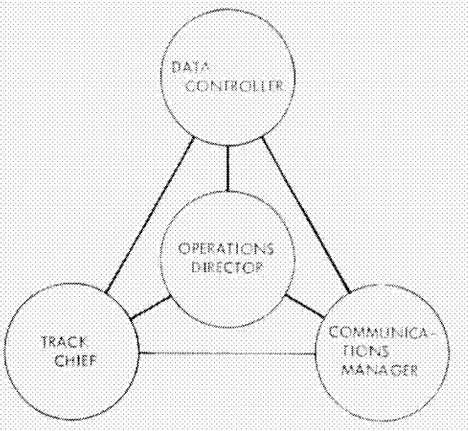


Fig. 12. First level operations organization of the Space Flight Operations director

technical information to the operations team upon request, information on ways to complete a specific task, and on priorities. The advisory organization worked with the first-level organization, as shown in Fig. 13.

A network analysis team was set up as an ad hoc activity for *Mariner* Mars 1969. The team, directed by a chief who acted as an advisor to the operations director, functioned during critical mission phases, staffed with selected volunteers from the development sections of the DSIF, ground computer facility, and flight operations facility.

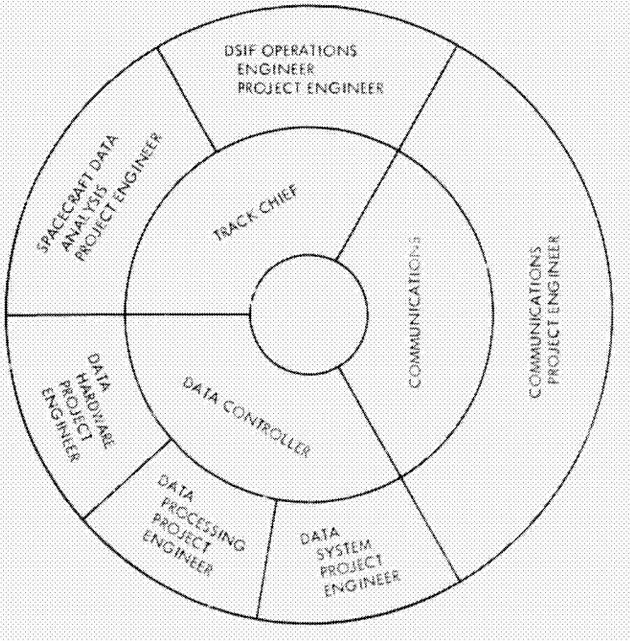


Fig. 13. Advisory organization integration

The problems that the network analysis team worked on dictated that the team interface with the DSN operational organization in two ways. When the problem was isolated to station or facility, the analyst worked directly with the appropriate advisor. When the problem could not be isolated, the analysis team chief established a working group of analysts and advised the operations director of the recommended course of action. Figure 14 shows diagrammatically the organization of the DSN operations control team. The DSN operations director interfacing with the flight project management exercised control and directed the DSN in support of commitments to the project.

The real-time coordination of the tracking station computers, the telemetry and command processor, and the data input system is handled through the track chief and station controller with assistance from track advisors and analysts as required. The communications processor and all other communications coordination is in the province of the communications manager and the communications controllers.

The data controller and data chief coordinate activities relating to data processing system computers and associated equipment and software. The support chief monitors and coordinates the environmental control systems, and off-line distribution and flow of processed data, and keeps the operations control team informed of the DSN status by means of large-scale off-line status displays. The monitor chief participates with the data chief in control of the data distribution system computers and monitors and advises the DSN operations director/operations control chief of DSN systems performance.

The chief of the network analysis team and his team of supporting network specialists maintain a constant analytical vigilance over the DSN systems in order to make rapid failure analysis/recovery recommendations to the operations control team, or to assume the failure analysis/recovery responsibility at the request of the operations director.

Training for the personnel of the TDS and MOS was planned in a jointly prepared mission operations plan. Training largely preceded and was intended to be distinct from the incidental experience gained during the test programs that were to follow. The DSN participated in two aspects of training. First was the training of its own personnel in executing mission-dependent operational procedures and operating mission-dependent equipment. Such training was conducted primarily at JPL for personnel of the ground communications and flight operations facilities. Key operators from various DSIF stations supporting this project were brought first to Goldstone and then to JPL for a 3-wk training period at DSS 12 and CTA-21. Upon returning to their respective stations, they assumed lead roles in on-site training of DSS personnel.

The second aspect of DSN training was to provide lectures and demonstrations for the familiarization of MOS personnel with equipment, software, data formats, and facilities of the flight operations facility. An essential element of this training was the lectures on data flow through the telemetry, tracking and command systems, and the operations interfaces.

Correct operation of the DSN depends on a large body of operational procedures which are for the most part mission-independent and evolved over the years during support of many missions. Some new procedures were used which were developed in connection with new system capabilities, while some were tailored for the *Mariner* Mars 1969 project to accommodate mission-dependent equipment and software.

Operation of the DSN telemetry system required procedures to accommodate data-rate mode changes in the telemetry and command processors at the Deep Space Stations and in the 7044 computer of the data processing system in the flight operations facility. The capabilities provided the telemetry system by the telemetry and command processor at the Deep Space Station, the high-speed data lines, and the 7044 computing system in the SFOF flight operations facility required development of procedures for accommodating the various data rates (8⅓ and 33⅓ bits/s on the engineering channel, and 66⅔ and 270 bits/s on the science channel). A routine procedure followed for protection of the telemetry system during critical phases by the ground communications facility was to provide special coverage on NASCOM circuits. Such coverage ensures that circuits and switching points are carefully monitored in order to switch quickly to backup circuits if required.

The DSN command system used the project-supplied RWV units for which command libraries of punched tapes were provided. Procedures for the correct operation of these units were developed and tested. Command sequences generated in the flight operations facility and transmitted to the Deep Space Station were handled by procedures which included, in addition to provisions for the generation, provisions for verification of correct transmission and receipt at the Deep Space Station and for monitoring the actual commands in process in the unit.

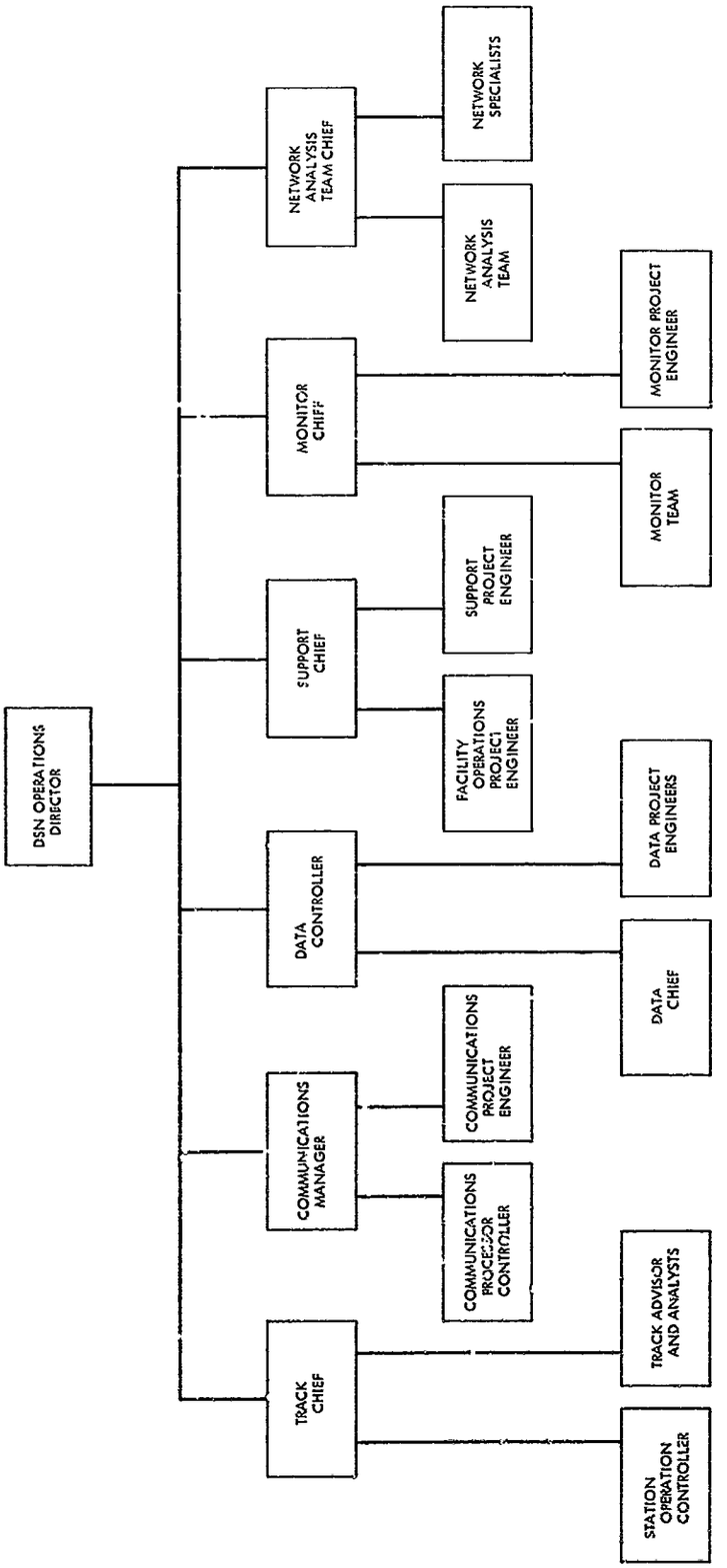


Fig. 14. Deep Space Network operations control team

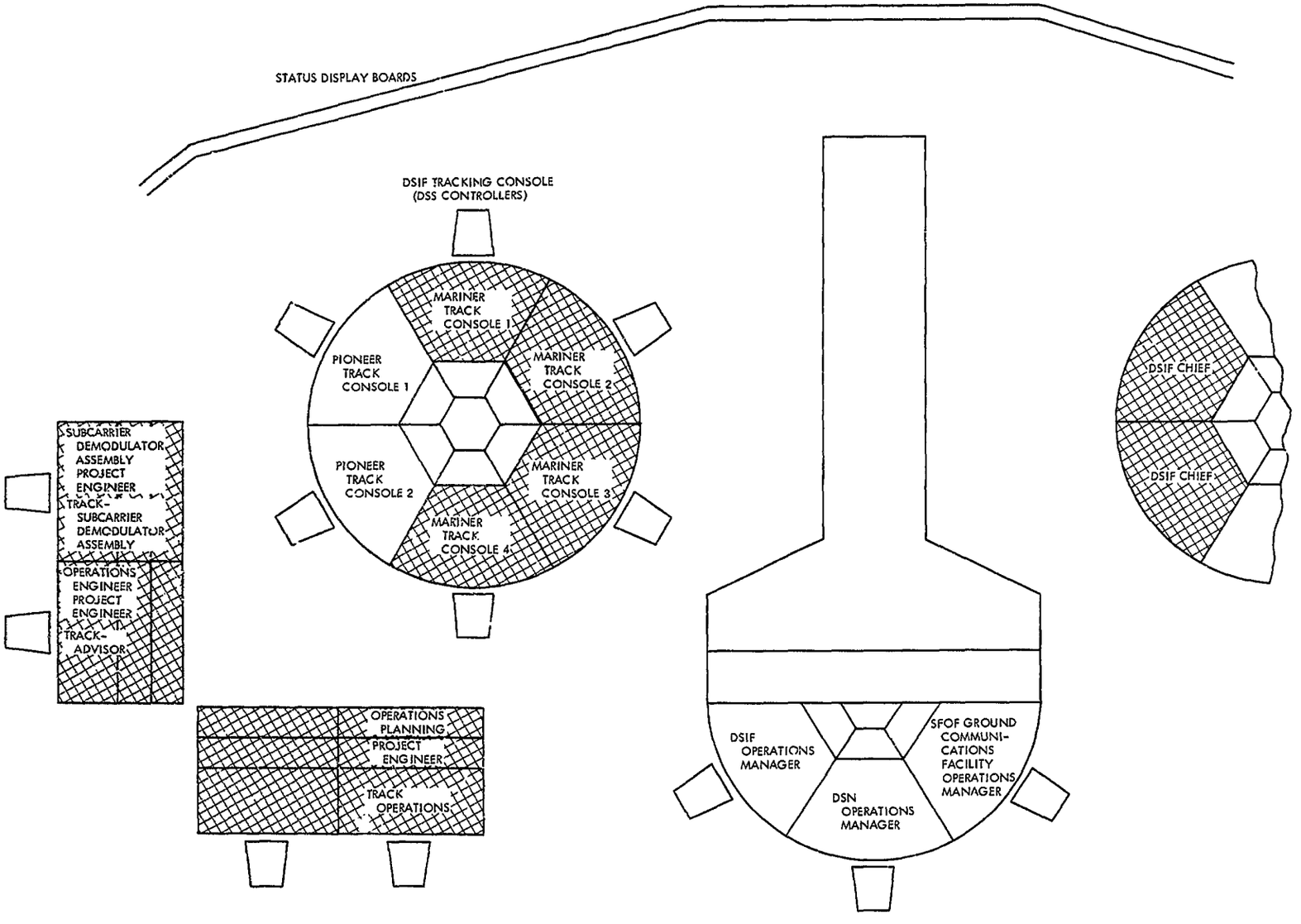


Fig. 15. Deep Space Instrumentation Facility operations control team

The Space Flight Operations director was provided a special voice circuit (red phone) for inhibiting any command activity.

The DSN tracking system operates in a largely mission-dependent manner in data acquisition. The principal mission-dependent activities for which procedures were developed are the generation and transmission of frequency predicts, procedures for initial acquisition of the spacecraft, programming the ground transmitter power level during the early phases of flight and, at encounter, the transmitter tuning strategy to be followed at occultation exit.

As part of the DSN operations control system, procedures were developed to direct the activities of the DSN operations team. As shown in Fig. 15, control of the DSIF by the DSIF chief was capable of accomplishment during periods of high activity by having the position manned by two persons. One DSIF chief directed command activities while the other interfaced with the DSN operations director and other members of the DSN operations team. Direction of the stations was through the DSS controllers at the round console, while the advisers and analysts were available nearby. Direction of the central processing system was managed in a similar manner by the data controllers (DACON) who manned positions at the round console opposite the DSIF chiefs. Again, during periods of high activity, one data controller worked with the DSN operations director while the other assisted him in working with the data chief who was in direct control of the computers. The communications activities were handled by the communications manager, following fairly routine procedures.

V. Tracking and Data System Preflight Testing

The TDS completed a series of internal training and test exercises before supporting the project operations. The philosophy related to the types of testing was standardized to apply to all elements of TDS supporting this mission. The testing was, in general, completed in November 1968 to ensure that the TDS was ready to support the combined mission operations testing which started in early December. The TDS ran operational tests throughout the mission to ensure that proficiency in various specialty items was maintained at a high level.

The training was defined to cover classroom-type instruction, as well as simulated operations. The testing followed a building block approach, starting at the facility level and proceeding through to system level testing. This applied to both engineering and operationally oriented testing.

A series of lectures was completed in August and September 1968 related to the theory of operation of the hardware and software peculiar to the *Mariner* Mars 1969 project. This training was provided for the senior operators from each of the supporting elements of the TDS, who then provided on-the-job training for their support personnel. This training included operators from each of the Deep Space Stations supporting *Mariner* Mars 1969.

Instruction in operational procedures developed for support of the project was completed in September 1968. Orientation lectures, conducted for all TDS personnel supporting this mission, covered two subjects. The first related to the spacecraft and its mission. The second covered the TDS, concentrating on the overall configuration and new technology which would be in effect during this mission. The second lecture was video-taped and shown at intervals from September 1968 until launch.

The integration tests were designed to demonstrate that the engineering features of the system/subsystem were met. The tests started at the facility level with testing of the mission-dependent hardware and software in the intended operational environment. The tests demonstrated items such as signal compatibility and bit error rates. After the facility tests were complete, the system level integration testing commenced. This testing covered groupings of the various facilities to determine the response time and loading of the various DSN systems.

Upon completion of the integration tests, the facilities were transferred to the operational organization. The operational verification tests were completed to demonstrate that the hardware could be operated in conjunction with the procedures. This testing was completed independently from the mission sequence, since the TDS may be called upon at any place in the sequence to provide a committed response time for a certain operation. The verification tests again started at the facility level and proceeded to the system level.

Configuration verification tests were essentially terminated for *Mariner* Mars 1969 in November 1968. To ensure that the configuration tested still existed at launch, the tests were completed at each facility as close to the actual launch as possible. This test resulted in a configuration freeze which was placed into effect at each facility.

Glossary

AAC	automatic aperture control
AC–	*Atlas/Centaur*
ACE	attitude control electronics
ACS	attitude control subsystem
A/D	analog-to-digital
ADC	analog-to-digital converter
AEOT	analog end of tape
AFETR	Air Force Eastern Test Range
AGC	automatic gain control
AGS	approach guidance subsystem
APC	automatic phase control
A/PW	analog-to-pulse-width
ATR	analog tape recorder
BCE	bench checkout equipment
BER	bit error rate
BPF	band pass filter
CAD	coherent amplitude detector
CAV	composite analog video
CC	coded commands
CC&S	central computer and sequencer
CTA	compatibility test area
CW	continuous wave or cordwood
DAS	data automation subsystem
DASC	data acquisition and storage console
DC	direct command
DE	development ephemeris
DIS	data input system
DN	data number
DPE	dynamic phase error
DPMMP	double precision matrix manipulation program
DPODP	double precision orbit determination program
DSE	development support equipment
DSIF	Deep Space Instrumentation Facility
DSN	Deep Space Network
DSS	Deep Space Station
DTL	diode transistor logic
DTM	development test model
DTR	digital tape recorder
DV	digital video
EA	electronic assembly
EB	electron beam
ECI	engineering change instruction
ECR	engineering change requirement
EDTL	environmental and dynamics testing laboratory
EMI	electromagnetic interference
EOS	Electro-Optical Systems, Inc.
ESA	explosive safe area
ESF	explosive safe facility
ET	ephemeris time
ETL	environmental test laboratory
EVT	extreme value theory
EXTR	exactor program
FA	flight acceptance
FAV	full analog video
FCS	flight command subsystem
FEPS	far-encounter planet sensor
FET	field effect transistor
FM	frequency modulation
FOV	field-of-view
FPAC	flight path analysis and command
FPS	flight power subsystem
FTS	flight telemetry subsystem
GCA	gyro control assembly
GCF	ground communications facility
GD/C	General Dynamics/Convair
GTS	ground telemetry system
HGA	high-gain antenna
HSDL	high-speed data line
IC	integrated circuit
IDCP	image data conditioning program
IPL	image processing laboratory
IR	infrared

Glossary (contd)

IRR	infrared radiometer subsystem
IRS	infrared spectrometer subsystem
J-FACT	joint-flight acceptance composite test
LCE	launch complex equipment
LEC	Lockheed Electronics Company
LeRC	Lewis Research Center
LGA	low-gain antenna
LMSC	Lockheed Missile and Space Company
LOS	line-of-sight
LSB	least significant bit
LTS	laboratory test set
LVS	Launch Vehicle System
MA&E	mission analysis and engineering
MC	midcourse maneuver
MCFR	media-conversion film recorder
MD	mission dependent
MID	mission independent
MMT	multi-mission telemetry
MOFR	mission operations functional requirements
MOS	Mission Operations System
MSB	most significant bit
MSFN	Manned Space Flight Network
MTF	modulation transfer function
NAMG	narrow-angle Mars gate
NRZ	non-return-to-zero
O/L	out-of-lock
OOGP	optical observable generator program
OSE	operational support equipment
OSSA	Office of Space Sciences and Applications
PAS	pyrotechnic arming switch
PC	printed circuit
PCE	power conditioning equipment
PCU	pyrotechnic control unit
PDP	project development plan
PFR	problem failure report
PIFOV	planet in field-of-view
PLB	propellant loading and instrumentation building
PLL	phase-locked loop
PMT	photomultiplier tube
PN	pseudo-noise
PPP	pre-processor program
PRD	project requirements document
PS	propulsion subsystem
PS&L	power switching and logic
PTM	proof test model
PU	propellant utilization
QA	quality assurance
QC	quantitative commands
RER	receiver exciter ranging
RFI	radio frequency interference
RFS	radio frequency subsystem
RT	real time
RWV	read write verify
RZ	return-to-zero
SAF	spacecraft assembly facility
SAT	select at test
SCAN	scan control subsystem
SCR	silicon controller rectifier
SCS	scan control subsystem
SDA	subcarrier demodulator assembly
SFOD	space flight operations director
SFOF	Space Flight Operations Facility
SFOP	space flight operations plan
SIRD	support instrumentation requirements document
SIT	separation initiated timer
SN	serial number
SNR	signal-to-noise ratio
SPAC	spacecraft performance analysis and command
SPE	static phase error
SSAC	space science analysis and command

Glossary (contd)

STC	system test complex
STCDS	system test complex data system
STCE	system test complex equipment
STM	structural test model
STS	system level test set
TA	type approval
TAG	technical analysis group
TCD	telemetry command data
TCFM	temperature-control flux monitor
TCM	thermal control model
TCP	telemetry and command processor
TDA	tracking and data acquisition
TDS	tracking and data system
TFR	trouble failure report
TI	Texas Instruments
TIG	tungsten inert gas
TLM	telemetry
T/R	transformer-rectifier
TTL	transistor transistor logic
TV-1	picture processing area
TV-A	wide-angle TV camera
TV-B	narrow-angle TV camera
TVC	thrust vector control
TVCA	thrust vector control assembly
TVS	television subsystem
TWT	travelling wave tube
TWTA	travelling wave tube amplifier
UIS	universal isolation switch
USNO	United States Naval Observatory
UT	universal time
UV	ultraviolet
UVS	ultraviolet spectrometer subsystem
VCO	voltage controlled oscillator
VHF	very high frequency
VLI	video level indicator

NASA — JPL — Comi., L.A., Calif.